MCR-69-611 Copy No.

CONTRACT NAS5-15208

Aerospace Systems Pyrotechnic Shock Data

(Ground Test and Flight)

Final Report

7 March 1970

Volume IV

Lockheed Data and Analyses

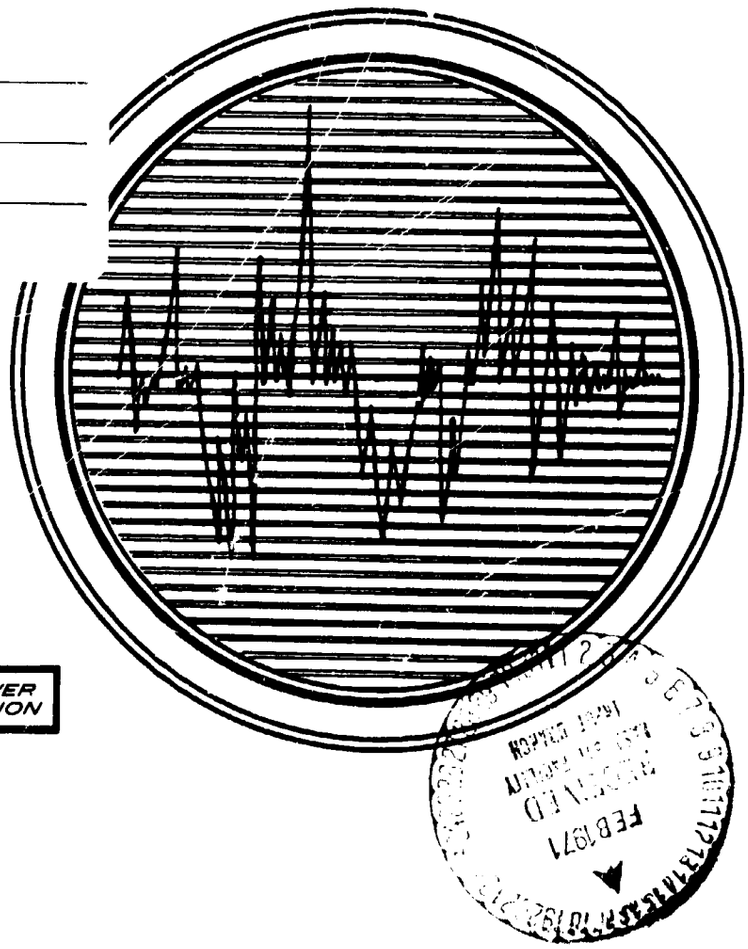

Prepared by

MARTIN MARIETTA CORPORATION DENVER DIVISION

for

GODDARD SPACE FLIGHT CENTER
GREENBELT, MARYLAND

FINAL REPORT

For

Aerospace Systems Pyrotechnic Shock Data (Ground Test and Flight)

June 1968 to March 1970

Volume IV

Contract No.: NAS5-15208

NASA, Goddard Space Flight Center

Contracting Officer: W. S. Kramer

Technical Monitor: William F. Bangs

Prepared by: Space System Dynamics Unit
Martin Marietta Corporation
Denver, Colorado

Contributing Authors: William J. Kacena III
Dr. M. B. McGrath
W. P. Rader

Approved:

F. A. Smith
Technical Director

Wilfred L. Kershaw
Program Manager

Prepared for: Goddard Space Flight Center
Greenbelt, Maryland

FINAL REPORT

for

COMPILATION OF PYROTECHNIC SHOCK DATA
(17 March, 1969 to 15 September, 1969)

Contract No: RC9-439031

Prepared by

LOCKHEED MISSILES & SPACE COMPANY
1111 Lockheed Way
Sunnyvale, California 94088

Authors: A. L. Ikola
G. G. Jacquemin
D. V. Retzloff

Project Leader: A. L. Ikola
A. L. Ikola

Group Leader: B. G. Wrenn
B. G. Wrenn

Department Manager: G. H. Moore
G. H. Moore

for

Martin Marietta Corporation
Denver, Colorado 80201

Contracting Officer: M. E. Weaver M/S C-0850

Technical Monitor: F. A. Smith

FOREWORD

The Martin Marietta Corporation, Denver Division performed a contract for the Goddard Spaceflight Center entitled "Aerospace Systems Pyrotechnic Shock Data (Ground Test and Flight)". This contract involved compilation and analysis of available industry wide pyrotechnic shock data. A total of 30 companies contributed. Because of the large volume of data available from Lockheed Missiles and Space Company, they were awarded a subcontract by the Martin Marietta Corporation to compile and analyze their data which are contained in Volumes IV and V. The results of these analyses have been included in the discussion contained in the summary document, Volume I. In addition, these analyses were considered in the preparation of the Design Guidelines Document, Volume VI.

GENERAL INDEX

NOTE: 1. Each section has complete Table of Contents.

2. See report format in "General Introduction."

GENERAL SUMMARY

GENERAL SUMMARY

The Pyrotechnic Shock Data Compilation presented in this report was prepared in compliance with Contract Number RC9-439031 granted to Lockheed Missiles & Space Company (LMSC) by Martin Marietta Corporation on 17 March, 1969.

The pyrotechnic shock data presented in this compilation was summarized from twenty-two Lockheed Missiles & Space Company reports. In order to present this data in a practical manner, it was subdivided into six groups to cover, respectively: separation joints, fairing jettisoning, pin actuators, external payloads, electronic box testing and shock testing devices. Information was also gathered from several other reports for use in general discussions and analyses.

A total of 445 shock spectra are presented together with 955 oscillograms. In addition, a large number of supplementary shock spectra were used to show various types of comparisons such as attenuation, repeatability, etc. This data was selected from about 500 shock spectra and approximately 1400 oscillograms (as quoted in the Second Quarterly Report) by eliminating duplication, most doubtful data, and data for which only insufficient documentation could be provided. It should be noted that this amount of data is considerably in excess of the contract specifications which required 250 to 350 shock spectra and 400 to 600 oscillograms.

In preparing this document, it was found convenient to follow the general pattern of the Lockheed Missiles & Space Company reports from which the data was taken. Each report was summarized and its data re-evaluated for the purpose of this compilation.

Sufficient analysis of the data was performed to describe the effects of pyrotechnic shocks. Definite trends were shown in several areas of interest which has led to a better understanding of the phenomenon.

The available data has a potential for more extensive analysis. This is discussed in Section VII of this report.

GENERAL SUMMARY (Cont.)

The following topics were considered for analysis on the basis of the Data available in this report:

1. Shock environment created by separation joints of various design.
2. Determination of the shock attenuation trend versus distance from the source.
3. Comparison of the environments generated by various fairing jettison mechanisms.
4. Comparison of the environment generated by pin pushers, pin pullers and explosive nuts.
5. Transmission of the shock environment through the interface between vehicle and external payload.
6. Reduction of the shock environment through equipment attachment brackets and effect of vibration isolators on the equipment shock level.
7. Analysis of pyroshock test facilities.

Some topics of a more general nature are also discussed. In particular, the application of statistical methods for determining test repeatability and confidence factors derived from full scale vehicle qualification testing.

The methods in use at Lockheed Missiles & Space Company for dealing with pyrotechnic shocks are described in a special section followed by information about instrumentation and data processing systems.

Finally, the structural and equipment failures which resulted from pyroshock tests are briefly discussed.

An effort has been made to point out the areas where more investigation appears to be needed to improve the state-of-the-art so that better shock predictions and improved design of structures and equipment may be achieved. The areas which merit special attention are:

1. Transmission of shocks through various types of structures. Influence of structural modes.

GENERAL SUMMARY (Cont.)

2. Shock attenuation versus distance from shock source for various types of structure.
3. Internal box environments at components and their mounting brackets.
4. Alternate methods of simulating pyro shock and correlation with known vehicle environments.
5. Evaluation of attenuation devices such as isolators, force limiting brackets, energy absorbers, snubbers, etc.
6. Statistical analysis of failure rate from components which are shock sensitive (relays, diodes, etc.).
7. Other methods of analysis such as Fourier Transform.

All shock spectrum data used in this compilation was processed on the UNIVAC 1108. This data, stored on punched cards, is available for further processing.

Although the pyrotechnic shock environment has been considered extremely important by Lockheed Missiles & Space Company for a number of years, the severity of this type of event has been somewhat underestimated by the industry at large. It is hoped that this compilation will help in placing this significant phenomena in proper focus.

SECTION NO. I

SUBJECT:

GENERAL INTRODUCTION

SECTION I

GENERAL INTRODUCTION

The Pyrotechnic Shock Data Compilation presented in this report was prepared in compliance with Contract Number RC9-439031 granted to Lockheed Missiles & Space Company by Martin Marietta Corporation on 17 March 1969. The compilation was performed in accordance with "Proposal for Compilation of Pyrotechnic Shock Data," LMSC/A943052, as modified by TWX LMSC/686607, dated 6 January 1969.

Contractual agreement provided a period of six months to complete the assembly and presentation of this data.

The majority of Lockheed Missiles & Space Company's effort was directed toward completing the data compilation. Significant effort was also devoted to analyzing the data. Areas of interest were treated as thoroughly as possible within the limitations of the contract.

Test data gathered at Lockheed Missiles & Space Company over a period of eight years was selected from twenty-two reports and replotted to meet contractual requirements. The reports were condensed into a form suitable for this publication. The data was available either as oscillograms or shock spectra or both. However, due to the use of several data processing systems, the shock spectrum presentation existed in various formats, either linear or log plots with non-consistent amplitude scales.

To replot the shock spectra in the required format, all available data was read at the appropriate frequencies by means of a Gerber Reader which provided a decimal output on punched cards. The cards were then processed on the UNIVAC 1108 with the help of a special program which rescaled the data and stored it on a tape for plotting. All shock spectrum plotting was performed automatically on the Stromberg Carlson 4020 High Speed Plotter. To obtain the desired format each plot was made in two halves which were later spliced together.

This report is subdivided into eight sections identified by Roman numerals.

SECTION I

GENERAL INTRODUCTION (Cont.)

The data compilation presented in Section II contains all oscillograms and shock spectra. It is divided into six subsections labeled A through F. Each subsection covers a particular aspect of pyrotechnic shocks described in a set of LMSC reports. Each report is presented as a separate entity with its own index, summary, introduction and analysis. The subsection links them together, also in a report form, with index, summary and, whenever pertinent, analysis showing some salient point common to the set of reports. The subsections (A through F) are then connected in the same fashion to form the Pyrotechnic Shock Data Compilation: Section II.

Sections III to VII complete the report to treat several important topics of a more general nature and Section VIII is a general conclusion.

A brief description of the contents of the report follows in order to provide the reader with an orientation background. This description covers Section II to Section VIII. It should be used in connection with the general index and with each subsection and report indexes for greater details.

SECTION II - Subsection A: Separation Joint

A set of seven reports covering Lockheed Missiles & Space Company's experience with a variety of pyrotechnic separation joints.

1. Ground tests and flight data.
2. Booster adapter separation and fairing jettison tests.
3. Modification to separation joint for shock reduction purpose.
4. Separation joint design for shock reduction purpose.
5. Special payload shroud separation. Hoop tension joint and cutters.
6. Booster adapter separation joint.
7. Satellite vehicle/booster separation test.

SECTION I

GENERAL INTRODUCTION (Cont.)

SECTION II - Subsection B: Fairing Jettison

A set of three reports covering two types of fairings and three actuator mechanisms.

1. Standard fairing - pin pusher actuated.
2. Standard fairing - comparison with a spring type pin puller
3. New fairing - spring-explosive nut mechanism.

SECTION II - Subsection C: Pin Actuators

A set of two reports discussing both pin pushers and pin pullers.

1. Shock environment simulation using pin pullers.
2. Study of pin puller isolation.

SECTION II - Subsection D: External Payloads

A set of two reports presenting data from tests of two external equipment pods.

1. Pod and equipment under separation joint shock.
2. Pod and other equipment under separation joint shock test.

SECTION II - Subsection E: Equipment Box Test

A set of six reports covering testing of electronic boxes and their attachment brackets. All test conducted for separation joint shocks were carried out on the Barrel Tester.

1.	Electronic box	Bay 2
2.	Three electronic boxes	Bay 2
3.	Bonded joint tests on special panel	Bays 1 and 2
4.	Electronic box	Bay 2 - inside barrel
5.	Equipment	Bay 1
6.	Electronic box on equipment	Bay 1

SECTION I

GENERAL INTRODUCTION (Cont.)

SECTION II - Subsection F: Development of Pyro Shock Test Facilities

A set of two reports covering a mechanical shock tester and a pyrotechnic shock tester.

1. Transfer Table shock tester.
2. Pyrotechnic Shock Barrel Tester.

SECTION III: General Analysis

This section contains analysis of a general nature performed with the available data. The following topics are treated:

1. List of analyses performed in Section II.
2. Test deviation, confidence levels and prediction of shock levels for full scale vehicle full ring separation tests.

SECTION IV: Lockheed Missiles & Space Company's Methods and Procedures

A discussion of LMSC's approach in dealing with pyro shock problems.

SECTION V: Instrumentation

Short description of the type of instrumentation generally used in pyrotechnic shock testing at LMSC. Method of data reduction is also discussed.

SECTION VI: Pyro Shock Failures

A survey of failures experienced at LMSC during shock qualification testing.

SECTION VII: Recommendation for Further Study

LMSC's opinion on the type of studies which should be carried out in order to advance the state-of-the-art in view of providing a satisfactory practical solution to the pyro shock problems.

SECTION VIII: General Conclusion

General remarks about the contents of this report.

SECTION NO. II.A

REPORT NOS. 606A, 674, 768, 790, 1080, 1340, 1377

SUBJECT:

SEPARATION JOINTS

SECTION II.A

SUMMARY

This section contains seven reports (No. 606A, 674, 768, 790, 1080, 1340 and 1377) which cover various tests and experiments carried out in the course of separation joint development. Some of this testing includes also sensor fairing jettison which is reported in greater detail in Section II.B. However, some discussion of test results is also presented in this section from the point of view of structural response to the shocks.

The development of separation joints covers several phases such as joint mechanical and pyrotechnic design, testing methods, comparison between flight and ground test results.

An effort is made in this section to determine the characteristics of the shock attenuation versus distance from the source. However, this summary analysis allows only to define a trend because in each test, too few data points are available to define the attenuation with good confidence.

The seven reports which form this section are as follows:

Report No. 606A covers flight test telemetry data for both booster adapter separation and sensor fairing jettison. The data was insufficient to validate a conclusion that the shock levels in space were different from those obtained at sea level. However, on the basis of unpublished data from a classified vehicle, the opinion is expressed that sea level atmospheric conditions have no significant effect on the environment generated by pyrotechnic shocks.

Report No. 674 covers the results of separation and fairing jettison tests carried out on a flight vehicle at the Santa Cruz Test Base. The tests were conducted for the purpose of improving confidence on the whole vehicle system. The vehicle system performed satisfactorily prior to and after the test thereby demonstrating no detrimental effect from the shock environment. The vehicle was flown successfully.

General shock data gathered during ground testing is presented in this report and an attempt was made to determine an attenuation curve on both shock spectrum and peak g bases.

Report No. 768 covers a series of full ring booster adapter separation tests conducted to evaluate methods of reducing the environment generated by the standard vehicle separation joint. The general results obtained from these tests indicated that the modified separation joints produced only insignificant shock reductions.

Report No. 790 covers a series of tests to evaluate three new separation joint configurations designed for shock level reduction. In all cases, the shock environment was significantly reduced but these types of joints were found difficult to incorporate into the present vehicle structure without extensive redesign and analysis. However, these joints could be used in new vehicle designs.

Report No. 1080 covers tests performed on a special spacecraft structure which is protected during launch by a shroud. The shroud release mechanism is activated by pyrotechnic devices. The separation system consists of a preloaded strap and four strap cutters designed so as to reduce the pyrotechnic shock environment. The shock levels recorded during tests were significantly lower than those generated by the standard separation joint.

Report No. 1340 covers booster adapter separation development testing carried out on a fully operational development test vehicle. The pyrotechnic shock environment was measured at selected locations on the vehicle in order to obtain environmental data. No failure of any kind occurred during testing and all systems remained operational.

Report No. 1377 covers tests performed for separation of a payload from the booster vehicle. These tests were carried out with a simulated spacecraft structure which included mass and c.g. simulated equipment of interest in order to gather environmental data. Although the data contained considerable scatter, a general attenuation curve was defined that would provide conservative estimates of the shock level at any point in the structure.

Repeatability of the shock environment for two firings is also investigated with the data from these tests.

In the analysis of the data presented in this section, special attention was paid to the development of a curve of shock attenuation versus distance from the shock source which would be applicable to the type of structure normally encountered on spacecraft and other similar vehicles.

An attempt at producing such a curve was found to be very difficult because of the interaction between vehicle modes and the high frequency shock response. Considerable additional analysis will be required in order to improve our estimating technique in this area.

TABLE OF CONTENTS

SECTION II.A

LIST OF TABLES

SECTION II.A

LIST OF FIGURES

SECTION II.A

SECTION NO. II.A.1

REPORT NO. 606A

SUBJECT:

FLIGHT DATA ANALYSIS OF BOOSTER SEPARATION AND FAIRING JETTISON EVENTS

SECTION II.A.1

SUMMARY

The primary purpose of Report 606A was to present the results of the data analysis which was completed on data taken from a flight vehicle during the booster adapter separation and horizon sensor fairing ejection events. These results were to be compared with results obtained from identical measurement locations during ground booster-adapter separation and horizon sensor fairing ejection tests on a similar vehicle. The purpose was to verify the ground test shock levels and to determine the effect of the atmosphere on the shock amplitudes. Agreement between flight and ground measurements would indicate that the extensive ground test data was valid and could be used to establish design and test criteria.

The range settings of the accelerometers that were to measure the shock in the forward rack on the guidance module which originated from the horizon sensor fairing ejection were set very high. In addition, the data channels were very noisy and therefore the shock data was lost in the noise level of the telemetry data channel.

Measurements were also made at the end of the aft rack (aft bulkhead) and at the engine cone/aft rack interface. Although the range settings for these accelerometers were more compatible with the shock levels, the noise level was still quite high and, combined with electrical interference, masked the shock data so as to make a correlation to ground test data almost impossible.

The test results were mostly inconclusive and flight data from identical measurements on a later, classified flight were used to fulfill the purpose of the measurement program as outlined above. In brief, measurements from the classified vehicle showed very good correlation with the ground test data above 500 Hz. It was later shown that the data did not correlate below 500 Hz because of low frequency components in the telemetry channel noise signal.

The results of the test program, including the classified vehicle measurements, showed that the density of the atmosphere has little or no effect on the shock levels above 500 Hz. The test results are inconclusive with respect to atmospheric damping below 500 Hz, however it is quite doubtful that the difference in atmospheric density could affect the shock amplitude to any significant degree.

TABLE OF CONTENTS

SECTION II.A.1

LIST OF TABLES

SECTION II.A.1

LIST OF FIGURES

SECTION II.A.1

II.A.1.1 INTRODUCTION

Data from tests of various separation system primacord joint configurations revealed that these pryotechnic devices yielded high acceleration shocks of characteristics which were not duplicated by qualification test methods that were available at the time report 606A was written. A test program was initiated to provide a definition of the shock environment which existed in the boost vehicle as a result of the detonation of these and other pyrotechnic devices (e.g., horizon sensor fairing pin pushers).

The test program was conducted in two phases. First, ground tests were performed on a vehicle which contained extensive shock measurement instrumentation (Section II.A.2). Second, selected measurements were made during the flights of two vehicles, one of which was classified. The results from the unclassified flight vehicle test are presented in this report, 606A.

Of special interest (in addition to defining the proper shock environment for use in establishing future design and test criteria) it was desired to determine the effect, if any, of the atmosphere on the shock amplitude.

II.A.1.2 DISCUSSION AND ANALYSIS

II.A.1.2.1 Test Configuration and Instrumentation

The test was conducted on a flight vehicle which was instrumented with six shock accelerometers and one noise transducer* to measure the shock environment generated during the booster adapter separation event and the horizon sensor door ejection event. A summary of the instrumentation is presented in Table II.A.1.1 and illustration of the instrumentation locations for the booster adapter separation event is shown in Figure II.A.1.1. Accelerometers for the ground test of a similar vehicle were located in exactly the same positions as the accelerometers for the flight vehicle test (see Section II.A.2).

Data from accelerometers 1, 2 and 7 was lost due to system electrical noise. Accelerometer 6 was purposely shorted to determine the system noise level during the shock.

Each of the measurement channels were calibrated to determine their roll-off characteristics. The roll-off is illustrated in Figure II.A.1.2. Each of the shock spectra should be adjusted upward at the higher frequencies to correct for the roll off. For example, the shock spectra for accelerometers 5 and 6 should be multiplied by a factor of 1/.80 = 1.25 at 2500 Hz to obtain the proper shock response level.

II.A.1.2.2 Test Results

The results of this test are presented in the form of shock spectra with their corresponding oscillograms in Figures II.A.1.3 to II.A.1.7. The shock spectra are presented for a Q of 50 for accelerometer 3 and for Q's of 5, 16.6, 50, 100 and 10^8 for accelerometers, 4, 5, and 6. The results from this flight test may be compared with results from the same accelerometer locations of the ground test which are presented in Figures II.A.2.22 to II.A.2.25.

* - The noise transducer consisted of a shorted accelerometer

Figure II.A.1.3 presents the results from accelerometer number 3 which was located in the longitudinal direction at the engine cone - aft rack interface. The calibration of the flight data channel for this transducer was incorrect. Artificial scale factors were used to show the general shape of the shock spectrum. As indicated in the figure, the data below 100 Hz is largely noise. The oscillogram and shock spectrum from the corresponding ground measurement is shown in Figure II.A.2.22.

Figure II.A.1.4 presents the results from accelerometer number 4 which was located in the radial direction at the engine cone - aft rack interface. This is the best data of all the measurements. Although system noise is very strong at 2500 Hz, the shock transient is clearly observable in the oscillogram and shows up at 800 Hz in the shock spectrum. The oscillogram and shock spectrum from the corresponding ground measurement is shown in Figure II.A.2.23.

Figure II.A.1.5 presents the results from accelerometer number 5 which was located in the longitudinal direction on the aft bulkhead of the aft rack. The oscillogram and shock spectrum from the corresponding ground measurement is shown in Figure II.A.2.24. Comparison of the ground and flight measurements shows that the flight spectrum for accelerometer number 5 is much higher than would be expected from the ground test data. Very high g spikes appear in the flight oscillogram. These spikes are believed to be electrical in nature and are not representative of the actual shock.

Figures II.A.1.6 and II.A.1.7 present the results from accelerometer number 6 which was shorted to measure the effect of shock on the noise level of the data. The measurement which produced the shock spectrum of Figure II.A.1.6 was taken before the shock and the measurement of Figure II.A.1.7 was taken during the shock. Comparison of the two spectra indicates that the shock did not raise the system noise level.

II.A.1.2.3 Analysis

Figures II.A.1.8 to II.A.1.10 present the results of an analysis to show the error which results in reading narrow band data in 1/3 octave bands at the 1/3 octave center frequency. The three figures indicate that reading the data in this manner can produce significant error. For example, the shock spectrum for accelerometer number 3 at the 1/3 octave center frequency of 2000 Hz reads 3000 g's. If an error in the frequency of only five percent were possible to accumulate during the data acquisition and data reduction processes, the actual reading could have occurred anywhere in the frequency range of 1900 to 2100 Hz. Thus the actual g level might have been anywhere from 1000 to 8250 g's. The total possible error which could result from reading two plots from two similar measurements at the 1/3 octave center frequencies could thus be as much as a factor of 8.25.

Another method which is used at LMSC to read shock spectra is to read the peak shock spectrum value in a 1/3 octave band. This method is more conservative but reduces the error due to frequency shift. As an example, if the maximum peak were read in the 1800 to 2240 Hz band, there would have been no error in the reading even if the frequency of the peak were shifted by as much as five percent (1900 to 2200 Hz) since the 1/3 octave band (1800 to 2240 Hz) includes this range.

The data also shows, because of its transient characteristics, that the shock spectrum amplitude is only slightly dependent on the (Q) used in the analysis. See Section II.A.7 for more information on Q vs amplitude.

II.A.1.3 CONCLUSIONS

Because of the noise content in the TM channels the data presented in this report for a flight vehicle is generally of poor quality.

The shock measurements which were intended to measure the shock from horizon sensor fairing ejection were not obtained as the levels were below the TM noise threshold.

A comparison of the shock spectrum of the noise channel before and during shock indicated that the shock did not increase the noise level.

A study of the channel roll-off characteristics of the flight data indicated a roll-off of the signal by as much as 20 percent at 2500 Hz on some channels.

A study of the error which is possible by reading that data at the 1/3 octave center frequencies showed that reading two sets of data from identical measurement locations in this manner can result in a reading error of a factor of 8.25 by virtue of a five percent shift in frequency in data acquisition and reduction.

Comparison of the data from this vehicle and that from the flight of the similar, classified vehicle with a ground test vehicle in which measurements were made in the same locations indicates good correlation above 500 Hz. This indicates that atmospheric density has little effect in this frequency region on the shock amplitude. Below 500 Hz, the results are inconclusive because of the low frequency noise content in the TM channel, however, it is believed that the atmospheric density also had very little effect below 500 Hz.

The test results of this report, in conjunction with the ground test results and the test results from the classified vehicle, indicated potentially damaging shock levels can be generated at equipment by the booster adapter separation event and the horizon sensor fairing ejection event.

A recommendation was made soon after this report was written that, in view of the high shock levels, equipment should be reviewed for its susceptibility to pyro shock and that susceptible equipment be either moved to another location or shock mounted. Additional pyro shock tests were recommended to evaluate shock mounts.

On the basis of this test series, the barrel tester* was recommended for qualifying equipment for pyro shock over other suggested methods because of the importance of duplicating the actual environment as closely as possible.

It was further recommended that shock spectra, not peak g's, should be used to establish qualification test requirements because the shock spectrum provides a more reliable and comprehensive definition of the excitation which exists throughout the frequency range and takes into consideration the number of excitation cycles.

* See Section II.F.2

TABLE II.A.1.1

ACCELEROMETERS AND LOCATIONS

Test Accelerometer Number	Station	Direction	Distance to Shock Source	Accelerometer Type
3	411	Longitudinal	27.0	ENDEVCO 2225
4	411	Radial	27.0	ENDEVCO 2225
5	462	Longitudinal	78.0	ENDEVCO 2225
6	462	Radial	78.0	ENDEVCO 2225

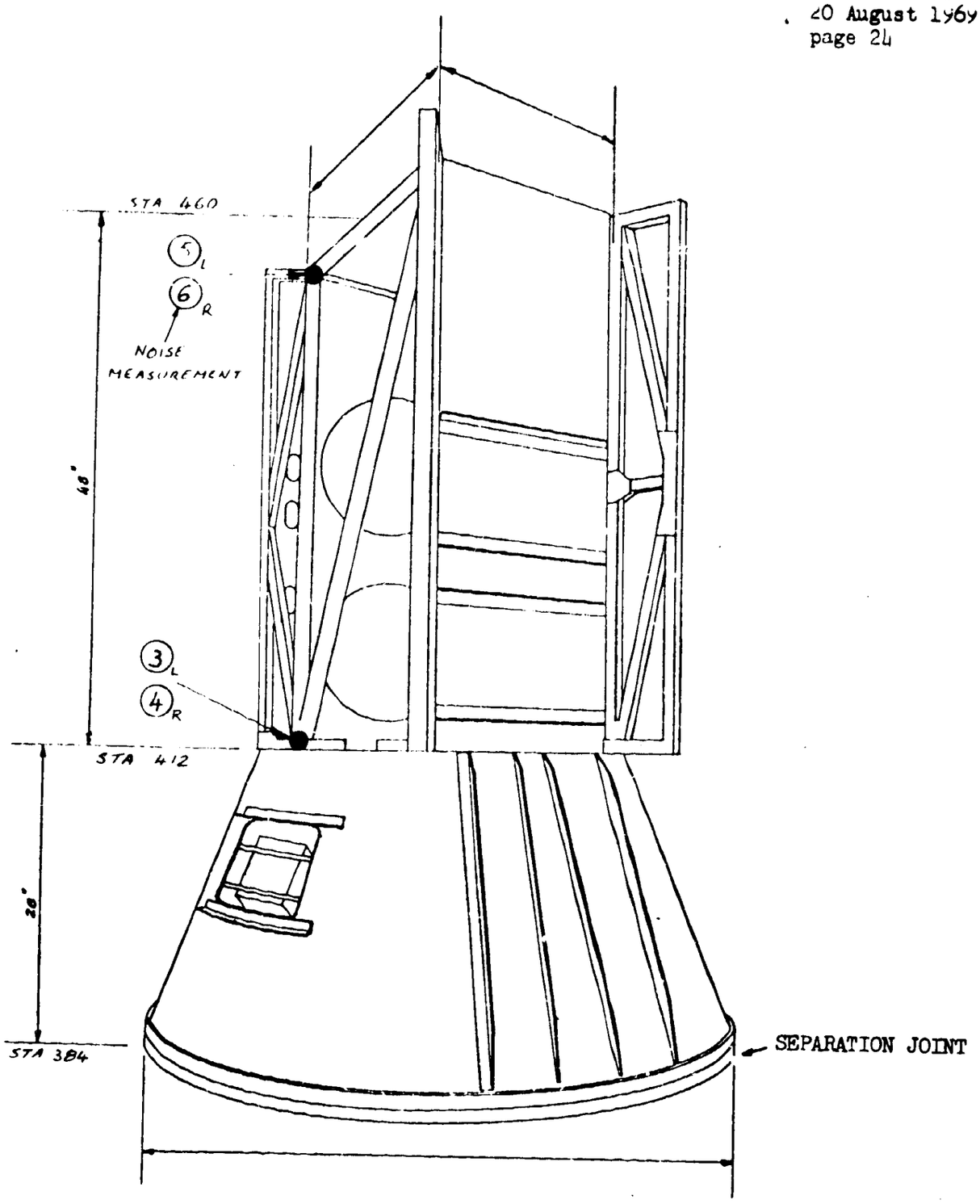

Figure II.A.1.1 VEHICLE STRUCTURE AND INSTRUMENTATION LOCATIONS

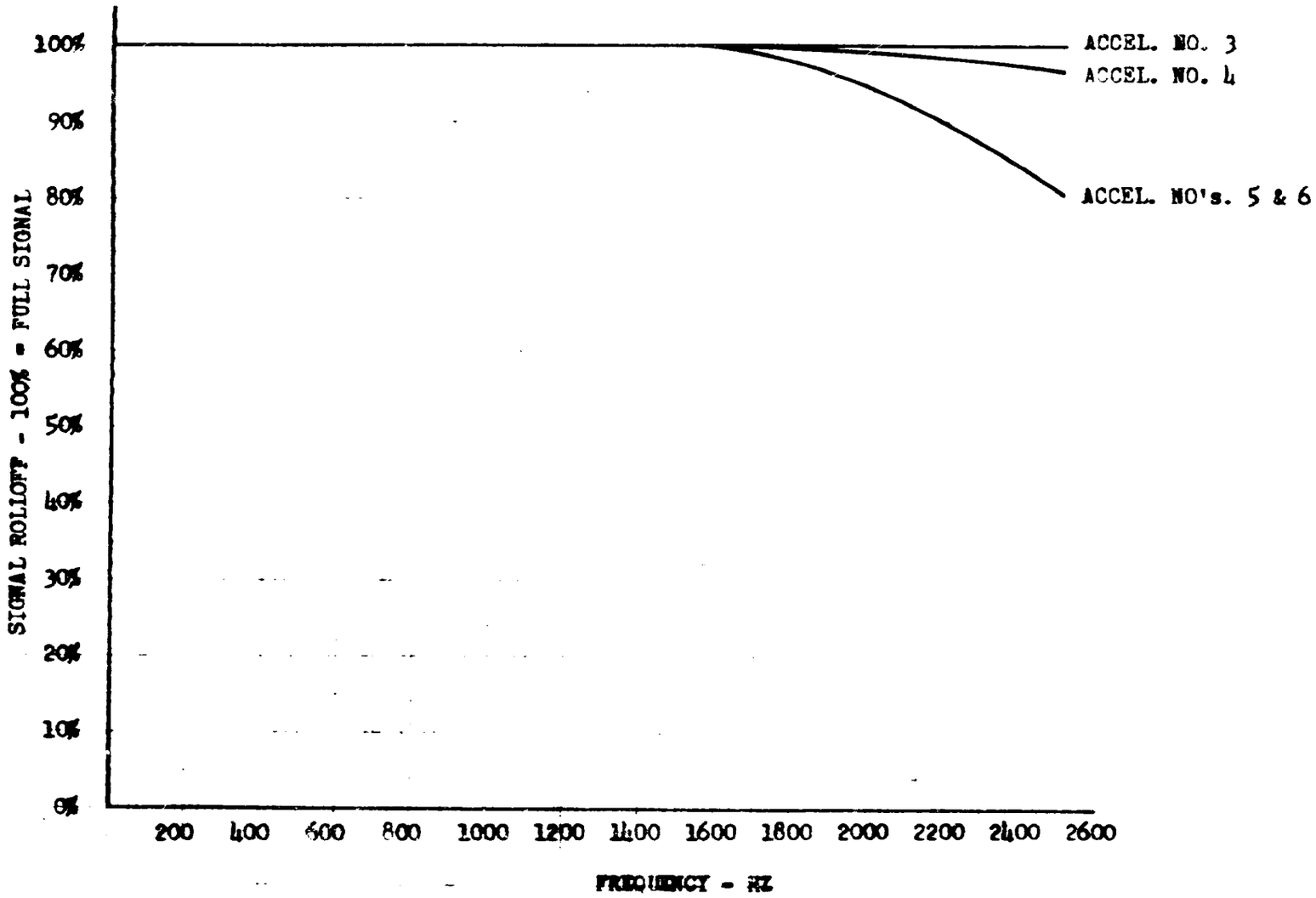

Figure II.A.1.2 - CHANNEL CALIBRATIONS

SHOCK TEST ANALYSIS DATA SHEET T1.A.1.3

TEST ITEM 606A-32 PART NO. STRUCTURE

SERIAL NO. TEST DATE NOV 11 1963

SHOCK AXIS LONGITUDINAL SHOCK NO. 1

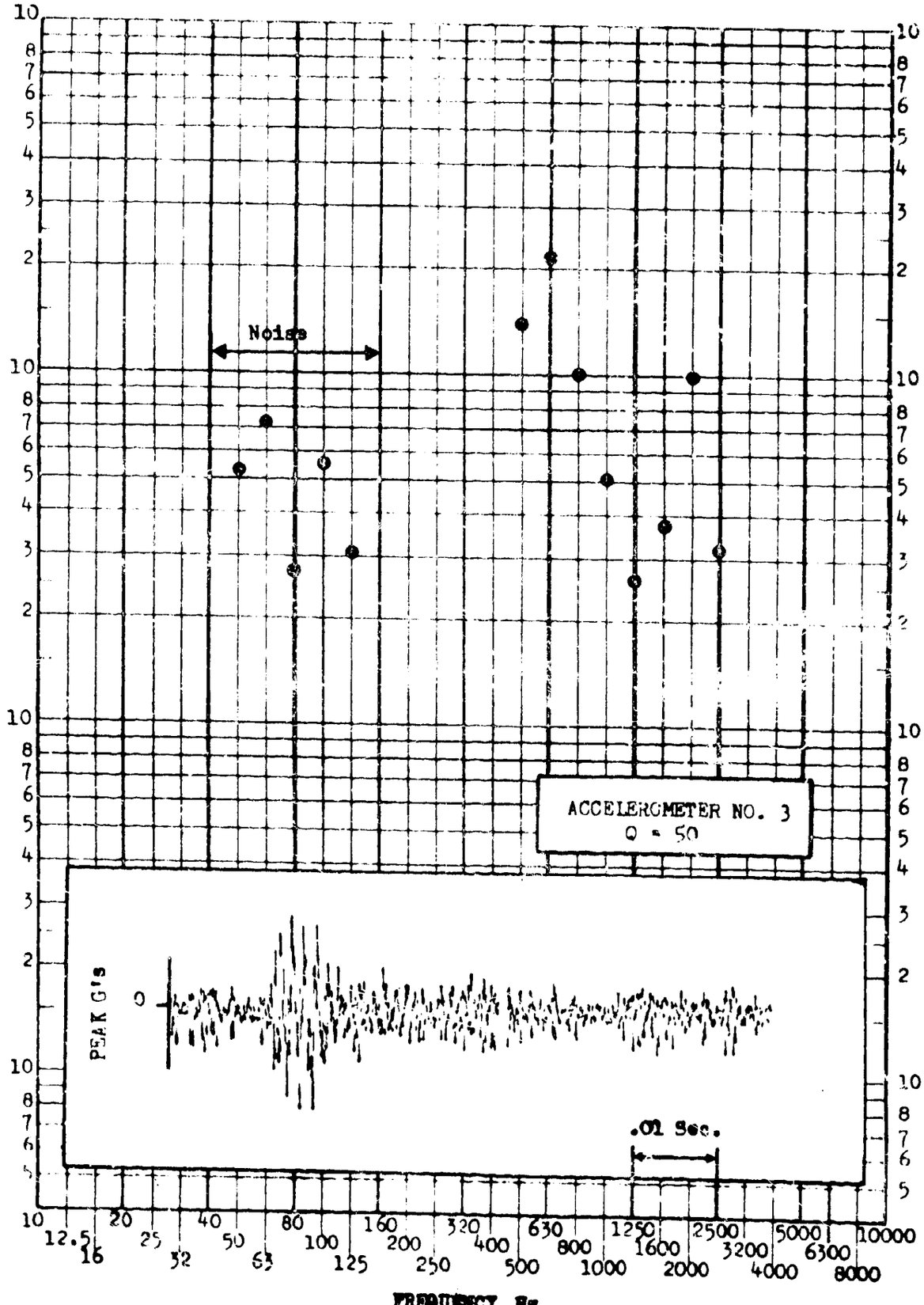

SHOCK TEST ANALYSIS DATA SHEET II.A.1.4

TEST ITEM 606A-25,26,27,28
SERIAL NO. —
SHOCK AXIS RADIAL —

PART NO. STRUCTURE —
TEST DATE NOV 11 1963
SHOCK NO. 1 —

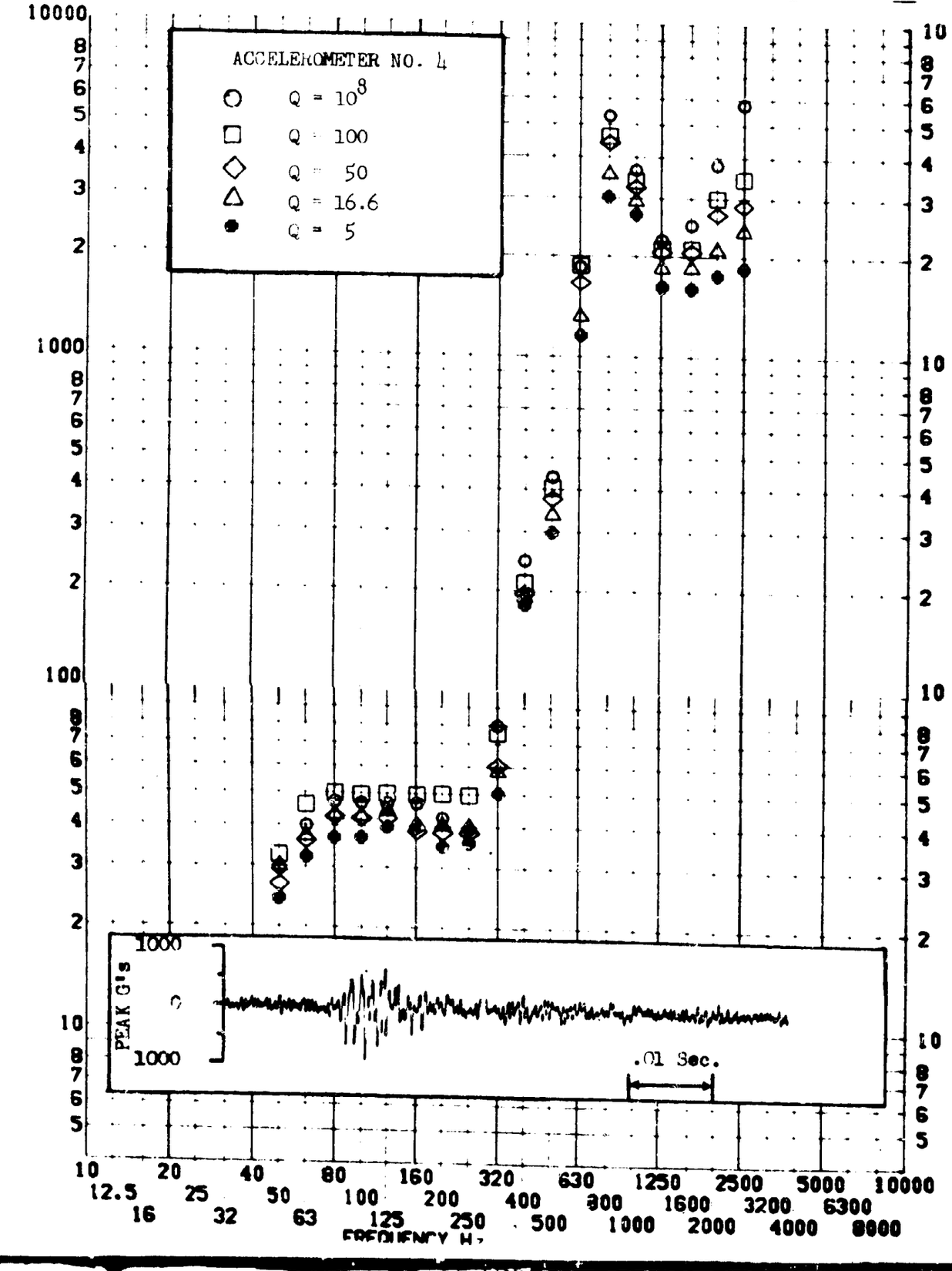

SHOCK TEST ANALYSIS DATA SHEET II.A.1.5

TEST ITEM 606A-35,36,37,38,39 PART NO. STRUCTURE
SERIAL NO. TEST DATE NOV 11 1963
SHOCK AXIS LONGITUDINAL SHOCK NO. 1

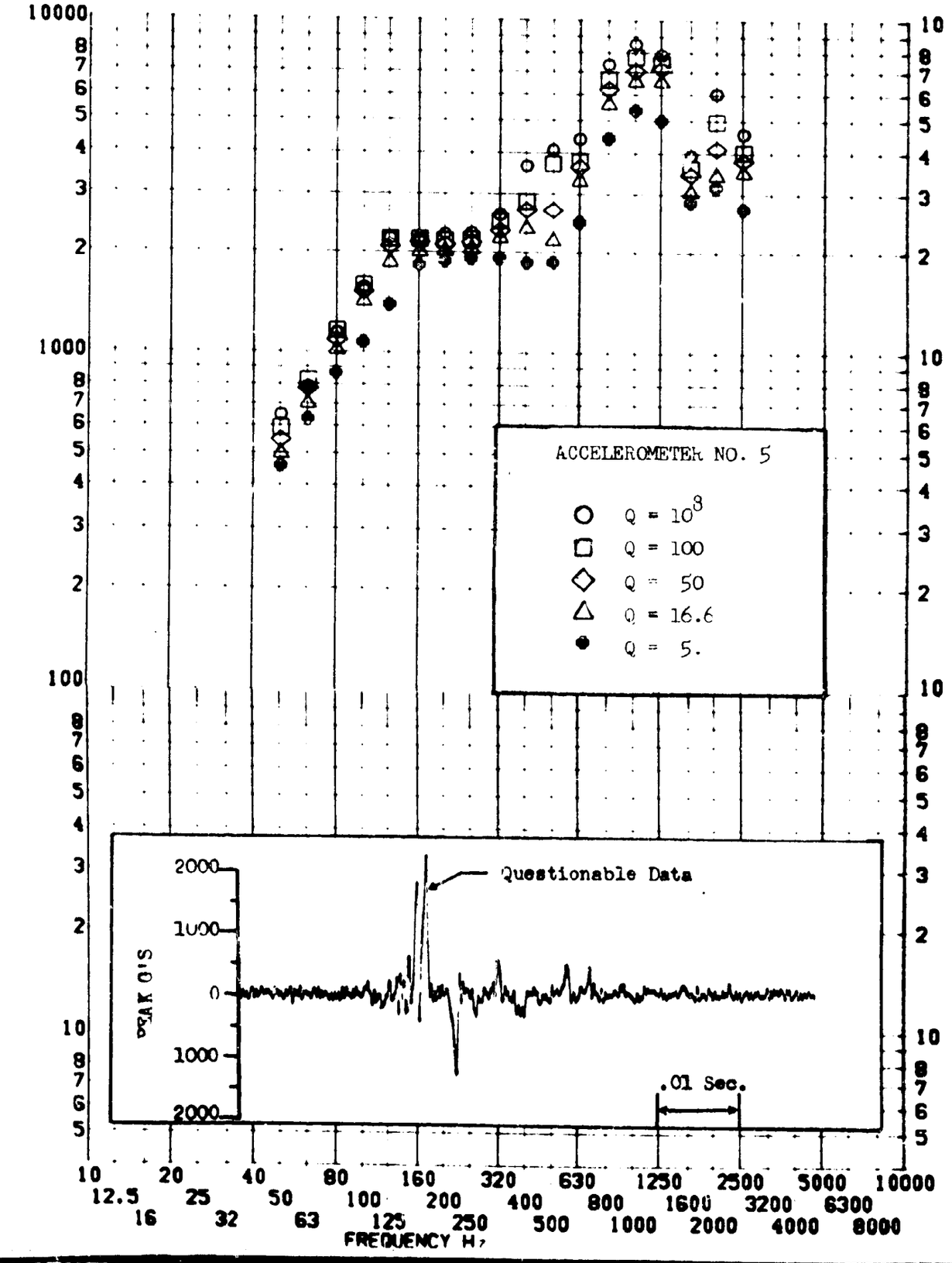

SHOCK TEST ANALYSIS DATA SHEET II.A.1.6

TEST ITEM 606A-17,18,19,20
SERIAL NO.
SHOCK AXIS RADIAL

PART NO. STRUCTURE
TEST DATE NOV 11 1963
SHOCK NO. PRE-SHOCK

RESPONSE G-S

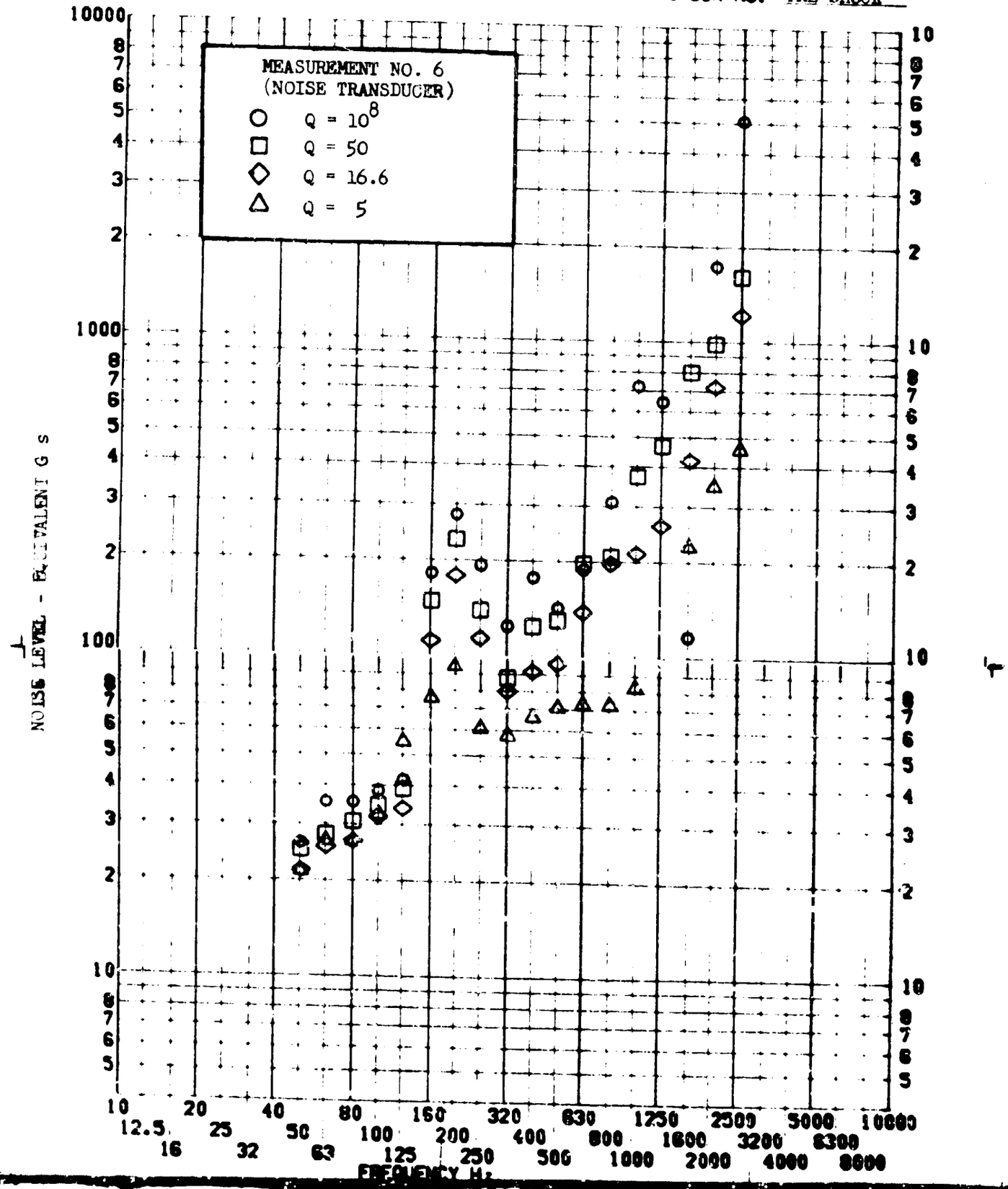

SHOCK TEST ANALYSIS DATA SHEET II.A.1.7

TEST ITEM 606A-21,22,23,24
SERIAL NO. —
SHOCK AXIS RADIAL —

PART NO. STRUCTURE —
TEST DATE NOV 71 1/23
SHOCK NO. 1 —

RESPONSE G-S

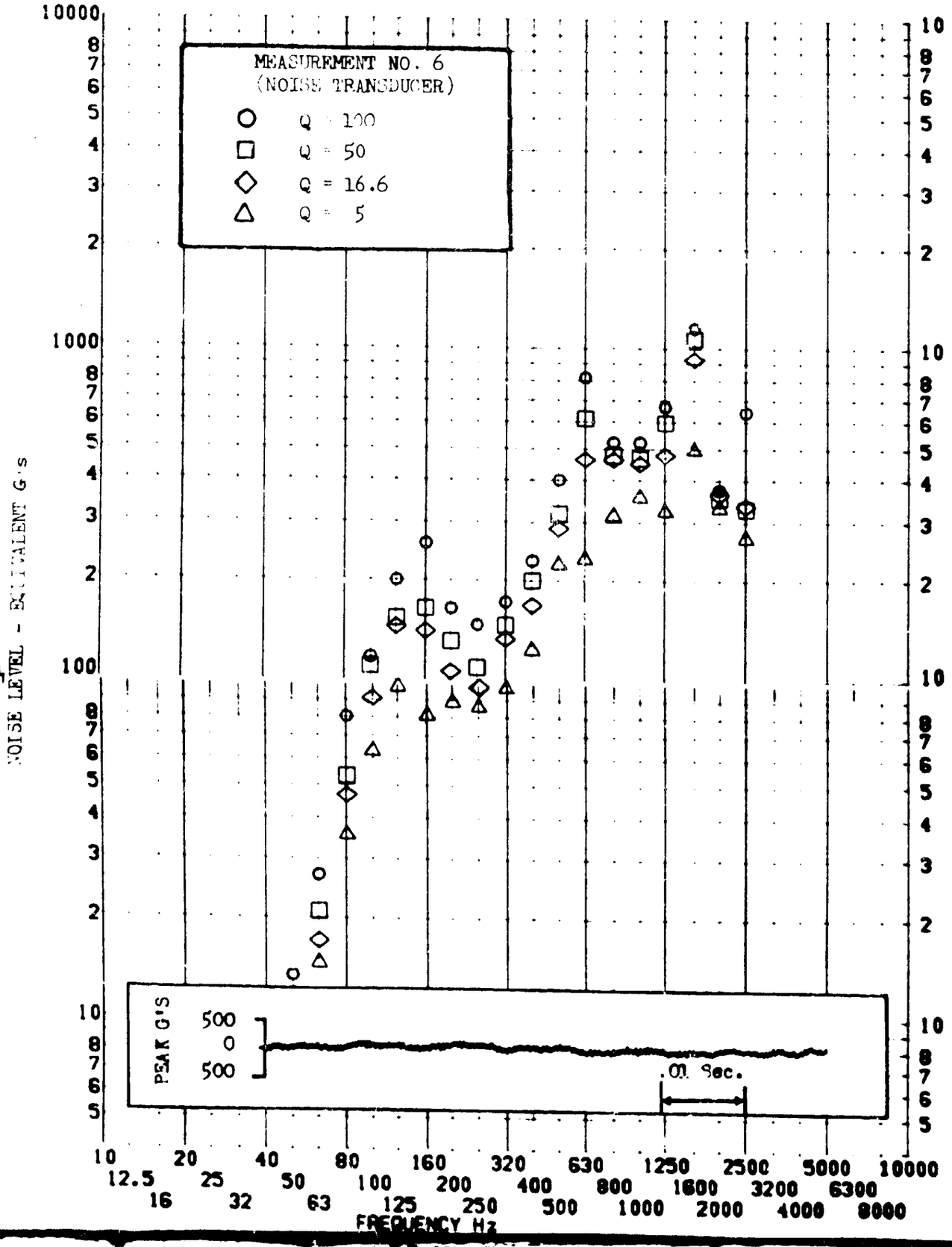

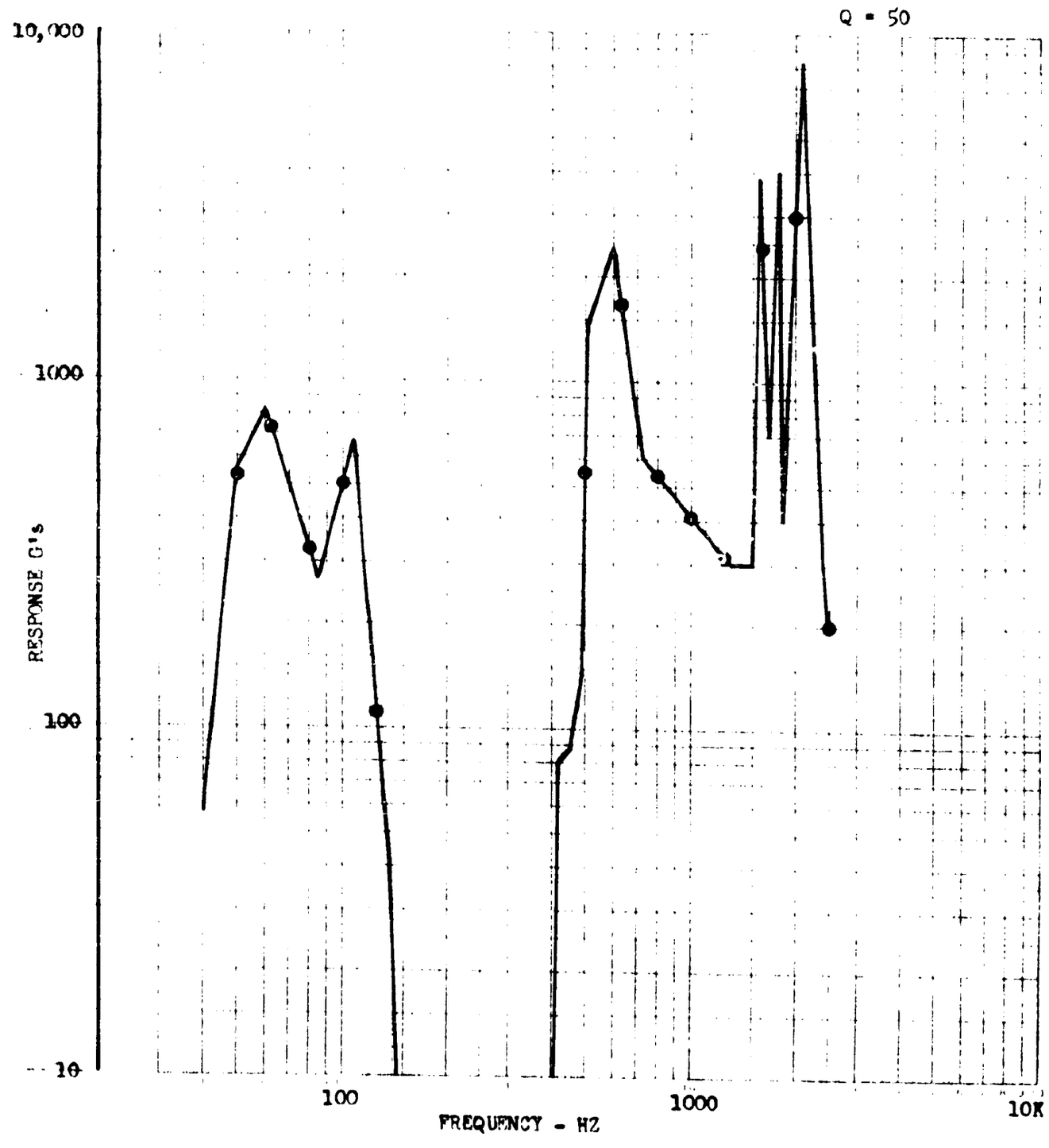

Figure II.A.1.8 COMPARISON OF NARROW BAND AND 1/3 OCTAVE ANALYSIS - ACCEL. NO. 3

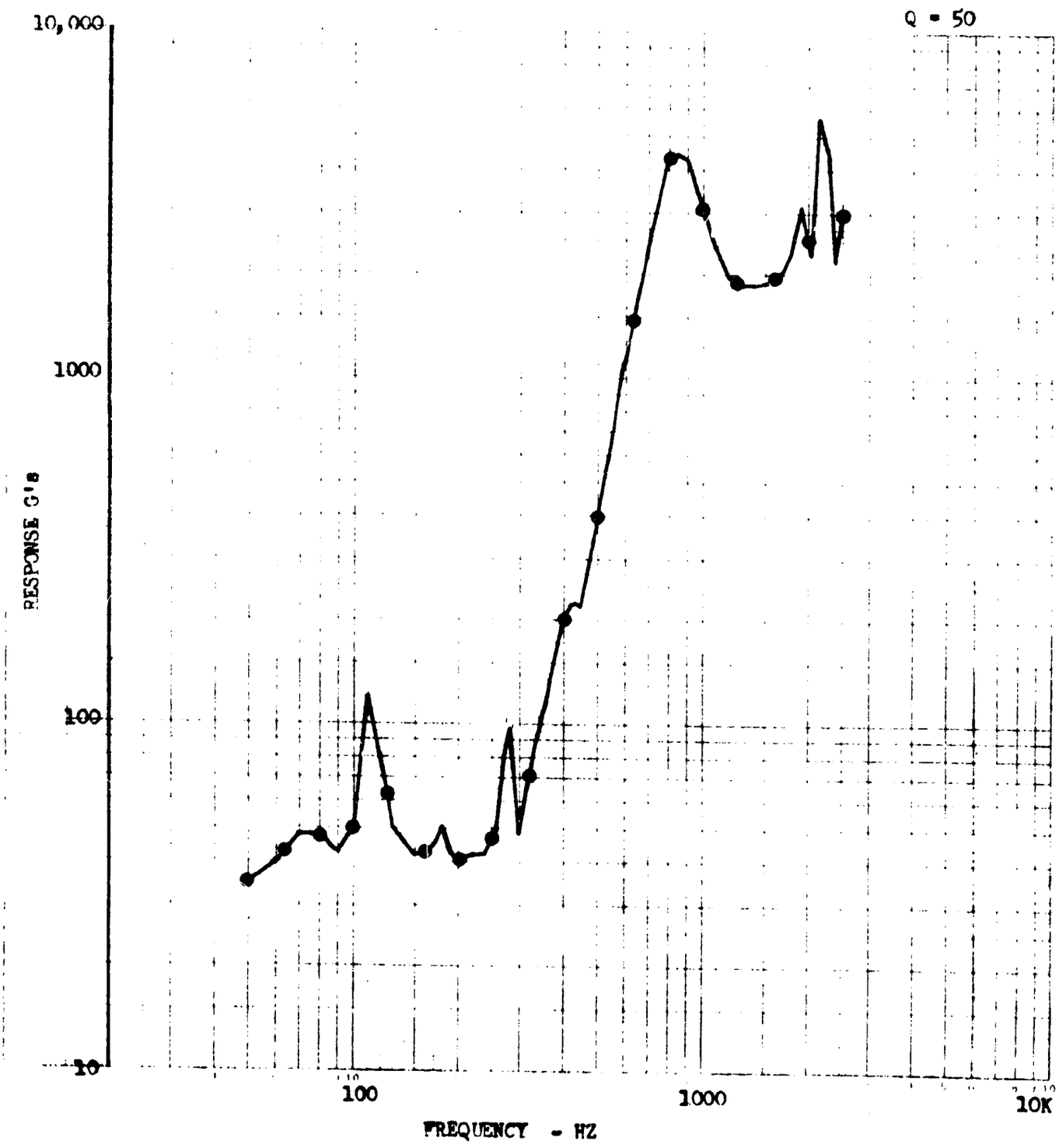

Figure II.A.1.9 COMPARISON OF NARROW BAND AND 1/3 OCTAVE ANALYSIS - ACCEL. NO. 4

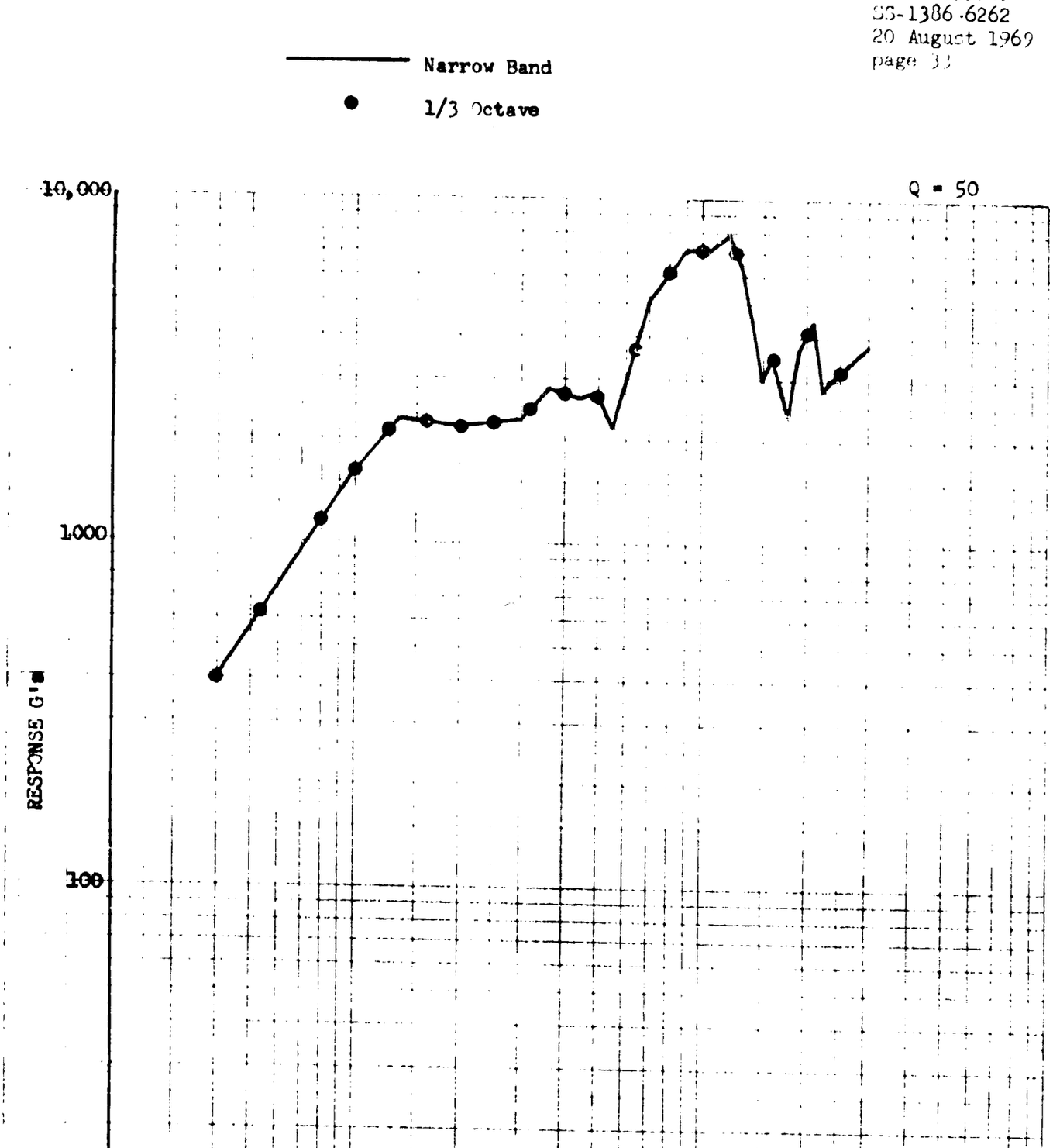

Figure II.A.1.10 COMPARISON OF NARROW BAND AND 1/3 OCTAVE ANALYSIS - ACCEL. NO. 5

SECTION NO. II.A.2

REPORT NO. 674

SUBJECT:

BOOSTER ADAPTER AND HORIZON SENSOR FAIRING SEPARATION

- CONFIDENCE AND ENVIRONMENTAL DETERMINATION TESTS

SECTION II.A.2

SUMMARY

Two booster separation and two horizon sensor fairing ejection tests were conducted on a flight vehicle at Santa Cruz Test Base as a means of confidence testing and to determine the pyro shock environment in the vehicle. At the time that these tests were conducted no facility was available to test components for pyro shock and a full scale vehicle test was the only available means of accomplishing the test objective.

As a result of the test, shock attenuation versus distance along structure was established for the booster separation event based on peak g readings from the oscillograms. A more detailed comparison with attenuation versus distance for shock spectra indicates that the attenuation versus distance developed from peak g readings of oscillograms cannot be used with certainty for predicting attenuation versus distance for any particular frequency since the response at any frequency depends on the modal characteristics at the measurement locations and these modal characteristics are different for each location.

The attenuation versus distance curve which has been developed here can, however, be used as a general indication of the overall shock reduction as a function of distance along structure. The curve indicates that the peak shock levels decrease exponentially; the shock levels at 22 inches from the joint are reduced to half of what the peak shock levels are at 4.6 inches from the joint.

TABLE OF CONTENTS

SECTION II.A.2

LIST OF TABLES

SECTION II.A.2

LIST OF FIGURES

SECTION II.A.2

Figures

LIST OF FIGURES (Cont.)

SECTION II.A.2

FORM MSC 9787 A

LIST OF FIGURES (Cont.)

SECTION II.A.2

II.A.2.1 INTRODUCTION

Two sets of separation tests were carried out, respectively labelled (1A, 2A) and (1. 2). They are briefly described below:

In Test 1A, the pin pushers which eject the horizon sensors were fired (two pin pushers for each fairing). In Test 2A, the booster adapter separation joint was detonated.

For Test 2, the booster adapter separation joint thickness was increased from .082 inch to .088 inch. The purpose of the thicker separation joint was an attempt to produce the highest flight shock level since previous experimental tests had shown that joint thickness had an influence on shock levels. In addition, a blank engine cone panel was replaced by an equipment panel which had a configuration similar to that which would be used for subsequent vehicles.

For Tests 1 and 2 some of the accelerometer range settings as well as some of the locations were changed.

II.A.2.2 DISCUSSION AND ANALYSIS

II.A.2.2.1 Test Configuration and Instrumentation

The test specimen consisted of a complete functional vehicle. This included a booster adapter mock-up. The entire vehicle with booster adapter mock-up was suspended vertically in a test stand at SCTB. For the booster separation tests the booster adapter was allowed to free-fall. The fall was arrested by cables.

The booster separation joint is illustrated in Figure II.A.2.1. The separation joint consists of a 10 grain/foot MDF charge which is contained in a circumferential back-up ring. Detonation of the charge induces failure in the adapter skin at the indicated notches. Test 2 was conducted with a standard skin thickness of .082 inch and Test 2A with a skin thickness of .088 inch, .003 inch above the maximum tolerance thickness for flight hardware.

A detail of the horizon sensor fairing system is given in Figure II.A.2.2. The location of the horizon sensor fairing system with respect to the forward rack is detailed in Figure II.A.2.6.

Endevco 2225 and Glenite 314 TMV piezoelectric accelerometers were mounted in the locations shown by station number in Figure II.A.2.3 for Tests 1A and 2A and in Figure II.A.2.4 for Tests 1 and 2. Exact locations for the booster separation tests (2 and 2A) are shown in Figure II.A.2.5 and for the horizon sensor fairing tests (1 and 1A) in Figure II.A.2.6. Some of the locations were used for both tests.

The transducers were attached to magnesium blocks by means of studs. The blocks were in turn either bolted onto the vehicle structure or bonded with an adhesive.

II.A.2.2.2 Analysis Methods

The data was analyzed primarily be means of high speed oscillograph records. Shock spectra were made from some of the accelerometer measurements from Tests 1 and 2. This consisted of four shock spectra out of twelve measurements for Test 1 (Figures II.A.2.10 to II.A.2.13) and twelve shock spectra out of twenty-four measurements for Test 2 (Figures II.A.2.14 to II.A.2.25). Figures II.A.2.26 to II.A.2.29 are comparisons of shock levels and shock spectra from booster separation and horizon sensor fairing ejection for selected accelerometer locations. The high speed oscillograms for test series 1 (Tests 1A and 2A) and for the balance of Tests 1 and 2 are presented in Figures II.A.2.30 to II.A.2.36.

Peak g readings for each of the measurements are presented in Table II.A.2.6. The peak g readings from accelerometers mounted on main structure are presented in Table II.A.2.7 as a function of distance from the shock source for booster separation and fairing ejection. These readings are also presented in Figure II.A.2.7. The data points for the booster separation test have been averaged for each case where more than one measurement was taken at the same distance from the source. A smooth curve was then constructed based on the average shock levels. This curve was then normalized so that the averaged shock as recorded at 5 inches from the joint corresponded to 100 percent and the rest of the curve drawn in accordingly (Figure II.A.2.8). This curve then represents the shock attenuation as a function of distance along structure which can be expected from detonation of the ten grain MDF booster separation joint.

Presented in Figure II.A.2.9 are three shock spectra from Test 2 of accelerometers 5, 20 and 19 which were located 4.6, 26.6 and 112.2 inches from the separation joint respectively. The peak g shock levels from the real time oscillograms of these measurements were used to construct the shock attenuation versus distance curve of Figure II.A.2.8. The purpose of Figure II.A.2.9 is to show shock attenuation versus distance with frequency as an additional parameter.

II.A.2.2.3 Test Conditions and Results

Test Series 1, Test 1A

The horizon sensor fairings were ejected in this test. The two fairings are mounted to the outside of the Agena forward equipment section. They protect the horizon sensor heads from environments encountered during the ascent phase of flight. Each fairing, located as shown in Figure II.A.2.6, is held against the outside skin by means of two pyrotechnic pin pushers . Local structural reinforcement is provided by plates which span the rings at Stations 247 and 273. Detonation of the pin pushers removes the shear attachment between the fairings and the plates and allows the fairings to jettison.

Results of Test 1A can be observed in the real time oscillograms of Figure II.A.2.32. Peak g levels have been entered in Table II.A.2.6. The oscillograms indicate that the shock originating from the horizon sensor fairing ejection is significantly attenuated in the aft area of the vehicle.

Test Series 1, Test 2A

A standard 10 grain/foot MDF primacord was used in booster adapter separation Test 2A. A sketch of the separation joint configuration is shown in Figure II.A.2.1. Detonation of the charge causes the adapter skin to fail at the three notches which run circumferentially around the adapter.

Real time oscillograms of the Test 2A booster separation shock measurements are presented in Figures II.A.2.33 to II.A.2.35. Peak g levels are recorded in Table II.A.2.6. The accelerometers located near the separation joint (5, 6, 7 and 8), as well as accelerometer 12, fell off in testing. This invalidated these measurements.

Examination of the oscillograph records indicates that although the shock was significantly attenuated going from the separation joint to the forward rack, a substantially larger number of peak excitation cycles were present in the forward section than were observed on the engine cone near the shock source.

Test Series 2, Test 1

Test 1 was another horizon sensor fairing ejection test. The only difference between this test and the previous horizon sensor fairing ejection test was in relocation of four of the accelerometers and substitution of a panel with equipment for a blank engine cone panel.

Real time oscillograms were produced for all twelve measurements and shock spectra for four of the measurements. The four shock spectra along with their corresponding oscillograms, are shown in Figures II.A.2.10 to II.A.2.13. The rest of the oscillograms are presented in Figure II.A.2.30. Peak amplitudes for Test 1 are summarized in Table II.A.2.6.

Again, no measurable excitation was evident in the aft section which confirmed that the pin pusher detonation is a local effect. The four shock spectra confirmed the presence of the 500 cycle mode observed in Test 1A. The radial measurements were observed to be predominantly higher than the axial measurements.

Test Series 2, Test 2

As in Test 2A, a standard 10 grain MDF primacord was used in Test 2, however, the joint thickness was increased from .082 inch to .088 inch to attempt to produce the highest shock which might be encountered in flight. As in Test 1, a blank engine cone panel was replaced with an equipment panel and a number of accelerometers were relocated. The accelerometers near the booster adapter were bolted to the structure to prevent them from breaking loose as in Test 2A.

Real time oscillographs were produced for all twenty-four of the measurements as well as shock spectra for twelve of the measurements. The shock spectra with their corresponding oscillograms are presented in Figures II.A.2.14 to II.A.2.25 and the rest of the oscillograms in Figure II.A.2.31. Table II.A.2.6 summarizes the peak amplitudes as observed from the real time oscillograms.

Table II.A.2.6 indicates that there was little difference in the shock levels of the two booster adapter separation tests. This test confirmed the presence of a proportionately greater number of peak excitation cycles in the forward section. Even though these excitations are lower in amplitude, they are nevertheless an important consideration in arriving at a suitable shock test criteria which will qualify equipment for this environment.

The shock spectra of Figures II.A.2.26 to II.A.2.29 compare shock levels (from accelerometers 1A, 2A, 18 and 19) in the forward area from booster separation and horizon sensor fairing ejection. These comparisons indicate that the horizon sensor fairing ejection produces the more severe environment.

II.A.2.2.4 Shock Attenuation Versus Distance

Figure II.A.2.8, which was derived as indicated in Section II.A.2.2.2, indicates the shock attenuation as a function of distance along structure based on peak g levels from the oscillograms.

Since the attenuation curve is based on peak g levels, application of this figure should be limited to cases where it is desired to determine the general severity between measurement locations or to set equipment operating ranges. When it is desired to determine the severity of shock between measurements at a particular frequency as, for example, applying shock attenuation to shock spectra, the attenuation curve of Figure II.A.2.8 can cause significant errors in predictions.

This is illustrated in Figure II.A.2.9 which presents shock spectra of measurements which were used to define the shock attenuation curve at three different locations along the structure and the predicted shock spectra based on the shock spectrum at five inches from the joint.

Based on the attenuation curve of Figure II.A.2.8, the shock spectrum of measurement 20, 26.6 inches from the source, would be reduced to 41 percent of the level of the shock spectrum of measurement 5. Figure II.A.2.9 shows this generally not to be the case. In fact, at 800 Hz, the shock spectrum from measurement 20 is 440 percent higher than the predicted spectrum whereas at 6300 Hz the shock level from measurement 20 is only 37 percent of the predicted shock level.

The predicted shock spectrum of measurement 19, 112.2 inches from the source is seen to agree more closely with the predicted spectrum, but individual 1/3 octave band consideration still indicates a considerable error in predicted values in some bands.

II.A.2.3 CONCLUSIONS

The vehicle full scale booster separation and horizon sensor fairing ejection tests were successful in developing confidence in the vehicle to withstand major pyro events in lieu of a satisfactory component pyrotechnic test facility.

The horizon sensor fairing ejection shock levels were localized to the forward area with little or no shock observed aft of the booster adapter separation plane.

Shock levels from the horizon sensor fairing event are generally more severe in the forward rack than shock levels from the booster adapter separation event.

Calculation of shock attenuation as a function of distance indicates that the shock attenuates along the structure exponentially with 50 percent reduction occurring at 22 inches from the separation joint based on 100 percent levels at 4.6 inches from the joint.

The shock attenuation-distance curve developed in this report can be used to determine equipment operating ranges and to determine general levels of severity between shock measurements.

The shock attenuation curve should be used cautiously in predicting the reduction in shock spectrum levels since it does not consider frequency as a parameter.

A shock spectrum analysis accounts for the number of cycles at every frequency and thus is a desirable method of measuring pyro shock.

TABLE II.A.2.1
ACCELEROMETER AND LOCATIONS - STRUCTURE
TEST 1A AND 2A

Accelerometer Number	Station	Direction	Distance to Shocksource A	Distance to Shocksource B	Accelerometer Type
1	273	R	7.0	112.4	Kistler 802
2	273	L	7.0	112.4	Kistler 802
3	247	L	19.0	138.4	Kistler 802
4	247	R	19.0	138.4	Kistler 802
5	390	L	124.0	4.6	Kistler 802
6	390	R	124.0	4.6	Kistler 802
7	390	L	124.0	4.6	Kistler 802
8	390	R	124.0	4.6	Kistler 802
9	437	L	171.0	51.6	Kistler 802
10	412	L	146.0	26.6	Kistler 802
11	412	R	146.0	26.6	Kistler 802
12	396.5	R	130.5	11.1	Endevco 2225
13					Glenite 314 TMV
14					Glenite 314 TMV
15	396.5	L	130.5	11.1	Endevco 2225
16					Glenite 314 TMV
17					Glenite 314 TMV
18	273.2	R	7.2	112.2	Endevco 2225
19	273.2	L	7.2	112.2	Endevco 2225
20	412	L	146.0	26.6	Endevco 2225
21	412	R	146.0	26.6	Endevco 2225
22	462.5	L	196.5	77.1	Endevco 2225
23	462.5	R	196.5	77.1	Endevco 2225
24					Endevco 2225

N Boxes

TABLE II.A.2.2

ACCELEROMETERS AND LOCATIONS - STRUCTURE
TESTS 1 AND 2

Accelerometer Number	Station	Direction	Distance to Shocksource 1	Distance to Shocksource 2	Accelerometer Type
1A	266	R	0	119.4	Kistler 802
2A	266	L	0	119.4	Kistler 802
3A					Kistler 802
4A					Kistler 802
5	390	L	124	4.6	Kistler 802
6	390	R	124	4.6	Kistler 802
7	390	L	124	4.6	Kistler 802
8	390	R	124	4.6	Kistler 802
9A					Kistler 802
10	412	L	146	26.6	Kistler 802
11	412	R	146	26.6	Kistler 802
12	396.5	R	130.5	11.1	Endevco 2225
13					Glenite 314 TMV
14					Glenite 314 TMV
15	396.5	R	130.5	11.1	Endevco 2225
16					Glenite 314 TMV
17					Glenite 314 TMV
18	273.2	R	7.2	112.2	Endevco 2225
19	273.2	L	7.2	112.2	Endevco 2225
20	412	L	146.0	26.6	Endevco 2225
21	412	R	146.0	26.6	Endevco 2225
22	462.5	L	196.5	77.1	Endevco 2225
23	462.5	R	196.5	77.1	Endevco 2225
24					Endevco 2225

N Boxes

TABLE II.A.2.3

ACCELEROMETERS AND LOCATION - BOXES
TESTS 1A AND 2A

Accelerometer Number	Box	Direction	Location Station	Distance to Shocksource A	Distance to Shocksource B	Accelerometer Type
1	Structure					Kistler 802
2	Structure					Kistler 802
3	Structure					Kistler 802
4	Structure					Kistler 802
5	Structure					Kistler 802
6	Structure					Kistler 802
7	Structure					Kistler 802
8	Structure					Kistler 802
9	Structure					Kistler 802
10	Structure					Kistler 802
11	Structure					Kistler 802
12	Structure					Endevco 2225
13	D timer bracket	R	267	2.0	118.4	Glenite 314 TMV
14	Aux. rack eq beam	L	231	35	154.4	Glenite 314 TMV
15	Structure					Endevco 2225
16	Aux. rack eq beam	L	231	35	154.4	Glenite 314 TMV
17	S/A J-Box	R	398	132	12.6	Glenite 314 TMV
18	Structure					Endevco 2225
19	Structure					Endevco 2225
20	Structure					Endevco 2225
21	Structure					Endevco 2225
22	Structure					Endevco 2225
23	Structure					Endevco 2225
24	S/A J-Box	L	398	132	12.6	Endevco 2225

TABLE II.A.2.4

ACCELEROMETERS AND LOCATIONS - BOXES
TESTS 1 AND 2

Accelerometer Number	Box	Direction	Location	Distance to Shocksource A	Distance to Shocksource B	Accelerometer Type
1A	Structure					Kistler 802
2A	Structure					Kistler 802
3A	Magnetometer box	L	402	136	16.6	Kistler 802
4A	Magnetometer box	R	402	136	16.6	Kistler 802
5	Structure					Kistler 802
6	Structure					Kistler 802
7	Structure					Kistler 802
8	Structure					Kistler 802
9A	Magnetometer box	R	407	141	21.6	Kistler 802
10	Structure					Kistler 802
11	Structure					Kistler 802
12	Structure					Endevco 2225
13	"D" Timer bracket	R	267	1.0	118.4	Glenite 314 TMV
14	Aux. Rack eq beam	L	231	35	154.4	Glenite 314 TMV
15	Structure					Endevco 2225
16	Aux. Rack eq beam	L	231	35	154.4	Glenite 314 TMV
17	S/A J-Box	R	398	132	12.6	Glenite 314 TMV
18	Structure		273			Endevco 2225
19	Structure		273			Endevco 2225
20	Structure					Endevco 2225
21	Structure					Endevco 2225
22	Structure					Endevco 2225
23	Structure					Endevco 2225
24	S/A J-Box	L	398	132	12.6	Endevco 2225

TABLE II.A.2.5

SUMMARY OF TESTS

Test Number	Configuration	Explosive Size	Test Purpose	Shock Isolation
2A	1	10 Gr/ft MDF	Booster Separation	None
1A	1	SQUIBS	Fairing Jett.	None
2	2 *	10 Gr/ft MDF	Booster Separation	None
1	2	SQUIBS	Fairing Jett.	None

* Some accelerometers relocated

Table II.A.2.6

OSCILLOGRAM PEAK G READINGS - ARRANGED BY ACCELEROMETER NUMBER

ACCEL. NO.	STATION	DIRECTION	TEST SERIES 1		TEST SERIES 2	
			BOOSTER SEP. (TEST 2A)	FAIRING EJEC. (TEST 1A)	BOOSTER SEP. (TEST 2)	FAIRING EJEC. (TEST 1)
1A	266	RAD.			378	648
1	273	RAD.	175	282		
2A	266	LONG.			370	430
2	273	LONG.	245	118		
3A*	402	LONG.			535	NO DATA
3	247	LONG.	234	193		
4A*	402	RAD.			535	NO DATA
4	247	RAD.	191	313		
5	390	LONG.	NO DATA		3900	
6	390	RAD.	NO DATA		4065	
7	390	LONG.	NO DATA		2580	
8	390	RAD.	NO DATA		3655	
9A*	407	RAD.			280	
9	437	LONG.	52			
10	412	LONG.	2070		1090	
11	412	RAD.	1755		1400	
12	396.5	RAD.	NO DATA		2800	
13*	267	RAD.	72	43	73	34
14*	231	LONG.	70	39	70	43
15	396.5	RAD.	1008	NO DATA	NO DATA	NO DATA
16*	231	LONG.	37	7	45	10
17*	398	RAD.	637	NO DATA	700	5
18	273.2	RAD.	85	288	108	190
19	273.2	LONG.	100	140	150	110
20	412	LONG.	1300	NO DATA	1585	NO DATA
21	412	RAD.	920		1020	
22	462.5	LONG.	190		190	
23	462.5	RAD.	78		145	
24*	398	LONG.	246		230	

*ACCELEROMETER MOUNTED ON EQUIPMENT

Table II.A.2.7

OSCILLOGRAM PEAK G READINGS - ARRANGED BY DISTANCE FROM SHOCK SOURCE

BOOSTER SEPARATION				FAIRING EJECTION			
DISTANCE FROM SOURCE (INCHES)	ACCEL. NO.	TEST 2A	TEST 2	DISTANCE FROM SOURCE (INCHES)	ACCEL. NO.	TEST 1A	TEST 1
4.6	5	NO DATA	3900	11.0	1A		548
4.6	6	NO DATA	4065	11.0	2A		430
4.6	7	NO DATA	2580	14.7	1	282	
4.6	8	NO DATA	3655	14.7	2	118	
11.1	12	NO DATA	2800	14.7	18	280	190
11.1	15	1008	NO DATA	14.7	19	140	110
26.6	10	2070	1090	18.1	3	193	
26.6	11	1765	1400	18.1	4	313	
26.6	20	1300	1585				
26.6	21	920	1020				
51.6	9	520					
77.1	22	190	190				
77.1	23	78	145				
112.2	18	85	108				
112.2	19	100	150				
112.4	1	175					
112.4	2	245					
119.4	1A		378				
119.4	2A		370				
138.4	3	234					
138.4	4	191					

Table II.A.2.8

SHOCK SPECTRUM INVENTORY

Location	Orientation	Accelerometer Number	Accelerometer Model	Shock Spectra Plot Number H/S Jettison	Shock Spectra Plot Number Separation
Guidance Module Longeron	Lateral	1A	Kistler 802	674/52	674/56
Guidance Module Longeron	Longitudinal	2A	Kistler 802	674/53	674/57
Magnetometer Box (Engine Cone)	Longitudinal	3A	Kistler 802		674/58
Magnetometer Box (Engine Cone)	Lateral	4A	Kistler 802		674/59
Engine Cone - Quad. II	Longitudinal	5	Kistler 802		674/60
Engine Cone - Quad. II	Lateral	6	Kistler 802		674/61
Fwd Rack Longeron	Lateral	18	Endevco 2225	674/54	674/62
Fwd Rack Longeron	Longitudinal	19	Endevco 2225	674/55	674/63
Engine Mounting Ring	Longitudinal	20	Endevco 2225		674/64
Engine Mounting Ring	Lateral	21	Endevco 2225		674/65
Aft Bulkhead	Longitudinal	22	Endevco 2225		674/66
Aft Bulkhead	Lateral	23	Endevco 2225		674/67
		Test No. 1 and 2		1	2

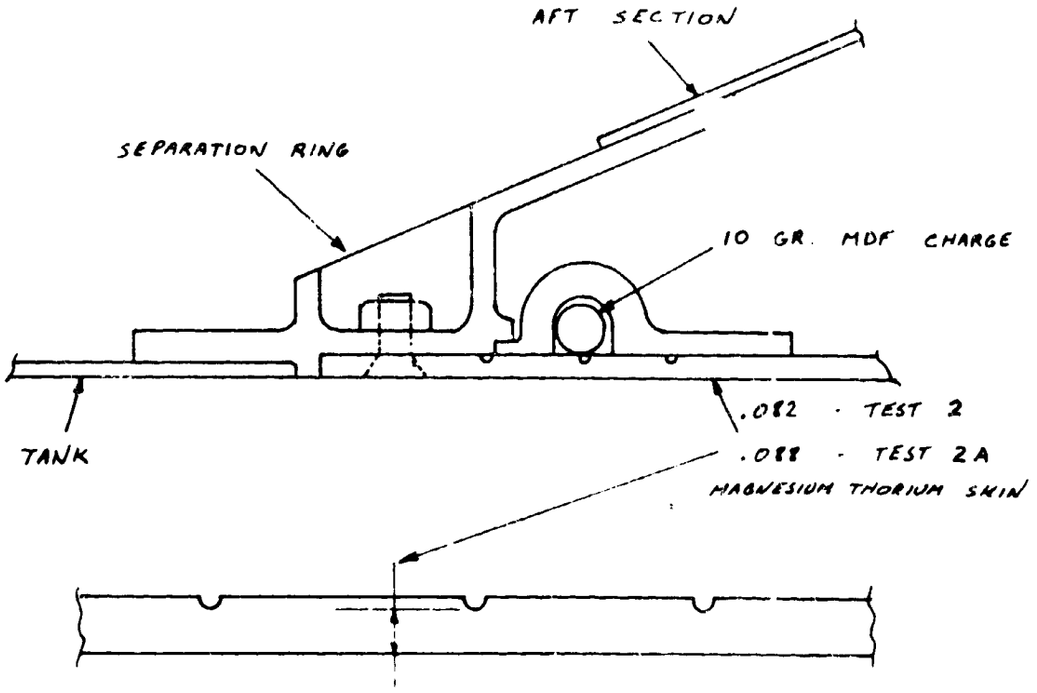

Figure II.A.2.1 STANDARD JOINT CONFIGURATION

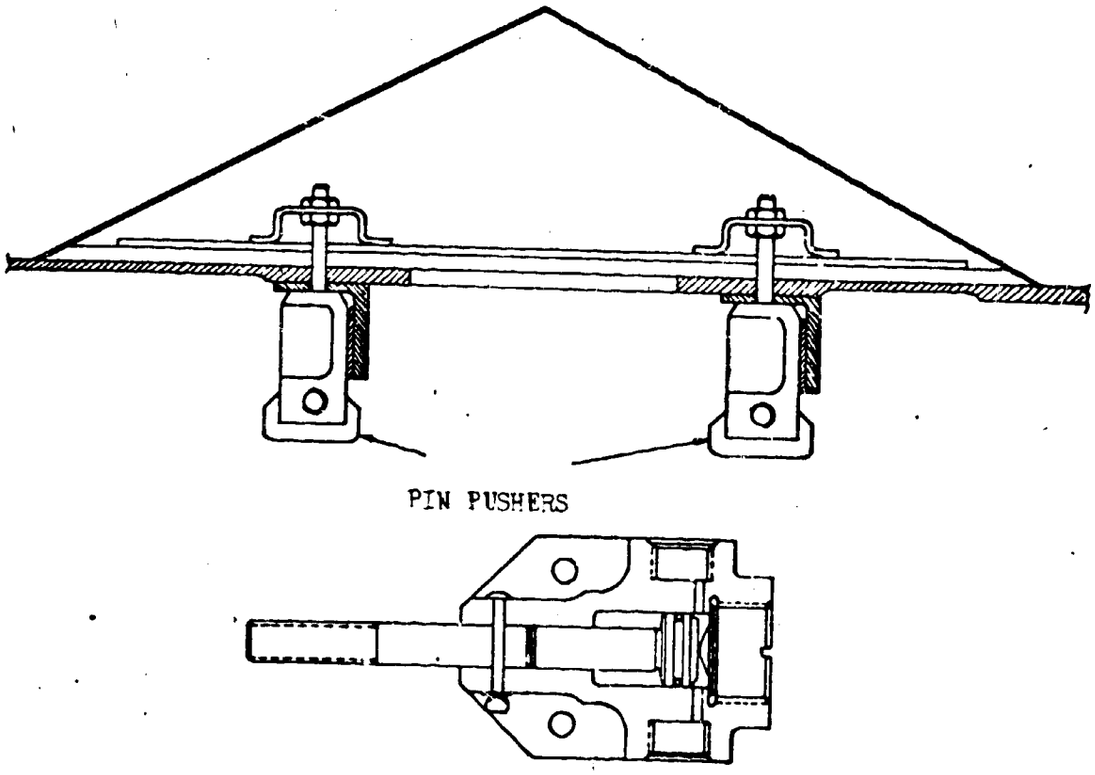

Figure II.A.2.2 HORIZON SENSOR FAIRING EJECTION DETAIL

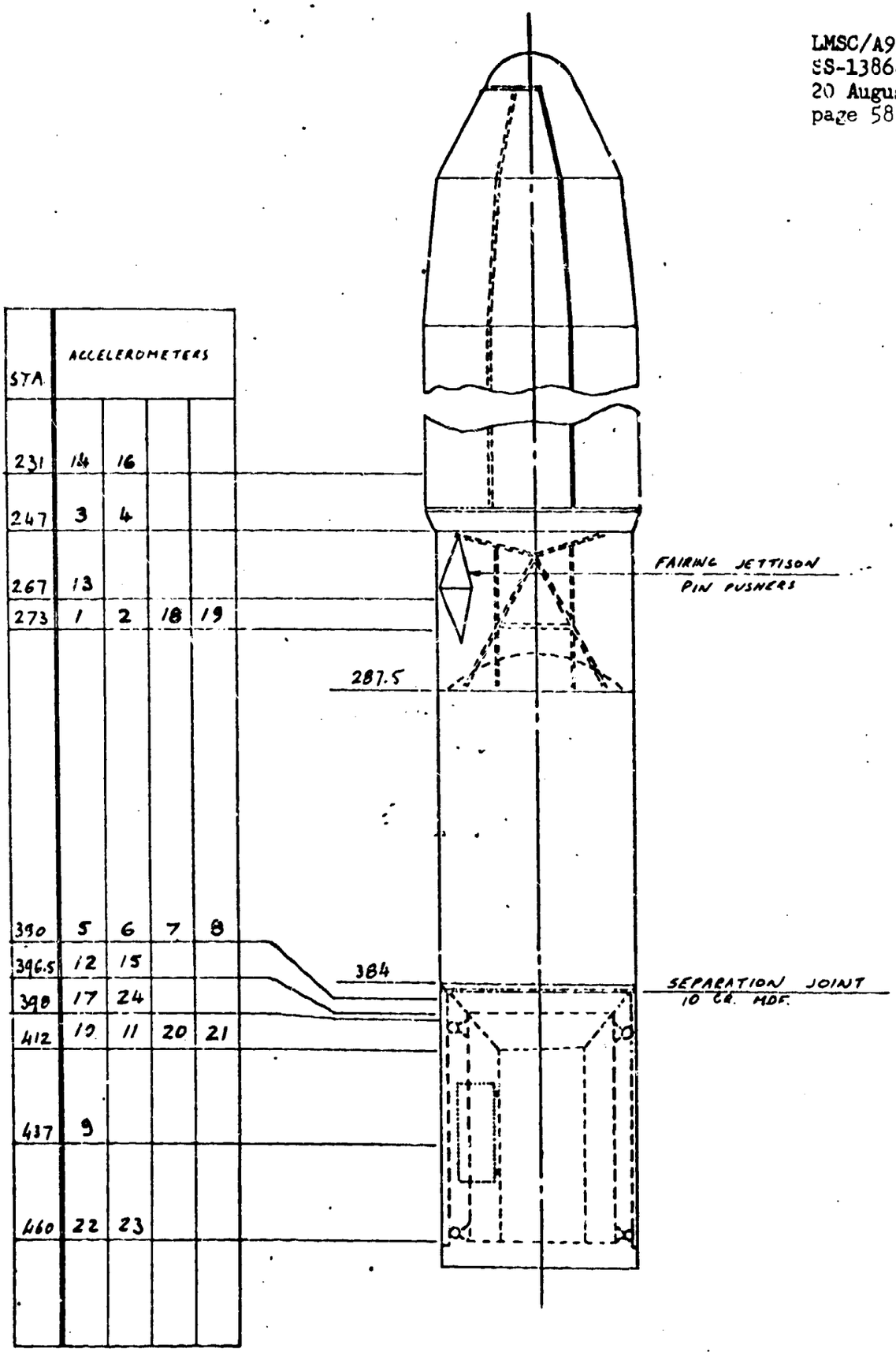

Figure II.A.2.3 INSTRUMENTATION LOCATIONS BY STATION NUMBER, TESTS 1A AND 2A

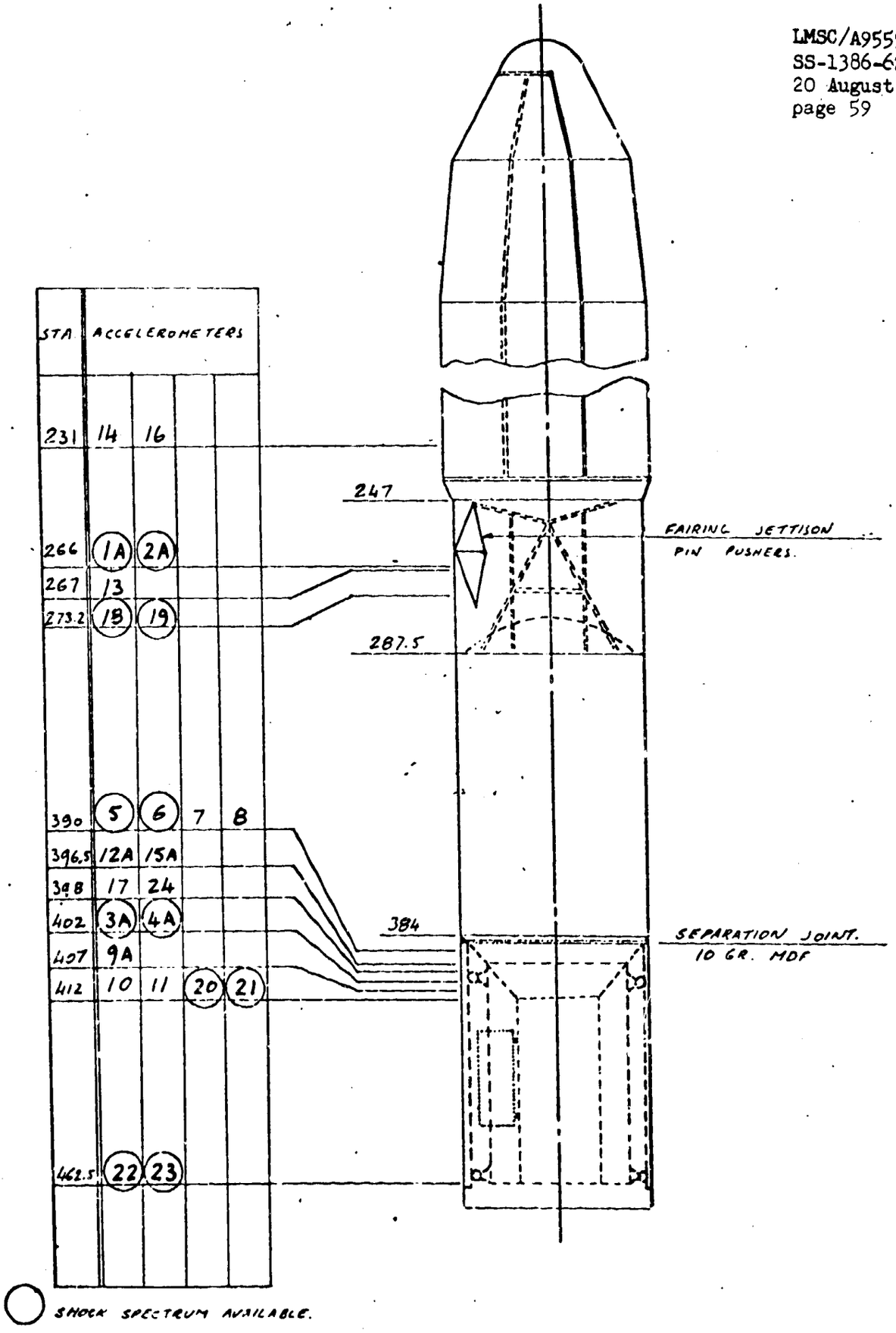

Figure II.A.2.4 INSTRUMENTATION LOCATIONS BY STATION NUMBER, TESTS 1 AND 2

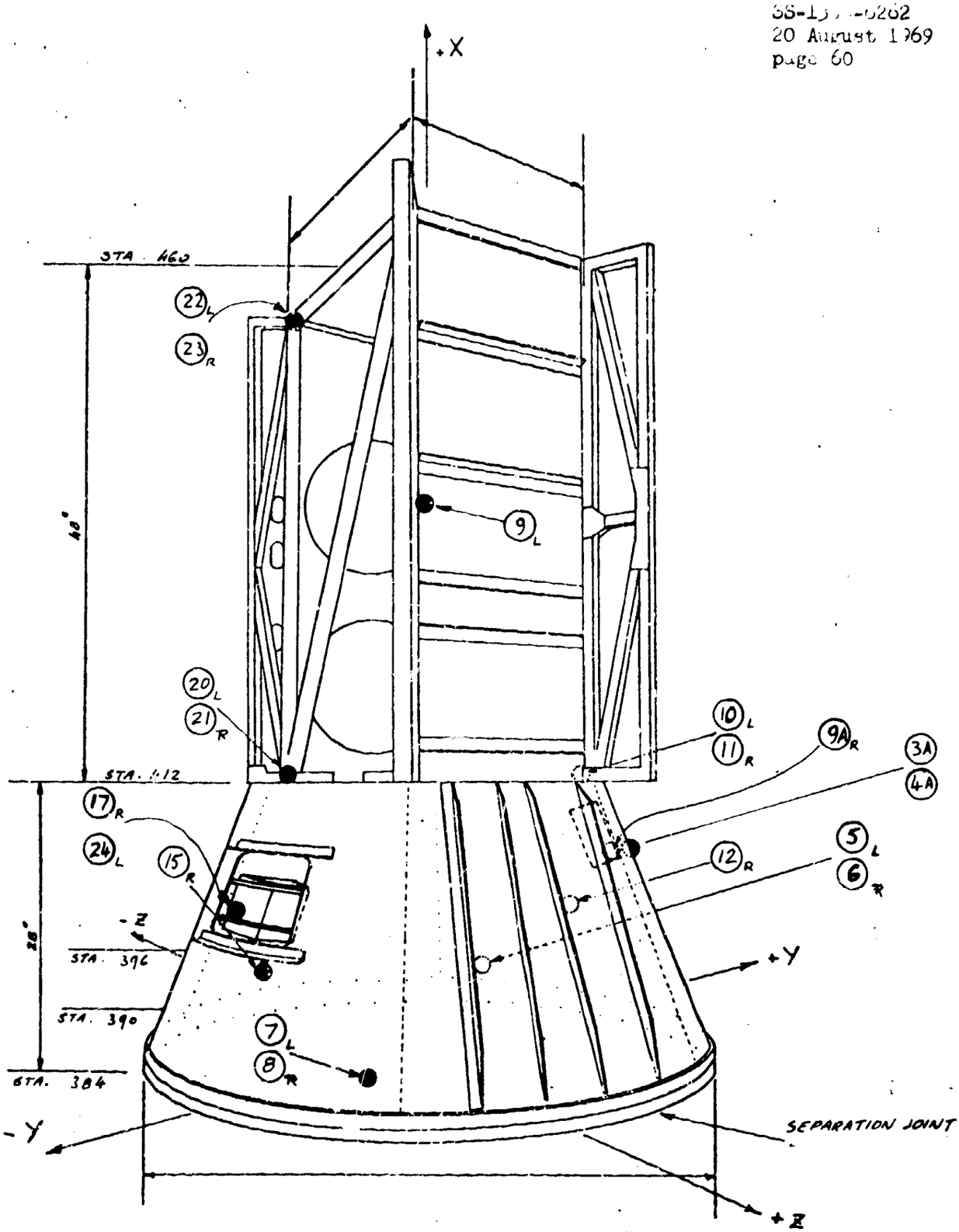

Figure II.A.2.5 AFT-RACK INSTRUMENTATION LOCATIONS, BOOSTER SEPARATION TESTS

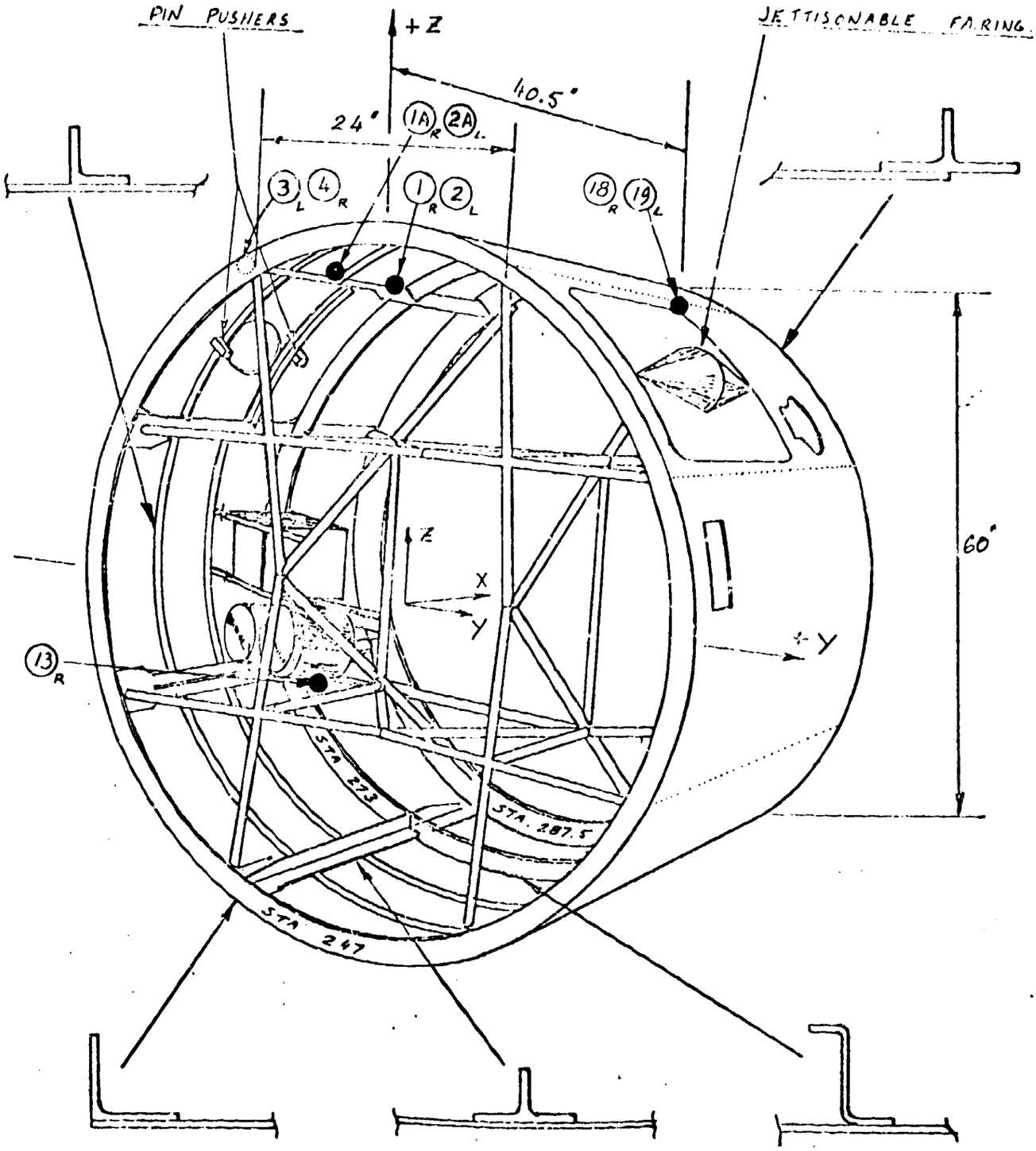

Figure II.A.2.6 FORWARD RACK INSTRUMENTATION LOCATIONS, HORIZON SENSOR FAIRING TESTS

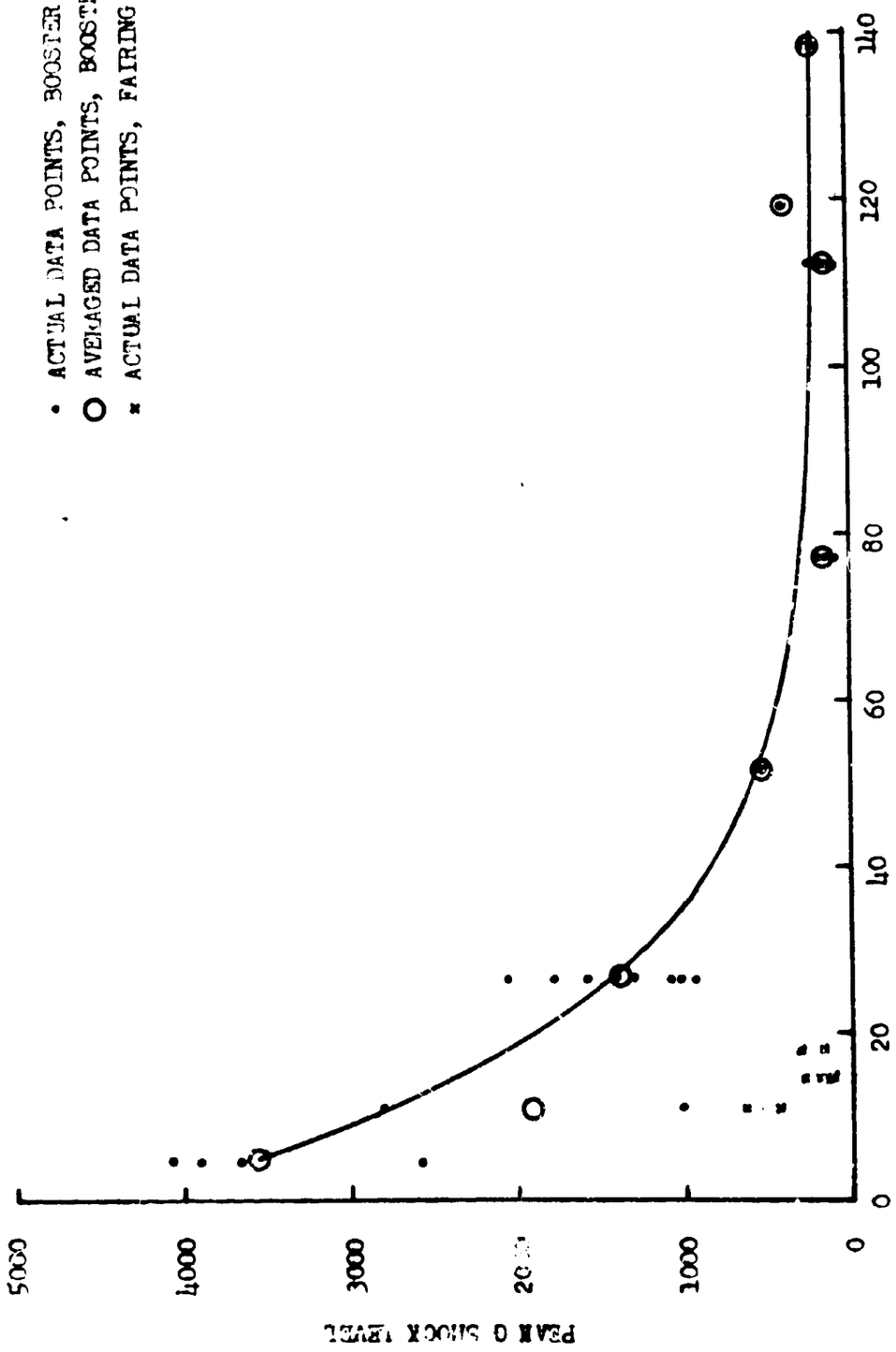

Figure II.A.2.7 PEAK G SHOCK LEVELS AS A FUNCTION OF DISTANCE FROM SOURCE

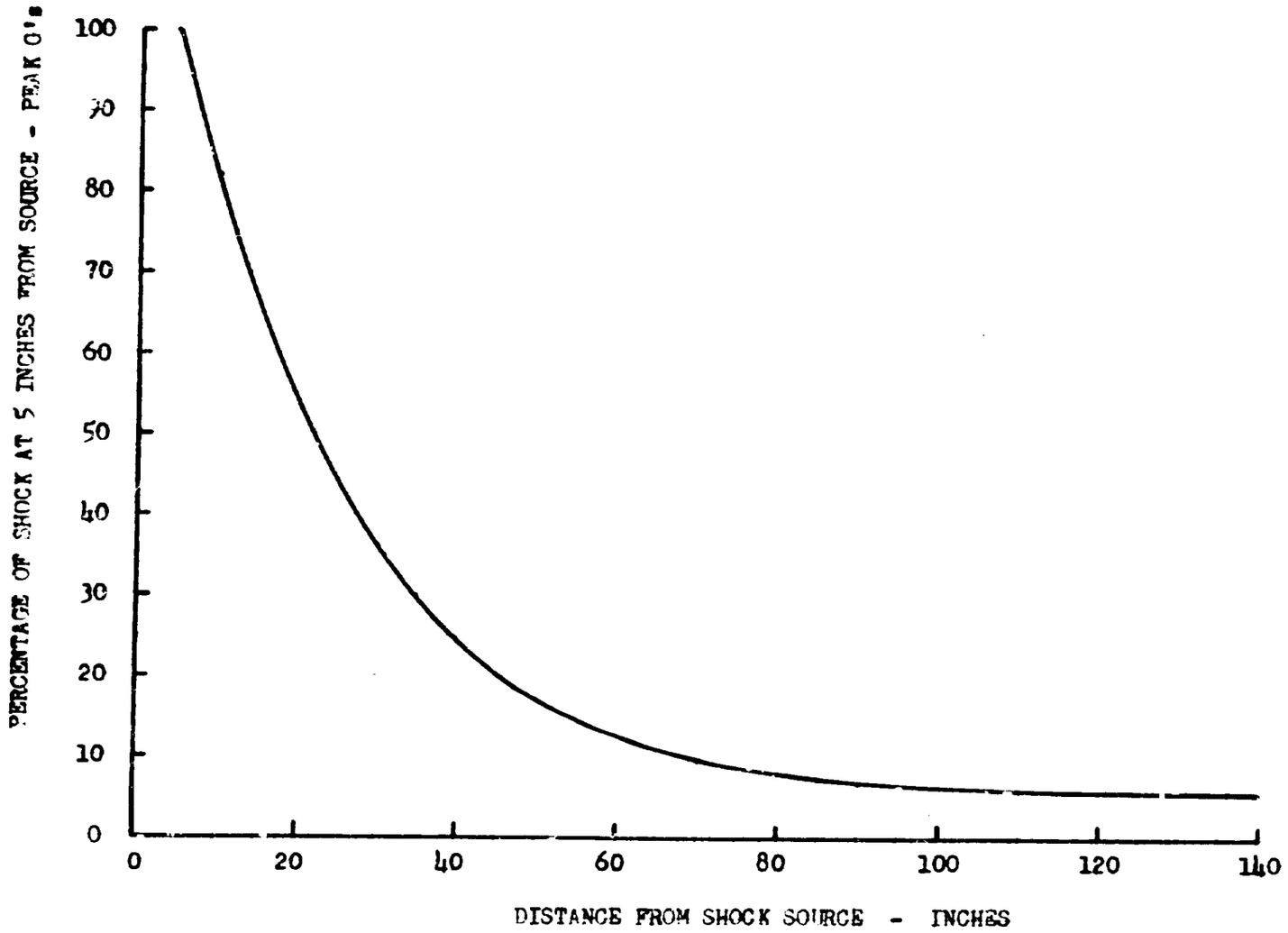

Figure II.A.2.8 PERCENTAGE OF PEAK G SHOCK LEVEL VERSES DISTANCE FROM SHOCK SOURCE

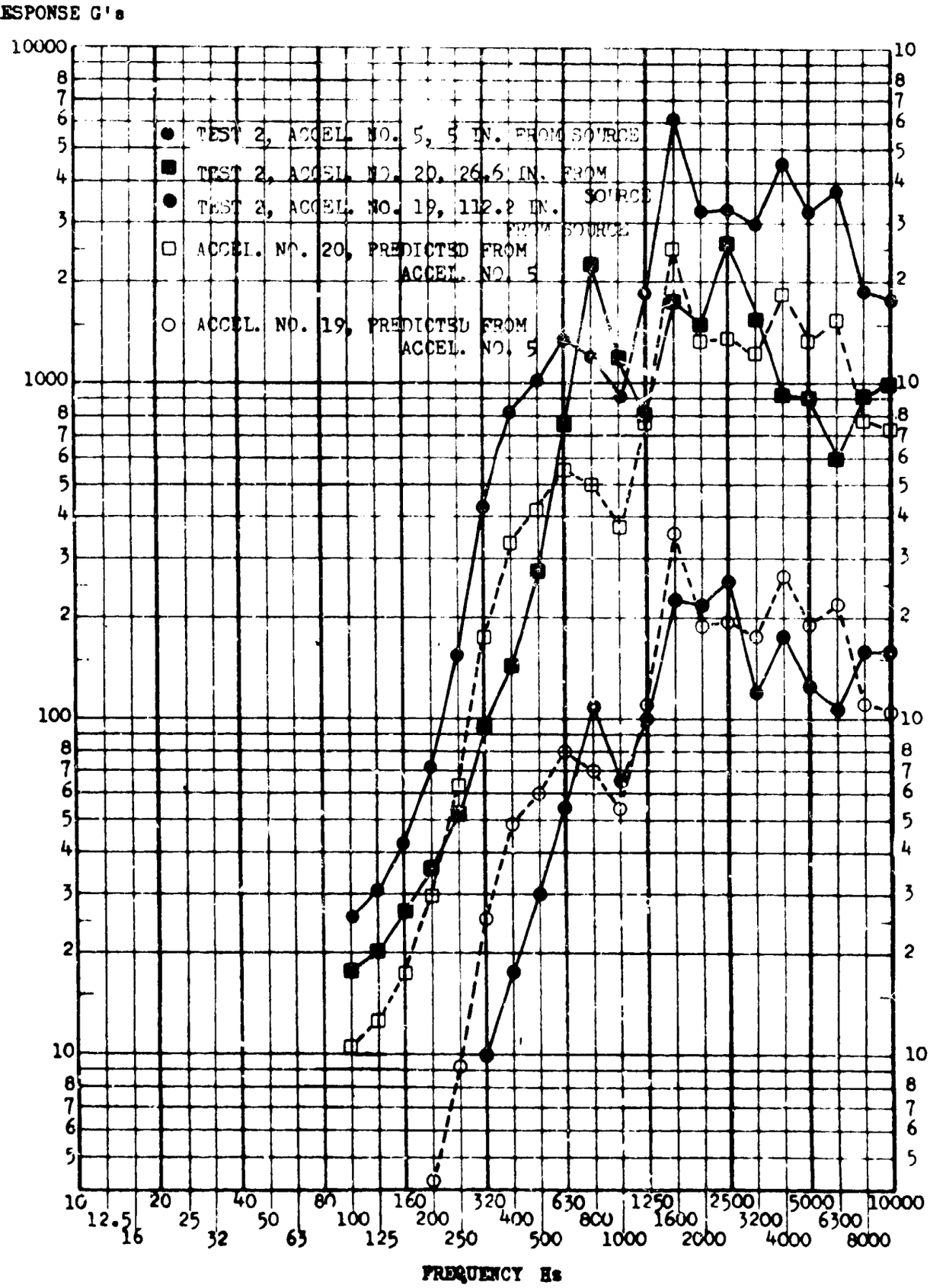

Figure II.A.2.9 EXAMPLE OF APPLICATION OF PEAK G SHOCK ATTENUATION TO SHOCK SPECTRUM

SHOCK TEST ANALYSIS DATA SHEET II.A.2.10

TEST ITEM 674-52
SERIAL NO.
SHOCK AXIS LATERAL

PART NO. STRUCTURE
TEST DATE 17 OCT 1963
SHOCK NO. 1

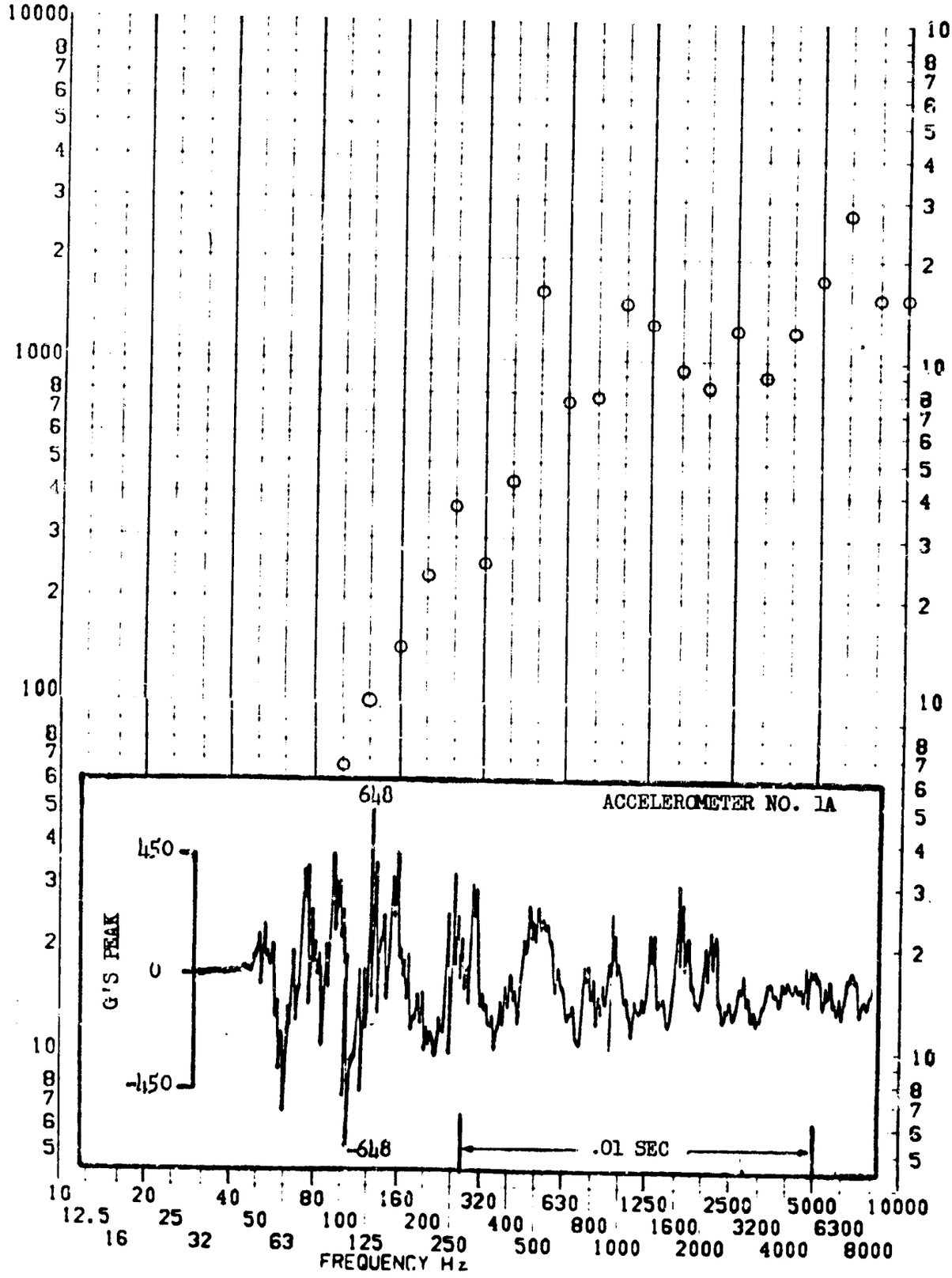

SHOCK TEST ANALYSIS DATA SHEET II.A.2.11

TEST ITEM 674-53 PART NO. STRUCTURE
SERIAL NO. TEST DATE 17 OCT 1963
RESPONSE G-S SHOCK AXIS LONGITUDINAL SHOCK NO. 1

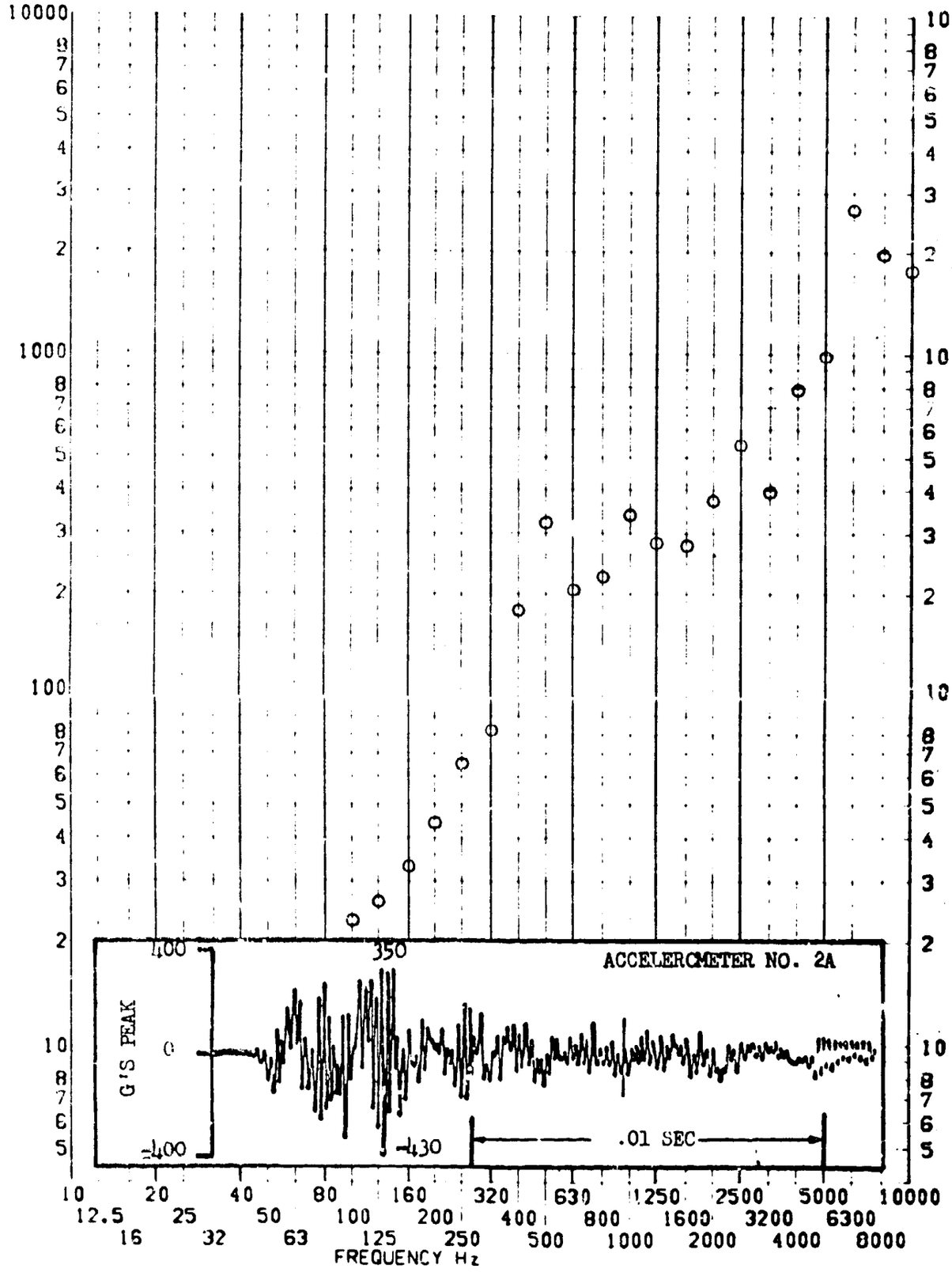

SHOCK TEST ANALYSIS DATA SHEET II.A.2.12

TEST ITEM 674-54
SERIAL NO.
SHOCK AXIS LATERAL

PART NO. STRUCTURE
TEST DATE 17 OCT 1963
SHOCK NO. 1

RESPONSE G-S

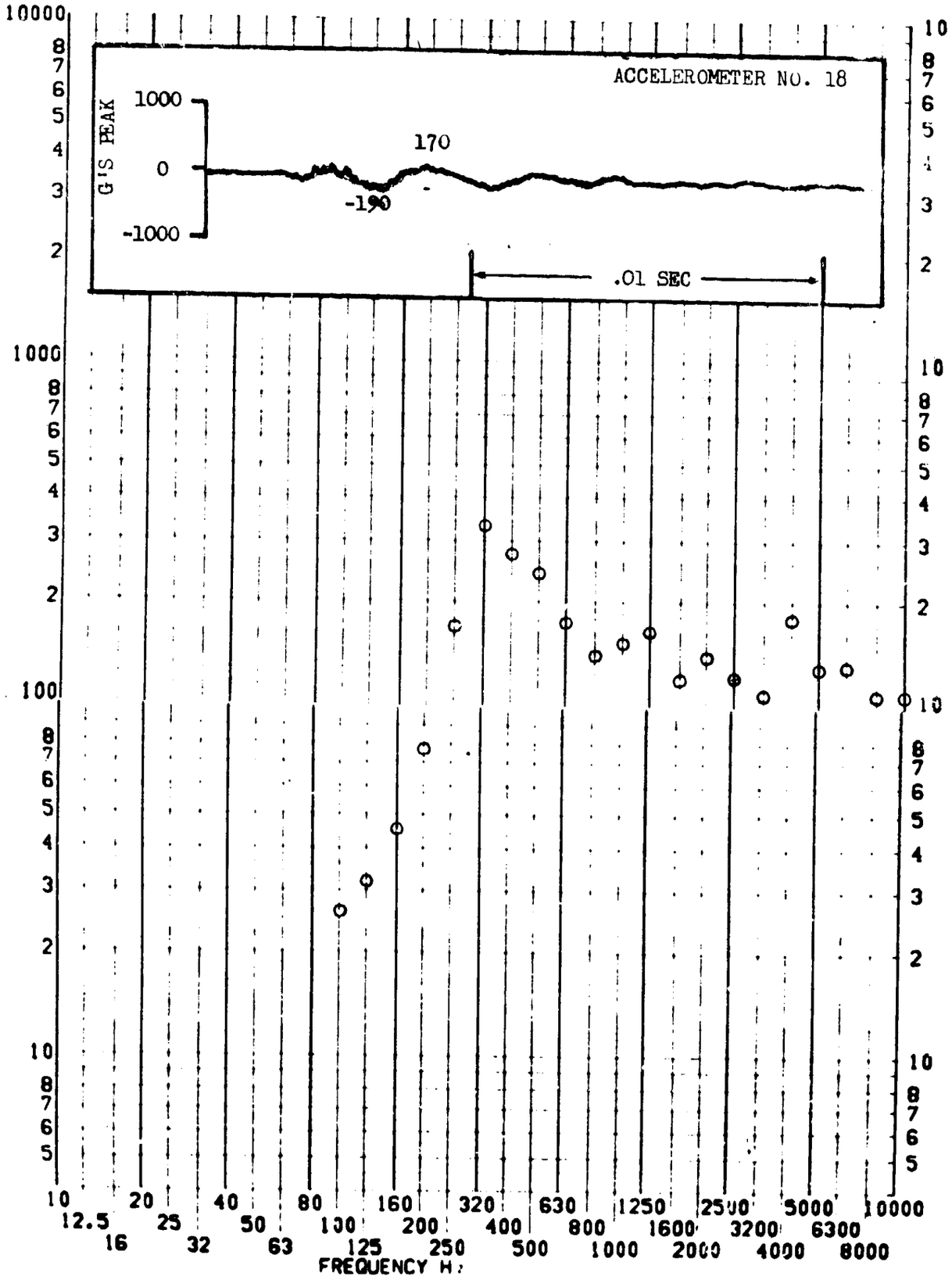

SHOCK TEST ANALYSIS DATA SHEET II.A.2.13

TEST ITEM 674-55
SERIAL NO.
SHOCK AXIS LONGITUDINAL

PART NO. STRUCTURE
TEST DATE 17 OCT 1963
SHOCK NO. 1

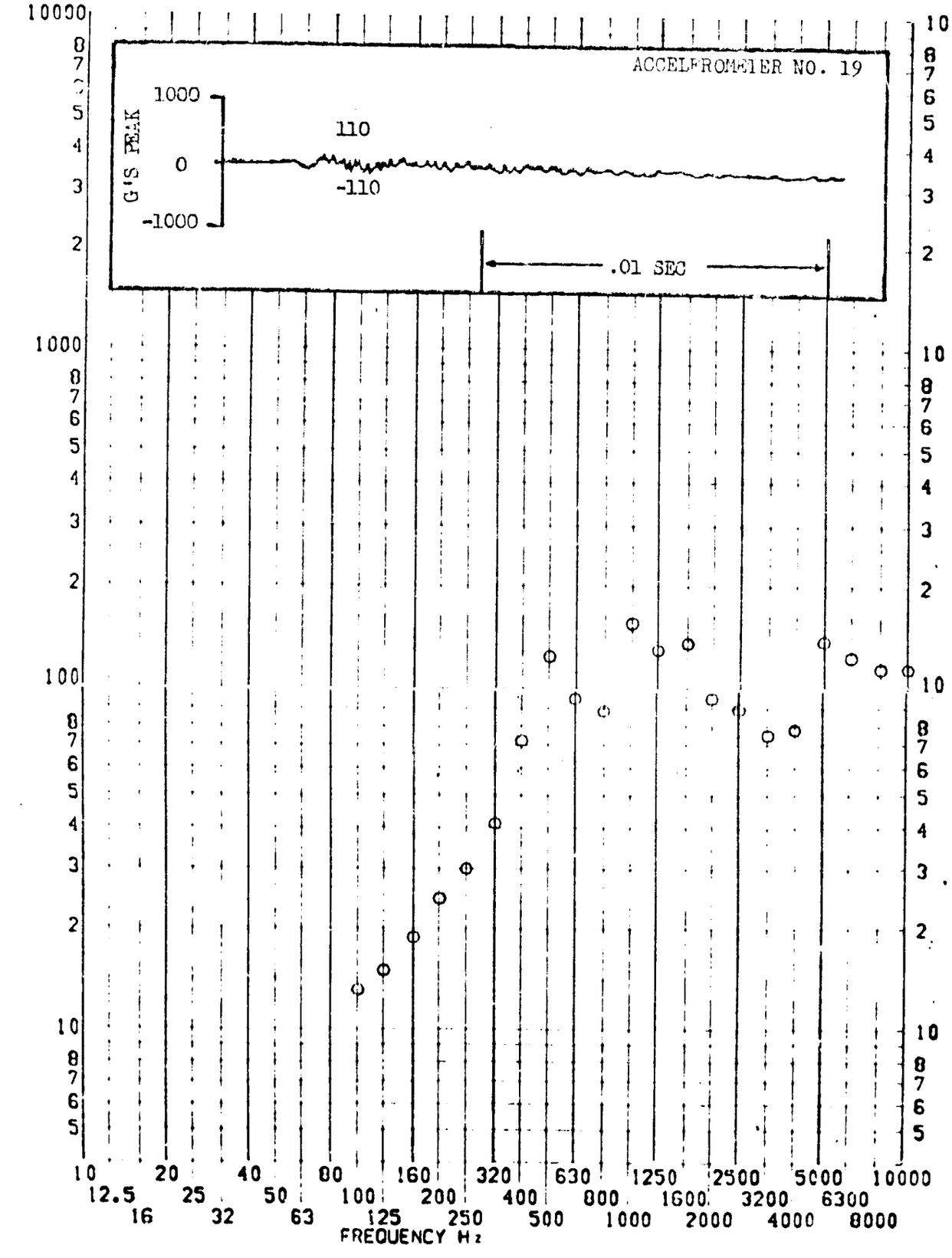

SHOCK TEST ANALYSIS DATA SHEET II.A.2.14

TEST ITEM 674-56
SERIAL NO.
SHOCK AXIS LATERAL

PART NO. STRUCTURE
TEST DATE 17 OCT 1963
SHOCK NO. 2

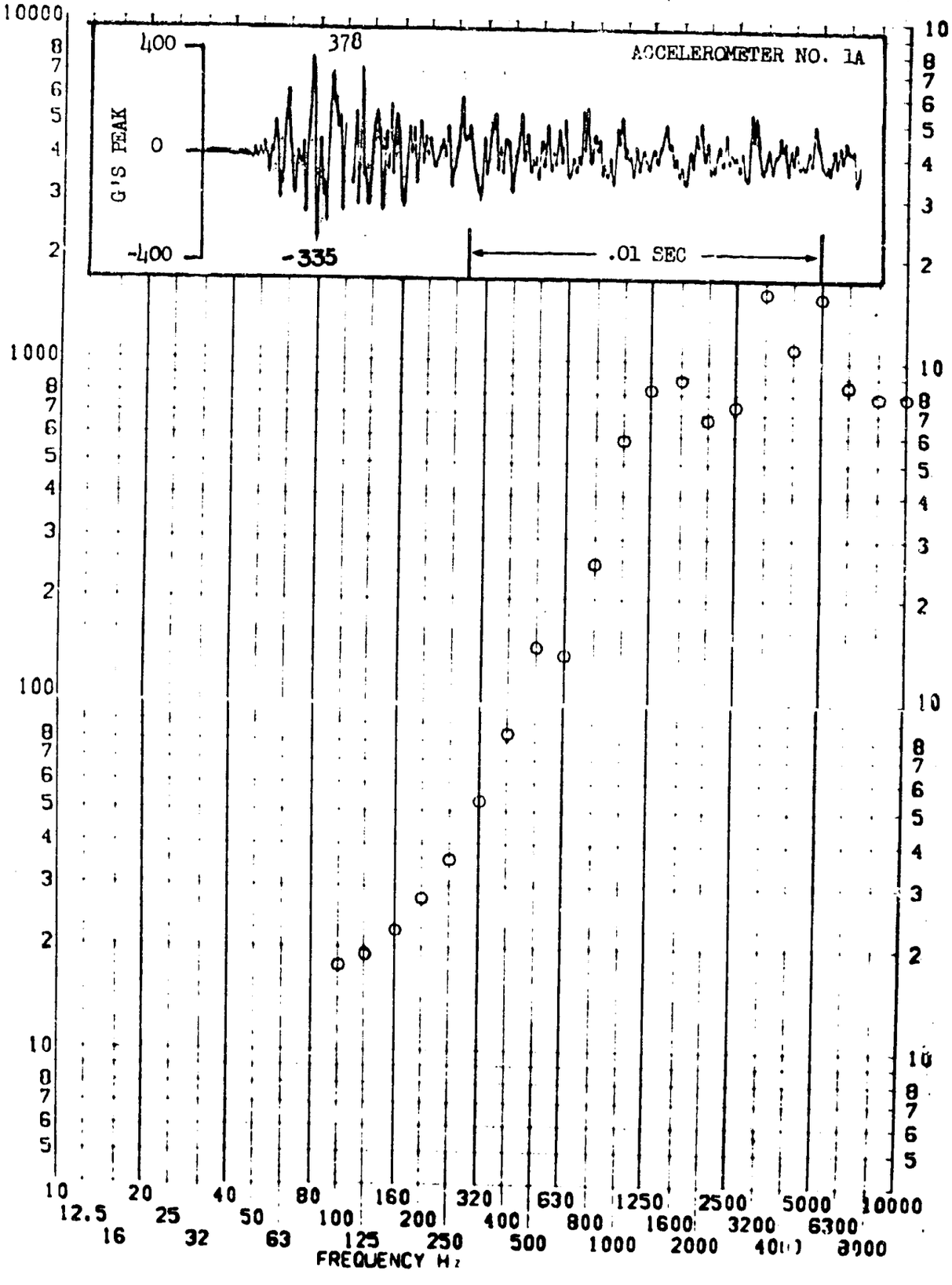

SHOCK TEST ANALYSIS DATA SHEET II.A.2.15

TEST ITEM 647-57
SERIAL NO.
SHOCK AXIS LONGITUDINAL

PART NO. STRUCTURE
TEST DATE 17 OCT 1963
SHOCK NO. 2

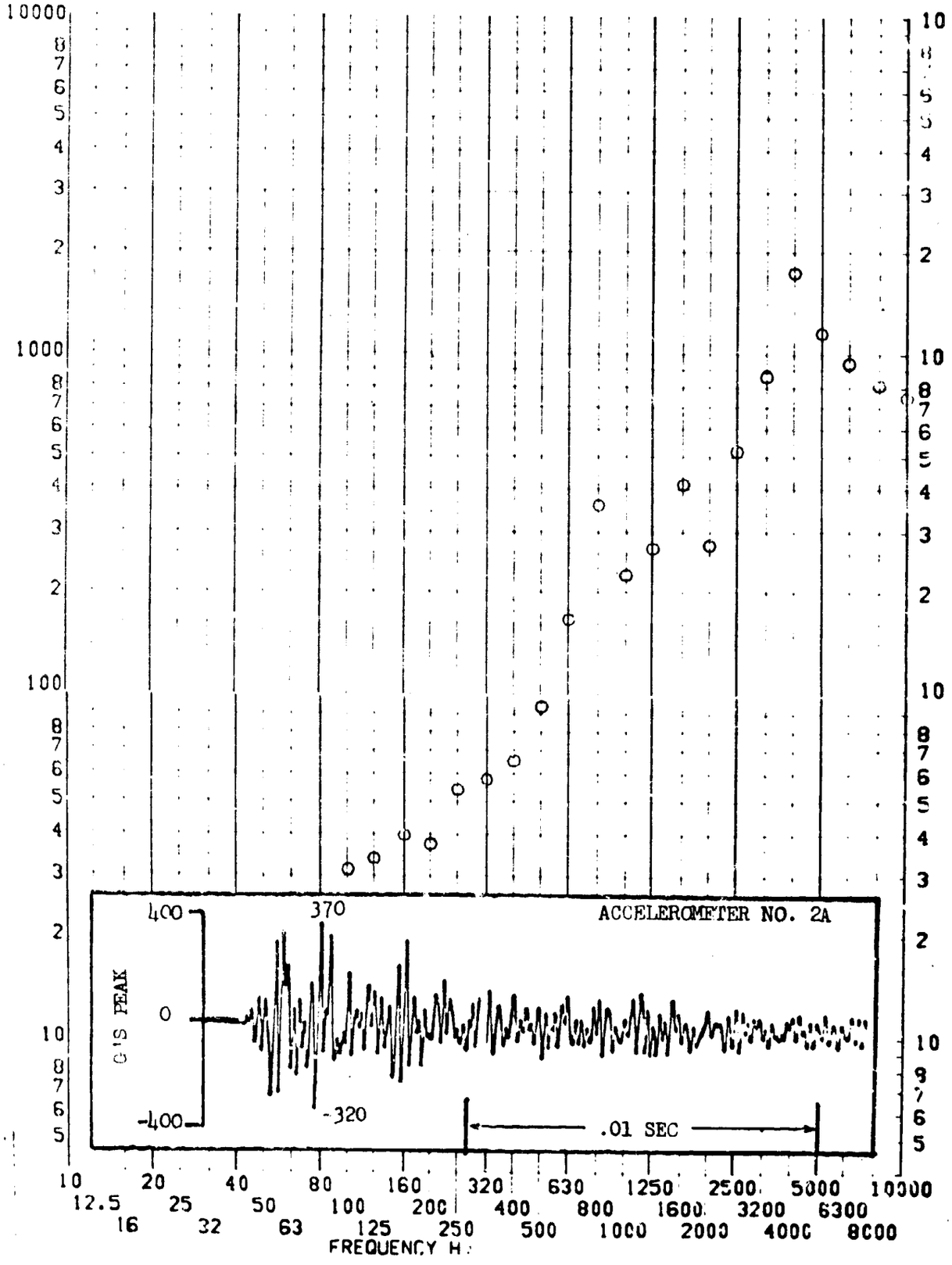

SHOCK TEST ANALYSIS DATA SHEET II.A.2.16

TEST ITEM 674-58 PART NO. EQUIPMENT
SERIAL NO. TEST DATE 17 OCT 1963
RESPONSE G-S SHOCK AXIS LONGITUDINAL SHOCK NO. 2

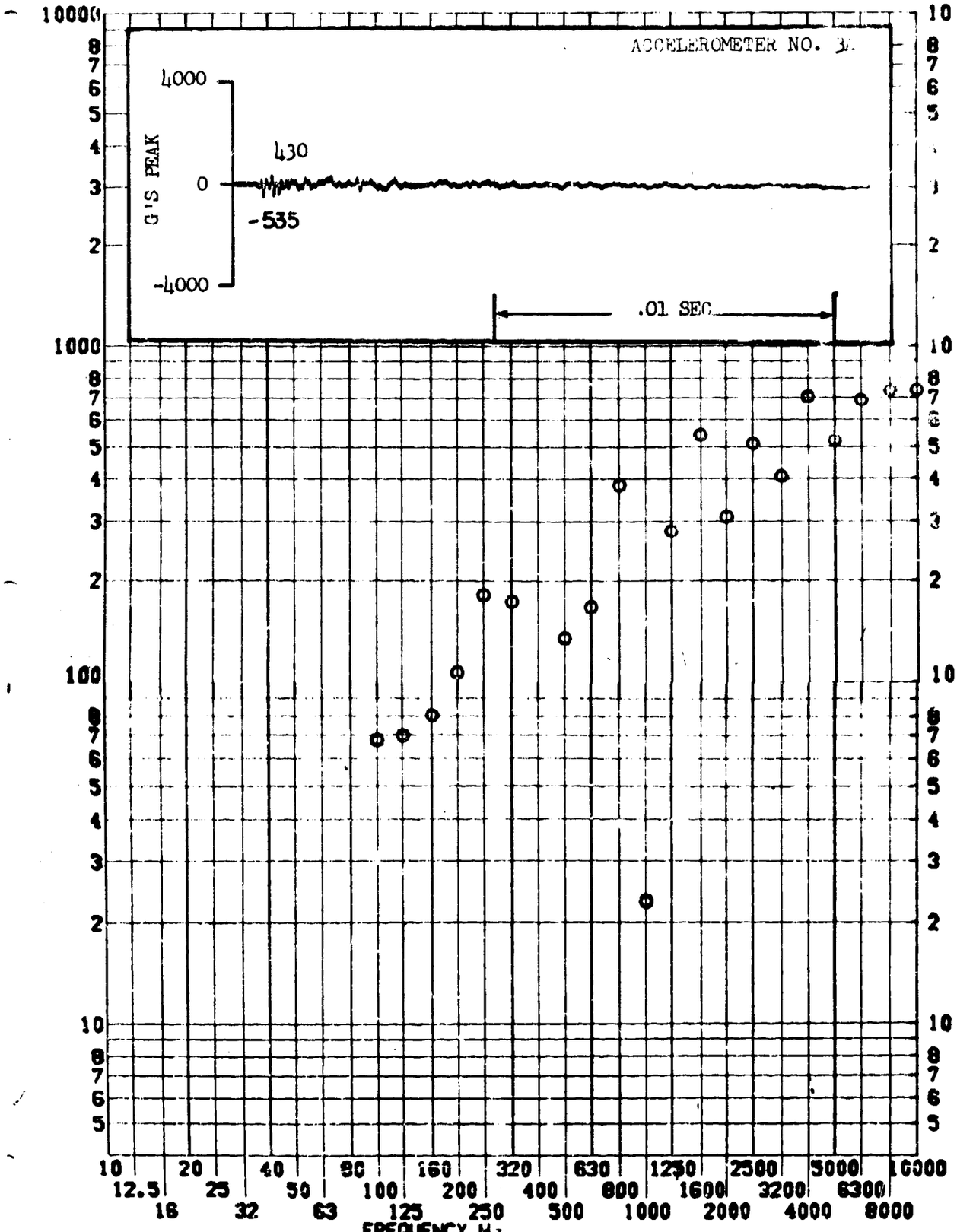

SHOCK TEST ANALYSIS DATA SHEET II.A.2.17

TEST ITEM 674-59
SERIAL NO.
SHOCK AXIS LATERAL

PART NO. EQUIPMENT
TEST DATE 17 OCT 1963
SHOCK NO. 2

RESPONSE G-S

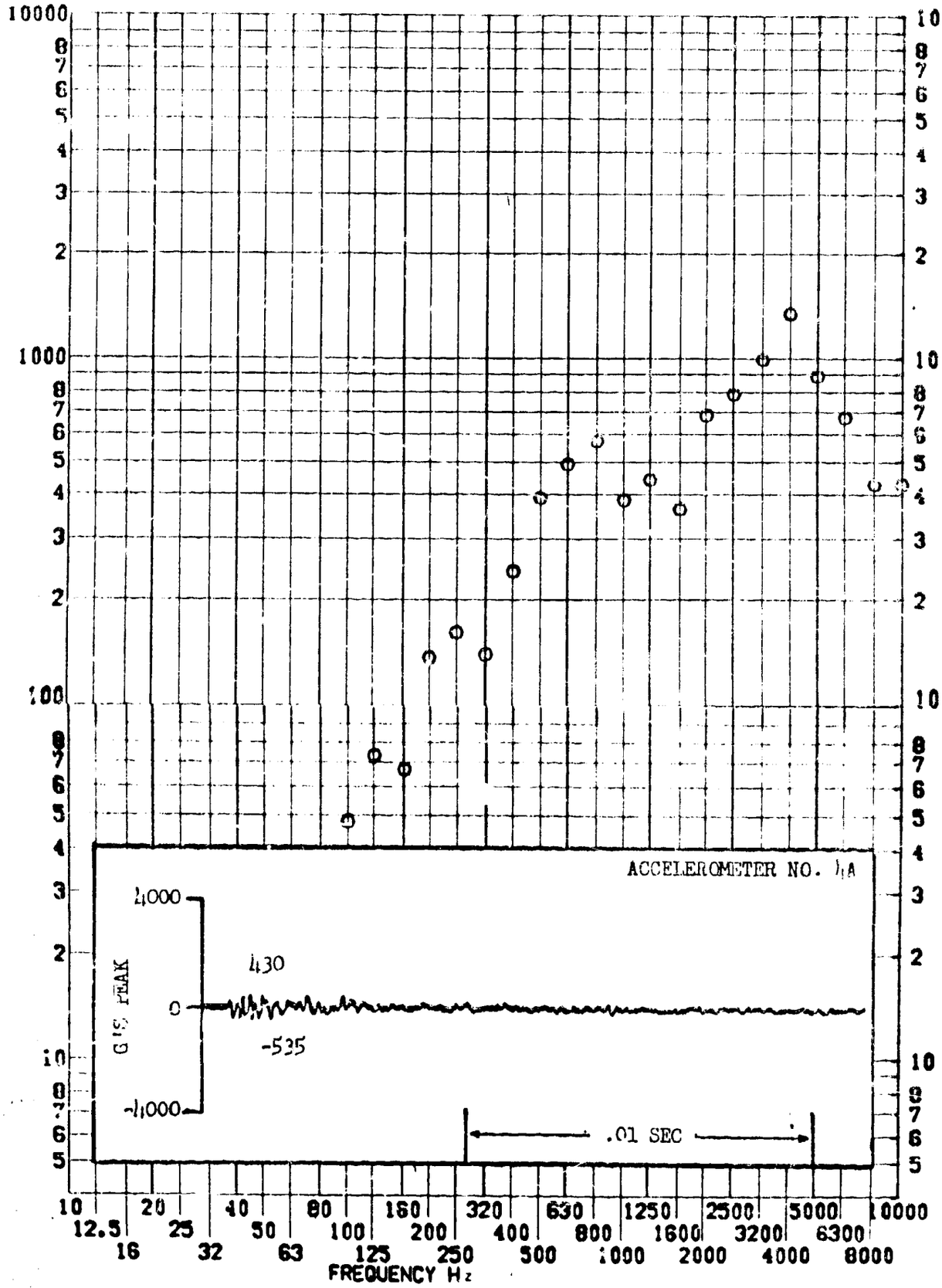

SHOCK TEST ANALYSIS DATA SHEET II.A.2.18

TEST ITEM 674-60
SERIAL NO.
SHOCK AXIS LONGITUDINAL

PART NO. STRUCTURE
TEST DATE 17 OCT 1963
SHOCK NO. 2

RESPONSE G-S

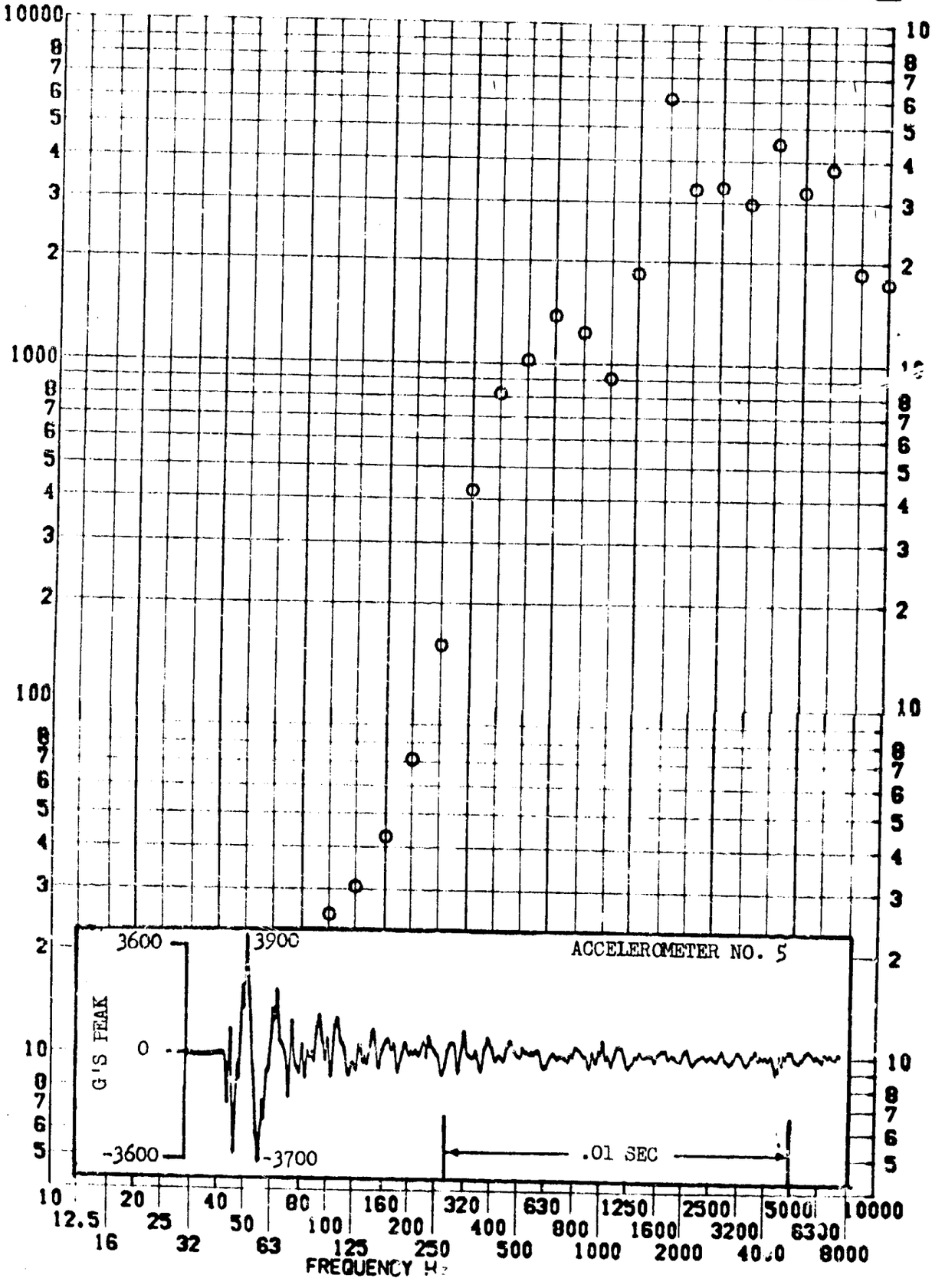

SHOCK TEST ANALYSIS DATA SHEET II.A.2.19

TEST ITEM 574-51 PART NO. STRUCTURE
SERIAL NO. TEST DATE 17 OCT 1963
RESPONSE G-S SHOCK AXIS RADIAL SHOCK NO. 2

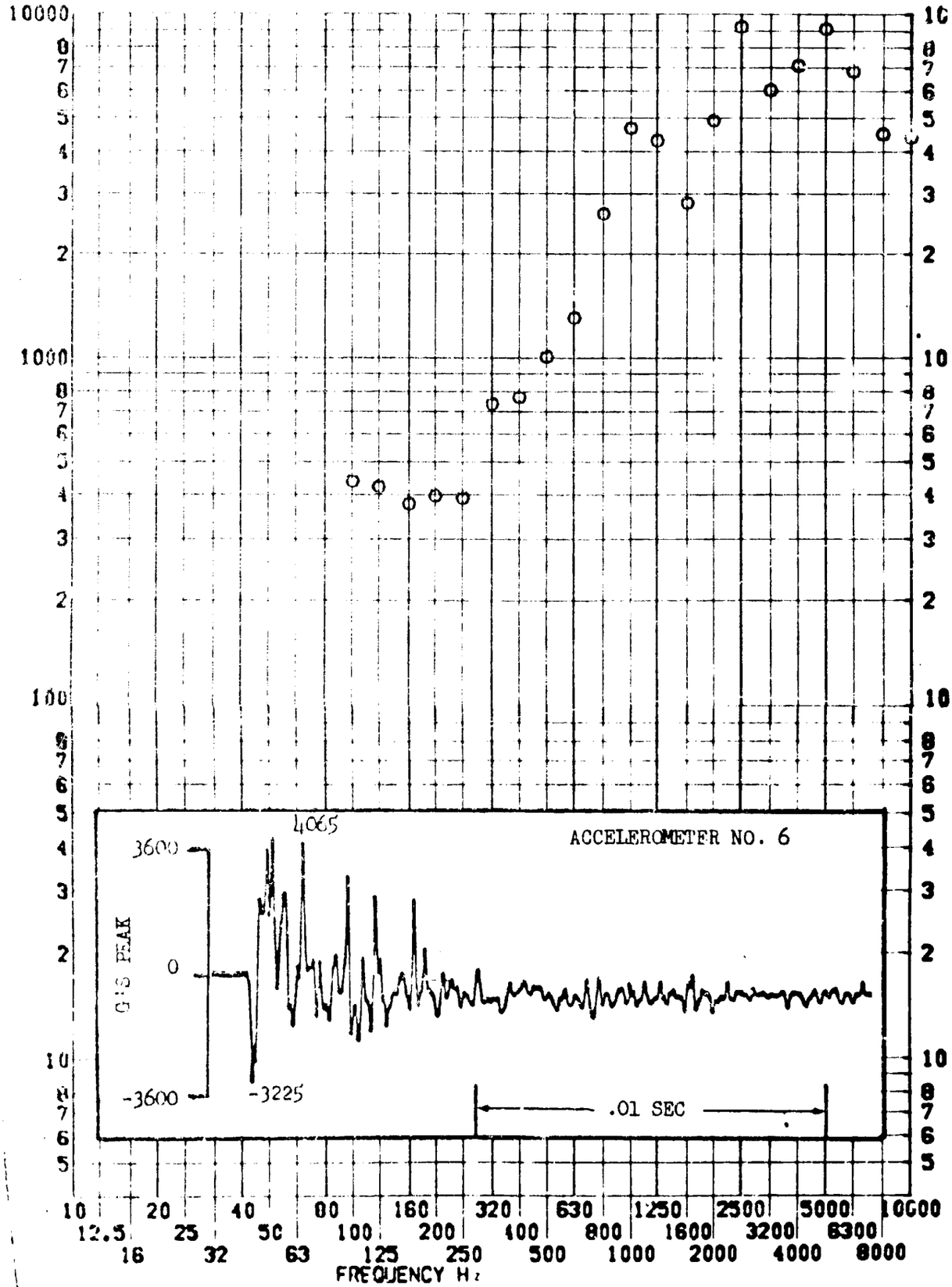

SHOCK TEST ANALYSIS DATA SHEET II.A.2.20

TEST ITEM 674-62
SERIAL NO.
SHOCK AXIS LATERAL

PART NO. STRUCTURE
TEST DATE 17 OCT 1963
SHOCK NO. 2

RESPONSE G-S

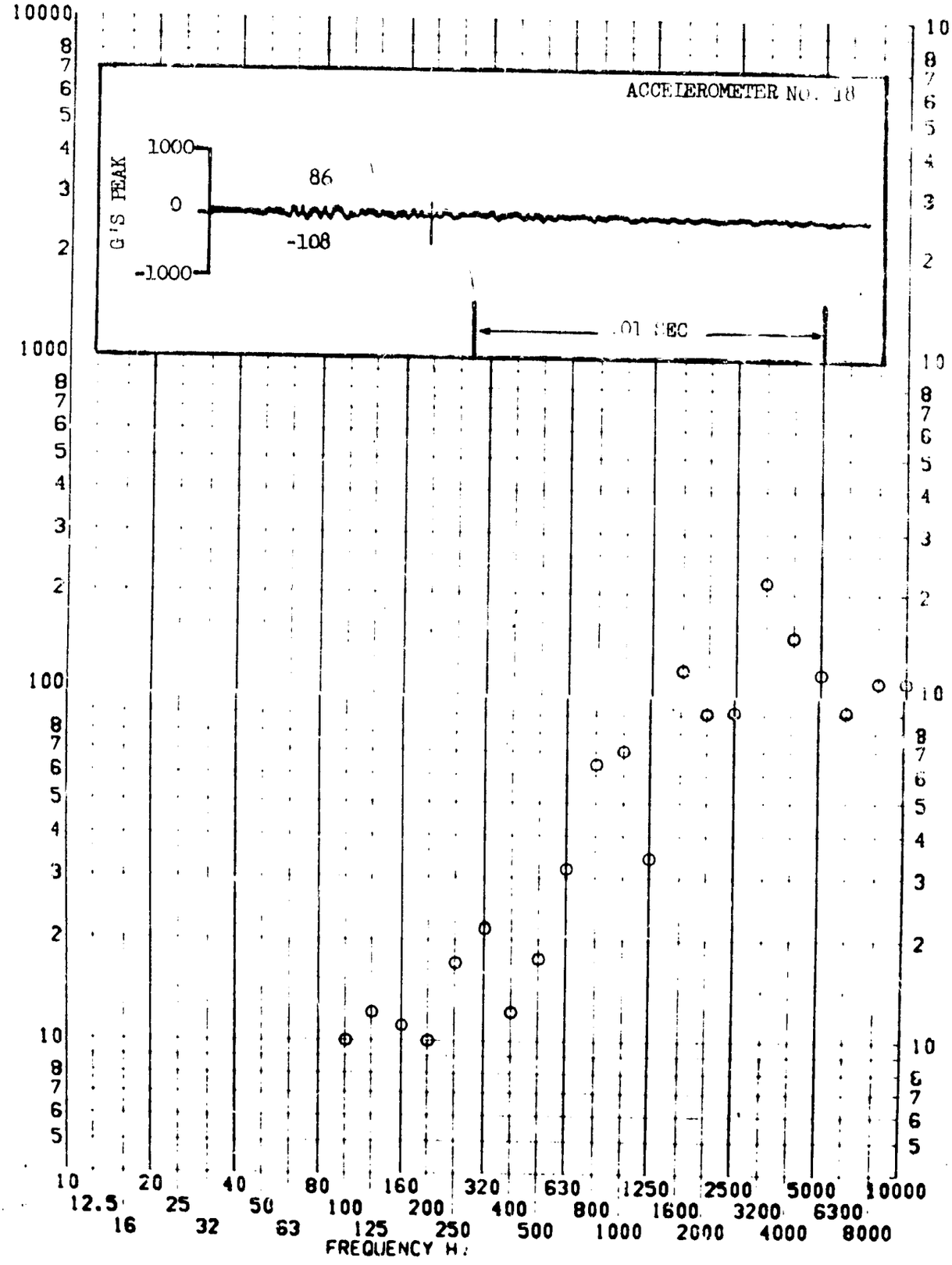

SHOCK TEST ANALYSIS DATA SHEET TT.A.2.21

TEST ITEM 674-63
SERIAL NO.
SHOCK AXIS LONGITUDINAL

PART NO. STRUCTURE
TEST DATE 17 OCT 1963
SHOCK NO. 2

RESPONSE G-S

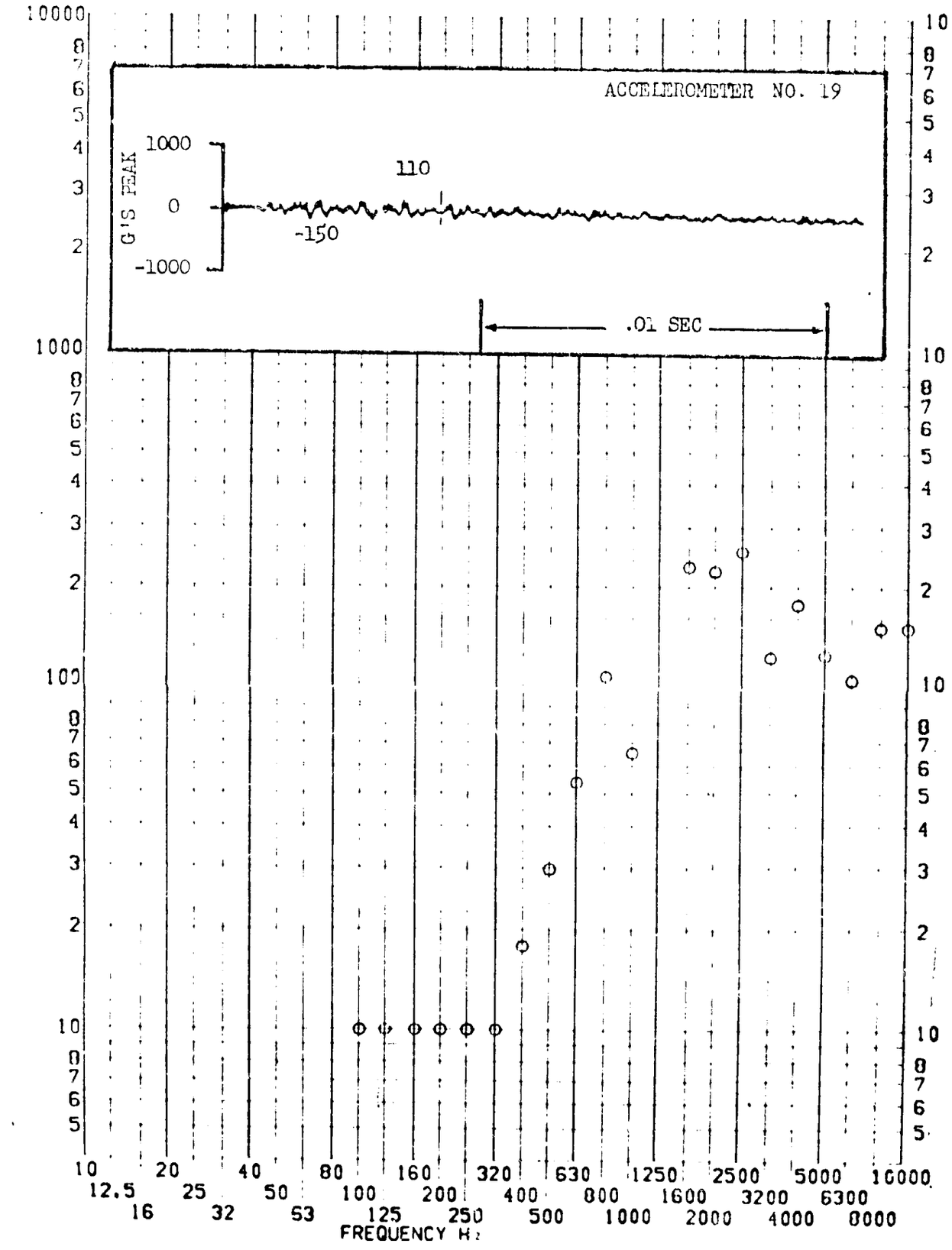

SHOCK TEST ANALYSIS DATA SHEET II.A.2.22

TEST ITEM 674-64
SERIAL NO.
SHOCK AXIS LONGITUDINAL

PART NO. STRUCTURE
TEST DATE 17 OCT 196[illegible]
SHOCK NO. 2

RESPONSE G-S

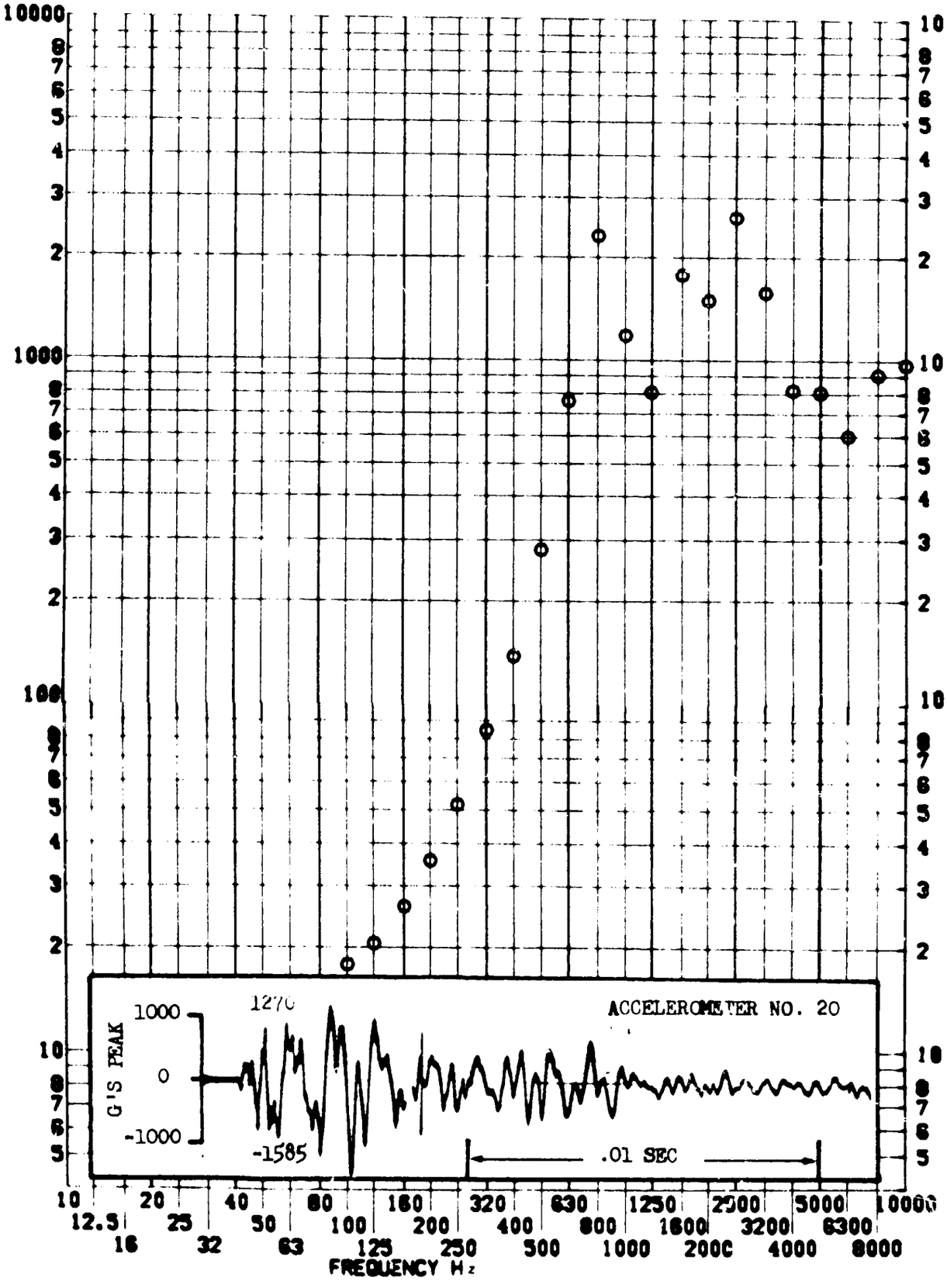

SHOCK TEST ANALYSIS DATA SHEET II.A.2.23

TEST ITEM 674-65
SERIAL NO.
SHOCK AXIS LATERAL

PART NO. STRUCTURE
TEST DATE 17 OCT 1963
SHOCK NO. 2

RESPONSE G-S

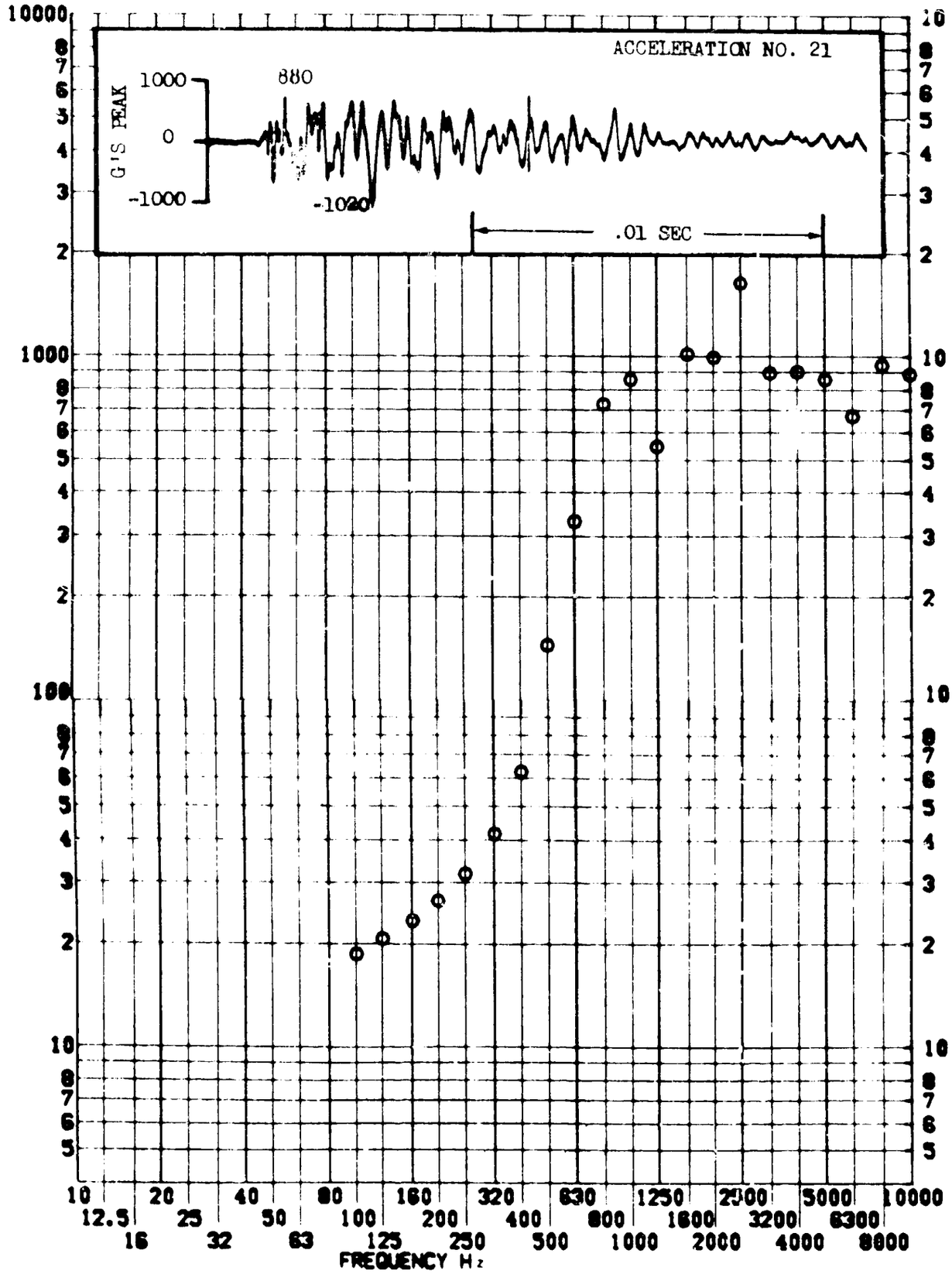

SHOCK TEST ANALYSIS DATA SHEET II.A.2.2h

TEST ITEM 674-66
SERIAL NO.
SHOCK AXIS LONGITUDINAL

PART NO. STRUCTURE
TEST DATE 17 OCT 1963
SHOCK NO. 2

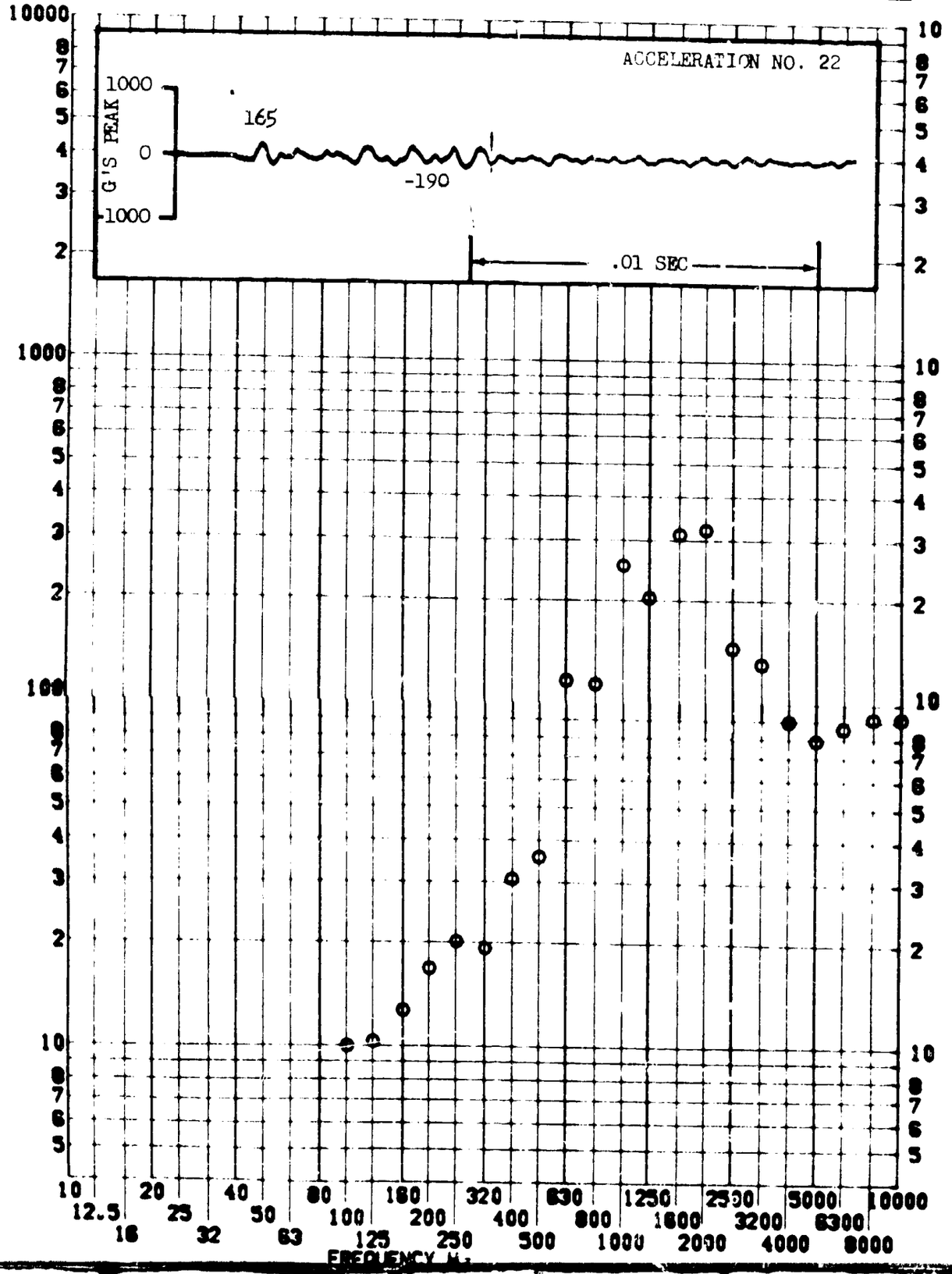

SHOCK TEST ANALYSIS DATA SHEET II.A.2.25

TEST ITEM 674-67
SERIAL NO.
SHOCK AXIS LATERAL

PART NO. STRUCTURE
TEST DATE 17 OCT 1963
SHOCK NO. 2

RESPONSE G-S

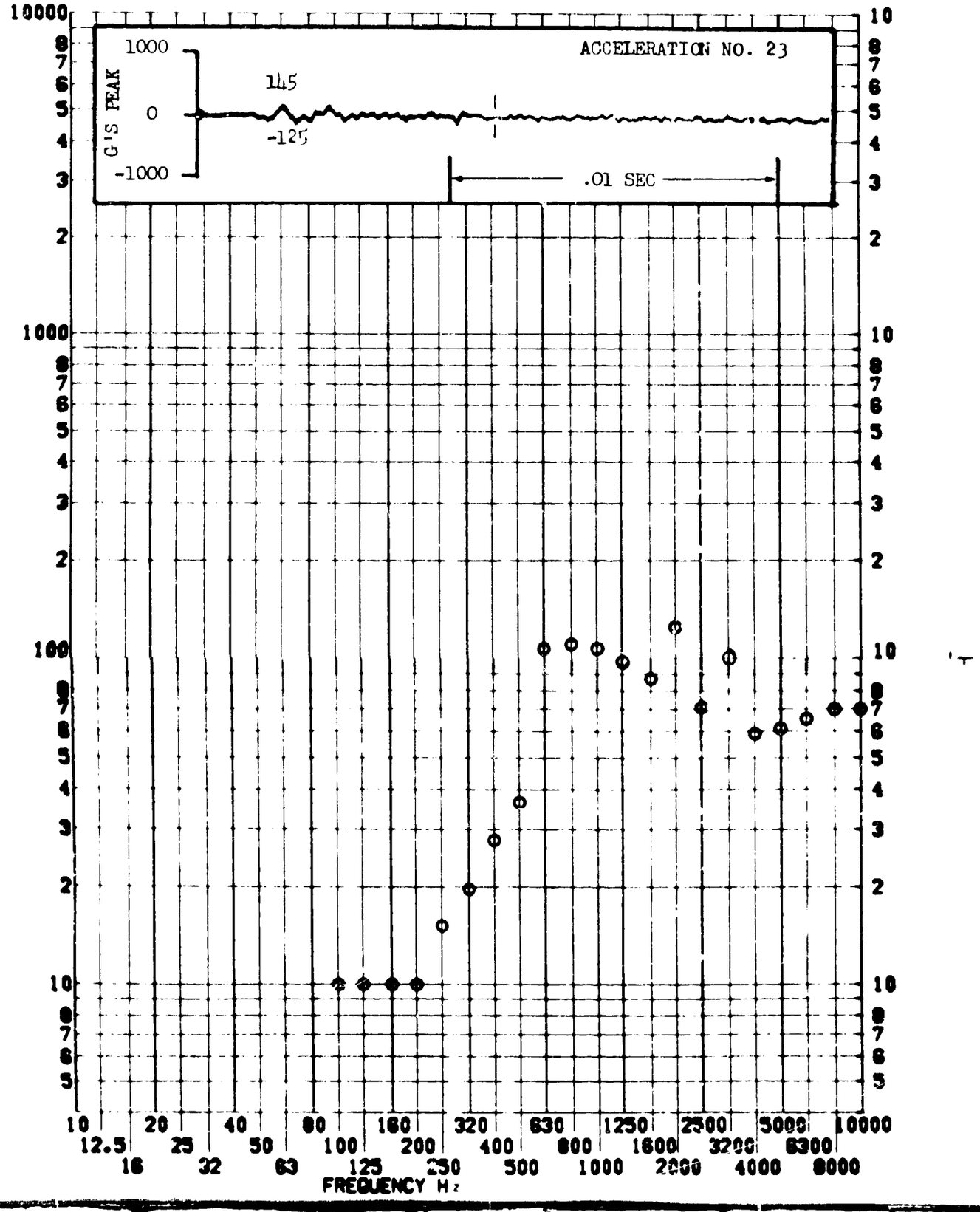

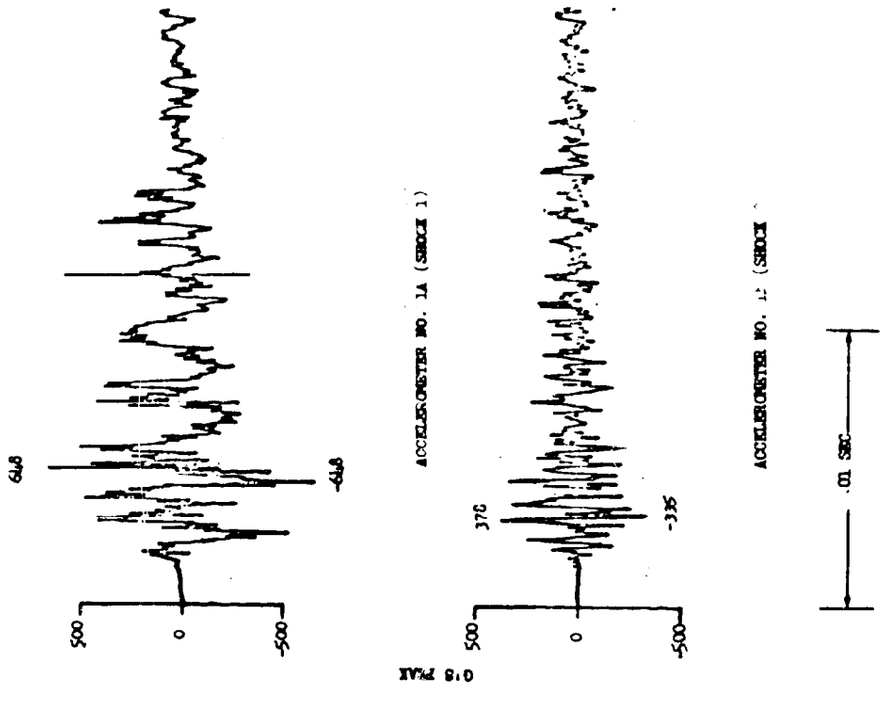
ACCELEROMETER NO. 1A (SHOCK 1)
ACCELEROMETER NO. 1A (SHOCK
0.1 SEC

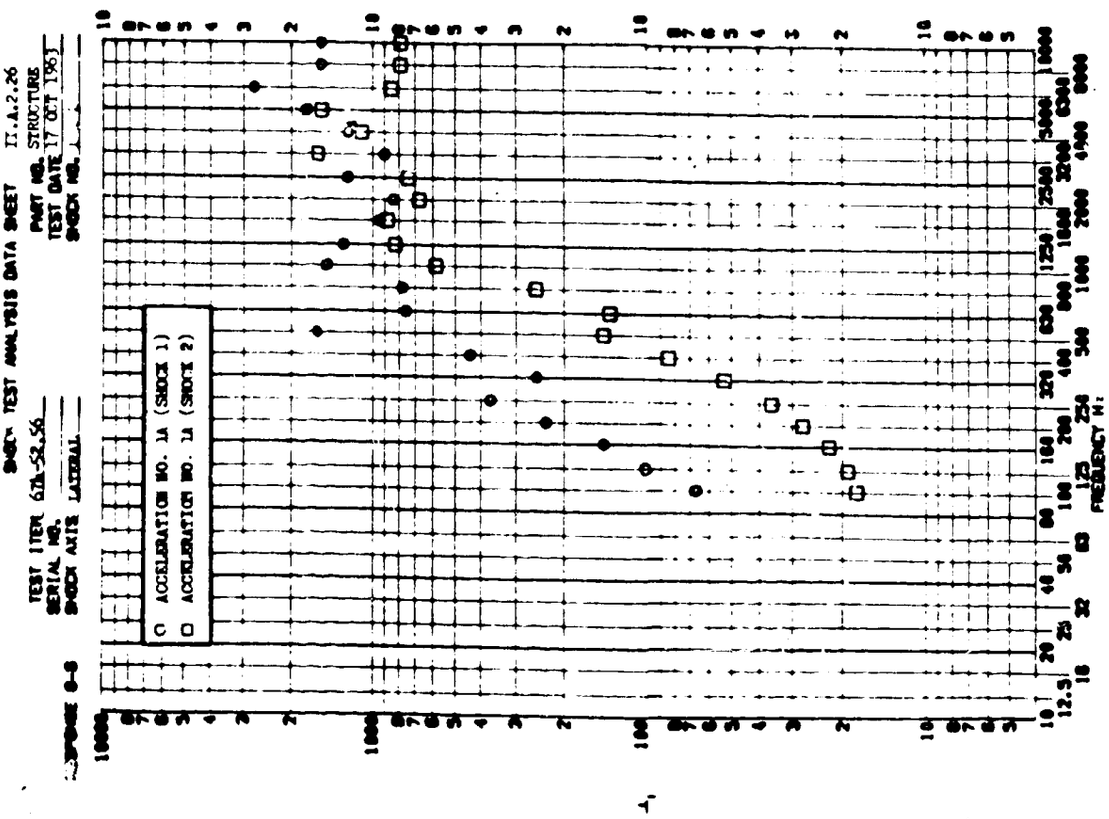
SHOCK TEST ANALYSIS DATA SHEET
TEST ITEM 62A-52.56
SERIAL NO.
SHOCK AXIS LATERAL
PART NO. STRUCTURE
TEST DATE 17 OCT 1963
SHOCK NO.
ACCELERATION NO. 1A (SHOCK 1)
ACCELERATION NO. 1A (SHOCK 2)
FREQUENCY IN

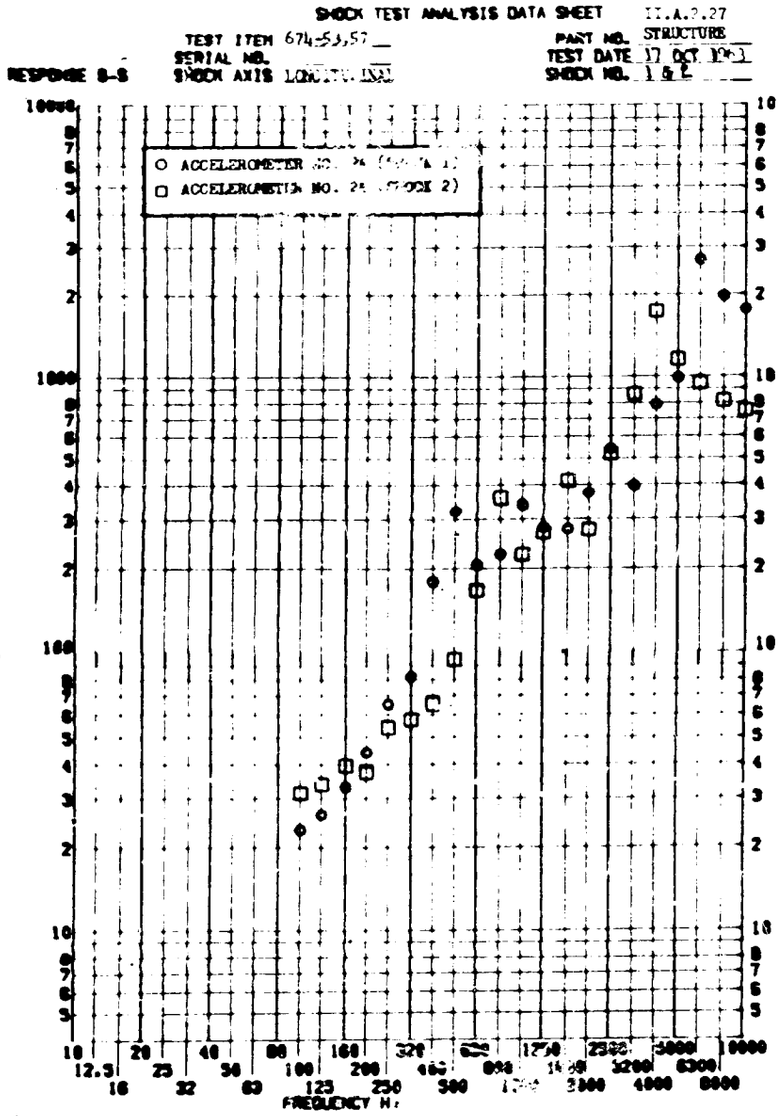

ACCELEROMETER NO. 2A (SHOCK 1)

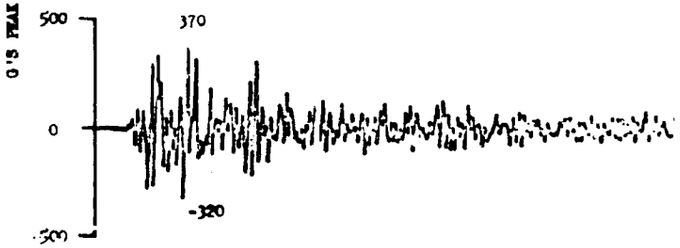

ACCELEROMETER NO. 2A (SHOCK 2)

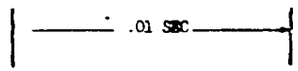

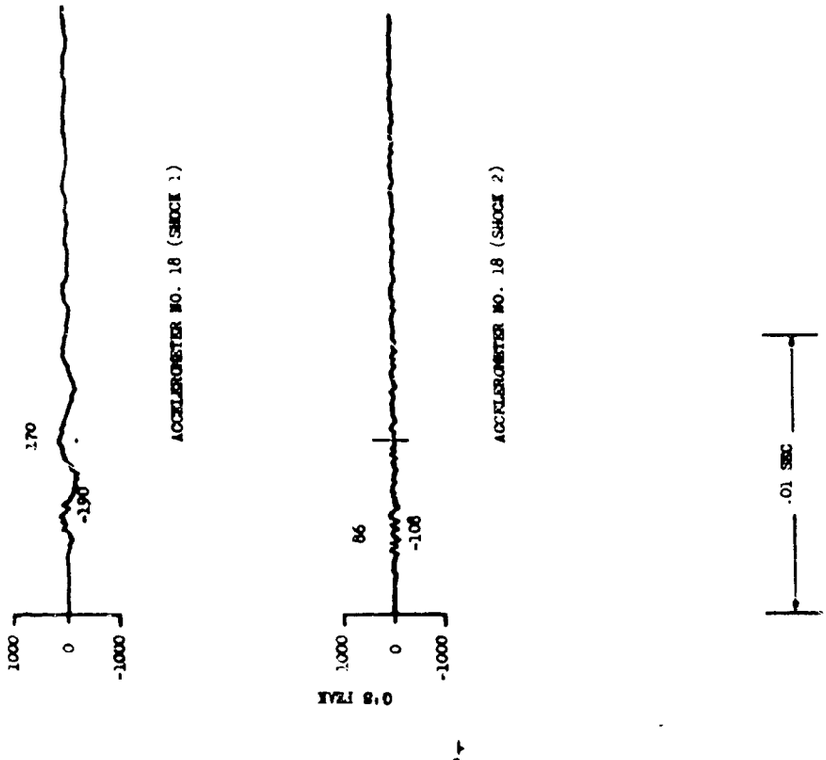
ACCELEROMETER NO. 18 (SHOCK 1)
170
-190
1000
0
-1000
ACCELEROMETER NO. 18 (SHOCK 2)
86
-108
1000
0
-1000
.01 SEC

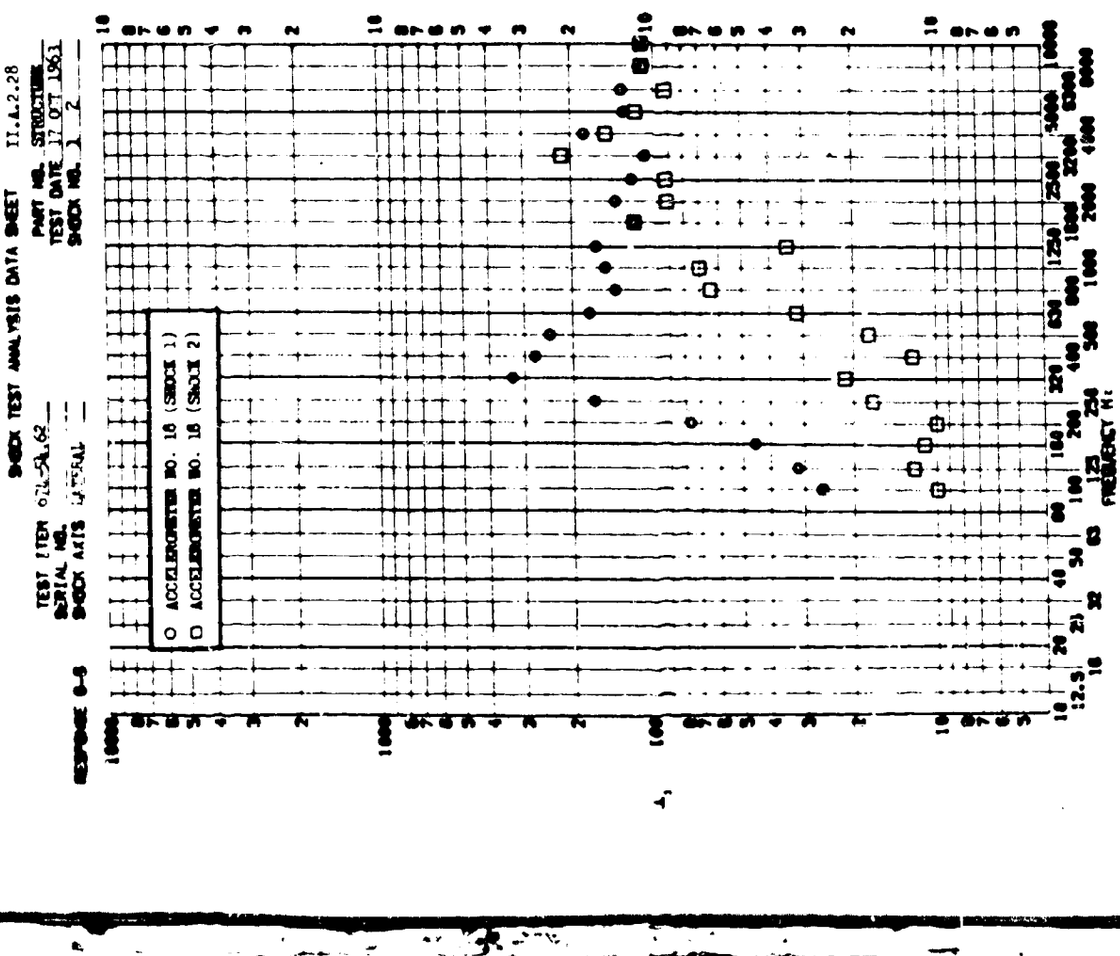
SHOCK TEST ANALYSIS DATA SHEET
TEST ITEM
SERIAL NO.
SHOCK AXIS
PART NO. STRUCTURE
TEST DATE 17 OCT 1961
SHOCK NO. 1 2
RESPONSE G-S
ACCELEROMETER NO. 18 (SHOCK 1)
ACCELEROMETER NO. 18 (SHOCK 2)
FREQUENCY H

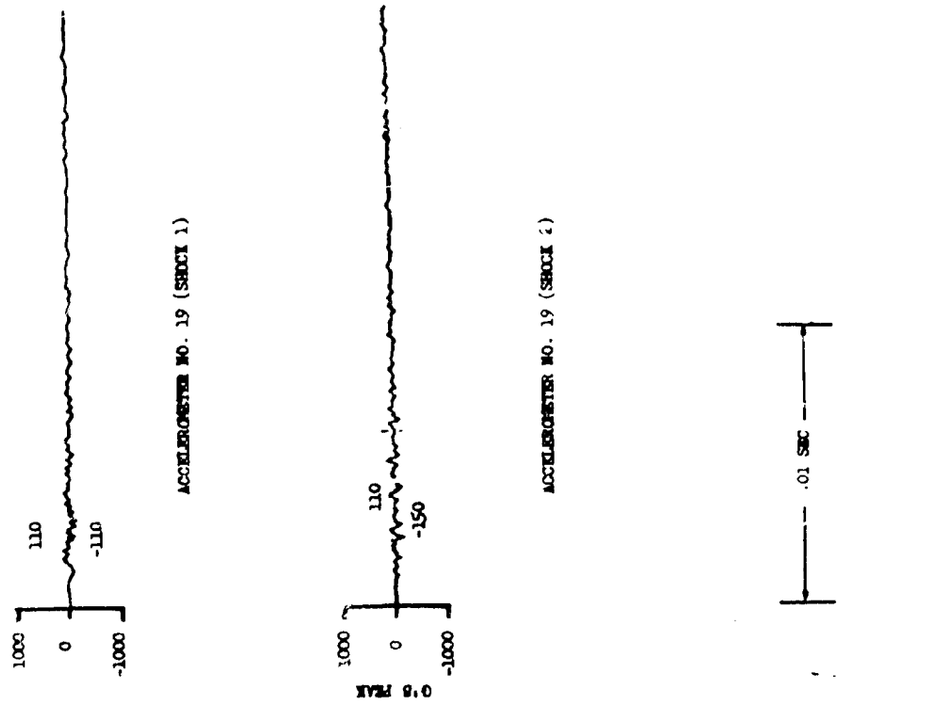
ACCELEROMETER NO. 19 (SHOCK 1)
110
-110
1000
0
-1000
ACCELEROMETER NO. 19 (SHOCK 2)
110
-150
1000
0
-1000
0.1 SEC

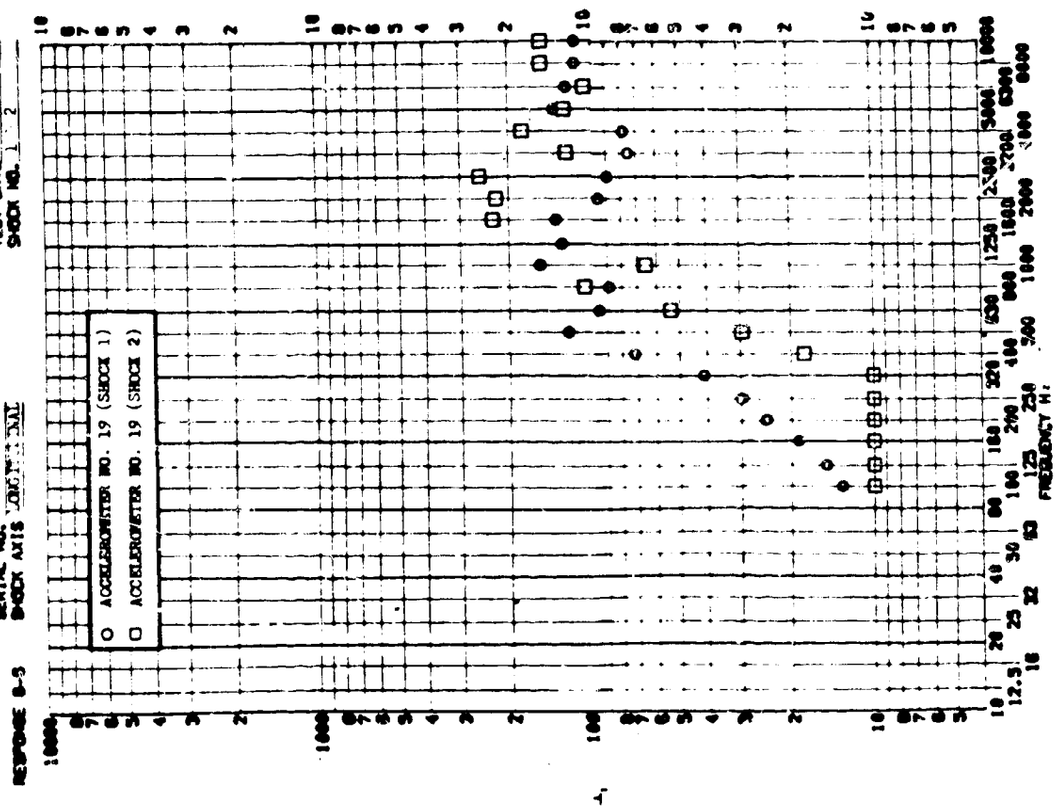
SHOCK TEST ANALYSIS DATA SHEET
TEST ITEM 674-55.63
SERIAL NO.
SHOCK AXIS
PART NO. STRUCTURE
TEST DATE 17 OCT 1967
SHOCK NO. 1 2
RESPONSE G-S
ACCELEROMETER NO. 19 (SHOCK 1)
ACCELEROMETER NO. 19 (SHOCK 2)
FREQUENCY H

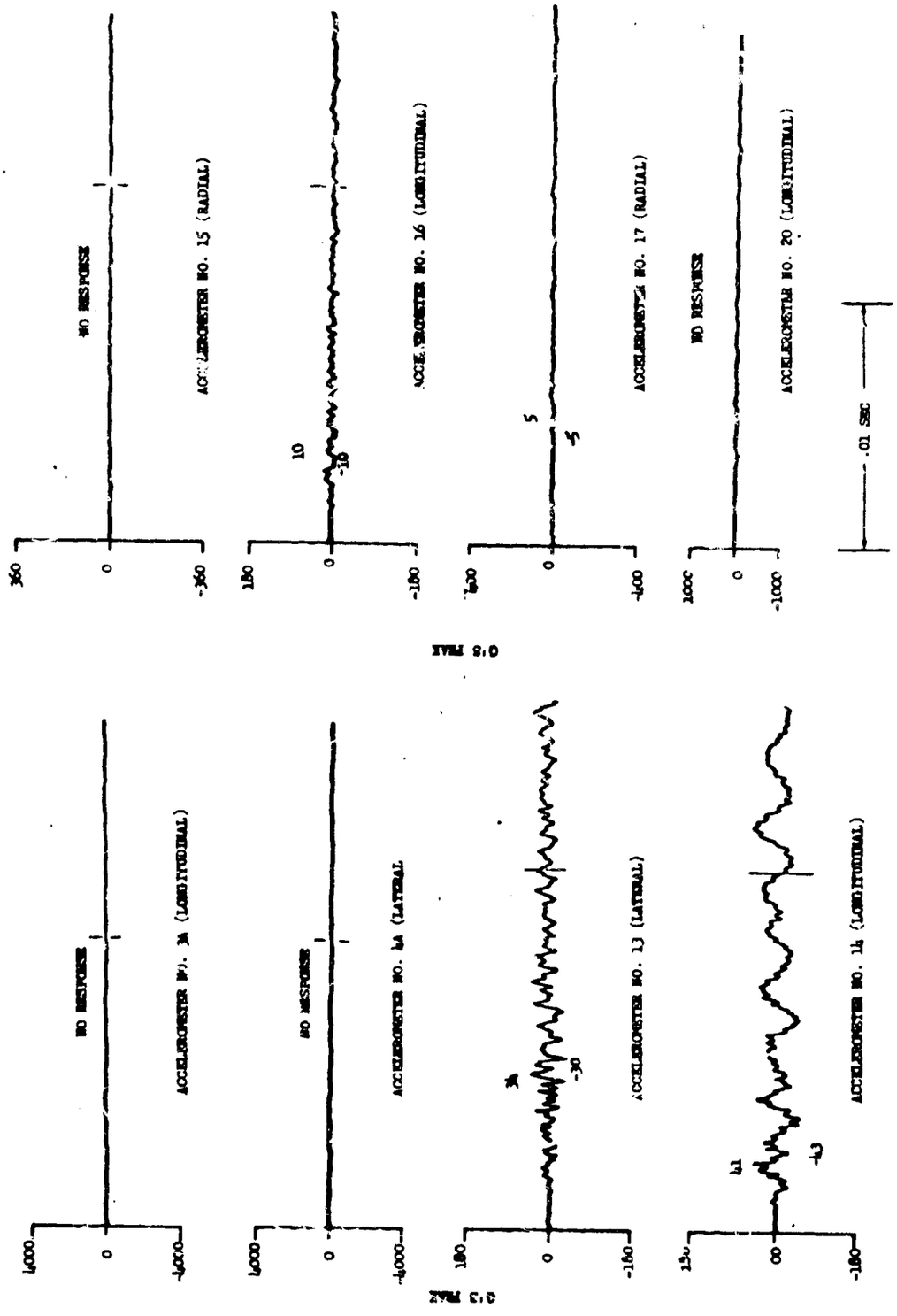

Figure IV.4.2.30 Shock Levels During Test No. 1

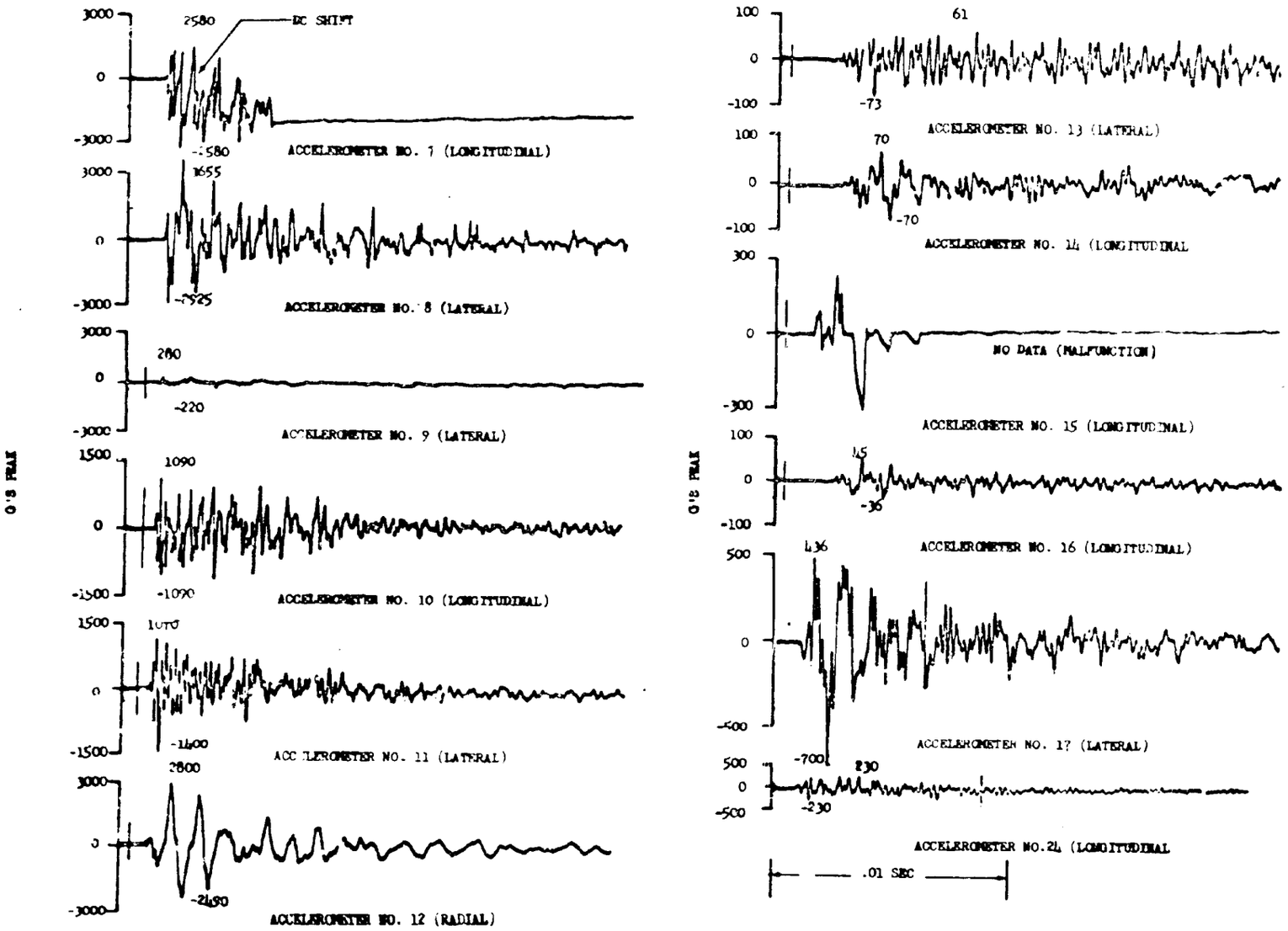

Figure II.A.2.31 Shock Levels From Test No. 2

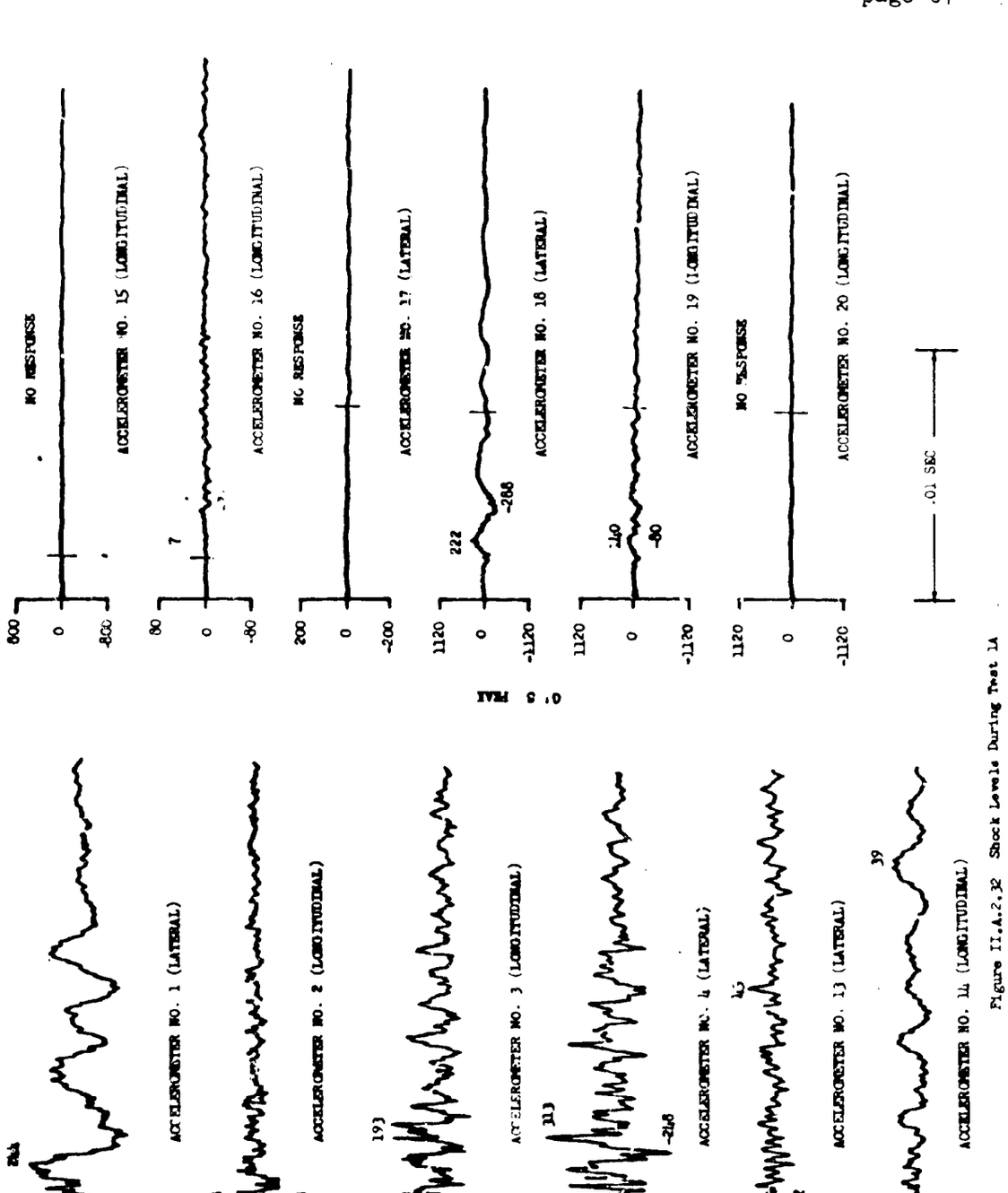

Figure II.A.2.32 Shock Levels During Test 14

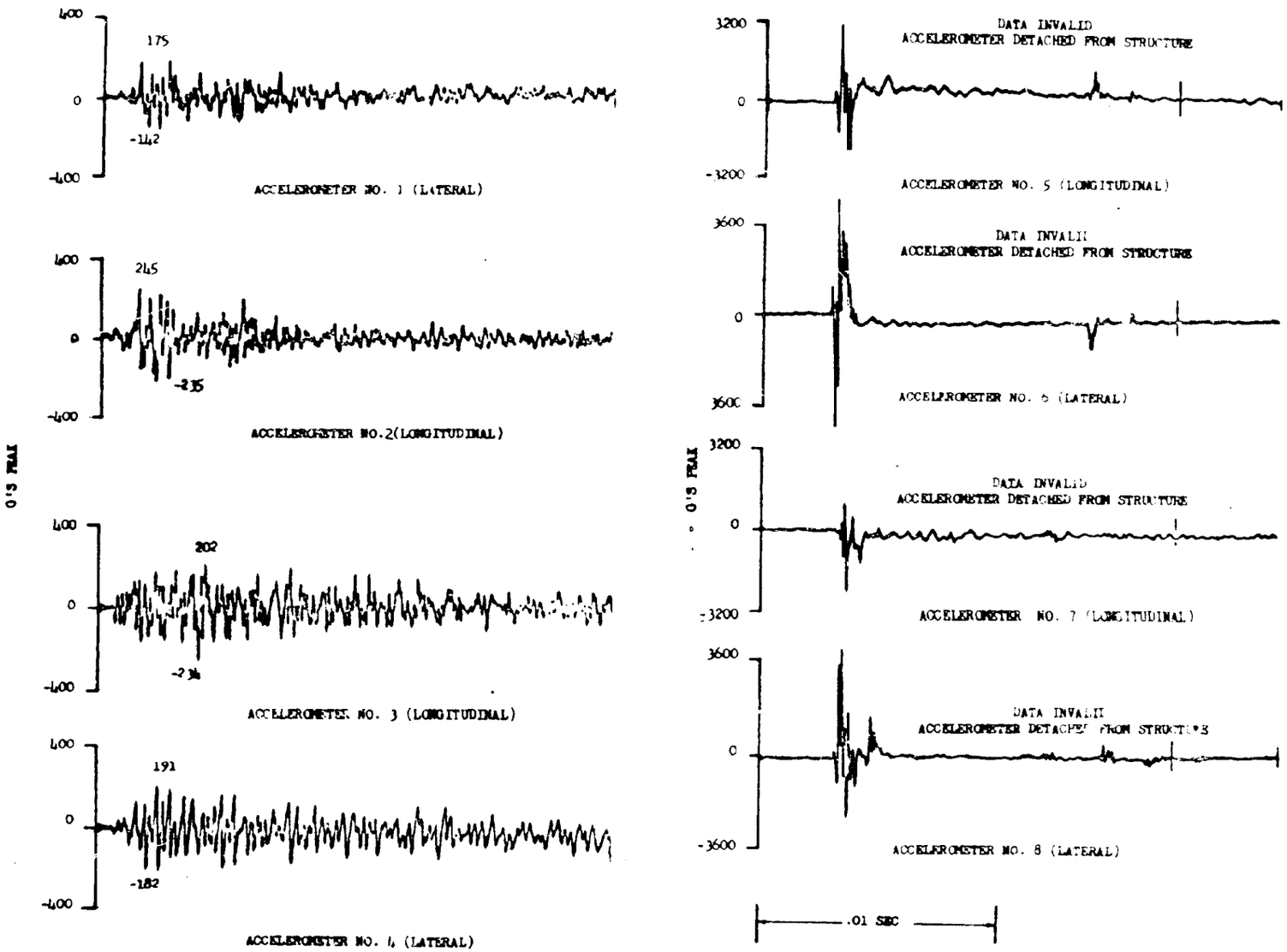

Figure II.A.2.33 Shock Levels During Test No. 2A

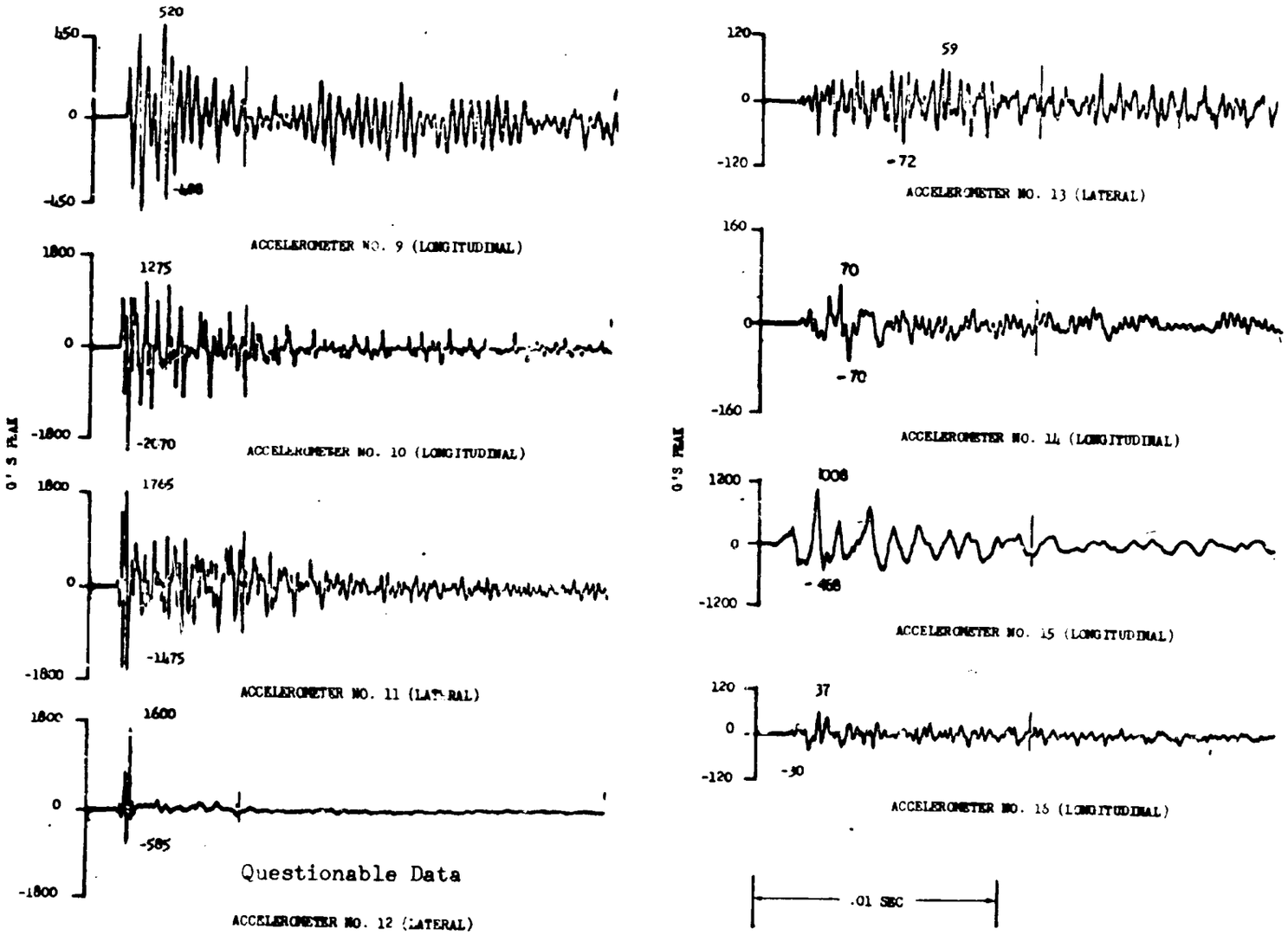

Figure II.A.2.34 Shock Levels During Test No. 2A

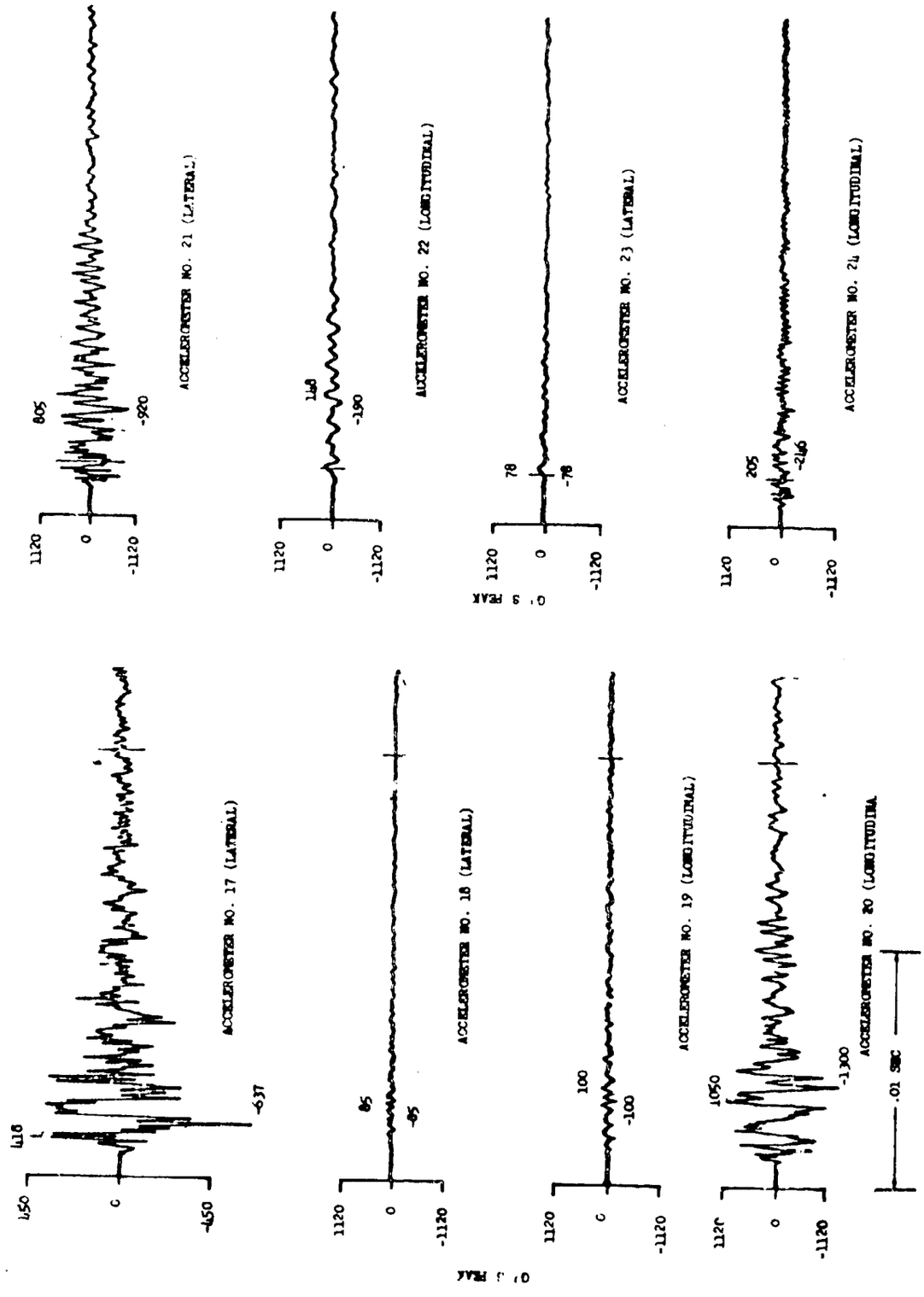

Figure II.A.2.35 Shock Levels During Test No. 2A

SECTION NO. II.A.3

REPORT NO. 768

SUBJECT:

EVALUATION OF DIFFERENT METHODS OF REDUCING PYROSHOCK ENVIRONMENT ON EQUIPMENT LOCATED NEAR SEPARATION JOINT

SECTION II.A.3

SUMMARY

A series of full ring booster adapter separation tests was conducted to evaluate methods of reducing the shock environment on vehicle equipment during the pyrotechnic separation of the booster adapter joint.

Two phases of testing were pursued. The first was a joint redesign investigation wherein the geometry of the existing separation joint was altered. The second was an evaluation of rubber shock isolators for equipment mounting.

During the joint redesign phase, reductions in shock levels by factors of from 1.52 to 2.68 (50th percentile values - see Table II.A.3.3) were noted with the greatest reduction achieved when the tang on the explosive housing ring was removed from the proximity of the lip on the engine cone casting (see Figure II.A.3.1, configurations 3 and 7). However, since the shock reduction factors were based on only one baseline firing with a standard joint, the shock reduction was insignificant when compared with the spread in shock levels which would occur were a representative sample of baseline tests conducted.

During the rubber shock isolator evaluation phase, 50th percentile reduction factors of all measurements, taken on isolated equipment, varied from 1.8 at 125 Hz to 7.4 at 500 Hz (Table II.A.3.4). This reduction was significant and a recommendation was made to evaluate several commercial isolators for possible use in isolation of shock sensitive equipment. During the test without shock isolators, measurements from the base of the bracket were compared to measurements from the base of equipment to determine the effectiveness of the normal mounting brackets in reducing the shock. Average bracket reduction factors ranged up to 9.5 at 800 Hz with an overall reduction over the frequency spectrum of 3.65.

TABLE OF CONTENTS

SECTION II.A.3

LIST OF TABLES

SECTION II.A.3

LIST OF FIGURES

SECTION II.A.3

LIST OF FIGURES (Cont.)

SECTION II.A.3

LIST OF FIGURES (Cont.)

SECTION II.A.3

II.A.3.1 INTRODUCTION

The ground rules for this series of tests was to find a means of reducing significantly the shock environment to which equipment was subjected during the pyrotechnic vehicle separation event by means of a simple fix which could have immediate application to a simple vehicle retro-fit.

The first eight tests were an attempt to reduce the shock by modifying the separation joint. Test 1 of the series was conducted with a standard joint. Tests 2 through 8 were then compared to Test 1.

Shock mounts were installed under five pieces of equipment in Test 9 in an attempt to reduce the booster separation shock loading. The shock mounts were removed in Test 10 and measurements made in the same locations as Test 9. The results of this test were compared to the results of Test 9 to determine the shock isolator effectiveness.

II.A.3.2 DISCUSSION AND ANALYSIS

II.A.3.2.1 Test Set-Up and Instrumentation

The test specimen consisted of an aft rack with only the equipment of interest mounted on it. A mock-up booster adapter housed the aft rack and attached at the booster adapter separation joint. The assembly was hung vertically in a test stand at SCTB and when the joint was fired, the booster adapter was allowed to free-fall. The fall was arrested by cables attached to the adapter.

In the first eight tests, various modifications of the standard separation joint were used to conduct a shock reduction study. The eight configurations are illustrated in Figure II.A.3.1. The location of the Endevco 2225 piezoelectric transducers for the first eight tests is shown in Figure II.A.3.2 and listed in Table II.A.3.1.

Tests 9 and 10 were a study of shock isolation by means of rubber shock isolators which were placed beneath the feet of selected equipment. The box locations on the engine thrust cone are illustrated in Figure II.A.3.3 along with accelerometer locations. More detailed drawings of the equipment and the accelerometer locations are included in Figure II.A.3.4 along with a typical shock isolator detail.

II.A.3.2.2 Analysis Methods

II.A.3.2.2.1 Joint Redesign Phase

The data from Tests 1 through 8 were analyzed by means of high speed oscillograph records of the accelerometer measurements. These oscillograms are included in Figures II.A.3.46 to II.A.3.52. The maximum 0 to peak g level was recorded from these oscillograms for each test for each of twelve measurements made on structure near the booster separation joint. The maximum g levels from Tests 2 through 8 were ratioed to Test 1 to obtain the shock reduction factors (Table II.A.3.3). These factors were then plotted on a log-normal probability grid for each test to determine the 50th percentile shock reduction (Figure II.A.3.5). The 50th percentile value represents the most probable value (not necessarily the average value) of shock reduction for that particular configuration.

II.A.3.2.2.2 Shock Isolator Phase

The data from Tests 9 and 10 were analyzed by means of high speed oscillograph records and shock spectra of the accelerometer measurements. The oscillograms and shock spectra are presented in Figures II.A.3.9 to II.A.3.45.

The shock isolator test series, Tests 9 and 10, were conducted to determine not only the shock reduction which could be realized by use of the isolators, but also to determine the shock reduction through the equipment mounting brackets alone.

The isolator reduction factors were determined for each 1/3 octave band beginning with the 90 to 112 Hz band by taking the ratio of the hard-mount equipment measurements (Test 10) to the soft-mount equipment measurements (Test 9). To compensate for the difference in shock levels between tests, the above ratio was multiplied by the ratio of the measurement taken at the base of the equipment during the soft-mount test to the measurement taken at the same location during the hard-mount test. These factors are presented in Table II.A.3.4. The ratios were then used to produce probability plots for each 1/3 octave band (Figure II.A.3.6). From these probability plots the 50th percentile values were selected which represented the most probable reduction factors. These factors are presented in Figure II.A.3.7 as a function of frequency.

To determine the shock reduction through the equipment mounting bracket for each 1/3 octave band, in the test without isolators the measurement taken from the base of the equipment bracket was ratioed to the measurement taken from the accelerometer at the base of the equipment which was oriented in the same direction as the accelerometer at the base of the equipment mounting bracket. The reduction factors which were obtained for each equipment were then averaged (Table II.A.3.5). The average reduction factors as a function of frequency for equipment brackets are presented in Figure II.A.3.8.

II.A.3.2.3 Test Conditions and Results

II.A.3.2.3.1 Joint Redesign Tests

Each of the joint configurations tested are illustrated in Figure II.A.3.1. Test results for Tests 1 through 7 are presented in Table II.A.3.3 as maximum 0 to peak g readings of the real time oscillograms. Also presented in this table are the shock reduction factors for Tests 2 through 7 based on the standard joint separation test levels of Test 1. No data were received from Test 8 due to a recording system malfunction.

Test 1

Test 1 used a standard separation joint to establish the base for determination of the shock reduction in the next seven tests in which the separation joint would be modified in an attempt to attenuate the shock.

The test was accomplished satisfactorily. Measuremsnts taken from this test were to be used as a base for determining the shock reduction in the next seven tests.

Test 2

For Test 2 the forward tang of the explosive housing ring was removed to check the effect that retention of the explosive housing ring would have on the shock level.

Test 2 resulted in a 1.52 shock reduction factor (50th percentile value). There appeared to be less attenuation in the shock levels in locations further removed from the separation joint than was observed in locations in relatively close proximity to the joint.

Test 3

The configuration tested during this shot was very similar to that of Test 2. The tang of the explosive housing ring was again removed but a back-up stiffener was added to determine if retention of the ring in this manner produced results comparable with the standard joint configuration.

The data from four of the accelerometers was lost. This reduced the confidence in the calculated reduction factors. The existing data indicated that the addition of the back-up stiffener reduced the shock levels by a 50th percentile factor of 2.30. However, it was noted that most of the data from the accelerometers located furthermost from the joint (the furthermost data indicated the least attenuation in Test 2) was lost. A point by point comparison of the available data from Test 3 with corresponding data of Test 2 indicated only a slight additional decrease in shock was obtained during Test 3 (see Table II.A.3.3).

Test 4

Five grain FLSC was installed in the standard joint configuration to compare the shock which originated from this charge with the usual 10 gr MDF. To obtain the proper separation distance for the FLSC it was necessary to notch the skin on the outside rather than on the inside.

The 50th percentile shock reduction factor for this test was 1.66. The shock reduction was attributed to the reduced explosive charge rather than to the cutting action of the FLSC since the FLSC and MDF both removed all the metal between the outermost notches in the adapter skin. The amount of shock reduction appeared to be independent of the distance from the separation joint since approximately the same reductions were noted on all accelerometers.

Test 5

Test 5 was conducted with the same separation joint as was used in baseline Test 1 with the exception that four different gas shields were added behind the explosive housing ring. This test was intended to check the results of Test 2.

The results of this test showed very close agreement with those of Test 2. The 50th percentile shock reduction factor was 1.89 while the Test 2 value was 1.52. The same trends were noticed in the Test 2 and Test 5 data.

Test 6

The Test 6 joint configuration differed from the standard joint in that the skin was pre-cut at the center groove. Tape was used to hold the sections together until detonation. This test was intended to determine the amount of shock produced by cutting the metal.

After detonation the joint was noted to have separated along the two outer notches in the same manner as the standard joint configuration. It was therefore impossible to evaluate the effect of the metal cutting during the test. However it is significant to note that since only a 1.71 50th percentile shock reduction factor was realized, the actual separation action was probably identical to the standard test. The test also showed that venting of the explosive gases will not reduce the shock environment.

Test 7

Contact between the explosive housing ring lip and the thrust cone casting was eliminated in Test 7 by moving the explosive housing ring 3/16 of an inch away from the retaining ring. The results of Test 7 were to be compared to Test 2 to determine if greater shock reduction could be obtained with this joint design.

This configuration produced the greatest shock reduction of any of the phase 1 configurations. A 50th percentile shock reduction factor of 2.68 was noted. The amount of shock reduction was also relatively independent of the distance of the measurement from the separation joint. Extensive cracking of the explosive housing ring was noted during this test. During Tests 2 and 3, no cracking was observed and only minor cracking occurred during Test 5. During Tests 2 and 3, no cracking was observed and only minor cracking occurred during Test 5. During Tests 2, 3 and 5 the housing ring made contact with the lip on the thrust cone casting and was therefore restrained enough so that extensive cracking did not occur. During Test 7 there was no possibility of such contact which would act as a restraint against cracking. The lower shock levels during Test 7 were probably a result of elimination of the contact between the housing ring and the thrust cone casting. Similar test results had been noted in the past.

Test 8

The primacord was placed directly on the skin and secured by masking tape. The purpose of this test was to check the effect of the explosive housing ring by comparing the results of this test to the standard joint results.

No data was received from Test 8 because of a recording system malfunction.

II.A.3.2.3.2 Shock Isolator Phase

Test 9

Test 9 was intended to determine the amount of shock reduction which was possible through the use of rubber shock isolators as well as the effectiveness of the brackets in reducing the shock. A typical equipment shock mount is illustrated in Figure II.A.3.4. The shock mounts were fabricated from 1/8 inch thick silicon rubber with a durometer rating of 40. This conforms to MIL-R-5847D. Thermal contact shrink tube, LAC 22-4025, Type 1 was placed on all mounting bolts to eliminate any metal to metal contact between equipment and structure by which shock could be transmitted. Five equipment boxes were shock mounted at various locations on the thrust cone. They were: an Aft Safe arm J-box, Flight Instrumentation J-box, Magnetometer, Auxiliary Timer, and the Flight Control Electronics package. A standard separation joint configuration was fired for this test.

Test 10

For Test 10 the shock isolation materials, rubber gromets, and shrink tubing were removed from the Test 9 configuration and the five boxes remounted in the conventional manner. As for Test 9, a standard separation joint was fired. The results of Test 10 would provide the standard shock levels to which the results of Test 9 could be compared to determine the effectiveness of the shock mounts and of the equipment brackets.

Results of Tests 9 and 10

It was immediately evident after visual inspection of the oscillograph records of the two tests that a substantial reduction of the shock had been obtained with the shock isolators. A comparison based on shock spectra of the shock measurements indicated a maximum 50th percentile reduction factor of 7.4 at 500 Hz (Figure II.A.3.7) for all brackets from which measurements were taken. The average reduction over the 100 to 10,000 Hz range was 3.2 based on the 50th percentile values.

A comparison of the shock spectra of measurements taken at the base of the equipment mounting brackets and measurements taken at the equipment base during Test 10 indicated average shock reduction factors of up to 9.5 at 800 Hz with an overall average shock reduction factor over the 100 to 10,000 Hz range of 3.65.

II.A.3.3 CONCLUSIONS

1. Data which came from tests in which the explosive housing tang was eliminated showed a general reduction in the shock environment.

2. Best results were obtained in Test 7 when the tang was moved away from the retaining lip. A 50th percentile shock reduction factor of 2.68 was noted for this test. This factor is based on the maximum 0 to peak g level from real time oscillographs of all accelerometers.

3. In general the shock reduction from the joint redesign phase of testing was insignificant when compared with the spread in shock levels which would occur were a representative sample of baseline firings conducted. Thus none of the redesigns produced a separation joint which would be worthwhile incorporating into future vehicles.

4. The use of shock isolators for equipment proved to be effective in lessening the equipment shock environment by reducing the shock by a factor of 7.4 (50th percentile value) at 500 Hz and on an overall average by a factor of 3.2 over the entire frequency spectrum of analysis. These factors were based on measurements taken at the base of equipments before and after shock mounting.

5. Equipment brackets contributed significantly themselves to reducing the shock levels. Average shock reduction factors of up to 9.5 (at 800 Hz) were noted with an overall average reduction factor of 3.65 over the entire analysis frequency spectrum. (The isolator reduction was in addition to this although the factors are not additive.)

6. It was recommended that several commercially available isolators be evaluated for possible use in isolation of shock sensitive instruments.

FORM LMSC 67072

TABLE II.A.3.1

ACCELEROMETERS AND LOCATIONS

Tests	1 to 8					9 and 10			
Accel. No.	Quad.	Sta. (in.)	Direction	Distance to Shock Source (inches)	Accel. Type	Box	Direction	Location	Distance to Shock Source (inches)
1					Endevco 2225	Aft Safe Arm-J-Box	R	Frame	18.5
2					Endevco 2225	Aft Safe Arm-J-Box	R	Box	18.5
3	II	390	R	6	Endevco 2225	Aft Safe Arm-J-Box	L	Box	18.5
4	II	390	T	6	Endevco 2225	Flt. Inst. J-Box	R	Frame	18.5
5	II	390	L	6	Endevco 2225	Flt. Inst. J-Box	R	Box	18.5
6	II	390	T	6	Endevco 2225	Flt. Inst. J-Box	L	Box	18.5
7	IV	396	T	12	Endevco 2225	Magnetometer	R	Frame	18.5
8	IV	396	L*	12	Endevco 2225	Magnetometer	R	Box	18.5
9					Endevco 2225	Magnetometer	L	Box	18.5
10	II	412	L	28	Endevco 2225	Aux. Timer	R	Frame	24.0
11	II	412	R	28	Endevco 2225	Aux. Timer	R	Box	24.0
12	I	396.5	R	12.5	Endevco 2225	Aux. Timer	L	Box	24.0
13					Endevco 2225	Flt. Control Electron.	R	Frame	25.0
14					Endevco 2225	Flt. Control Electron.	L	Box	25.0
15	III	396.5	R	12.5	Endevco 2225	Flt. Control Electron.	R	Box	25.0
20	IV	412	L	28	Endevco 2225				
21	IV	412	T	28	Endevco 2225				

* Radial for Tests 1 to 4

TABLE II.A.3.2

SUMMARY OF TESTS

Test Number	Separation Joint Configuration	Explosive Size	Test Purpose	Shock Isolation
1	1	10 Gr. MDF	Structure	No
2	2	10 Gr. MDF	Structure	No
3	3	10 Gr. MDF	Structure	No
4	4	5 Gr. FLSC	Structure	No
5	5	10 Gr. MDF	Structure	No
6	6	10 Gr. MDF	Structure	No
7	7	10 Gr. MDF	Structure	No
8*	8	10 Gr. MDF	Structure	No
9	1	10 Gr. MDF	Box Qual.	Yes
10	1	10 Gr. MDF	Box Qual.	No

* All Data Lost

TABLE II.A.3.3

PEAK G AND REDUCTION FACTORS OVER TEST 1 BASELINE

ACCEL. NO.	TEST 1	TEST 2		TEST 3		TEST 4		TEST 5		TEST 6		TEST 7	
	PEAK G	PEAK G	RED. FACT.	PEAK G	RED. FACT.	PEAK G	RED. FACT.	PEAK G	RED. FACT.	PEAK G	RED. FACT.	PEAK G	RED. FACT.
V 3	2000	600	3.34	600	3.34	1200	1.67	1000	2.00	1500	1.33	540	3.71
V 4	5100	3000	1.70	2180	2.34	2450	2.08	2500	2.04	3150	1.62	2000	2.65
V 5	1400	1000	1.40	890	1.57	1000	1.40	800	1.75	1100	1.27	350	4.00
V 6	1300	600	2.17	no data	----	800	1.63	500	2.60	800	1.63	350	3.71
V 7	1850	1900	.98	990	1.87	1500	1.23	1300	1.42	1100	1.68	1150	1.61
V 8	4100	1450	2.83	990	4.15	2500	1.64	1000	4.10	1050	3.90	850	4.82
V 10	1200	1200	1.00	560	2.14	900	1.33	1260	.95	450	2.67	600	2.00
V 11	1200	no data	----	760	1.58	600	2.00	480	2.50	540	2.22	660	1.82
V 12	no data	700	----	560	----	550	----	800	----	600	----	600	----
V 15	1400	1450	.97	no data	----	550	2.50	850	1.65	750	1.87	D.C. Shift	----
V 20	1200	1380	.87	no data	----	840	1.43	1200	1.00	1850	.65	900	1.33
V 21	no data	no data	----	no data	----	600	----	540	----	480	----	570	----
50th Percentile Reduction Factors			1.52		2.30		1.68		1.89		1.71		2.68

TABLE II.A.3.4

SHOCK ISOLATOR REDUCTION FACTORS

ACCEL. NO. / 1/3 OCT. BAND C.F.	2	3	5	6	8	9	14	15	50th PERCENTILE REDUCTION FACTORS
100	1.78	1.45	1.61	1.02	10.97	3.01		2.00	1.9
125	2.25	1.63	1.65	0.96	9.14	2.78		1.04	1.8
160	3.15	3.54	2.64	2.09	3.85	3.09		0.80	2.8
200	3.77	4.23	2.70	2.25	8.80	6.05		0.75	3.6
250	3.11	4.75	3.13	3.25	15.27	4.28	BAD DATA	0.41	3.7
320	3.35	2.67	5.69	5.59	9.16	2.36		0.27	3.7
400	3.21	2.68	2.90	10.11	10.48	6.67		1.02	4.3
500	4.60	6.24	4.11	17.63	10.64	25.90		1.73	7.4
630	2.74	6.08	2.71	12.40	13.78	11.62		1.24	5.2
800	1.99	2.18	1.34	4.17	3.77	1.87		0.63	2.0
1000	7.00	1.56	2.05	6.59	6.58	1.35		0.27	2.8
1250	4.07	1.17	1.82	6.47	3.68	2.12	1.24	0.69	2.3
1600	5.04	2.61	2.56	3.85	9.59	1.26	1.40	0.84	2.6
2000	3.90	1.38	3.06	3.40	3.18	1.48	1.01	1.71	2.2
2500	6.86	3.36	1.80	1.98	4.51	1.37	1.83	1.01	2.35
3200	9.06	2.31	3.59	1.40	5.28	3.94	2.12	1.00	3.0
4000	6.53	2.71	1.21	1.79	1.39	2.99	1.96	1.05	2.1
5000	2.81	3.17	8.23	7.93	3.59	5.93	1.23	0.98	3.4
6300	7.53	4.04	4.99	7.61	2.63	4.37	1.90	1.84	3.9
8000	1.99	1.56	3.81	3.53	4.63	4.66	1.35	1.63	2.6
									AVERAGE = 3.2

TABLE II.A.3.5

EQUIPMENT MOUNTING BRACKET REDUCTION FACTORS

ACCEL. NO. / 1/3 OCT. BAND C.F.	2	5	8	14	Total	Ave.
100	3.90	.69	.42		5.01	1.67
125	3.43	.94	.39		4.76	1.59
160	2.18	.94	.45		3.57	1.19
200	1.45	.97	.46		2.88	0.96
250	1.29	1.34	.30		2.93	0.98
320	2.32	.89	.25		3.46	1.15
400	2.57	1.55	.38		4.50	1.50
500	1.51	2.70	.68		4.89	1.63
630	1.84	5.61	.79		8.24	2.75
800	4.37	22.86	1.22		28.45	9.48
1000	4.88	18.11	1.73		24.72	8.24
1250	2.94	7.08	1.85	13.80	25.67	6.42
1600	2.85	7.22	.60	13.90	24.57	6.14
2000	3.84	5.60	1.62	15.60	26.66	6.67
2500	2.80	6.94	.80	15.90	26.44	6.61
3200	2.47	3.18	.71	12.60	18.96	4.74
4000	2.53	7.22	.78	6.07	16.60	4.15
5000	3.43	2.23	.78	6.68	13.12	3.28
6300	1.72	2.43	.94	2.51	7.60	1.90
8000	2.11	2.59	.42	2.34	7.46	1.87
					Average =	3.65

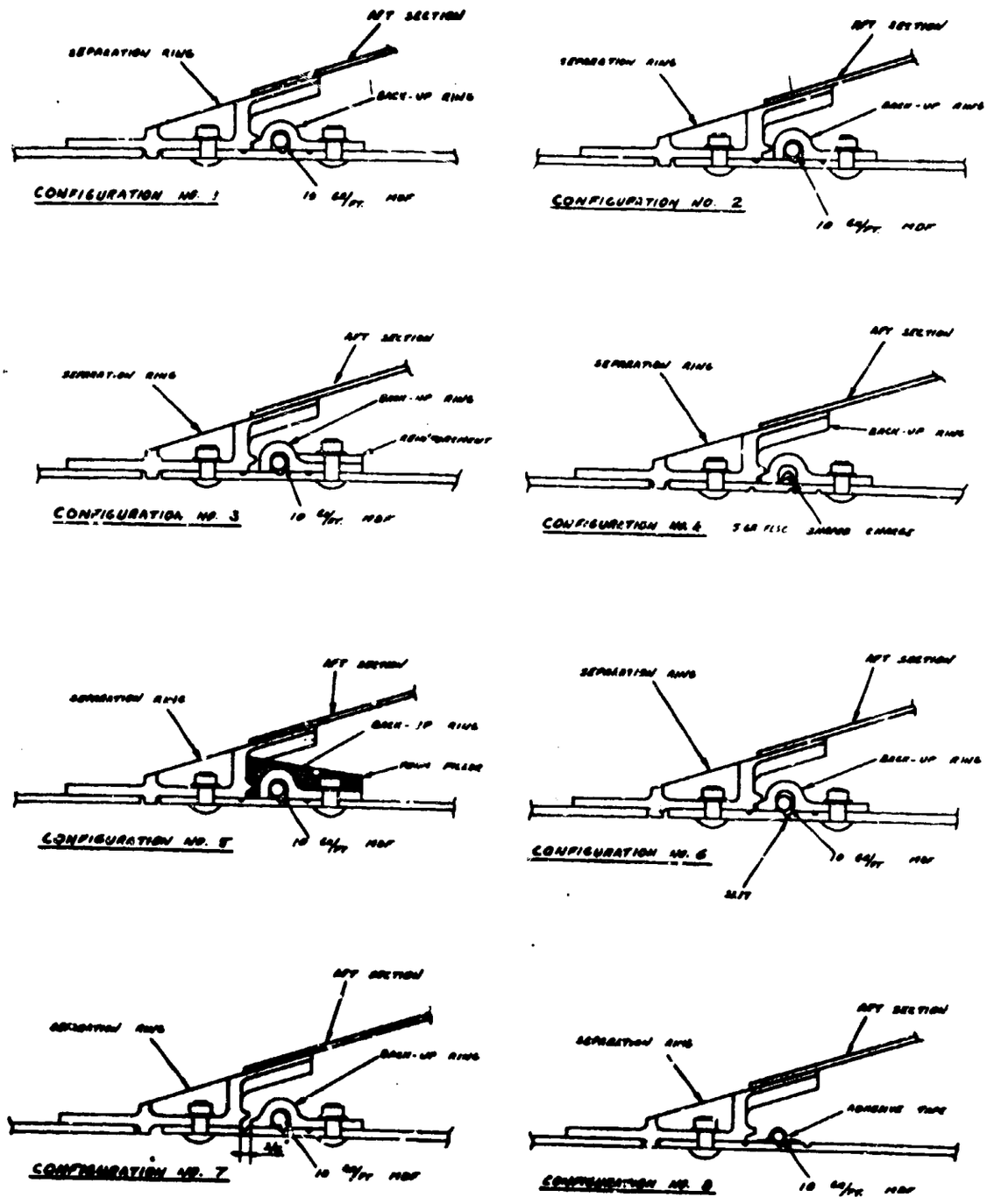

Figure II.A.3.1 SEPARATION JOINT DETAILS

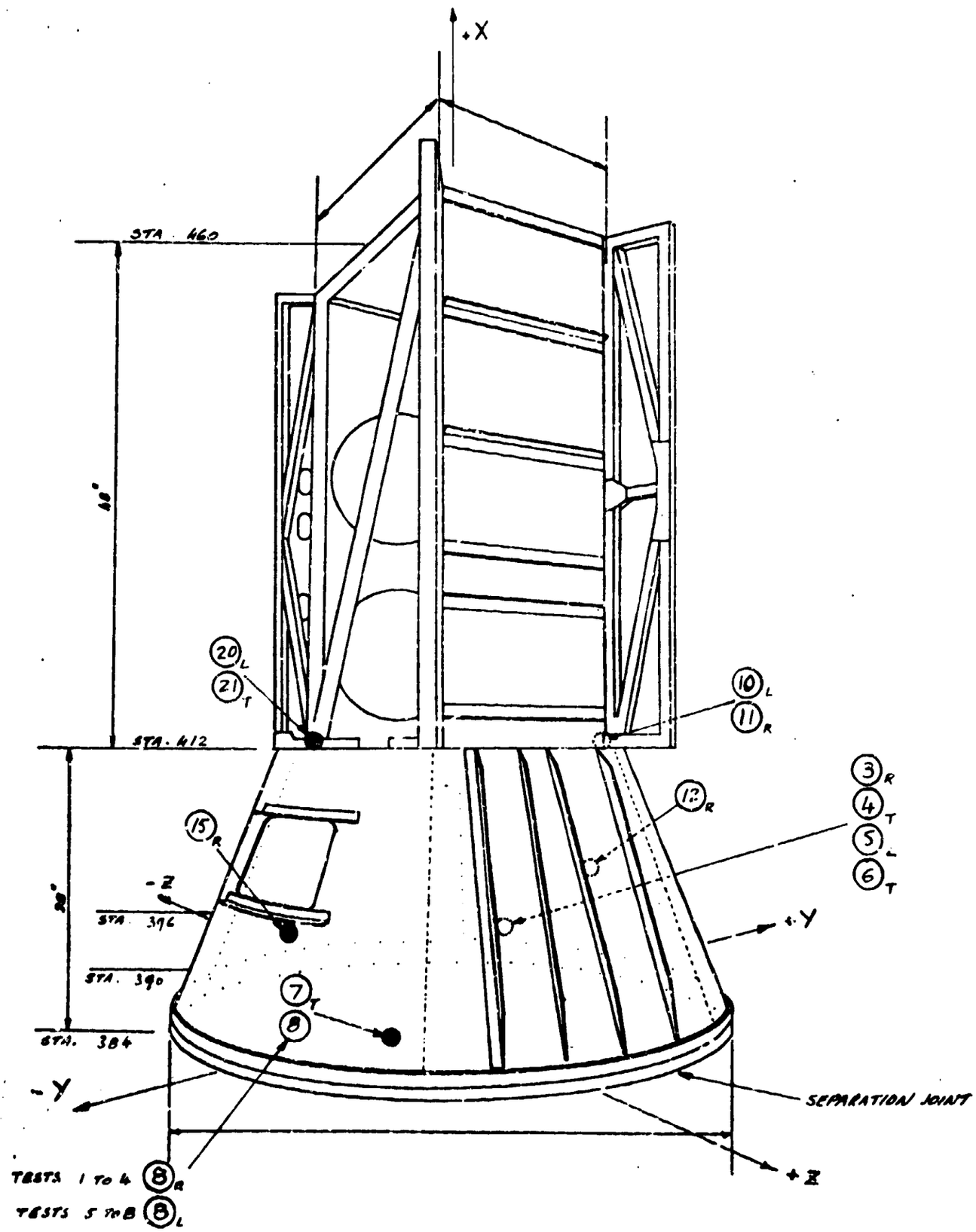

Figure II.A.3.2 TEST CONFIGURATION AND ACCELEROMETER LOCATIONS, TESTS 1 TO 8

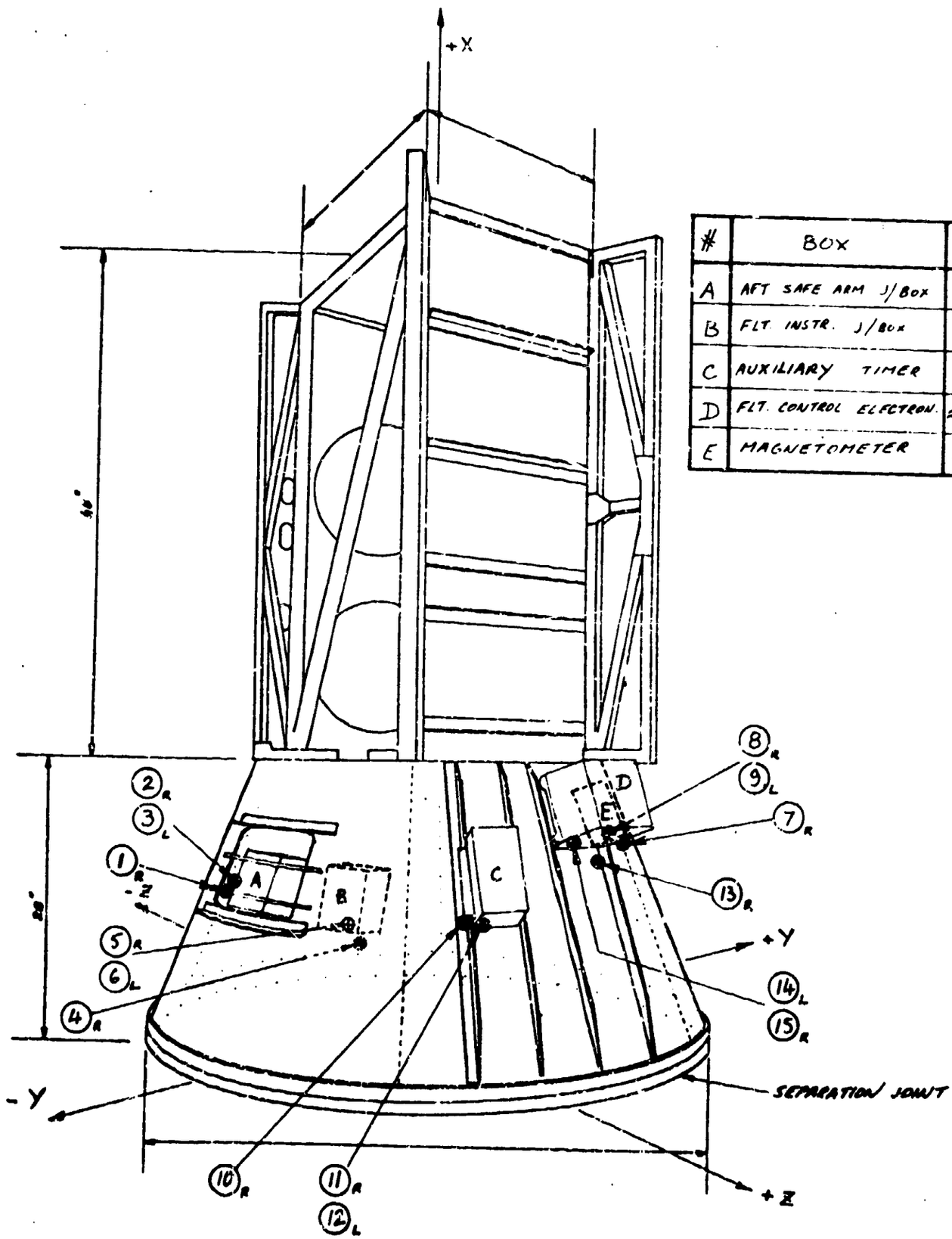

#	BOX	WT. LB.
A	AFT SAFE ARM J/BOX	4.5
B	FLT. INSTR. J/BOX	3.6
C	AUXILIARY TIMER	4.5
D	FLT. CONTROL ELECTRON.	≈ 10
E	MAGNETOMETER	2.0

Figure II.A.3.3 TEST CONFIGURATION AND ACCELEROMETER LOCATIONS, TESTS 9 and 10

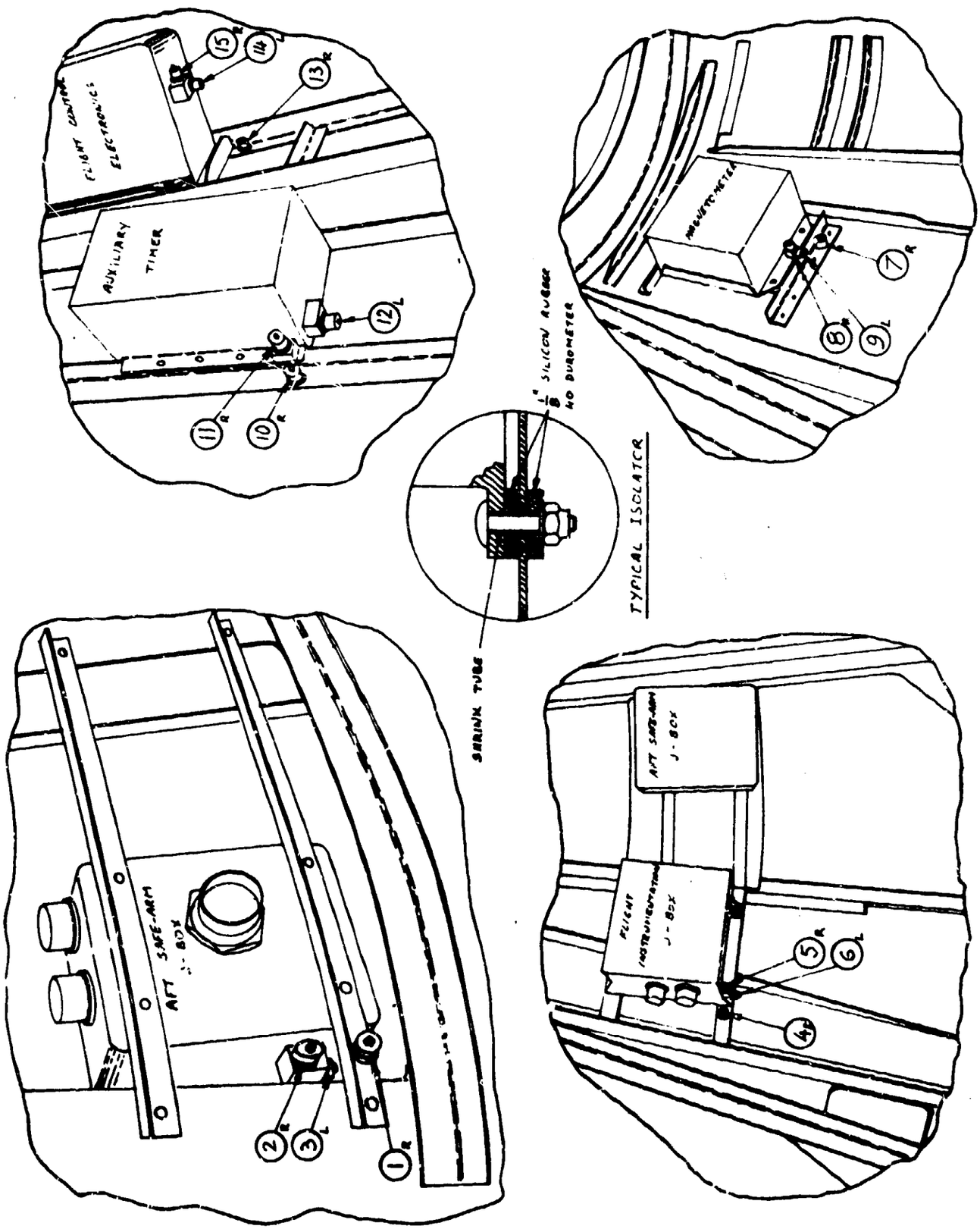

Figure II.A.3.4 DETAIL OF ACCELEROMETER LOCATIONS ON EQUIPMENT AND A TYPICAL ISOLATOR

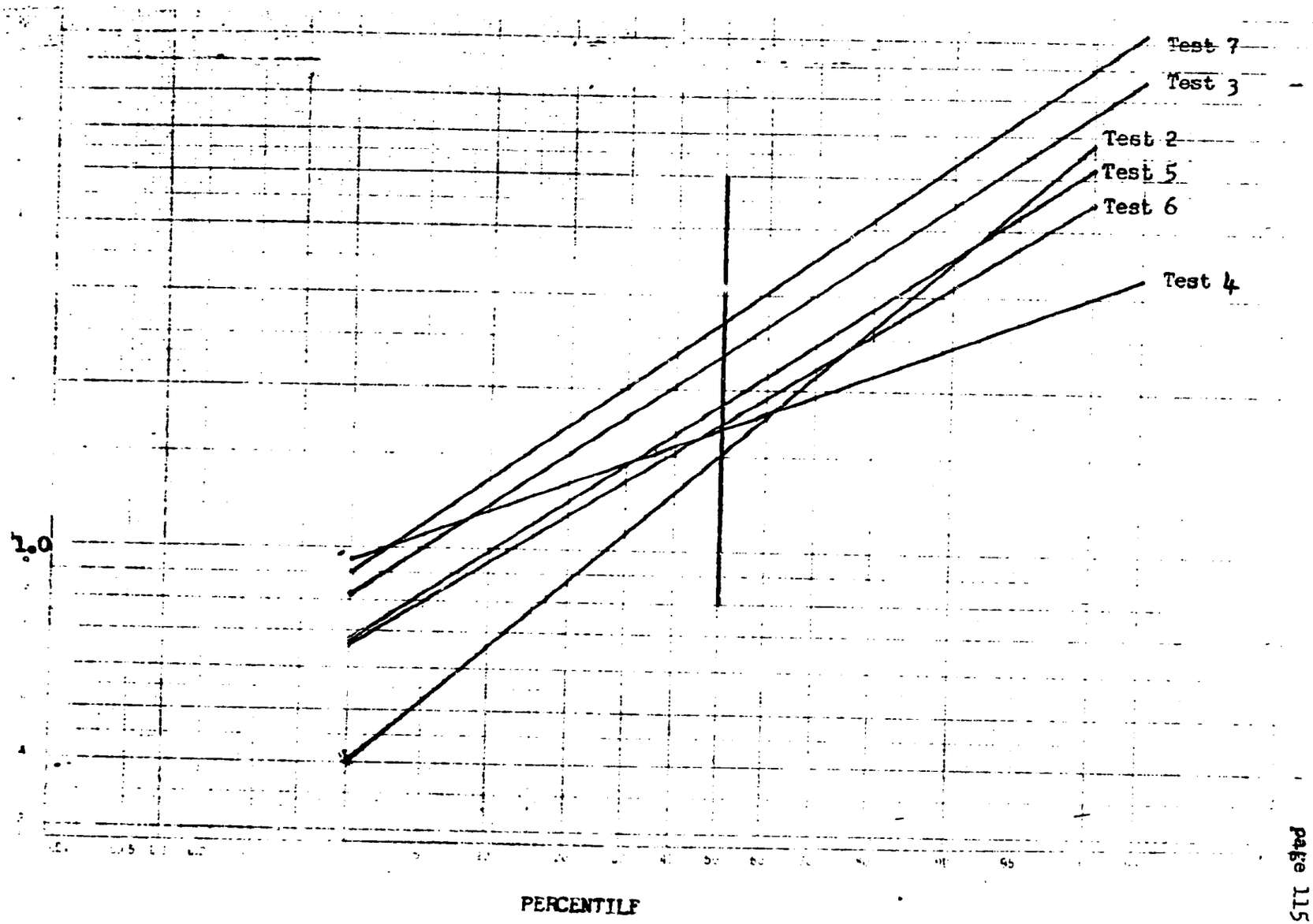

SHOCK REDUCTION FACTOR

Figure II.A.3.5 DERIVATION OF 50TH PERCENTILE SEPARATION JOINT REDUCTION FACTORS, TESTS 2 TO 7

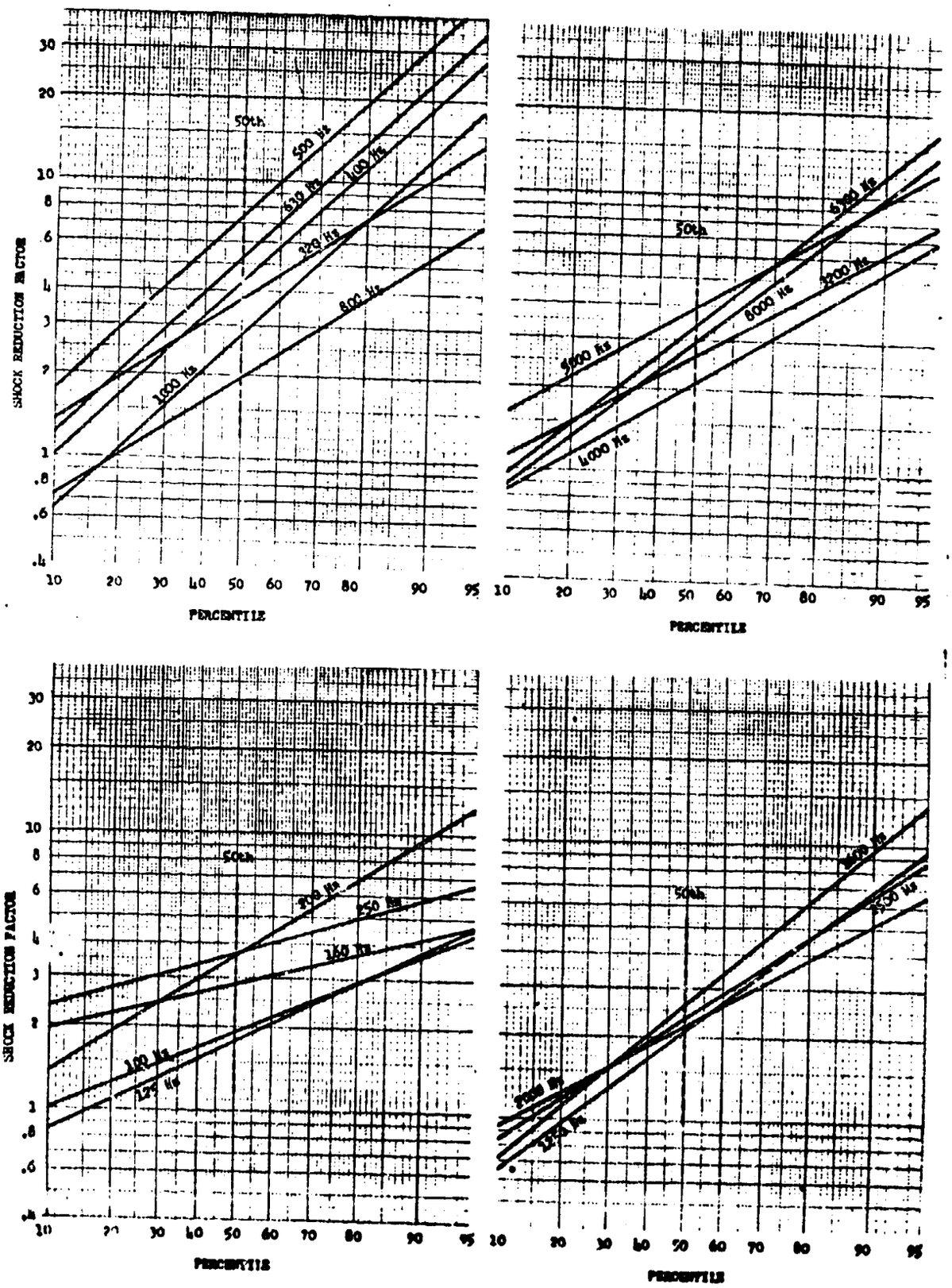

Figure II.A.3.6 DERIVATION OF 50TH PERCENTILE ISOLATOR REDUCTION FACTORS, TESTS 9 AND 10

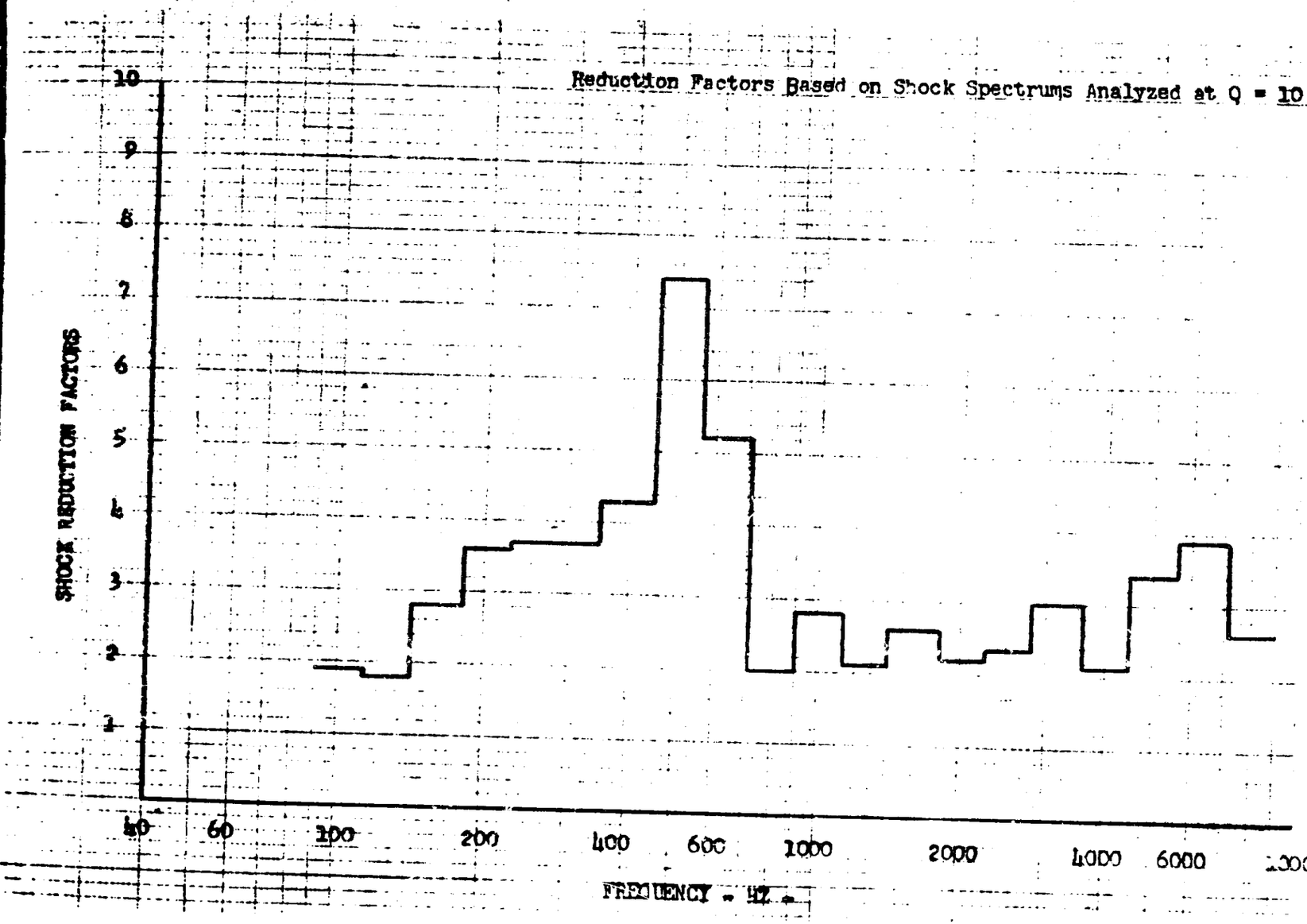

Figure II.A.3.7 50TH PERCENTILE SHOCK ISOLATOR REDUCTION FACTORS

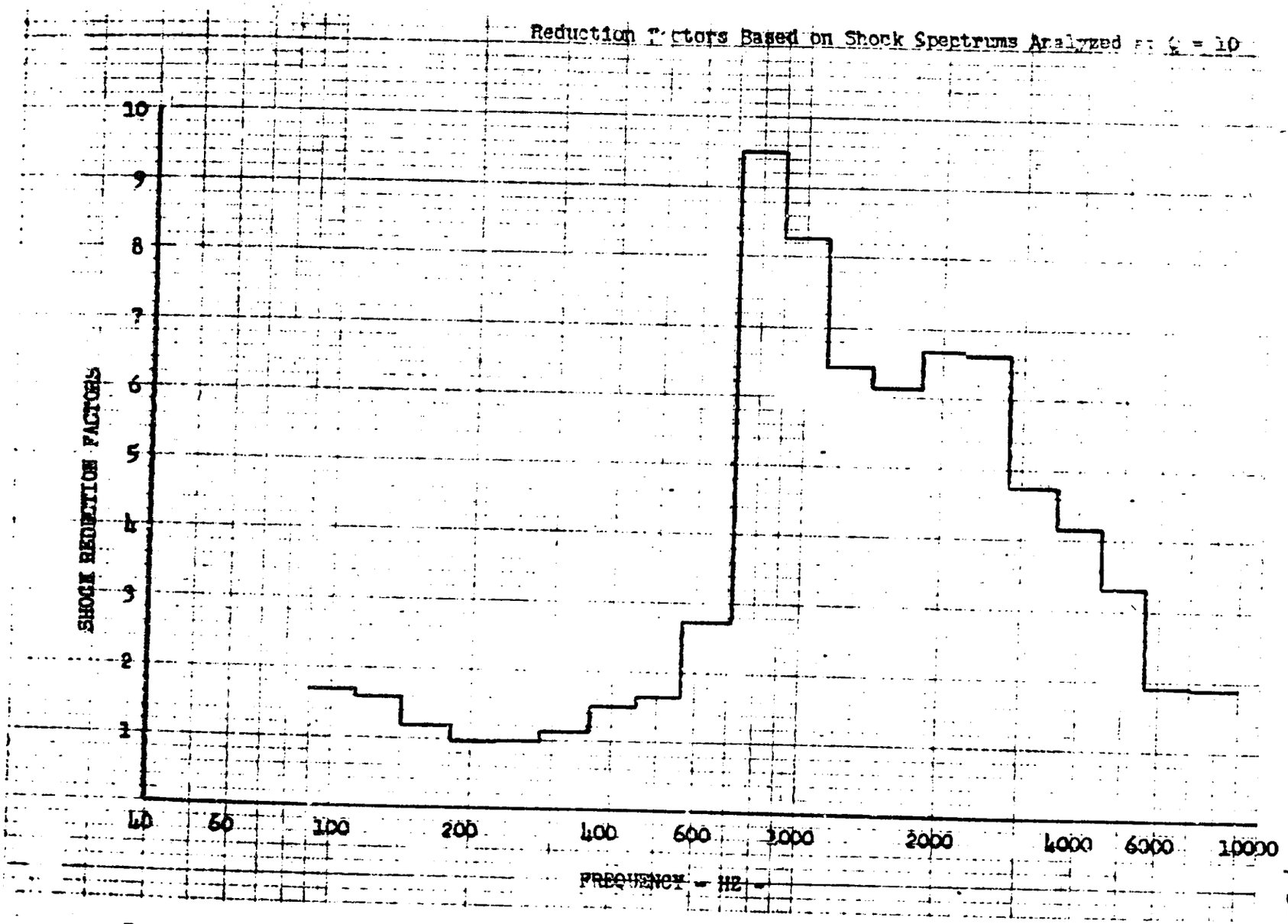

Figure II.A.3.8 AVERAGE EQUIPMENT MOUNTING BRACKET REDUCTION FACTORS

SHOCK TEST ANALYSIS DATA SHEET II.A.3.9

TEST ITEM 768-241
SERIAL NO. 1
SHOCK AXIS Radial

PART NO. Box A Frame
TEST DATE 25 May 1964
SHOCK NO. 9

RESPONSE G-S

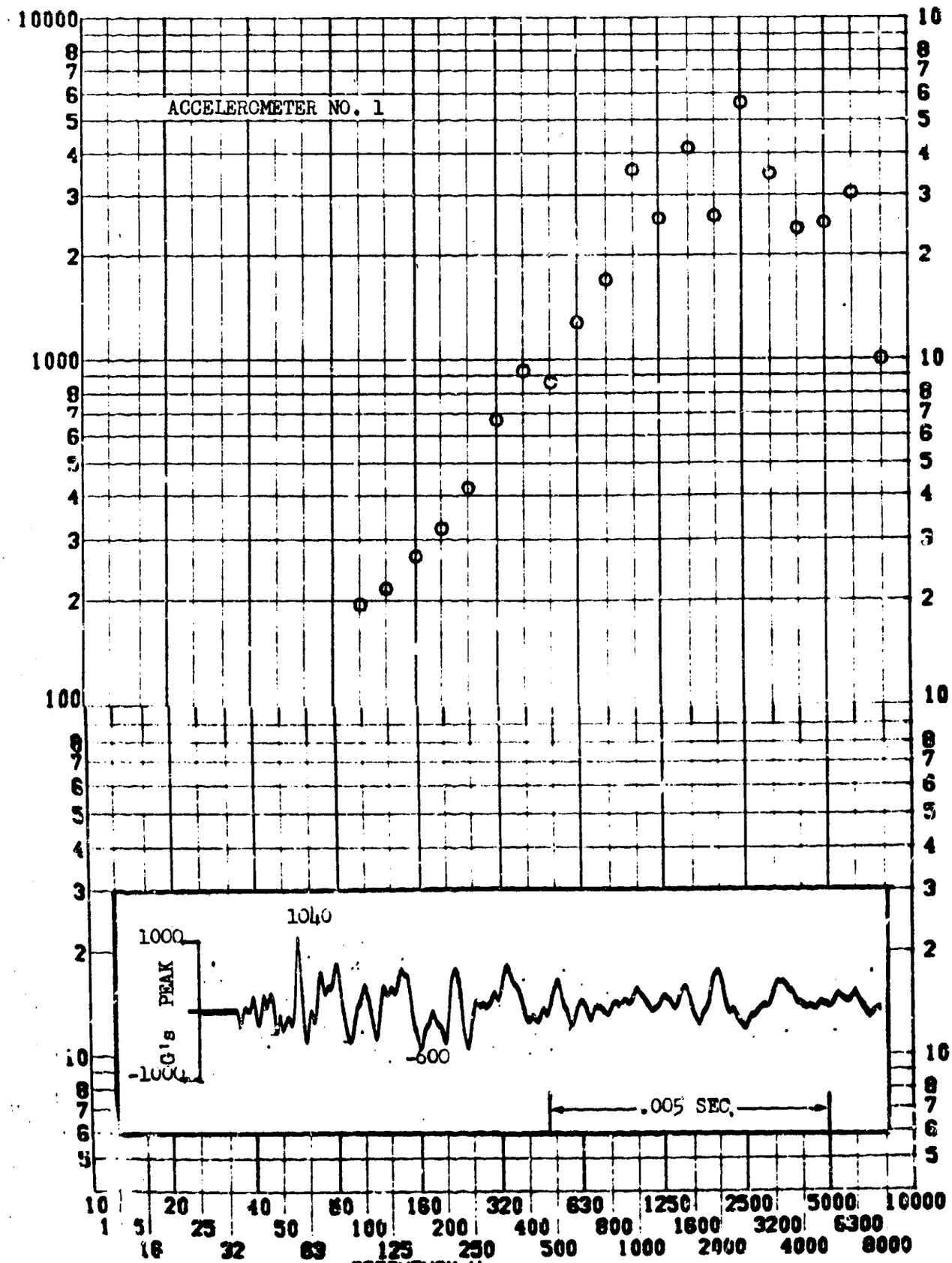

SHOCK TEST ANALYSIS DATA SHEET II.A.3.10

TEST ITEM 768-243
SERIAL NO. 2
SHOCK AXIS Radial

PART NO. Box A
TEST DATE 25 May 1964
SHOCK NO. 9

RESPONSE G-S

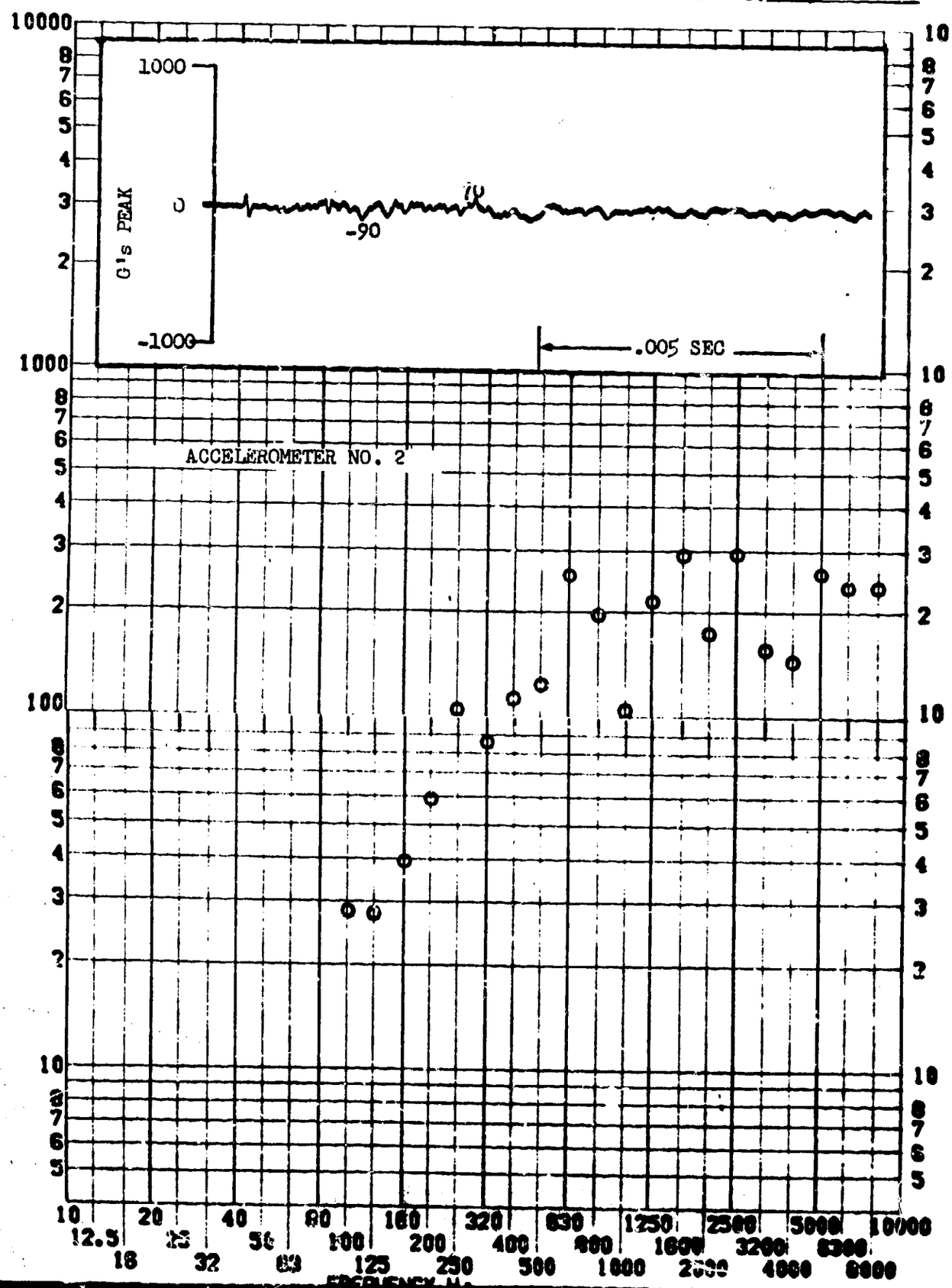

SHOCK TEST ANALYSIS DATA SHEET II.A.3.11

TEST ITEM 768-245
SERIAL NO. 3
SHOCK AXIS Long

PART NO. Box A
TEST DATE 25 May 1964
SHOCK NO. 9

RESPONSE G-S

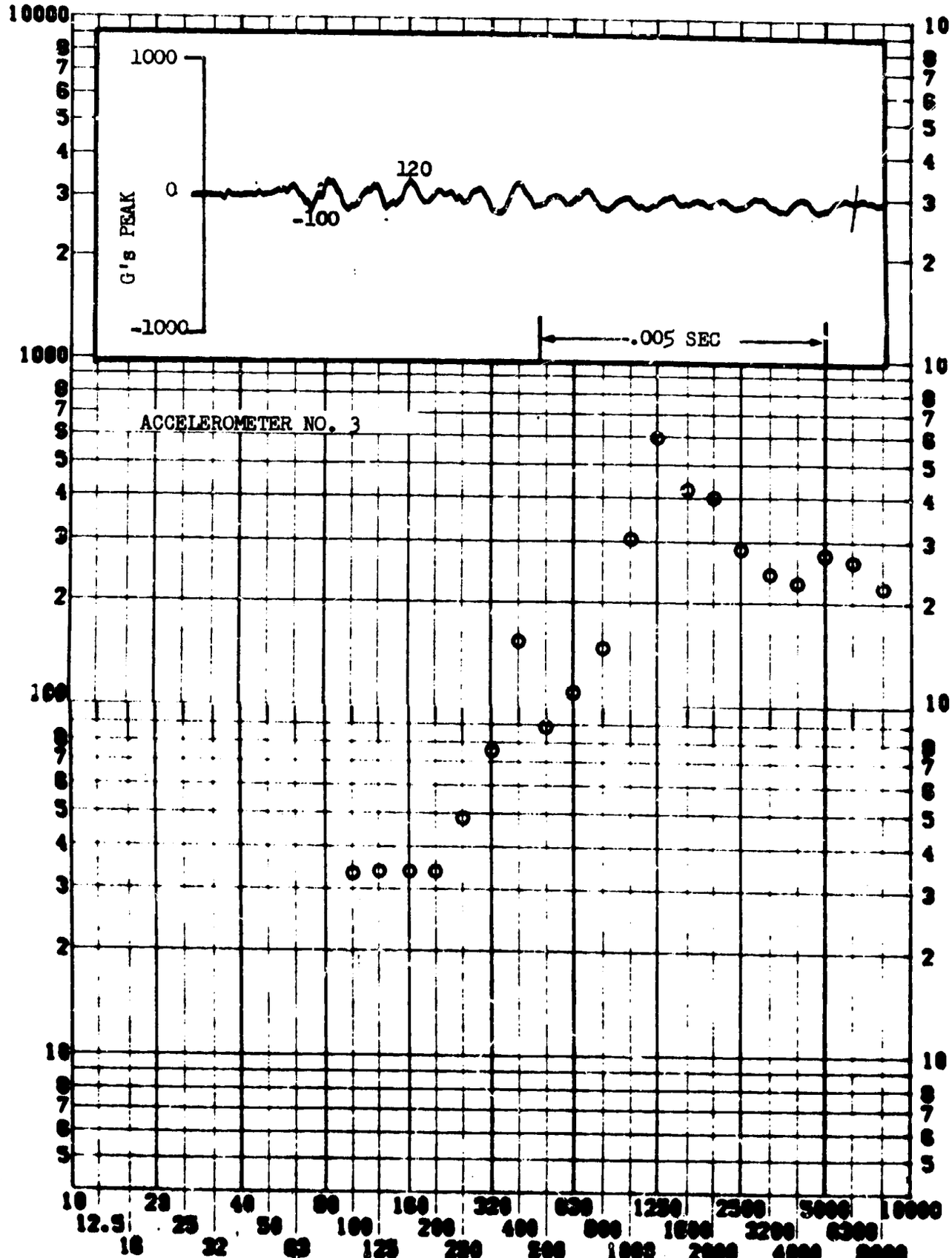

SHOCK TEST ANALYSIS DATA SHEET II.A.3.12

TEST ITEM 768-247
SERIAL NO. 4
SHOCK AXIS Radial

PART NO. Box B Frame
TEST DATE 25 May 1964
SHOCK NO. 9

RESPONSE G-S

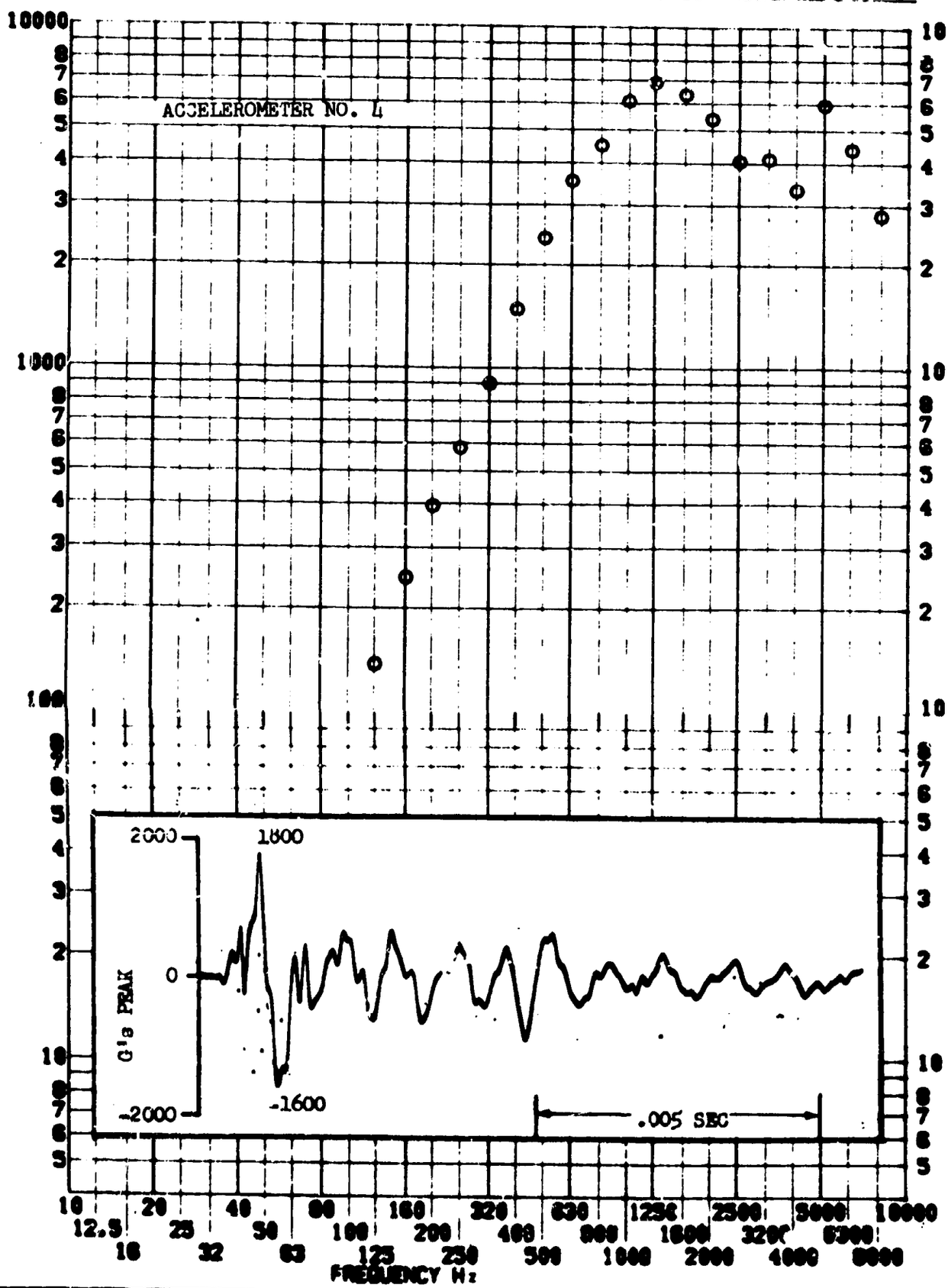

SHOCK TEST ANALYSIS DATA SHEET II.A.3.13

TEST ITEM 768-249
SERIAL NO. 5
SHOCK AXIS Radial

PART NO. Box B
TEST DATE 25 May 1964
SHOCK NO. 9

RESPONSE G-S

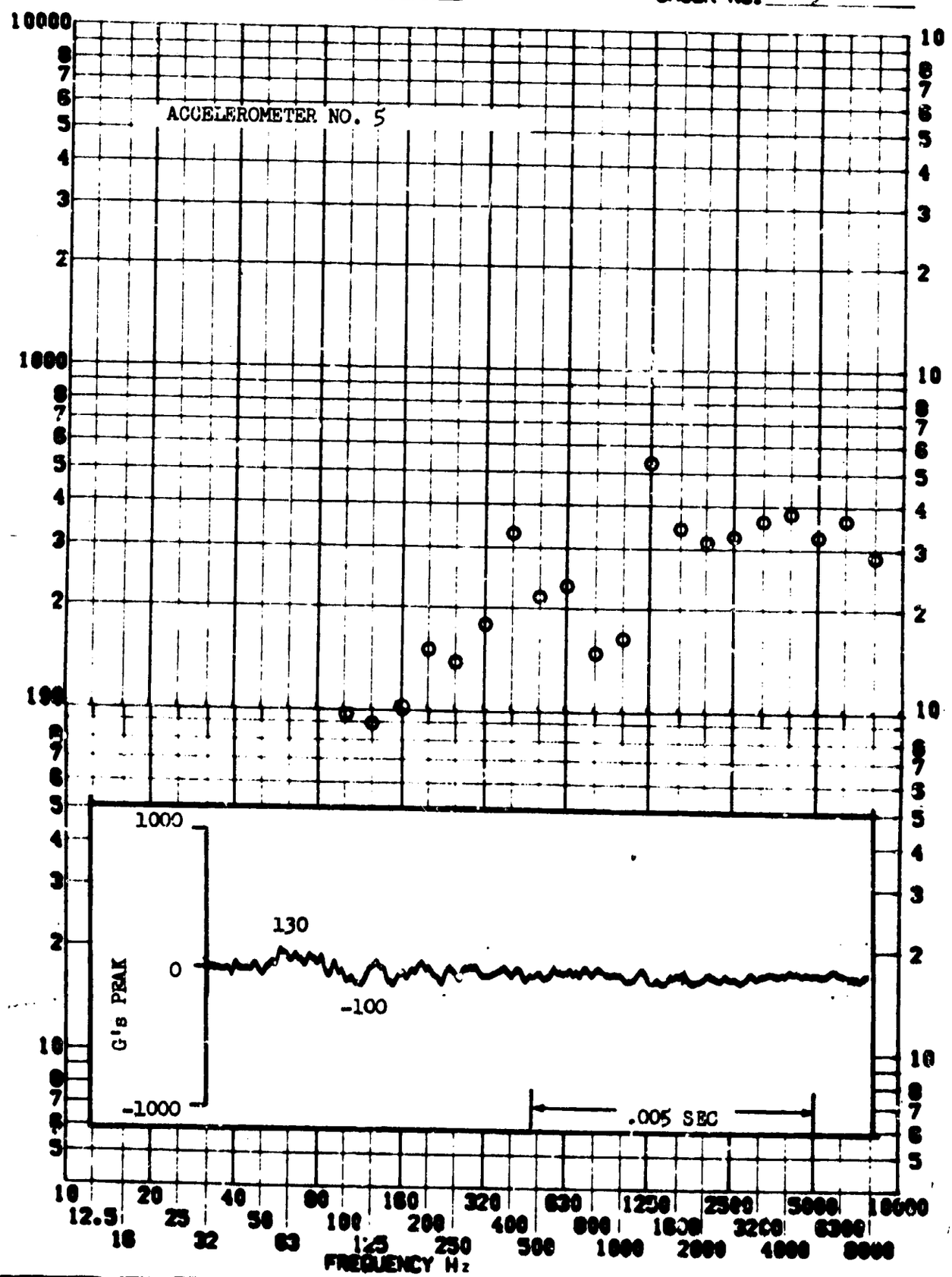

SHOCK TEST ANALYSIS DATA SHEET II.A.3.14

TEST ITEM 768-251
SERIAL NO. 6
SHOCK AXIS Long

PART NO. Box B
TEST DATE 25 May 1964
SHOCK NO. 9

RESPONSE G-S

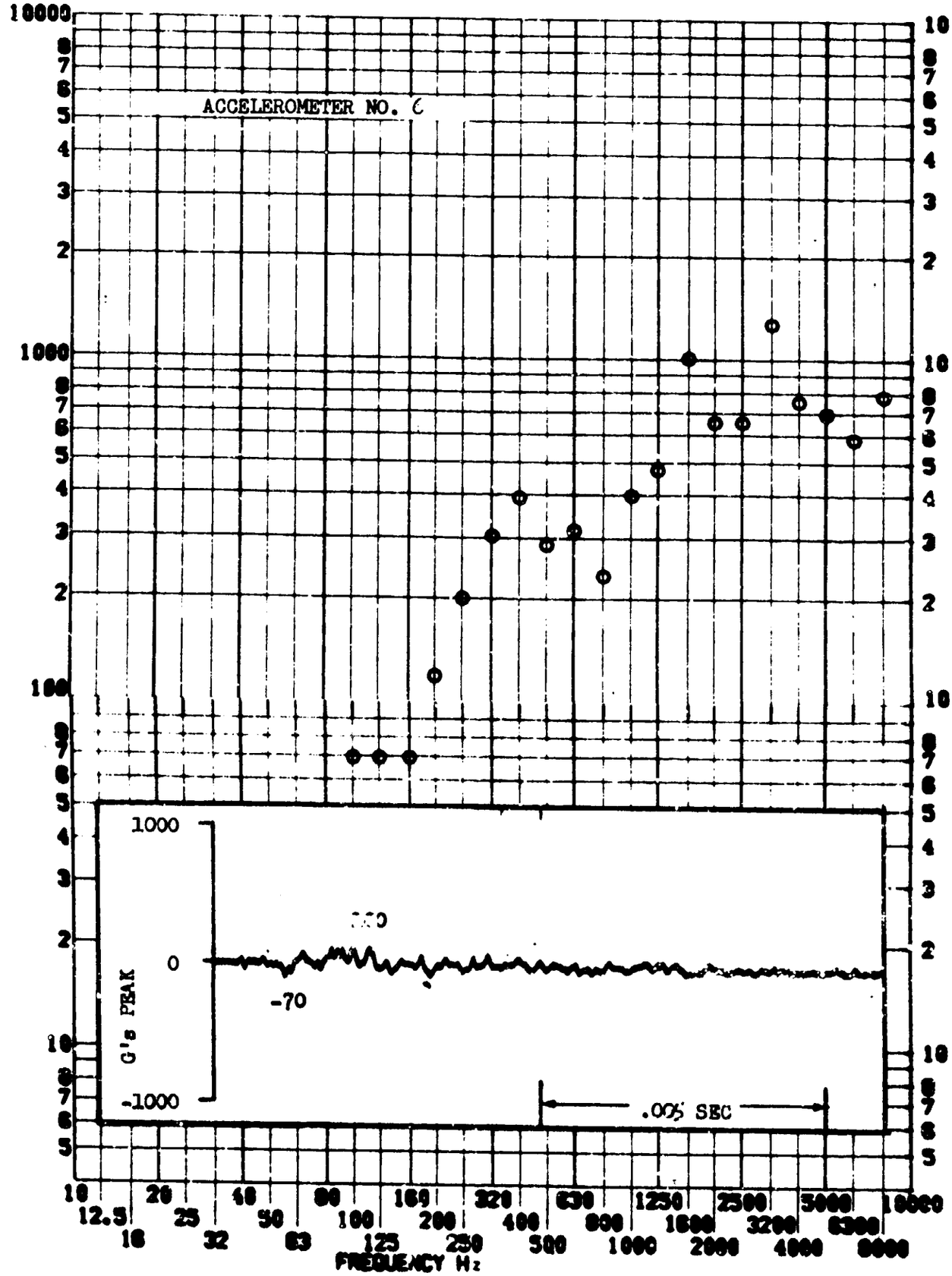

SHOCK TEST ANALYSIS DATA SHEET II.A.3.15

TEST ITEM 768-253
SERIAL NO. 7
SHOCK AXIS Radial

PART NO. Box B Frame
TEST DATE 25 May 1964
SHOCK NO. 9

RESPONSE G-S

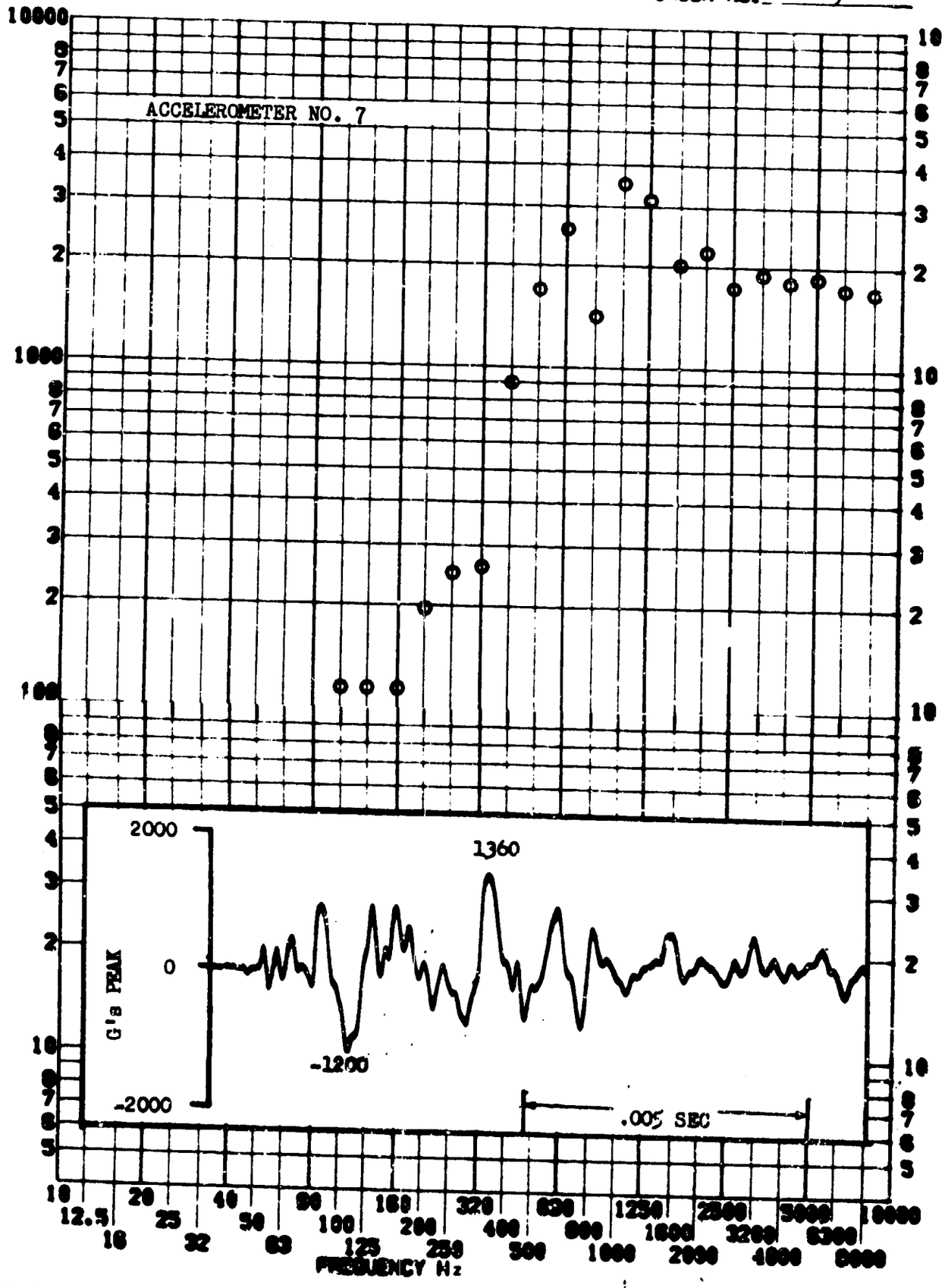

SHOCK TEST ANALYSIS DATA SHEET II.A.3.16

TEST ITEM 768-255
SERIAL NO. 8
SHOCK AXIS Radial

PART NO. Box E
TEST DATE 25 May 1964
SHOCK NO. 9

RESPONSE G-S

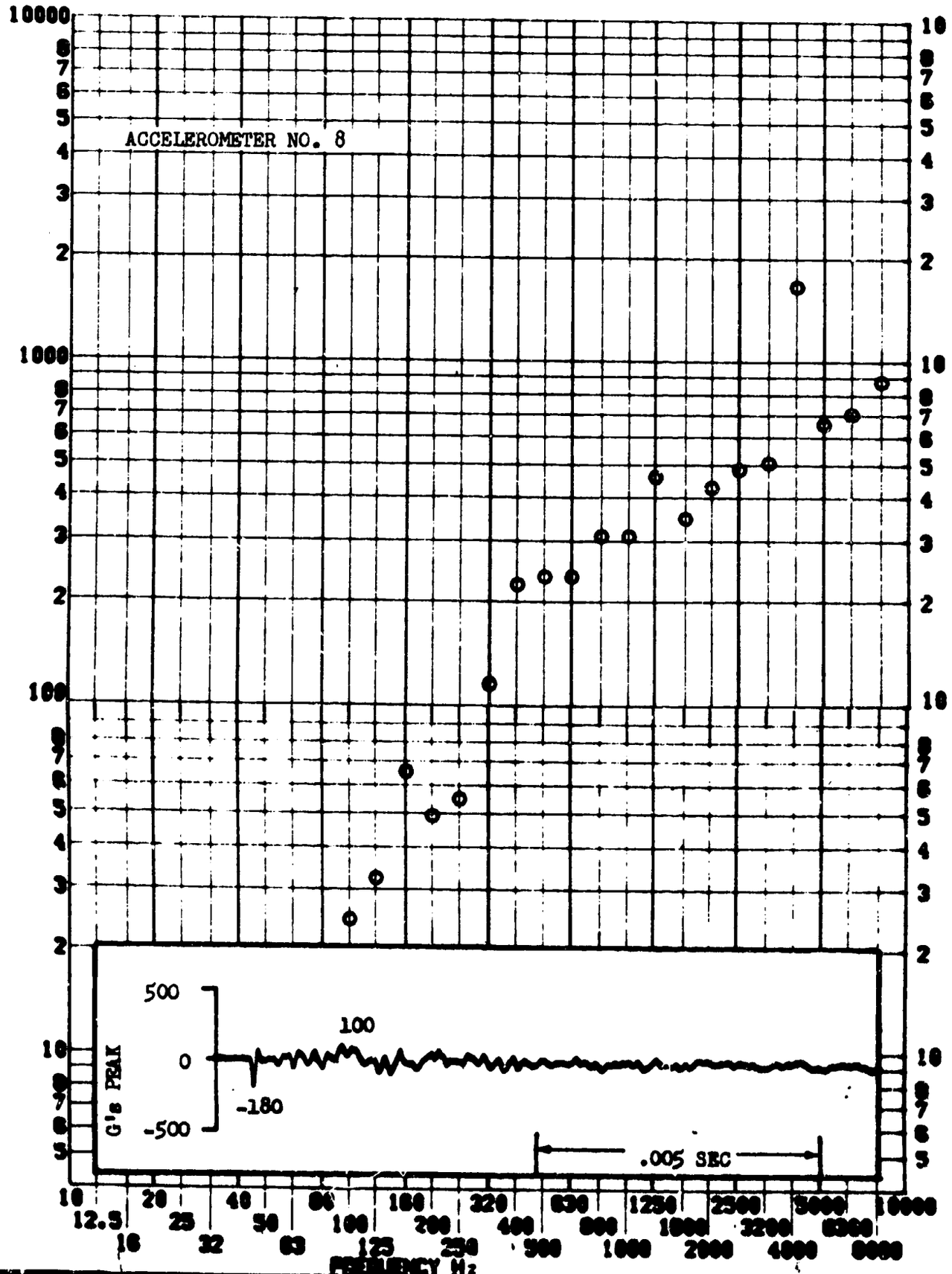

SHOCK TEST ANALYSIS DATA SHEET II.A.3.17

TEST ITEM 768-257
SERIAL NO. 9
SHOCK AXIS Long

PART NO. Box E
TEST DATE 25 May 1964
SHOCK NO. 9

RESPONSE G-S

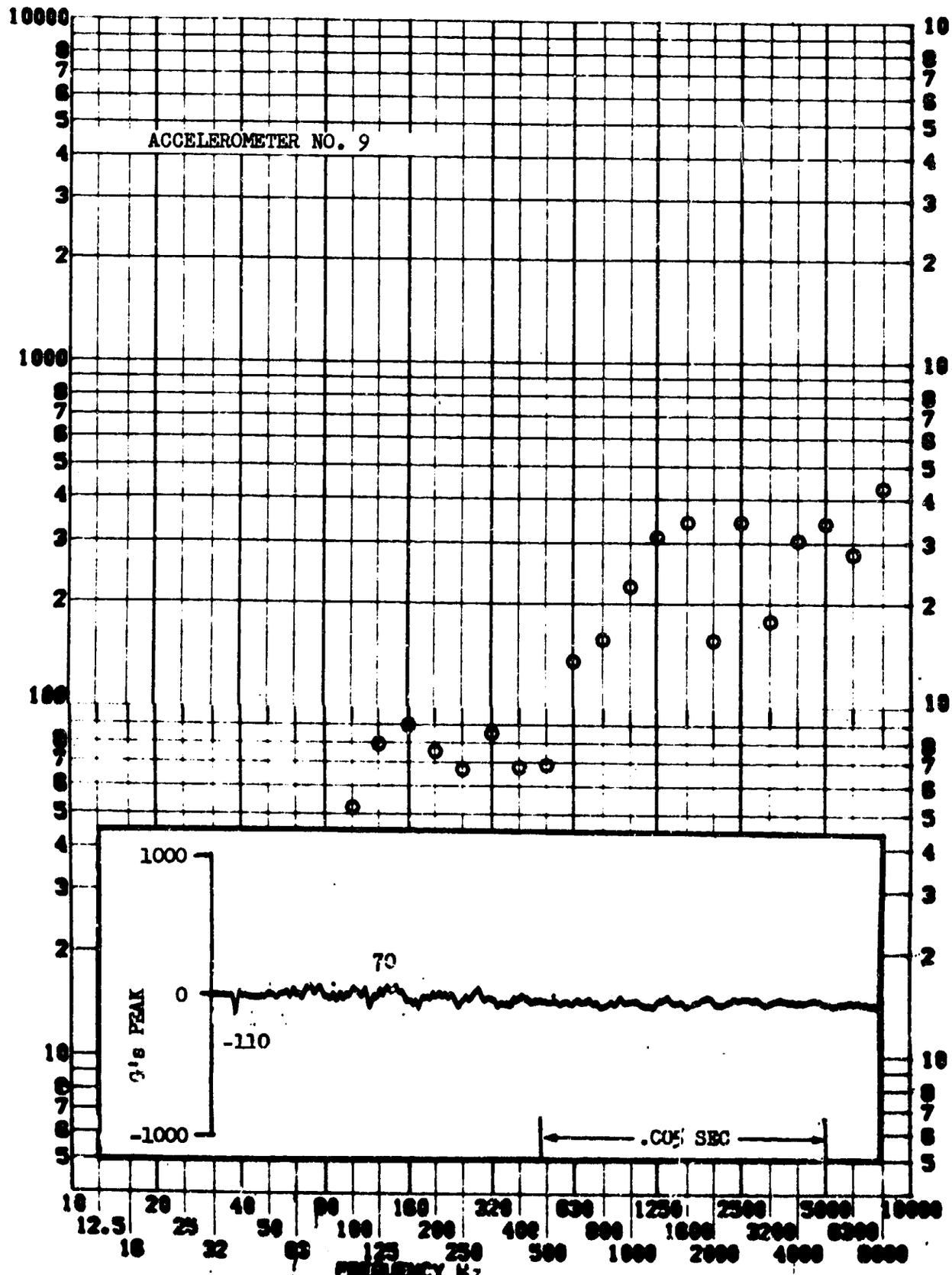

SHOCK TEST ANALYSIS DATA SHEET II.A.3.18

TEST ITEM 768-259
SERIAL NO. 13
SHOCK AXIS Radial

PART NO. Box D Frame
TEST DATE 25 May 1964
SHOCK NO. 9

RESPONSE G-S

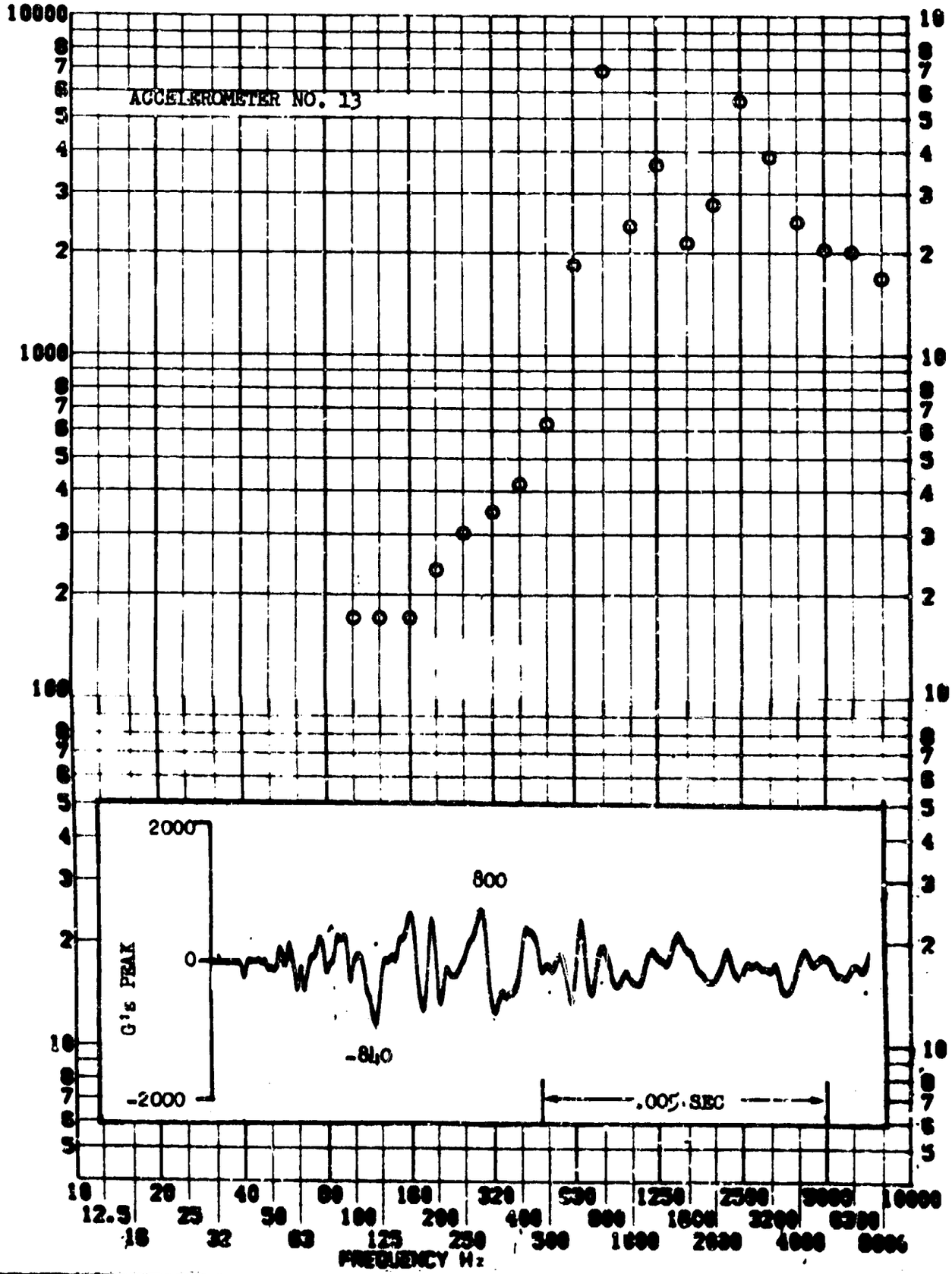

SHOCK TEST ANALYSIS DATA SHEET II.A.3.19

TEST ITEM 768-261
SERIAL NO. 14
SHOCK AXIS Long

PART NO. Box D
TEST DATE 25 May 1964
SHOCK NO. 9

RESPONSE G-S

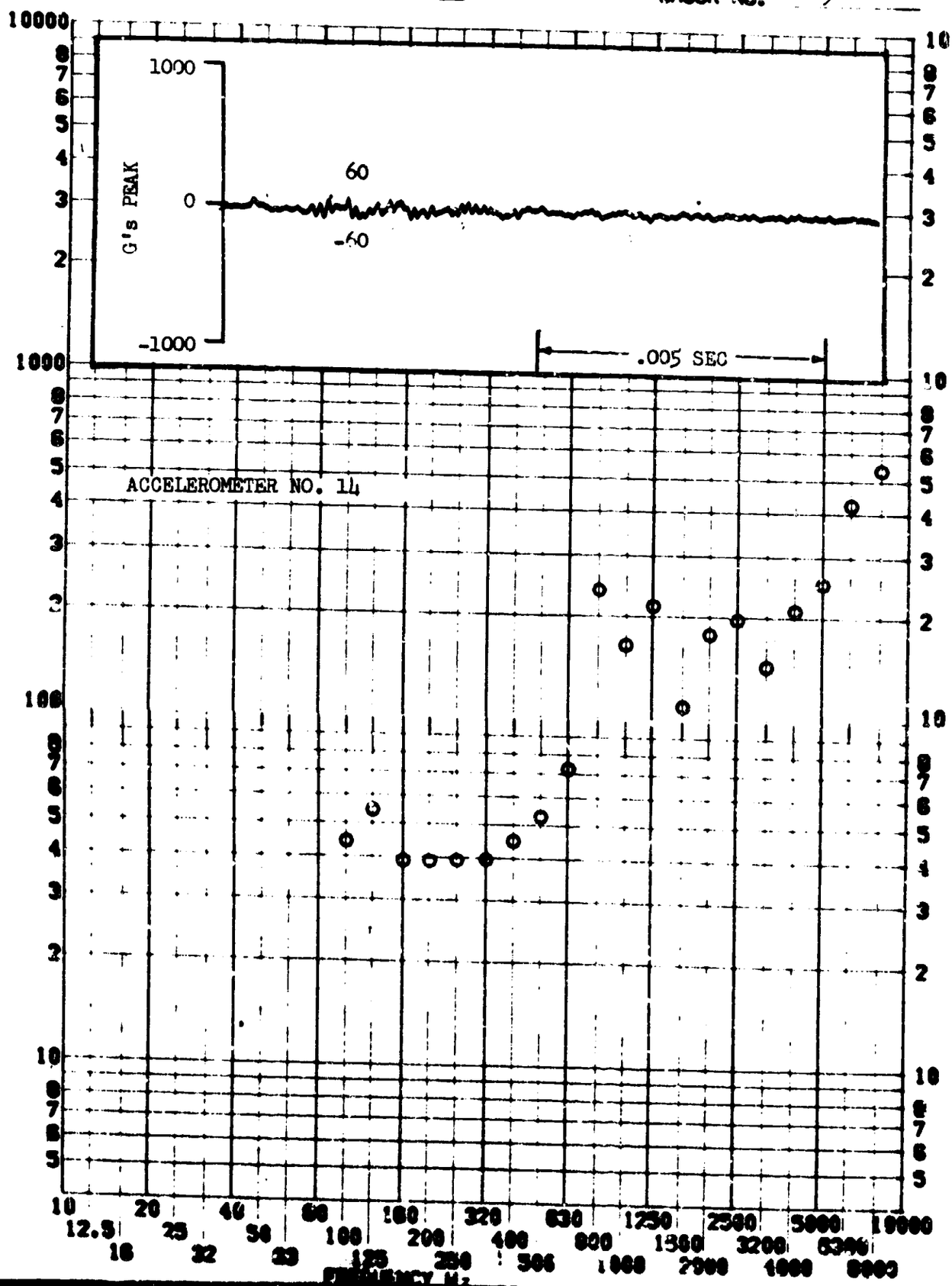

SHOCK TEST ANALYSIS DATA SHEET II.A.3.20

TEST ITEM 768-263
SERIAL NO. 15
SHOCK AXIS Radial

PART NO. Box D
TEST DATE 25 May 1964
SHOCK NO. 9

RESPONSE G-S

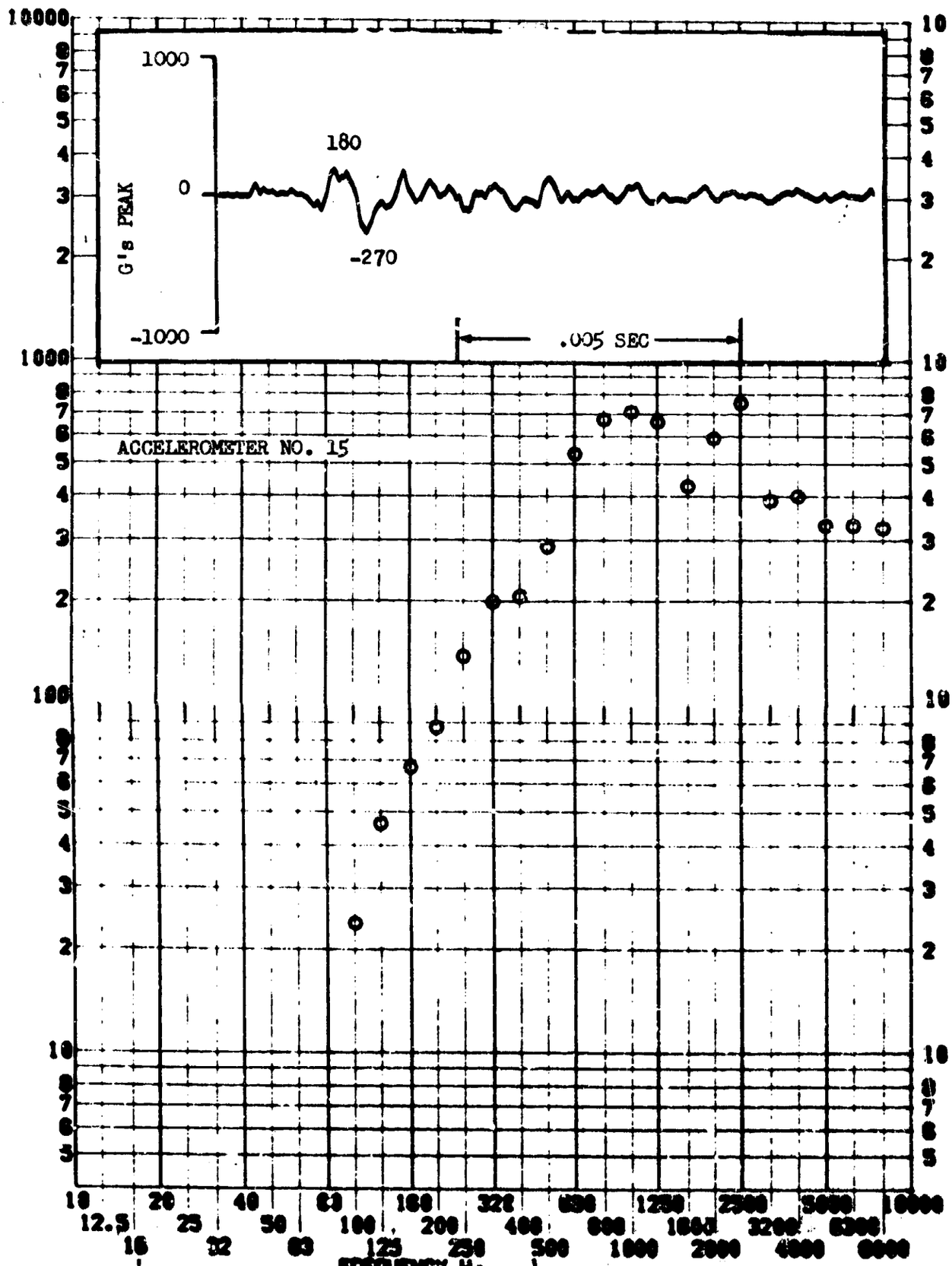

SHOCK TEST ANALYSIS DATA SHEET II.A.3.21

TEST ITEM 768-242
SERIAL NO. 1
SHOCK AXIS Radial

PART NO. Box A Frame
TEST DATE 25 May 1964
SHOCK NO. 10

RESPONSE G-S

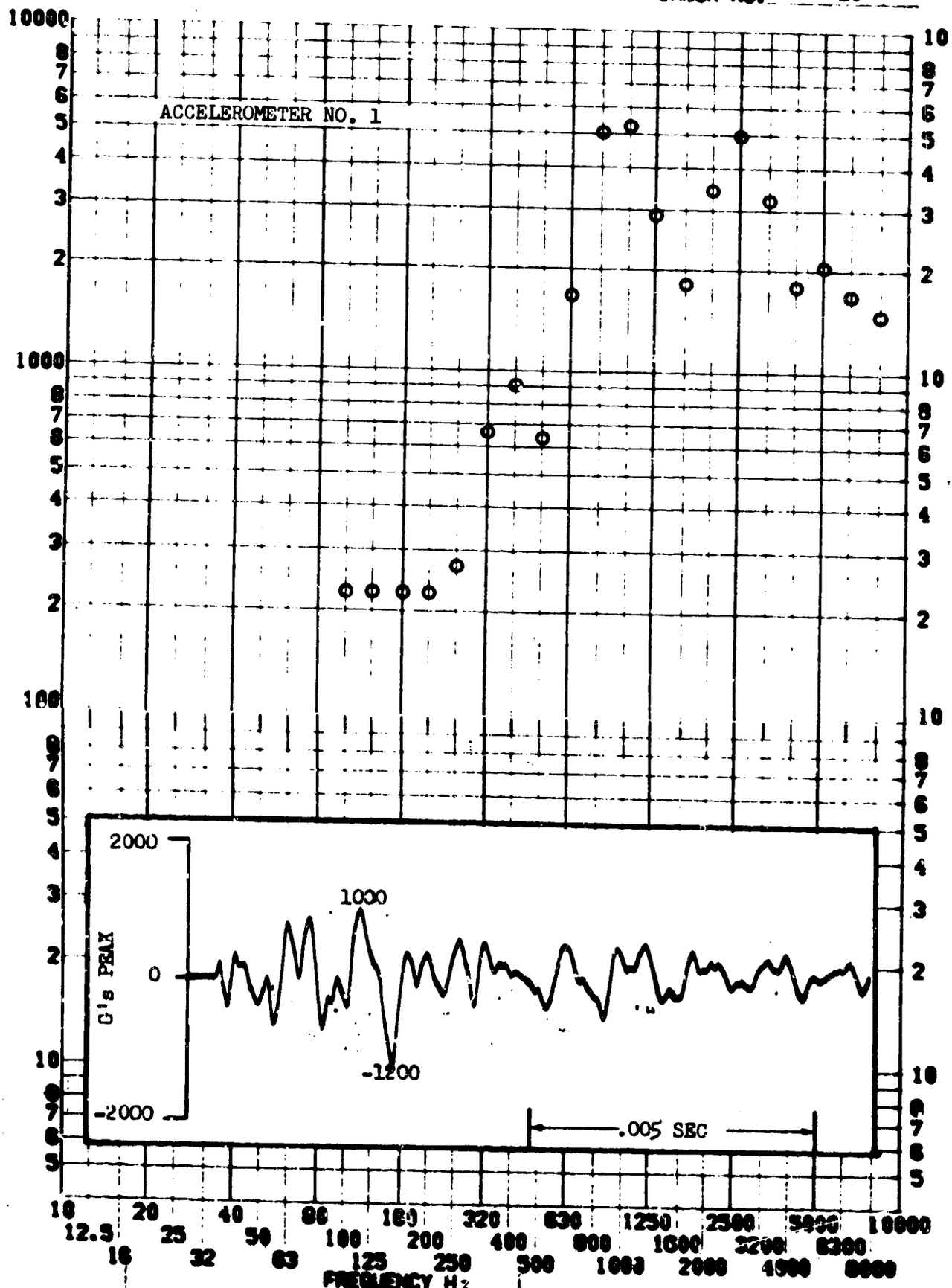

SHOCK TEST ANALYSIS DATA SHEET II.A.3.22

TEST ITEM 768-244 PART NO. Box A
SERIAL NO. 2 TEST DATE 25 May 1964
RESPONSE G-S SHOCK AXIS Radial SHOCK NO. 10

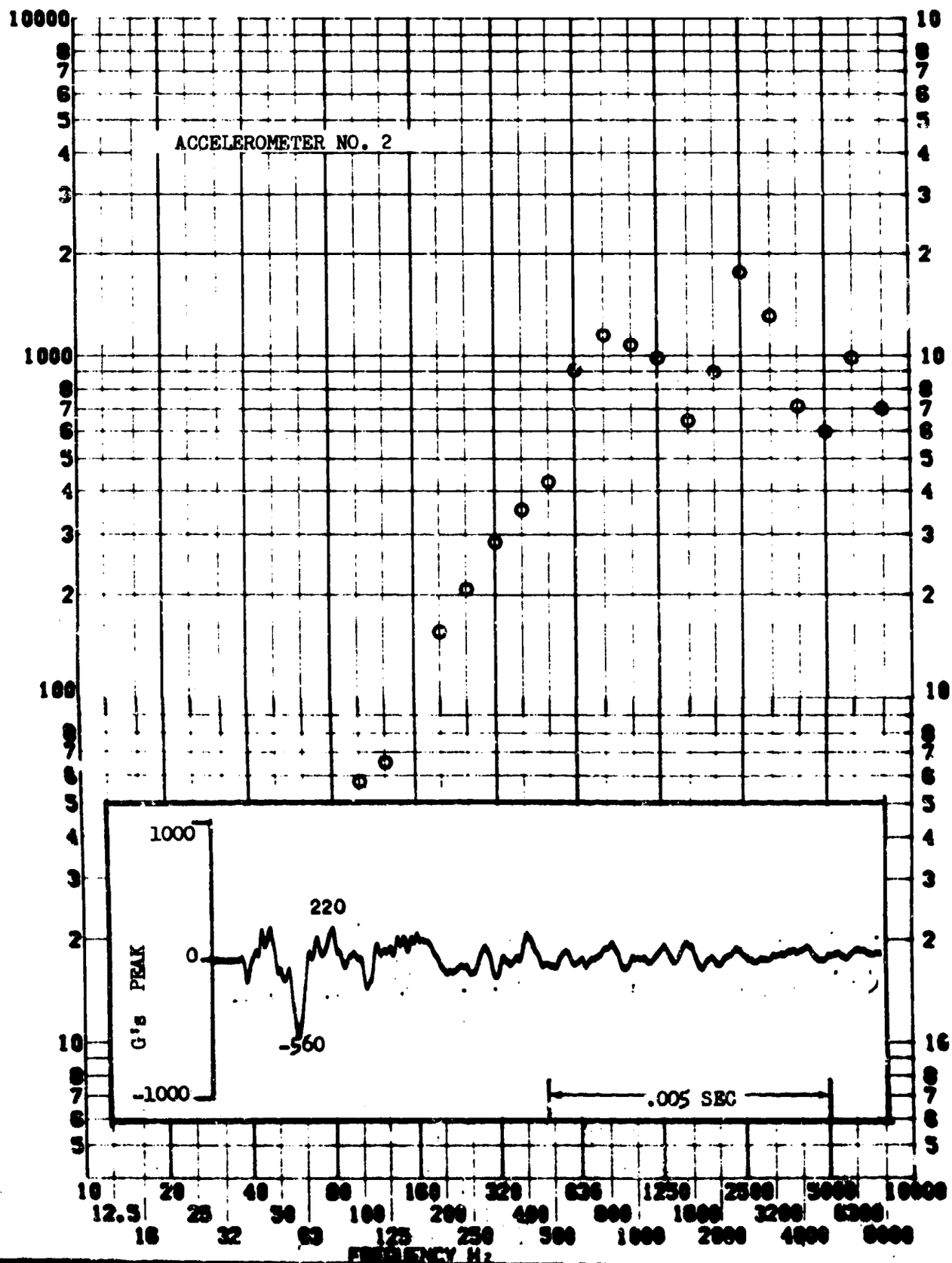

SHOCK TEST ANALYSIS DATA SHEET II.A.3.23

TEST ITEM 768-246
SERIAL NO. 3
SHOCK AXIS Long

PART NO. Box A
TEST DATE 25 May 1964
SHOCK NO. 10

RESPONSE G-S

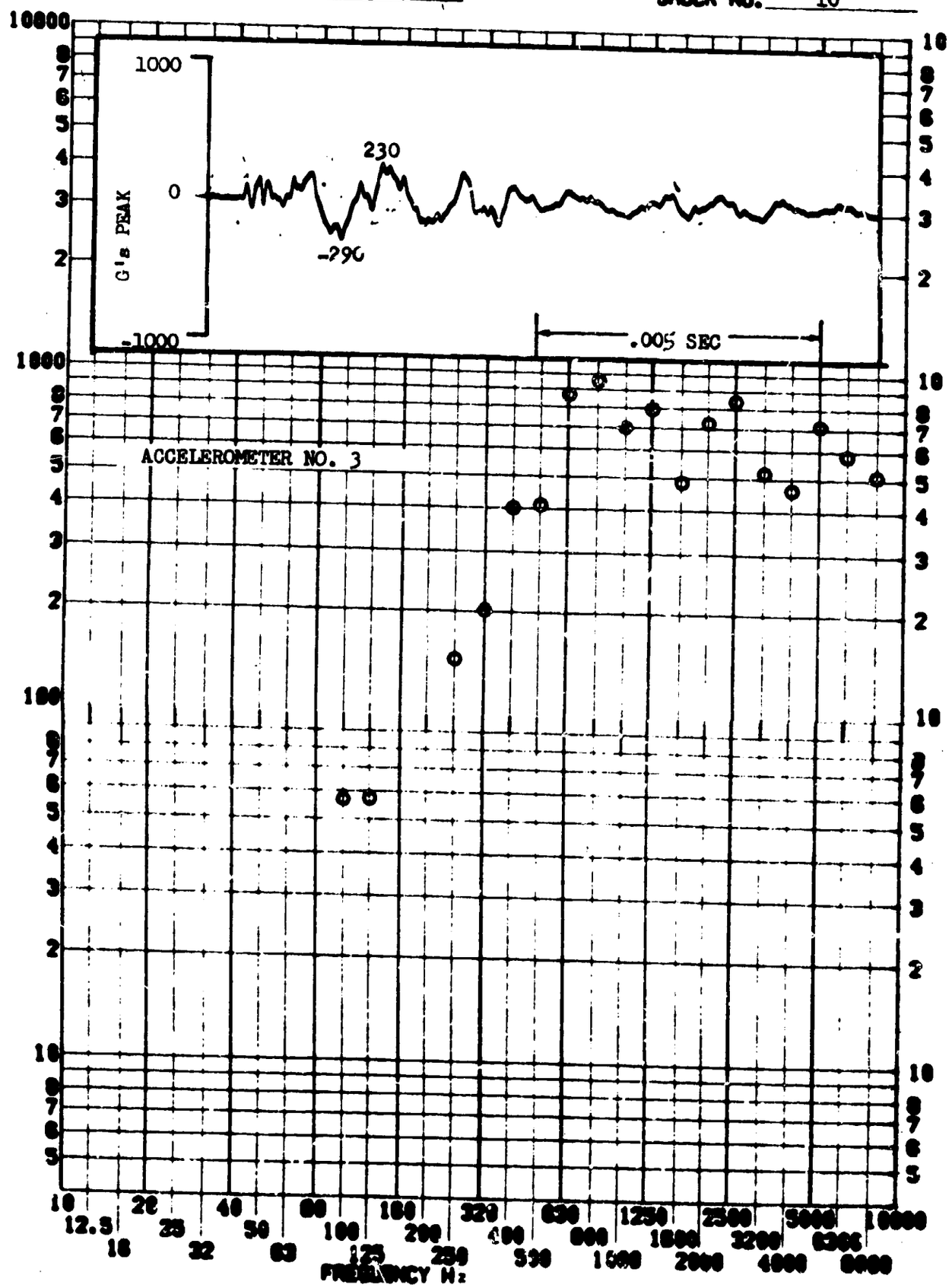

SHOCK TEST ANALYSIS DATA SHEET II.A.3.24

TEST ITEM 768-248
SERIAL NO. 4
SHOCK AXIS Radial

PART NO. Box B Frame
TEST DATE 25 May 1964
SHOCK NO. 10

RESPONSE G-S

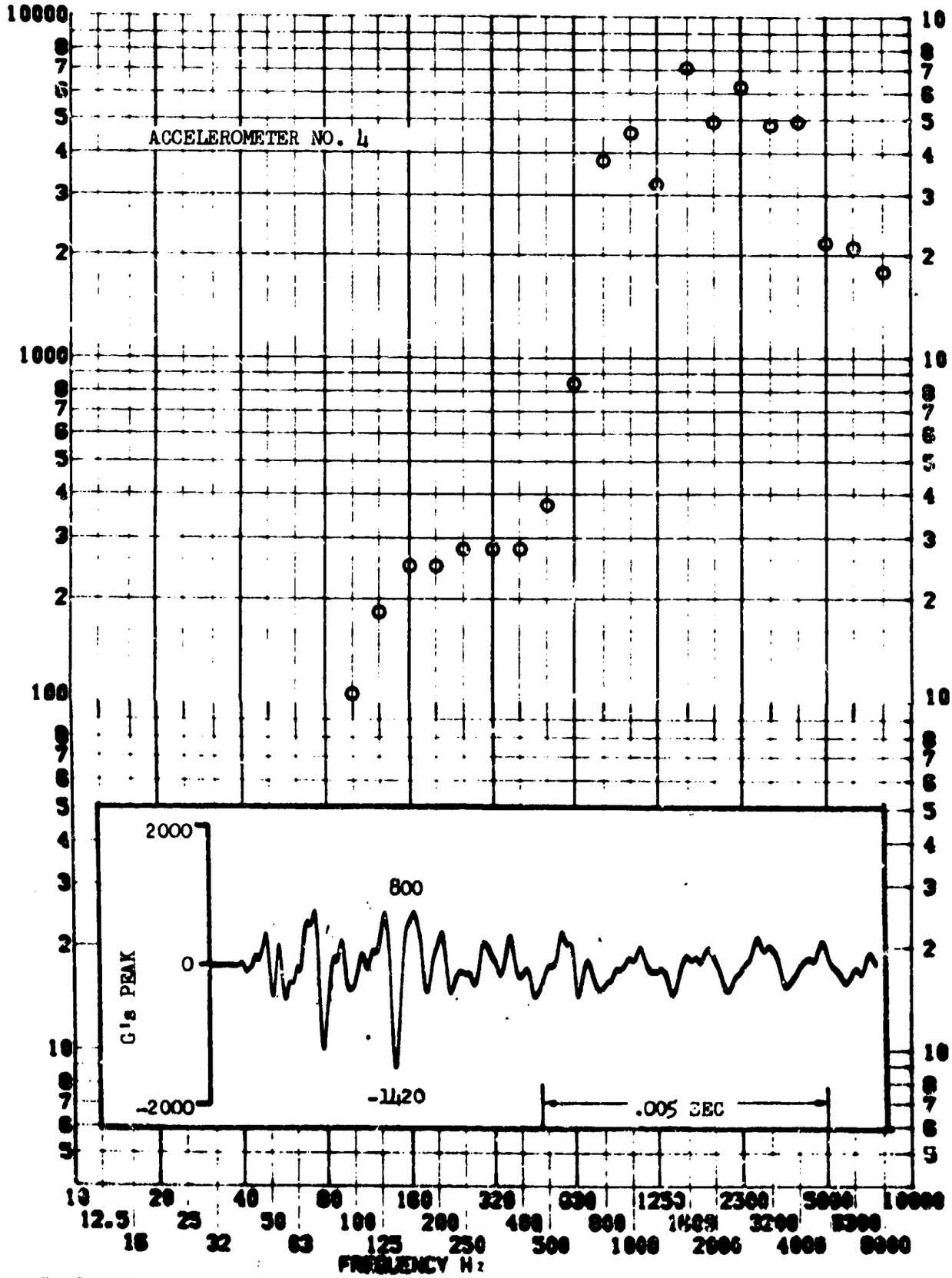

SHOCK TEST ANALYSIS DATA SHEET II.A.3.25

TEST ITEM 768-250
SERIAL NO. 5
SHOCK AXIS Radial

PART NO. Box B
TEST DATE 25 May 1964
SHOCK NO. 10

RESPONSE G-S

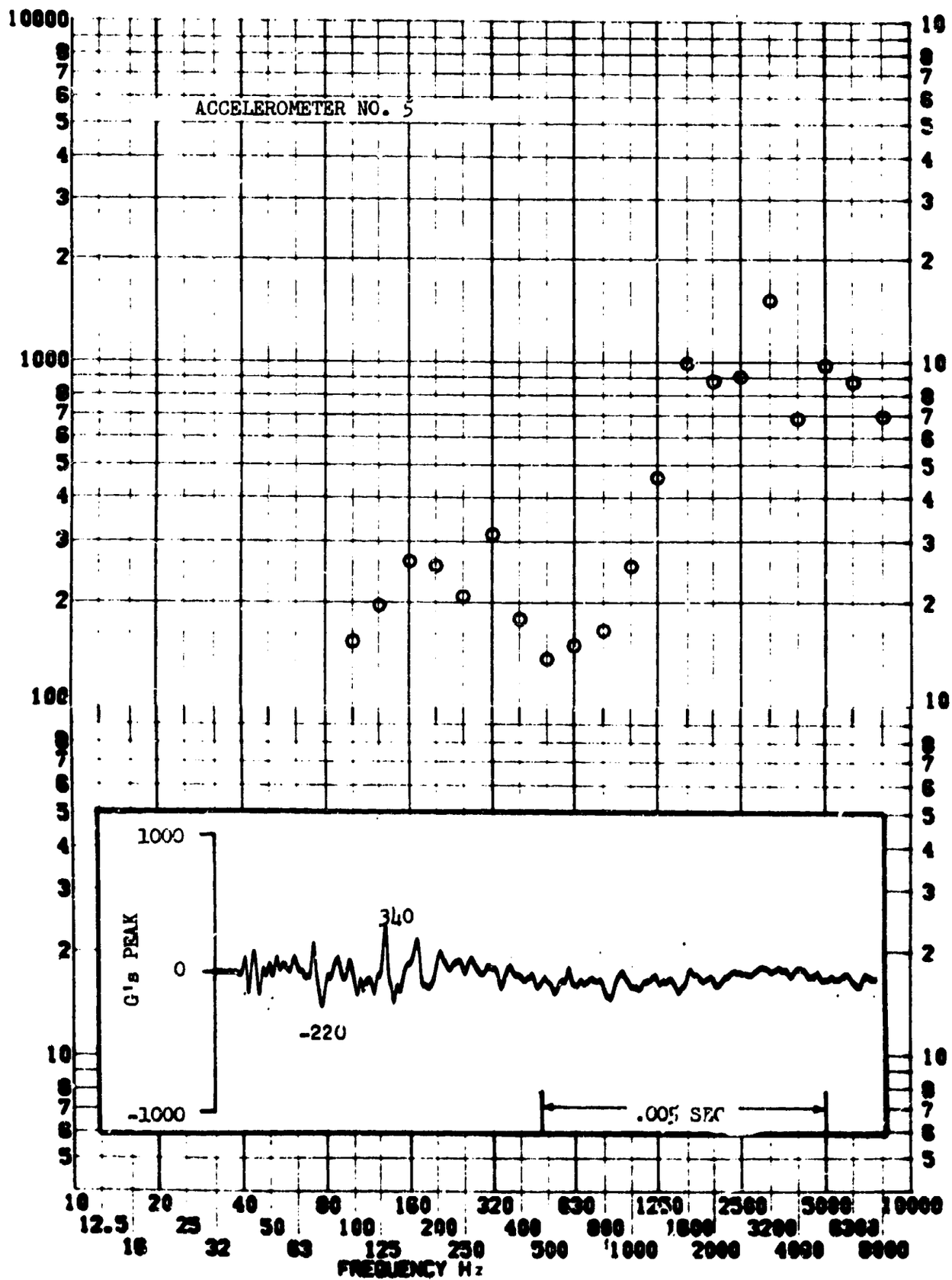

SHOCK TEST ANALYSIS DATA SHEET II.A.3.26

TEST ITEM 768-252
SERIAL NO. 6
SHOCK AXIS Long

PART NO. Box B
TEST DATE 25 May 1964
SHOCK NO. 10

RESPONSE G-S

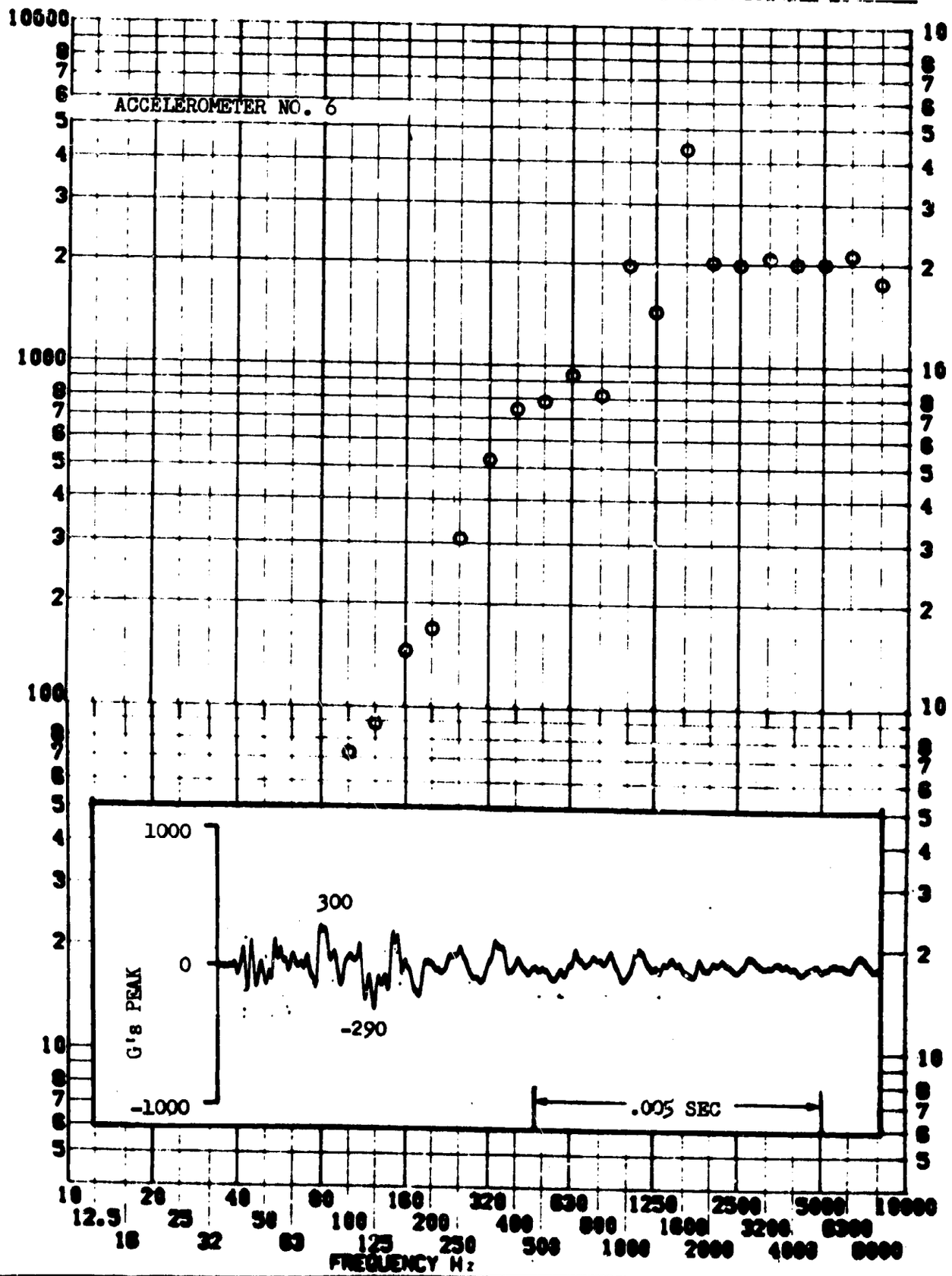

SHOCK TEST ANALYSIS DATA SHEET II.A.3.27

TEST ITEM 768-254
SERIAL NO. 7
SHOCK AXIS Radial

PART NO. Box E Frame
TEST DATE 25 May 1964
SHOCK NO. 10

RESPONSE G-S

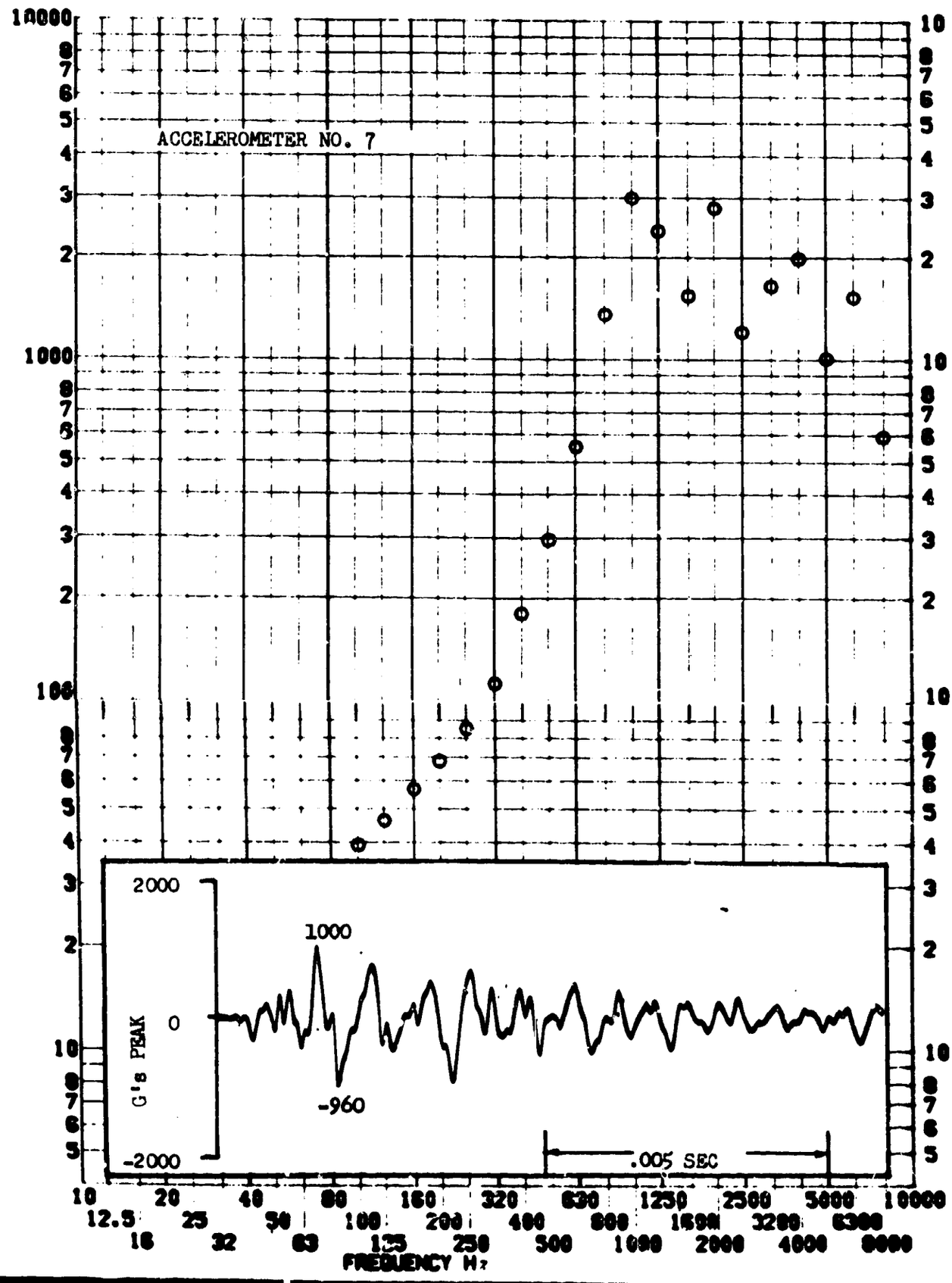

SHOCK TEST ANALYSIS DATA SHEET II.A.3.28

TEST ITEM 768-256
SERIAL NO. 8
SHOCK AXIS Radial

PART NO. Box E
TEST DATE 25 May 1964
SHOCK NO. 10

RESPONSE G-S

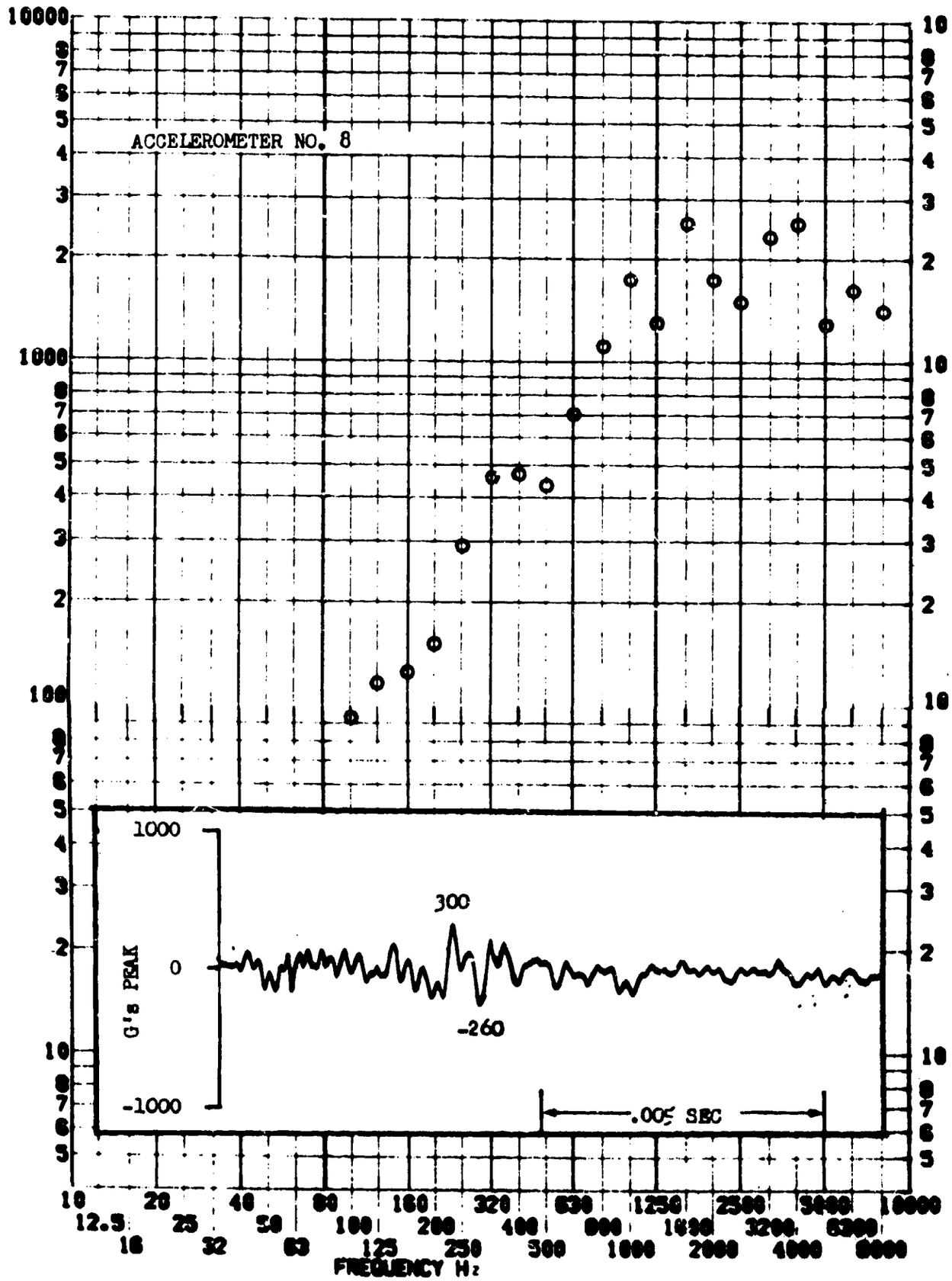

SHOCK TEST ANALYSIS DATA SHEET II.A.3.29

TEST ITEM 768-258
SERIAL NO. 9
SHOCK AXIS Long
PART NO. Box E
TEST DATE 25 May 1964
SHOCK NO. 10

RESPONSE G-S

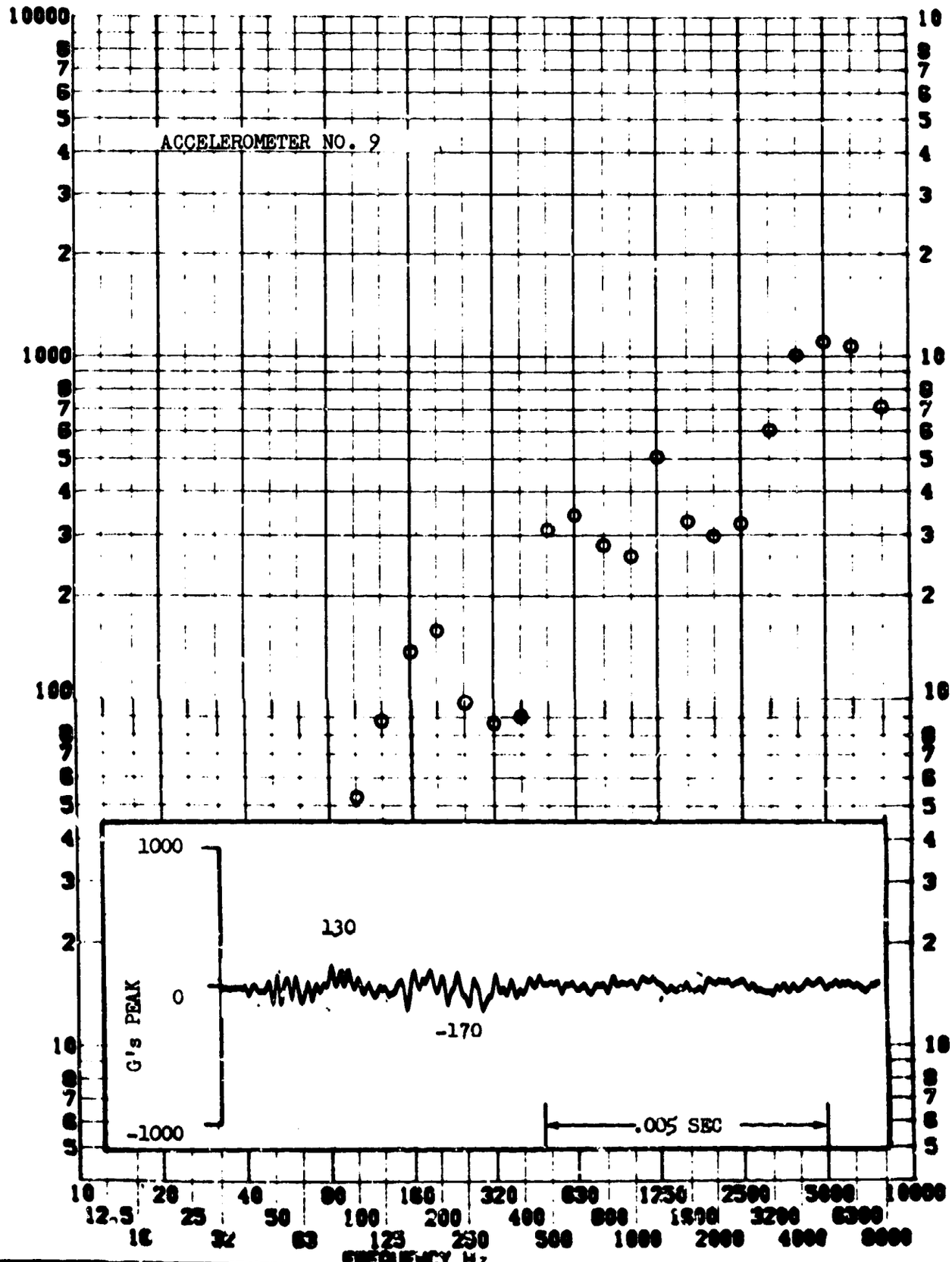

SHOCK TEST ANALYSIS DATA SHEET II.A.3.30

TEST ITEM 768-260
SERIAL NO. 13
SHOCK AXIS Radial

PART NO. Box D Frame
TEST DATE 25 May 1964
SHOCK NO. 10

RESPONSE G-S

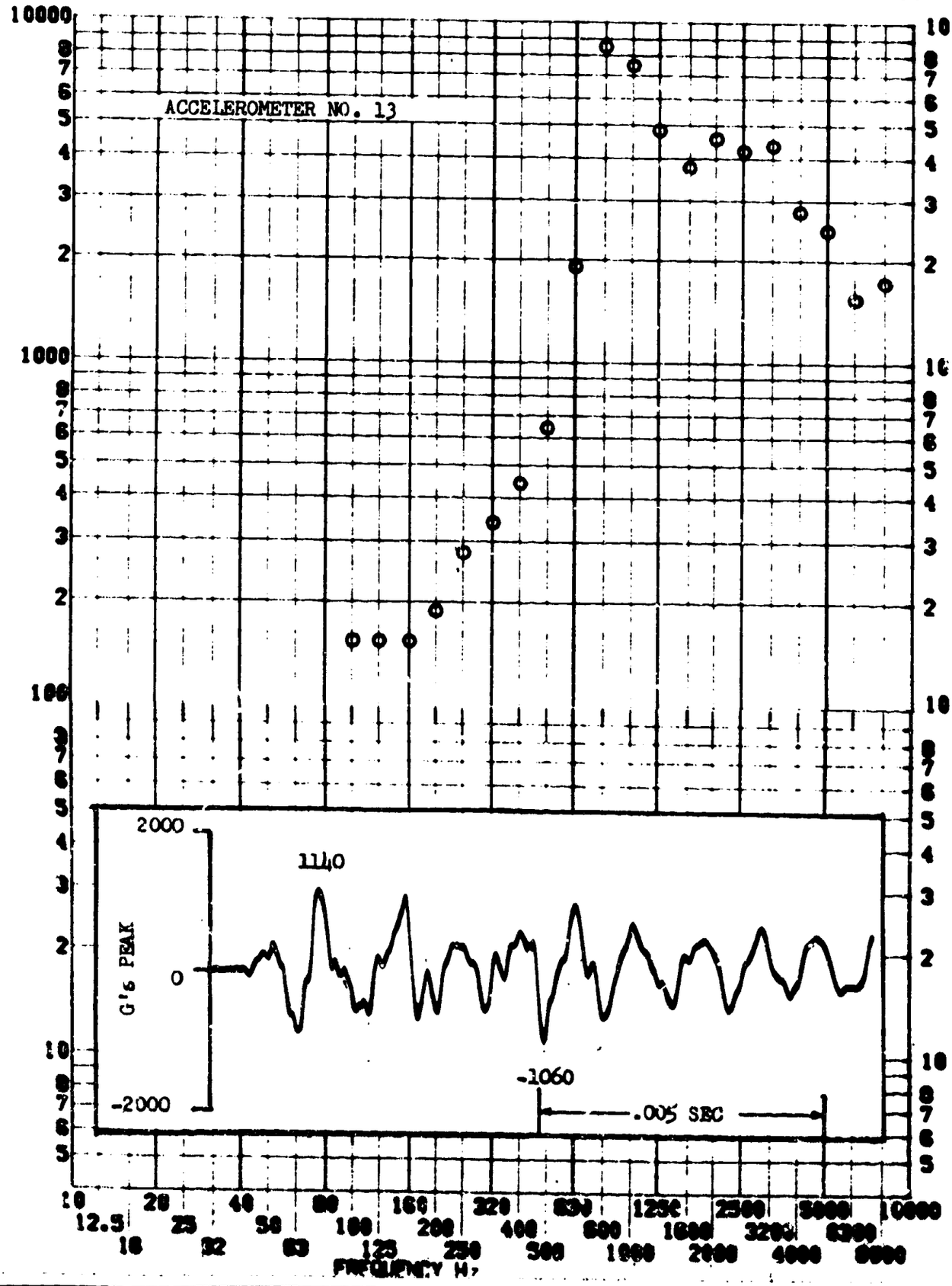

SHOCK TEST ANALYSIS DATA SHEET II.A.3.31

TEST ITEM 768-262
SERIAL NO. 14
SHOCK AXIS Long

PART NO. Box D
TEST DATE 25 May 1960
SHOCK NO. 10

RESPONSE G-S

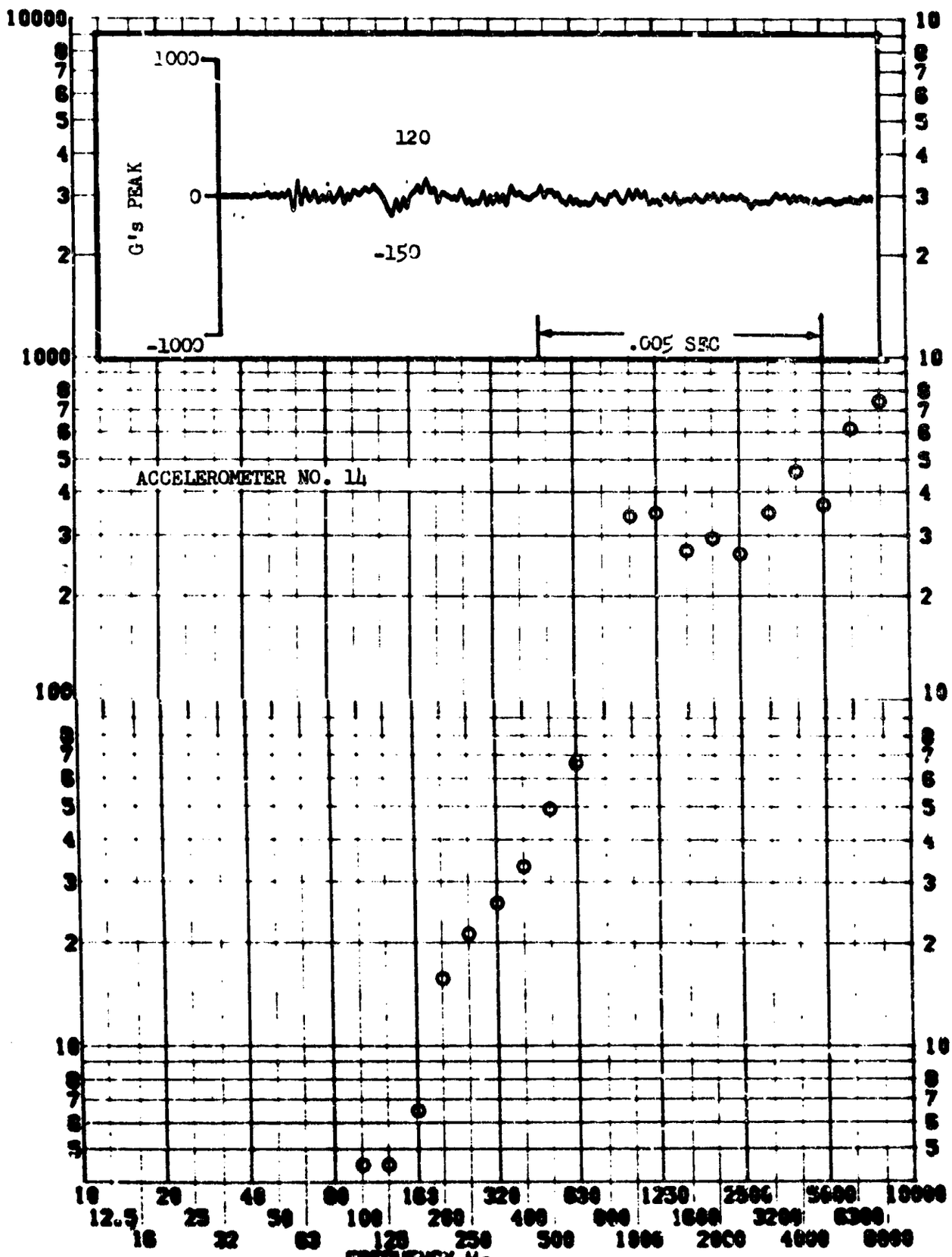

SHOCK TEST ANALYSIS DATA SHEET II.A.3.32

TEST ITEM 768-264
SERIAL NO. 15
SHOCK AXIS Radial

PART NO. Box D
TEST DATE 25 May 1964
SHOCK NO. 10

RESPONSE G-S

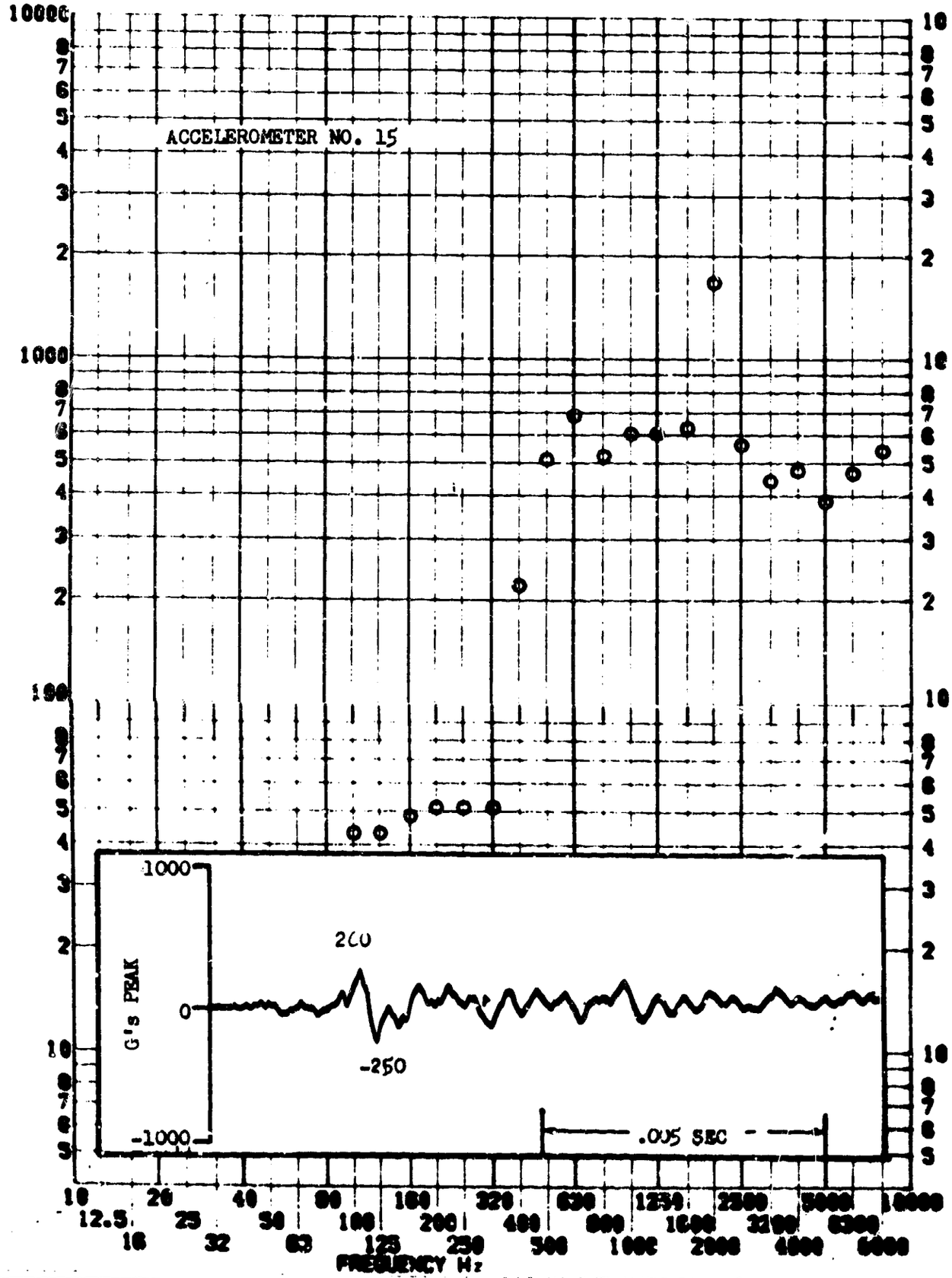

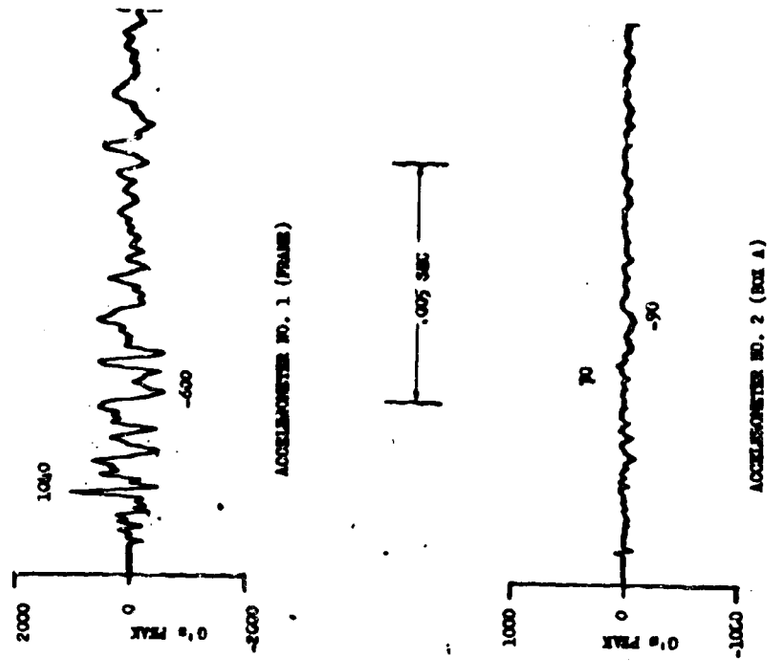
ACCELEROMETER NO. 1 (FRAME)
ACCELEROMETER NO. 2 (BOX A)
.005 SEC
0-PEAK
0-PEAK

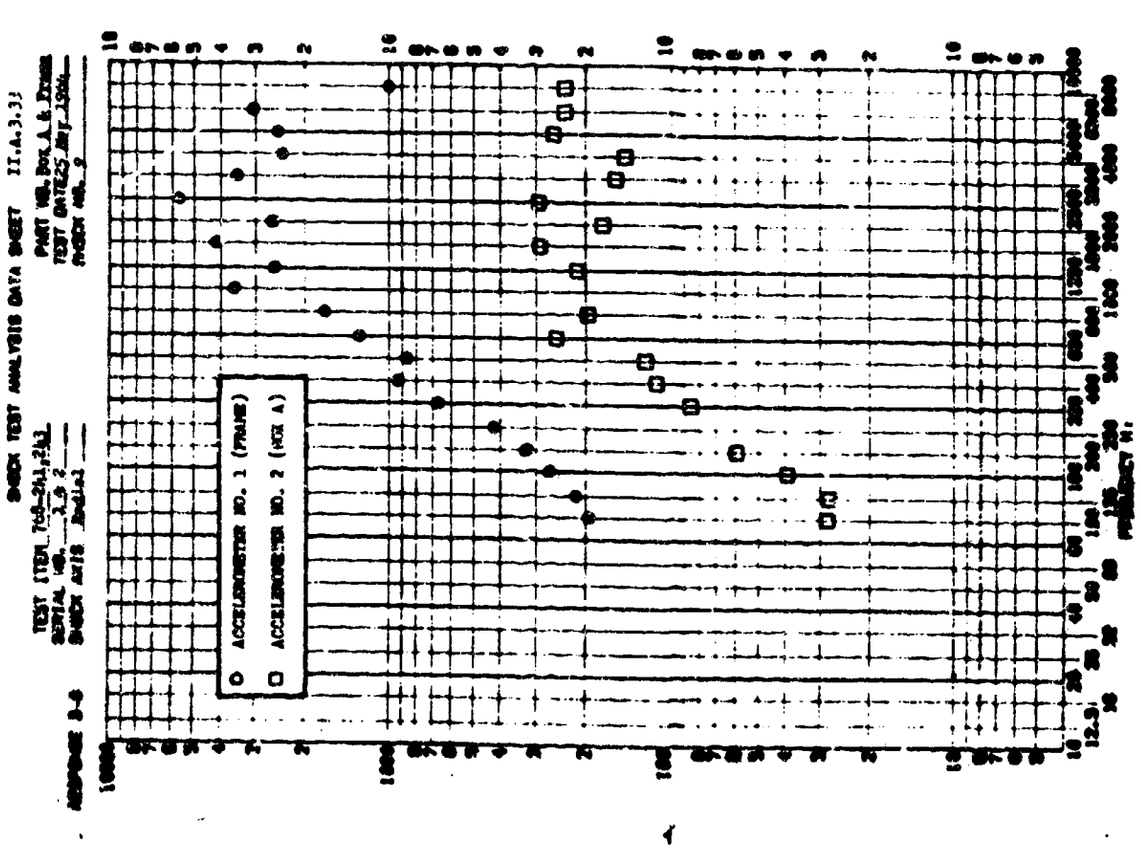
SHOCK TEST ANALYSIS DATA SHEET
ACCELEROMETER NO. 1 (FRAME)
ACCELEROMETER NO. 2 (BOX A)

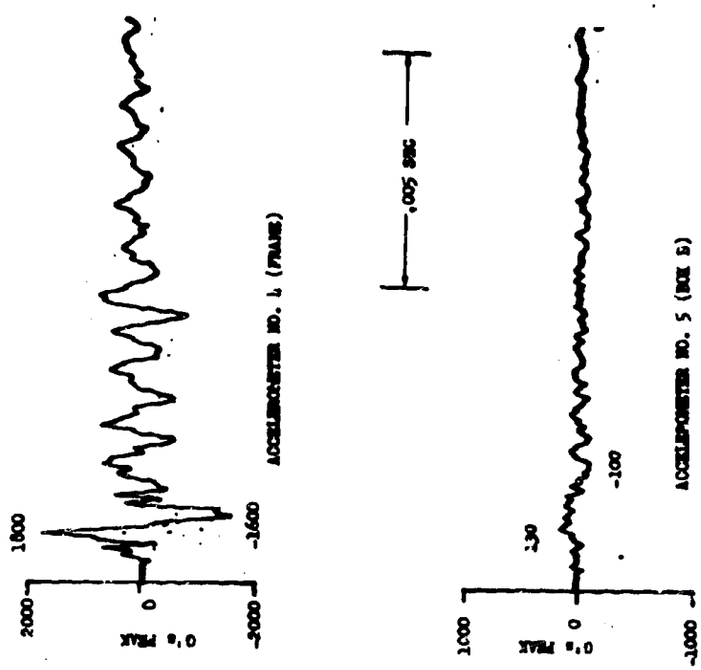
ACCELEROMETER NO. 4 (FRAME)
2000
1600
0
-1600
-2000
0.6 PEAK
.005 SEC
ACCELEROMETER NO. 5 (BOX B)
1000
500
0
-500
-1000
0.7 PEAK

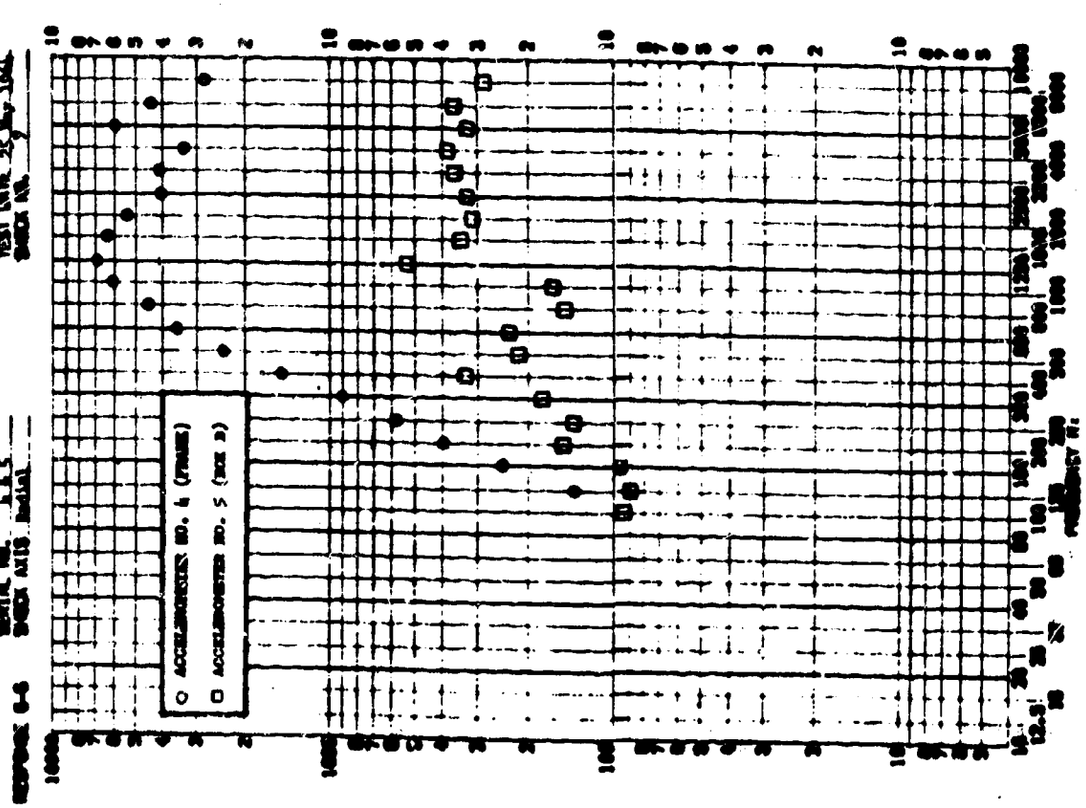
SHOCK TEST ANALYSIS DATA SHEET
ACCELEROMETER NO. 4 (FRAME)
ACCELEROMETER NO. 5 (BOX B)

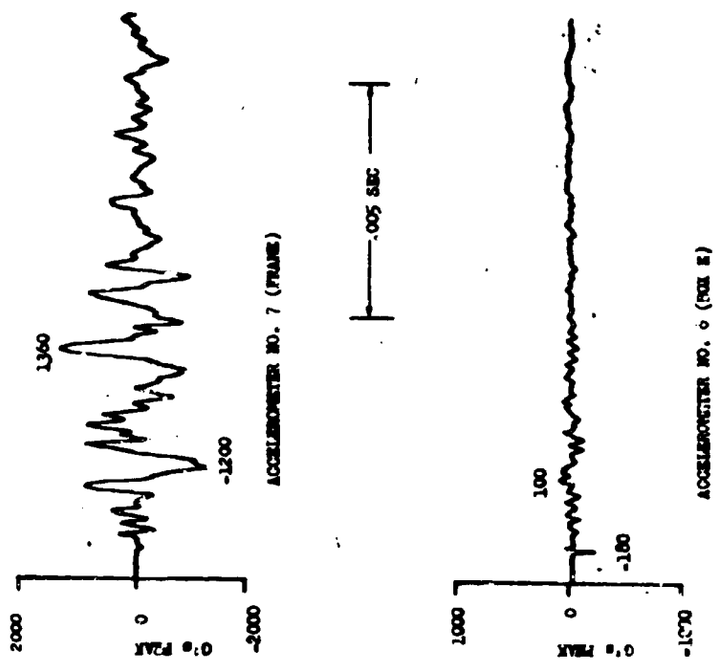
ACCELEROMETER NO. 7 (FRAME)
1360
-1200
2000
0
-2000
0.6 PEAK
.005 SEC
ACCELEROMETER NO. 6 (BOX E)
100
-180
1000
0
-1000
0.6 PEAK

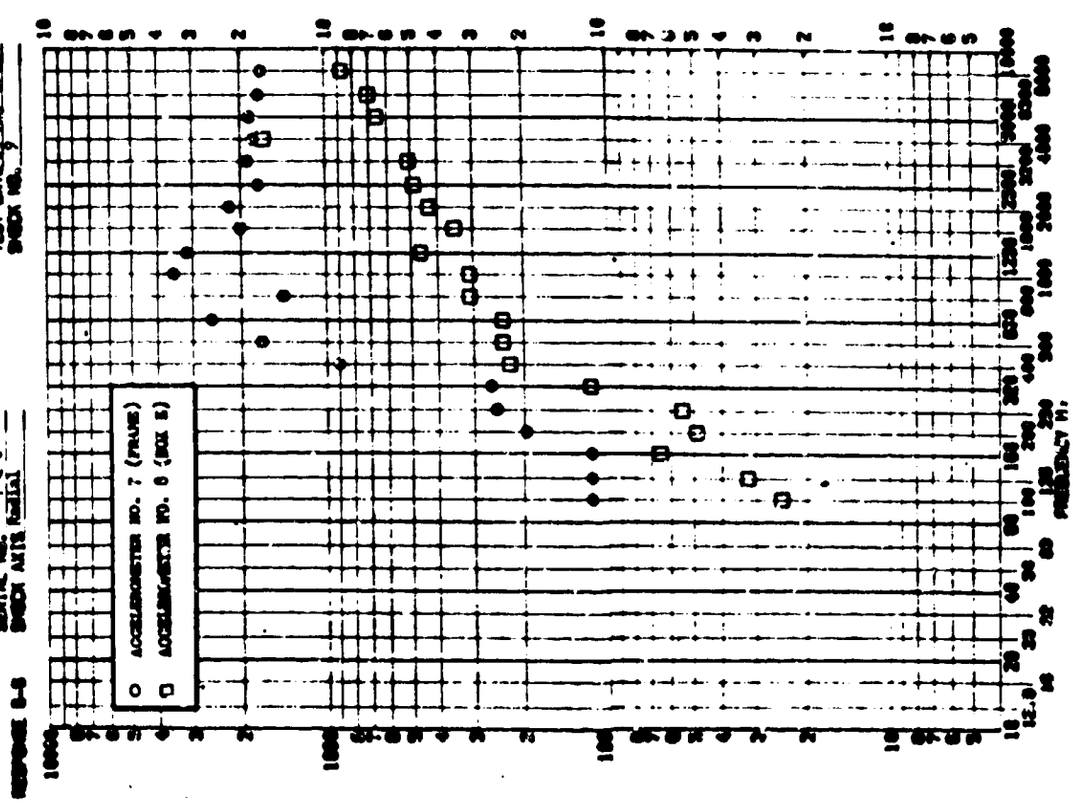
SHOCK TEST ANALYSIS DATA SHEET
TEST ITEM 768-253-255
SERIAL NO.
SHOCK AXIS
PART NO., Box E & Frame
TEST DATE 25 May 1969
SHOCK NO.
RESPONSE G-S
ACCELEROMETER NO. 7 (FRAME)
ACCELEROMETER NO. 6 (BOX E)
FREQUENCY H

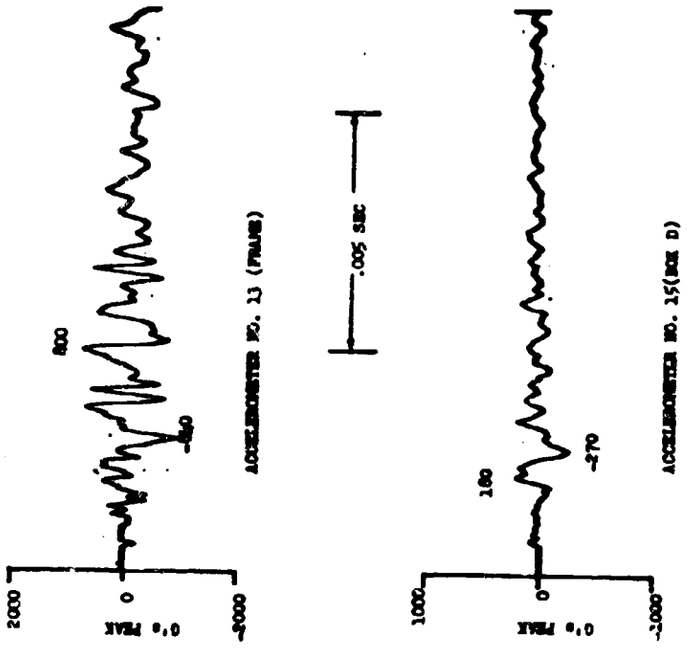
800
-80
0% PEAK
2000
0
-2000
ACCELEROMETER NO. 13 (FRAME)
.005 SEC
180
-270
0% PEAK
1000
0
-1000
ACCELEROMETER NO. 15(BOX D)

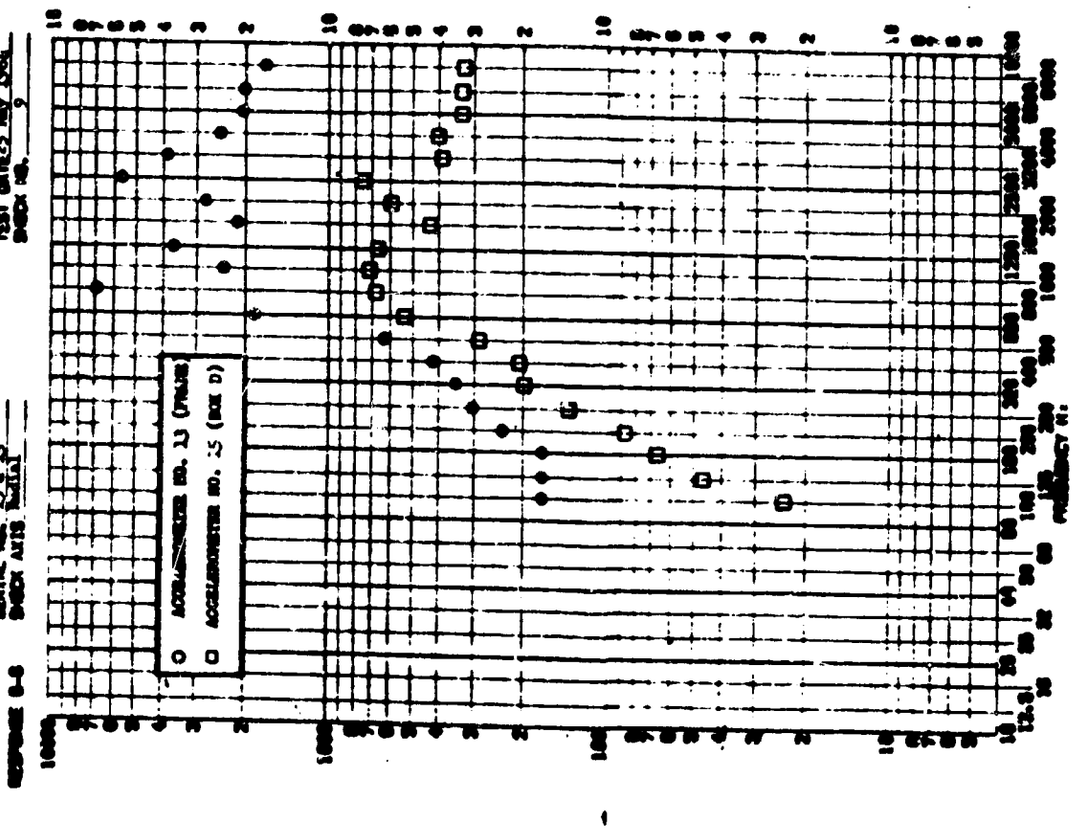
SHOCK TEST ANALYSIS DATA SHEET
ACCELEROMETER NO. 13 (FRAME)
ACCELEROMETER NO. 15 (BOX D)

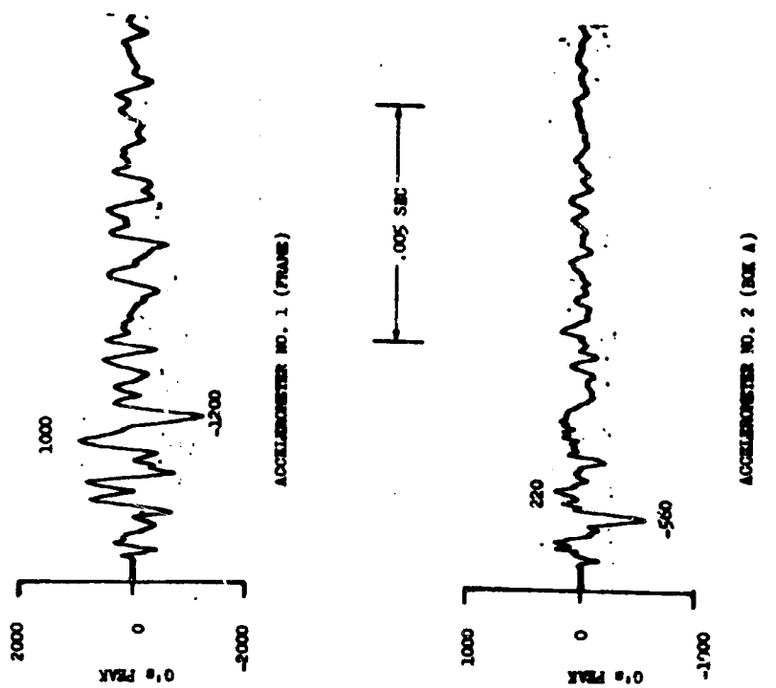
ACCELEROMETER NO. 1 (FRAME)
1000
-1200
0
2000
-2000
0-e PEAK
.005 SEC
ACCELEROMETER NO. 2 (BOX A)
220
-560
0
1000
-1000
0-e PEAK

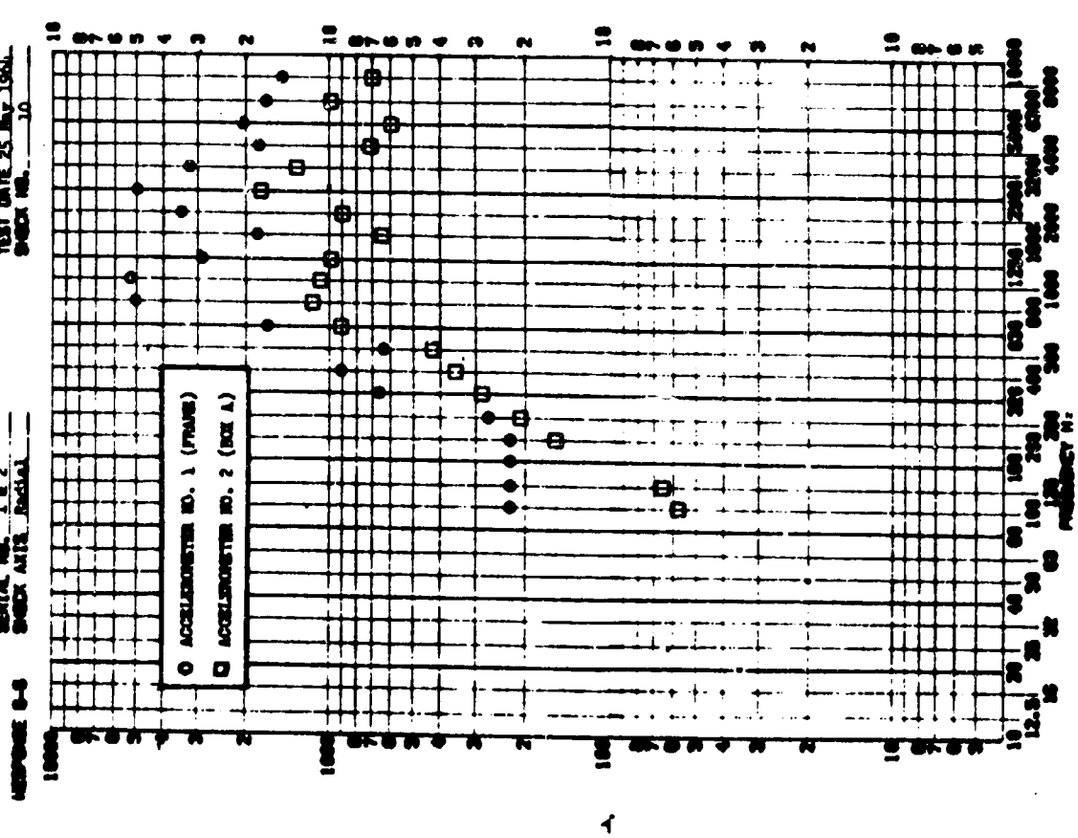
SHOCK TEST ANALYSIS DATA SHEET
ACCELEROMETER NO. 1 (FRAME)
ACCELEROMETER NO. 2 (BOX A)

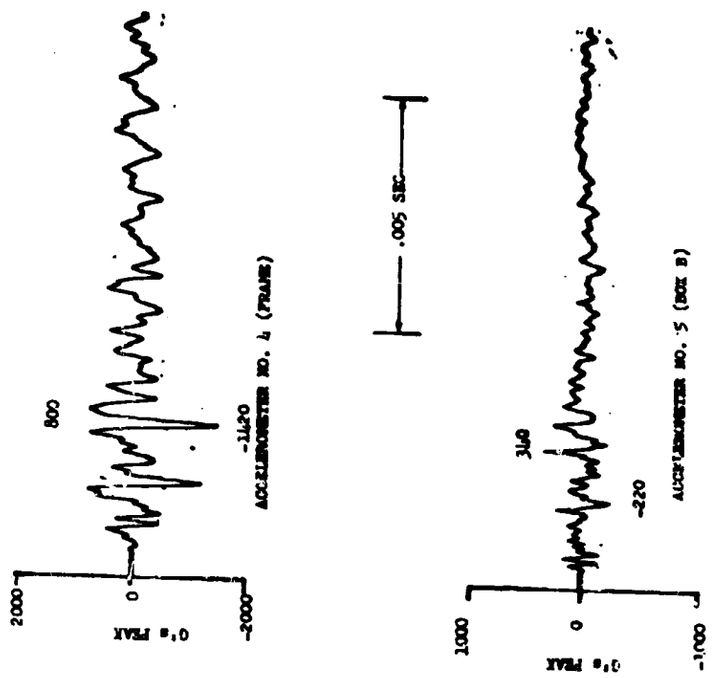
800
-1120
ACCELEROMETER NO. 4 (FRAME)
2000
0
-2000
0-g PEAK
.005 SEC
340
-220
ACCELEROMETER NO. 5 (BOX B)
1000
0
-1000
0-g PEAK

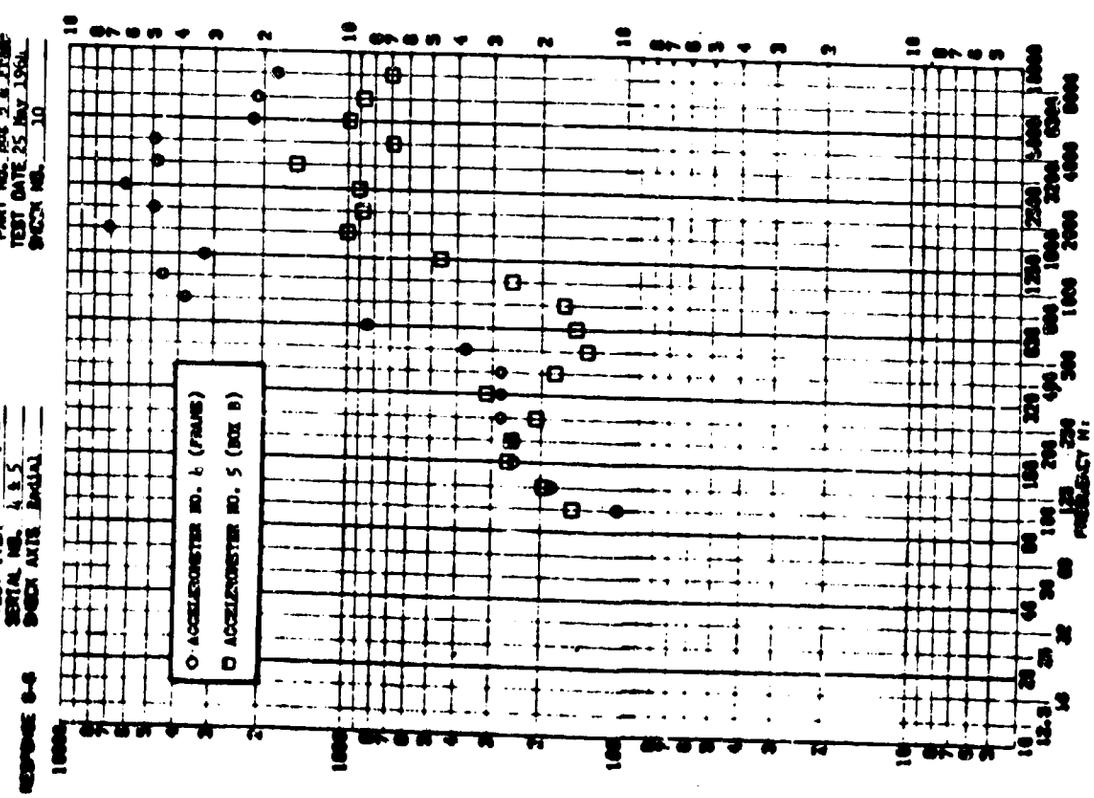
SHOCK TEST ANALYSIS DATA SHEET II.A.3.38
TEST ITEM 768-240,249
SERIAL NO. 4 & 5
SHOCK AXIS Radial
PART NO. Box 2 & Frame
TEST DATE 25 May 1968
SHOCK NO. 10
RESPONSE G-S
ACCELEROMETER NO. 4 (FRAME)
ACCELEROMETER NO. 5 (BOX B)
FREQUENCY H:

SHOCK TEST ANALYSIS DATA SHEET II.A.3.39

TEST ITEM 768-254,256 PART NO. Box E & Frame
SERIAL NO. 7 & 8 TEST DATE 25 May 1964
SHOCK AXIS Radial SHOCK NO. 10

ESPOOCE 8-8

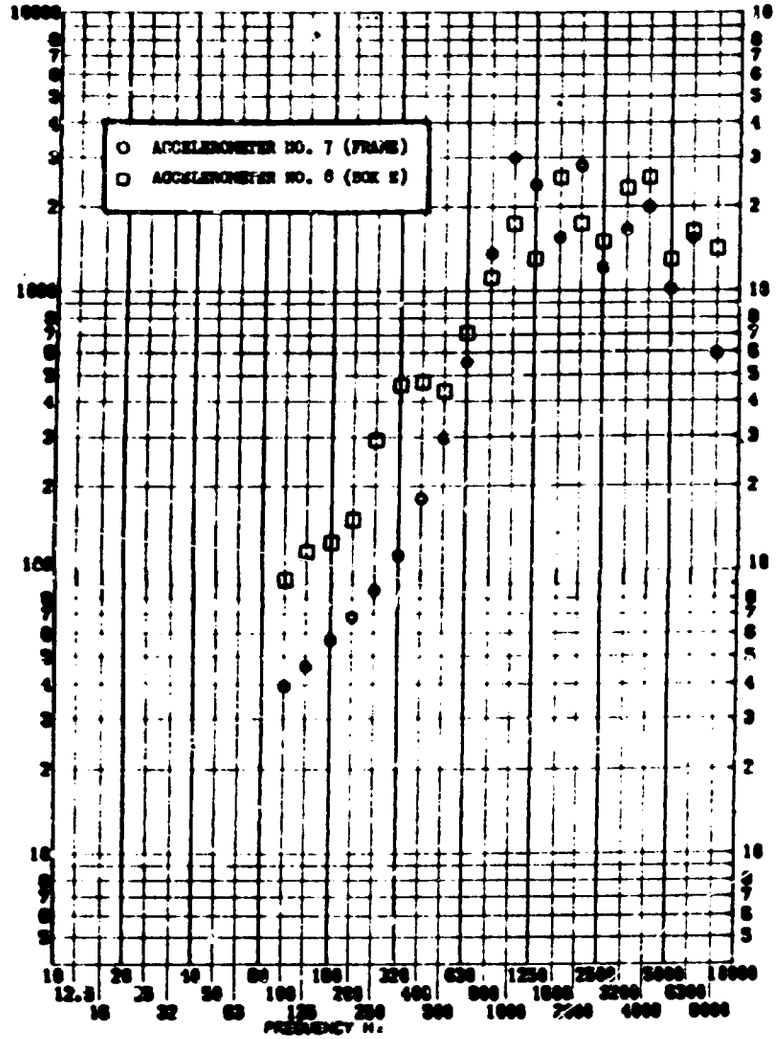

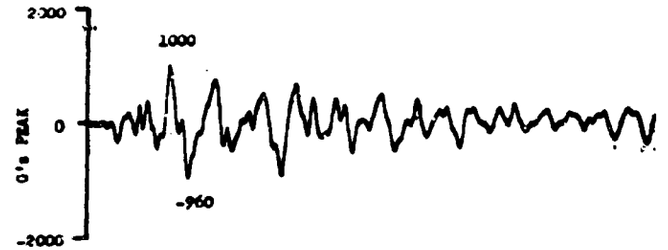

ACCELEROMETER NO. 7 (FRAME)

.005 SEC

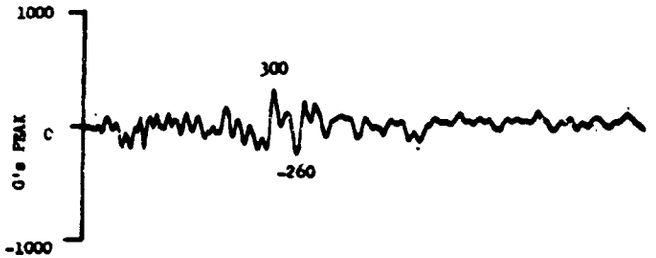

ACCELEROMETER NO. 8 (BOX E)

LMSC/A955903
SS-1386-6262
20 August 1969
page L-9

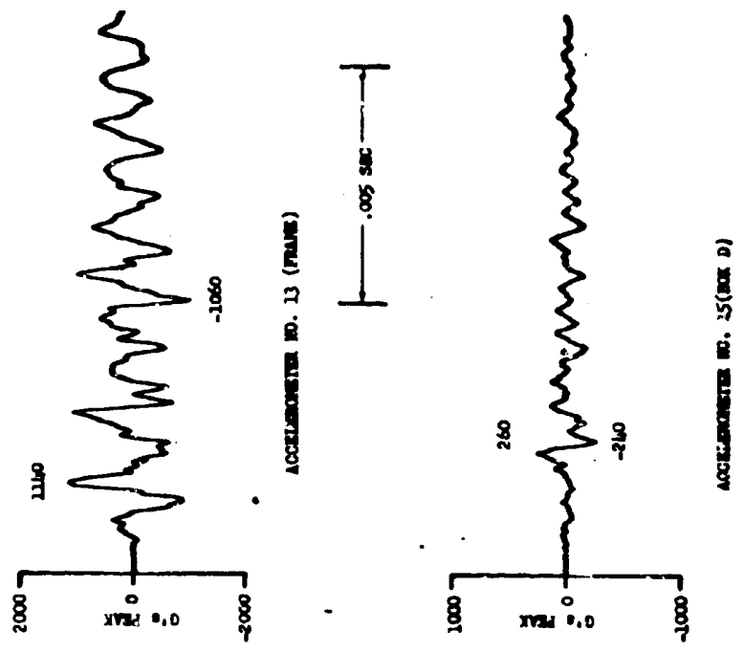
1140
-1060
0% PEAK
2000
-2000
ACCELEROMETER NO. 13 (FRAME)
.005 SEC
260
-240
0% PEAK
1000
-1000
ACCELEROMETER NO. 15(BOX D)

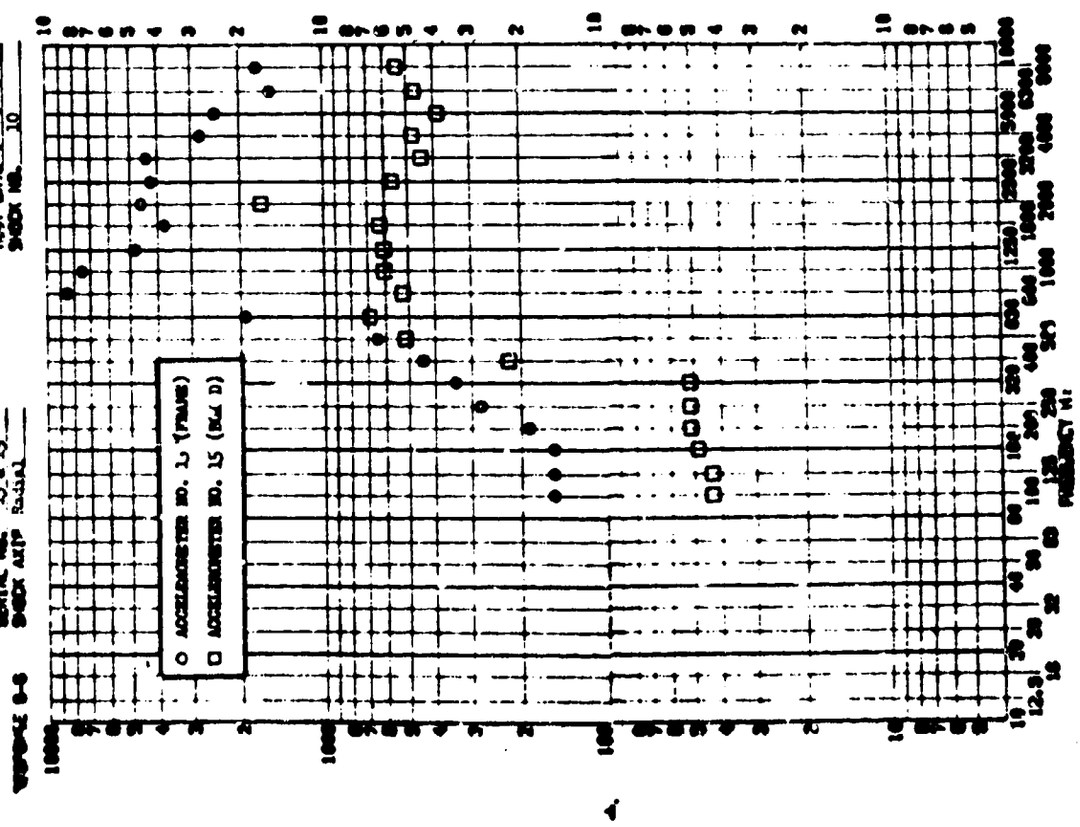
SHOCK TEST ANALYSIS DATA SHEET II.A.3.40
TEST ITEM 768-200,264
SERIAL NO. 13 & 15
SHOCK AXIS Radial
PART NO. Box D & Frame
TEST DATE 25 May 1966
SHOCK NO. 10
ACCELEROMETER NO. 13 (FRAME)
ACCELEROMETER NO. 15 (BOX D)
FREQUENCY IN

SHOCK TEST ANALYSIS DATA SHEET II.4.3.41

TEST ITEM 768-241,242,243,244 PART NO. STRUCTURE & EQUIPMENT
SERIAL NO. TEST DATE 25 MAY 1964
RESPONSE G-S SHOCK AXIS RADIAL SHOCK NO. 9 & 10

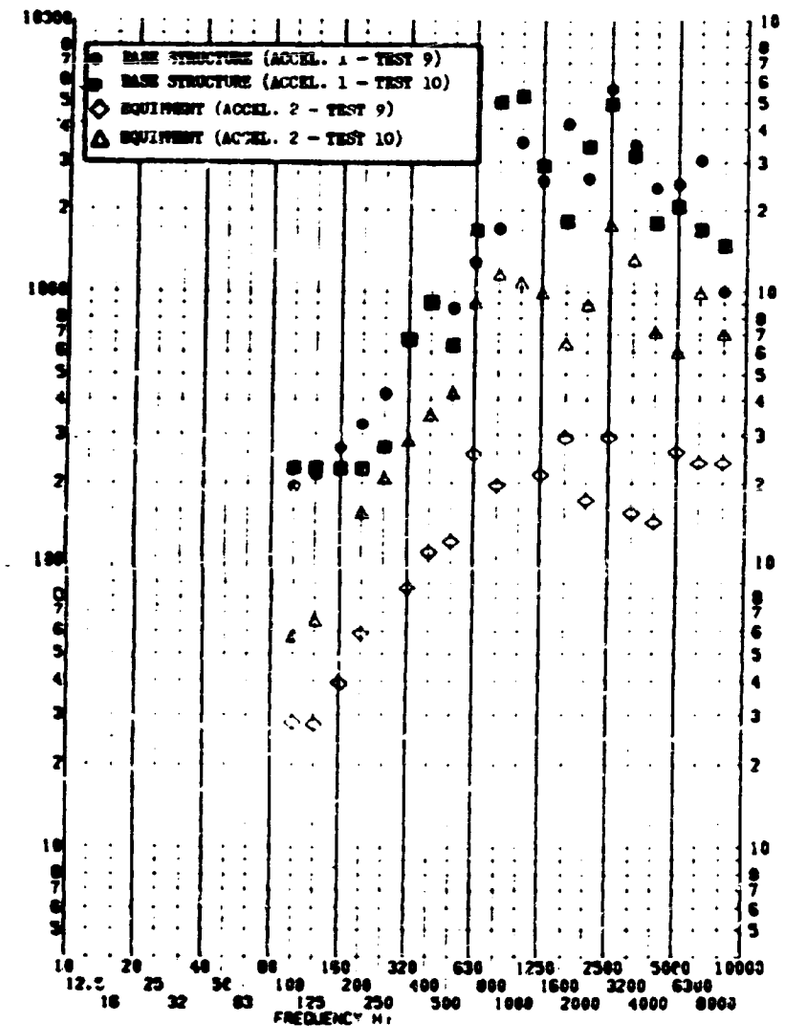

SHOCK TEST ANALYSIS DATA SHEET

TEST ITEM 768-241,242,245,246 PART NO. STRUCTURE & EQUIPMENT
SERIAL NO. TEST DATE 25 MAY 1964
RESPONSE G-S SHOCK AXIS RADIAL & LONGITUDINAL SHOCK NO. 9 & 10

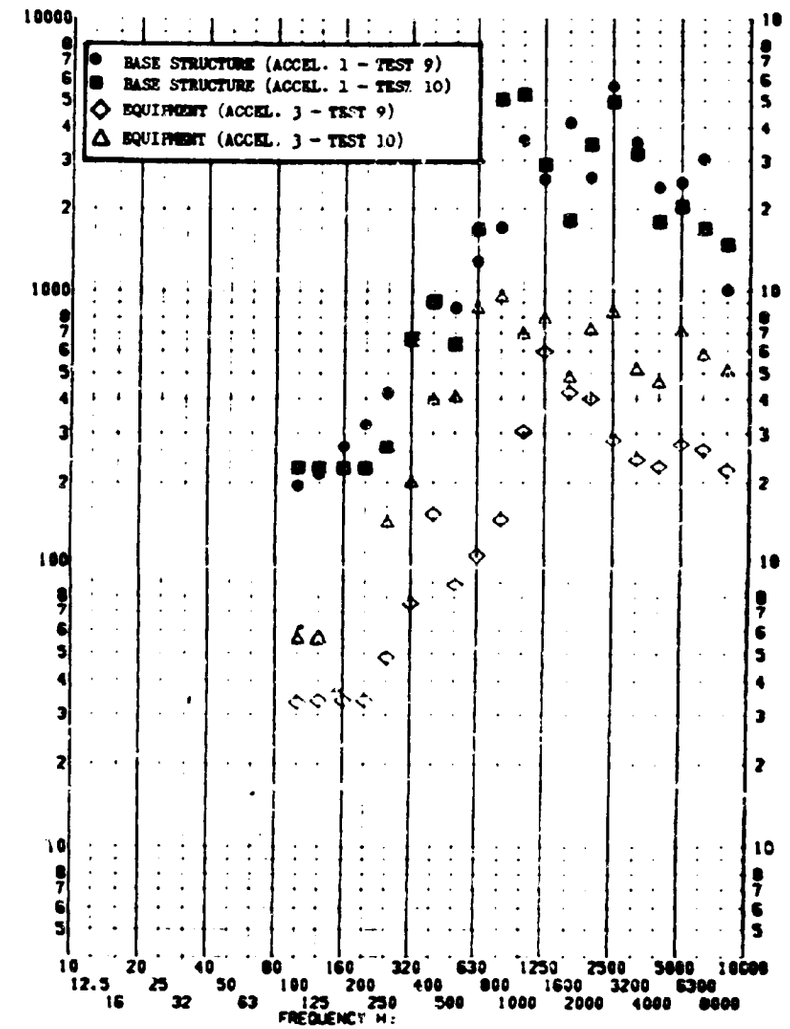

SHOCK TEST ANALYSIS DATA SHEET II.A.3.42

TEST ITEM 768-247,248,249,250 PART NO. STRUCTURE & EQUIPMENT
SERIAL NO. TEST DATE 25 MAY 1964
RESPONSE G-S SHOCK AXIS RADIAL SHOCK NO. 9 & 10

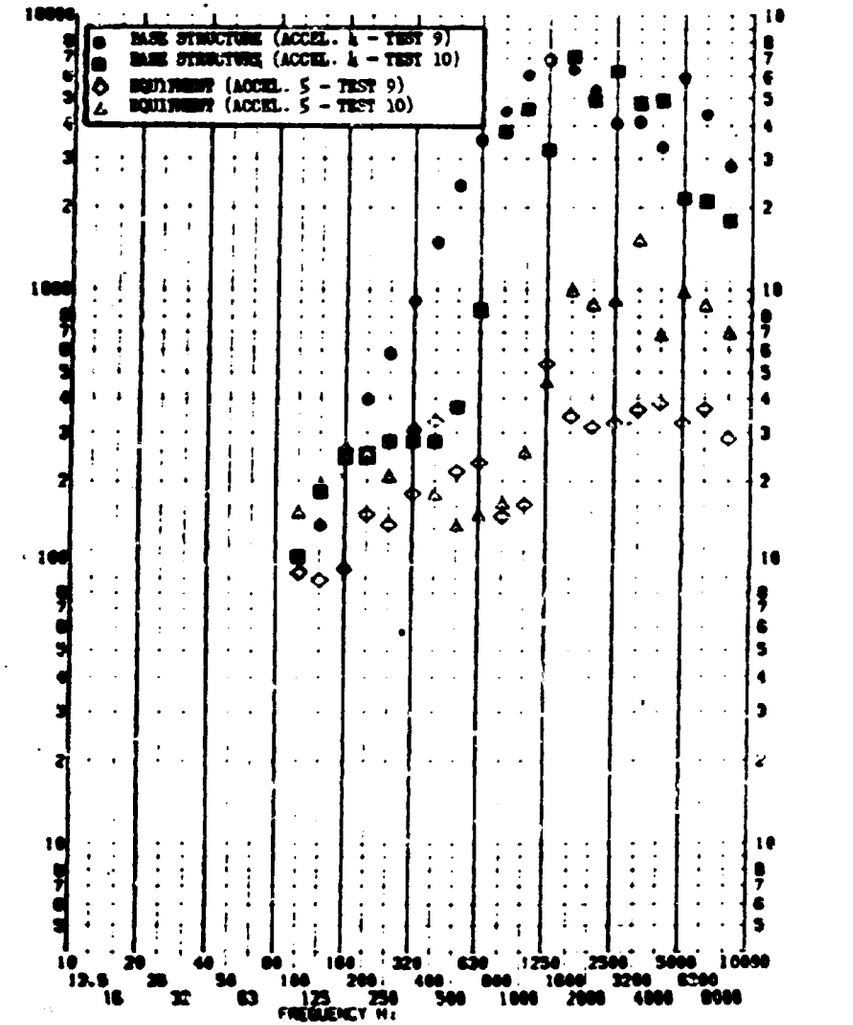

SHOCK TEST ANALYSIS DATA SHEET

TEST ITEM 768-247,248,251,252 PART NO. STRUCTURE & EQUIPMENT
SERIAL NO. TEST DATE 25 MAY 1964
RESPONSE G-S SHOCK AXIS RADIAL & LONGITUDINAL SHOCK NO. 9 & 10

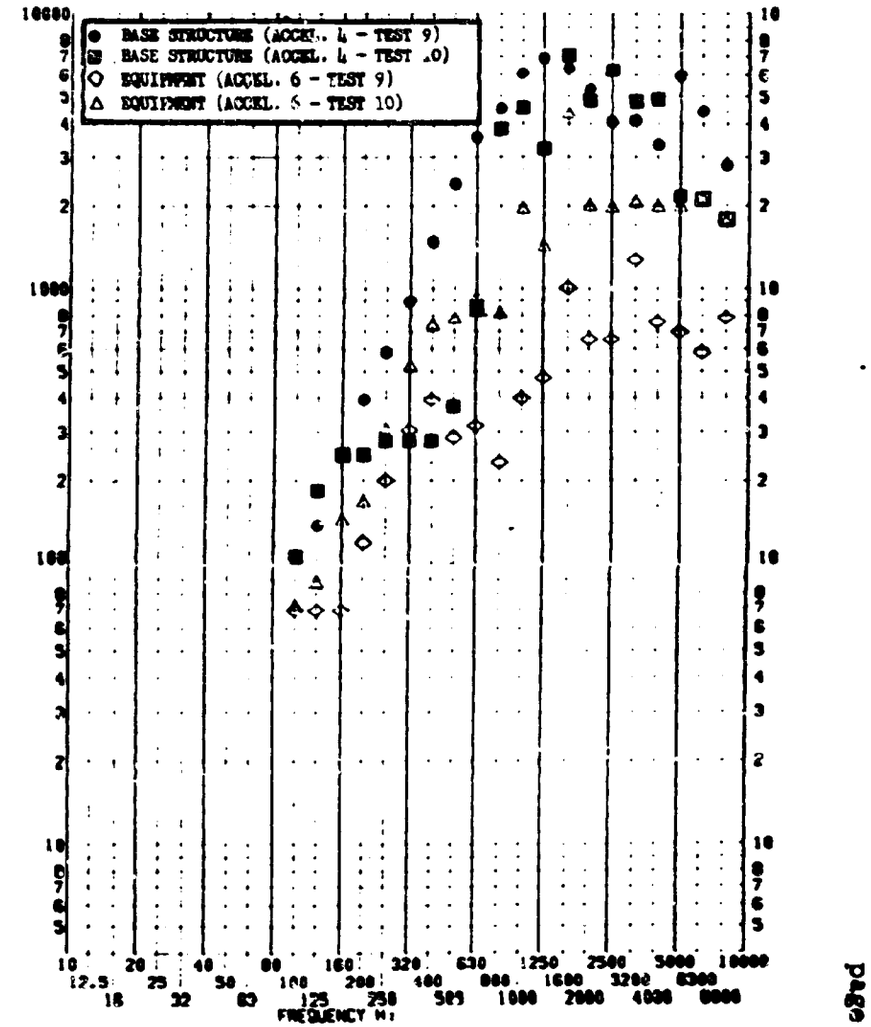

SHOCK TEST ANALYSIS DATA SHEET II.a.3.43

TEST ITEM 768-253,254,255,256 PART NO. STRUCTURE & EQUIPMENT
SERIAL NO. TEST DATE 25 OCT 1964
RESPONSE G-S SHOCK AXIS RADIAL SHOCK NO. 9 & 10

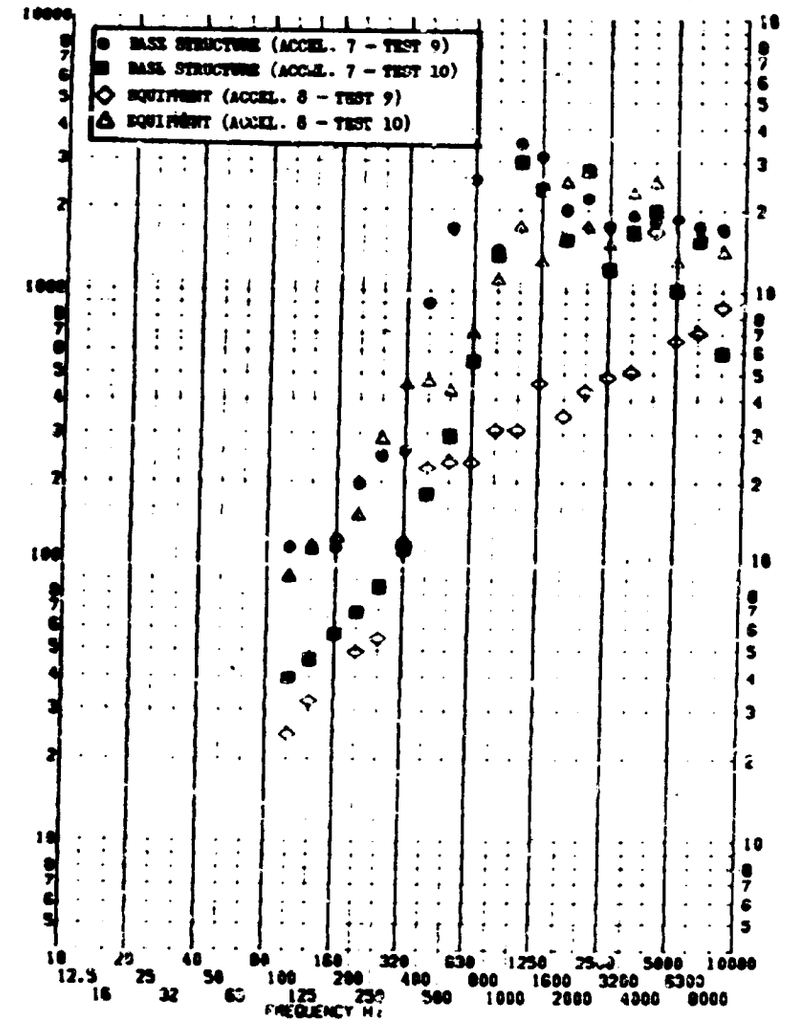

SHOCK TEST ANALYSIS DATA SHEET

TEST ITEM 768-253,254,257,258 PART NO. STRUCTURE & EQUIPMENT
SERIAL NO. TEST DATE 25 OCT 1964
RESPONSE G-S SHOCK AXIS RADIAL & LONGITUDINAL SHOCK NO. 9 & 10

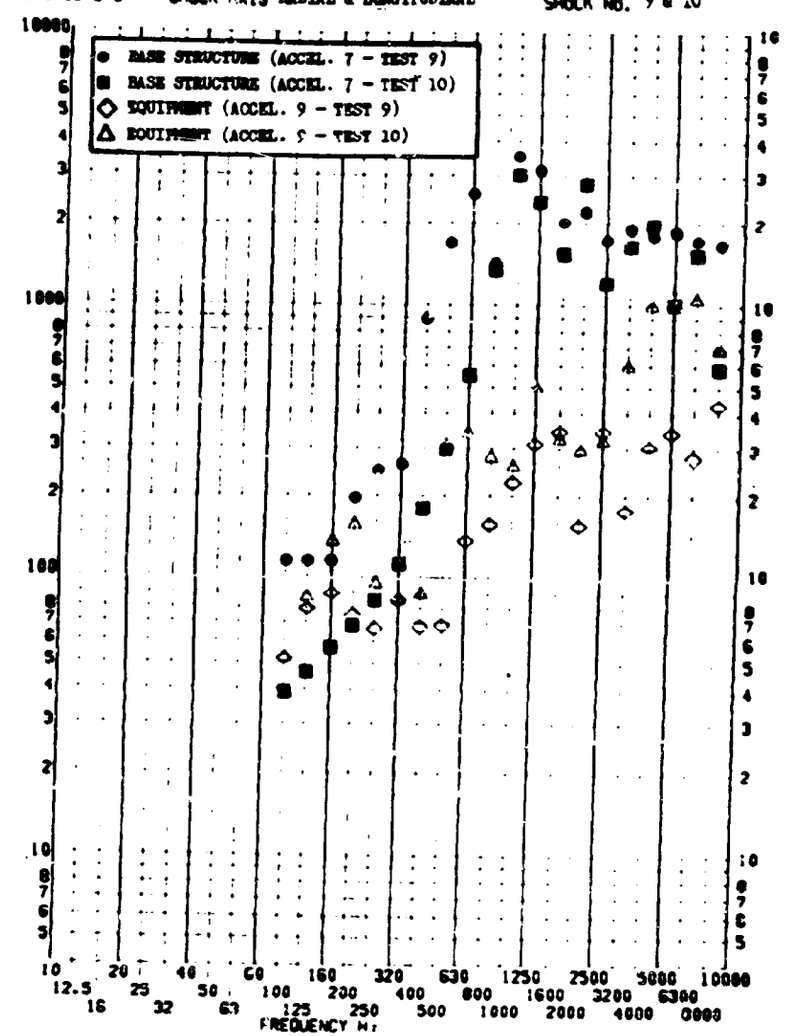

SHOCK TEST ANALYSIS DATA SHEET II.A.3.14

TEST ITEM 766-259,260,261,262
SERIAL NO.
SHOCK AXIS RADIAL

PART NO. STRUCTURE & EQUIPMENT
TEST DATE 25 OCT 1964
SHOCK NO. 9 & 10

RESPONSE G-S

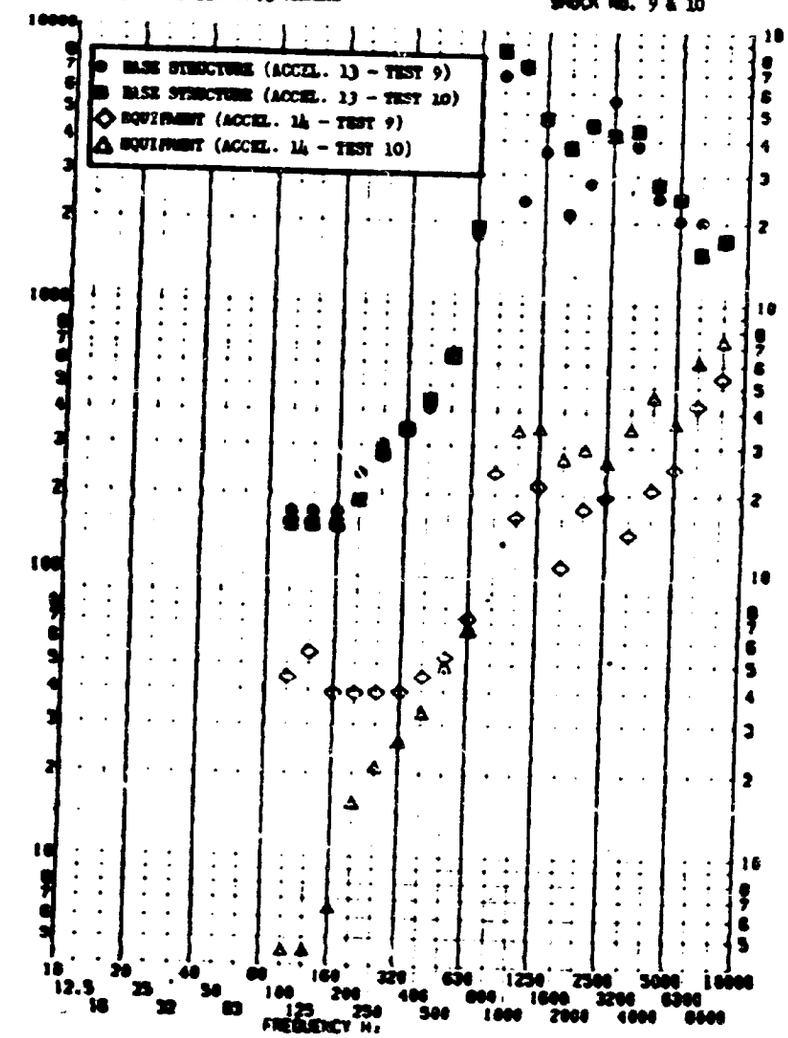

SHOCK TEST ANALYSIS DATA SHEET

TEST ITEM 766-259,260,263,264
SERIAL NO.
SHOCK AXIS RADIAL & LONGITUDINAL

PART NO. STRUCTURE & EQUIPMENT
TEST DATE 25 OCT 1964
SHOCK NO. 9 & 10

RESPONSE G-S

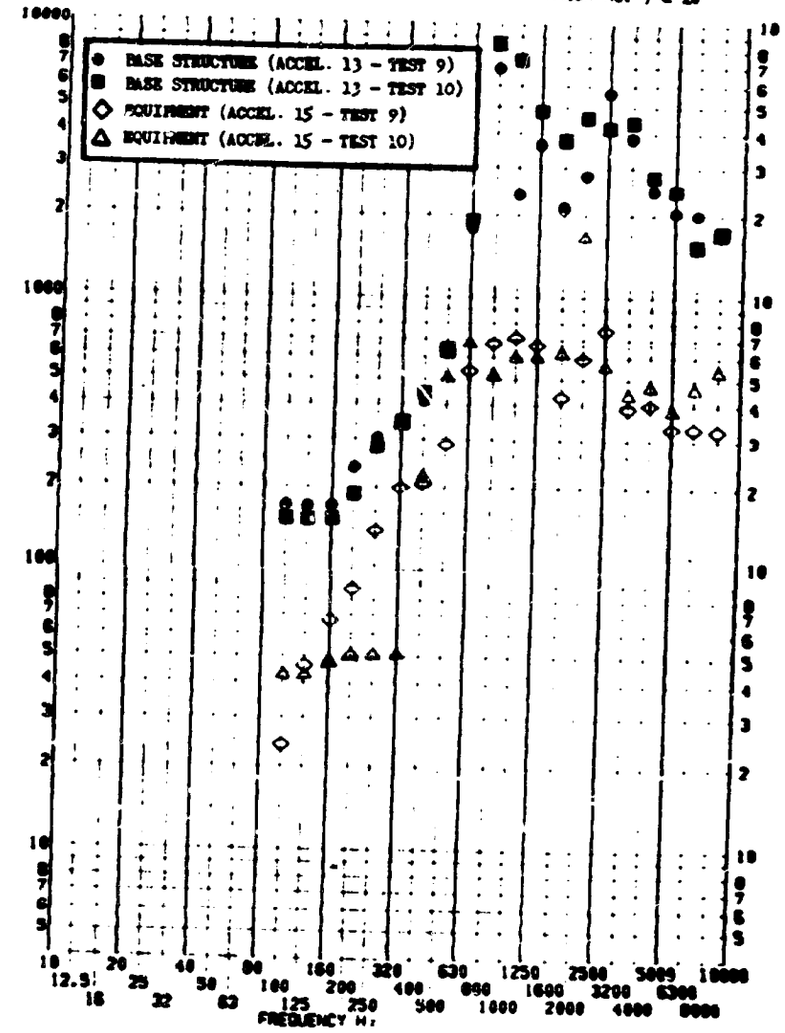

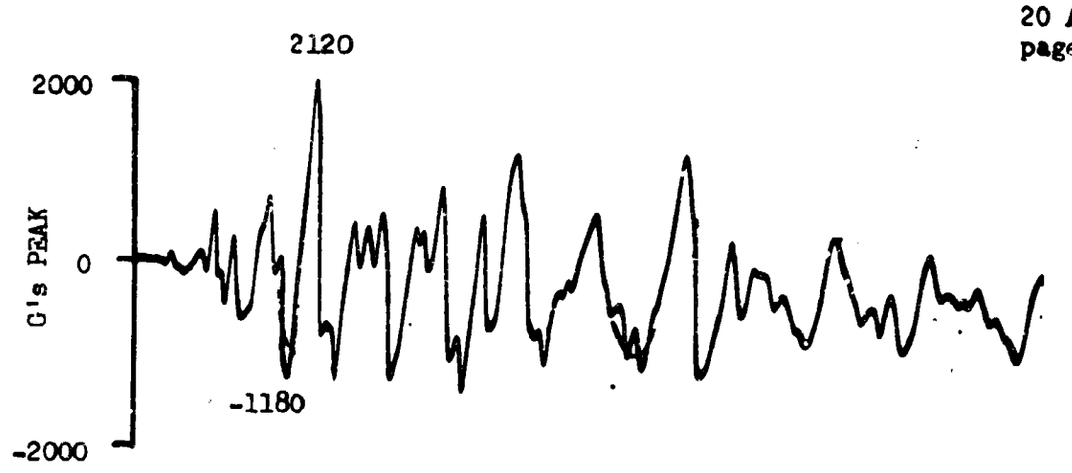

ACCELEROMETER NO. 10 (RADIAL ON FRAME)

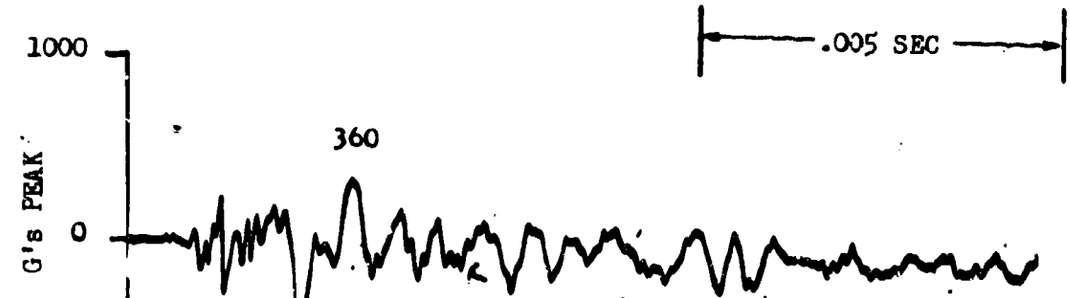

ACCELEROMETER NO. 11 (RADIAL ON BOX C)

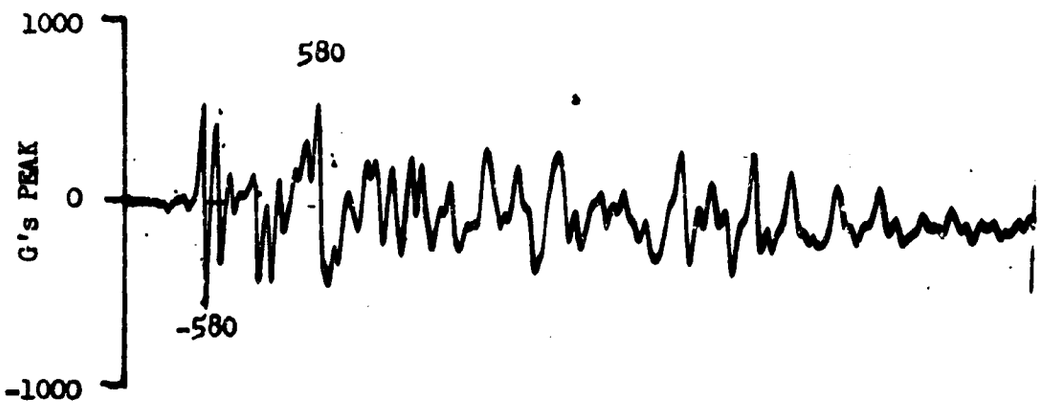

ACCELEROMETER NO. 12 (LONG. ON BOX C)

Figure II.A.3.45 SHOCK LEVELS FOR TEST NO. 10

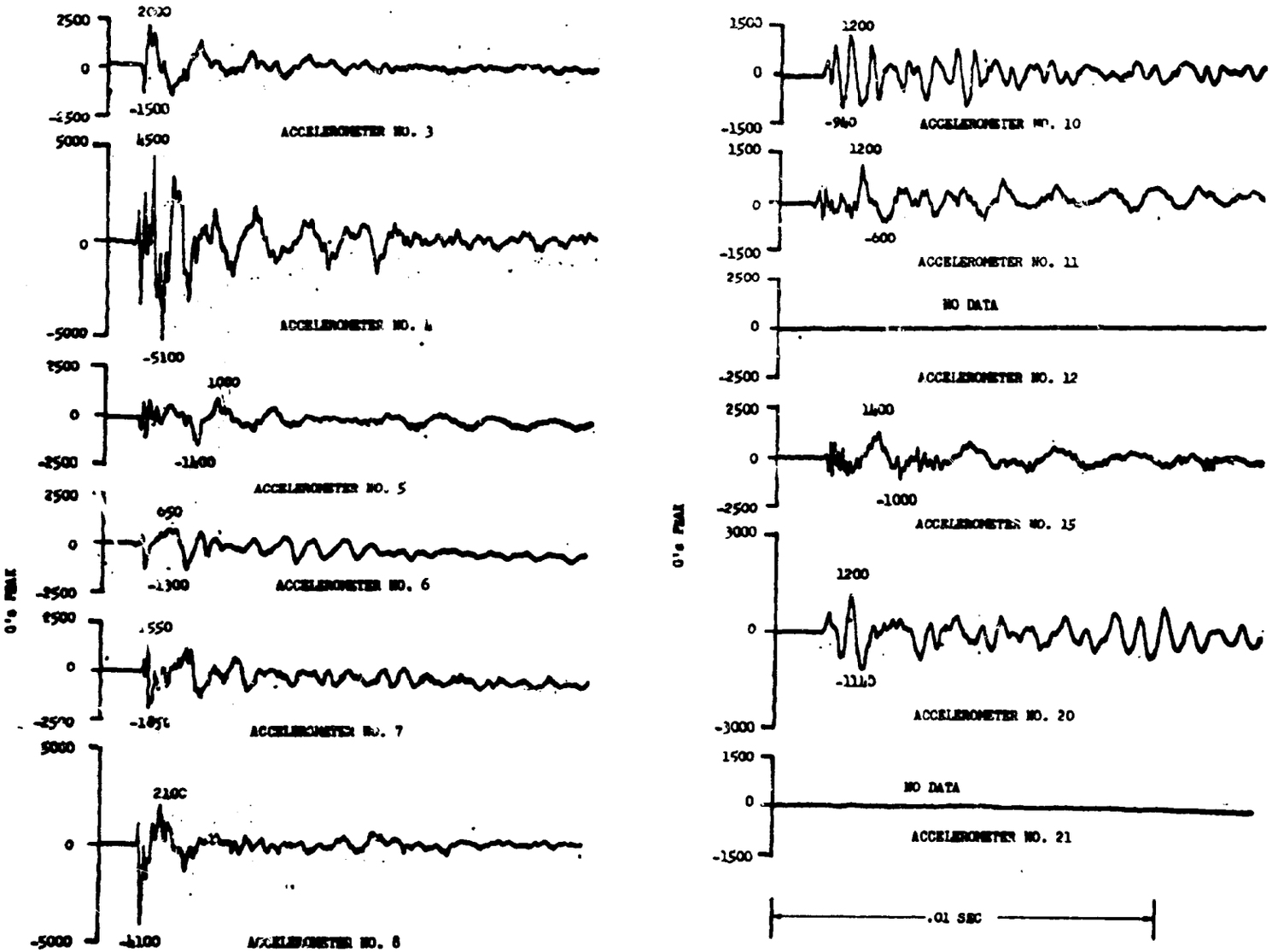

Figure II.A.3.46 Shock Levels for Test No. 1

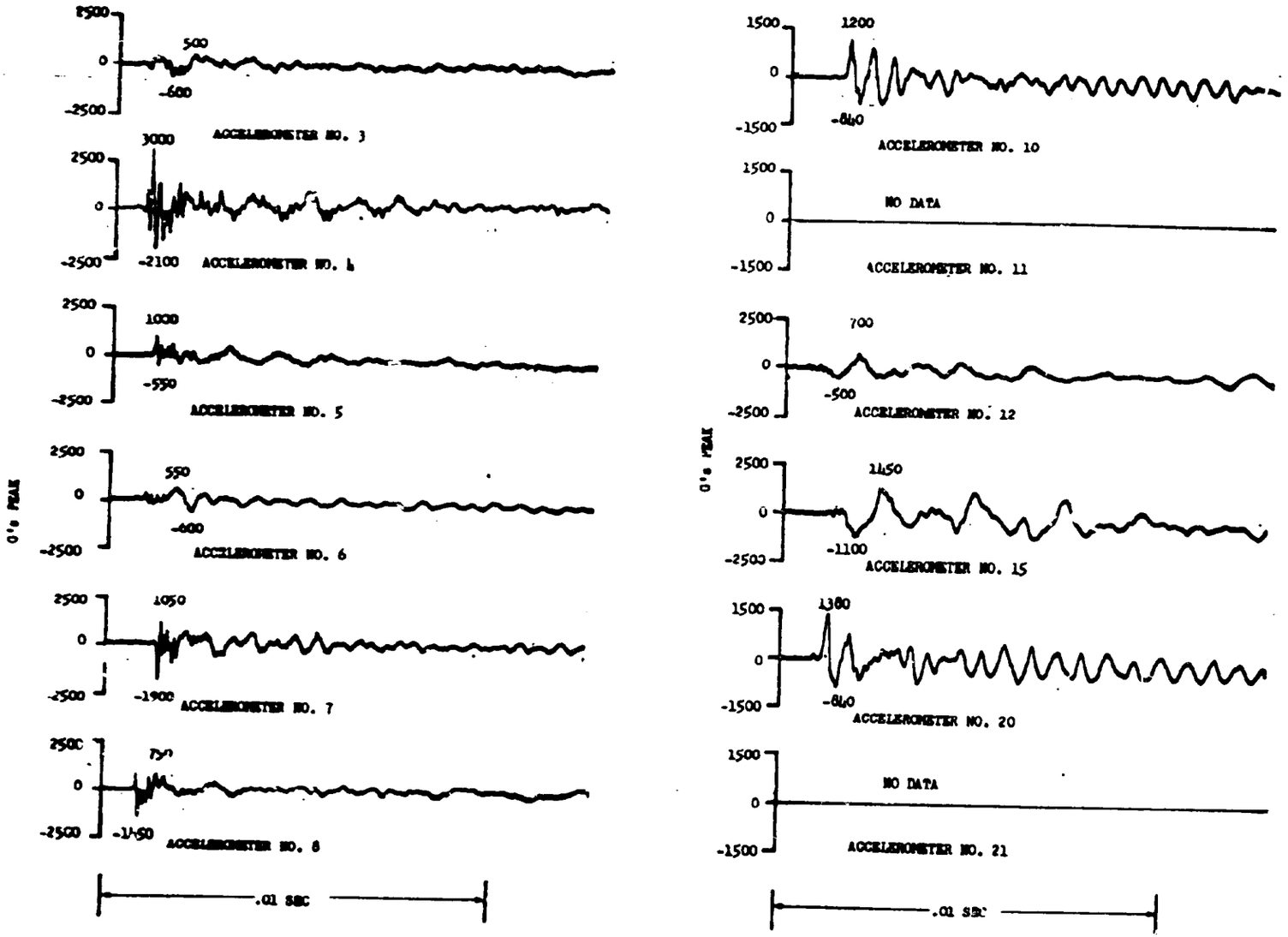

Figure II.A.3.47 Shock Levels from Test No. 2

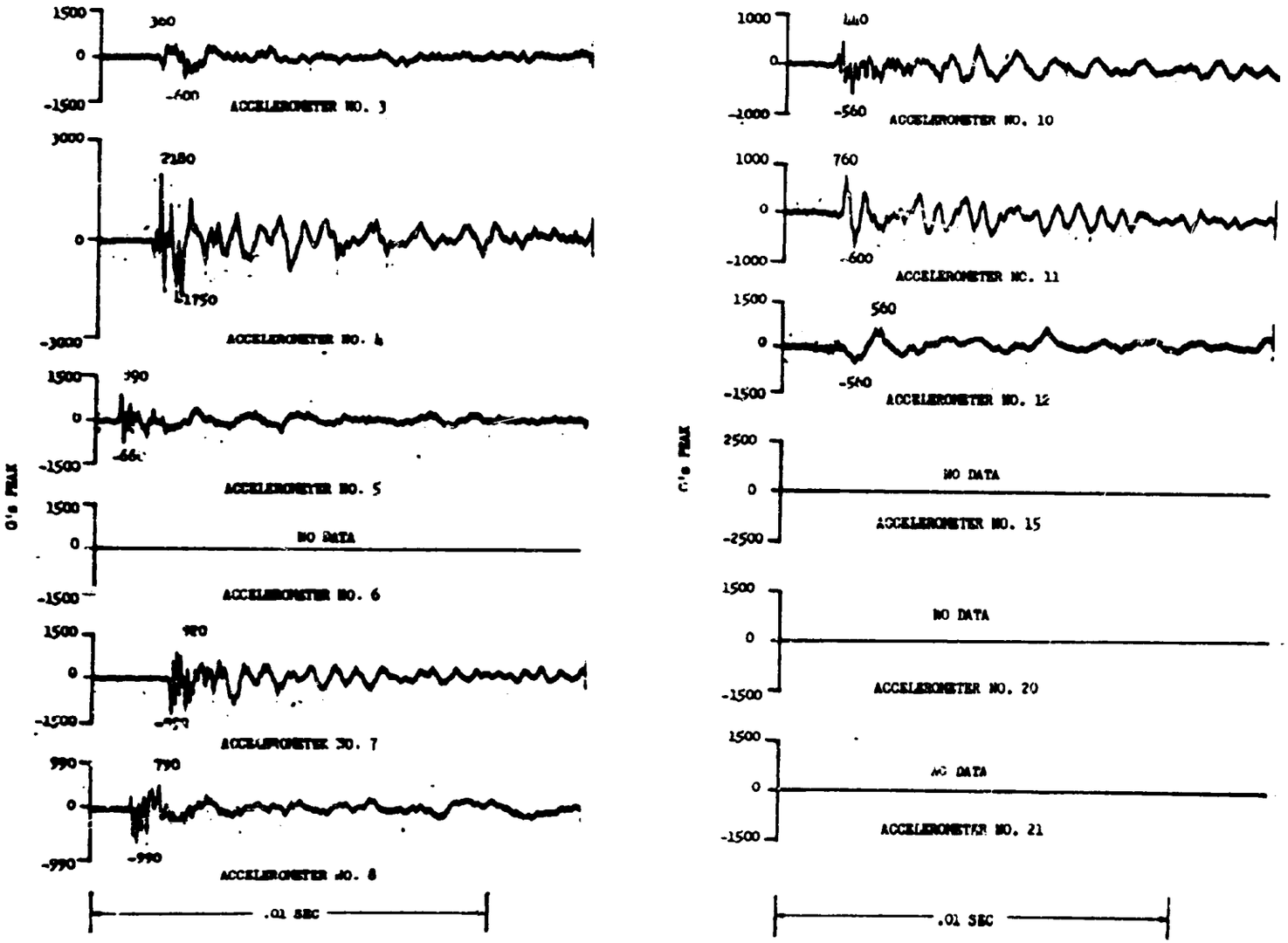

Figure II.A.3.48 Shock Levels from Test 3

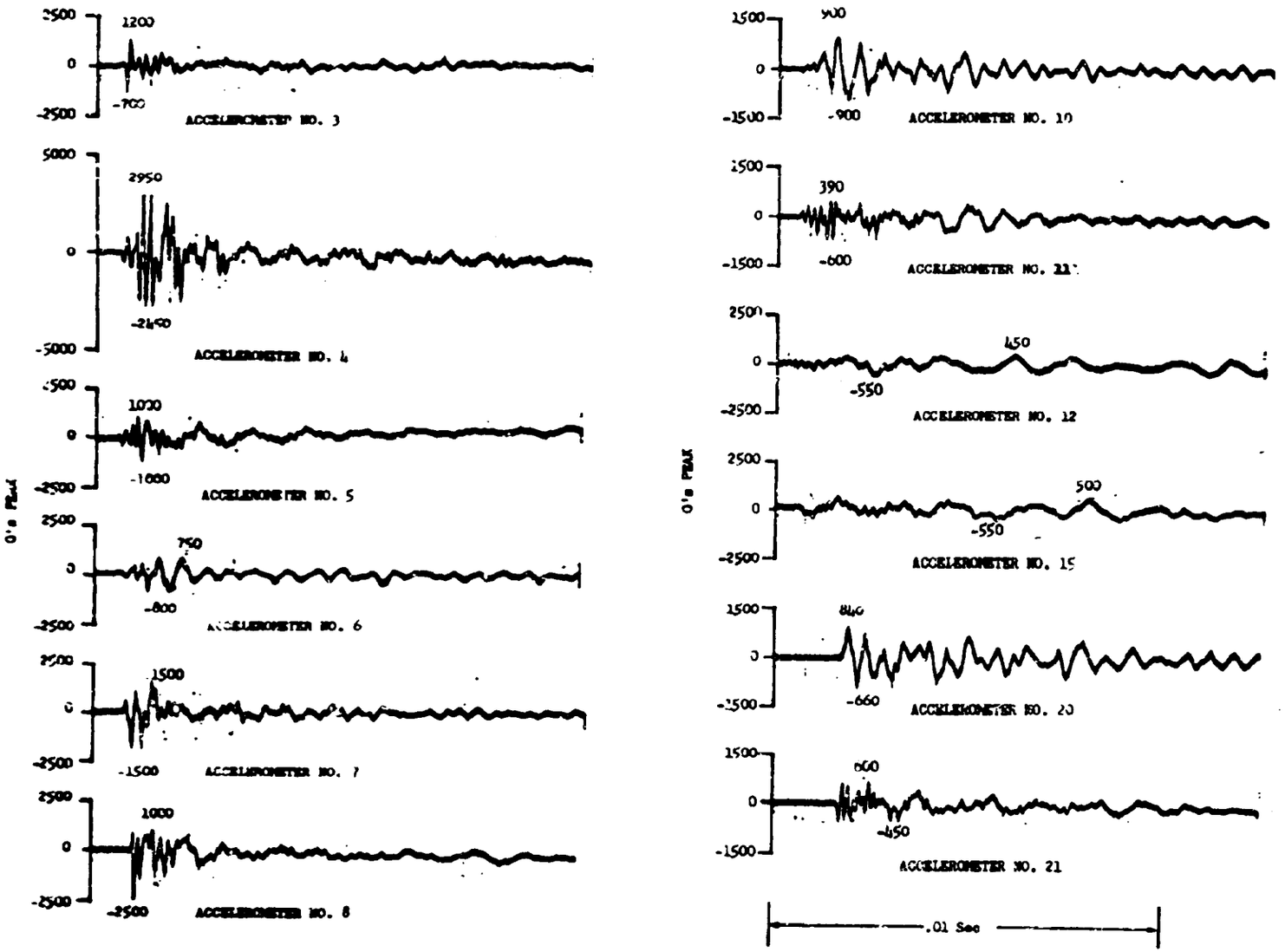

Figure II.A.3.49 Shock Levels from Test No. 4

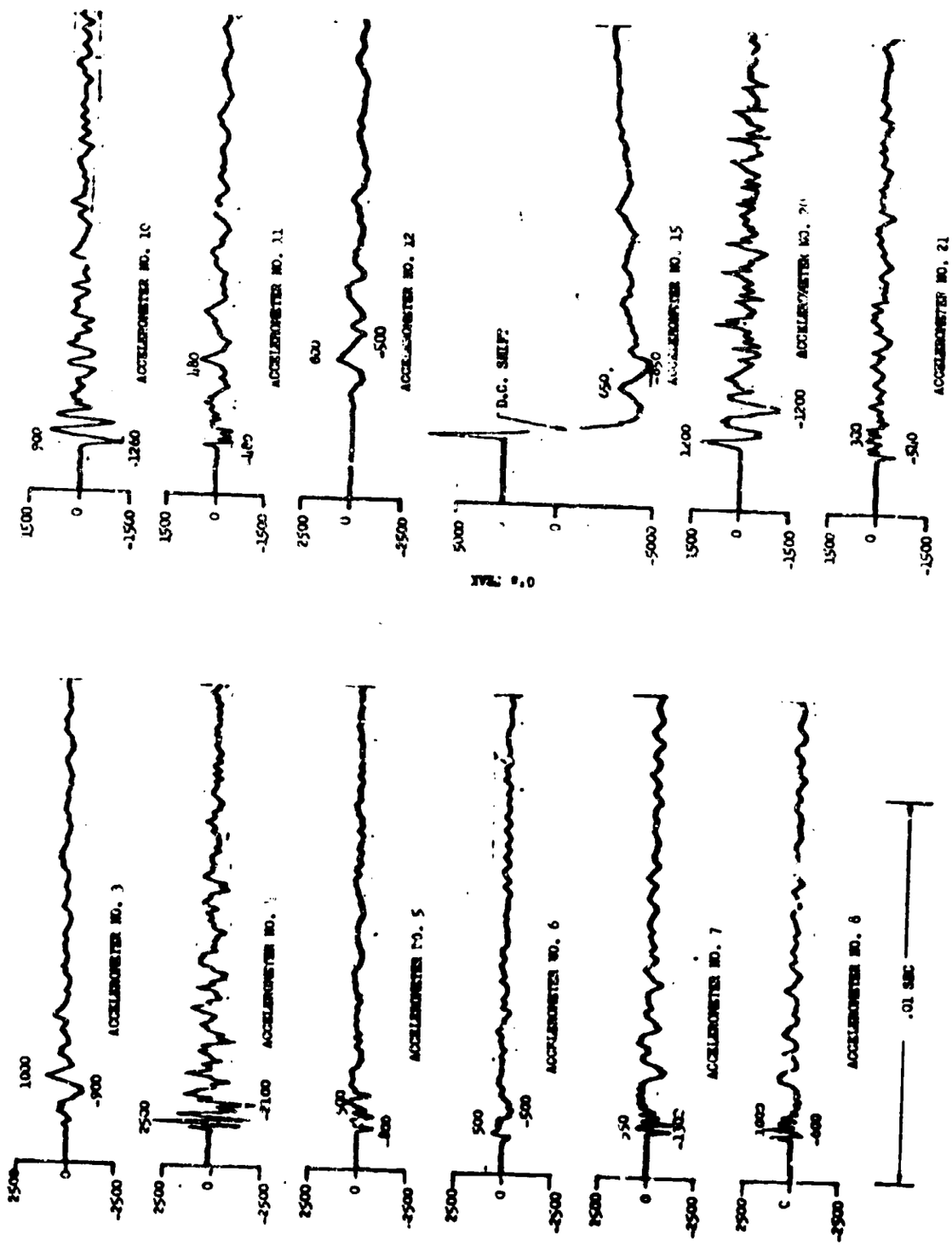

Figure II.A.3.5G Shock Levels from Test No. 5

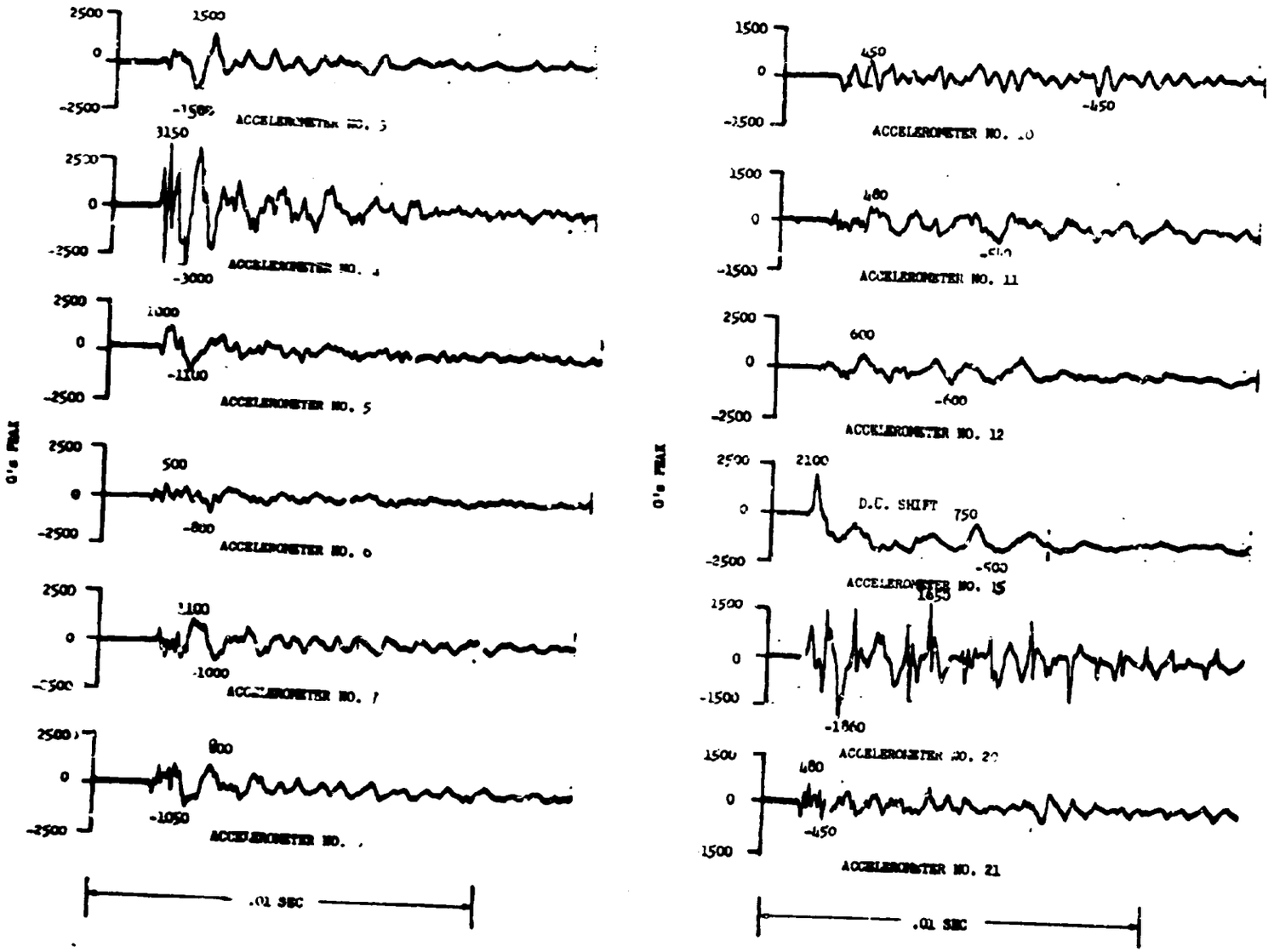

Figure II.A.3.51 Shock Levels from Test No. 6

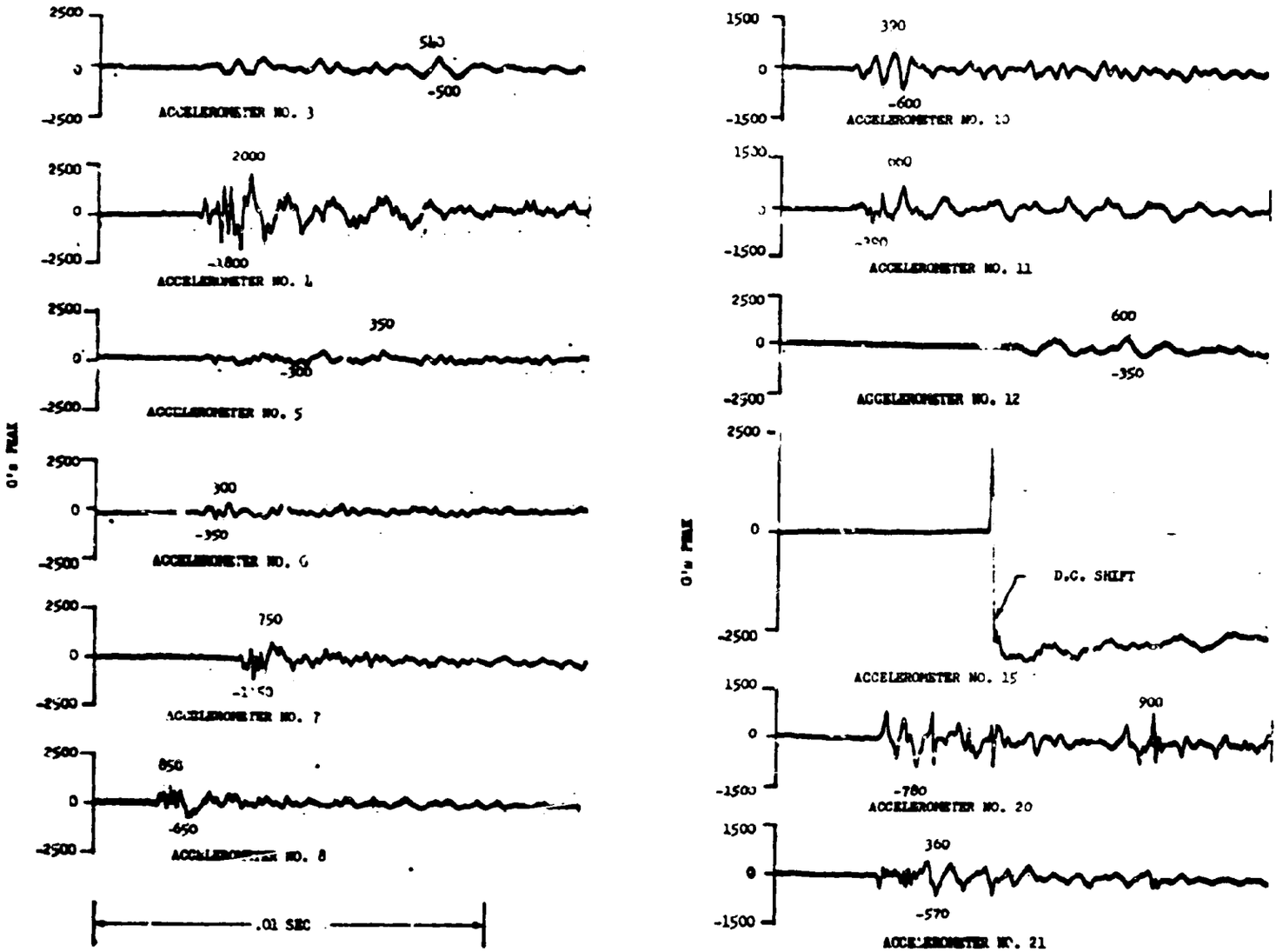

Figure II.A.3.52 Shock Levels from Test No. 7

SECTION NO. II.A.4

REPORT NO. 790

SUBJECT:

DYNAMIC EVALUATION OF THE V-BAND, EXPANDER TUBE,

AND SPRING CLAMP SEPARATION JOINTS

SECTION II.A.4

SUMMARY

A series of five booster adapter separation tests were conducted to evaluate three separation joint configurations (Figure II.A.4.1) with the intention of reducing significantly the shock originating from booster adapter separation. A summary of the tests which were performed is presented in Table II.A.4.2. The shock levels produced by the separation joints from Tests 2, 3 and 4 were compared with the shock levels obtained at the same measurement locations during the standard MDF separation joint Test 1. Comparisons were made by averaging all the measurements from each test by 1/3 octave bands.

The results of these tests (Figure II.A.4.3) indicate that the spring clamp joint most significantly reduced the shock levels over the entire frequency spectrum with shock reduction ranging from a factor of 1.4 in the 90 to 112 frequency band on up to 14.8 in the 710 to 900 Hz band. The average reduction over the entire frequency spectrum was 6.70. The spring clamp configuration, although it produced the desired shock reduction, did not provide the axial support that was needed in the booster adapter separation joint.

The expander tube configuration proved to be very comparable to the spring clamp in its ability to reduce the shock environment. Shock reduction ranged from a factor of 1.50 in the 140 to 180 Hz range to 12.83 in the 710 to 900 Hz range with an average reduction over the frequency spectrum of 5.95.

The V band produced the least shock reduction. The V band produced higher shock levels than the standard joint below 355 Hz by as much as a factor of 3.14, while above 355 Hz the V band reduced the shock by only as much as a factor of 5.33 in the 1800 to 2250 Hz range. The higher shock levels produced by the V band separation in the low frequencies would have required that all thrust cone and aft rack equipment be requalified to the higher shock levels were this configuration to replace the standard MDF joint.

TABLE OF CONTENTS

SECTION II.A.4

LIST OF TABLES

SECTION II.A.4

LIST OF FIGURES

SECTION II.A.4

LIST OF FIGURES (Cont.)

SECTION II.A.4

LIST OF FIGURES (Cont.)

SECTION II.A.4

II.A.4.1 INTRODUCTION

Booster adapter separation shock development tests were conducted with three different joint configurations (shown in Figure II.A.4.1). Five tests were conducted (see Table II.A.4.2 for testing sequence). Measurements were made at seven locations as shown in Figure II.A.4.2. Data was lost from one of the measurements from the baseline test, therefore only the six good data channels were used for comparison. The fifth test (referred to as Test 4A) was a test of the V-band under ascent heating conditions. The purpose of this test was to confirm that the V-band would operate properly in the ascent thermal environment. The data from this test was not used for comparison with the standard joint test. The analysis was based on shock spectra of each of the measurements.

II.A.4.2 DISCUSSION AND ANALYSIS

II.A.4.2.1 Test Set-Up and Instrumentation

The test specimen consisted of an aft rack, engine thrust cone, and booster adapter segment. The booster adapter segment was modified to accept installation of the test specimen separation joint rings. The separation joint configurations are shown in Figure II.A.4.1.

Seven Endevco 2225 piezoelectric accelerometers were located as shown in Figure II.A.4.2 and indicated in Table II.A.4.1. Flow charts of the data acquisition and data reduction systems which were used in these tests are shown in Section V of this report.

II.A.4.2.2 Analysis Methods

The data from Tests 1 through 4 was analyzed by means of high speed oscillograph records and shock spectra of the seven accelerometer measurements. The oscillograms, along with their respective shock spectra, are presented in Figures II.A.4.4 to II.A.4.30. Only oscillograph records were obtained from Test 4A, the elevated temperature test of the V-band, since the oscillograms indicated that the elevated temperatures had little effect on the shock levels. These oscillograms are presented in Figure II.A.4.42. The shock spectrum data from the spring clamp, expander tube, and V-band joints were then compared to the data of the standard separation joint.* This was accomplished by averaging the shock spectrum data in each 1/3 octave band from the accelerometers which corresponded to the six accelerometers of the standard separation joint test (see Table II.A.4.4). The shock spectrum data from the standard joint was then ratioed to the averaged data from each of the three separation tests by 1/3 octaves. Figure II.A.4.3 presents the results of this analysis. Anything above 1.0 on the vertical axis represents a reduction under the standard MDF separation joint shock levels whereas anything below 1.0 represents an increase over the standard joint shock levels. Peak g readings for all tests and all measurements are presented in Table II.A.4.3.

* Figures II.A.4.31 through II.A.4.37.

II.A.4.2.3 Test Conditions and Results

Test 1

Test 1 was conducted with the standard pyrotechnic separation joint. A 10 grain/foot MDF which goes around the entire circumference of the booster adapter fractures the adapter skin at the separation plane to produce separation. See Figure II.A.4.1 for details of the standard joint.

Test 1 apparently produced nominal shock levels representative of levels obtained during previous tests of the same joint. No data was received from accelerometer No. 30. The data from the remaining six accelerometers was averaged and compared with data from each of the three experimental joint configurations. Data from the other joints was normalized to the standard joint shock which is represented as the straight line at 1.0 in Figure II.A.4.3.

Test 2

Test 2 was performed with the spring clamp joint which is illustrated in Figure II.A.4.1. Deployment and disengagement of the forward and aft rings results from the unwrapping spring action of the clamp subsequent to the firing of two explosive nuts engaged on a common stud.

The results of Test 2 are presented in Table II.A.4.4 as an average of the six accelerometer shock levels by 1/3 octave bands and in Figure II.A.4.3 as a ratio between the standard joint and the spring clamp joint. Figure II.A.4.3 indicates that this joint configuration was most effective of all the joints tested in reducing the separation joint shock levels. Shock reduction was most effective above 560 Hz with a maximum reduction by a factor of 14.8 in the 710 to 900 Hz range. Shock reduction below 560 Hz varied from 3.54 down to 1.4. Average shock reduction over the entire frequency spectrum was 6.7.

Unfortunately the spring clamp joint does not provide the structural support in the axial direction which is required at the separation joint and, until the spring clamp system could be modified to provide the needed support, it could not be incorporated into the vehicle.

Test 3

Test 3 was achieved with the expander tube joint illustrated in Figure II.A.4.1. Booster adapter separation resulted from the squib activated value release of high pressure nitrogen within a confined elastic expander tube. The resultant expansion of the expander tube causes a series of 28 curved 6 1/4 inch by 3 7/16 inch notched beryllium panels to fracture at the separation plane.

The results of Test 3 are presented in Tables II.A.4.3 and II.A.4.4 and in Figure II.A.4.3. Figure II.A.4.3 indicates that the expander tube joint was almost as effective as the spring clamp joint in reducing the shock levels. As with the spring clamp joint, the expander tube joint was most effective in the higher frequencies with a maximum shock reduction of 12.83 in the 710 to 900 Hz range. The shock reduction in the lower frequencies, while less than in the higher frequencies (as low as 1.9 in the 140 to 180 Hz range), were greater than for the spring clamp. The average shock reduction for the expander tube over the entire frequency range was 5.95 as compared to 6.70 for the spring clamp.

Tests 4 and 4A

Tests 4 and 4A were conducted with the V-band joint illustrated in Figure II.A.4.1. The clamp strap was stressed to 16,000 psi tension to insure adequate engagement of the segmented clamp shoes with the forward and aft rings. Booster-adapter separation with the V-band was achieved by the release of band tension through the simultaneous firing of two diametrically opposed explosive nuts. Test 4 was conducted at ambient temperature while Test 4A was conducted at elevated temperatures to simulate the ascent thermal environment.

The results of Test 4 and 4A are presented in Tables II.A.4.3 and II.A.4.4 and Figure II.A.4.3. Comparison of the oscillographs of Test 4 and Test 4A (Table II.A.4.3) indicate very little difference in shock levels between the two tests. As a result it was not necessary to produce shock spectra for Test 4A and no comparisons were made for that test.

Comparison of the V-band tests with the spring clamp and the expander tube tests (Figure II.A.4.3) indicate that the V-band was not as effective in reducing the shock levels. In the higher frequencies a maximum shock reduction of only 5.33 was noted while below 355 Hz the shock levels were greater than were observed with the standard MDF joint. An amplification of 3.1 was observed in the 90 to 112 Hz band. The high levels in the low frequency region are almost certainly due to a low frequency (approximately 100 Hz) ring mode vibration which is created when the pre-load tension is released in the V-band. All radially mounted accelerometers showed the motion.

If the V-band joint configuration were selected for use it would have been necessary to increase the severity of the vibration criteria which was used in the vehicle environmental specification at that time for engine-cone mounted equipment.

II.A.4.3 CONCLUSIONS

The spring clamp and the expander tube were most effective in reducing the shock levels which originate from booster-adapter separation.

The spring clamp separation joint does not provide the required structural stiffness in the axial direction. Additional modifications would have to be made to this joint followed by additional testing before it could replace the standard MDF joint.

The V-band showed the least shock reduction. In the lower frequencies the shock levels are more severe than they are for the standard MDF joint.

In general all three of the new joints tested demonstrated effectiveness in reducing the overall shock environment which originates from booster-adapter separation.

TABLE II.A.4.1

ACCELEROMETERS & LOCATIONS

Accelerometer No.	Station	Direction	Distance to Shock Source	Accelerometer Type
3	390	Radial	6	ENDEVCO 2225
5	390	Longitudinal	6	ENDEVCO 2225
10	412	Longitudinal	28	ENDEVCO 2225
11	412	Radial	28	ENDEVCO 2225
15	396	Radial	12	ENDEVCO 2225
20	412	Longitudinal	28	ENDEVCO 2225
30	398	Radial	4	ENDEVCO 2225

TABLE II.A.4.2

SUMMARY OF TESTS

Test No.	Configuration	Explosive Size	Test Purpose	Shock Isolation	Joint Type
1	1	10 Gr/Ft MDF	Structure	None	STD Joint
2	2	2XP Nuts	Structure	None	Spring Clamp Hot
3	3	SQUIB	Structure	None	Expander Tube
4	4	2XP Nuts	Structure	None	Cold V Band
4A	4	2XP Nuts	Structure	None	Hot V Band

TABLE II.A.4.3

SUMMARY OF PEAK G READINGS

Accelerometer No.	Distance to Shock Source (Inches)	PEAK G READINGS				
		TEST 1 Standard Joint	TEST 2 Spring Clamp	TEST 3 Expander Tube	TEST 4 V-Band Ambient	TEST 4A V-Band Heated
3	6	2100	190	130	570	570
5	6	1300	150	215	480	510
10	28	1200	176	100	260	310
11	28	1200	134	60	180	200
15	12	1400	105	360	560	440
20	28	1140	585	90	200	400
30	4		50	348	900	930

TABLE II.A.4.4

AVERAGED 1/3 OCTAVE SHOCK SPECTRUM DATA

1/3 OCTAVE BAND CENTER FREQUENCY	TEST NUMBER 1	2	3	4
100	46	33	21	142
125	69	48	42	124
160	110	77	73	142
200	166	95	92	200
250	245	111	111	246
320	401	171	206	418
400	759	217	258	502
500	1398	394	473	812
630	2468	254	447	912
800	3902	264	304	1076
1000	2422	416	331	928
1250	2753	337	310	873
1600	3165	402	425	981
2000	3839	359	303	719
2500	3326	417	416	824
3200	3120	350	346	810
4000	2911	299	323	830
5000	3004	298	355	820
6300	4179	313	466	804
8000	3095	393	724	913
10000	3634	435	474	1022

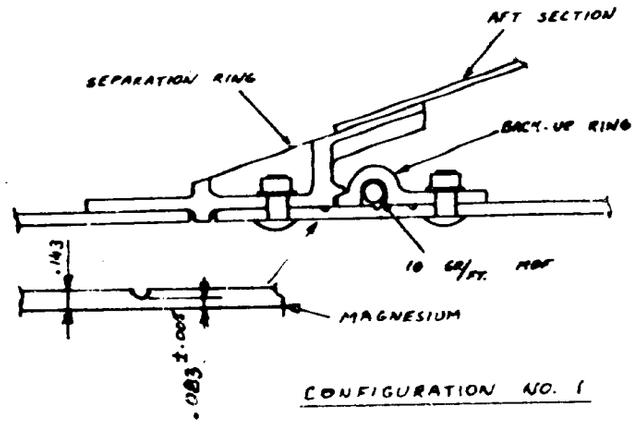

CONFIGURATION NO. 1

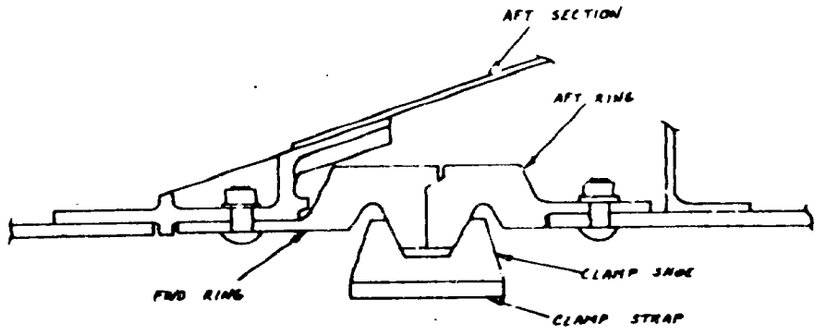

CONFIGURATION NO. 4

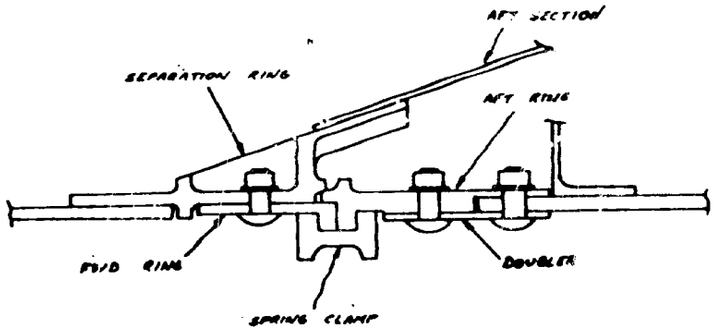

CONFIGURATION NO. 2

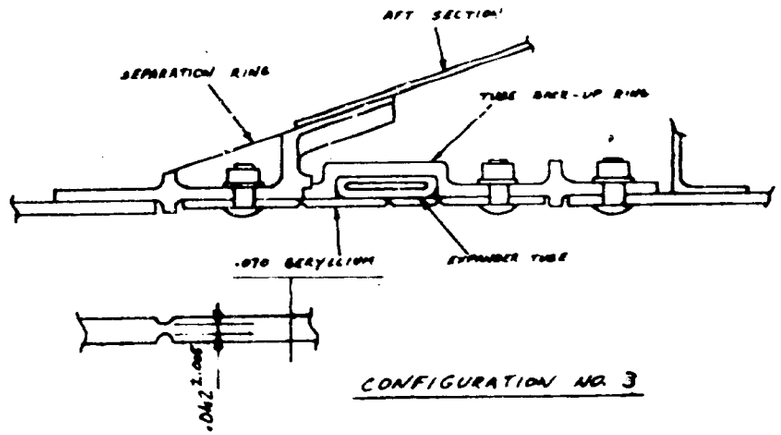

CONFIGURATION NO. 3

Figure II.A.4.1 BOOSTER SEPARATION JOINT CONFIGURATIONS

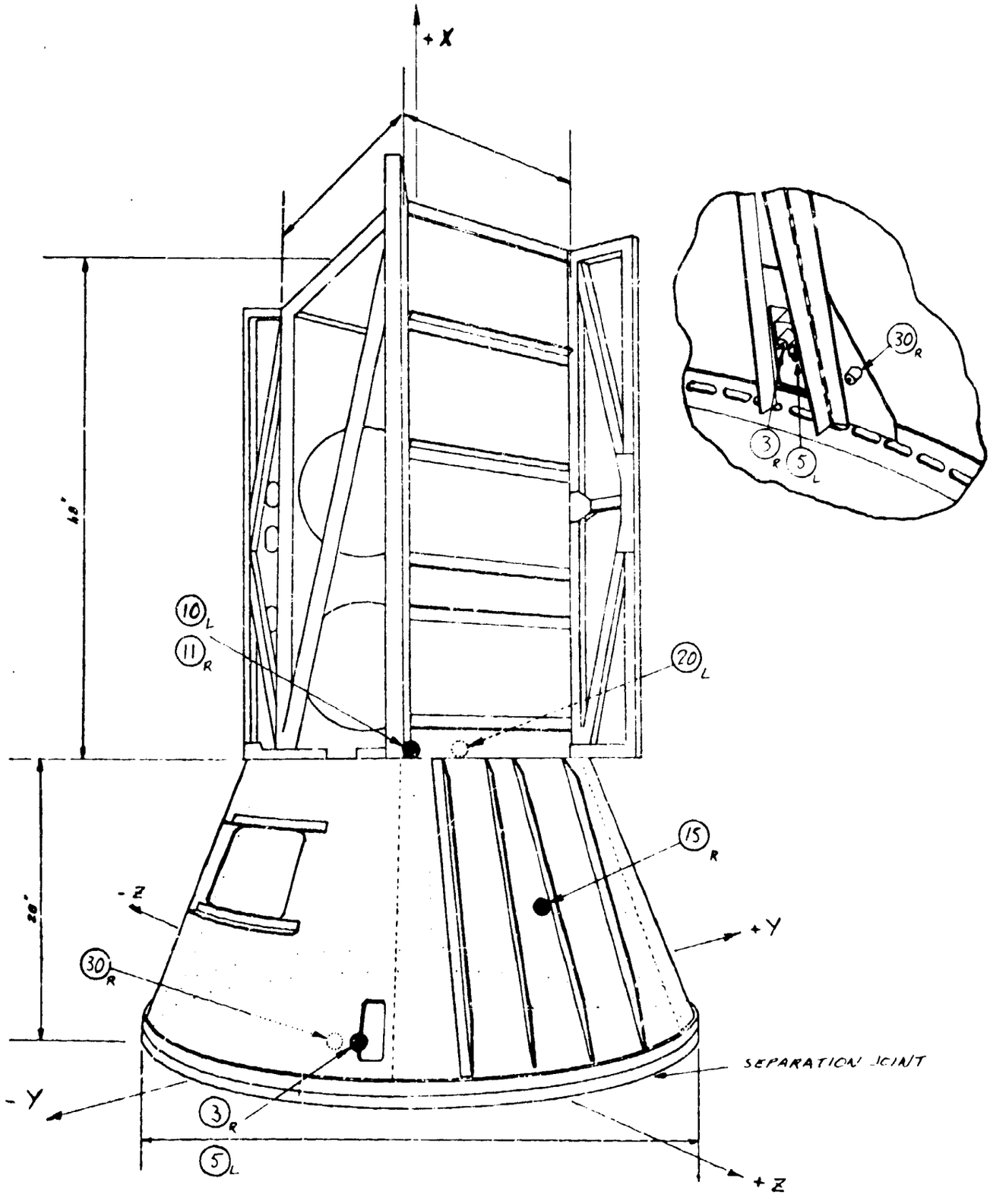

Figure II.A.4.2 TEST CONFIGURATION AND INSTRUMENTATION LOCATIONS

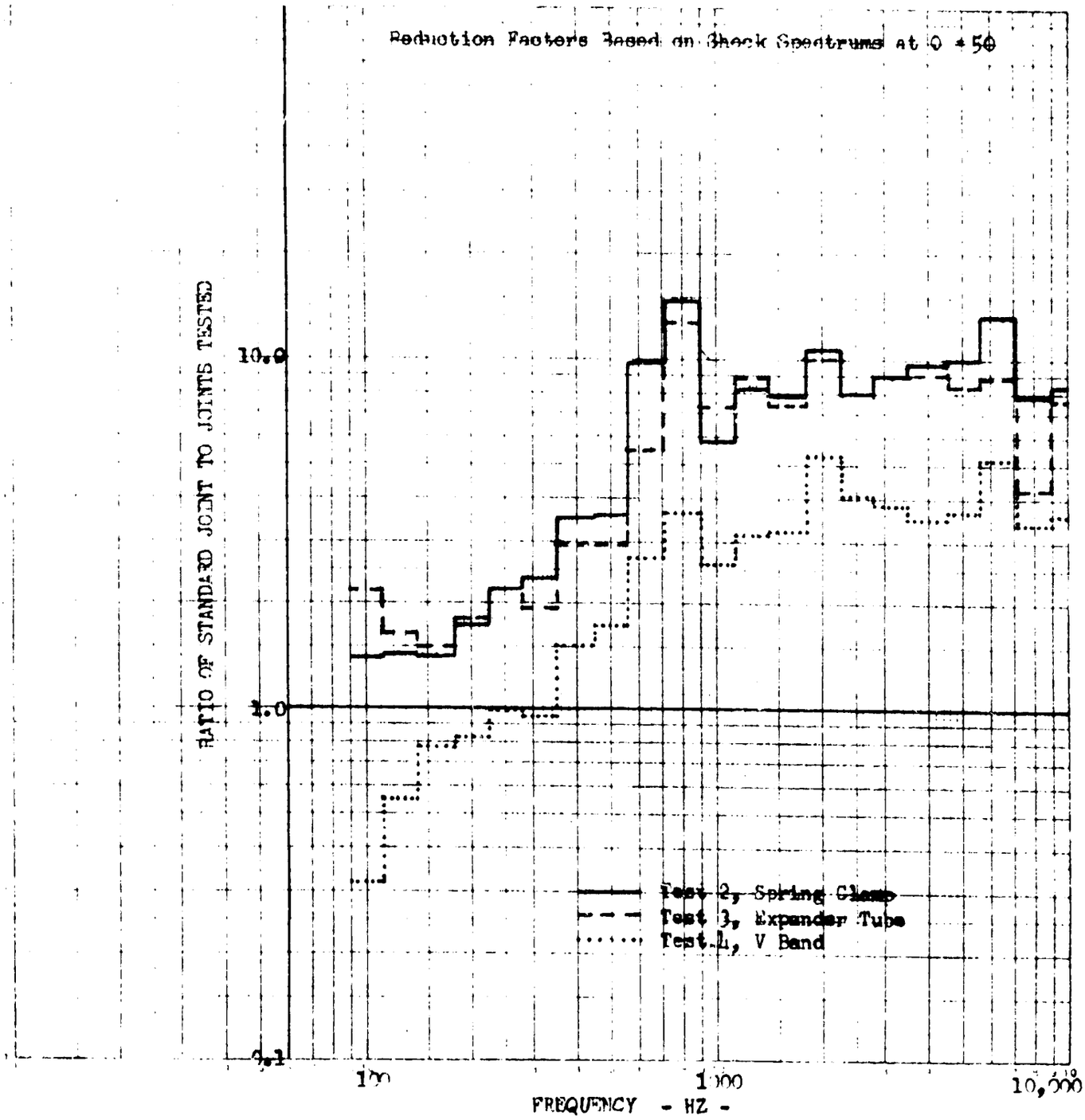

Figure II.A.4.3 COMPARISON OF AVERAGED 1/3 OCTAVE SHOCK SPECTRUM DATA

SHOCK TEST ANALYSIS DATA SHEET II.A.4.4

TEST ITEM 790-143
SERIAL NO.
SHOCK AXIS RADIAL

PART NO. STRUCTURE
TEST DATE 6-23-64
SHOCK NO. 1

RESPONSE G-S

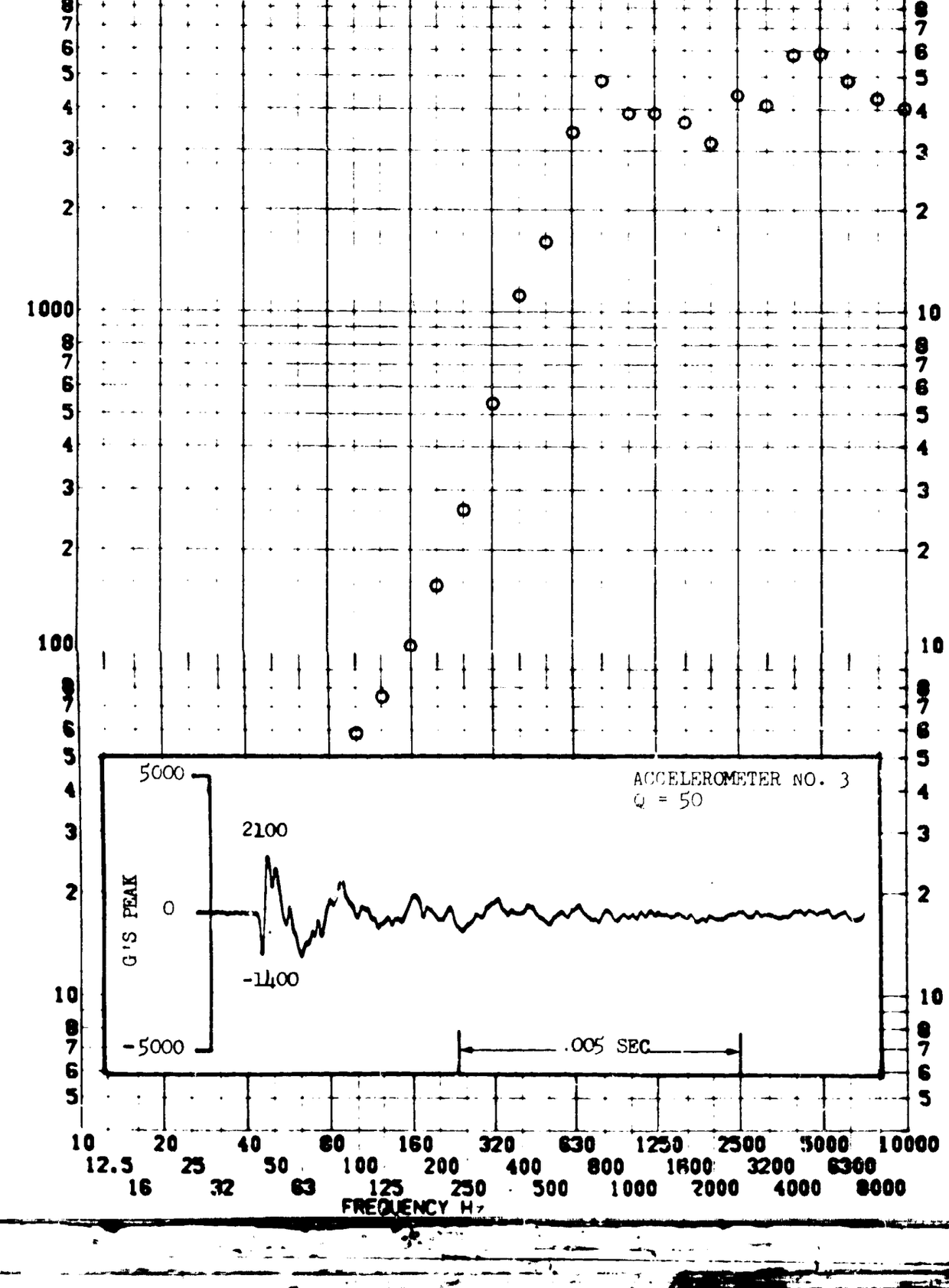

SHOCK TEST ANALYSIS DATA SHEET II.A.4.5

TEST ITEM 790-155
SERIAL NO.
SHOCK AXIS LONGITUDINAL

PART NO. STRUCTURE
TEST DATE 6-23-64
SHOCK NO. 1

RESPONSE G-S

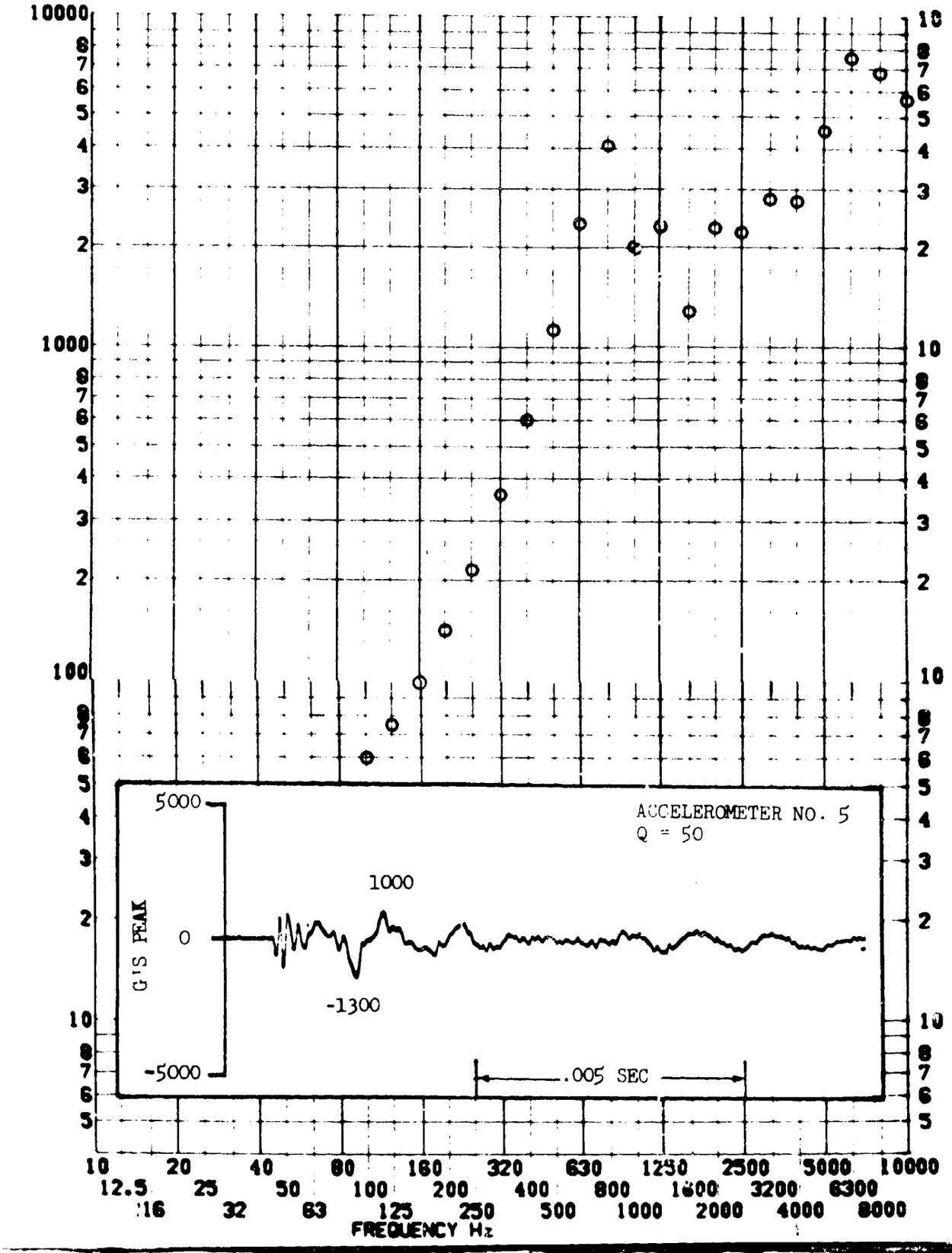

SHOCK TEST ANALYSIS DATA SHEET II.A.4.6

TEST ITEM 790-151
SERIAL NO.
SHOCK AXIS LONGITUDINAL

PART NO. STRUCTURE
TEST DATE 6-23-64
SHOCK NO. 1

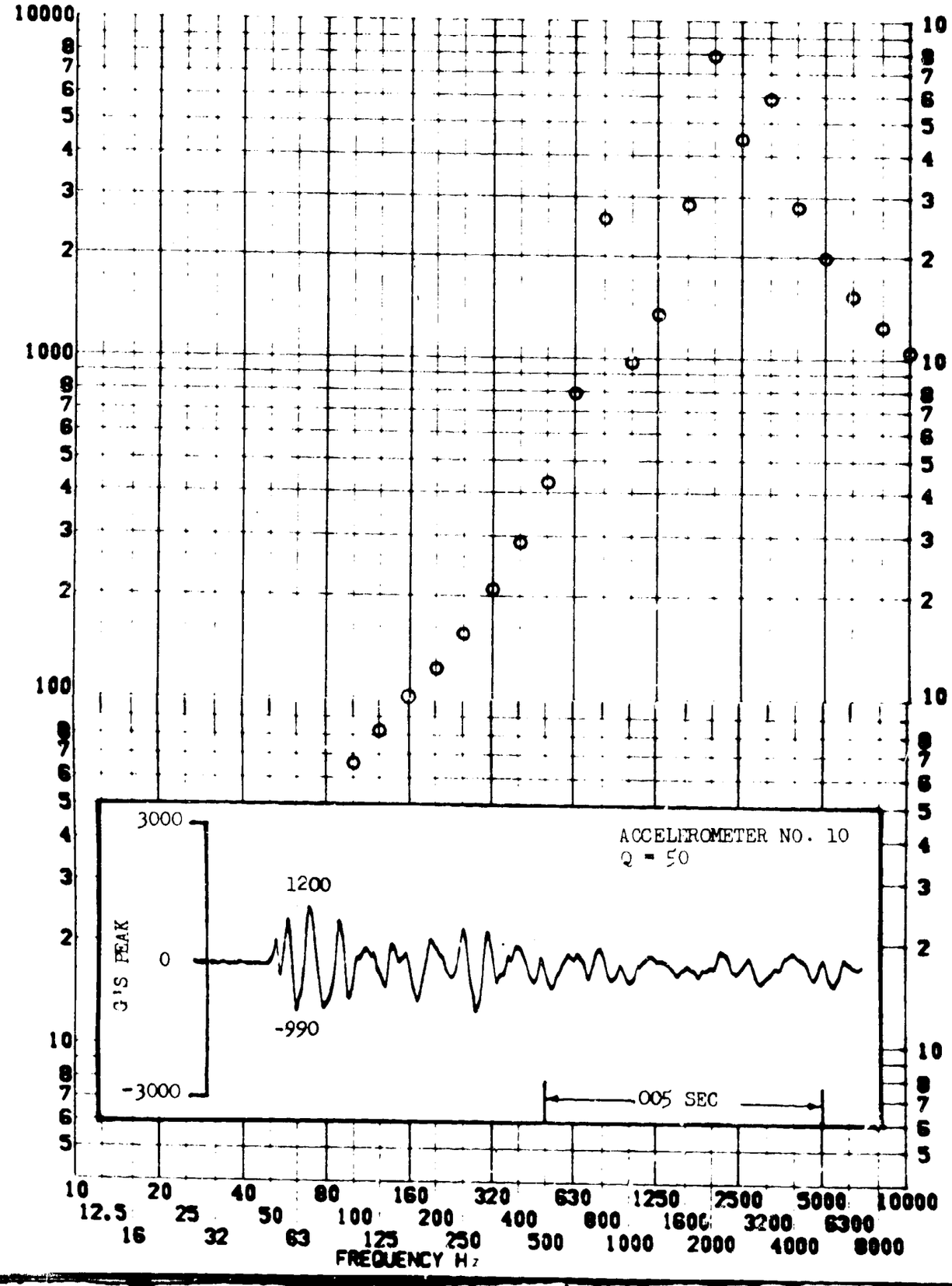

SHOCK TEST ANALYSIS DATA SHEET II.A.4.7

TEST ITEM 790-147
SERIAL NO.
SHOCK AXIS RADIAL

PART NO. STRUCTURE
TEST DATE 6-23-64
SHOCK NO. 1

RESPONSE G-S

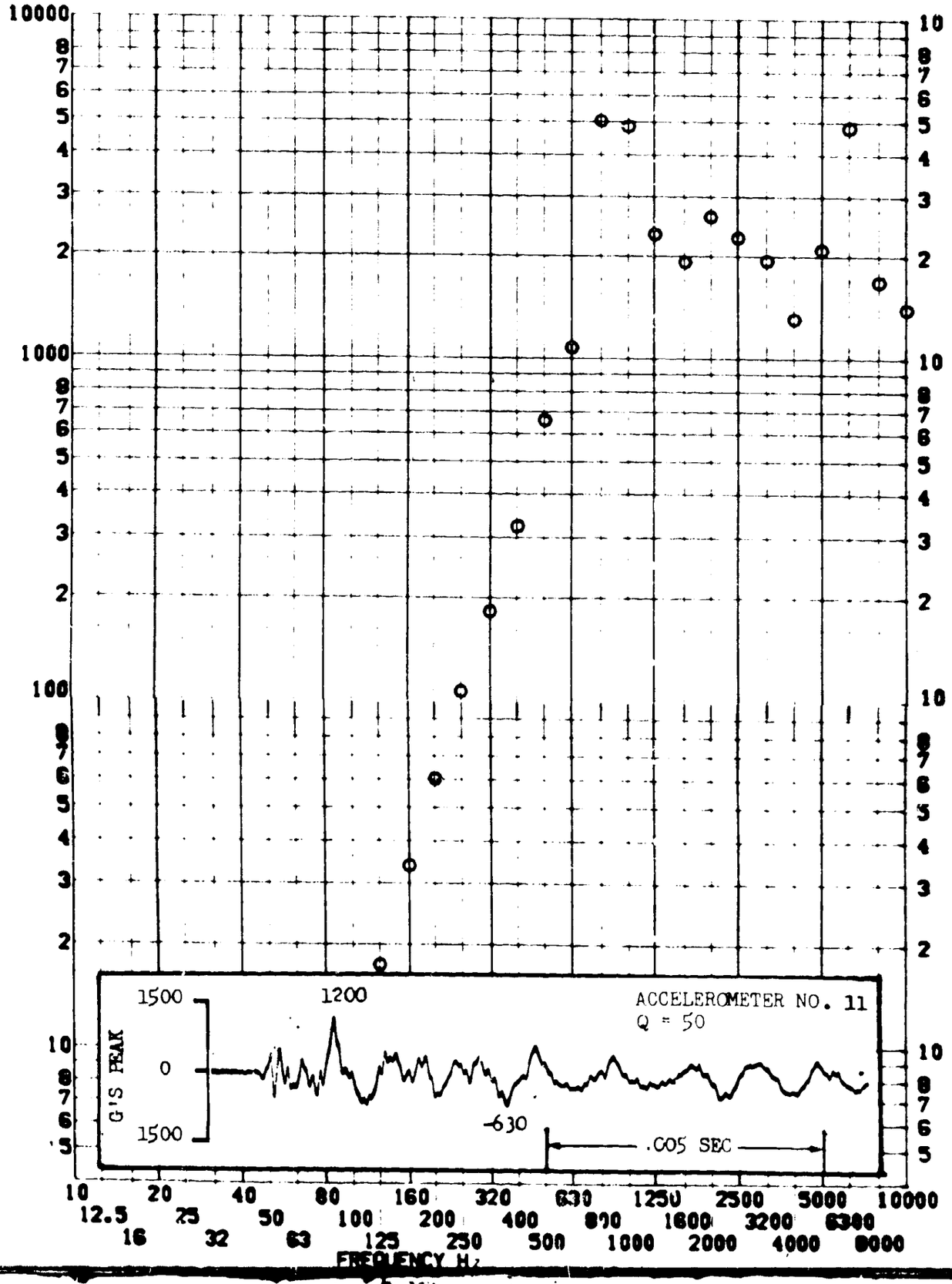

SHOCK TEST ANALYSIS DATA SHEET II.A.4.8

TEST ITEM 790-159
SERIAL NO.
SHOCK AXIS RADIAL

PART NO. STRUCTURE
TEST DATE 6-23-64
SHOCK NO. 1

RESPONSE G-S

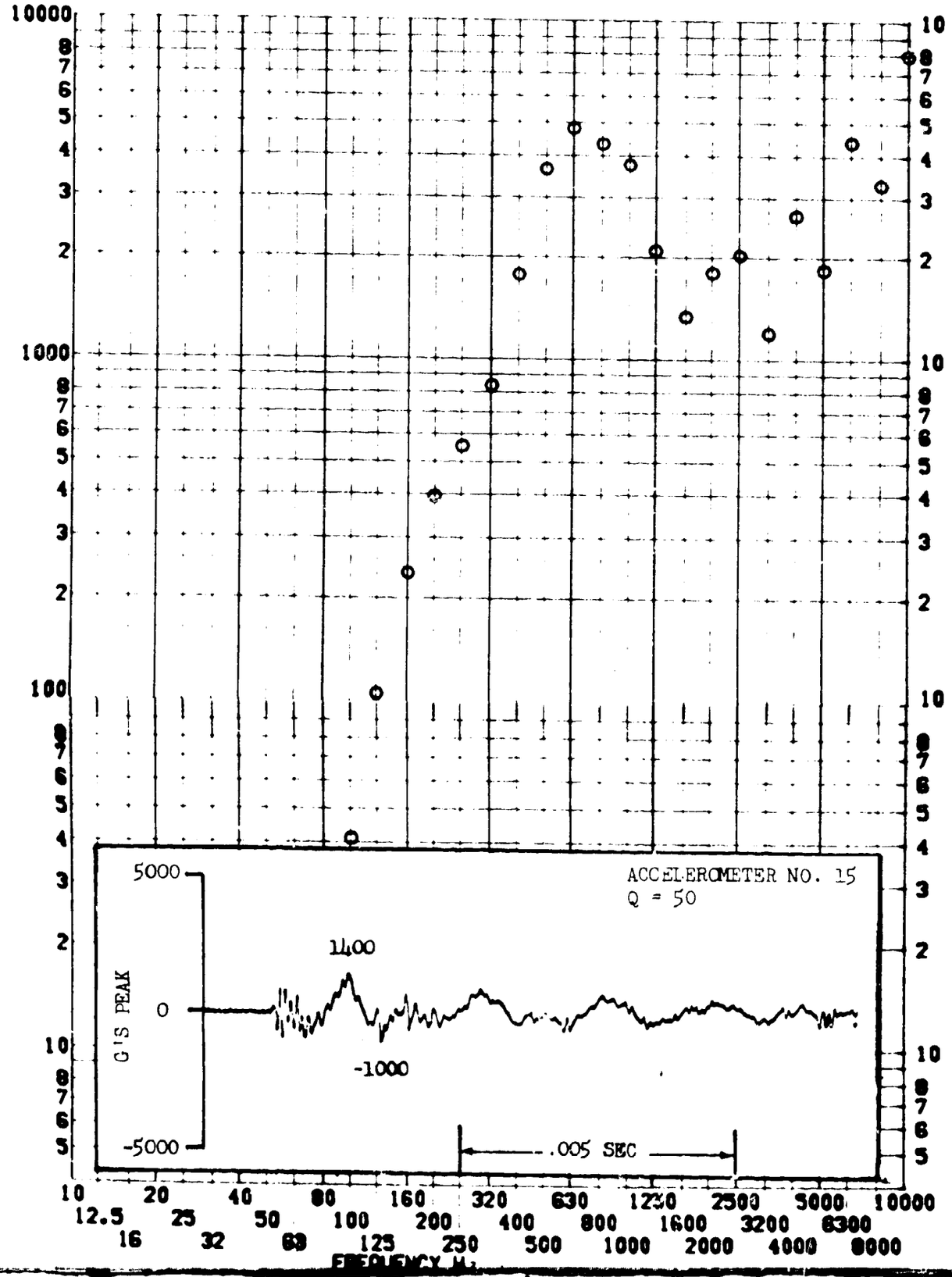

SHOCK TEST ANALYSIS DATA SHEET II.A.4.9

TEST ITEM 790-163
SERIAL NO.
SHOCK AXIS LONGITUDINAL

PART NO. STRUCTURE
TEST DATE 6-23-64
SHOCK NO. 1

RESPONSE G-S

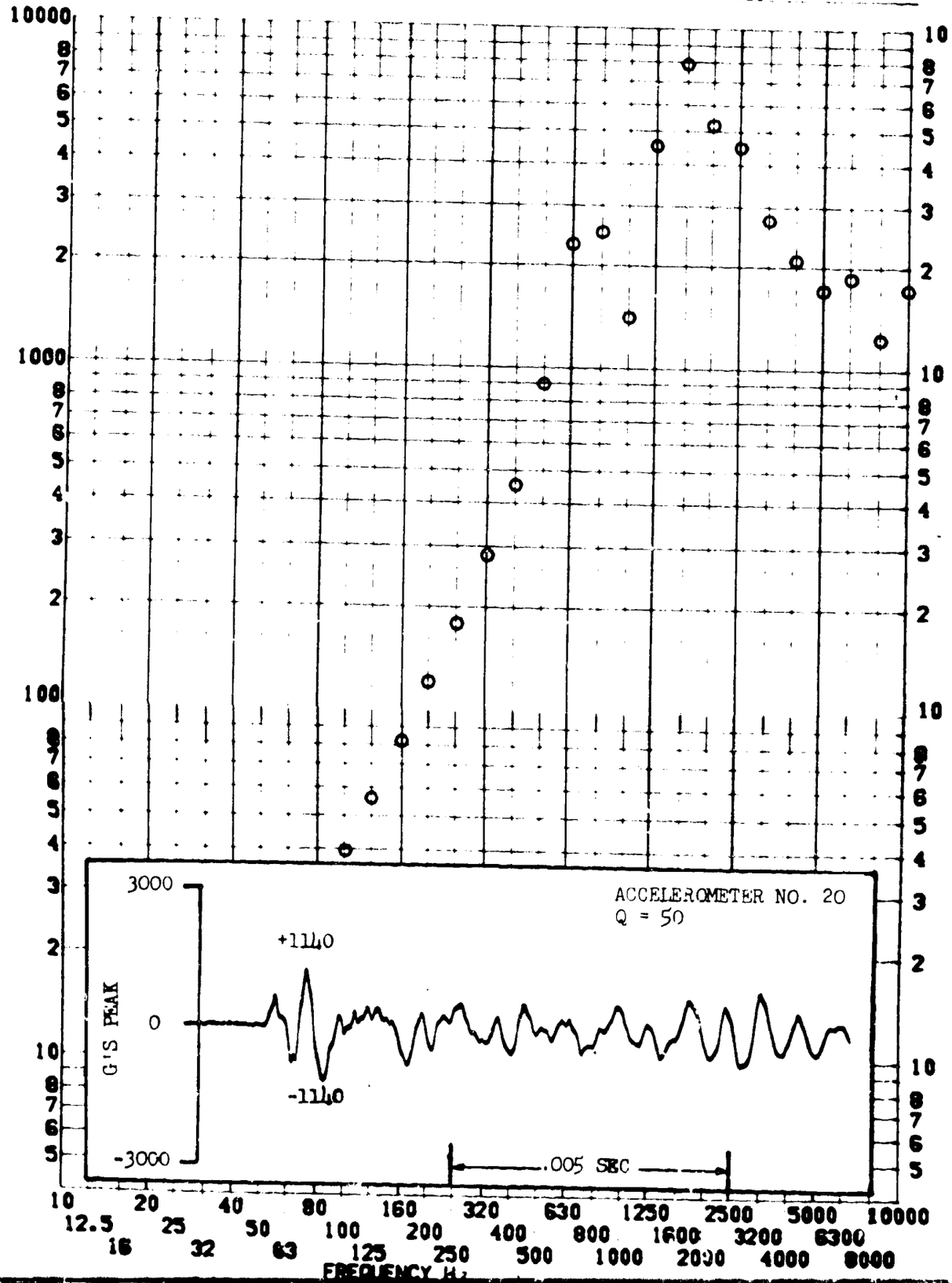

SHOCK TEST ANALYSIS DATA SHEET II.A.4.10

TEST ITEM 790-146
SERIAL NO.
SHOCK AXIS RADIAL

PART NO. STRUCTURE
TEST DATE 6-23-64
SHOCK NO. 2

RESPONSE G-S

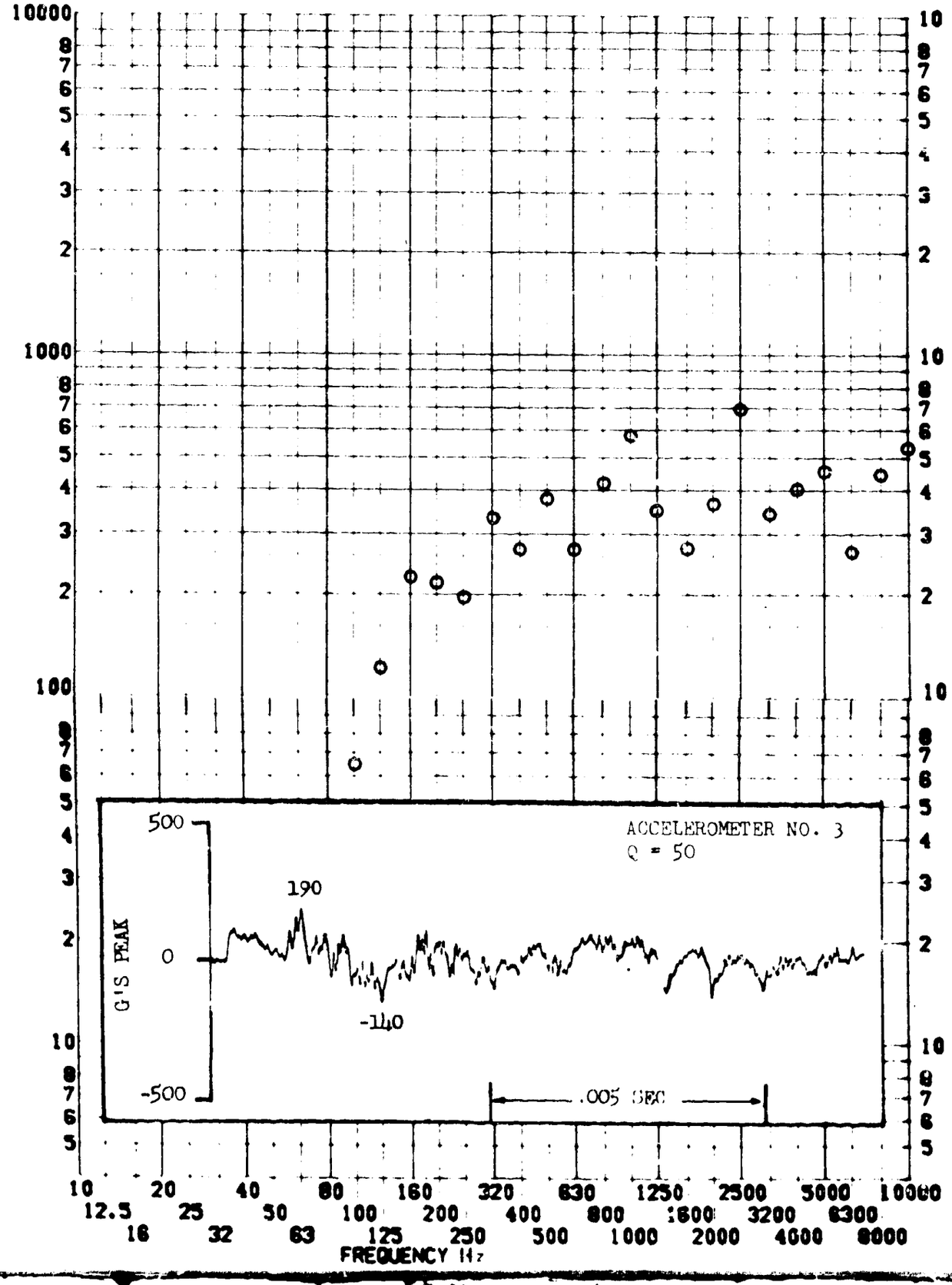

SHOCK TEST ANALYSIS DATA SHEET II.A.4.11

TEST ITEM 790-157
SERIAL NO.
SHOCK AXIS LONGITUDINAL

PART NO. STRUCTURE
TEST DATE 23 JUNE 1961
SHOCK NO. 2

RESPONSE G-S

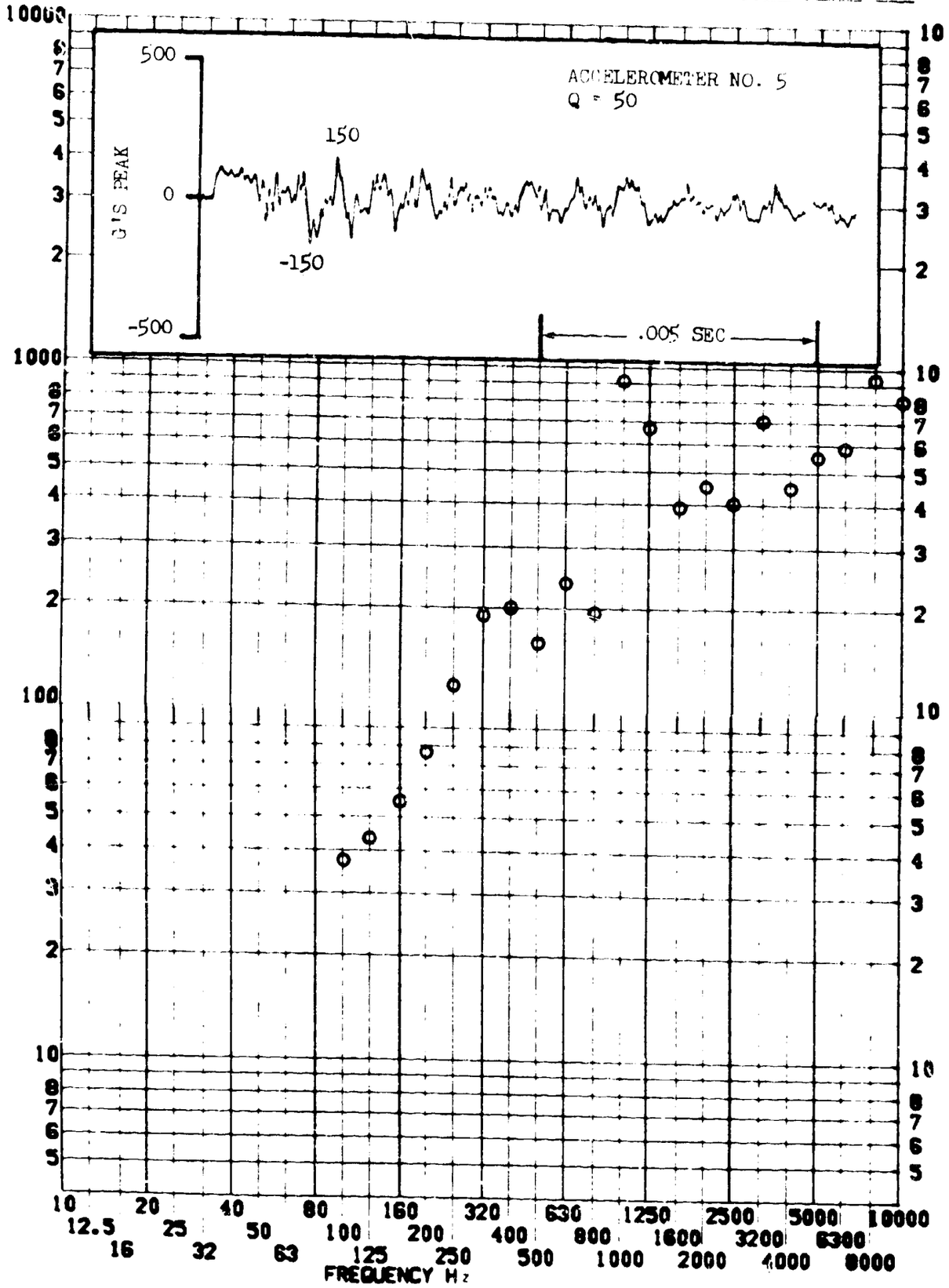

SHOCK TEST ANALYSIS DATA SHEET II.A.4.12

TEST ITEM 790-153
SERIAL NO.
SHOCK AXIS LONGITUDINAL

PART NO. STRUCTURE
TEST DATE 23 JUNE 1964
SHOCK NO. 2

RESPONSE G-S

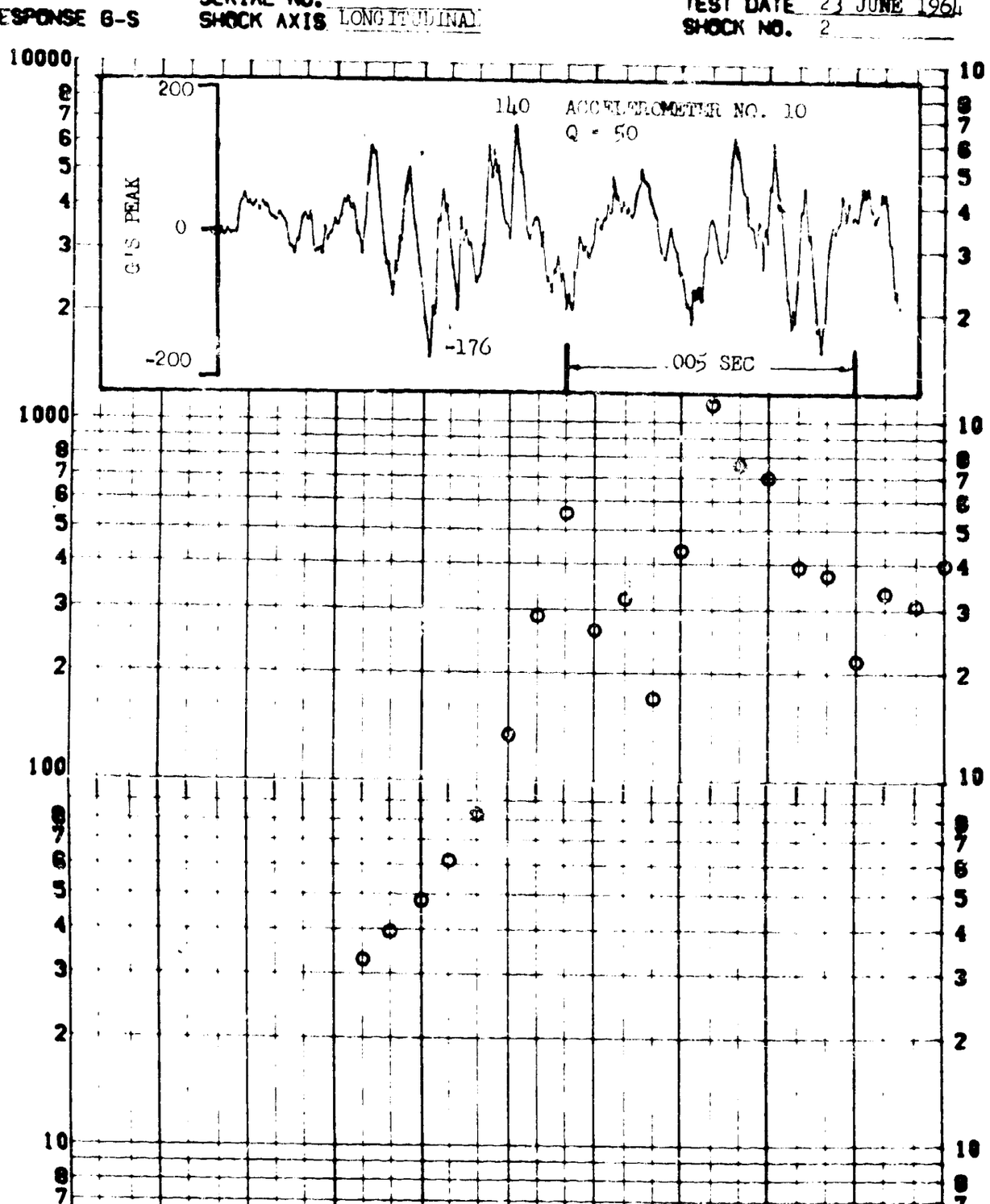

SHOCK TEST ANALYSIS DATA SHEET II.A.4.13

TEST ITEM ZSQ-119 PART NO. STRUCTURE
SERIAL NO. TEST DATE 23 JUNE 1964
RESPONSE G-S SHOCK AXIS RADIAL SHOCK NO. 2

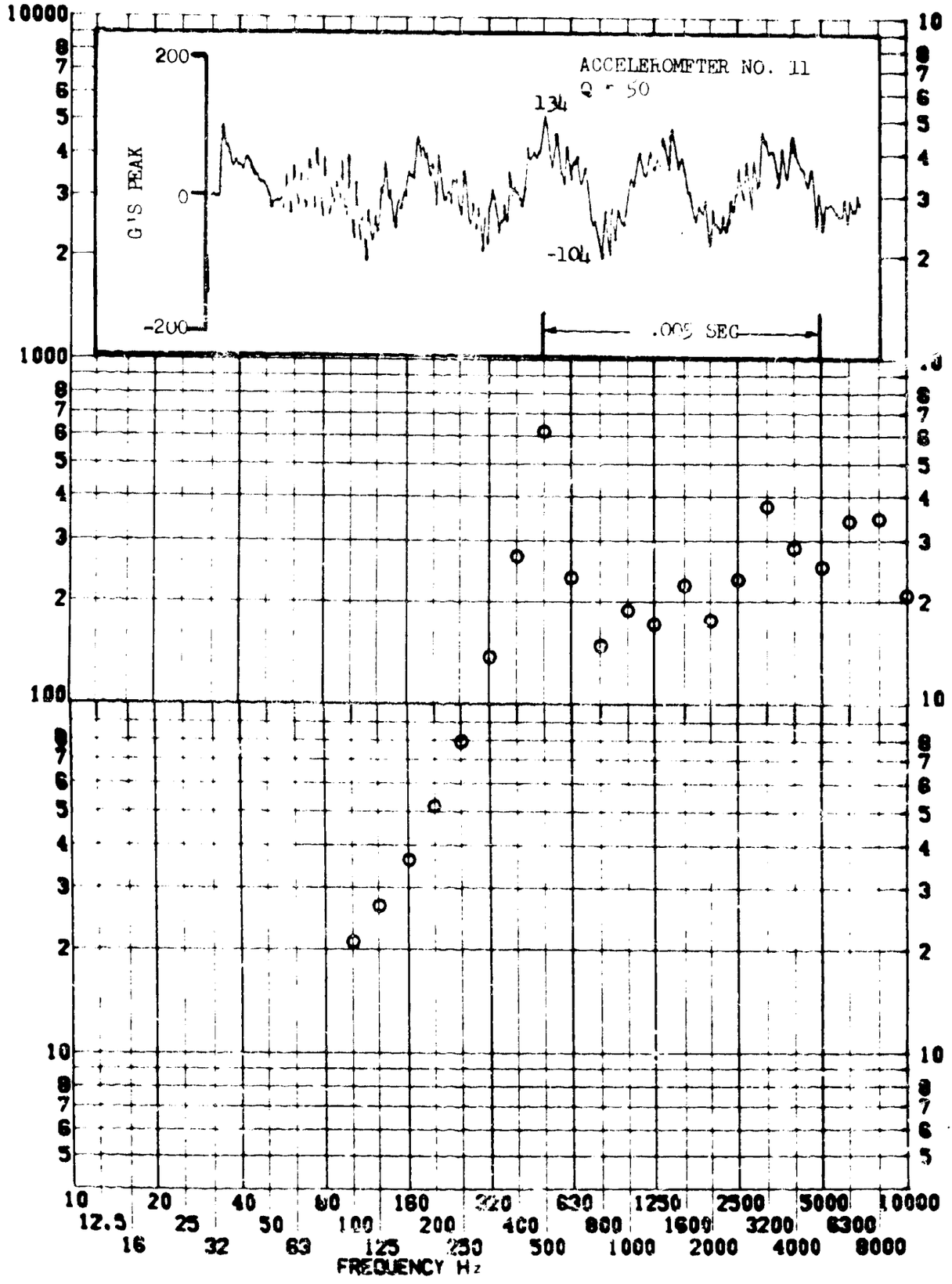

SHOCK TEST ANALYSIS DATA SHEET II.A.4.14

TEST ITEM 790-161 PART NO. STRUCTURE
SERIAL NO. TEST DATE 23 JUNE 1964
RESPONSE G-S SHOCK AXIS RADIAL SHOCK NO. 2

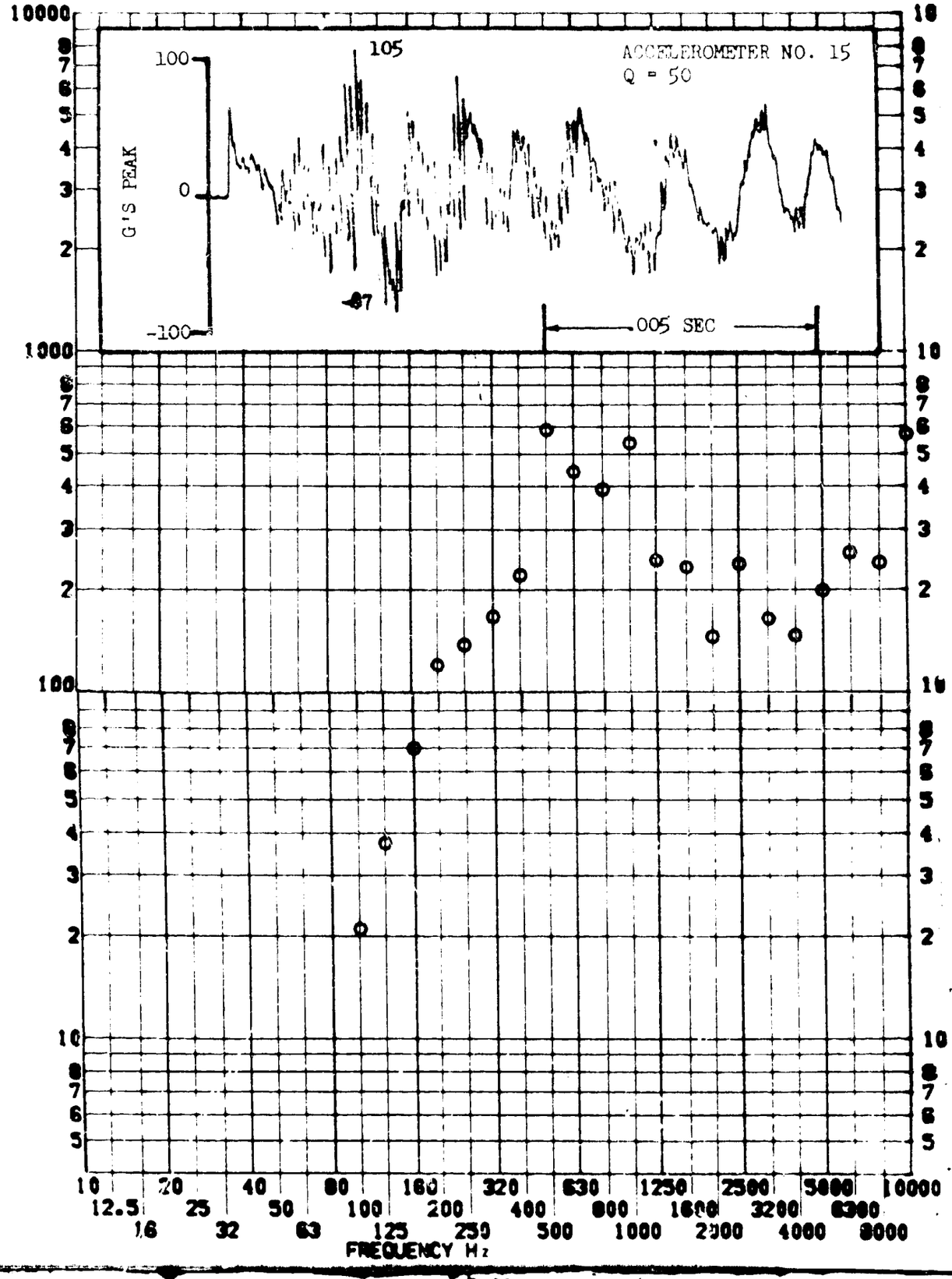

SHOCK TEST ANALYSIS DATA SHEET II.A.4.15

TEST ITEM 790-141
SERIAL NO.
SHOCK AXIS RADIAL

PART NO. STRUCTURE
TEST DATE 23 JUNE 1964
SHOCK NO. 2

RESPONSE G-S

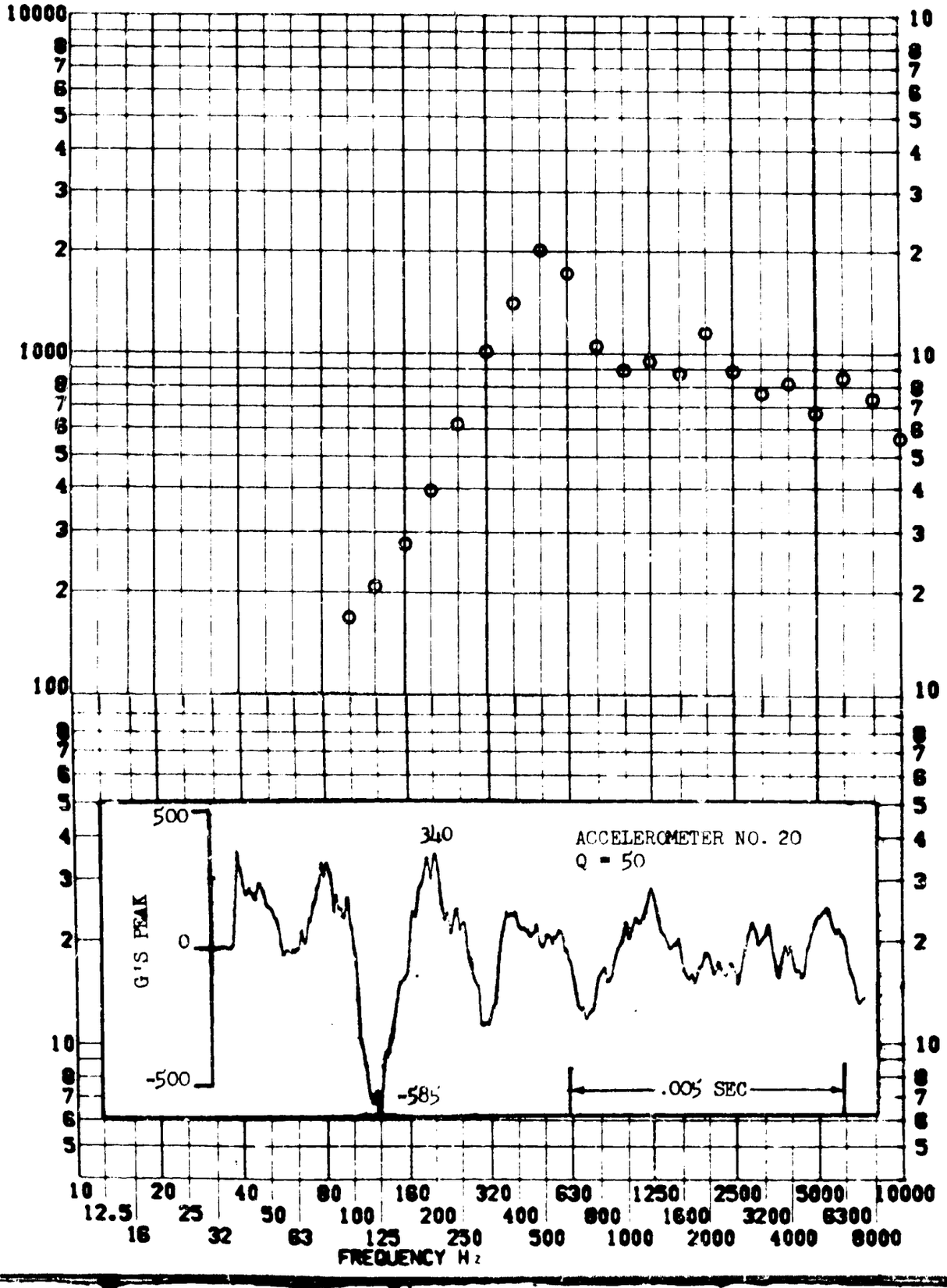

SHOCK TEST ANALYSIS DATA SHEET II.A.4.16

TEST ITEM 790-165
SERIAL NO.
SHOCK AXIS LONGITUDINAL

PART NO. STRUCTURE
TEST DATE 23 JUNE 1964
SHOCK NO. 2

RESPONSE G-S

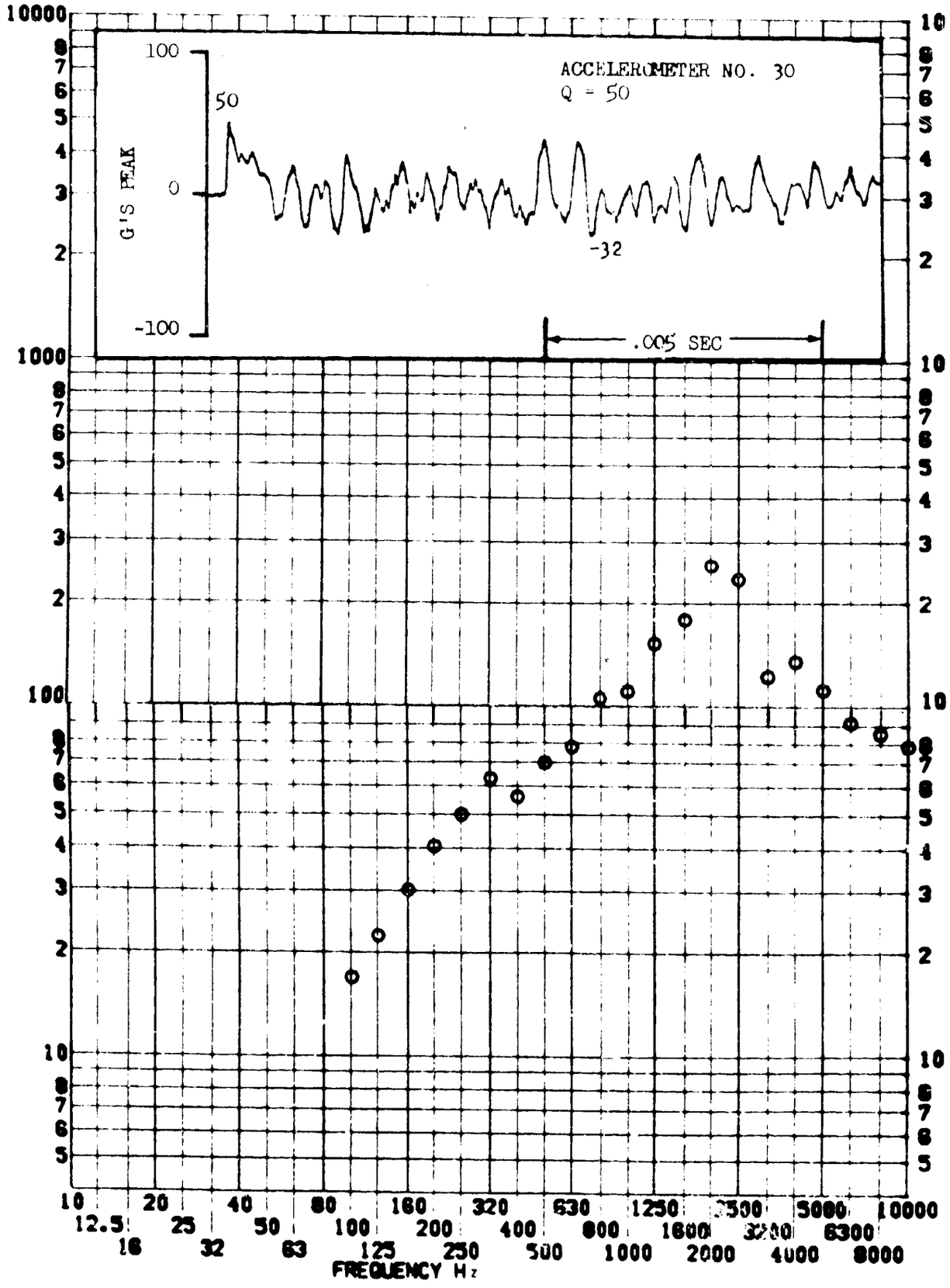

SHOCK TEST ANALYSIS DATA SHEET II.A.4.17

TEST ITEM 020-115
SERIAL NO.
SHOCK AXIS RADIAL

PART NO. STRUCTURE
TEST DATE 23 JUNE 1964
SHOCK NO. 3

RESPONSE G-S

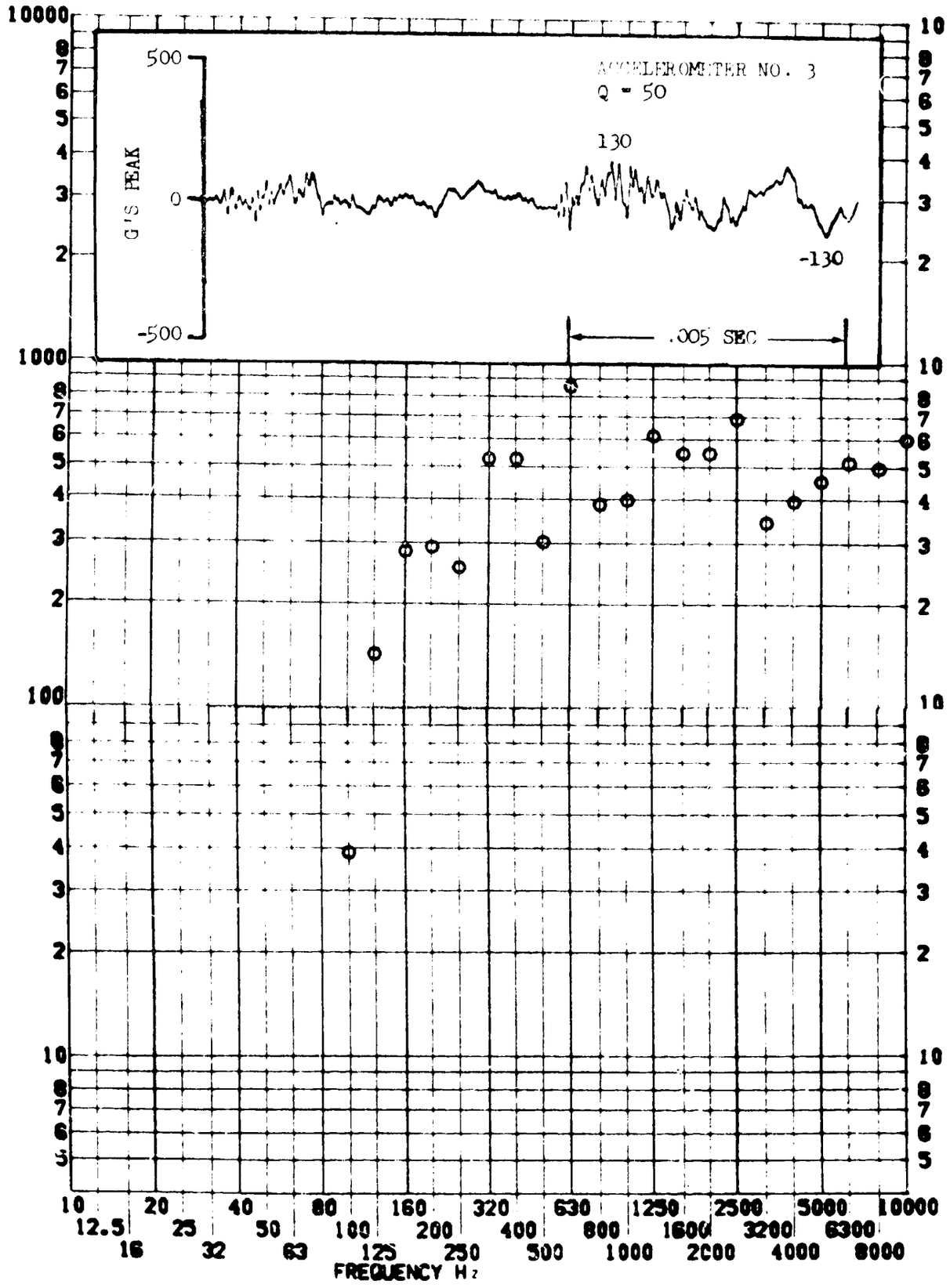

SHOCK TEST ANALYSIS DATA SHEET II.A.4.18

TEST ITEM 790-158 PART NO. STRUCTURE

SERIAL NO. TEST DATE 23 JUNE 1964

RESPONSE G-S SHOCK AXIS LONGITUDINAL SHOCK NO. 3

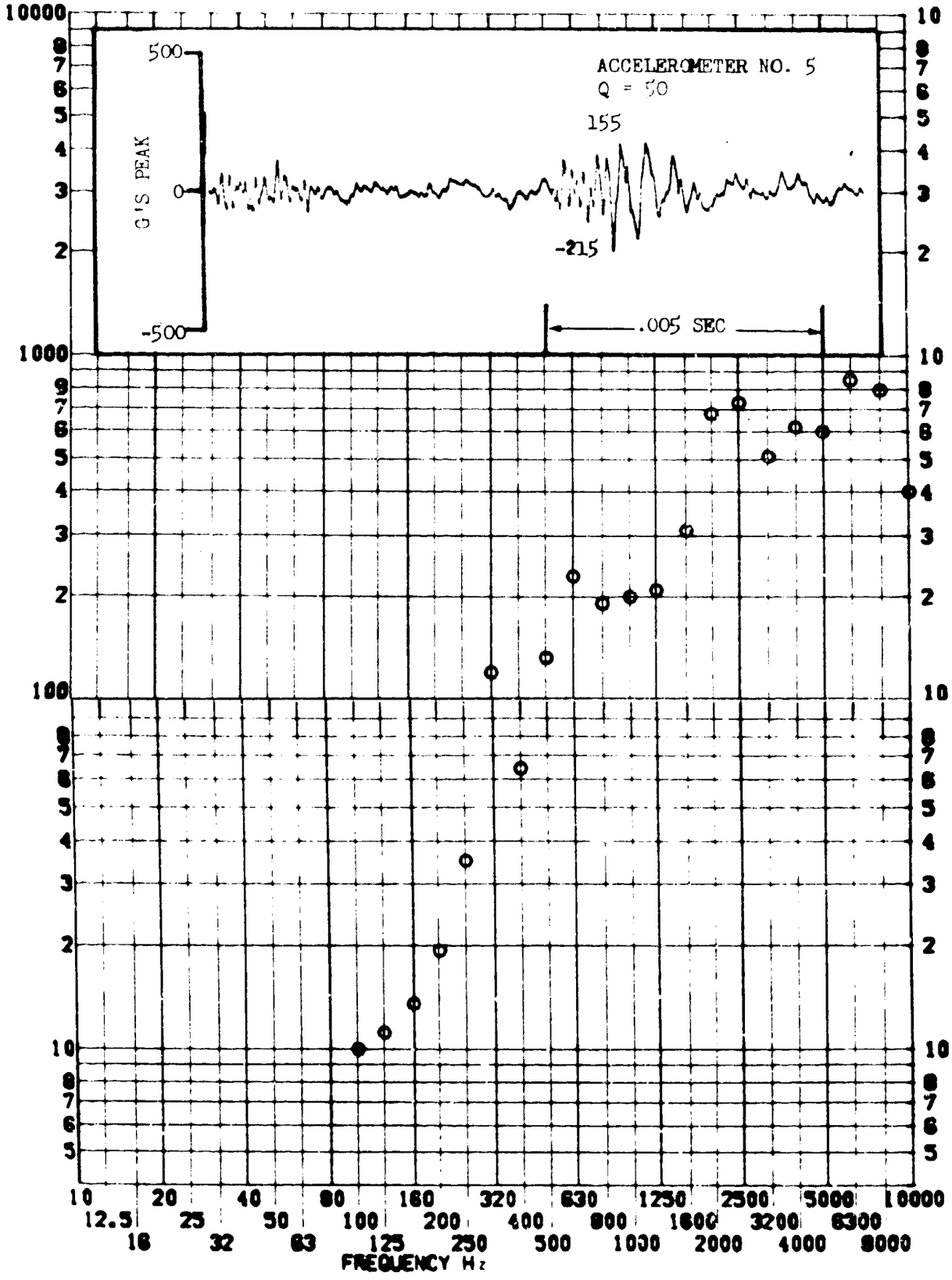

SHOCK TEST ANALYSIS DATA SHEET II.A.4.19

TEST ITEM 790-154
SERIAL NO.
SHOCK AXIS LONGITUDINAL

PART NO. STRUCTURE
TEST DATE 23 JUNE 1964
SHOCK NO. 3

RESPONSE G-S

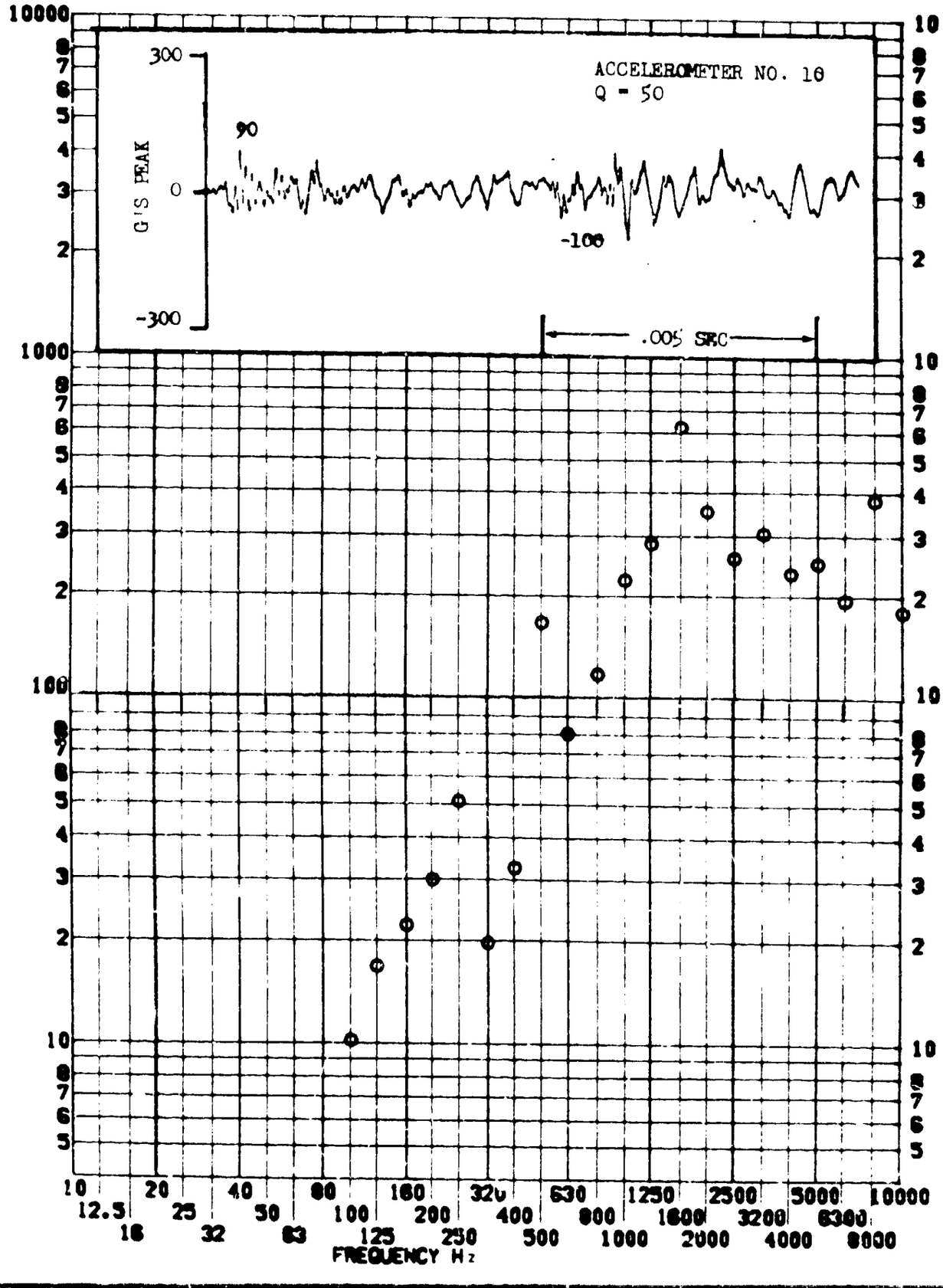

SHOCK TEST ANALYSIS DATA SHEET II.A.4.20

TEST ITEM 790-150
SERIAL NO.
SHOCK AXIS RADIAL

PART NO. STRUCTURE
TEST DATE 23 JUNE 1964
SHOCK NO. 3

RESPONSE G-S

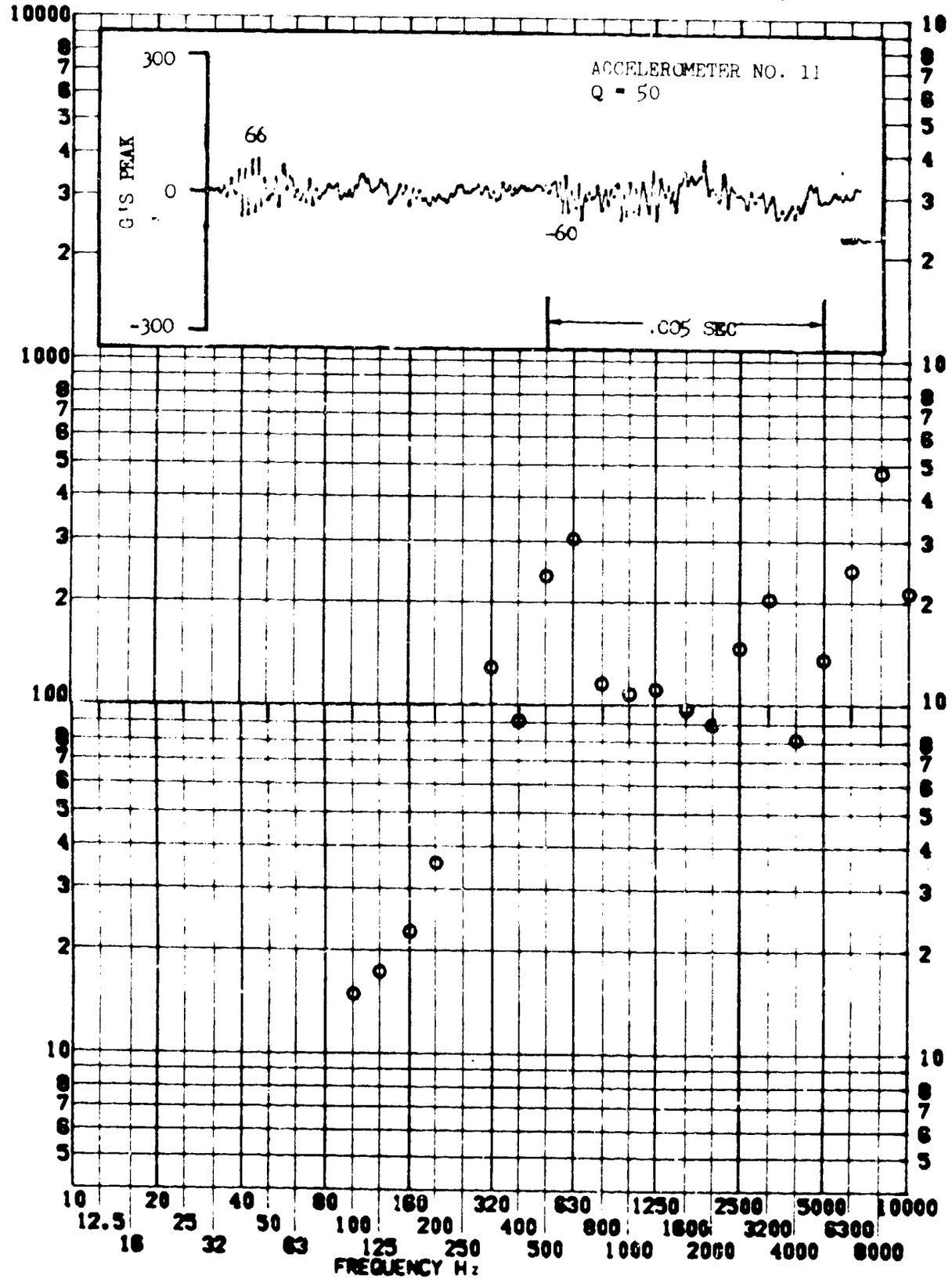

SHOCK TEST ANALYSIS DATA SHEET II.A.4.21

TEST ITEM 790-162 PART NO. STRUCTURE

SERIAL NO. TEST DATE 23 JUNE 1964

SHOCK AXIS RADIAL SHOCK NO. 3

RESPONSE G's

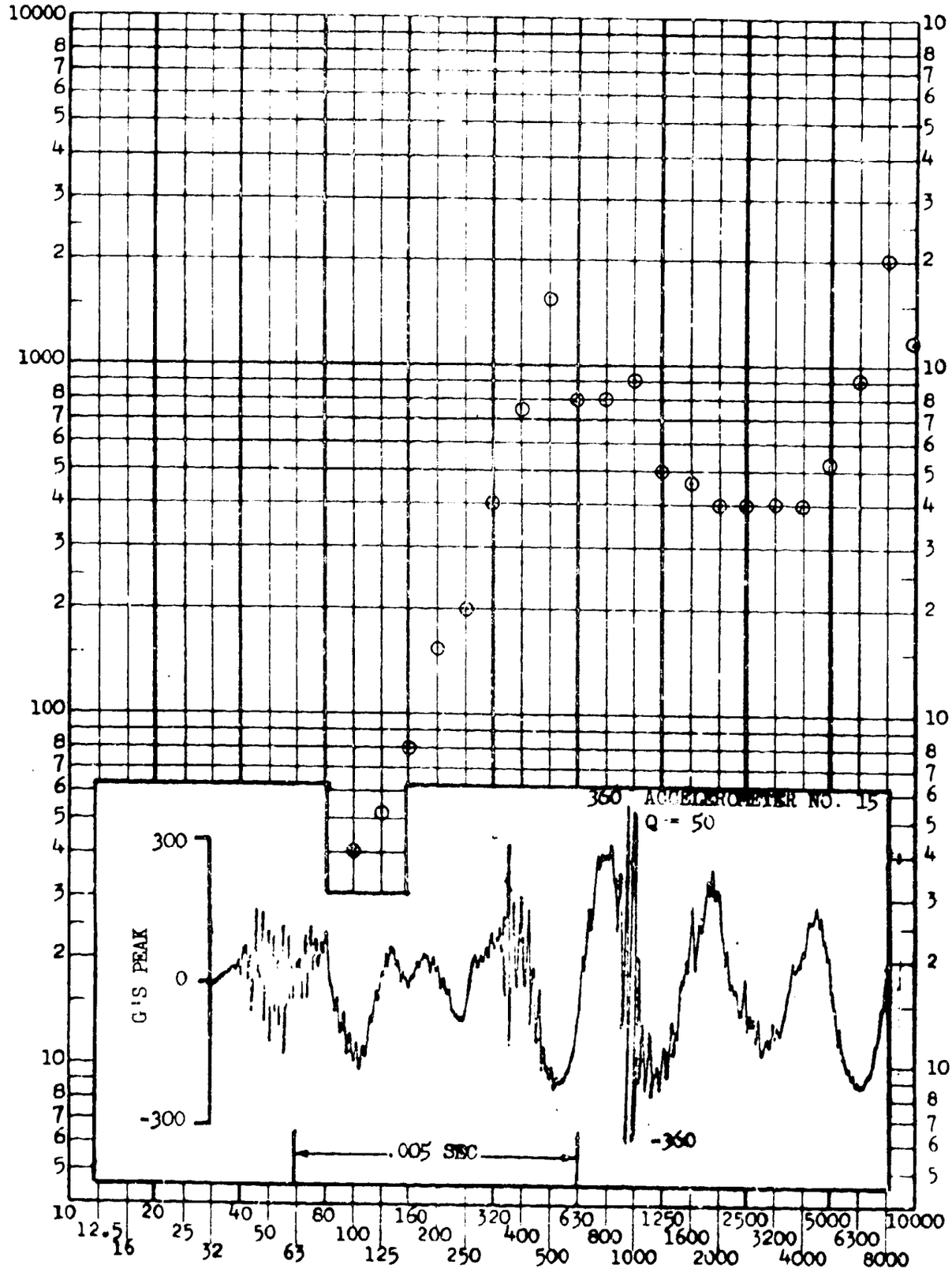

FREQUENCY Hz

SHOCK TEST ANALYSIS DATA SHEET II.A.4.22

TEST ITEM 790-166
SERIAL NO.
SHOCK AXIS LONGITUDINAL

PART NO. STRUCTURE
TEST DATE 23 JUNE 1964
SHOCK NO. 3

RESPONSE G-S

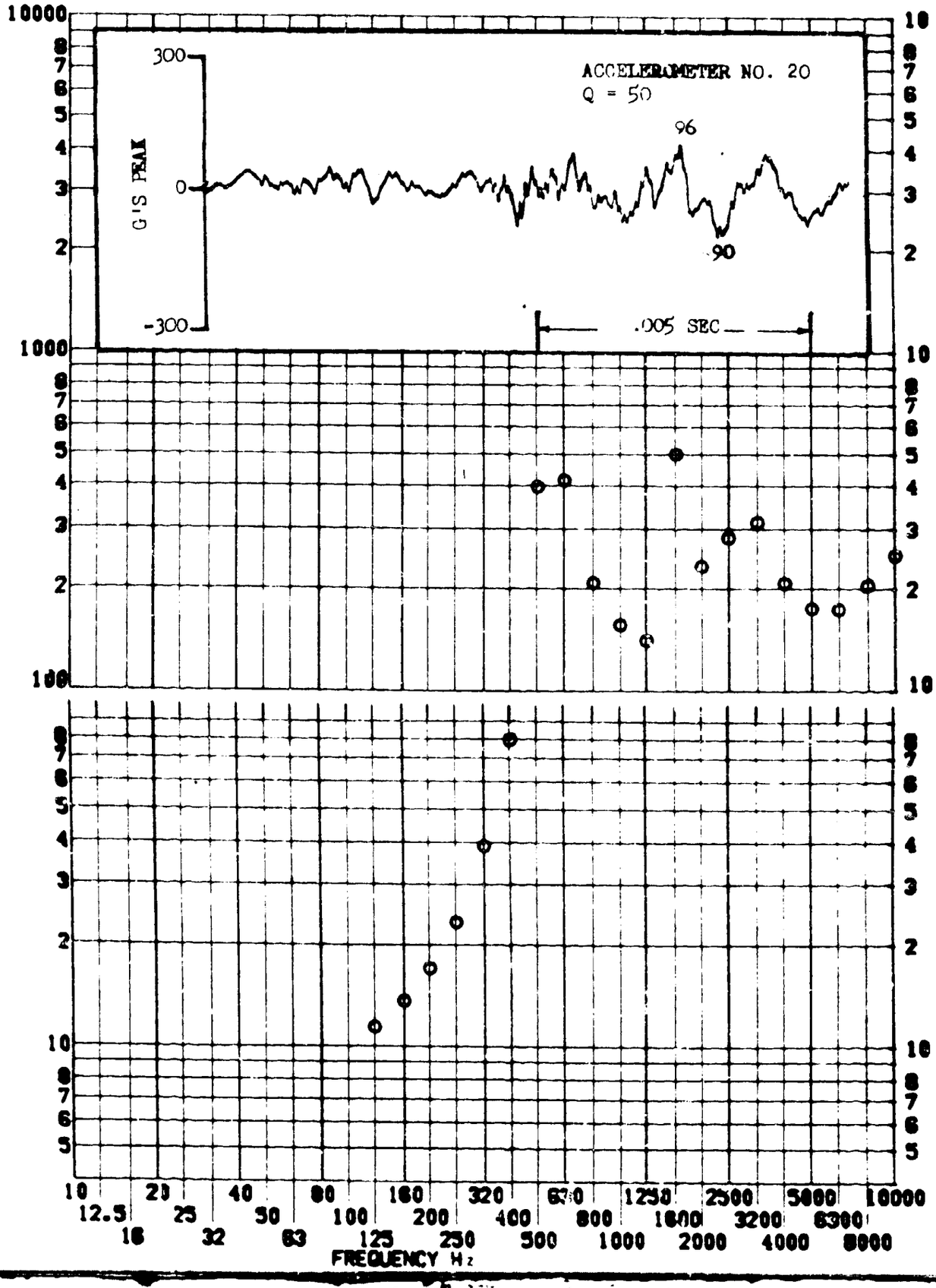

SHOCK TEST ANALYSIS DATA SHEET II.A.4.23

TEST ITEM 790-142 PART NO. STRUCTURE
SERIAL NO. TEST DATE 23 JUNE 1964
RESPONSE G-S SHOCK AXIS RADIAL SHOCK NO. 3

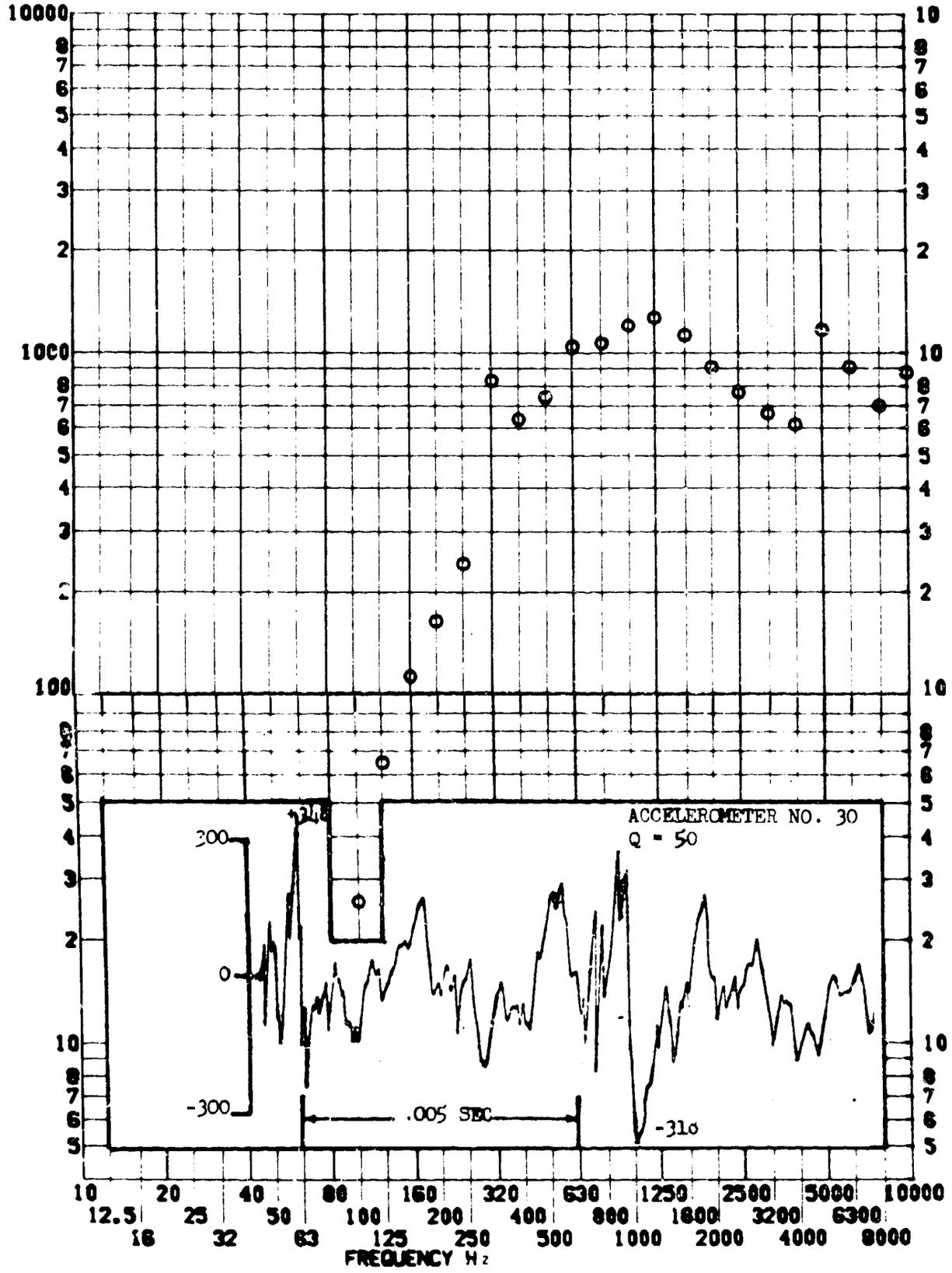

SHOCK TEST ANALYSIS DATA SHEET II.A.4.24

TEST ITEM 790-144 PART NO. STRUCTURE
SERIAL NO. TEST DATE 23 JUNE 1964
RESPONSE G-S SHOCK AXIS RADIAL SHOCK NO. 4

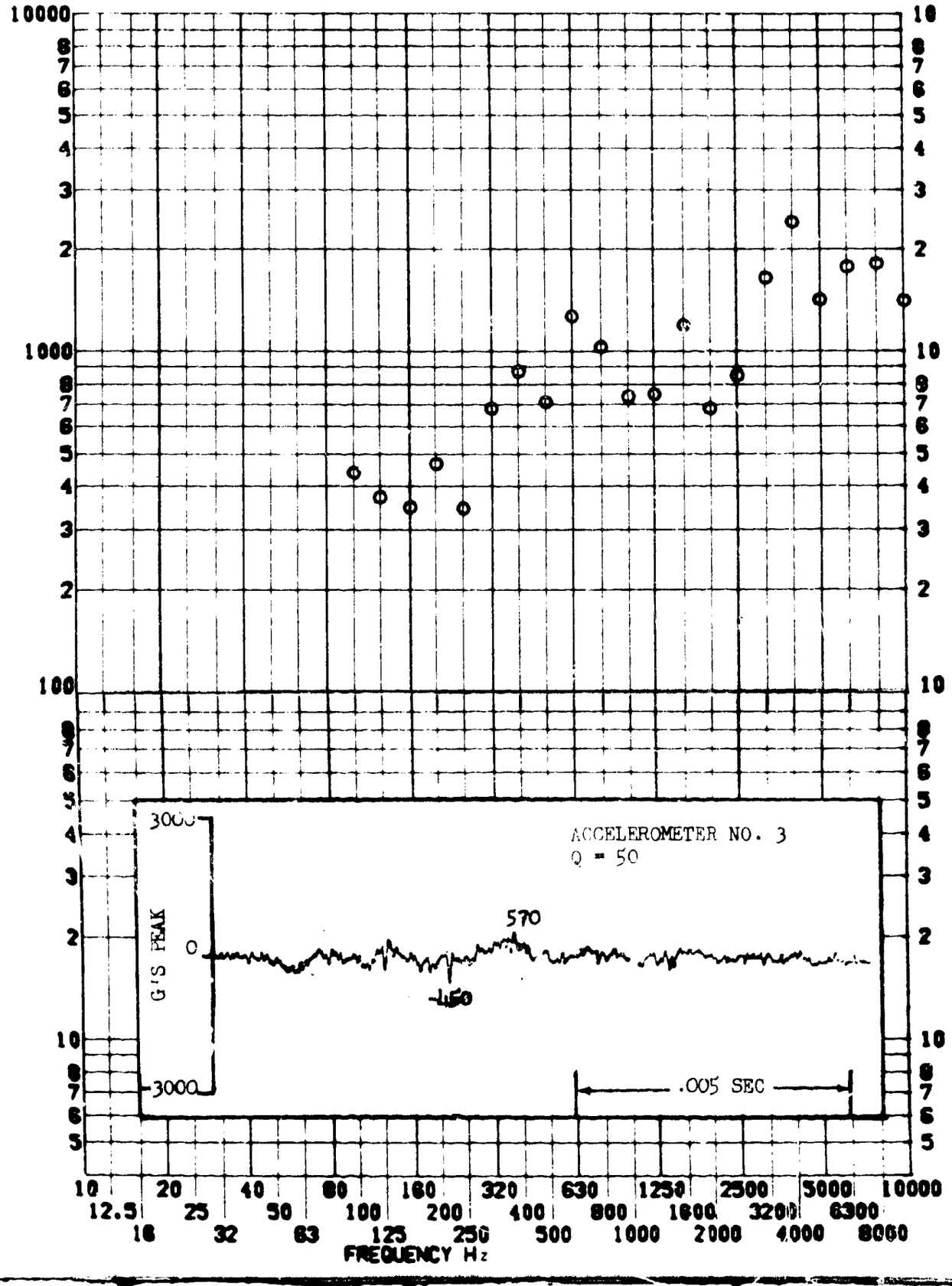

SHOCK TEST ANALYSIS DATA SHEET TT.A.4.25

TEST ITEM 790-156
SERIAL NO.
SHOCK AXIS LONGITUDINAL

PART NO. STRUCTURE
TEST DATE 23 JUNE 1964
SHOCK NO. 4

RESPONSE G-S

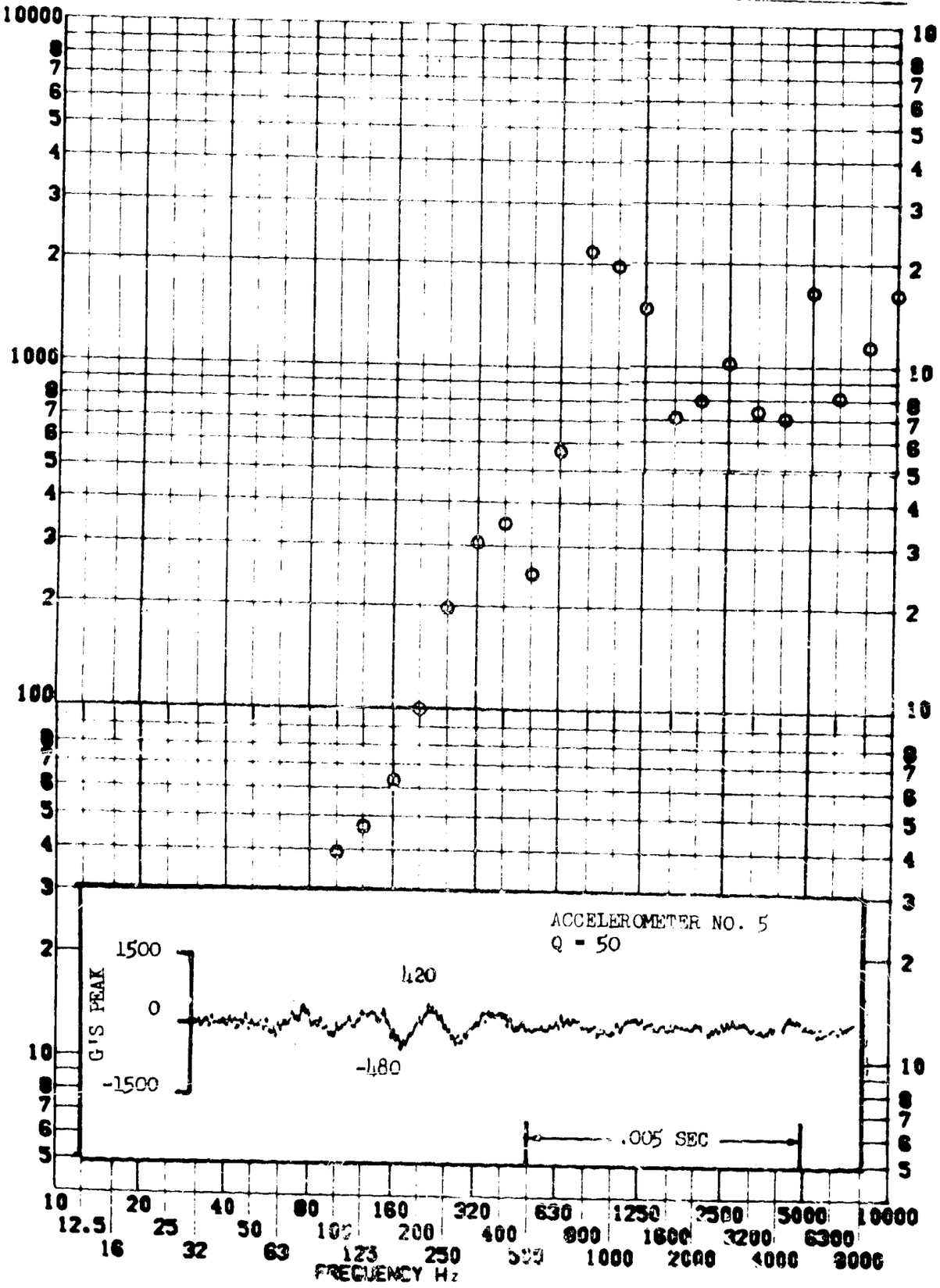

SHOCK TEST ANALYSIS DATA SHEET II.A.4.26

TEST ITEM 790-152 PART NO. STRUCTURE
SERIAL NO. TEST DATE 23 JUNE 1964
RESPONSE G-S SHOCK AXIS LONGITUDINAL SHOCK NO. 4

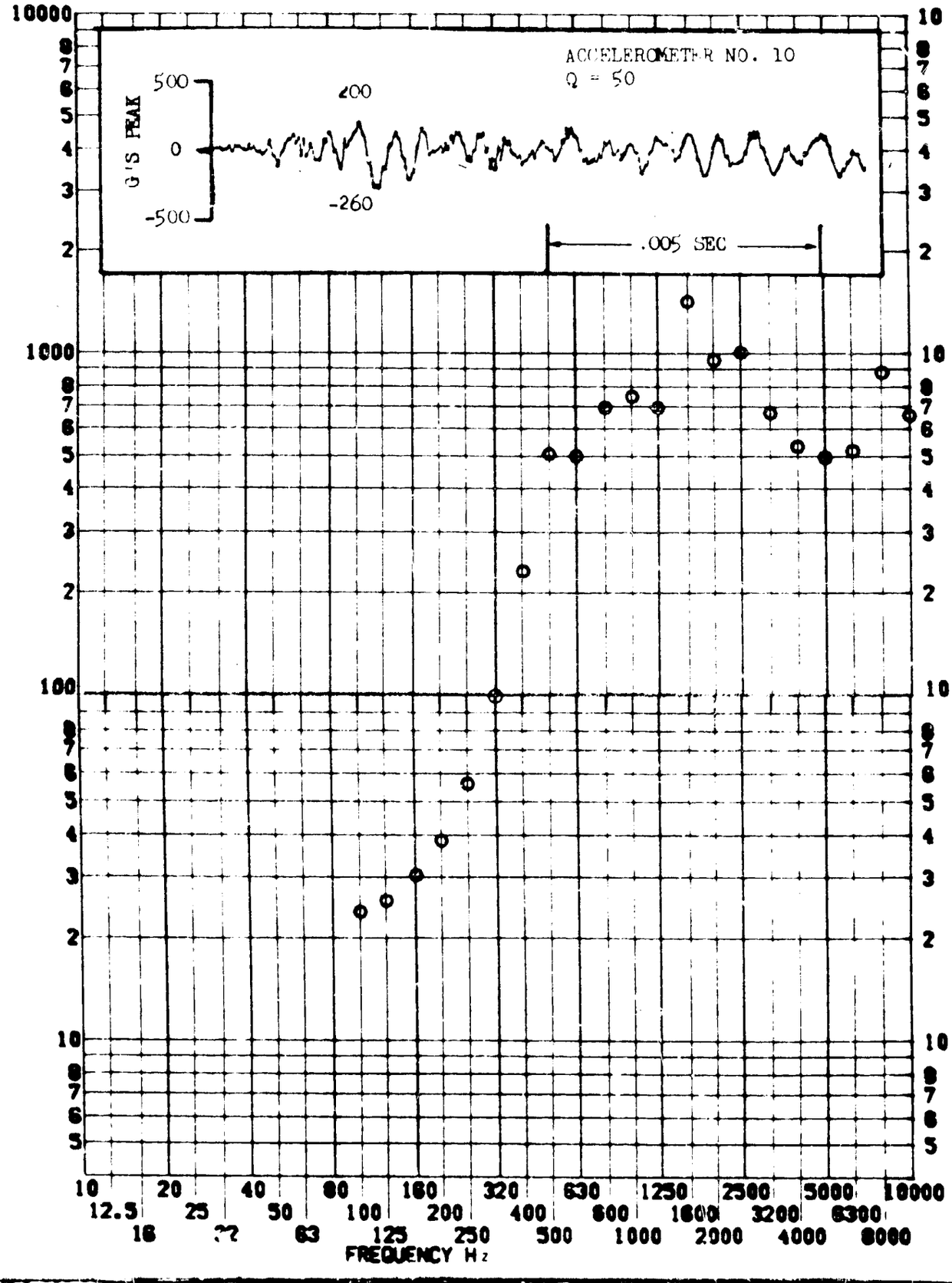

SHOCK TEST ANALYSIS DATA SHEET II.A.4.27

TEST ITEM 790-148
SERIAL NO.
SHOCK AXIS RADIAL

PART NO. STRUCTURE
TEST DATE 23 JUNE 1961
SHOCK NO. 1

RESPONSE G-S

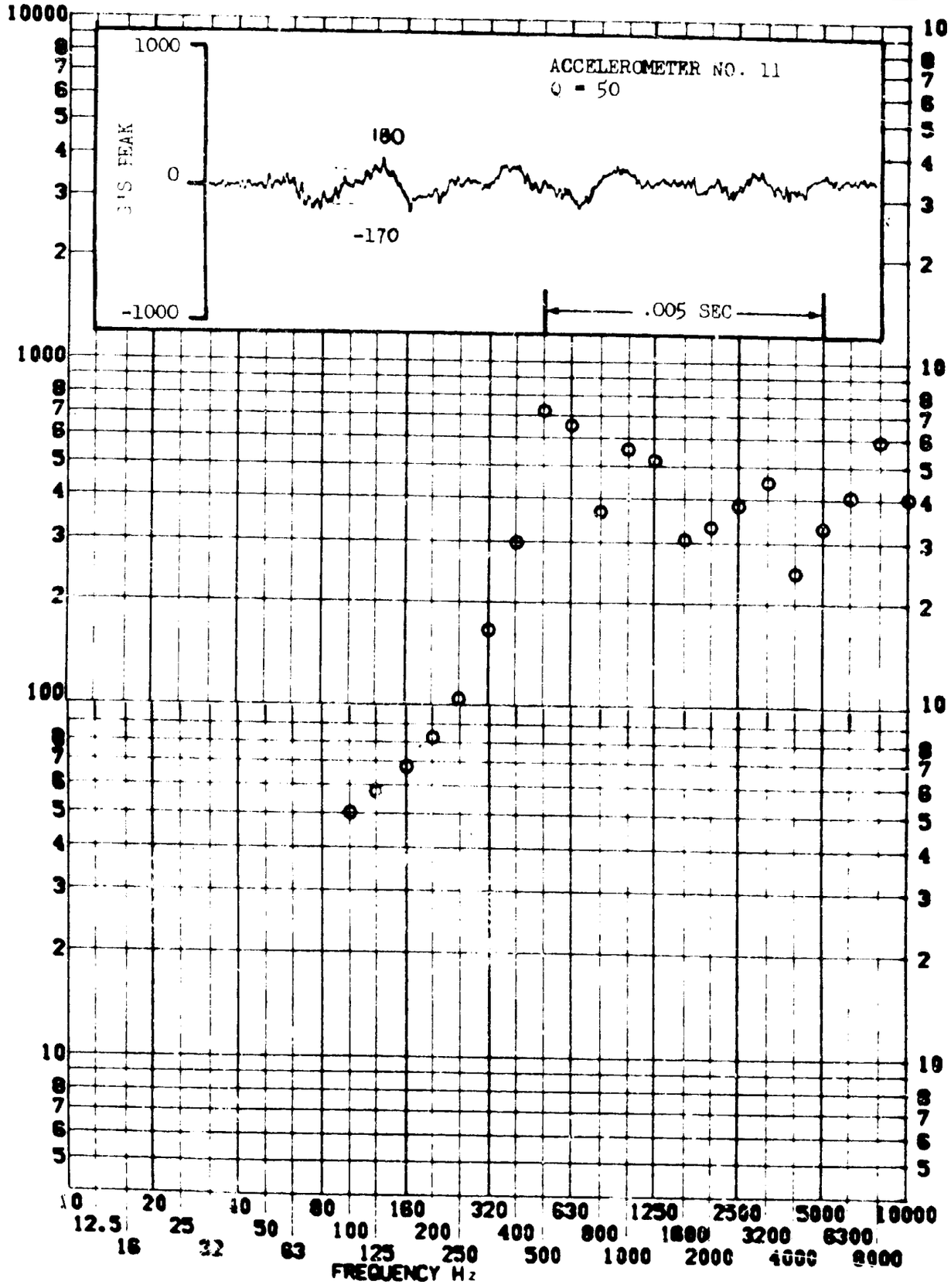

SHOCK TEST ANALYSIS DATA SHEET II.A.4.28

TEST ITEM 790-160
SERIAL NO.
SHOCK AXIS RADIAL

PART NO. STRUCTURE
TEST DATE 23 JUNE 1964
SHOCK NO. 4

RESPONSE G-S

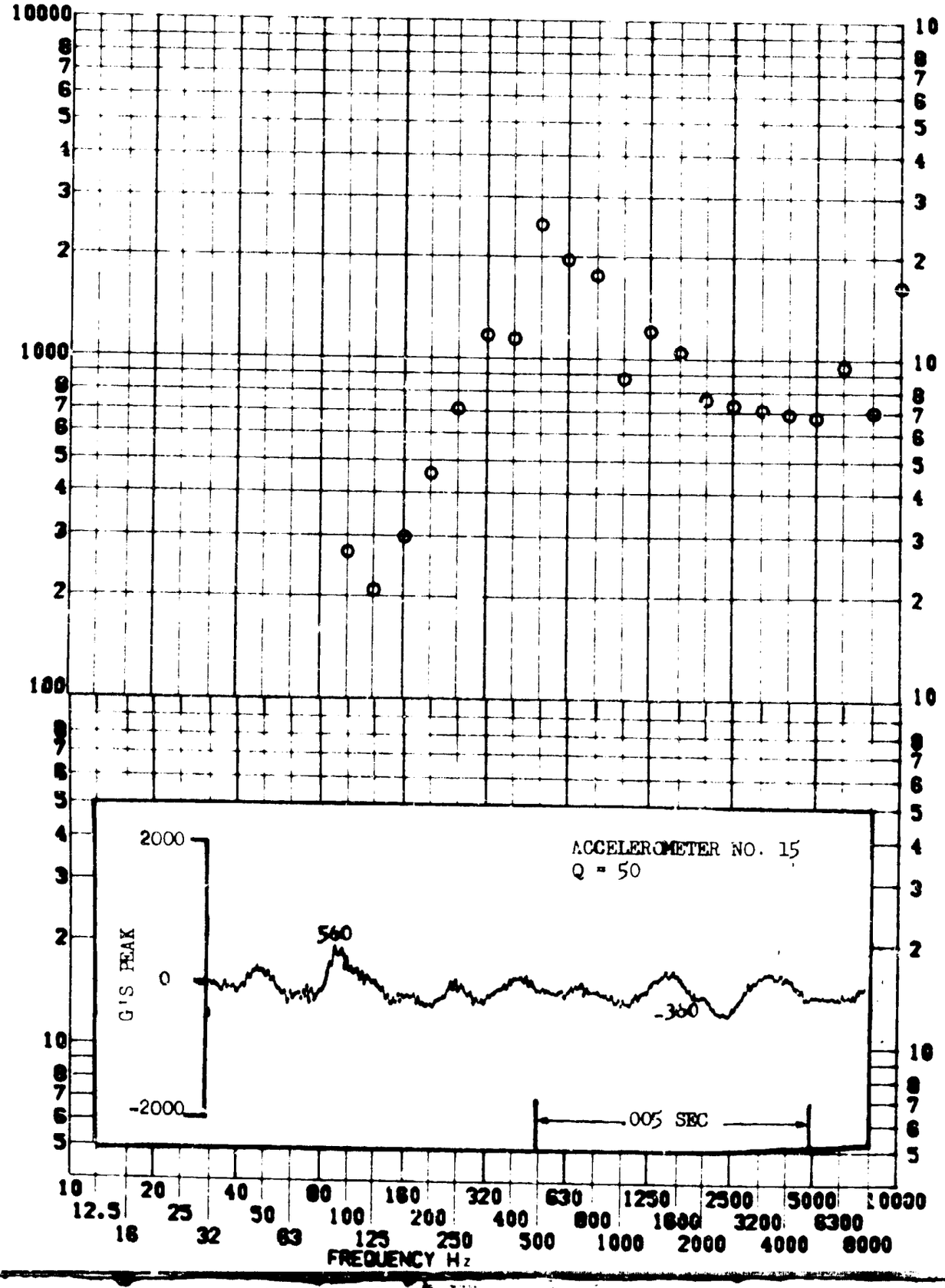

SHOCK TEST ANALYSIS DATA SHEET T.I.A.4.29

TEST ITEM 790-164
SERIAL NO.
SHOCK AXIS LONGITUDINAL

PART NO. STRUCTURE
TEST DATE 23 JUNE 1964
SHOCK NO. 4

RESPONSE G-S

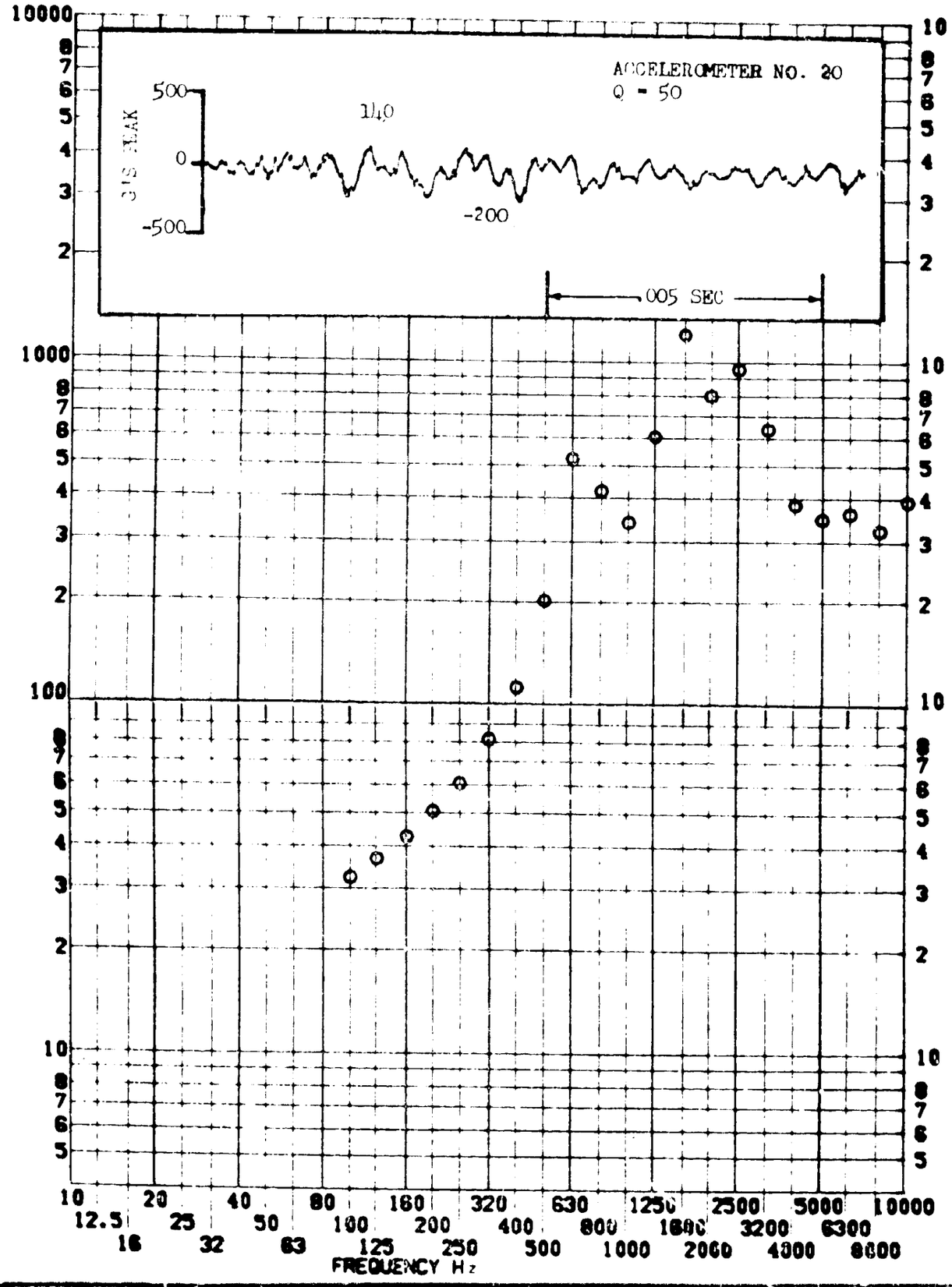

SHOCK TEST ANALYSIS DATA SHEET II.A.4.30

TEST ITEM 790-140
SERIAL NO.
SHOCK AXIS RADIAL

PART NO. STRUCTURE
TEST DATE 23 JUNE 1964
SHOCK NO. 4

RESPONSE G-S

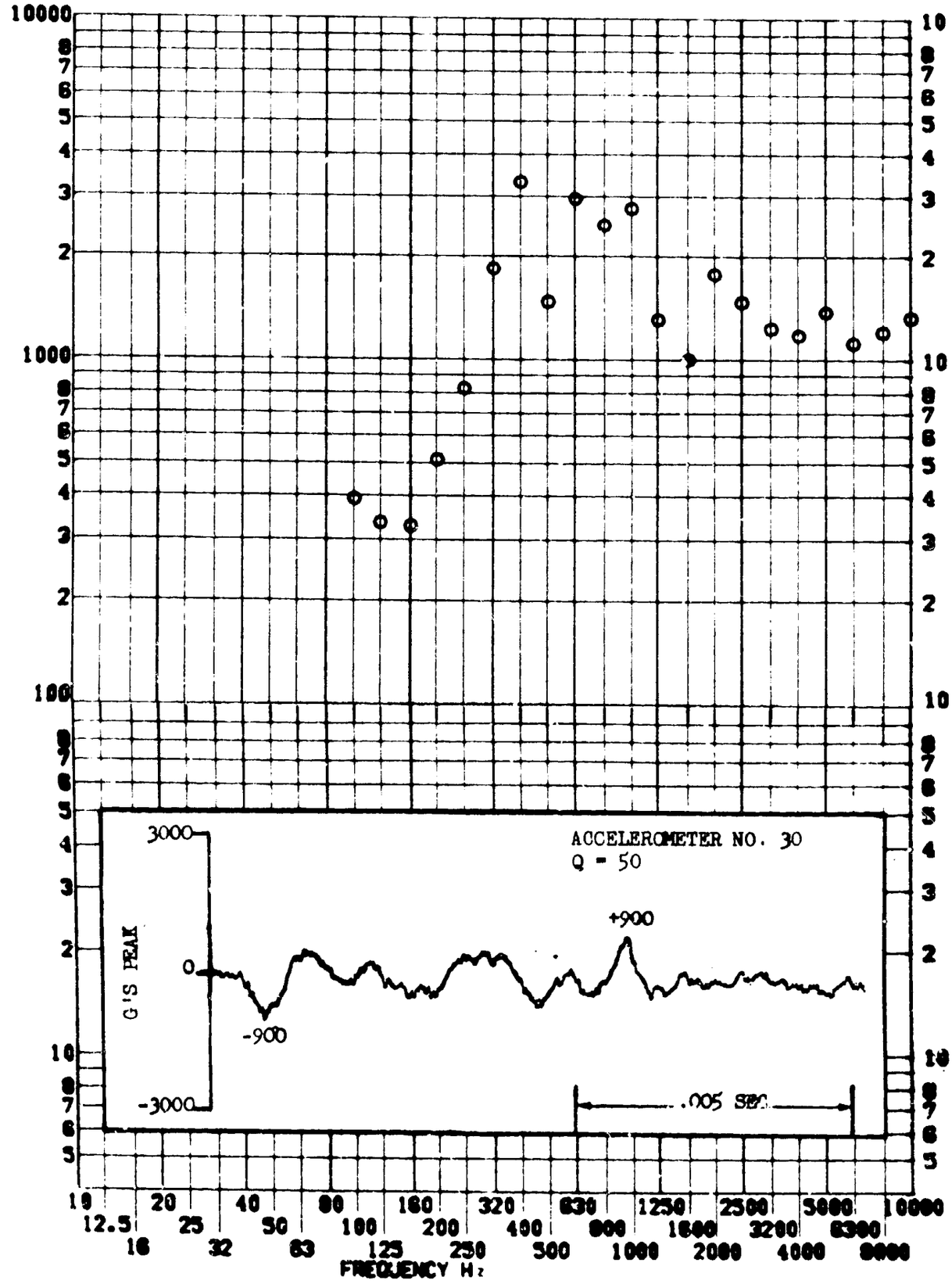

SHOCK TEST ANALYSIS DATA SHEET II.A.4.31

TEST ITEM 790-143,144,145,146
SERIAL NO.
SHOCK AXIS RADIAL

PART NO. STRUCTURE
TEST DATE 23 JUNE 1964
SHOCK NO. 1,2,3,& 4

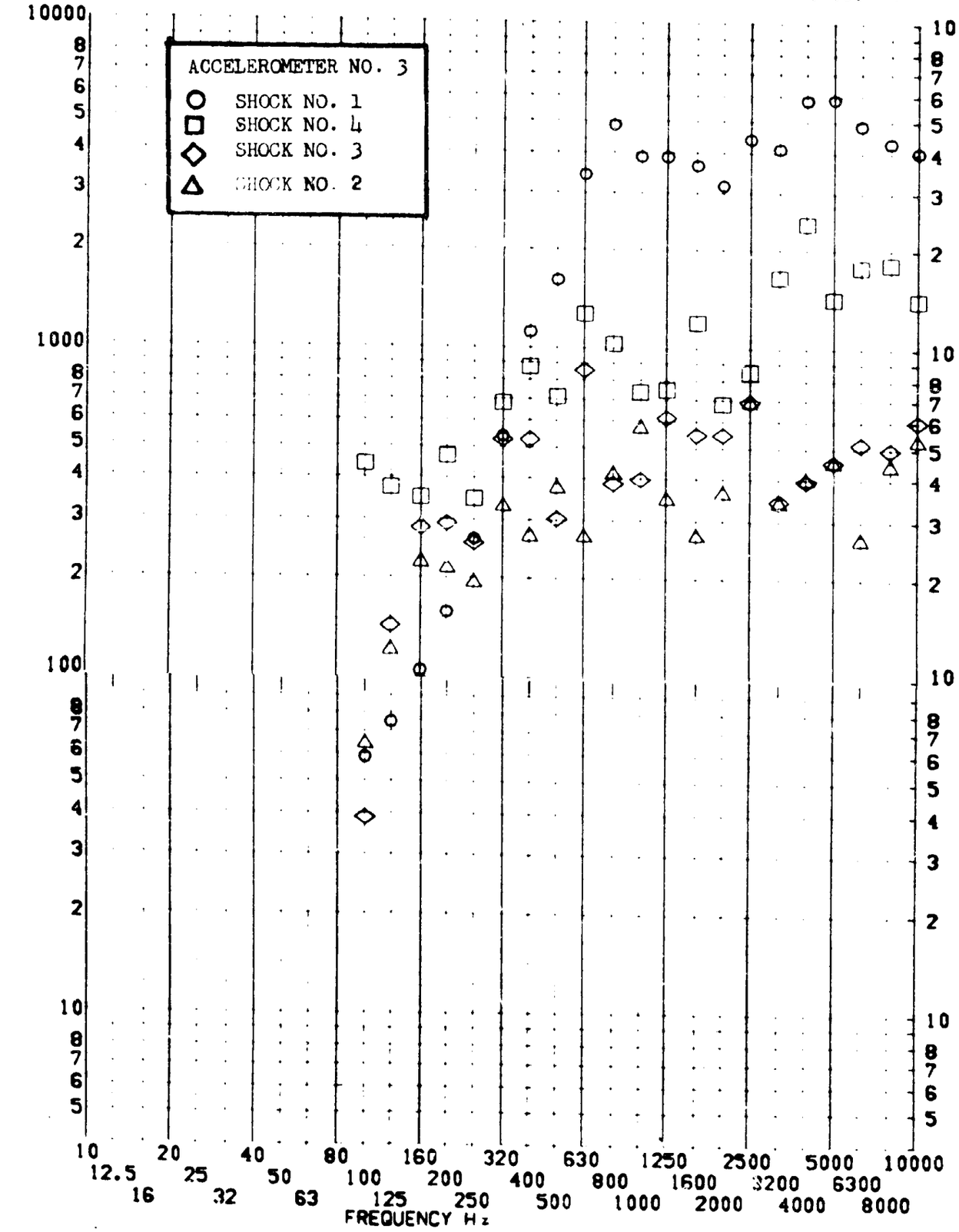

SHOCK TEST ANALYSIS DATA SHEET II.A.4.32

TEST ITEM 790-155,156,157,158
SERIAL NO.
SHOCK AXIS LONGITUDINAL

PART NO. STRUCTURE
TEST DATE 23 JUNE 1964
SHOCK NO. 1,2,3,4

RESPONSE G-S

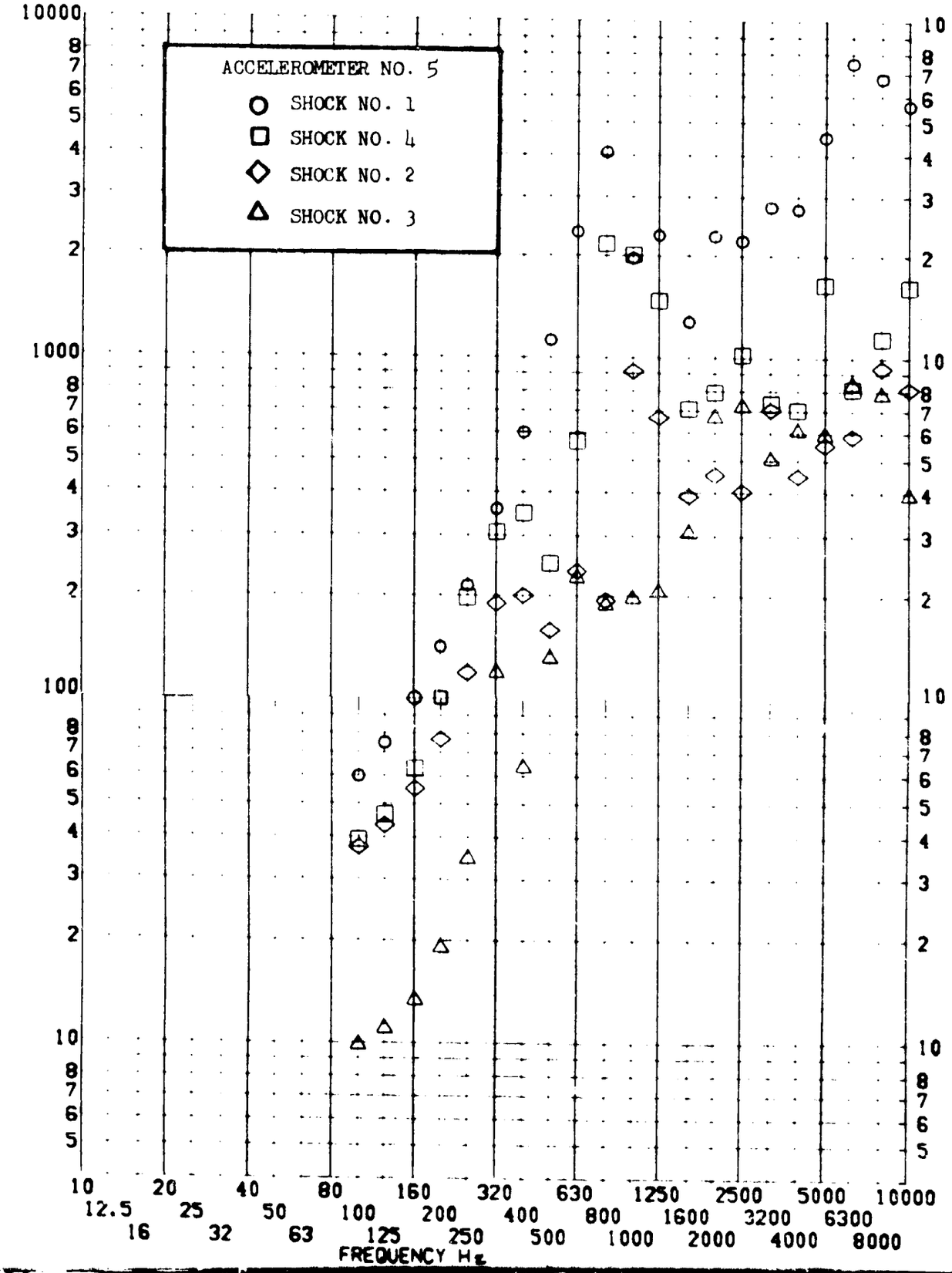

SHOCK TEST ANALYSIS DATA SHEET II.A.4.33

TEST ITEM 790-151,152,153,154
SERIAL NO.
SHOCK AXIS LONGITUDINAL

PART NO. STRUCTURE
TEST DATE 23 JUNE 1964
SHOCK NO. 1,2,3 & 4

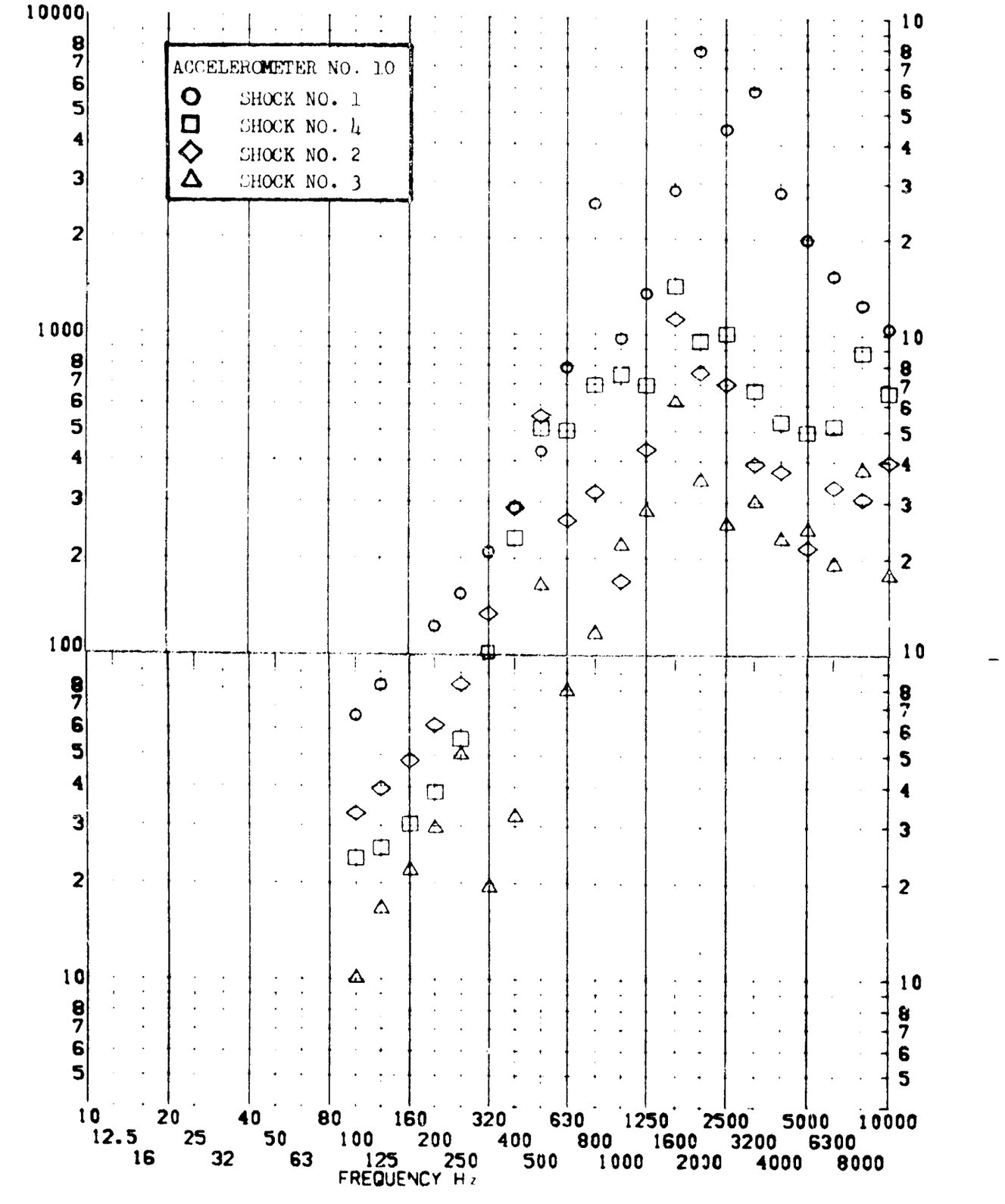

SHOCK TEST ANALYSIS DATA SHEET II.A.4.34

TEST ITEM 790-147,148,149,150 PART NO. STRUCTURE

SERIAL NO. — TEST DATE 23 JUNE 1961

SHOCK AXIS RADIAL SHOCK NO. 1,2,3, & 4

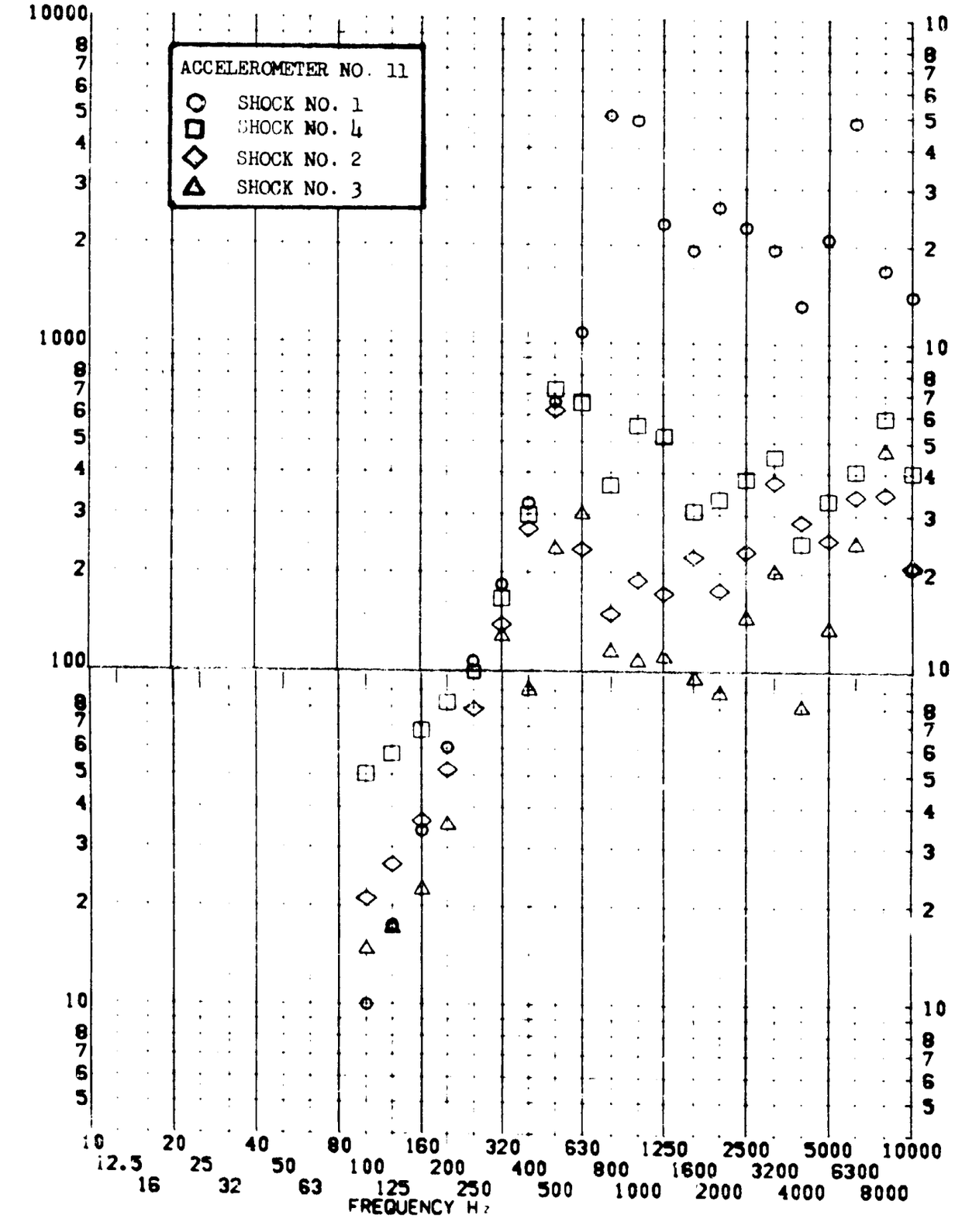

SHOCK TEST ANALYSIS DATA SHEET II.A.4.35

TEST ITEM 790-159,160,161,162
SERIAL NO.
SHOCK AXIS RADIAL

PART NO. STRUCTURE
TEST DATE 23 JUNE 1964
SHOCK NO. 1,2,3,4

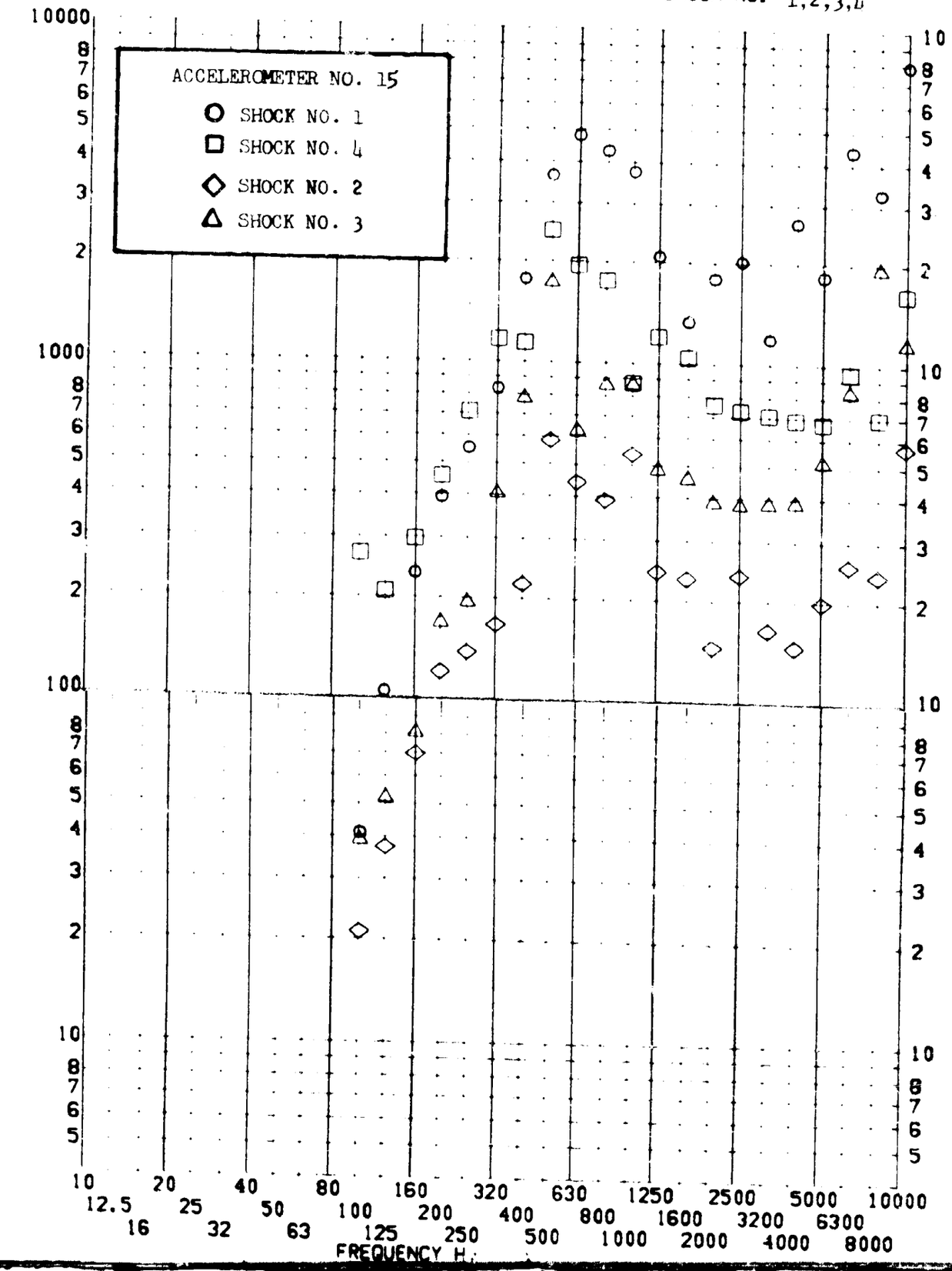

SHOCK TEST ANALYSIS DATA SHEET II.A.4.36

TEST ITEM 790-163,164,165,166
SERIAL NO.
SHOCK AXIS LONGITUDINAL

PART NO. STRUCTURE
TEST DATE 23 JUNE 1964
SHOCK NO. 1,2,3 & 4

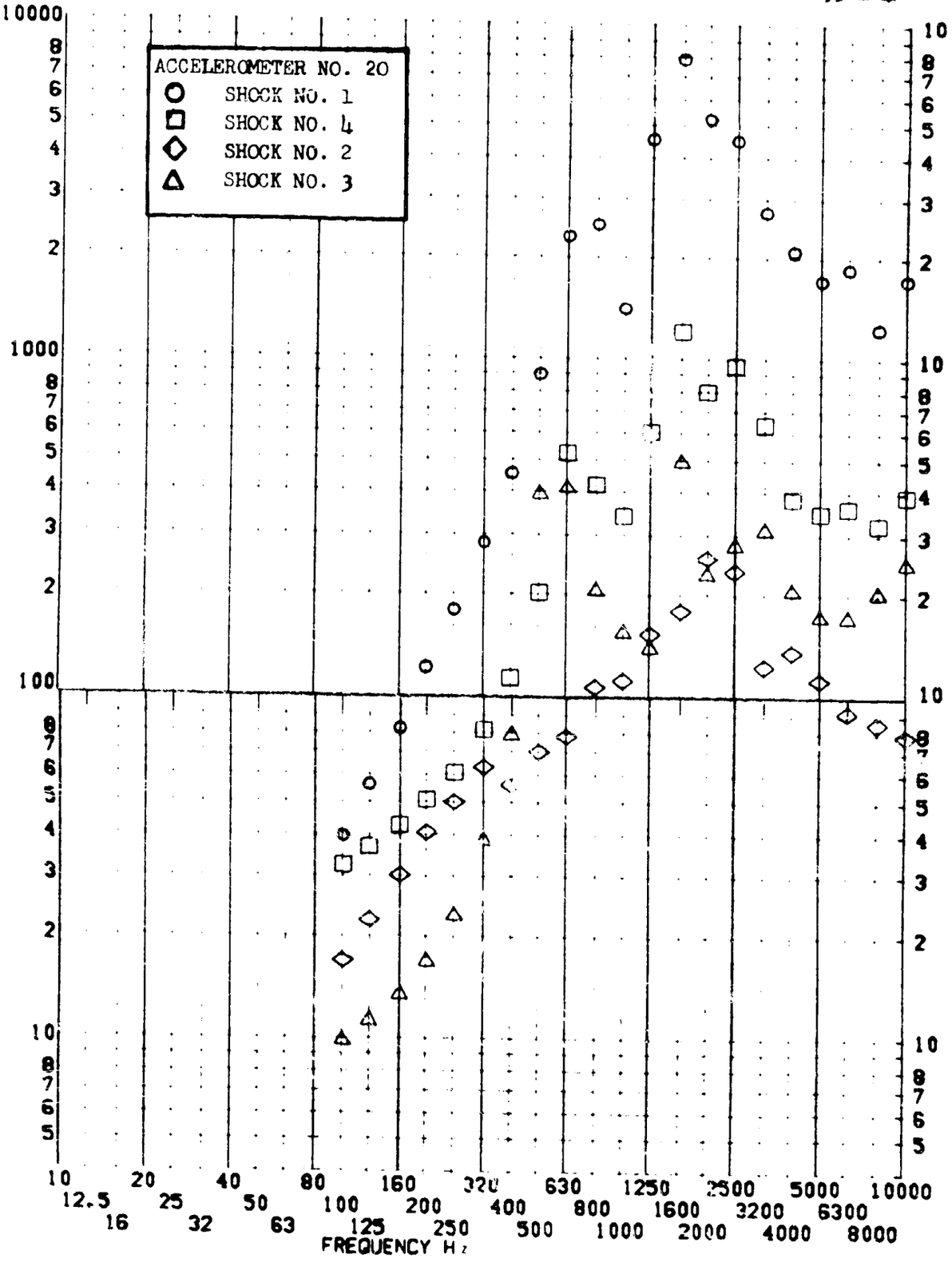

SHOCK TEST ANALYSIS DATA SHEET II.A.4.37

TEST ITEM 790-140,141,142
SERIAL NO.
SHOCK AXIS AXIAL

PART NO. STRUCTURE
TEST DATE 23 JUNE 1964
SHOCK NO. 2,3,&4

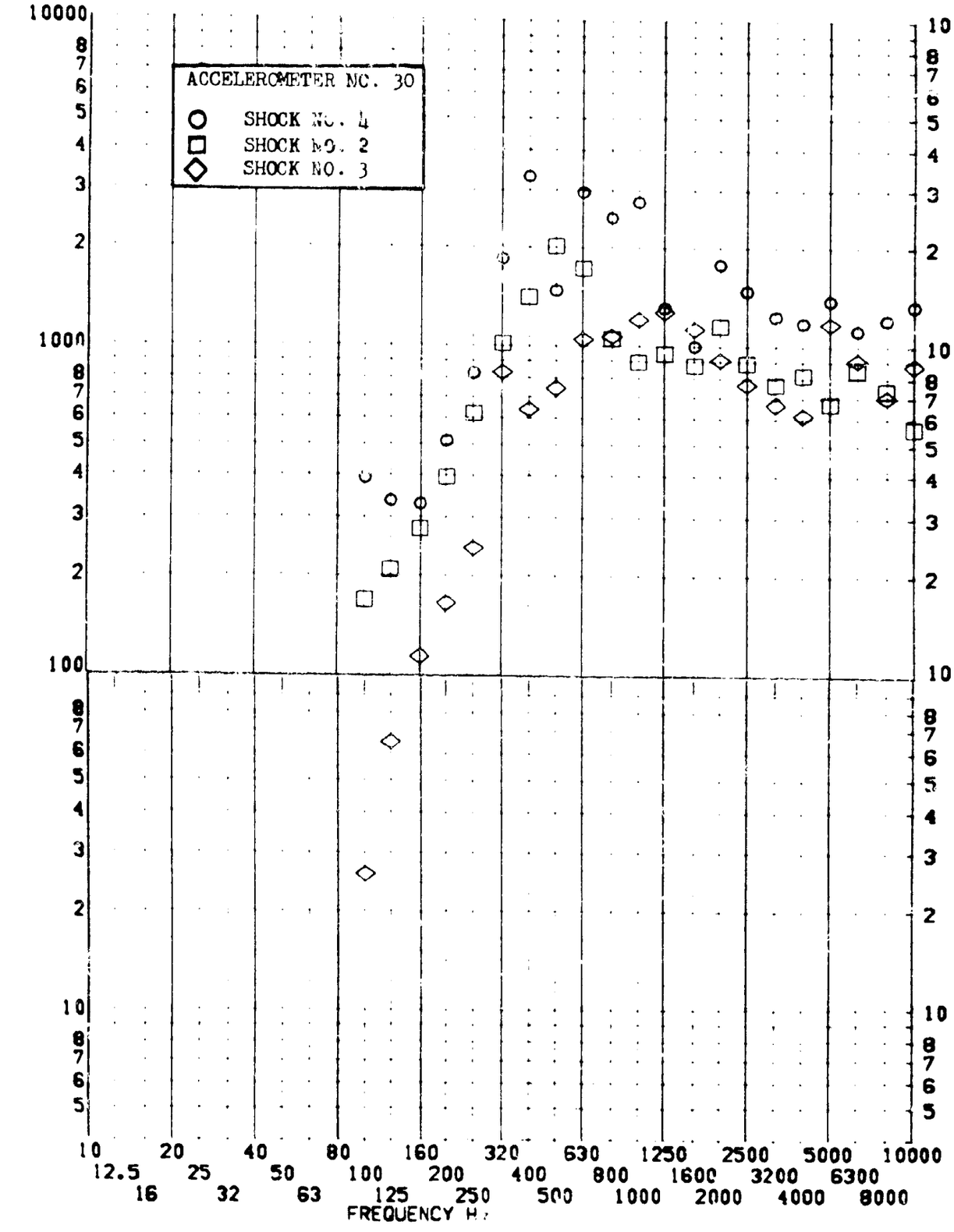

SHOCK TEST ANALYSIS DATA SHEET II.A.4.38

TEST ITEM 790-167,168
SERIAL NO.
SHOCK AXIS LONGITUDINAL

PART NO. STRUCTURE
TEST DATE 23 JUNE 1964
SHOCK NO. 4

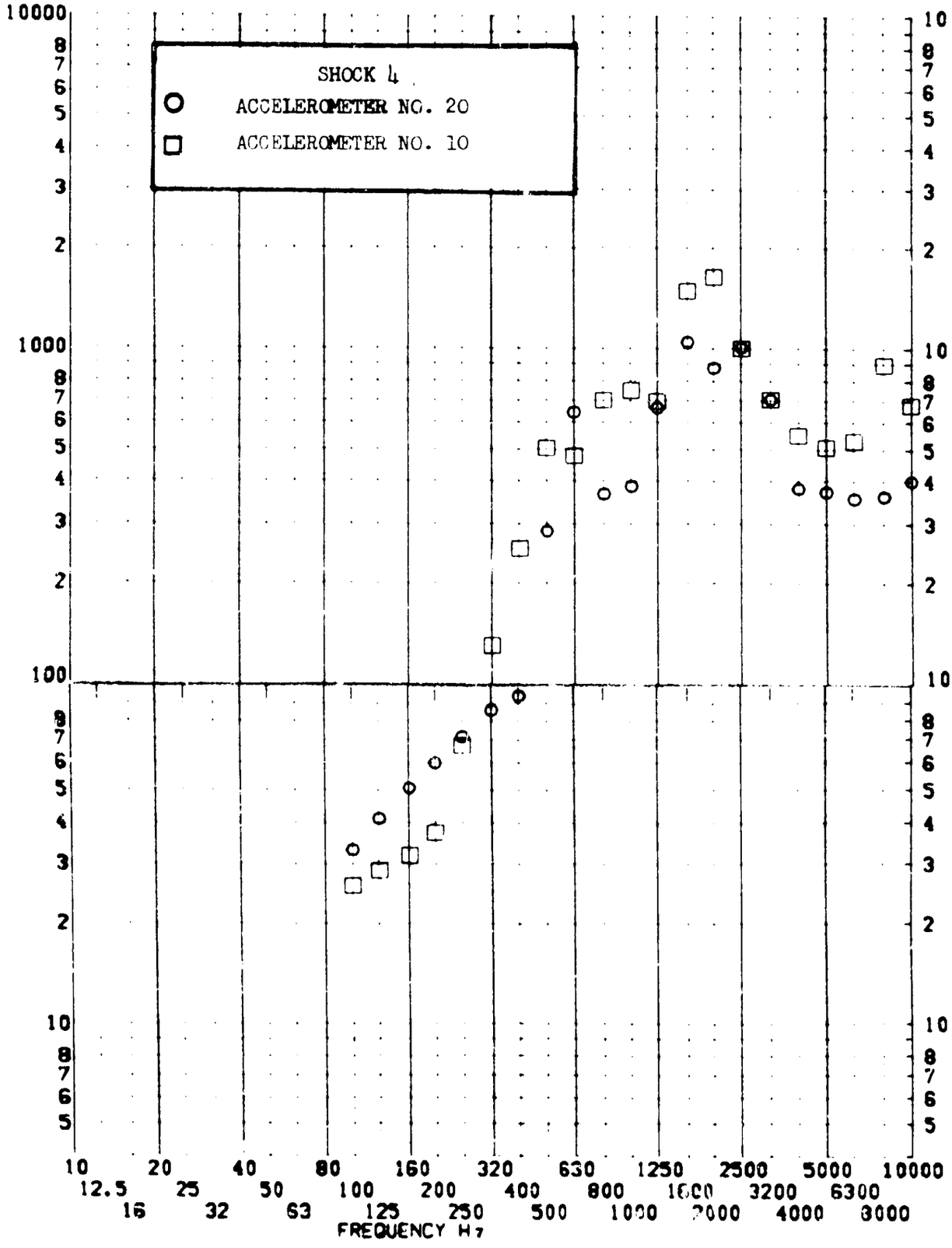

SHOCK TEST ANALYSIS DATA SHEET II.A.4.39

TEST ITEM 790-169,170
SERIAL NO.
SHOCK AXIS LONGITUDINAL

PART NO. STRUCTURE
TEST DATE 23 JUNE 1964
SHOCK NO. 2 & 3

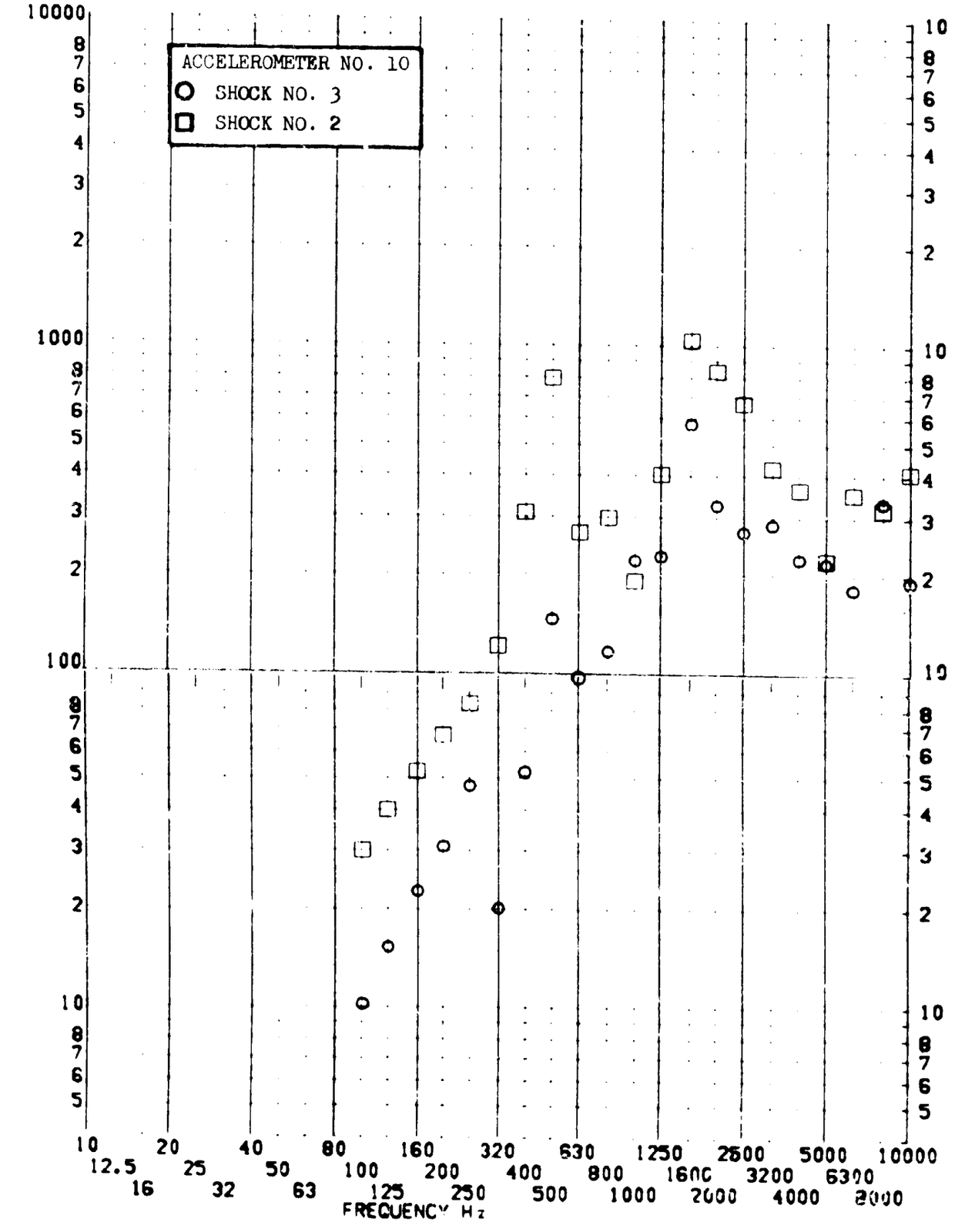

SHOCK TEST ANALYSIS DATA SHEET II.A.4.40

TEST ITEM 790-171,172
SERIAL NO.
SHOCK AXIS RADIAL

PART NO. STRUCTURE
TEST DATE 23 JUNE 1964
SHOCK NO. 2 & 3

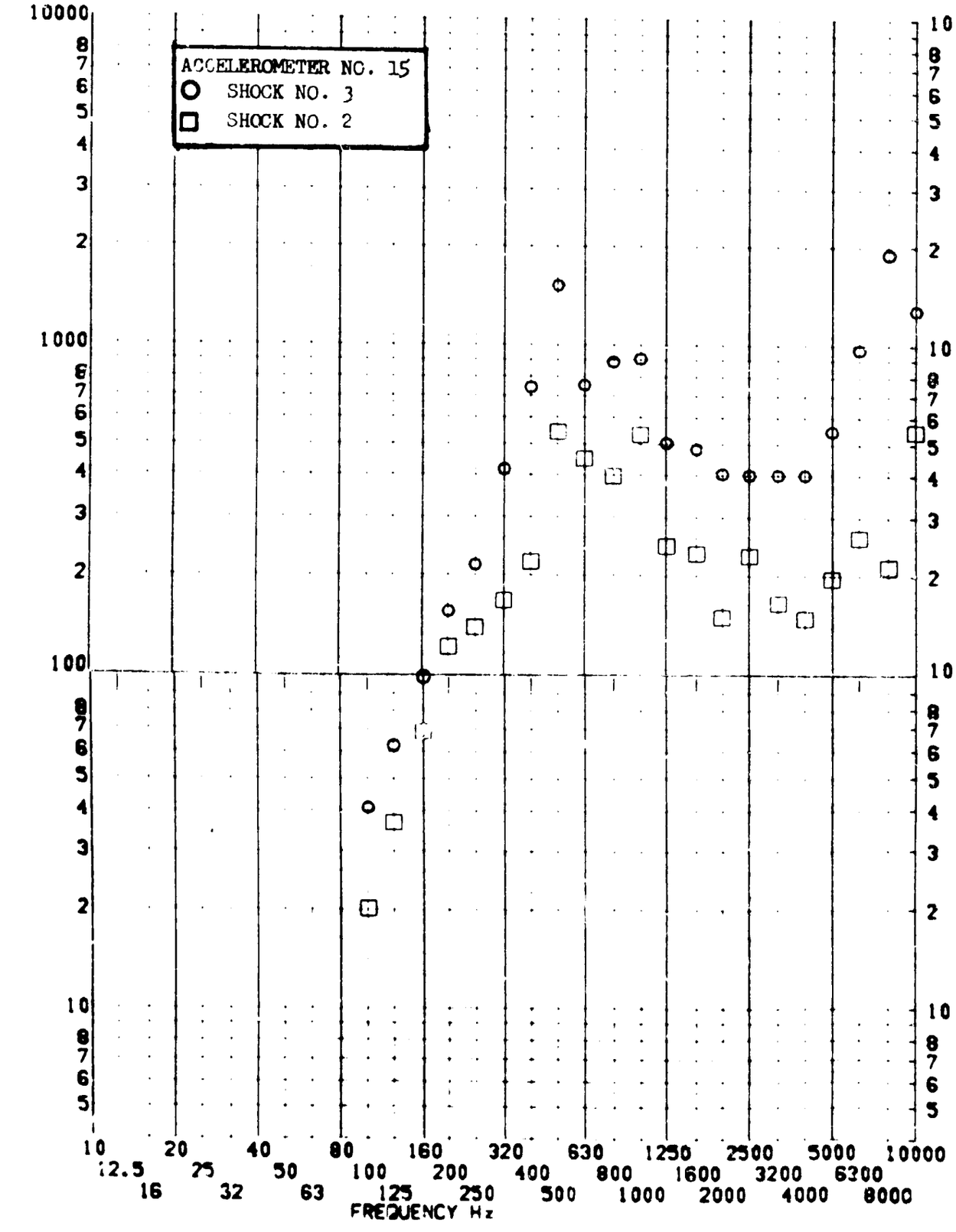

SHOCK TEST ANALYSIS DATA SHEET II.A.4.41

TEST ITEM 790-173,174
SERIAL NO.
SHOCK AXIS LONGITUDINAL

PART NO. STRUCTURE
TEST DATE 23 JUNE 1964
SHOCK NO. 2 & 3

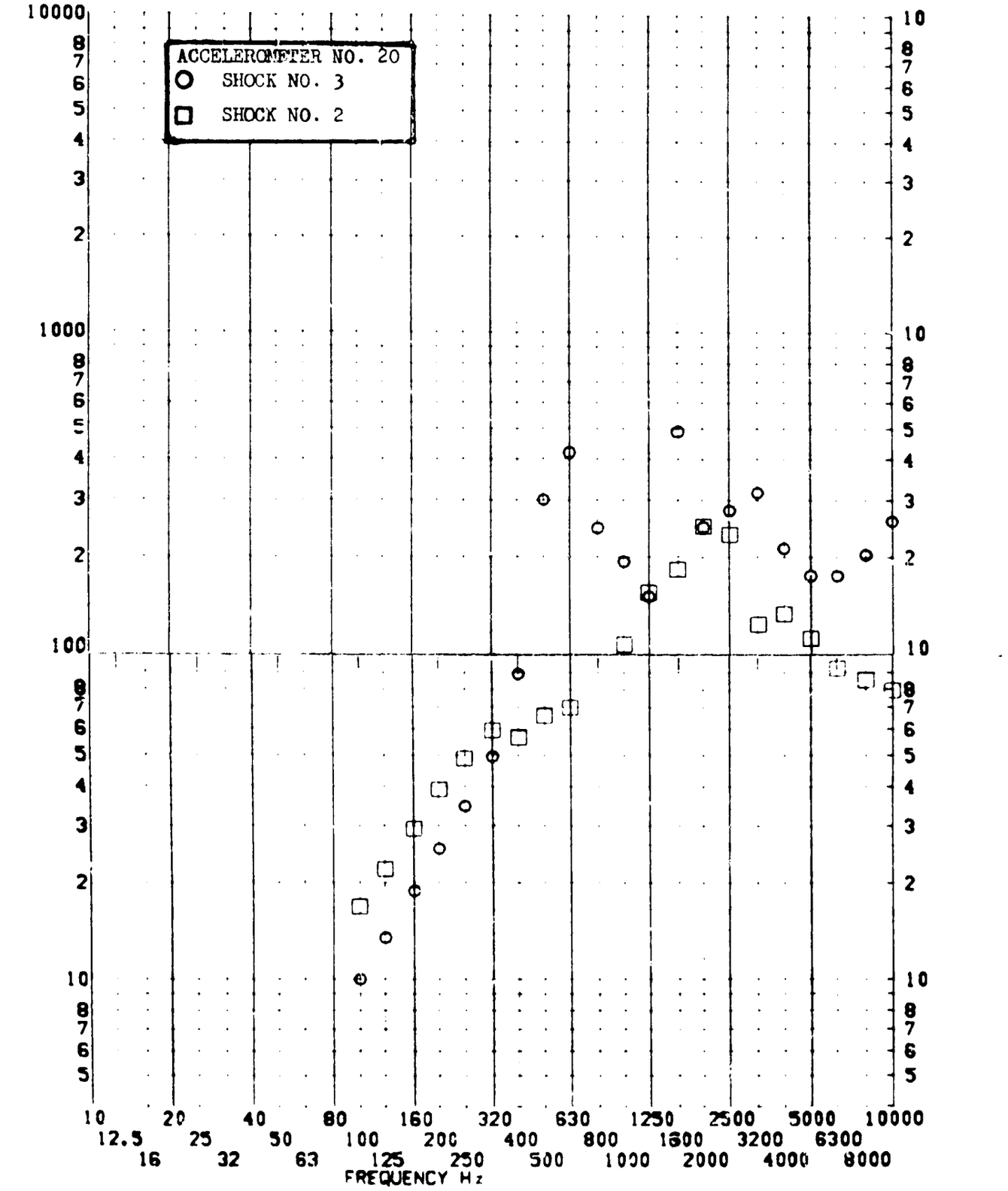

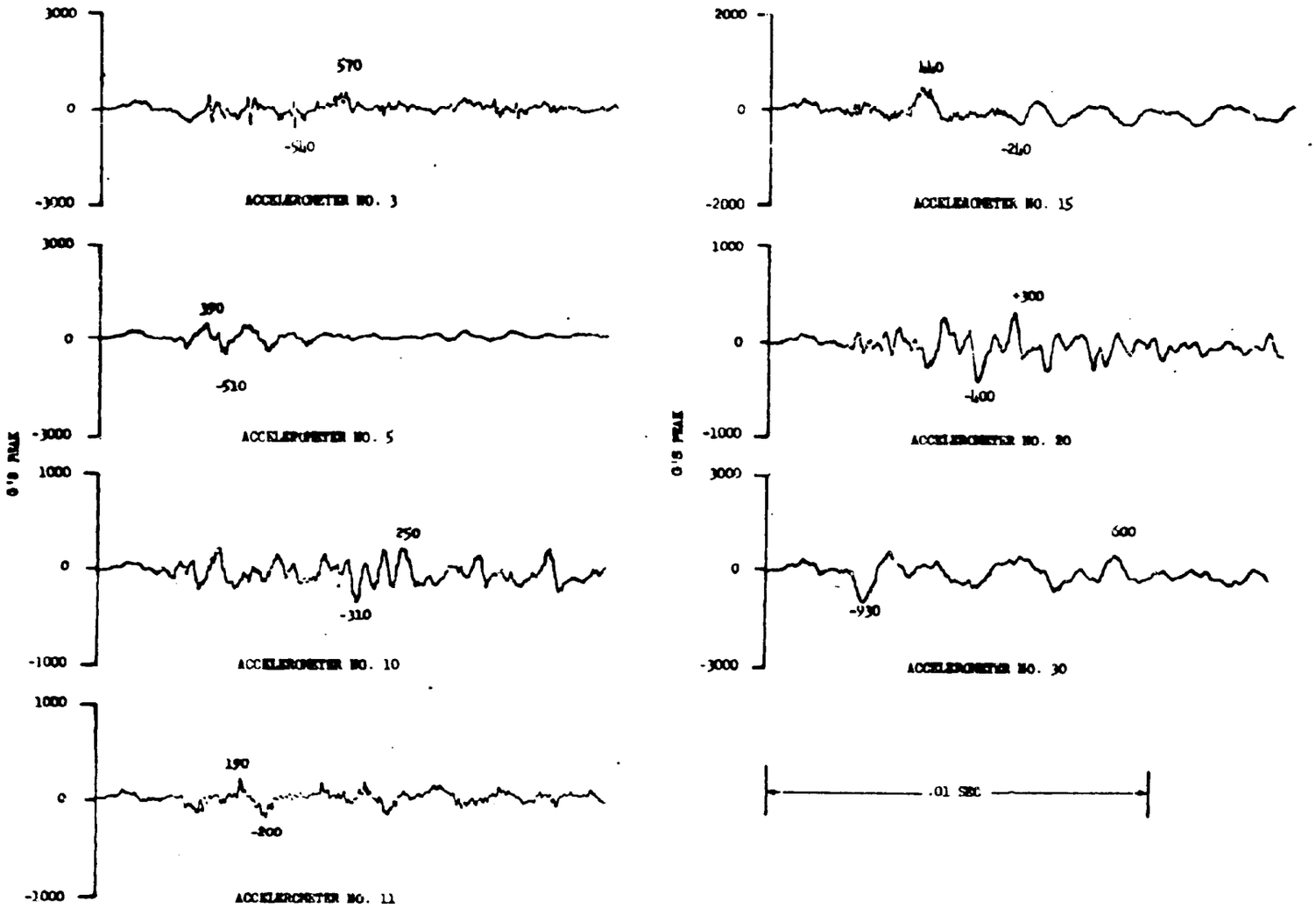

Figure II.A.4.42 Shock Levels During V-Band Separation at Temperature

SECTION NO. II.A.5

REPORT NO. 1080

SUBJECT:

PAYLOAD AHEAD OF FORWARD RACK - SHROUD SEPARATION

SECTION II.A.5

SUMMARY

This report covers pyrotechnic tests performed on a spacecraft equipment structure which is protected during launch by a shroud. The pyrotechnic event under consideration is the separation of the shroud which is achieved by four strap cutters severing a stainless steel strip of metal. The release of the band tension allows the strap to be thrown out from the shroud. The strap cutters are pyrotechnic devices which provide the shock environment investigated here. Removal of the shroud is performed as a secondary operation which does not entail pyrotechnic shock.

The pyrotechnic tests were carried out on an actual flight frame. Two firings were performed. From the first firing, shock spectrums and oscillograms are available for five accelerometers: three on the equipment frame and two on the equipment rack below the separation joint. From the second firing, 10 oscillograms are available for accelerometers located on the equipment frame.

No data recording problems were encountered and the available results appear reliable. However this data was generated for specific equipment installations; it is therefore not well suited for analytical purpose. An attempt was made to define the trend of the shock level attenuation versus distance from the shock source. A general trend could be established from the shock spectrum data but no conclusive results could be obtained from the oscillograms.

The strap/strap-cutter separation joint was selected for this application because it produces a much lower pyrotechnic shock than the standard separation joint. The reduction in shock level varies between 2 and 10 over the frequency range.

TABLE OF CONTENTS

SECTION II.A.5

LIST OF TABLES

SECTION II.A.5

LIST OF FIGURES

SECTION II.A.5

Figures

Shock Spectra and Oscillograms

II.A.5.1 INTRODUCTION

The test set-up was primarily intended for the determination of the environment to which some specific equipment would be subjected. As a result, the readings of only a small number of accelerometers were recorded.

The test installation was set up from actual flight hardware including a forward equipment rack, spacecraft frame and shroud.

Two tests were performed on the entire configuration. For Test 1, Figure II.A.5.1, five accelerometers monitored the environment level at various points of the structure while Test 2, Figure II.A.5.2, had ten accelerometers, three reading environment at the end of the structure and seven reading environment at the interface of equipment. Details of the accelerometers are given on Table II.A.5.1.

A total explosive charge of approximately 40 Gr was fired for each test, the four strap cutters being fired simultaneously.

II.A.5.2 DISCUSSION AND ANALYSIS

II.A.5.2.1 Test Configuration and Instrumentation

The test set-up consisted of an actual spacecraft frame complete with shroud, mounted on a forward equipment rack as shown on Figure II.A.5.1 and II.A.5.2. The four strap cutters (Figure II.A.5.3) were mounted inboard of the strap to fire outboard. The stainless steel strap was mounted under a tensile preload so that it would spring off the vehicle upon firing of the strap cutters.

Two tests were carried out on the entire configuration.
For Test 1, Figure II.A.5.1, five accelerometers monitored the environment level at various points of the structure while Test 2, Figure II.A.5.2, had ten accelerometers, three reading environment at the end of the structure and seven reading environment at the interface of equipment. Details of the accelerometers are given on Table II.A.5.1.

A total explosive charge of approximately 40 Gr was fired for each test, the four strap cutters were fired simultaneously.

II.A.5.2.2 Technical Discussion

Upon completion of the tests, inspection of the specimen showed that no failure occurred. All accelerometer readings were found to be reliable and free from noise and other anomalies.

Shock spectra were established only for the data of Test 1. They are presented on Figures II.A.5.7 to II.A.5.11. The data was reduced for Q = 5 and Q = 25. Both values are available for comparison purpose on Figures II.A.5.7 to II.A.5.11.

Oscillograms are presented on Figure II.A.5.12 for each accelerometer of shock No. 2.

II.A.5.2.3 Analysis

An attempt was made to determine the trend of the shock attenuation versus distance from the shock source. This was accomplished first

from the shock spectrum of Test 1, taking peaks in each octave band from 200 to 6400 cps, Figure II.A.5.4, then for both tests combined by taking peak g levels from oscillogram data, Figure II.A.5.5.

Although based on only three points per curve, the data of Figure II.A.5.4 tends toward the general shape of an attenuation curve, even though unexpected results are shown for the readings closer to the shock source. The data taken from the oscillogram, Figure II.A.5.5, also tends toward the same trend for the accelerometers reading the structure environment. However, the amount of data available is not sufficient to be conclusive.

The strap separation joint generates a shock level which is lower than the standard separation joint. Figure II.A.5.6 shows a comparison of shock level envelopes for the two types of joint. It will be noted that the standard joint uses about 157 grains of explosive (5 foot diameter, 10 gr/ft) while the four strap cutters have only 40 grains (1 foot x 40 gr) collectively. The reduction in shock level provided by the strap system is significant. As can be seen on Figure II.A.5.6, it varies over the frequency range with reduction factors from about 2 to 10.

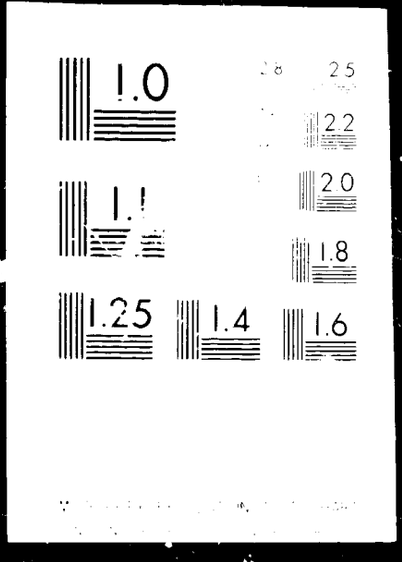

II.A.5.3 CONCLUSION

The tests successfully demonstrated that the structure and equipment under consideration were capable of surviving the pyrotechnic shock environment.

The scope of the test was limited to investigating points of interest to the designers. As a result, the amount of available data is insufficient to perform a general analysis of the environment to which this frame is subjected. The attempt at determining a curve of shock attenuation versus distance from the shock source remains largely inconcludsive although it indicates the generally expected trend.

The strap/strap-cutter separation joint provides a much lower shock environment than the standard separation joint. Reduction by factors of from 2 to 10 are shown to exist over the frequency range.

TABLE II.A.5.1

ACCELEROMETERS AND LOCATIONS

Accelerometer Number	Test Number	Station	Direction	Distance to Shock source	Accelerometer Type
1	1	132	Y	113.0	Endevco 2225
2	1	220	Y	25.0	Endevco 2225
3	1	230	Y	15.0	Endevco 2225
6	1	251.5	R, X	6.5	Endevco 2225
15	2	132	X	113.0	Endevco 2225
16	2	132	Y	113.0	Endevco 2225
17	2	132	Z	113.0	Endevco 2225
18	2	221	X	24.0	Endevco 2225
19	2	221	Y	24.0	Endevco 2225
20	2	221	Z	24.0	Endevco 2225
21	2	181	X	64.0	Endevco 2225
22	2	181	Z	64.0	Endevco 2225
23	2	192	X	53.0	Endevco 2225
24	2	192	Z	53.0	Endevco 2225

TABLE II.A.5.2

SUMMARY OF TESTS

Test Number	Configuration	Explosive Size	Test Purpose	Shock Isolation
1 *	Separation	40 Gr/ft *	Structure	None
2	Separation	40 Gr/ft	Structure and Equipment	None

* V Band Separation Test

TABLE II.A.5.3

SUMMARY OF OSCILLOGRAMS PEAK G LEVELS

Accelerometer	G Level	d inch*	Symbols
1Y	96	-113	x
2Y	510	25	x
3Y	400	15	x
6X	590	6.5	x
6R	400	6.5	x
15X	100	-113	x
16Y	194	-113	x
17Z	160	-113	x
18X	147	24	o
19Y	173	24	o
20Z	166	24	o
21X	80	64	o
22Z	133	64	o
23X	67	53	o
24Z	67	53	o

* Distance to Shock Source - inches

x Structure

o Equipment

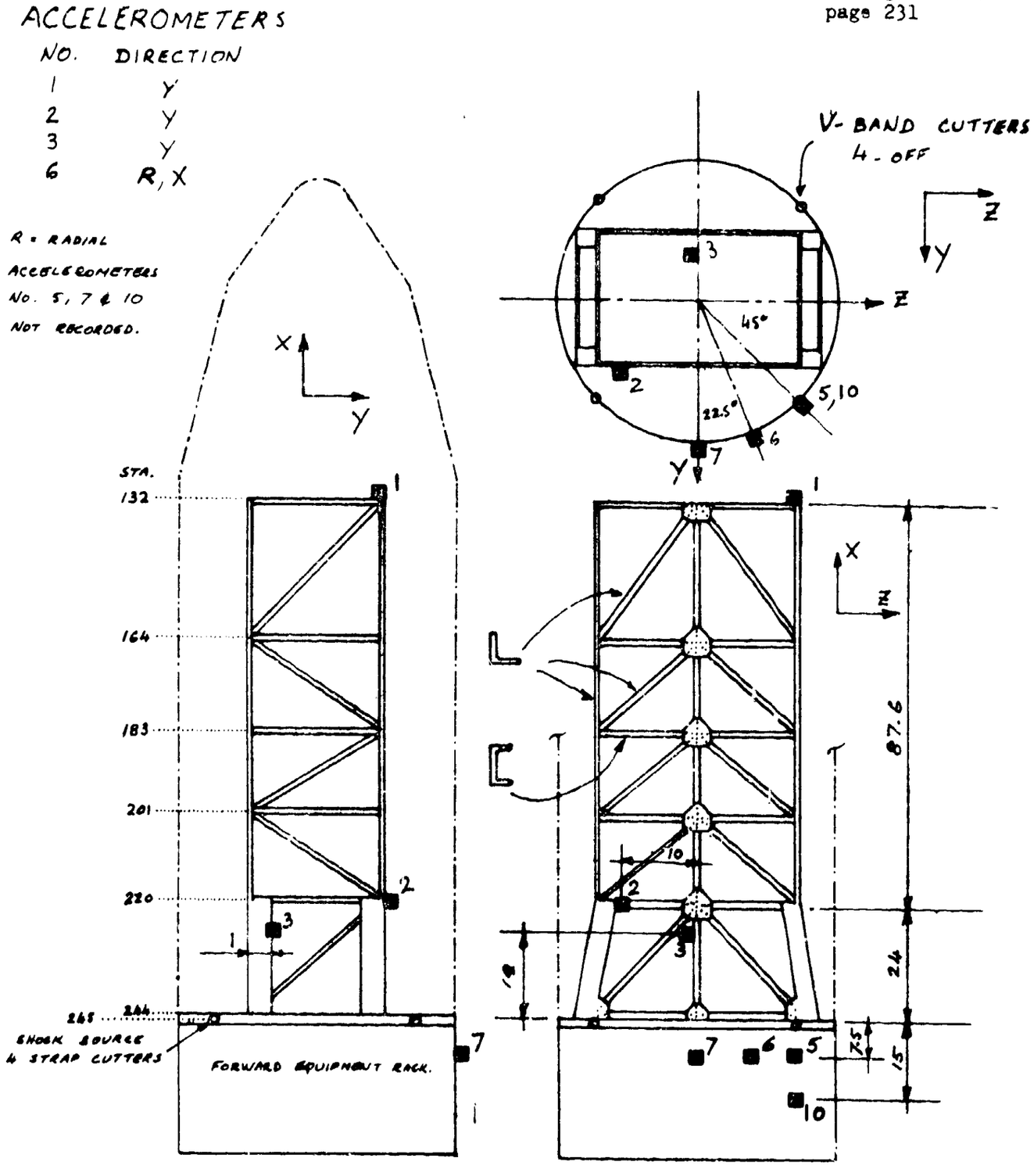

Figure II.A.5.1 TEST 1 CONFIGURATION AND INSTRUMENTATION

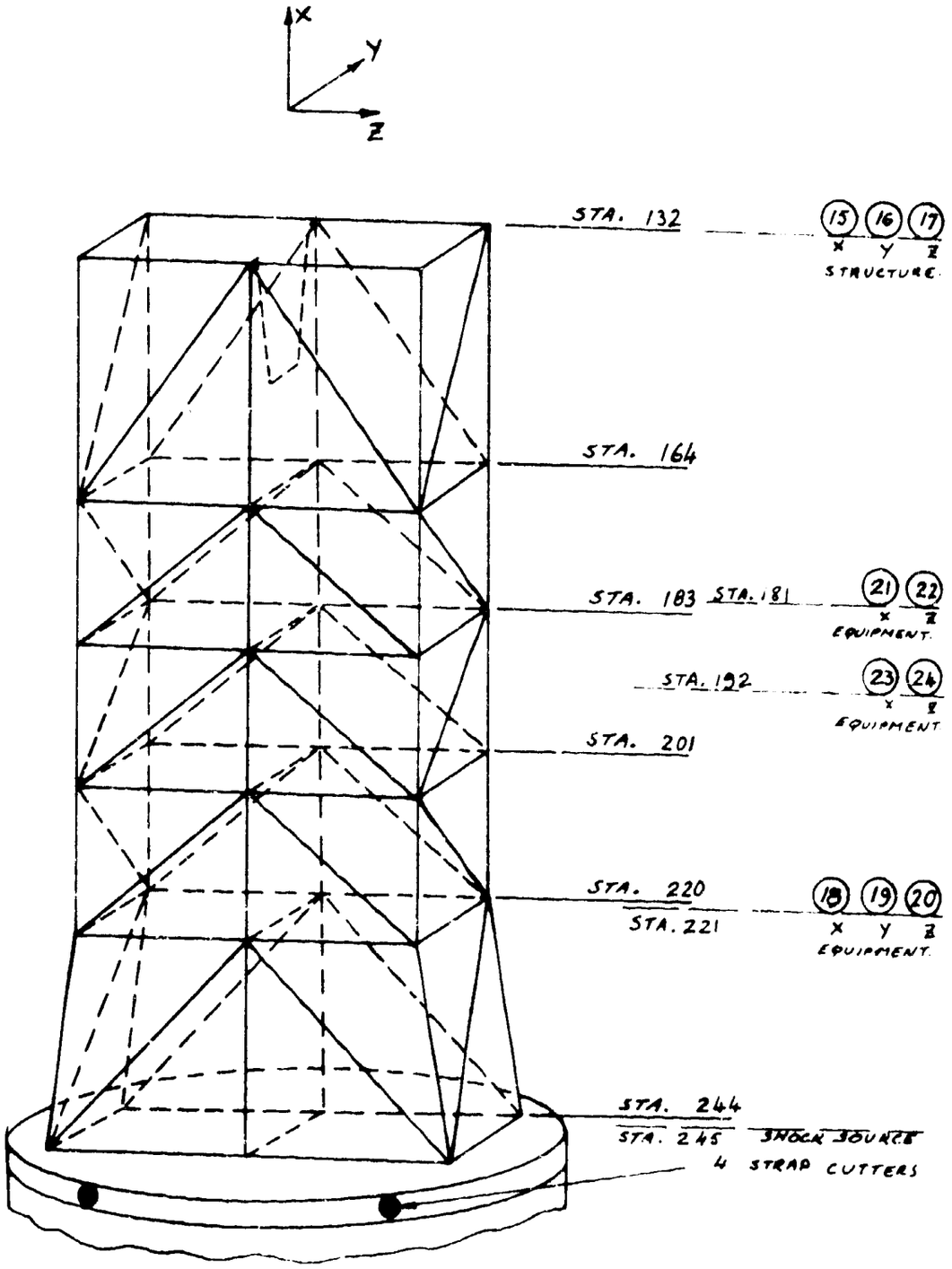

Note: Exact accelerometer locations within framework are not known.

Figure II.A.5.2 TEST 2 CONFIGURATION AND INSTRUMENTATION

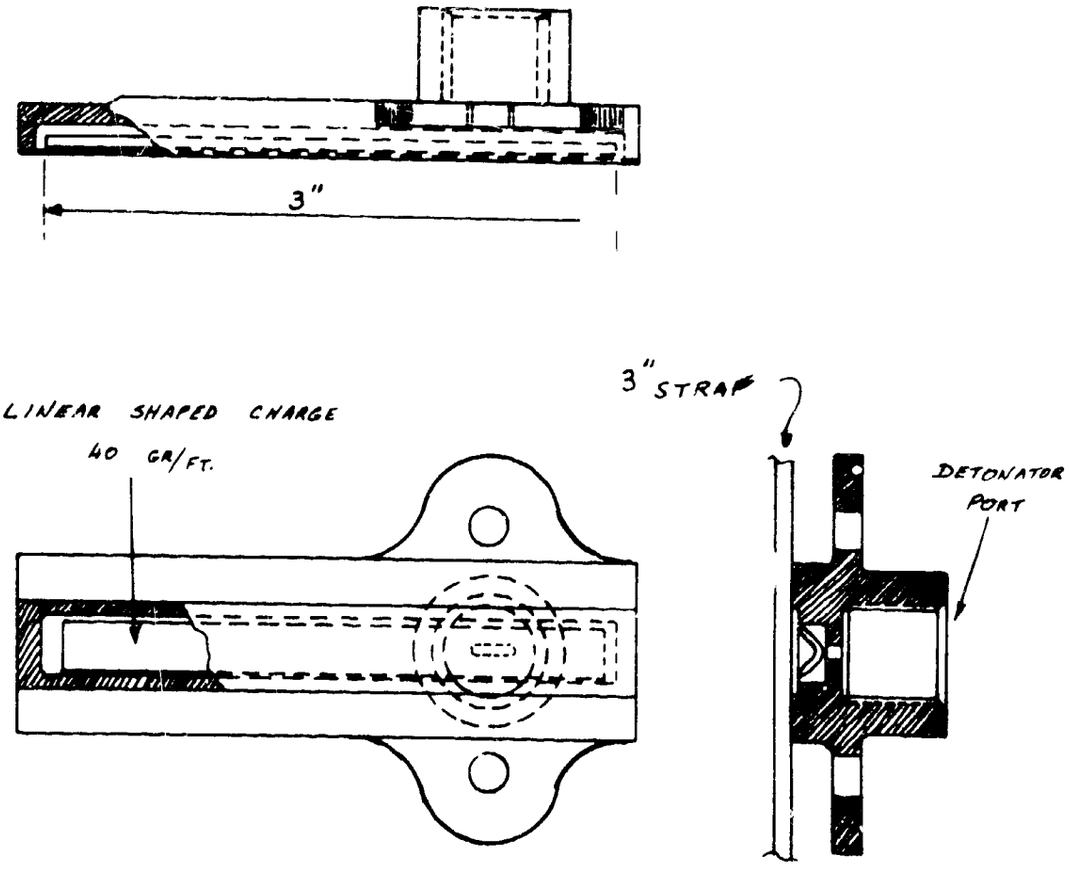

Figure II.A.5.3 TYPICAL STRAP CUTTER - SCALE: FULL SCALE

Data based on peak values in each
octave band as read on shock spectrum.
Q = 25

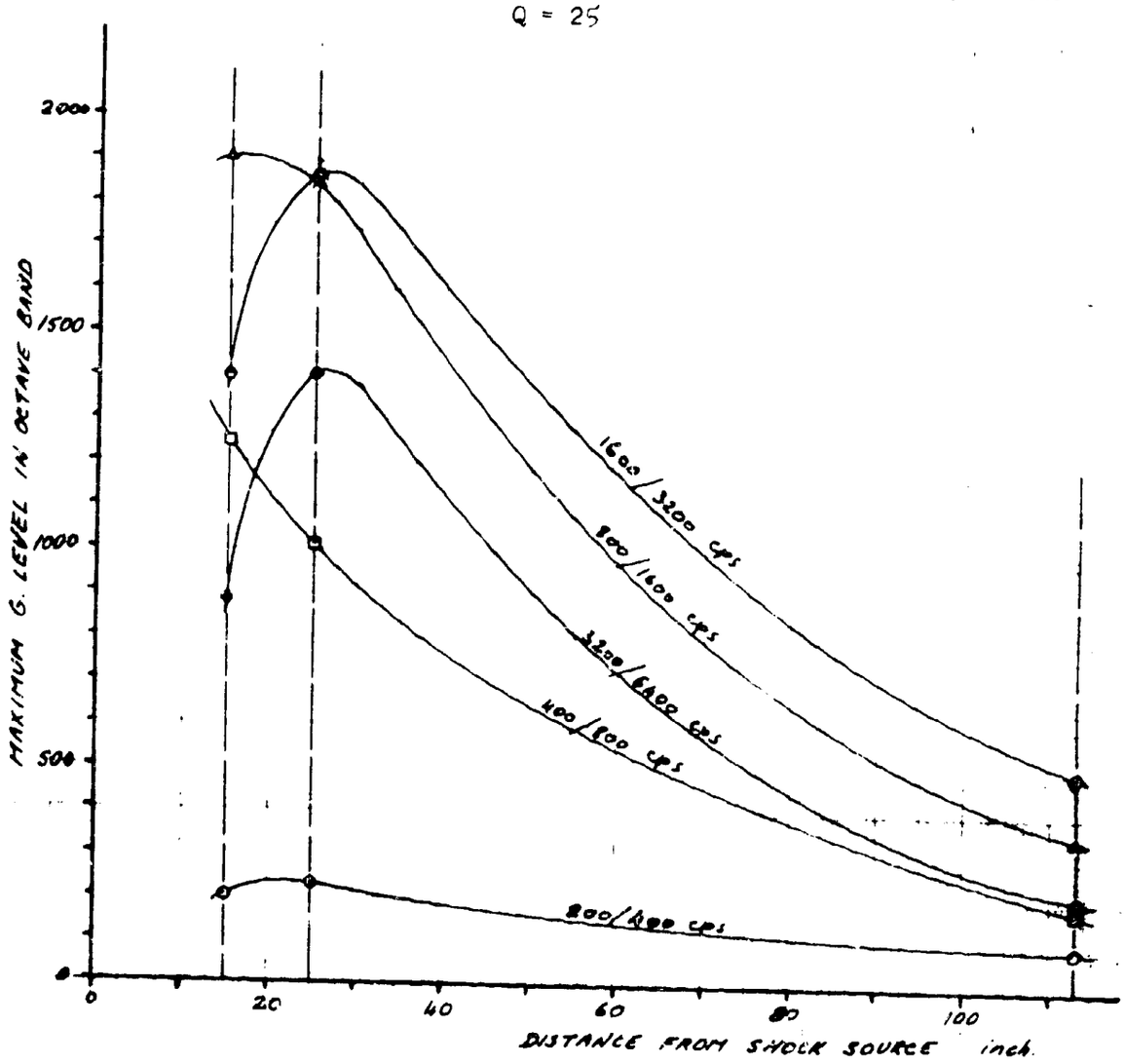

Figure II.A.5.4 TREND OF ATTENUATION VERSUS DISTANCE FROM SHOCK SOURCE FOR EACH OCTAVE BAND

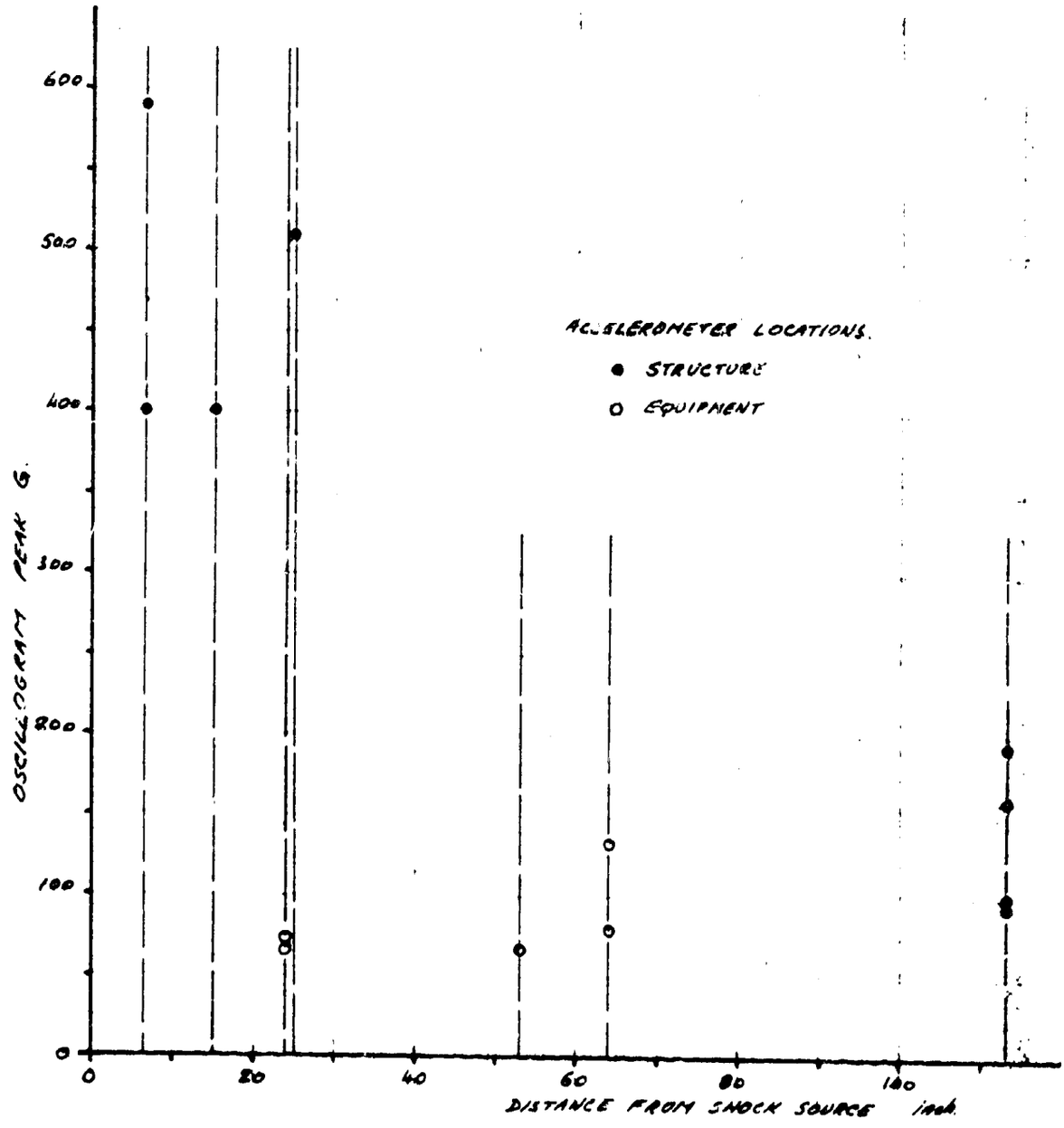

Figure II.A.5.5 DISTRIBUTION OF PEAK G LEVEL VERSUS DISTANCE FROM SHOCK SOURCE DERIVED FROM OSCILLOGRAM DATA

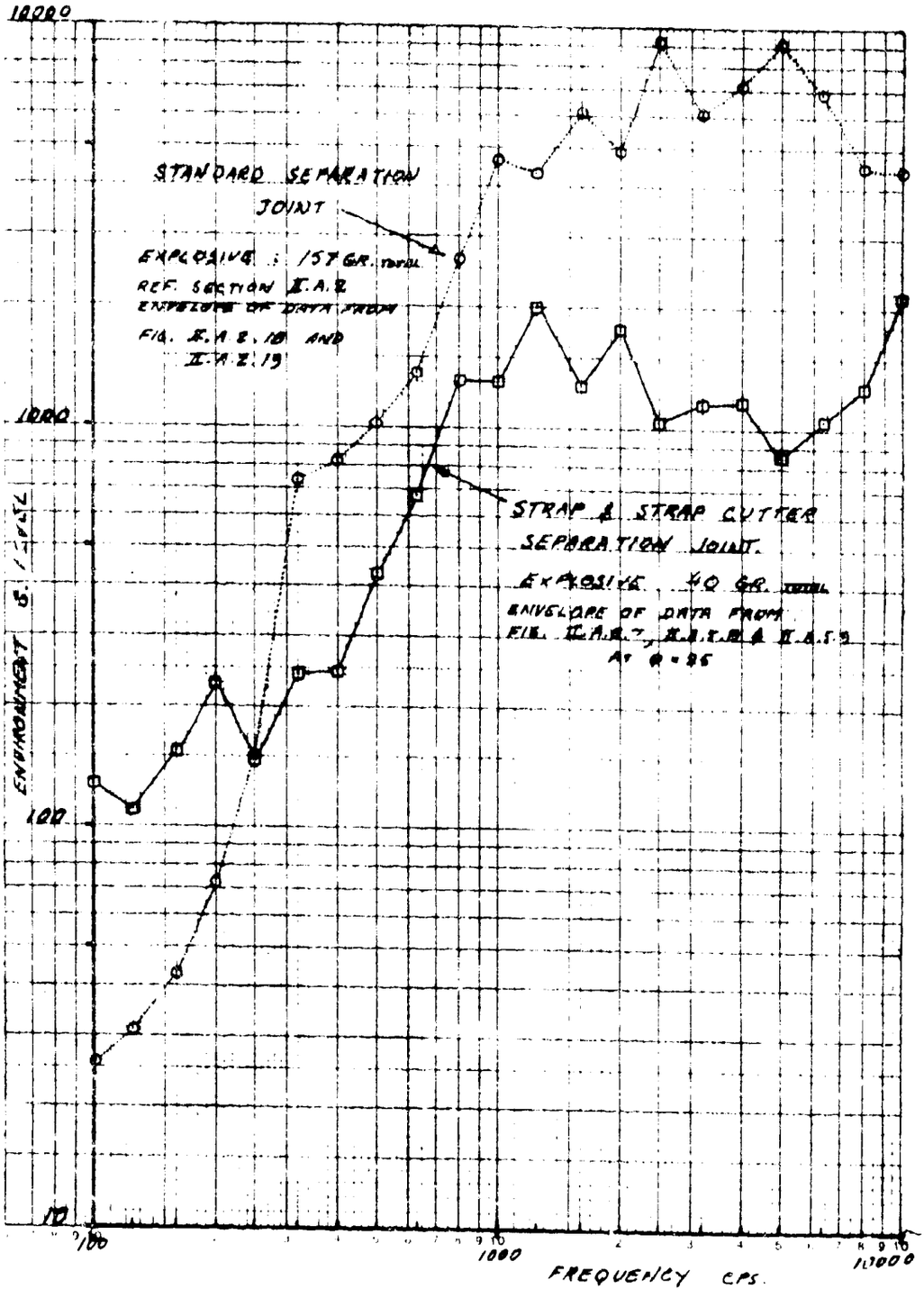

Figure II.A.5.6 COMPARISON OF SHOCK ENVIRONMENTS - STANDARD AND STRAP + CUTTER SEPARATION JOINT

SHOCK TEST ANALYSIS DATA SHEET II.A.5.7

TEST ITEM 1080-130.111
SERIAL NO.
SHOCK AXIS LATERAL

PART NO. STRUCTURE
TEST DATE 27 JAN 1966
SHOCK NO. 1

RESPONSE G-S

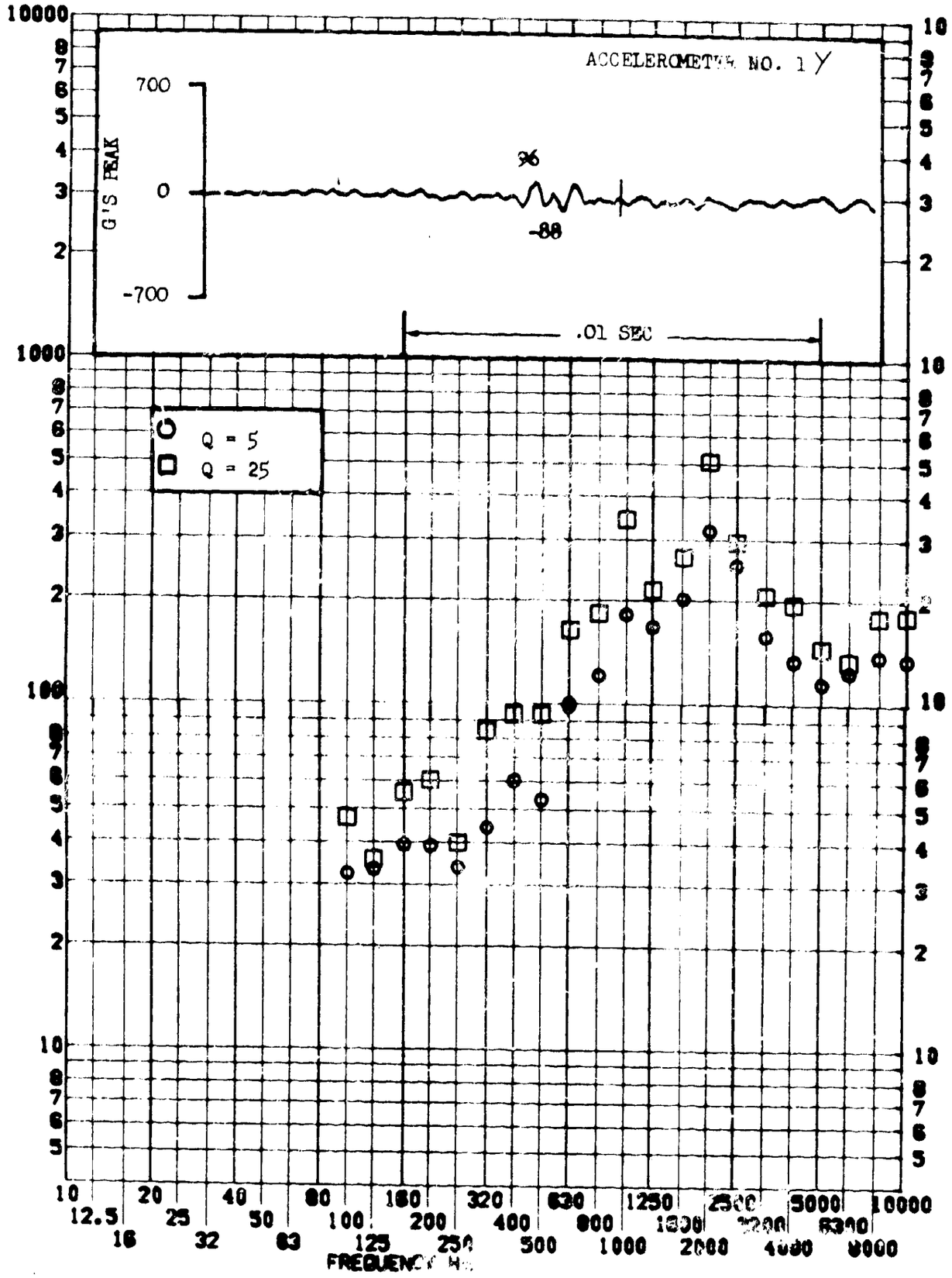

SHOCK TEST ANALYSIS DATA SHEET II.A.5.8

TEST ITEM 1080-132,133
SERIAL NO.
SHOCK AXIS LATERAL

PART NO. STRUCTURE
TEST DATE 27 JAN 1966
SHOCK NO. 1

RESPONSE G-S

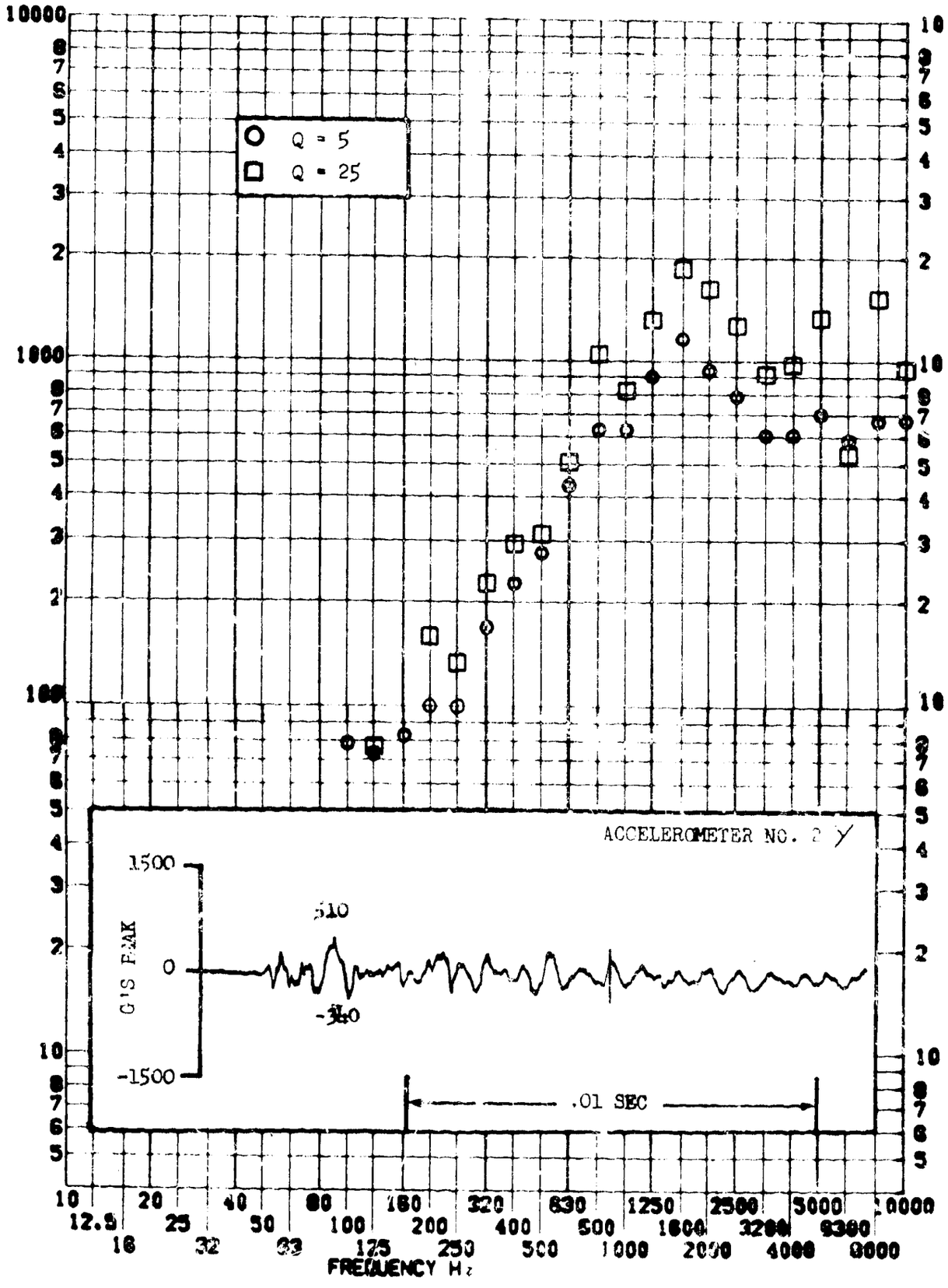

SHOCK TEST ANALYSIS DATA SHEET II.A.5.9

TEST ITEM 1080-134,135
SERIAL NO.
SHOCK AXIS LATERAL

PART NO. STRUCTURE
TEST DATE 27 JAN 1966
SHOCK NO. 1

RESPONSE G-S

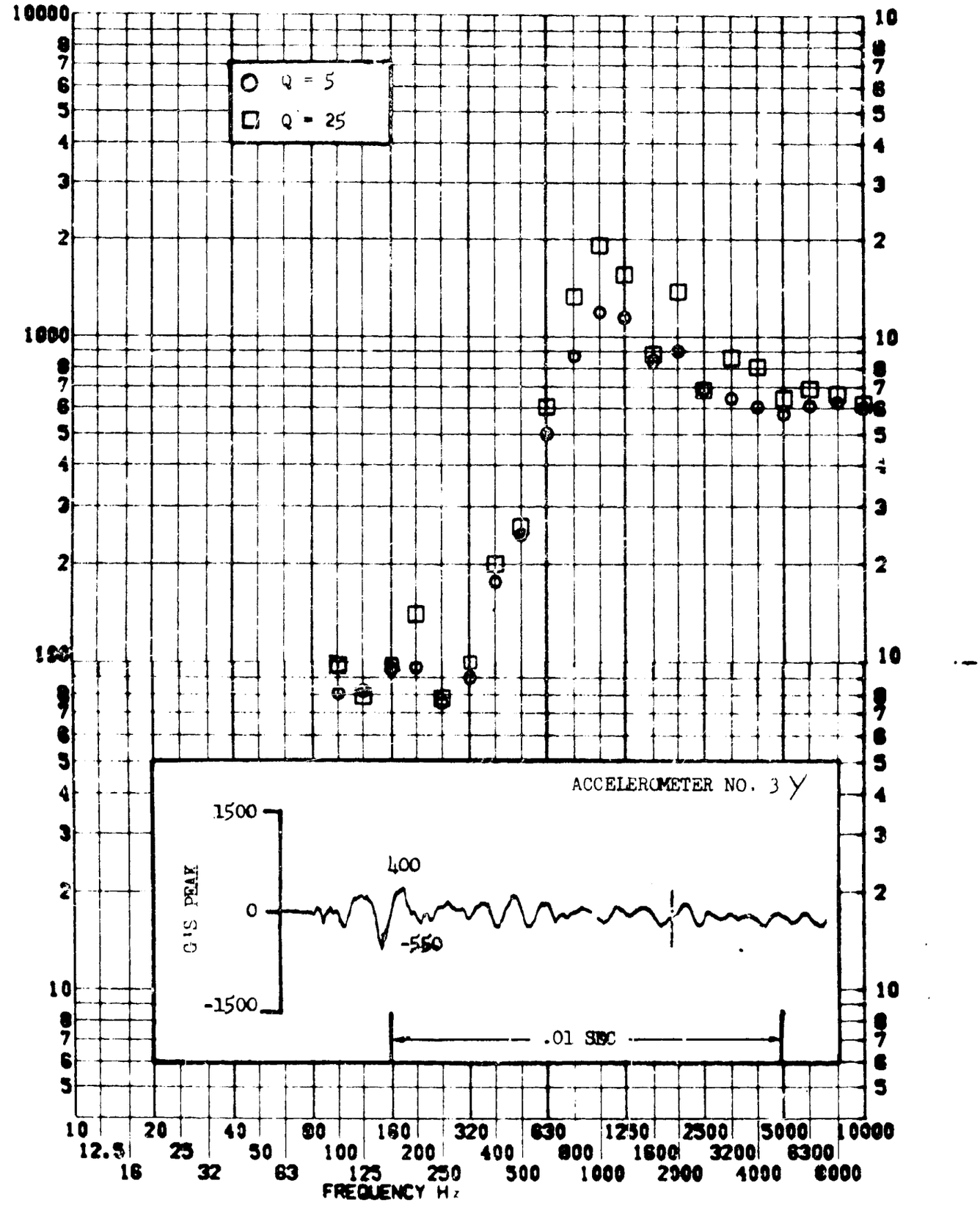

SHOCK TEST ANALYSIS DATA SHEET II.A.5.10

TEST ITEM 1080-136,137
SERIAL NO.
SHOCK AXIS LATERAL

PART NO. STRUCTURE
TEST DATE 27 JAN 1966
SHOCK NO. 1

RESPONSE G-S

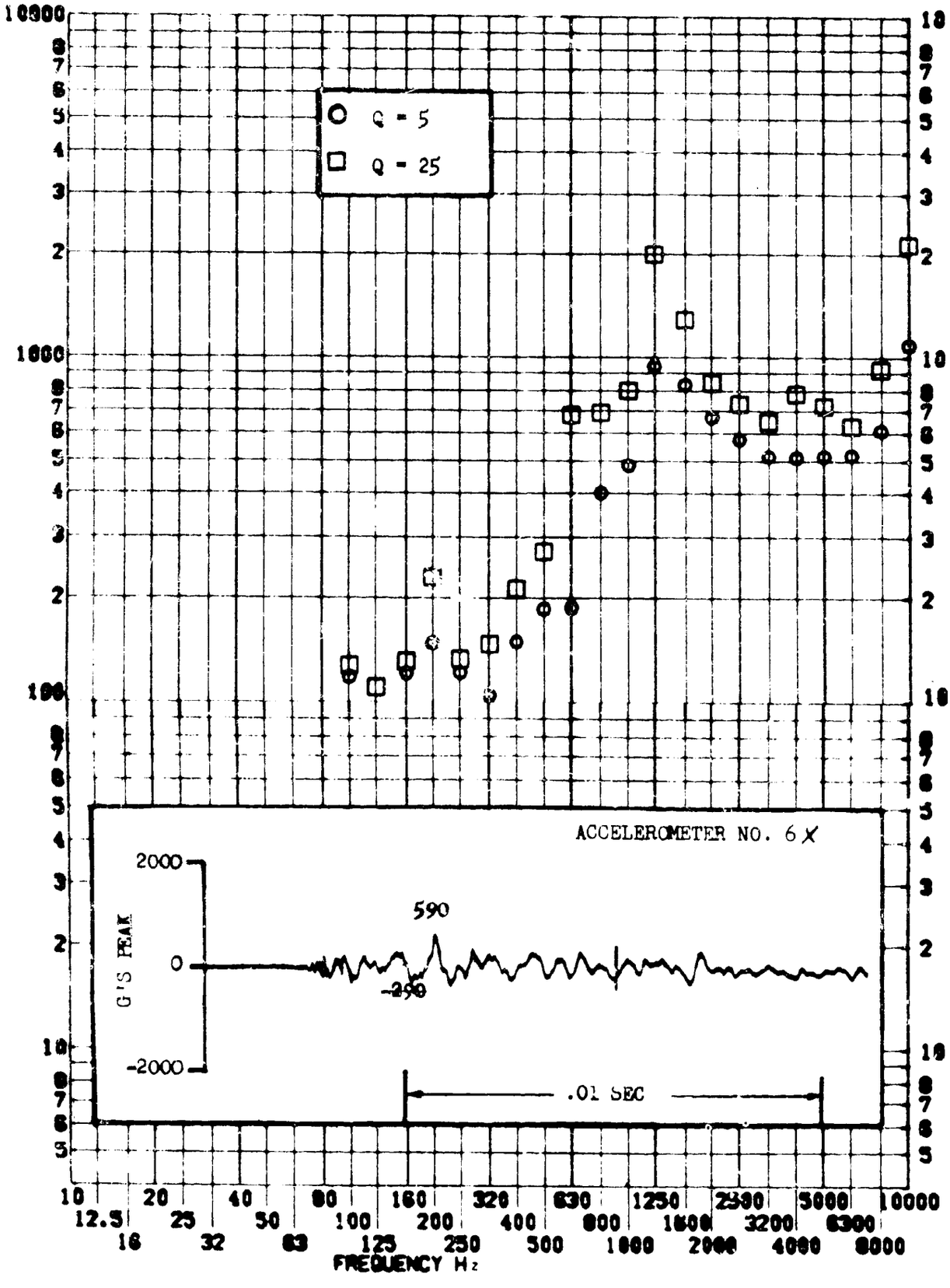

SHOCK TEST ANALYSIS DATA SHEET II.A.5.11

TEST ITEM 1080-138,139
SERIAL NO.
SHOCK AXIS RADIAL

PART NO. STRUCTURE
TEST DATE 27 JAN 1966
SHOCK NO. 1

RESPONSE G-S

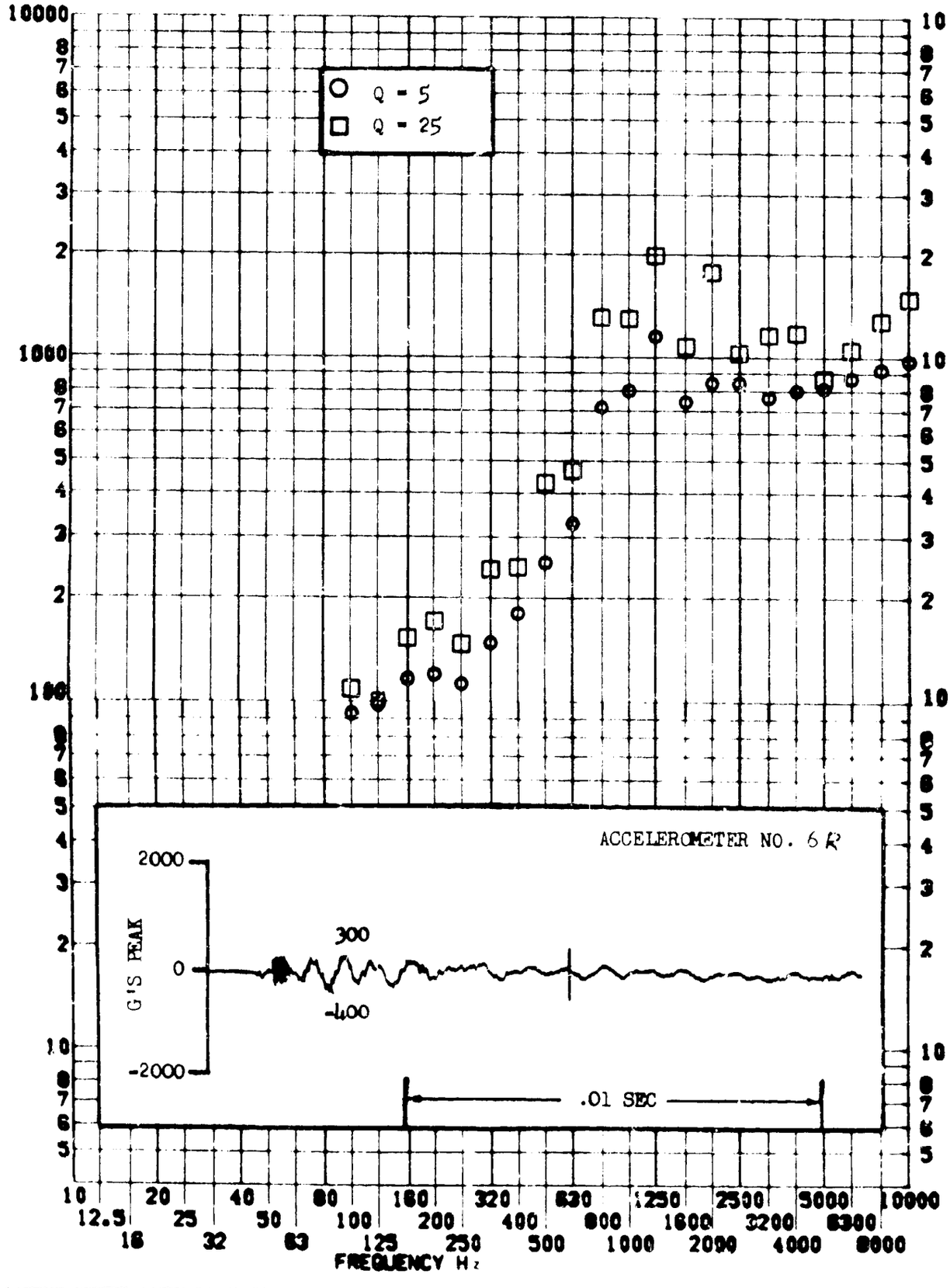

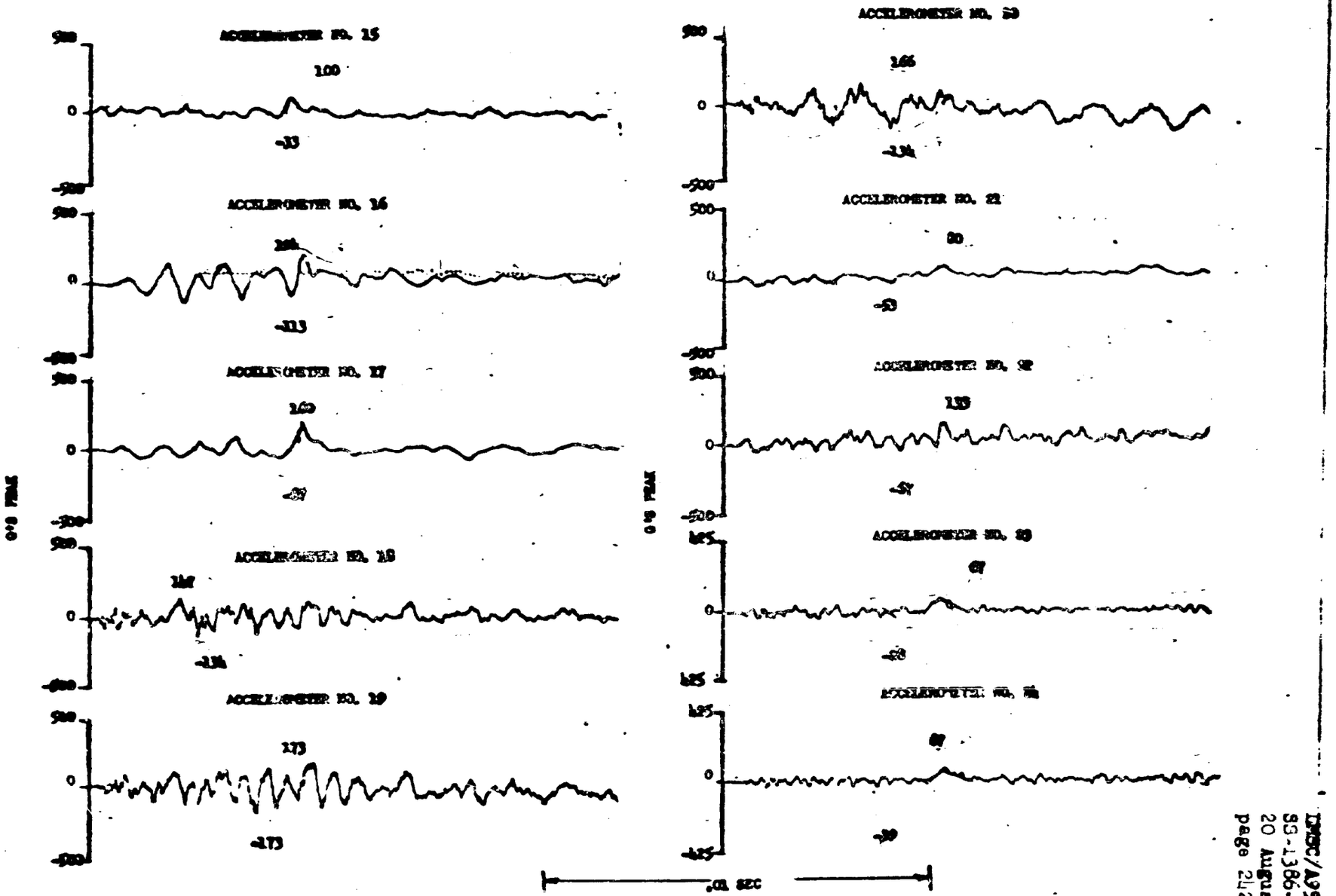

Figure II.A.5.12 Oscillograms Item 1080 - Accelerometers 15 to 24 (Test 2)

SECTION NO. II.A.6

REPORT NO. 1340

SUBJECT:

BOOSTER ADAPTER FUNCTIONAL/ENVIRONMENTAL

DETERMINATION TEST

SECTION II.A.6

SUMMARY

Two booster adapter separation tests were performed on the development test vehicle (DTV) to determine the pyro shock environment at selected locations on the vehicle structure and to demonstrate confidence that the vehicle and its equipment could survive the separation event.

The tests were satisfactorily performed and no structural or equipment degradations were noted after either test.

Included in this report are real time oscillograms and shock spectra for selected accelerometers for both tests.

TABLE OF CONTENTS

SECTION II.A.6

LIST OF TABLES

SECTION II.A.6

LIST OF FIGURES

SECTION II.A.6

LIST OF FIGURES

SECTION II, A.6

II.A.6.1 INTRODUCTION

A fully equipped vehicle was used for these tests. The vehicle was suspended by bungee cords. A section of adapter was added at the aft end of the vehicle to complete the booster adapter separation joint and a catcher box was positioned around and to the rear of the separation joint to catch the debris. The separation joint was a 10 grain/foot MDF and is shown in Figure II.A.6.3.

II.A.6.2 DISCUSSION AND ANALYSIS

II.A.6.2.1 Test Configuration and Instrumentation

A sketch of the test specimen is shown in Figures II.A.6.1 and II.A.6.2. The specimen consisted of a standard aft rack and booster adapter with a section of booster added aft ofthe separation joint. The explosive separation joint consisted of 10 grain/foot MDF encased in a ring about the circumference of the vehicle. The separation joint is detailed in Figure II.A.6.3.

A total of thirteen Endevco 2225 piezoelectric accelerometers were mounted in the locations shown in Figures II.A.6.1 and II.A.6.2 and summarized in Tables II.A.6.1 and II.A.6.2. The mounting blocks for accelerometers 3, 4 and 5 were bolted directly to the vehicle structure for Test 2. The shocks were measured through signal conditioning equipment and recorded on magnetic tape at 60 inches/second tape speed for subsequent playback and analysis. Details on the data acquisition and data reduction systems are illustrated in Section V.

II.A.6.2.2 Data Analysis

The recorded data was used to produce oscillograms of all measurements and shock spectrums of selected measurements. Peak g readings from the oscillograms have been summarized in Table II.A.6.4.

No analysis was performed on the data other than to check the repeatability of the two tests by comparing the shock spectrum of two measurements from both tests and to check the accuracy of a 1/3 octave analysis by comparing the 1/3 octave shock spectrum with the narrow band shock spectrum from which the 1/3 octave shock spectrum came. The data has been organized so that it can be used for a repeatability study in conjunction with other tests of the same type and to determine shock attenuation as a function of distance by use of the peak g information or the shock spectra.

II.A.6.2.3 Test Results

Test 1

Shock spectra and corresponding oscillograms from Test 1 are presented in Figures II.A.6.5 to II.A.6.10. Oscillograms from measurements for which shock spectra were not prepared are presented in Figure II.A.6.24. Peak g readings from the oscillograms are summarized in Table II.A.6.4.

Following the test the vehicle structure was visually inspected. No structure or equipment degradation was observed. The oscillograms indicated that the range settings should be lowered for the next test.

Test 2

Shock spectra with their corresponding oscillograms are presented in Figures II.A.6.11 to II.A.6.22. Oscillograms for the rest of the measurements are presented in Figure II.A.6.24. Peak g readings are summarized in Table II.A.6.4. Accelerometer 2 was relocated, accelerometer 14 was replaced by accelerometer 13 in a different position, and the range settings were lowered for this test.

II.A.6.2.4 Repeatability

Shock spectra from measurements 8 and 9 from Test 1 have been compared to measurements 8 and 9 from Test 2 in Figures II.A.6.22 and II.A.6.23 as a check on repeatability between the two tests. The two figures indicate somewhat higher shock levels were obtained in Test 2, however the two tests are reasonably similar with the exception of the spike observed at 60 cycles in Test 1. This is most likely due to 60 Hz noise in the instrumentation system resulting from the high range setting of the accelerometers, since Test 2, in which all the range settings were lowered, did not exhibit this phenomenon.

II.A.6.2.5 Comparison of 1/3 Octave with Narrow Band Shock Spectrums

The shock spectra presented in this report were read from narrow band shock spectra in 1/3 octave intervals. The narrow band shock spectra were produced in 5 cycle bandwidths from 0 to 500 Hz, 20 cycle bandwidths from 500 to 2500 Hz, and 100 cycle bandwidths from 2500 to 10,000 Hz. The data was then read at the 1/3 octave center frequencies to produce the 1/3 octave shock spectra of this report. To show the error which can be introduced by analyzing the data in 1/3 octaves, one of the shock spectra was plotted in 1/3 octaves and in the original narrow bands (Figure II.A.6.4).

Figure II.A.6.4 indicates that the 1/3 octave analysis may be off by as much as a factor of 1.70 (at 1000 Hz) in any 1/3 octave band by virtue of the method in which the shock spectrum was read.

II.A.6.3 CONCLUSIONS

The vehicle demonstrated its ability to survive the booster adapter separation event without degradation to equipment or structure.

Data collected provided a good definition of the pyro shock environment which originates from booster separation. This data can be used in conjunction with data from other similar booster adapter separation tests to determine repeatability between tests and attenuation characteristics.

Reading shock spectra by 1/3 octaves can introduce errors in the shock levels by as much as a factor of 1.7. This should be taken into consideration whenever these shock spectrums are used.

TABLE II.A.6.1

ACCELEROMETERS AND LOCATIONS, TEST 1

	Accelerometer No.	Station	Direction	Distance to Shocksource	Accelerometer Type
	1	414	X	30	ENDEVCO 2225
	2	414	R	30	ENDEVCO 2225
	3	386	Z	2	ENDEVCO 2225
*	4	386	X	2	ENDEVCO 2225
	5	386	Y	2	ENDEVCO 2225
	6	414	X	30	ENDEVCO 2225
	7	414	R	30	ENDEVCO 2225
	8	404.5	X	20.5	ENDEVCO 2225
	9	404.5	R	20.5	ENDEVCO 2225
	10	437	X	53.0	ENDEVCO 2225
	11	460	X	76	ENDEVCO 2225
	12	460	R	76	ENDEVCO 2225
	14	271	Y	-113	ENDEVCO 2225

Shock Source at Sta 384

* Bonded triax accelerometer block broken by shock. No data.

TABLE II.A.6.2

ACCELEROMETERS AND LOCATIONS, TEST 2

	Accelerometer No.	Station	Direction	Distance to Shocksource	Accelerometer Type
	1	414	X	30	ENDEVCO 2225
	2	412	X	28	ENDEVCO 2225
	3	386	Z	2	ENDEVCO 2225
*	4	386	X	2	ENDEVCO 2225
	5	336	Y	2	ENDEVCO 2225
	6	414	X	30	ENDEVCO 2225
	7	414	R	30	ENDEVCO 2225
	8	404.5	X	20.5	ENDEVCO 2225
	9	404.5	R	20.5	ENDEVCO 2225
	10	437	X	53	ENDEVCO 2225
	11	460	X	76	ENDEVCO 2225
	12	460	R	76	ENDEVCO 2225
	13	271	X	-113	ENDEVCO 2225

Shock Source at

* Triax accelerometer block bolted to structure.

TABLE II.A.6.3

SUMMARY OF TESTS

Test Number	Configuration	Explosive Size	Test Purpose	Shock Isolation
1	1	10 Gr/ft MDF	Structure	None
2	1	10 Gr/ft MDF	Structure	None

TABLE II.A.6.4

OSCILLOGRAM PEAK G READINGS

Accelero-meter No.	DIRECTION	STATION	PEAK G READING TEST 1	TEST 2
1	X	414	625	1280
2	X	412	*	590
2	RADIAL	414	480	*
3	Z	386	NO DATA	4390
4	X	386	NO DATA	2610
5	Y	386	NO DATA	3940
6	X	414	NO DATA	350
7	RADIAL	414	600	660
8	X	404.5	144	135
9	RADIAL	404.5	74	88
10	X	437	140	182
11	X	460	160	52
12	RADIAL	460	73	NO DATA
13	X	271	*	210
14	Y	271	57	*

* NOT INSTRUMENTED

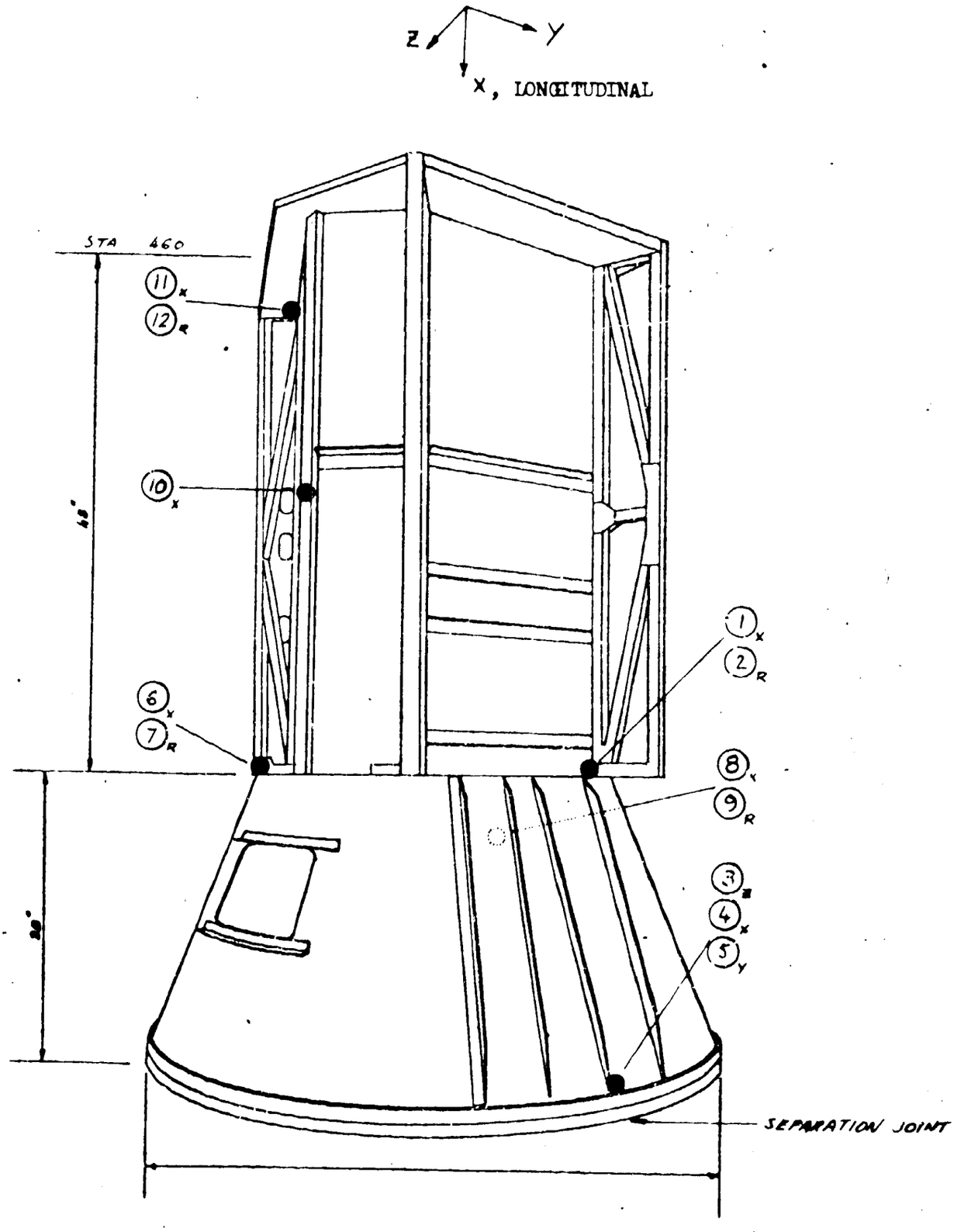

Figure II.A.6.1 TEST 1 CONFIGURATION AND INSTRUMENTATION LOCATIONS

DESIGNATE AXIS TO BE CONSISTENT WITH SHOCK SPECTRUMS

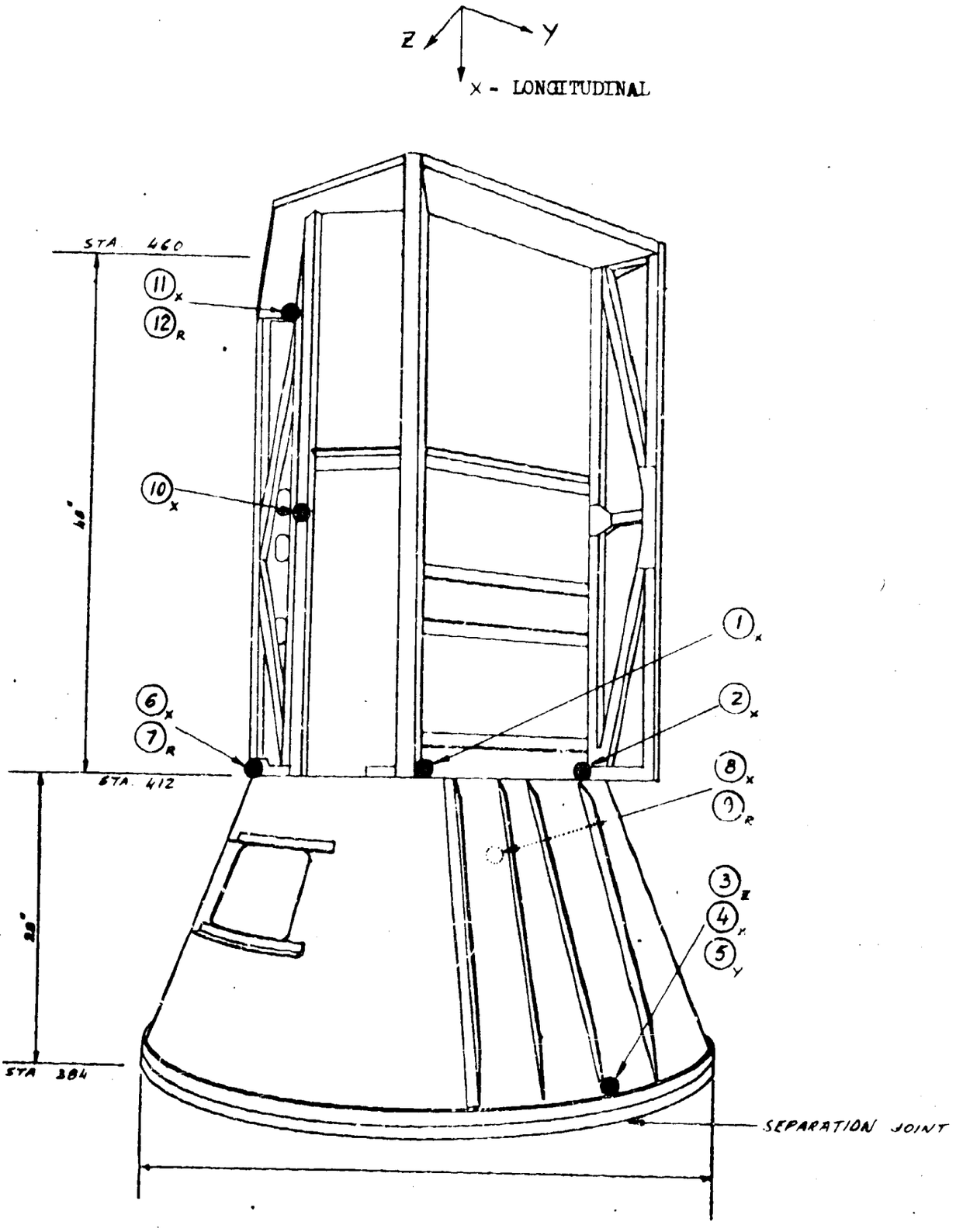

Figure II.A.6.2 TEST 2 CONFIGURATION AND INSTRUMENTATION LOCATIONS

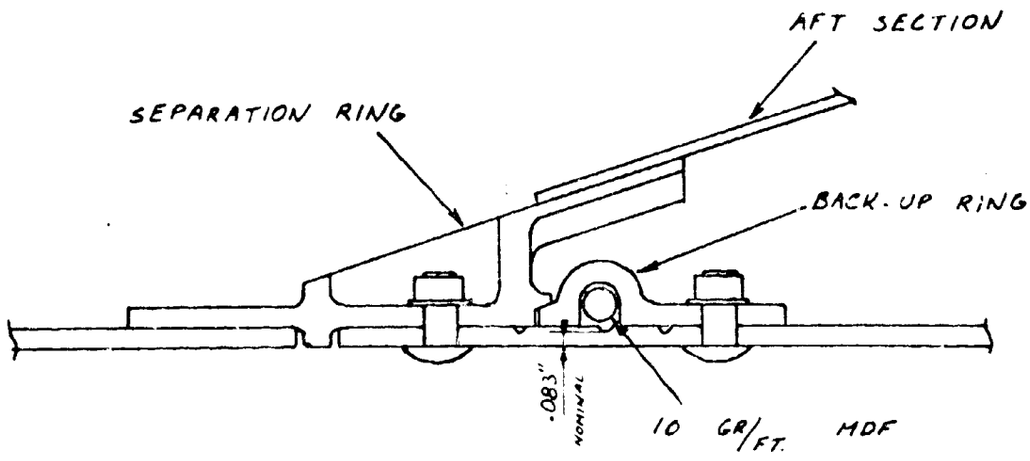

Figure II.A.6.3 SEPARATION JOINT DETAIL

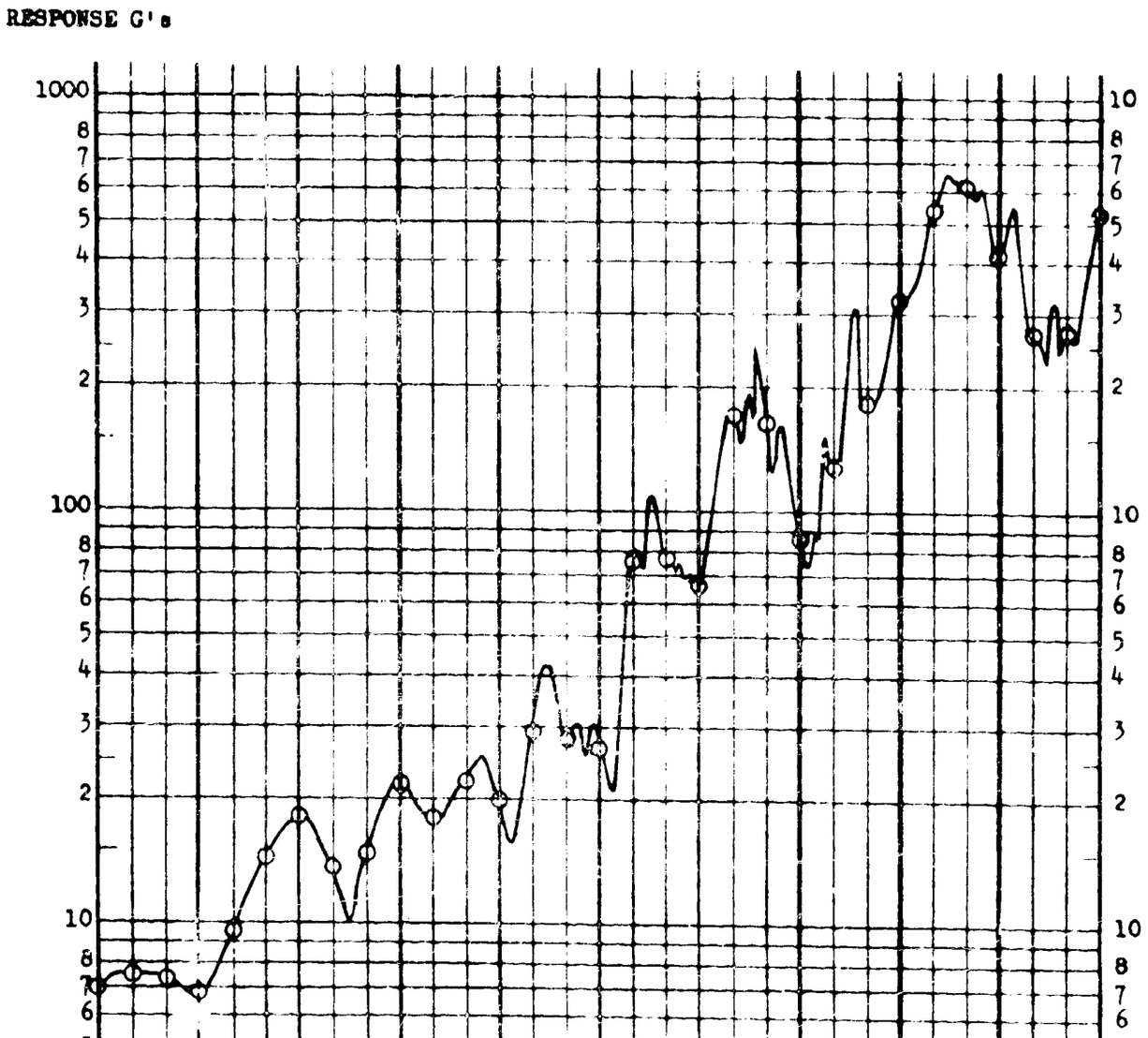

Figure II.A.6.4 COMPARISON OF 1/3 OCTAVE WITH NARROW BAND SHOCK SPECTRUM (ACCELEROMETER 8, SHOCK 2)

SHOCK TEST ANALYSIS DATA SHEET II.A.6.5

TEST ITEM 1340-175
SERIAL NO.
SHOCK AXIS RADIAL

PART NO. STRUCTURE
TEST DATE 10-22-68
SHOCK NO. 1

RESPONSE G-S

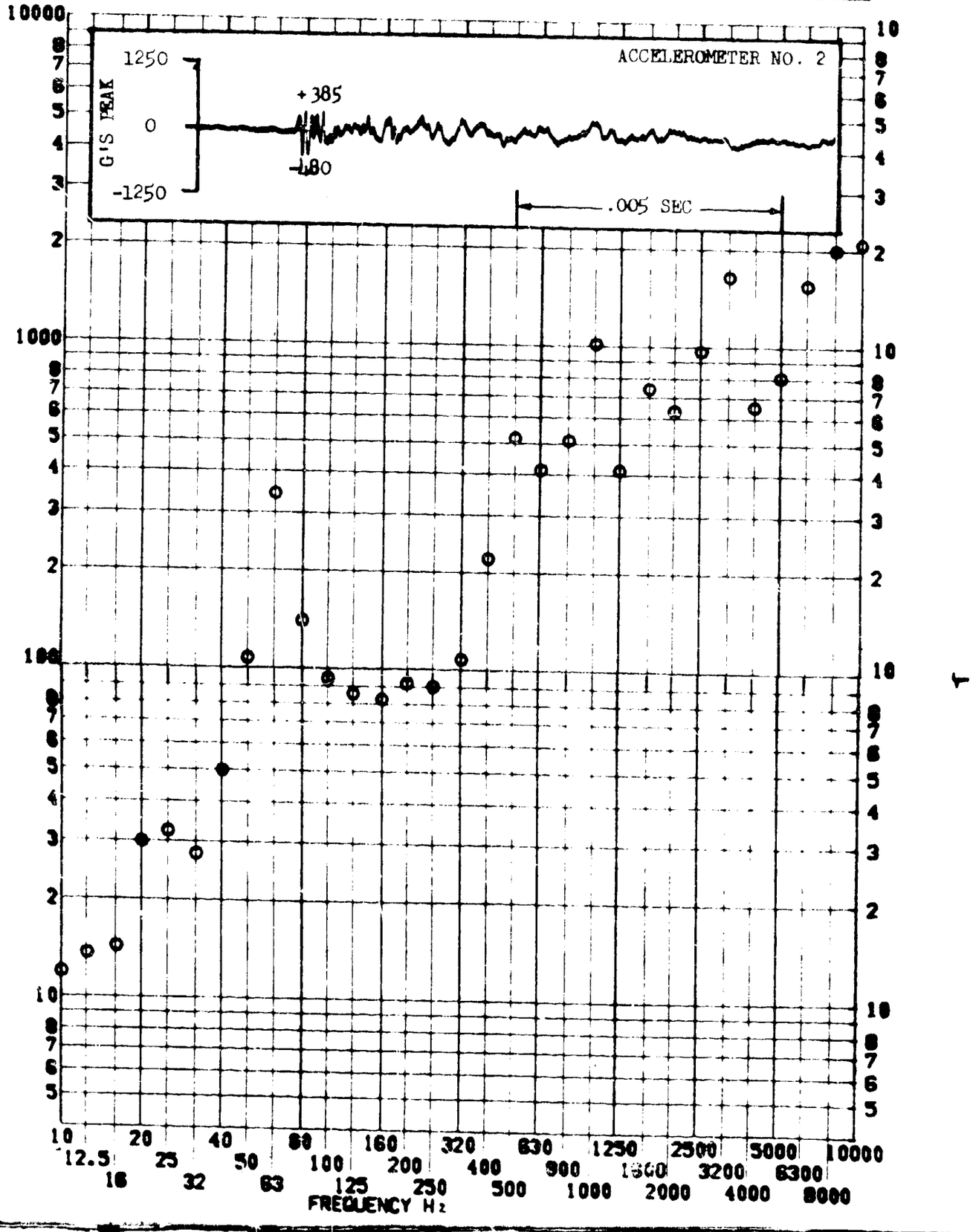

SHOCK TEST ANALYSIS DATA SHEET II.A.6.6

TEST ITEM 1340-176
SERIAL NO.
SHOCK AXIS LONGITUDINAL

PART NO. STRUCTURE
TEST DATE 10-22-66
SHOCK NO. 1

RESPONSE G-S

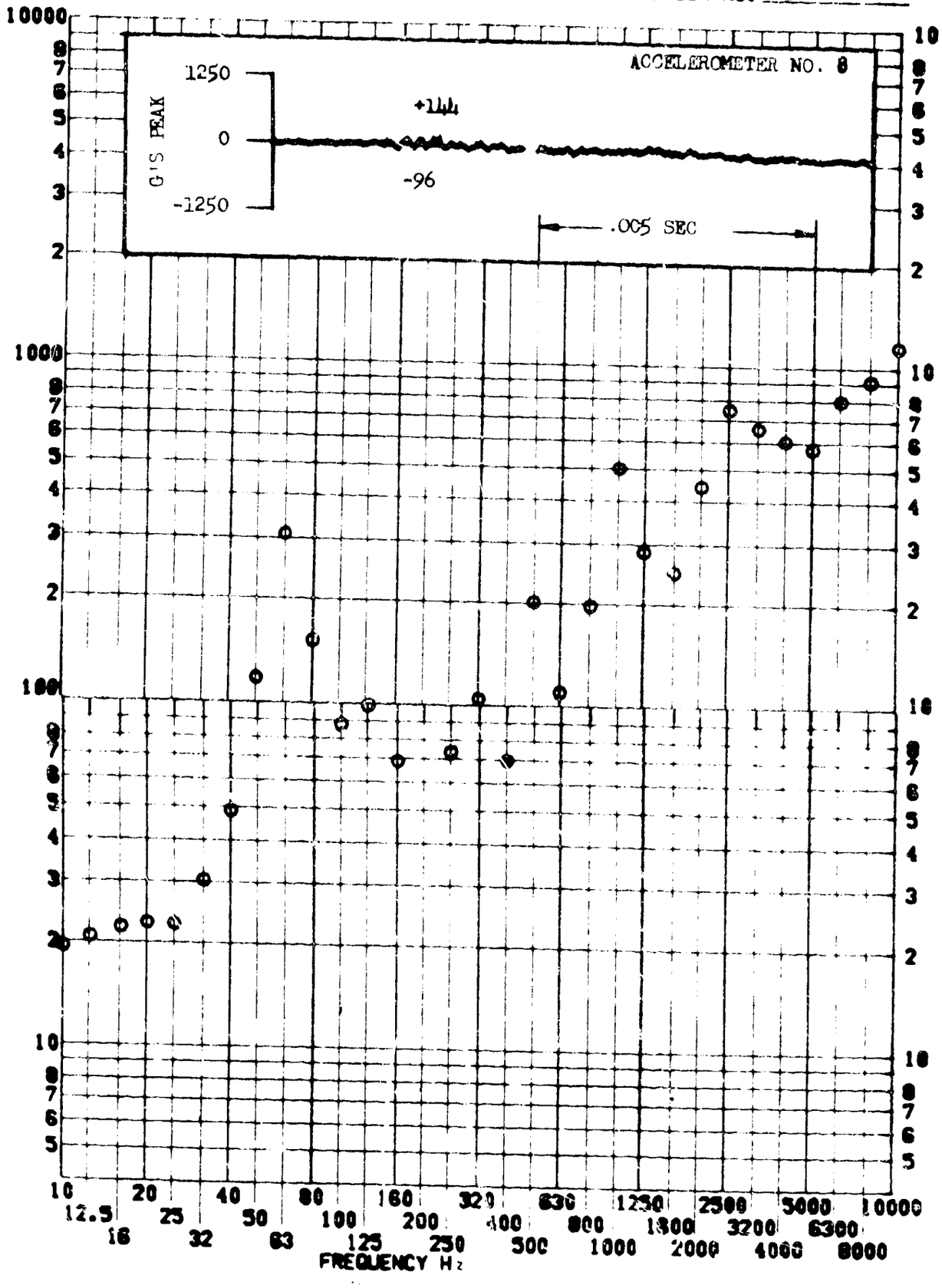

SHOCK TEST ANALYSIS DATA SHEET II.A.6.7

TEST ITEM 1340-177
SERIAL NO.
SHOCK AXIS RADIAL

PART NO. STRUCTURE
TEST DATE 10-22-68
SHOCK NO. 1

RESPONSE G-S

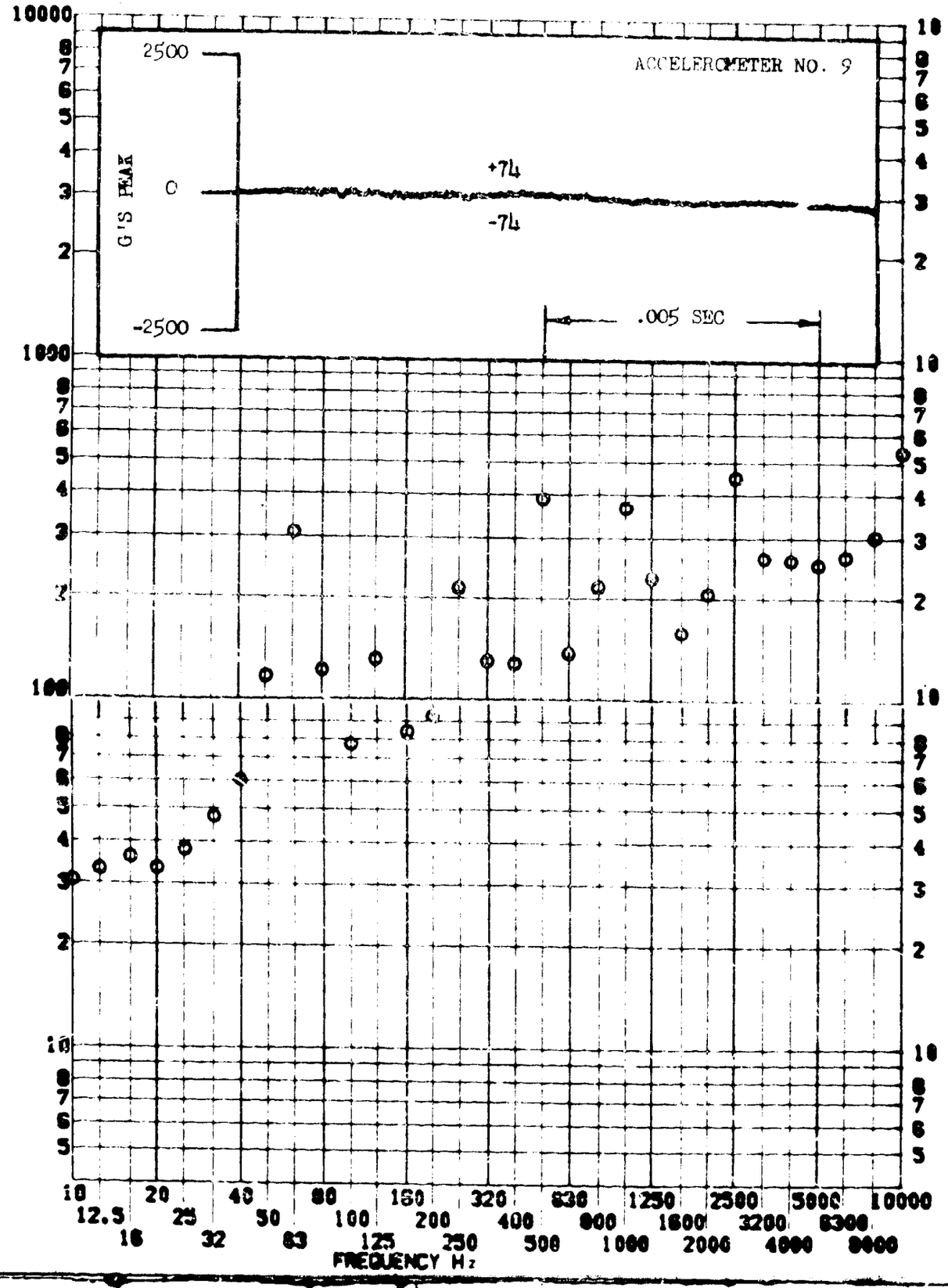

SHOCK TEST ANALYSIS DATA SHEET II.A.6.8

TEST ITEM 2040-178
SERIAL NO.
SHOCK AXIS LONGITUDINAL

PART NO. STRUCTURE
TEST DATE 10-22-68
SHOCK NO. 1

RESPONSE G-S

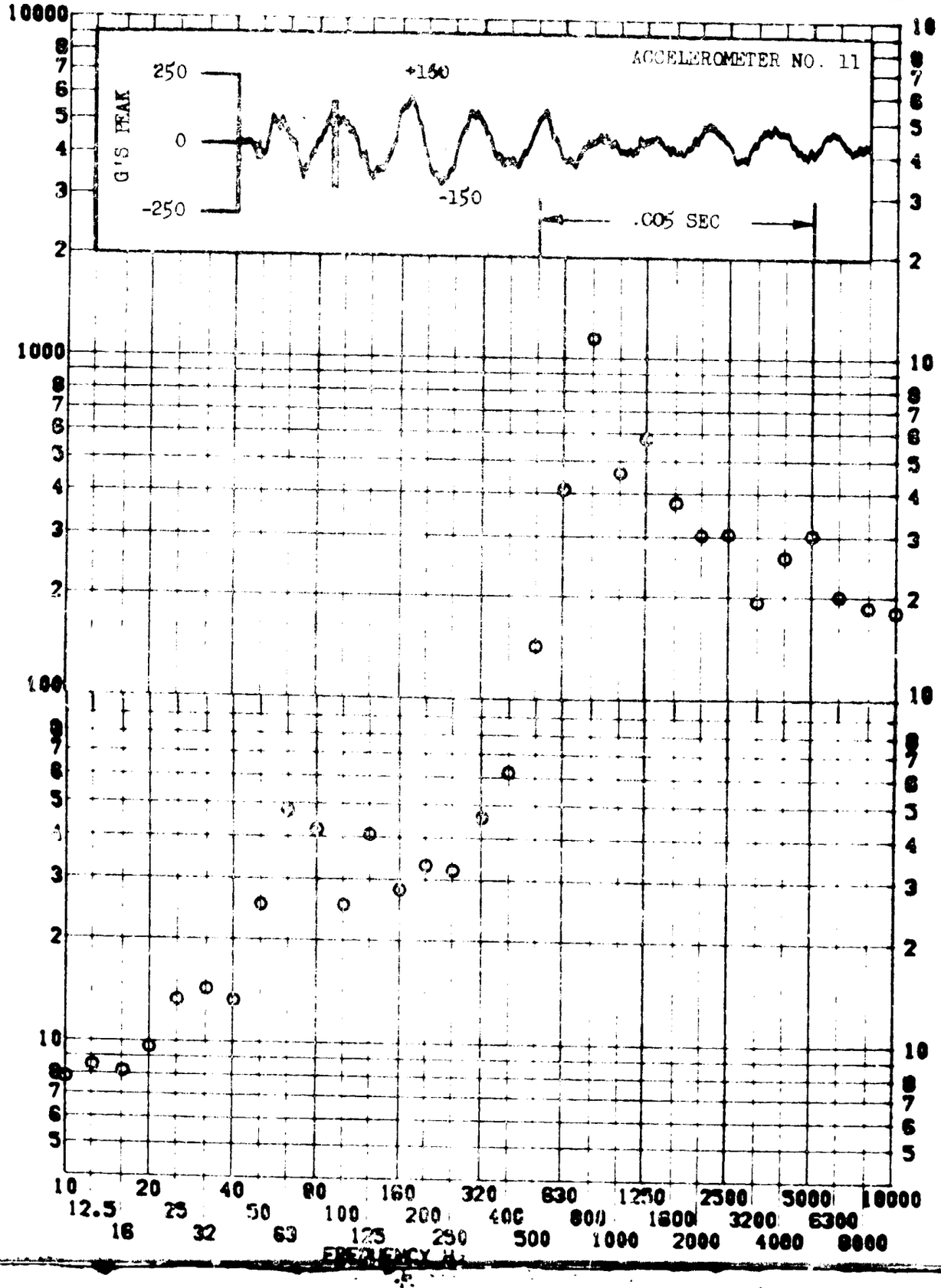

SHOCK TEST ANALYSIS DATA SHEET II.A.6.9

TEST ITEM 1340-179
SERIAL NO.
SHOCK AXIS RADIAL

PART NO. STRUCTURE
TEST DATE 10-22-68
SHOCK NO. 1

RESPONSE G-S

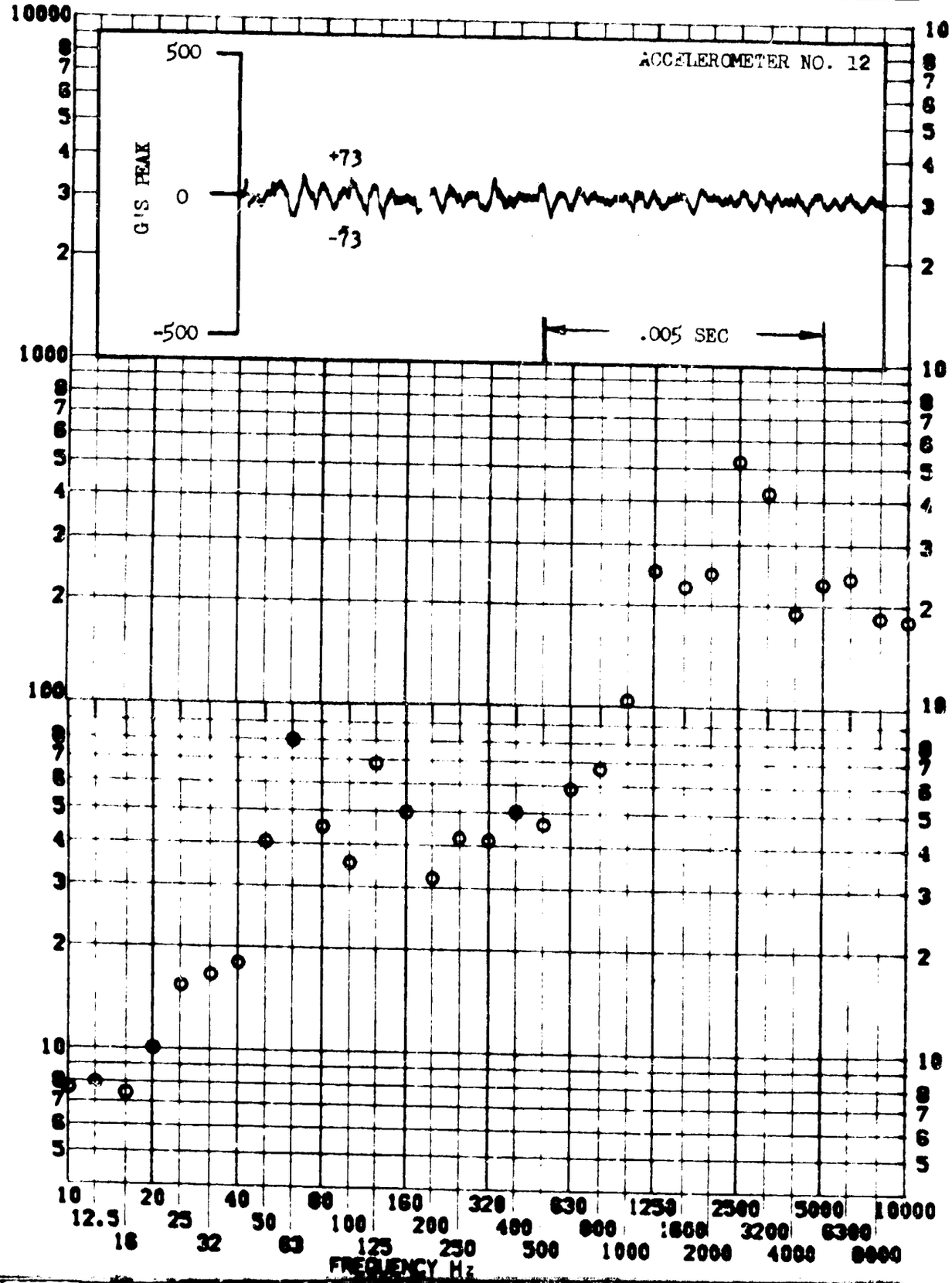

SHOCK TEST ANALYSIS DATA SHEET II.A.6.10

TEST ITEM 1340-180
SERIAL NO.
SHOCK AXIS Y

PART NO. STRUCTURE
TEST DATE 10-22-68
SHOCK NO. 1

RESPONSE G-S

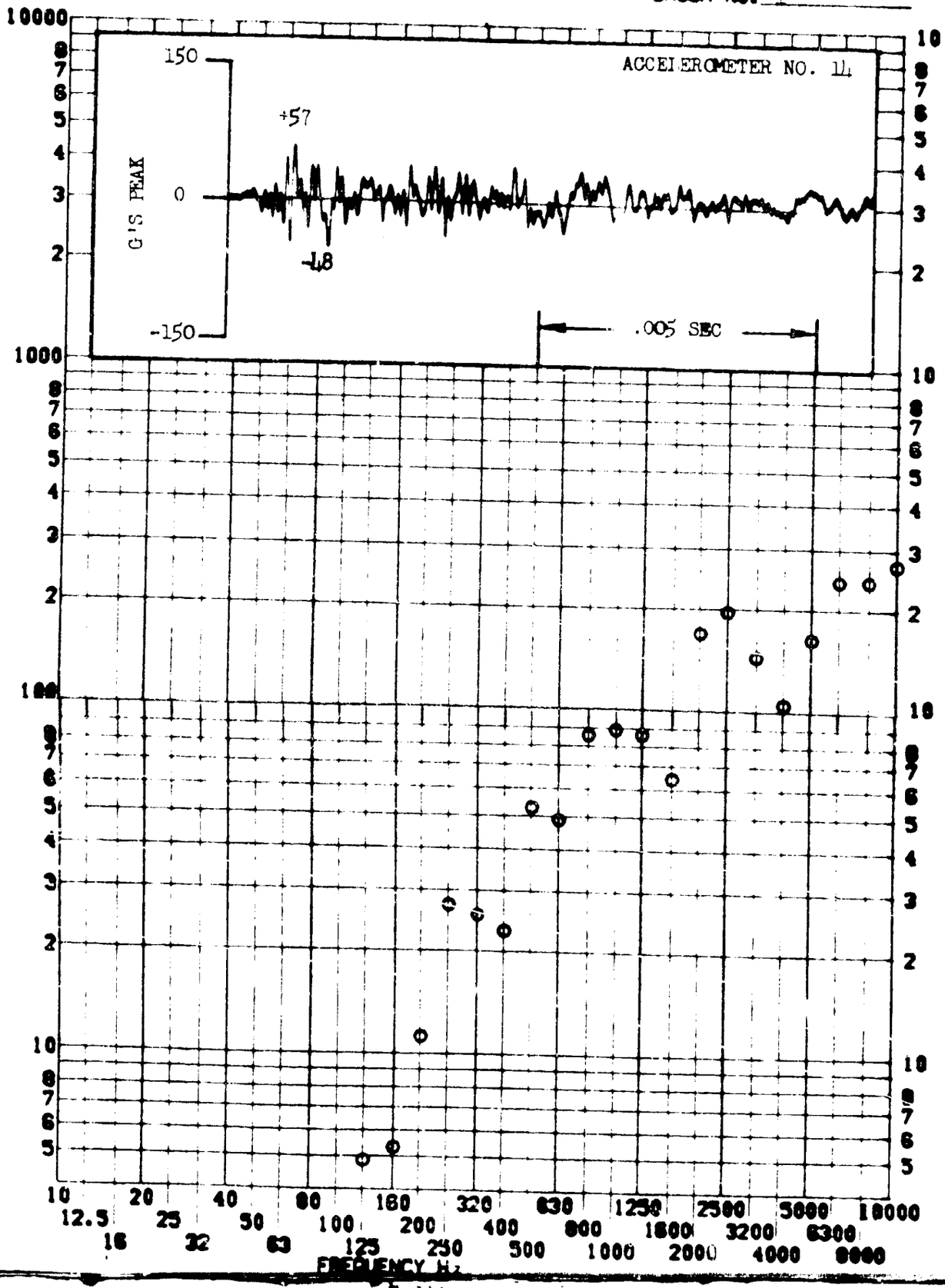

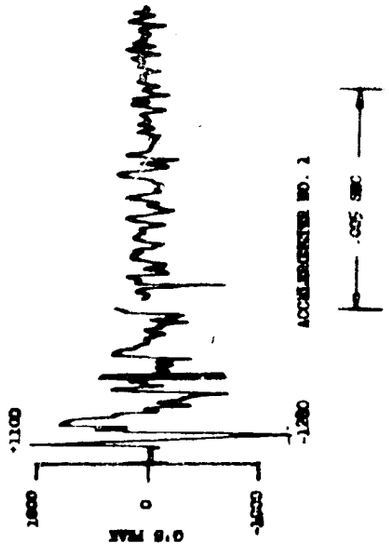
ACCELEROMETER NO. 1
.005 SEC
+1100
-1200
1800
0
-1800
0.5 MAX

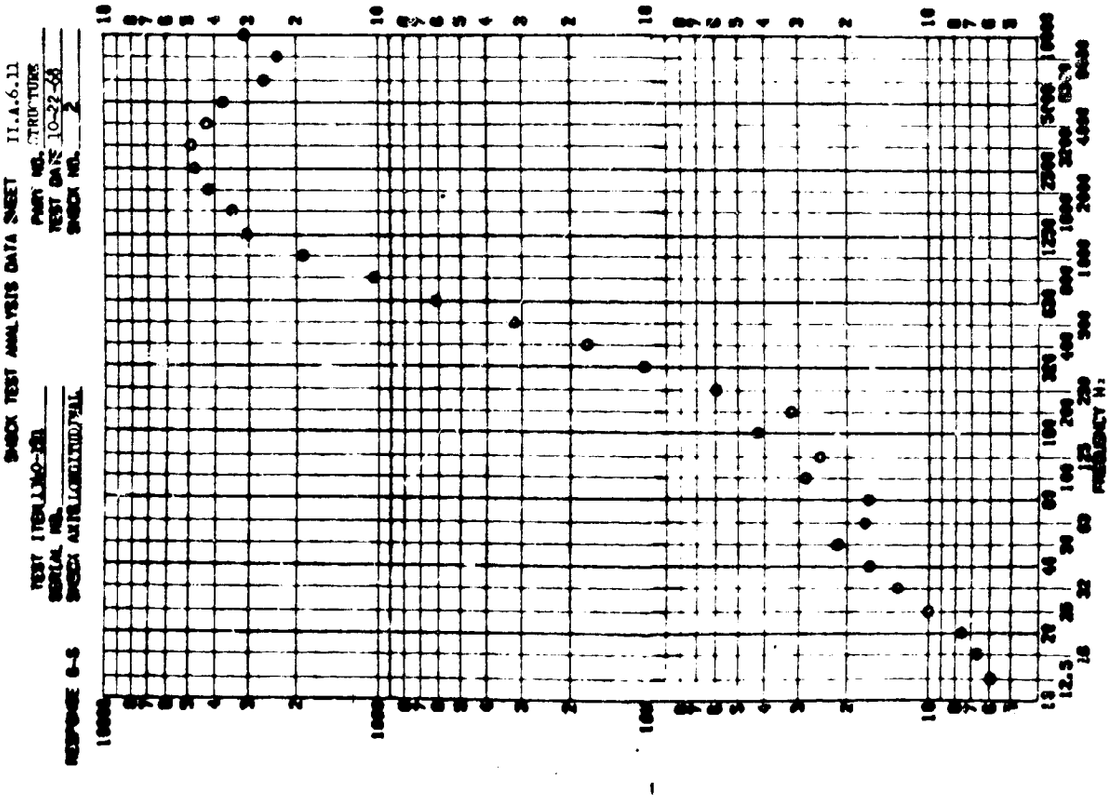
SHOCK TEST ANALYSIS DATA SHEET 11.4.6.11
TEST ITEM
SERIAL NO.
SHOCK AXIS
PART NO.
TEST DATE 10-22-68
SHOCK NO. 2
RESPONSE G-S
FREQUENCY H:

SHOCK TEST ANALYSIS DATA SHEET II.A.6.12

TEST ITEM [illegible]
SERIAL NO.
RESPONSE G-S SHOCK AXIS LONGITUDINAL

PART NO. STRUCTURE
TEST DATE 10-22-68
SHOCK NO. 2

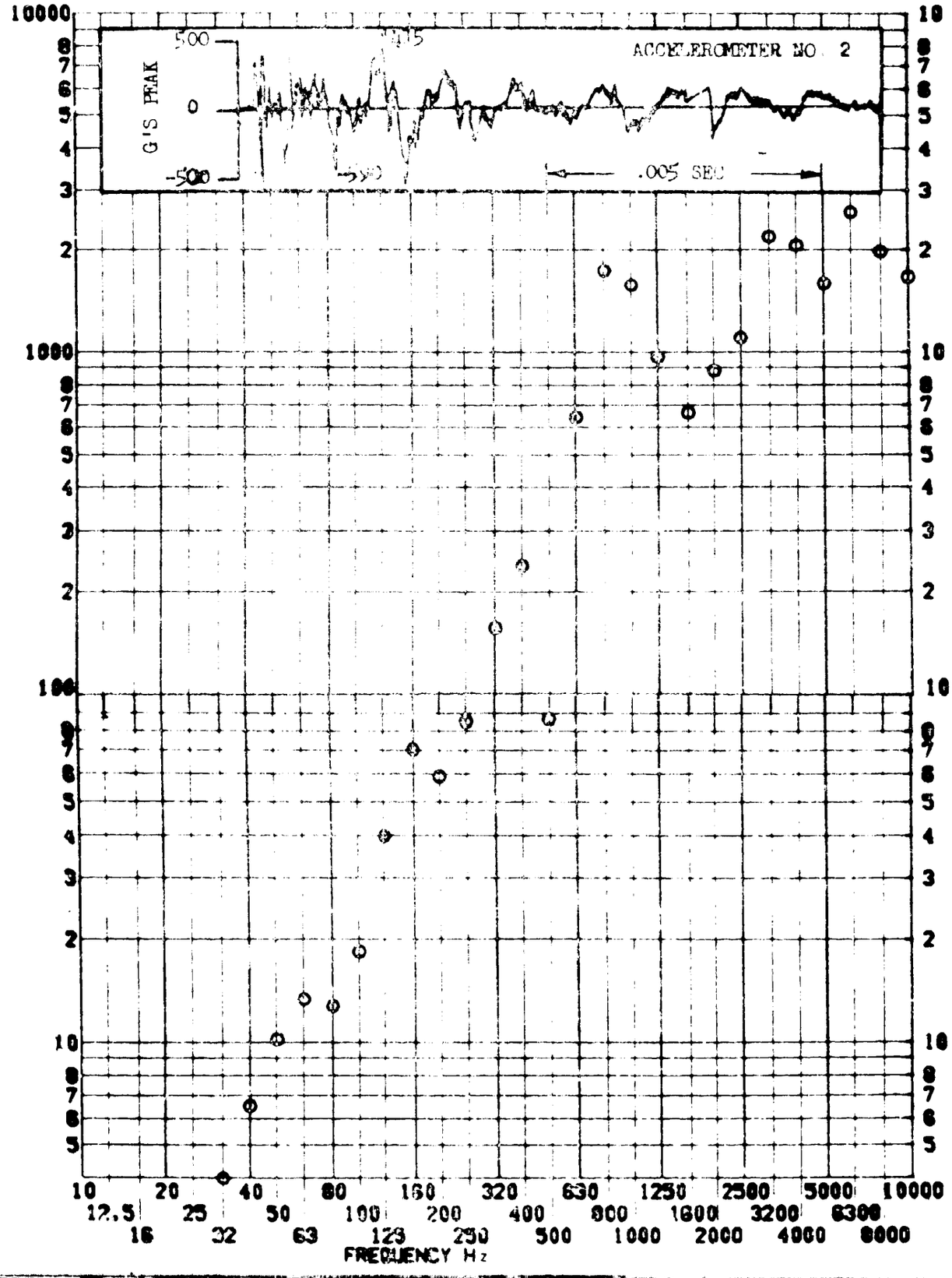

SHOCK TEST ANALYSIS DATA SHEET II.A.6.13

TEST ITEM 1340-182
SERIAL NO.
SHOCK AXIS Z

PART NO. STRUCTURE
TEST DATE 10-22-68
SHOCK NO. 2

RESPONSE G-S

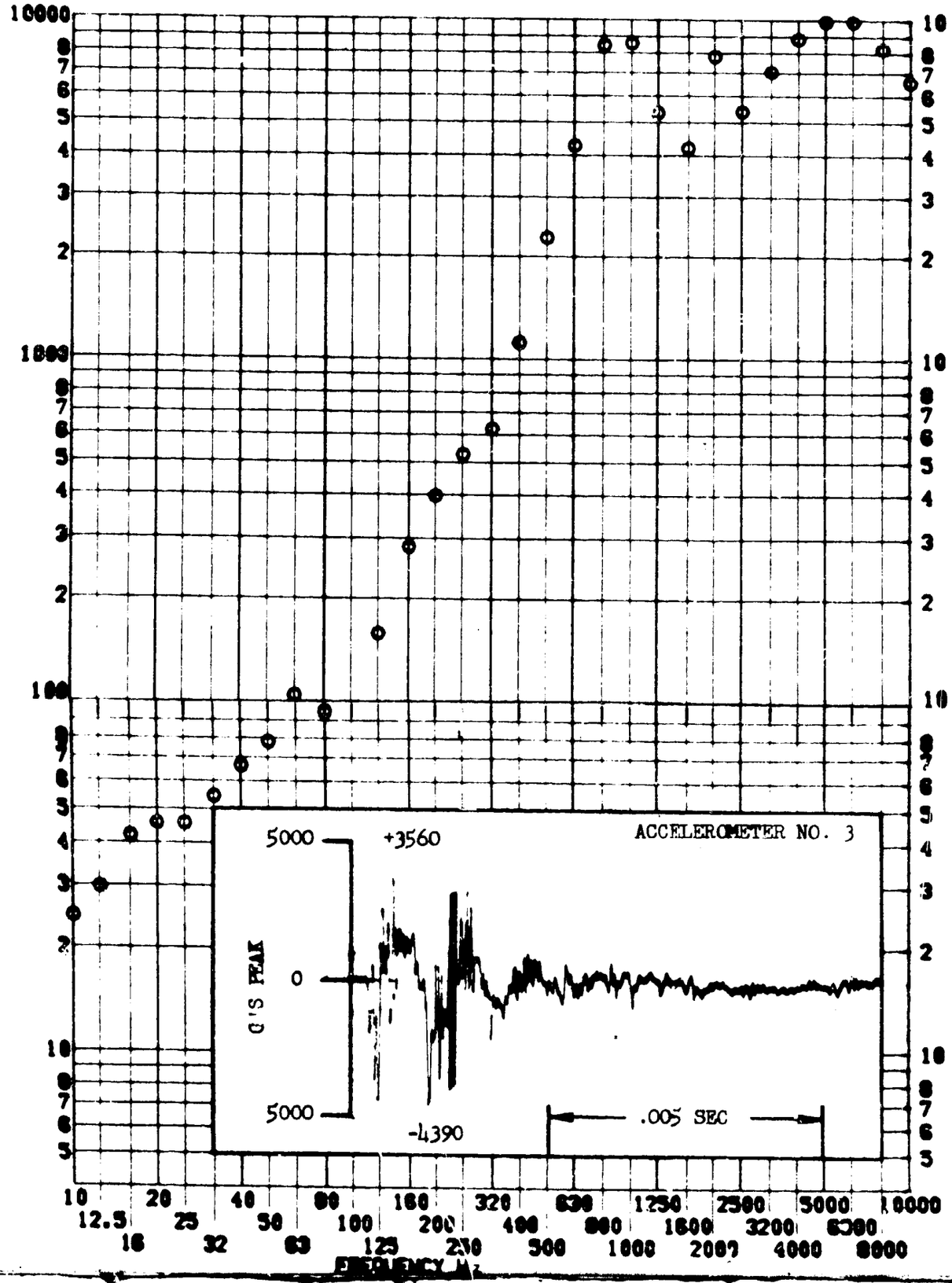

SHOCK TEST ANALYSIS DATA SHEET II.A.6.14

TEST ITEM 1340-183
SERIAL NO.
SHOCK AXIS LONGITUDINAL

PART NO. STRUCTURE
TEST DATE 10-22-68
SHOCK NO. 2

RESPONSE G-S

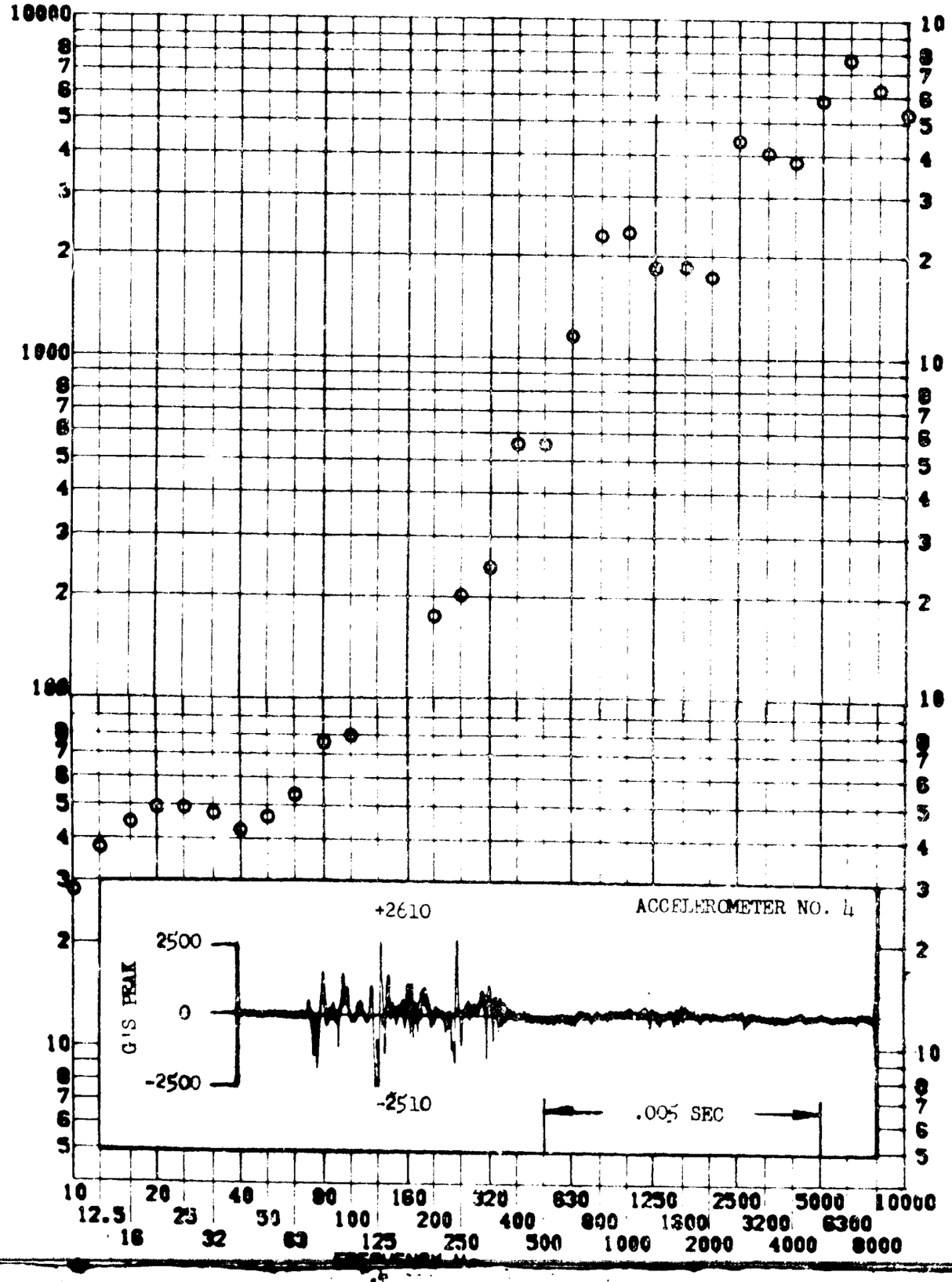

SHOCK TEST ANALYSIS DATA SHEET II.A.6.15

TEST ITEM 1340-184
SERIAL NO.
SHOCK AXIS Y

PART NO. STRUCTURE
TEST DATE 10-22-68
SHOCK NO. 2

RESPONSE G-S

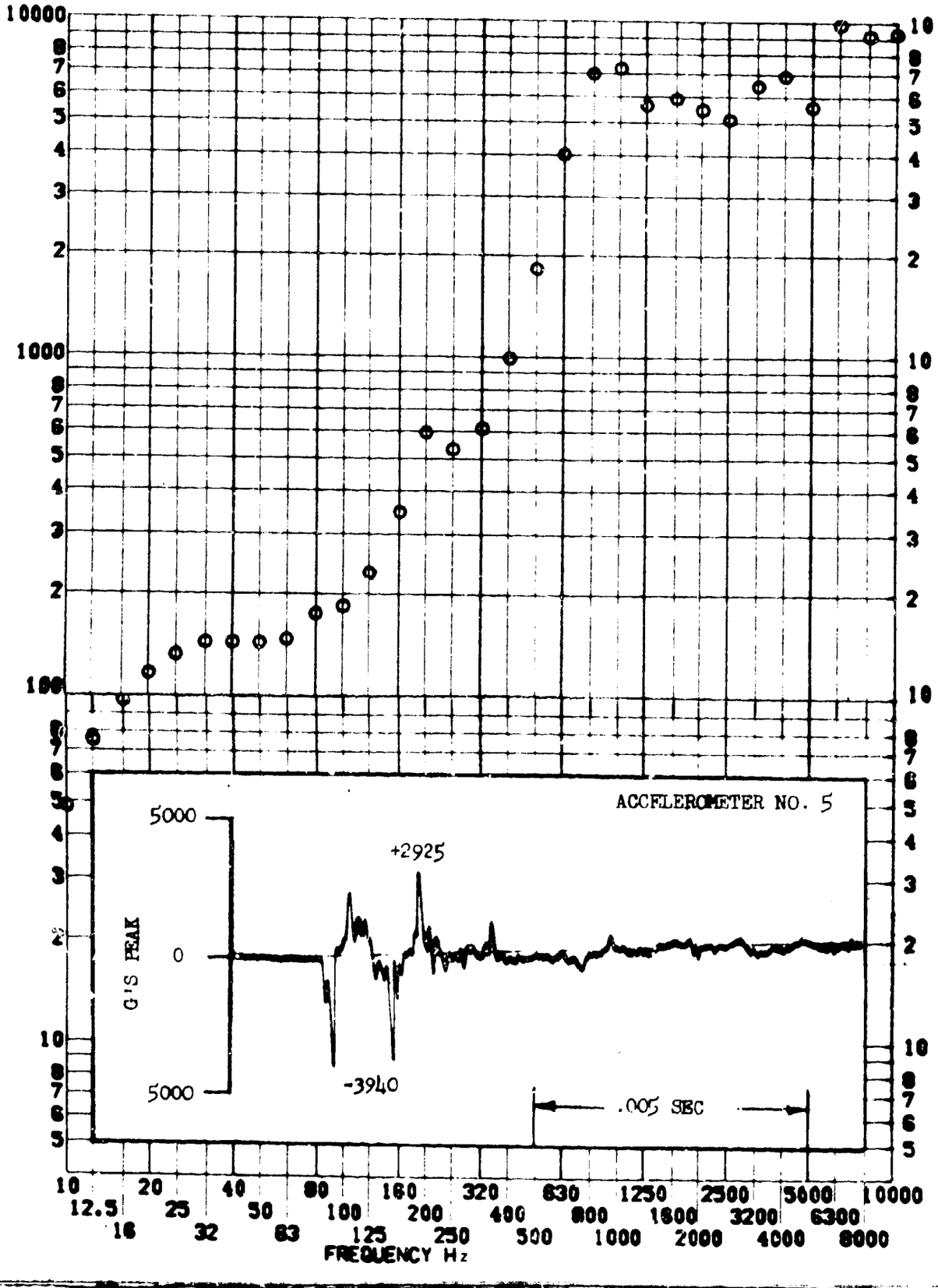

SHOCK TEST ANALYSIS DATA SHEET II.A.6.16

TEST [illegible]
SERIAL NO. [illegible]
SHOCK AXIS [illegible]

PART NO. STRUCTURE
TEST DATE 10-22-68
SHOCK NO. 2

RESPONSE G-S

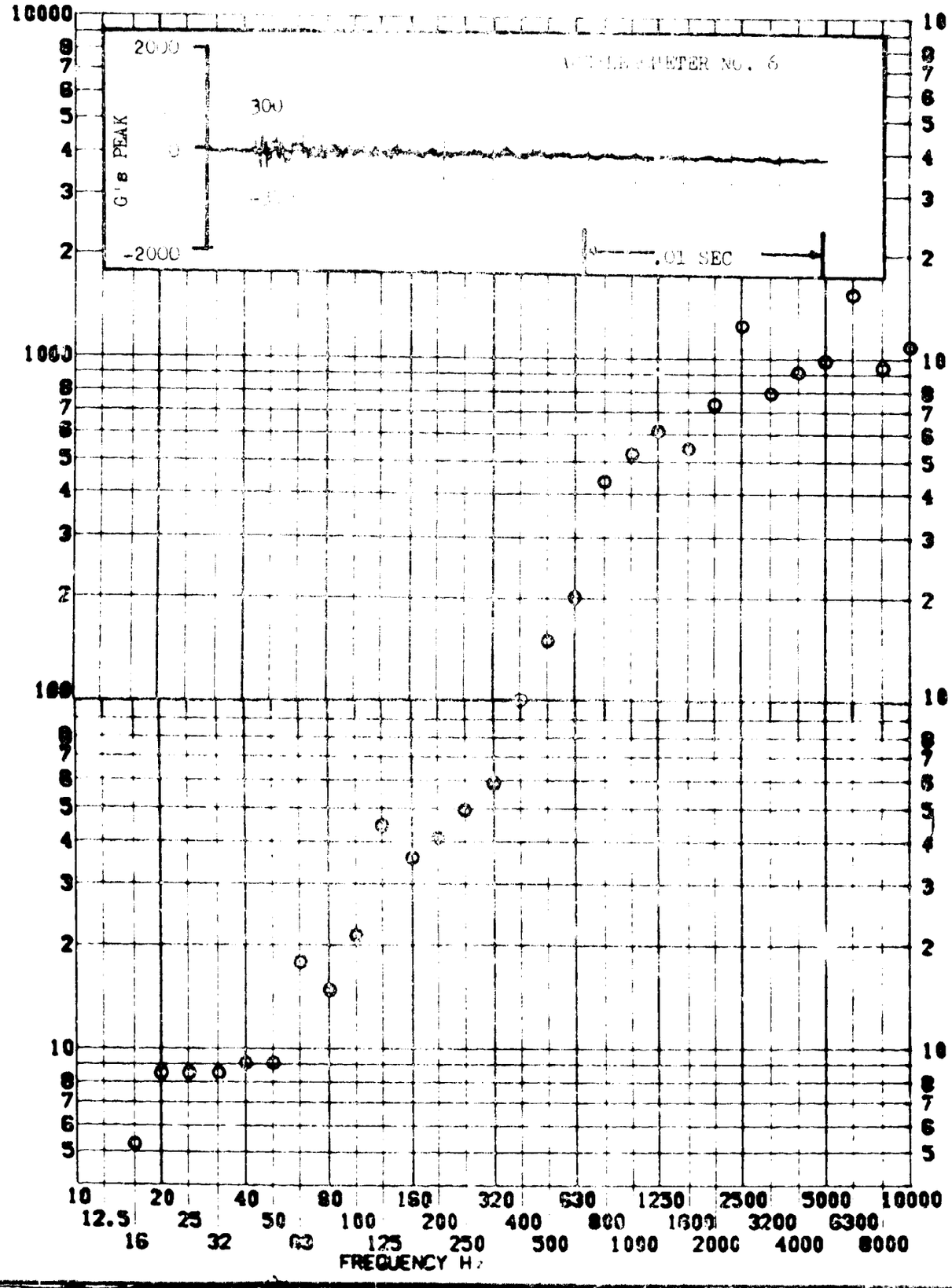

SHOCK TEST ANALYSIS DATA SHEET II.A.6.17

TEST ITEM 1340-186
SERIAL NO.
SHOCK AXIS RADIAL

PART NO. STRUCTURE
TEST DATE 10-22-68
SHOCK NO. 2

RESPONSE G-S

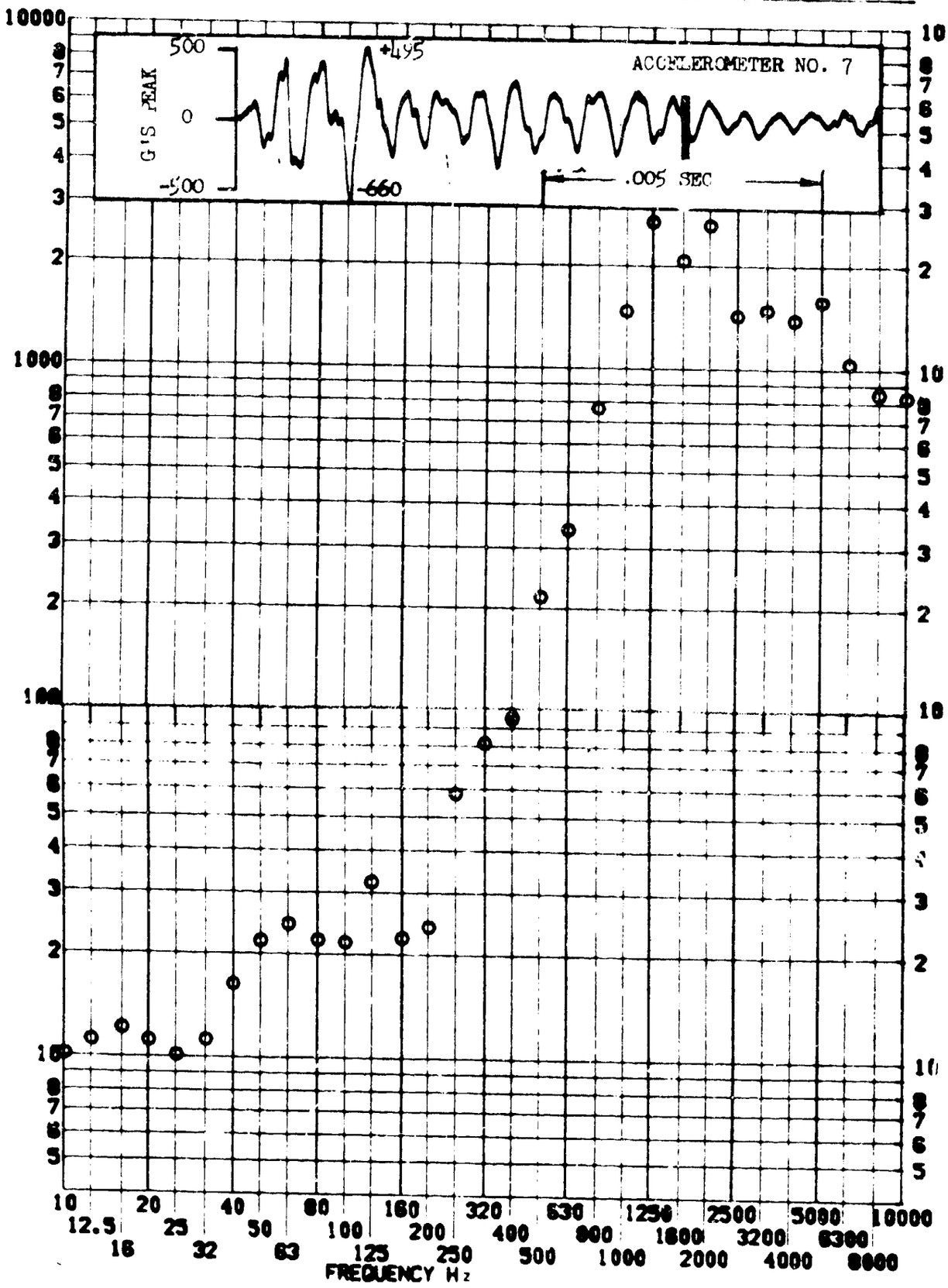

SHOCK TEST ANALYSIS DATA SHEET II.A.6.13

TEST ITEM 1340-187
SERIAL NO.
SHOCK AXIS LONGITUDINAL

PART NO. STRUCTURE
TEST DATE 10-22-68
SHOCK NO. 2

RESPONSE G-S

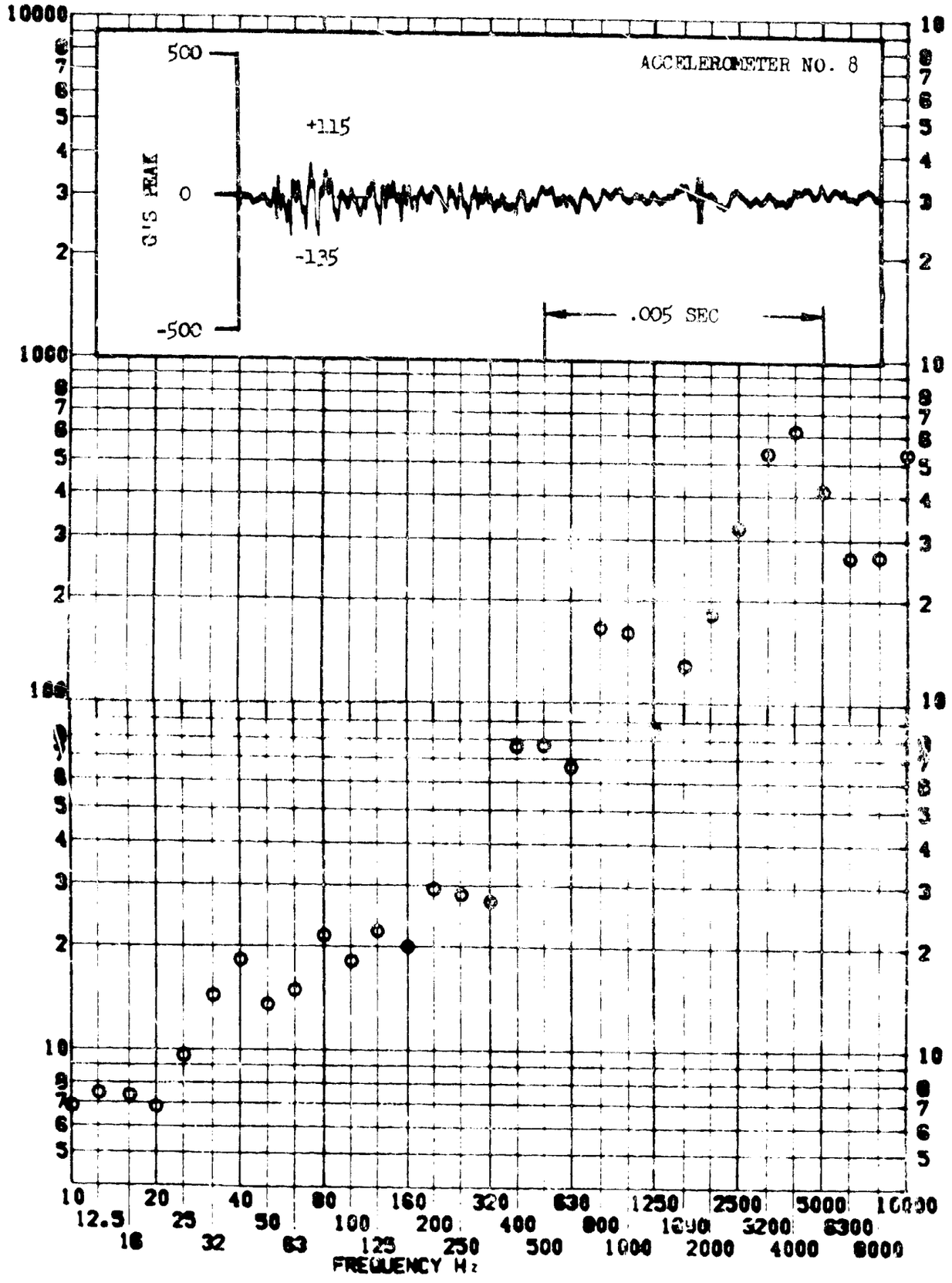

SHOCK TEST ANALYSIS DATA SHEET II.A.6.19

TEST ITEM 1340-188
SERIAL NO.
SHOCK AXIS RADIAL

PART NO. STRUCTURE
TEST DATE 10-22-68
SHOCK NO. 2

RESPONSE G-S

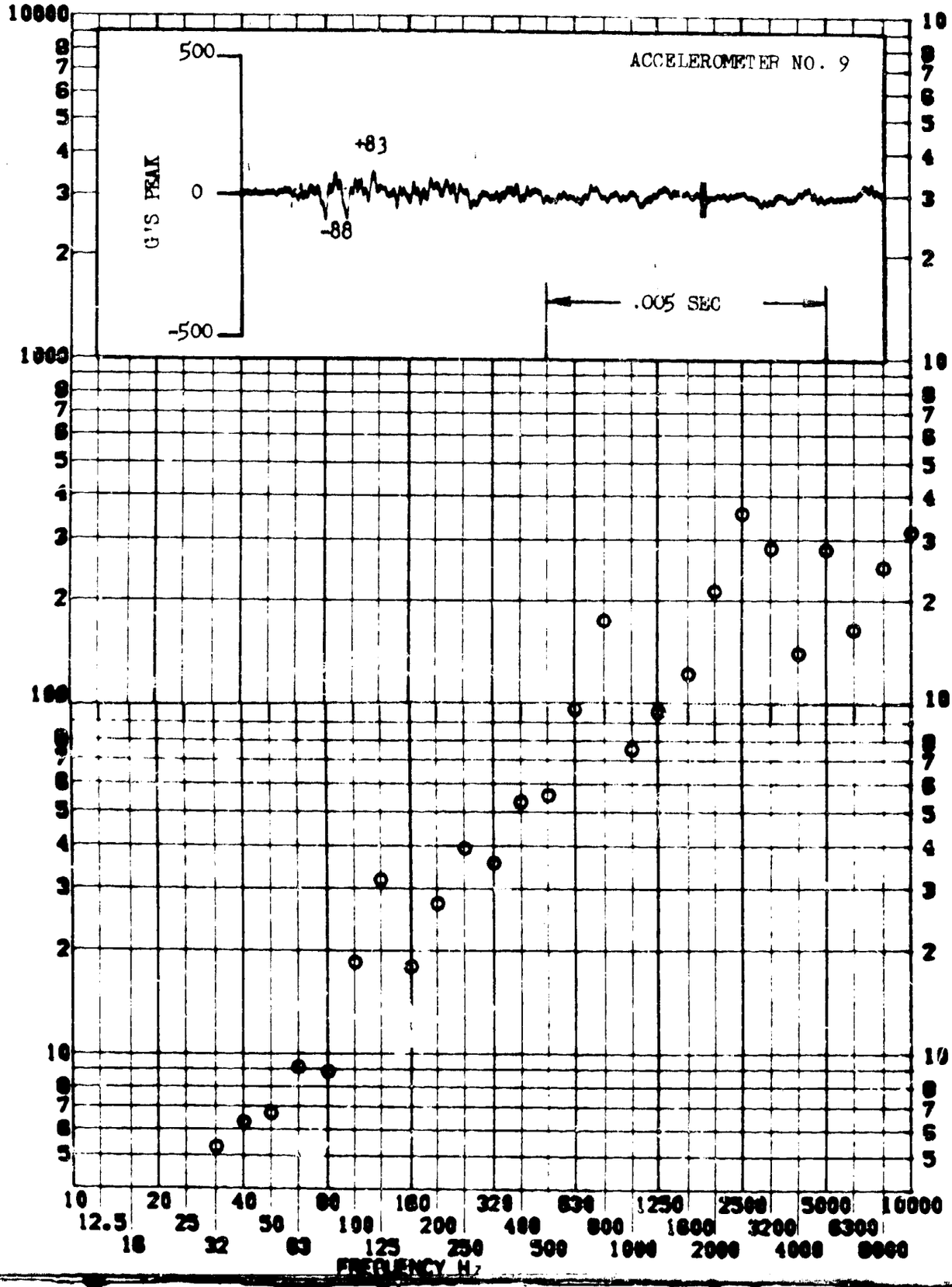

SHOCK TEST ANALYSIS DATA SHEET II.A.6.20

TEST [illegible]
SERIAL NO.
SHOCK AXIS LONGITUDINAL

PART NO. STRUCTURE
TEST DATE 10-22-68
SHOCK NO. 2

RESPONSE G-S

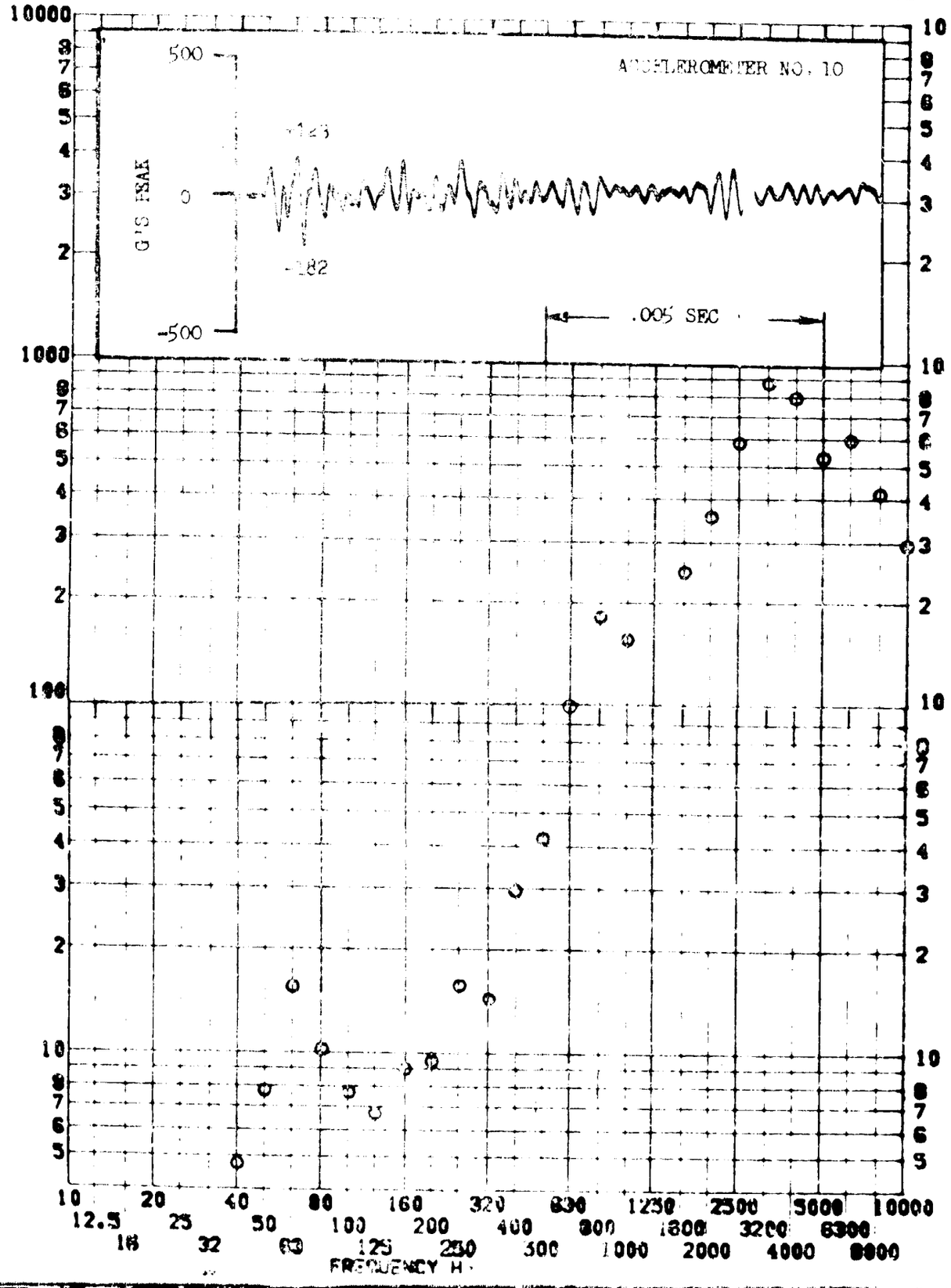

SHOCK TEST ANALYSIS DATA SHEET II.A.6.21

TEST ITEM 1310-190
SERIAL NO.
SHOCK AXIS LONGITUDINAL

PART NO. STRUCTURE
TEST DATE 10-22-68
SHOCK NO. 2

RESPONSE G-S

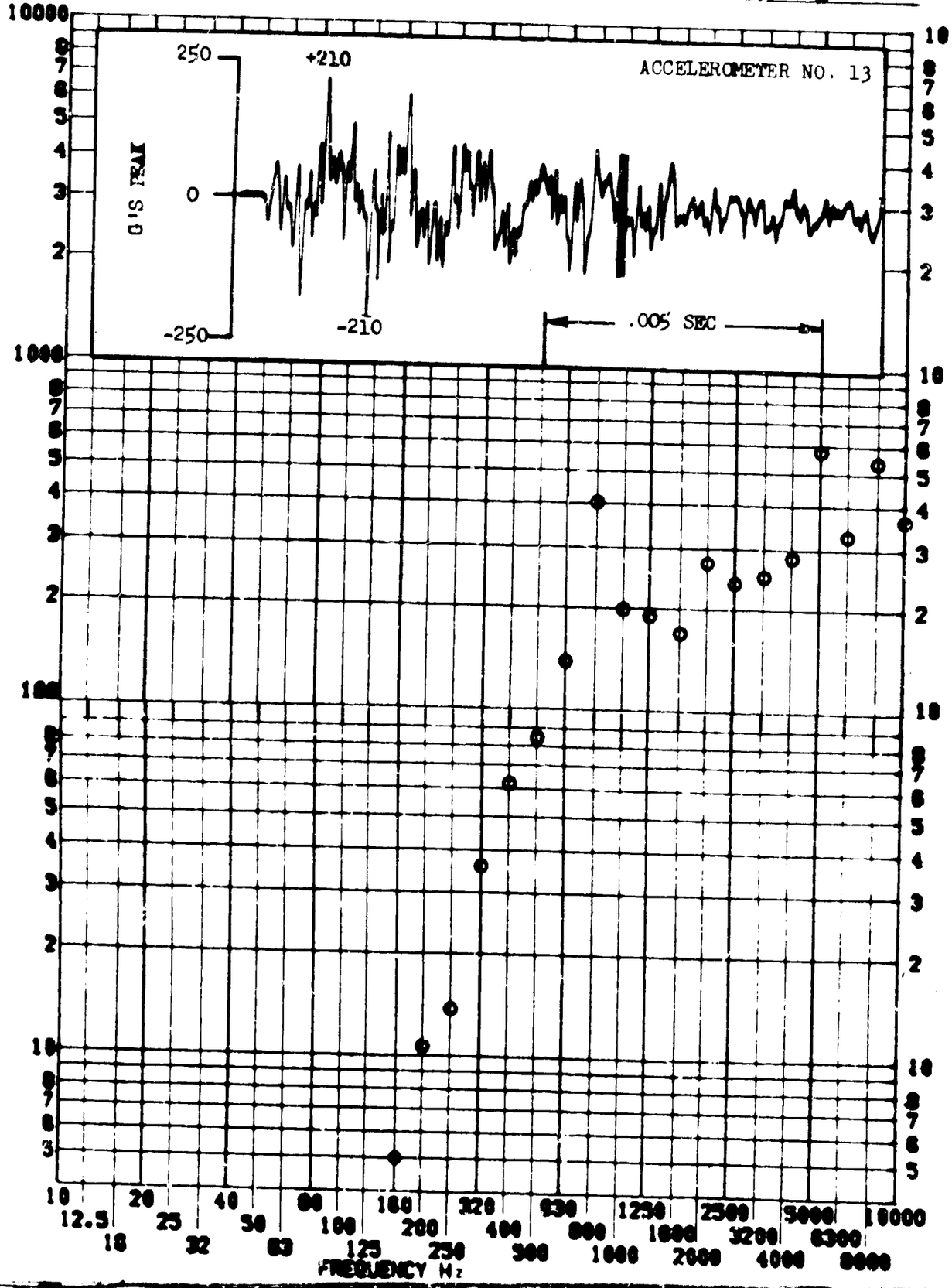

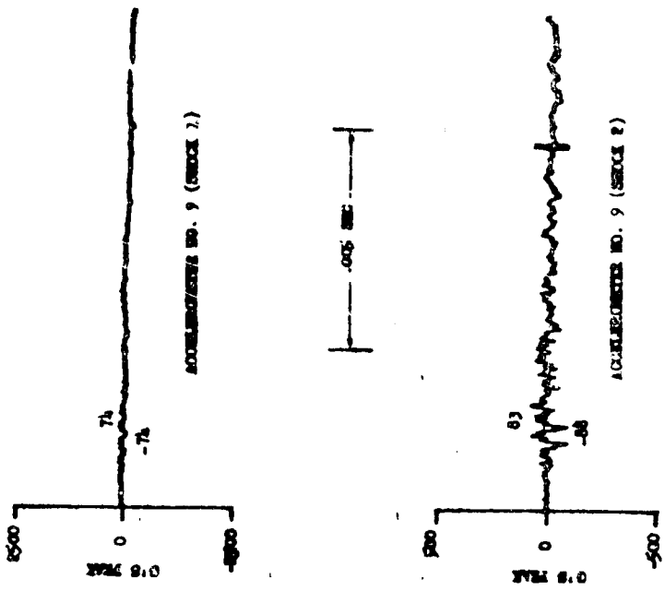
74
-74
500
0
-500
0.5 MSEC
83
-88
500
0
-500
0.5 MSEC

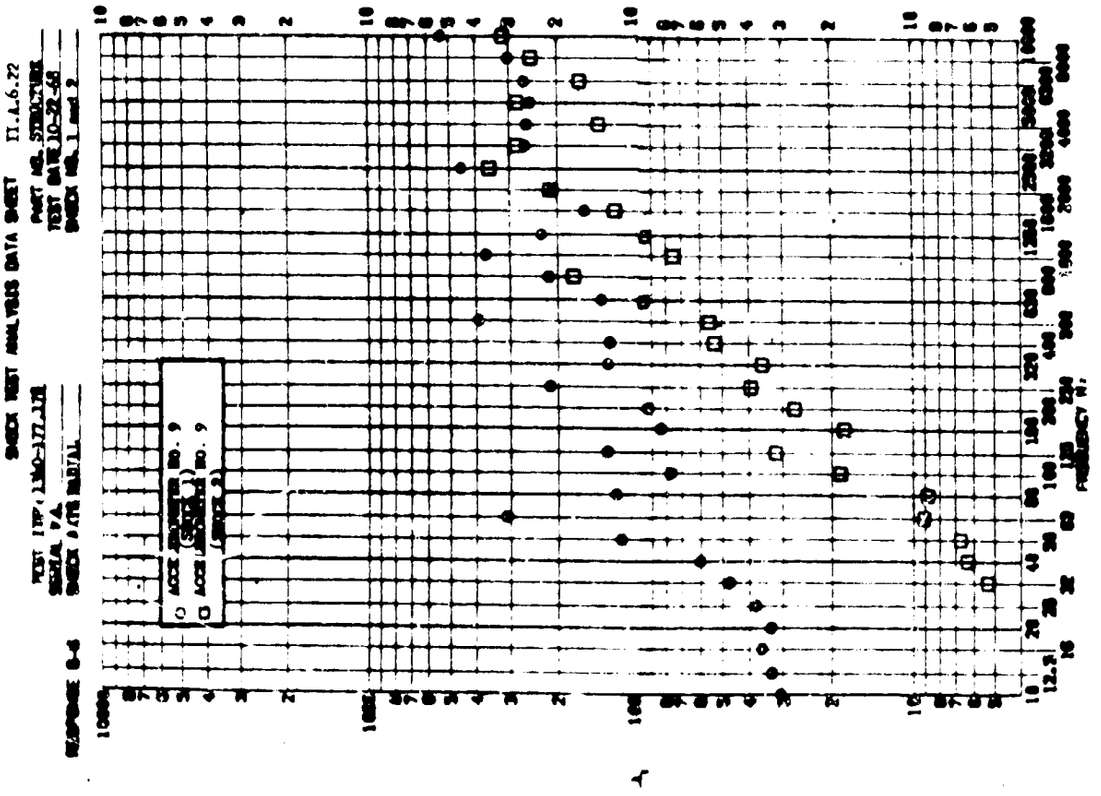
SHOCK TEST ANALYSIS DATA SHEET
ACC RESPONSE NO. 9
ACC RESPONSE NO. 9
FREQUENCY IN

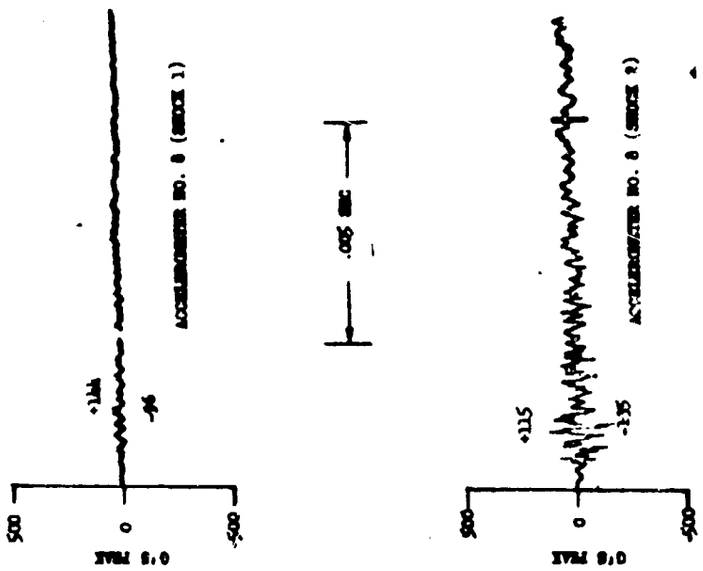
ACCELEROMETER NO. 8 (SHOCK 1)
.005 SEC
ACCELEROMETER NO. 8 (SHOCK 2)

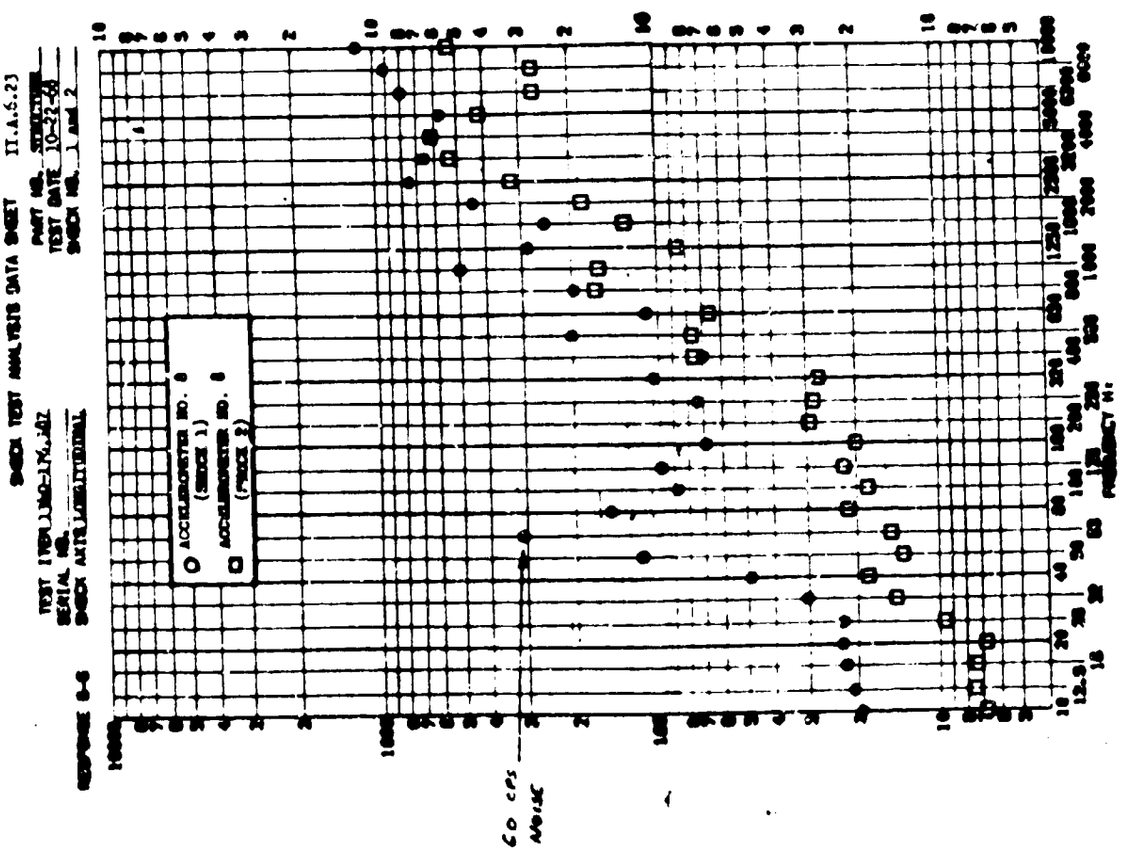
SHOCK TEST ANALYSIS DATA SHEET
ACCELEROMETER NO. 8 (SHOCK 1)
ACCELEROMETER NO. 8 (SHOCK 2)
FREQUENCY, Hz

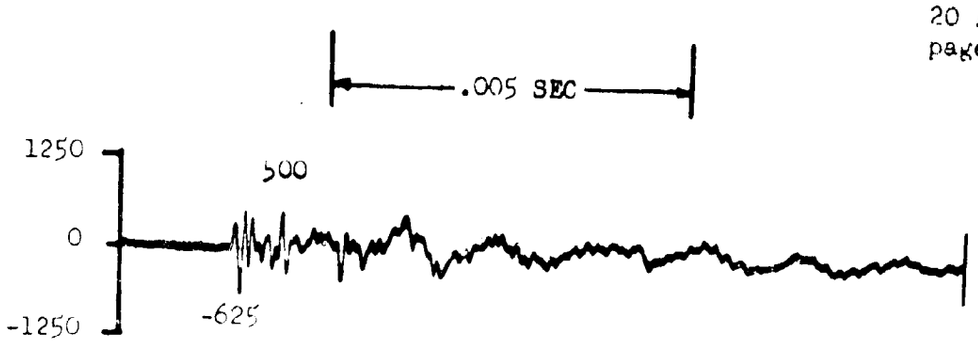

ACCELEROMETER NO. 1 (Longitudinal) TEST 1

ACCELEROMETER NO. 7 (Radial) TEST 1

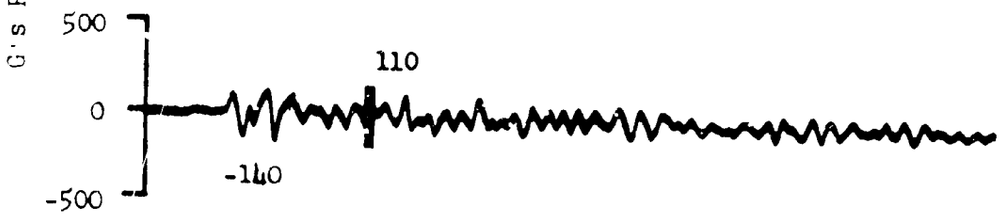

ACCELEROMETER NO. 10 (Longitudinal) TEST 1

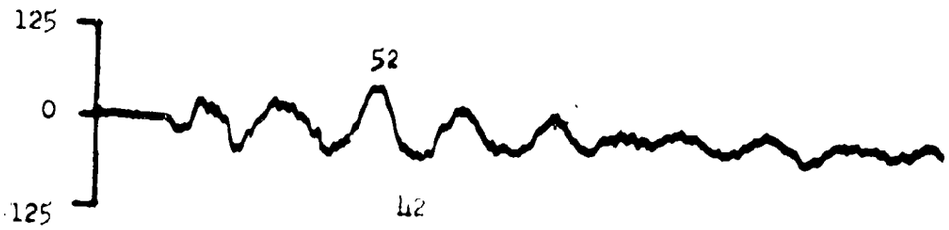

ACCELEROMETER NO. 11(Longitudinal) TEST 2

Figure II.A.6.24 SHOCK LEVELS FROM TEST 1 AND 2

SECTION NO. II.A.7

REPORT NO. 1377

SUBJECT:

SATELLITE VEHICLE BOOSTER SEPARATION TESTS

SUMMARY

Two Satellite Vehicle (SV)/booster separation tests were performed with a specimen which simulated the spacecraft structure. The specimen included mass and c.g. simulated equipment of interest.

The objectives of these tests were to functionally test the SV/booster separation joint and to gather shock environmental data from the Satellite Vehicle structure and equipment.

Data analysis included a listing of the peak g levels for all oscillograph measurements, shock attenuation as a function of distance from the joint and its application to other tests of similar structure, an evaluation of shock attenuation as a function of frequency, and an evaluation of shock spectrum g levels for different analysis Q (amplification) values.

The objectives of the SV/booster separation tests were satisfied. The separation tests were accomplished as planned with satisfactory results.

The data values from primary structure were too scattered to establish a well-defined shock attenuation curve, however general trends were definitely observable and a test of the attenuation curves that were generated indicated they were completely satisfactory for conservatively estimating the shock levels at any point on the structure.

An analysis of shock attenuation as a function of frequency yielded somewhat inconclusive and sometimes conflicting results. Generally shock was attenuated more with increasing frequency.

An analysis of shock spectra for different values of Q indicated that amplification varies little with frequency. Factors were calculated based on shock spectra for Q's of 5, 10, 25 and 50 which can be used to determine the factor which should be used to multiply a shock spectrum of one Q to obtain a shock spectrum for any other Q.

TABLE OF CONTENTS

SECTION II.A.7

LIST OF TABLES

SECTION II.A.7

LIST OF FIGURES

SECTION II.A.7

LIST OF FIGURES (Cont.)

SECTION II.A.7

LIST OF FIGURES (Cont.)

SECTION II.A.7

LIST OF FIGURES (Cont.)

SECTION II.A.7

LIST OF FIGURES (Cont.)

SECTION II.A.7

LIST OF FIGURES (Cont.)

SECTION II.A.7

LIST OF FIGURES (Cont.)

SECTION II.A.7

LIST OF FIGURES (Cont.)

SECTION II.A.7

LIST OF FIGURES (Cont.)

SECTION II.A.7

II.A.7.1 INTRODUCTION

These were the first tests of the separation system of this SV/booster. Pyrotechnic events of this nature quite often subject structure and equipment near the source to a severe shock environment. This environment must be defined to determine the possibility of equipment damage or malfunction during flight.

The pyroshock environment for this SV/booster combination was defined by measurement of the generated shock from the pyrotechnic detonation on a test specimen that simulated the spacecraft structure and equipment of interest.

Measurements were placed on primary structure, at truss interfaces and at equipment interfaces. The primary structure measurements were mainly intended to determine attenuation characteristics of the main structure.

II.A.7.2 DISCUSSION AND ANALYSIS

II.A.7.2.1 Test Configuration and Instrumentation

A sketch of the SV/booster separation test specimen is shown in Figure II.A.7.1. The specimen consisted of a short section of simulated shroud, a Satellite Control aft section containing simulated equipment packages, and a booster forward section. The entire assembled test specimen approximated a cylinder 190 inches high and 120 inches in diameter. The aft section consisted of a booster adapter, a Reaction Control Module (RCM) and an equipment section which contained simulated equipment modules. A typical equipment installation is shown in Figure II.A.7.2.

The pyrotechnic separation joint was located in the forward ring of the booster adapter on the aft section. A detail drawing of the separation joint is shown in Figure II.A.7.3. The joint consisted of two 2.5 grains/foot RDX explosive cords seated in adjacent circumferential grooves in the forward ring and covered with beryllium break plates which lapped the booster adapter and the RCM. The portion of the test specimen above the separation joint was counter-weighted to lift the vehicle away from the booster skirt immediately upon separation.

A total of 62 ENDEVCO Corporation piezoelectric accelerometers were mounted at 39 locations on the test specimen as shown in Tables II.A.7.1,2,3 and Fig.II.A.7.4. Forty Model 2220 and twenty-two Model 2225 accelerometers were used in the two tests. All transducers were of the single-axis type and were mounted to measure shock excitation in one of three directions: longitudinal (parallel to vehicle axis), radial (along a radius of the vehicle cross section) and tangential (lateral and at 90 degrees to the radial direction). The shock transients produced at the accelerometer locations by the pyrotechnic separations were processed through the signal-conditioning equipment illustrated in Figure V.2 in another section of this report and recorded on magnetic tape at 60 inches/second tape speed for subsequent playback and analysis as illustrated in Figure V.3

II.A.7.2.2 Test Conditions and Results

Table II.A.7.3 contains a summary of the tests performed. Both tests 1 and 2 were conducted with a separation joint which consisted of two 2.5 grains/foot RDX explosive cords seated in adjacent circumferential grooves in the forward ring and covered with beryllium break plates which lapped the booster adapter and the Reaction Control Module (RCM). A sketch of the separation joint configuration is shown in Figure II.A.7.3. The detonations of the two RDX strips occurred sequentially with a time lapse of 15 milliseconds between detonations.

The data from both tests 1 and 2 were analyzed by means of high speed oscillograms and shock spectra The shock spectrums are based on a Q of 25. The oscillograms, along with their respective shock spectra, are presented in Figures II.A.7.13 to II.A.7.182. These figures include composites of the shock spectra of the same measurement for tests 1 and 2 whenever a measurement is repeated. Peak g levels for each oscillogram have been tabulated in Tables II.A.7.4 and II.A.7.5.

II.A.7.2.3 Data Analysis

II.A.7.2.3.1 Shock Attenuation Versus Distance from Shock Source

Figure II.A.7.5 shows the peak g shock levels as a function of distance from the shock source. Separate curves are shown for the longitudinal measurements and for the radial and tangential measurements.

Measurements were made on primary structure with the objective of obtaining attenuation data. Figure II.A.7.5 was derived by plotting the peak g values obtained from the primary structure oscillograms (Tables II.A.7.4 and II.A.7.5). Data from both tests were used. A curve was then constructed using the average of the longitudinal and of the radial and tangential measurements for each location (5, 24, 43 and 62 inches from the source). The ordinate of these curves was then normalized so that the average of the measurements 5 inches from the joint corresponded to 100 percent and the curves reconstructed (Figure II.A.7.6). All other measurements were also normalized and

plotted in Figure II.A.7.6 to show their relative location with respect to the attenuation curves.

These attenuation curves may be used in several ways to determine the peak shock level expected at a given distance from the source. To determine the expected shock level on primary structure the curves of Figure II.A.7.6 can be used directly. To determine the maximum expected shock levels on primary structure, truss structure, or equipment for any location of this test or any other test of similar structure and a similar separation joint, it is only necessary to know the shock level at 5 inches from the source and the distance from the source. If more than one measurement is made at the source, the highest measurement should be used for best assurance that the method will yield values which are conservative enough to cover the highest shock levels which might be encountered. The highest shock level at 5 inches from the source should be used to reconstruct the radial/tangential curve of Figure II.A.7.6 in terms of g's. From this curve the maximum anticipated peak shock levels at any distance can be determined.

This method assumes that the primary structure measurements are more severe for a corresponding distance from the source than are any other measurements. To test this and the general application of this method, all the peak g levels from test 2 (except in cases where only test 1 data were available) from each accelerometer and each axis were plotted in Figure II.A.7.7. The primary structure measurements were differentiated from the truss and equipment locations. The more conservative of the shock attenuation curves of Figure II.A.7.6 was then constructed in Figure II.A.7.7 based on the highest peak g reading at 5 inches from the joint as was stipulated in the conditions. Figure II.A.7.7 thus indicates that application of this method gives a conservative estimate of the shock at any location since all other measurements (with only two exceptions) fall below the curve.

If an average shock reduction is desired for points on primary structure for this and other tests, it is necessary to use the average of the measurements at 5 inches from the joint to construct the attenuation curve. It should be noted that if the average of the radial and tangential measurements at 5 inches from the joint were used to construct the attenuation curve, the result would be a curve which would fall through the average of the radial and tangential measurements at all primary structure locations. This was the curve which was used to derive the original shock attenuation curve of Figure II.A.7.6.

Notice also that there is a large body of measurements which fall below the attenuation curve of Figure II.A.7.7 by a factor (on the average) of 7. These measurements correspond to locations on equipment. Thus it must be kept in mind that application of this method to equipment locations may give highly conservative levels; a factor of 7 is an indication of the amount of this conservatism.

II.A.7.2.3.2 Shock Attenuation as a Function of Frequency

An attempt was made to establish a relationship between shock attenuation as a function of distance and frequency. The envelope of all axes of the shock sprectra for measurements 1, 2, 3 and 4 were read in 1/3 octave points (Table II.A.7.6). Shock spectra are presented in Figure II.A.7.8 to indicate how much the characteristics of a shock spectrum can vary even when measurements are made on similar structure. The accelerometers which produced the spectra of Figure II.A.7.8 were all placed on the same primary structure with the intention of collecting attenuation data. Yet these spectra exhibit vastly different characteristics. Even though the spectra are from measurements which are spaced at 20 inch intervals from the source, the spectra overlap in any areas.

Figure II.A.7.9 illustrates what happens when an attempt is made to predict a shock spectrum at some distance from the source based on a spectrum obtained from a measurement at the source and a shock attenuation curve constructed from peak g measurements. Here, a shock

spectrum obtained from an envelope of shock spectra of all axes at measurement location 1, 5 inches from the source on the primary structure, is used to predict the shock spectrum for measurement location 4, 62 inches from the source on the same primary structure. (Table II.A.7.6, 9 percent of location 1 levels based on attenuation curve of Figure II.A.7.6 . For comparison, an envelope of all axes of the actual shock spectra from measurement location 4 is included. The figure indicates that this method was good for predicting the maximum g level but that the spectra are not at all similar and, in fact the predicted spectrum falls below the actual spectrum over much of the frequency range. Thus it is not possible to predict with accuracy the entire shock spectrum at some location simply by enveloping the measurements at some other location and applying a shock attenuation curve.

Figure II.A.7.10 is the result of a study to determine how the attenuation varied with frequency as an additional parameter to distance. These spectra result when the spectra from three of the primary structure locations (24, 43 and 62 inches from the source) from both tests 1 and 2 are averaged and ratioed to the averaged spectrum from the location 1 measurements in octave bands (Table II.A.7.7).

As Figure II.A.7.8 indicated, it is not possiole to predict with any accuracy how the shock attenuates with frequency for different measurement locations without some additional information. There is a trend for the shock to attenuate more at higher frequencies and at greater distances from the source but no number can be assigned to the amount of attenuation on the bases of these measurements. More measurements are needed to resolve this.

Figure II.A.7.10 does indicate that frequency attenuation is dependent on the mode of the structure on which the measurements are made. A preliminary calculation of the first breathing mode of the structure on which the measurements were located yields a frequency of 480 Hz. Measurement 3 which was located 43 inches from the source on a ring

shows amplification at the 500 Hz octave band center frequency. This is consistent with the location of the measurements since measurement 3 was located on a ring and recorded the ring mode whereas measurement 1 was located on a longeron. Thus, additional test data as well as additional analysis is needed to more accurately define how shock is attenuated with frequency.

7.2.3.3 Amplification (Q) Factor

Shock spectra were produced for different Q values for selected measurements to determine how spectra analyzed at different Q valu could be related to each other. Shock spectra were produced for Q of 5, 10, 25 and 50 for measurements 1, 3, 4 and 35 (all axes). The shock spectra for Q's of 5, 10 and 50 are not included in this report but were used in the analysis. The shock spectra were read in octave bands at the octave band center frequencies. The data for Q's of 5, 10 and 50 for each measurement were then normalized to the data which were analyzed at a Q of 25. The normalized data are presented in Table II.A.7.8. The data in each octave band were then averaged for each value of Q. The averaged data also appear in Table II.A.7.8. This table shows that the spread in the averaged data for each value of Q as a function of frequency appears to be quite small. For example the averaged normalized data for a Q of 5 is 0.71. The mean deviation is 0.027 or only 4 percent. Furthermor the spread does not seem to be a function of frequency but rather appears to be random in nature. Thus the relationship between shock spectra for different values of Q seems to be independent of frequency and shock spectra analyzed at different Q values can be related by constant factors. It only remains to determine what thos factors are.

Figure II.A.7.11 is a plot of the average factors of Table II.A.7.8. The actual data points are also plotted. As the figure shows, a straight line can easily be drawn through the data points. This plo makes it possible to determine the relationship between shock spectra of different values of Q simply by taking the ratio of the

correction factor corresponding to the Q of the desired spectrum to the correction factor corresponding to the Q of the known spectrum to obtain a new factor. The known spectrum is then multiplied by the new factor to obtain the desired spectrum.

The formula for the correction factor curve is $y = 0.425 \log x + 0.41$ where y is the correction factor and x is the amplification, Q. Thus to determine the factor which should be multiplied times a given spectrum at a given Q to obtain the corresponding spectrum for a new Q, the formula is:

$$A_o = \frac{y_o}{y_1} = \frac{0.425 \log x_o + 0.41}{0.425 \log x_1 + 0.41}$$

where:

A_o = required factor

y_o = correction factor of Figure II.A.7.11 for the desired spectrum

y_1 = correction factor of Figure II.A.7.11 for the given spectrum

x_o = amplification (Q) of the desired spectrum

x_1 = amplification (Q) of the given spectrum

This can be simplified to: $A_o = \frac{1.04 \log x_o + 1}{1.04 \log x_1 + 1}$

and $A_o \cong \frac{\log x_o + 1}{\log x_1 + 1}$ is sufficiently accurate for most analysis.

It should be noted that these formulae and Figure II.A.7.11 from which they were derived are intended to be used only as an estimate of the shock spectrum levels. This method does not account for peaks in high Q spectra which are the result of only a few cycles of data. Highly damped systems (low Q) do not respond as much to those few cycles as would a lightly damped (high Q) system. Thus, for example, when this formula is applied to predict a high Q spectrum from a low Q spectrum and the derived high Q spectrum is compared with the actual high Q

spectrum, peaks may be observed in the actual high Q spectrum which exceed the level of the derived high Q spectrum.

7.2.3.4 Data Repeatability

Shock spectra from this test were used in a data repeatability study (see Section III.A of this report). Shock spectra from identical measurements, tests 1 and 2, were summarized by 1/3 octave bands (Table II.A.7.9). Values from the two tests were ratioed. The ratios were input into a statistical program which gave a one sigma deviation expressed in dB as a function of grequency (Figure II.A.7.12). Generally the deviation was no greater than 4 dB in any 1/3 octave band.

II.A.7.3 CONCLUSIONS

The basic objectives of the test, to functionally test the SV/booster separation joint and to gather environmental data, were satisfactorily met.

The attenuation-distance curves of Figure II.A.7.6 can be used with good confidence to predict the maximum anticipated peak g level at any location. However, prediction of peak g levels at equipment interfaces where the shock must travel through truss-work can result in peak g levels which may be on an average of seven times too high.

The attenuation-distance curves should not be used to predict shock spectrum levels since shock spectrum characteristics are highly dependent on the structure on which the measuremtn is made.

Because of the dependency of shock spectra on the modal characteristics of the structure, the relationship of attenuation to frequency, with the few measurements which were made and the small amount of analysis which time allowed, was not completely resolved. Generally, the shock was attenuated more at the higher frequencies, but more data and more analysis is needed to determine the role of frequency in shock attenuation.

Indications from a study in which shock spectra were produced at varying Q's was that the Q did not vary with freq. but that shock spectra at different Q values are related to each other by a constant which can be applied to the entire spectrum. A very simple formula and its corresponding curve were derived empirically to estimate a shock spectrum at any Q if the shock spectrum another Q is known.

TABLE II.A.7.1

ACCELEROMETERS AND LOCATIONS - STRUCTURE

Accelerometer No.	Bay	Direction	Distance to Shock Source (inches)	Accelerometer Type
1	6 - 7	L - R - T	5	ENDEVCO 2225
2	6 - 7	L - R	24	ENDEVCO 2225
3	6 - 7	L - R	43	ENDEVCO 2225
4	6 - 7	L - R - T	62	ENDEVCO 2225
5	6 - 7	L - R	33	ENDEVCO 2225
6	6 - 7	L - R	46	ENDEVCO 2220
7	8 - 9	L - R	33	ENDEVCO 2225
8	8 - 9	L - R	46	L 2220 R 2225
9	1 - 12	L - R	33	L 2220 R 2225
10	1 - 12	L - R	46	L 2220 R 2220

* **L - Longitudinal**
R - Radial
T - Tangential

TABLE II.A.7.2

ACCELEROMETERS AND LOCATIONS - EQUIPMENT

Accelerometer No.	Box	Direction	Bay Location	Distance to Shock Source (inches)	Accelerometer Type
11	Sec. battery module	R	1	76	ENDEVCO 2220
12	Elec. distrib. module	R	2	52	ENDEVCO 2220
13	Elec. distrib. module	L - R	2	72	ENDEVCO 2220
14	OTEX module	R	4	40	ENDEVCO 2220
15	Altitude ref. module	R	6	50	ENDEVCO 2220
16	Altitude ref. module	R	6	50	ENDEVCO 2220
17	Altitude ref. module	R	6	38	ENDEVCO 2220
18	Altitude ref. module	L - R	6	38	ENDEVCO 2220
19	Altitude ref. module	R	6	36	ENDEVCO 2220
20	T and T module	L - R	7	45	ENDEVCO 2220
21	Prim. cmd. module	L	8	54	ENDEVCO 2220
22	Prim. cmd. module	L - R	8	45	ENDEVCO 2220
23	Prim. cmd. module	R	8	54	ENDEVCO 2220
24	BRAC module	R	9	42	ENDEVCO 2220
25	BRAC module	L - R	9	62	ENDEVCO 2220
26	BRAC module	L	9	56	ENDEVCO 2220

* L - Longitudinal
R - Radial
T - Tangential

TABLE II.A.7.2 (Cont.)

ACCELEROMETERS AND LOCATIONS - EQUIPMENT

Accelerometer No.	Box	Direction	Bay Location	Distance to Shock Source (inches)	Accelerometer Type
27	BRAC module	R	9	50	ENDEVCO 2220
28	Ascent TLM module	L	10	44	ENDEVCO 2220
29	Ascent module	R	10	58	ENDEVCO 2220
30	Prim. battery module	R	12	42	ENDEVCO 2220
31	Prim. battery module	R	12	50	ENDEVCO 2220
32	BRAC thruster	R	6	14	ENDEVCO 2225
33	Sol. array module	L - R	6 - 7	18	ENDEVCO 2225
34	Thr. cont. actuator	L - R - T	-	115	ENDEVCO 2220

* L - Longitudinal
R - Radial
T - Tangential

TABLE II.A.7.3

SUMMARY OF TESTS

Test No.	Configuration	Explosive Size	Test Purpose	Shock Isolation
1	Bcoster separation	2 1/2 gr/ft dual chord	Struct. box	No
2	Booster separation	2 1/2 gr/ft dual chord	Struct. box	No

TABLE II.A.7.4

OSCILLOGRAM PEAK G READINGS

ACCEL. NO.	AXES	DISTANCE FROM SHOCK SOURCE	LOCATION	PEAK G READING TEST 1	PEAK G READING TEST 2
1	L R T	5 in.	PRIMARY STRUCTURE	7400 2800 2200	7600 2500 3000
2	L R	24	PRIMARY STRUCTURE	750 1500	800 1450
3	L R	43	PRIMARY STRUCTURE	760 450	[illegible] [illegible]
4	L R T	62	PRIMARY STRUCTURE	300 320 [illegible]	[illegible] [illegible] 180
5	L R	33	TRUSS STRUCTURE	110 180	130 180
6	L R	46	TRUSS STRUCTURE	110 200	110 190
7	L R	33	TRUSS STRUCTURE	100 150	100 140
8	L R	46	TRUSS STRUCTURE	110 180	110 200
9	L R	33	TRUSS STRUCTURE	290 280	260 250
10	L R	46	TRUSS STRUCTURE	170 180	120 170
11	R	76	SEC. BATTERY MODULE	150	150
12	R	52	ELEC. DIST. MODULE	170	100
13	L R	72	ELEC. DIST. MODULE	75 120	65 80
14	R	40	OTEX MODULE	NO DATA	225
15	R	50	ATTITUDE REF. MODULE	30	40
16	R	50	ATTITUDE REF. MODULE	70	70
17	R	38	ATTITUDE REF. MODULE	60	45
18	L R	38	ATTITUDE REF. MODULE	110 130	120 NO DATA
19	R	36	ATTITUDE REF. MODULE	155	315
20	L R	45	T & T MODULE	40 90	40 NO DATA
21	L	54	PRIMARY COMMAND MODULE	55	NO DATA
22	L R	45	PRIMARY COMMAND MODULE	20 10	29 30
23	R	54	PRIMARY COMMAND MODULE	40	62

* L - Longitudinal
  R - Radial
  T - Tangential

TABLE II.A.7.5

OSCILLOGRAM PEAK G READINGS

ACCEL. NO.	AXIS	DISTANCE FROM SHOCK SOURCE	LOCATION	PEAK G READING	
				TEST 1	TEST 2
24	R	42 in.	BRAC MODULE	NO DATA	10
25	L	62	BRAC MODULE	50	55
	R			NO DATA	53
26	L	56	BRAC MODULE	60	70
27	R	50	BRAC MODULE	NO DATA	175
28	L	44	ASCENT TLM MODULE	200	300
29	R	38	ASCENT TLM MODULE	90	150
30	R	42	PRIMARY BATTERY MODULE	230	230
31	R	50	PRIMARY BATTERY MODULE	110	145
32	R	14	BRAC [illegible]	105	150
33	L	18	SOLAR ARRAY MODULE	1150	NO DATA
	R			1450	1250
34	L	115	THRUST CONTROL ACTUATOR	25	*
	P			150	*
	T			135	*
35	L	16	BOOSTER SKIRT	2100	2000
	R			1900	1600
36	L	25	BOOSTER SKIRT	[illegible]	1300
	R			[illegible]	850
37	L	53	BOOSTER SKIRT	NO DATA	1150
	R			[illegible]	460
38	L	33	REACTION CONTROL TANK	*	1100
	R			*	1430
39	L	33	BRAC TANK	*	1850
	R			*	850

* NO INSTRUMENTATION

L - Longitudinal
R - Radial
T - Tangential

TABLE II.A.7.6

1/3 OCTAVE ENVELOPES AND A PREDICTED ENVELOPE

OF PRIMARY STRUCTURE SHOCK SPECTRUMS BY 1/3 OCTAVE

1/3 OCTAVE BAND CENTER FREQUENCY	ENVELOPE G LEVEL				
	1 L,R,T	2 L,R	3 L,R	4 L,R,T	PREDICTED 4 L,R,T
200	113	95	36	32	10
250	163	90	63	49	15
320	183	107	189	139	17
400	277	151	718	693	25
500	492	257	881	467	44
630	718	559	953	470	65
800	885	843	588	567	80
1000	1676	1010	802	421	151
1250	3566	735	526	421	321
1600	3219	1182	928	1234	290
2000	2867	2720	1141	2901	258
2500	3117	2855	1151	1203	281
3200	4507	2351	1622	810	406
4000	8155	1805	1865	832	735
5000	14,904	2859	1020	1026	1340
6300	22,590	9051	1288	893	2037
8000	26,866	7555	1182	606	2420
10,000	22,764	5492	649	630	2050

TABLE II.A.7.7

DERIVATION OF FIGURE II.A.7. , ATTENUATION ALONG PRIMARY STRUCTURE AS A FUNCTION OF FREQUENCY

1/3 Octave Band Center Frequency	Avg. Shock Level Test 1 and 2				% of 5" Shock Level, 1/3 Octaves			% of 5" Shock Level, Octave Avg.		
	5" 1 L, R, T	24" 2 L, R	43" 3 L, R	62" 4 L, R, T	24"	43"	62"	24"	43"	62"
200	123	78	26	19	63	21	16			
250	182	88	47	33	48	26	18	64	43	28
320	165	135	134	81	82	83	49			
400	239	215	356	355	90	149	148			
500	348	324	493	227	93	141	65	89	133	57
630	567	481	612	281	85	108	49			
800	877	695	573	449	79	65	51			
1000	1462	766	586	358	53	40	24	53	42	29
1250	2533	696	518	350	28	20	14			
1600	2737	1149	754	743	42	28	27			
2000	2699	1614	934	1263	60	35	47	80	50	51
2500	2812	1634	1075	830	58	38	29			
3200	2772	1785	1198	528	64	43	19			
4000	4208	2044	1416	618	48	34	15	77	29	15
5000	7579	3256	875	913	43	12	12			
6300	12660	5795	1116	817	46	6	7			
8000	16996	5212	1048	565	31	6	3	37	0	4
10,000	15297	5256	651	507	35	4	3			

TABLE II.A.7.6

NORMALIZED AND AVERAGED TEST 1 AND 2 PRIMARY STRUCTURE SHOCK SPECTRUM DATA
BY OCTAVE BANDS - DATA NORMALIZED TO Q = 25

Octave Band Center Frequency	1 L	1 R	1 T	3 L	3 R	4 L	4 R	4 T	35 L	35 F	Average, All Measurements
Q = 5											
125	-	.69	-	.94	1.08	.80	-	-	.46	.[illegible]	.[illegible]4
250	-	.56	.54	1.08	.92	.87	.88	.67	.58	.[illegible]7	.75
500	.68	.96	.93	.57	.57	.63	.53	.92	.62	.62	.70
1000	.80	.80	.67	.57	.71	.72	.78	.51	.57	.[illegible]7	.69
2000	.66	.92	.66	.70	.50	.53	.41	.46	.73	.72	.65
4000	.85	.89	.80	.70	.56	.90	.80	.57	.55	.[illegible]3	.73
8000	.73	.55	.56	.67	.62	.77	.81	.70	.89	.[illegible]4	.70
									Average, all frequencies		.71
Q = 10											
125	-	.85	-	1.00	1.08	.87	-	-	.93	.[illegible]4	.90
250	-	.68	.62	1.08	1.00	.91	.88	.75	.79	.[illegible]3	.83
500	.87	.97	.96	.86	.[illegible]3	.88	.60	.96	.[illegible]8	.[illegible]7	.84
1000	.95	.92	.87	.72	.86	.89	.87	.67	.[illegible]7	.88	.84
2000	.93	1.00	.81	.75	.65	.69	.63	.62	.[illegible]7	.86	.[illegible]7
4000	.96	1.00	.94	.85	.75	.85	.83	.77	.78	.79	.85
8000	.86	.77	.78	.93	.71	.92	.94	.76	.96	.84	.85
									Average, all frequencies		.82

TABLE II.A.7.8 (CONT'D.)

NORMALIZED AND AVERAGED TEST 1 AND 2 PRIMARY STRUCTURE SHOCK SPECTRUM DATA
BY OCTAVE BANDS - DATA NORMALIZED TO Q = 25

Octave Band Center Frequency	1 L	1 R	1 T	3 L	3 R	4 L	4 R	4 T	35 L	35 R	Average, All Measurements
Q = 50											
125	-	1.08	-	1.00	1.08	1.20	-	-	1.15	1.11	1.10
250	-	1.20	1.31	1.08	1.00	1.14	1.06	1.00	1.05	1.14	1.11
500	1.13	1.03	1.00	1.07	1.04	1.25	1.20	1.20	1.20	1.07	1.12
1000	1.08	1.08	1.13	1.14	1.14	1.07	1.22	1.11	1.33	1.06	1.14
2000	1.07	1.00	1.15	1.12	1.30	1.17	1.18	1.38	1.23	1.14	1.17
4000	1.08	1.11	1.23	1.30	1.12	1.00	1.15	1.15	1.10	1.05	1.13
8000	1.09	1.06	1.11	1.00	1.08	1.23	1.22	1.20	1.02	1.20	1.12
										Average, all frequencies	1.13

TABLE II.A.7.9

PEAK SHOCK SPECTRA RESPONSE g's O-P

22 Locations - 2 Tests

Frequency -Hz-	ACCELERATION 13R Test 1	Test 2	RATIO Test 1 / Test 2	ACCELERATION 16R Test 1	Test 2	RATIO Tests 1/2	ACCELERATION 18X Test 1	Test 2	RATIO Tests 1/2	ACCELERATION 20Y Test 1	Test 2	RATIO Tests 1/2
200	6.8	7.2	.95	9.6	8.3	1.16	8.4	1.0	.82	5.6	5.2	1.06
250	9.4	9.7	.97	15.0	14.2	1.06	7.8	1.0	.76	4.8	4.5	1.09
320	13.5	10.8	1.26	22.5	18.5	1.22	13.3	1.0	1.29	5.1	7.0	.74
400	30.8	19.5	1.97	31.1	39.6	.79	11.7	14.2	.80	7.2	17.8	.41
500	63.3	62.9	1.01	48.5	58.6	.83	25.0	11.3	2.15	25.9	34.0	.76
630	53.2	60.3	.89	37.1	44.5	.84	28.6	30.7	.91	24.9	34.7	.72
800	74.0	85.4	.87	38.7	97.0	.40	57.8	54.2	1.04	22.4	28.5	.79
1000	121.	184.	.66	104.	148.	.70	72.4	75.5	.94	30.0	27.5	1.09
1250	141.	165.	.86	123.	101.	1.22	76.2	89.2	.84	22.0	19.0	1.15
1600	262.	316.	.83	106.	82.6	1.29	268.	247.	1.06	16.6	31.2	.54
2000	380.	322.	1.18	124.	114.	1.08	268.	265.	.99	21.9	58.5	.38
2500	225.	267.	.84	92.	101.	.92	310.	382.	.79	51.9	46.6	1.11
3200	205.	179.	1.14	119.	93.1	1.28	567.	675.	.82	61.1	90.8	.68
4000	349.	252.	1.38	111.	103.	1.08	489.	948.	.51	110.	189.	.58
5000	474.	321.	1.47	393.	347.	1.13	445.	425.	1.03	217.	387.	.57
6300	242.	200.	1.21	303.	357.	.85	224.	219.	1.00	299.	190.	1.57
8000	201.	182.	1.10	630.	507.	1.24	199.	242.	.80	134.	173.	.78
10,000	176.	161.	1.20	748.	757.	.99	294.	309.	.93	122.	213.	.58

TABLE II.A.7.9

(CONT'D.)

Frequency - Hz -	ACCELERATION 22R Test 1	Test 2	RATIO Test 1 / Test 2	ACCELERATION 26X Test 1	Test 2	RATIO Tests 1/2	ACCELERATION 29R Test 1	Test 2	RATIO Tests 1/2	ACCELERATION 31R Test 1	Test 2	RATIO Tests 1/2
200	5.5	2.6	2.16	19.5	28.6	.68	23.4	18.8	1.21	20.0	20.1	1.00
250	9.9	3.3	2.94	20.8	26.1	.80	18.4	12.9	1.38	16.2	13.0	1.25
320	6.3	3.9	1.63	17.0	20.1	.85	37.1	24.1	1.50	18.8	14.7	1.27
400	7.8	8.1	.95	40.5	56.1	.72	63.8	23.0	2.68	22.8	21.0	1.08
500	33.2	23.1	1.43	55.3	47.8	1.16	67.3	45.8	1.43	31.3	23.8	1.31
630	13.8	13.5	1.02	69.4	74.1	.94	66.0	50.9	1.26	37.3	45.1	.83
800	20.7	14.1	1.47	153.	206.	.75	96.4	61.6	1.52	54.9	56. 3	.98
1000	58.8	48.9	1.20	87.7	83.1	1.05	156.	112.	1.36	46.8	31.6	1.48
1250	44.5	44.5	1.00	102.	91.6	1.11	109.	77.	1.38	45.3	33.7	1.34
1600	58.8	48.2	1.22	54.6	52.7	1.04	120.	147.	.80	85.1	76.1	1.11
2000	117.	70.0	1.66	62.1	55.9	1 11	230.	218.	1.03	130.	139.	.94
2500	85.7	76.4	1.12	132.	136.	.97	208.	360.	.57	173.	176.	.99
3200	97.9	76.1	1.28	158.	155.	1.02	332.	464.	.70	136.	130.	1.05
4000	147.	136.	1.08	210.	210.	1.00	366.	503.	.71	437.	347.	1.26
5000	243.	176.	1.38	367	309.	1.19	379.	484.	.77	778.	580.	1.34
6300	161.	167.	.97	328.	351.	.94	316.	344.	.90	378.	350.	1.08
8000	138	108.	1.28	428.	558.	.77	639	831.	.75	643.	433.	1.48
10,000	118	121.	.98	230.	293.	.79	490.	1074.	.45	107.	106.	1.00

TABLE II.A.7.9

(CONT'D.)

Frequency -Hz-	ACCELERATION 2X Test 1	Test 2	RATIO Test 1 / Test 2	ACCELERATION 3X Test 1	Test 2	RATIO Tests 1/2	ACCELERATION 4X Test 1	Test 2	RATIO Tests 1/2	ACCELERATION 4T Test 1	Test 2	RATIO Tests 1/2
200	65	95	.69	18	16	1.11	16	22	.76	32	33	.99
250	80	77	1.04	25	28	.89	22	26	.89	67	50	1.33
320	145	90	1.60	45	40	1.12	27	39	.73	209	139	1.50
400	280	150	1.88	138	130	1.06	94	158	.61	891	694	1.28
500	458	257	1.77	139	126	1.10	174	194	.92	249	468	.54
630	600	560	1.07	373	434	.86	328	471	.72	272	321	.85
800	600	466	1.28	610	562	1.07	639	567	1.15	459	502	.92
1000	570	642	.89	774	803	.97	305	343	.91	488	422	1.15
1205	753	501	1.50	629	577	1.09	216	269	.82	425	422	1.01
1600	988	683	1.14	691	577	1.20	317	521	.63	522	683	.77
2000	783	767	1.02	824	722	1.14	645	643	1.02	716	633	1.13
2500	834	798	1.05	1293	1157	1.12	553	534	1.06	432	425	1.02
3200	1610	1249	1.29	1929	1622	1.19	393	428	.94	441	393	1.12
4000	2349	1655	1.41	2246	1865	1.20	423	464	.93	558	470	1.25
5000	3055	2543	1.24	1194	1021	1.17	543	851	.66	1322	1027	1.28
6300	2935	3227	.91	1592	1288	1.23	806	894	.92	866	817	1.06
8000	4335	2793	1.54	1555	1182	1.31	700	606	1.18	501	578	.87
10,000	5941	3978	1.49	842	649	1.29	391	418	.96	436	515	.85

TABLE II.A. 7.9

3 (CONTD.)

Frequency -Hz-	ACCELERATION 35X			ACCELERATION 36X			ACCELERATION 36R			ACCELERATION LR		
	Test 1	Test 2	RATIO Test 1 / Test 2	Test 1	Test 2	RATIO Tests 1/2	Test 1	Test 2	RATIO Tests 1/2	Test 1	Test 2	RATIO Tests 1/2
200	138	98	1.43	81	45	1.78	137	109	1.25	147	113	1.29
250	195	233	.85	132	51	2.54	305	212	1.43	245	163	1.50
320	195	164	1.21	144	97	1.48	286	319	.90	193	163	1.18
400	346	331	1.07	413	228	1.80	854	695	1.23	240	278	.87
500	453	300	1.54	449	182	2.45	1494	908	1.64	331	404	.82
630	594	485	1.25	449	380	1.31	927	662	1.40	620	602	1.03
800	622	526	1.21	378	296	1.28	1326	878	1.50	1039	886	1.17
1000	622	575	1.10	445	488	.91	2040	2002	1.02	1834	1676	1.09
1250	522	581	.92	854	698	1.22	1929	999	1.92	3589	3566	1.01
1600	793	861	.94	836	1022	.82	1770	940	1.87	3261	3220	1.01
2000	1270	2020	.65	1101	1654	.67	1143	1160	.99	2092	2611	.81
2500	2216	2647	.86	2285	1888	1.21	2310	1013	2.26	1517	1986	.77
3200	4851	4801	1.03	4886	3547	1.37	1485	1089	1.34	1558	1639	.95
4000	10862	9778	1.14	4124	3174	1.30	2257	2322	.97	1949	2367	.83
5000	12503	7650	1.66	3525	3682	.96	3450	3477	1.05	3611	4900	.74
6300	7400	5499	1.37	3486	3677	.95	2932	3328	.88	6232	10437	.60
8000	4626	3451	1.37	2824	3174	.89	2614	2349	1.11	15204	13865	1.09
10,000	3557	3592	1.01	2015	2509	.81	4461	1640	2.69	14251	12550	1.13

TABLE II.A.7.9

4 (CONT'D.)

Frequency -Hz-	ACCELERATION 5R			ACCELERATION 7R			ACCELERATION 8R			ACCELERATION 9R		
	Test 1	Test 2	RATIO Test 1 / Test 2	Test 1	Test 2	RATIO Tests 1/2	Test 1	Test 2	RATIO Tests 1/2	Test 1	Test 2	RATIO Tests 1/2
200	12	13	.94	10	13	.77	31	14	2.2	82	80	1.03
250	28	21	1.34	13	19	.71	49	32	1.53	114	116	.99
320	61	46	1.34	34	32	1.08	82	43	1.90	163	126	1.29
400	83	67	1.24	50	79	.64	113	132	.86	232	294	1.08
500	109	122	.90	166	146	1.13	120	181	.68	322	290	1.11
800	234	211	1.11	124	142	.88	293	221	1.32	369	431	.77
1000	180	177	1.02	365	547	.67	367	550	.67	493	541	.97
1250	243	274	.89	317	392	.81	497	319	1.55	628	398	1.57
1600	322	379	.85	639	664	.96	465	459	1.01	714	532	1.34
2000	403	370	1.09	503	437	1.15	545	614	.89	547	586	.93
2500	587	693	.85	388	507	.78	580	720	.81	639	553	1.15
3200	624	481	1.30	413	330	1.25	445	416	1.07	675	471	1.43
4000	563	551	1.02	577	435	1.32	784	668	1.17	596	580	1.03
5000	605	593	1.02	820	805	1.02	985	608	1.61	759	681	1.11
6300	523	176	3.01	699	428	1.63	724	429	1.68	982	986	1.00
8000	515	599	.86	550	393	1.46	412	331	1.24	814	781	1.04
10,000	399	681	.59	480	339	1.24	335	272	1.23	791	647	1.22

TABLE II.A.7.9

(CONT'D.)

Frequency - Hz -	ACCELERATION 10R			ACCELERATION 12R		
	Test 1	Test 2	RATIO Tests 1/2	Test 1	Test 2	RATIO Tests 1/2
200	35	15	2.34	11	13	.83
250	54	22	2.39	12	18	.67
320	880	42	1.90	17	16	1.01
400	134	119	1.34	27	26	1.02
500	147	86	1.71	37	22	1.65
630	125	134	.94	61	26	2.28
800	245	565	.44	54	56	.97
1000	441	294	1.49	147	191	.77
1250	428	468	.92	102	504	.20
1600	547	635	.86	175	254	.69
2000	462	440	.92	419	306	1.36
2500	859	672	1.27	377	255	1.47
3200	577	734	.79	427	344	1.23
4000	572	549	1.04	702	656	1.07
5000	741	632	1.17	746	623	1.20
6300	949	624	1.51	535	307	1.73
8000	762	580	1.31	606	616	.98
10000	397	248	1.59	481	278	1.72

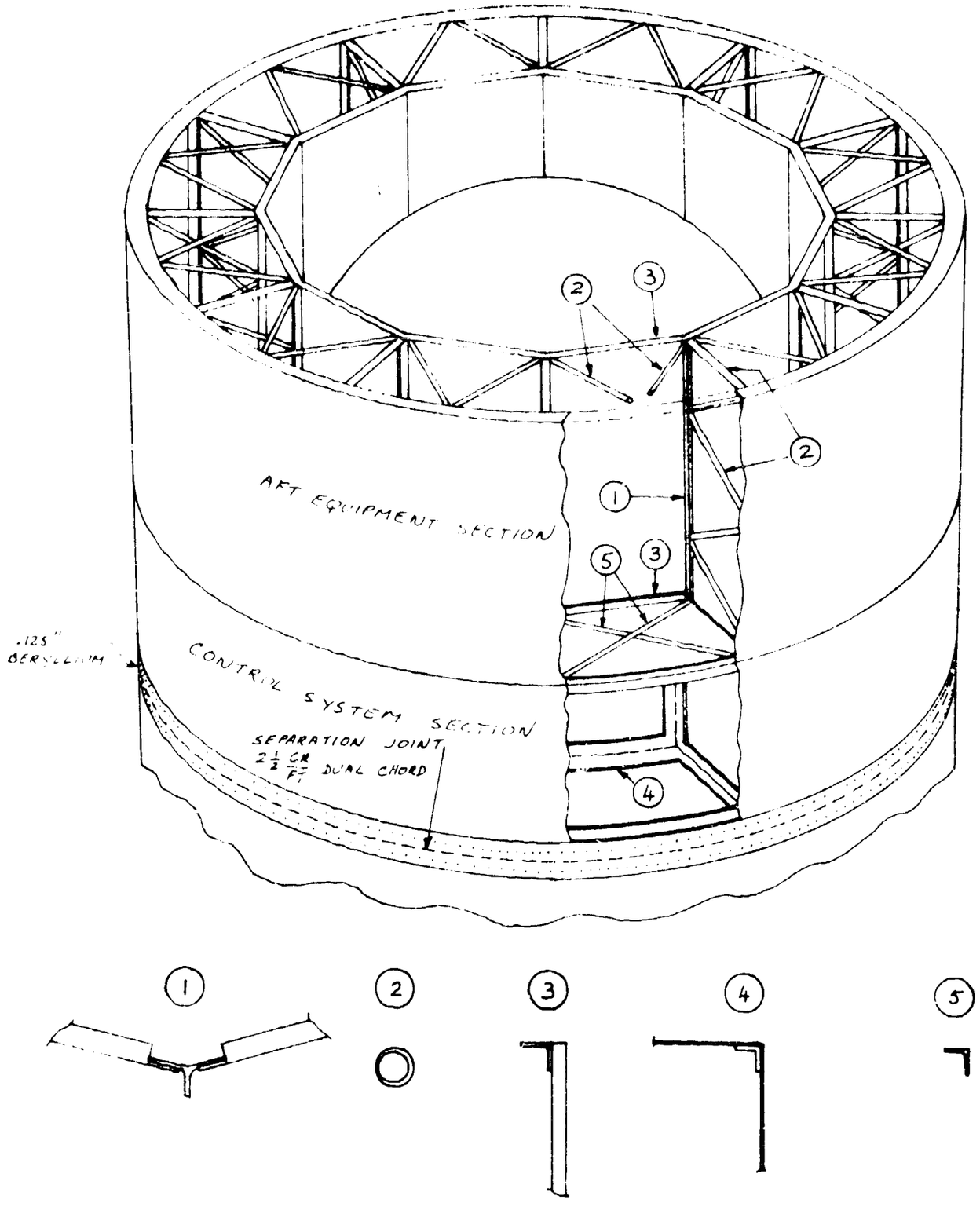

Figure II.A.7.1 TEST SPECIMEN

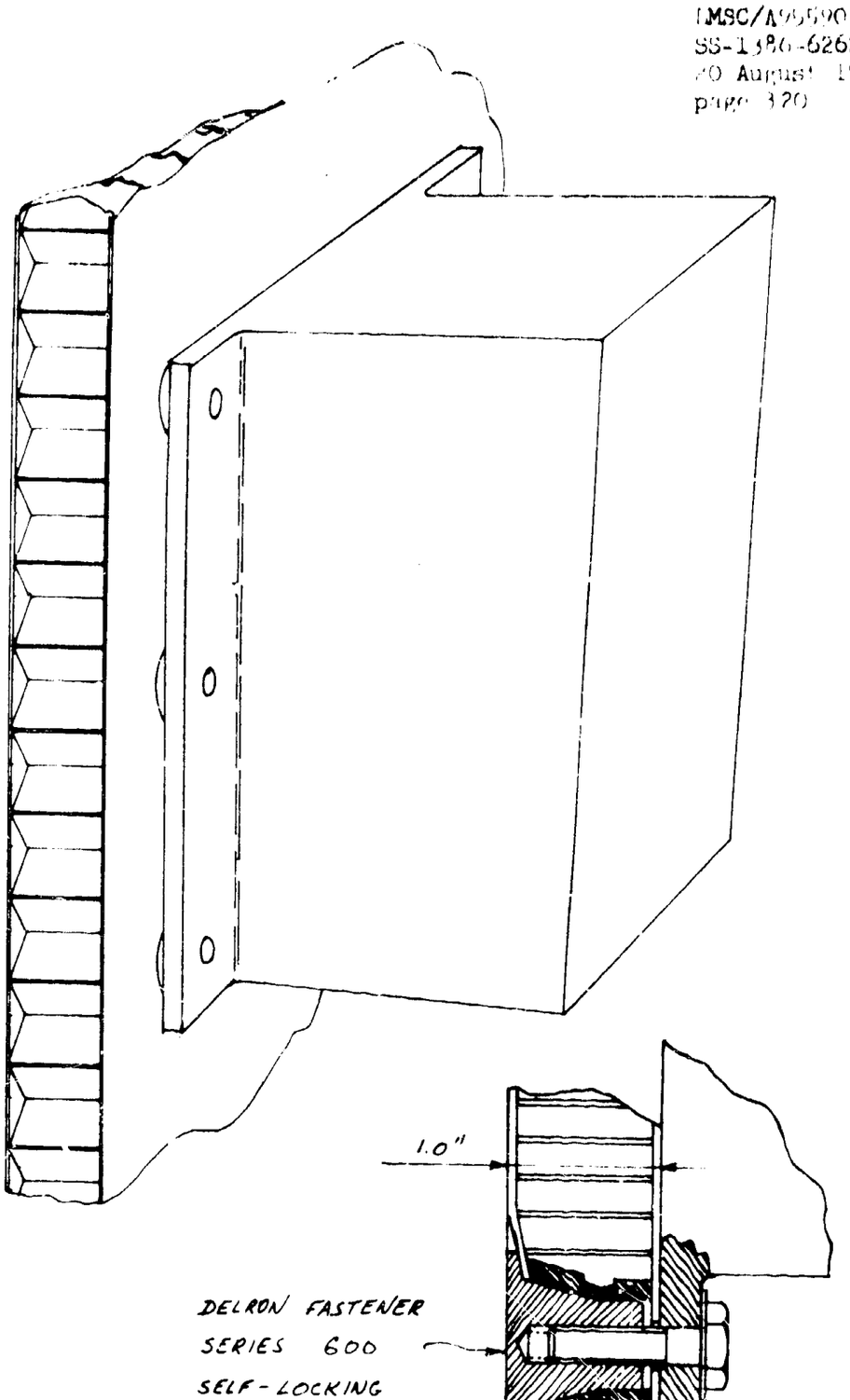

Figure II.A.7.2 TYPICAL EQUIPMENT INSTALLATION

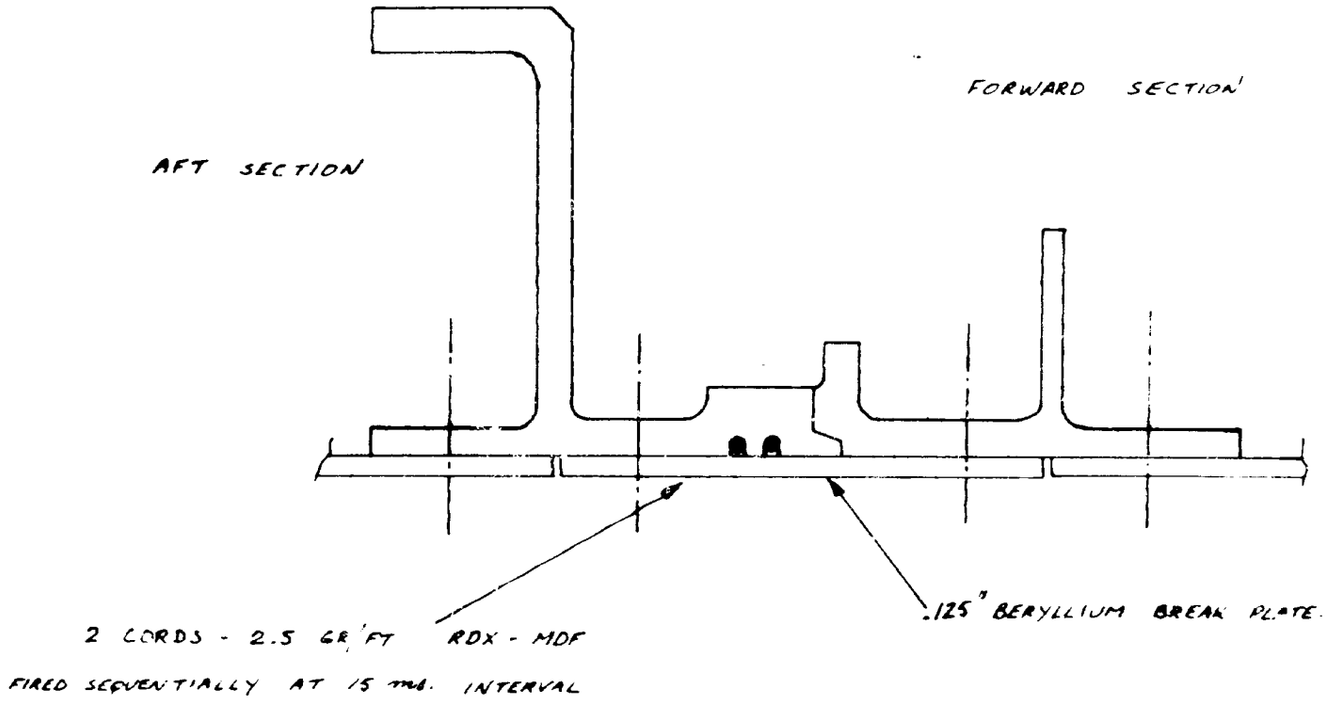

Figure II.A.7.3 SEPARATION JOINT DETAIL

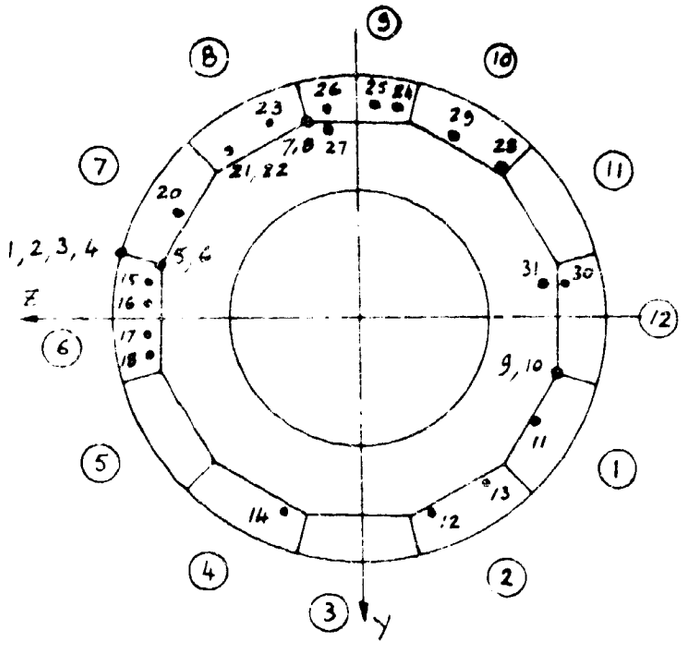

ACCELEROMETERS

#	L	R	T
1	•	○	•
2	•	•	
3	•	•	
4	•	○	○
5	○	•	
6	•	○	
7	•	•	
8	○	•	
9	•	•	
10	○	•	
11		•	
12		•	
13	○	•	
14		•	
15		•	
16		•	
17		•	
18	○	•	
19		•	
20	•	•	
21	•		
22	•	•	
23		•	
24		•	
25	•	•	
26	•		
27		•	
28	•		
29		•	
30		•	
31		•	
32		•	
33	•	•	
34	•	•	○

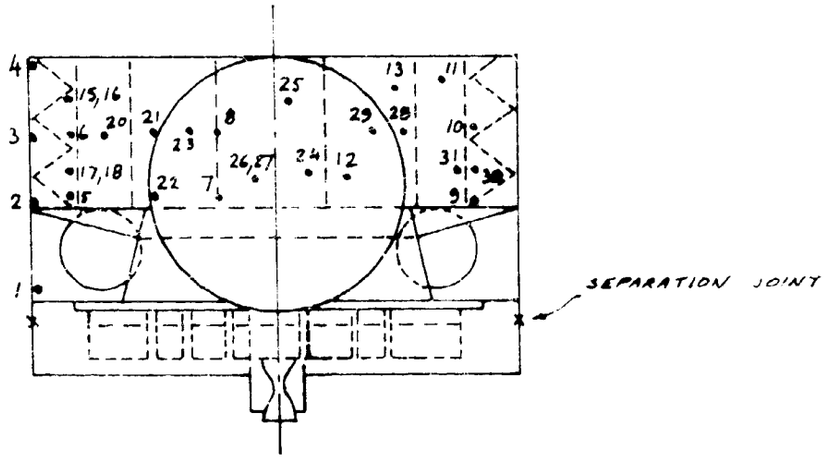

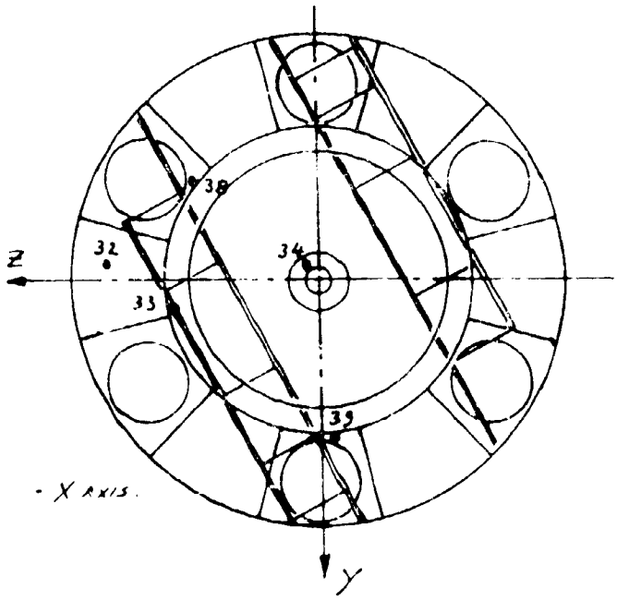

L . LONGITUDINAL - X AXIS.

R . RADIAL

T . TANGENTIAL

Figure II.A.7.4. INSTRUMENTATION LOCATIONS

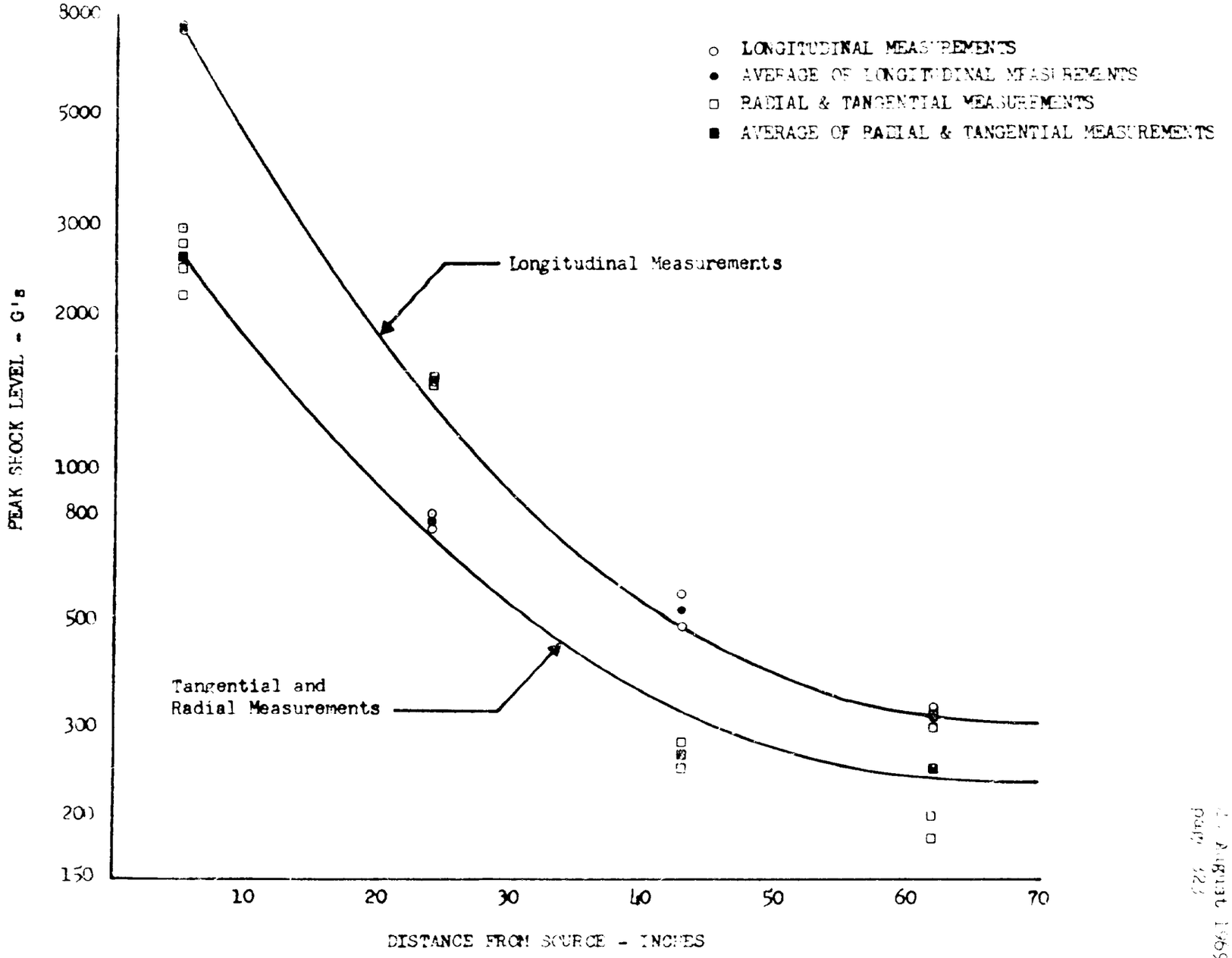

Figure II.A.7.5 PEAK G SHOCK LEVEL VERSUS DISTANCE FROM SOURCE

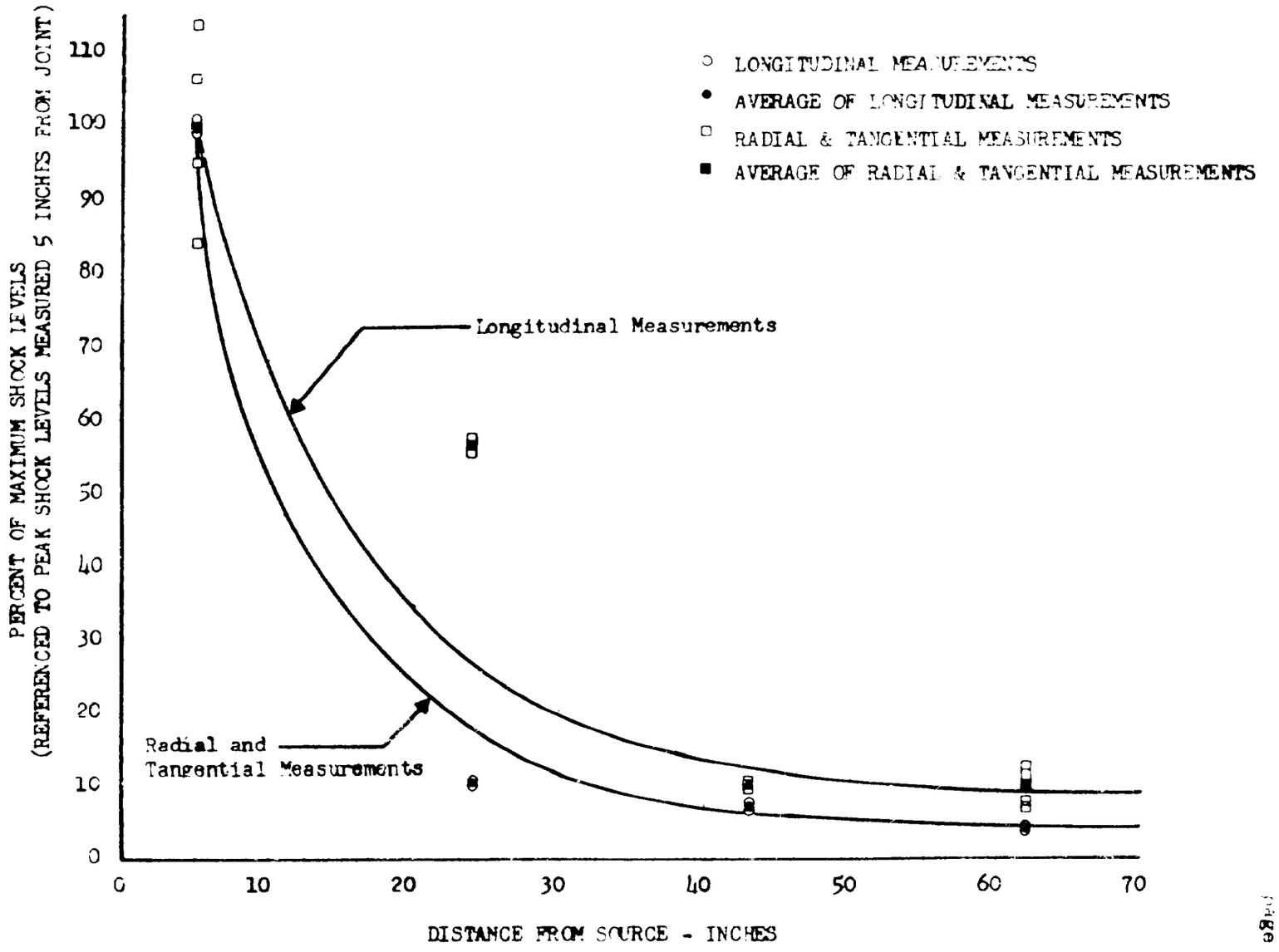

Figure II.A.7.6 PEAK G SHOCK ATTENUATION VERSUS DISTANCE FROM THE SOURCE

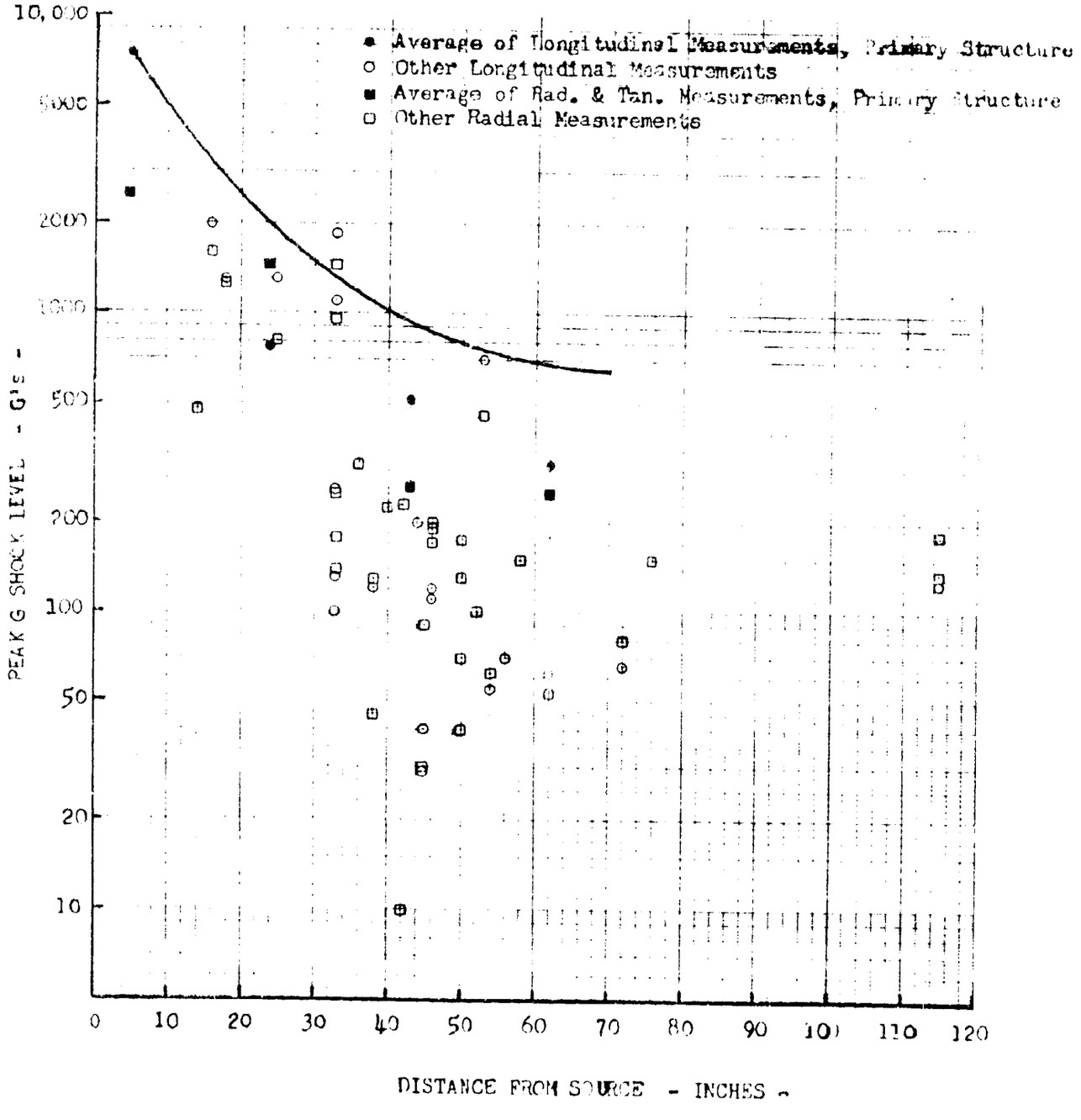

Figure II.A.7.7 TEST OF APPLICATION OF SHOCK ATTENUATION - DISTANCE METHOD IN PREDICTING PEAK G LEVEL AT ANY LOCATION

RESPONSE G's

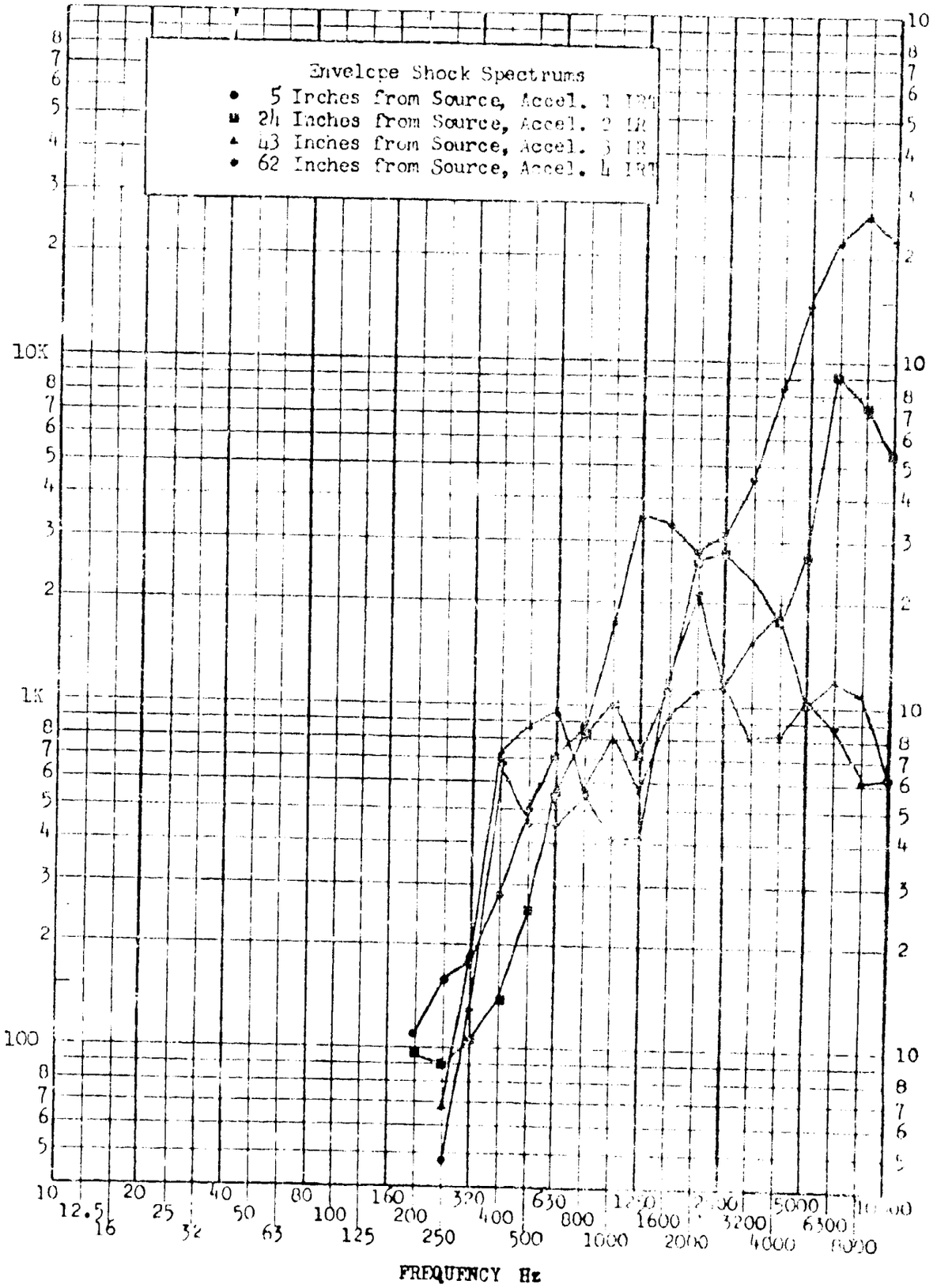

Figure II.A.7.8 PRIMARY STRUCTURE ENVELOPE SHOCK SPECTRUMS

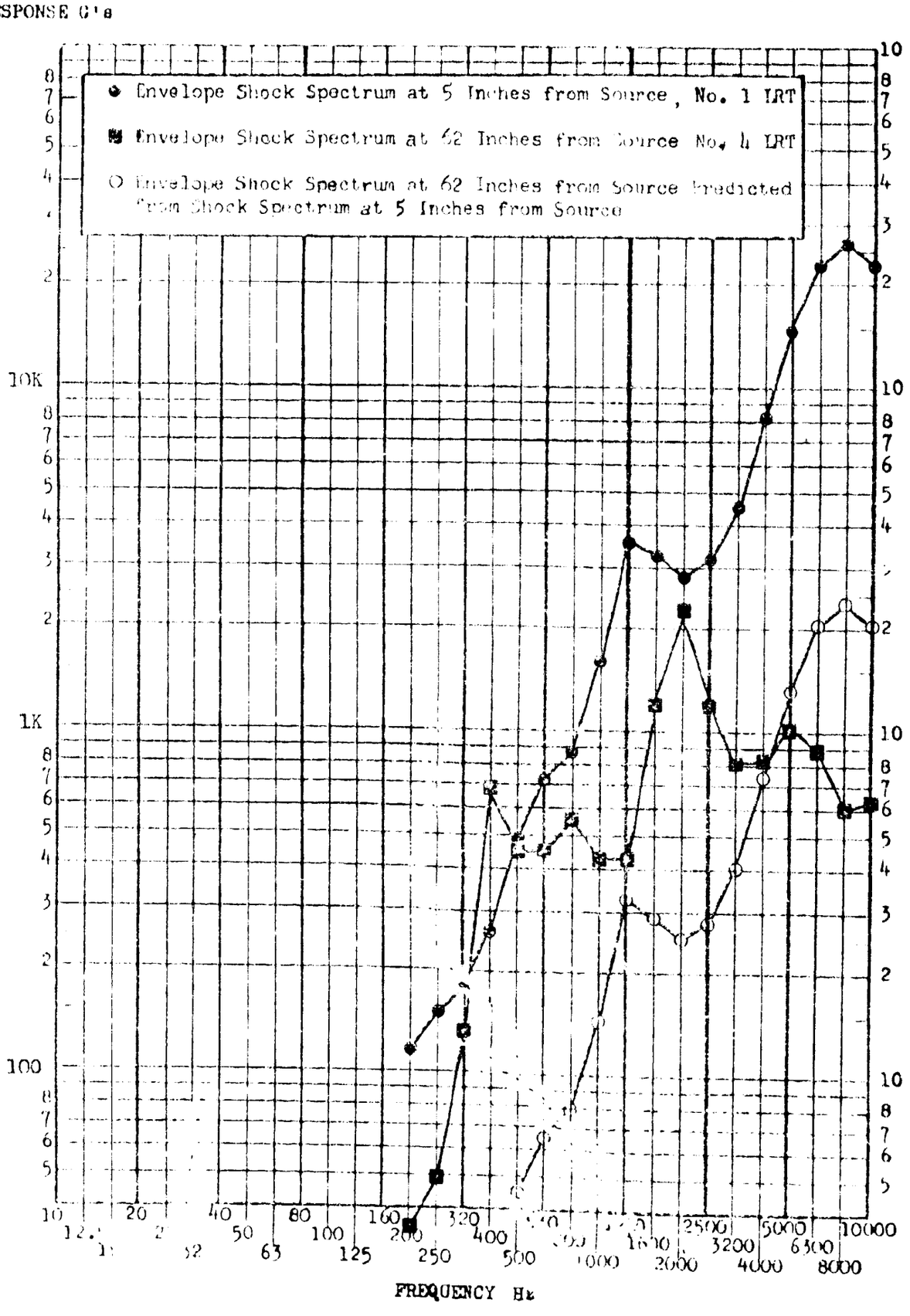

Figure II.A.7.9. ILLUSTRATION OF ATTEMPT TO PREDICT SHOCK SPECTRUM BY PEAK G ATTENUATION-DISTANCE METHOD

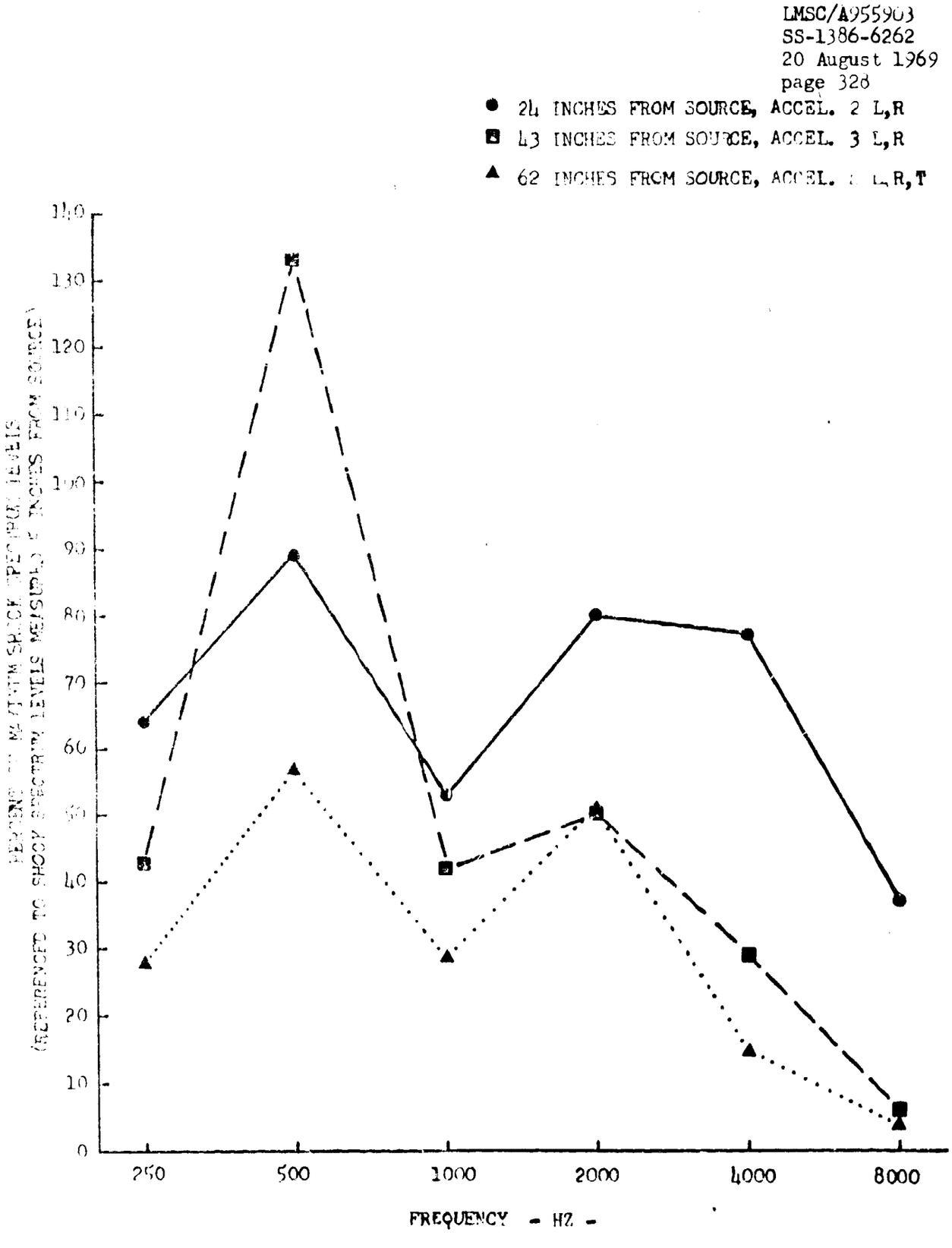

Figure II.A.7.10 ATTENUATION VERSUS FREQUENCY ALONG PRIMARY STRUCTURE

Shock Spectrum Desired = $\frac{\text{Correction Factor at Q of Desired Spectrum}}{\text{Correction Factor at Q of Given Spectrum}} \times \text{Given Spectrum}$

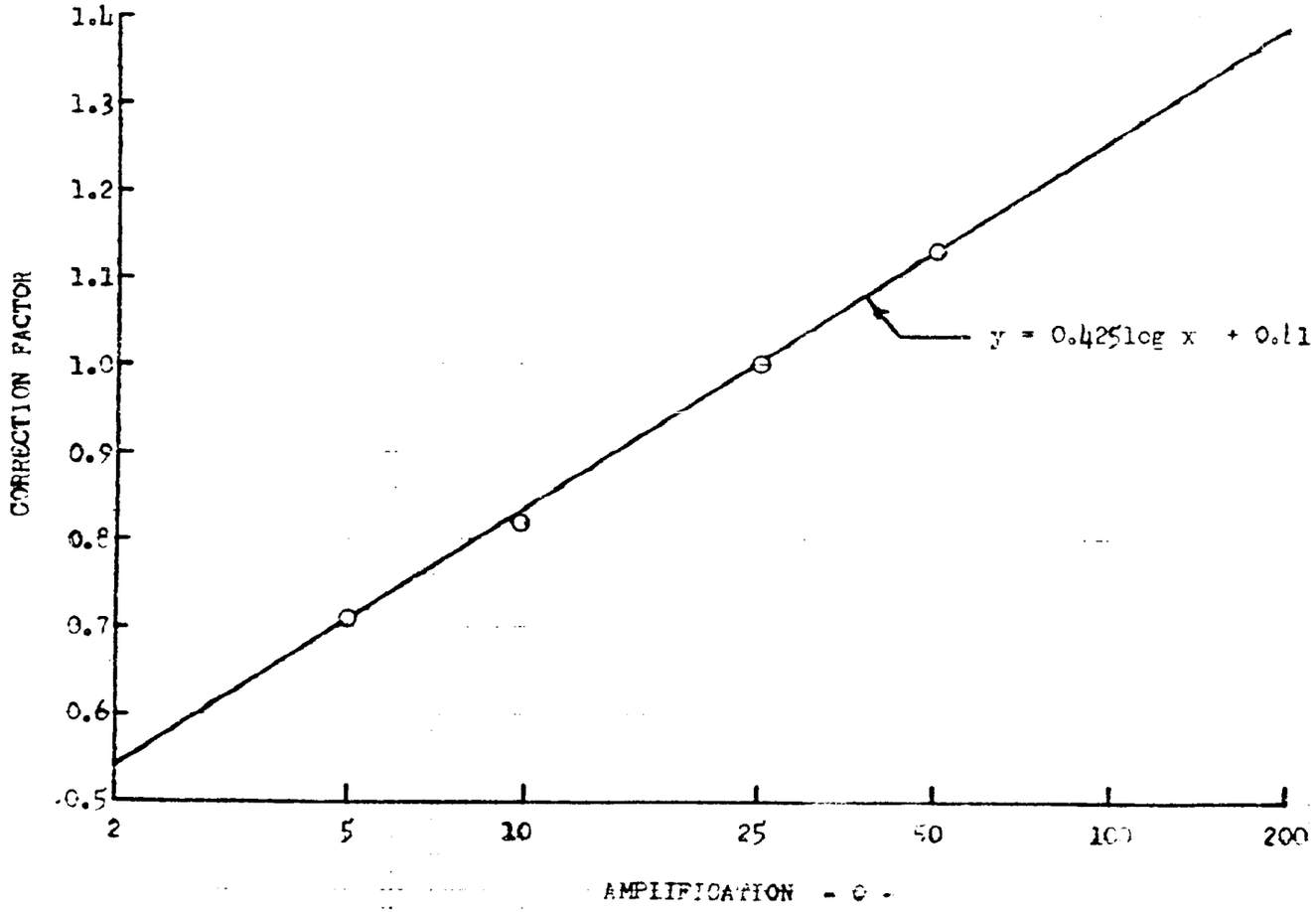

Figure II.A.7.11 RELATIONSHIP BETWEEN SHOCK SPECTRUM OF DIFFERENT Q VALUES

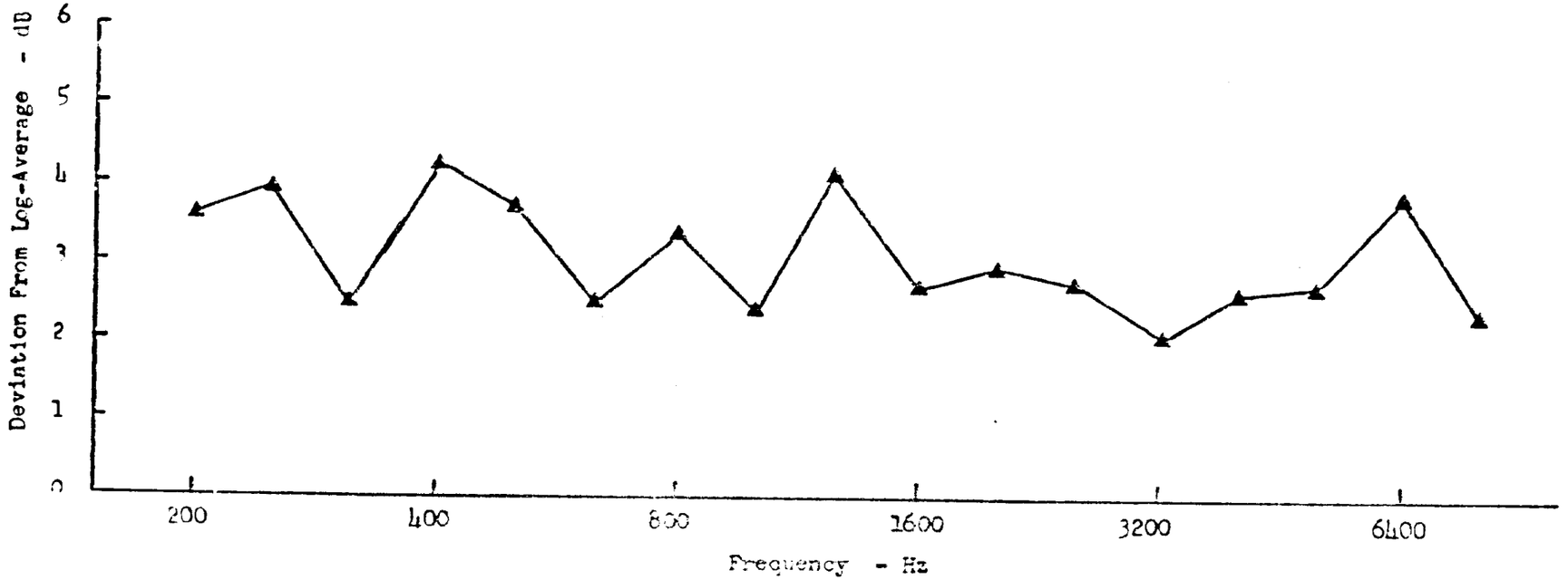

Figure II.A.7.12 STANDARD DEVIATION EXPRESSED AS dB FOR 2 TESTS, 22 LOCATIONS

SHOCK TEST ANALYSIS DATA SHEET NO. II.A.7.13

TEST ITEM 1377-433
SERIAL NO.
SHOCK AXIS LONGITUDINAL

PART NO. STRUCTURE
TEST DATE 11 FEB 1269
SHOCK NO. 1

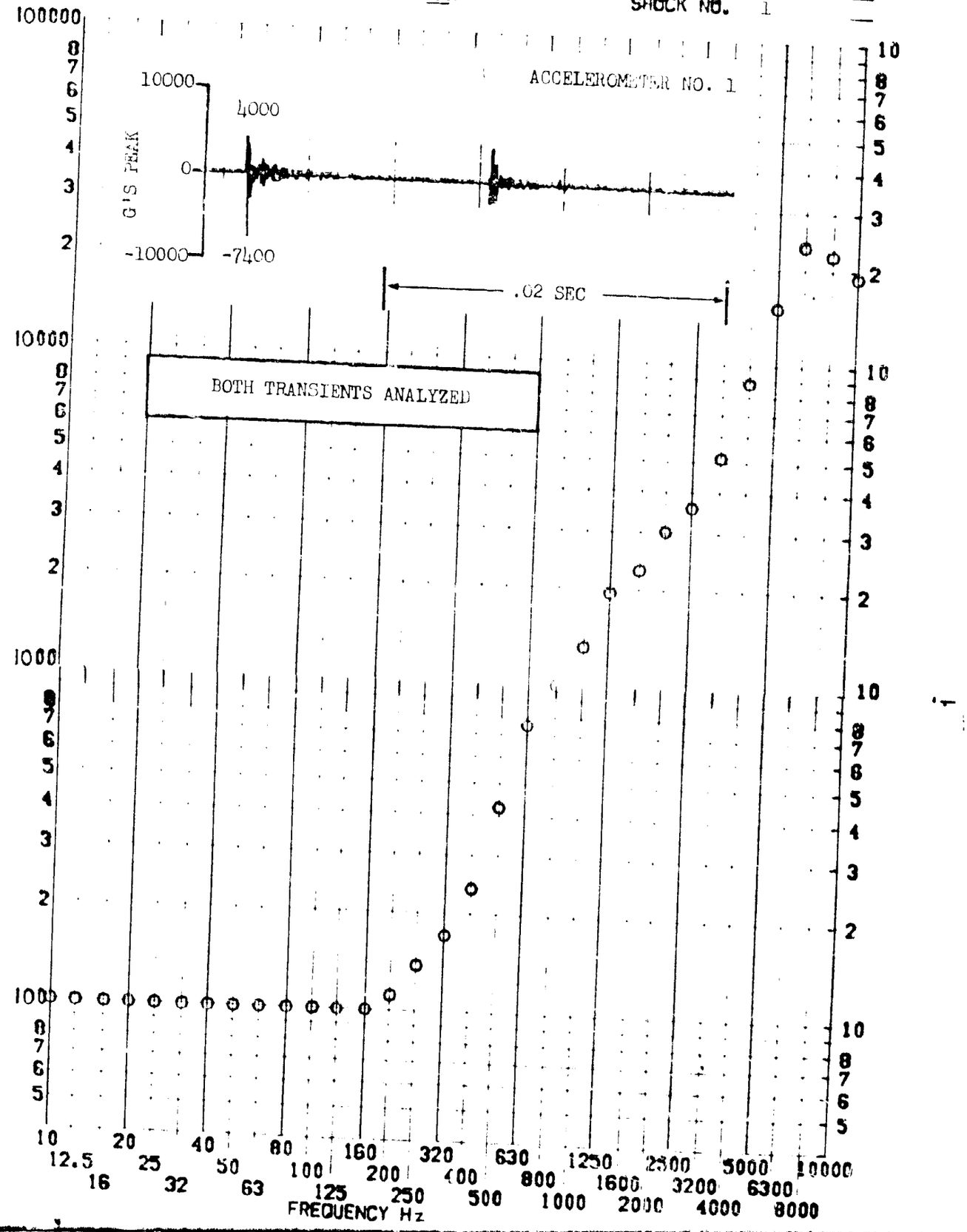

SHOCK TEST ANALYSIS DATA SHEET NO. II.A.7.14

TEST ITEM 1377-434
SERIAL NO.
SHOCK AXIS LONGITUDINAL

PART NO. STRUCTURE
TEST DATE 11 FEB 1969
SHOCK NO. 1

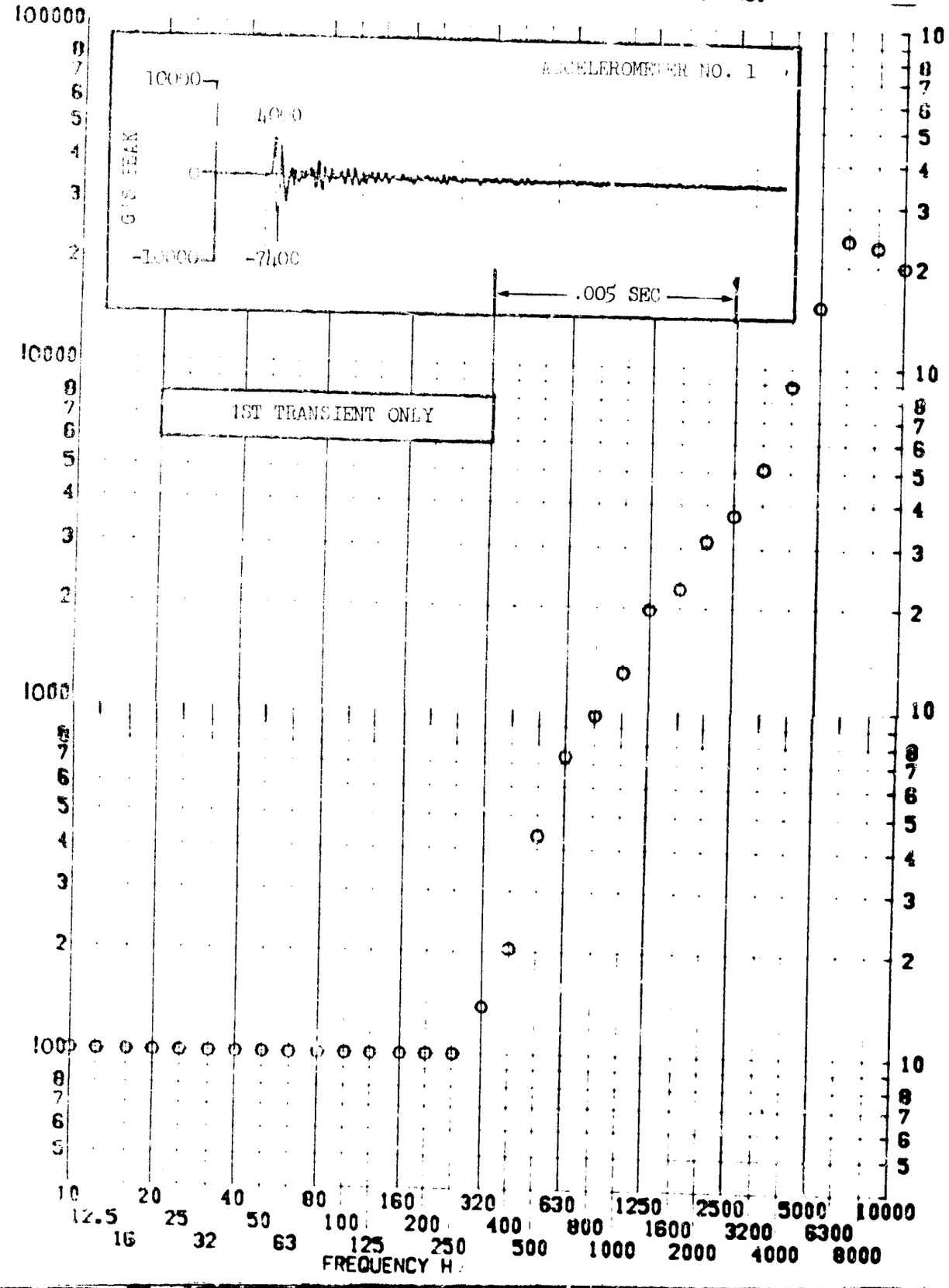

SHOCK TEST ANALYSIS DATA SHEET NO. II.A.7.15

TEST ITEM 1377-460
SERIAL NO.
SHOCK AXIS LONGITUDINAL

PART NO. STRUCTURE
TEST DATE 11 FEB 1969
SHOCK NO. 2

RESPONSE G-S

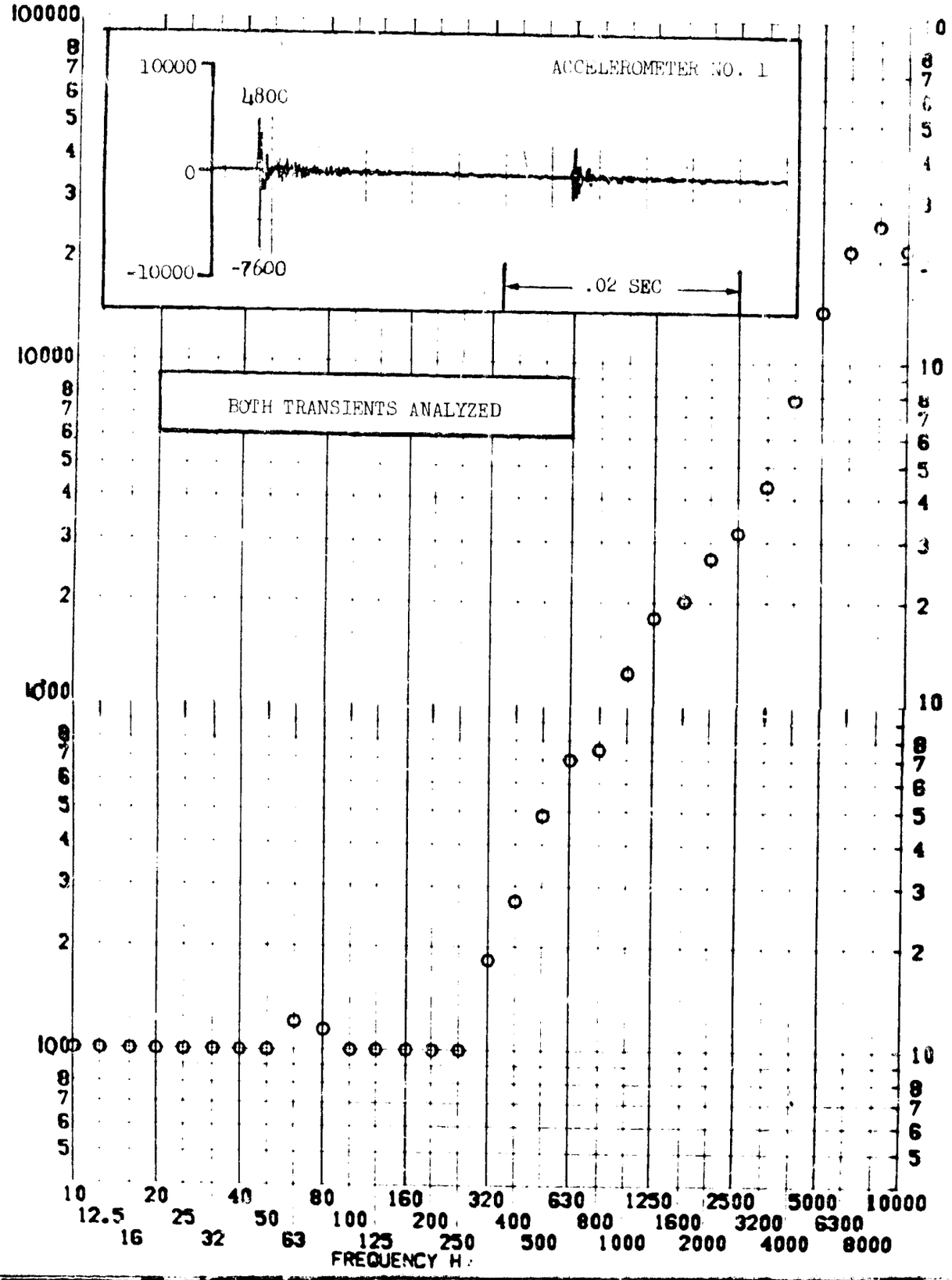

SHOCK TEST ANALYSIS DATA SHEET NO. II.A.7.16

TEST ITEM 1377-433,434,460
SERIAL NO.
SHOCK AXIS LONGITUDINAL

PART NO. STRUCTURE
TEST DATE [illegible]
SHOCK NO. 1 & 2

RESPONSE G-S

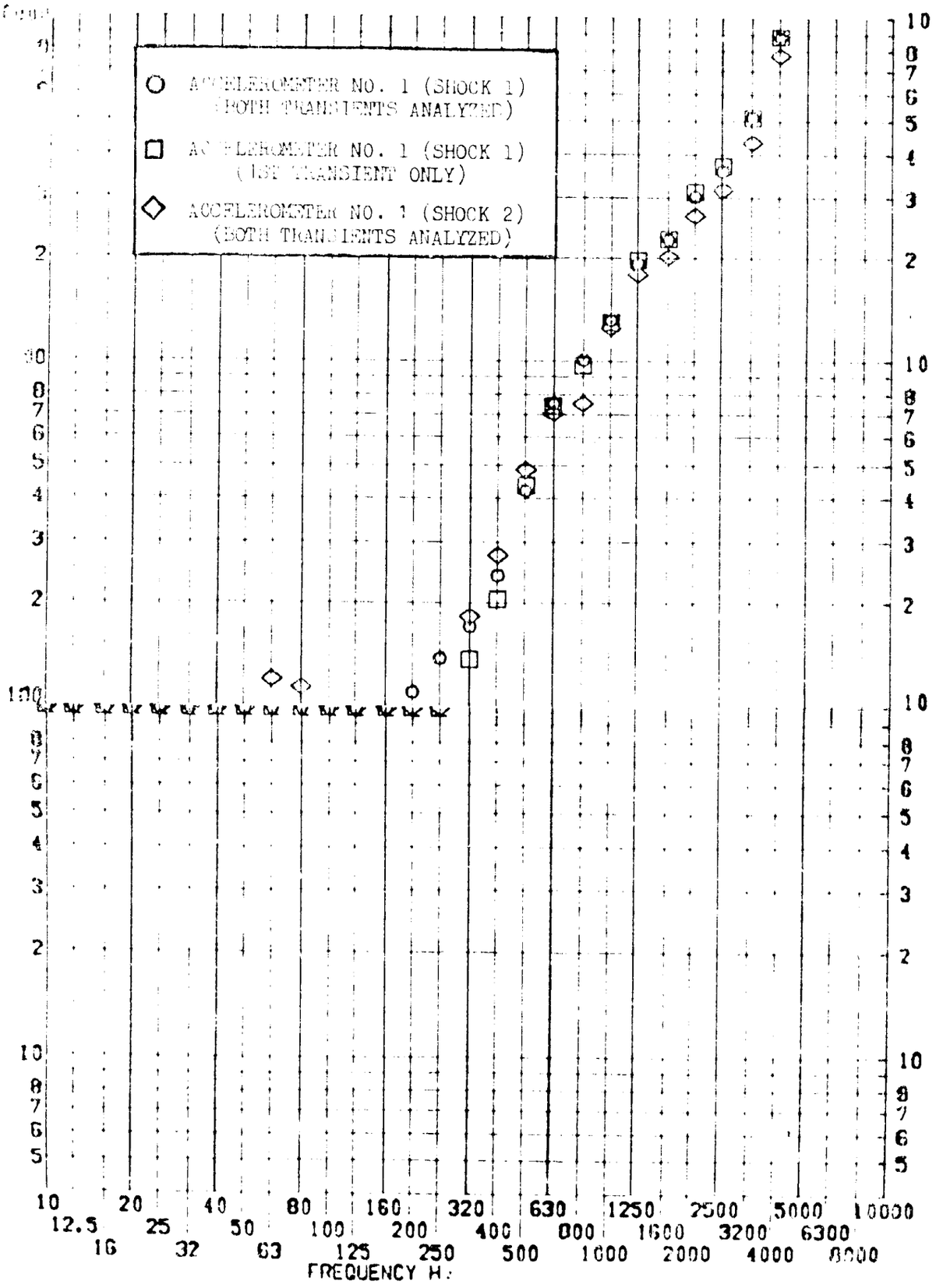

SHOCK TEST ANALYSIS DATA SHEET NO. II.A.7.17

TEST ITEM 1377-435
SERIAL NO.
SHOCK AXIS RADIAL

PART NO. STRUCTURE
TEST DATE 11 FEB 1969
SHOCK NO. 1

RESPONSE G-S

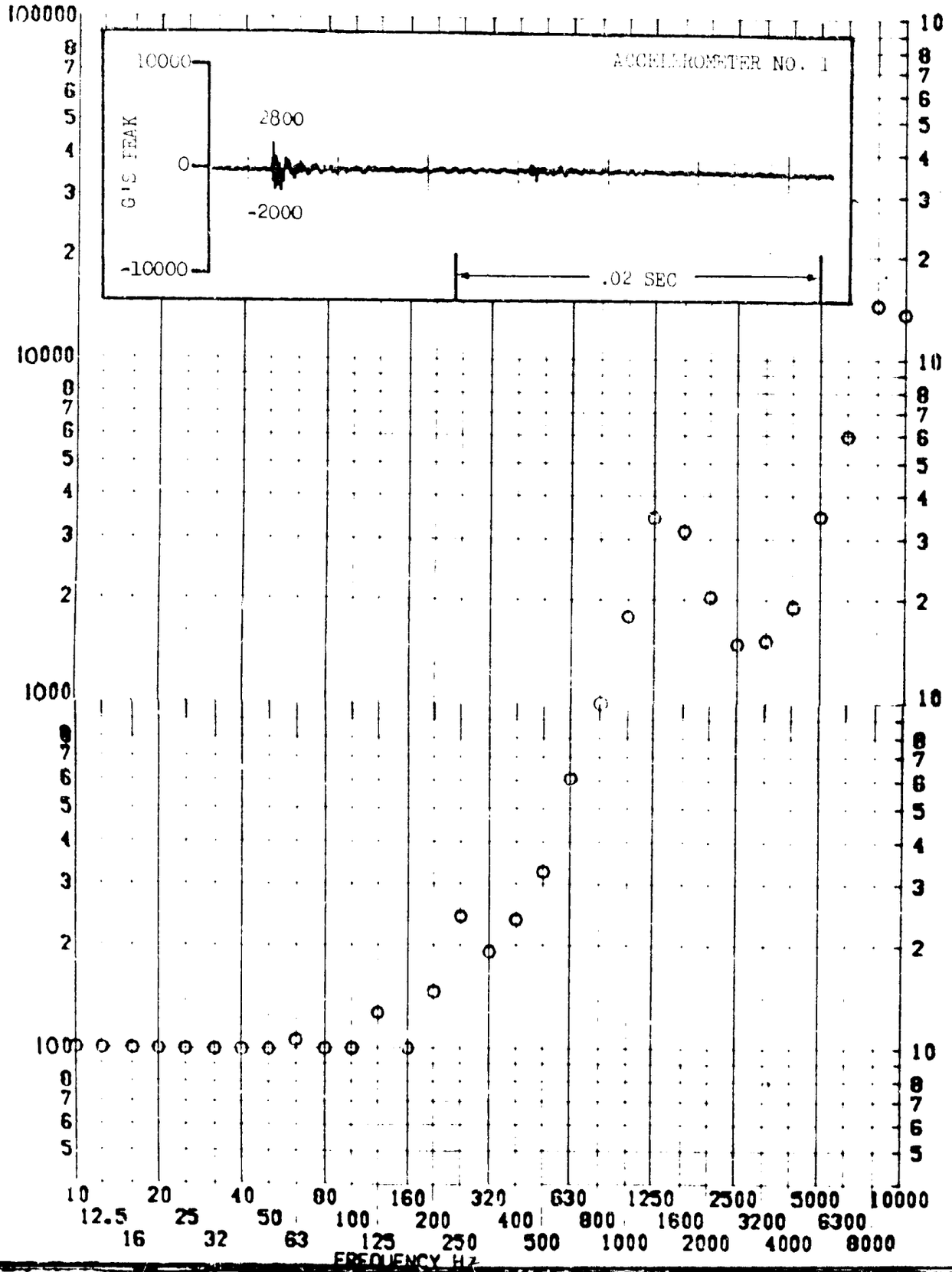

SHOCK TEST ANALYSIS DATA SHEET NO. II.A.7.18

TEST ITEM 1377-461
SERIAL NO.
SHOCK AXIS RADIAL

PART NO. STRUCTURE
TEST DATE 11 FEB 1969
SHOCK NO. 2

RESPONSE G-S

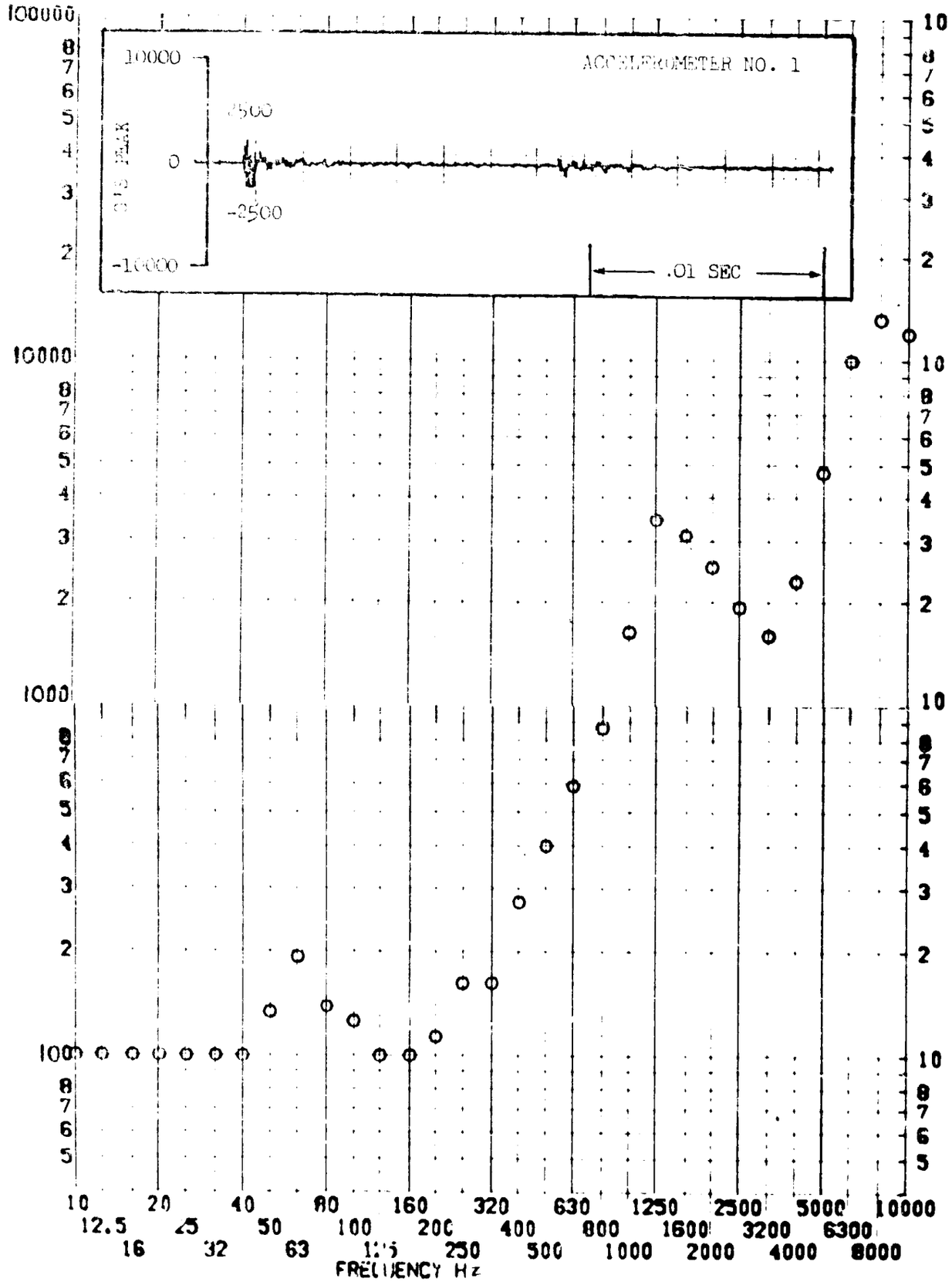

SHOCK TEST ANALYSIS DATA SHEET NO. II.A.7.19

TEST ITEM 1377-435,461 PART NO. STRUCTURE
SERIAL NO. TEST DATE 11 FEB 1969
SHOCK AXIS RADIAL SHOCK NO. 1 & 2

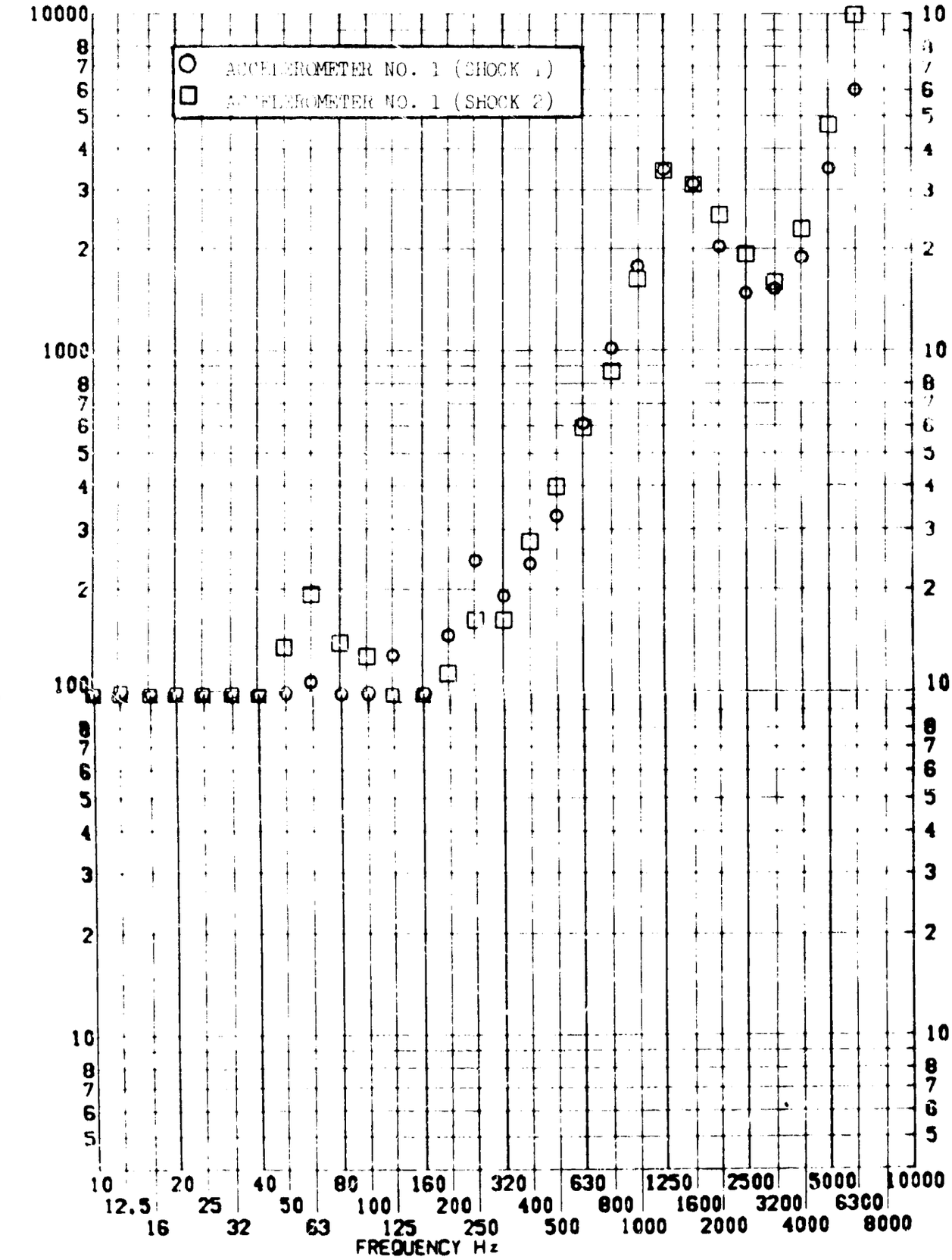

SHOCK TEST ANALYSIS DATA SHEET NO. II.A.7.20

TEST ITEM 1377-436
SERIAL NO.
SHOCK AXIS TANGENTIAL

PART NO. STRUCTURE
TEST DATE 11 FEB 1969
SHOCK NO. 1

RESPONSE G-S

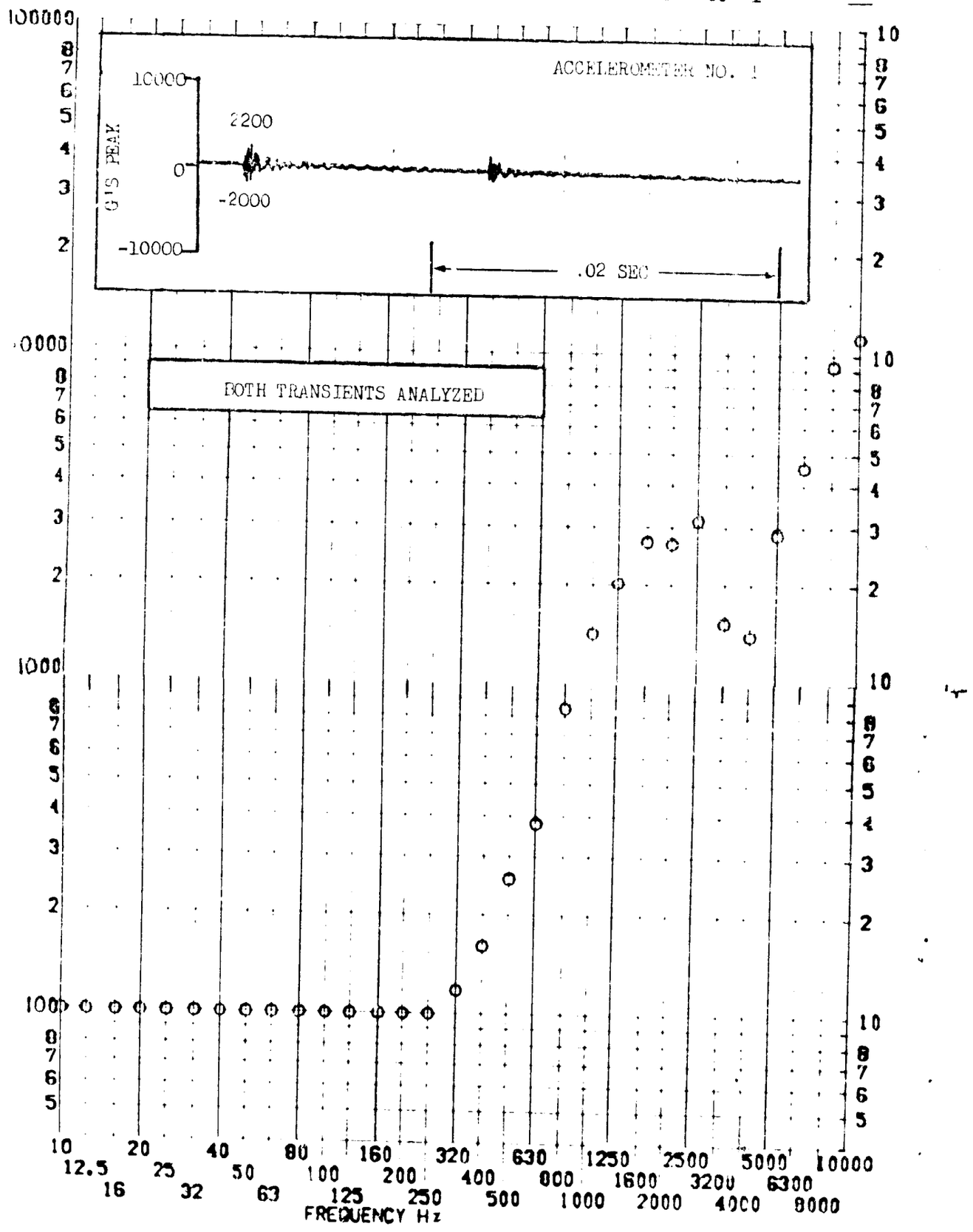

SHOCK TEST ANALYSIS DATA SHEET NO. II.A.7.21

TEST ITEM 1377-437
SERIAL NO.
SHOCK AXIS TANGENTIAL
PART NO. STRUCTURE
TEST DATE 11 FEB 1969
SHOCK NO. 1

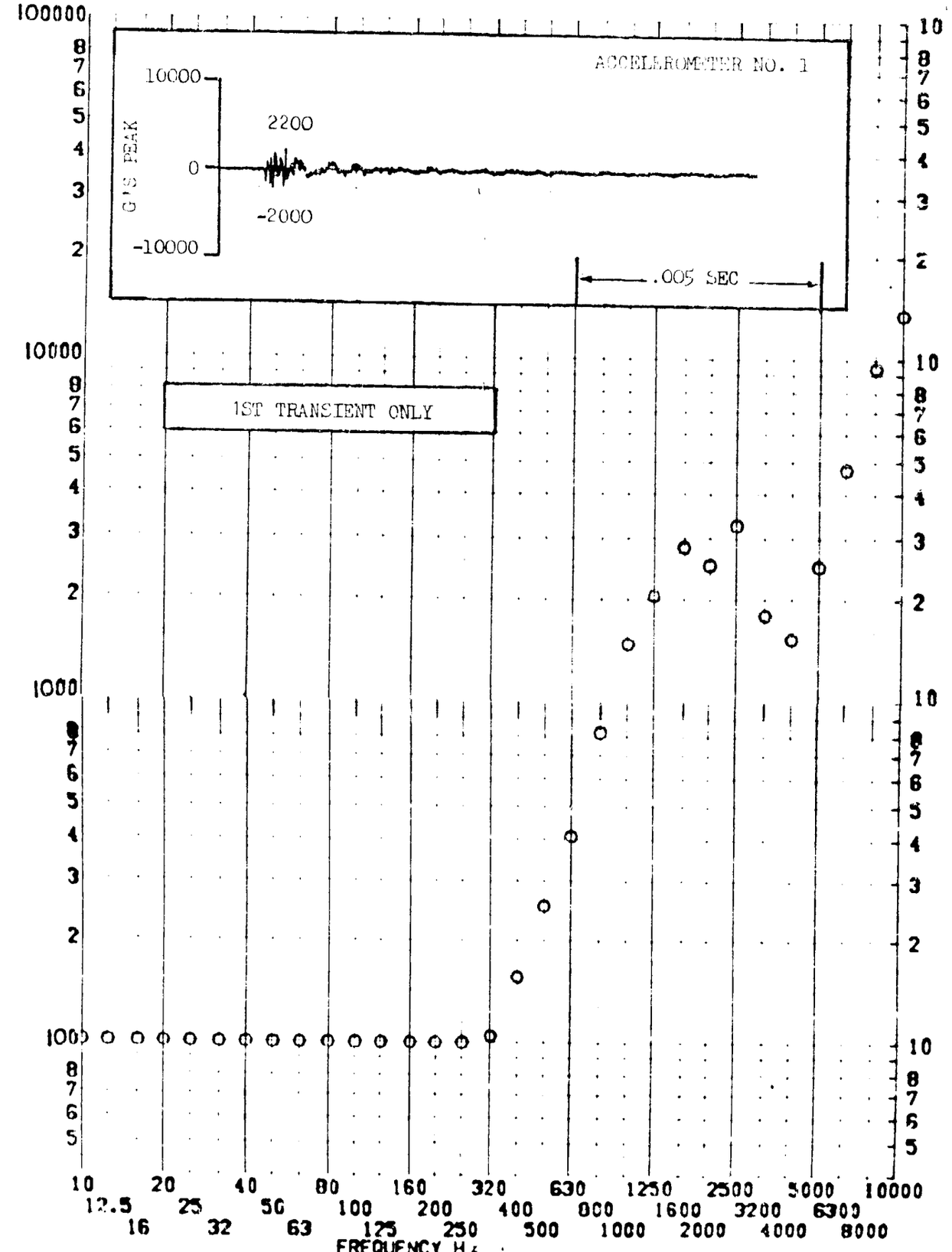

LMSC/A[illegible] 69-1356-6262 2 Aug[illegible] 1969

SHOCK TEST ANALYSIS DATA SHEET NO. II.A.[illegible].23

TEST ITEM 1377-402
SERIAL NO.
SHOCK AXIS [illegible]

PART NO. STRUCTURE
TEST DATE [illegible]
SHOCK NO. 2

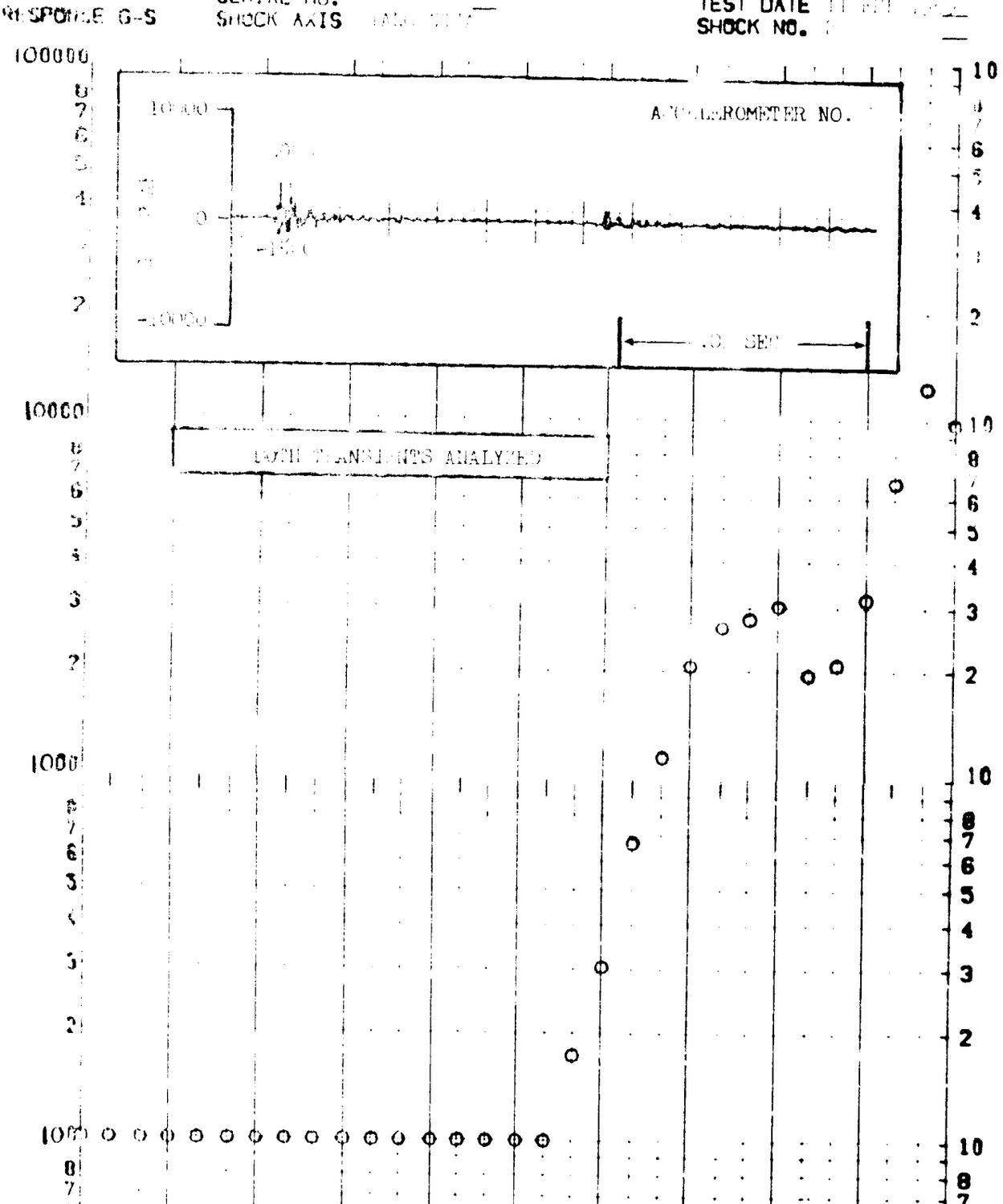

SHOCK TEST ANALYSIS DATA SHEET NO. 11.A.1.1

TEST ITEM 1377-436,437,462 PART NO. STRUCTURE

SERIAL NO. TEST DATE 11 FEB 1969

SHOCK AXIS TANGENTIAL SHOCK NO. 1 & 2

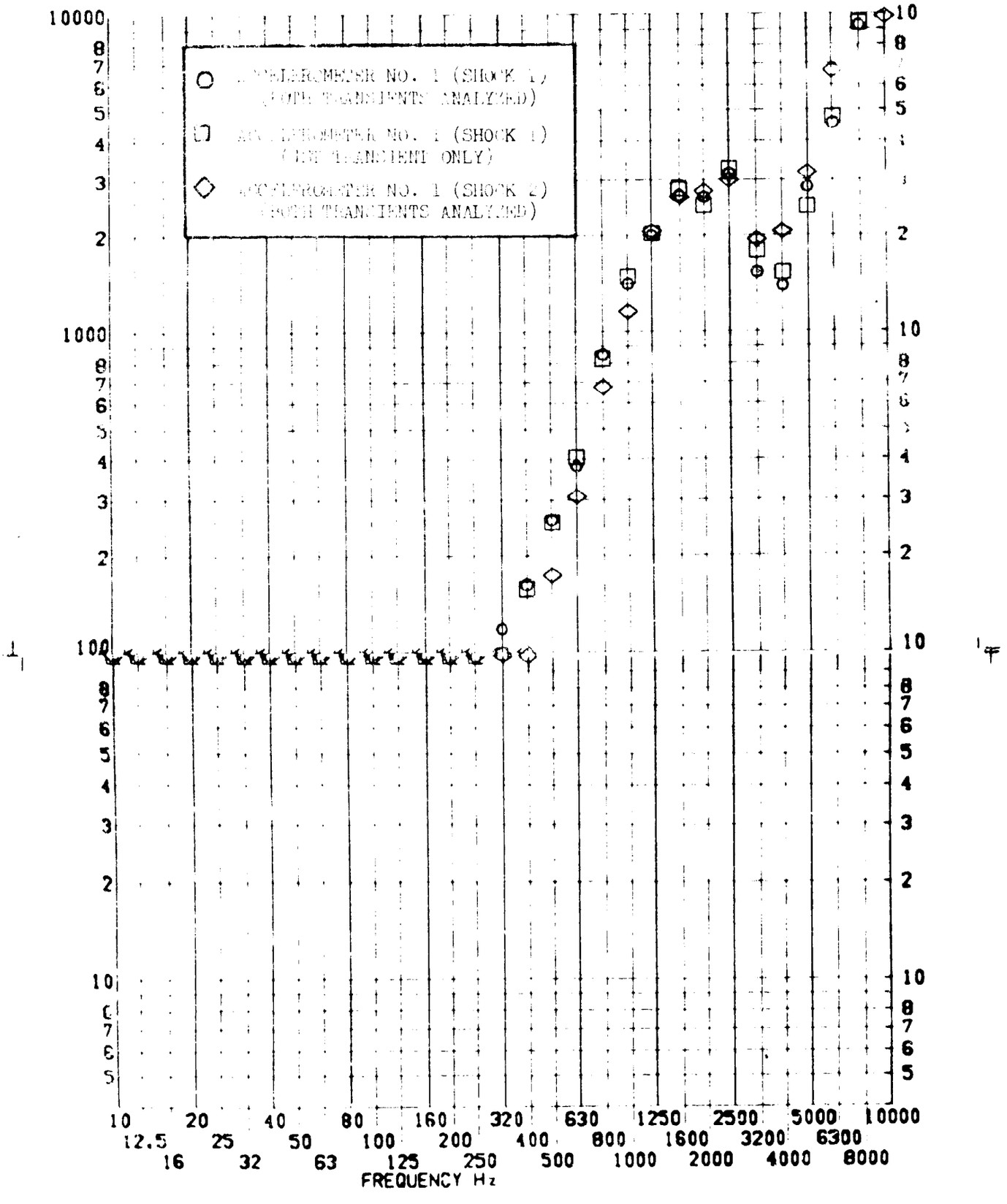

SHOCK TEST ANALYSIS DATA SHEET NO. II.A.7.24

TEST ITEM 1377-433
SERIAL NO.
SHOCK AXIS LONGITUDINAL

PART NO. STRUCTURE
TEST DATE 11 FEB 1962
SHOCK NO. 1

RESPONSE G-S

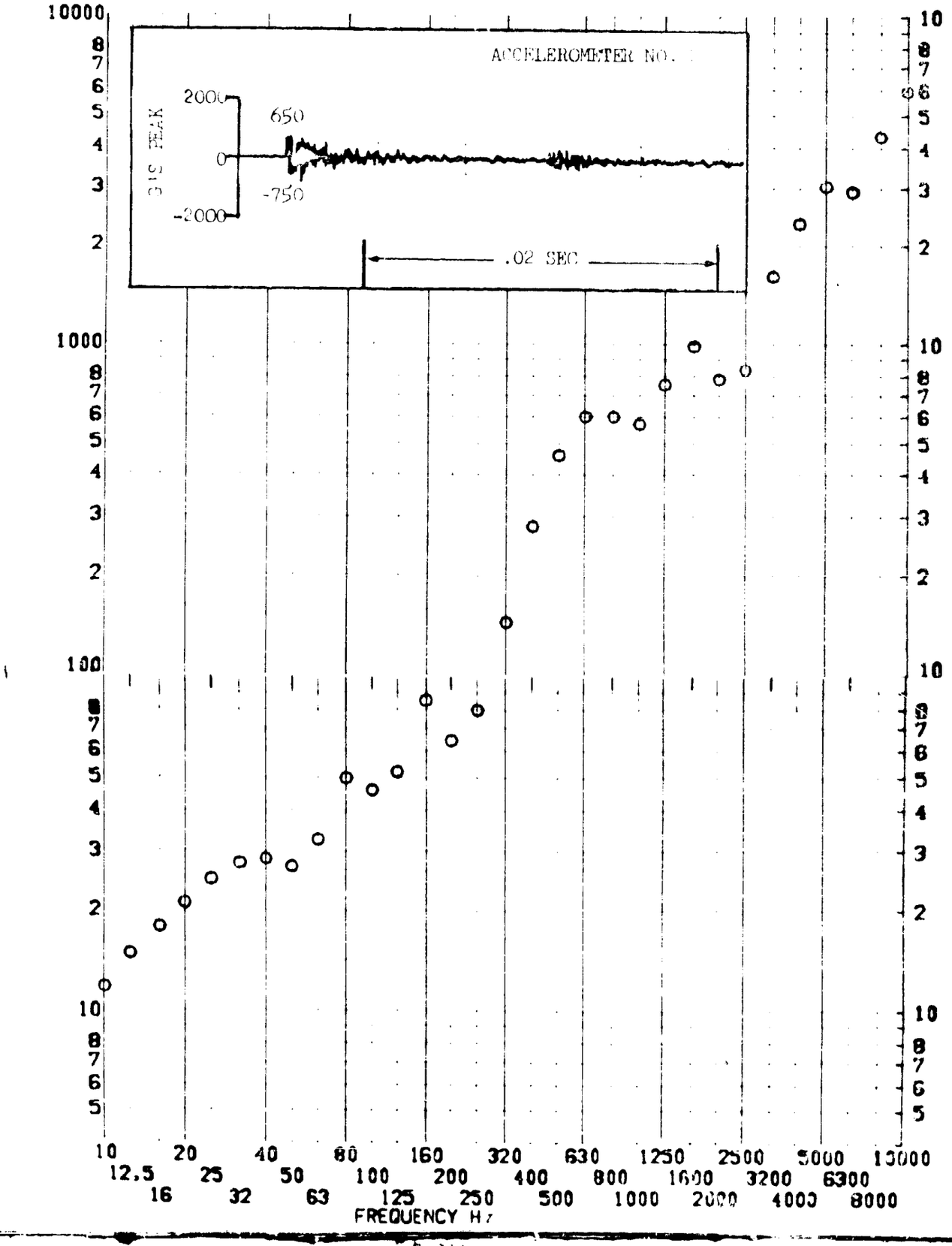

SHOCK TEST ANALYSIS DATA SHEET NO. II.A.7.25

TEST ITEM 1377-463
SERIAL NO.
SHOCK AXIS LONGITUDINAL

PART NO. STRUCTURE
TEST DATE 11 FEB 1969
SHOCK NO. 2

RESPONSE G-S

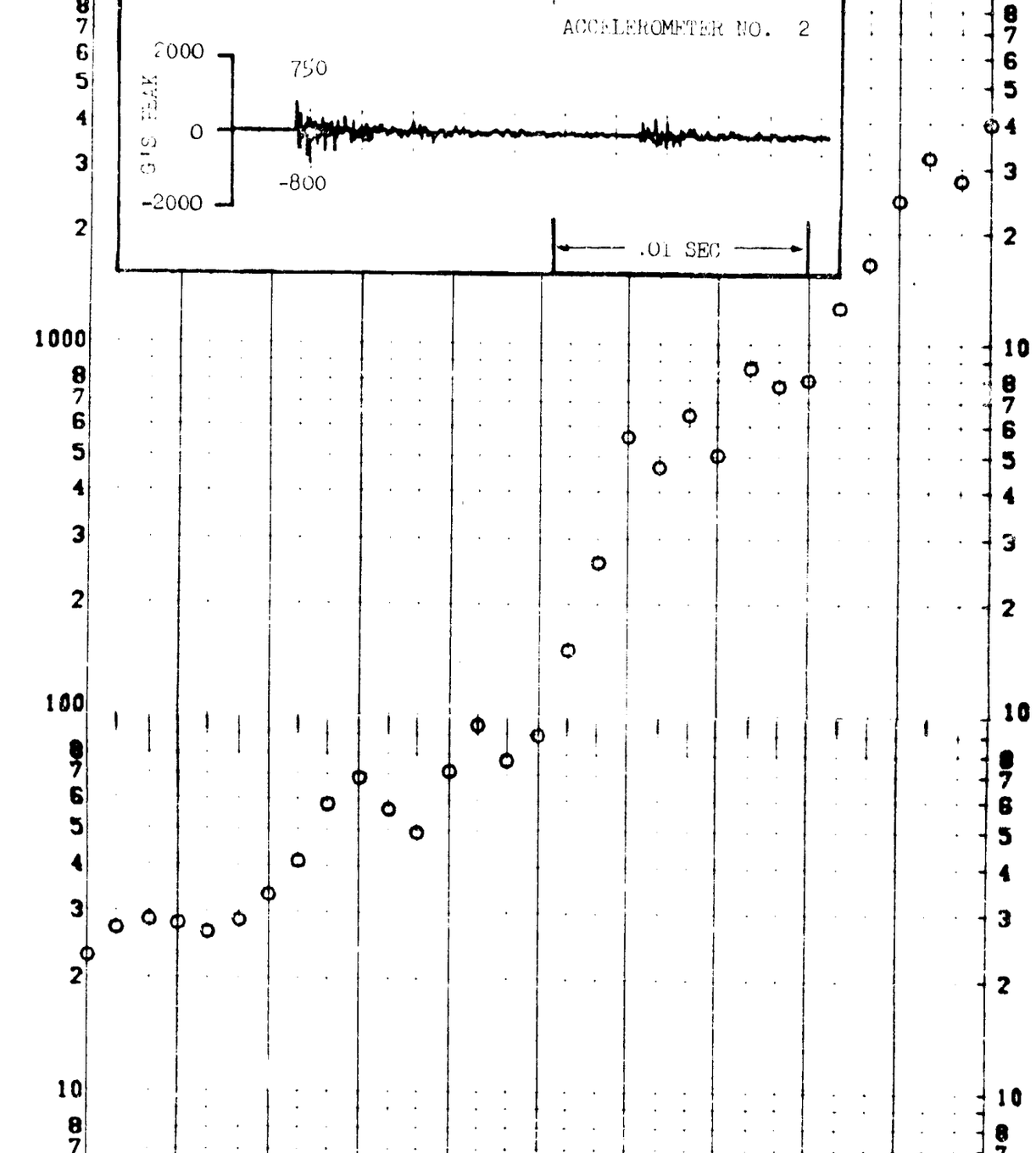

SHOCK TEST ANALYSIS DATA SHEET NO. II.A.7.26

TEST ITEM 1377-436,463 PART NO. STRUCTURE
SERIAL NO. TEST DATE 11 FEB 1969
SHOCK AXIS [illegible] SHOCK NO. 1 & 2

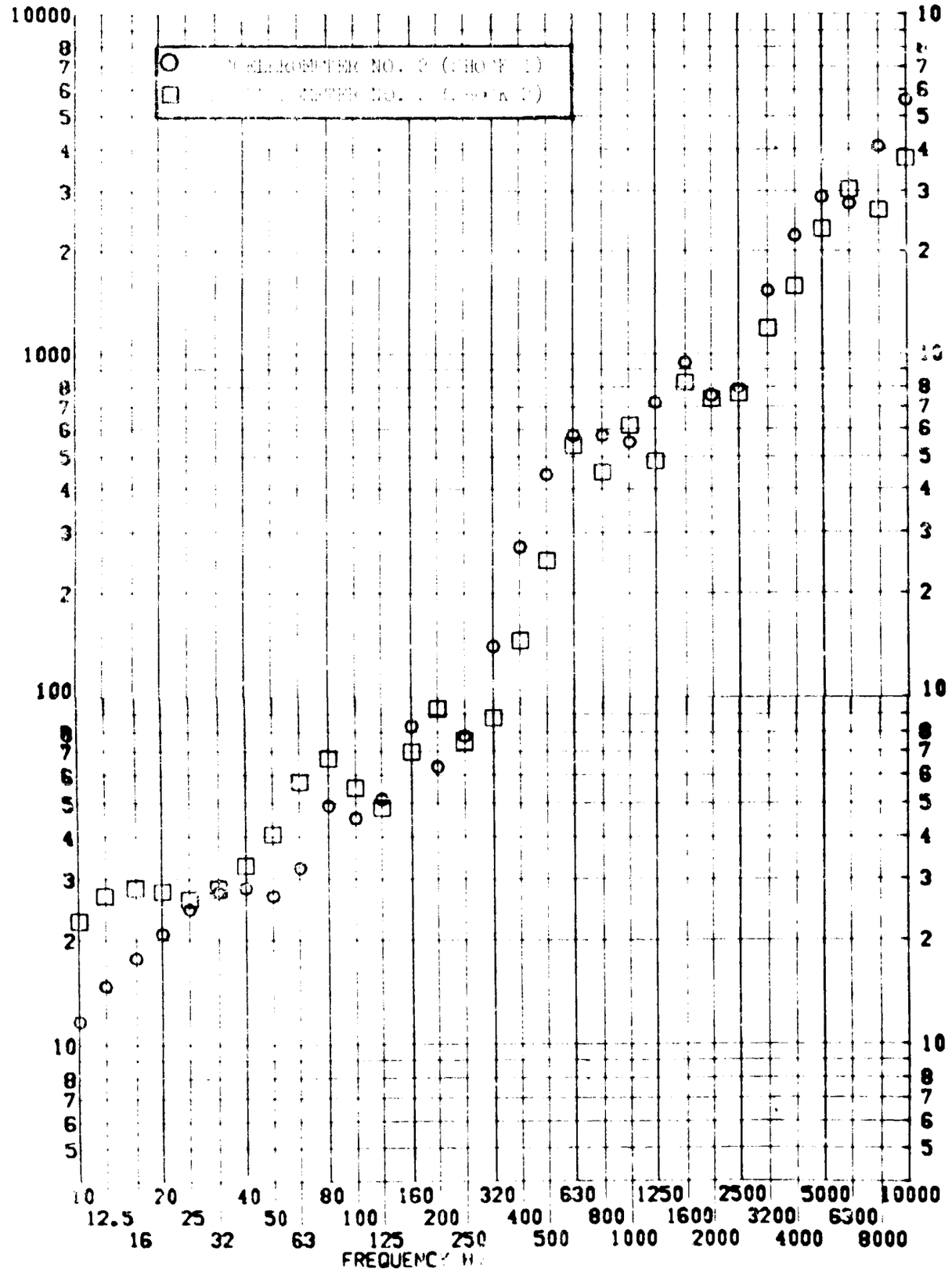

SHOCK TEST ANALYSIS DATA SHEET NO. II.A. 22

TEST ITEM 1377-439
SERIAL NO.
SHOCK AXIS RADIAL

PART NO. STRUCTURE
TEST DATE 11 FEB 1969
SHOCK NO. 1

RESPONSE G-S

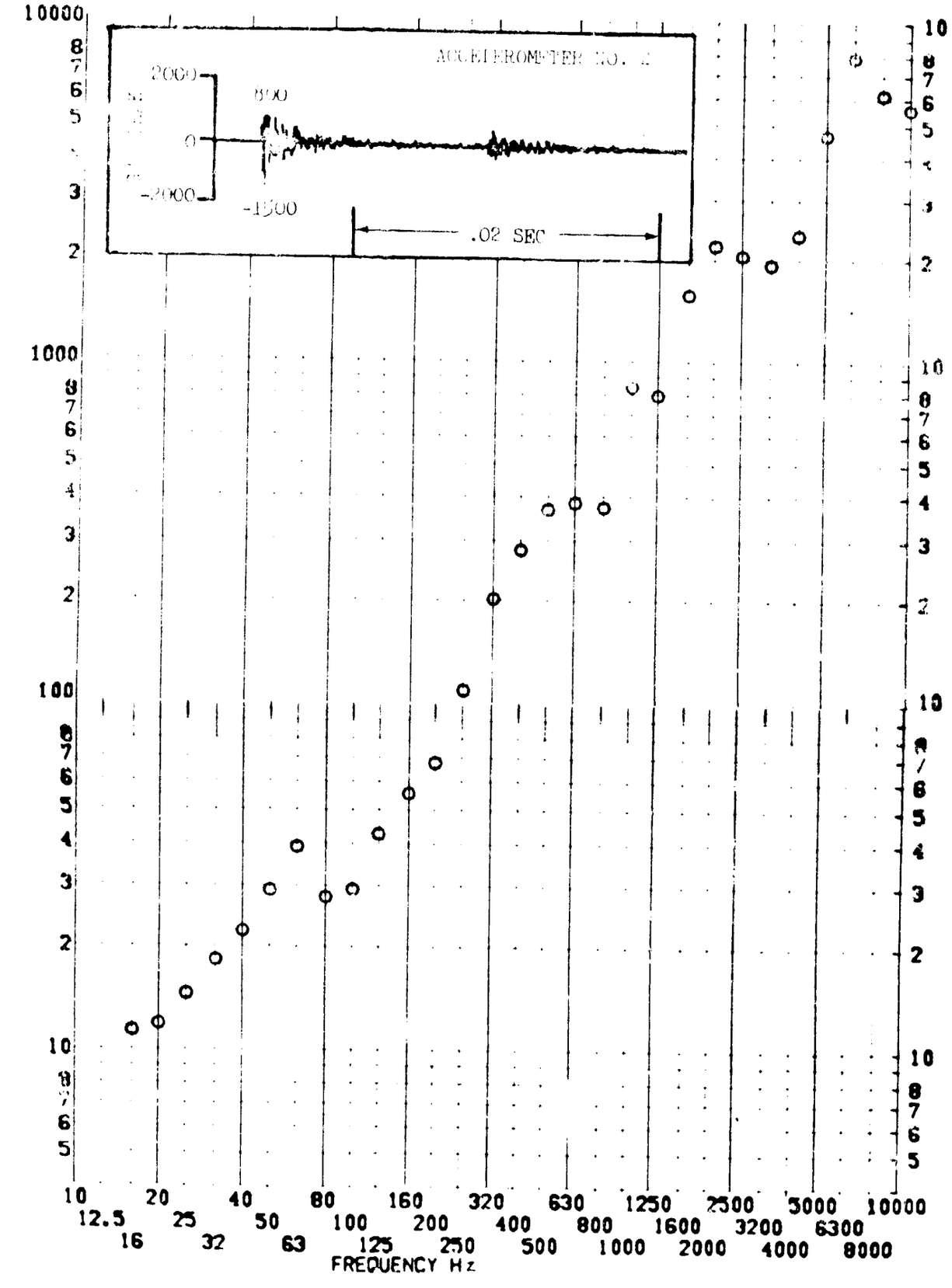

SHOCK TEST ANALYSIS DATA SHEET NO. II.A.7.28

TEST ITEM 1577-4A3
SERIAL NO.
SHOCK AXIS RADIAL

PART NO. STRUCTURE
TEST DATE 11 FEB 1969
SHOCK NO. 2

RESPONSE G-S

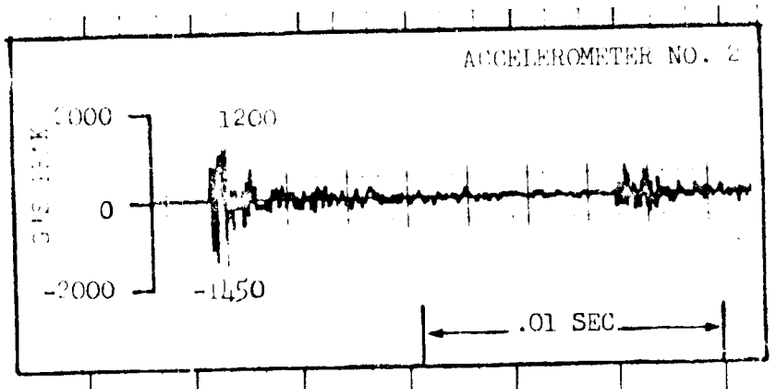

10000 8 7 6 5 4 3 2 1000 8 7 6 5 4 3 2 100 9 8 7 6 5 4 3 2 10 8 7 6 5

10 8 7 6 5 4 3 2 10 8 7 6 5 4 3 2 10 8 7 6 5 4 3 2 10 8 7 6 5

10 20 40 80 160 320 630 1250 2500 5000 10000
12.5 25 50 100 200 400 800 1600 3200 6300
16 32 63 125 250 500 1000 2000 4000 8000

FREQUENCY H

7

SHOCK TEST ANALYSIS DATA SHEET NO. II.A.7.29

TEST ITEM 1377-439,464 PART NO. STRUCTURE

SERIAL NO. — TEST DATE 11 FEB 1969

SHOCK AXIS RADIAL — SHOCK NO. & 2 —

SPONSE G-S

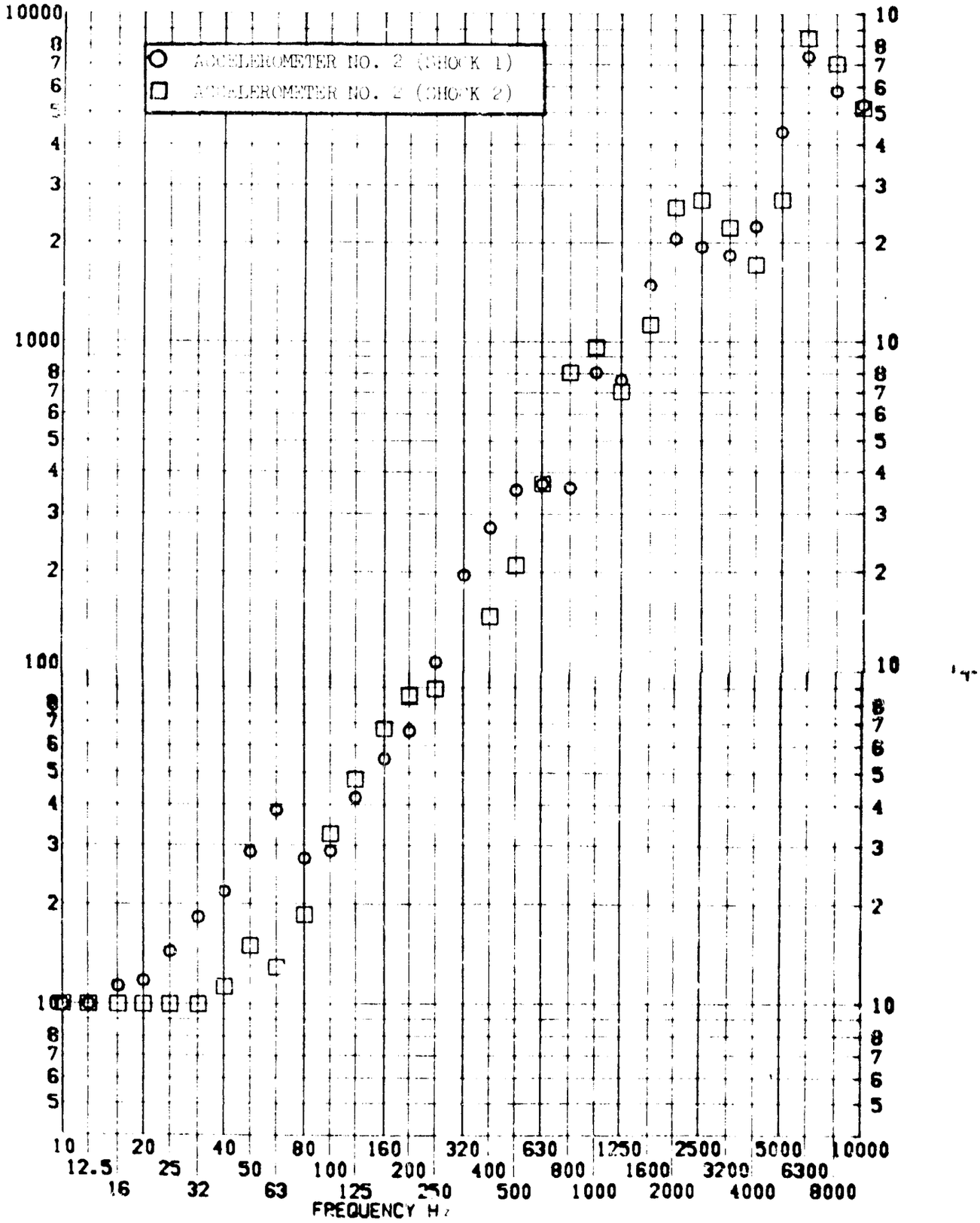

SHOCK TEST ANALYSIS DATA SHEET NO. II.A.T.30

TEST ITEM 1377-440 PART NO. STRUCTURE

SERIAL NO. TEST DATE 11 FEB 1962

RESPONSE G-S SHOCK AXIS LONGITUDINAL SHOCK NO. 1

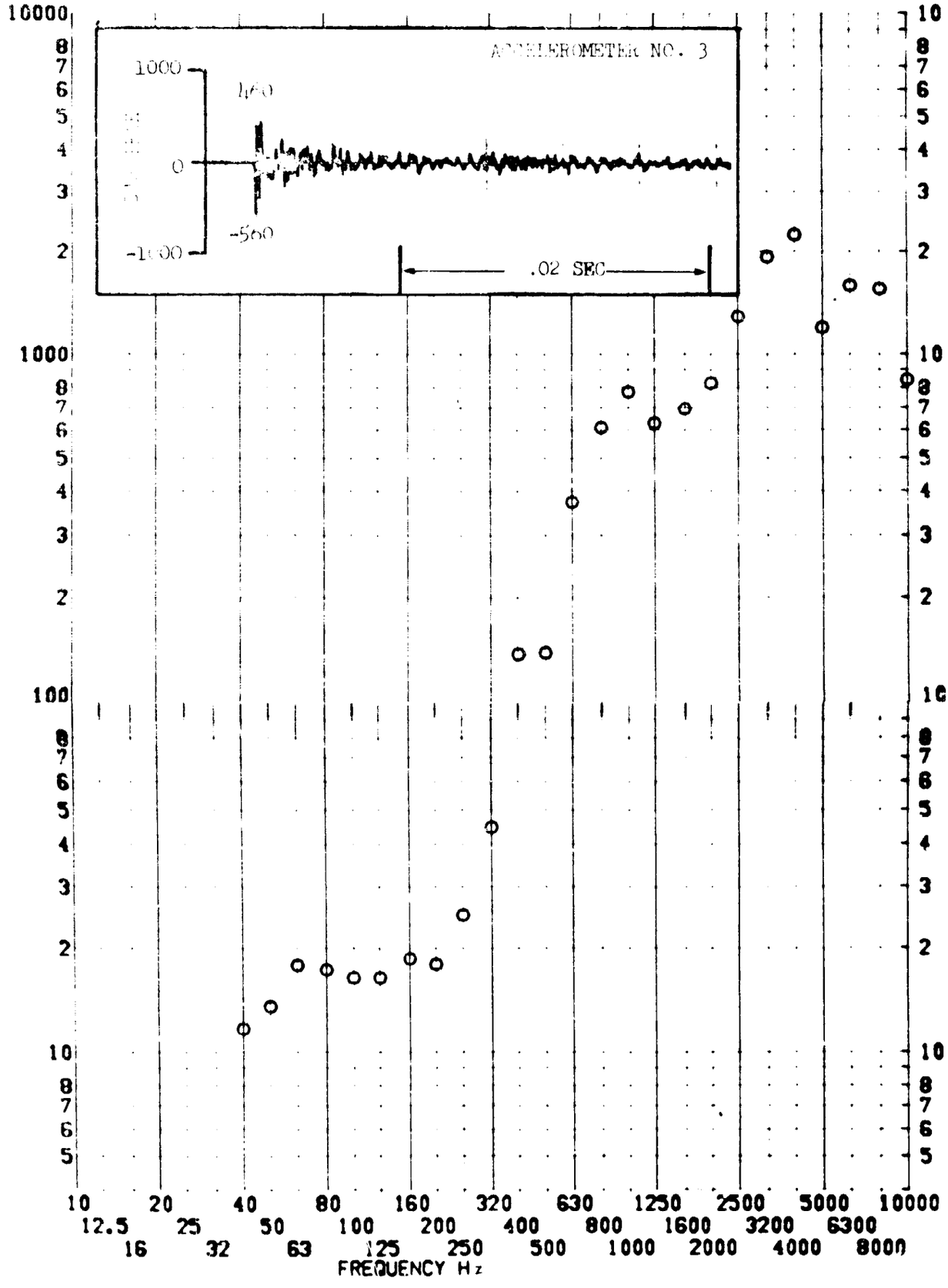

SHOCK TEST ANALYSIS DATA SHEET NO. 11.A.7.31

TEST ITEM 1377-469 **PART NO.** STRUCTURE

SERIAL NO. **TEST DATE** 11 FEB 1969

RESPONSE G-S **SHOCK AXIS** LONGITUDINAL **SHOCK NO.** 2

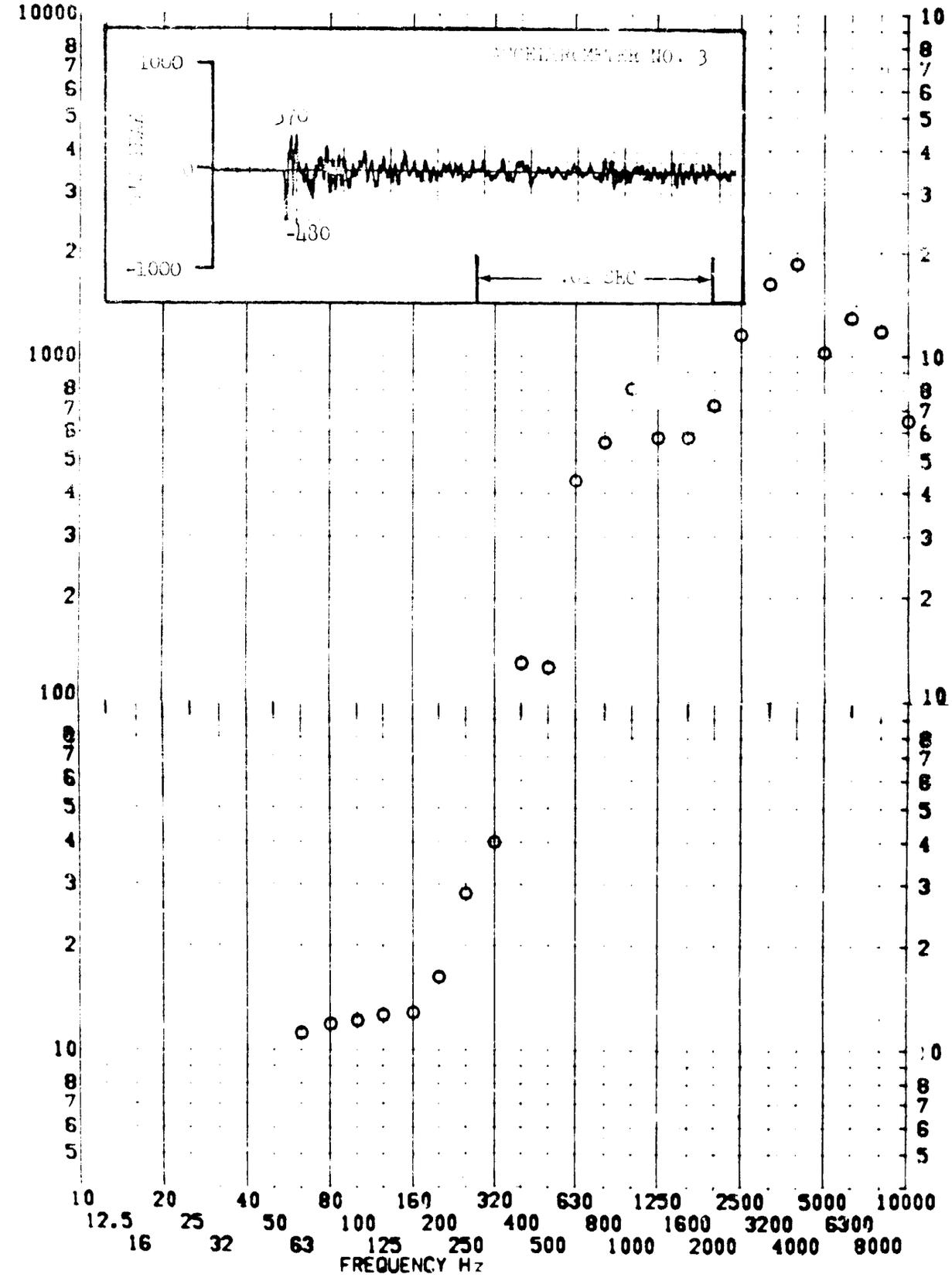

SHOCK TEST ANALYSIS DATA SHEET NO. II.A.7.32

TEST ITEM 1377-440,465 PART NO. STRUCTURE
SERIAL NO. TEST DATE 11 FEB 1969
SHOCK AXIS LONGITUDINAL SHOCK NO. 1 & 2

RESPONSE G-S

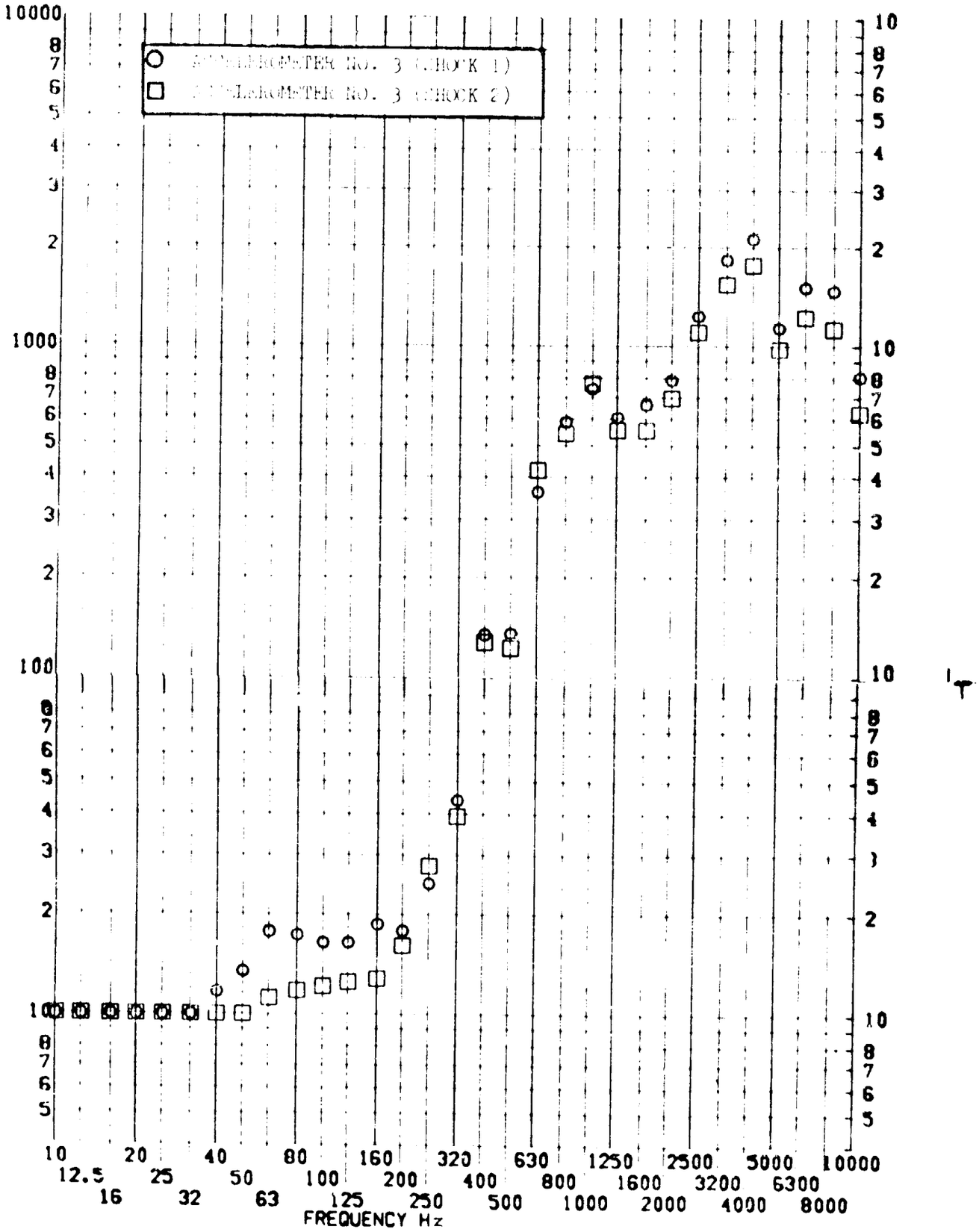

SHOCK TEST ANALYSIS DATA SHEET NO. II.A.7.33

TEST ITEM 1377-4.41 PART NO. STRUCTURE
SERIAL NO. TEST DATE 11 FEB 1969
RESPONSE G-S SHOCK AXIS RADIAL SHOCK NO. 1

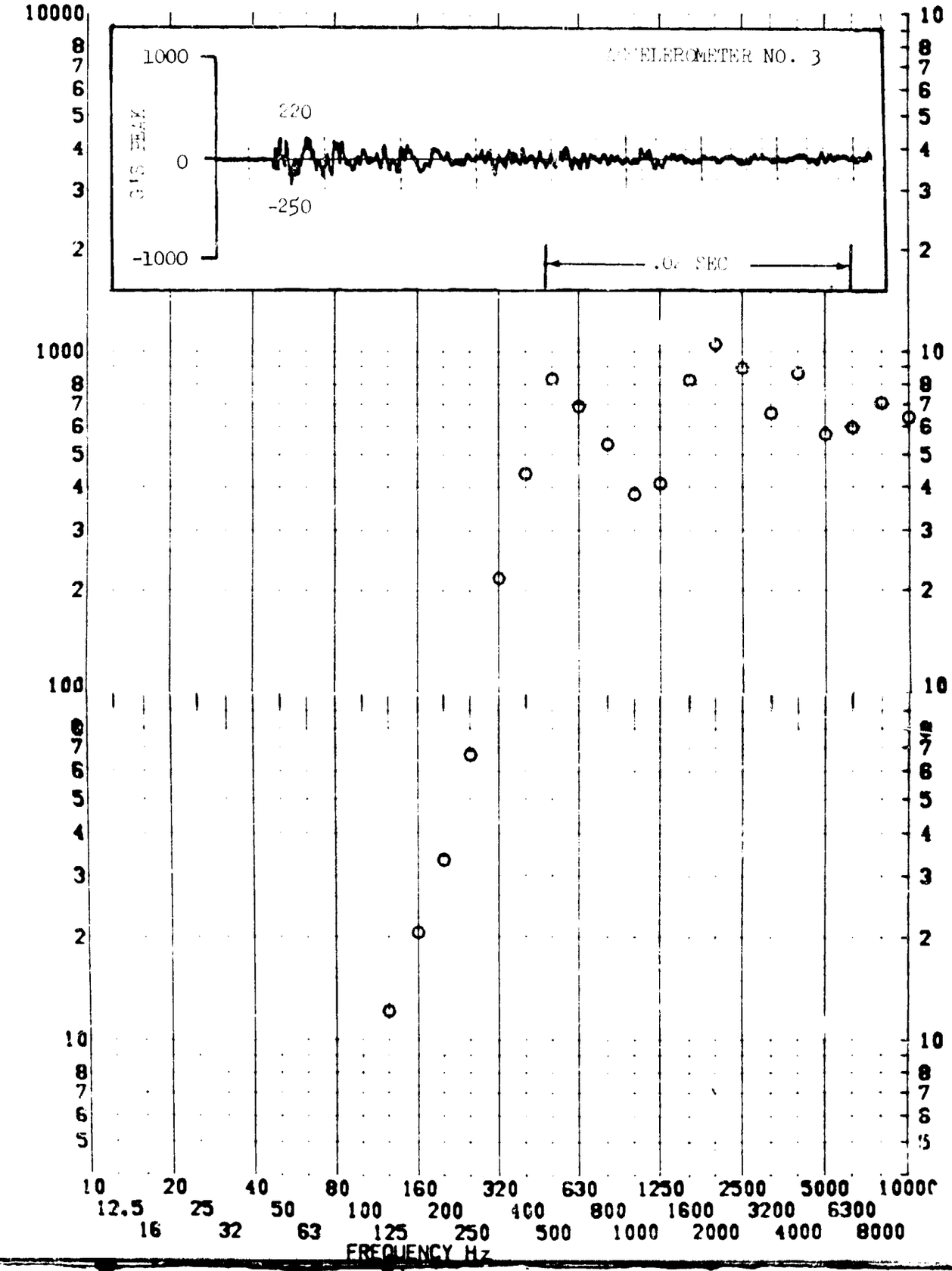

SHOCK TEST ANALYSIS DATA SHEET NO. II.A.7.34

TEST ITEM 1377-1[illegible]
SERIAL NO.
SHOCK AXIS RADIAL

PART NO. STRUCTURE
TEST DATE 11 FEB 1962
SHOCK NO. 2

RESPONSE G-S

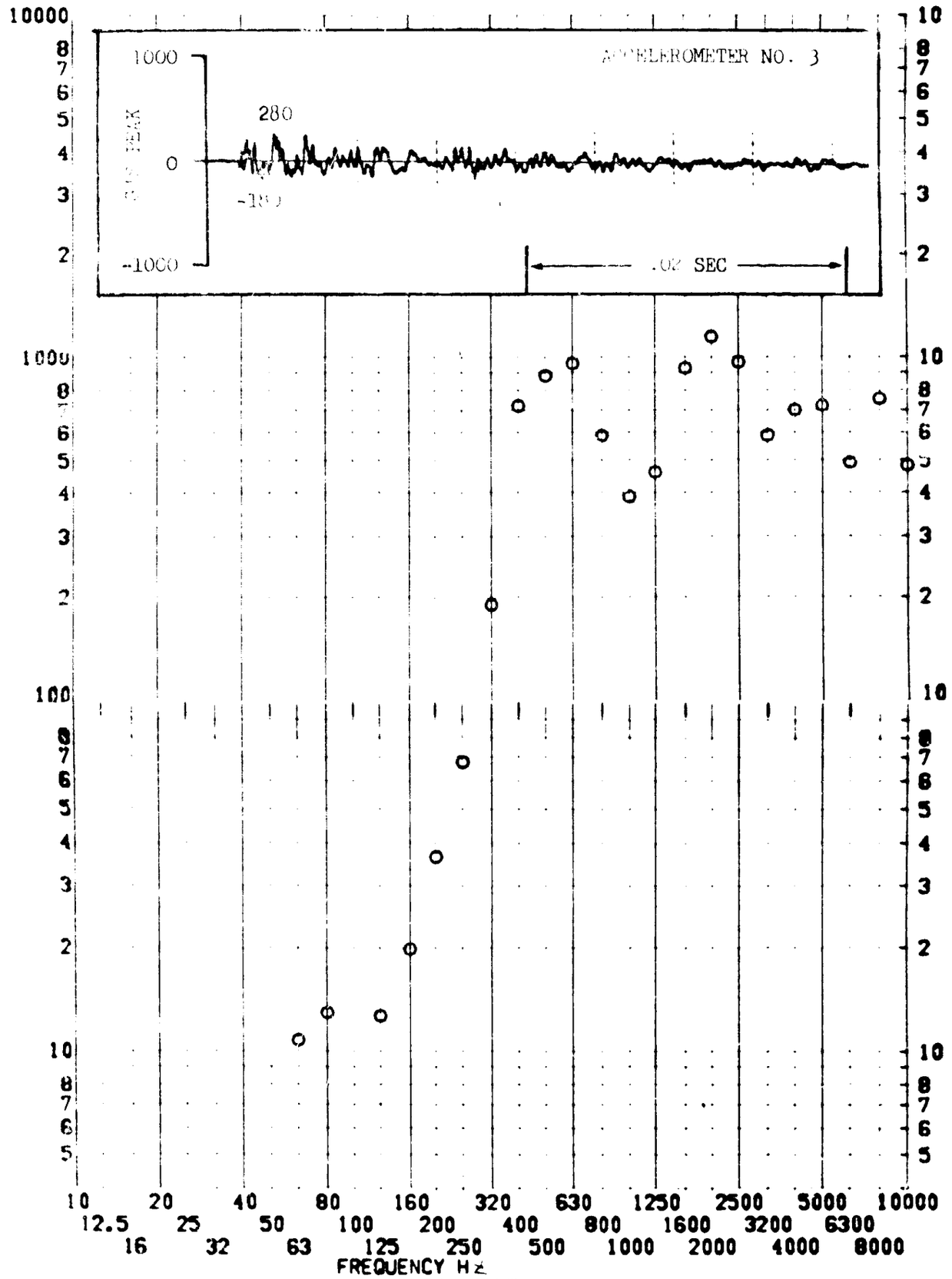

SHOCK TEST ANALYSIS DATA SHEET NO. II.A.7.3

TEST ITEM 1377-441,466 PART NO. STRUCTURE
SERIAL NO. — TEST DATE 11 FEB 1962
SHOCK AXIS RADIAL SHOCK NO. 1 & 2

RESPONSE G-S

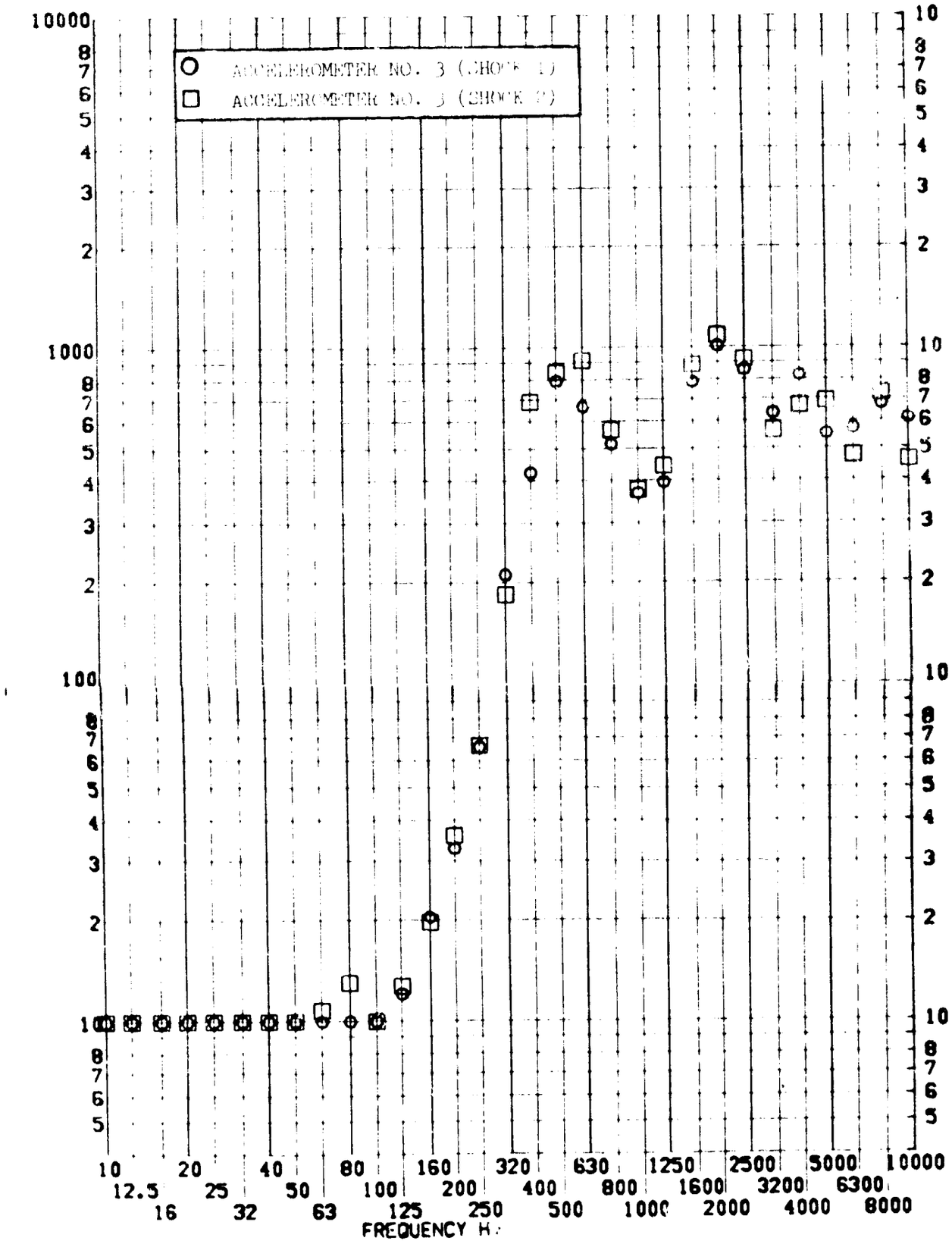

SHOCK TEST ANALYSIS DATA SHEET NO. II.A.7.36

TEST ITEM 1377-442 PART NO. STRUCTURE

SERIAL NO. TEST DATE 11 FEB 1962

RESPONSE G-S SHOCK AXIS LONGITUDINAL SHOCK NO. 1

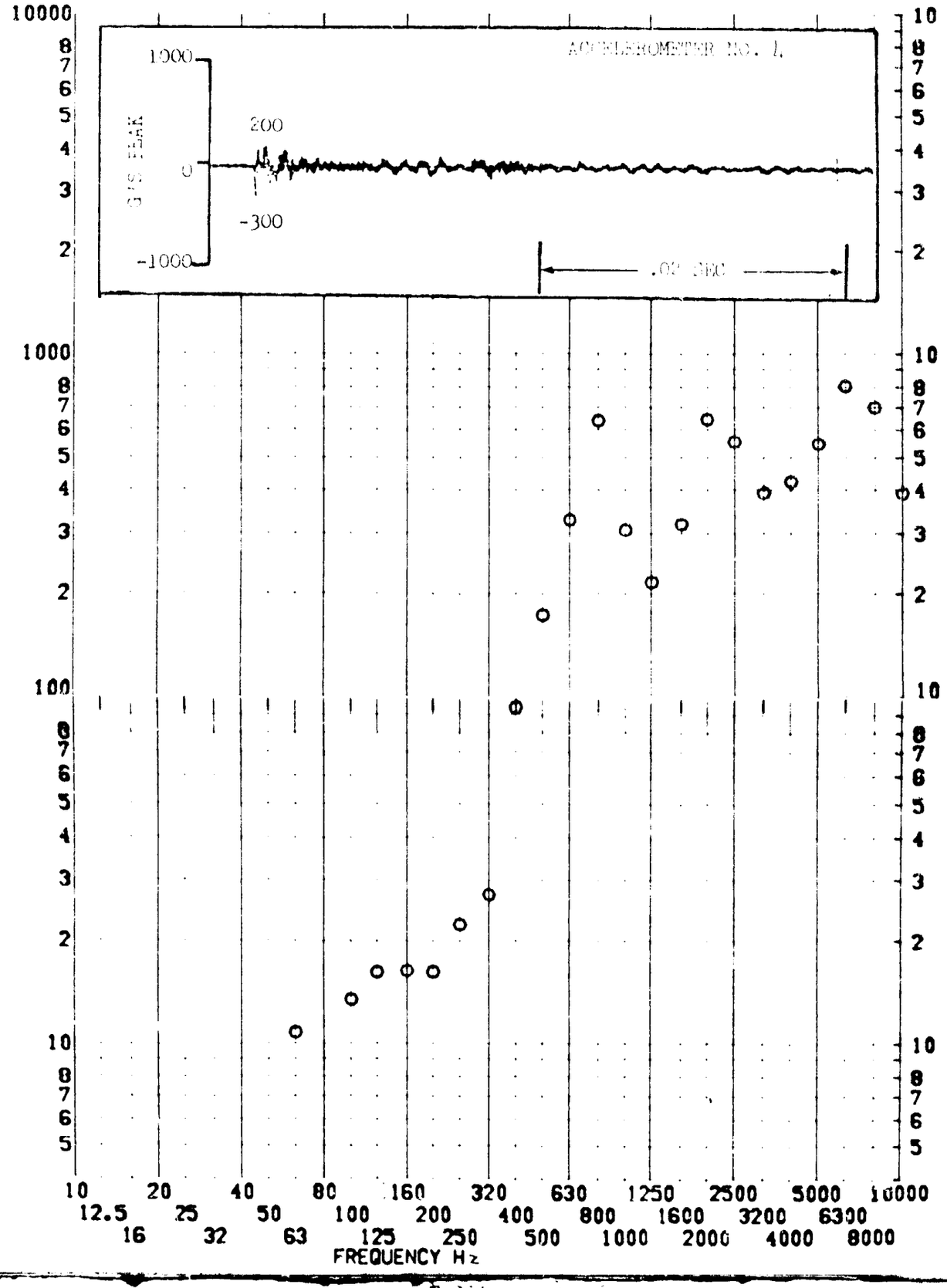

SHOCK TEST ANALYSIS DATA SHEET No. II.A.7.37

TEST ITEM 1377-667 PART NO. STRUCTURE

SERIAL NO. TEST DATE 21 FEB 1969

RESPONSE G-S SHOCK AXIS LONGITUDINAL SHOCK NO. 2

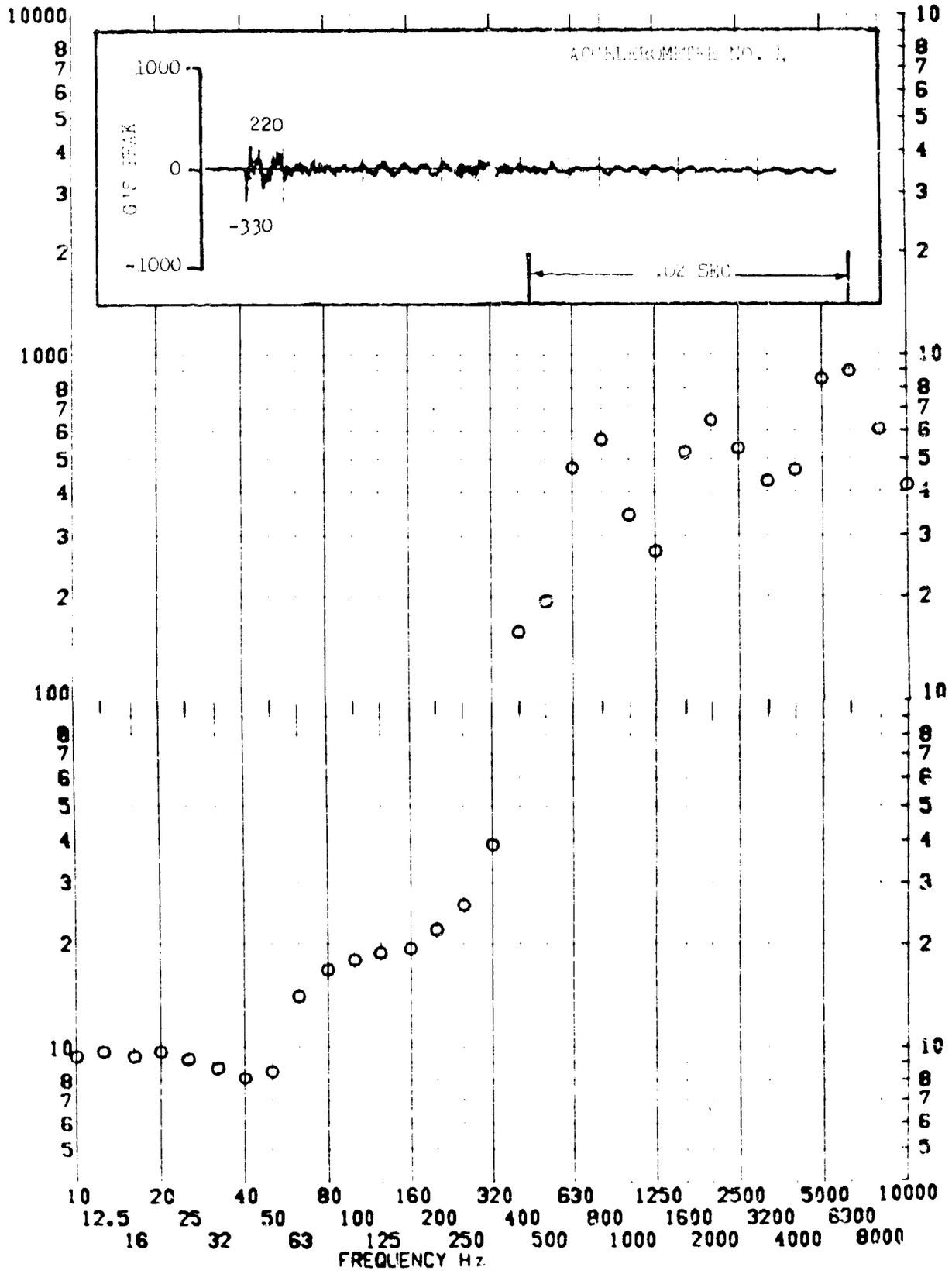

SHOCK TEST ANALYSIS DATA SHEET NO. II.A.7.38

TEST ITEM 1377-442.467 PART NO. STRUCTURE

SERIAL NO. — TEST DATE 11 FEB 1969

SHOCK AXIS LONGITUDINAL SHOCK NO. 1 & 2

RESPONSE G-S

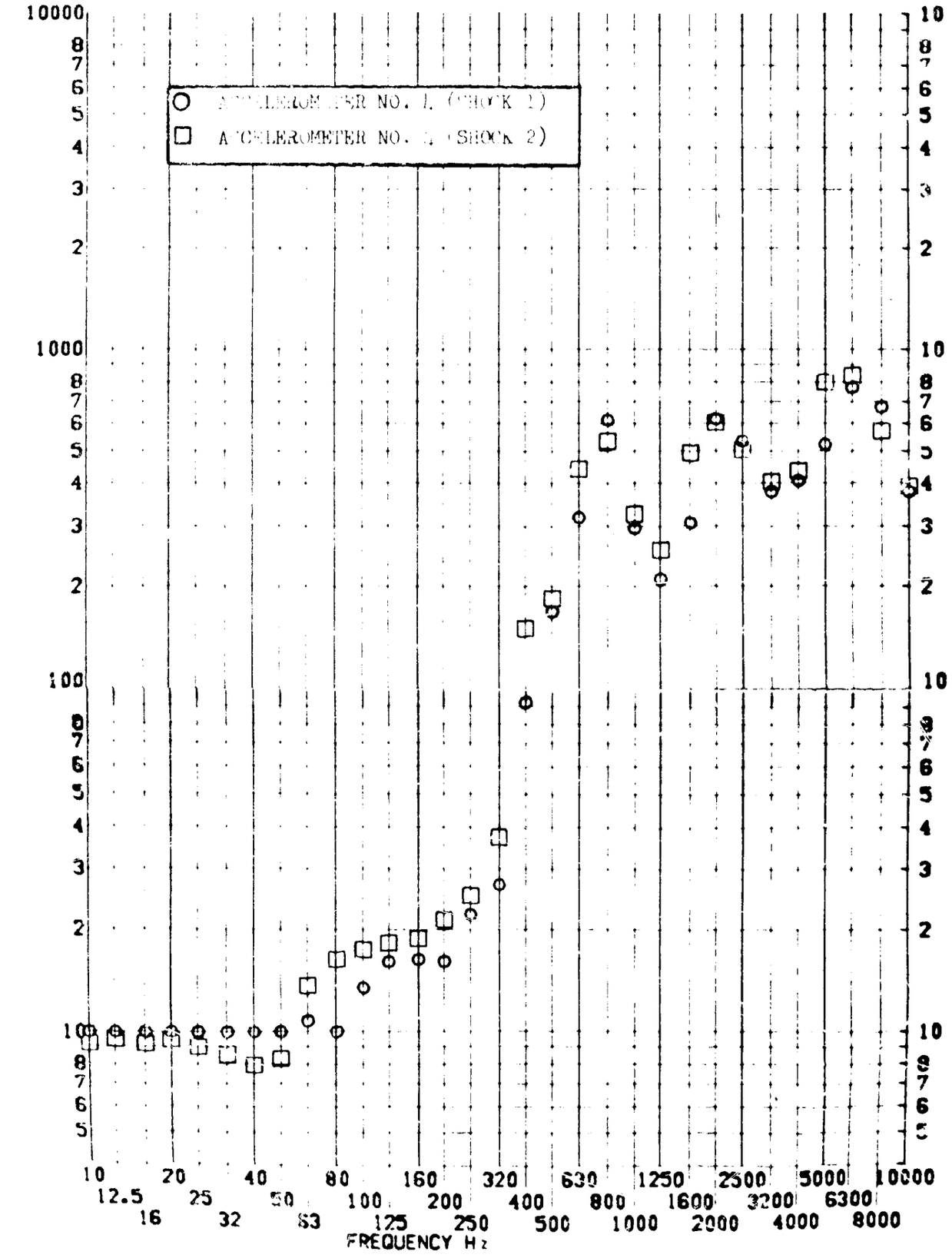

SHOCK TEST ANALYSIS DATA SHEET NO. II.A.7.39

TEST ITEM 1377-443
SERIAL NO.
SHOCK AXIS [illegible]

PART NO. STRUCTURE
TEST DATE 11 FEB 1969
SHOCK NO. 1

RESPONSE G-S

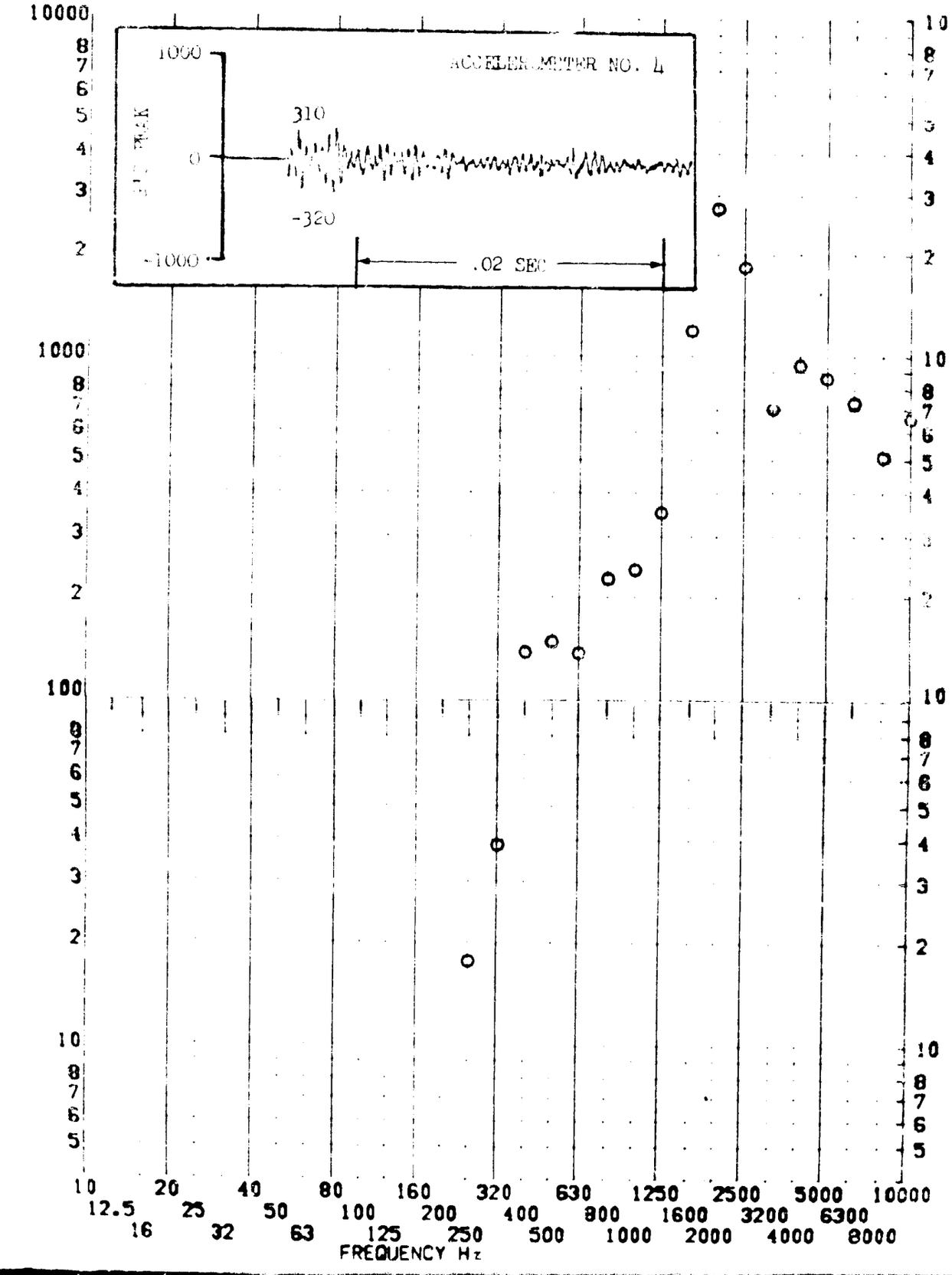

SHOCK TEST ANALYSIS DATA SHEET NO. II.A.7.40

TEST ITEM 1377-4[illegible]
SERIAL NO.
SHOCK AXIS RADIAL

PART NO. STRUCTURE
TEST DATE 14 FEB 1969
SHOCK NO. 2

RESPONSE G-S

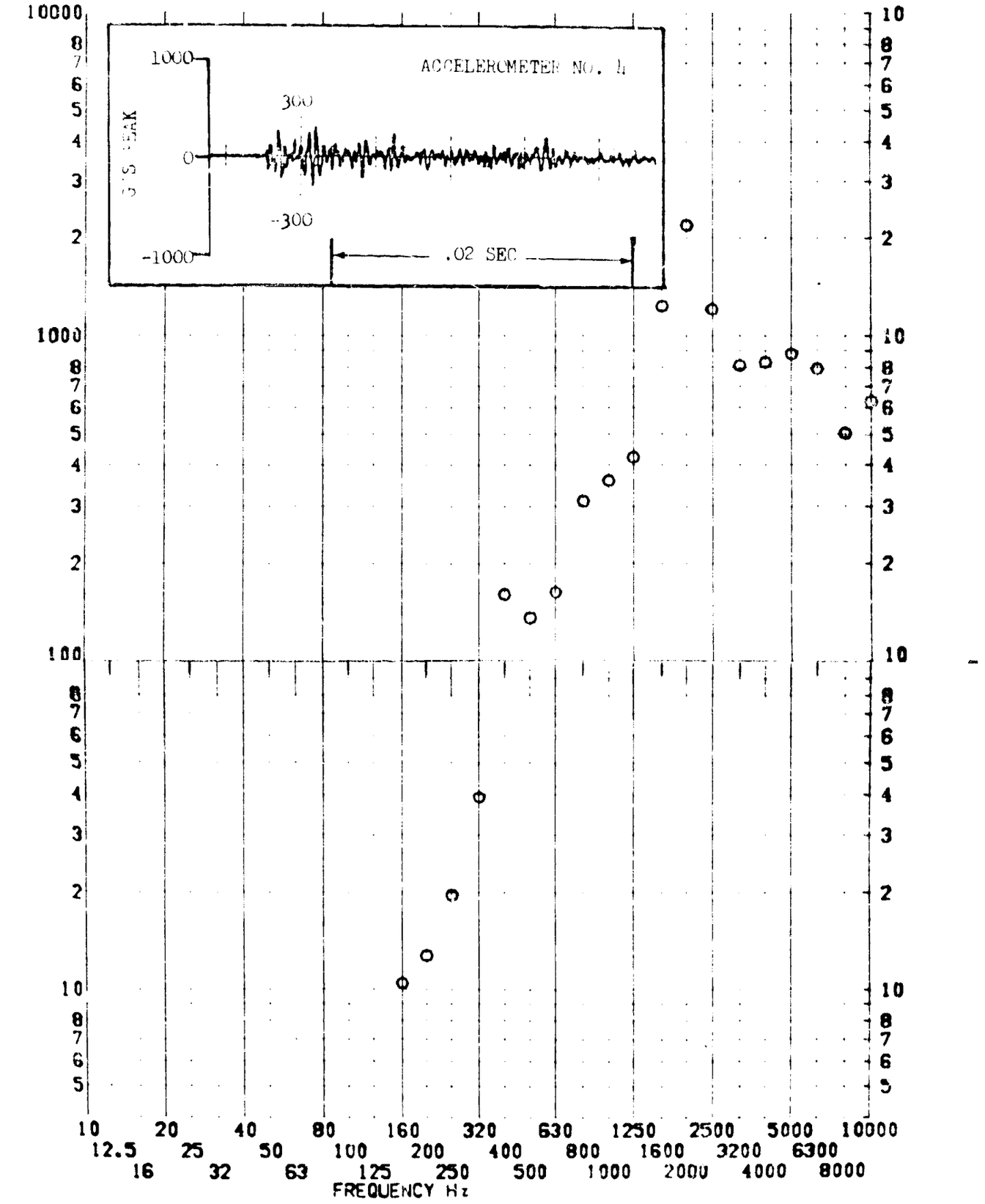

SHOCK TEST ANALYSIS DATA SHEET NO. II.A.7.41

TEST ITEM 1377-443,468 PART NO. STRUCTURE
SERIAL NO. — TEST DATE 11 FEB 1962
SHOCK AXIS RADIAL — SHOCK NO. 1 & 2 —

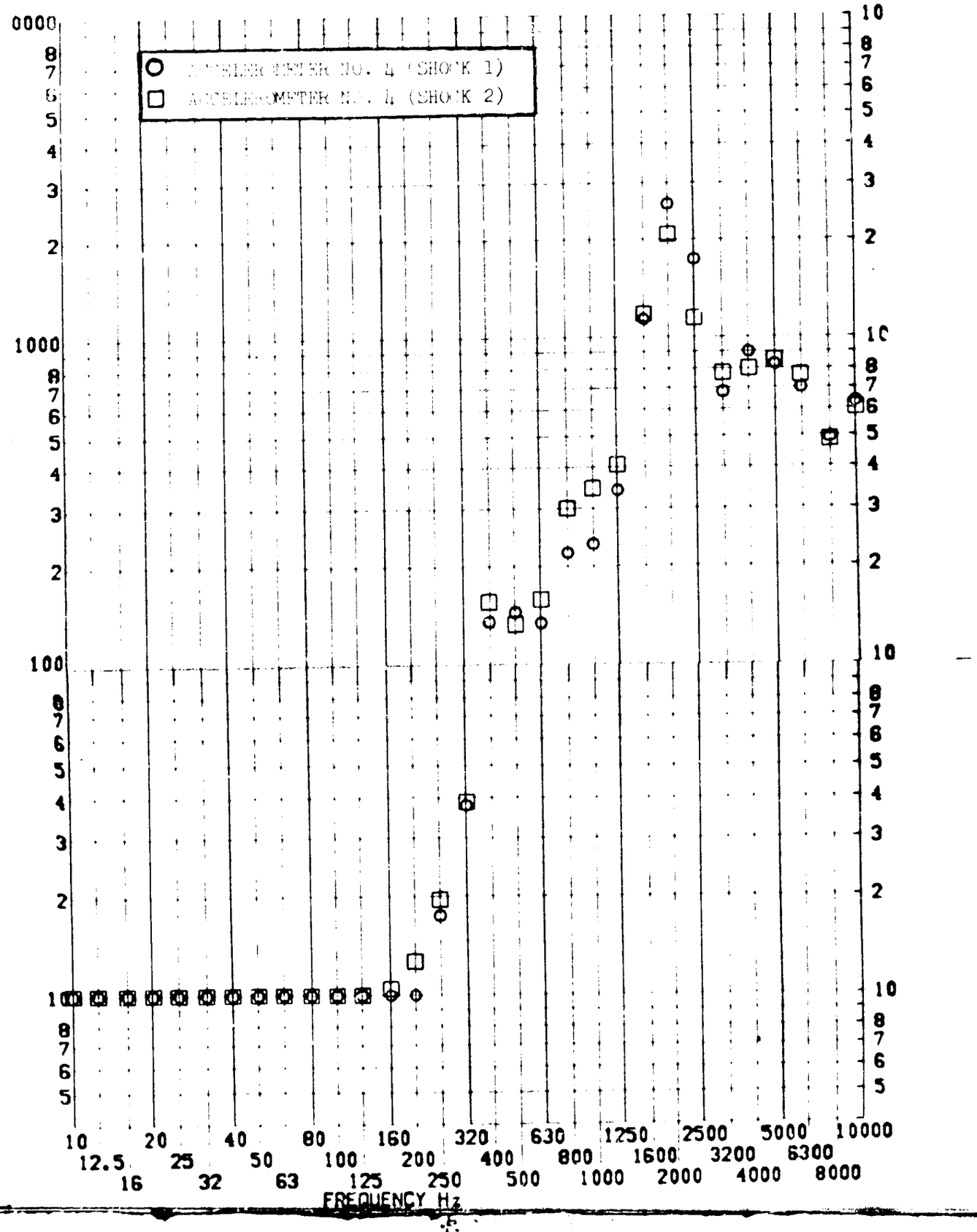

SHOCK TEST ANALYSIS DATA SHEET NO. II.A.7.42

TEST ITEM 1377-445
SERIAL NO.
SHOCK AXIS CONFIDENTIAL

PART NO. STRUCTURE
TEST DATE 11 FEB 1969
SHOCK NO. 1

RESPONSE G-S

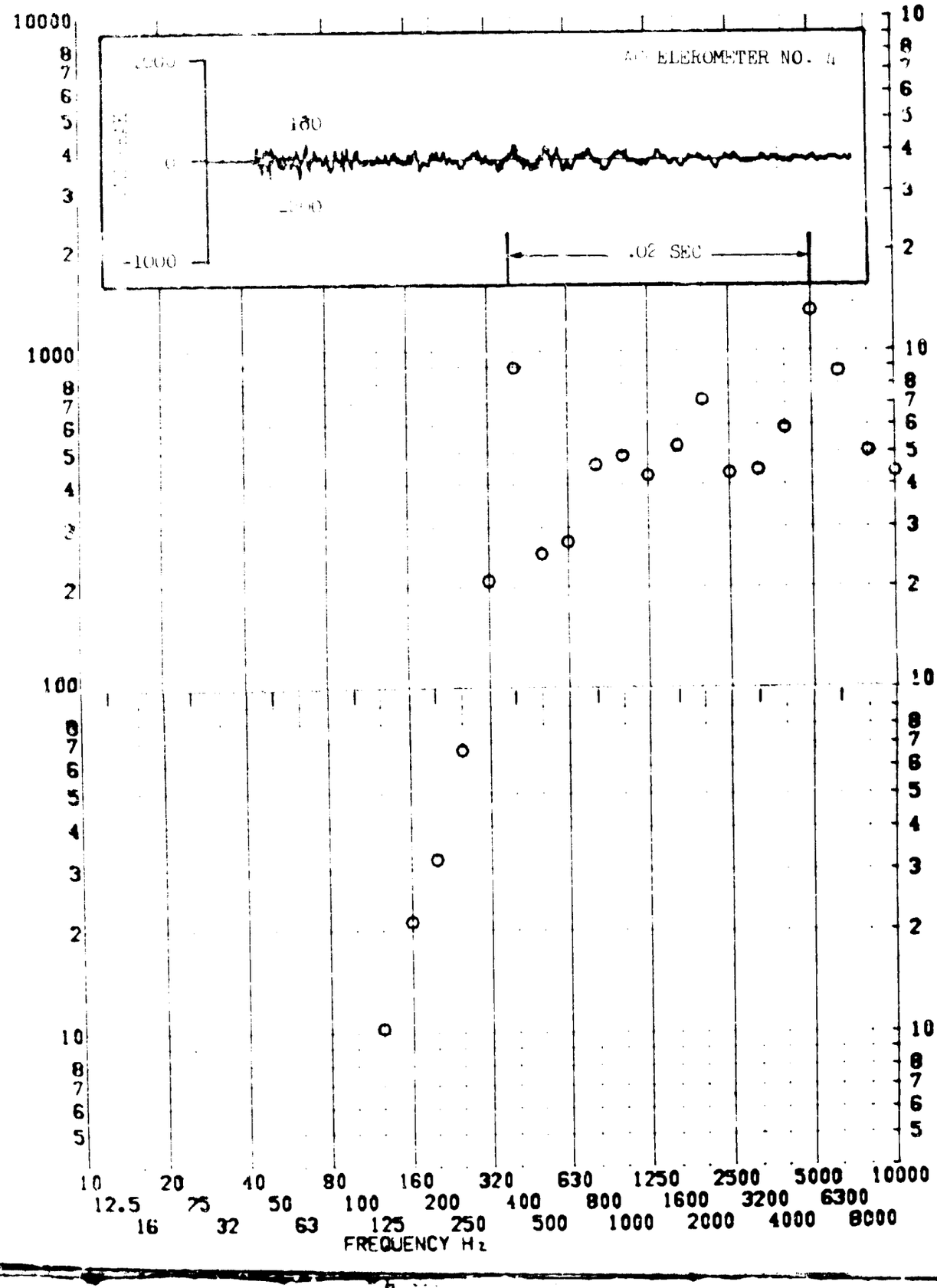

SHOCK TEST ANALYSIS DATA SHEET NO. II.A.7.43

TEST ITEM 1377-469 PART NO. STRUCTURE

SERIAL NO. TEST DATE 11 FEB 1962

RESPONSE G-S SHOCK AXIS TANGENTIAL SHOCK NO. 2

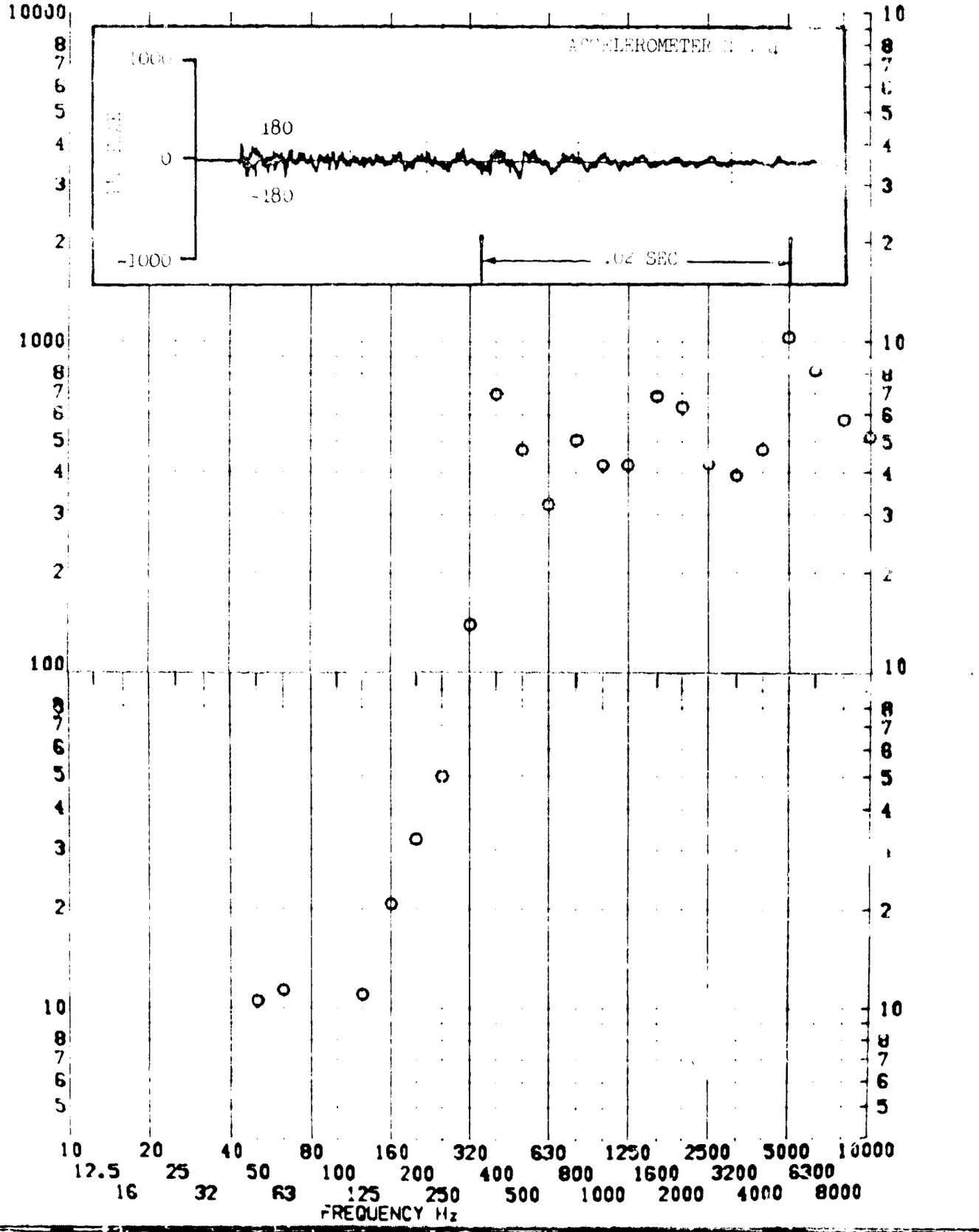

SHOCK TEST ANALYSIS DATA SHEET NO. II.A.7.44

TEST ITEM 1377-445,469
SERIAL NO. —
SHOCK AXIS TANGENTIAL

PART NO. STRUCTURE
TEST DATE 11 FEB 1969
SHOCK NO. 1 & 2

RESPONSE G-S

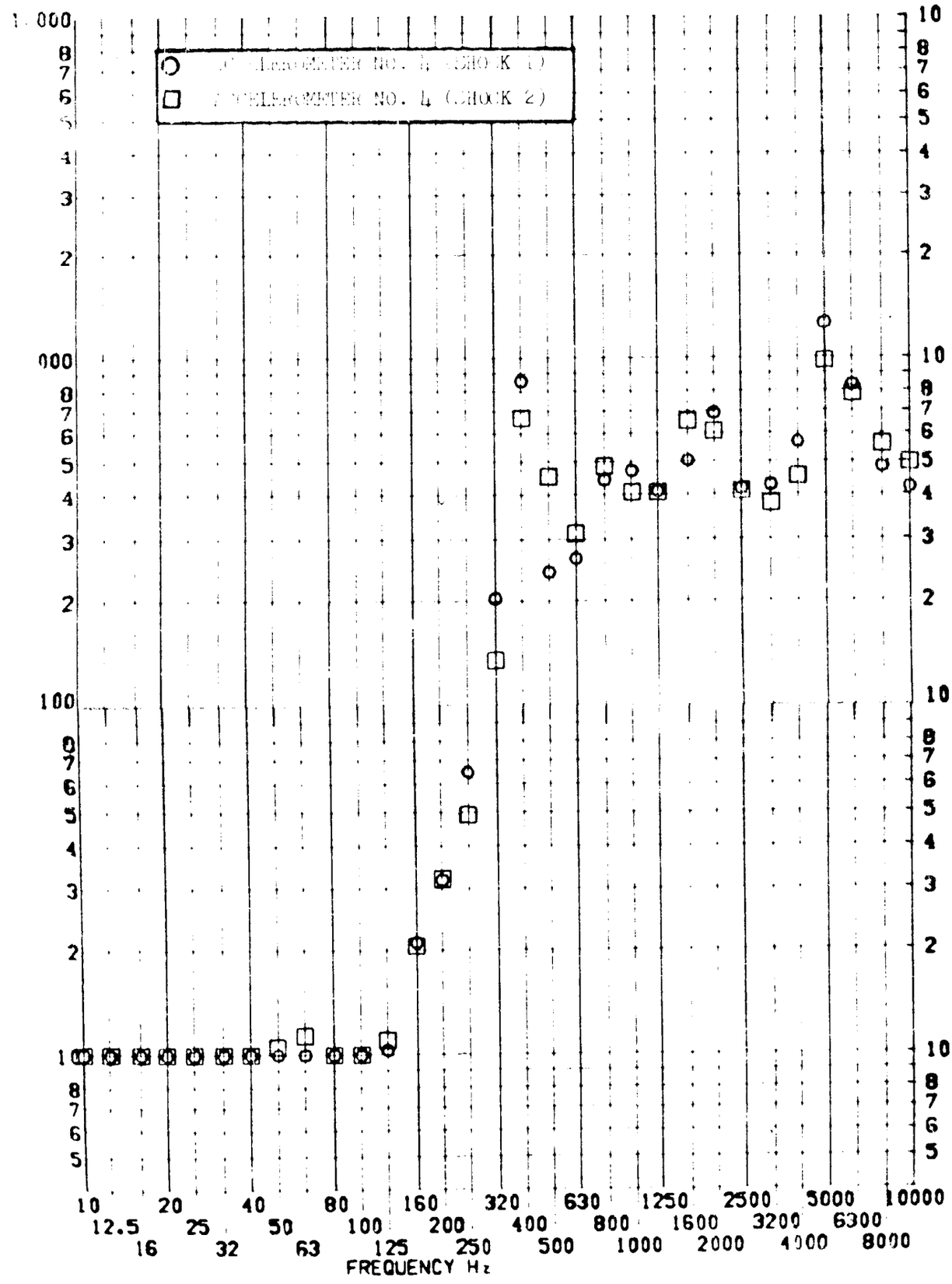

SHOCK TEST ANALYSIS DATA SHEET No. II.A.7.45

TEST ITEM 1377-446 PART NO. STRUCTURE

SERIAL NO. TEST DATE 11 FEB 1969

RESPONSE G-S SHOCK AXIS LONGITUDINAL SHOCK NO. 1

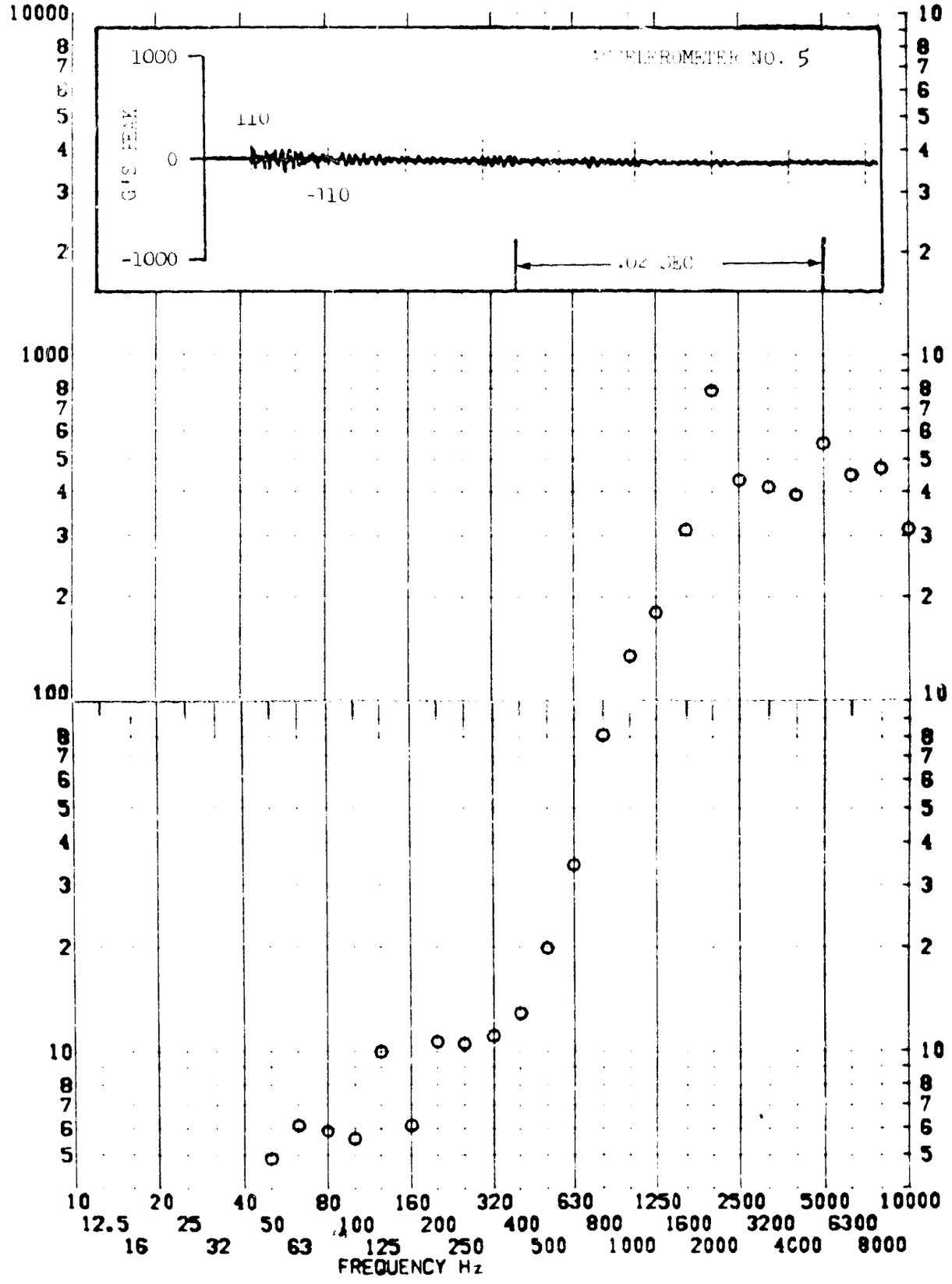

SHOCK TEST ANALYSIS DATA SHEET NO. II.A.7.46

TEST ITEM 1377-470
SERIAL NO.
SHOCK AXIS LONGITUDINAL

PART NO. STRUCTURE
TEST DATE 11 FEB 1969
SHOCK NO. 2

RESPONSE G-S

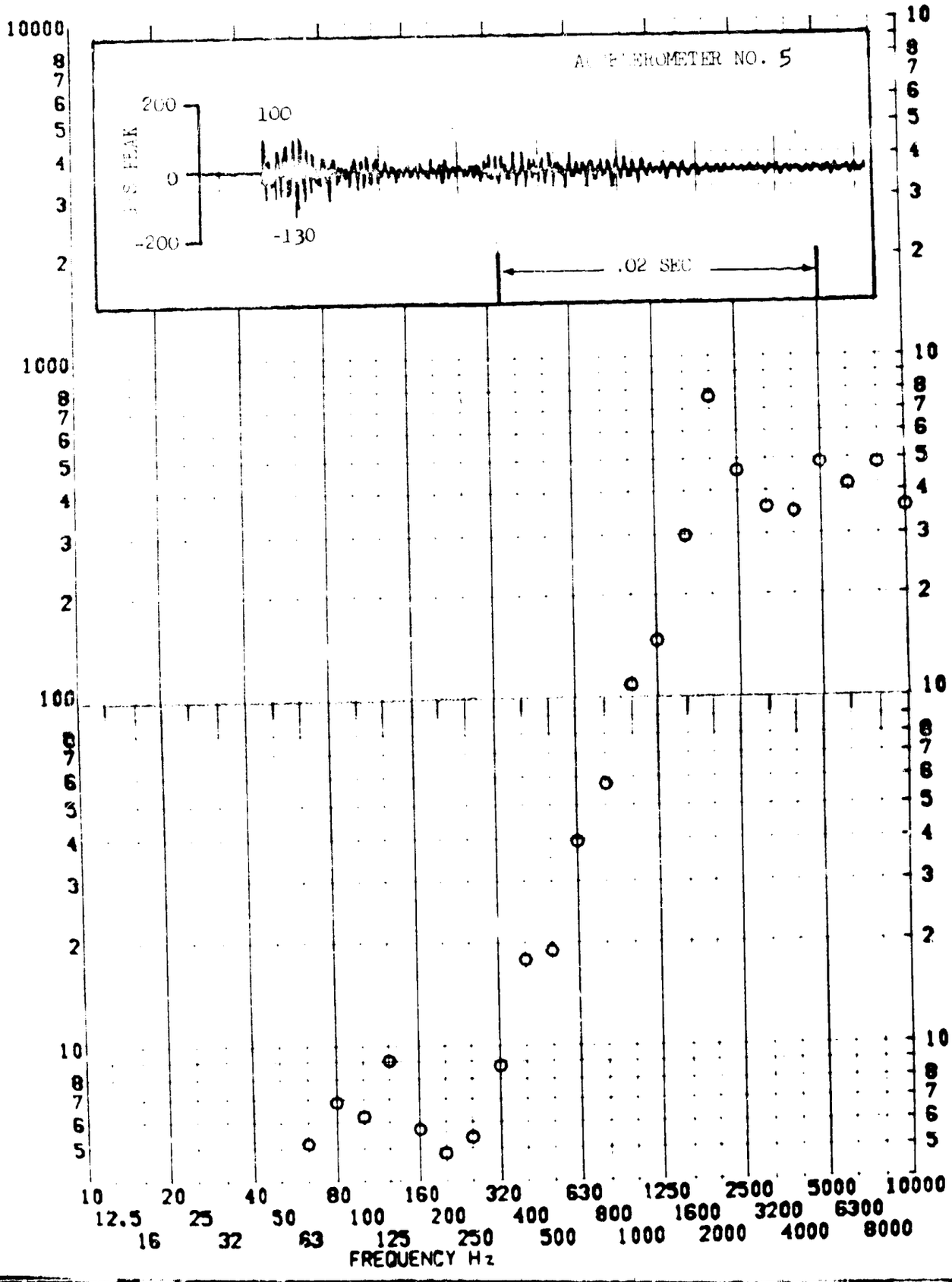

SHOCK TEST ANALYSIS DATA SHEET NO. II.A.7.47

TEST ITEM 1377-446,470
SERIAL NO. —
SHOCK AXIS LONGITUDINAL

PART NO. STRUCTURE
TEST DATE 11 FEB 1969
SHOCK NO. 1 & 2

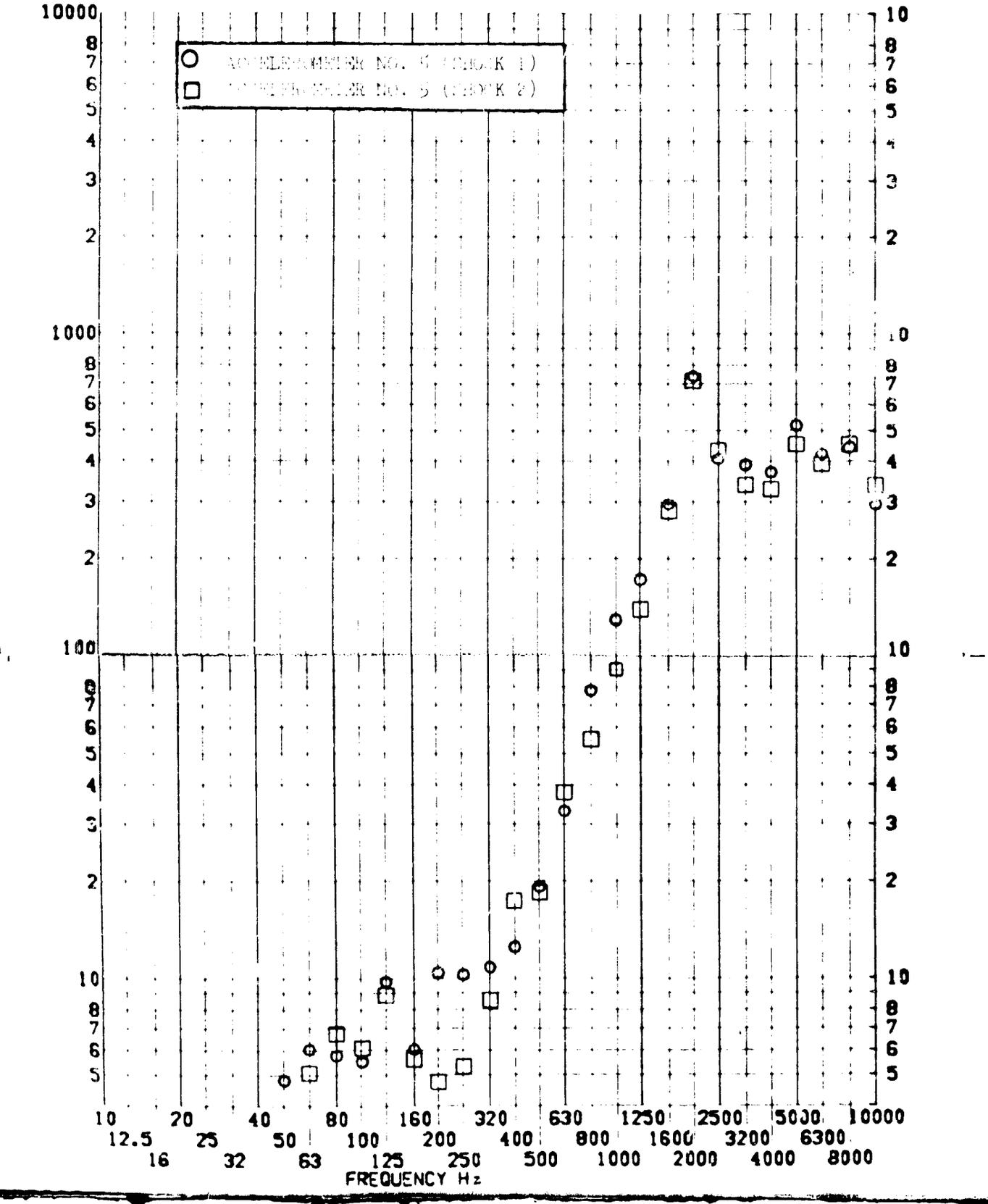

SHOCK TEST ANALYSIS DATA SHEET NO. II.A.7.48

TEST ITEM 1377-447 PART NO. STRUCTURE

SERIAL NO. TEST DATE 11 FEB 1969

RESPONSE G-S SHOCK AXIS RADIAL SHOCK NO. 1

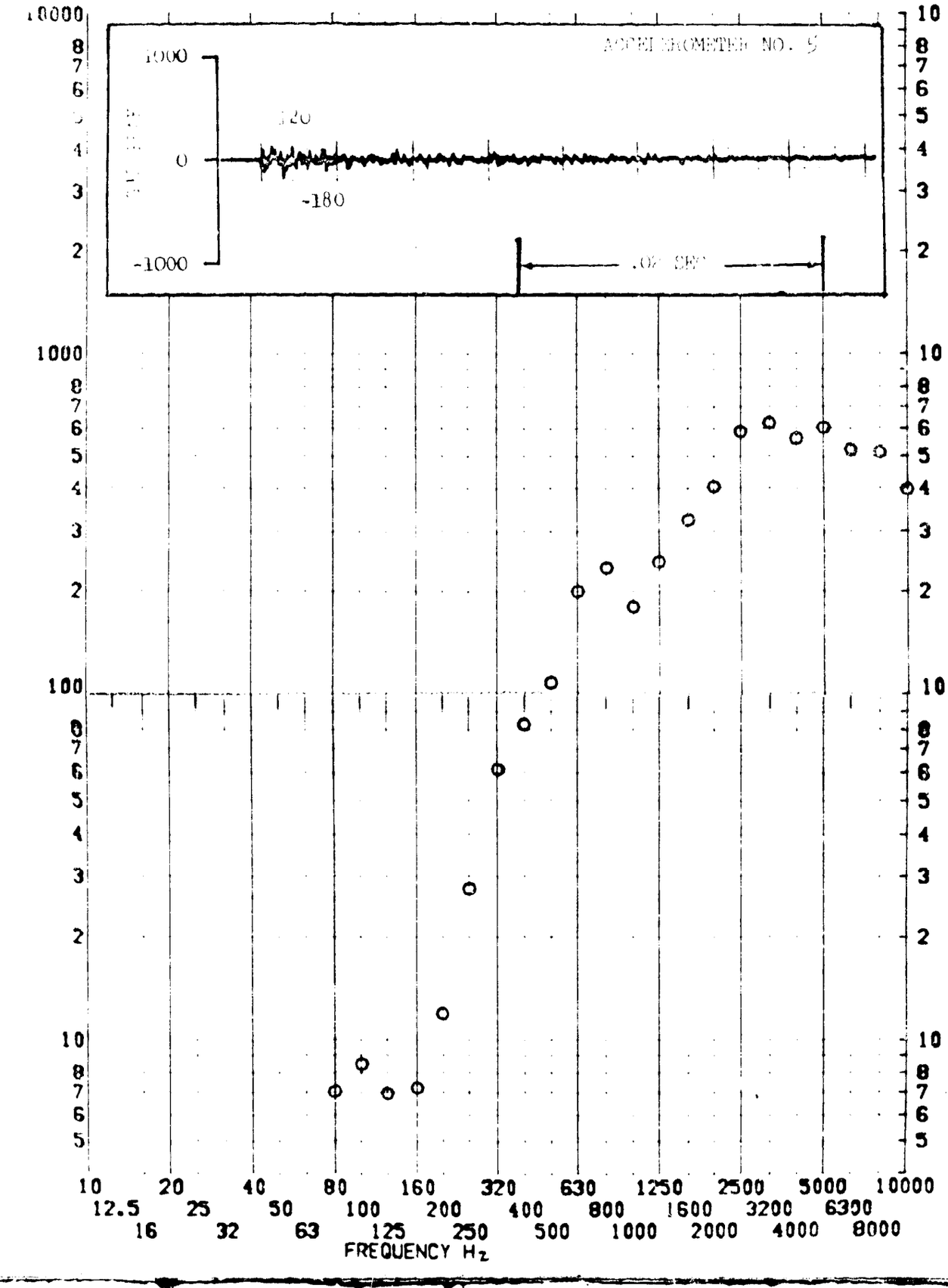

SHOCK TEST ANALYSIS DATA SHEET NO. II.A.7.49

TEST ITEM 1377-471 PART NO. STRUCTURE
SERIAL NO. TEST DATE 11 FEB 1969
RESPONSE G-S SHOCK AXIS RADIAL SHOCK NO. 2

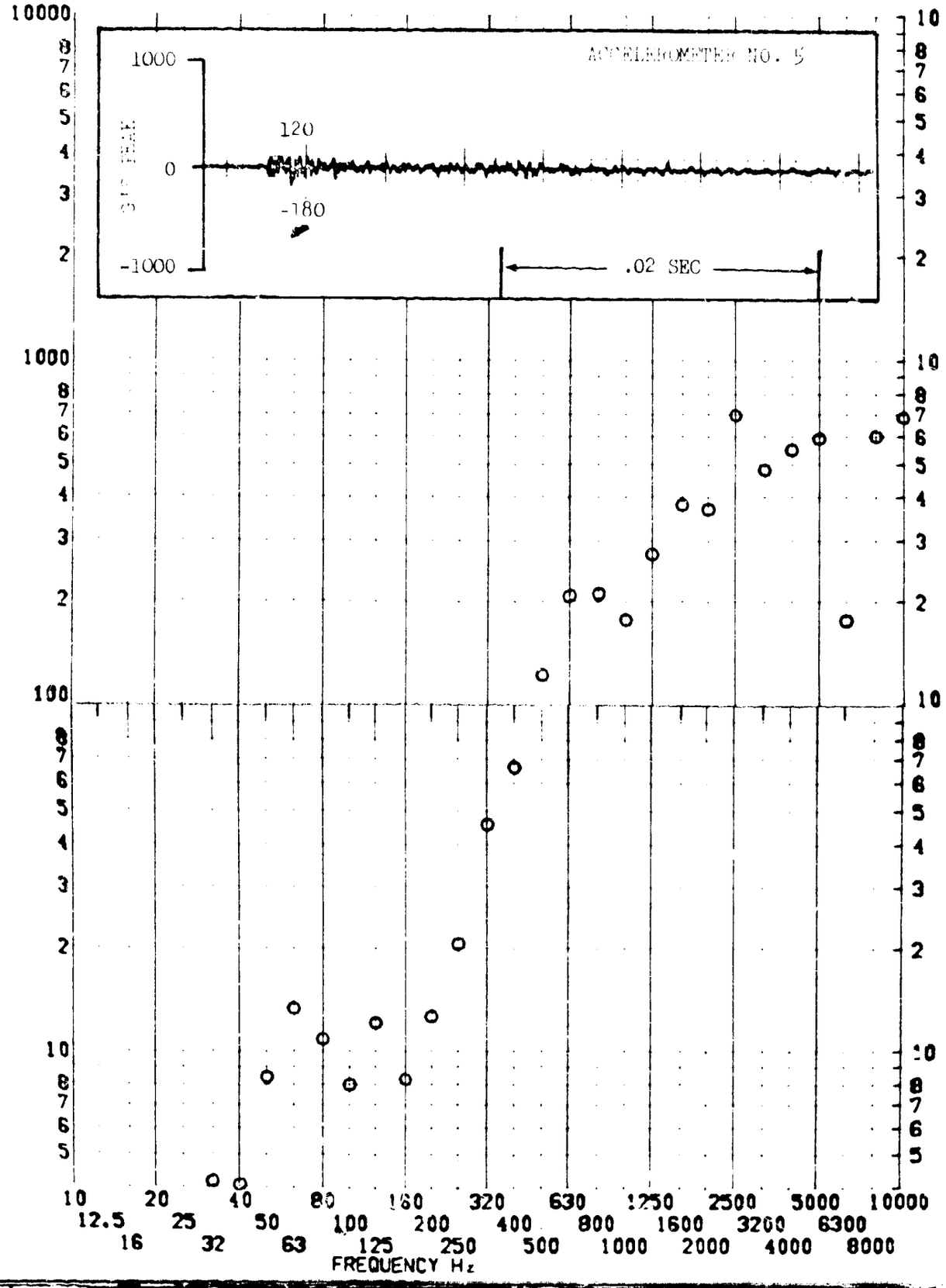

SHOCK TEST ANALYSIS DATA SHEET NO. II.A.7.50

TEST ITEM 1377-447,471 PART NO. STRUCTURE
SERIAL NO. — TEST DATE 11 FEB 1969
SHOCK AXIS AXIAL SHOCK NO. 1 & 2

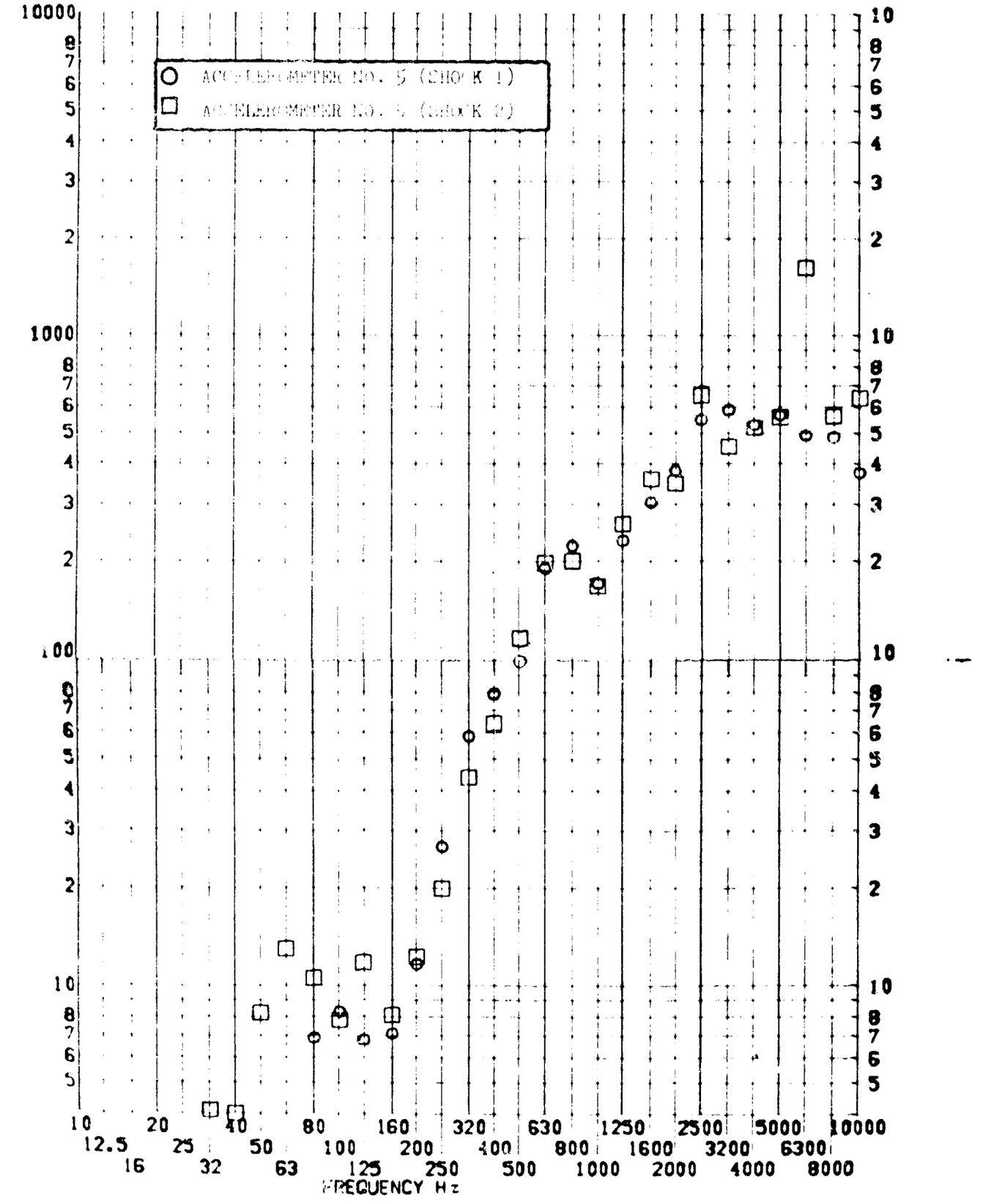

SHOCK TEST ANALYSIS DATA SHEET NO. II.A...91

TEST ITEM 1377-0L3 ___ PART NO. STRUCTURE ___
SERIAL NO. TEST DATE 11 FEB 1969
SHOCK AXIS LONGITUDINAL SHOCK NO. 1

RESPONSE G-S

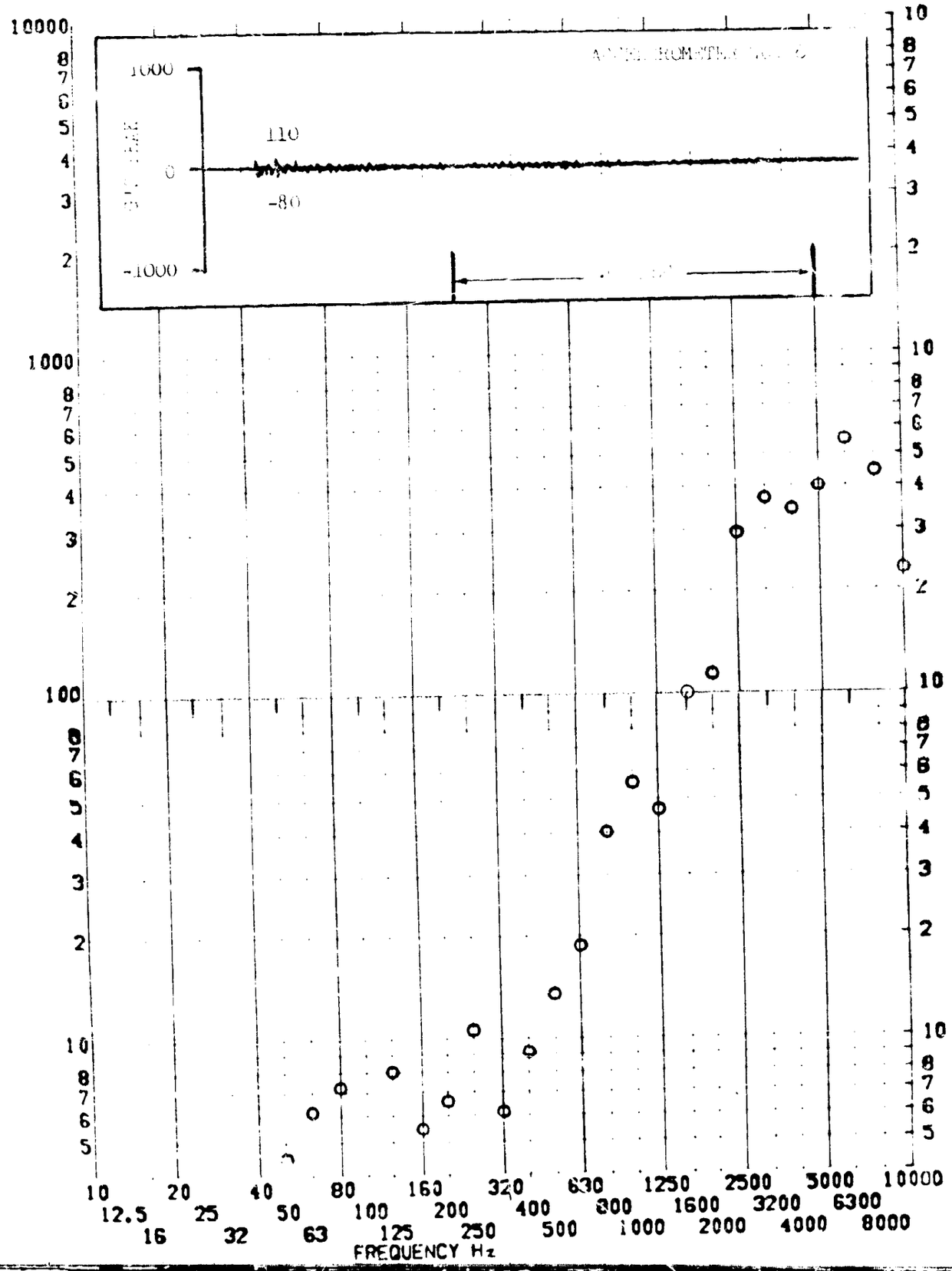

SHOCK TEST ANALYSIS DATA SHEET NO. II.A.7.52

TEST ITEM 1377-472 PART NO. STRUCTURE

SERIAL NO. TEST DATE 11 FEB 1969

SHOCK AXIS LONGITUDINAL SHOCK NO. 2

RESPONSE G-S

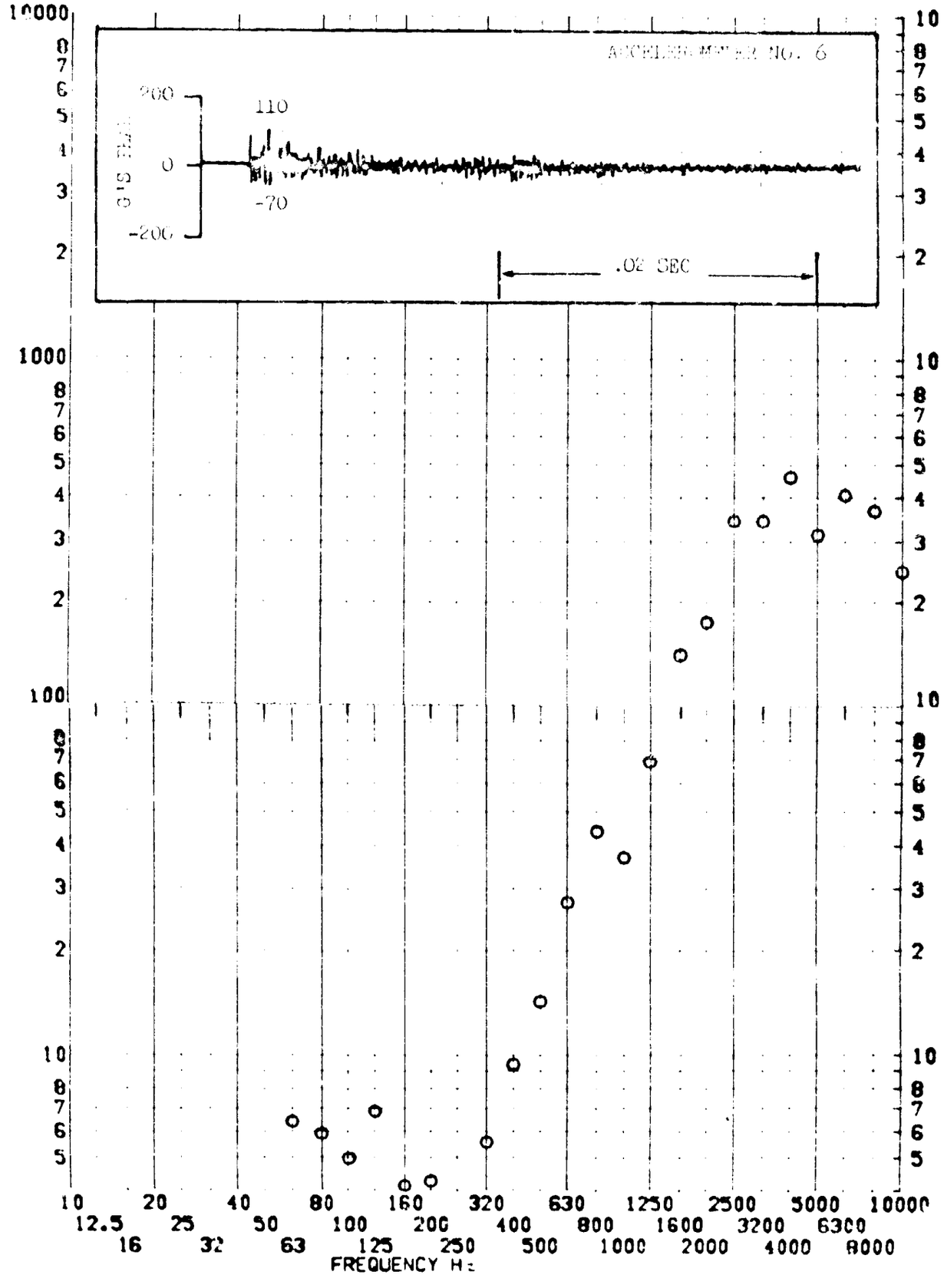

SHOCK TEST ANALYSIS DATA SHEET NO. II.A.7.53

TEST ITEM 1377-448,472 PART NO. STRUCTURE
SERIAL NO. TEST DATE 14 FEB 1962
SHOCK AXIS LONGITUDINAL SHOCK NO. 1 & 2

PONSE G-S

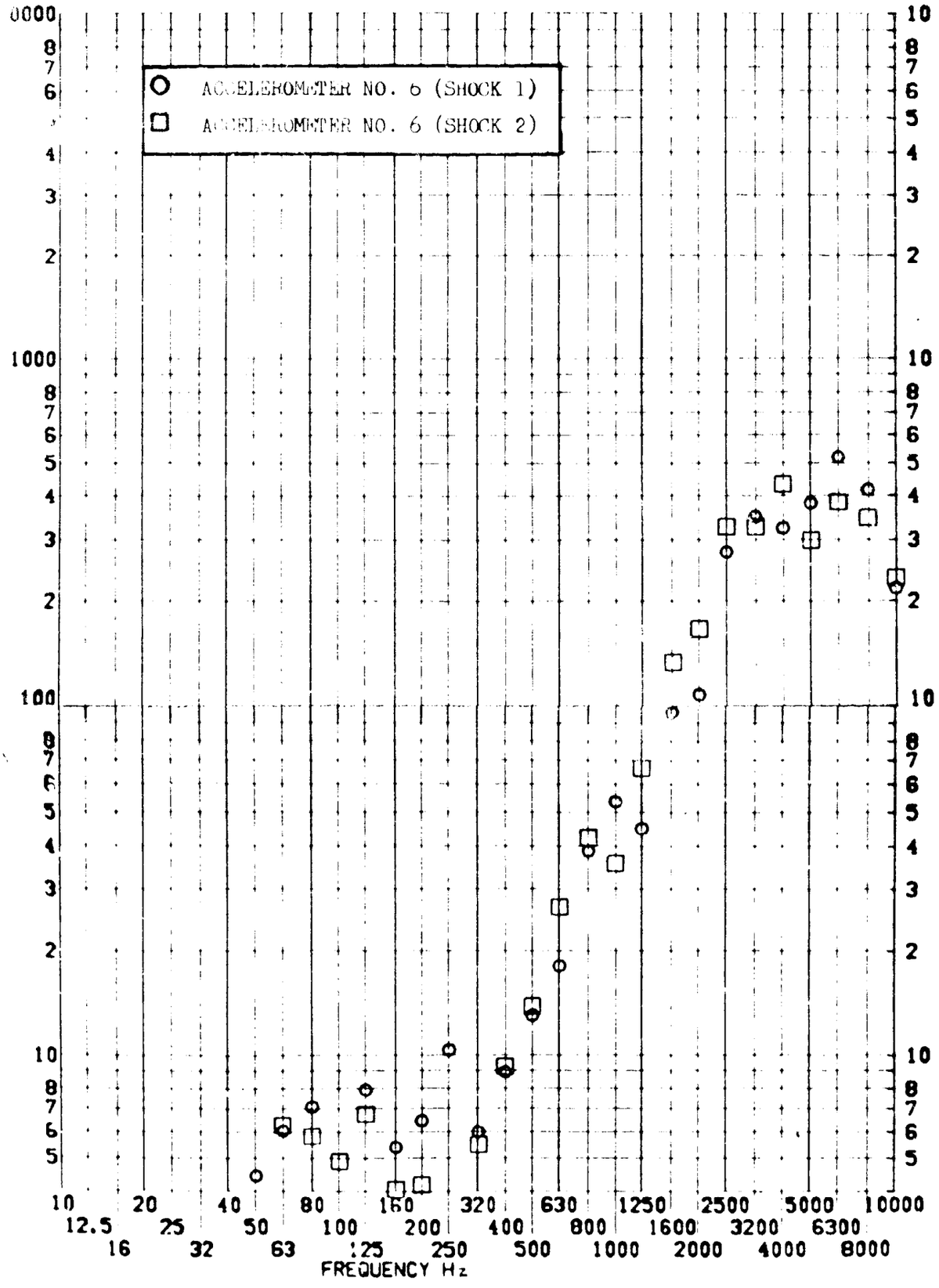

SHOCK TEST ANALYSIS DATA SHEET NO. II.A.7.54

TEST ITEM 1377-1A
SERIAL NO.
SHOCK AXIS RADIAL

PART NO. STRUCTURE
TEST DATE 21 FEB 1969
SHOCK NO. 1

RESPONSE G-S

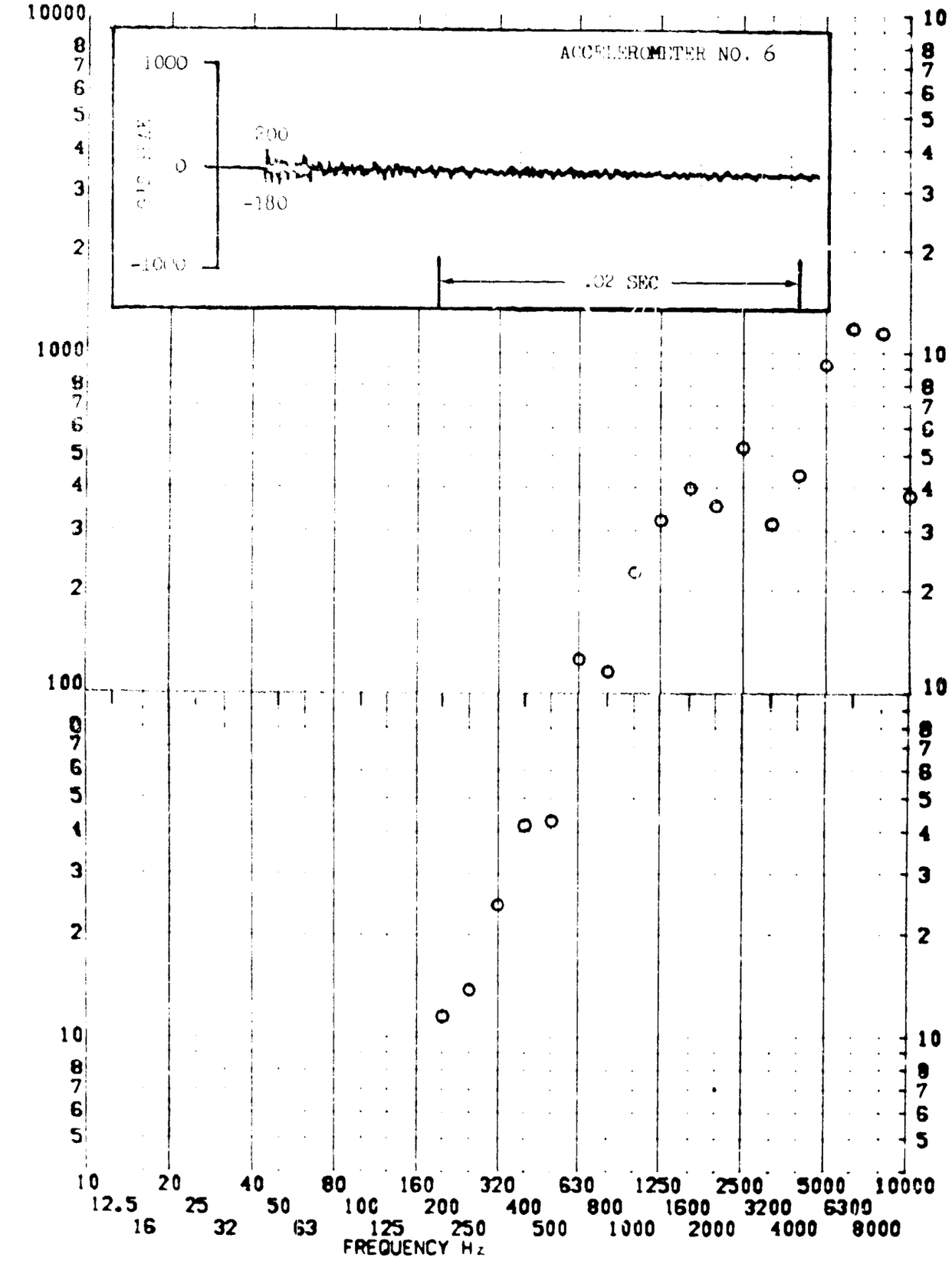

SHOCK TEST ANALYSIS DATA SHEET NO. II.A.7.5

TEST ITEM [illegible] PART NO. STRUCTURE

SERIAL NO. TEST DATE 11 FEB 1969

RESPONSE G-S SHOCK AXIS [illegible] SHOCK NO. 2

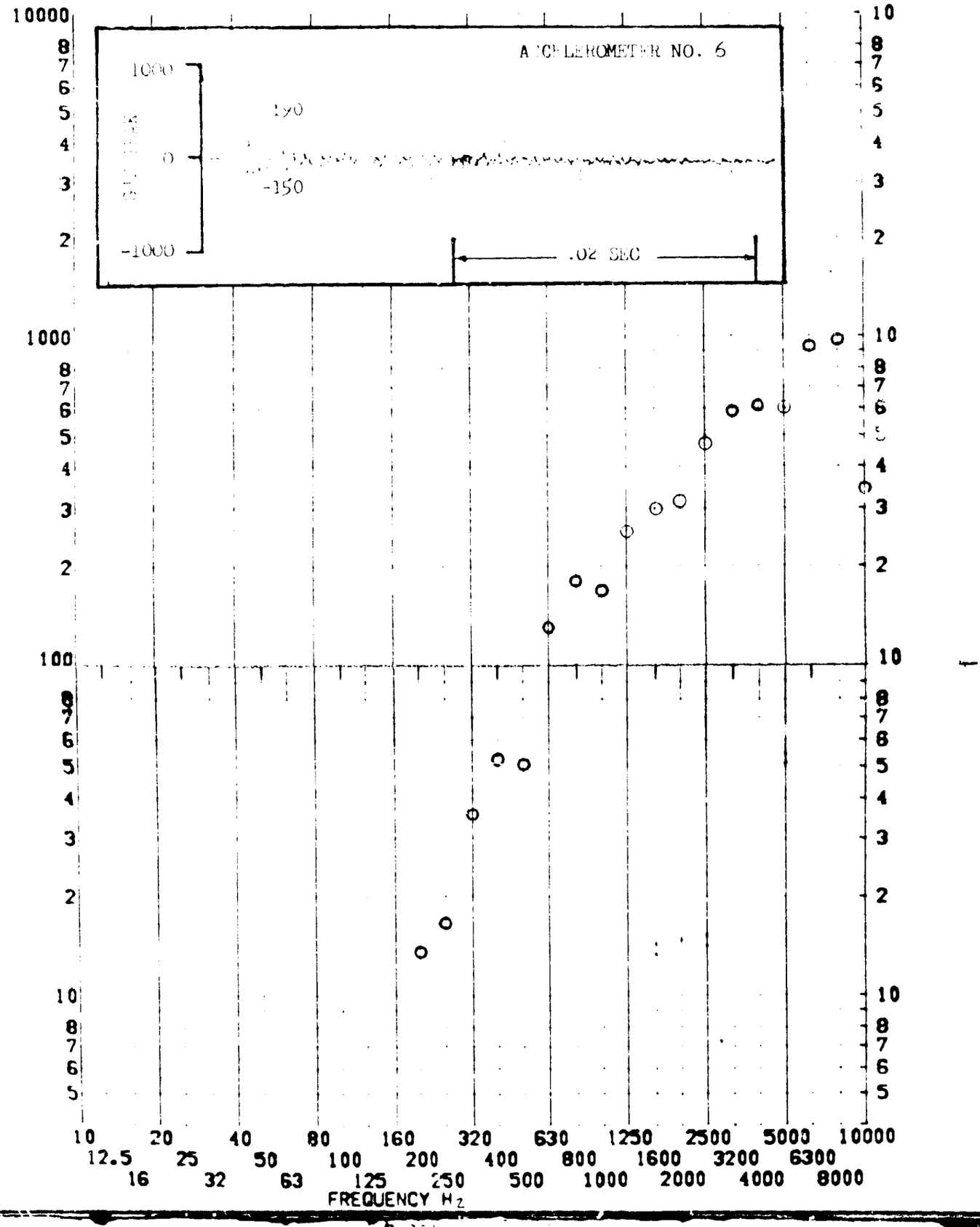

SHOCK TEST ANALYSIS DATA SHEET NO. II.A.7.56

TEST ITEM 1377-[illegible] PART NO. STRUCTURE

SERIAL NO. — TEST DATE 11 FEB 1969

SHOCK AXIS AXIAL SHOCK NO. 1 & 2

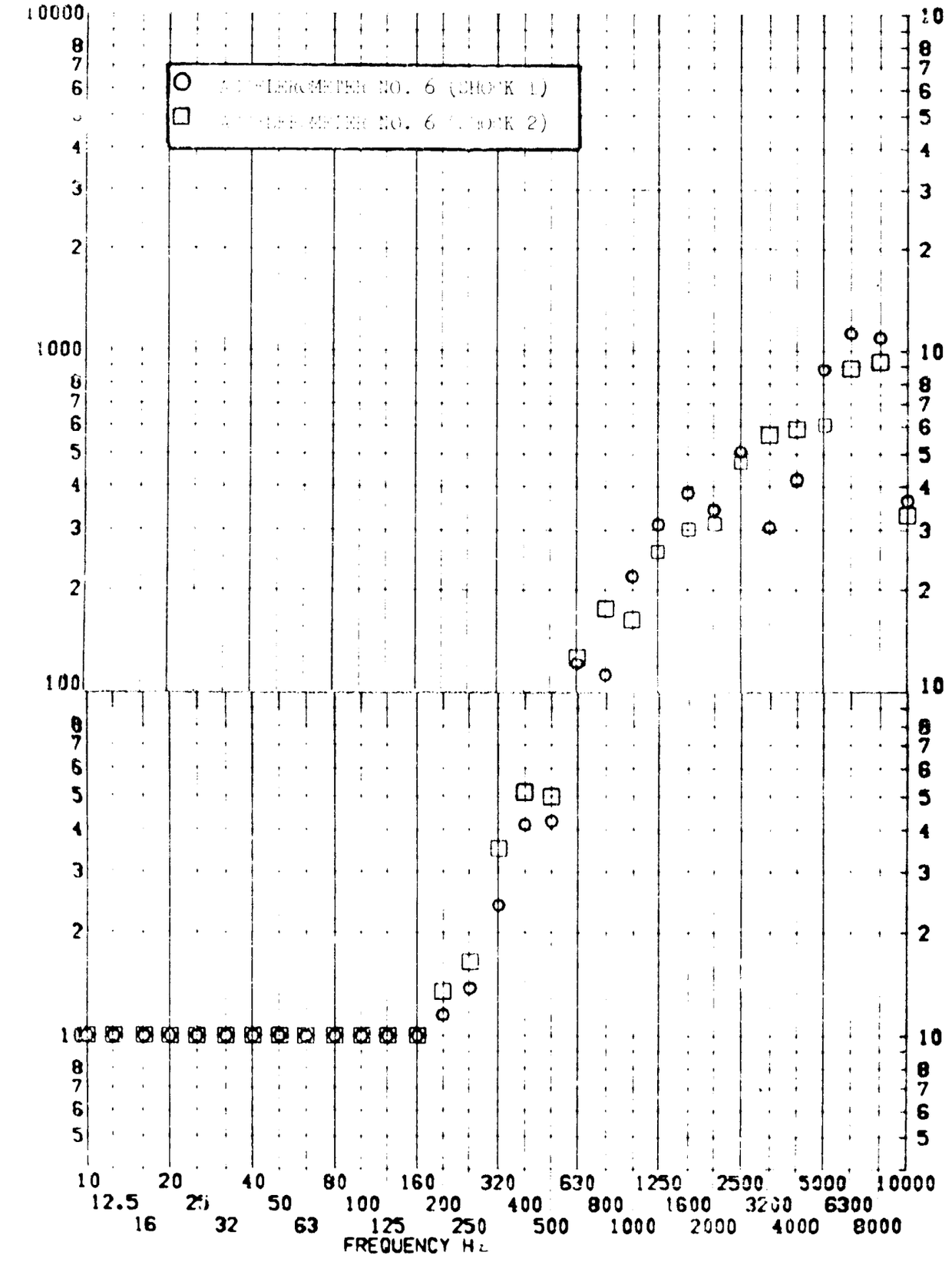

SHOCK TEST ANALYSIS DATA SHEET NO. II.A.7.57

TEST ITEM 377-45 PART NO. STRUCTURE

SERIAL NO. TEST DATE 11 FEB 1962

RESPONSE G-S SHOCK AXIS LONGITUDINAL SHOCK NO. 1

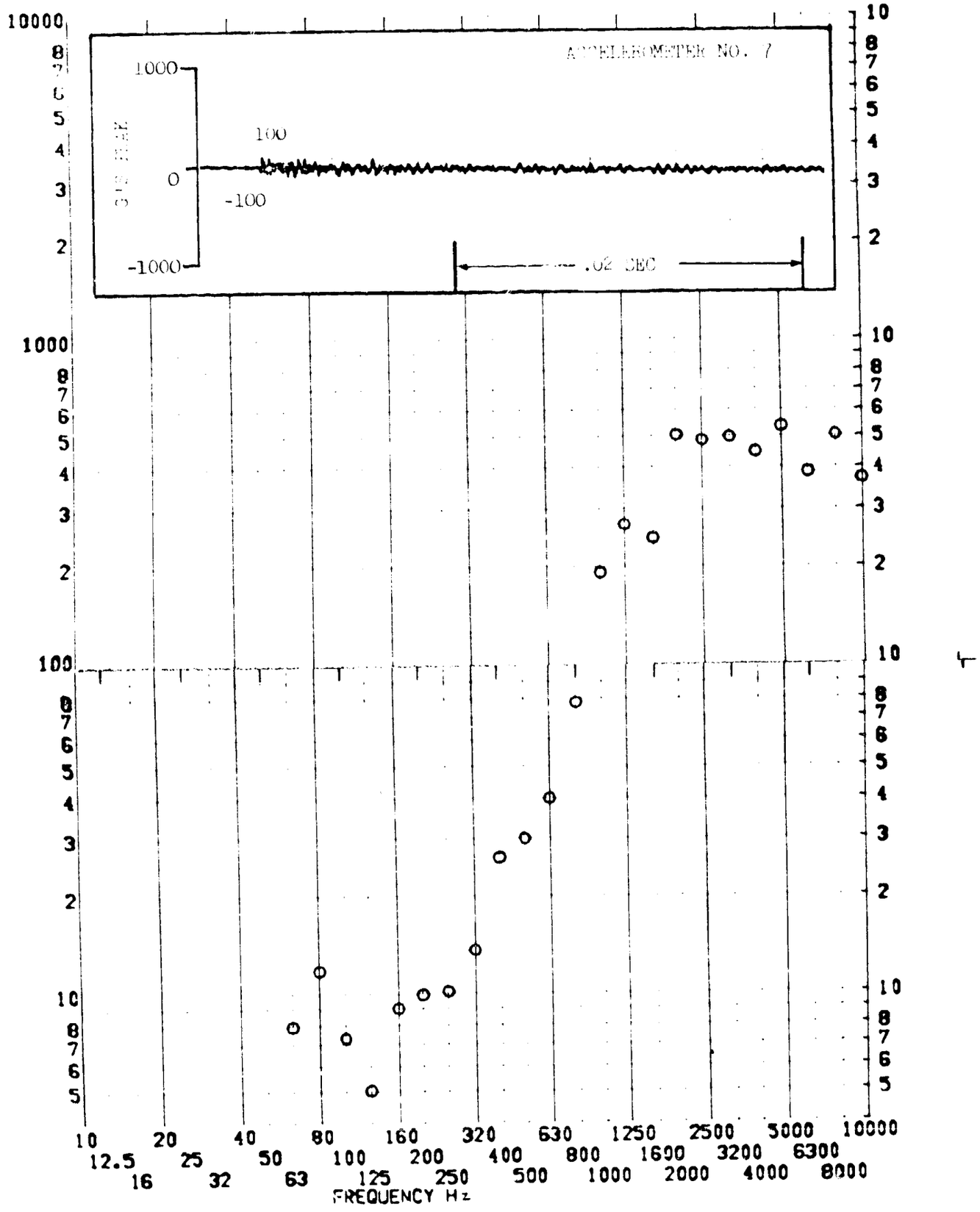

SHOCK TEST ANALYSIS DATA SHEET NO. II.A.7.58

TEST ITEM 1377-474
SERIAL NO.
SHOCK AXIS LONGITUDINAL

PART NO. STRUCTURE
TEST DATE 11 FEB 1969
SHOCK NO. 2

RESPONSE G-S

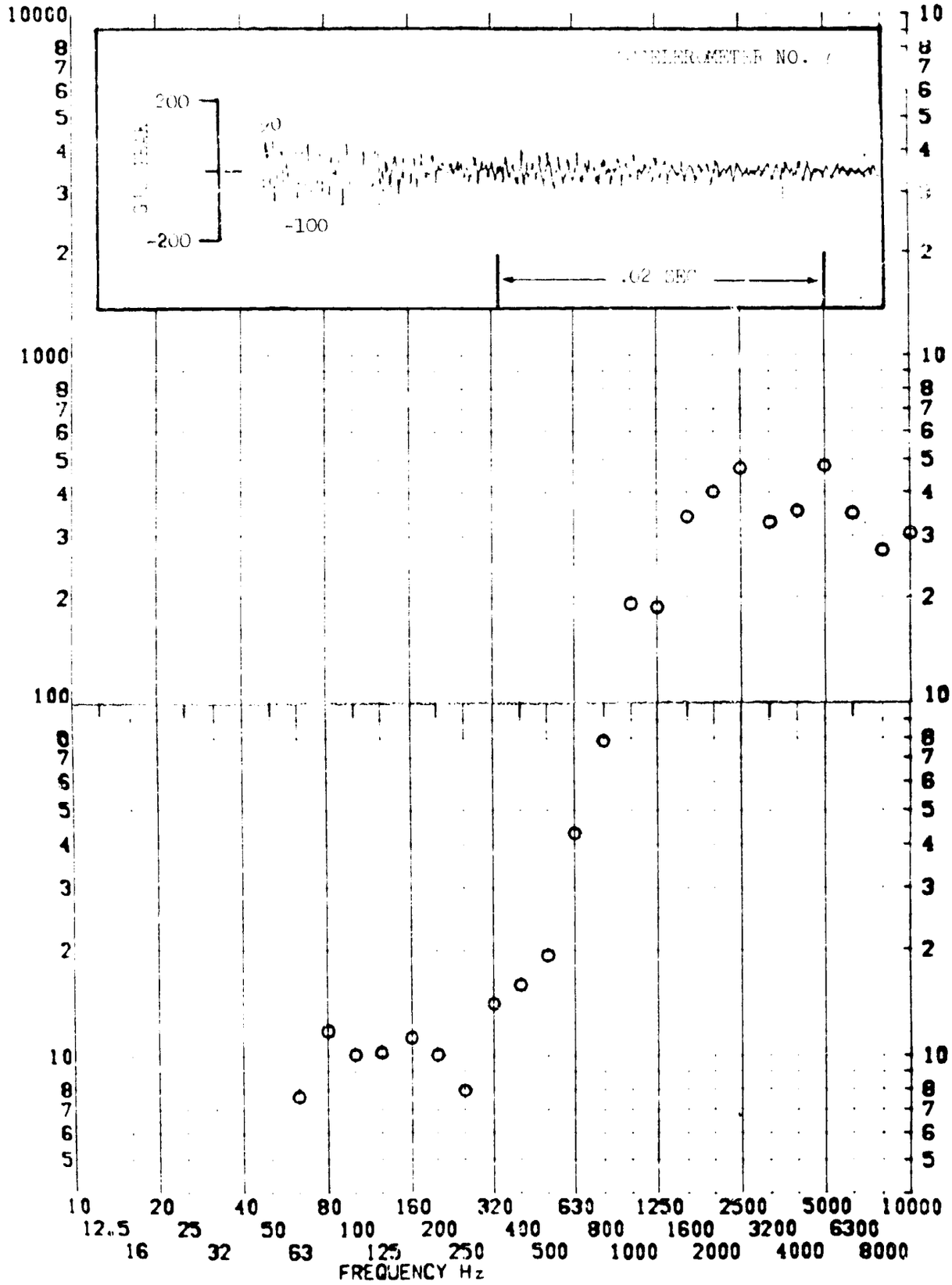

SHOCK TEST ANALYSIS DATA SHEET NO. II.A...59

TEST ITEM 1377-450,474 PART NO. STRUCTURE
SERIAL NO. TEST DATE 11 FEB 1962
SHOCK AXIS LONGITUDINAL SHOCK NO. 1 & 2

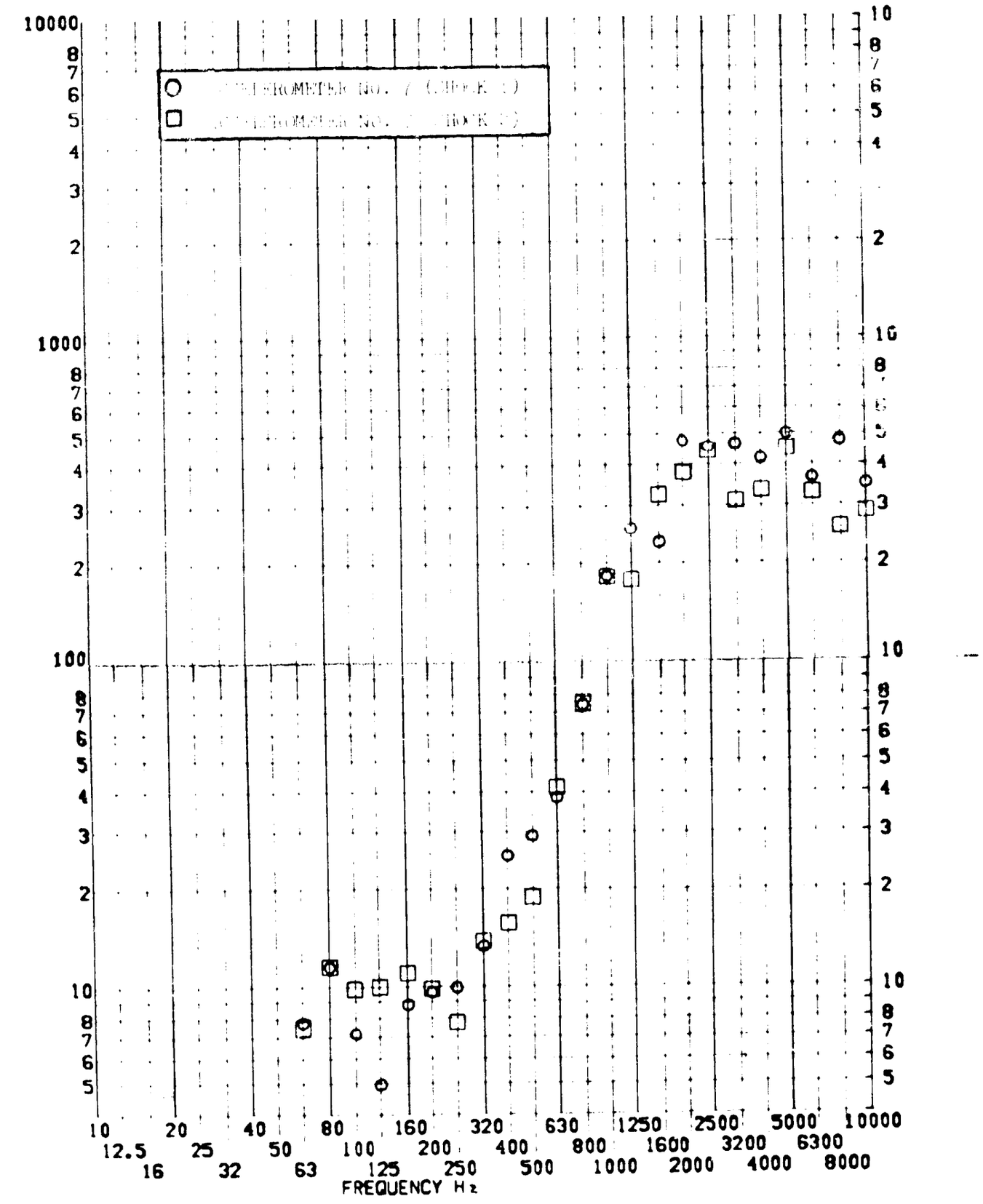

SHOCK TEST ANALYSIS DATA SHEET NO. 11.A.7.60

TEST ITEM 1377-451
SERIAL NO.
SHOCK AXIS RADIAL

PART NO. STRUCTURE
TEST DATE 11 FEB 1969
SHOCK NO. 1

RESPONSE G-S

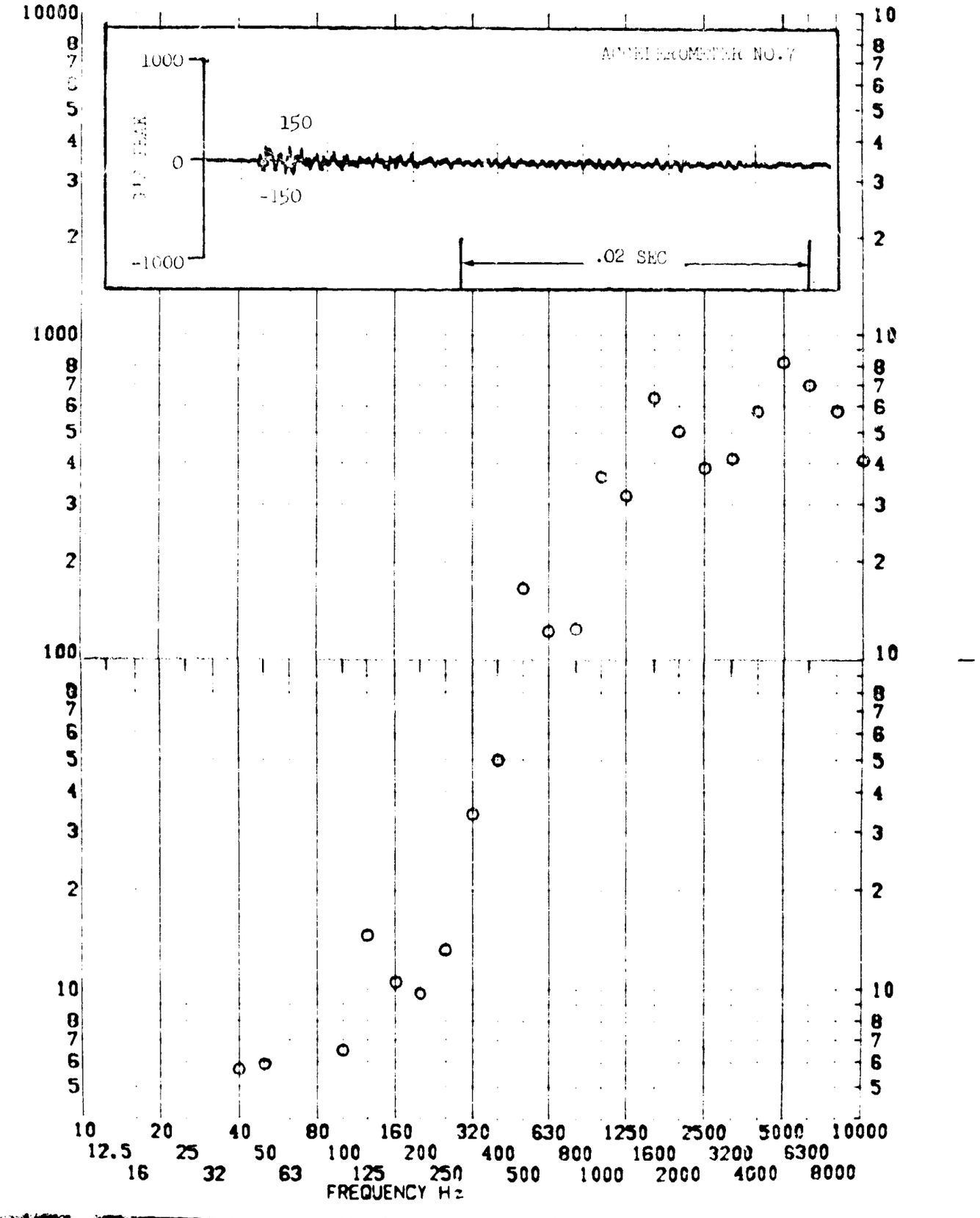

SHOCK TEST ANALYSIS DATA SHEET NO. II.A.7.61

TEST ITEM 1377-475 PART NO. STRUCTURE
SERIAL NO. TEST DATE 13 FEB 1962
SHOCK AXIS RADIAL SHOCK NO. 2

RESPONSE G-S

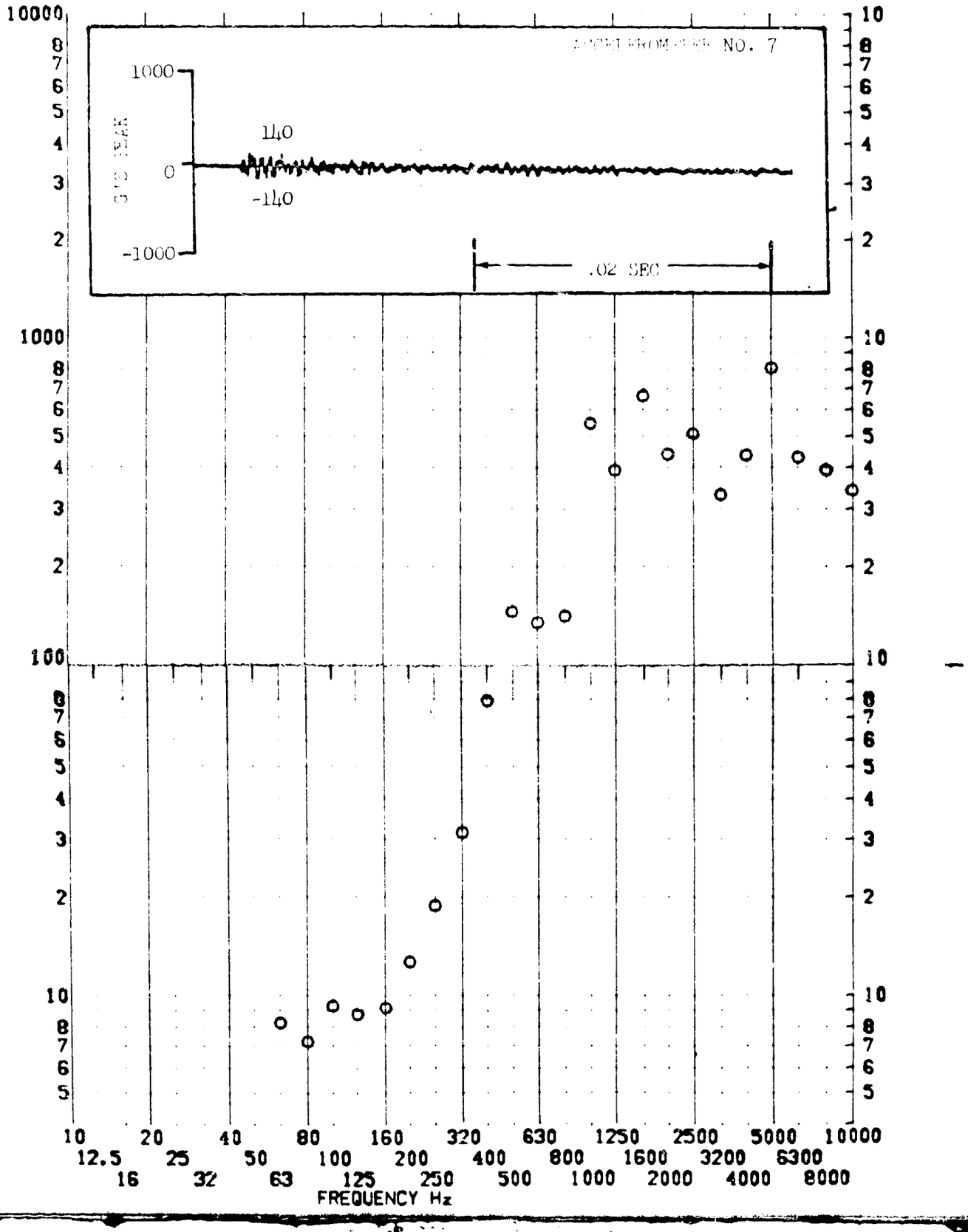

SHOCK TEST ANALYSIS DATA SHEET NO. II.A.7.62

TEST ITEM 1377-451,475 PART NO. STRUCTURE
SERIAL NO. — TEST DATE 11 FEB 1969
SHOCK AXIS RADIAL SHOCK NO. 1 & 2

RESPONSE G-S

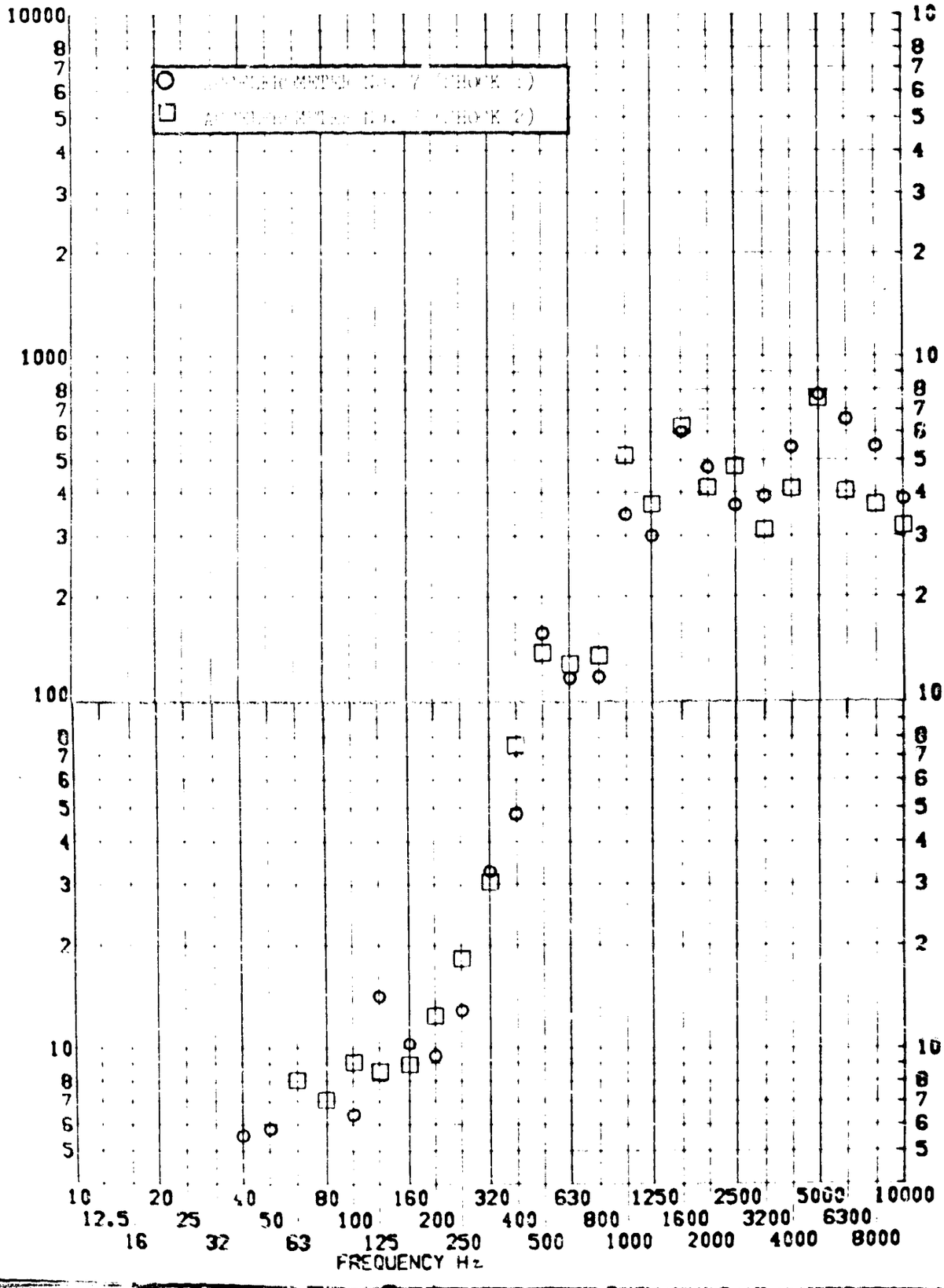

SHOCK TEST ANALYSIS DATA SHEET NO. II.A.7.03

TEST ITEM [illegible] PART NO. STRUCTURE

SERIAL NO. TEST DATE 12 FEB 1969

RESPONSE G-S SHOCK AXIS [illegible] SHOCK NO. 1

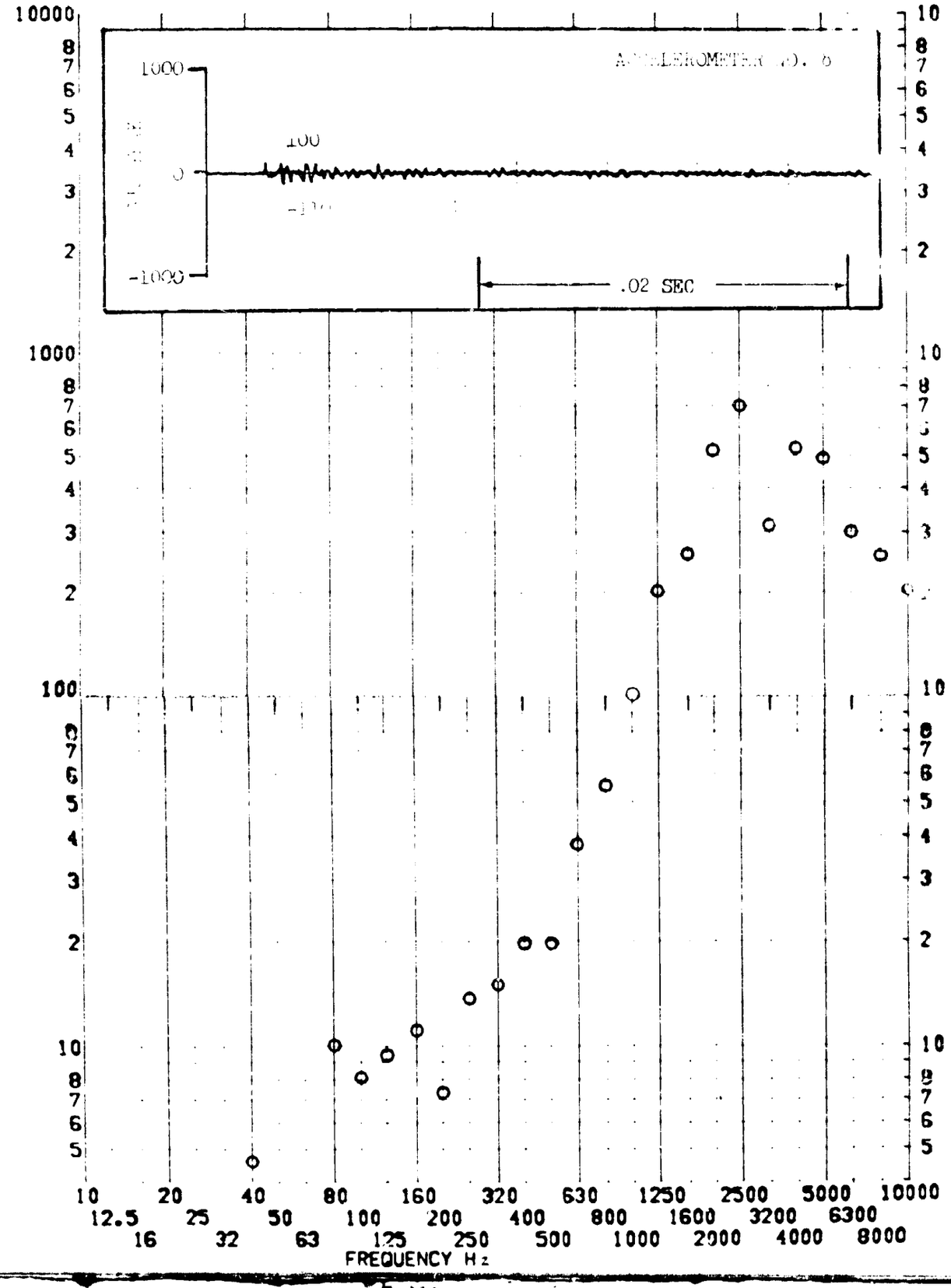

SHOCK TEST ANALYSIS DATA SHEET NO. II.A.7.64

TEST ITEM 377-476
SERIAL NO.
SHOCK AXIS LONGITUDINAL

PART NO. STRUCTURE
TEST DATE 11 FEB 1969
SHOCK NO. 2

RESPONSE G-S

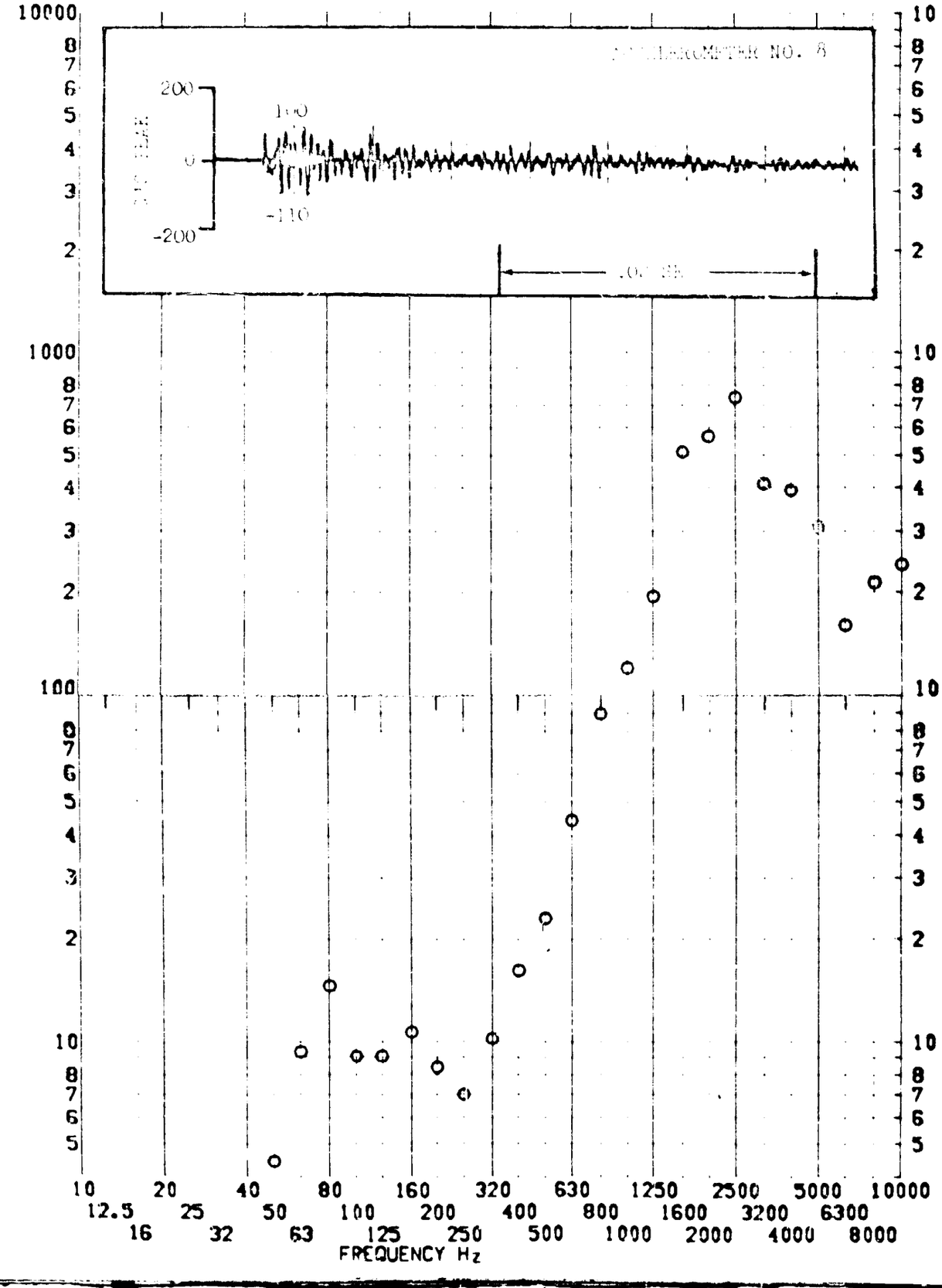

SHOCK TEST ANALYSIS DATA SHEET NO. II.A.7.65

TEST ITEM 1377-452,476 PART NO. STRUCTURE

SERIAL NO. TEST DATE FEB 1969

SHOCK AXIS LONGITUDINAL SHOCK NO. 1 & 2

RESPONSE G-S

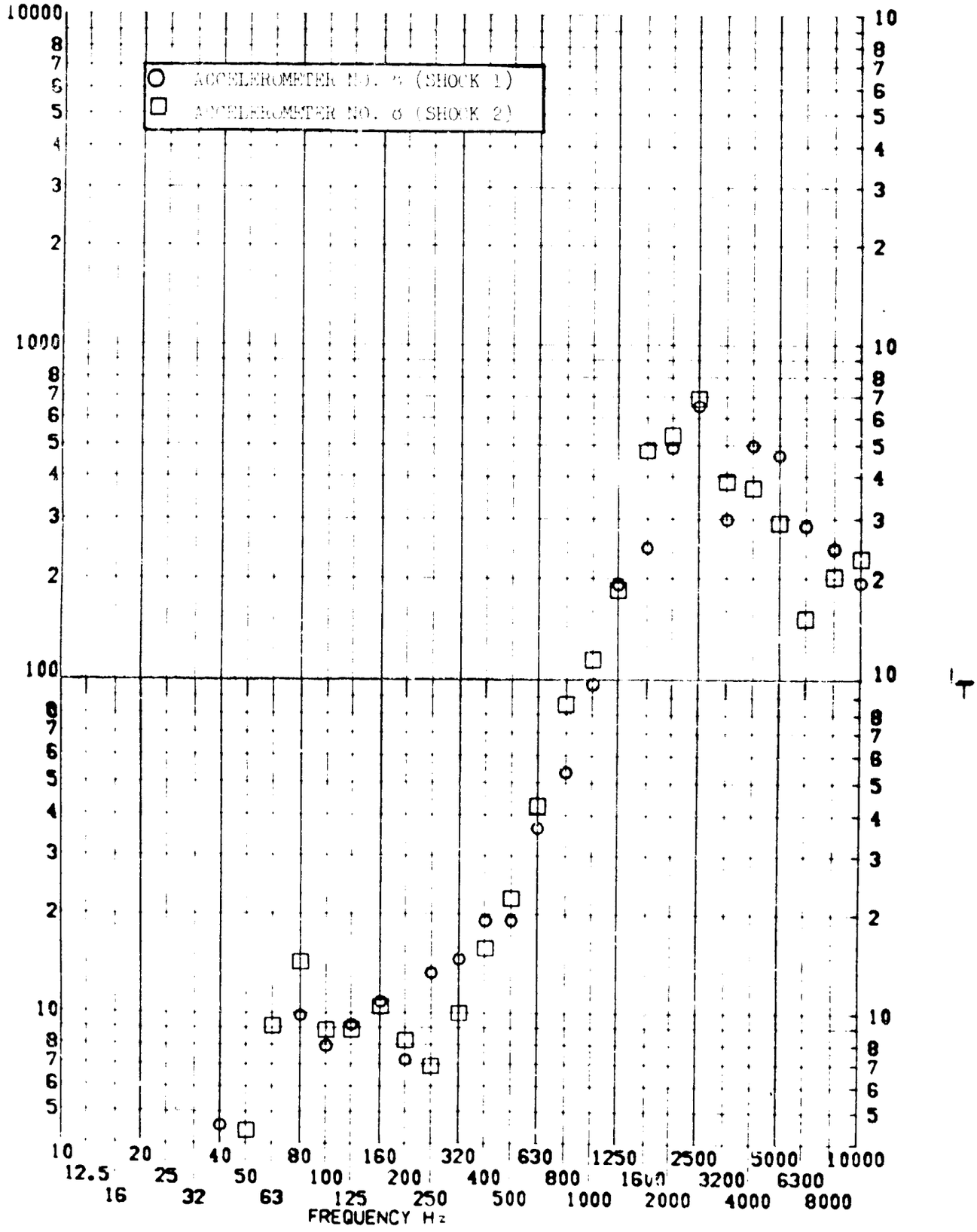

SHOCK TEST ANALYSIS DATA SHEET NO. 11.A./.66

TEST ITEM 1377-453
SERIAL NO.
SHOCK AXIS AXIAL

PART NO. STRUCTURE
TEST DATE 11 FEB 1967
SHOCK NO. 1

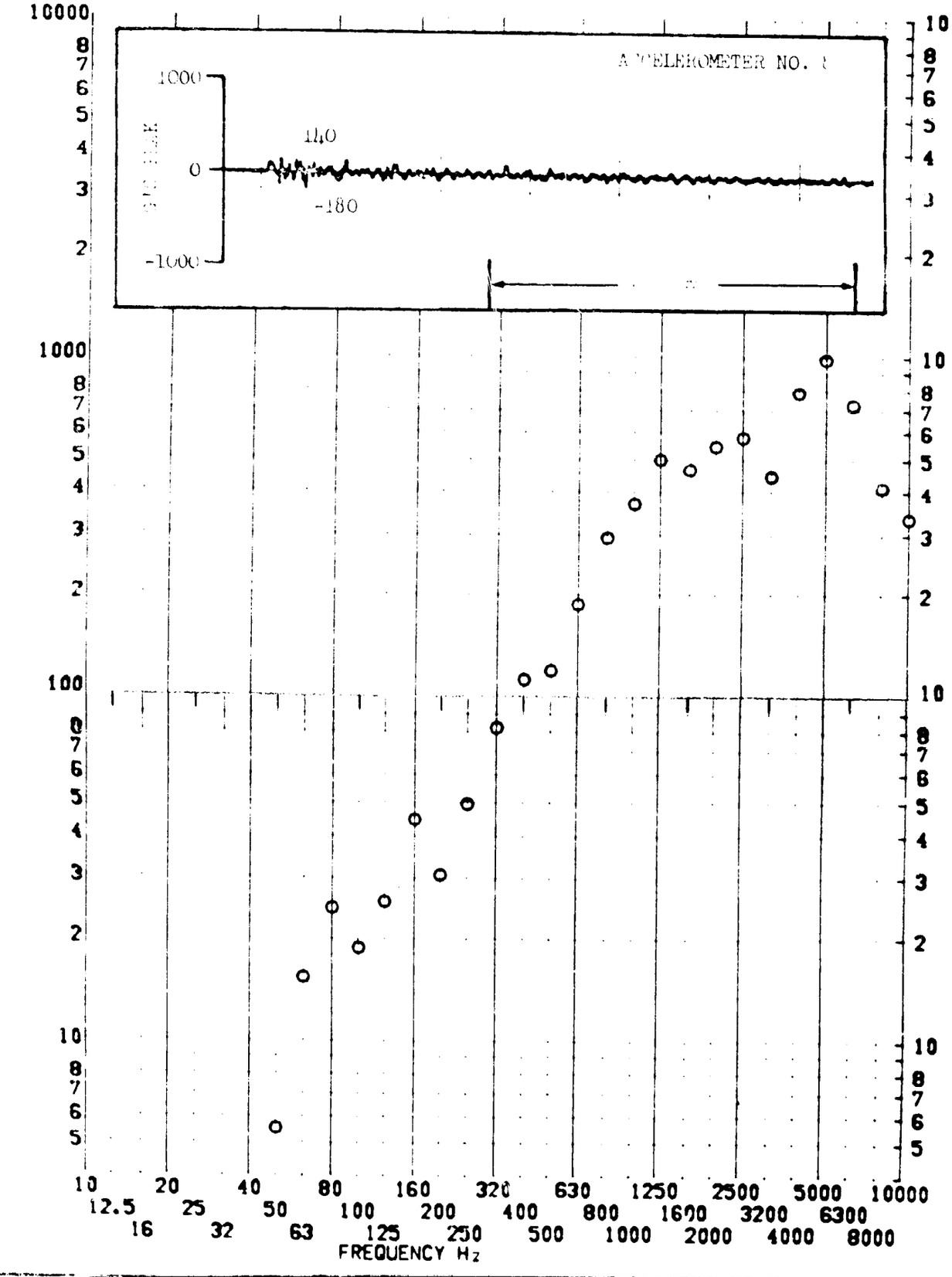

SHOCK TEST ANALYSIS DATA SHEET NO. II.A.7.67

TEST ITEM 137-477
SERIAL NO.
SHOCK AXIS [illegible]

PART NO. STRUCTURE
TEST DATE 11 FEB 1969
SHOCK NO. 2

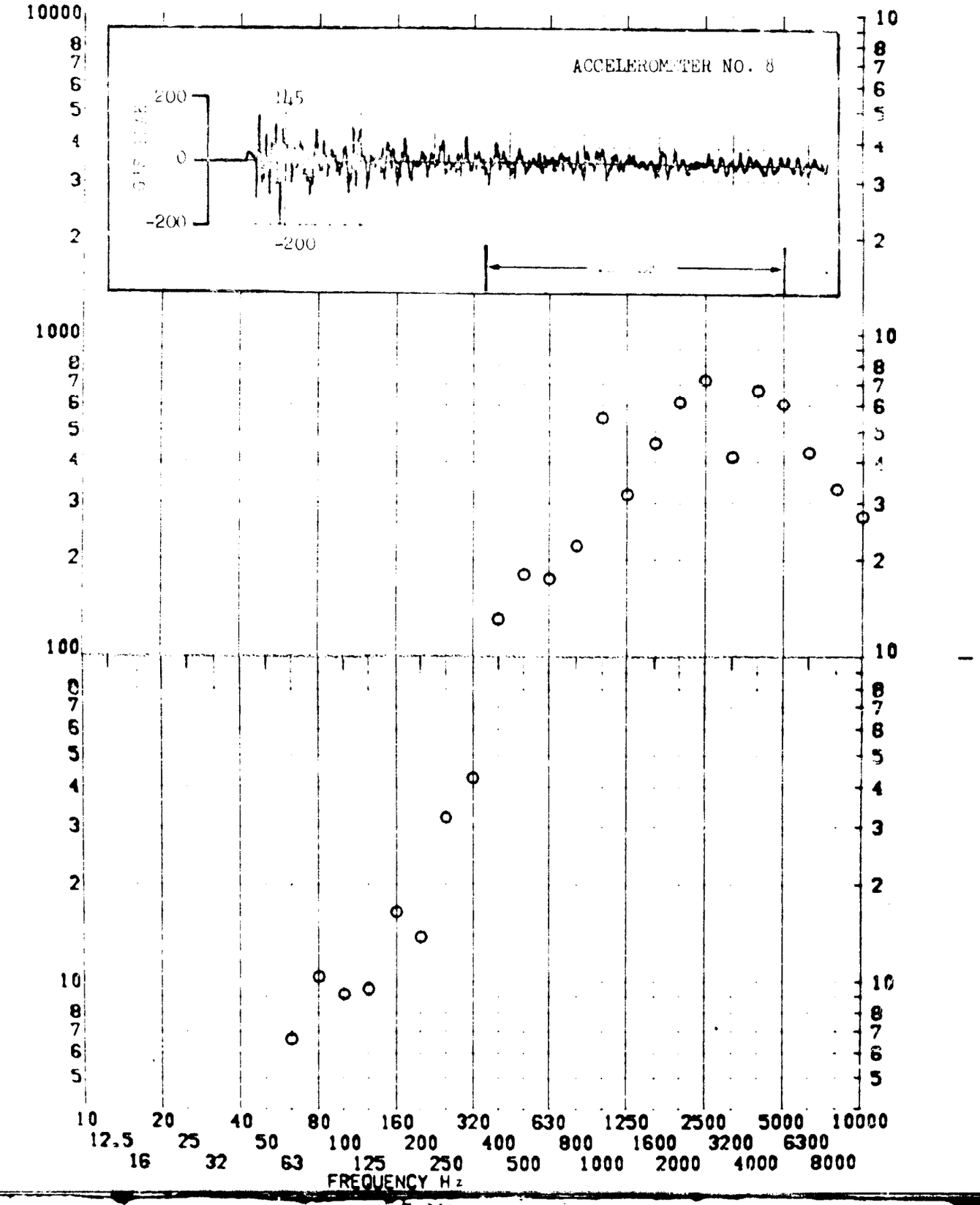

SHOCK TEST ANALYSIS DATA SHEET NO. II.A.7.68

TEST ITEM 1377-453.477 PART NO. STRUCTURE
SERIAL NO. — TEST DATE 11 FEB 1969
SHOCK AXIS RADIAL SHOCK NO. 2

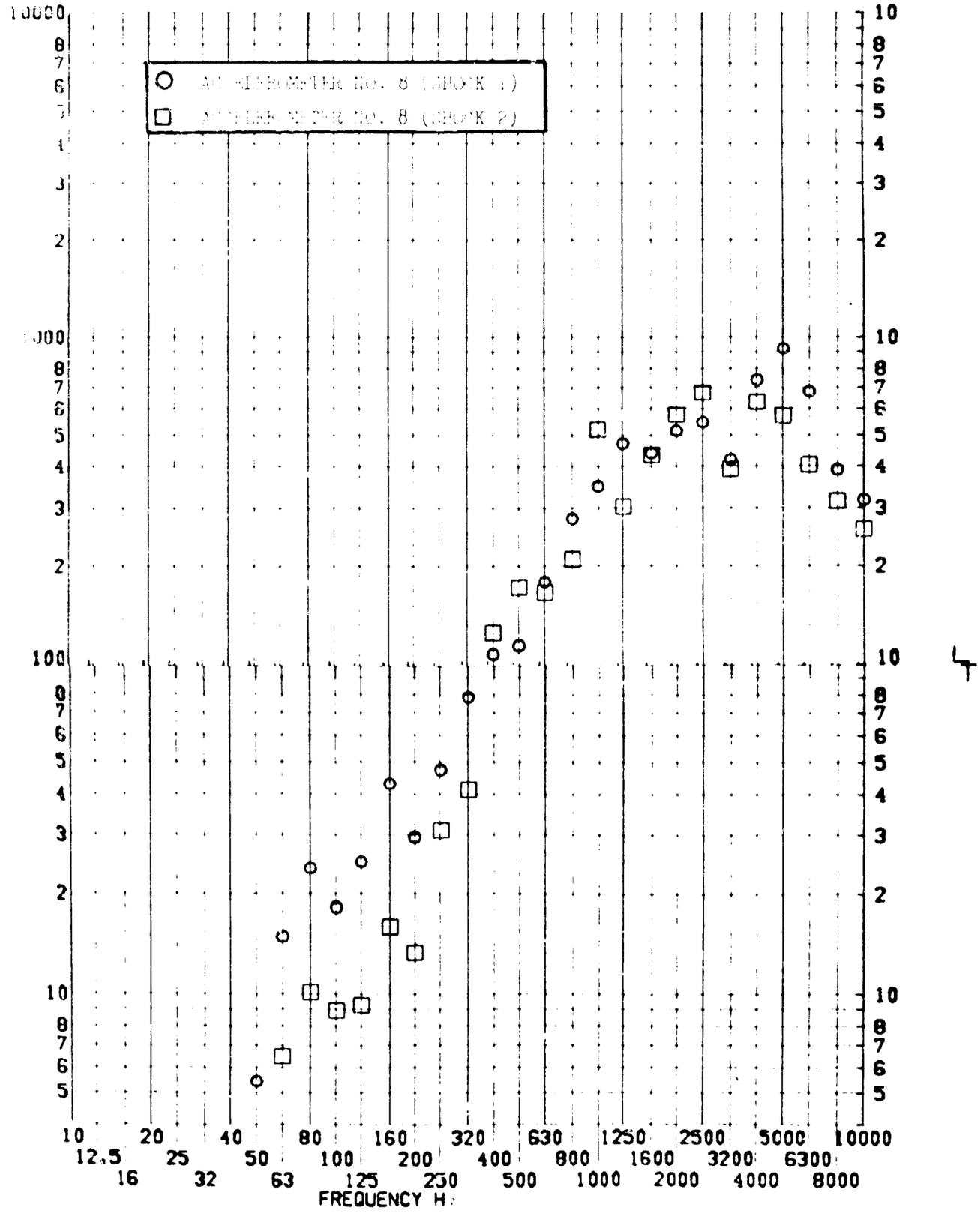

SHOCK TEST ANALYSIS DATA SHEET NO. II.A.7.69

TEST ITEM 377-451
SERIAL NO.
SHOCK AXIS LONGIT[illegible]

PART NO. STRUCTURE
TEST DATE 11 FEB 1962
SHOCK NO. 2

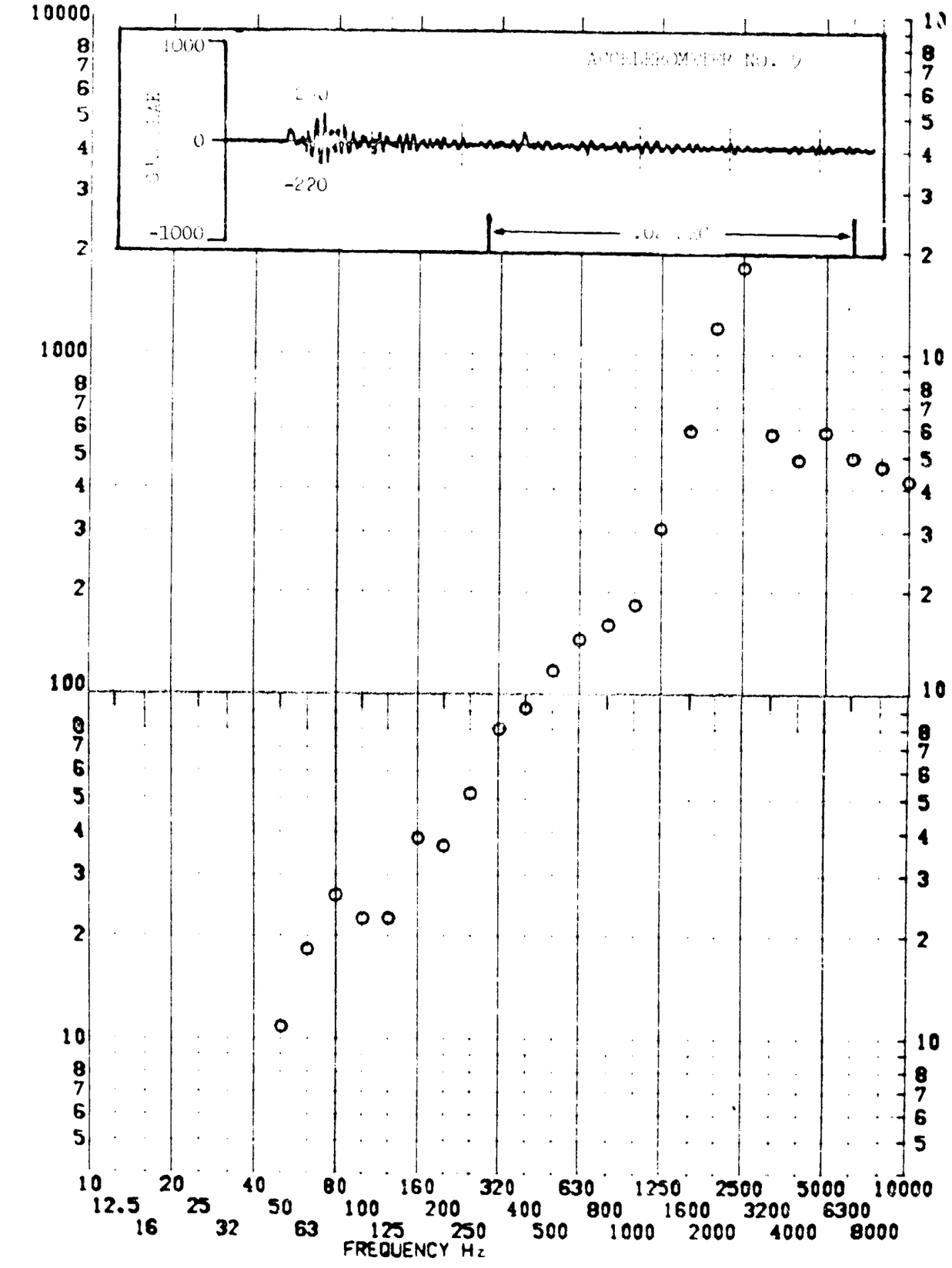

SHOCK TEST ANALYSIS DATA SHEET NO. II.A.7.70

STRUCTURE

TEST ITEM 1377-478

SERIAL NO.

SHOCK AXIS LONGITUDINAL

PART NO.

TEST DATE 11 FEB 1969

SHOCK NO. 4

RESPONSE G-S

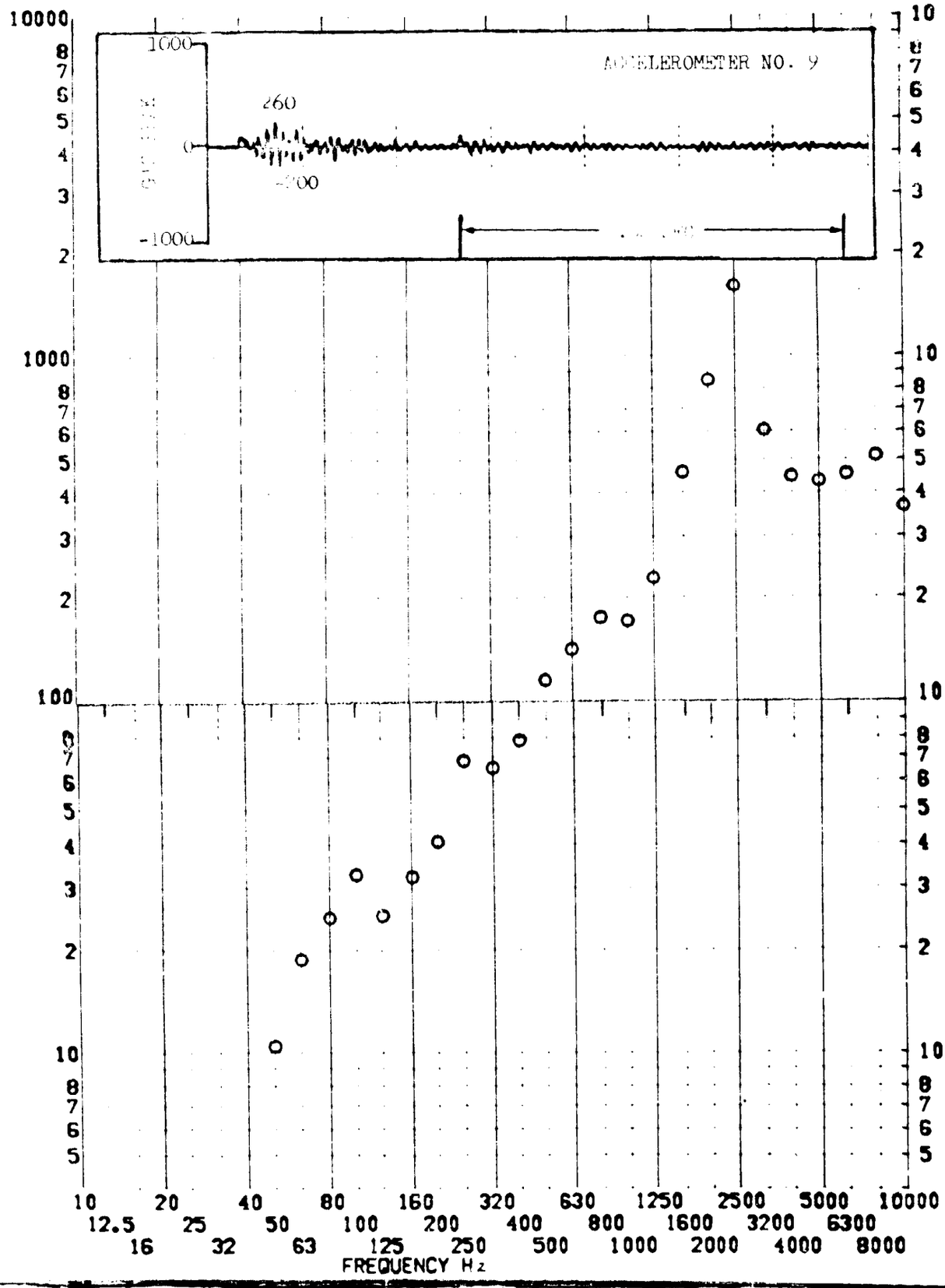

SHOCK TEST ANALYSIS DATA SHEET NO. H.A.F.71

TEST ITEM 1377-454,428 PART NO. ST30[illegible]
SERIAL NO. TEST DATE 1 FEB 1[illegible]
SHOCK AXIS LONGITUDINAL SHOCK NO. 1 & 2

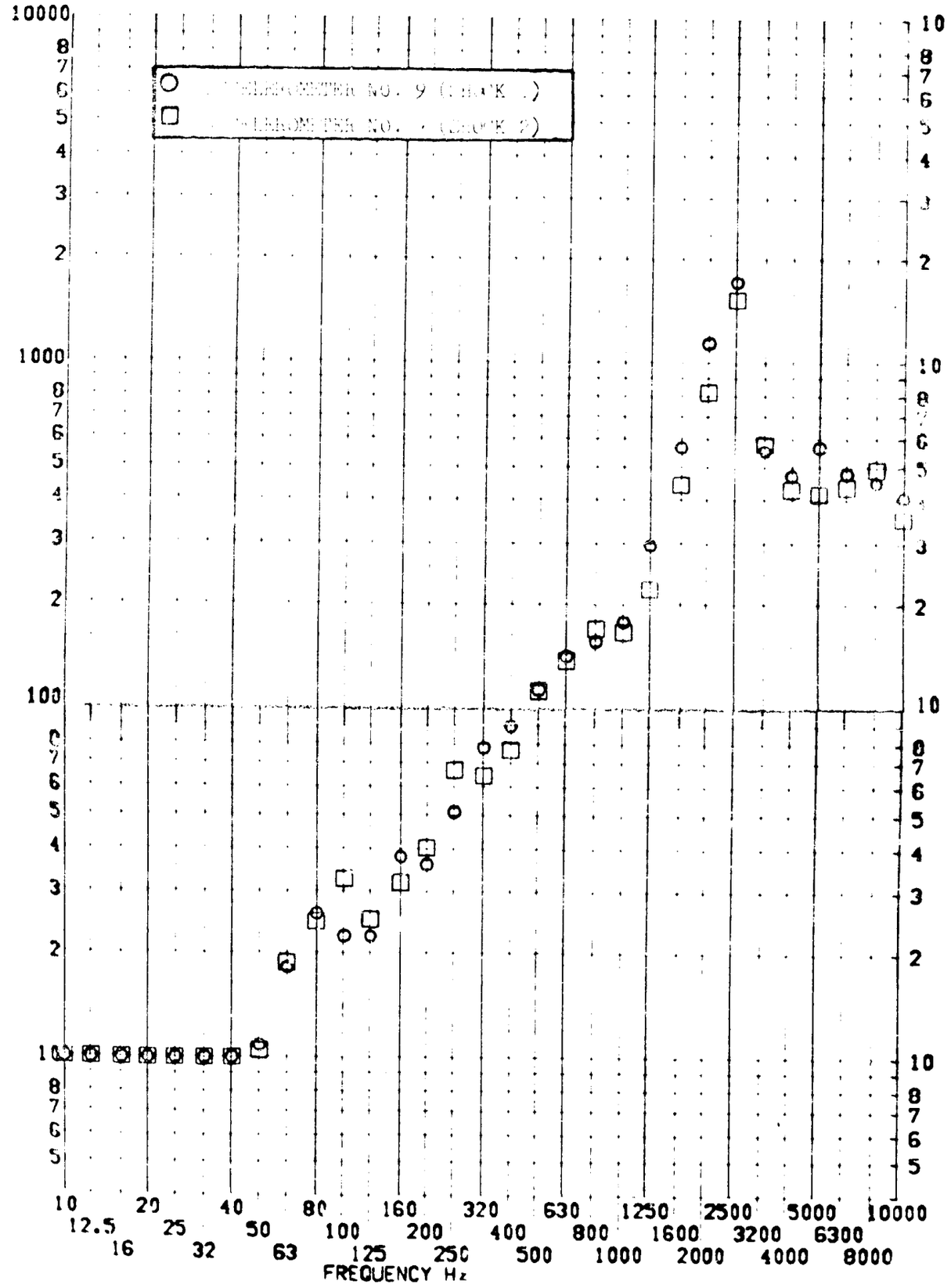

SHOCK TEST ANALYSIS DATA SHEET NO. II.A.7.7?

TEST ITEM [illegible] PART NO. STRUCTURE

SERIAL NO. [illegible] TEST DATE [illegible]

RESPONSE G-S SHOCK AXIS [illegible] SHOCK NO. [illegible]

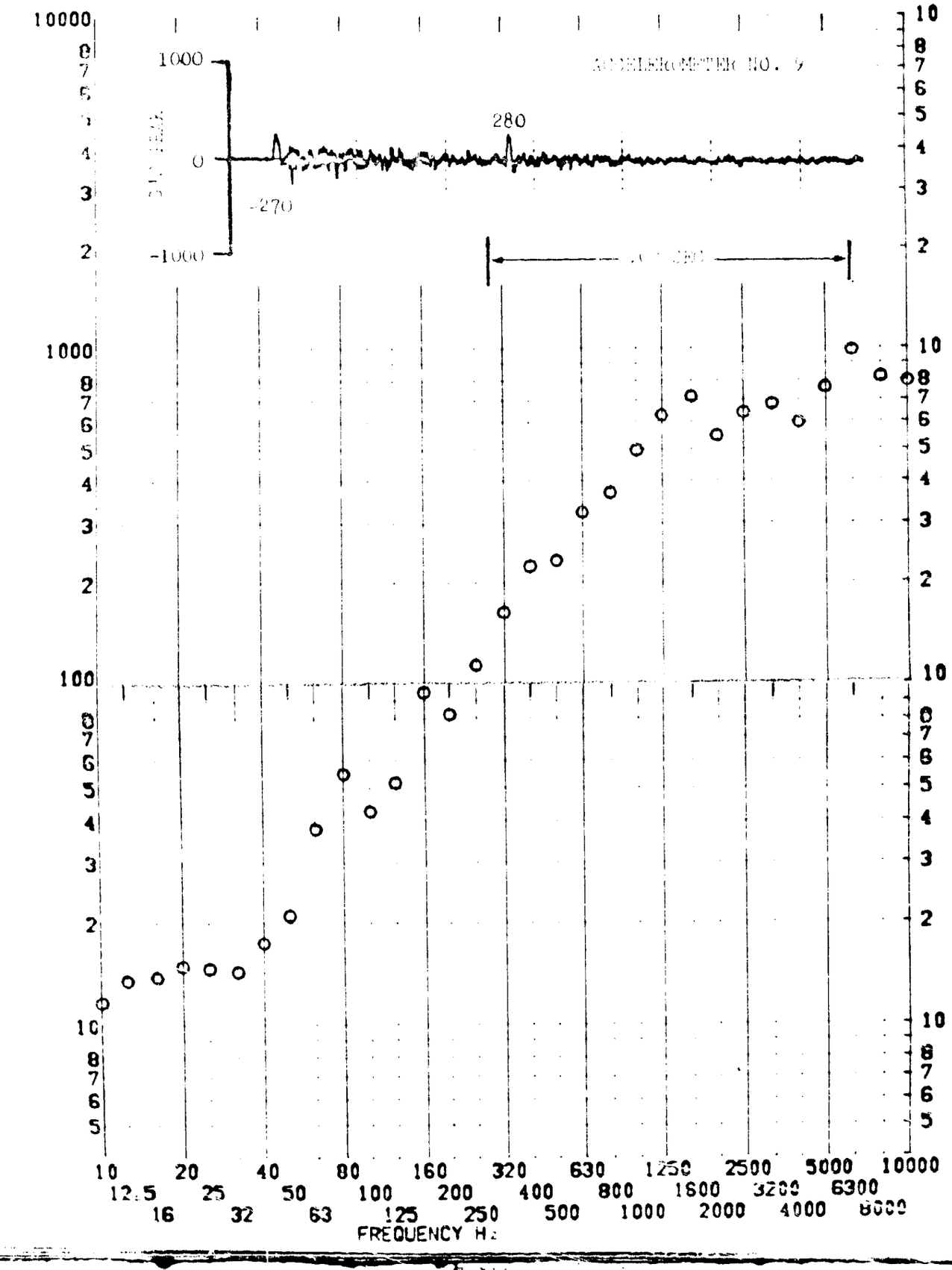

SHOCK TEST ANALYSIS DATA SHEET NO. 11.A.7.73

TEST ITEM 377-477
SERIAL NO.
SHOCK AXIS RADIAL

PART NO. STRUCTURE
TEST DATE 11 FEB 1969
SHOCK NO. 2

RESPONSE G-S

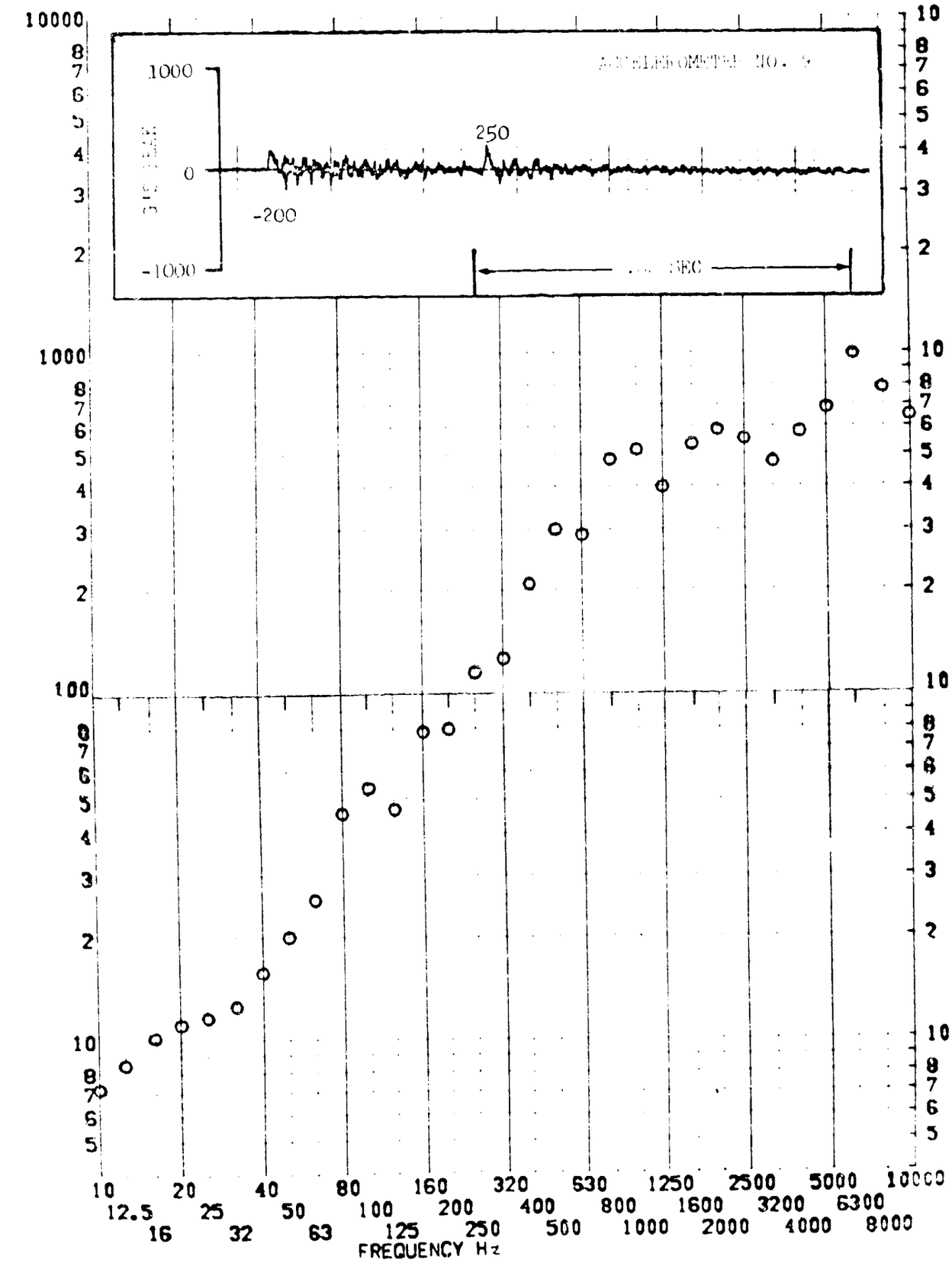

SHOCK TEST ANALYSIS DATA SHEET NO. II.A.7.74

TEST ITEM 1377-455,479 PART NO. STRUCTURE

SERIAL NO. — TEST DATE 11 FEB 1969

RESPONSE G-S SHOCK AXIS [illegible] SHOCK NO. [illegible] 2

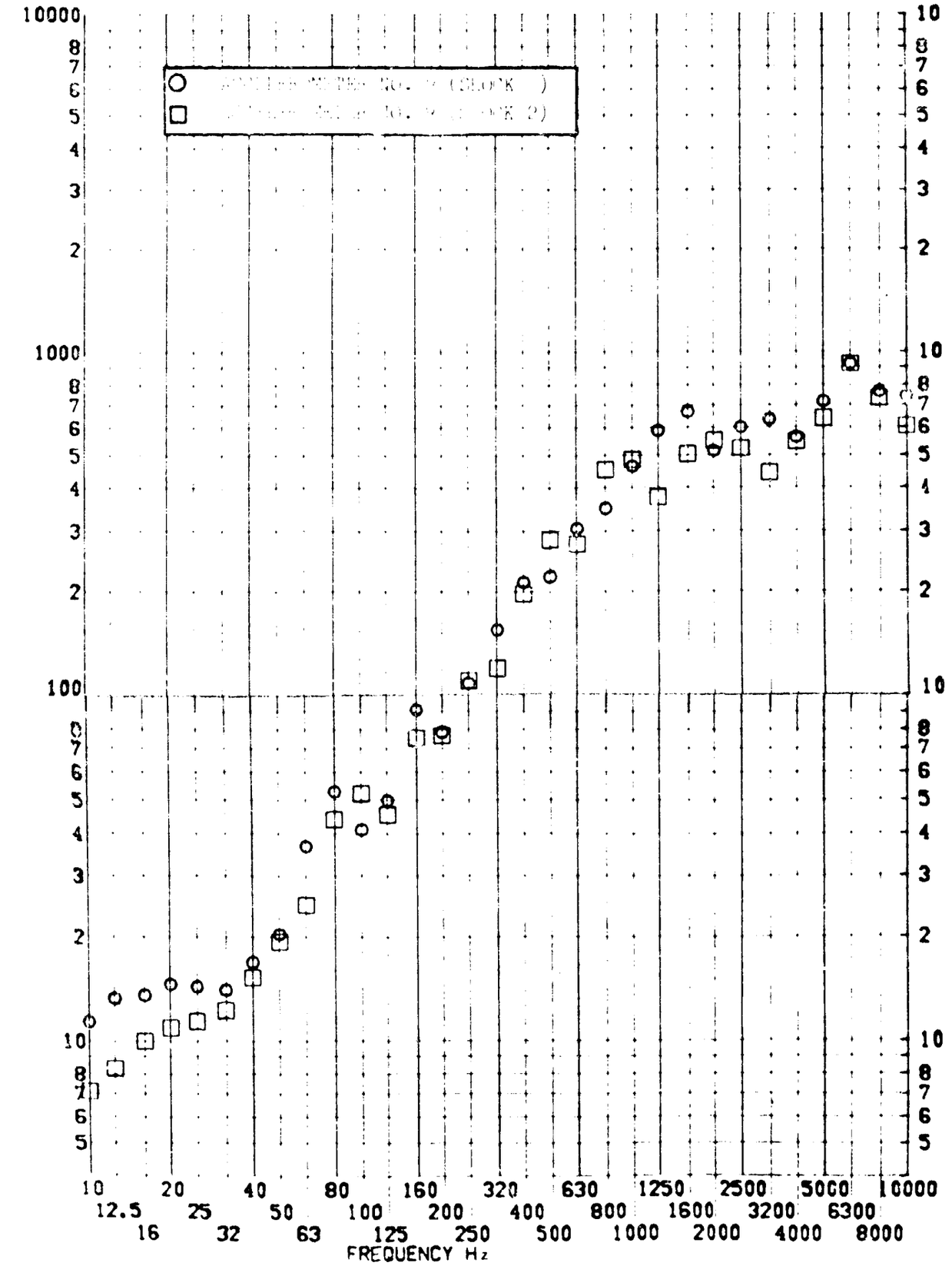

SHOCK TEST ANALYSIS DATA SHEET NO. [illegible]

TEST ITEM [illegible]
SERIAL NO. —
SHOCK AXIS [illegible]

PART NO. [illegible]
TEST DATE [illegible]
SHOCK NO. 1

RESPONSE G-S

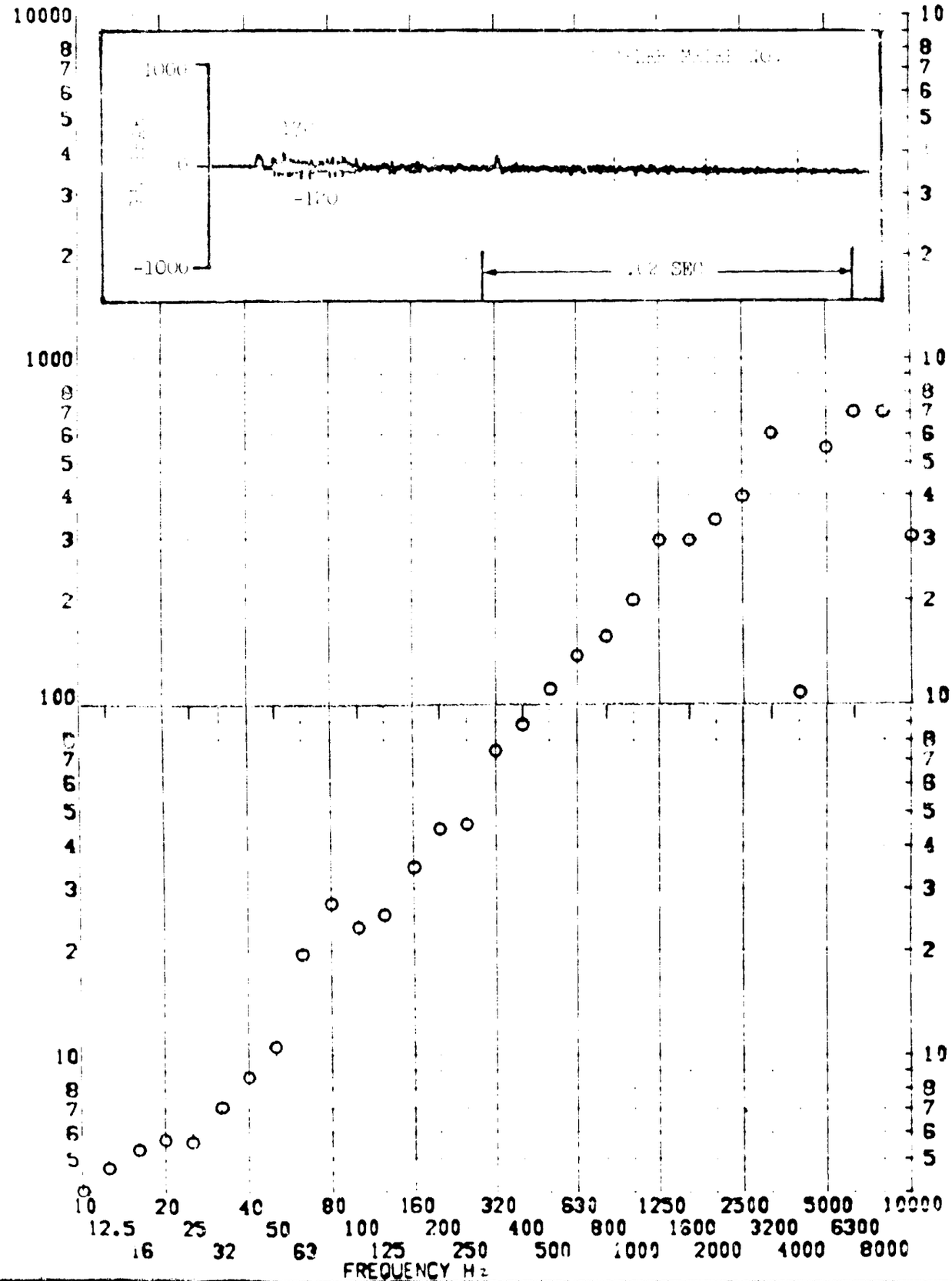

SHOCK TEST ANALYSIS DATA SHEET NO. II.A.7.76

TEST ITEM 1377-4,8 PART NO. STRUCTURE
SERIAL NO. TEST DATE 11 FEB 1969
RESPONSE G-S SHOCK AXIS LONGITUDINAL SHOCK NO. 2

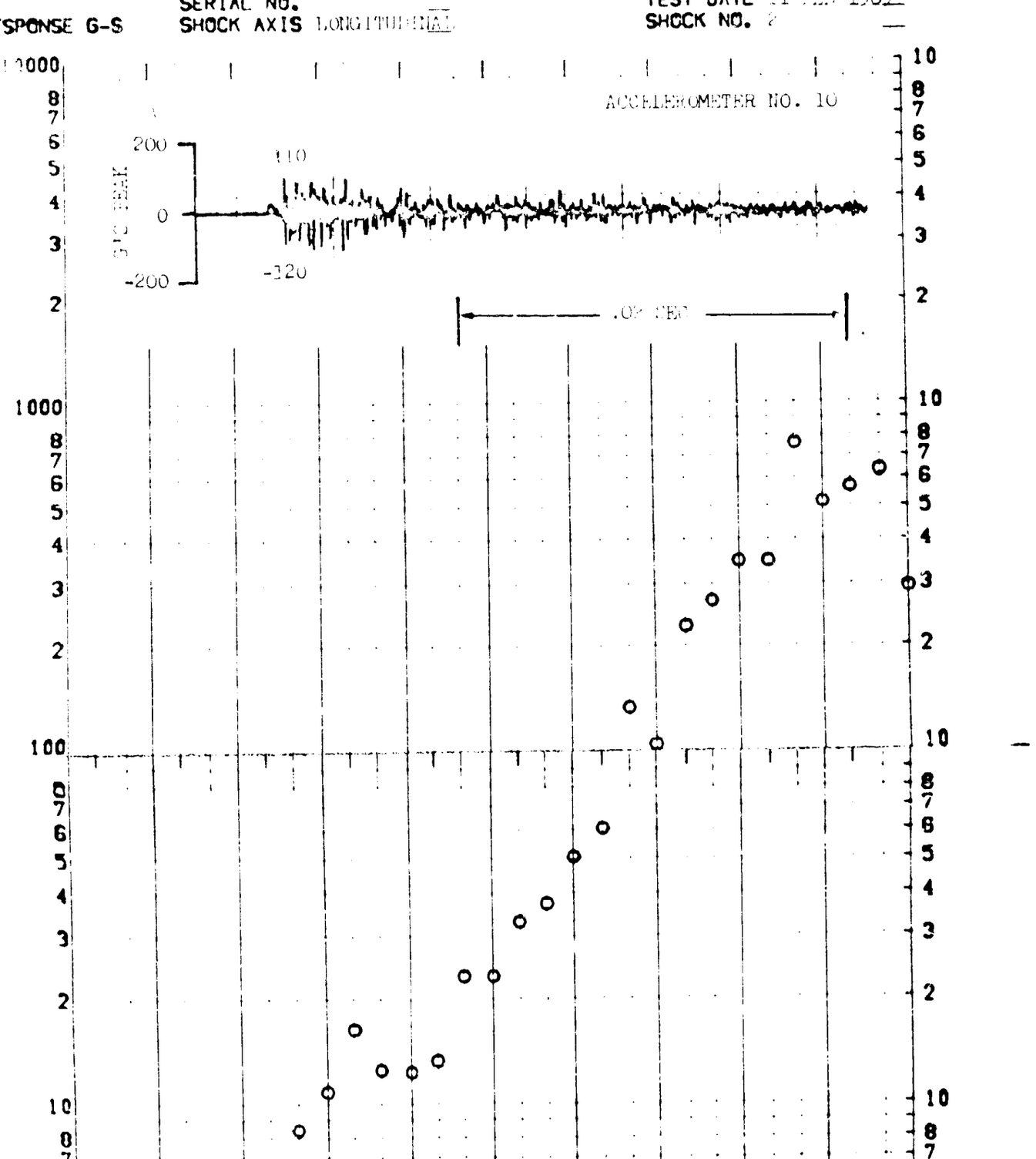

SHOCK TEST ANALYSIS DATA SHEET NO. II.A.7.77

TEST ITEM 1377-456,480 PART NO. STRUCTURE
SERIAL NO. TEST DATE 11 FEB 1969
SHOCK AXIS LONGITUDINAL SHOCK NO. 1 --

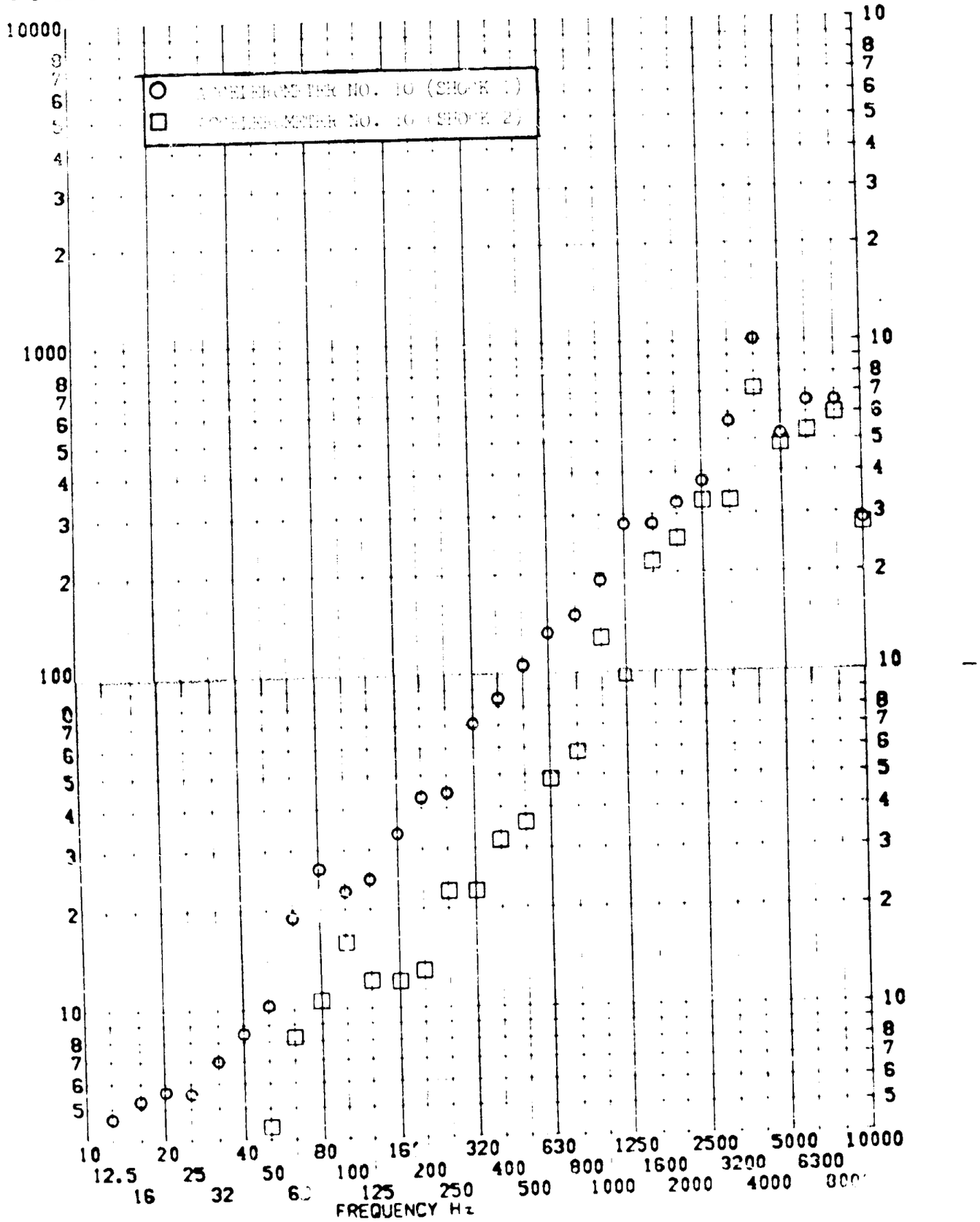

SHOCK TEST ANALYSIS DATA SHEET NO. II.A.7.76

TEST ITEM 1377-[illegible]
SERIAL NO.
SHOCK AXIS [illegible]

PART NO. STRUCTURE
TEST DATE 11 FEB 1969
SHOCK NO. 1

RESPONSE G-S

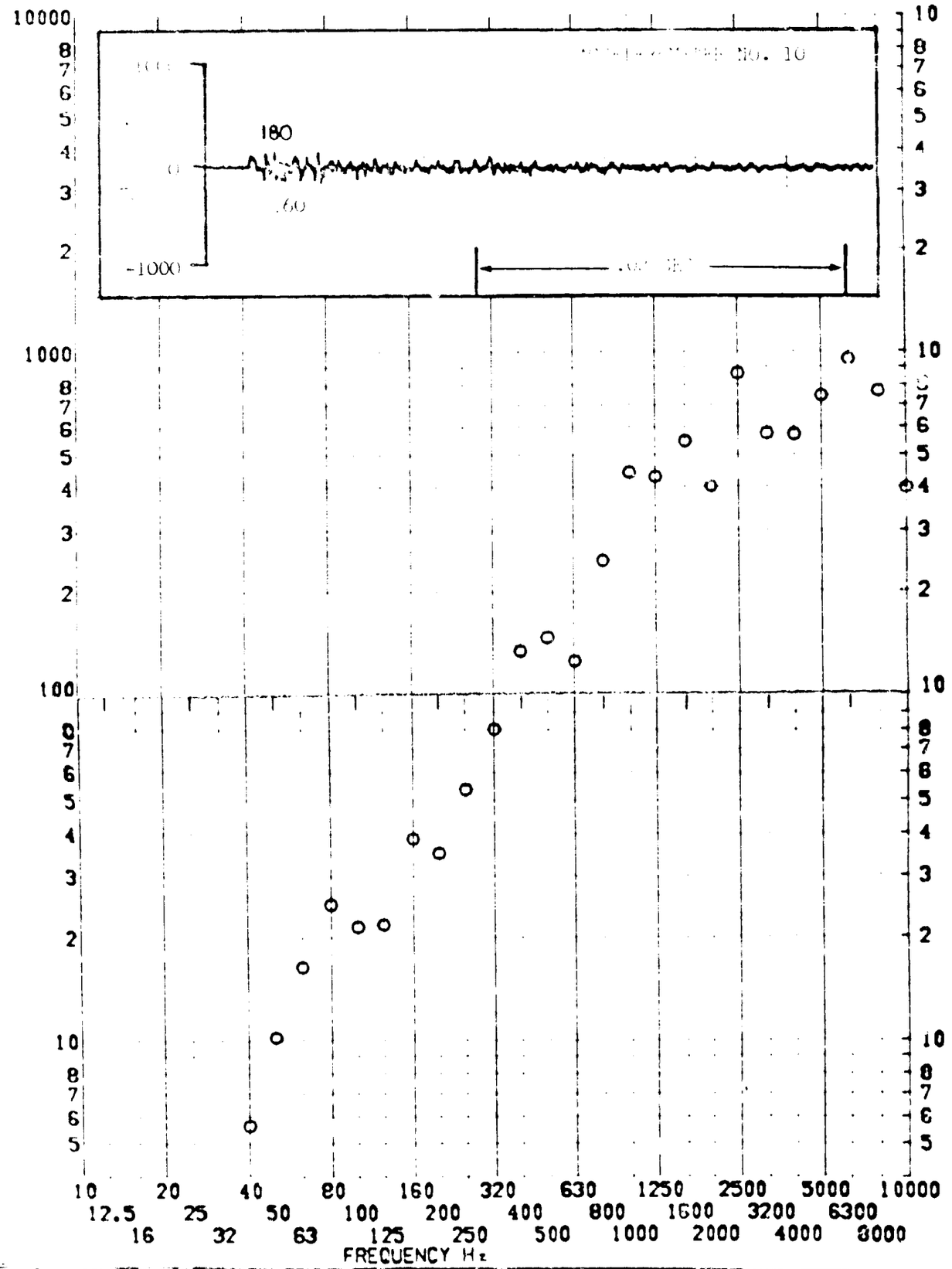

SHOCK TEST ANALYSIS DATA SHEET NO. [illegible]

TEST ITEM [illegible]
SERIAL NO. —
SHOCK AXIS RADIAL

PART NO. STRUCTURE
TEST DATE [illegible]
SHOCK NO. 2

RESPONSE G-S

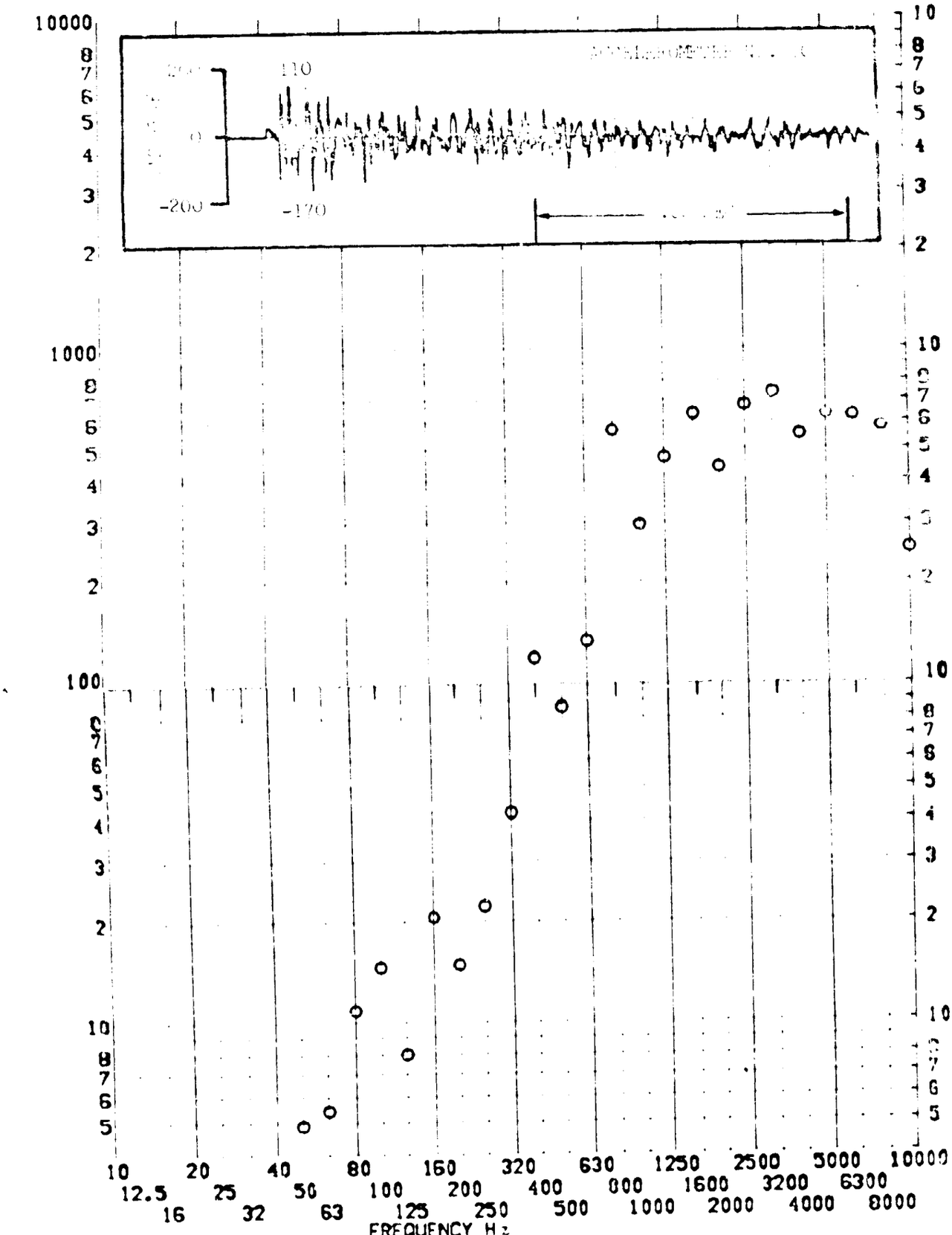

SHOCK TEST ANALYSIS DATA SHEET NO. II.A.7.80

TEST ITEM 377-481,457
SERIAL NO. —
SHOCK AXIS RADIAL —

PART NO. STRUCTURE
TEST DATE 11 FEB 1962
SHOCK NO. — —

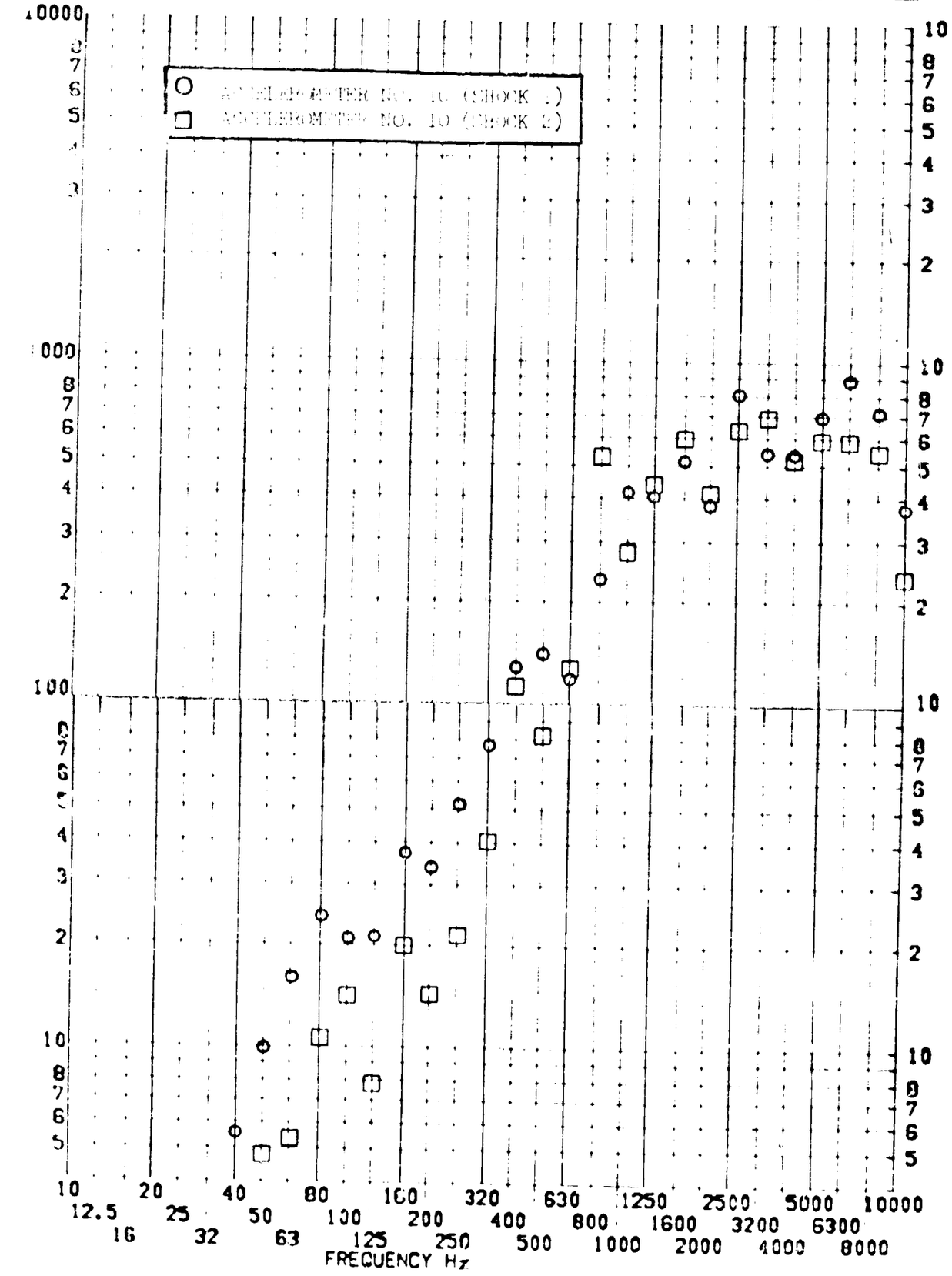

SHOCK TEST ANALYSIS DATA SHEET NO. 11.A.7.81

TEST ITEM [illegible] PART NO. EQUIPMENT

SERIAL NO. TEST DATE [illegible]

RESPONSE G-S SHOCK AXIS RADIAL SHOCK NO.

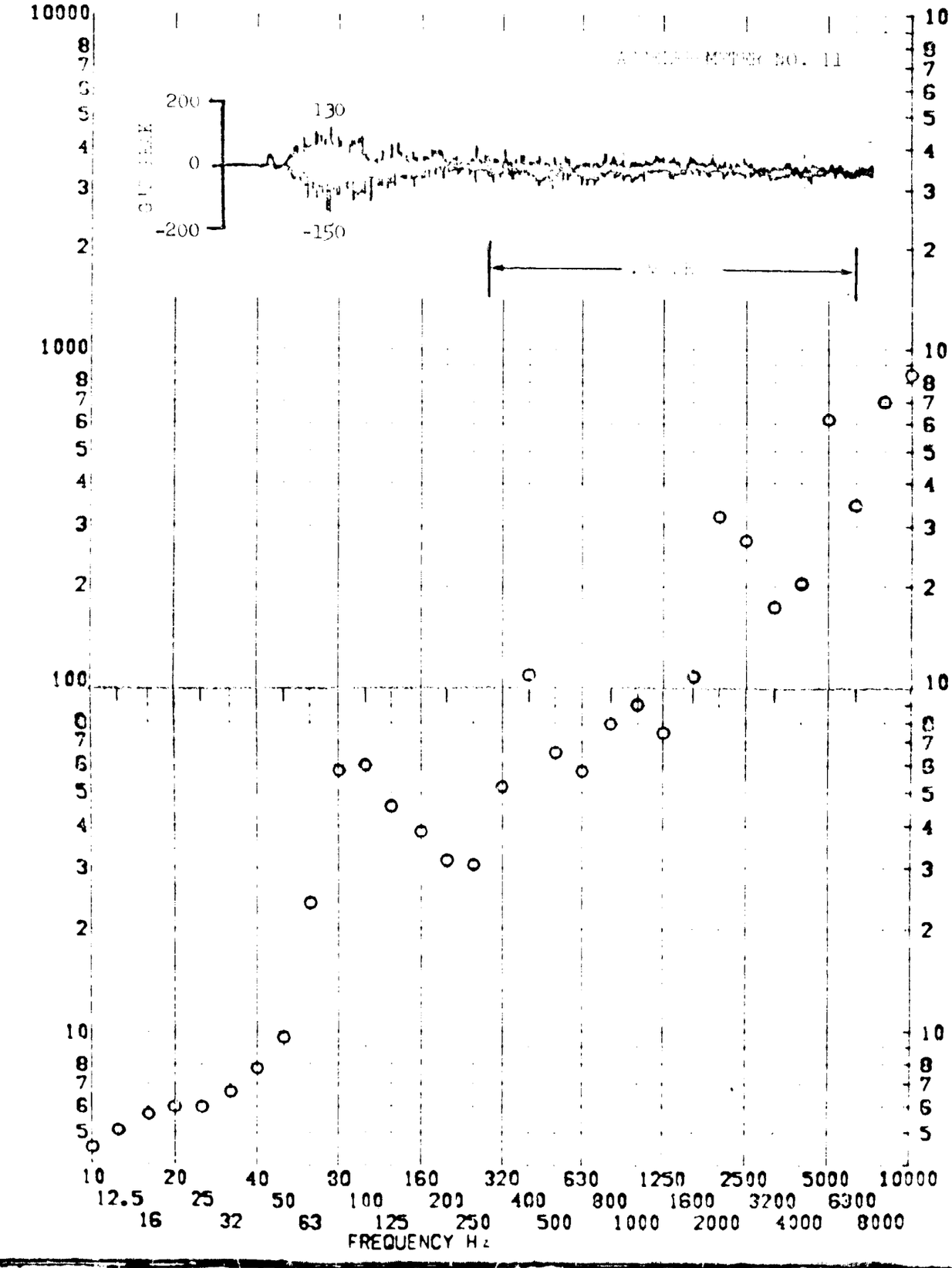

SHOCK TEST ANALYSIS DATA SHEET NO. [illegible].7.82

TEST ITEM 1377-482 PART NO. EQUIPMENT

SERIAL NO. TEST DATE 11 FEB 1969

SHOCK AXIS [illegible] SHOCK NO. 2

RESPONSE G-S

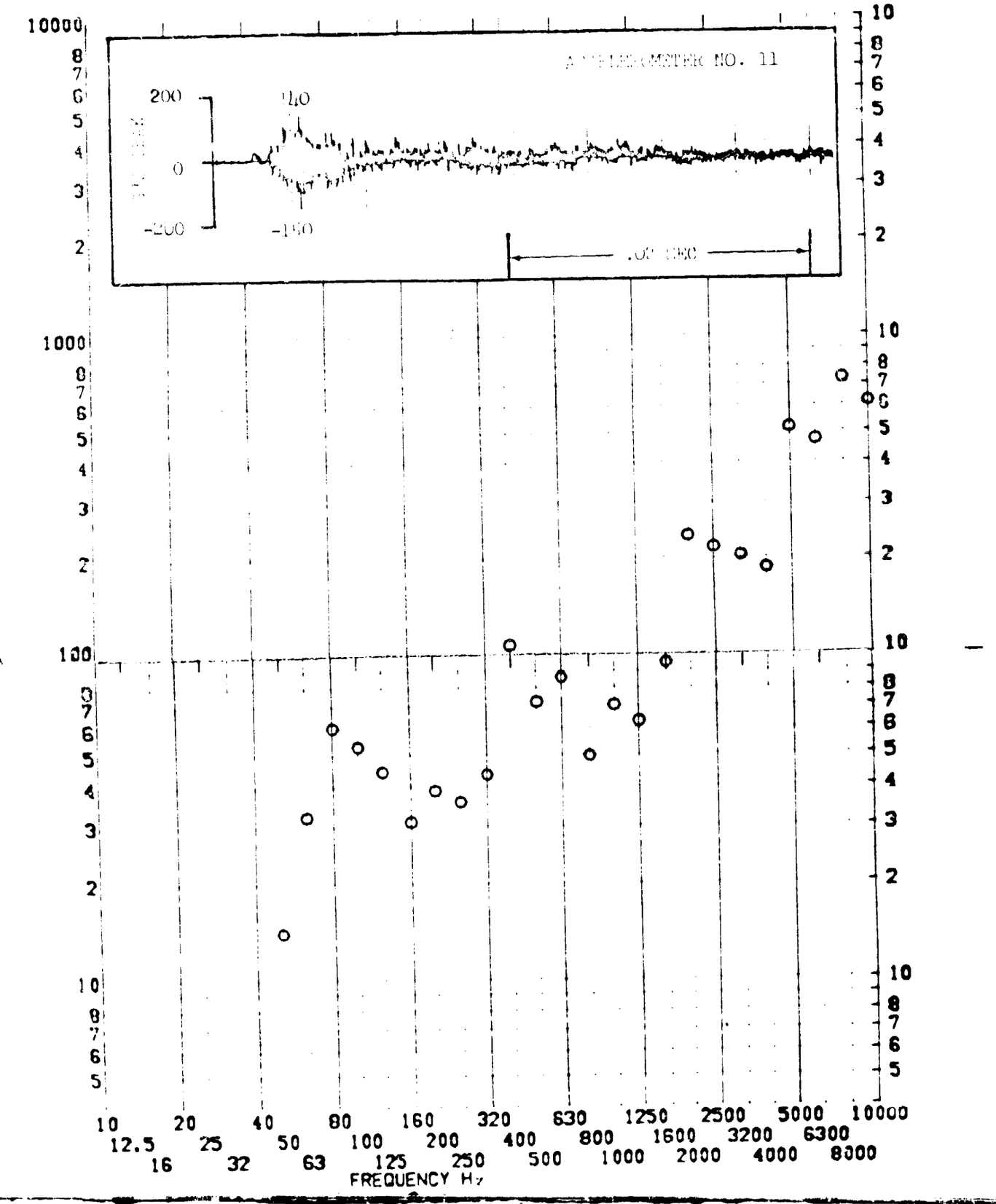

SHOCK TEST ANALYSIS DATA SHEET [illegible]

TEST ITEM [illegible] PART NO. [illegible]
SERIAL NO. [illegible] TEST DATE [illegible]
SHOCK AXIS [illegible] SHOCK NO. [illegible]

RESPONSE G-S

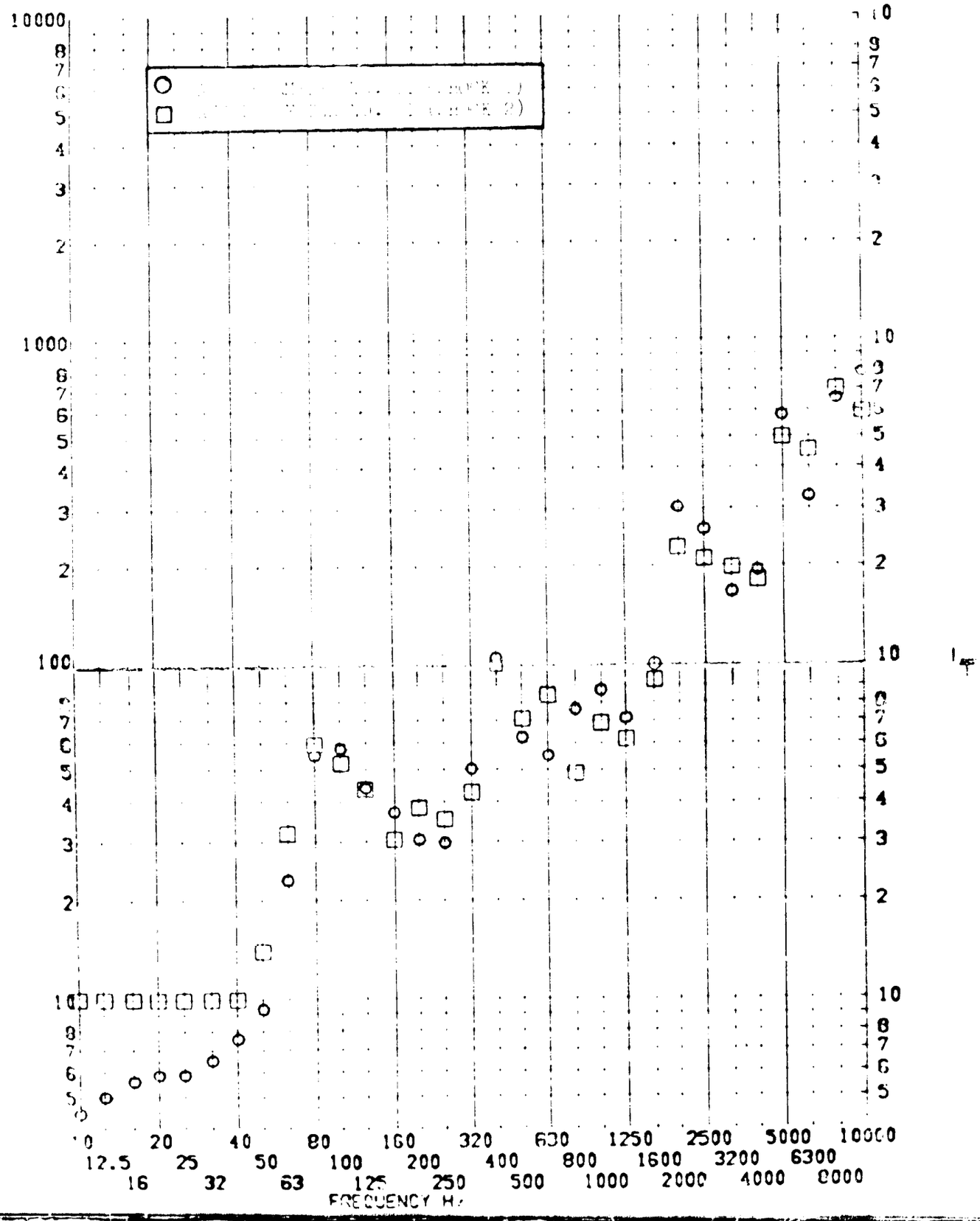

SHOCK TEST ANALYSIS DATA SHEET NO. H.A.7.84

TEST ITEM 1377-459
SERIAL NO.
SHOCK AXIS RADIAL

PART NO. EQUIPMENT
TEST DATE 11 FEB 1969
SHOCK NO. 1

RESPONSE G-S

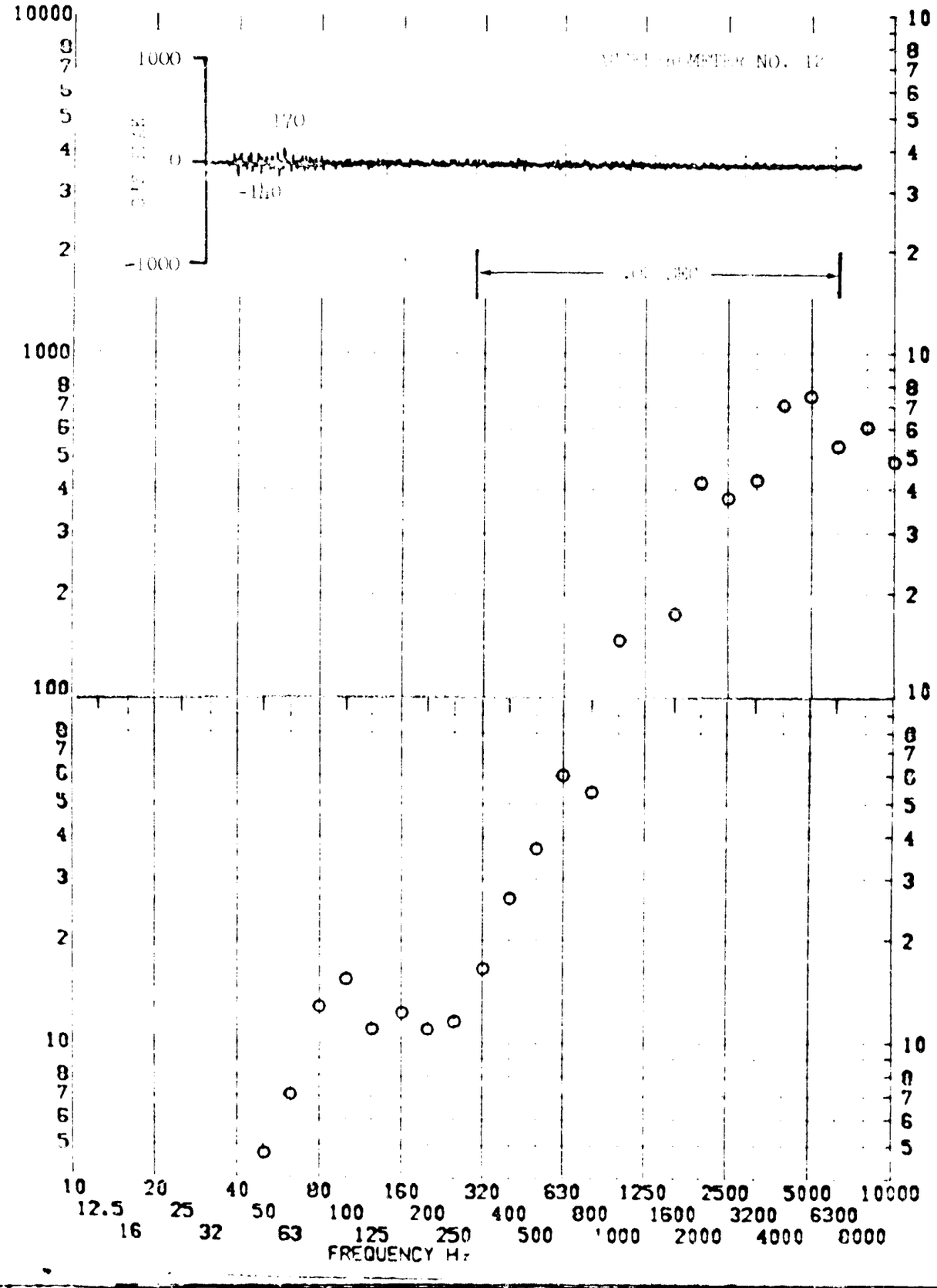

SHOCK TEST ANALYSIS DATA SHEET NO. [illegible].A.7.89

TEST ITEM 1377-483 PART NO. EQUIPMENT
SERIAL NO. TEST DATE [illegible] 1962
SHOCK AXIS RADIAL SHOCK NO. 2

RESPONSE G-S

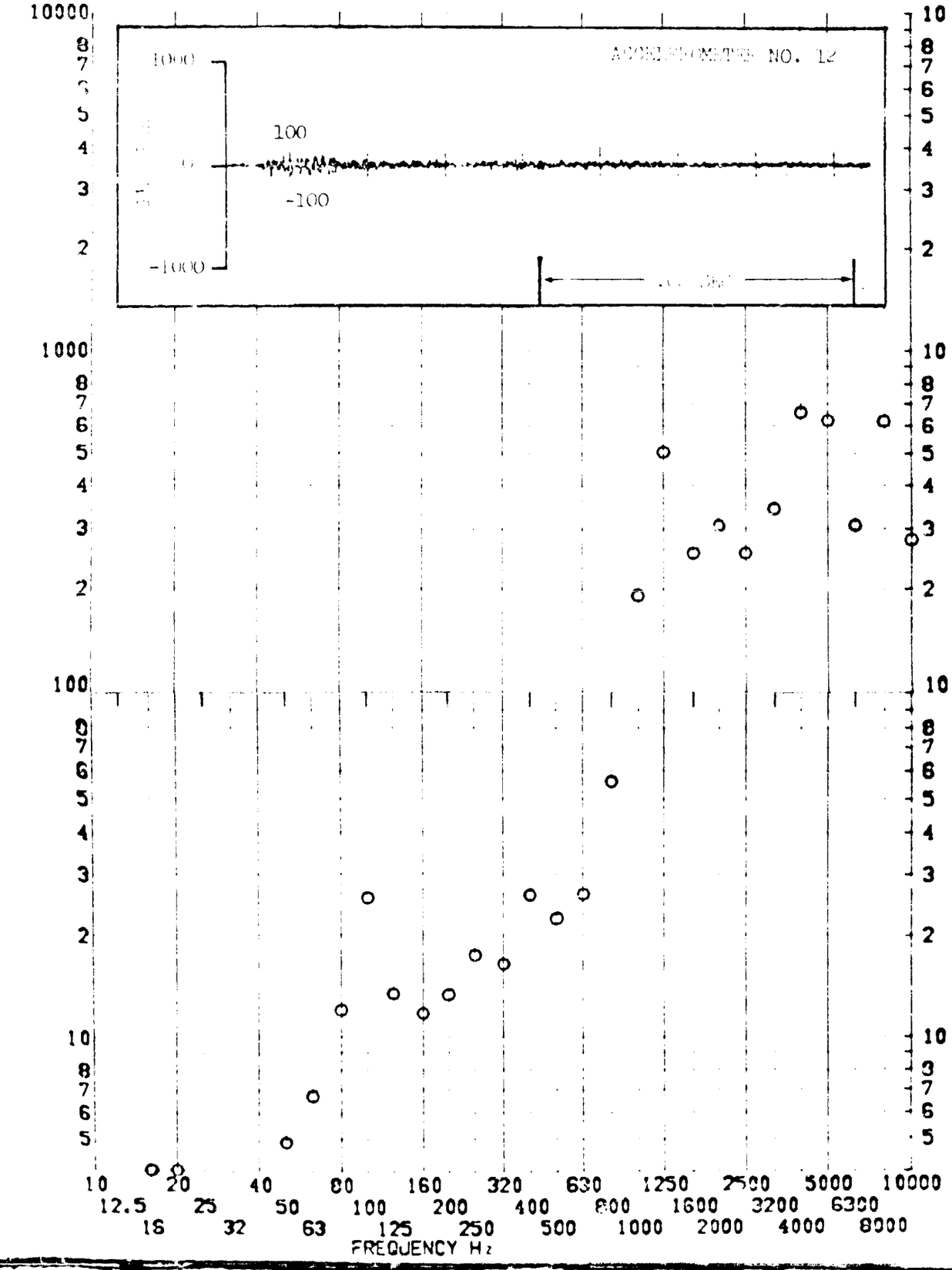

SHOCK TEST ANALYSIS DATA SHEET NO. II.A.7.66

TEST ITEM [illegible] PART NO. EQUIPMENT

SERIAL NO. — TEST DATE 11 FEB 1969

SHOCK AXIS [illegible] — SHOCK NO. 1 & 2 —

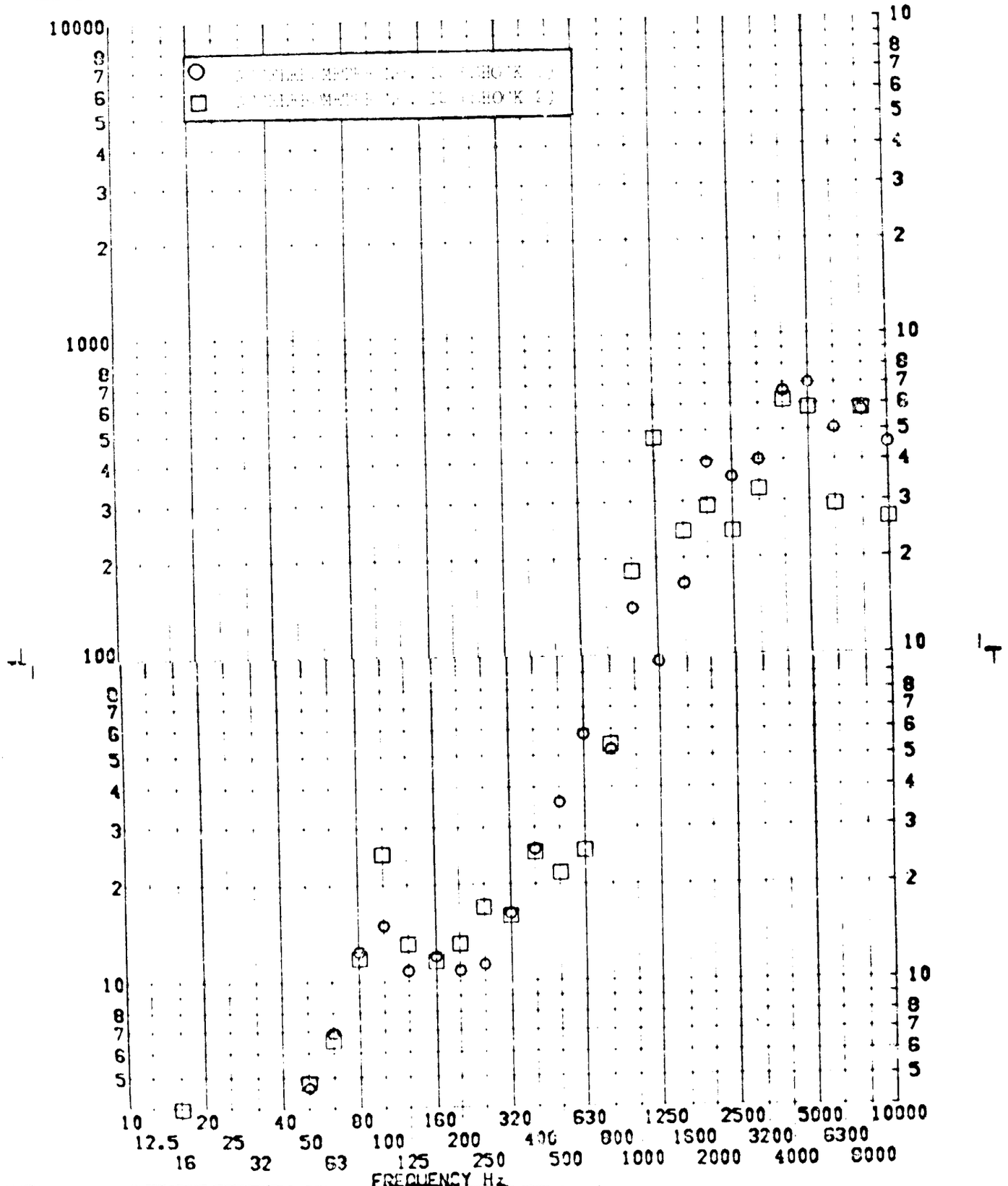

SHOCK TEST ANALYSIS DATA SHEET NO. [illegible]

TEST ITEM [illegible]
SERIAL NO.
SHOCK AXIS LONGITUDINAL

PART NO. EQUIPMENT
TEST DATE [illegible]
SHOCK NO. 1

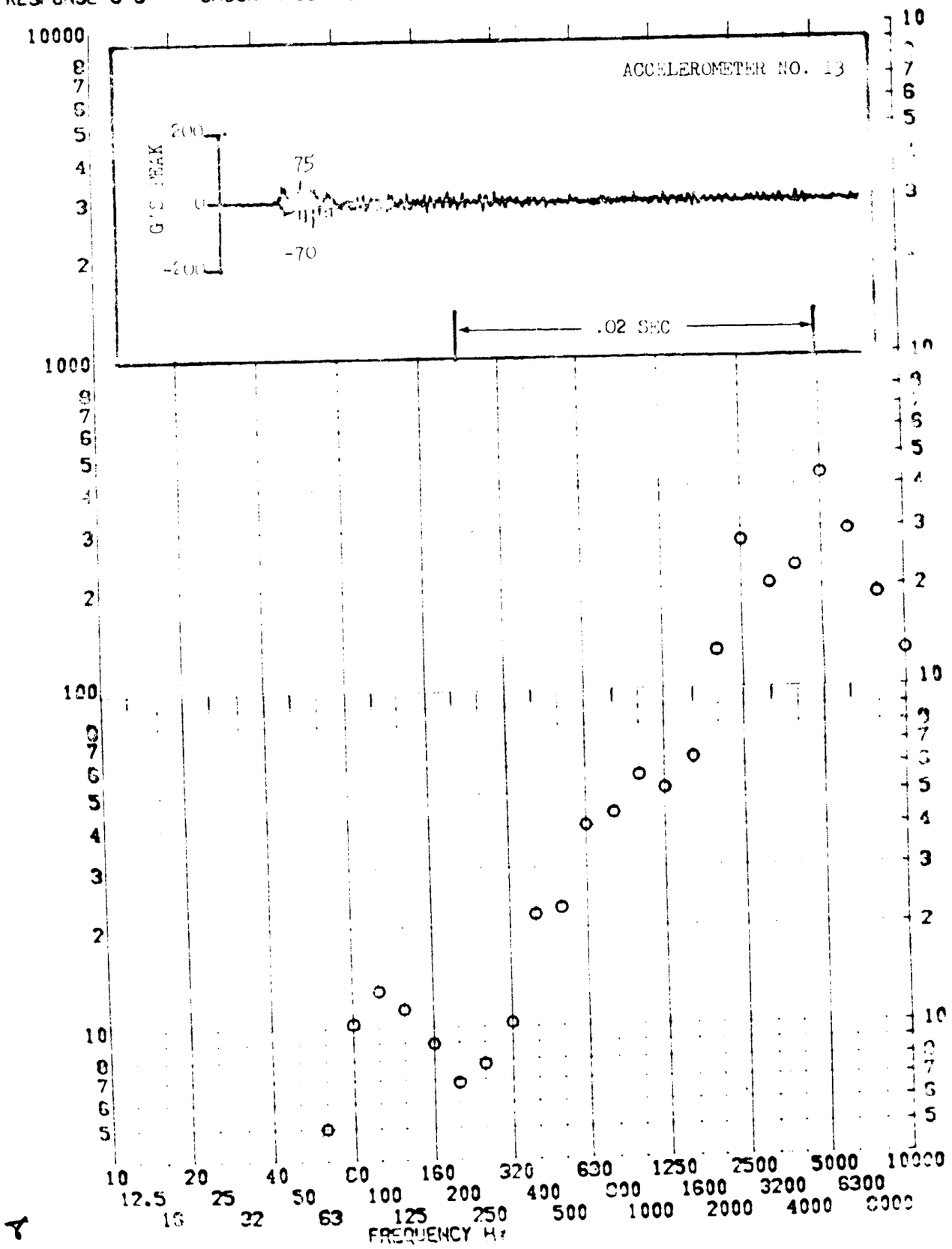

SHOCK TEST ANALYSIS DATA SHEET

NO. II.A.7.88

TEST ITEM	1377-484	PART NO.	EQUIPMENT
SERIAL NO.		TEST DATE	11 FEB 1969
SHOCK AXIS	LONGITUDINAL	SHOCK NO.	2

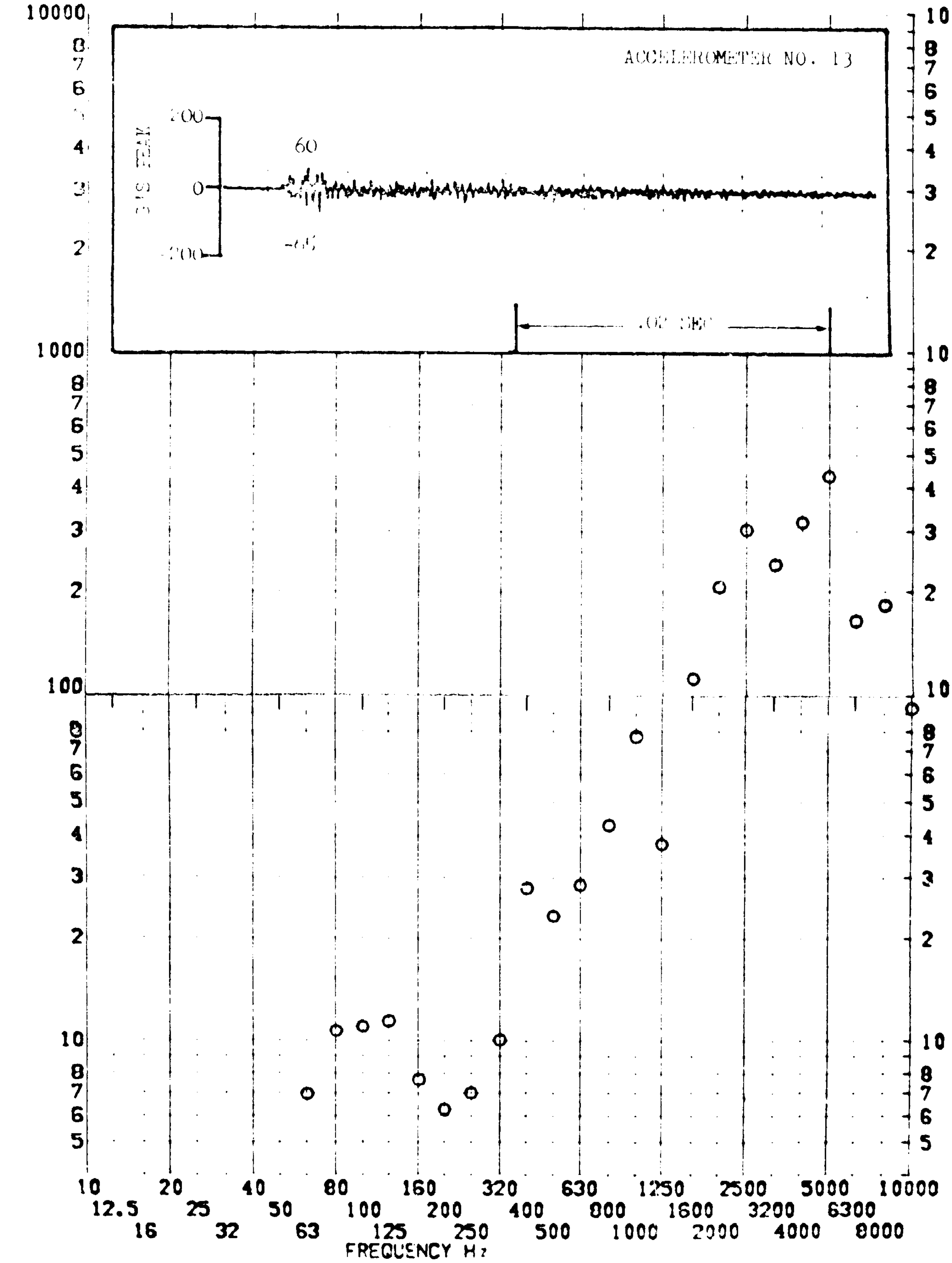

SHOCK TEST ANALYSIS DATA SHEET No. II.A./.89

TEST ITEM 1377-397,484
SERIAL NO.
SHOCK AXIS LONGITUDINAL

PART NO. EQUIPMENT
TEST DATE 11 FEB 1969
SHOCK NO. 1 & 2

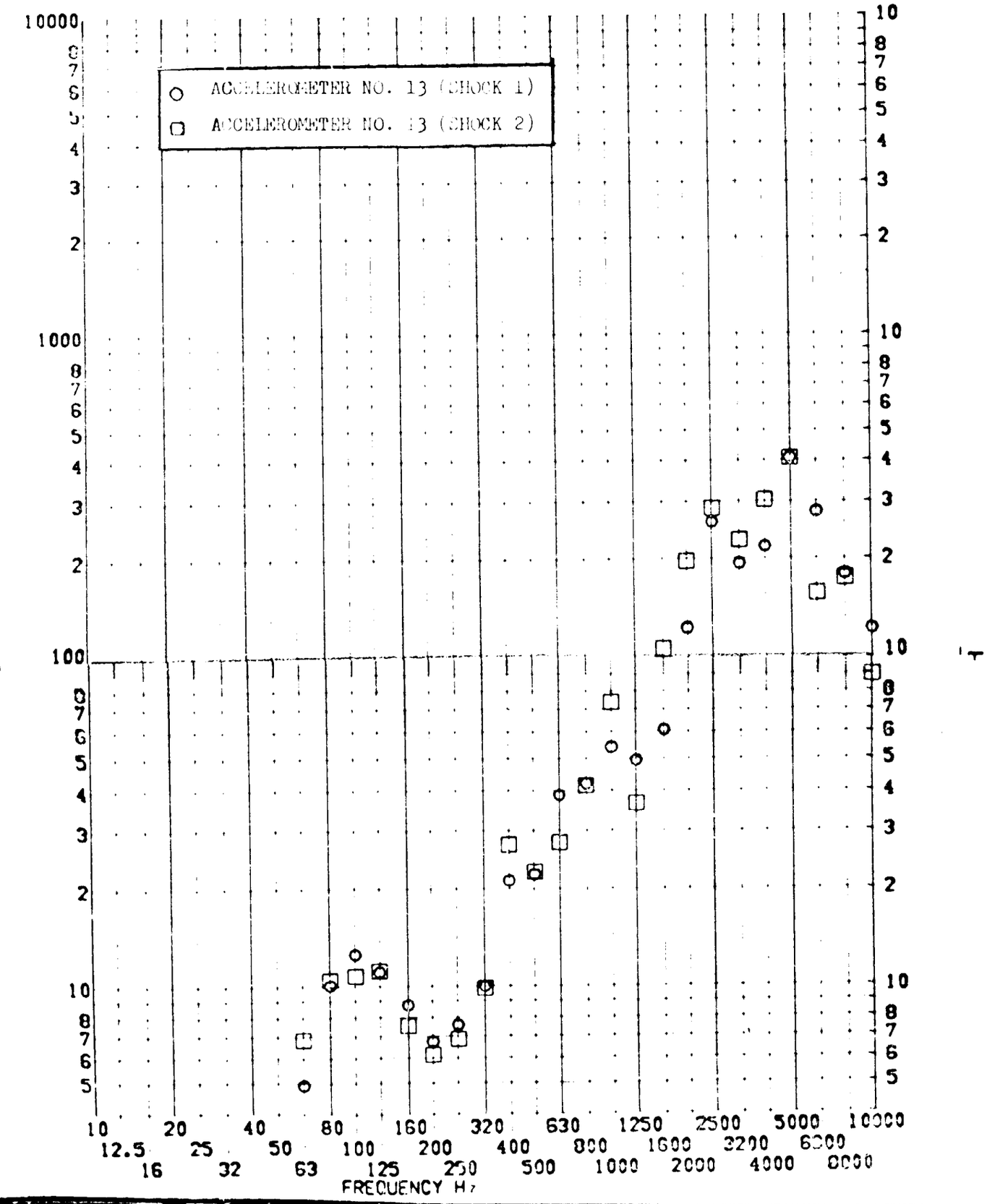

SHOCK TEST ANALYSIS DATA SHEET NO. II.A.7.90

TEST ITEM 1377-398
SERIAL NO.
SHOCK AXIS RADIAL

PART NO. EQUIPMENT
TEST DATE 11 FEB 1969
SHOCK NO. 1

RESPONSE G-S

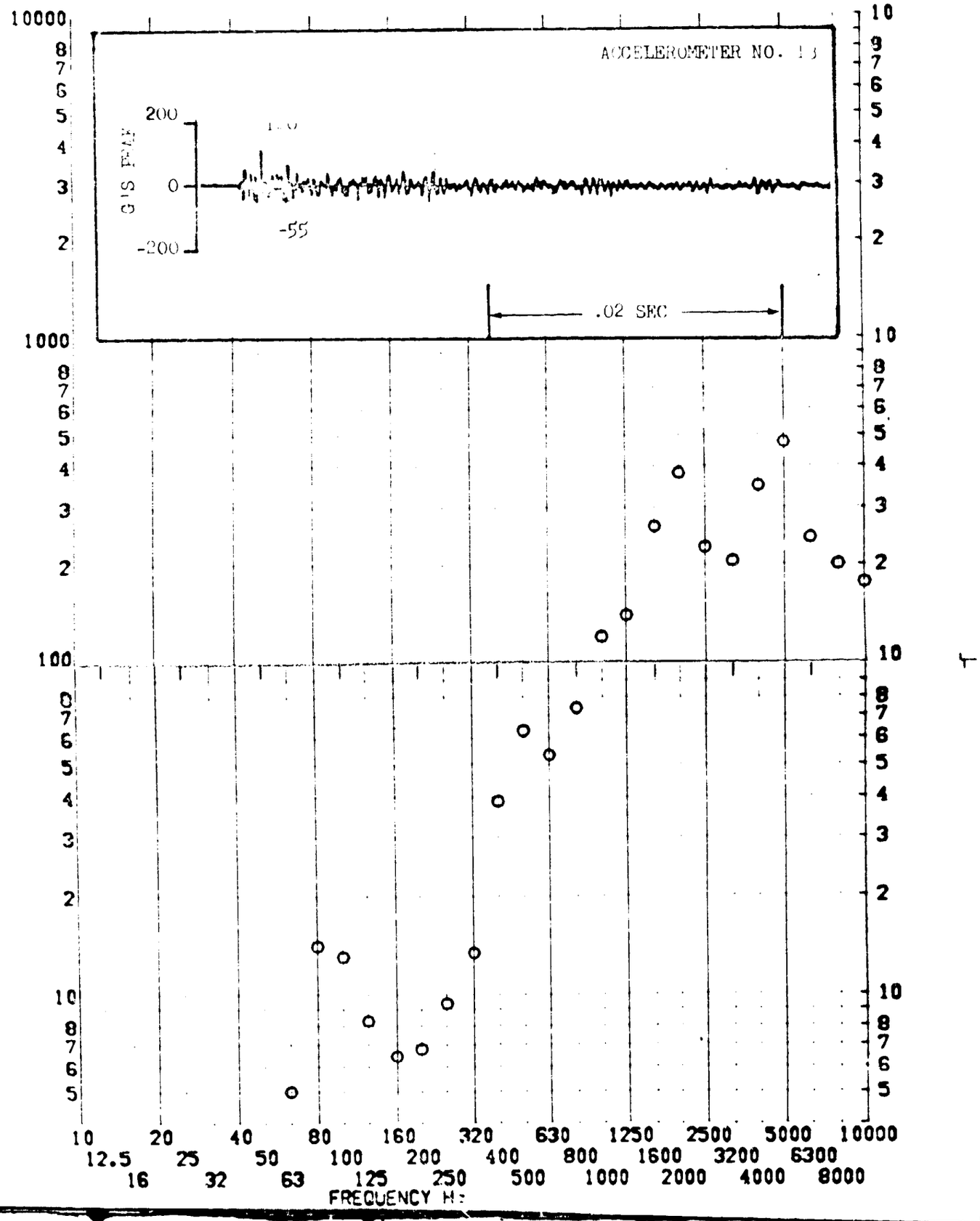

SHOCK TEST ANALYSIS DATA SHEET NO. 11.A.7.91

TEST ITEM 1377-485 PART NO. EQUIPMENT
SERIAL NO. TEST DATE 11 FEB 1969
RESPONSE G-S SHOCK AXIS RADIAL SHOCK NO. 2

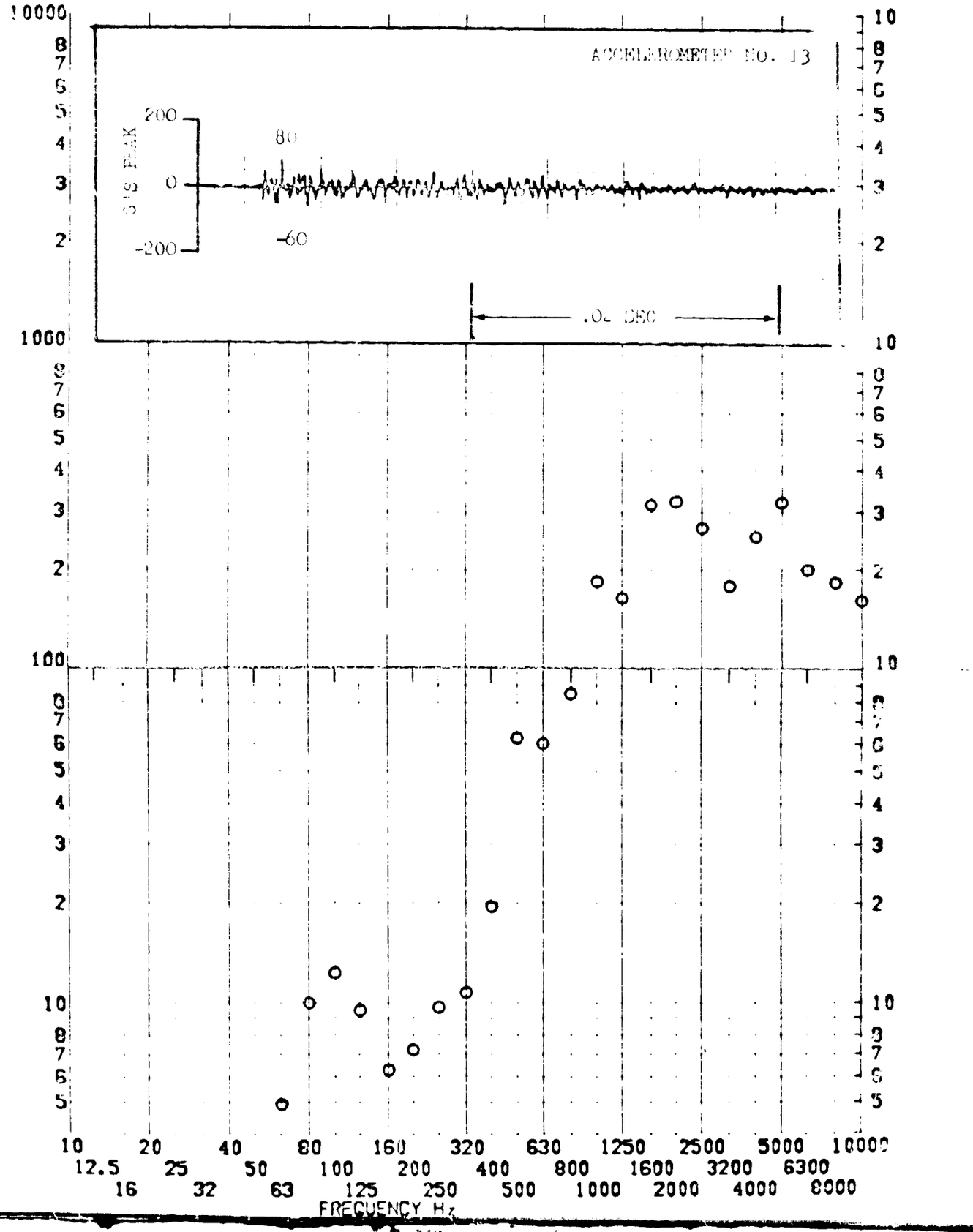

SHOCK TEST ANALYSIS DATA SHEET NO. 11.A.7.92

TEST ITEM 1377-398,485 PART NO. EQUIPMENT
SERIAL NO. — TEST DATE 11 FEB 1969
SHOCK AXIS RADIAL SHOCK NO. 1 & 2

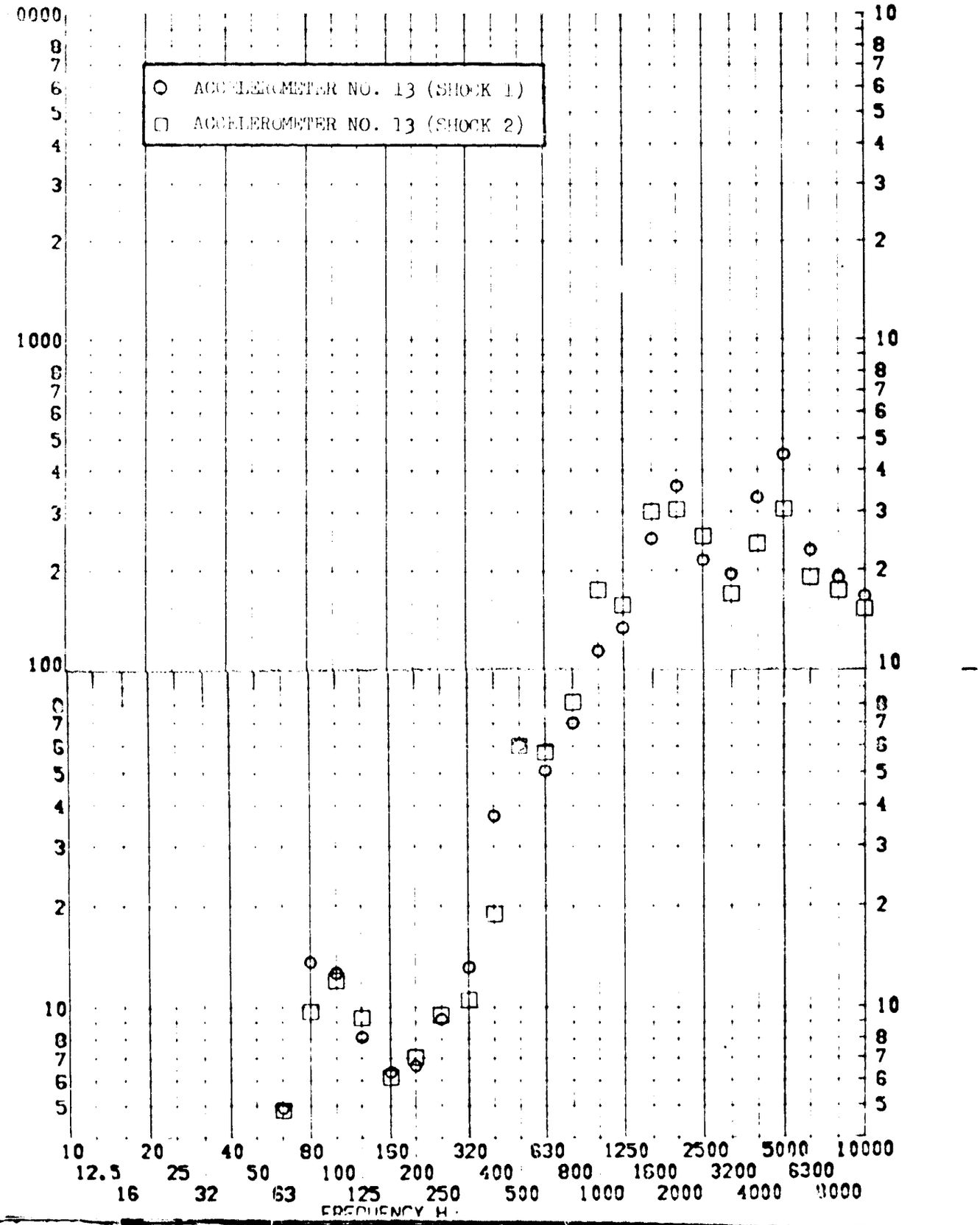

SHOCK TEST ANALYSIS DATA SHEET NO. II.A.7.93

TEST ITEM [illegible]
SERIAL NO. —
SHOCK AXIS RADIAL

PART NO. EQUIPMENT
TEST DATE 11 FEB 1969
SHOCK NO. 2

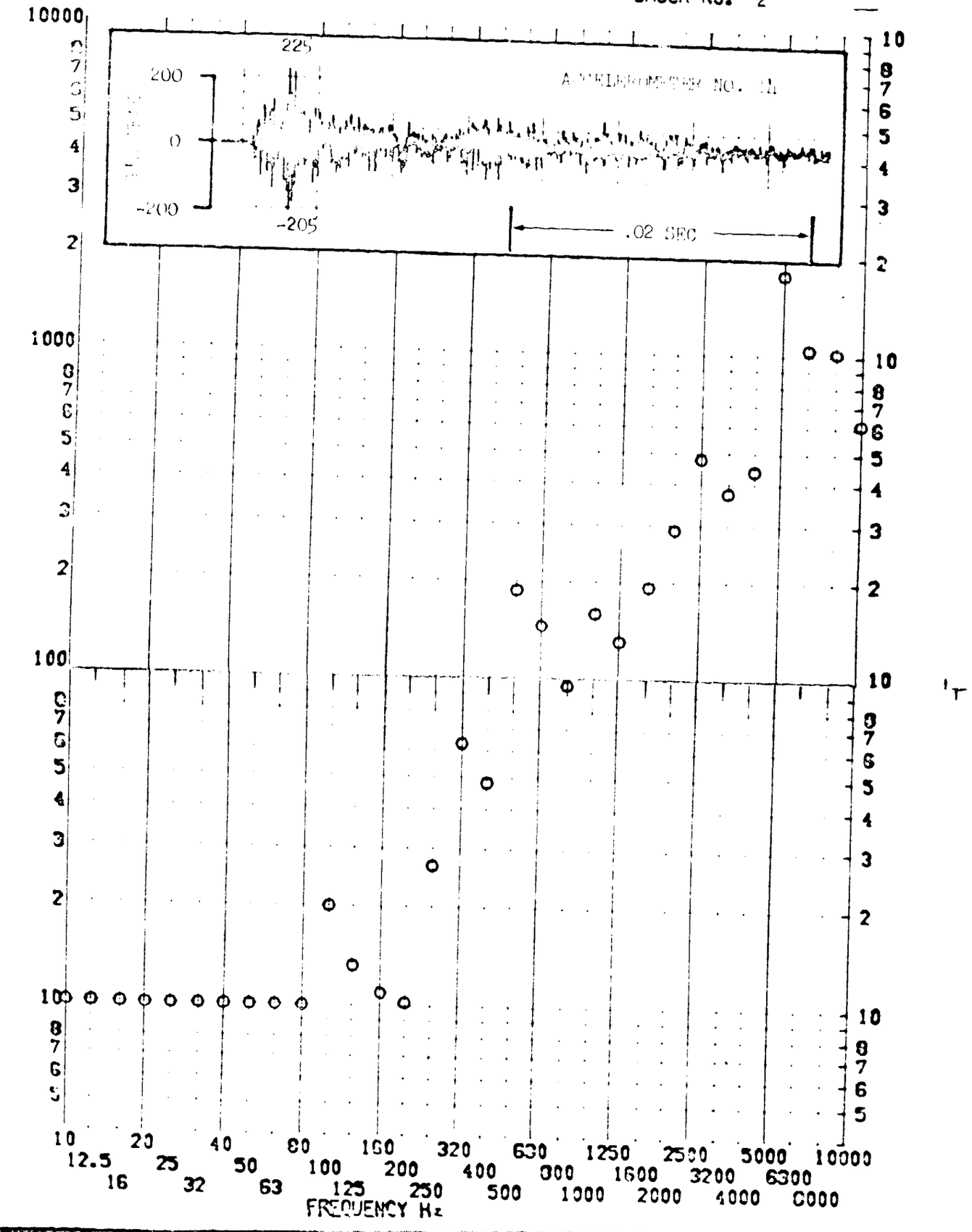

SHOCK TEST ANALYSIS DATA SHEET NO. II.A.7.94

TEST ITEM 1377-399
SERIAL NO.
SHOCK AXIS [illegible]

PART NO. EQUIPMENT
TEST DATE 11 FEB 1969
SHOCK NO. 1

RESPONSE G-S

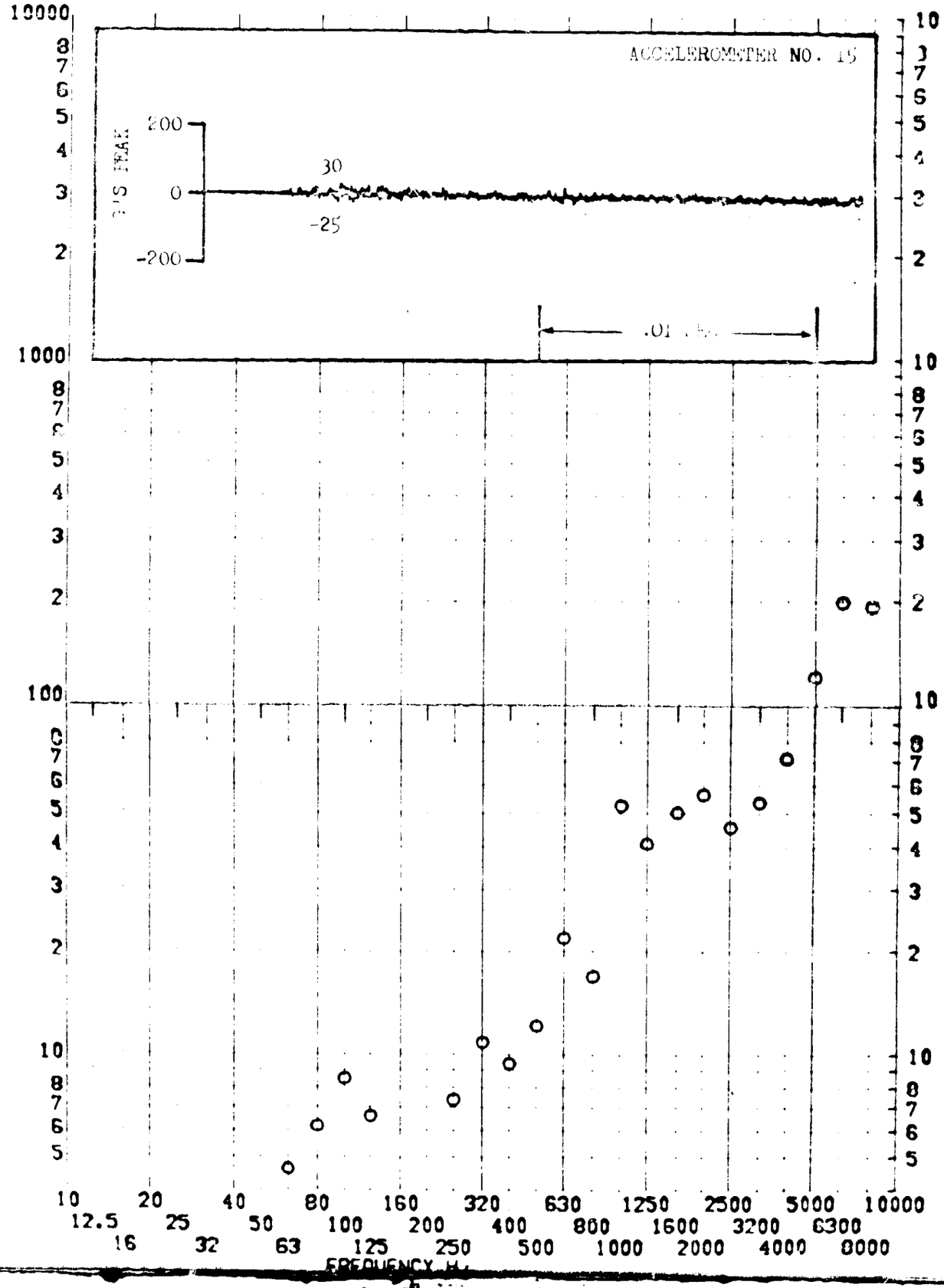

SHOCK TEST ANALYSIS DATA SHEET NO. H.A.7.99

TEST ITEM 1377-487
SERIAL NO.
SHOCK AXIS RADIAL

PART NO. EQUIPMENT
TEST DATE 11 FEB 1962
SHOCK NO. 2

RESPONSE G-S

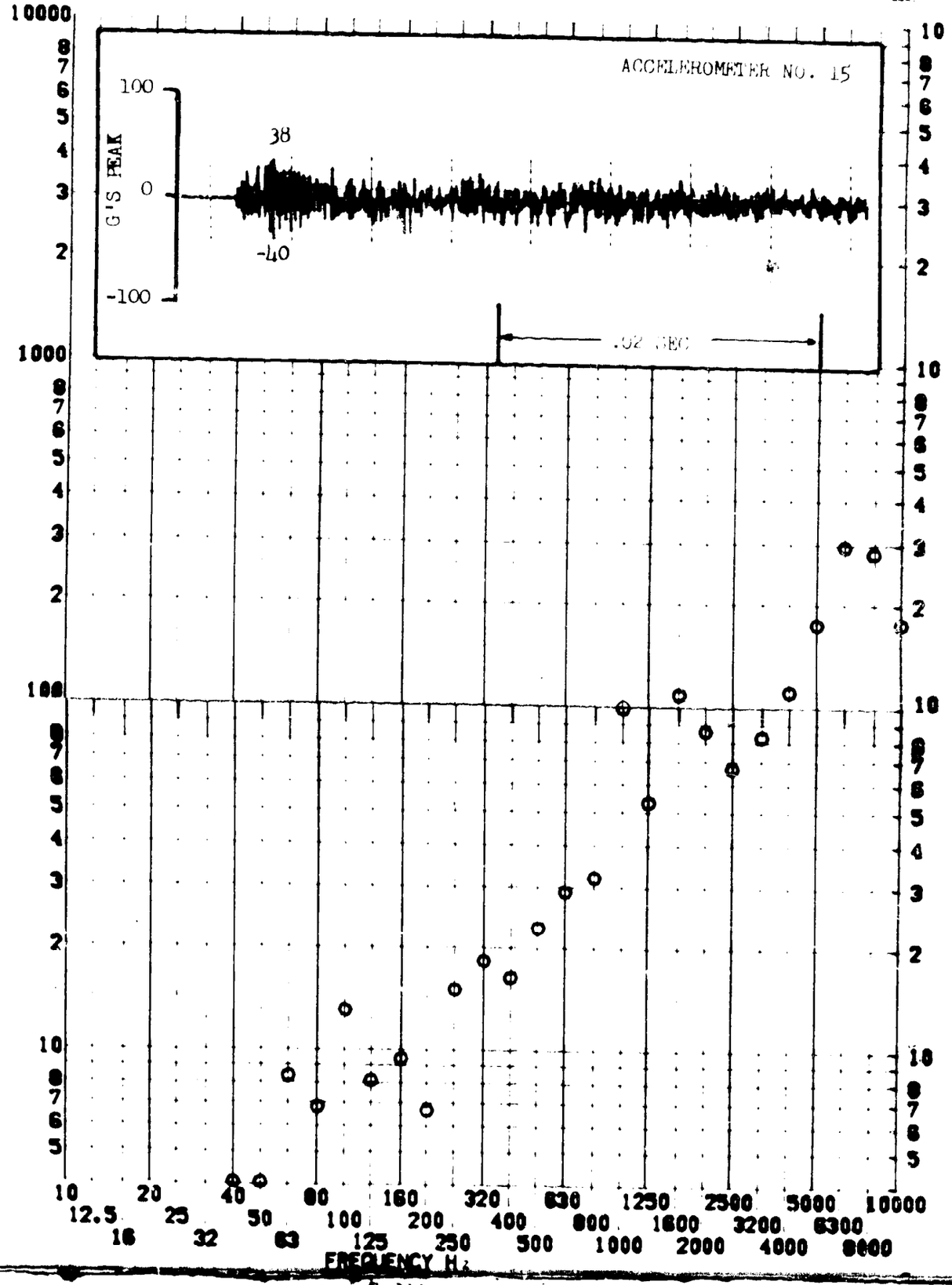

SHOCK TEST ANALYSIS DATA SHEET NO. 11.A.7.96

TEST ITEM 1377-399,487 PART NO. EQUIPMENT
SERIAL NO. — TEST DATE 11 FEB 1969
SHOCK AXIS RADIAL — SHOCK NO. 1 & 2 —

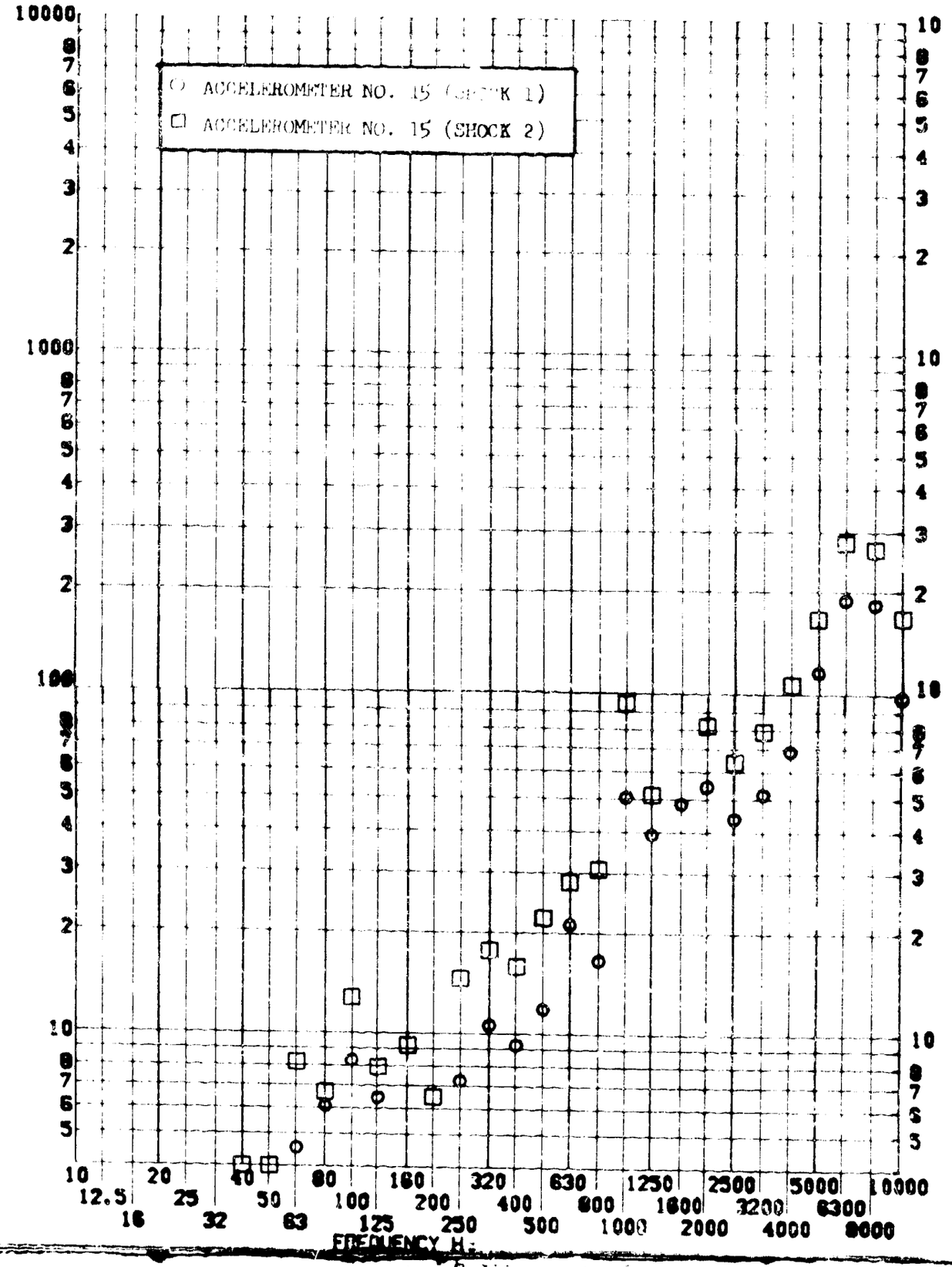

SHOCK TEST ANALYSIS DATA SHEET NO. II.A.7.97

TEST ITEM 13[illegible]-400
SERIAL NO.
SHOCK AXIS RADIAL

PART NO. EQUIPMENT
TEST DATE 11 [illegible] 1969
SHOCK NO. 1

RESPONSE G-S

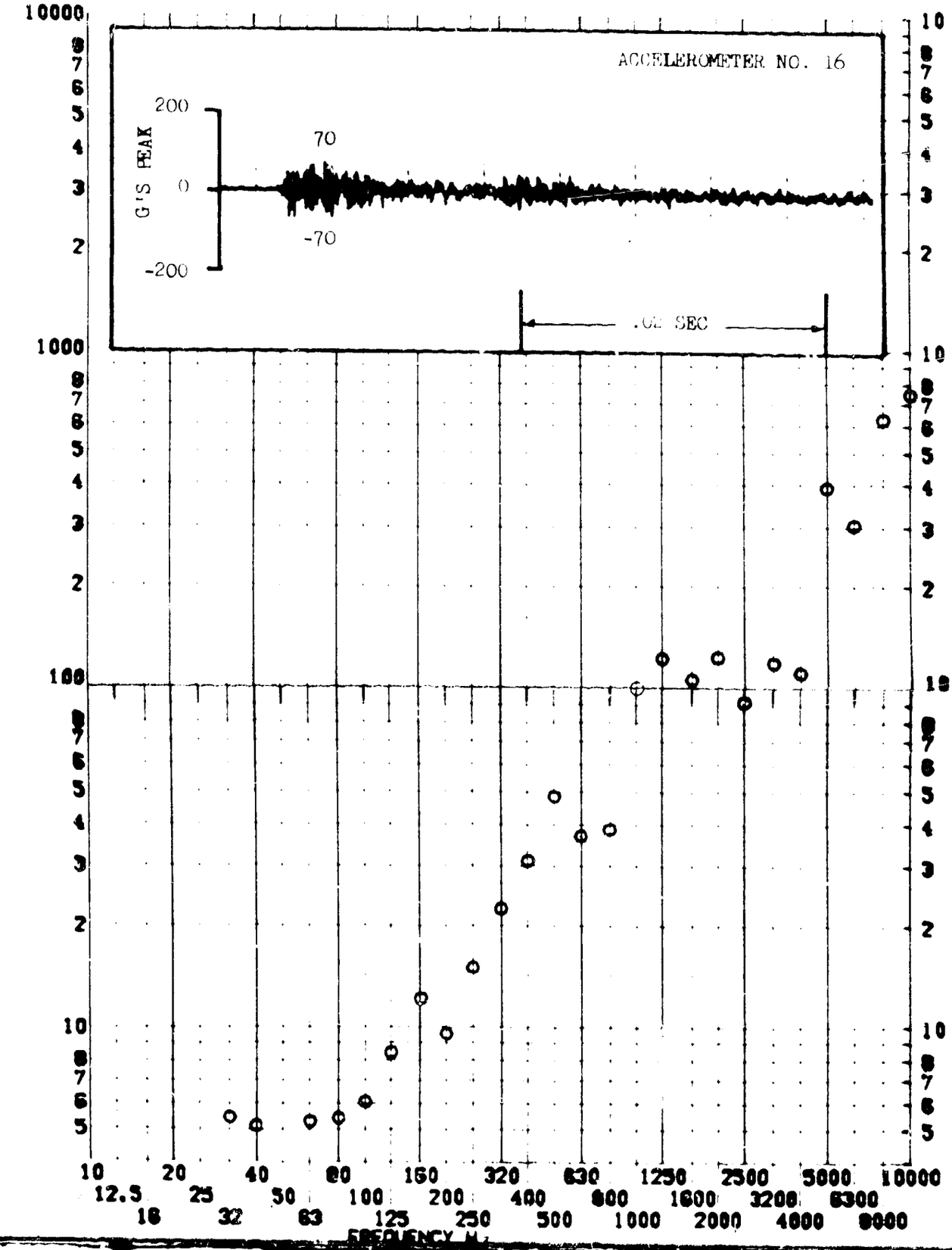

SHOCK TEST ANALYSIS DATA SHEET NO. H.A./.98

TEST ITEM [illegible]
SERIAL NO.
SHOCK AXIS RADIAL

PART NO. EQUIPMENT
TEST DATE [illegible]
SHOCK NO. 2

RESPONSE G-S

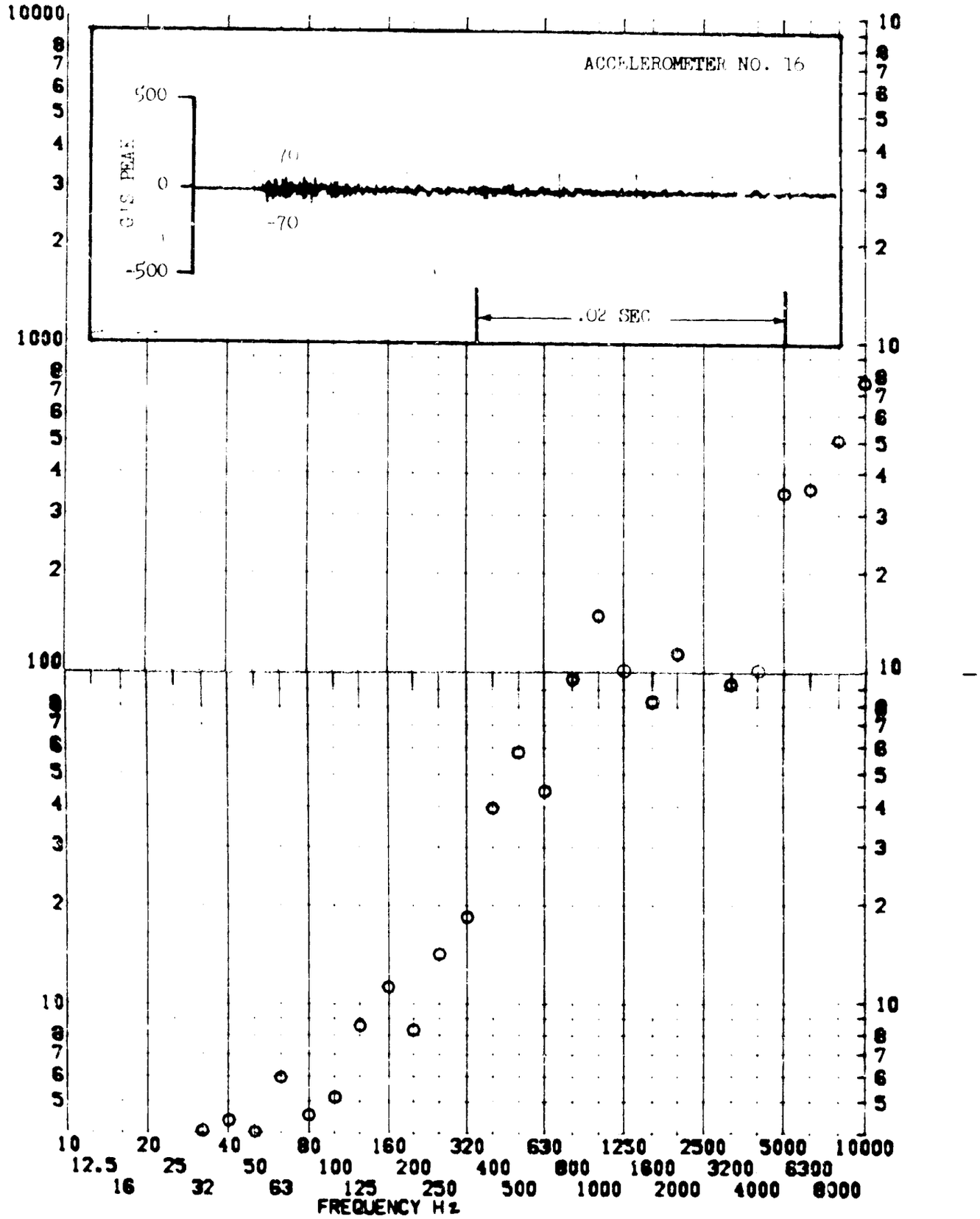

SHOCK TEST ANALYSIS DATA SHEET NO. 11.A.7.99

TEST ITEM 1377-400,420
SERIAL NO. —
SHOCK AXIS RADIAL —

PART NO. EQUIPMENT
TEST DATE 11 SEP 1969
SHOCK NO. 1 & 2 —

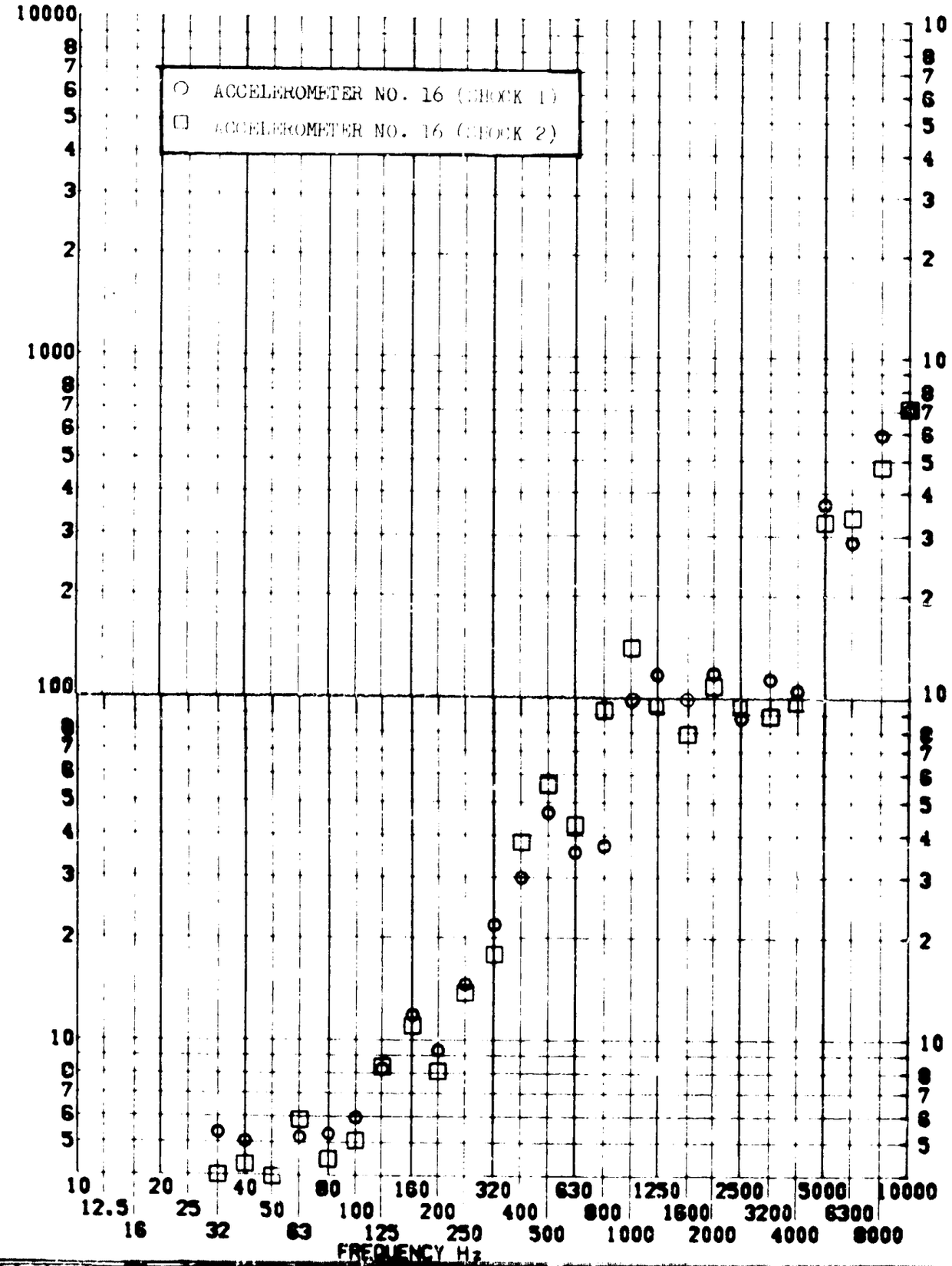

SHOCK TEST ANALYSIS DATA SHEET NO. H.A.-[illegible]

TEST ITEM 1377-401 _ PART NO. EQUIPMENT _
SERIAL NO. _ TEST DATE 11 FEB 1969
SHOCK AXIS RADIAL _ SHOCK NO. 1 _

RESPONSE G-S

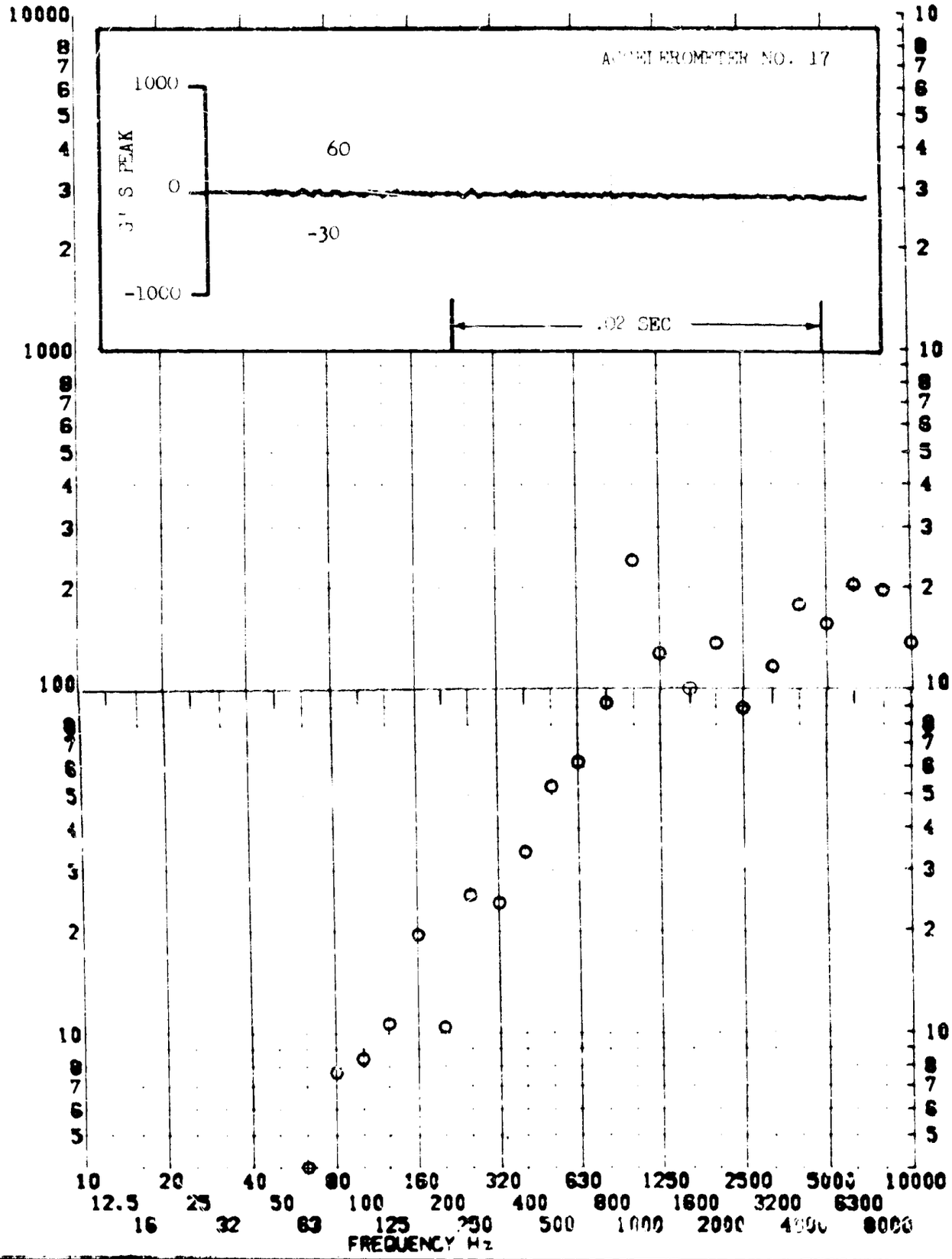

SHOCK TEST ANALYSIS DATA SHEET NO. [illegible]

TEST ITEM [illegible] PART NO. EQUIPMENT

SERIAL NO.

RESPONSE G-S SHOCK AXIS AXIAL TEST DATE [illegible] 1962

SHOCK NO. 2

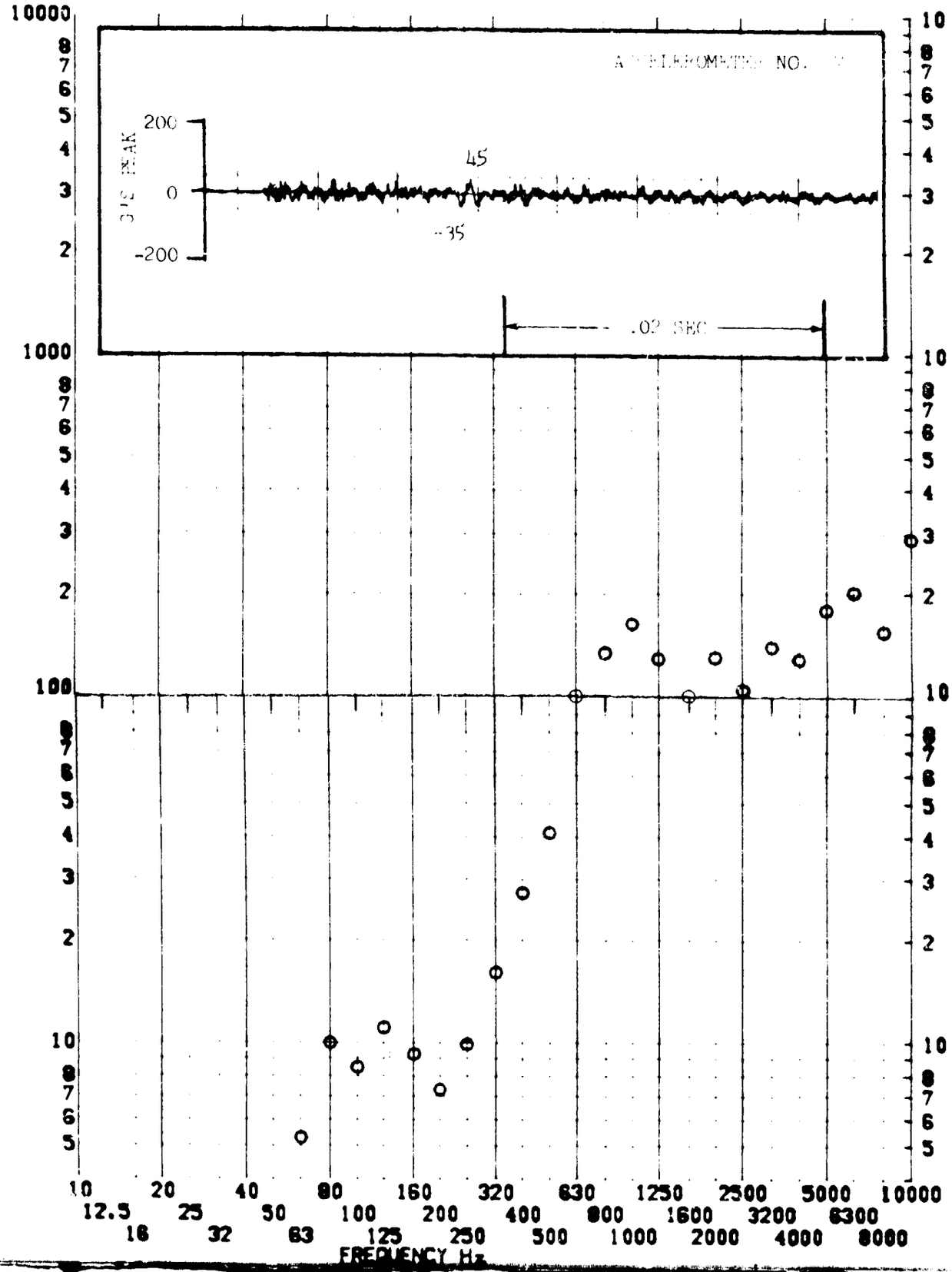

SHOCK TEST ANALYSIS DATA SHEET NO. [illegible]

TEST ITEM 377-401,488 PART NO. EQUIPMENT
SERIAL NO. — TEST DATE 11 FEB 1969
SHOCK AXIS RADIAL — SHOCK NO. 1 & 2 —

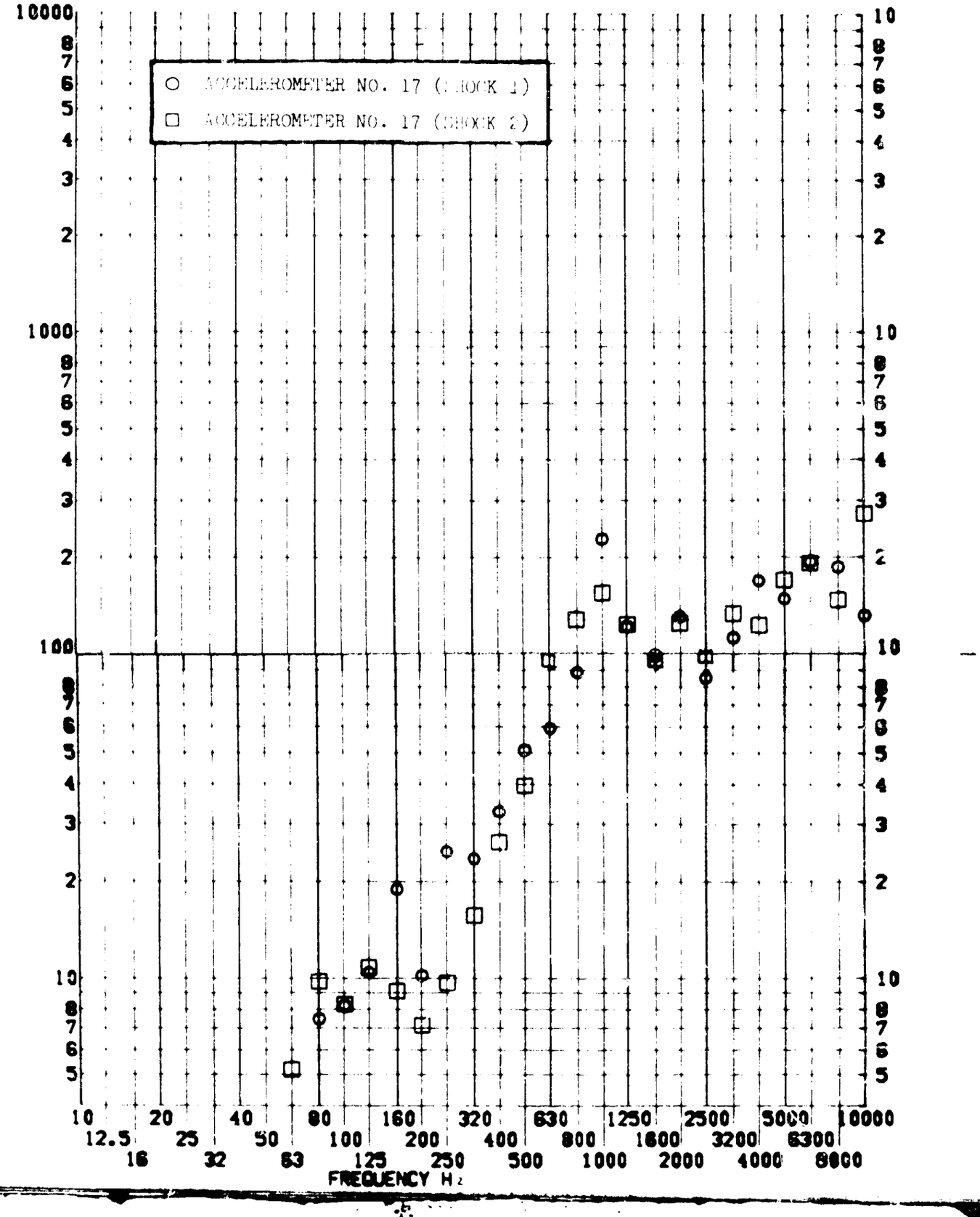

SHOCK TEST ANALYSIS DATA SHEET NO. 11.A.7.1??

TEST ITEM 1377-402 PART NO. EQUIPMENT

SERIAL NO. TEST DATE 11 FEB 1962

RESPONSE G-S SHOCK AXIS [illegible] SHOCK NO.

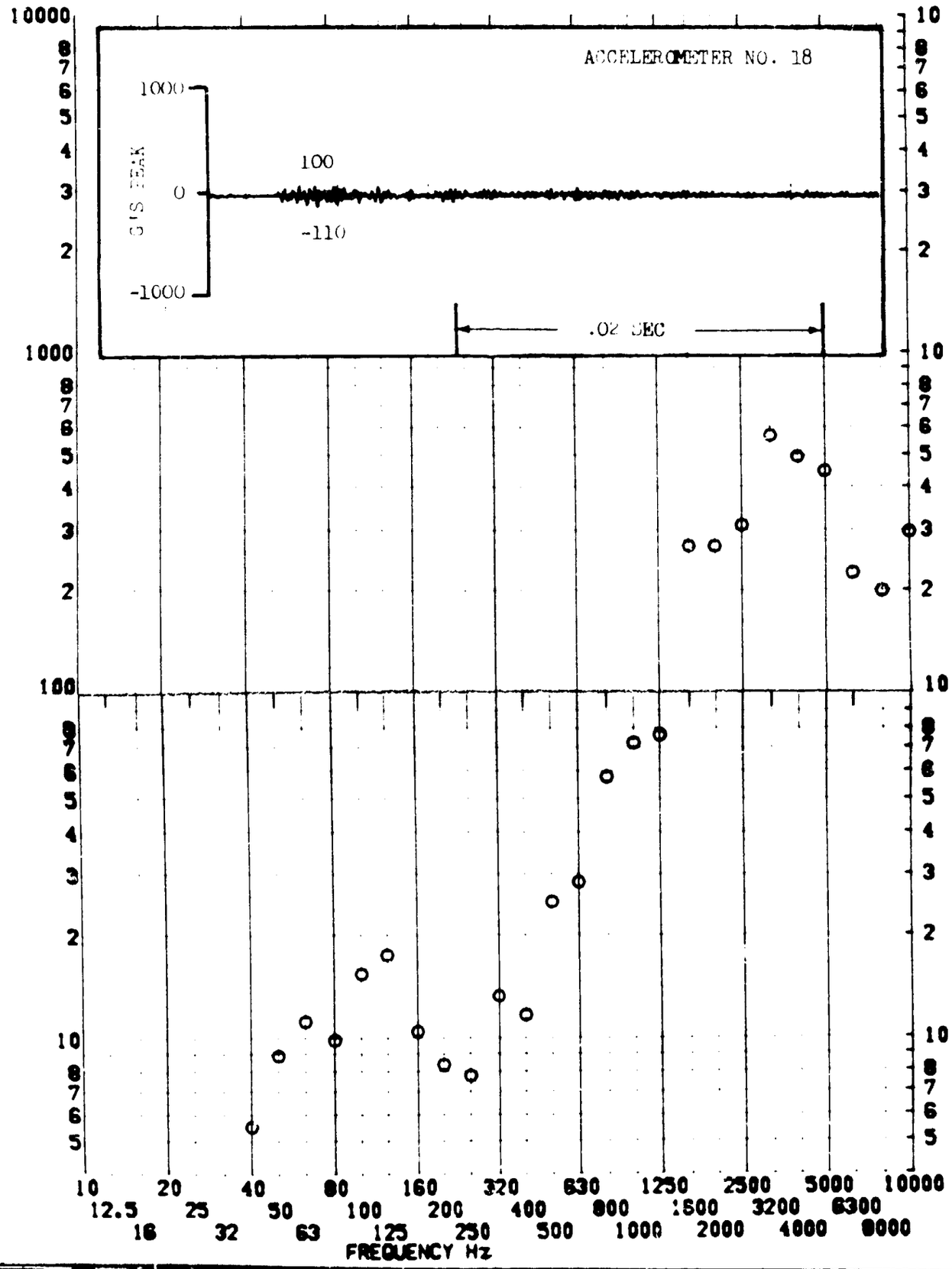

SHOCK TEST ANALYSIS DATA SHEET NO. [illegible]

TEST ITEM [illegible]
SERIAL NO.
SHOCK AXIS [illegible]

PART NO. EQUIPMENT
TEST DATE [illegible] 1969
SHOCK NO. 2

RESPONSE G-S

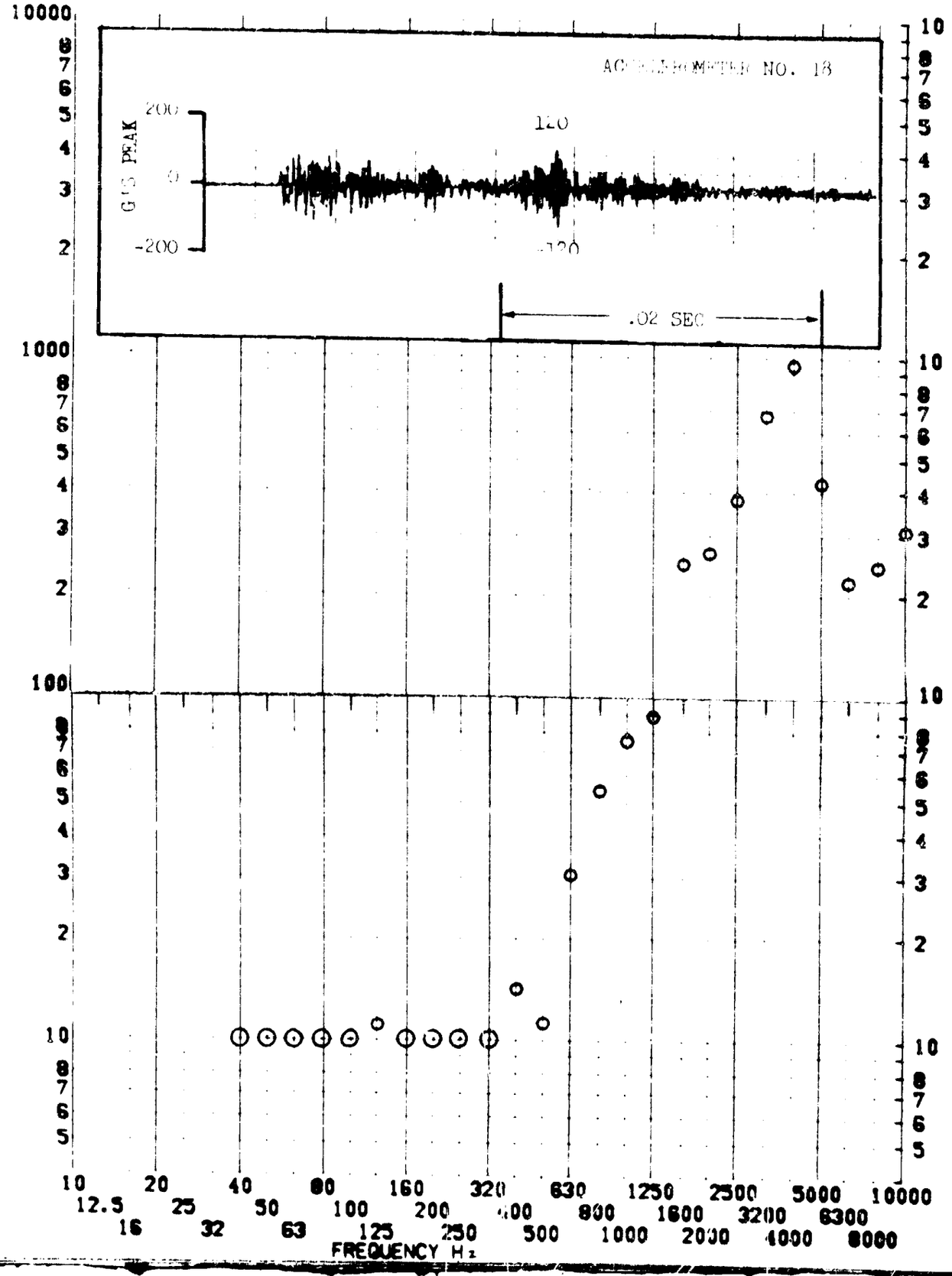

SHOCK TEST ANALYSIS DATA SHEET NO. II.A.7.105

TEST ITEM 1377-402,489
SERIAL NO.
SHOCK AXIS LONGITUDINAL

PART NO. EQUIPMENT
TEST DATE 11 FEB 1969
SHOCK NO. 1 & 2

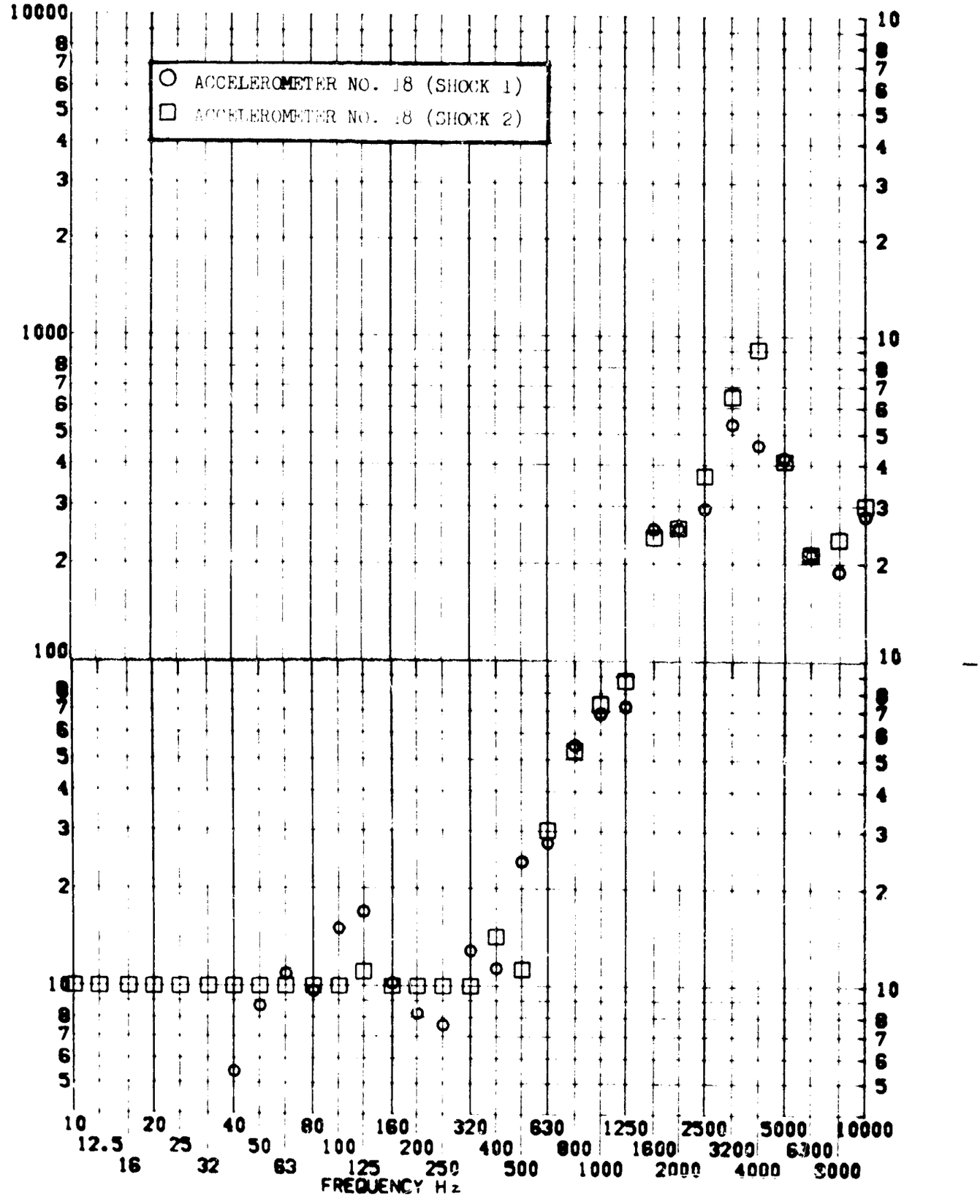

SHOCK TEST ANALYSIS DATA SHEET NO. [illegible]

TEST ITEM [illegible] PART NO. EQUIPMENT
SERIAL NO. TEST DATE [illegible] 1962
SHOCK AXIS RADIAL SHOCK NO. 3

RESPONSE G-S

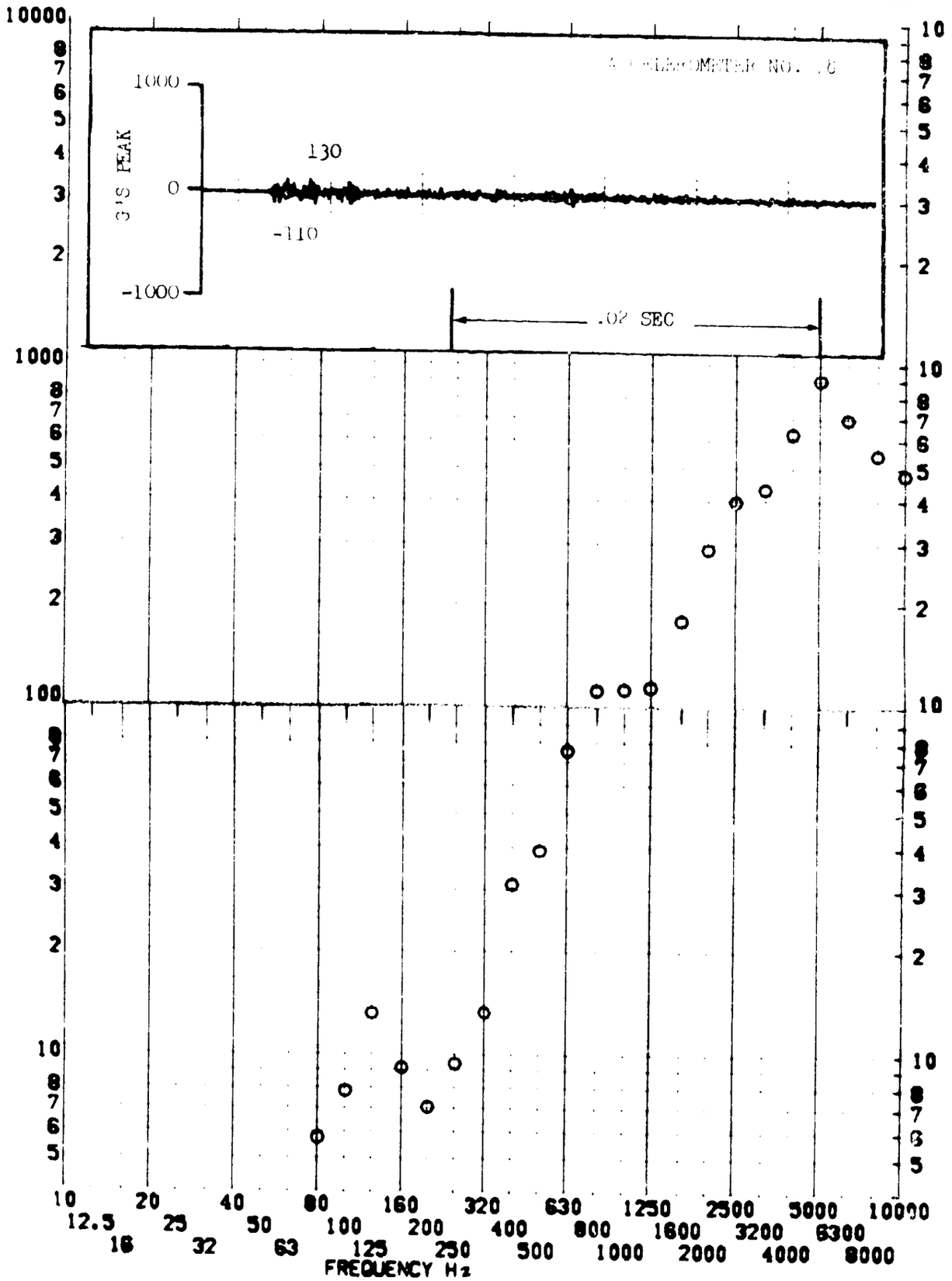

SHOCK TEST ANALYSIS DATA SHEET N[illegible]A-[illegible]

TEST ITEM 1377-491
SERIAL NO.
SHOCK AXIS RADIAL

PART NO. EQUIPMENT
TEST DATE 11 FEB 1962
SHOCK NO. 2

RESPONSE G-S

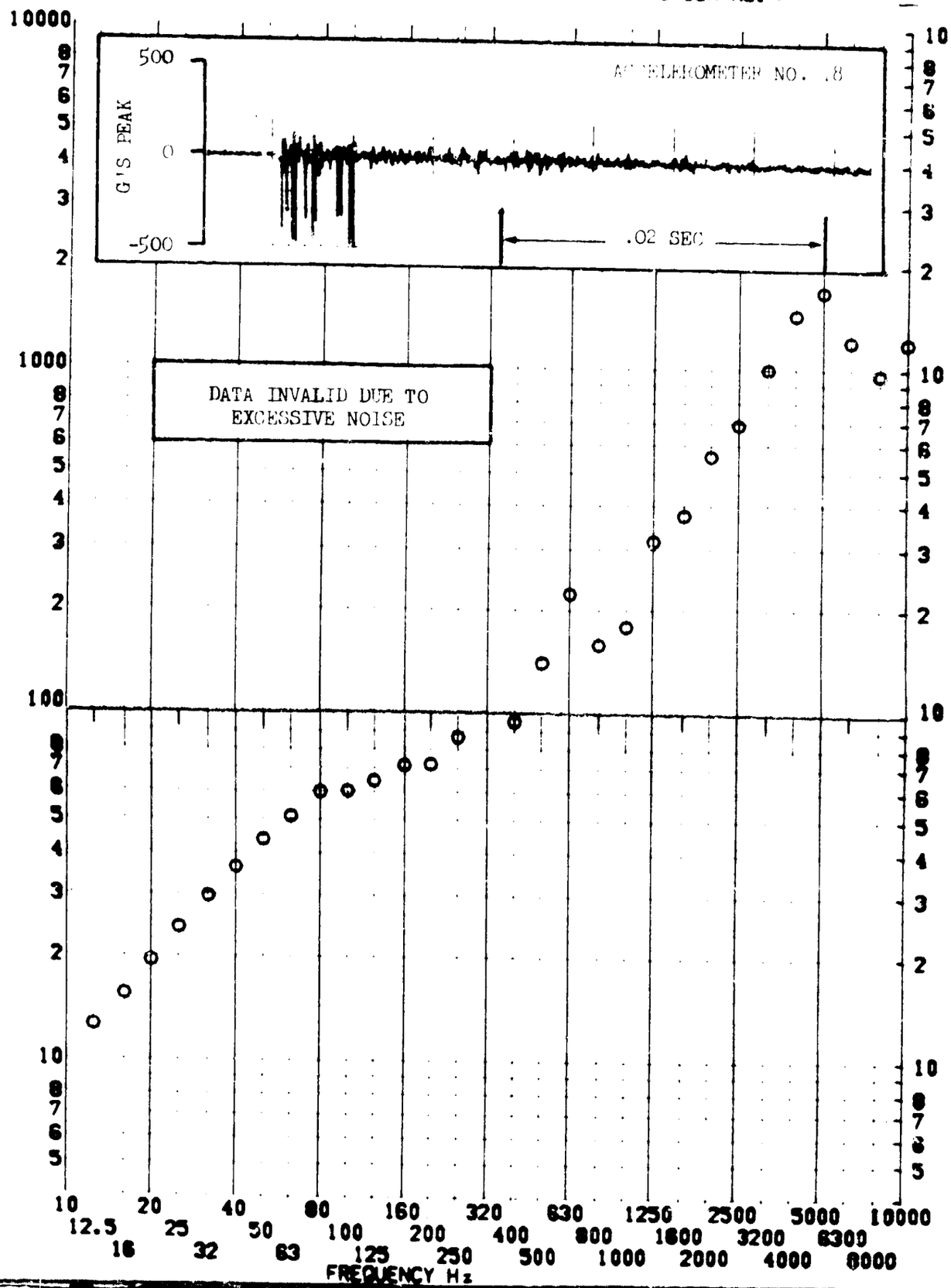

SHOCK TEST ANALYSIS DATA SHEET NO. H.A.Y.108

TEST ITEM [illegible]
SERIAL NO. —
SHOCK AXIS RADIAL —

PART NO. EQUIPMENT —
TEST DATE [illegible] 1969
SHOCK NO. 1 & 2 —

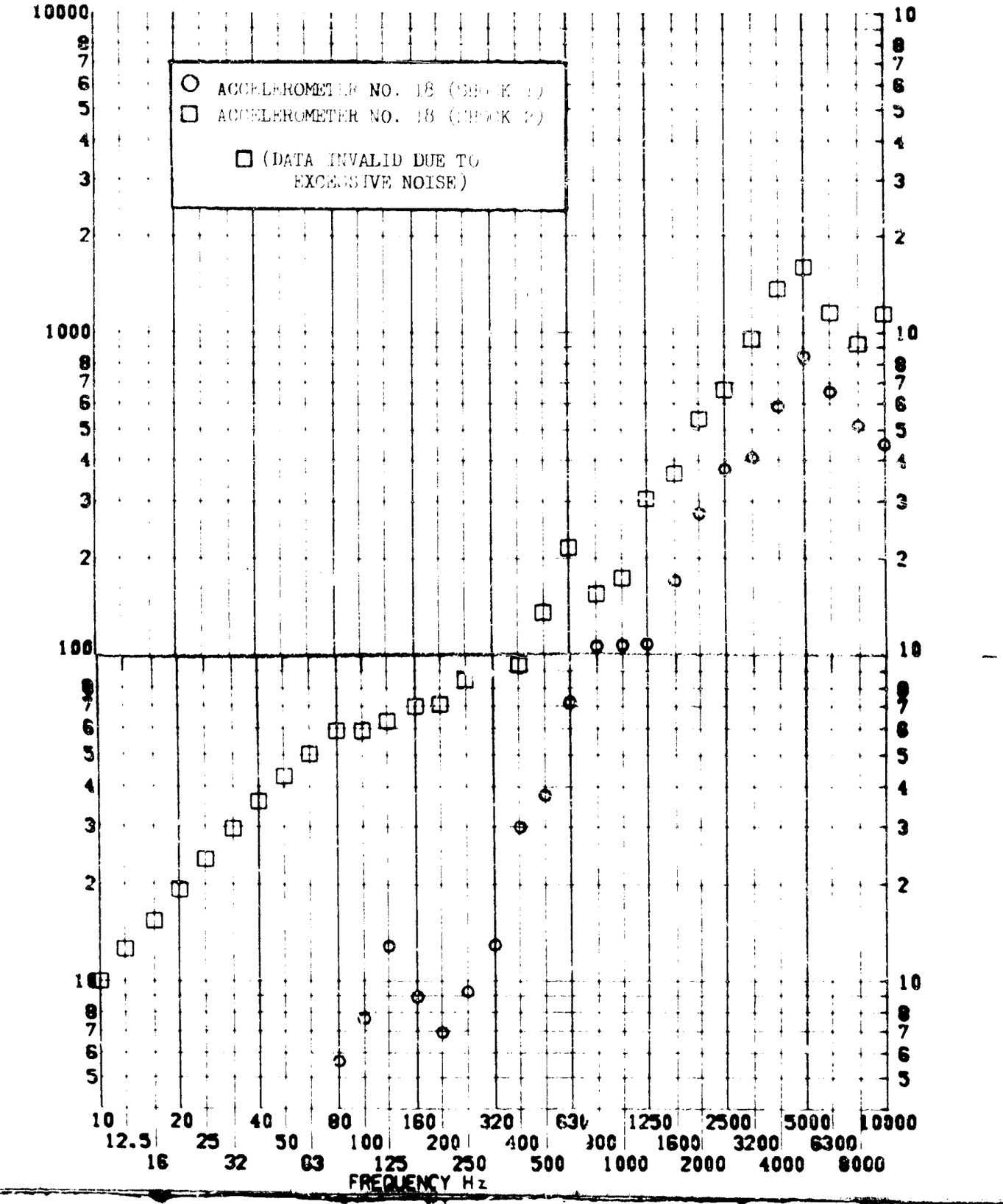

SHOCK TEST ANALYSIS DATA SHEET NO. H.A.[illegible].169

TEST ITEM 1377-404
SERIAL NO.
SHOCK AXIS [illegible]

PART NO. EQUIPMENT
TEST DATE 11 SEP 1969
SHOCK NO. 1

RESPONSE G-S

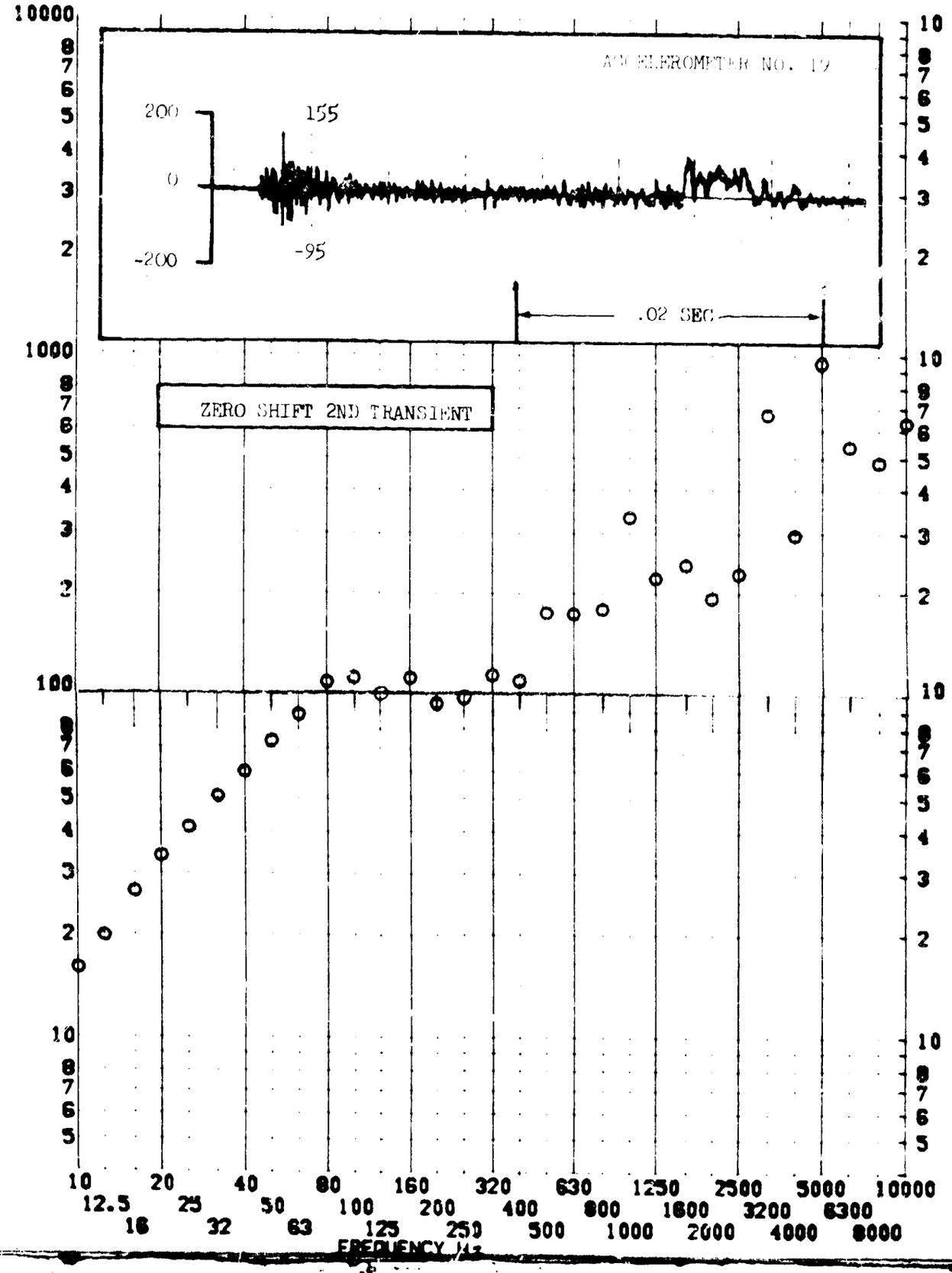

SHOCK TEST ANALYSIS DATA SHEET NO. [illegible]

TEST ITEM [illegible] PART NO. [illegible]
SERIAL NO. - TEST DATE [illegible] 8 1962
SHOCK AXIS [illegible] SHOCK NO. 1

RESPONSE G-S

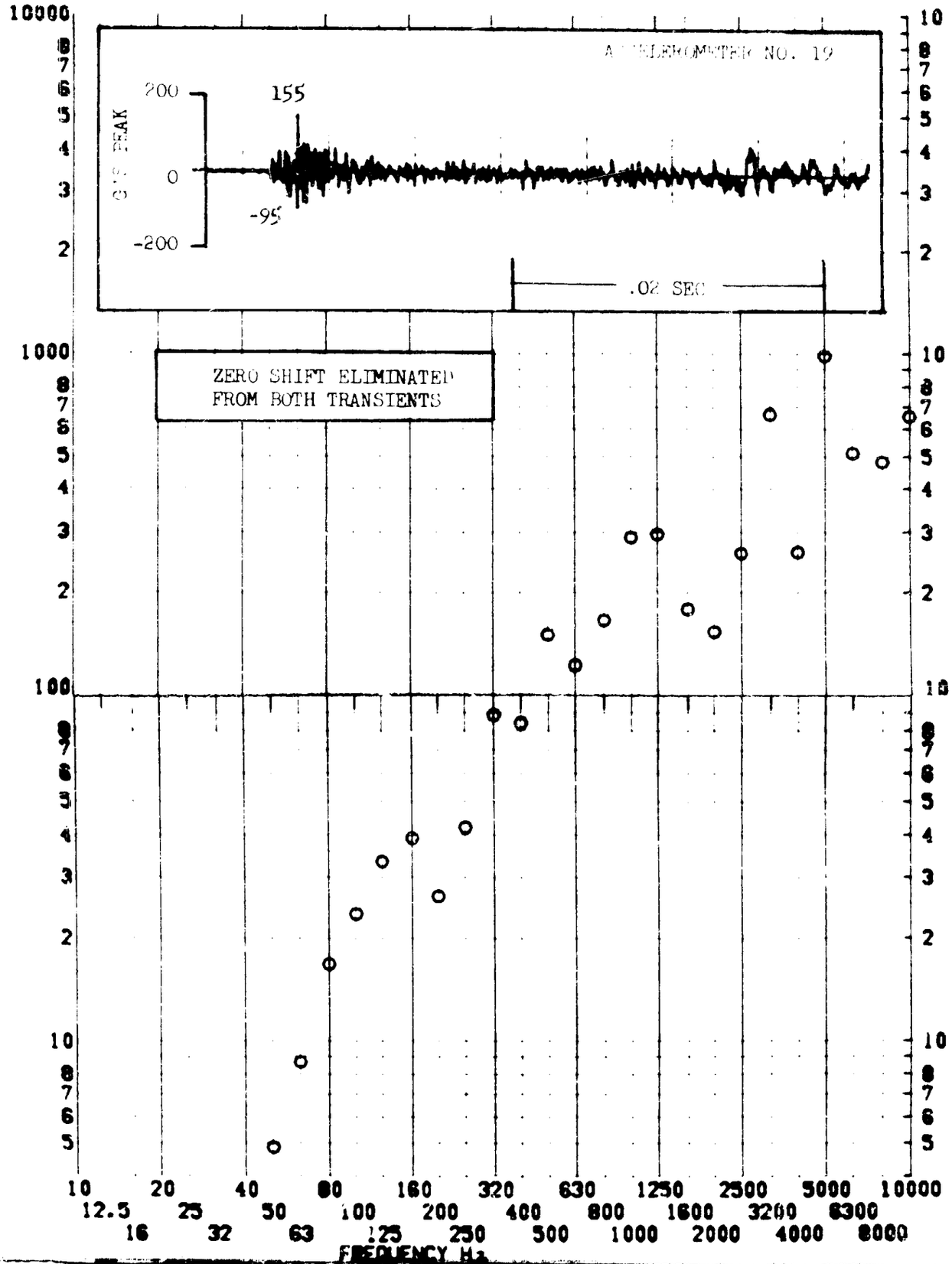

SHOCK TEST ANALYSIS DATA SHEET NO. [illegible]

TEST ITEM 1377-492
SERIAL NO.
SHOCK AXIS RADIAL

PART NO. [illegible]
TEST DATE 11 FEB 1969
SHOCK NO. 2

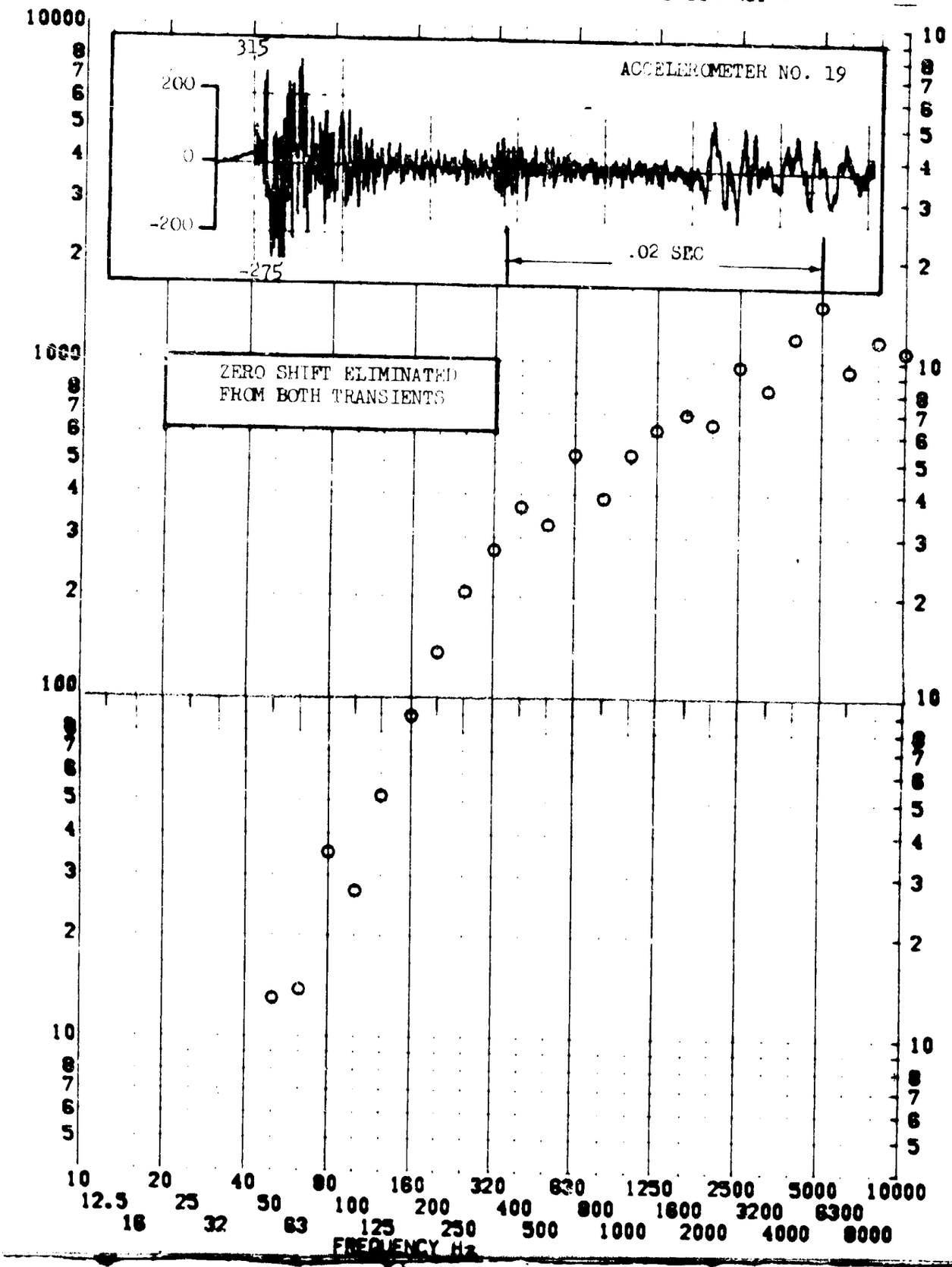

SHOCK TEST ANALYSIS DATA SHEET NO. II.A.7.1.2

TEST ITEM 1372-409,409,492 PART NO. EQUIPMENT
SERIAL NO. TEST DATE 11 FEB 1969
SHOCK AXIS RADIAL SHOCK NO.

RESPONSE G-S

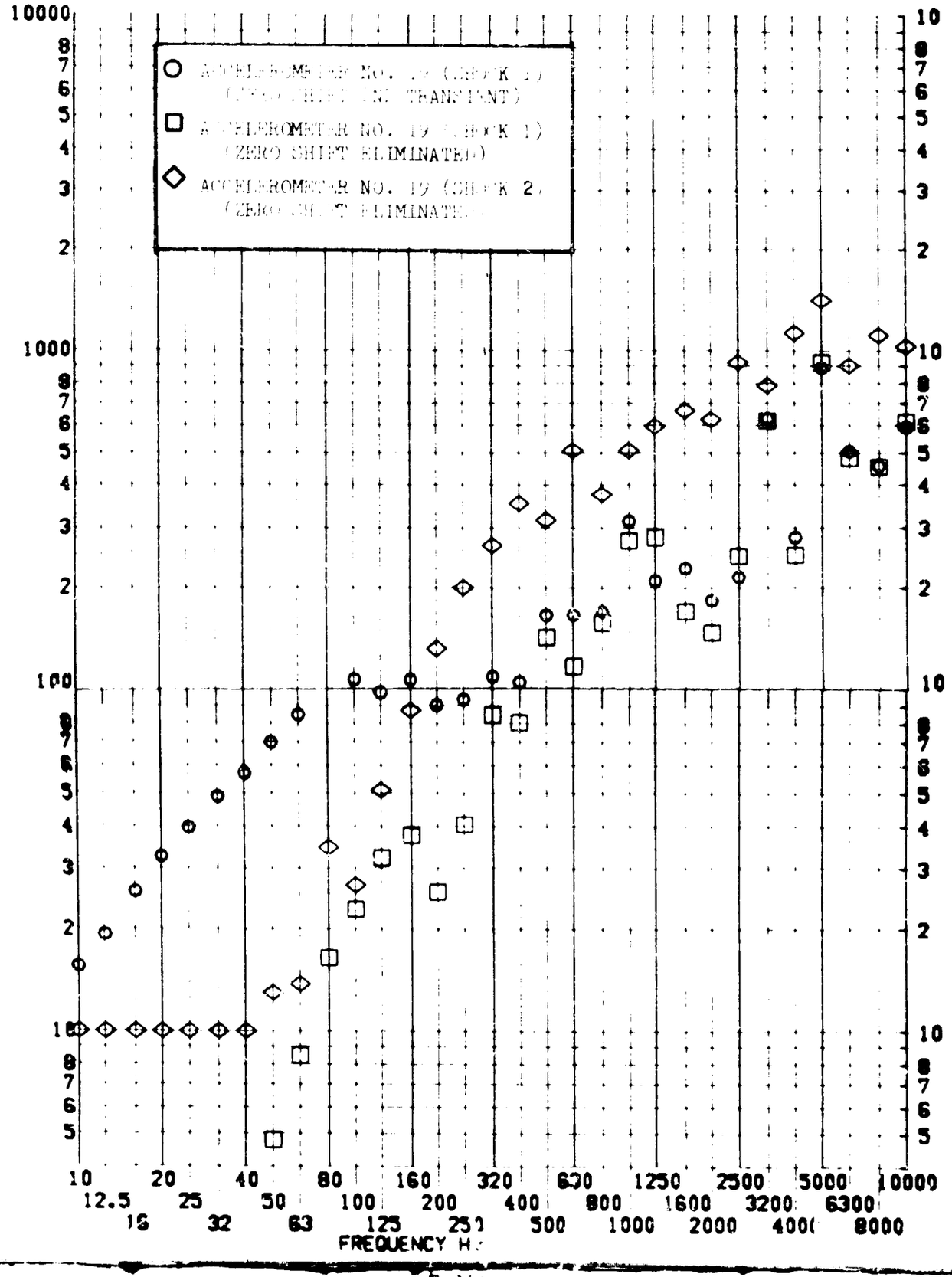

SHOCK TEST ANALYSIS DATA SHEET NO. H.A./.113

TEST ITEM 377-406
SERIAL NO.
SHOCK AXIS LONGITUDINAL

PART NO. EQUIPMENT
TEST DATE 11 FEB 1966
SHOCK NO. 1

RESPONSE G-S

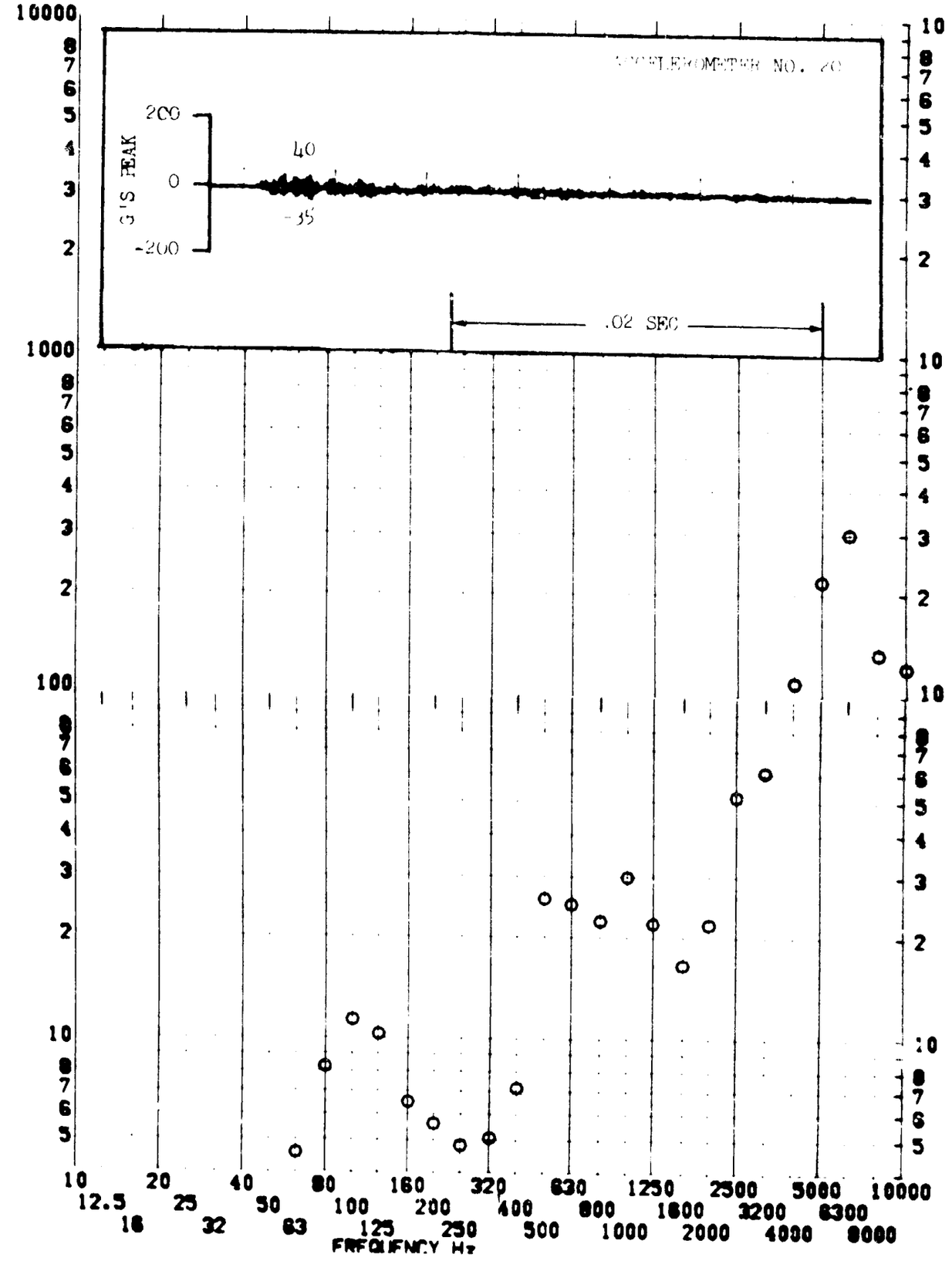

SHOCK TEST ANALYSIS DATA SHEET NO. T.A. ...

TEST ITEM 1377-493 PART NO. EQUIPMENT
SERIAL NO. TEST DATE 11 FEB 1969
RESPONSE G-S SHOCK AXIS LONGITUDINAL SHOCK NO. 2

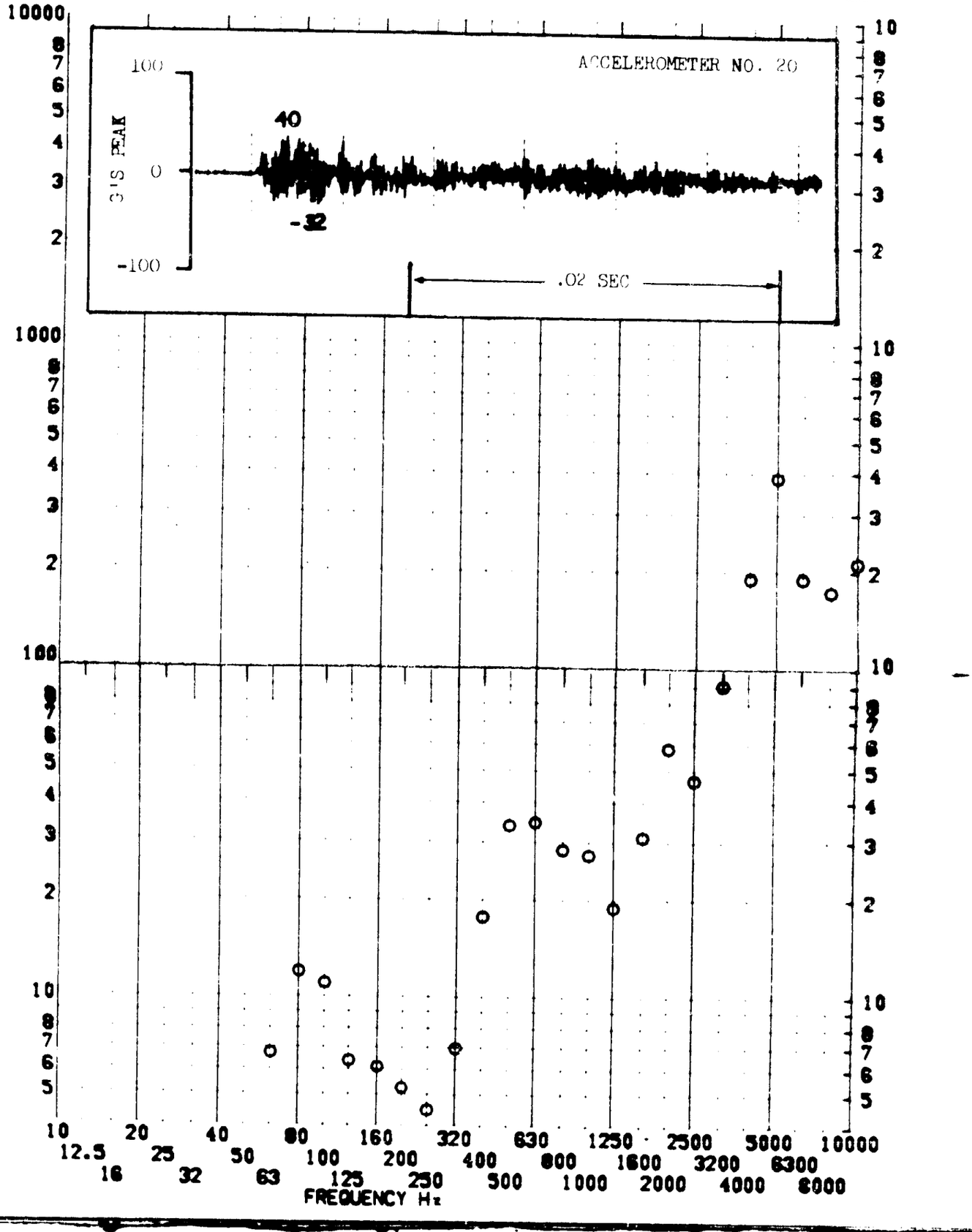

SHOCK TEST ANALYSIS DATA SHEET NO. II.A.7.115

TEST ITEM 1377-406,493
SERIAL NO.
SHOCK AXIS LONGITUDINAL

PART NO. EQUIPMENT
TEST DATE 11 FEB 1969
SHOCK NO. 1 & 2

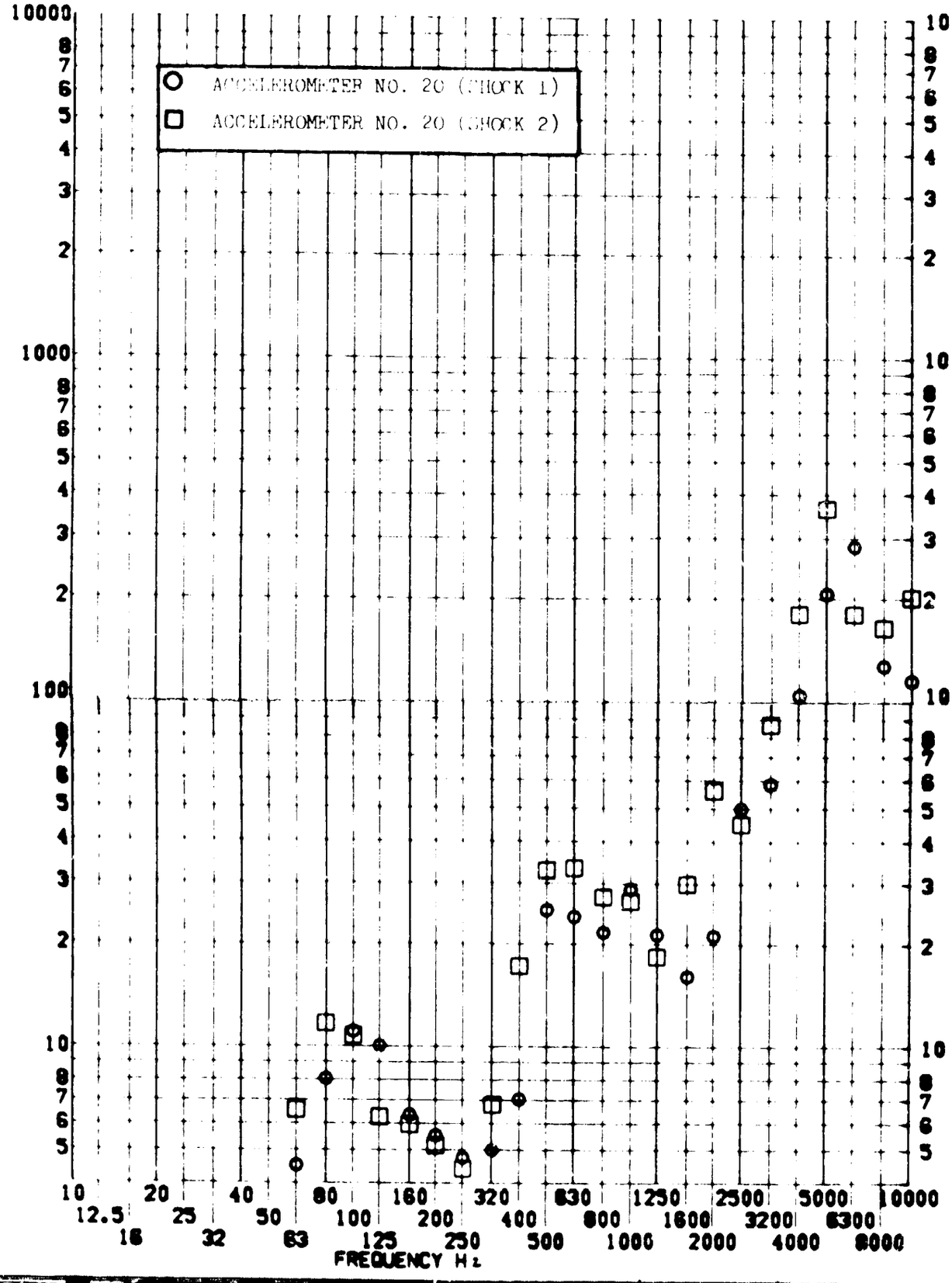

SHOCK TEST ANALYSIS DATA SHEET NO. II.A.7.16

TEST ITEM 1377-407
SERIAL NO.
SHOCK AXIS RADIAL

PART NO. EQUIPMENT
TEST DATE 11 FEB 1969
SHOCK NO. 1

RESPONSE G-S

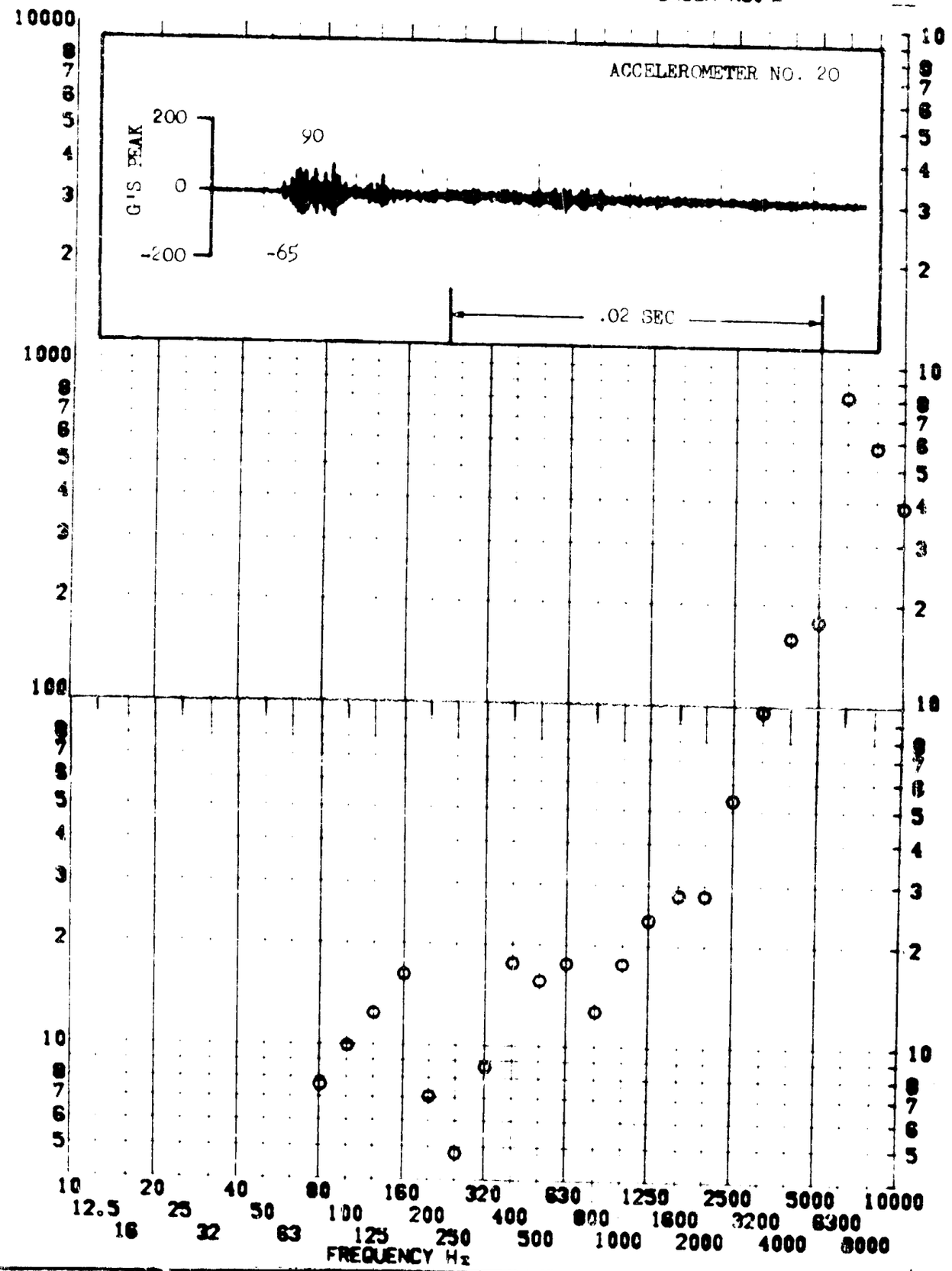

SHOCK TEST ANALYSIS DATA SHEET NO. II.A.7.117

TEST ITEM 1377-408 **PART NO.** EQUIPMENT

SERIAL NO. **TEST DATE** 11 FEB 1969

RESPONSE G-S **SHOCK AXIS** LONGITUDINAL **SHOCK NO.** 1

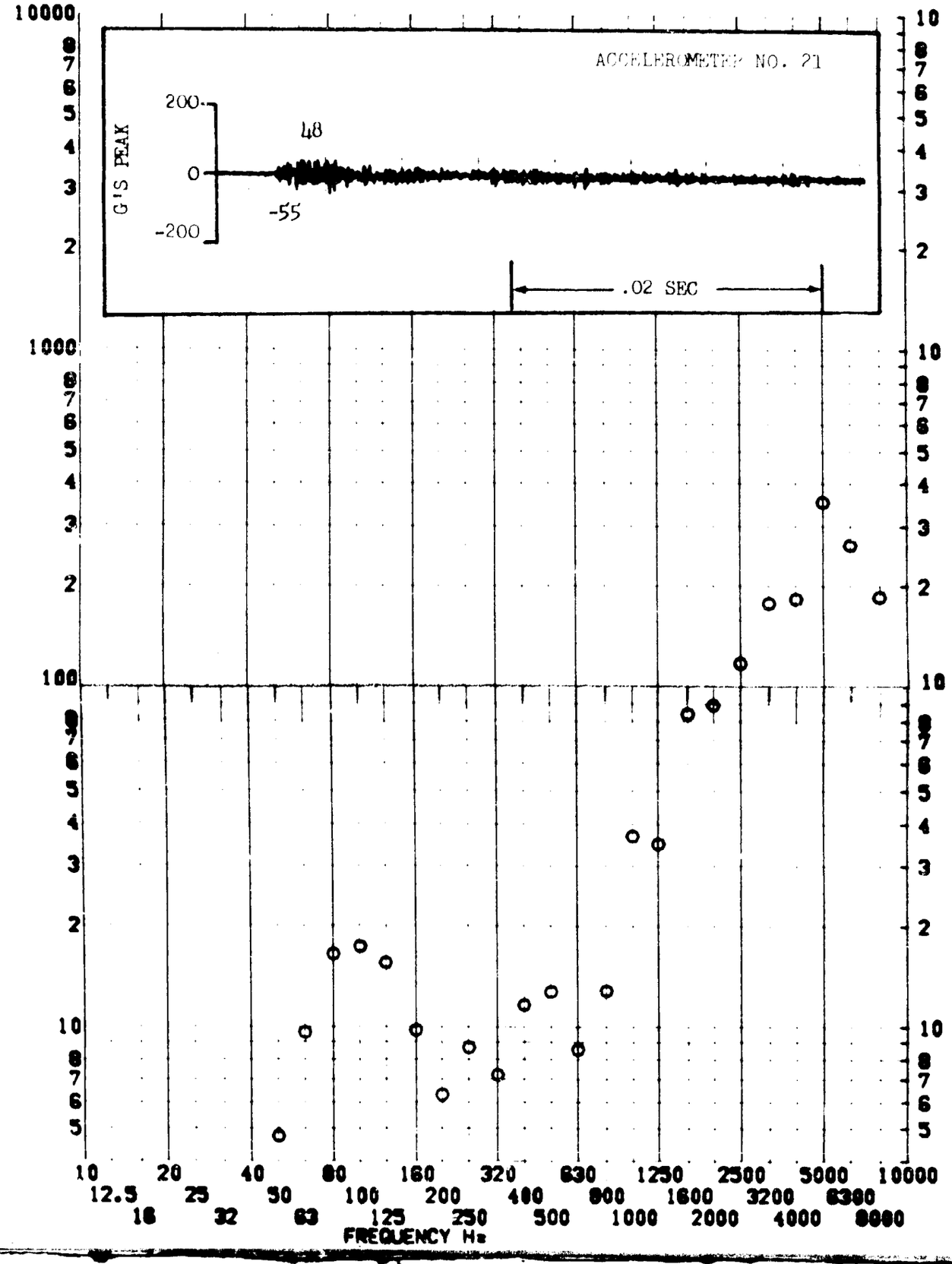

SHOCK TEST ANALYSIS DATA SHEET NO. [illegible]

TEST ITEM 1377-409
SERIAL NO.
SHOCK AXIS LONGITUDINAL

PART NO. EQUIPMENT
TEST DATE [illegible]
SHOCK NO. 1

RESPONSE G-S

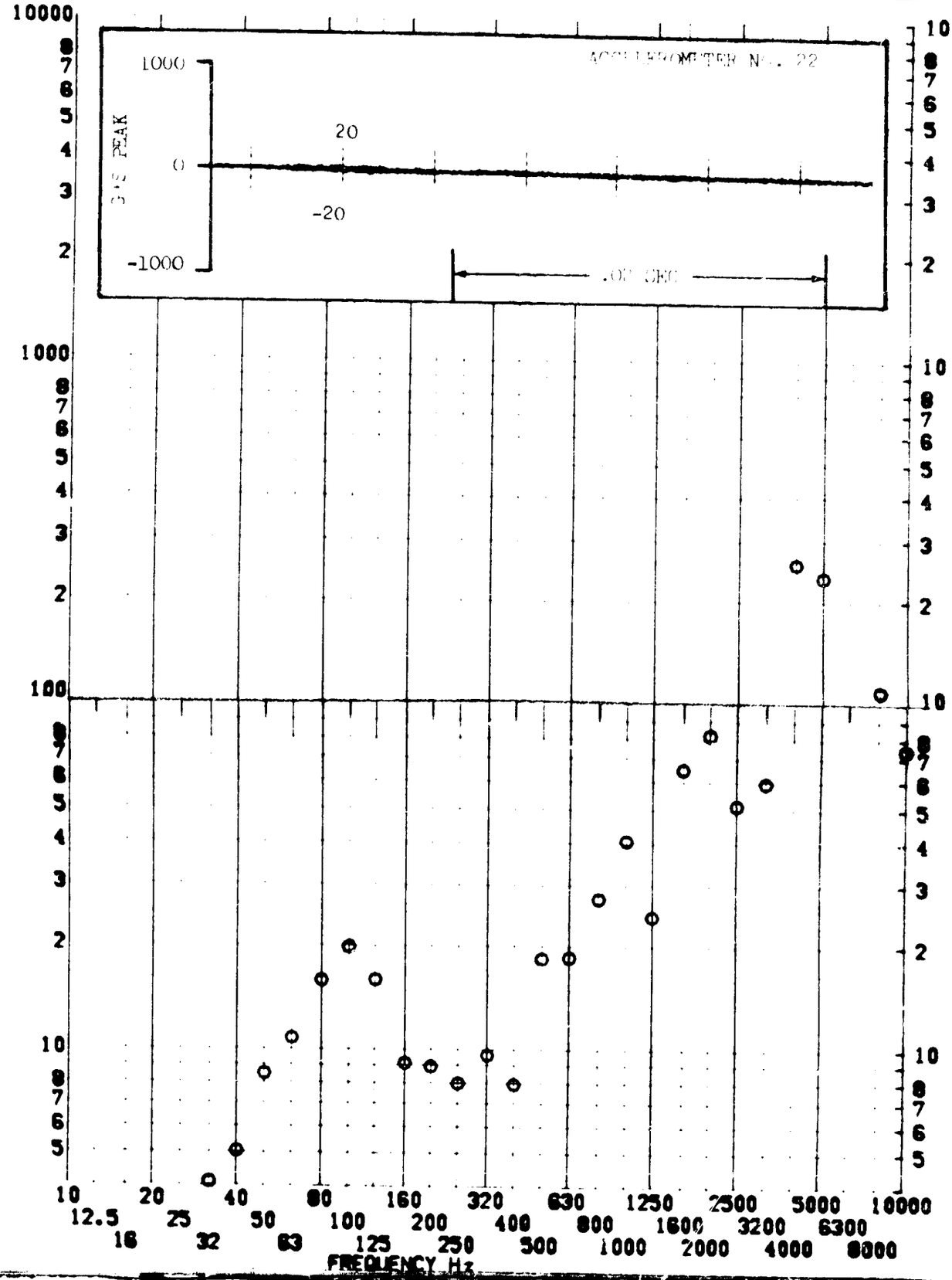

SHOCK TEST ANALYSIS DATA SHEET [illegible]

TEST ITEM 1377-494 PART NO. [illegible]
SERIAL NO. TEST DATE [illegible]
SHOCK AXIS [illegible] SHOCK NO. 2

RESPONSE G-S

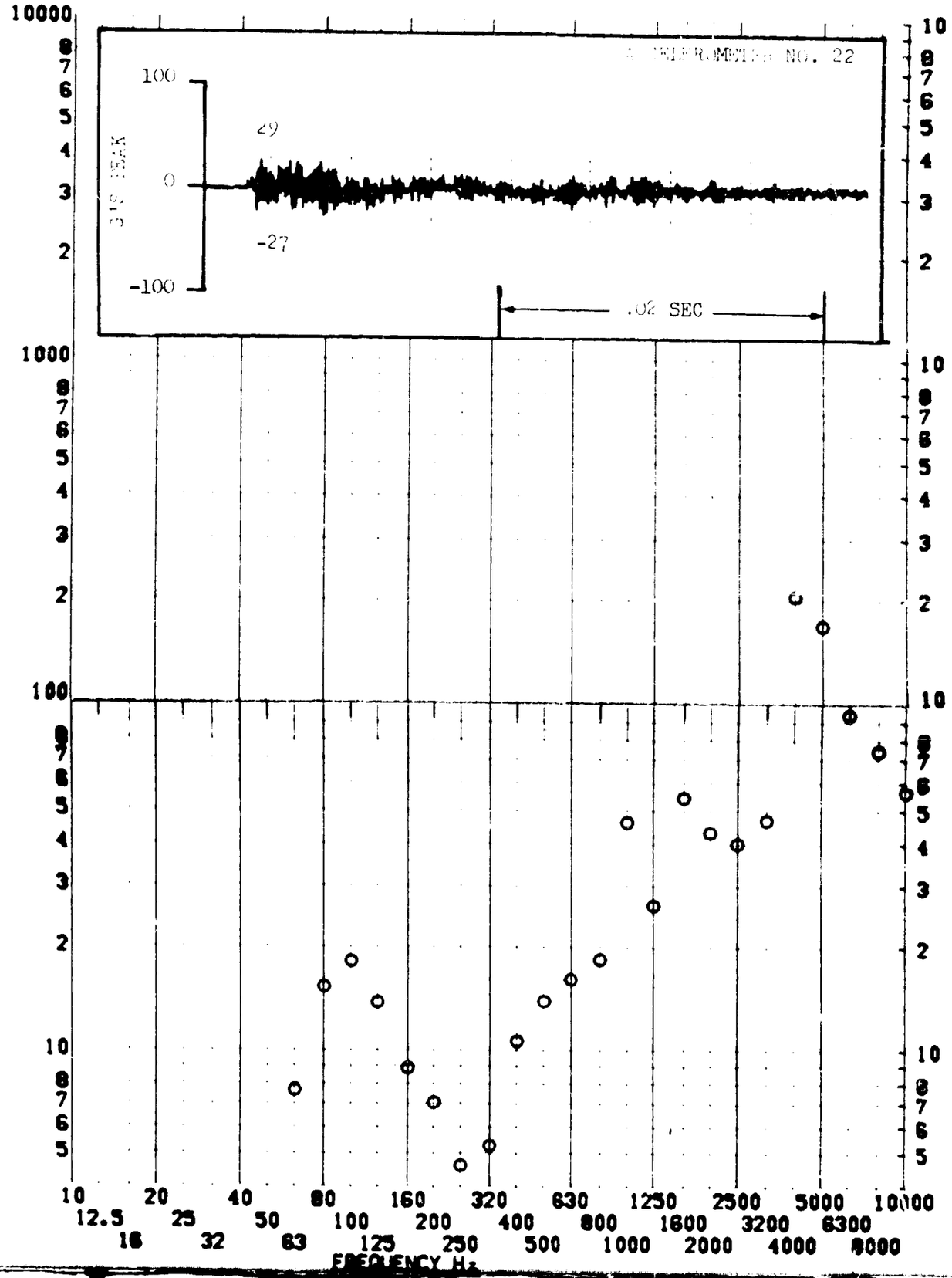

SHOCK TEST ANALYSIS DATA SHEET NO. II.A.7.120

TEST ITEM 377-469,491 PART NO. SPECIMEN

SERIAL NO. TEST DATE 11 SEP 1962

SHOCK AXIS LONGITUDINAL SHOCK NO. 1 & 2

RESPONSE G-S

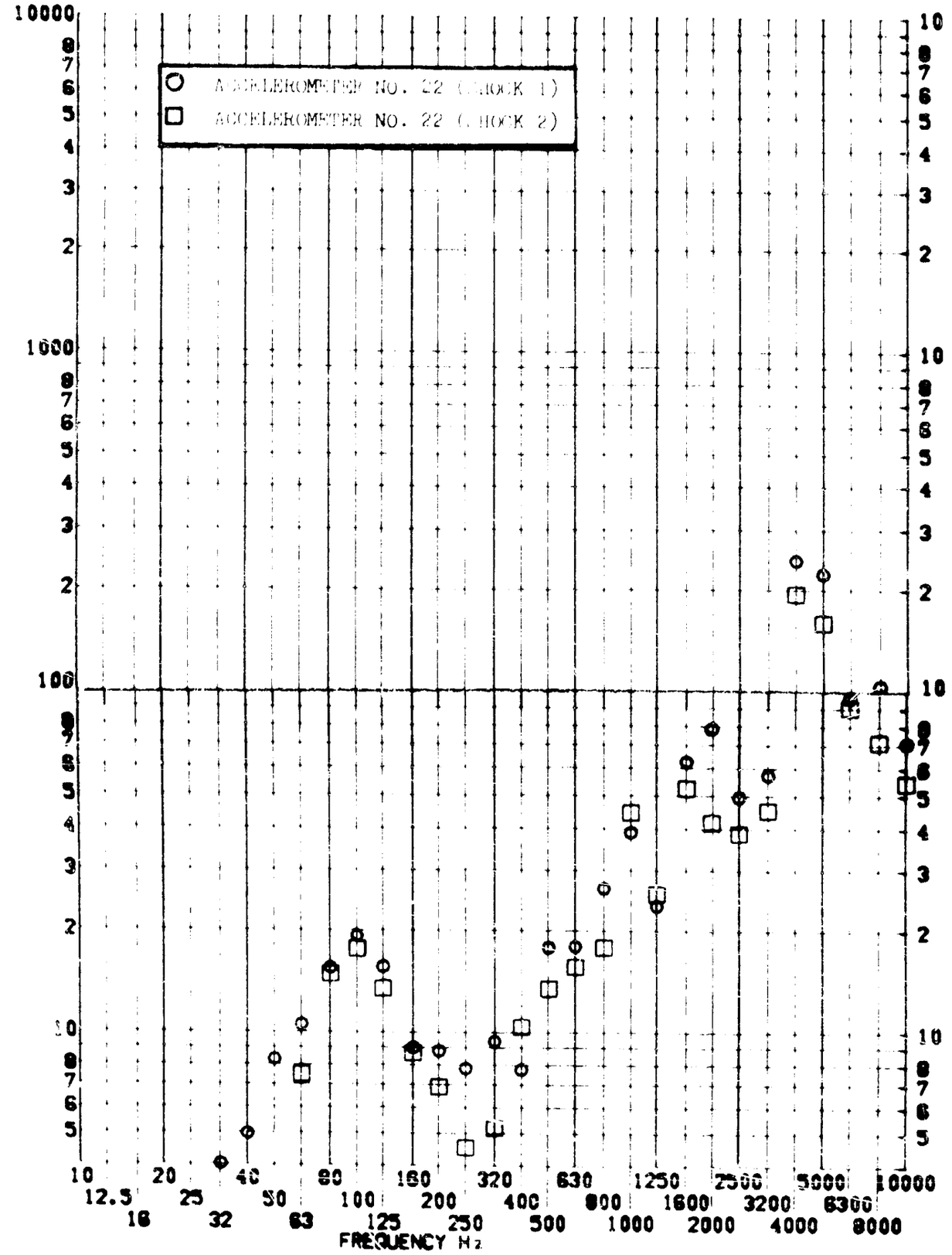

SHOCK TEST ANALYSIS DATA SHEET NO. II.A.7.1.1

TEST ITEM 1377-410
SERIAL NO.
SHOCK AXIS RADIAL

PART NO. EQUIPMENT
TEST DATE 11 FEB 1962
SHOCK NO. 1

RESPONSE G-S

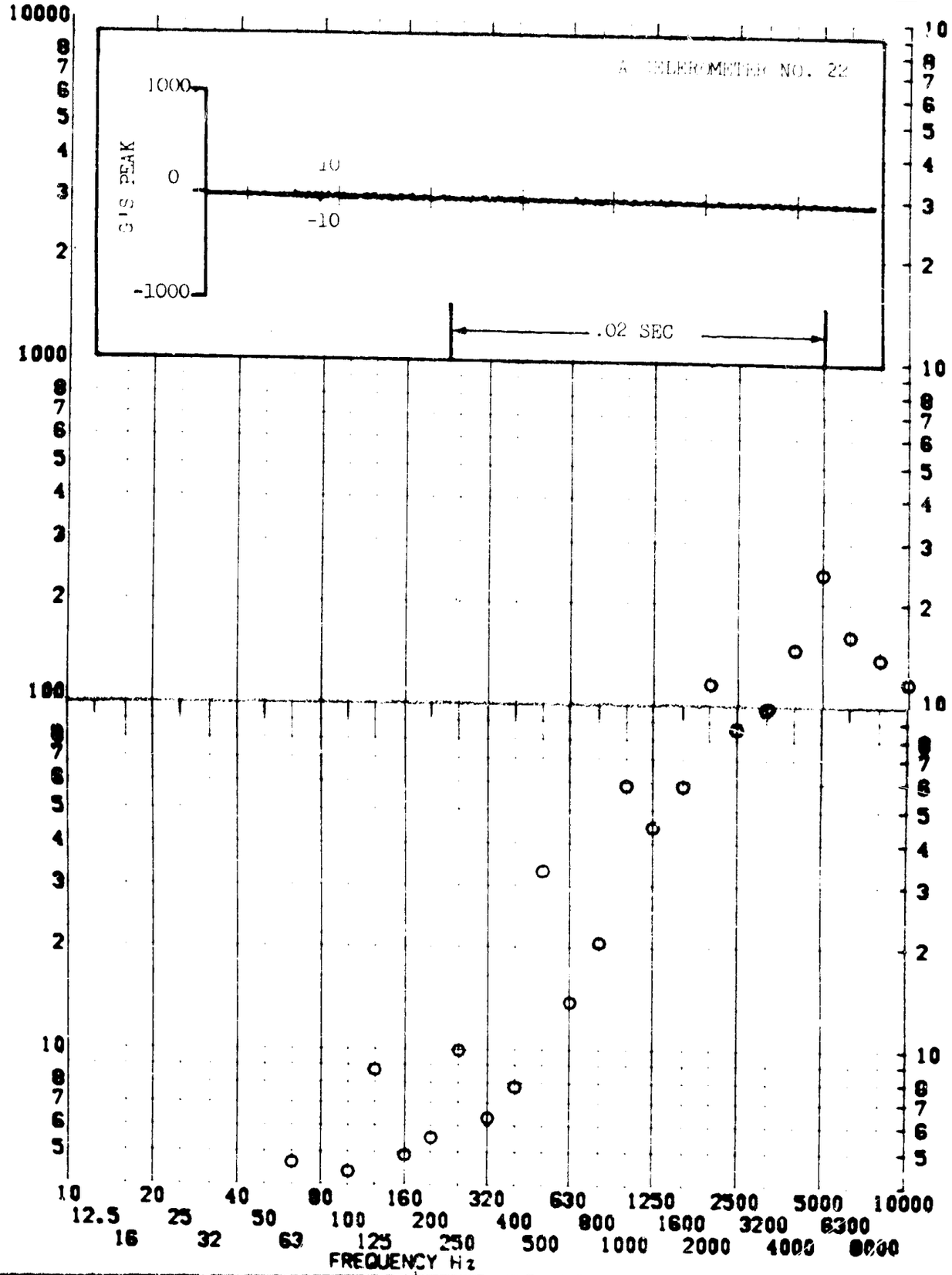

SHOCK TEST ANALYSIS DATA SHEET NO. T.A. ...

TEST ITEM ...-495 PART NO. EQUIPMENT

SERIAL NO. TEST DATE ... 1969

RESPONSE G-S SHOCK AXIS AXIAL SHOCK NO. 2

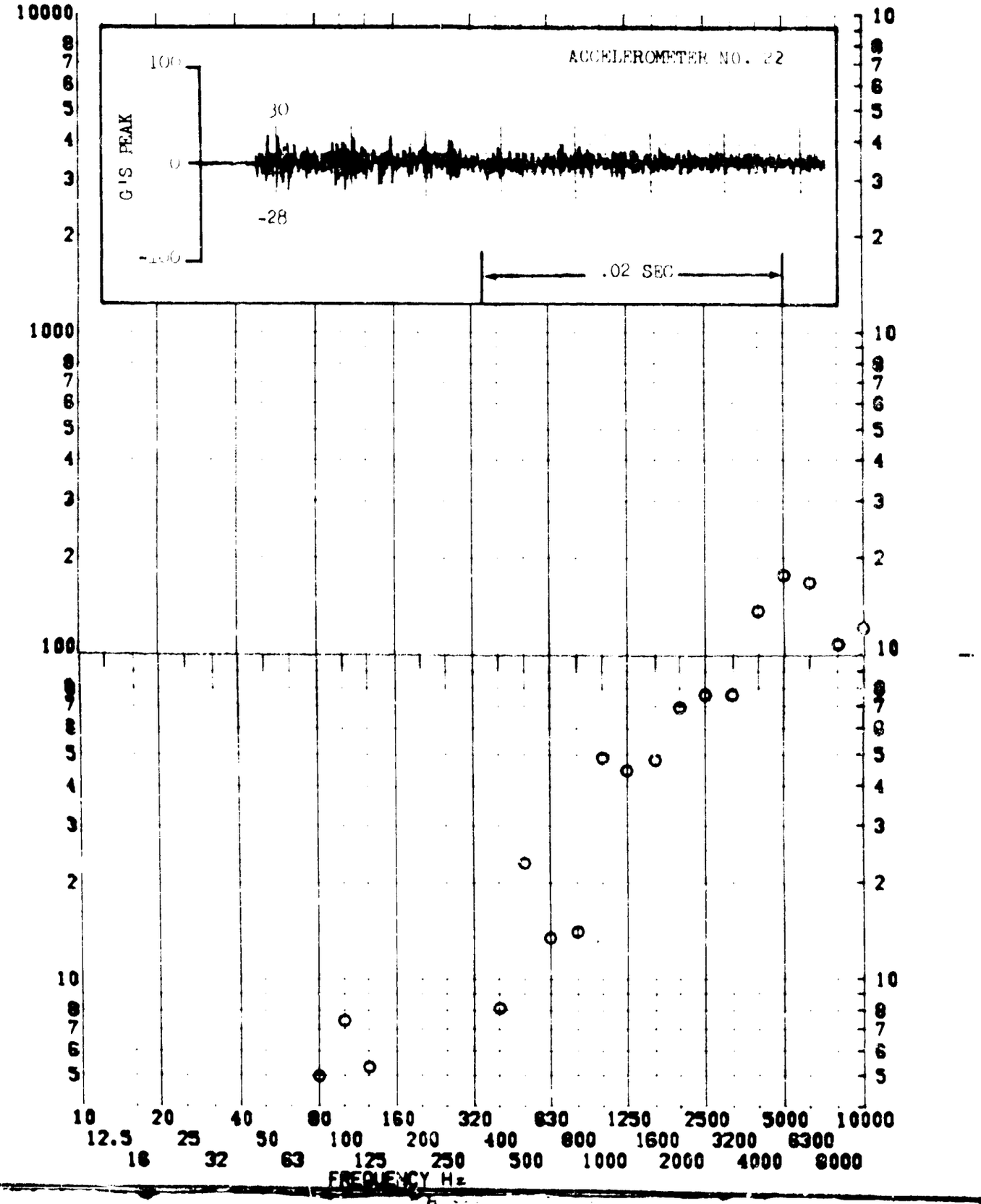

SHOCK TEST ANALYSIS DATA SHEET

No. 1 & 2 (123)

TEST ITEM 1377-410,422
SERIAL NO. —
SHOCK AXIS RADIAL —

PART NO. EQUIPMENT —
TEST DATE 11 FEB 1962
SHOCK NO. 1 & 2 —

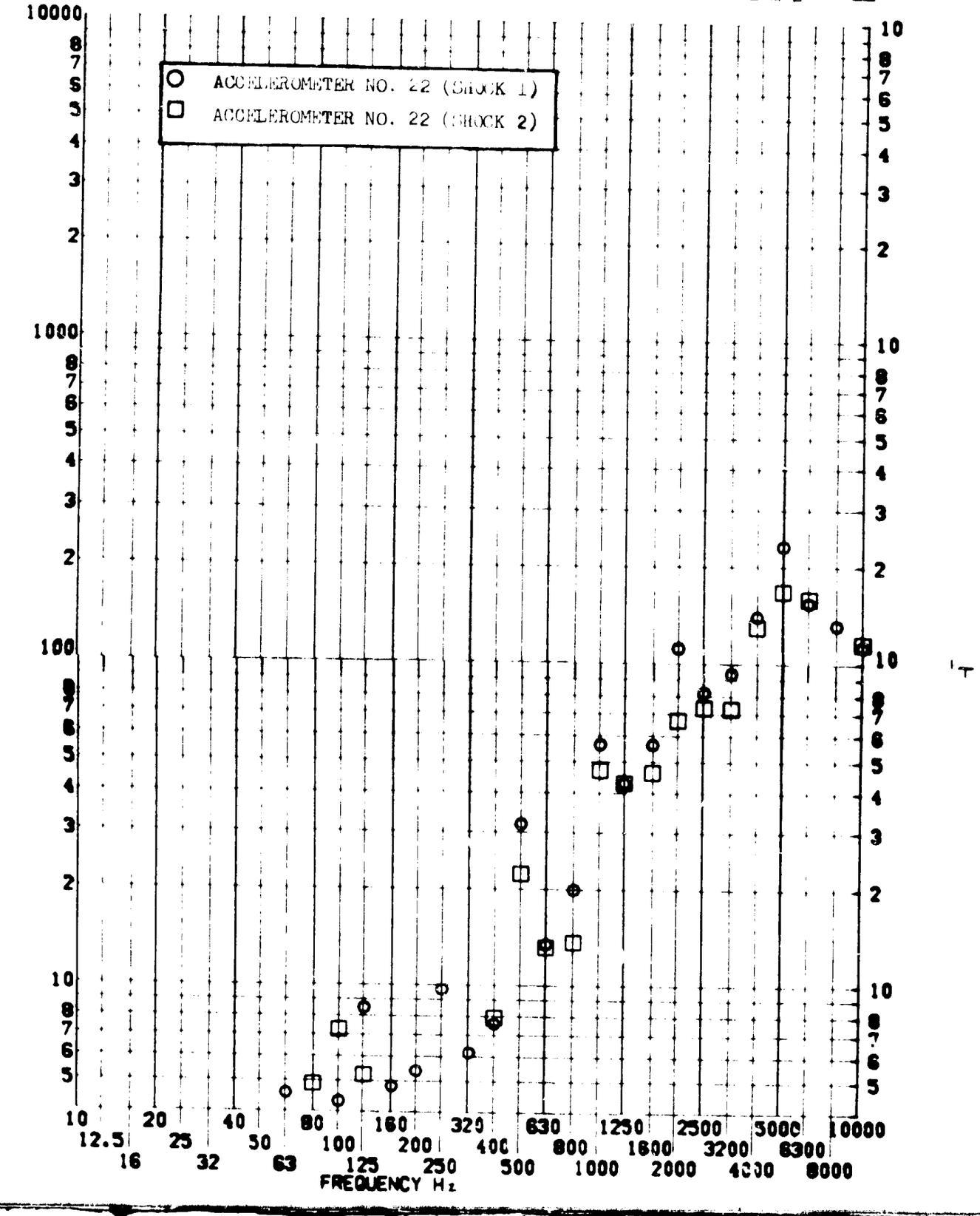

SHOCK TEST ANALYSIS DATA SHEET NO. S.A./. 2L

TEST ITEM 137-4... PART NO. EQUIPMENT

SERIAL NO. TEST DATE 1. FEB 1969

RESPONSE G-S SHOCK AXIS RADIAL SHOCK NO. 1

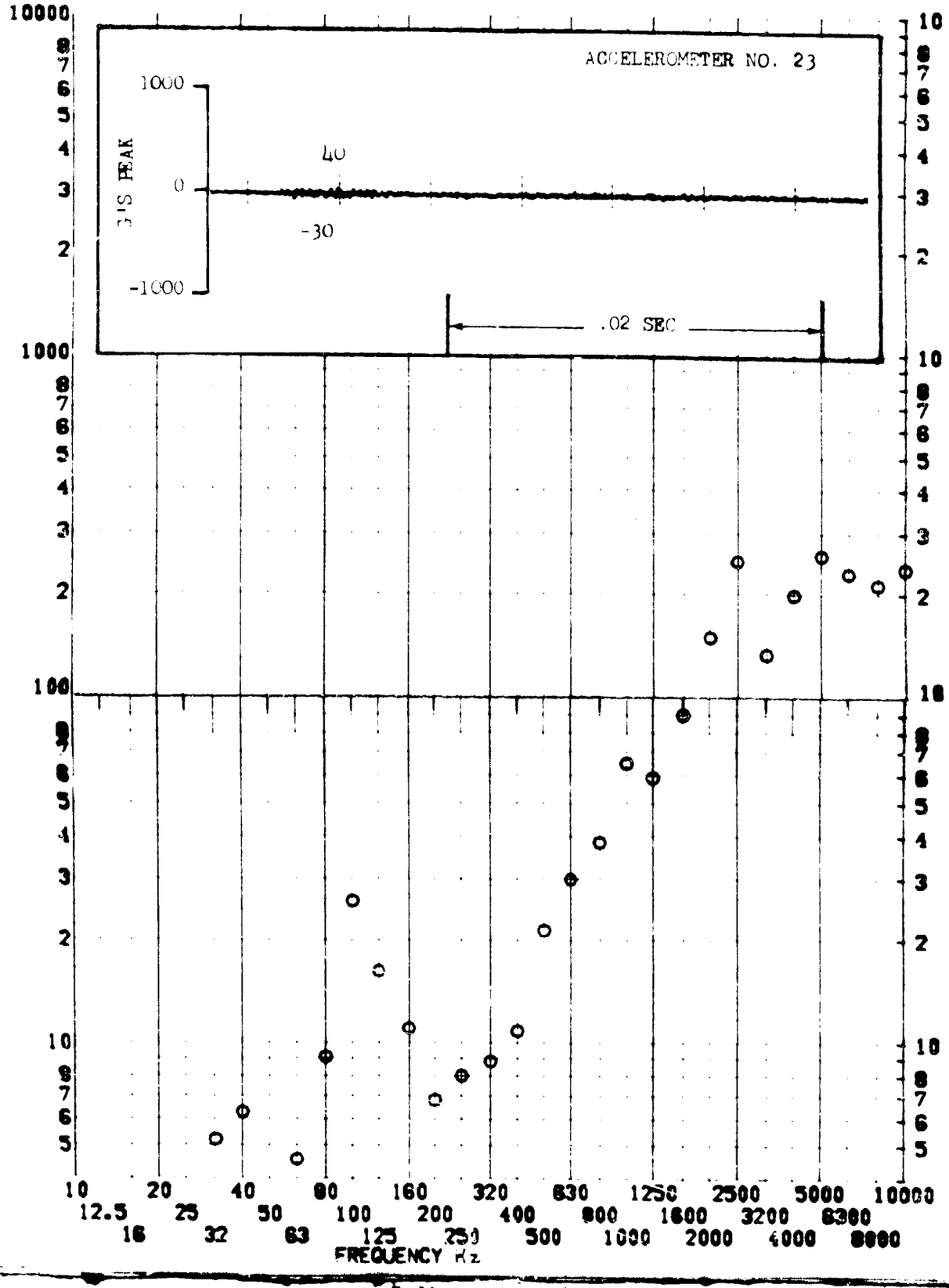

SHOCK TEST ANALYSIS DATA SHEET No. II.A.7.125

TEST ITEM 1377-496
SERIAL NO.
SHOCK AXIS RADIAL

PART NO. EQUIPMENT
TEST DATE [illegible] 1969
SHOCK NO. 2

RESPONSE G-S

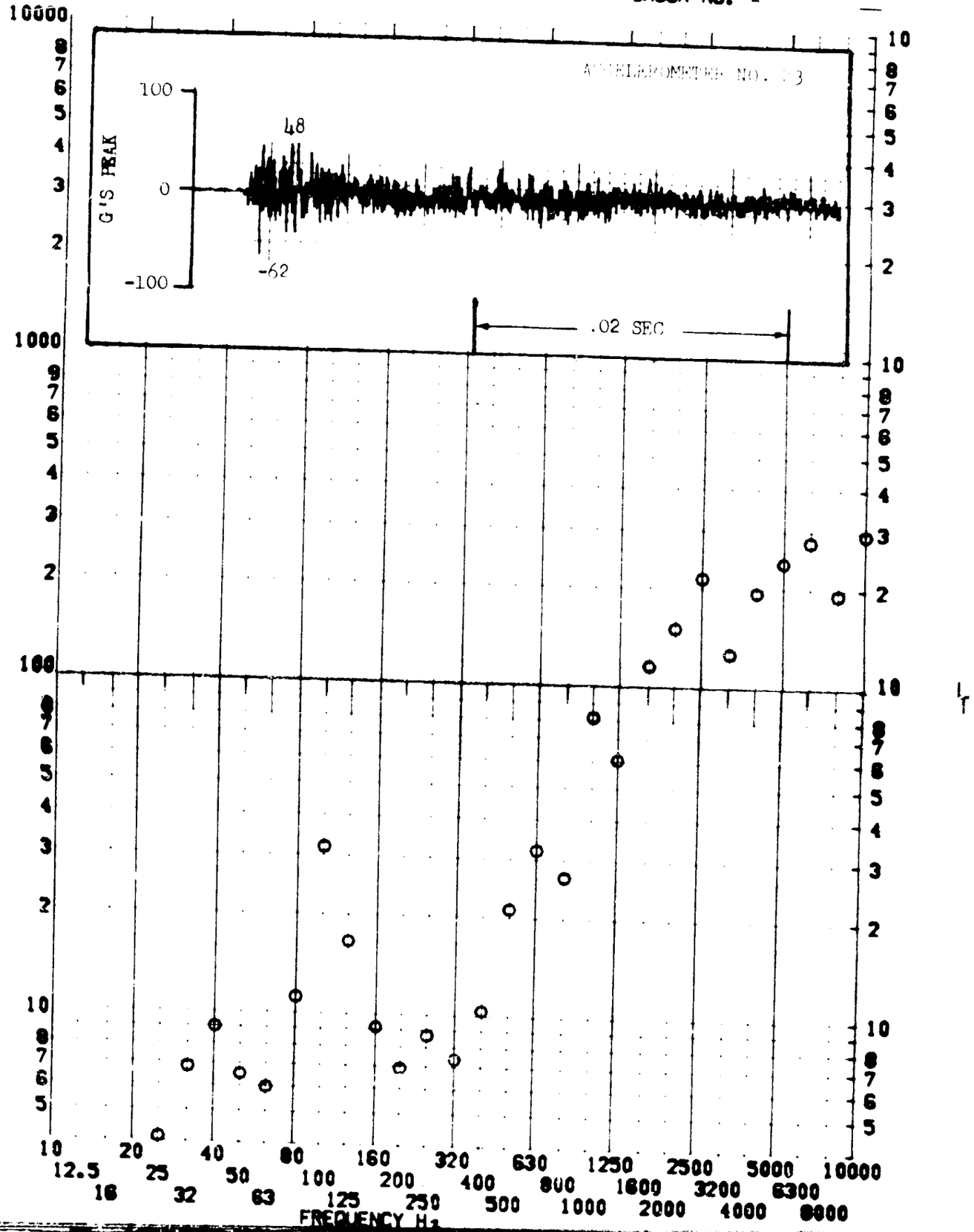

SHOCK TEST ANALYSIS DATA SHEET NO. [illegible]

TEST ITEM 377-411,496
SERIAL NO. —
SHOCK AXIS RADIAL —

PART NO. EQUIPMENT —
TEST DATE [illegible]
SHOCK NO. 1 & 2 —

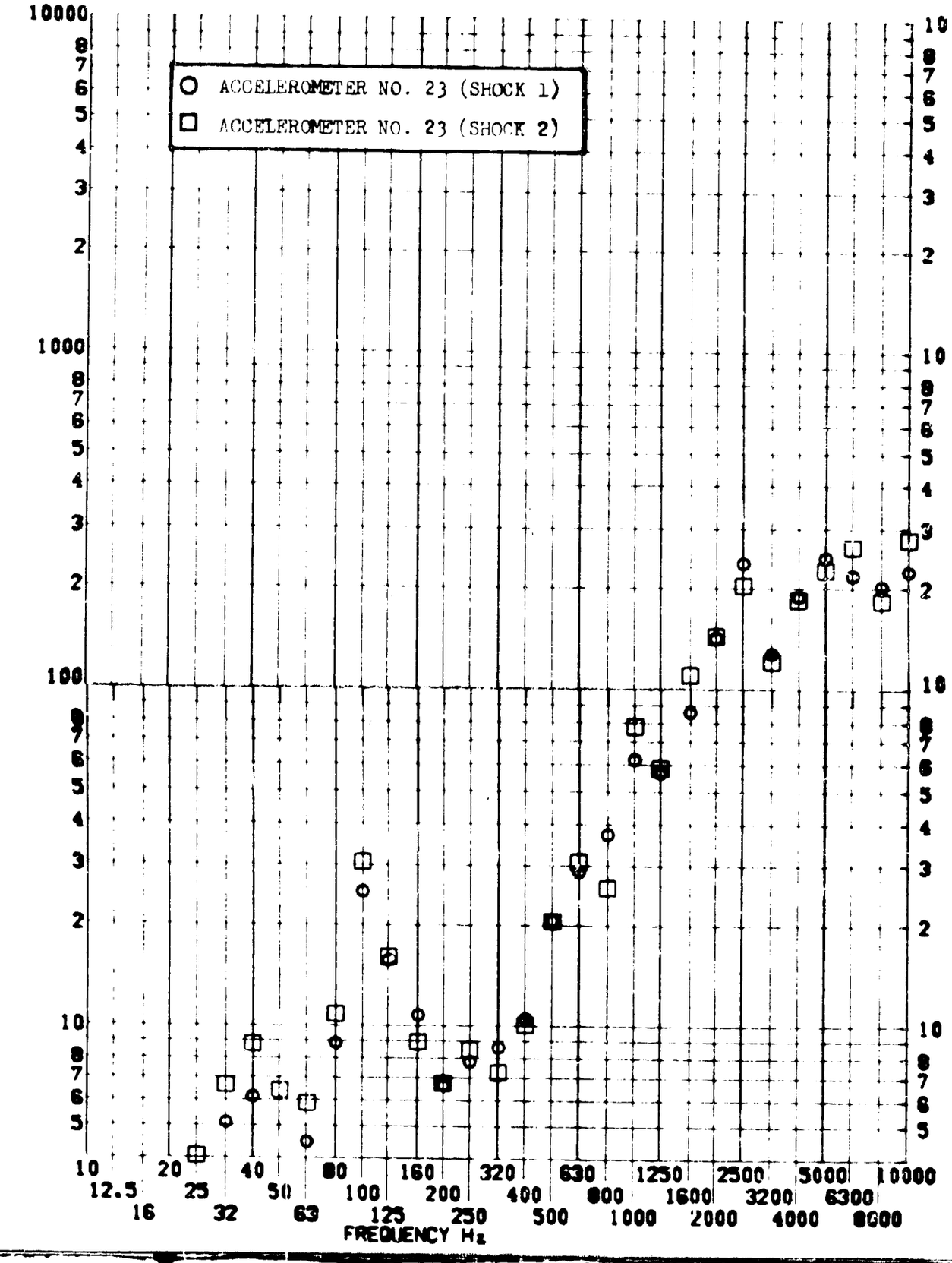

SHOCK TEST ANALYSIS DATA SHEET No. II.A.7.127

TEST ITEM 1377-412 PART NO. EQUIPMENT
SERIAL NO. — TEST DATE 11 SEP 1969
RESPONSE G-S SHOCK AXIS RADIAL SHOCK NO. 1

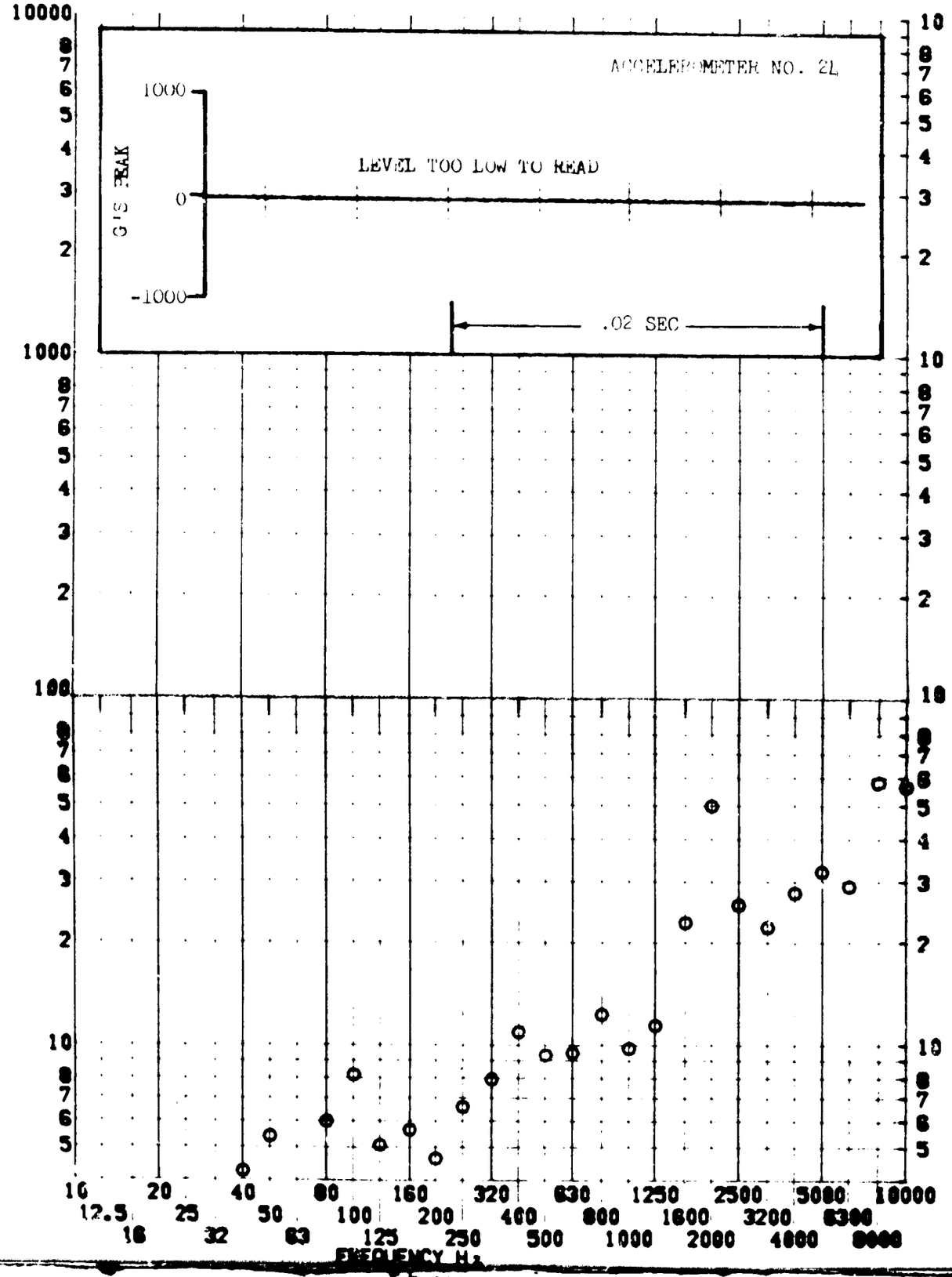

SHOCK TEST ANALYSIS DATA SHEET NO. H.A.7.128

TEST ITEM 1377-497
SERIAL NO.
SHOCK AXIS RADIAL

PART NO. EQUIPMENT
TEST DATE 11 FEB 1969
SHOCK NO. 2

RESPONSE G-S

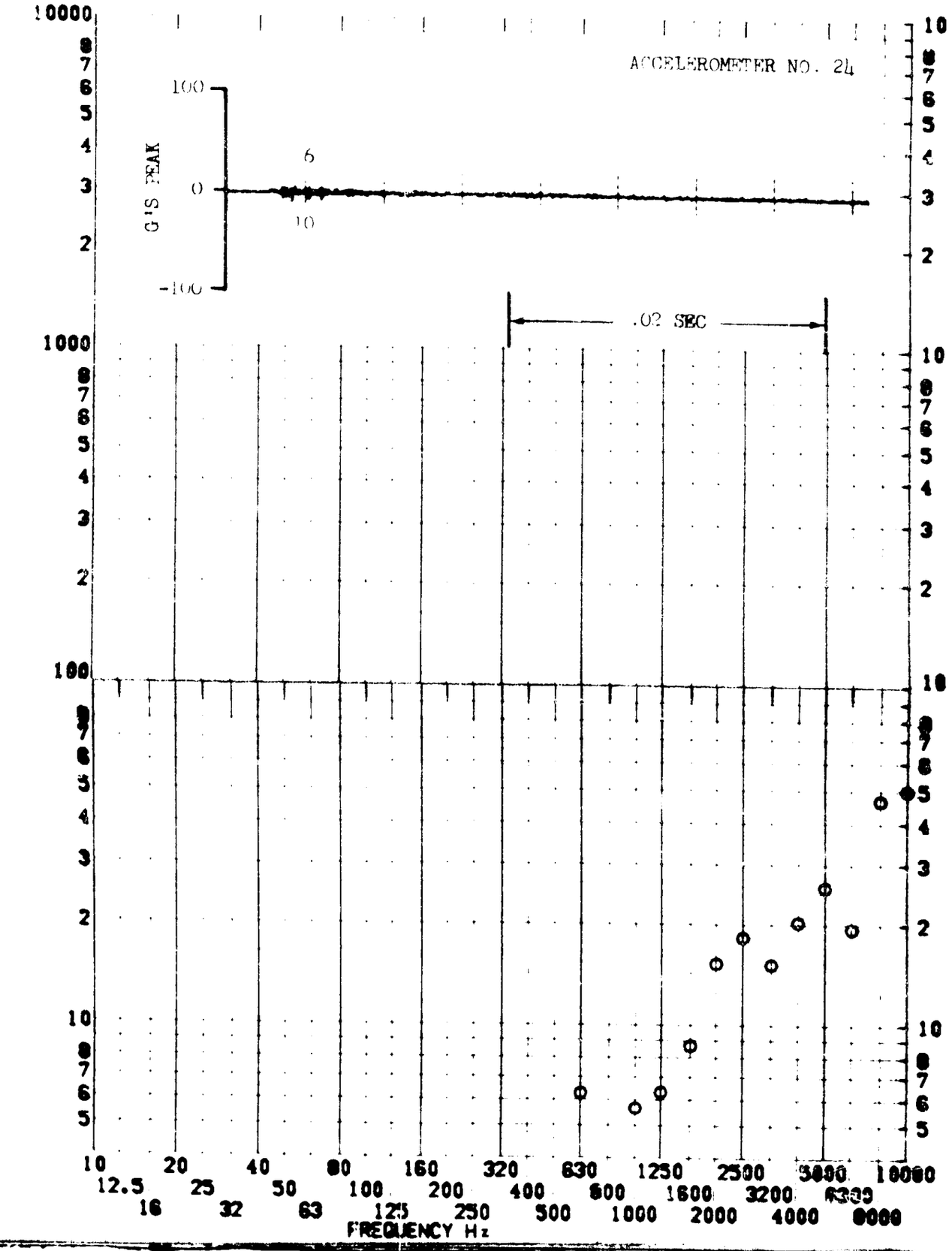

SHOCK TEST ANALYSIS DATA SHEET NO. II.A.7.129

TEST ITEM 1377-412,497
SERIAL NO. —
SHOCK AXIS RADIAL —

PART NO. EQUIPMENT
TEST DATE 11 FEB 1969
SHOCK NO. 1 & 2 —

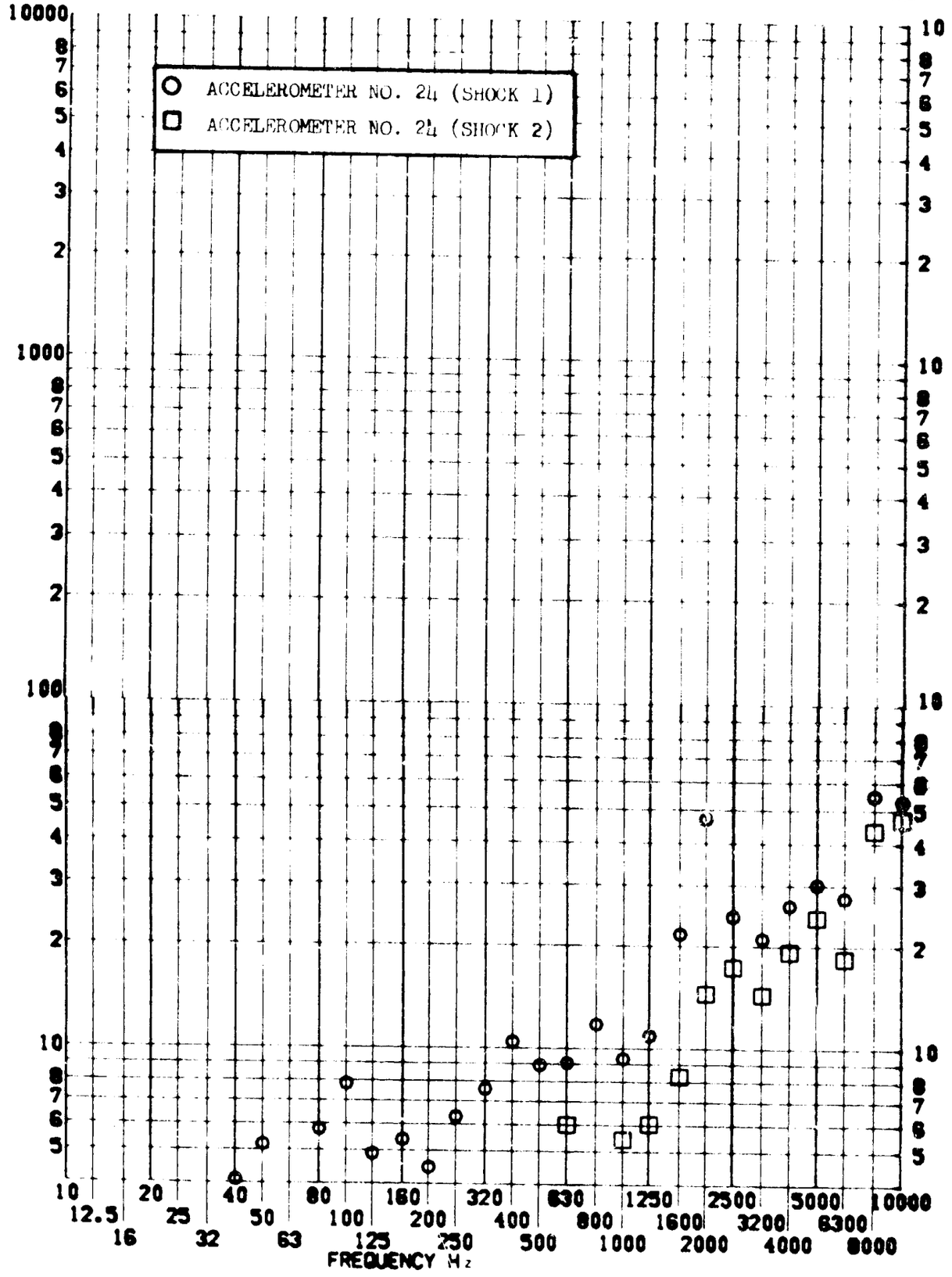

SHOCK TEST ANALYSIS DATA SHEET NO. [illegible].A. [illegible]30

TEST ITEM 137-413
SERIAL NO.
SHOCK AXIS LONGITUDINAL

PART NO. EQUIPMENT
TEST DATE 11 FEB 1969
SHOCK NO. 1

RESPONSE G-S

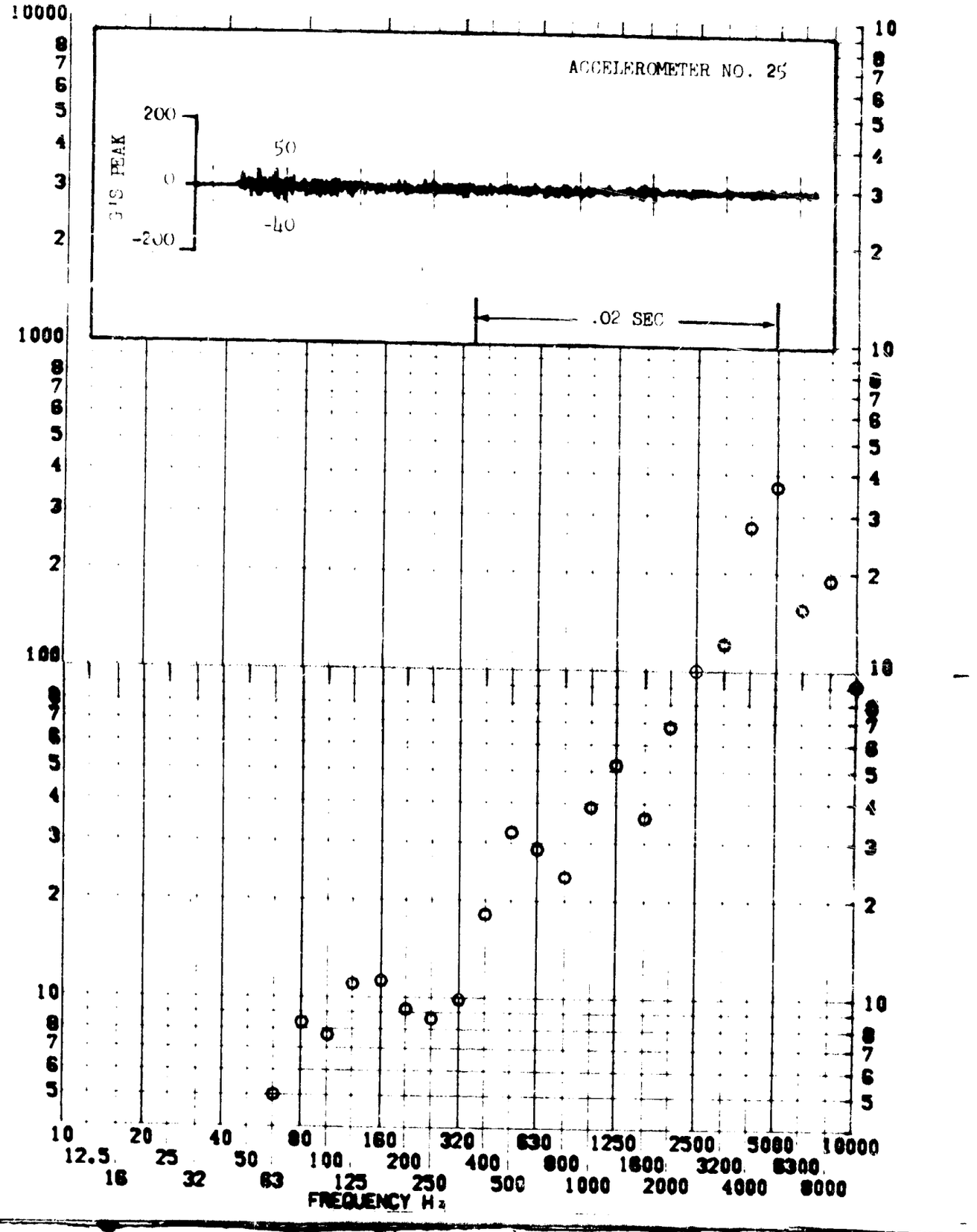

SHOCK TEST ANALYSIS DATA SHEET NO. II.A.7.151

TEST ITEM 1377-498 **PART NO.** EQUIPMENT
SERIAL NO. **TEST DATE** 11 FEB 1962
RESPONSE G-S **SHOCK AXIS** LONGITUDINAL **SHOCK NO.** 2

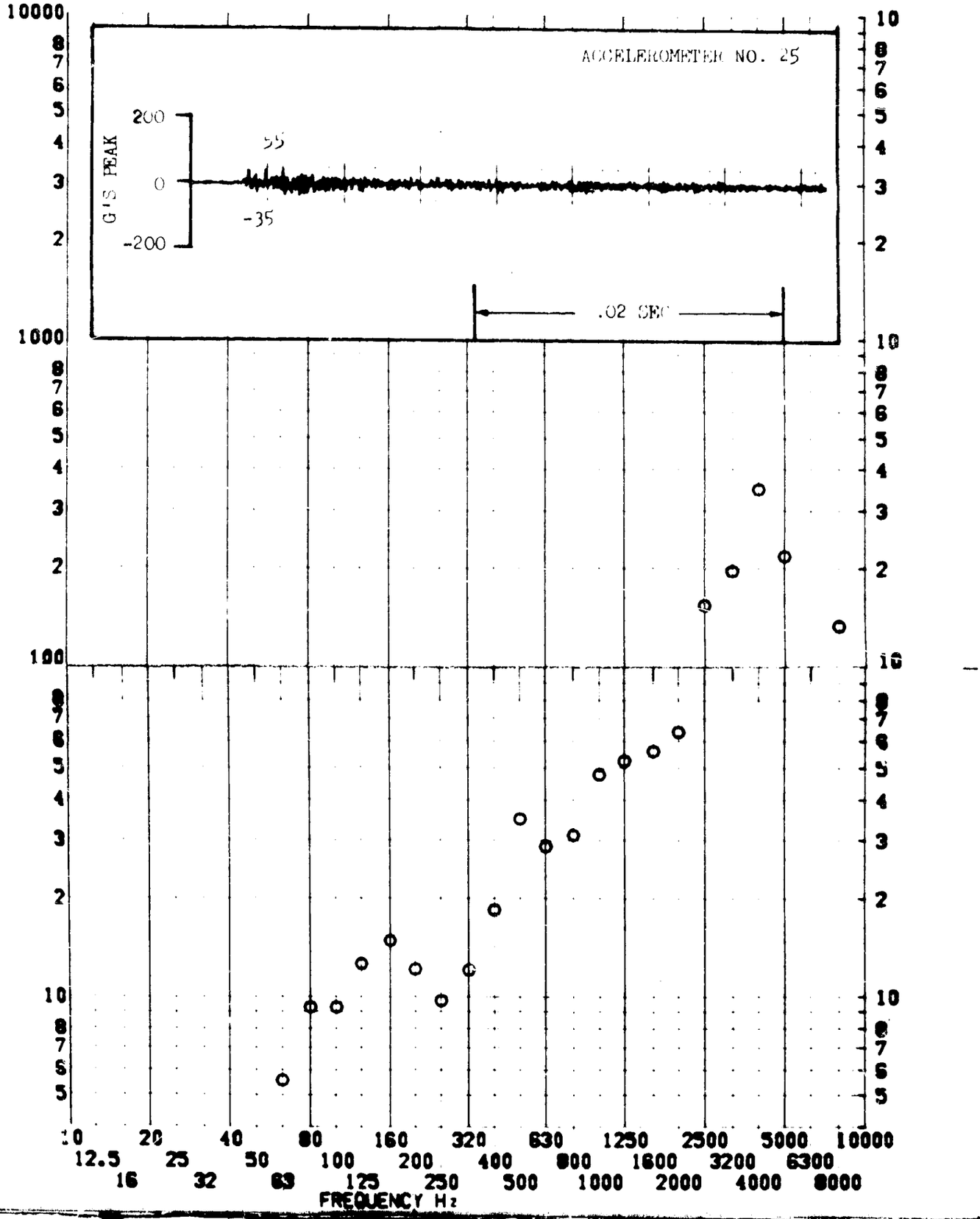

SHOCK TEST ANALYSIS DATA SHEET NO. II.A.7.132

TEST ITEM 1377-413,498
SERIAL NO.
SHOCK AXIS LONGITUDINAL

PART NO. EQUIPMENT
TEST DATE 11 FEB 1969
SHOCK NO. 1 & 2

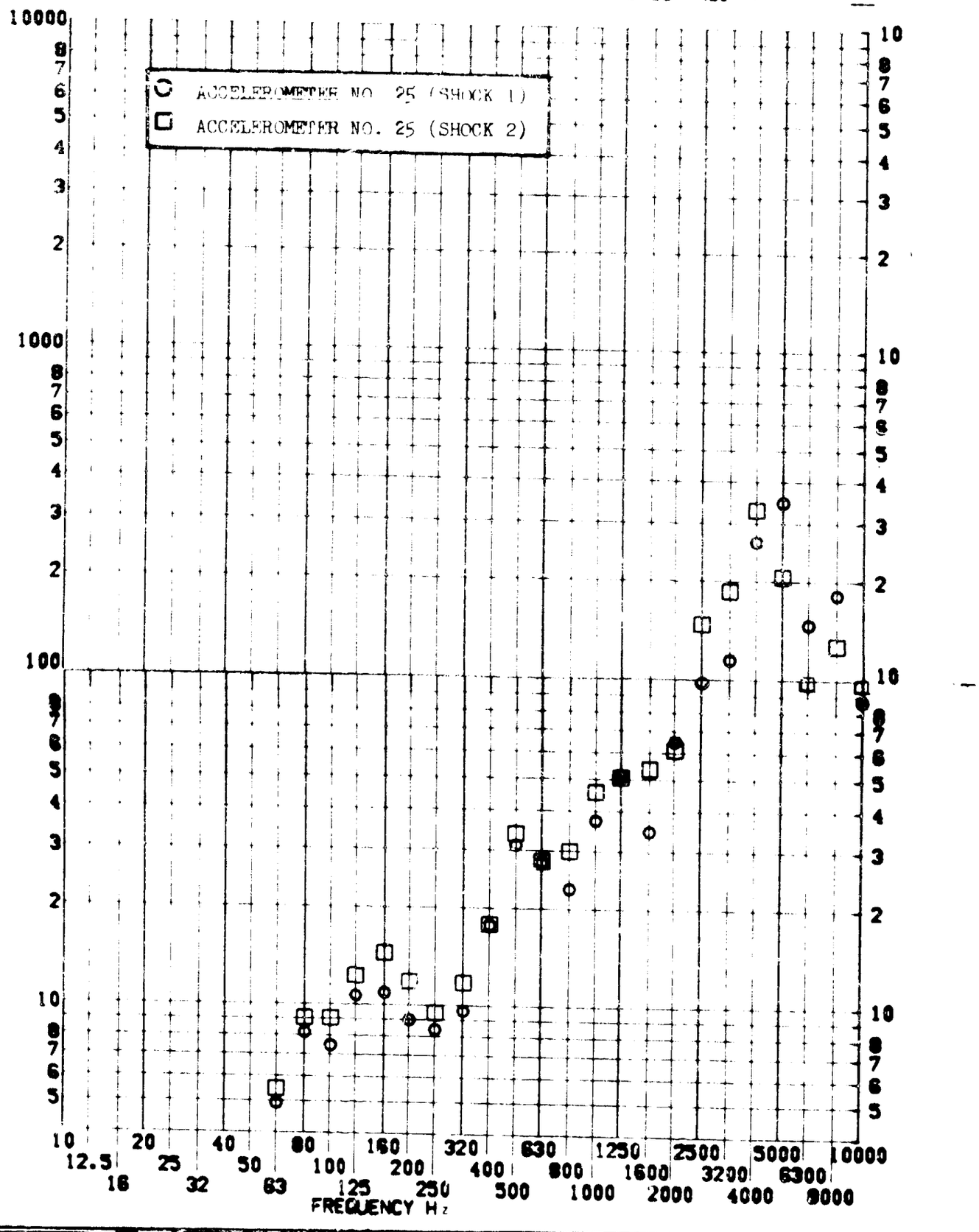

SHOCK TEST ANALYSIS DATA SHEET NO. II.A.7.1.3

TEST ITEM 1377-499
SERIAL NO.
SHOCK AXIS RADIAL
PART NO. EQUIPMENT
TEST DATE 11 FEB 1969
SHOCK NO. 2

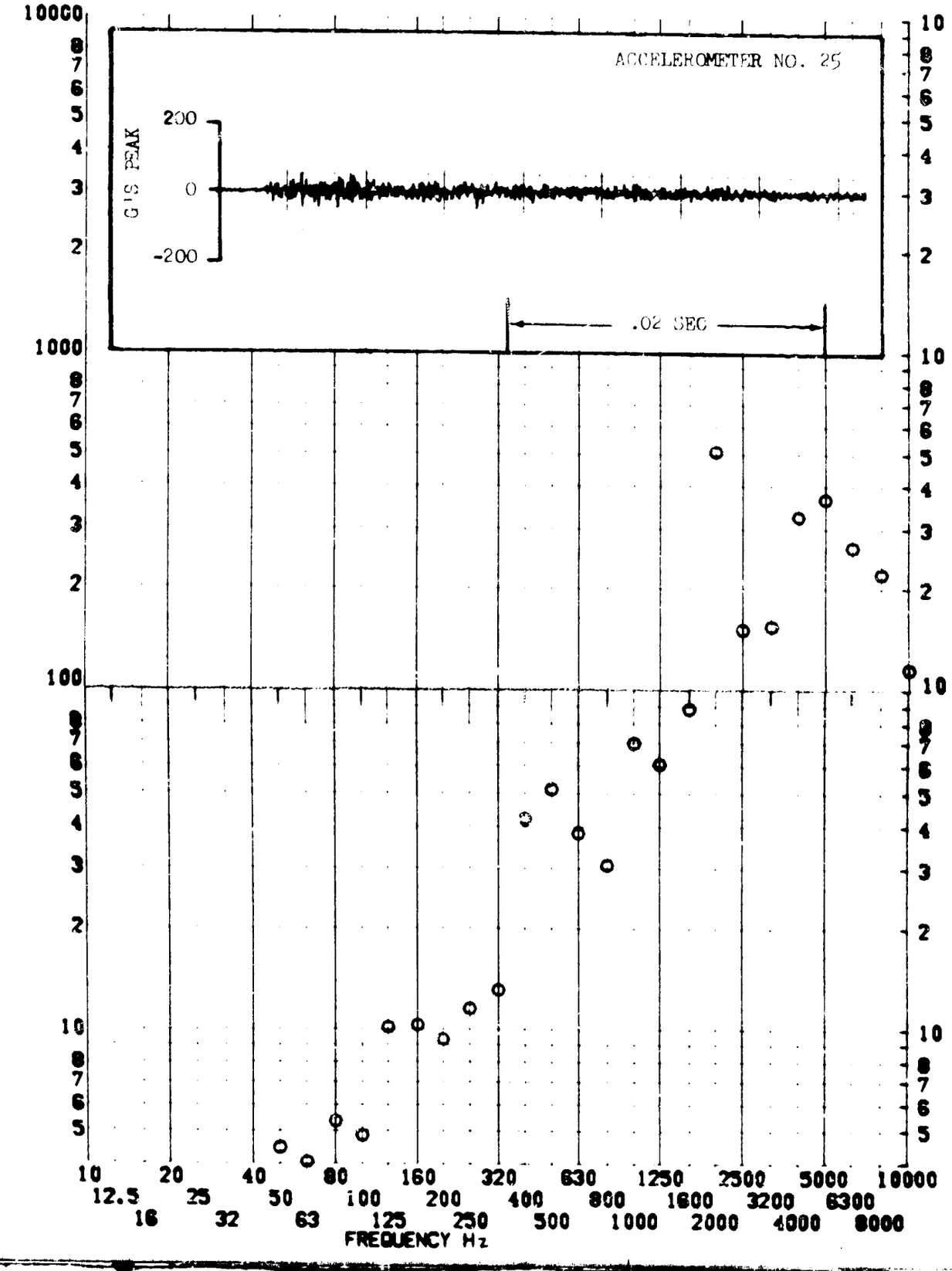

SHOCK TEST ANALYSIS DATA SHEET NO. L.A. .19

TEST ITEM [illegible]
SERIAL NO.
SHOCK AXIS L.V.T.

PART NO. EQUIPMENT
TEST DATE 11 FEB 1969
SHOCK NO. 1

RESPONSE G-S

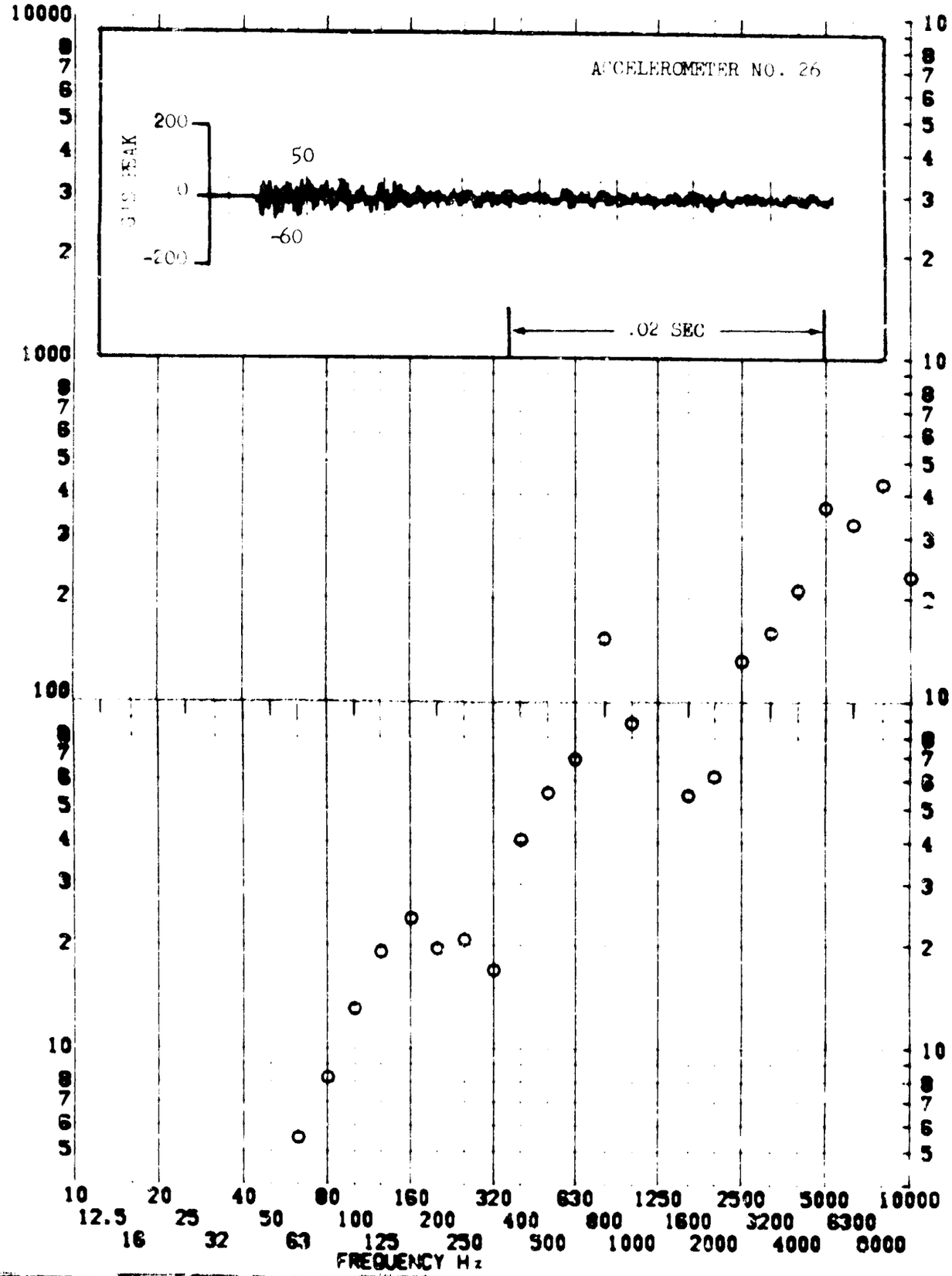

SHOCK TEST ANALYSIS DATA SHEET NO. H.A.-139

TEST ITEM 1377-500
SERIAL NO.
SHOCK AXIS LONGITUDINAL

PART NO. EQUIPMENT
TEST DATE 11 FEB 1969
SHOCK NO. 2

RESPONSE G-S

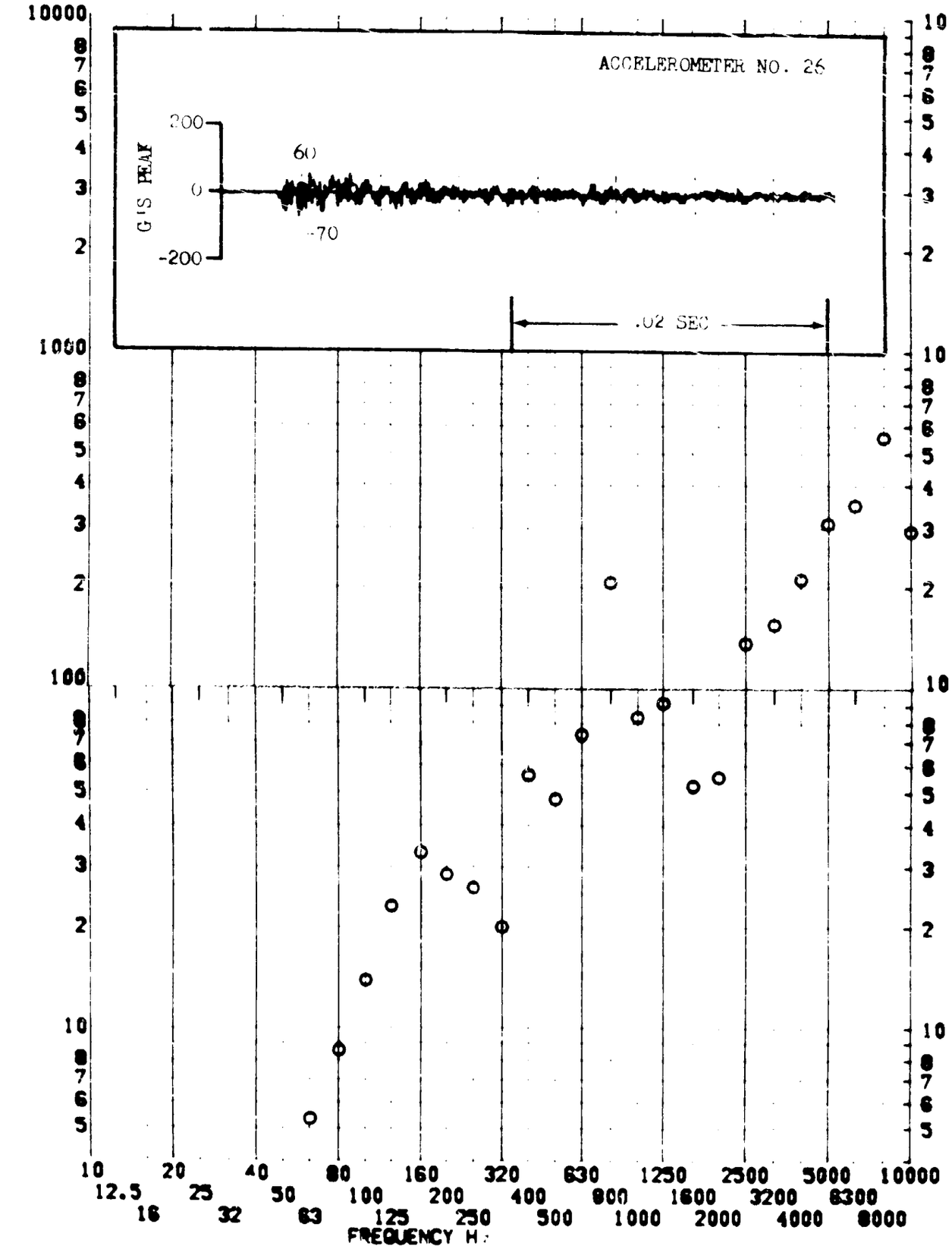

SHOCK TEST ANALYSIS DATA SHEET NO. T.A. .136

TEST ITEM 1377-414,500 PART NO. EQUIPMENT
SERIAL NO. TEST DATE 11 Feb 1969
SHOCK AXIS LONGITUDINAL SHOCK NO. 1 & 2

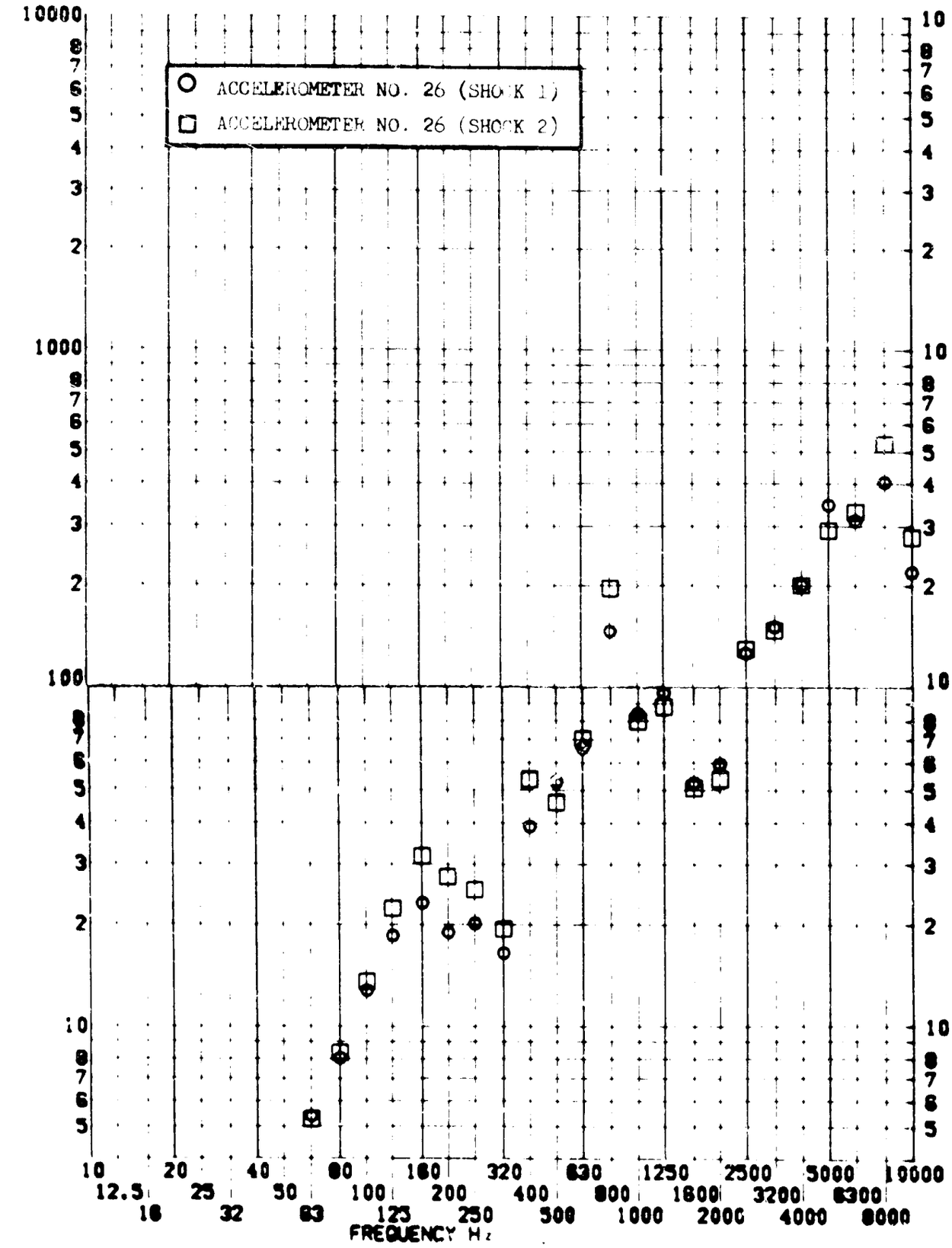

SHOCK TEST

TEST ITEM
SERIAL NO.
RESPONSE G-S SHOCK AXIS

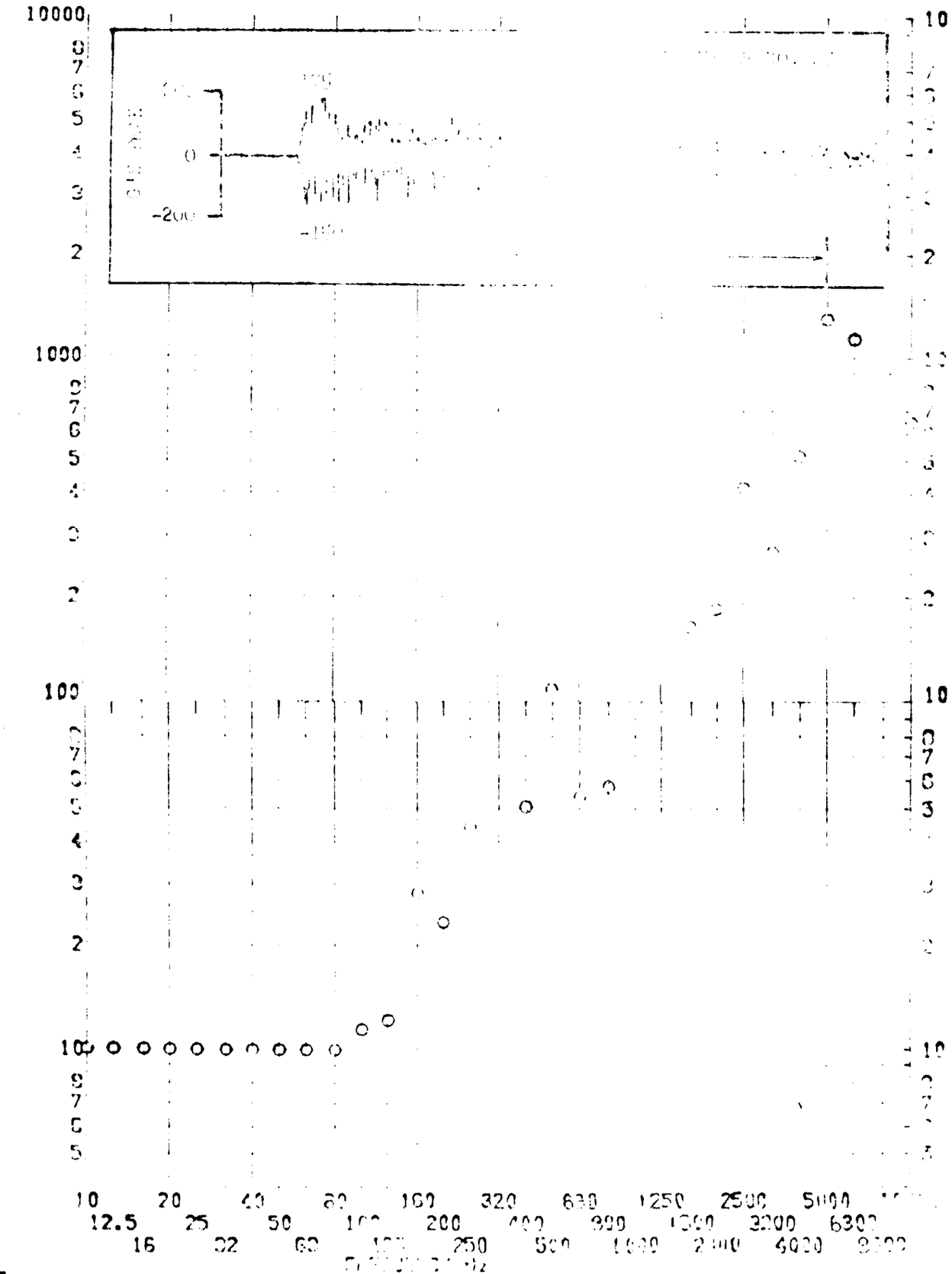

TEST ITEM
SERIAL NO.
RESPONSE G-S SHOCK AXIS
PART NO. EQUIPMENT
TEST DATE 1 FEB 1969
SPECIMEN NO. 1

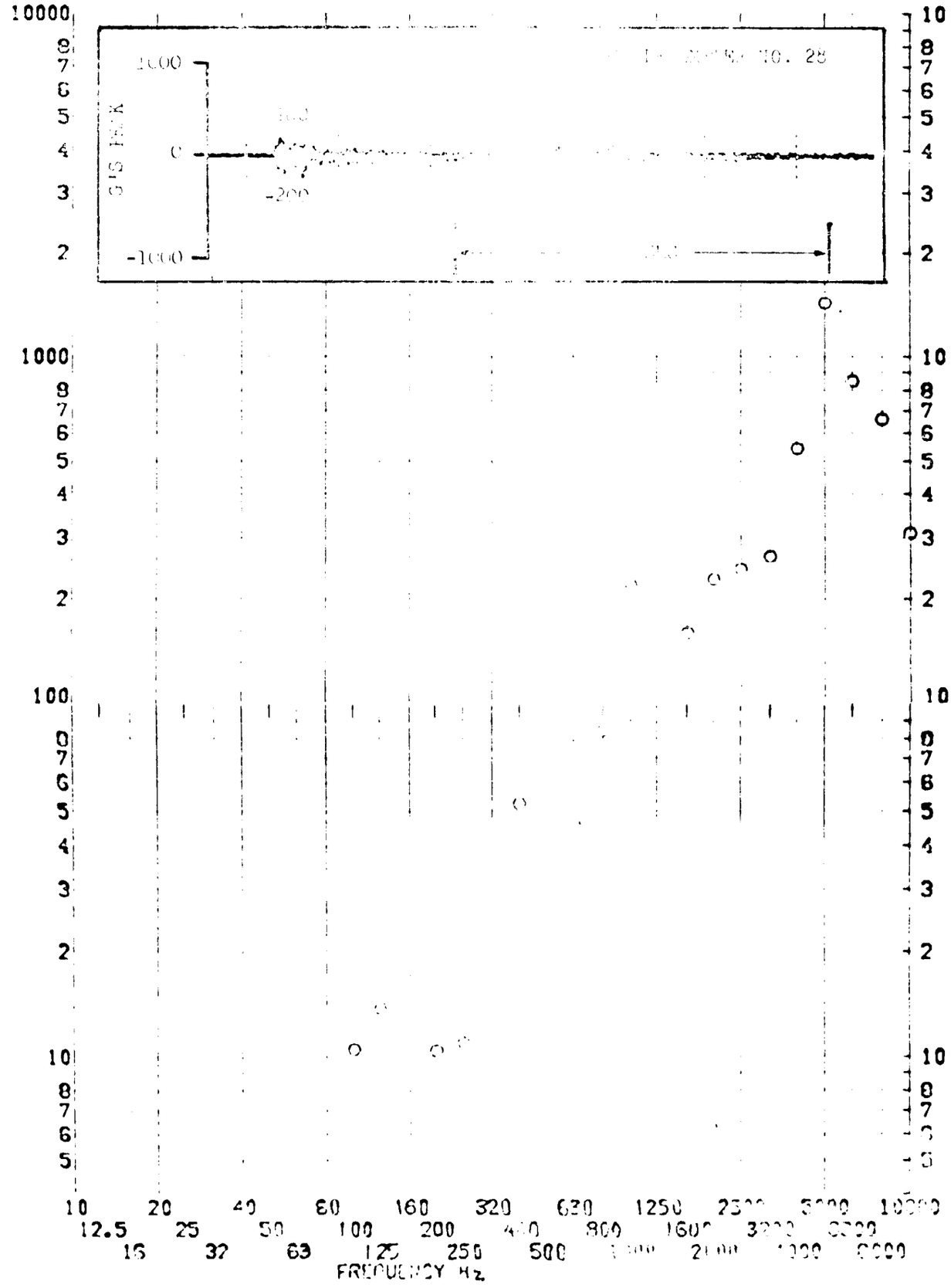

SHOCK TEST ANALYSIS DATA SHEET NO. H.A./.139

TEST ITEM 1377-502 PART NO. EQUIPMENT

SERIAL NO. _____ TEST DATE 11 FEB 1969

SHOCK AXIS LONGITUDINAL SHOCK NO. 2

RESPONSE G's

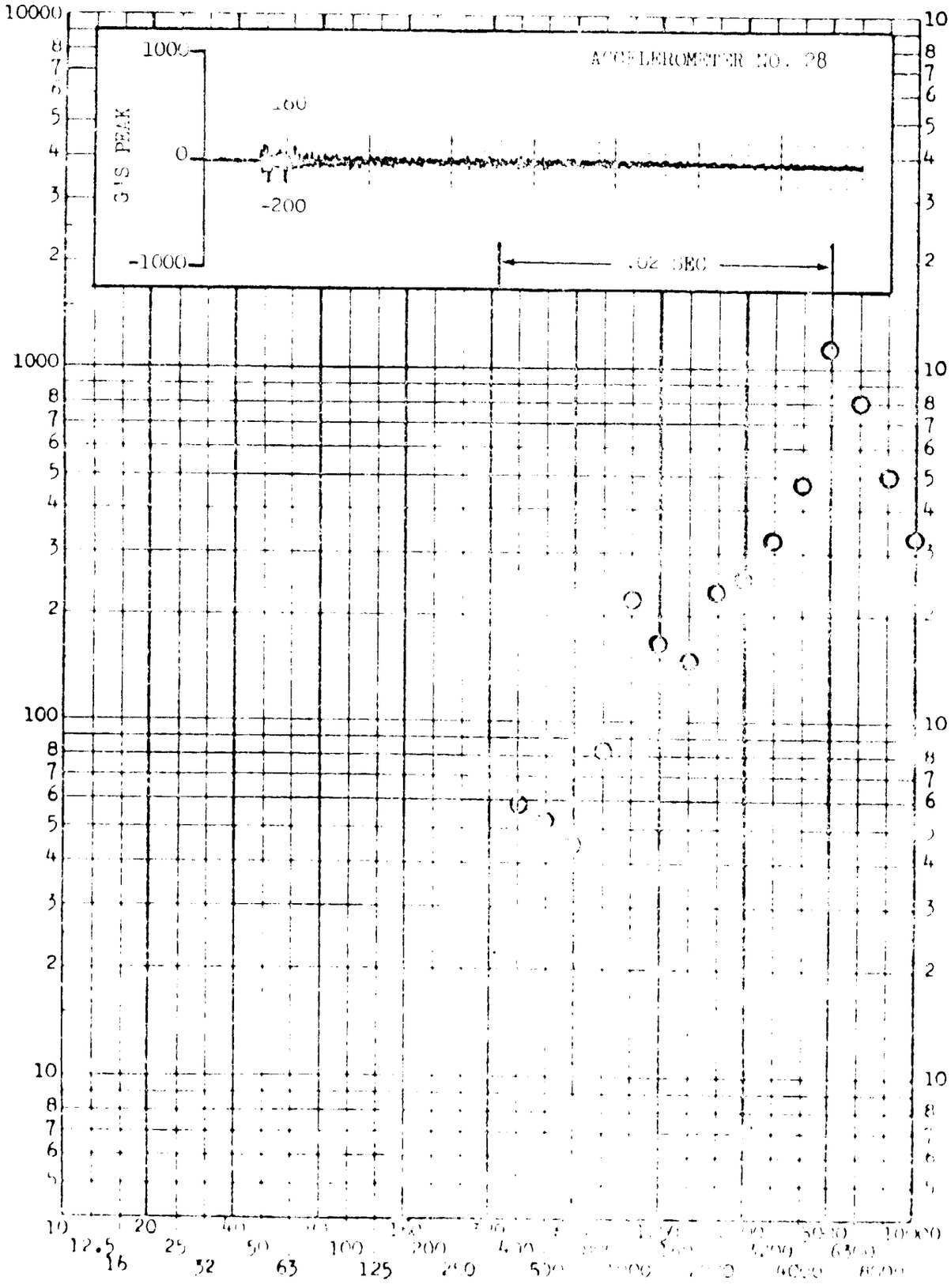

LMSC/A955903
SS-1386-6262
20 August 1969
page 458

SHOCK TEST DATA SHEET No. II.A./.140

TEST ITEM 1377-[illegible] TEST NO. EQUIPMENT

SERIAL NO. _____ TEST DATE 1 FEB 1969

SHOCK AXIS [illegible] CURVE NO. 2

RESPONSE G's

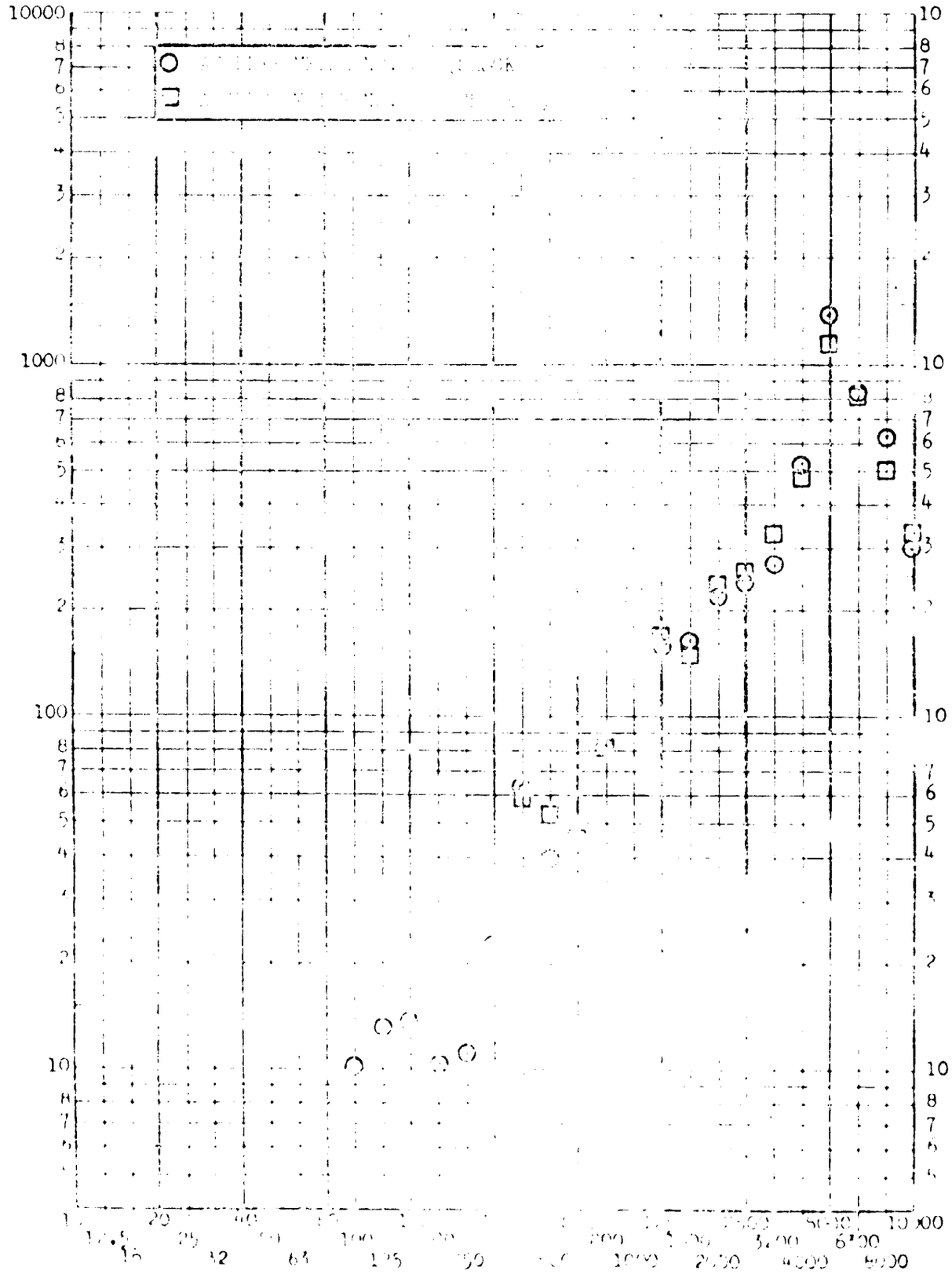

DEVELOPMENT ... 30 August 1969

SHOCK TEST ANALYSIS DATA SHEET

TEST ITEM 1377-...
SERIAL NO.
SHOCK AXIS

PART NO. EQUIPMENT
TEST DATE
SHOCK NO.

RESPONSE G-S

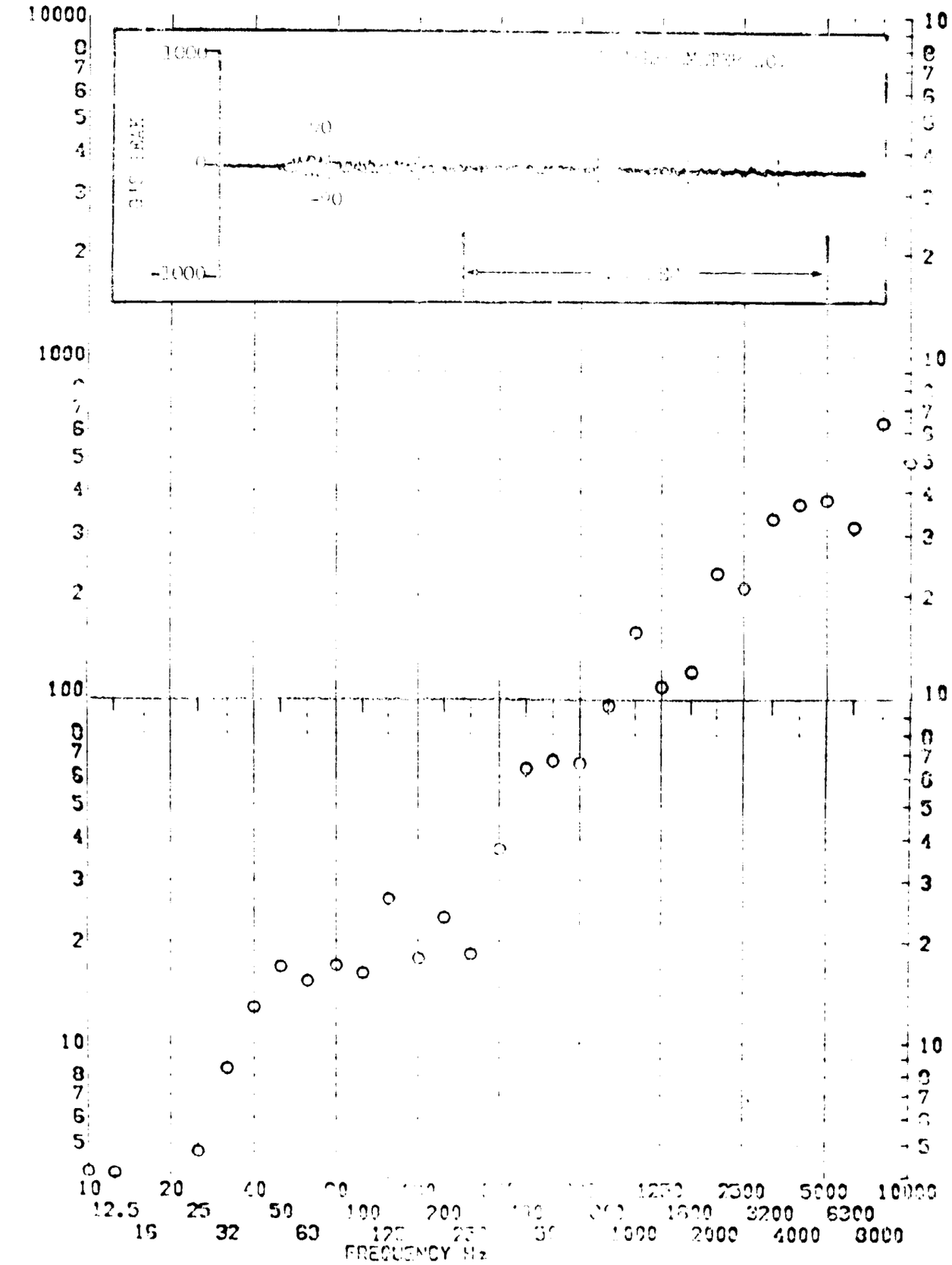

SHOCK TEST ANALYSIS DATA SHEET NO II.A.7.142

TEST ITEM 1377-503 PART NO. EQUIPMENT
SERIAL NO. TEST DATE 1 [illegible] 1969
SHOCK AXIS RADIAL SHOCK NO. 2

RESPONSE G-S

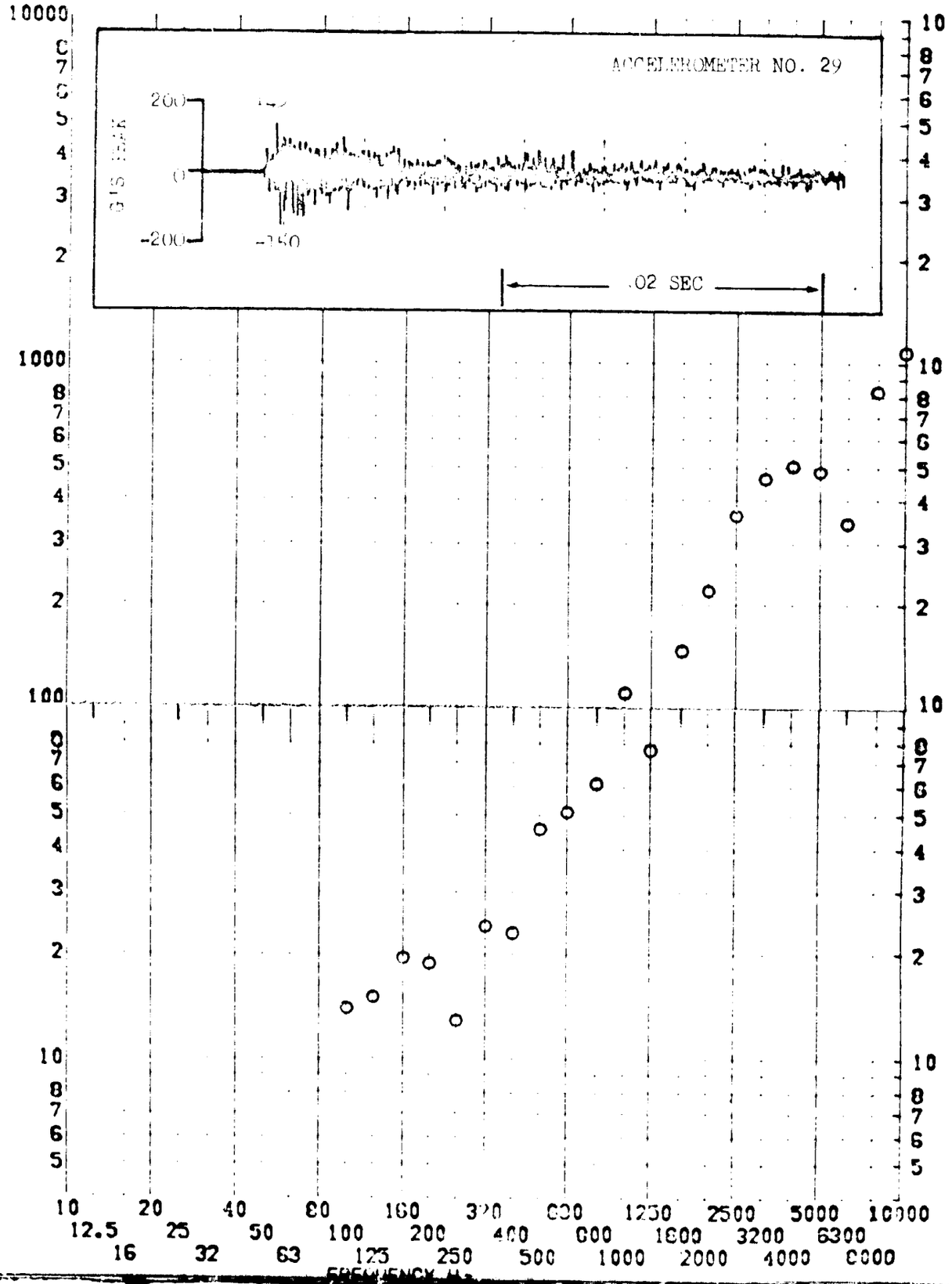

SHOCK TEST ANALYSIS DATA SHEET NO. 11.A.7.143

TEST ITEM [illegible] PART NO. EQUIPMENT

SERIAL NO. — TEST DATE 11 FEB 1962

SHOCK AXIS RADIAL SHOCK NO. 2

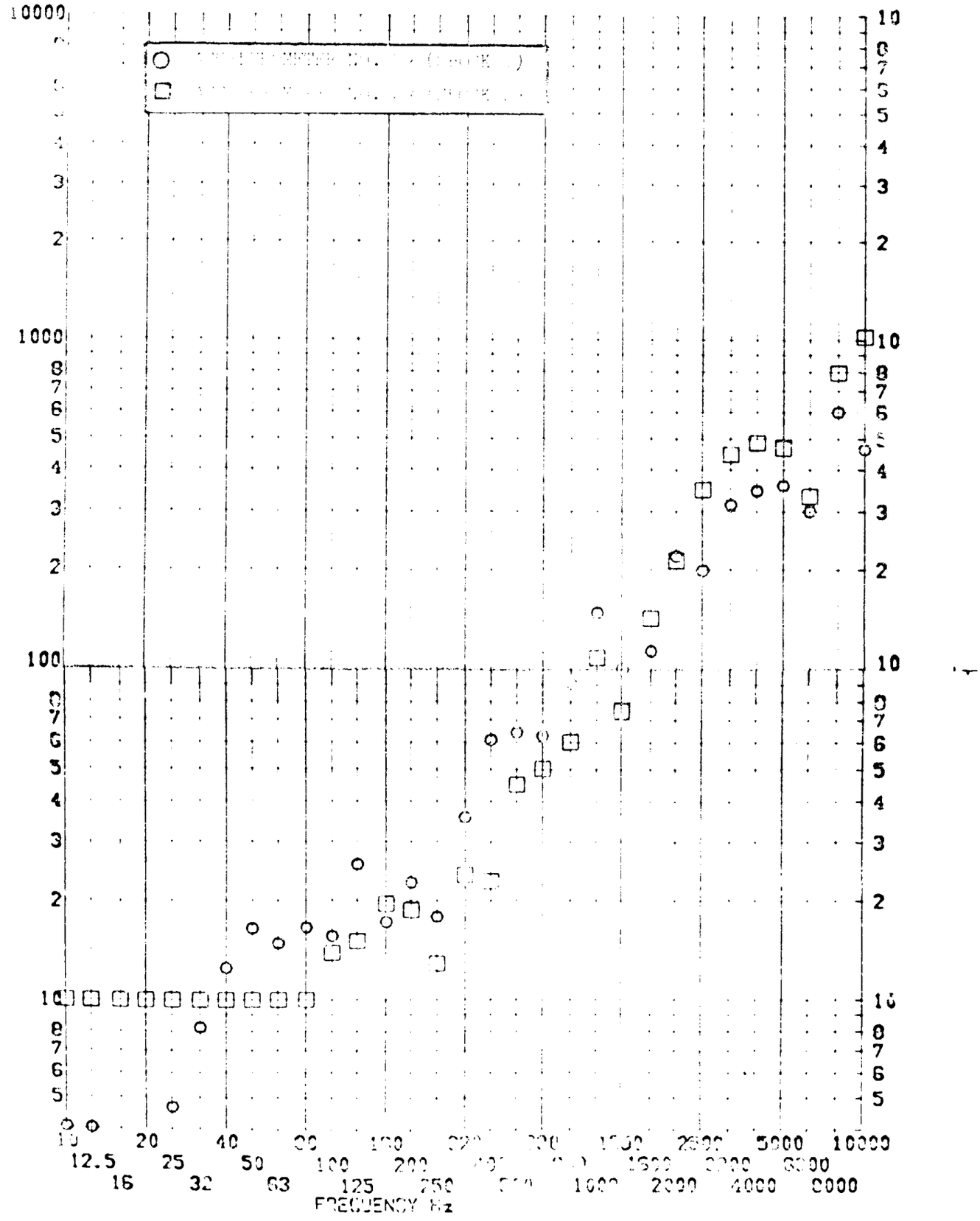

SHOCK TEST ANALYSIS DATA SHEET NO. II.A.[illegible]

TEST ITEM [illegible] PART NO. [illegible]
SERIAL NO. TEST DATE [illegible]
SHOCK AXIS [illegible] SHOCK NO. 1

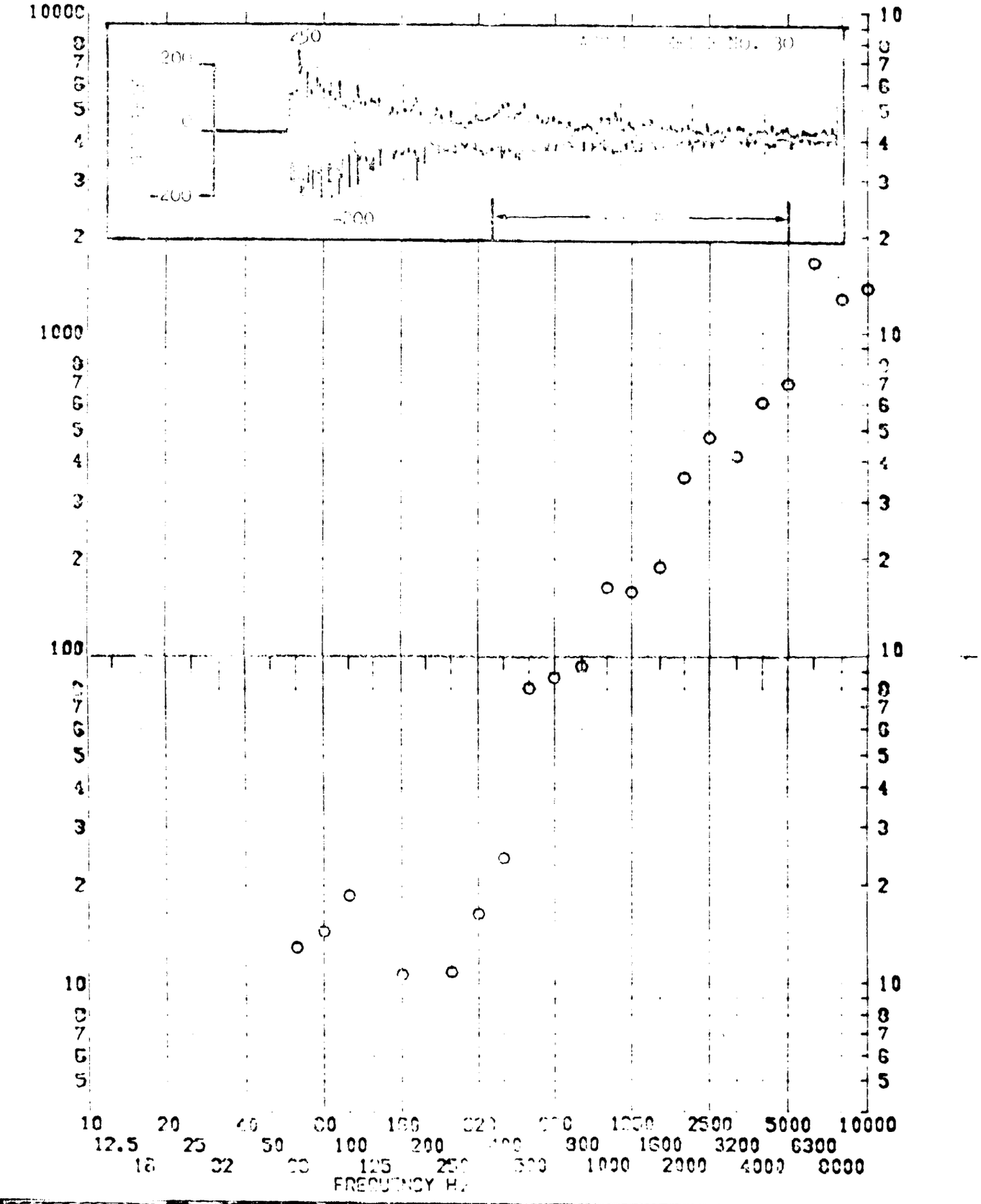

SHOCK TEST ANALYSIS DATA SHEET NO. [illegible]

TEST ITEM [illegible]
SERIAL NO.
SHOCK AXIS [illegible]

PART NO. [illegible]
TEST DATE [illegible]
SHOCK NO. 2

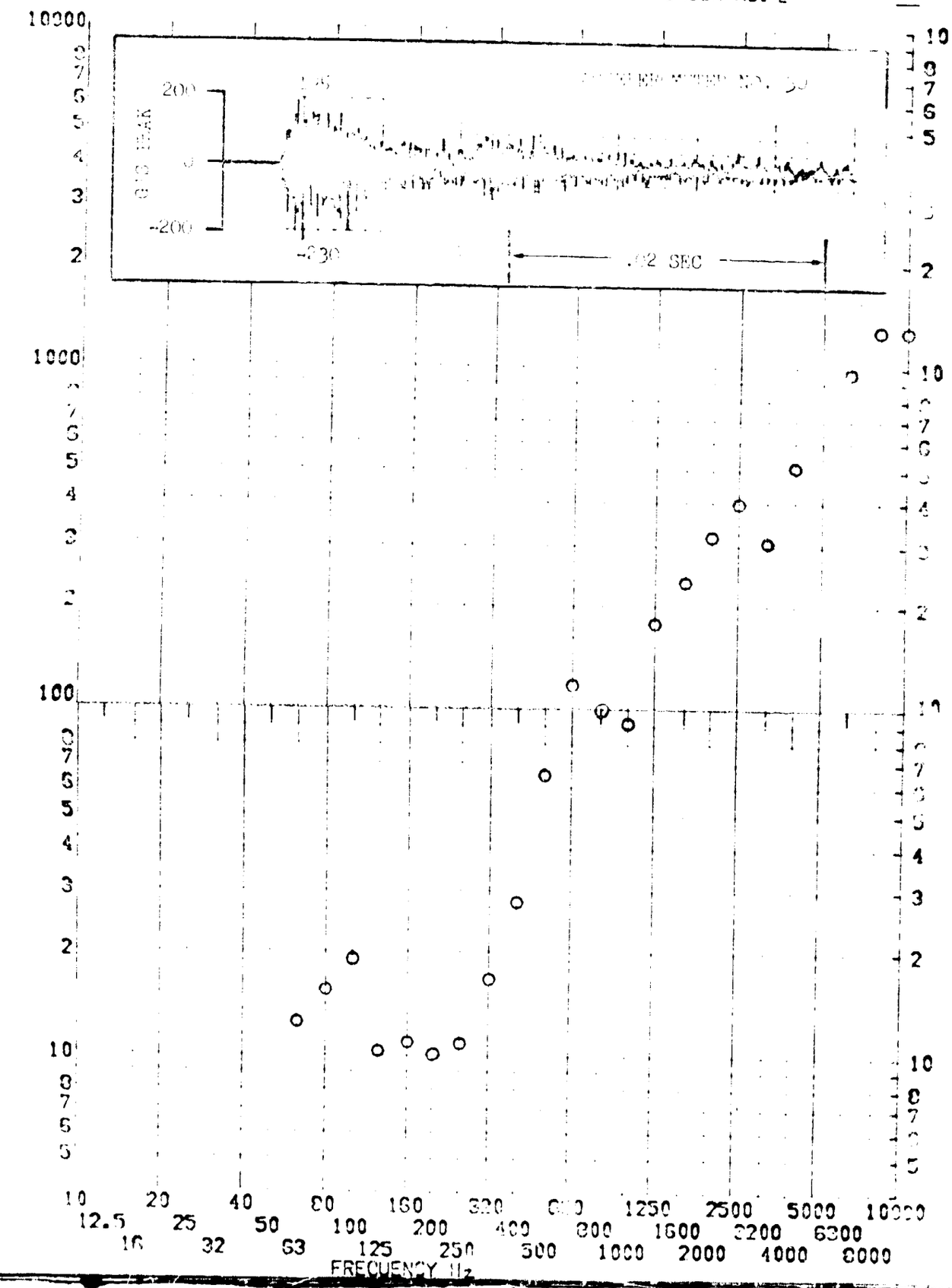

SHOCK TEST ANALYSIS DATA SHEET No. II.A.7.146

TEST ITEM [illegible] Sol
SERIAL NO. —
SHOCK AXIS [illegible] —

PART NO. EQUIPMENT
TEST DATE [illegible] FEB 1969
SHOCK NO. 1 & 2 —

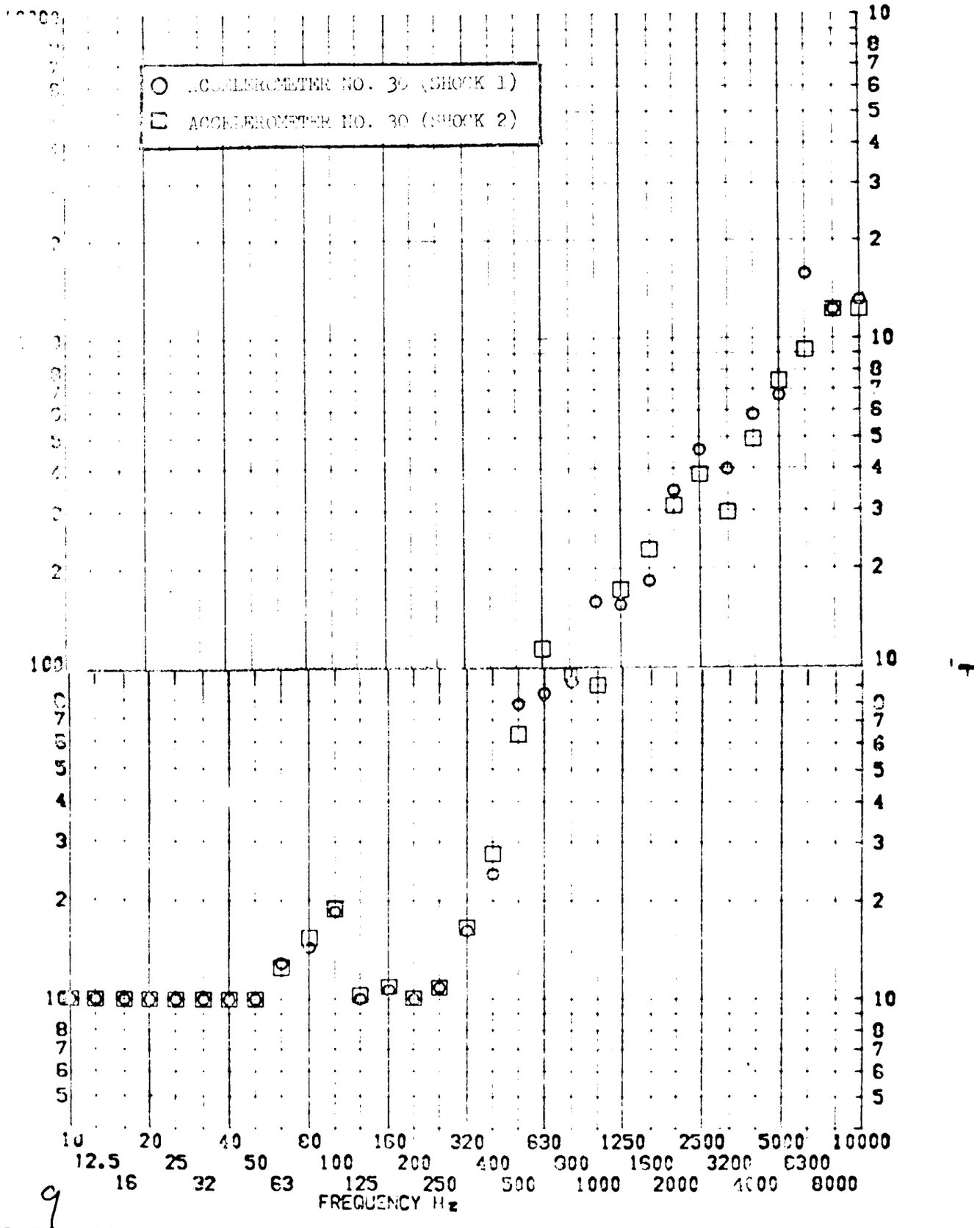

SHOCK TEST ANALYSIS DATA SHEET NO. 11.A.7.147

TEST ITEM 1377-418 PART NO. [illegible]
SERIAL NO. TEST DATE [illegible]
RESPONSE G-S SHOCK AXIS [illegible] SHOCK NO. 1

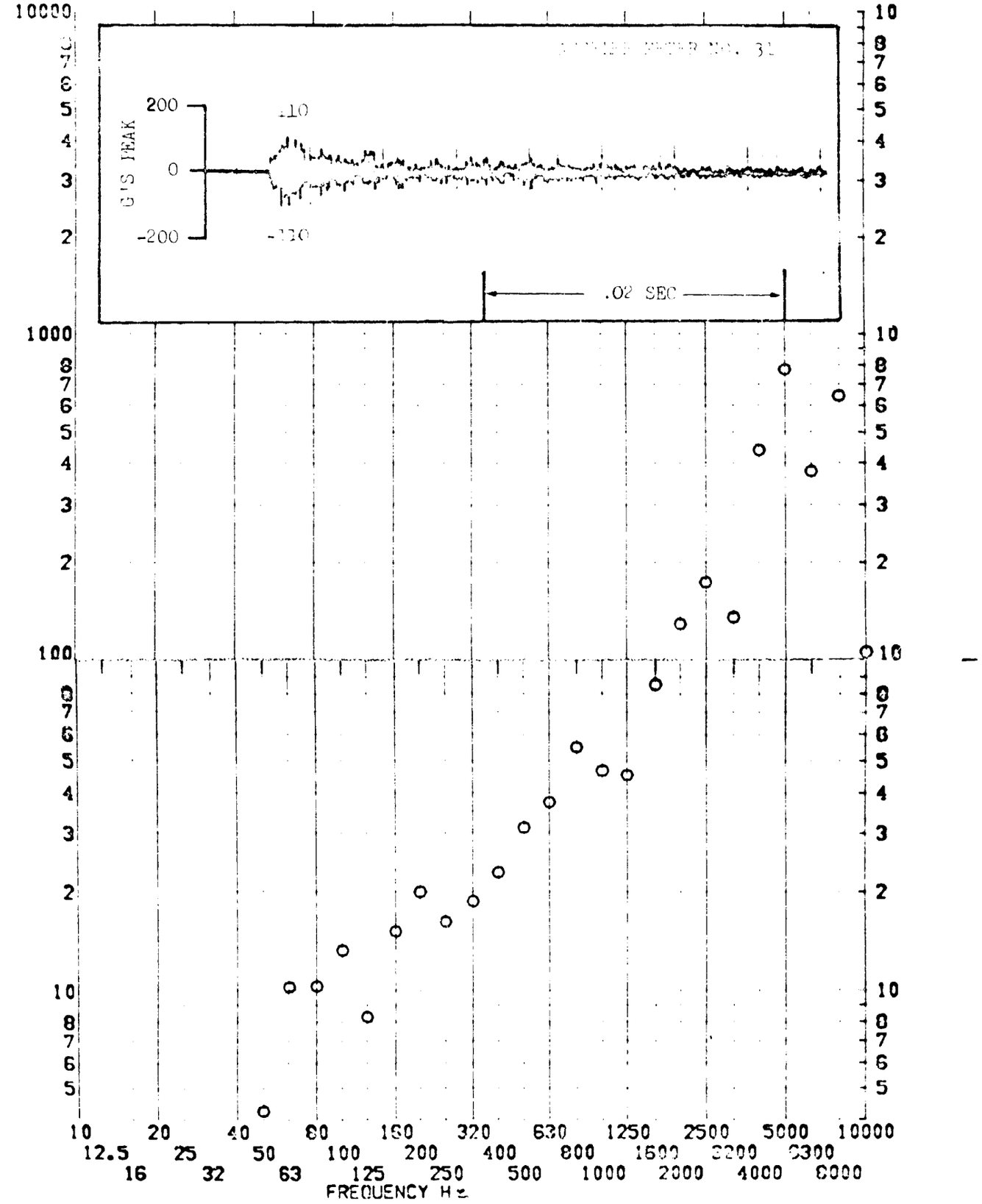

SHOCK TEST ANALYSIS DATA SHEET NO. II.A.7.148

TEST ITEM [illegible] PART NO. EQUIPMENT

SERIAL NO. TEST DATE 11 FEB 1969

RESPONSE G-S SHOCK AXIS [illegible] SHOCK NO. 2

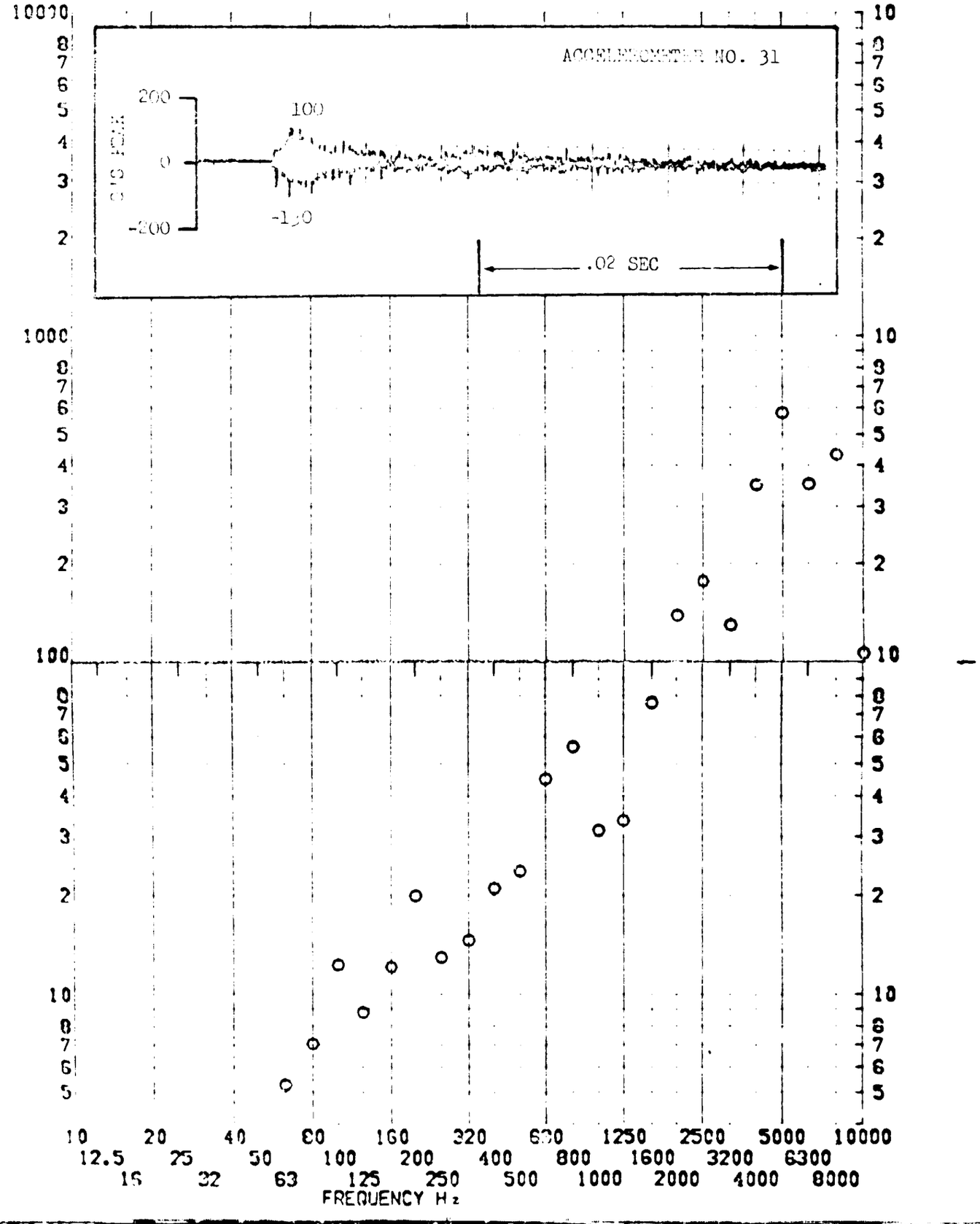

SHOCK TEST ANALYSIS DATA SHEET NO. U.A.7.149

TEST ITEM 1377-418,509 PART NO. EQUIPMENT
SERIAL NO. — TEST DATE [illegible]
SHOCK AXIS RADIAL — SHOCK NO. 1 & 2 —

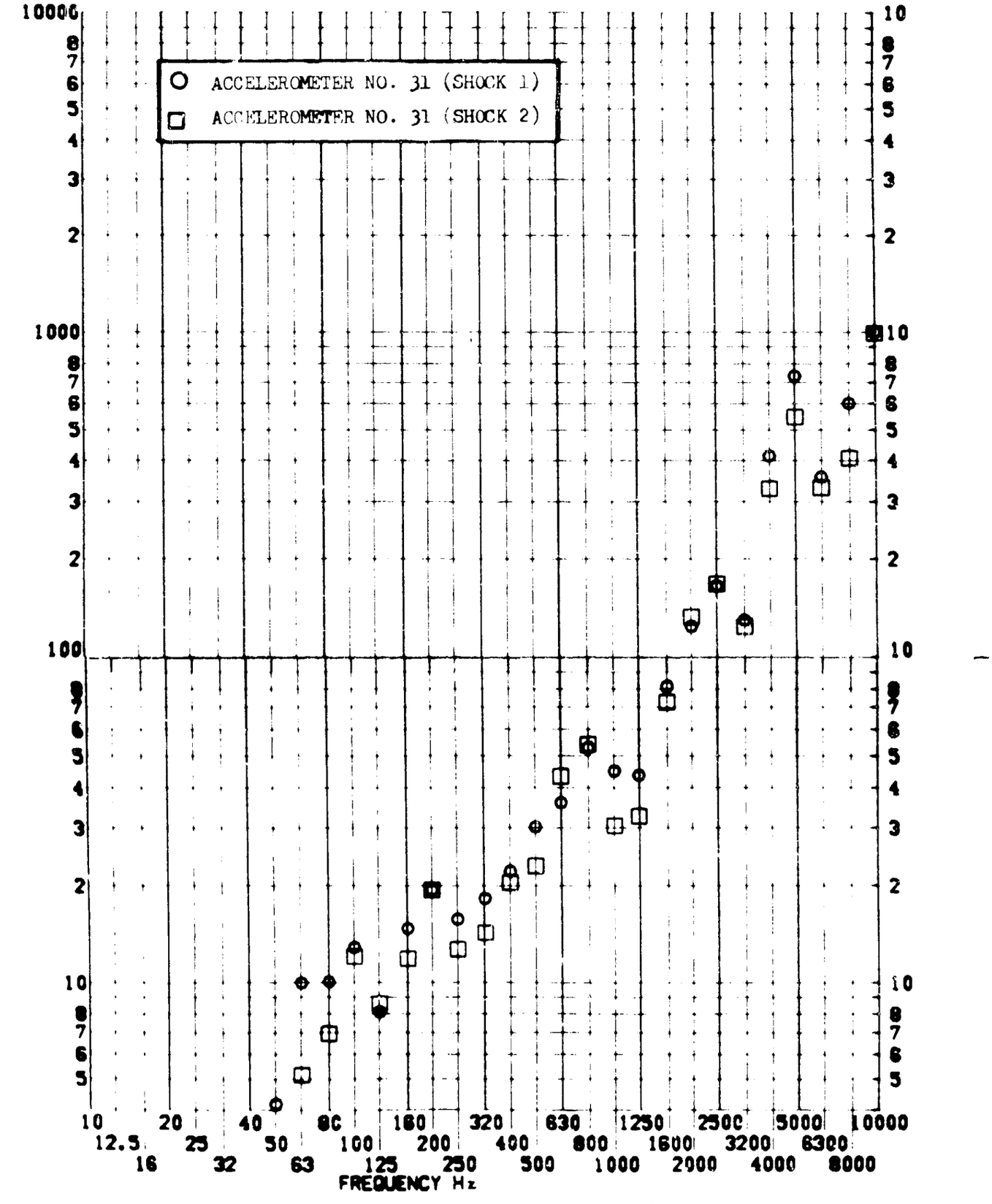

SHOCK TEST ANALYSIS DATA SHEET NO. II.A.7.150

TEST ITEM 1377-419 PART NO. EQUIPMENT

SERIAL NO. TEST DATE 11 FEB 1969

RESPONSE G-S SHOCK AXIS RADIAL SHOCK NO. 1

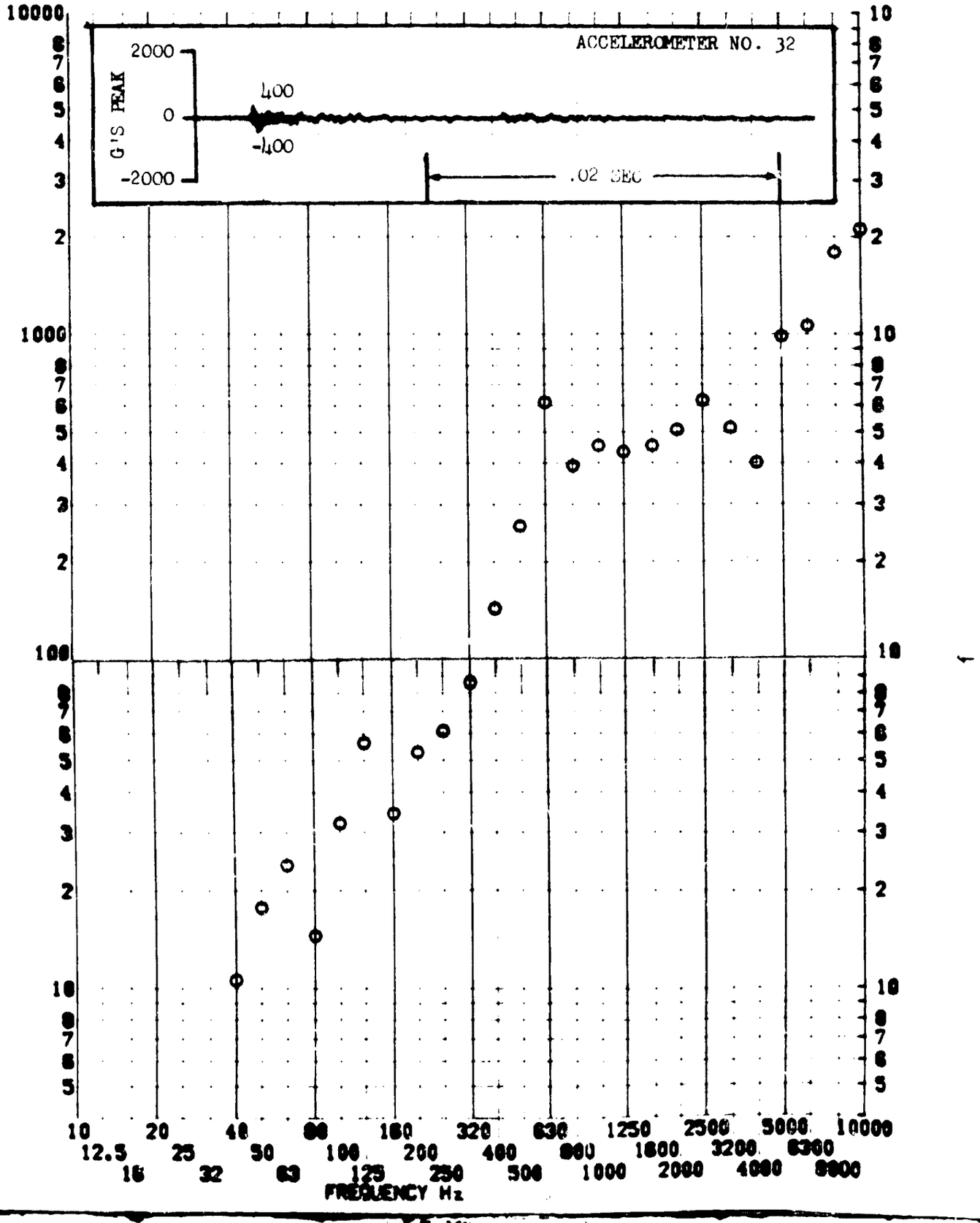

SHOCK TEST ANALYSIS DATA SHEET NO. H.A. .1-3

TEST ITEM 377-506 PART NO. EQUIPMENT

SERIAL NO. TEST DATE 11 FEB 1969

RESPONSE G-S SHOCK AXIS RADIAL SHOCK NO. 2

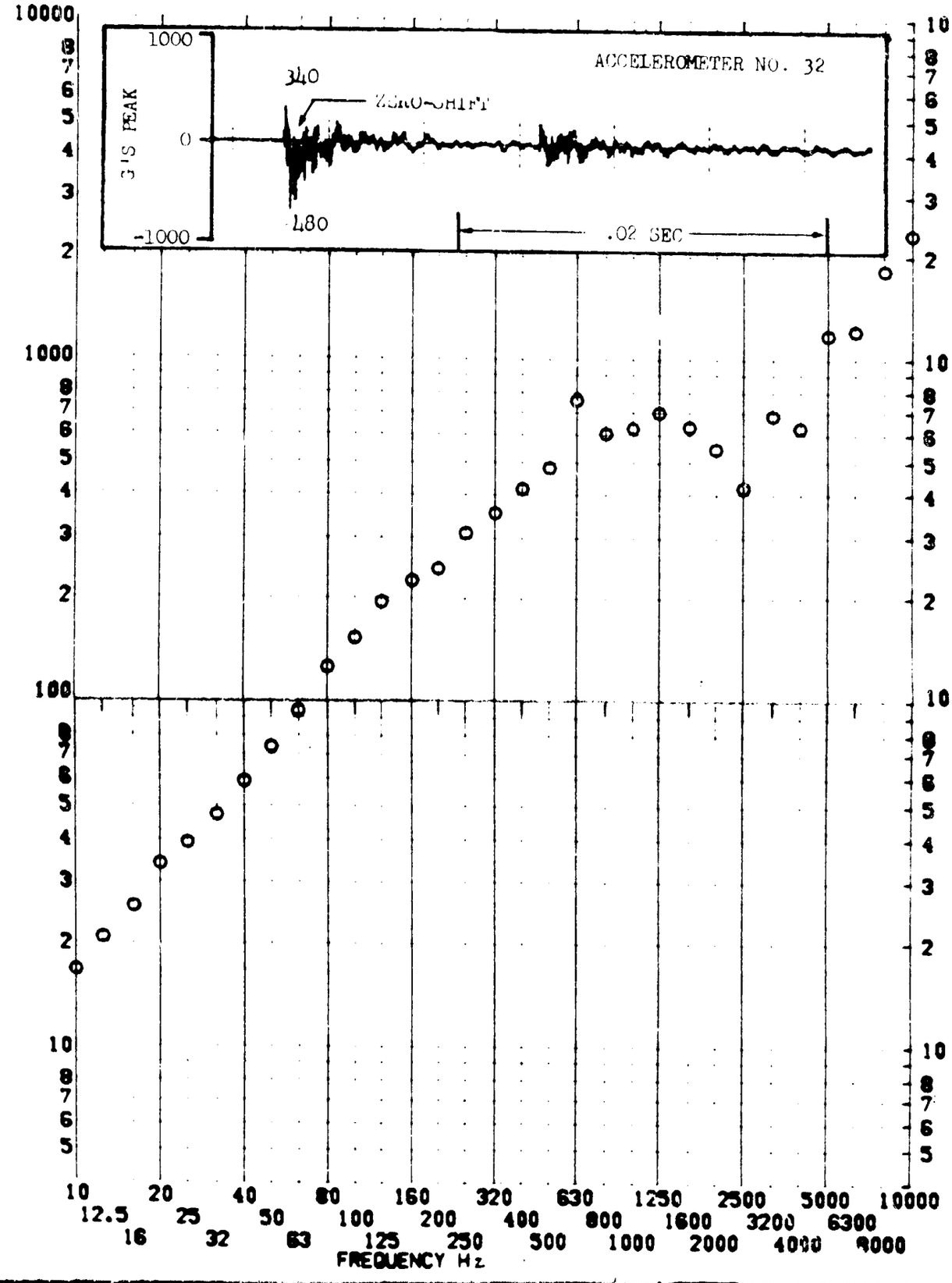

SHOCK TEST ANALYSIS DATA SHEET NO. II.A.7.15

TEST ITEM 1377-429,50[illegible]
SERIAL NO. —
SHOCK AXIS RADIAL —

PART NO. EQUIPMENT —
TEST DATE 11 FEB 1969
SHOCK NO. 1 & 2 —

RESPONSE G-S

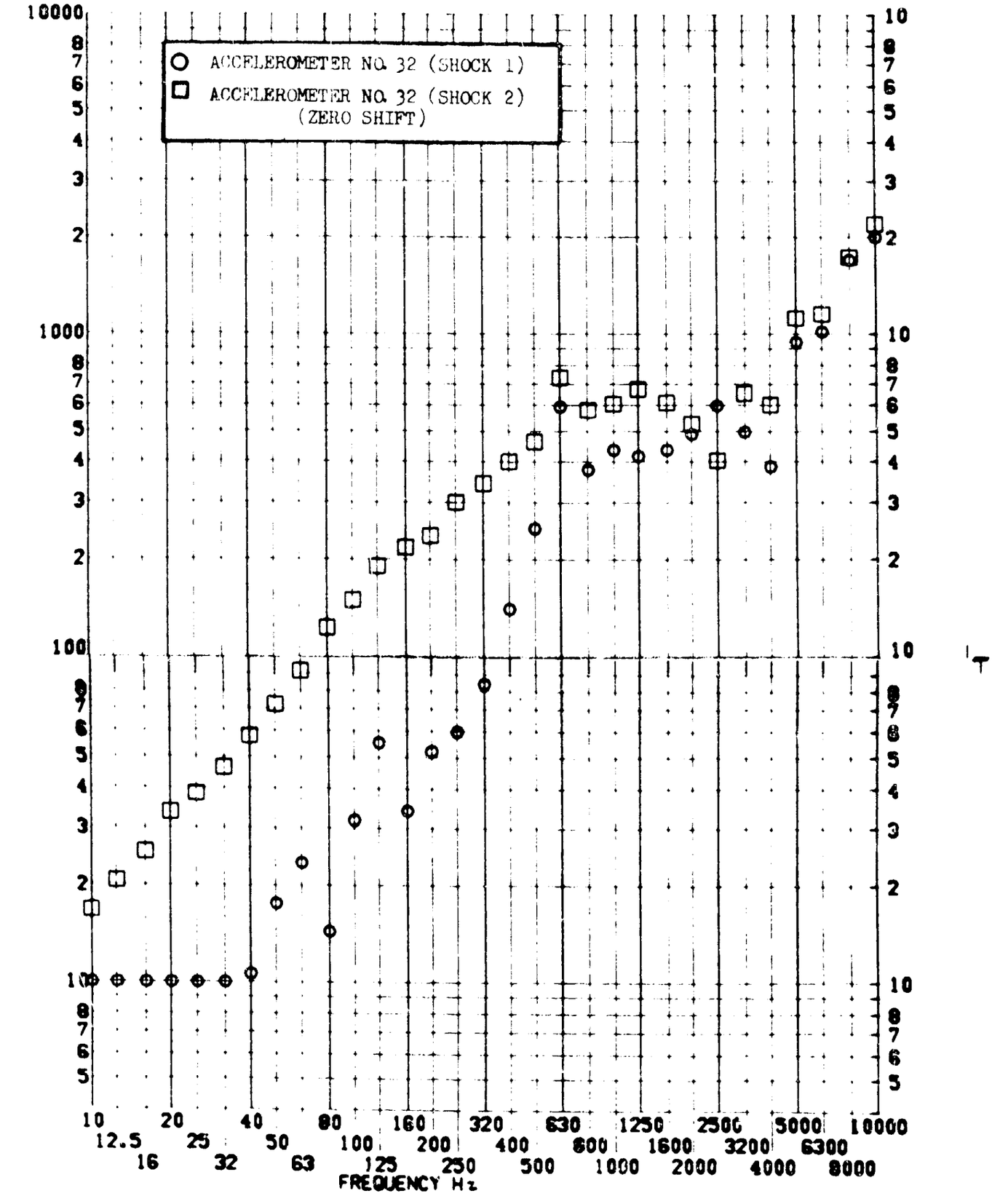

SHOCK TEST ANALYSIS DATA SHEET NO. [illegible]

TEST ITEM 1377-420
SERIAL NO.
SHOCK AXIS LONGITUDINAL

PART NO. [illegible]
TEST DATE [illegible]
SHOCK NO.

RESPONSE G-S

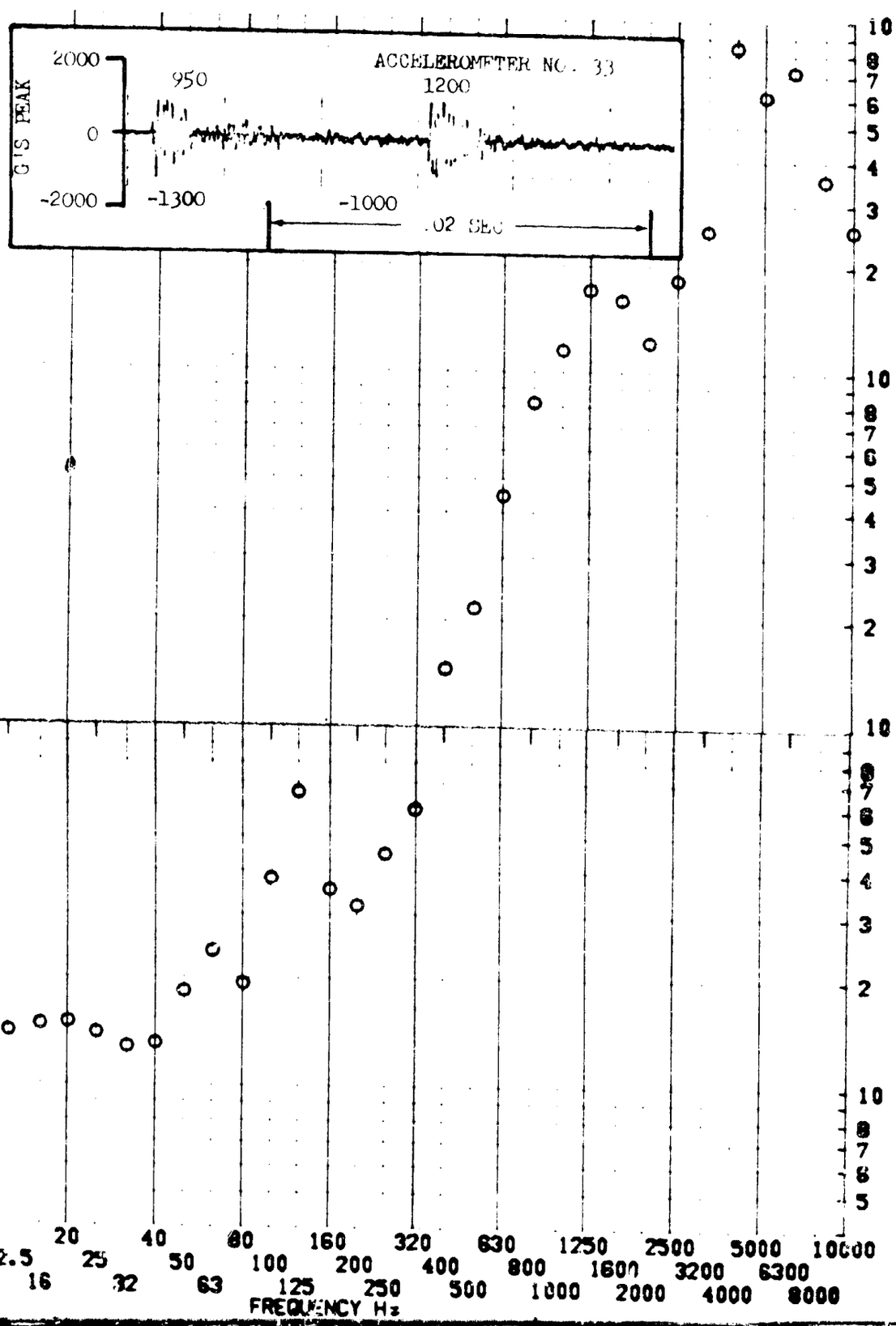

SHOCK TEST ANALYSIS DATA SHEET

TEST ITEM 1377-421
SERIAL NO.
SHOCK AXIS RADIAL

PART NO.
TEST DATE
SHOCK NO. 1

RESPONSE G-S

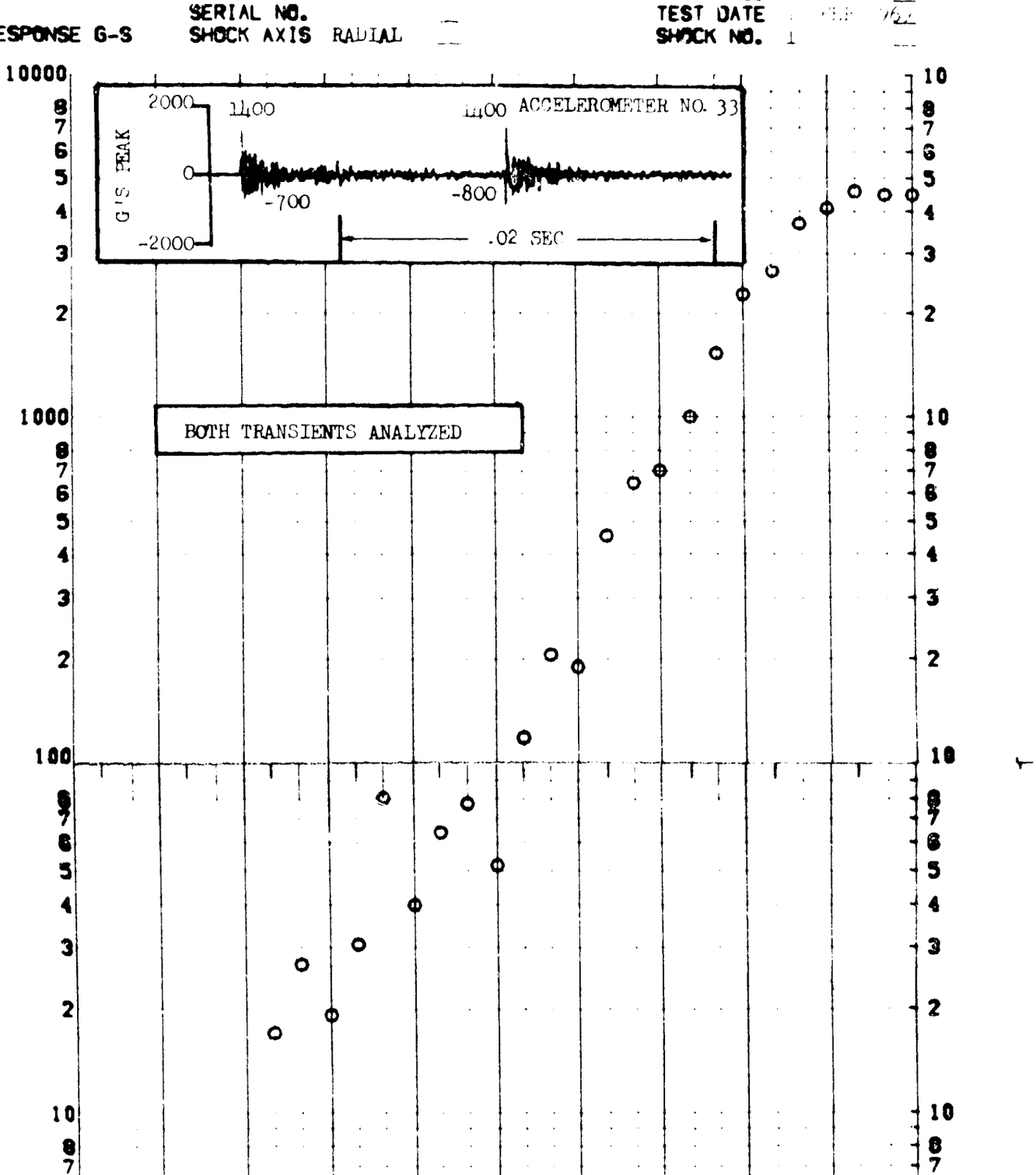

SHOCK TEST ANALYSIS DATA SHEET NO. II.A.7.[illegible]

TEST ITEM 1377-422 PART NO. EQUIPMENT
SERIAL NO. TEST DATE [illegible] 1967
SHOCK AXIS RADIAL SHOCK NO. 1

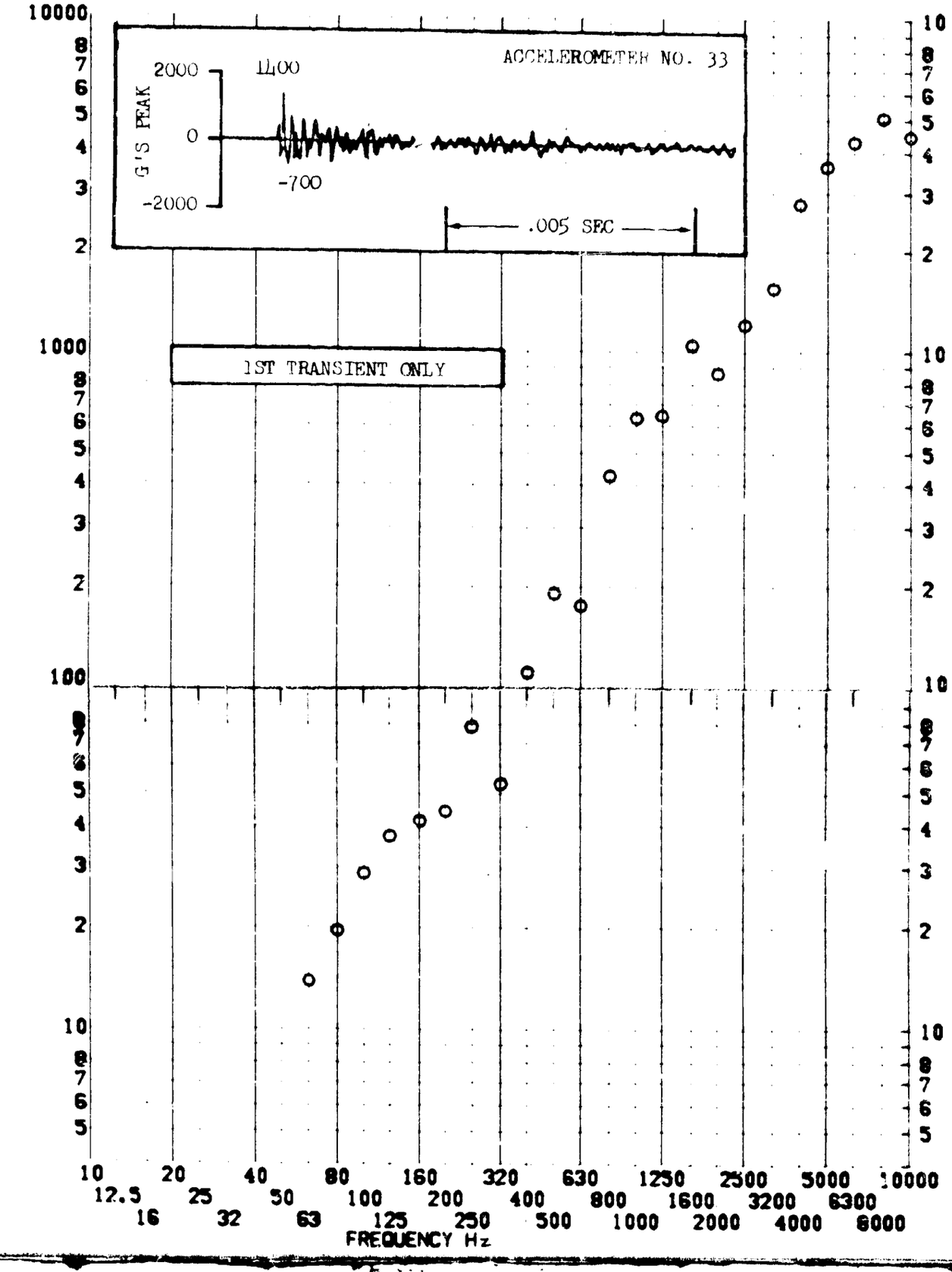

SHOCK TEST ANALYSIS DATA SHEET NO. II.A. .19[illegible]

TEST ITEM 1377-507
SERIAL NO.
SHOCK AXIS RADIAL

PART NO. [illegible]EMENT
TEST DATE [illegible]
SHOCK NO. 2

RESPONSE G-S

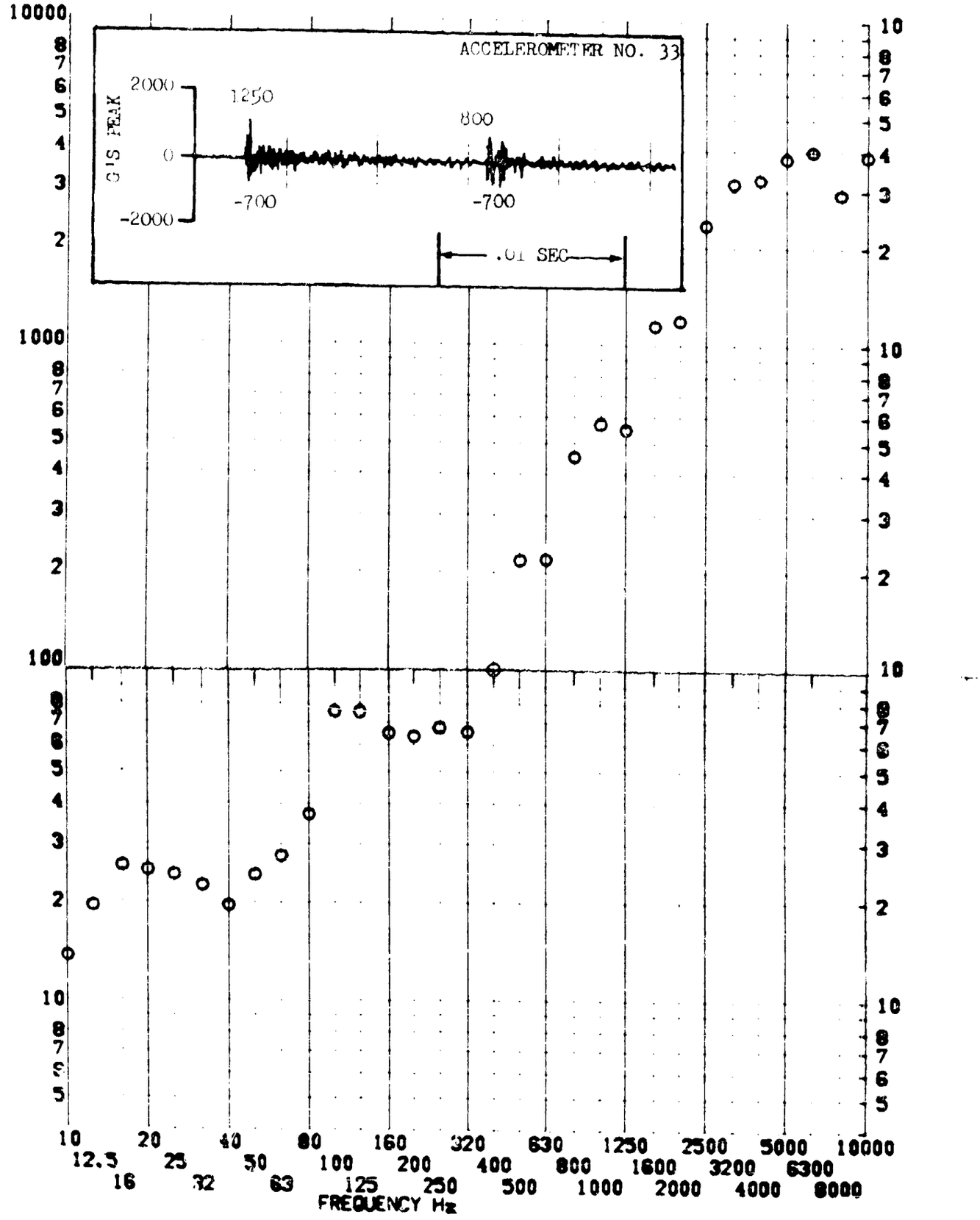

SHOCK TEST ANALYSIS DATA SHEET NO. II.A.7.15?

TEST ITEM 377-421,422,507 PART NO. EQUIPMENT
SERIAL NO. — TEST DATE 11 FEB 1970
SHOCK AXIS RADIAL — SHOCK NO. 1 & 2 —

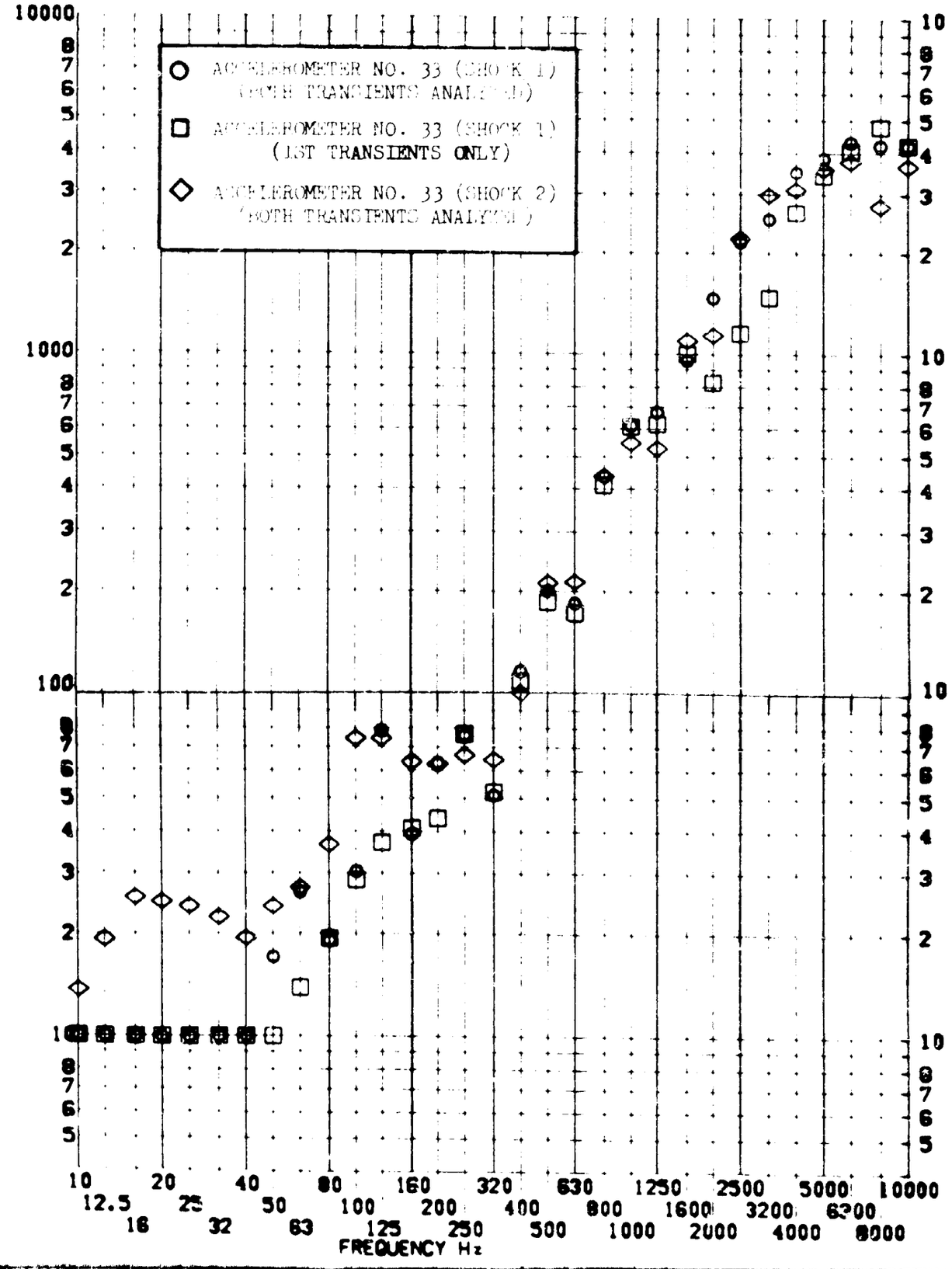

SHOCK TEST ANALYSIS DATA SHEET NO. II.A.7.158

TEST ITEM 1377-423
SERIAL NO.
SHOCK AXIS LONGITUDINAL

PART NO. EQUIPMENT
TEST DATE 10 [illegible] 1962
SHOCK NO. 1

RESPONSE G-S

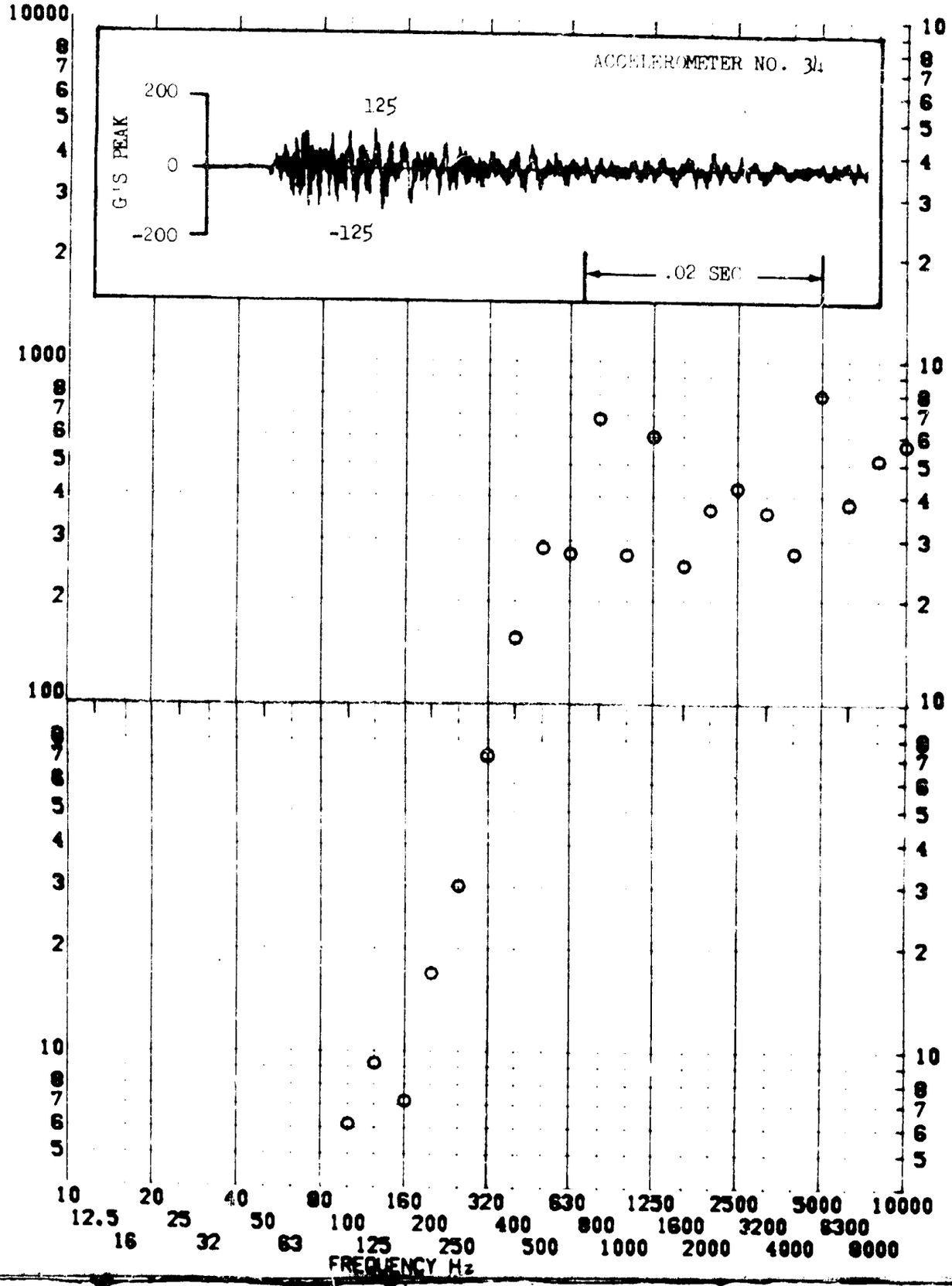

SHOCK TEST ANALYSIS DATA SHEET

TEST ITEM 1377-424
SERIAL NO.
SHOCK AXIS RADIAL

PART NO. EQUIPMENT
TEST DATE
SHOCK NO.

RESPONSE G-S

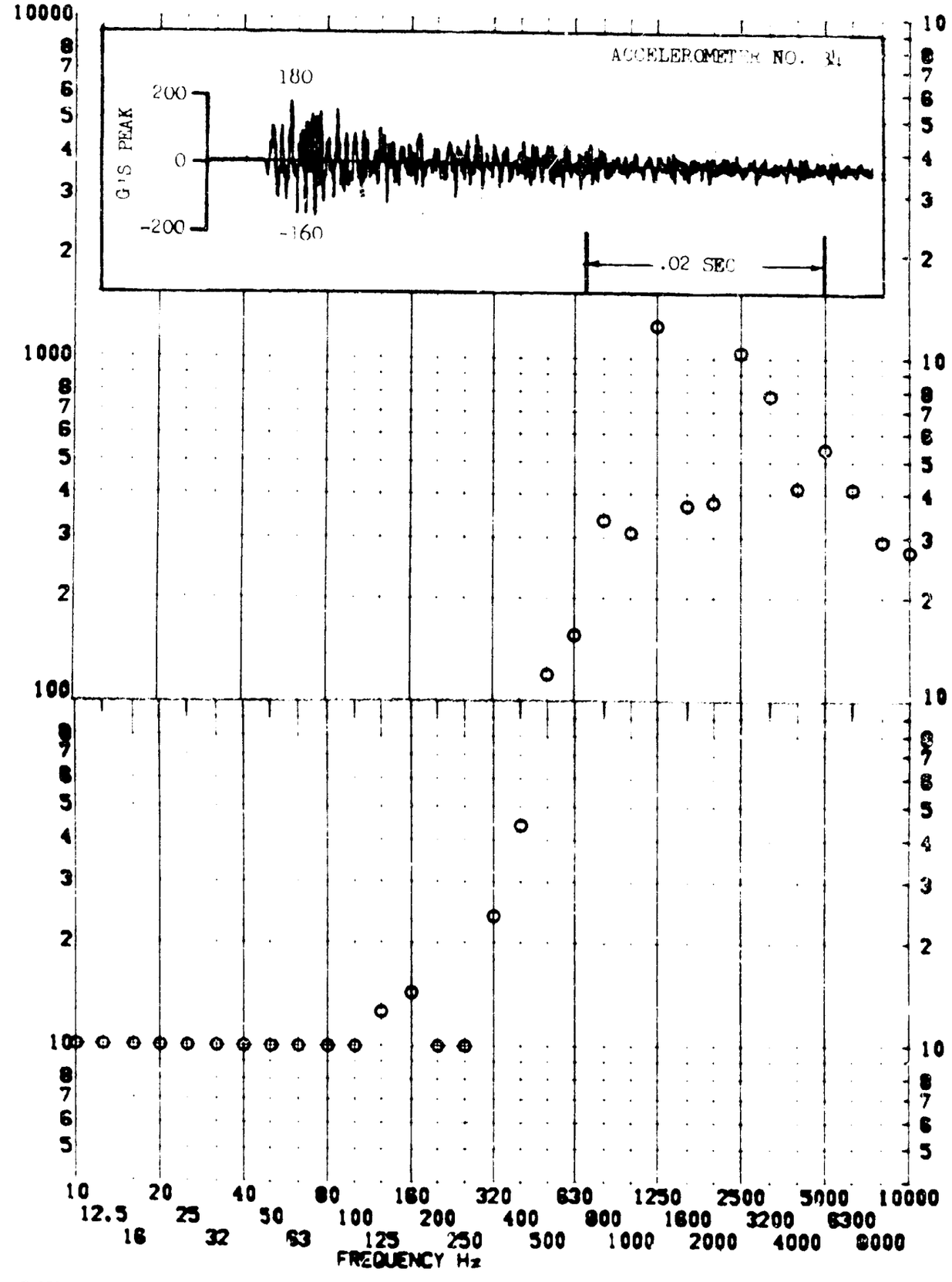

SHOCK TEST ANALYSIS DATA SHEET NO. [illegible]

TEST ITEM 1377-425 PART NO. EQUIPMENT
SERIAL NO. TEST DATE [illegible]
SHOCK AXIS TANGENTIAL SHOCK NO. 1

RESPONSE G-S

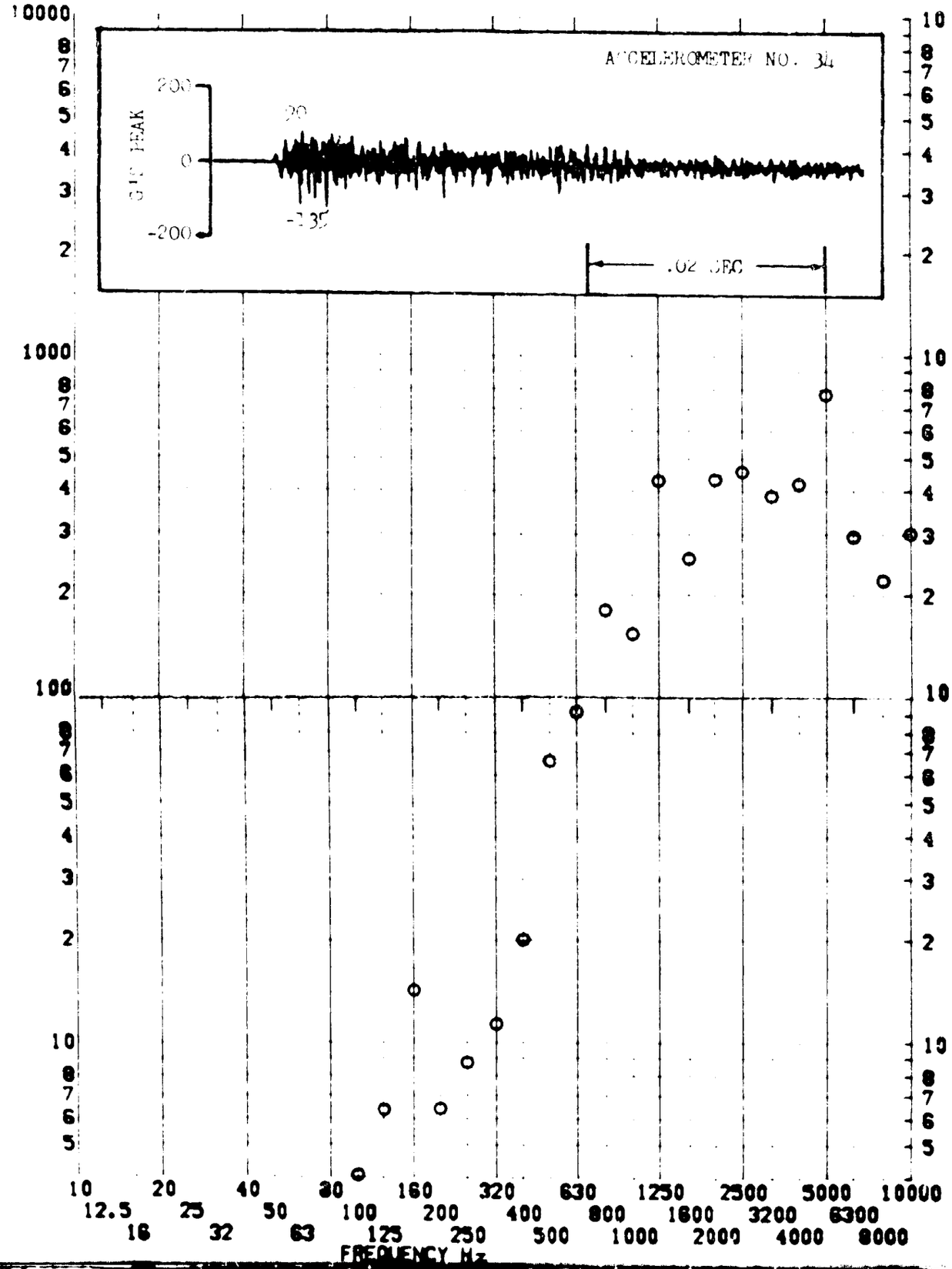

SHOCK TEST ANALYSIS DATA SHEET NO. H.A.[illegible]

TEST ITEM 1377-426
SERIAL NO.
SHOCK AXIS LONGITUDINAL

PART NO. STRUCTURE
TEST DATE 11 FEB 1962
SHOCK NO. 1

RESPONSE G-S

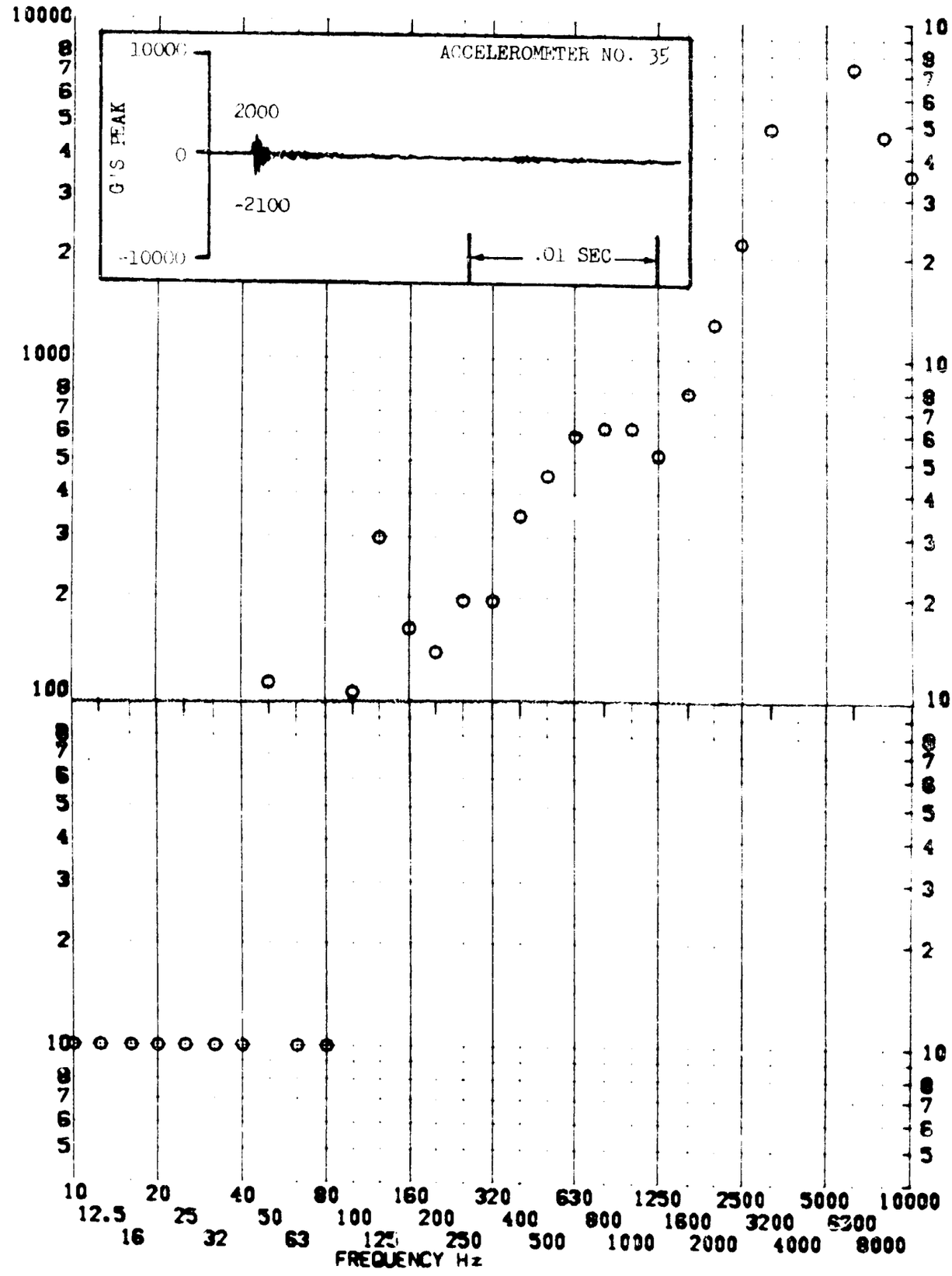

LMSC/A959903 SS-1386-6262 20 August 1969

SHOCK TEST ANALYSIS DATA SHEET

TEST ITEM 1377-506
SERIAL NO.
SHOCK AXIS LONGITUDINAL

PART NO. STRUCTURE
TEST DATE 11 FEB 1969
SHOCK NO. 2

RESPONSE G-S

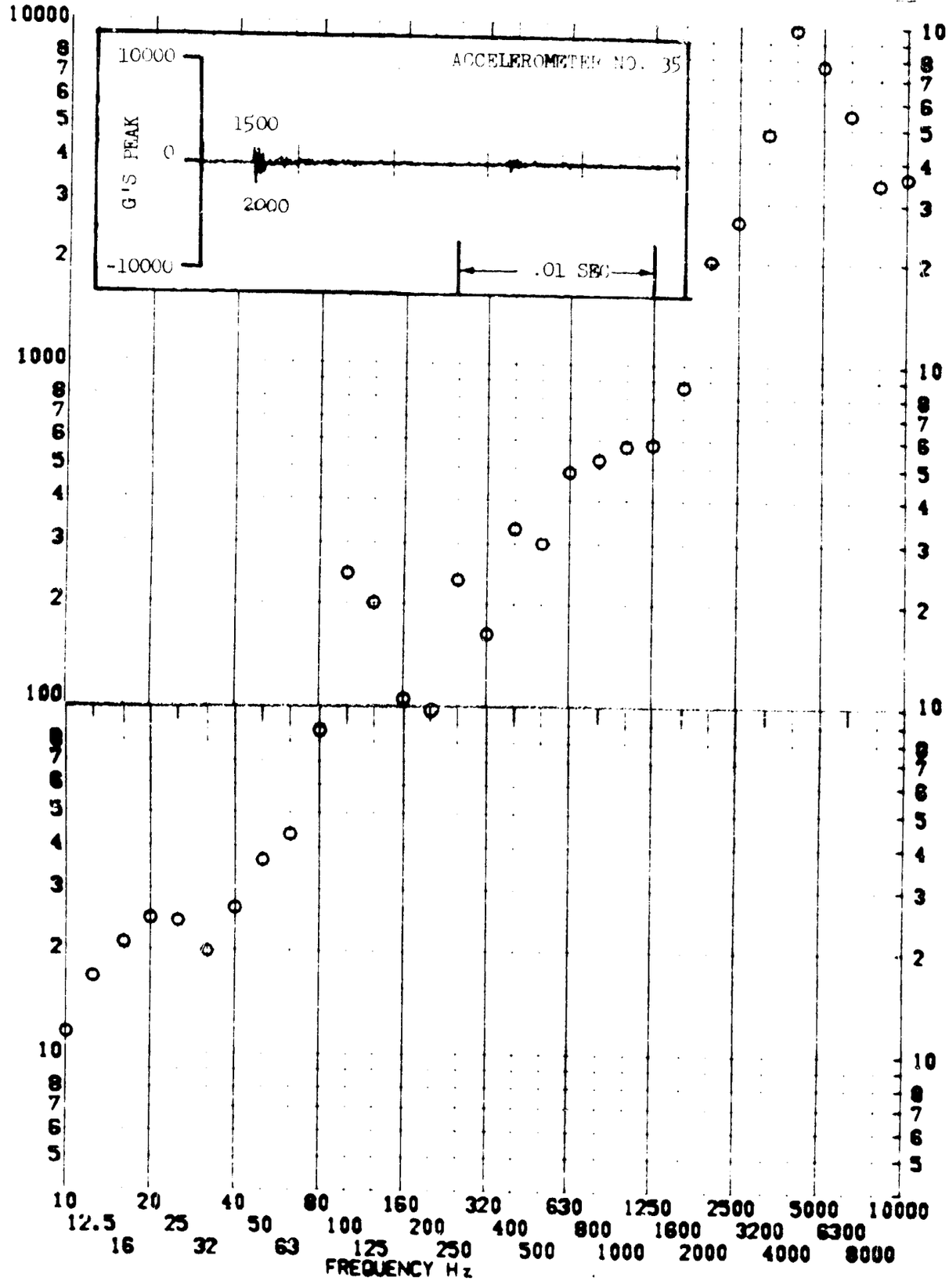

SHOCK TEST ANALYSIS DATA SHEET NO. II.A.7.163

TEST ITEM 1377-426,508
SERIAL NO.
SHOCK AXIS LONGITUDINAL

PART NO. STRUCTURE
TEST DATE 17 SEP 1969
SHOCK NO. 1 & 2

RESPONSE G-S

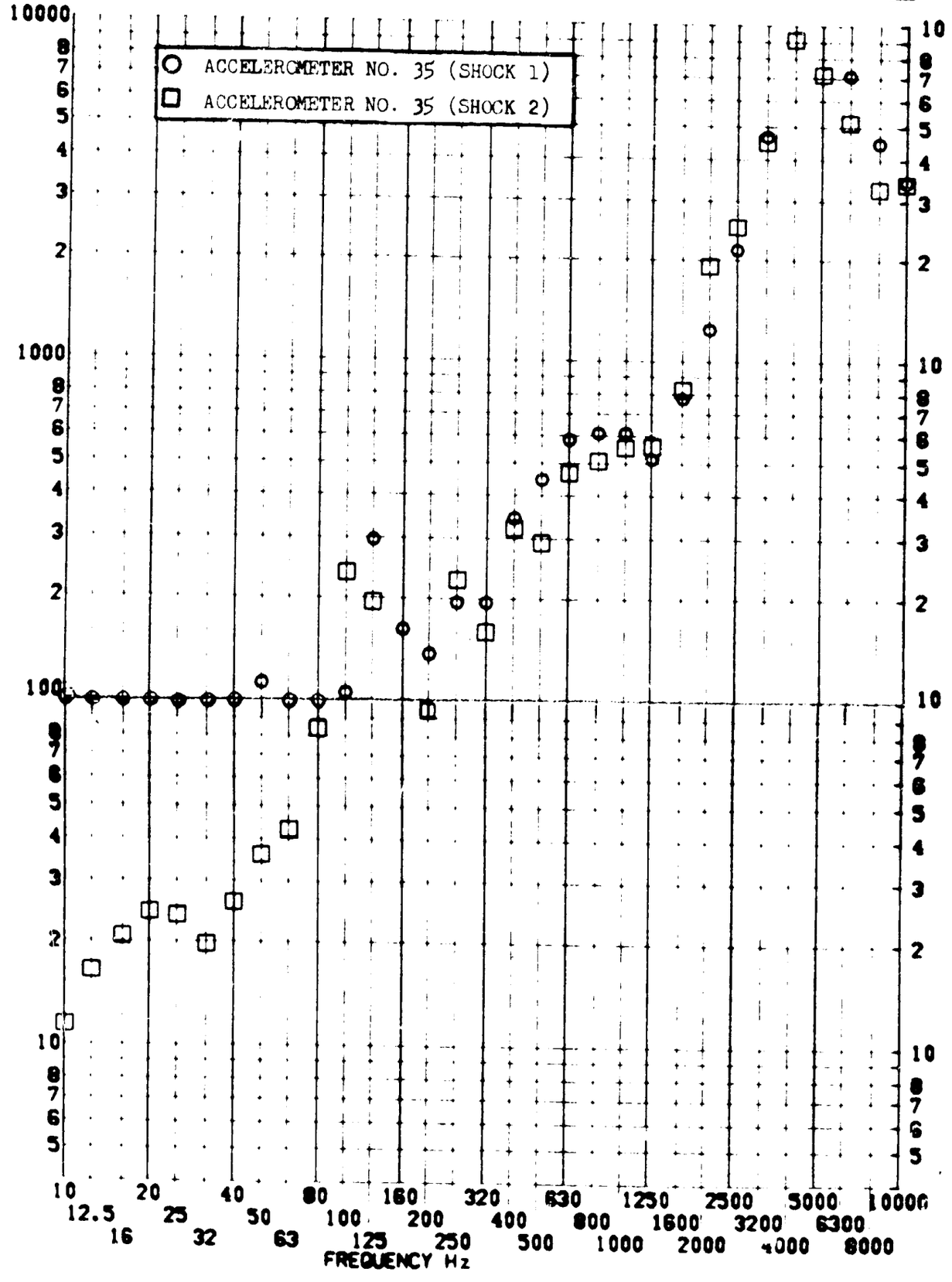

SHOCK TEST ANALYSIS DATA SHEET NO. II.A.7.16A

TEST ITEM 1377-427
SERIAL NO.
SHOCK AXIS RADIAL

PART NO. STRUCTURE
TEST DATE 11 FEB 1962
SHOCK NO. 1

RESPONSE G-S

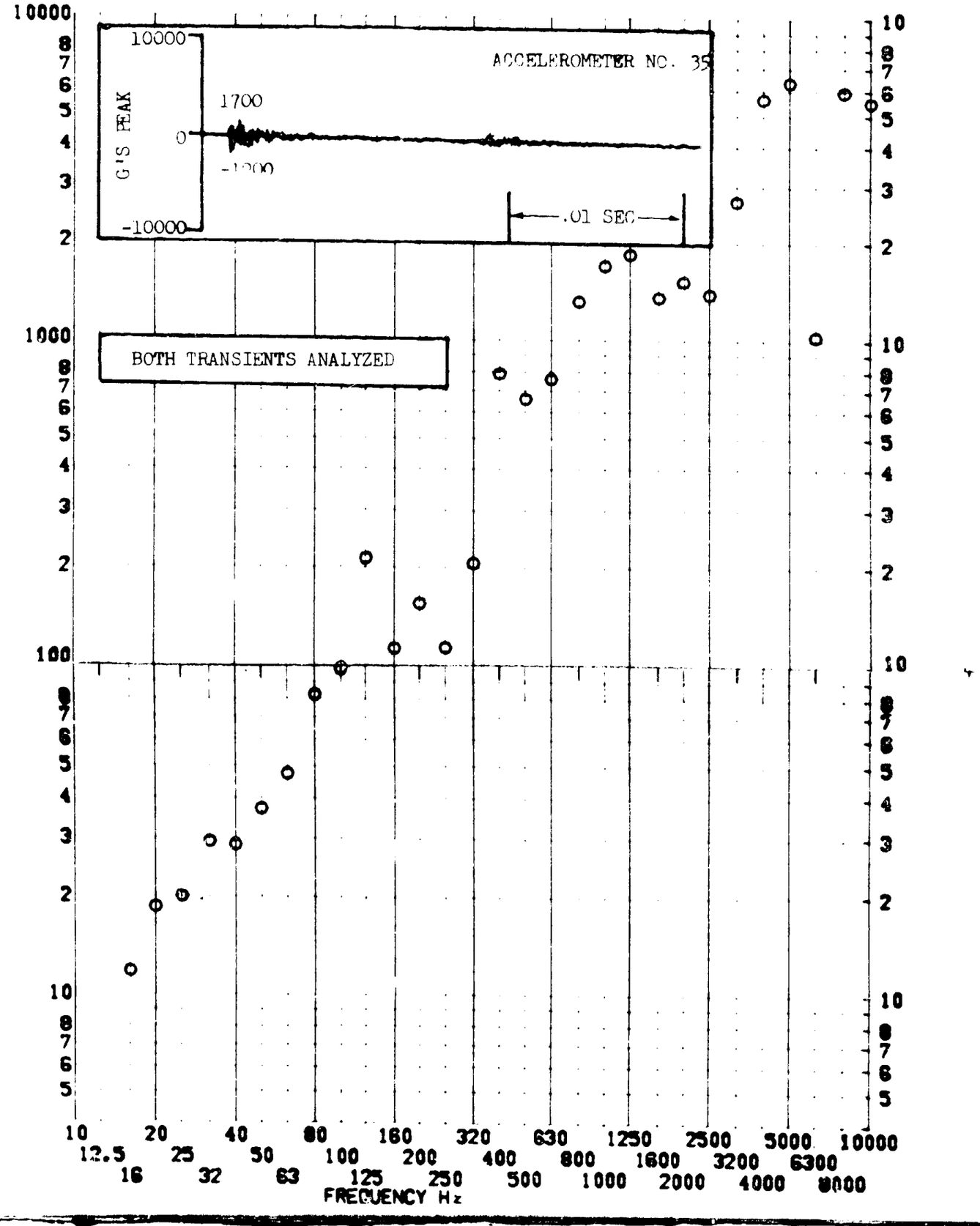

SHOCK TEST ANALYSIS DATA SHEET No. H.A.V.105

TEST ITEM 1377-428
SERIAL NO.
SHOCK AXIS RADIAL

PART NO. STRUCTURE
TEST DATE
SHOCK NO. 1

RESPONSE G-S

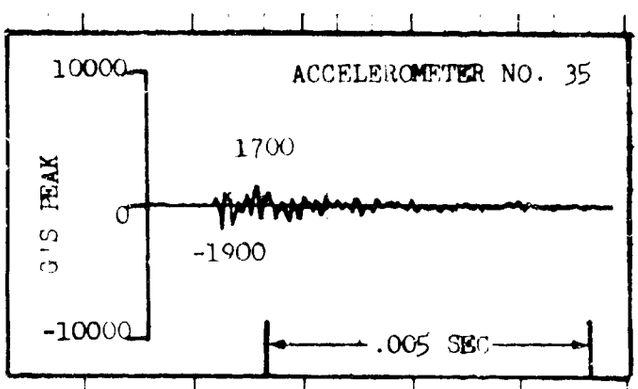

1ST TRANSIENT ONLY

10000 1000 100 10

10 20 40 80 160 320 630 1250 2500 5000 10000
12.5 25 50 100 200 400 800 1600 3200 6300
16 32 63 125 250 500 1000 2000 4000 8000

FREQUENCY Hz

SHOCK TEST ANALYSIS DATA SHEET NO. 11.A.7.166

TEST ITEM 1377-509 PART NO. STRUCTURE

SERIAL NO. TEST DATE 11 [illegible] 1969

SHOCK AXIS RADIAL SHOCK NO. 2

RESPONSE G-S

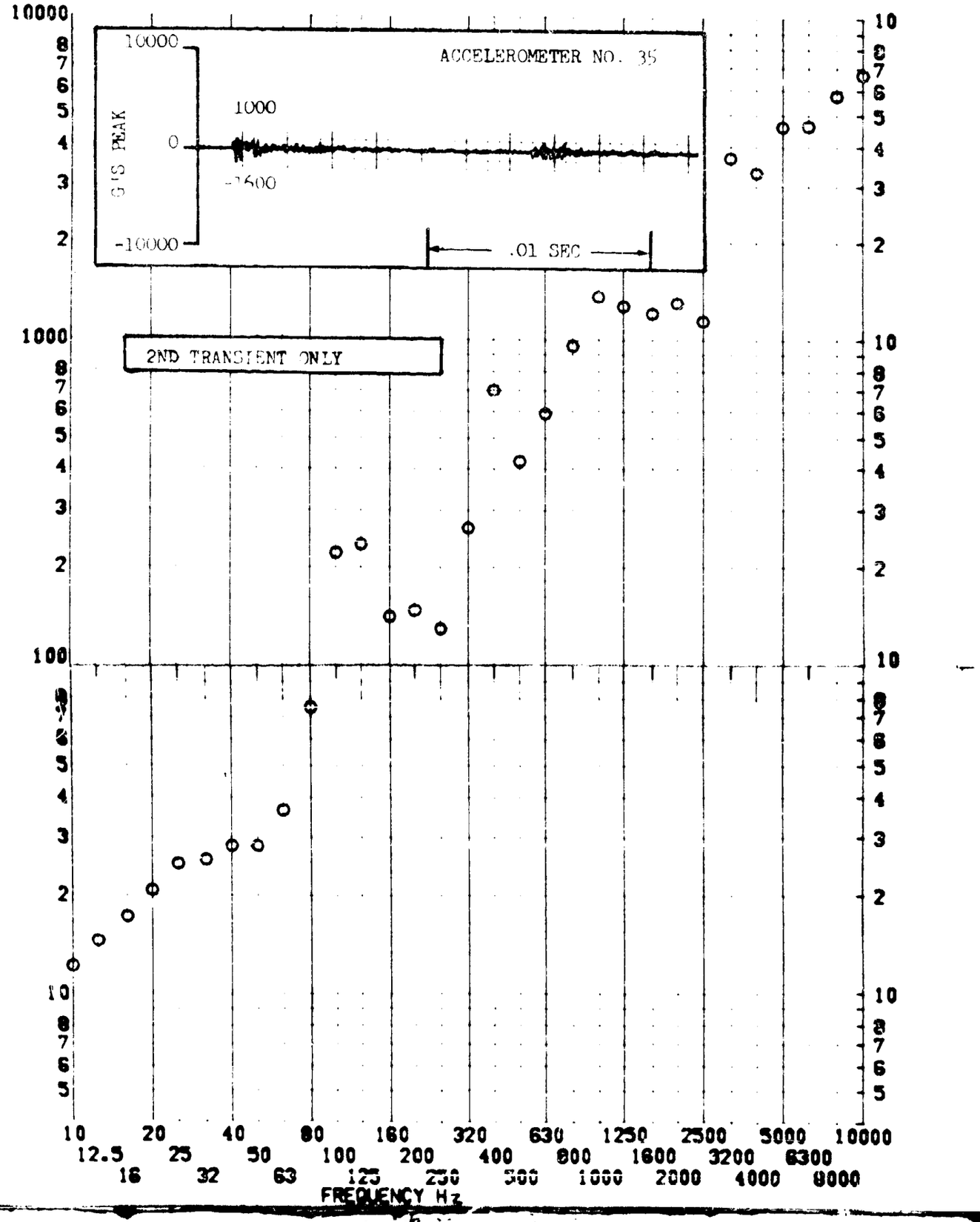

SHOCK TEST ANALYSIS DATA SHEET NO. H.A.7.167

TEST ITEM 1377-427,428,509
SERIAL NO.
SHOCK AXIS RADIAL

PART NO. STRUCTURE
TEST DATE 11 FEB 1962
SHOCK NO. 1 & 2

RESPONSE G-S

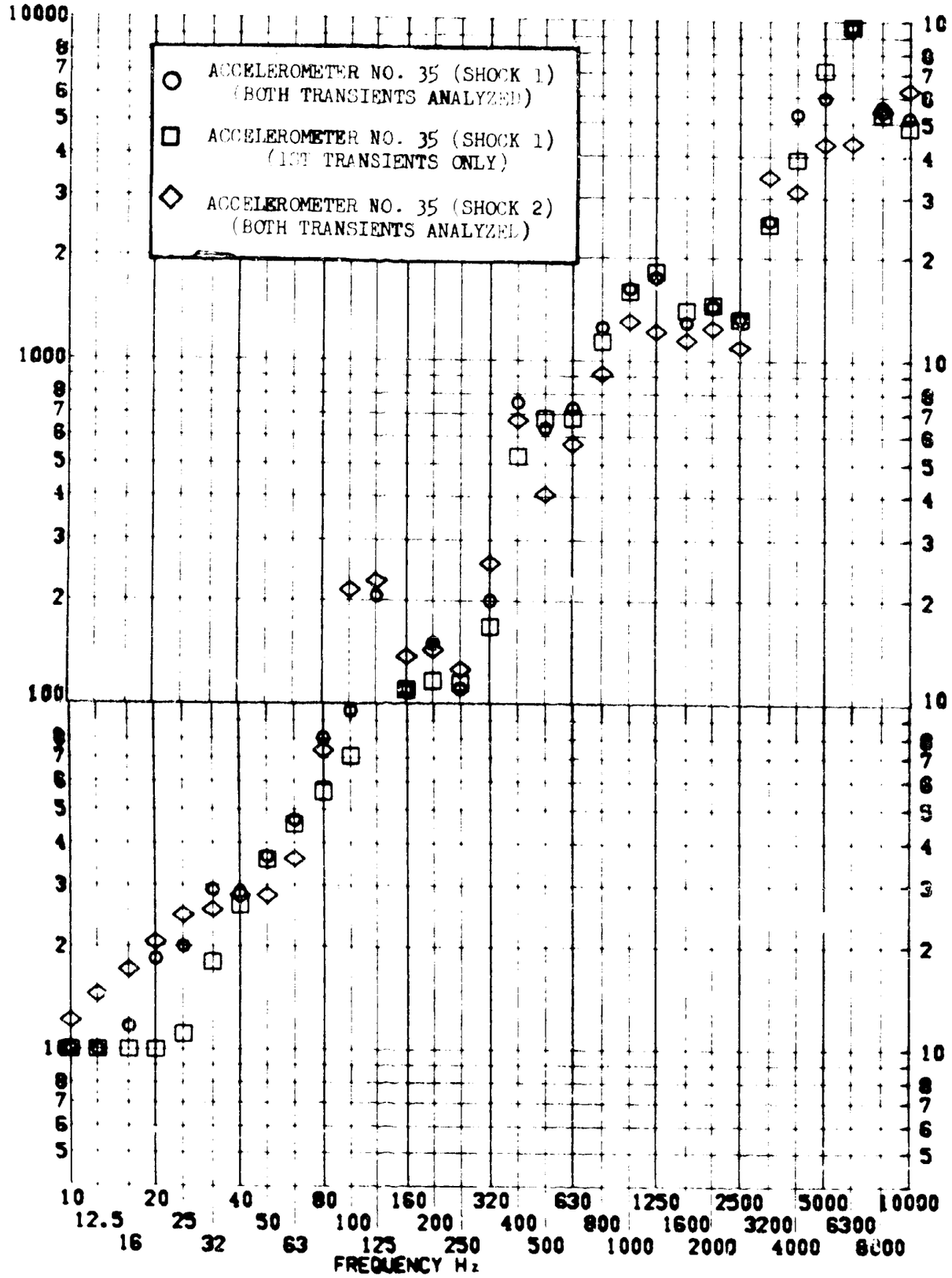

NO. 11.A.7.168

SHOCK TEST ANALYSIS DATA SHEET

TEST ITEM 1377-429 STRUCTURE
SERIAL NO. PART NO.
SHOCK AXIS LONGITU. TEST DATE 11 FEB 1962
RESPONSE G-S SHOCK NO. 1

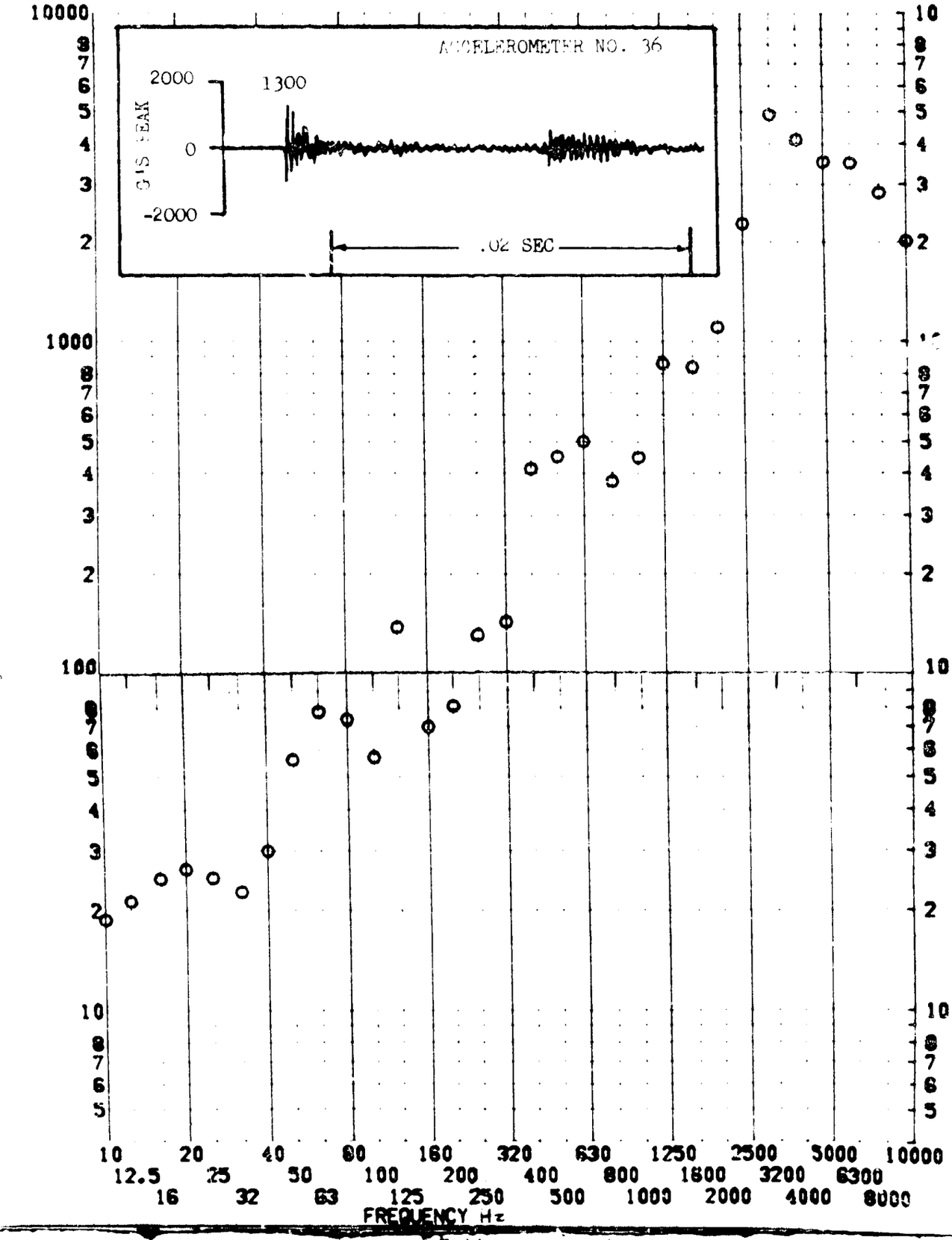

SHOCK TEST ANALYSIS DATA SHEET NO. [illegible]

TEST ITEM 377-510
SERIAL NO.
SHOCK AXIS LONGITUDINAL

PART NO. STRUCTURE
TEST DATE 11 FEB 1962
SHOCK NO. 2

RESPONSE G-S

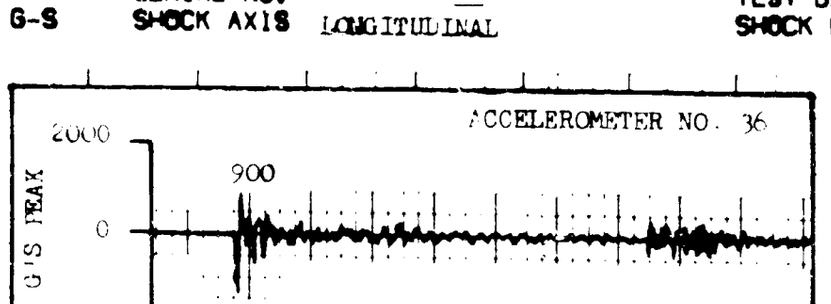

10000 1000 100 10

10 12.5 16 20 25 32 40 50 63 80 100 125 160 200 250 320 400 500 630 800 1000 1250 1600 2000 2500 3200 4000 5000 6300 8000 10000

FREQUENCY Hz

SHOCK TEST ANALYSIS DATA SHEET NO. II.A.4.1-1

TEST ITEM 1377-429,510
SERIAL NO.
SHOCK AXIS LONGITUDINAL

PART NO. STRUCTURE
TEST DATE 11 FEB 1972
SHOCK NO. 1 & 2

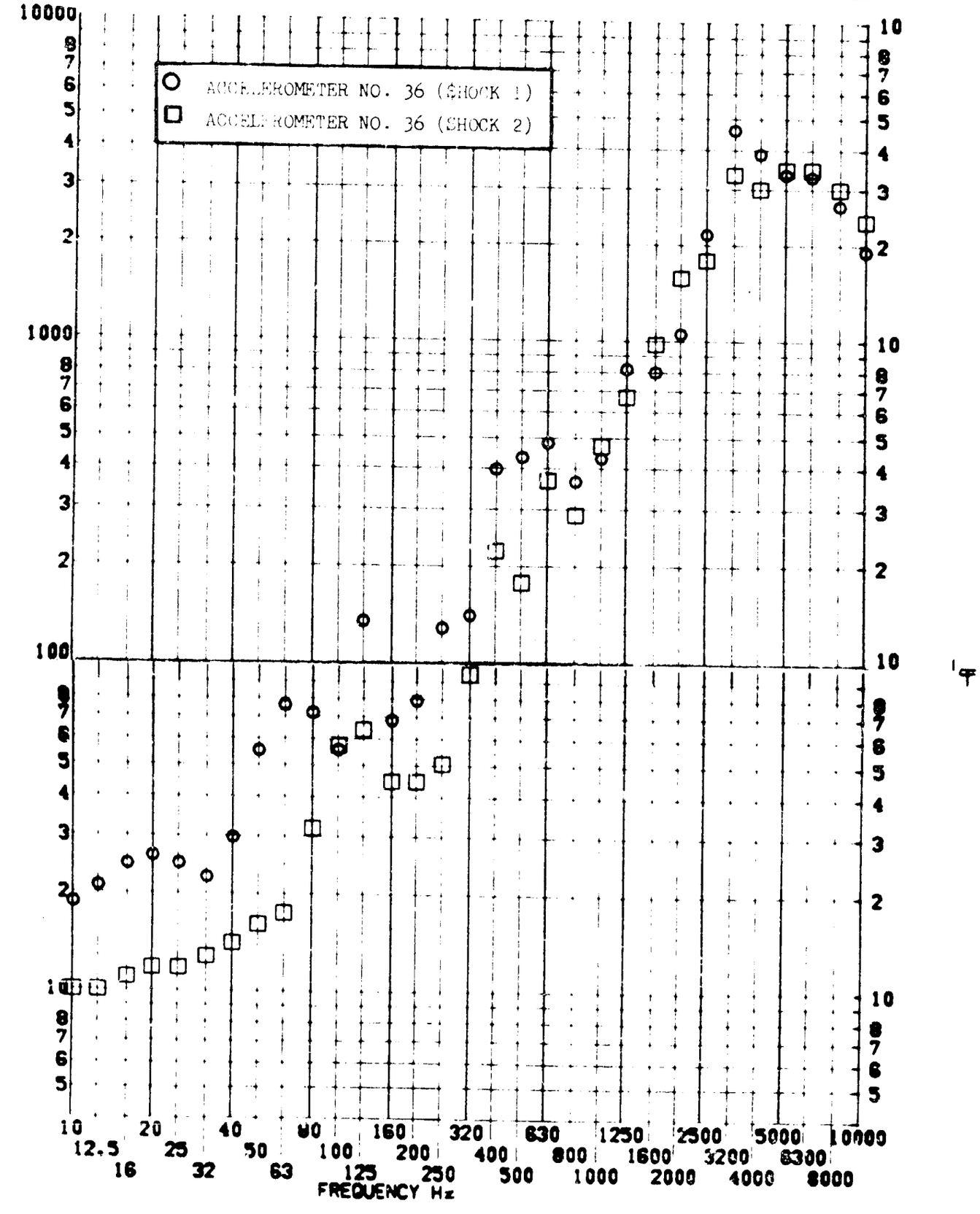

SHOCK TEST ANALYSIS DATA SHEET NO. I.A. . . 1

TEST ITEM 1377-430 **PART NO.** STRUCTURE

SERIAL NO. **TEST DATE** 11 FEB 1969

RESPONSE G-S **SHOCK AXIS** RADIAL **SHOCK NO.** 1

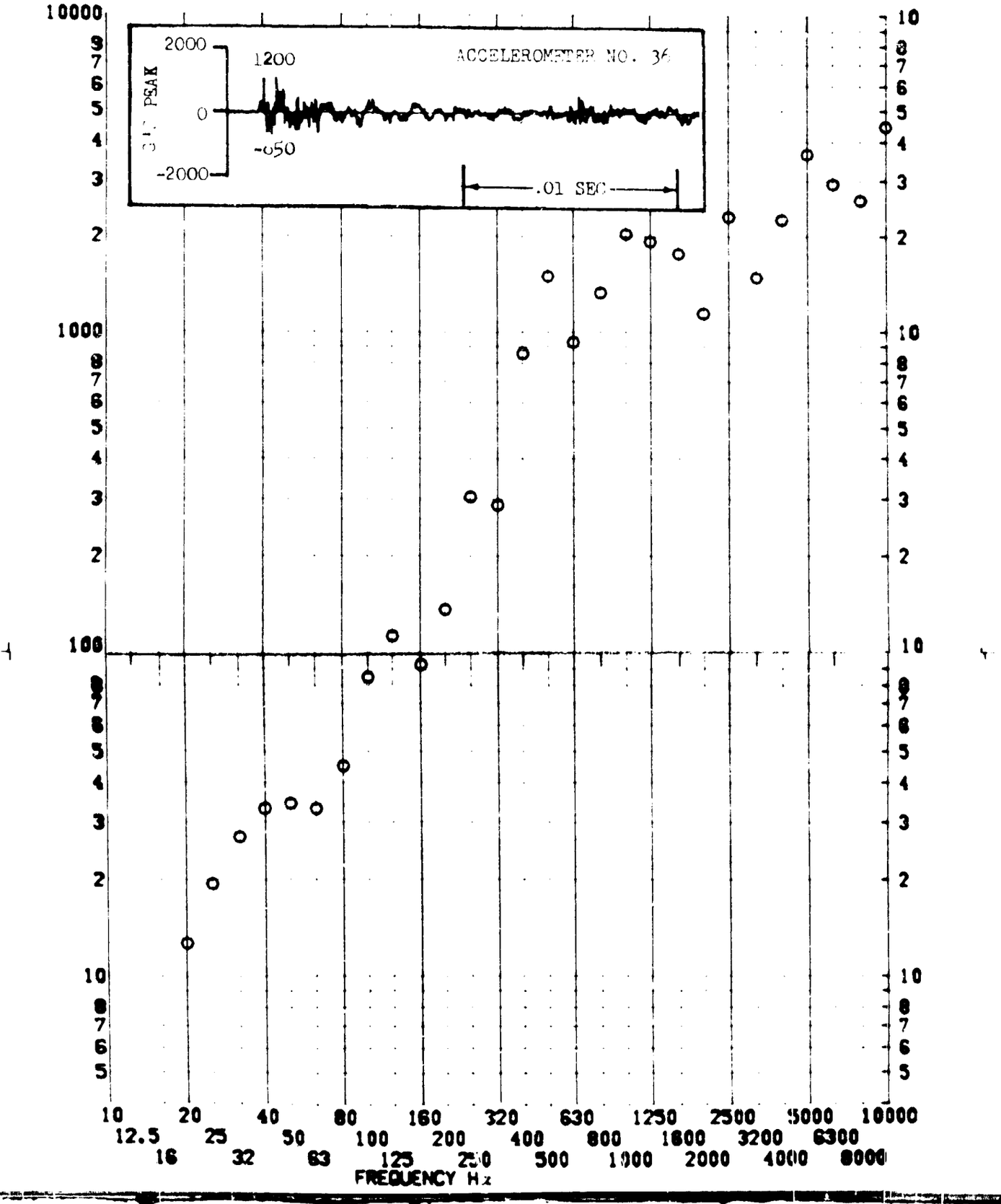

SHOCK TEST ANALYSIS DATA SHEET NO. I.A.7-172

TEST ITEM 1377-51 ___ **PART NO.** STRUCTURE ___
SERIAL NO. ___ **TEST DATE** 11 FEB 1969 ___
SHOCK AXIS RADIAL ___ **SHOCK NO.** 2 ___

RESPONSE G-S

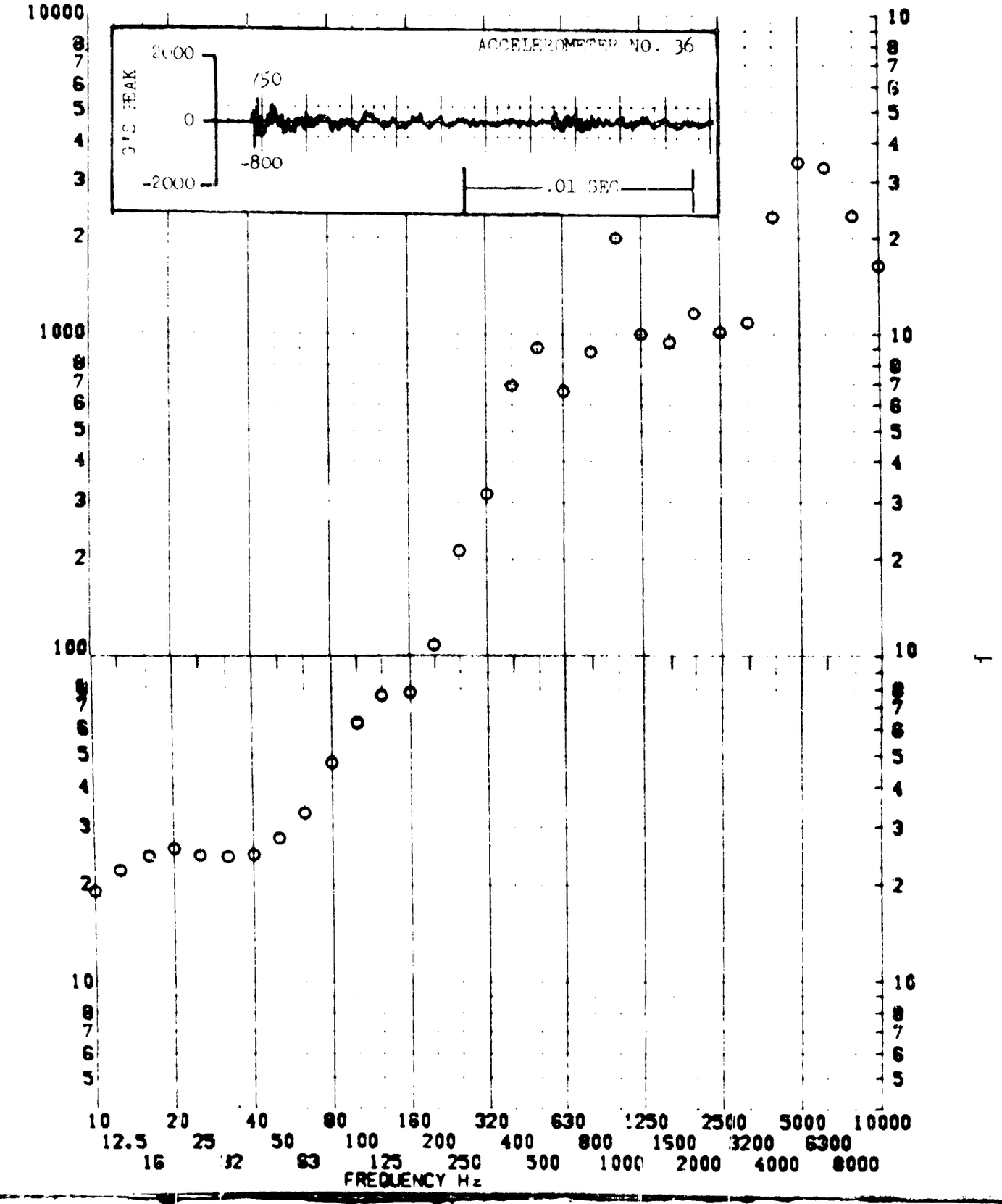

SHOCK TEST ANALYSIS DATA SHEET NO. II.A. .1 3

TEST ITEM 1377-430,511
SERIAL NO. —
SHOCK AXIS RADIAL —

PART NO. STRUCTURE
TEST DATE 11 FEB 1969
SHOCK NO. 1 & 2

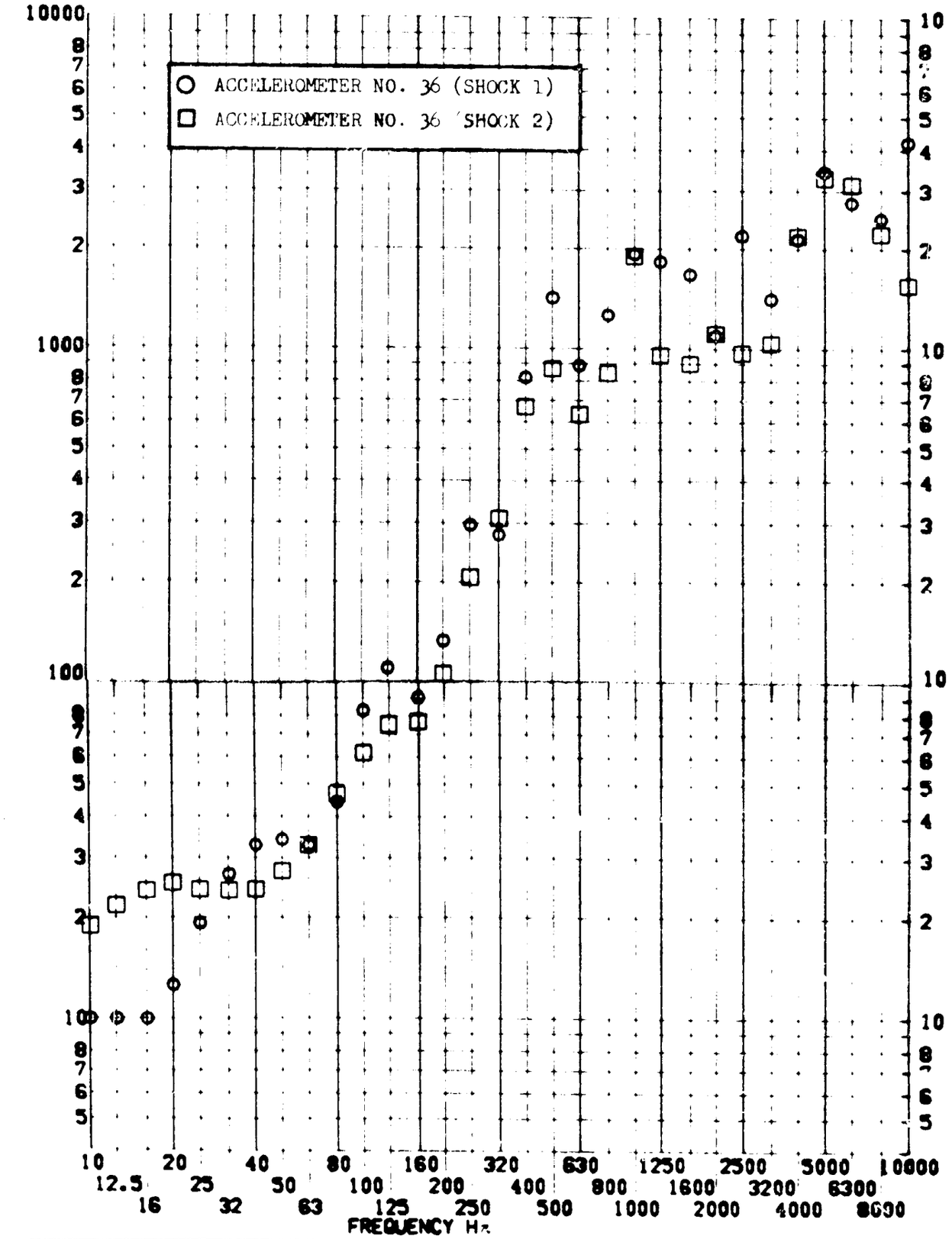

SHOCK TEST ANALYSIS DATA SHEET NO. II.A.1.4

TEST ITEM 1377-512
SERIAL NO.
SHOCK AXIS LONGITUDINAL

PART NO. STRUCTURE
TEST DATE 11 FEB 1962
SHOCK NO. 2

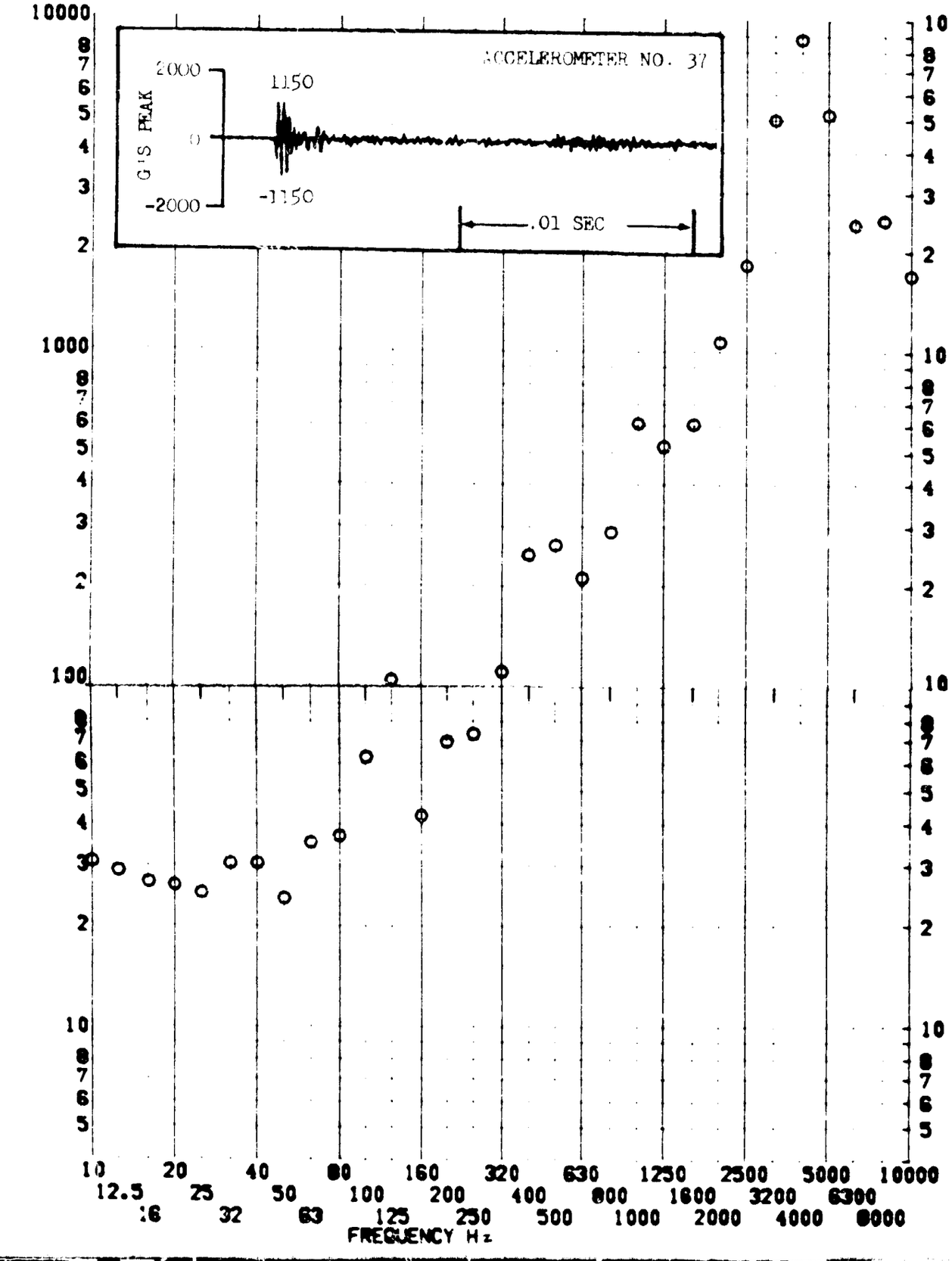

SHOCK TEST ANALYSIS DATA SHEET NO. [illegible]

TEST ITEM 1377-431
SERIAL NO.
SHOCK AXIS RADIAL

PART NO. STRUCTURE
TEST DATE 11 FEB 1967
SHOCK NO. 1

RESPONSE G-S

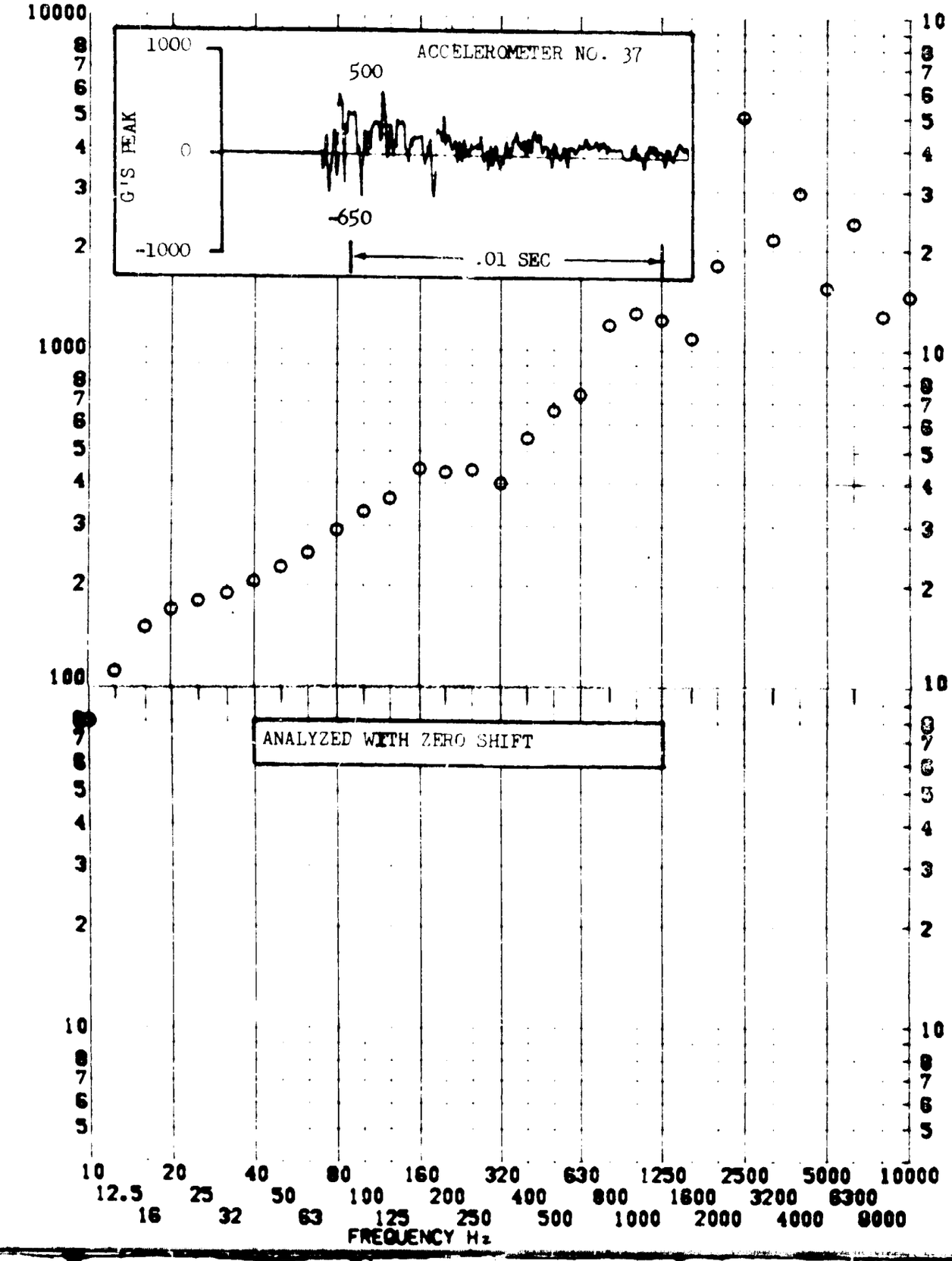

SHOCK TEST ANALYSIS DATA SHEET NO. II.A.7.76

TEST ITEM 1377-432
SERIAL NO.
SHOCK AXIS RADIAL

PART NO. STRUCTURE
TEST DATE 11 FEB 69
SHOCK NO.

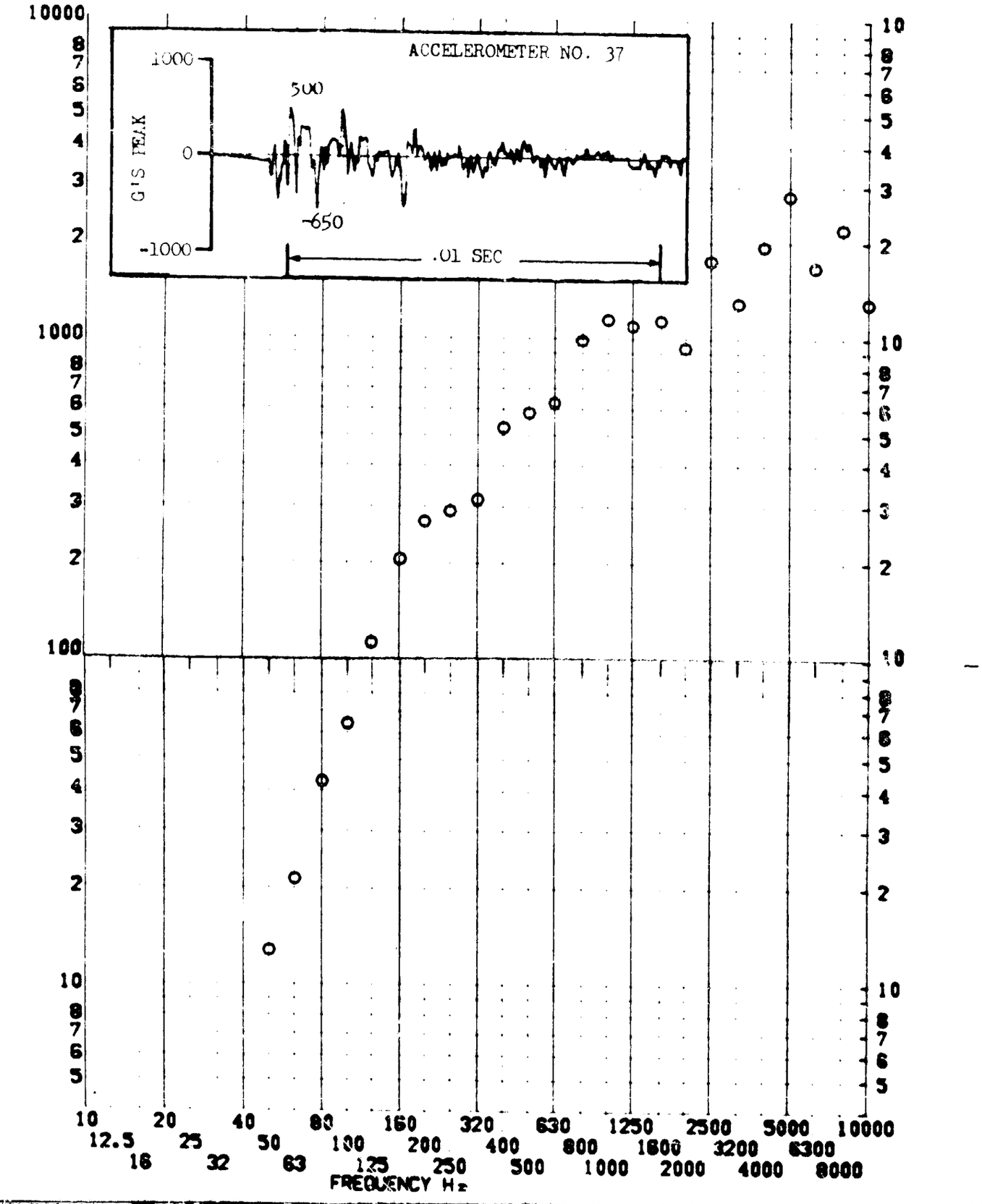

SHOCK TEST ANALYSIS DATA SHEET

TEST ITEM 1377-513
SERIAL NO.
SHOCK AXIS RADIAL

PART NO.
TEST DATE
SHOCK NO.

RESPONSE G-S

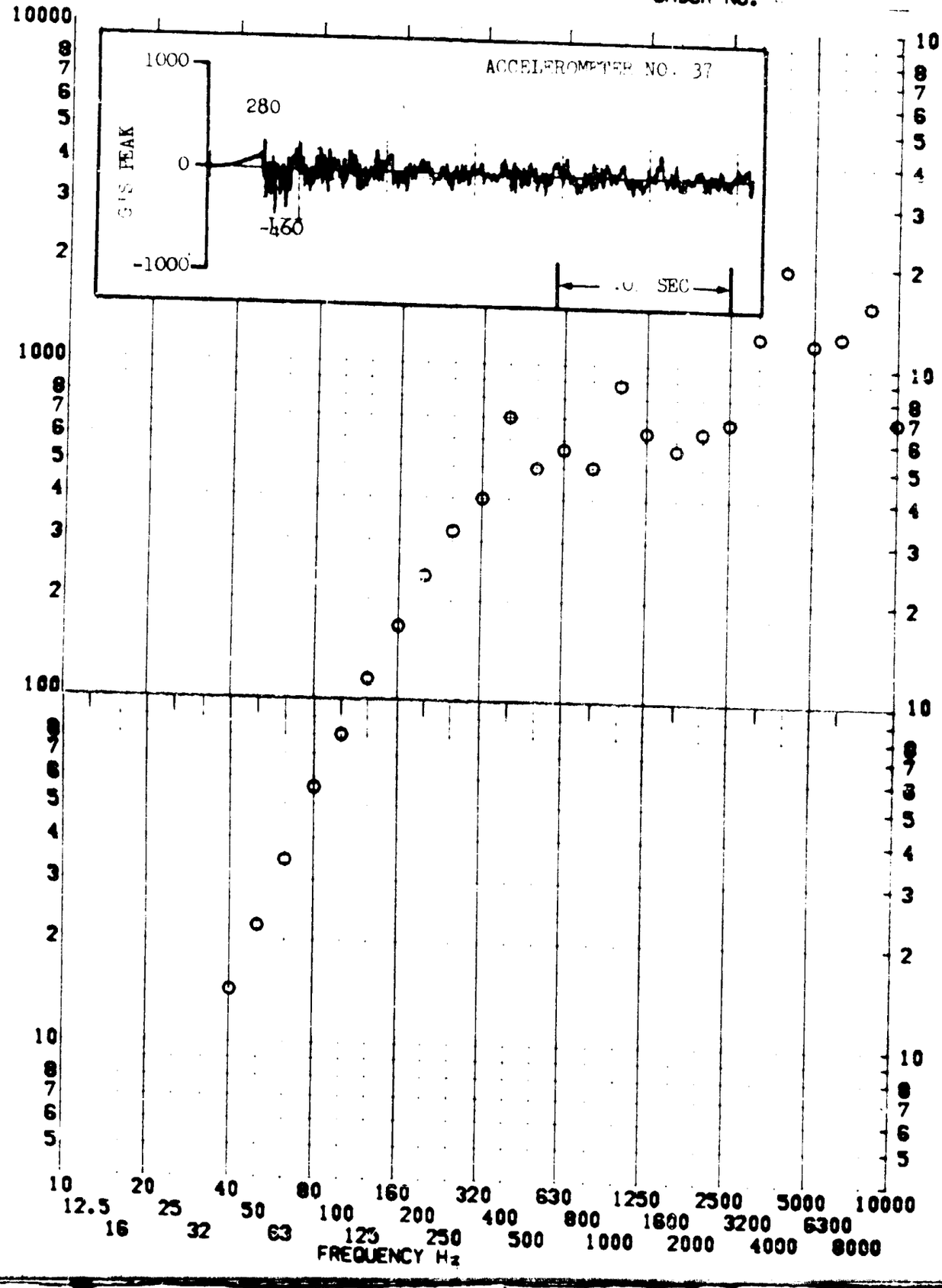

SHOCK TEST ANALYSIS DATA SHEET NO. H.A.T.178

TEST ITEM 1377-431,432,513 PART NO. STRUCTURE

SERIAL NO. TEST DATE 11 FEB 1969

SHOCK AXIS RADIAL SHOCK NO. 1 & 2

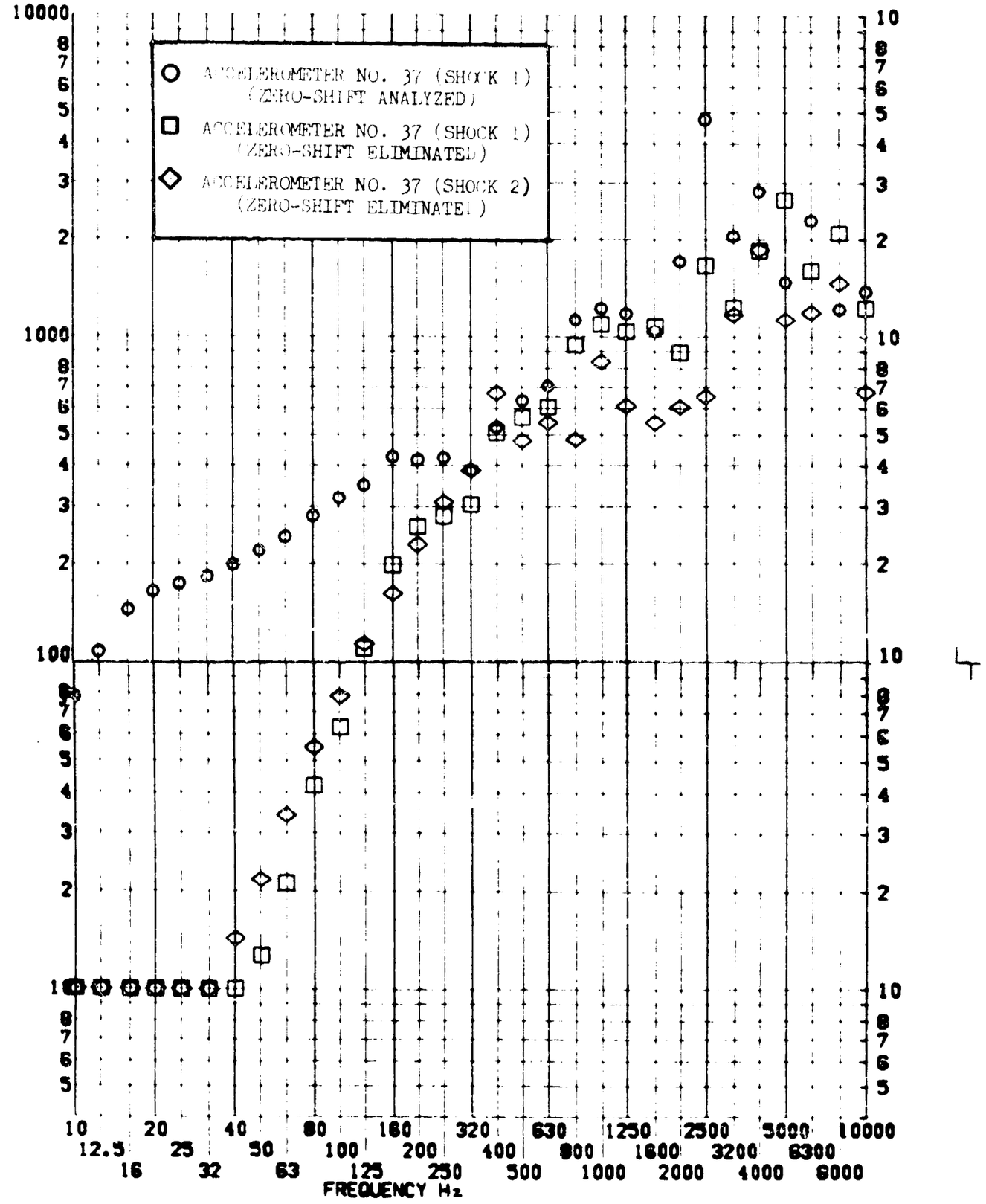

SHOCK TEST ANALYSIS DATA SHEET NO. II.A.7.179

TEST ITEM 1377-514
SERIAL NO.
SHOCK AXIS LONGITUDINAL

PART NO. EQUIPMENT
TEST DATE 11 FEB 1962
SHOCK NO. 2

RESPONSE G-S

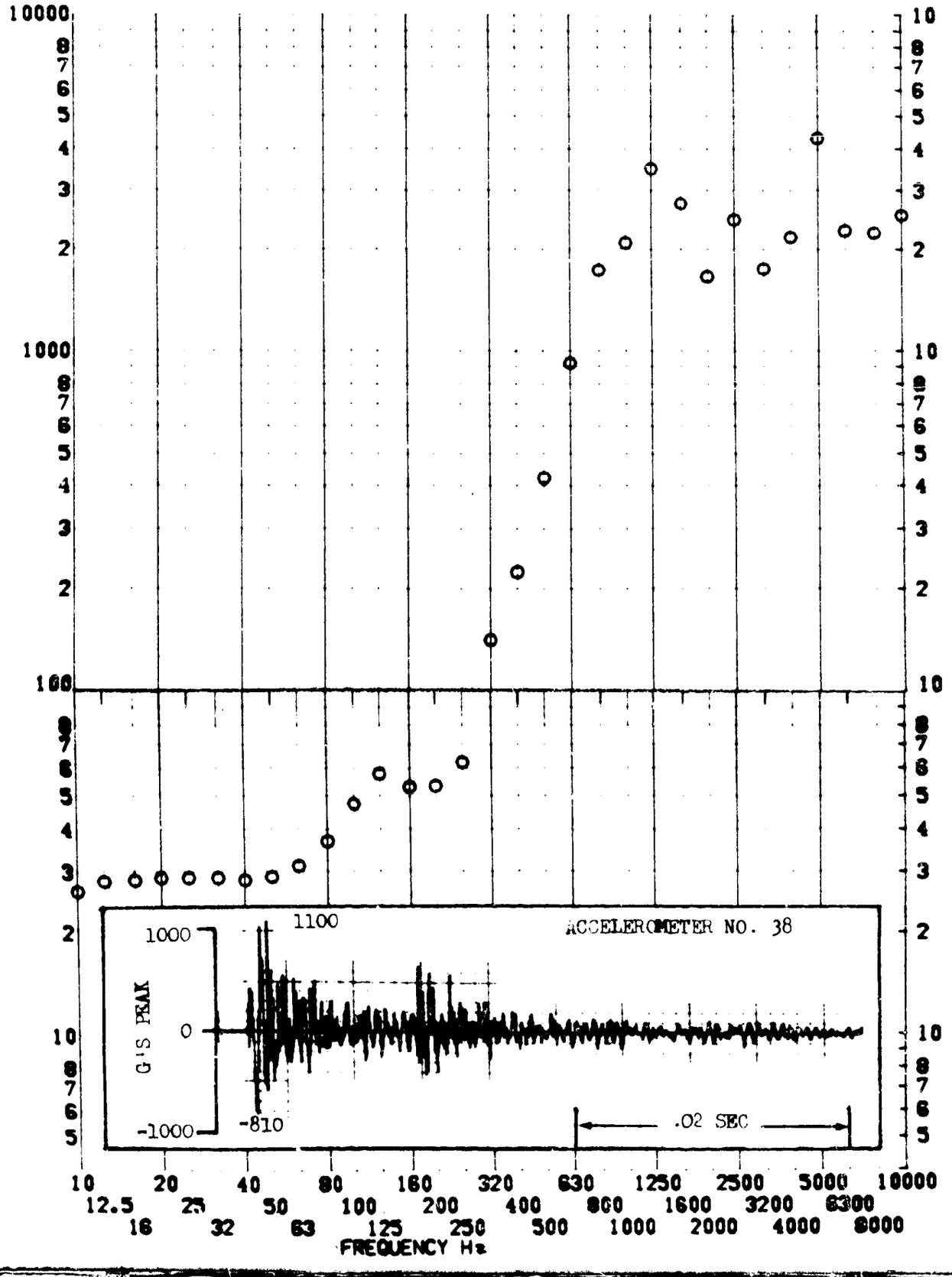

SHOCK TEST ANALYSIS DATA SHEET NO. II.A.7.18[illegible]

TEST ITEM 1377-515
SERIAL NO.
SHOCK AXIS RADIAL

PART NO. EQUIPMENT
TEST DATE 11 FEB 1969
SHOCK NO. 2

RESPONSE G-S

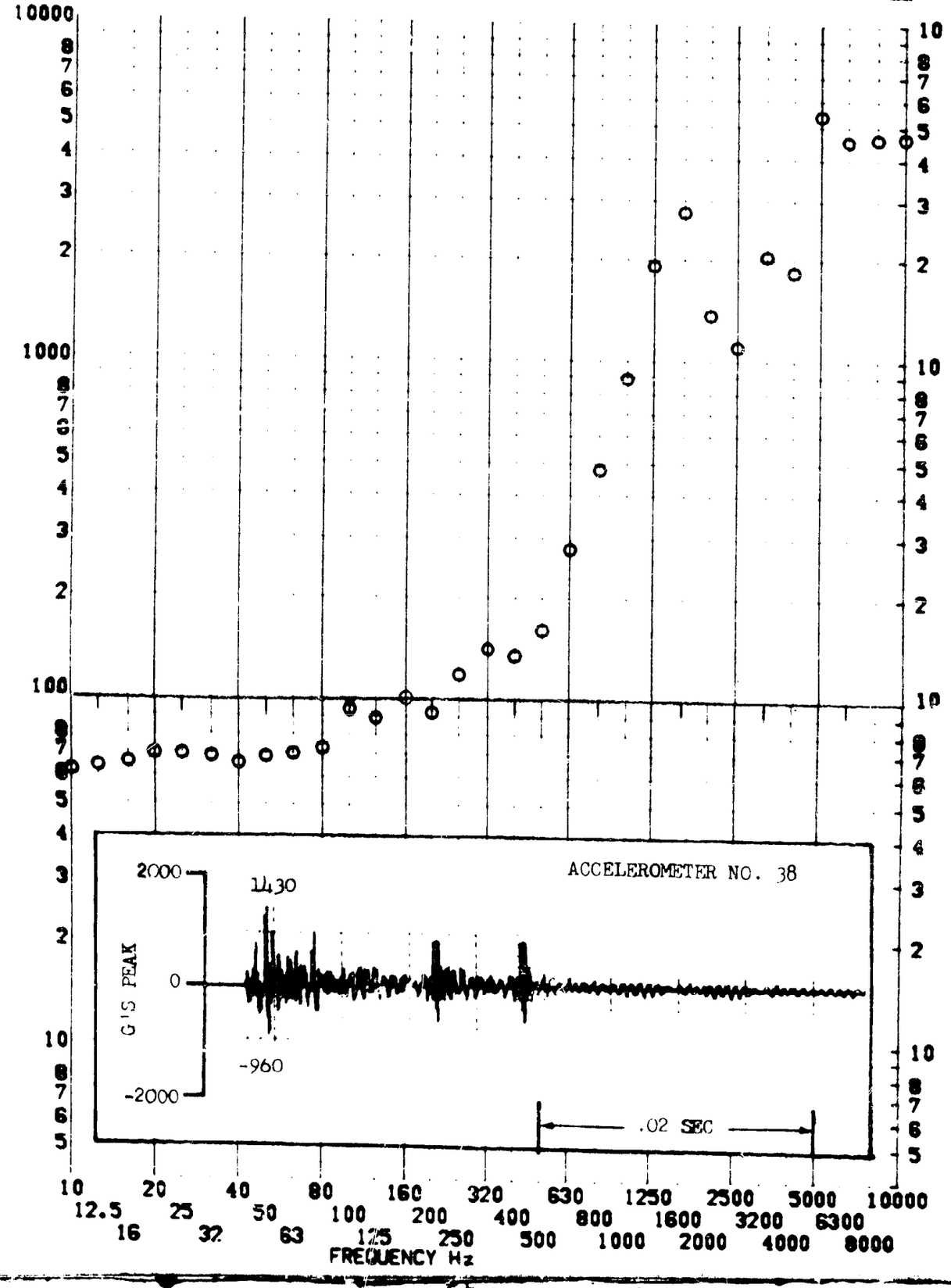

SHOCK TEST ANALYSIS DATA SHEET

TEST ITEM [illegible] PART NO. [illegible]
SERIAL NO. TEST DATE 11 FEB 1969
RESPONSE G-S SHOCK AXIS LONGITUDINAL SHOCK NO. 2

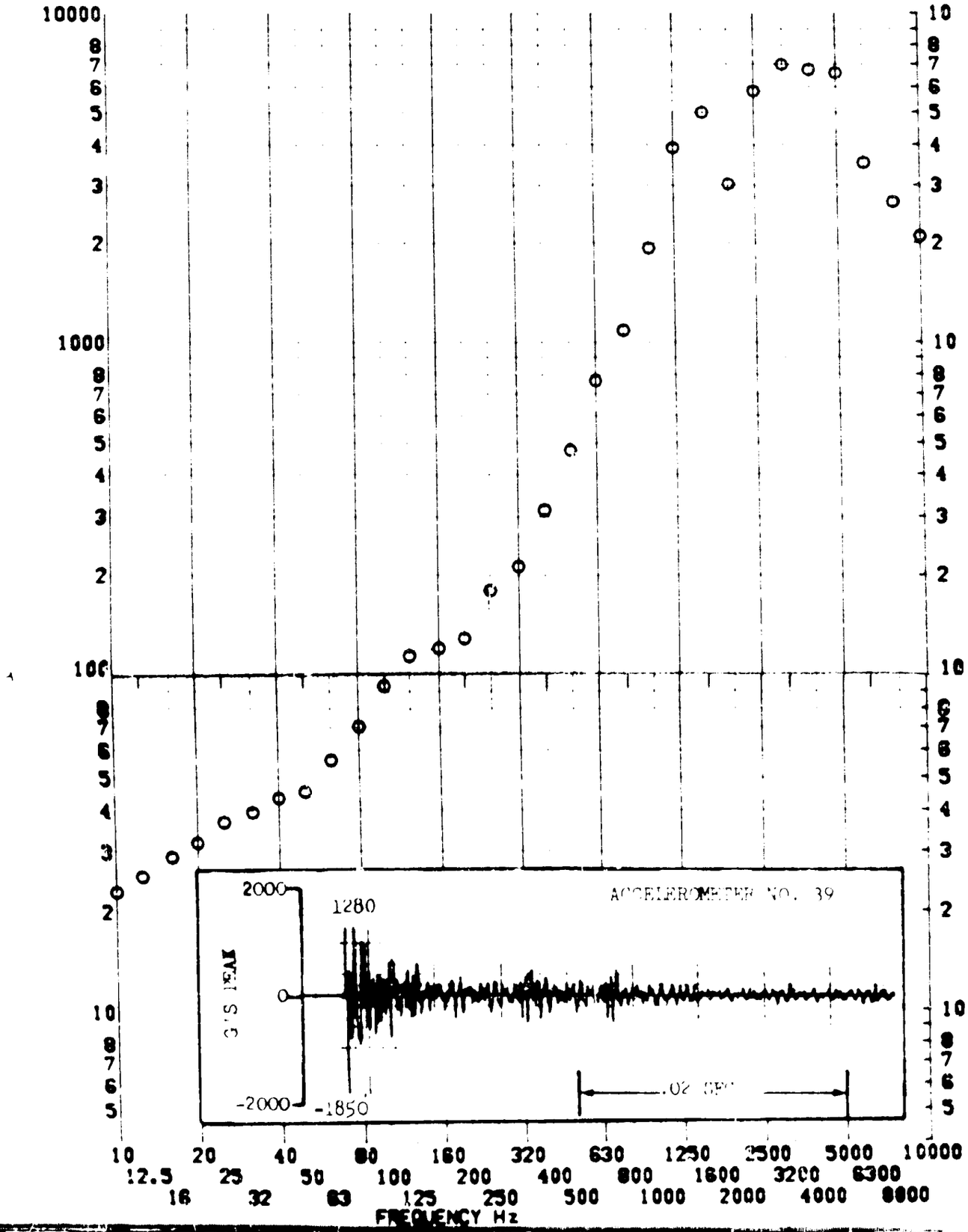

SHOCK TEST ANALYSIS DATA SHEET NO. II.A.7.1.2

TEST ITEM 1377-517 — **PART NO.** EQUIPMENT —
SERIAL NO. — **TEST DATE** [illegible] —
SHOCK AXIS RADIAL — **SHOCK NO.** 2 —

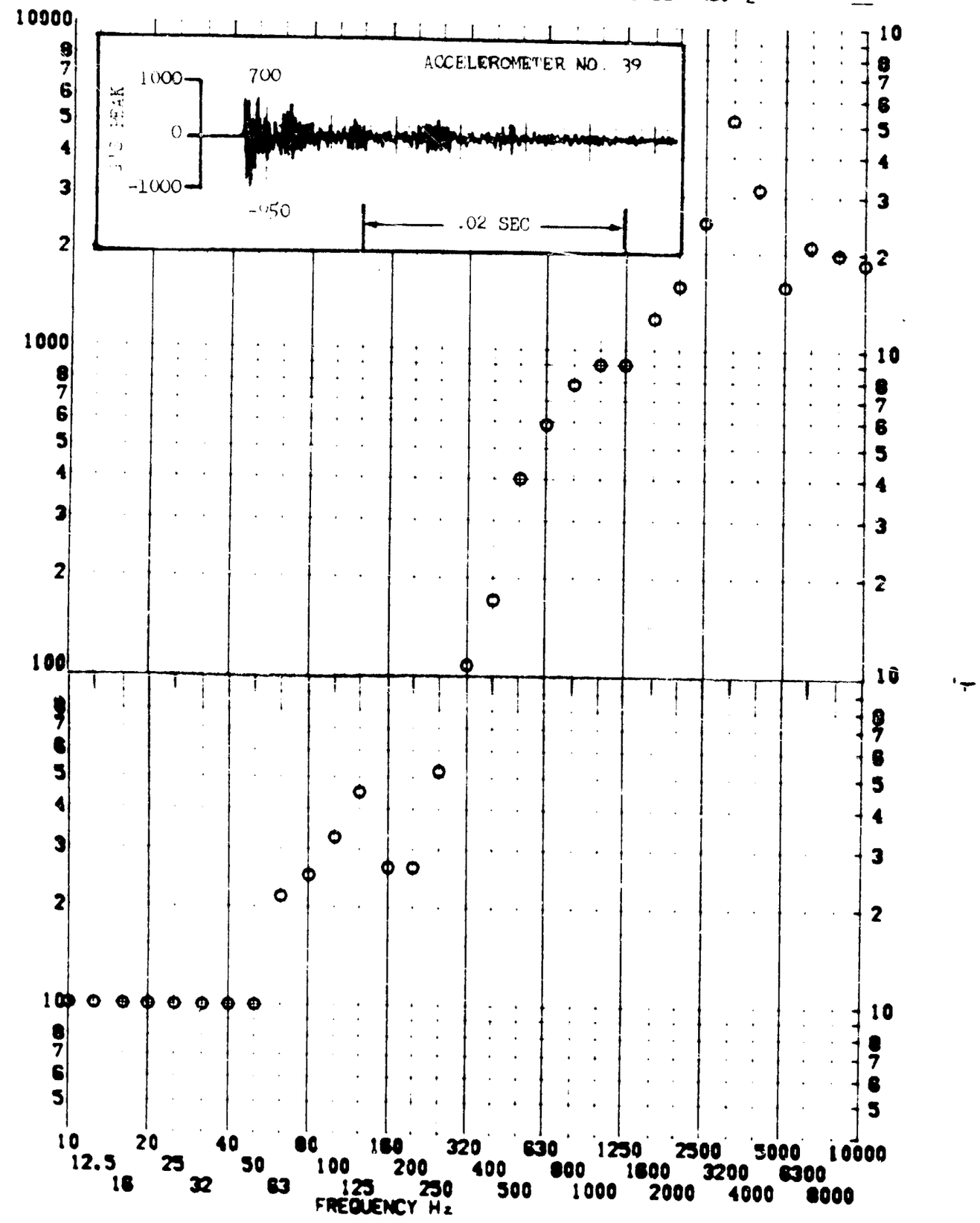

II.A.8 DISCUSSION AND ANALYSIS

II.A.8.1 General

This section covers three major topics of interest, namely:

a. Separation joint design.

b. Shock environment levels as a function of the distance from the shock source.

c. Repeatability of test results.

Correlation between flight pyrotechnic environment and ground level simulation testing is also an important topic. However, the only data which can be made available in this report is not reliable enough to allow a reasonable comparison to be made.

II.A.8.2 Separation Joints

Testing reported in this section covers twelve different separation joint configurations, as follows:

Section II.A.3 - Report 768 - Standard joint plus seven modifications.

Section II.A.4 - Report 790 - Standard joint plus three configurations: V band, spring band and inflatable tube.

Section II.A.5 - Report 1080 - Hoop tension strap and strap cutters.

In order to place the results of these experiments in their proper perspective, a shock attenuation grading based on oscillogram peak g's is provided for each configuration and expressed in terms of the standard joint shock level. Shock attenuation grading for the joints of Section II.A.3 are taken from Table II.A.3.3 while those of the joints of Section II.A.4 are calculated on Table II.A.1. The hoop tension strap and cutter joint of Section II.A.5 is graded by comparison of the curves of Figure II.A.1. The complete grading is presented on Table II.A.2.

Another comparison, based on shock spectrum data, is presented on Figure II.A.1 for the joints of Section II.A.4 and II.A.5 since no shock spectrums are available for the modifications to the standard joints of Section II.A.3. Pertinent data from Section II.A.3 is presented on Table II.A.3.

It will be noted that this method of solution is a very simplified evaluation of the relative attenuation. The use of more sophisticated methods was not considered necessary since only an indication of the severity was required. The values presented in this analysis reflect the general trend of the attenuation which may be achieved with various types of separation joints.

This analysis indicates that separation joints designed to minimize pyrotechnic shocks can provide as much as 90 percent attenuation with the environment generated by the standard joint. However, direct substitution is not necessarily possible and structural redesign may be required.

II.A.8.3 Shock Environment Level as a Function of Distance to Shock Source

In only two cases (Section II.A.6 and II.A.7) was the instrumentation intended to provide for some mapping of the shock environment throughout the structure. In all other cases, the tests were conducted for development purposes or equipment qualification and accelerometer locations did not provide sufficient data for extensive shock environment analysis. Thus, in most instances, the data necessary for determining shock attenuation versus distance came only as a secondary by-product of the tests.

The shock attenuation versus distance can be obtained either from the oscillogram data or from the shock spectra. These two methods of analysis are treated separately.

Attenuation versus Distance from Oscillogram Data

The peak G levels recorded on the oscillograms are used to define an overall shock attenuation versus distance which covers the whole frequency spectrum.

Useful data, in addition to that of Section II.A.6 and II.A.7, was also obtained from oscillogram records of Sections II.A.2, II.A.3, II.A.4 and II.A.5. All this data was normalized and collected as a plot of percent shock attenuation versus distance from shock source (presented on Figure II.A.2). The data is normalized to the shock environment at about five inches from the shock source which is the closest available reading. The approximate attenuation curve, which was derived from an earlier set of test results, is also plotted on Figure II.A.2. It may be noted that the somewhat more complete data presented here tends to indicate higher levels near the source. This could suggest that no appreciable attenuation occurs within about 20 inches from the source. This conclusion, however, appears to be conservative since the available data is not extensive enough to allow for a thorough analysis.

Attenuation versus Distance from Shock Spectrum Data

Shock spectrum data available in Section II.A.5, II.A.6 and II.A.7 presents an alternate method of examining the shock level attenuation versus distance from the shock source as a function of frequency. The analysis performed here is conservatively based on the maximum shock level in each octave band.

Attenuation curves from shock spectrum data in Section II.A.5, II.A.6 and II.A.7 are respectively plotted on Figure II.A.3, II.A.4 and II.A.5 with the data from which Figure II.A.4 is generated presented on Table II.A.2. Reference should be made to Figure II.A.5.1, II.A.6.1 and II.A.7.1 to examine the structures under test.

It will be noted that the three sets of attenuation curves indicate the existence of peak levels at some frequencies. Cross-plotting of the data shows this occurring between 1600 and 3200 cps on Figure II.A.3 and II.A.4 and around 500 cps on Figure II.A.5. The existence of these peaks suggests a possible relationship with the acoustic wave velocity through the material or with the explosive burning velocity which would provide frequency responses of the order observed in these tests.

From the oscillogram data, it was suggested that possibly no appreciable attenuation occurred within 20 inches from the source. This seems to be generally supported by the curves of Figure II.A.3 and to some extent by those of Figure II.A.5. Figure II.A.4 however, indicates very good attenuation within 20 inches from the source. This lack of correlation cannot be explained readily within the scope of this report. Further analysis is needed to examine the effect of several parameters such as structural stiffness, shock conduction paths and vehicle normal mode interaction.

Application of Shock Attenuation Data

Although the shock attenuation characteristics determined from shock testing on one particular type of structure cannot be readily generalized to any other type, experience has shown that the results are applicable to reasonably similar structures.

However, the attenuation curve derived from oscillogram data can introduce considerable error when applied to shock spectrum data. This is shown by an example treated in Section II.A.2.2.4 of this report of which Figure II.A.2.9 is repeated here as Figure II.A.6. The attenuated curves (dotted lines) can be compared with shock spectrums derived from accelerometer data at the same stations. Significant discrepancies are evident.

Further discussion of this subject may be found in Section II.A.7.2.3 of this report.

II.8.A.4 Repeatability of Test Results

In Section II.A.7 the results of two identical tests are suitable for examining the repeatability of the shock environment. A statistical analysis is performed in Section III of this report. Shock spectrums from identical measurements of Tests 1 and 2 were summarized by 1/3 octave bands, then ratioed. The ratios, input into a statistical program, were used to determine a one sigma deviation expressed in DB as a function of frequency. Generally, the deviation was no greater than 4 DB in any 1/3 octave band.

II.A.9 CONCLUSION

The data presented in this section is generally reliable. It is not unduly affected by recording disturbances. In spite of this, the shock spectra, derived from accelerometers placed on the same primary structure, may exhibit significantly different characteristics. It is assumed that local resonances may affect the response read by the instrumentation.

Significant reduction in the shock level generated by a separation joint is possible with different types of joints. (The spring clamp type is the most effective). Small modifications to the standard joint were found to have some beneficial effect but could not achieve the intended level of attenuation.

The practical determination of the shock attenuation versus distance from the source is shown to be dependent on many factors. The data available was sufficient to establish a trend. This problem deserves considerably more attention in order to determine a prediction method suitable for environmental purpose.

Repeatability of the shock environment for two successive shocks on the same instrumented equipment indicates a one sigma deviation not greater than 4 DB in any 1/3 octave band.

TABLE II.A.1

DETERMINATION OF ATTENUATION WITH RESPECT TO STANDARD JOINT

	Standard Joint	Spring Clamp	Expander Tube	V-Band
Accelerometer 3	2100	190	130	570
Accelerometer 5	1300	150	215	480
Mean G	1700	170	172	525
Percent Level	100	10	10.1	31
Attenuation	0	90	89.9	69

The attenuation is calculated from mean of readings of accelerometers No. 3 and 5 placed six inches from the shock source.

Data from Section II.A.4 - Table II.A.4.3

TABLE II.A. 2

COMPARISON OF ATTENUATION PROVIDED BY THE VARIOUS SEPARATION JOINTS CONSIDERED IN THIS STUDY

Section	Report No.	JOINT No.	Configuration Description	Percent Attenuation
II.A.3	768	1	Standard (10 GR MDF)	0 (Basis)
		2	Fwd tang removed	34
		3	Fwd tang removed - back up stiffener	56
		4	Standard - 5 GR FLSC	40
		5	Gas shield added	47
		6	Skin pre-cut	41
		7	3/16 inch separation between joint and ring	63
		8	Masking tape over primacord	No data
II.A.4	790	2	Spring clamp	90
		3	Expander tube	89.9
		4	V Band	69
II.A.5	1080	1	Hoop tension strap and cutters	70

TABLE [illegible]

[illegible] LEVELS [illegible] PEAK VALUES

[illegible] SECTION [illegible]

[illegible] PEAK [illegible]	[illegible] ← SPECTRAL FLAME [illegible] 15	[illegible] & 158	[illegible] 156
	65	3	
.25	122		
	223		
2	2		168
2	196	33	
3	333		
	270	52	876
	3.8	30	
	2		12
	42	80	2.82
	11		3016
			14.2
			1198
	459		795
	055	73	1019
	05	09	
	450	019	
	52	600	1652
	2	850	1778
	43	9	1
	2		

G LEVELS ARE ENVELOPES OF POSITIVE PEAKS.

[illegible] DATA IS PLOTTED ON FIGURE NO. II.A.1

TABLE II.A.4

SHOCK SPECTRUM PEAKS IN EACH OCTAVE BAND

Accer. No.	Shock	D* inches	Direction	200/400	400/800	800/1600	1600/3200	3200/6400
2	1	30	R	530	1000	980	1700	1700
3	1	20.5	X	105	200	500	750	800
9	1	20.5	R	220	390	370	450	270
11	1	76	X	62	1020	1020	380	300
12	1	76	R	50	68	260	520	420
14	1	- 113	Y	28	53	90	190	250
1	2	30	X	180	1050	3500	4800	4800
2	2	28	X	240	1700	1700	2200	2600
3	2	2	Z	1015	8300	8600	7900	10000
4	2	2	X	960	2300	2500	5400	7800
5	2	2	Y	1000	8000	8000	6700	6900
6	2	30	X	59	440	610	1300	1700
7	2	30	R	95	770	2800	2700	1700
8	2	20.5	X	29	78	170	530	620
9	2	20.5	R	39	180	180	360	280
10	2	53	X	17	185	250	780	780
13	2	- 113	X	62	400	400	270	580

* D = distance to shock source - inches

Reference: shock spectrum data from Section II.A.6.
This data is plotted on Figure II.A.4.

REF: SECTIONS II.A.3, II.A.4, II.A.5

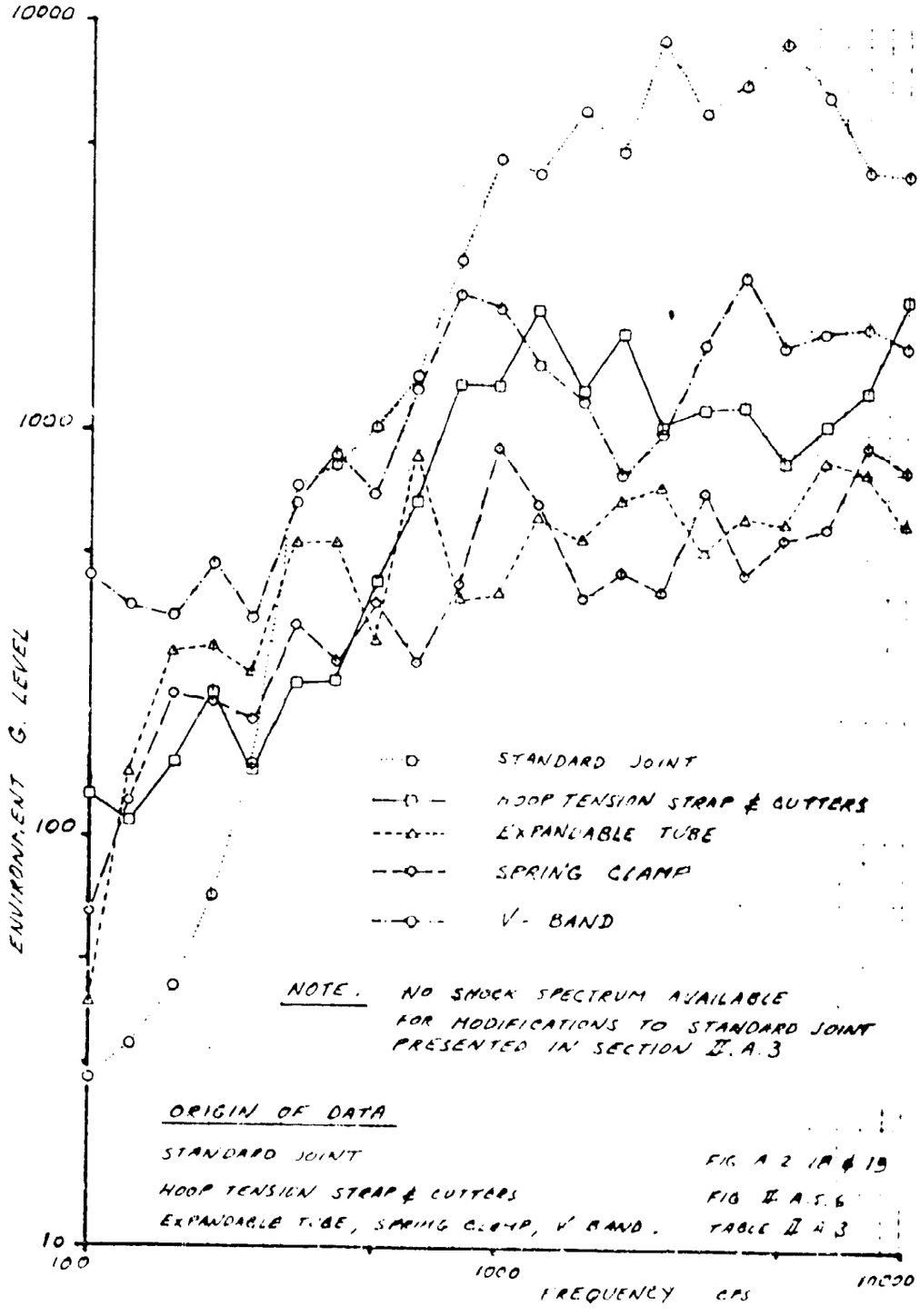

Figure II.A.1 COMPARISON OF HOOP LEVELS GENERATED BY STANDARD JOINT AND FOUR OTHER TYPES OF JOINTS

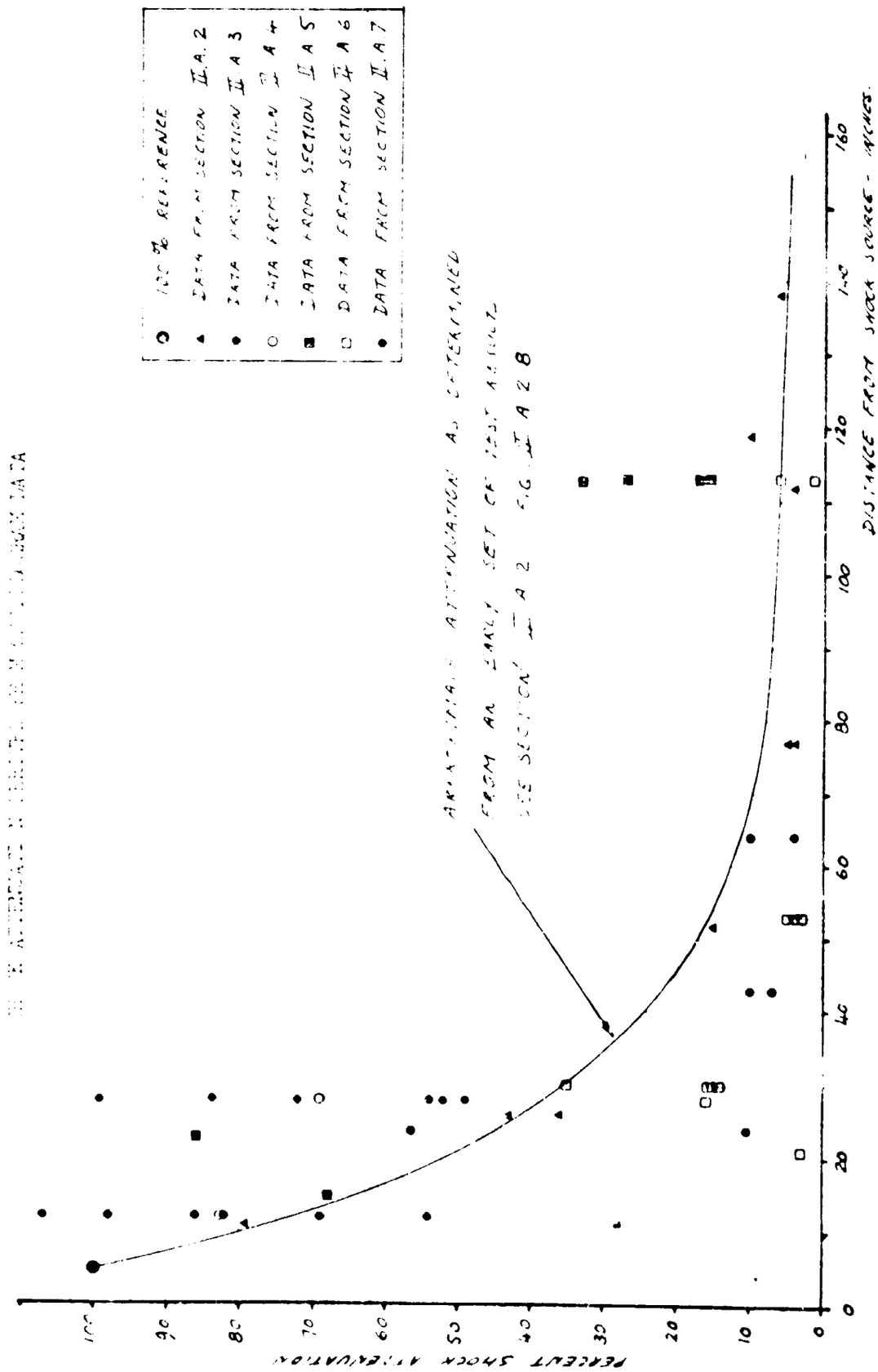

Figure II.A.2 SHOCK ATTENUATION VERSUS DISTANCE FROM SHOCK SOURCE

REF: SHOCK SPECTRUM DATA FROM SECTION II.A.5

Data based on peak values in each octave band as read on shock spectrum.

Q = 25

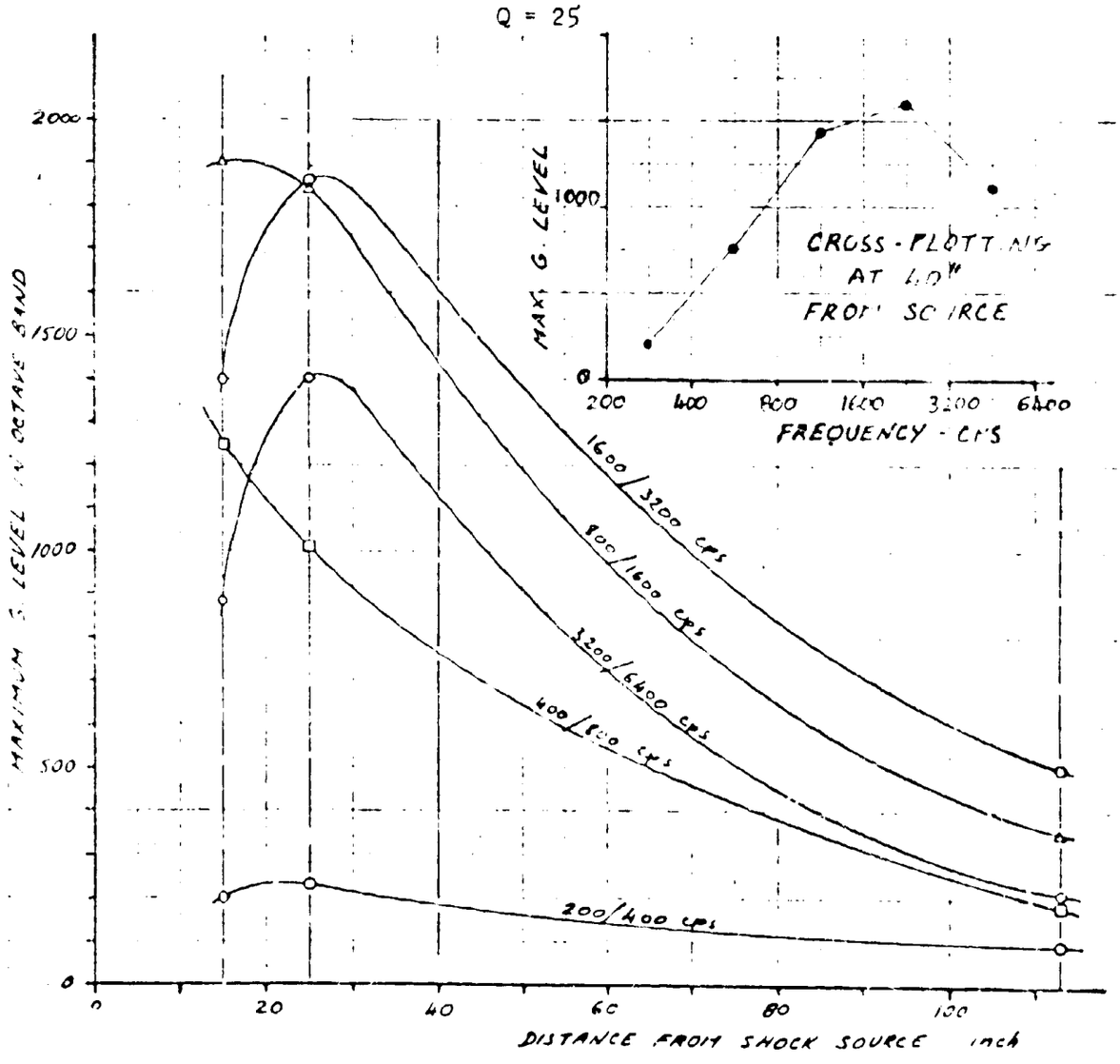

Figure II.A.3 TREND OF ATTENUATION VERSUS DISTANCE FROM SHOCK SOURCE FOR EACH OCTAVE BAND

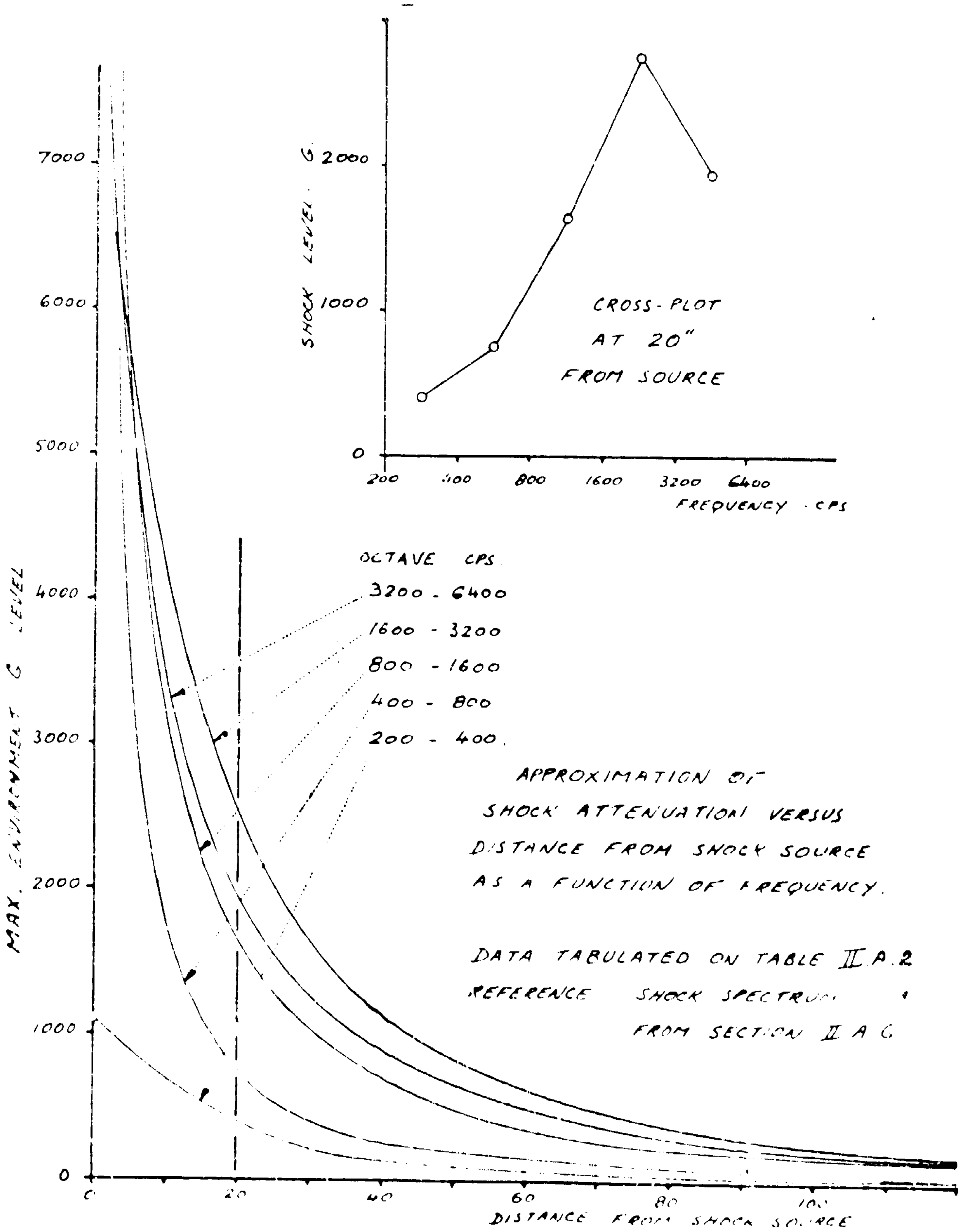

Figure II.A.1 APPROXIMATION OF SHOCK ATTENUATION VERSUS DISTANCE FROM SHOCK SOURCE AS A FUNCTION OF FREQUENCY

REF: SECTION II.A.7 - FIGURE II.A.7.10

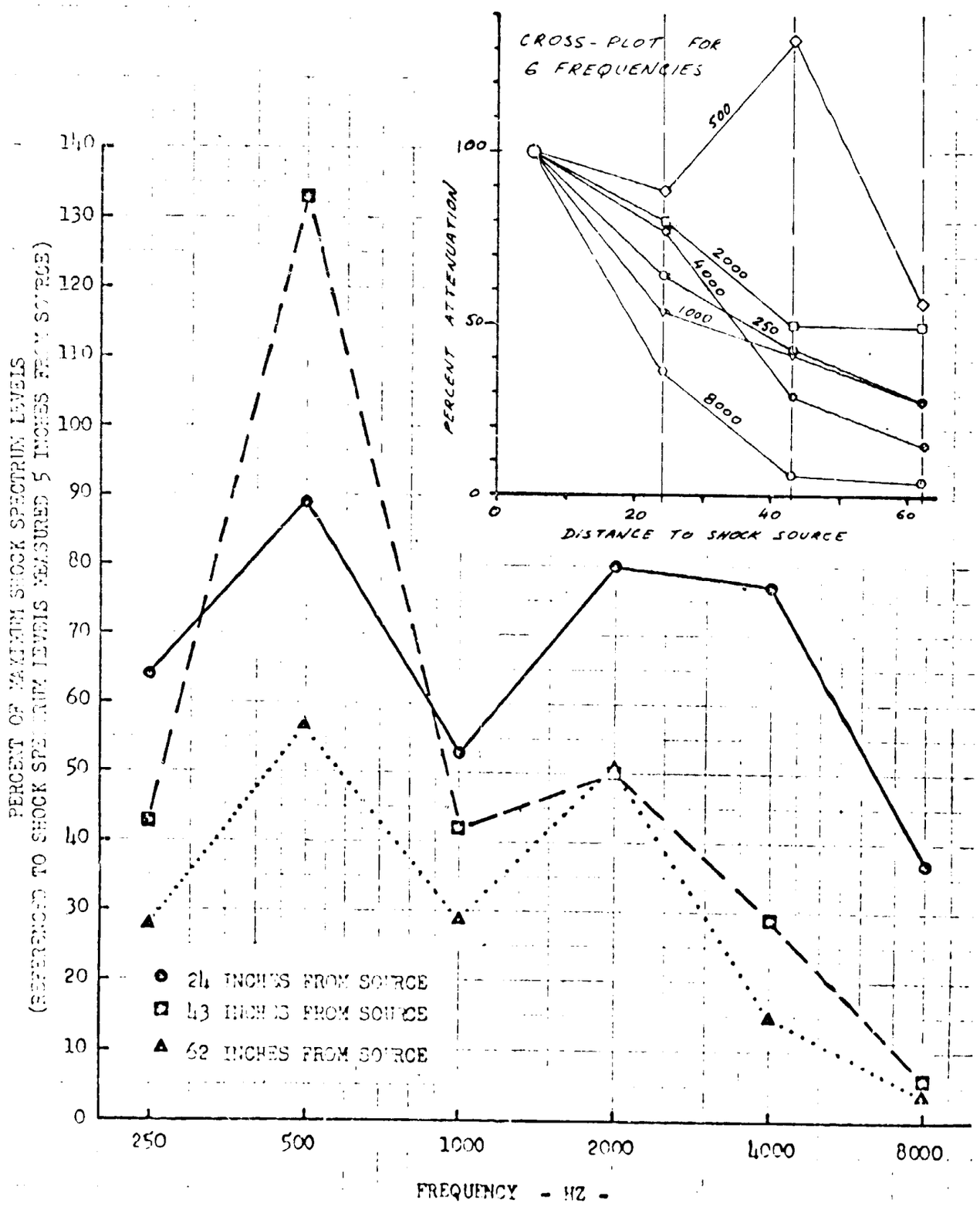

Figure II.A.5 ATTENUATION VERSUS FREQUENCY ALONG PRIMARY STRUCTURE

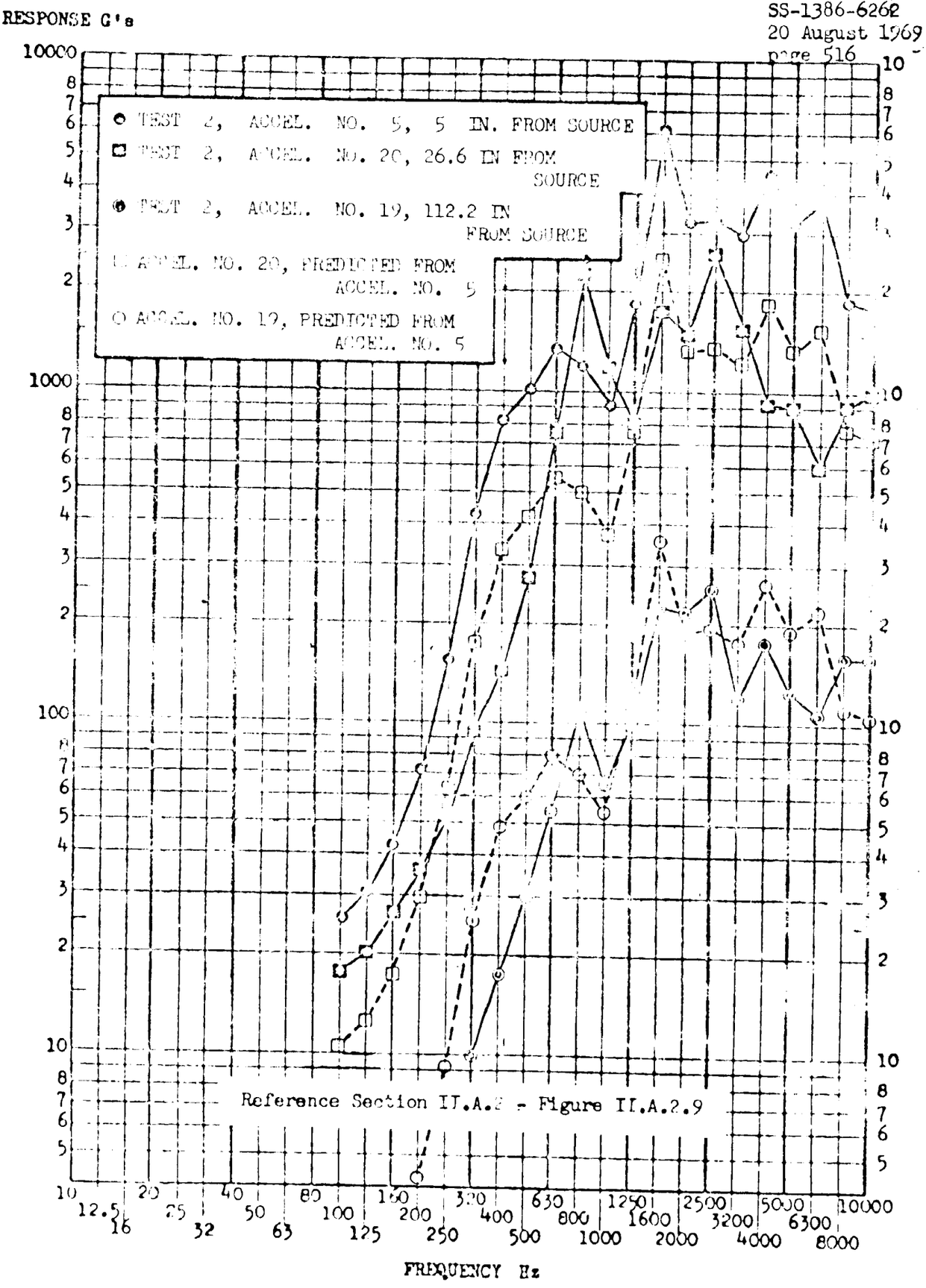

Figure II.A.6 EXAMPLE OF APPLICATION OF PEAK G SHOCK ATTENUATION TO SHOCK SPECTRUM

SECTION II.B

SUBJECT:

FAIRING DEPLOYMENT MECHANISMS

REPORT NO. 794, 867, 1353

SECTION II.B

SUMMARY

This section contains three reports (Nos. 794, 867 and 1353) covering a series of tests performed to reduce the shock environment from the fairing deployment mechanism activated by pyrotechnic devices such as pinpushers, pinpullers, and explosive nuts.

The first fairing deployment mechanism which was developed made use of two pin pushers mounted normal to the vehicle skin. Firing of 4 squibs (4 grains of explosive) expels the fairing away from the vehicle. With this relatively high quantity of explosive, combined with the general configuration arrangement, the pyrotechnic shock environment was considered unnecessarily high.

Report No. 794 covers various attempts at isolating shock source without altering the basic mechanism. Shock reduction by as much as 29 percent were shown possible. These results were not considered significant enough to incorporate into the design.

Report No. 867 covers a redesign of the fairing deployment mechanism where the pin pushers are eliminated and replaced by a spring loaded device operated in conjuction with a fall-away hinge. The release of the spring is obtained by firing a pin puller which frees the retaining rod. Reduction of the shock level is obtained by a combination of the following items:

1. Reduction by half of the quantity of explosive.
2. Using a spring as the primary force for ejecting the fairing.
3. Isolating the pinpuller with rubber mounts.

This system provides an average shock environment reduction of the order of 50 percent over the basic system.

Report No. 1353 covers a further improvement to the mechanism since obviously the pin puller expands far more energy than needed to free the retaining rod. The pin puller is therefore replaced by an explosive nut which achieves the same results without moving parts. This new deployment mechanism provides an average shock environment reduction of 95 percent over the basic system.

SECTION II.B

SUMMARY (Cont.)

Additional information and data about pin actuators are presented in Section II.C of this report.

TABLE OF CONTENTS

SECTION II.B

SECTION NO. II.B.1

REPORT NO. 794

SUBJECT:

PIN-PUSHER FAIRING DEPLOYMENT MECHANISM

SHOCK ALLEVIATION TESTS

SECTION II.B.1

SUMMARY

The standard fairing deployment mechanism makes use of two pin pushers each activated by two squibs. The force developed by the pin pushers is used to propel the fairing away from the vehicle. Since the energy generated by squib firing is much greater than needed to expel the fairing, a high shock environment level is created. A series of tests was carried out on a forward equipment rack to try various types of isolators in an attempt to reduce the shock level generated by the pin pushers. Several models of internal bumpers, energy absorbers and isolators were designed and tested.

A maximum reduction of about 29 percent was obtained with the combination of internal energy absorber and external isolator of test No. 13. Although some other modifications showed comparable but slightly lower reduction, there was no indication that reduction significantly greater than 29 percent could be obtained with this type of shock reduction device.

The data indicated that the shock environment created by the pin pushers was fairly repeatable.

TABLE OF CONTENTS

SECTION II.B.1

LIST OF TABLES

SECTION II.B.1

LIST OF FIGURES

SECTION II.B.1

Figures

OSCILLOGRAMS

II.B.1.1 INTRODUCTION

To reduce the shock environment in the forward equipment rack which was caused by the jettison of the horizon sensor fairings, several methods of shock reduction were tested. Essentially, the methods of reduction consisted of absorbing as much shock energy as possible inside the pin pushers and in installing elastic isolators at the pin-pusher structure interface.

The tests reported here were carried out with a forward equipment rack in order to simulate flight conditions more closely. The general test arrangement is hown in Figure II.B.1.1. The details of pin-pusher modification and installation are shown in Figures II.B.1.2 and II.B.1.3.

II.B.1.2 DISCUSSION AND ANALYSIS

II.B.1.2.1 Test Configuration and Instrumentation

An actual forward equipment rack containing all internal structure, less no equipment, was used for this test. Figure II.B.1.1 shows the general arrangement of the test specimen with locations of all accelerometers (Table II.B.1.1), and a schematic of the pin-pusher fairing deployment mechanism.

Figure II.B.1.2 shows a cross section of the pin pusher and a series of six different types of piston energy absorbing devices which were used in the tests.

Figure II.B.1.3 shows four types of hard mounted and isolated pin-pusher installation.

A first series of tests was carried out with the fairing mounted on a flat plate base (test 1 through 7). These tests exhibited some anomalies which made them unrelated to the vehicle conditions. This report covers only the results from tests 8 to 17 which are summarized on Table II.B.1.2. Three tests were carried out for each configuration.

Only oscillograms are available from this test. They are presented in Figures II.B.1.4 to II.B.1.9.

II.B.1.2.2 Technical Discussion

The internal modification to the pin-pusher assembly consisted of installing various types of energy absorbing washers on the back side of the piston in order to decelerate it at a lower rate and eliminate the metal to metal shock originating from striking the stop (see Figure II.B.1.2).

The external pin-pusher installation modifications were intended to reduce the shock level transmitted to the adjacent structure by shock isolation through either an impedance mismatch or energy absorption (see Figure II.B.1.3).

Internal and external modifications were tested either singly or in combination. Details of each configuration tested are given in Table II.B.1.3 for tests 8 through 17. Test 8 was carried out with the pin pushers rigidly mounted in order to serve as a basis for comparison with the subsequent tests.

II.B.1.2.3 Analysis

The data obtained from each set of three firings showed fair repeatability. Figures II.B.1.4 to II.B.1.9 show the oscillograms obtained from the second test series.

The peak g levels for each test at all accelerometer locations are presented in Table II.B.1.4 and each test configuration is rated in Table II.B.1.3 according to the average peak acceleration noted in Table II.B.1.5. The lowest shock level recorded in any one test was given the rating of 1. Higher recorded levels were given ratings greater than 1, according to their magnitude.

Oscillograms from accelerometers 5 and 6 show a strong vibration occurring in the tangential direction at about 500 cps. This vibration has been identified as the second plate mode of the shell structure, excited by the fairing reaction to the pyrotechnic event.

Shock spectrum data was not found necessary for this study because examination of the oscillograph records indicated that no major differences in amplitude and frequency content were present in any of the configurations under test.

In considering the results of this series of tests, it was concluded that a 29 percent maximum possible improvement did not warrant further analysis and development since it is too close to the data scatter. This deployment mechanism is therefore inadequate and must be redesigned along other lines.

In retrospect, the failure of this study in reducing the shock environment is due to the fact that the energy absorption systems did not allow for enough travel distance to dissipate the energy of the moving components.

II.B.1.3 CONCLUSION

Based on the limited analysis performed on the test data, the modifications incorporated in the test 13 series provided the best shock reduction (about 29 percent). The test configurations, listed in order of decreased rating are as follows: Test No. 13, 16, 15, 17, 14, 11, 12, 9 and 10.

Repeatability of the shock for each set of three firings was fair. It does not appear that a pin-pusher shock environment reduction much greater than 29 percent could be achieved from the configuration modifications investigated in this series of tests. These results are not considered significant enough to warrant a further stydy of these types of isolation. A new fairing deployment concept is required to provide a more significant reduction of the shock environment.

TABLE II.B.1.1

ACCELEROMETERS AND LOCATIONS

Accelerometer Number	Direction	Distance to Shock Source (inches)	Accelerometer Type
1	X	12	ENDEVCO 2225
2	R	12	ENDEVCO 2225
3	X	12	ENDEVCO 2225
4	X	12	ENDEVCO 2225
5	T	12	ENDEVCO 2225
6	T	14	ENDEVCO 2225

TABLE II.B.1.2

SUMMARY OF TESTS

Test No.	Configuration	Explosive Size	Test Purpose	Shock Isolation
8	1	4 squibs	Shock Reduction	none
9	2	4 squibs	Shock Reduction	yes
10	3	4 squibs	Shock Reduction	yes
11	4	4 squibs	Shock Reduction	yes
12	5	4 squibs	Shock Reduction	yes
13	6	4 squibs	Shock Reduction	yes
14	7	4 squibs	Shock Reduction	yes
15	8	4 squibs	Shock Reduction	yes
16	9	4 squibs	Shock Reduction	yes
17	10	4 squibs	Shock Reduction	yes

TABLE II.B.1.3

TEST DESCRIPTION AND RESULTS

Test Series #	Description of Pin Pusher Installation Modification	Rating
8	None - Control shots	-
9	"O"-ring bumper in pin pushers	8
10	No internal modification Rubber grommet mounting	9
11	"O"-ring bumper in pin pusher Rubber Grommet mounting	6
12	3 "O"-ring bumpers in pin pushers Rubber grommet mounting	7
13	"O"-ring bumper in pin pushers Rubber grommet mounting H/S panel gasket	1*
14	Lead conical washers in pin pushers Rubber grommet mounting	5
15	No internal modifications Rubber grommet mounting H/S panel rubber gasket	3
16	No internal modifications Laminated grommet mounting	2
17	Modified crush washer in pin pusher Laminated grommet mounting	4

* Lowest shock level

TABLE II.B.1.4

PEAK G LEVELS O TO PEAK

Test No.	Accelerometer No.					
	1	2	3	4	5	6
8-1	102	278	268	258	992	1011
8-2	152	254	220	206	831	560
8-3	102	229	244	178	1014	612
9-1	127	226	244	253	780	739
9-2	107	212	146	240	1060	677
9-3	148	179	269	319	1027	677
10-1	134	258	316	249	718	514
10-2	128	215	335	290	688	930
10-3	120	198	462	248	920	600
11-1	104	224	362	216	650	390
11-2	129	174	238	300	678	420
11-3	104	174	231	169	1017	604
12-1	159	242	476	332	606	286
12-2	103	146	446	256	860	524
12-3	175	172	314	257	765	438
13-1	69	163	108	124	465	240
13-2	129	163	177	297	675	266
13-3	84	171	131	188	984	706
14-1	122	145	207	239	800	328
14-2	100	173	147	231	1080	663
14-3	85	172	192	181	687	309
15-1	92	155	123	413	658	780
15-2	93	146	154	222	780	448
15-3	92	155	169	294	582	312
16-1	84	86	154	164	653	500
16-2	111	168	220	274	964	482
16-3	91	130	112	151	815	596
17-1	142	130	235	358	603	420
17-2	141	158	183	255	668	374
17-3	122	151	176	272	623	443

TABLE II.B.1.5

AVERAGE "G"'s 0 TO PEAK

Test No.	Accelerometer No.					
	1	2	3	4	5	6
8	119	256	244	214	945	728
9	127	195	207	280	1043	677
10	137	224	372	262	776	682
11	112	190	277	228	783	472
12	146	187	412	281	744	416
13	94	165	139	203	710	404
14	102	163	182	217	856	433
15	92	152	148	310	674	514
16	95	128	162	196	810	526
17	135	146	198	295	632	412

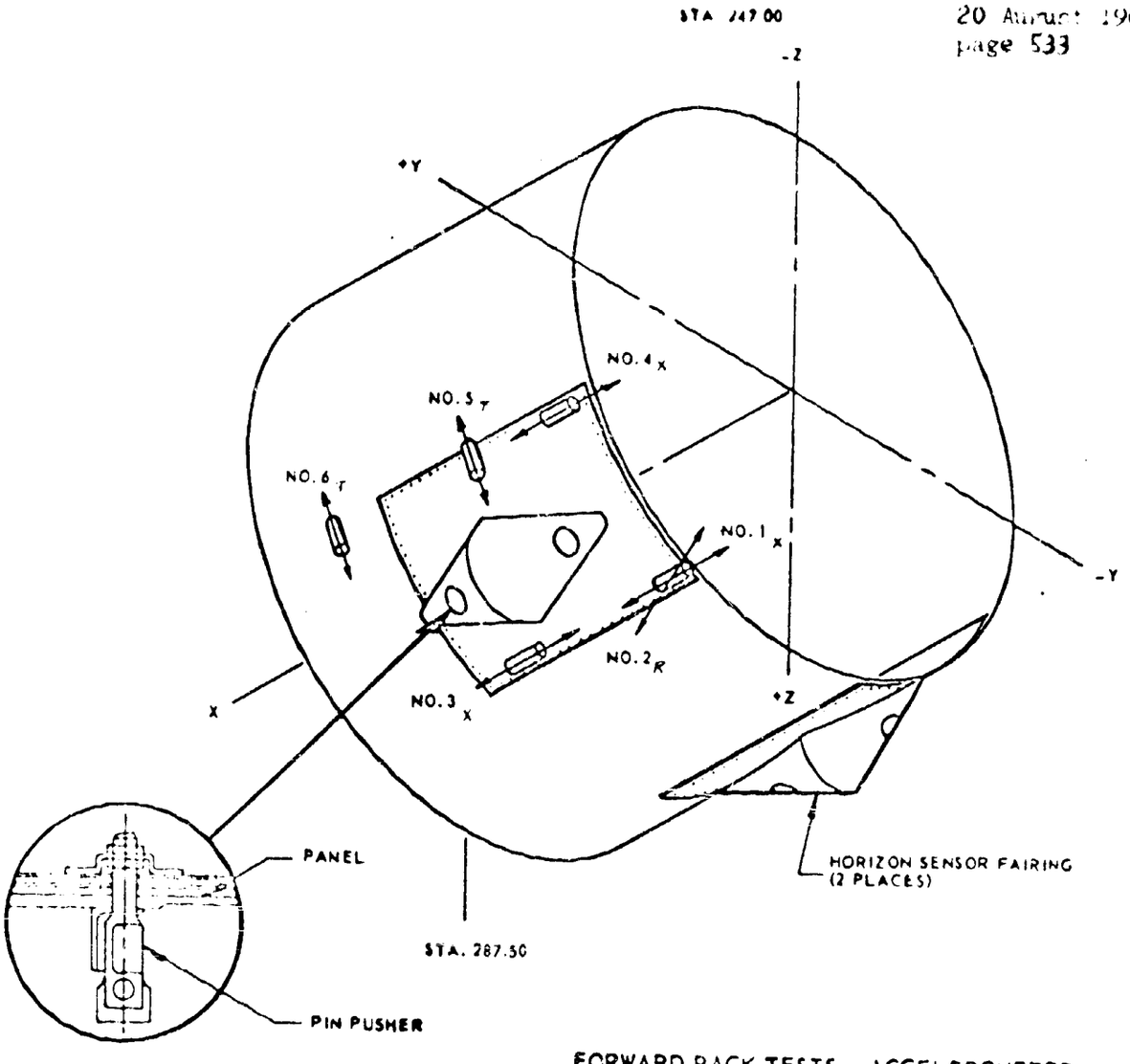

FORWARD RACK TESTS – ACCELEROMETER LOCATIONS AND SENSITIVE AXES

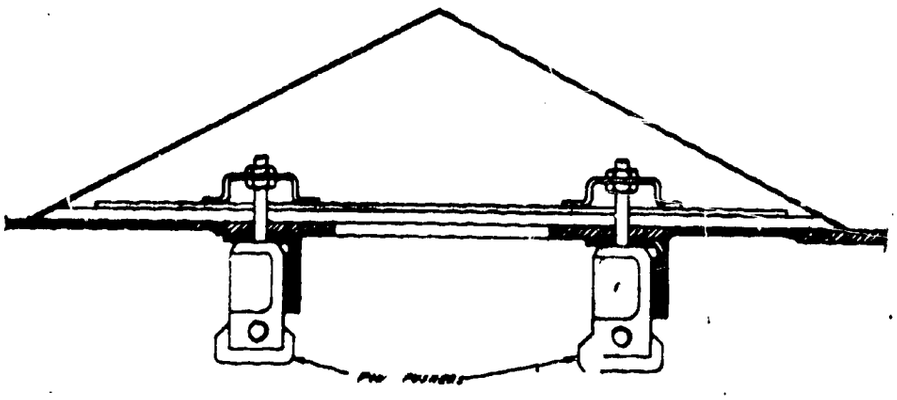

Figure II.B.1.1 TEST CONFIGURATION AND INSTRUMENTATION

TEST NO.	INTERNAL STOP CONFIGURATION	
1,	NONE	
2, 9, 11, & 13	"O" RING	
3, 4, 5	WASHER	
3A, 4A, 5A	TAPERED WASHER	
12	3 "O" RINGS	
14	CONICAL WASHER	
17	MODIFIED CONICAL WASHER	

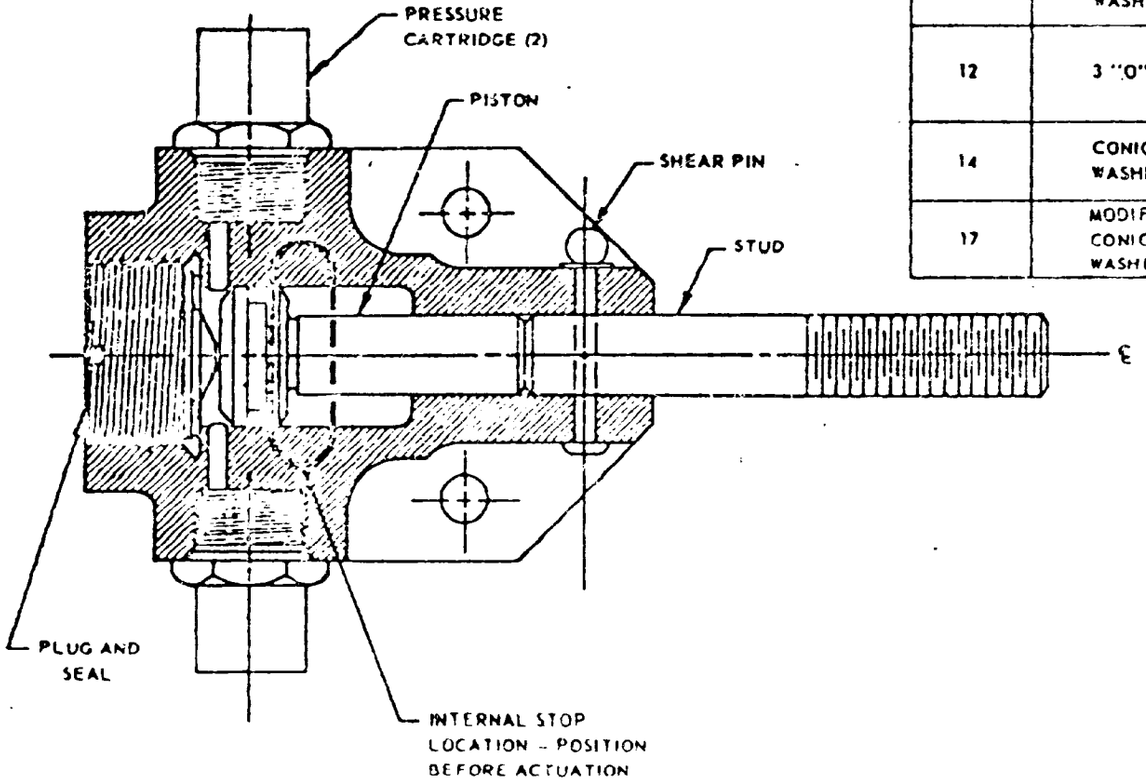

Figure II.B.1.2 PIN PUSHER GEOMETRY AND INTERNAL MODIFICATIONS

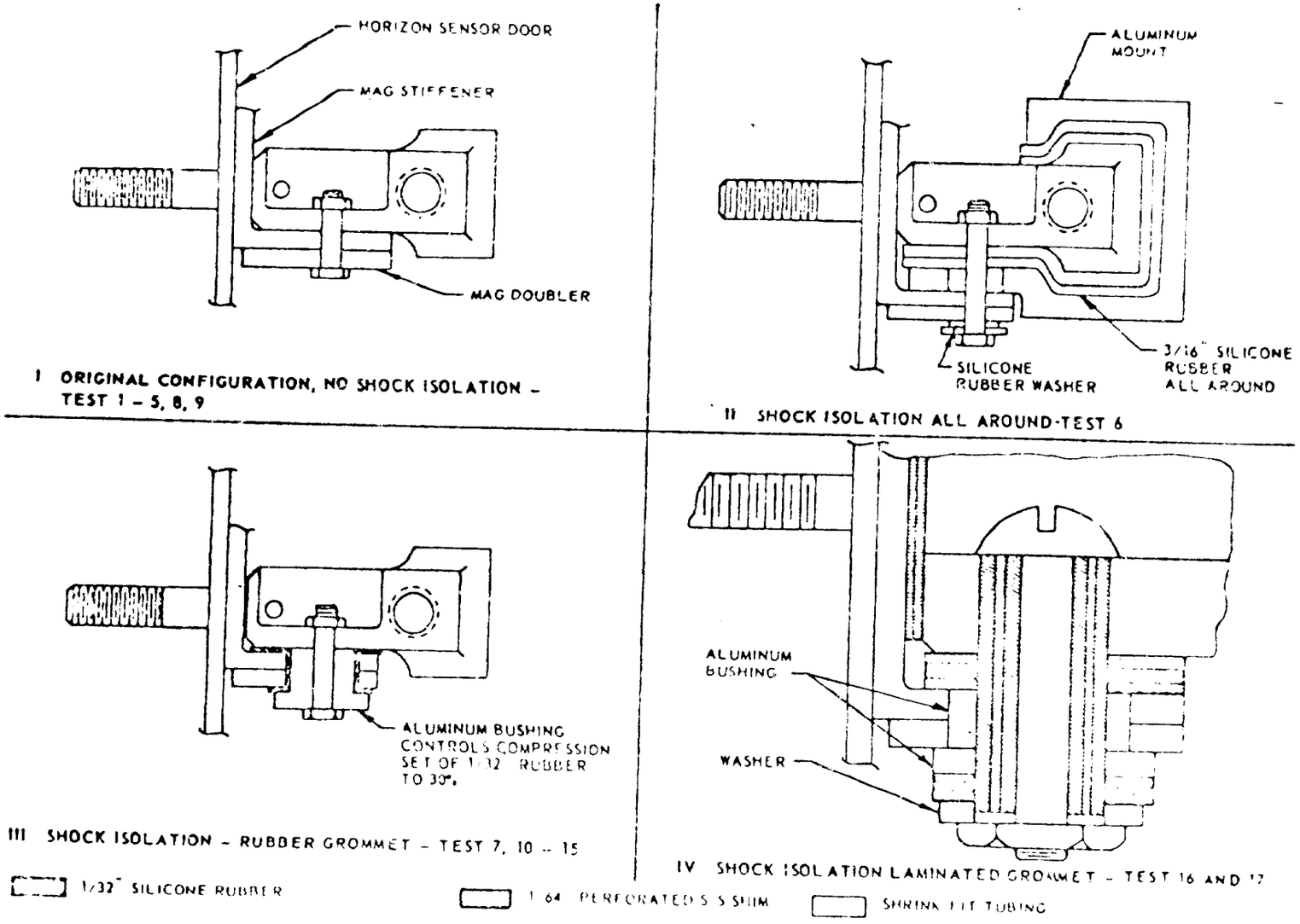

Figure II.B.1.3 PIN PUSHER SHOCK ISOLATORS

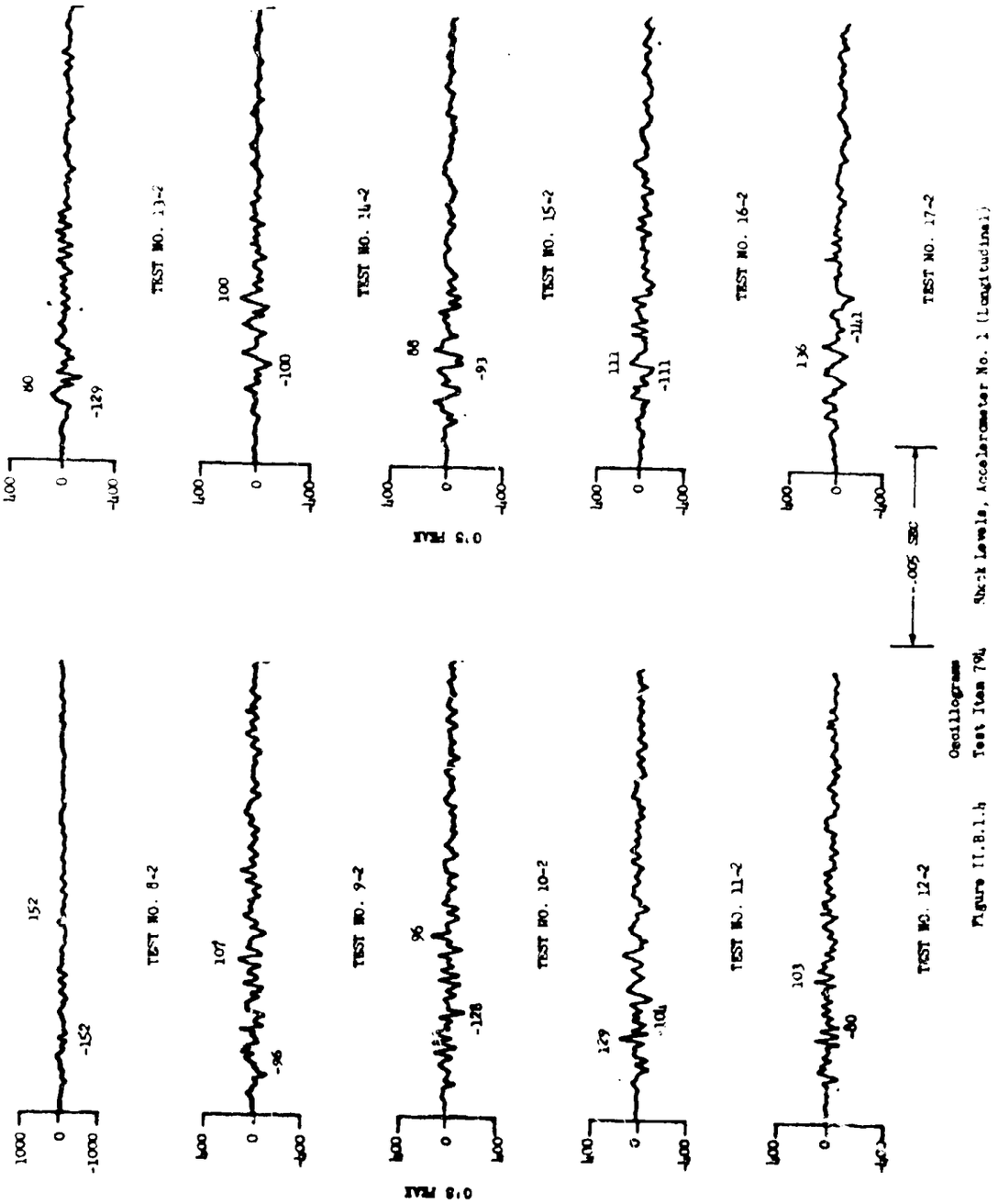

Figure II.B.1.h Test Item 7% Oscillograms Shock Levels, Accelerometer No. 2 (Longitudinal)

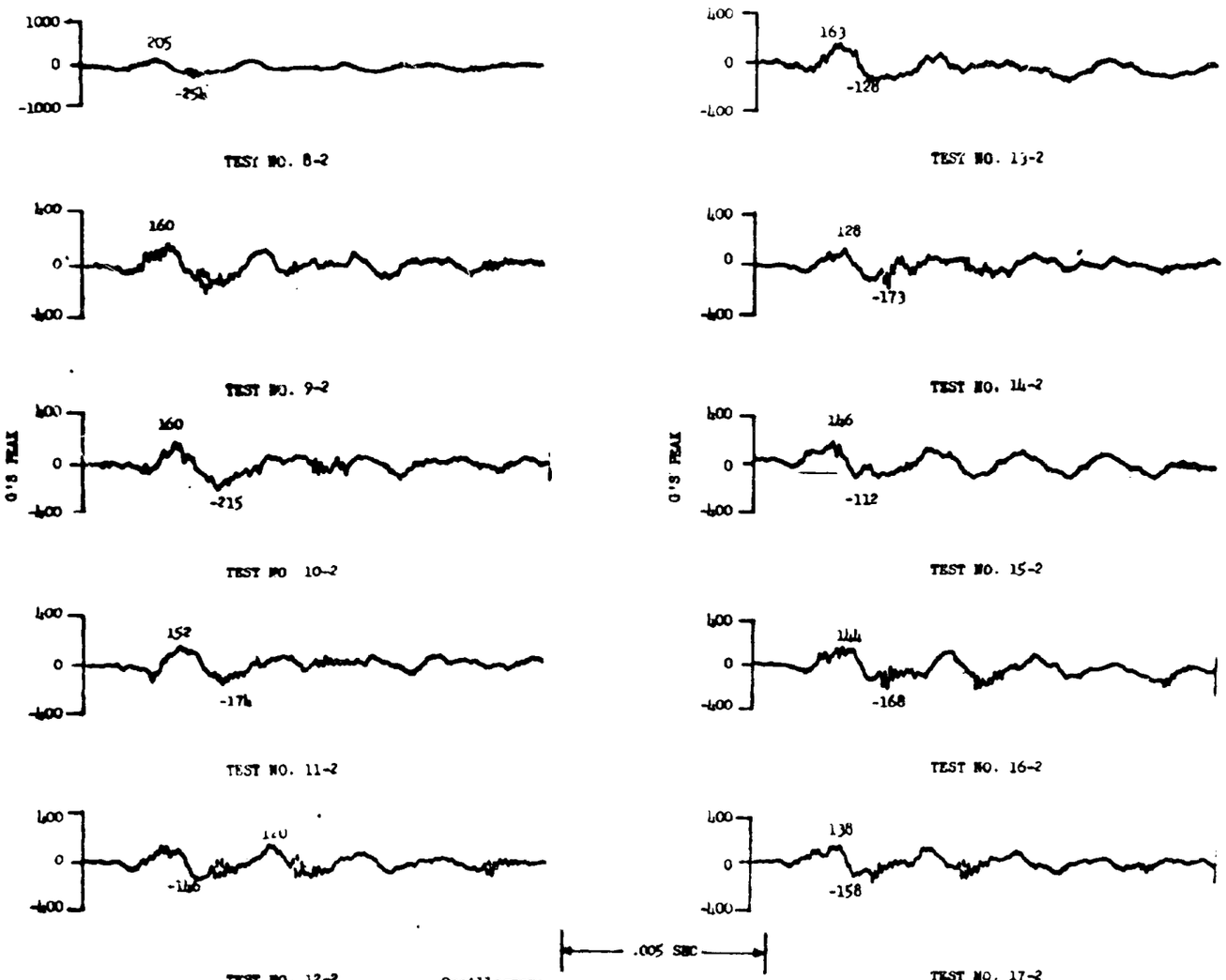

Figure II.B.1.5 Oscillograms Test Item 794 Shock Levels Accelerometer No. 2 (Radial)

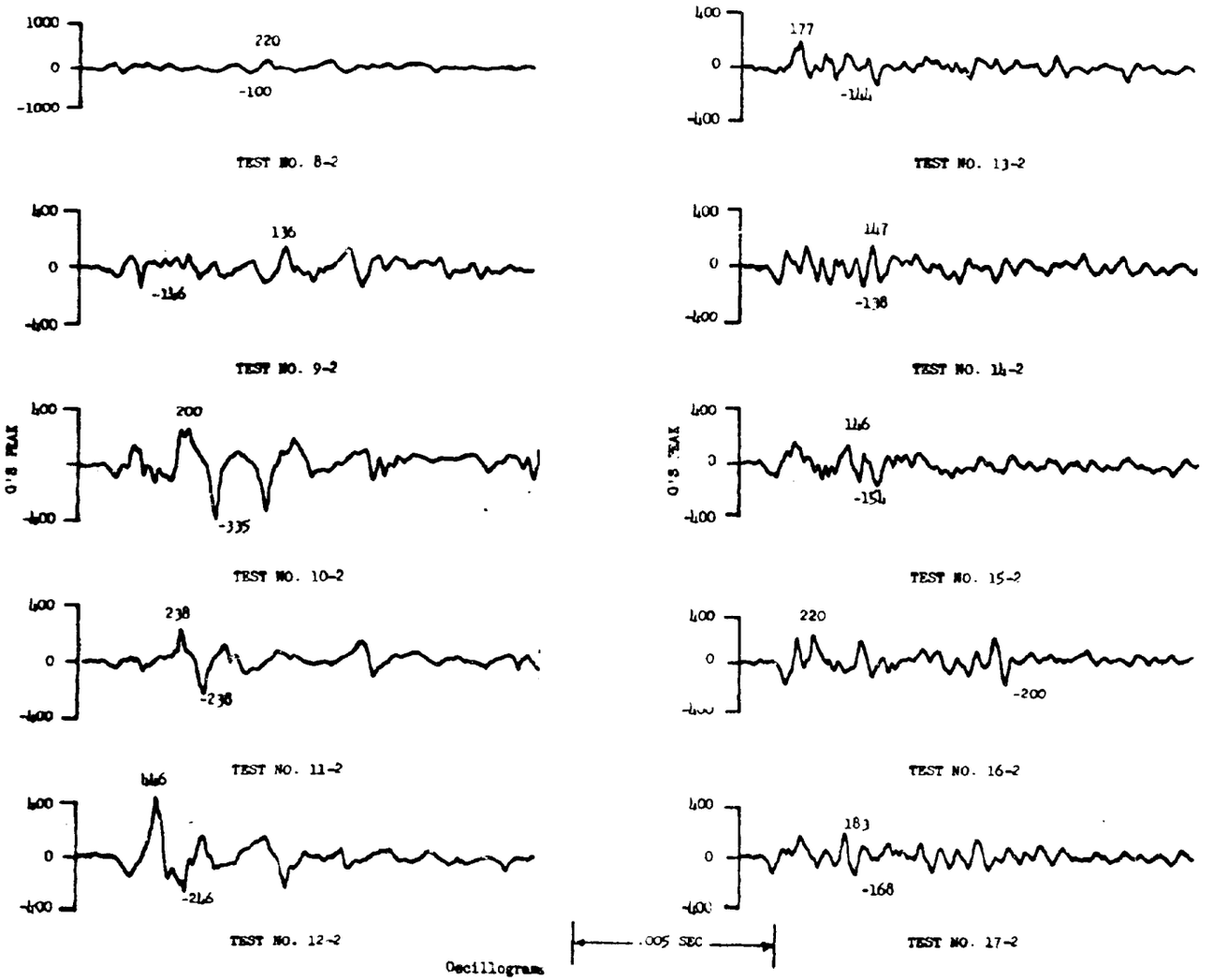

Oscillogram

Figure II.B.1.6 Test Item 794 Shock Levels, Accelerometer No. 3 (Longitudinal)

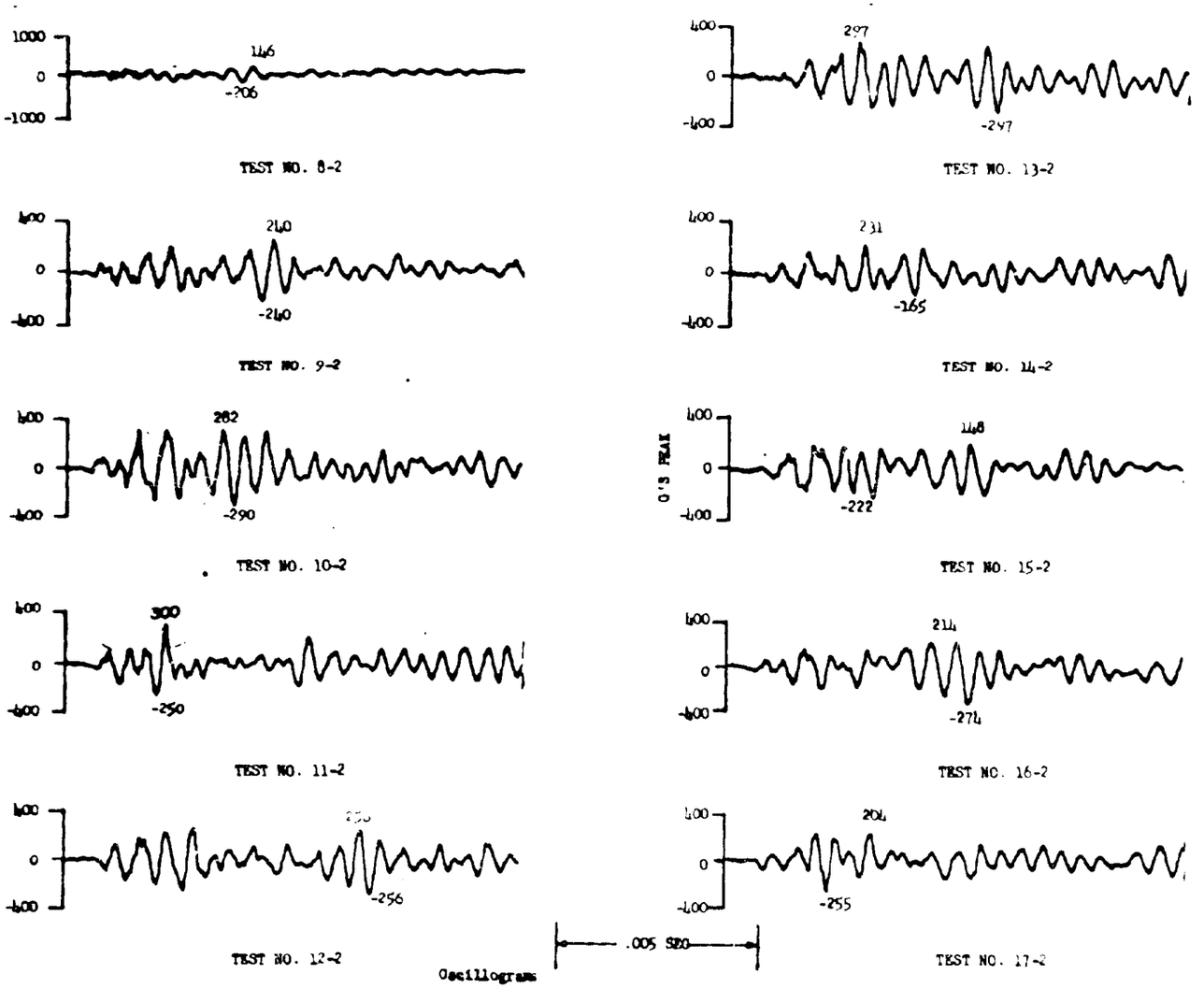

Figure II.B.1.7 Test Item 754 Shock Levels, Accelerometer No. 4 (Longitudinal)

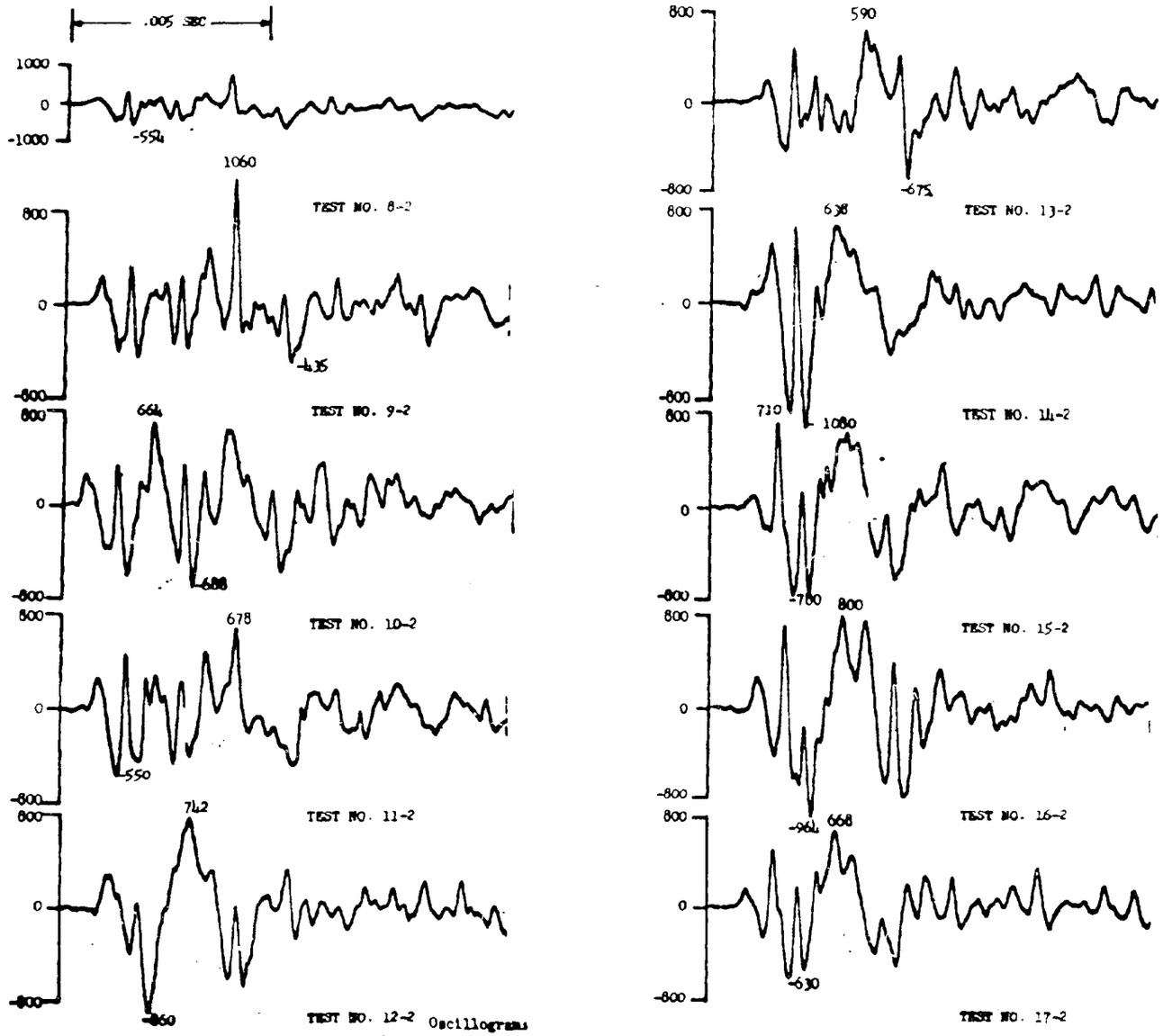

Figure II.B 1.8 Oscillograms Test Item 794 Shock Levels, Accelerometer No. 5 (Tangential)

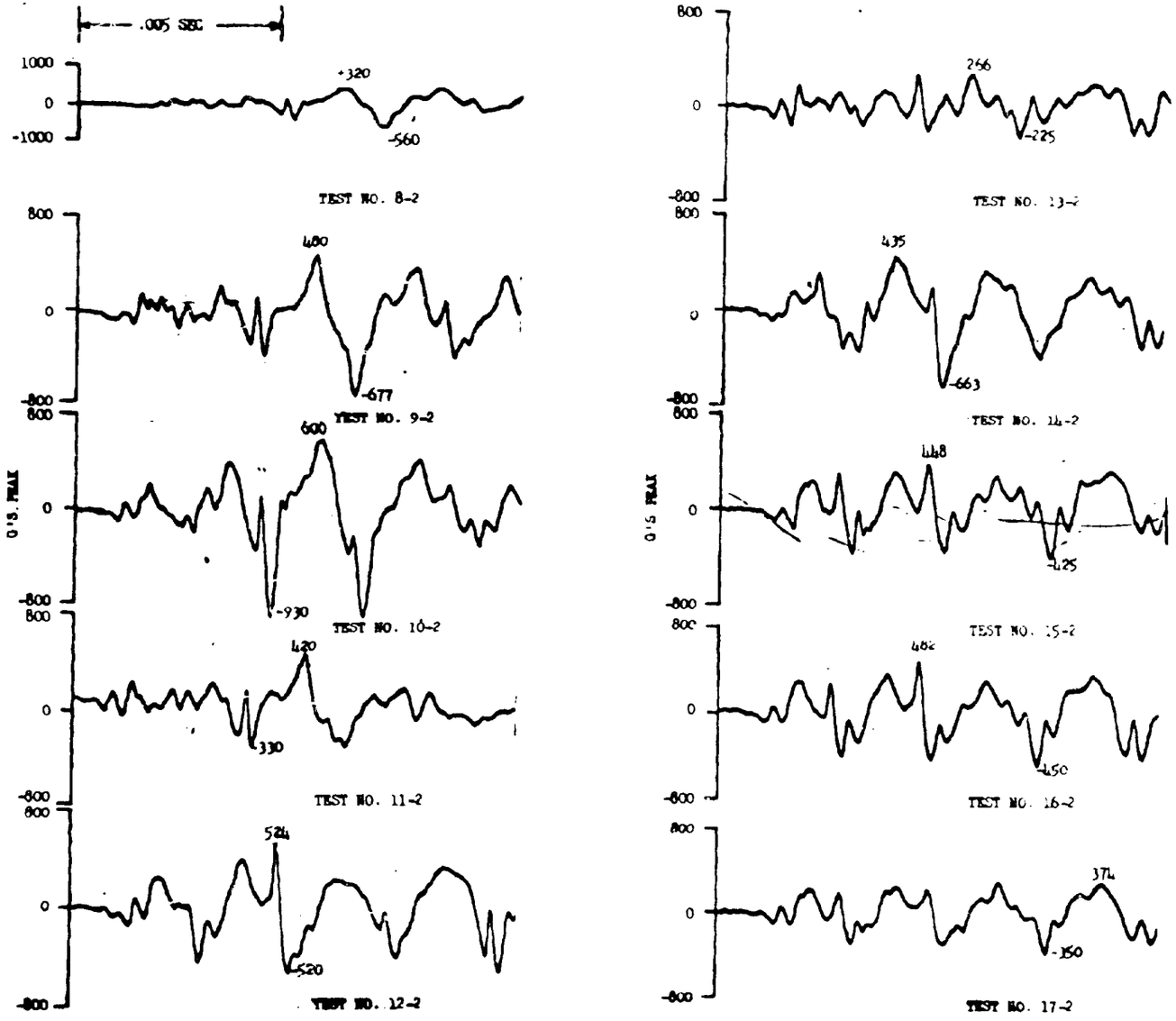

Figure II.B.1.9 Oscillograms Test Item 79L Shock Levels, Accelerometer No. 6 (Tangential)

SECTION NO. II.B.2

REPORT NO. 867

SUBJECT:

FAIRING JETTISON COMPARISON OF STANDARD PIN-PUSHER SYSTEM WITH A PIN-PULLER/SPRING/FALL-AWAY HINGE SYSTEM

SECTION II.B.2

SUMMARY

The test results presented in this section provide a comparison between two fairing deployment mechanisms which were tested on an actual equipment rack frame.

The standard mechanism makes use of two pin pushers mounted normal to the skin in such a manner that each fairing is expelled by the force developed by the four squibs. A high level environment is created by this system which makes use of eight squibs (two fairings) to activate the pin pushers.

Mechanism No. 2 was designed to reduce the pyrotechnic environment through use of one pin puller per fairing. The pin puller is used to trigger a cocked spring whose release, in combination with fall-away hinges, provides the force required to expel the fairing. The advantages of this system over the standard are:

1. Reduction by half of the quantity of explosive.
2. The primary force used for expelling each fairing is provided by a spring. (The force is very low in comparison to pin pushers.)
3. The pin pullers are isolated by rubber mounts and their attachment is in the plane of the skin rather than normal to it.

Four pyrotechnic tests were carried out, deploying fairing A and B separately for each configuration.

The test results indicate a significant reduction of the shock overall g level which drops to approximately one-half of its value with the standard mechanism.

An analysis has been carried out to compare shock spectrum and oscillogram data from deployment of A and B fairings. In general, mechanism No. 2 provides large level reduction for frequencies up to 1000 cps, while at high frequencies, an average reduction of the order to 25 percent is achieved. The pin puller and spring mechanism is therefore a significant improvement over the standard pin-puller mechanism.

TABLE OF CONTENTS

SECTION II.B.2

LIST OF TABLES

SECTION II.B.2

LIST OF FIGURES

SECTION II.B.2

LIST OF FIGURES

SECTION II.B.2

LIST OF FIGURES

SECTION II.B.2

LIST OF FIGURES

SECTION II.B.2

II.B.2.1 INTRODUCTION

A series of four fairing jettison tests were carried out on a forward equipment rack with two different deployment mechanisms. The instrumentation which consisted of 12 accelerometers remained unchanged throughout the tests. The two fairings were jettisoned separately for each configuration of the deployment mechanism.

The forward equipment rack structure is shown on Figure II.B.2.1 together with fairing and accelerometer locations. The fairing deployment mechanisms are shown on Figure II.B.2.2.

The standard deployment mechanism consists of two pin-pushers which "blast" the fairing away from the vehicle. The new mechanism uses a pin-puller to release a coked spring which in turn sends the fairing tumbling away from the vehicle.

II.B.2.2 DISCUSSION AND ANALYSIS

II.B.2.2.1 Test Configuration and Instrumentation

An actual forward equipment rack containing all internal structure but no equipment was used for this test.

Figure II.B.2.1 shows the arrangement of the test specimen with location of all accelerometers. Figure II.B.2.2 shows the two fairing release configurations. Configuration No. 1 (standard) makes use of two pin pushers per fairing. The fairing is thus expelled normally to the skin by the force developed by the explosion of the four squibs. Configuration No. 2 consists of a rubber mounted pin puller which releases the deployment mechanism upon firing two squibs. The orientation of the pin puller was selected to reduce as much as possible the second normal plate mode of the shell.

The instrumentation comprises 12 accelerometers as described on Table II.B.2.1, installed at various points of the structure as shown on Figure II.B.2.1 in order to provide a general mapping of the shock environment.

The test procedure as described on Table II.B.2.2, consisted of jettisoning one fairing at a time for each deployment mechanism configuration, with all accelerometers recording data.

Shock spectrum and oscillograms are presented in Figure II.B.2.5 to II.B.2.63.

II.B.2.2.2 Technical Discussion

Upon completion of the tests, inspection of the specimen showed that no failure occurred.

Accelerometer data was found generally satisfactory. However, some results did not correlate well between the two sets of tests (1 and 2, 3 and 4) and the cause of these inconsistencies could not be found. This data has been labeled "doubtful" and was excluded in the final analysis.

Reduction of the test data was performed on the UNIVAC 1108 after digitizing the analog tape.

II.B.2.2.3 Analysis

The analysis performed with the test data consisted of a comparison of the shock environment provided by each fairing deployment mechanism operation.

For the reasons described in paragraph II.B.2.2.2, the data from six accelerometers was used for jettison of the "A" fairing and from seven accelerometers for the "B" fairing. Analysis based on shock spectrum data is shown on Table II.B.2.3 and II.B.2.4 for fairings "A" and "B" respectively. This data is also plotted on Figure II.B.3 and II.B.4. A similar analysis based on oscillogram peaks and using the mean value of five accelerometers is shown on Table II.B.2.5.

Arithmetic mean values of the reduction ratios are plotted on Figure II.B.2.3 and II.B.2.4. The minimum reduction occurs during deployment of the fairing "A." The reduction is quoted as follows by taking the arithmetic mean maximum value of the reduction ratios in each octave band:

Octave	Reduction Ratio
200/400	.19
400/800	.37
800/1600	.50
1600/3200	.94
3200/6400	.72

Hence an overall mean reduction ratio of .54 may be compared with a value of .42 derived from oscillogram data. These reduction ratios provide a comparison of the environment level created by the pin-puller spring deployment mechanism in terms of the standard mechanism level.

II.B.2.3 CONCLUSION

The reduction in shock level provided by the pin-puller deployment mechanism was greater at low frequency. Over the frequency range investigated, an average reduction of about 50 percent is achieved.

Accounting for normal data scatter, it is seen that the environment level is reduced over the whole structure.

Although the data from five accelerometers could not be correlated with the remaining data and was not included in the analysis, the useful measurements exhibited good correlation so that a high degree of confidence is placed in the results.

TABLE II.B.2.1

ACCELEROMETERS AND LOCATIONS

Accelerometer No.	Station (inches)	Direction	Distance to Shock Source (Inches) Jettison A	Jettison B	Accelerometer Type
1	248	L	18	54	ENDEVCO 2225
2	260	T	15	52	ENDEVCO 2225
3	272	L	13	36	ENDEVCO 2225
4	248	R	44	12	ENDEVCO 2225
5	248	L	64	19	ENDEVCO 2225
6	256	R	55	8	ENDEVCO 2225
7	260	T	62	8	ENDEVCO 2225
8	270	L	64	18	ENDEVCO 2225
9	281	T	65	25	ENDEVCO 2225
10	255	T	43	79	ENDEVCO 2225
11	255	R	43	79	ENDEVCO 2225
12	255	T	87	62	ENDEVCO 2225

L = longitudinal
R = radial
T = tangential

TABLE II.B.2.2

SUMMARY OF TESTS

Test No.	Configuration	Explosive Size	Test Purpose	Shock Isolation	Jettison
1	1	4 squibs	Structure	None	A
2	2	4 squibs	Structure	None	B
3	3	2 squibs	Structure	Yes	B
4	4	2 squibs	Structure	Yes	A

Configurations:

1 Original geometry - jettison fairing A
2 Original geometry - jettison fairing B
3 Modified geometry - jettison fairing B
4 Modified geometry - jettison fairing A

See Figure II.B.2.5.1

Table II.B.2.3

RATIO OF NEW VERSUS STANDARD CONFIGURATION LEVELS

"A" FAIRING JETTISON

RATIO $\frac{\text{TEST 4}}{\text{TEST 1}}$

Accel.	Curve/Freq.	100	125	160	200	250	320	400	500	630	800	1000	1250	1600	2000	2500	3200	4000	5000	6300	8000	10000
5 L	85/84					.13		.13	.08	.12	.29	.26	.28	.53	.40	.65	.98	.64	.81	.76	.50	.84
7 T	93/92	.11	.15	.13	.07	.07	.08	.18	.19	.31	.51	.26	.21	.11	1.00	.67	.82	.49	.43	.58	.30	.35
8 L	97/96							.15	.16	.33	.37	.39	.59	.47	.71	.39	.33	.45	.66	1.00	1.18	1.03
9 T	101/100						.21	.09	.05	.16	.23	.18	.46	.43	.32	.83	.29	.37	.36	.48	.31	.36
10 T	105/104		.09	.06	.0092	.02	.01	.05	.10	.15	.13	.12	.15	.11	.27	.38	.26	.28	.24	.28	.11	.30
12 T	113/112			.17	.15	.26	.18	.29	.27	.39	.74	.65	.71	.96	1.31	2.73	.86	.87	.86	1.24	.90	.56
		.14	.12	.12	.06	.12	.19	.15	.11	.24	.37	.31	.40	.49	.67	.94	.59	.52	.56	.72	.66	.48

TABLE II.B.2.4

RATIO OF NEW VERSUS STANDARD CONFIGURATION LEVELS

"B" FAIRING JETTISON

RATIO $\frac{\text{TEST 3}}{\text{TEST 2}}$

Accel.	Curve/Freq.	100	125	160	200	250	320	400	500	630	800	1000	1250	1600	2000	2500	3200	4000	5000	6300	8000	10000
5 L	87/86			.05	.09	.18	.27	.13	.10	.03	.16	.12	.27	.34	.78	.83	.62	.44	.38	.51	.70	.59
6 R	91/90			.01	.02	.04	.02	.02	.04	.02	.01	.03	.02	.02	.07	.05	.03	.03	.09	.03	.02	.02
7 T	95/94	.12	.11	.01	.11	.14	.16	.19	.17	.19	.22	.23	.28	.37	.43	.64	.38	.29	.21	.43	.36	.48
8 L	99/98				.16	.20	.25	26	.24	.32	.44	.38	.49	.38	.92	.56	.45	.38	.48	.50	.45	.17
10 T	107/106			.09	.07	.10	.22	.21	.22	.19	.29	.30	.60	.73	.10	.67	.55	.55	.56	.49	.49	.37
11 R	111/110		.61	.42	.60	.32	.73	.40	.63	.44	.93	.88	1.05	1.06	1.41	1.26	1.32	1.52	1.23	1.37	1.63	1.23
12 T	115/114			.12	.12	.15	.17	.25	.16	.14	.16	.19	.28	.36	.63	.84	.36	.53	.35	.23	.34	.35
Arithmetic mean*		.12	.11	.06	.11	.16	.22	.20	.21	.22	.26	.25	.39	.44	.59	.72	.48	.44	.40	.44	.47	.40

* Accel. 11 R deleted

TABLE II.B.2.5

RATIO OF NEW VERSUS STANDARD CONFIGURATION LEVELS FROM OSCILLOGRAM PEAKS

Accelerometer No.	Doubtful Data	Fairing Jettison A		Fairing Jettison B		Ratio A	Ratio B	Mean
		1	4	2	3	4/1	3/2	A + B / 2
1 L	X	355	38	75	6	.1070	.0800	
2 T	X	560	18	45	4	.0321	.0889	
3 L	X	280	6	80	3	.0214	.0375	
4 R	X	90	11	190	9	.1222	.0474	
5 L		90	75	400	150	.8333	.375	.6040
6 R	X	150		1945	38		0195	
7 T		185	66	1010	260	.3567	.2574	.3070
8 L		92	54	265	100	.5869	.3773	.4821
9 T		75	20	75	76	.2667	1.0133	
10 T		368	92	112	47	.2500	.4196	.3348
11 R	X	265		92	100		1.0869	
12 T		100	52	224	53	.5200	.2366	.3783
						Mean reduction ratio		.4212

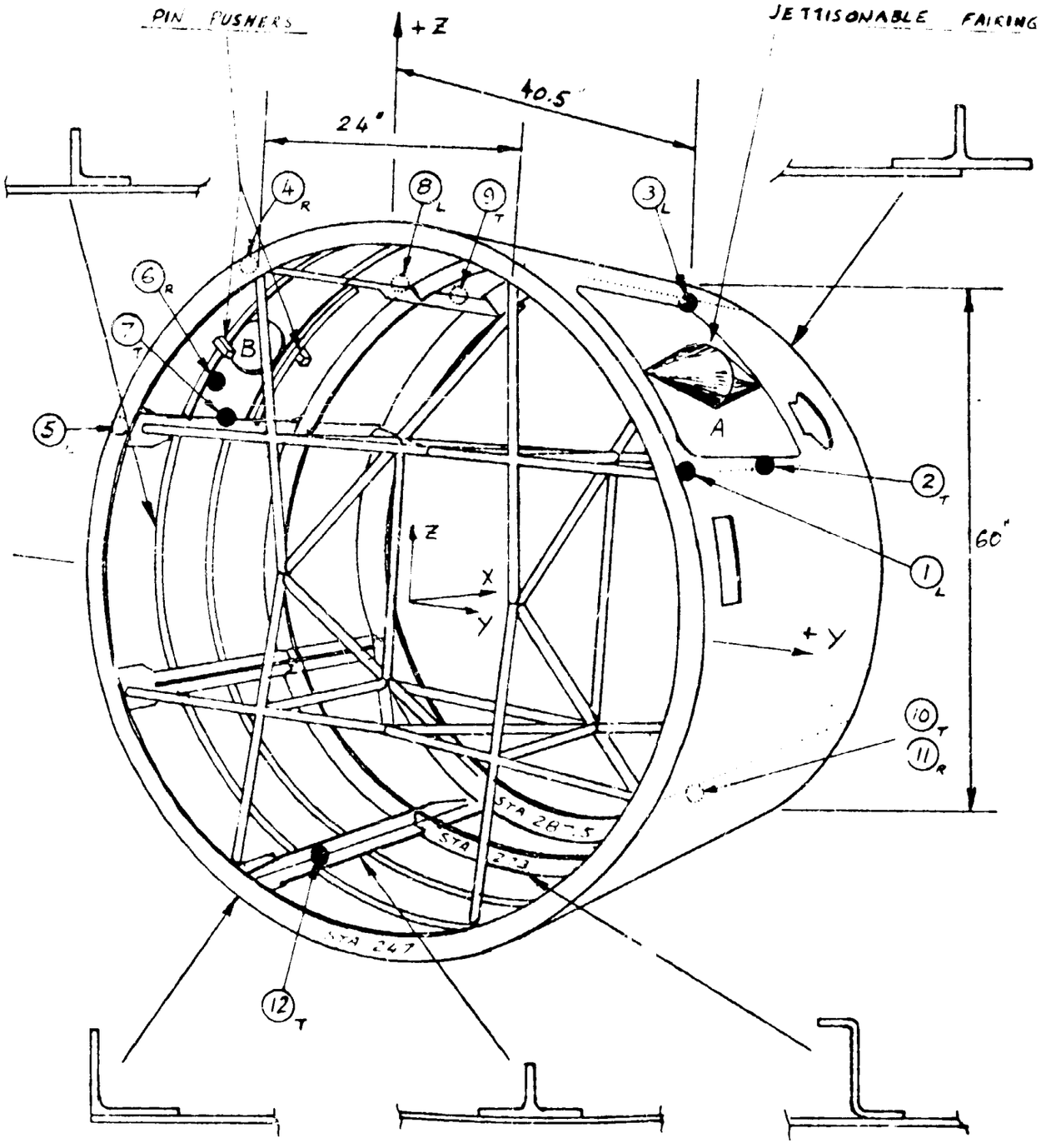

Figure II.B.2.1 TEST CONFIGURATION AND INSTRUMENTATION LOCATIONS

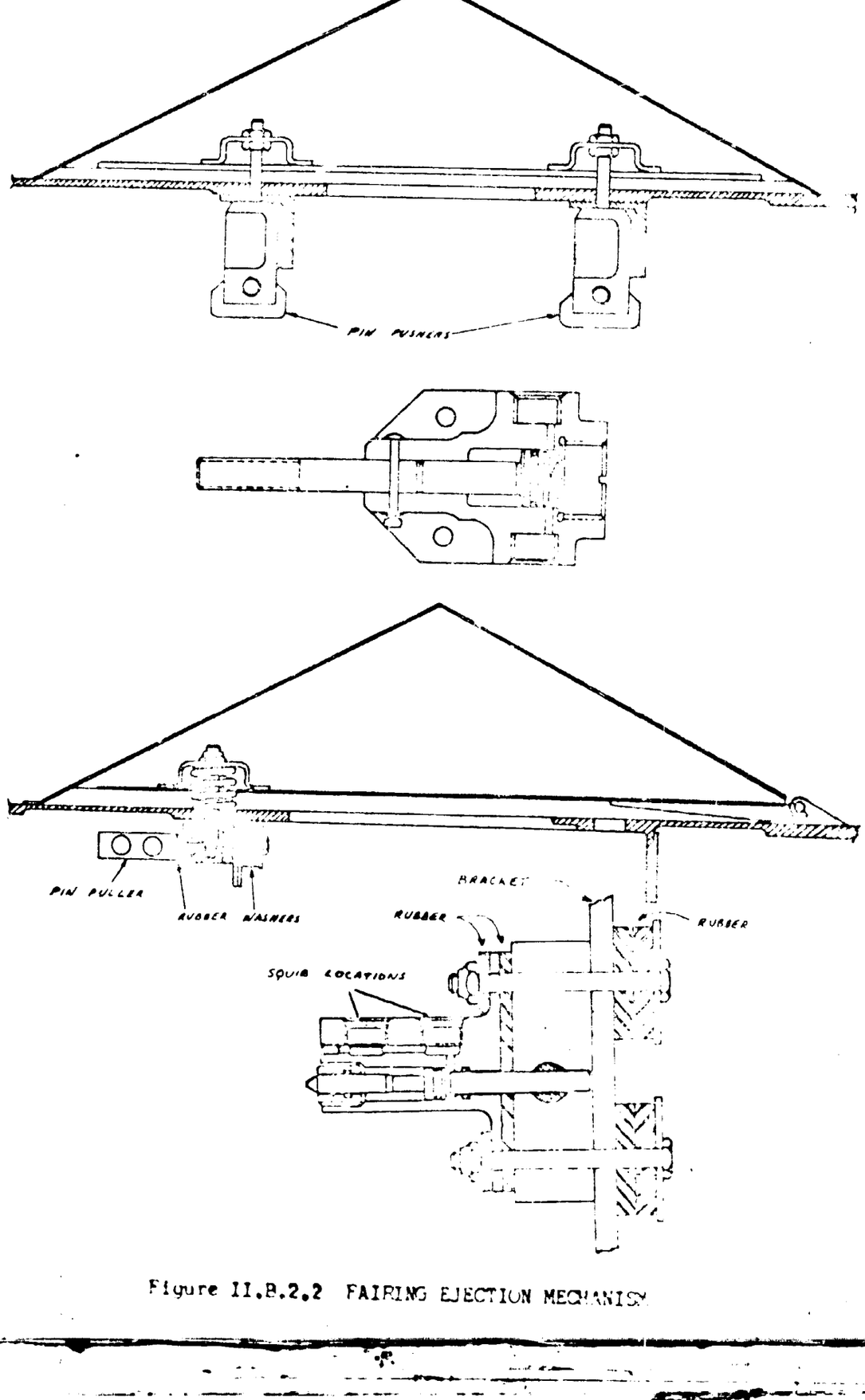

Figure II.B.2.2 FAIRING EJECTION MECHANISM

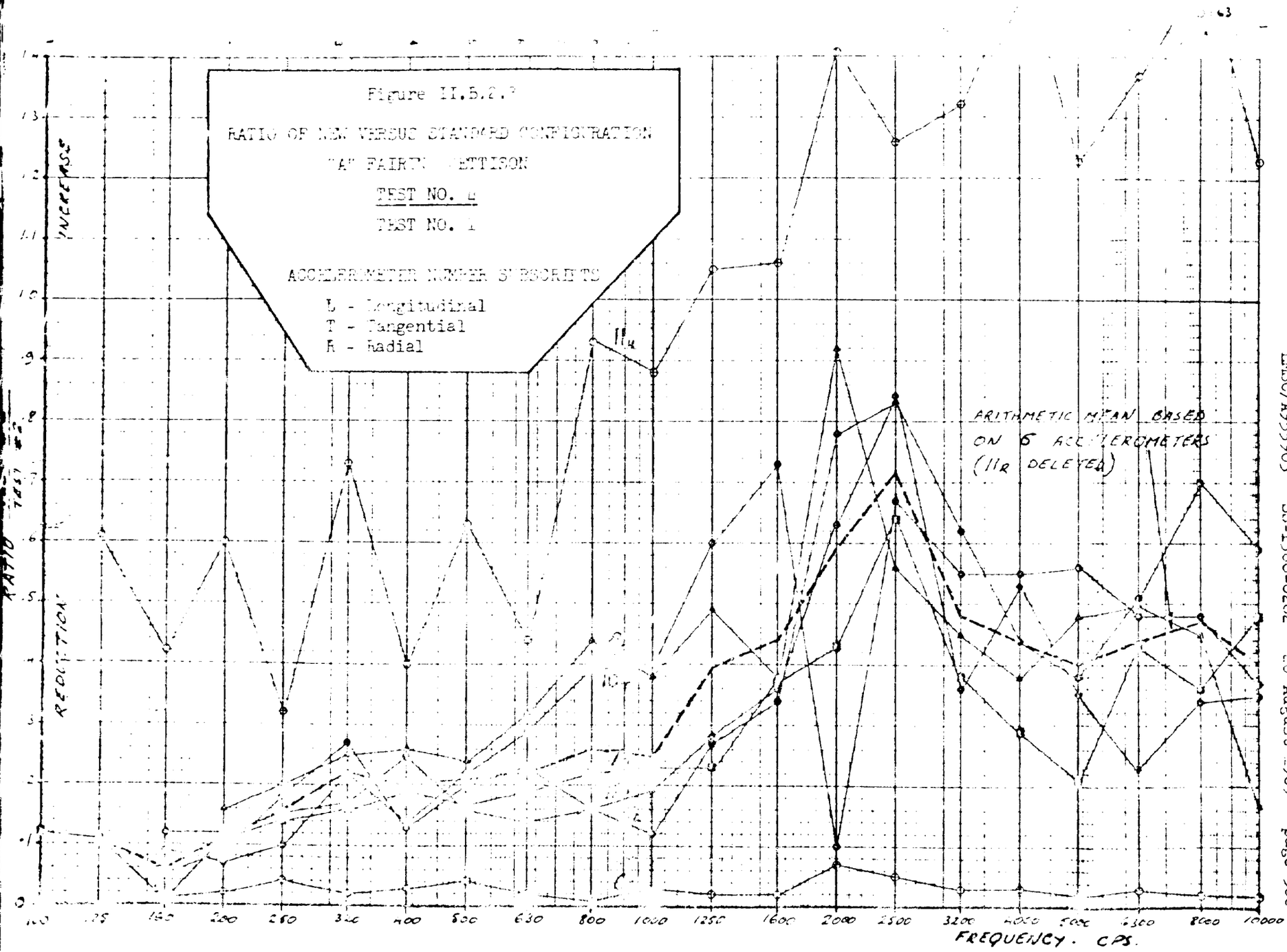
Figure II.5.2.3
RATIO OF MSM VERSUS STANDARD CONFIGURATION
"A" FAIRING JETTISON
TEST NO. 4
TEST NO. 1
ACCELEROMETER NUMBER SUBSCRIPTS
L - Longitudinal
T - Tangential
R - Radial
INCREASE
RESOLUTION
ARITHMETIC MEAN BASED ON 6 ACCELEROMETERS (11R DELETED)
FREQUENCY. CPS.

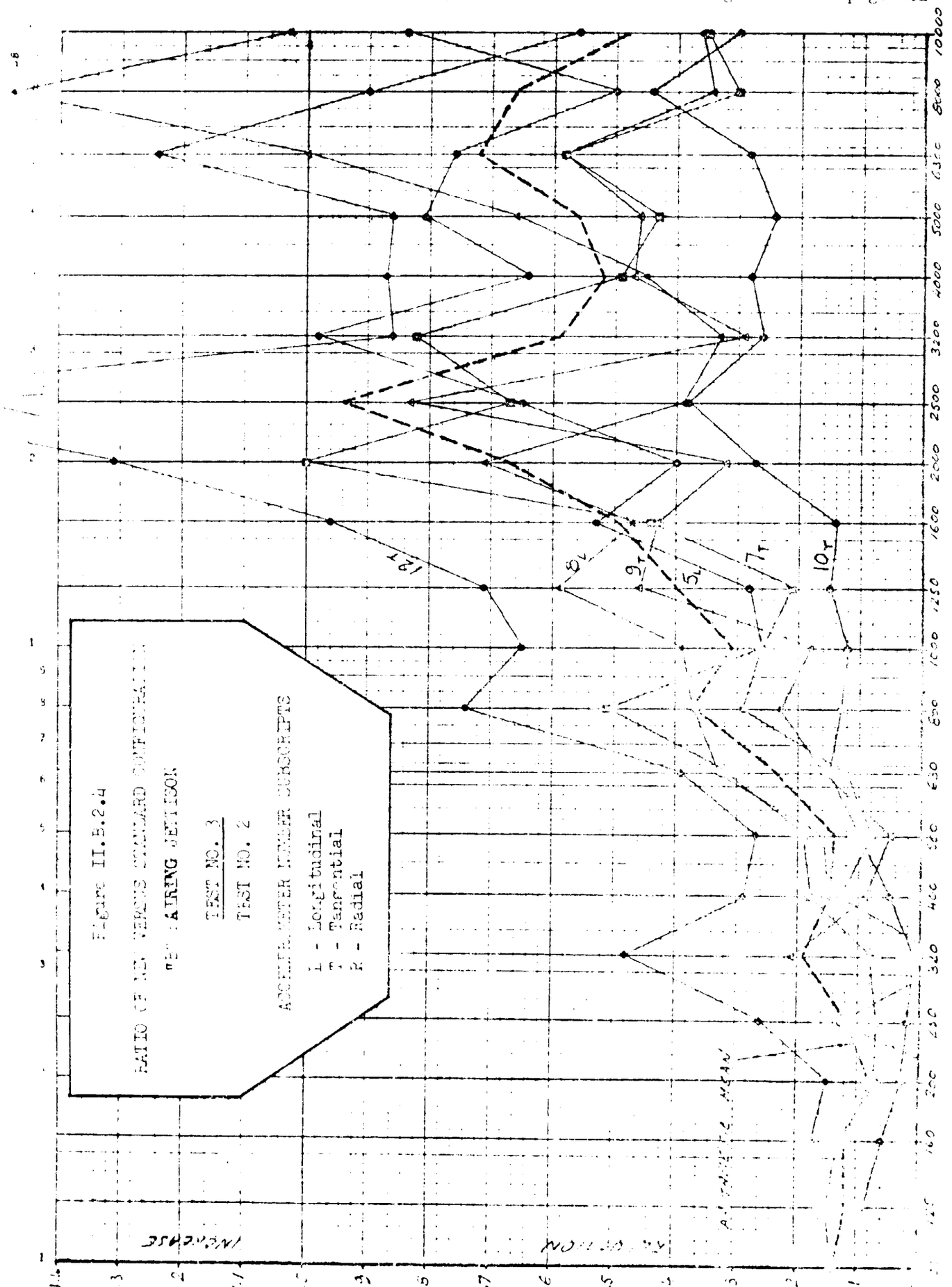
Figure II.B.2.4
RATIO OF RMS VERSUS STANDARD DEVIATION
RCS ABRING JETTISON
TEST NO. 3
TEST NO. 2
ACCELEROMETER NUMBER SUBSCRIPTS
L - Longitudinal
T - Tangential
R - Radial
FREQUENCY - CPS
8L
9T
5L
7T
10T

SHOCK TEST ANALYSIS DATA SHEET II.B.2.5

TEST ITEM 867-68
SERIAL NO.
SHOCK AXIS LATERAL

PART NO. STRUCTURE
TEST DATE 2 NOV 1964
SHOCK NO. 1

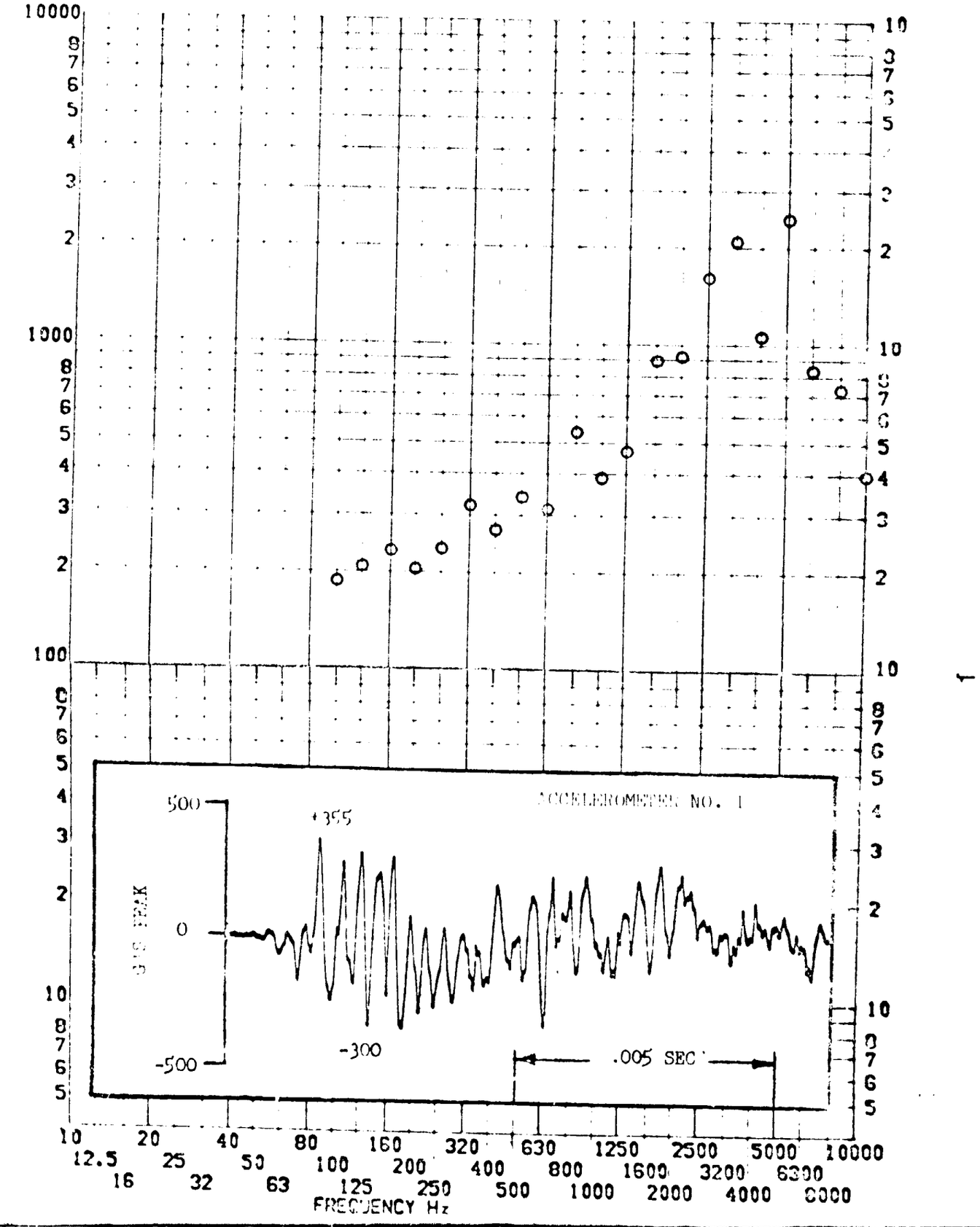

SHOCK TEST ANALYSIS DATA SHEET II.B.2.6

TEST ITEM 867-70 PART NO. STRUCTURE
SERIAL NO. TEST DATE NOV. 1964
SHOCK AXIS LATERAL SHOCK NO.

RESPONSE G-S

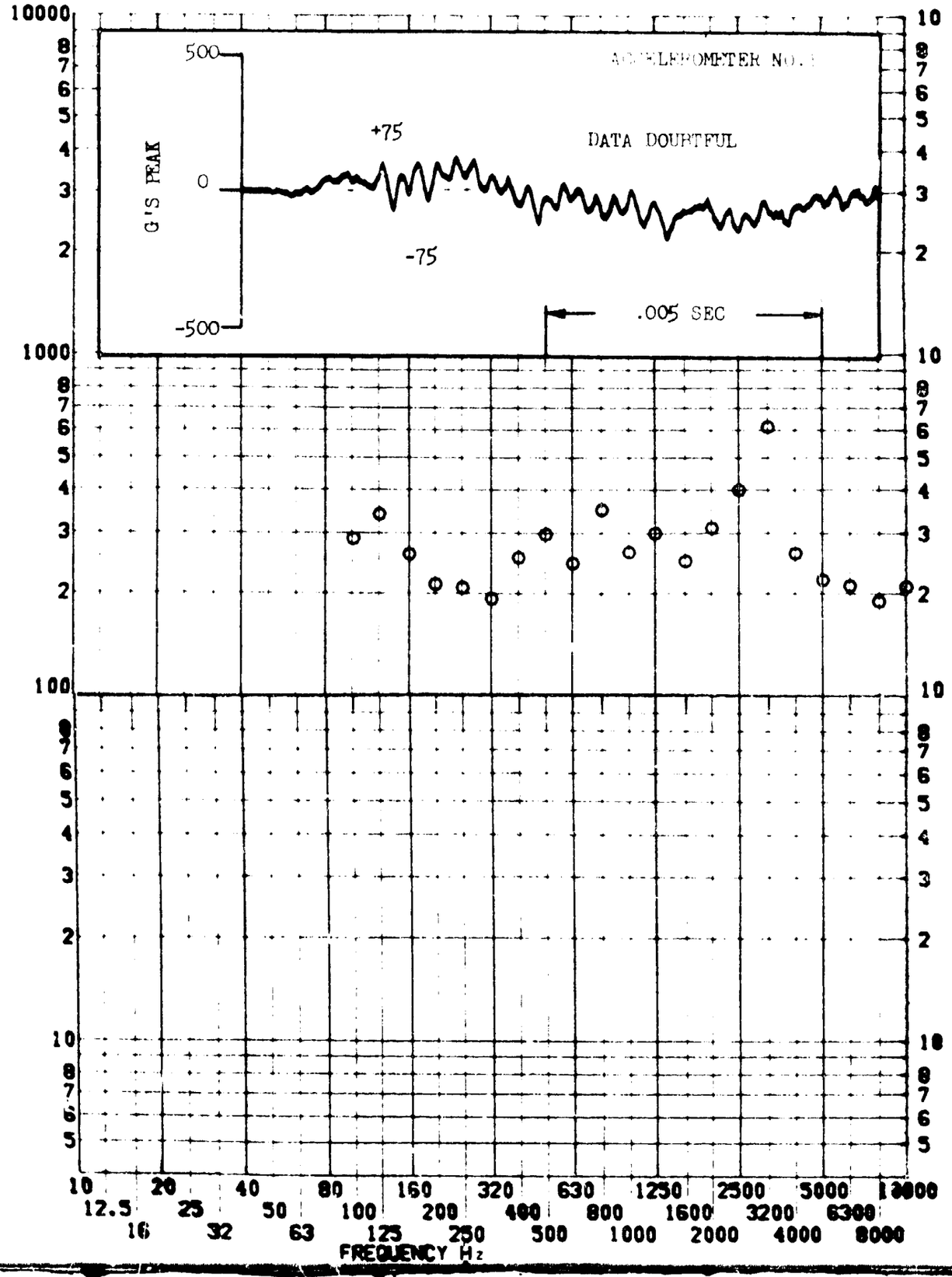

SHOCK TEST ANALYSIS DATA SHEET U.B.P.7

TEST ITEM C67-71 PART NO. STRUCTURE
SERIAL NO. TEST DATE 3 NOV 1964
SHOCK AXIS LATERAL SHOCK NO. 3

RESPONSE G-S

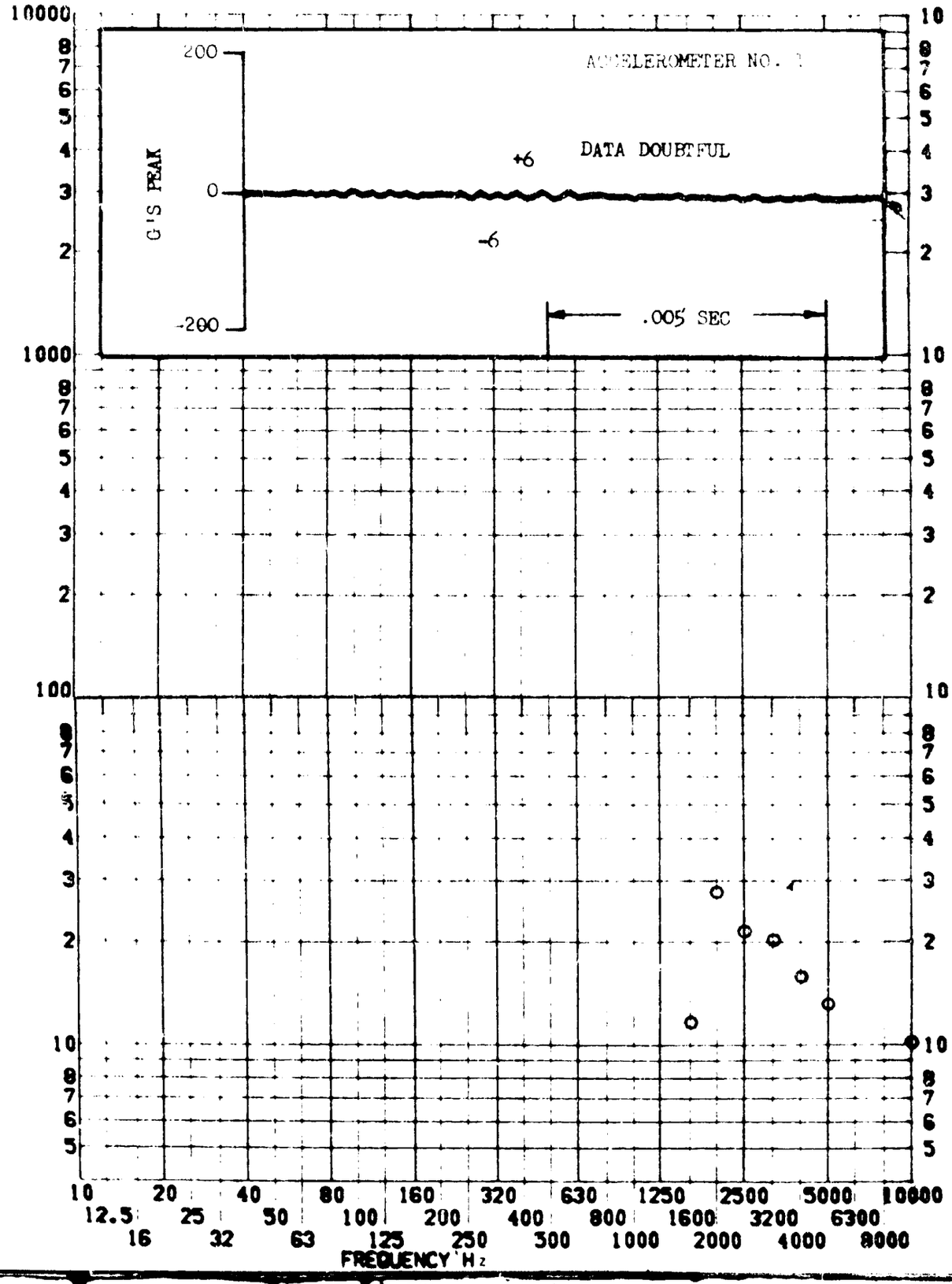

SHOCK TEST ANALYSIS DATA SHEET II.B.2.8

TEST ITEM 867-69 PART NO. STRUCTURE
SERIAL NO. TEST DATE 2 NOV 1964
RESPONSE 6-S SHOCK AXIS LATERAL SHOCK NO. 4

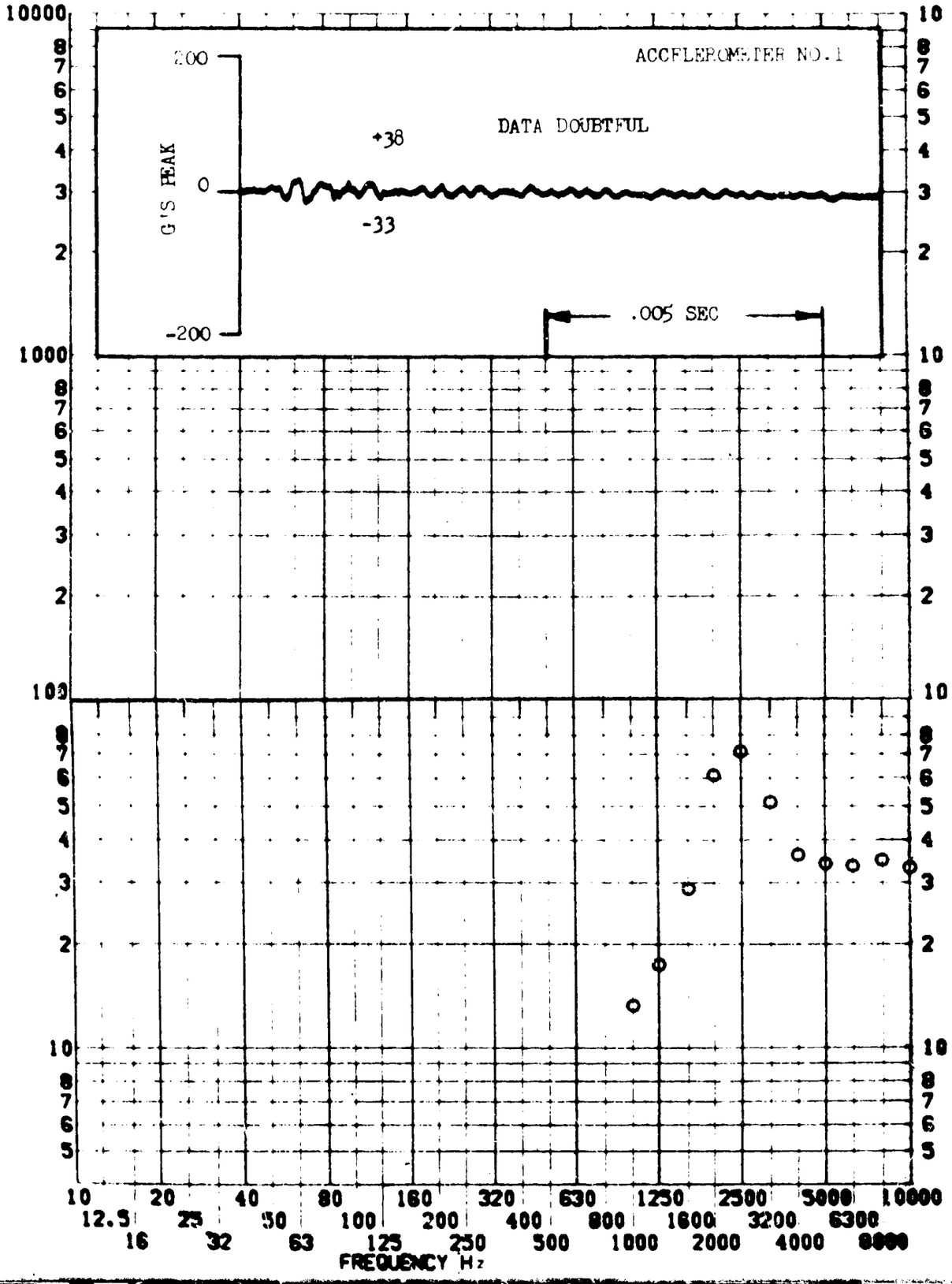

SHOCK TEST ANALYSIS DATA SHEET II.B.2.9

TEST ITEM 867-72
SERIAL NO.
SHOCK AXIS TANGENTIAL

PART NO. STRUCTURE
TEST DATE 2 NOV 1964
SHOCK NO.

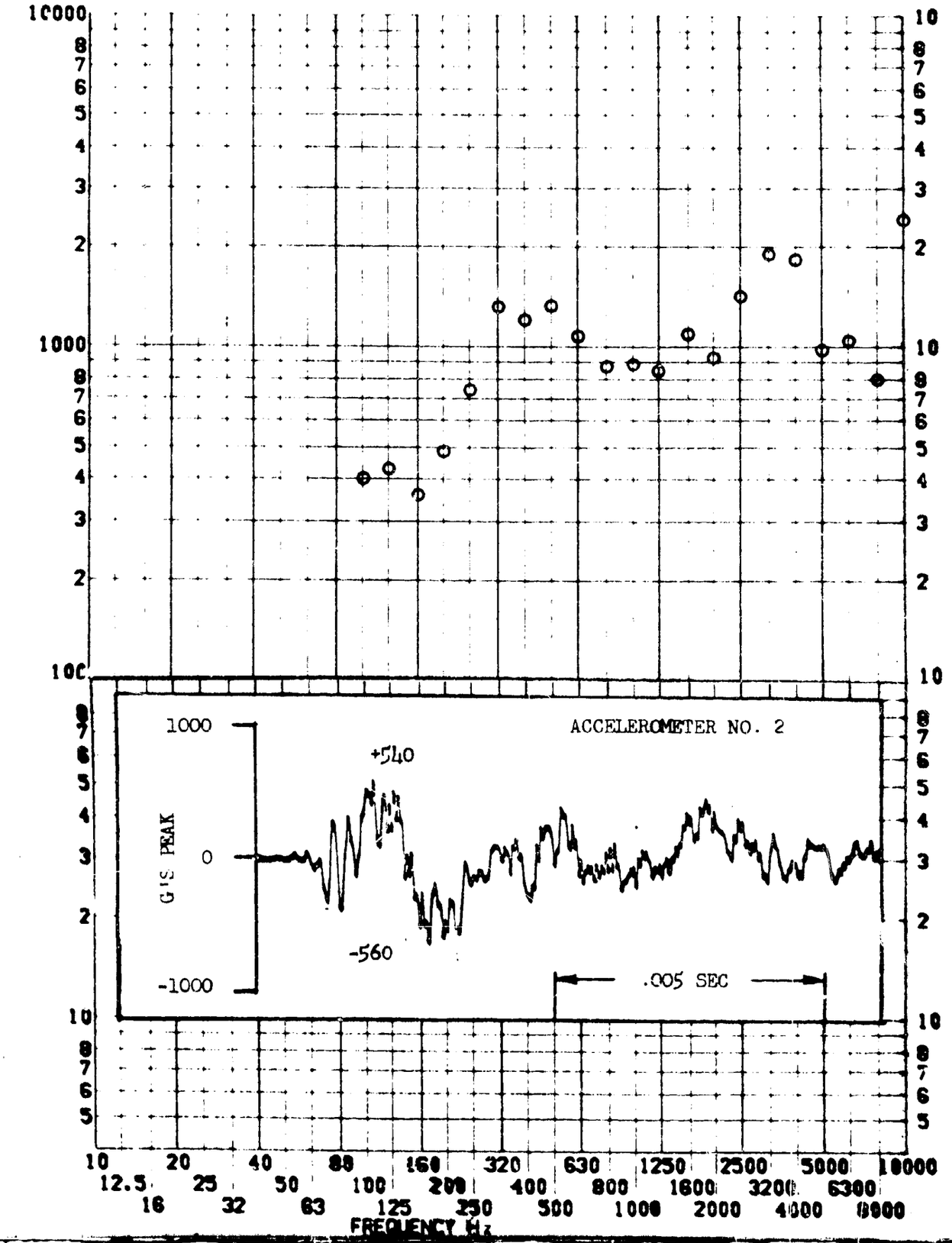

SHOCK TEST ANALYSIS DATA SHEET II.B.2.10

TEST ITEM 867-74
SERIAL NO.
SHOCK AXIS TANGENTIAL

PART NO. STRUCTURE
TEST DATE 2 NOV 1964
SHOCK NO. 2

RESPONSE G-S

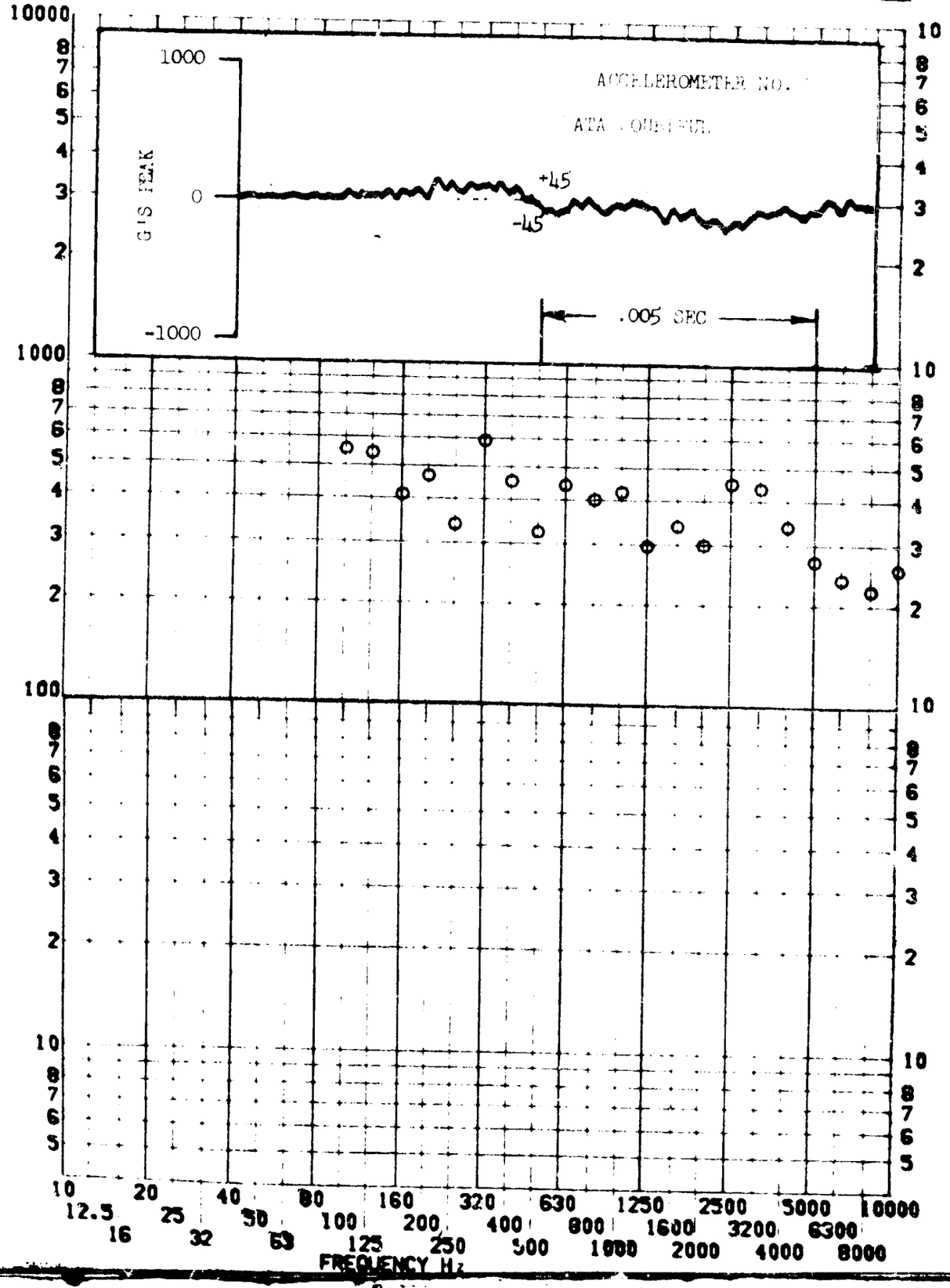

SHOCK TEST ANALYSIS DATA SHEET II.B.2.11

TEST ITEM 867-75
SERIAL NO.
SHOCK AXIS TANGENTIAL

PART NO. STRUCTURE
TEST DATE 2 NOV 1964
SHOCK NO. 3

RESPONSE G-S

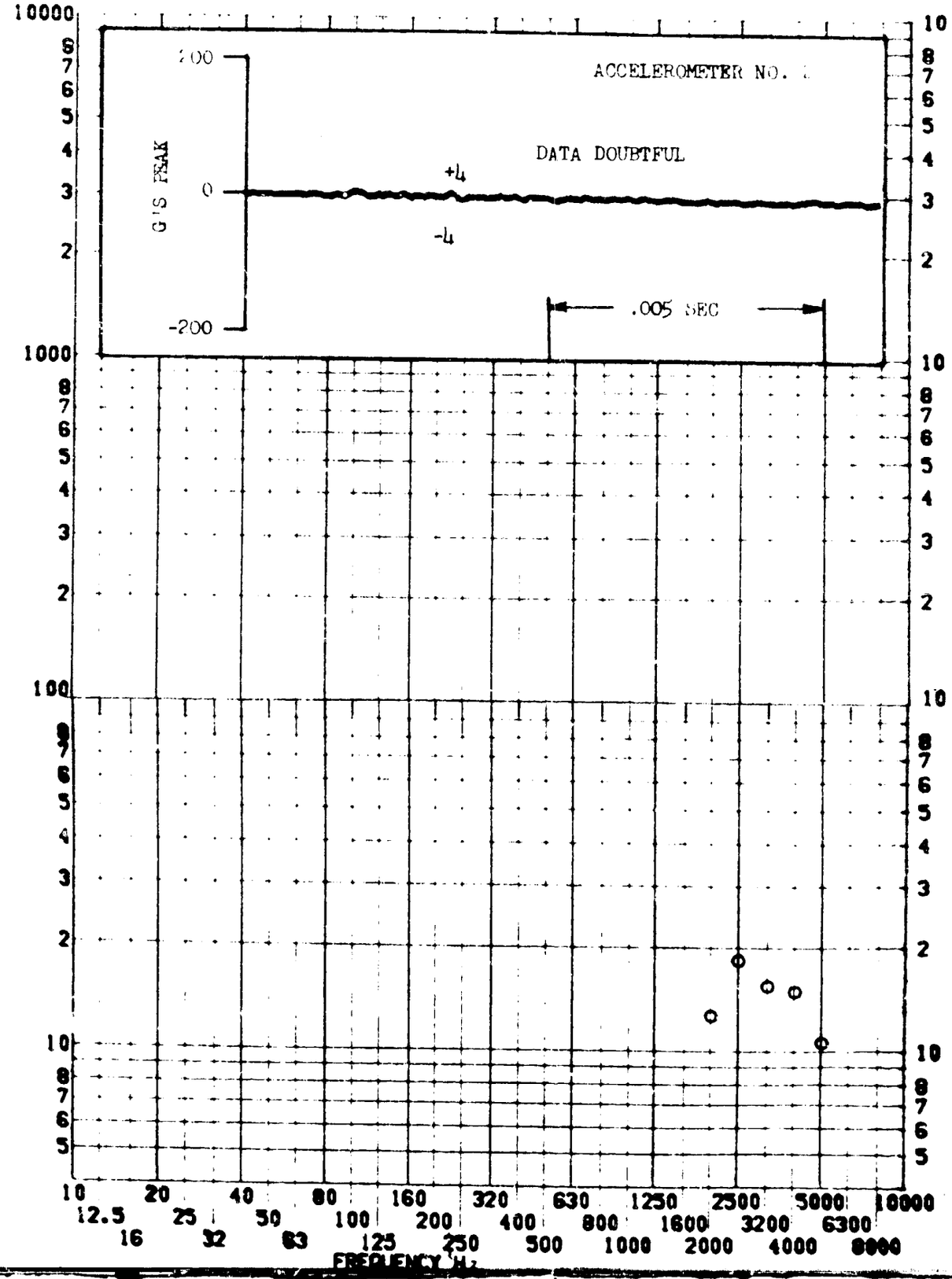

SHOCK TEST ANALYSIS DATA SHEET II.B.2.12

TEST ITEM 867-73
SERIAL NO. 2
SHOCK AXIS TANGENTIAL

PART NO. STRUCTURE
TEST DATE 2 NOV. 1961
SHOCK NO. A

RESPONSE G-S

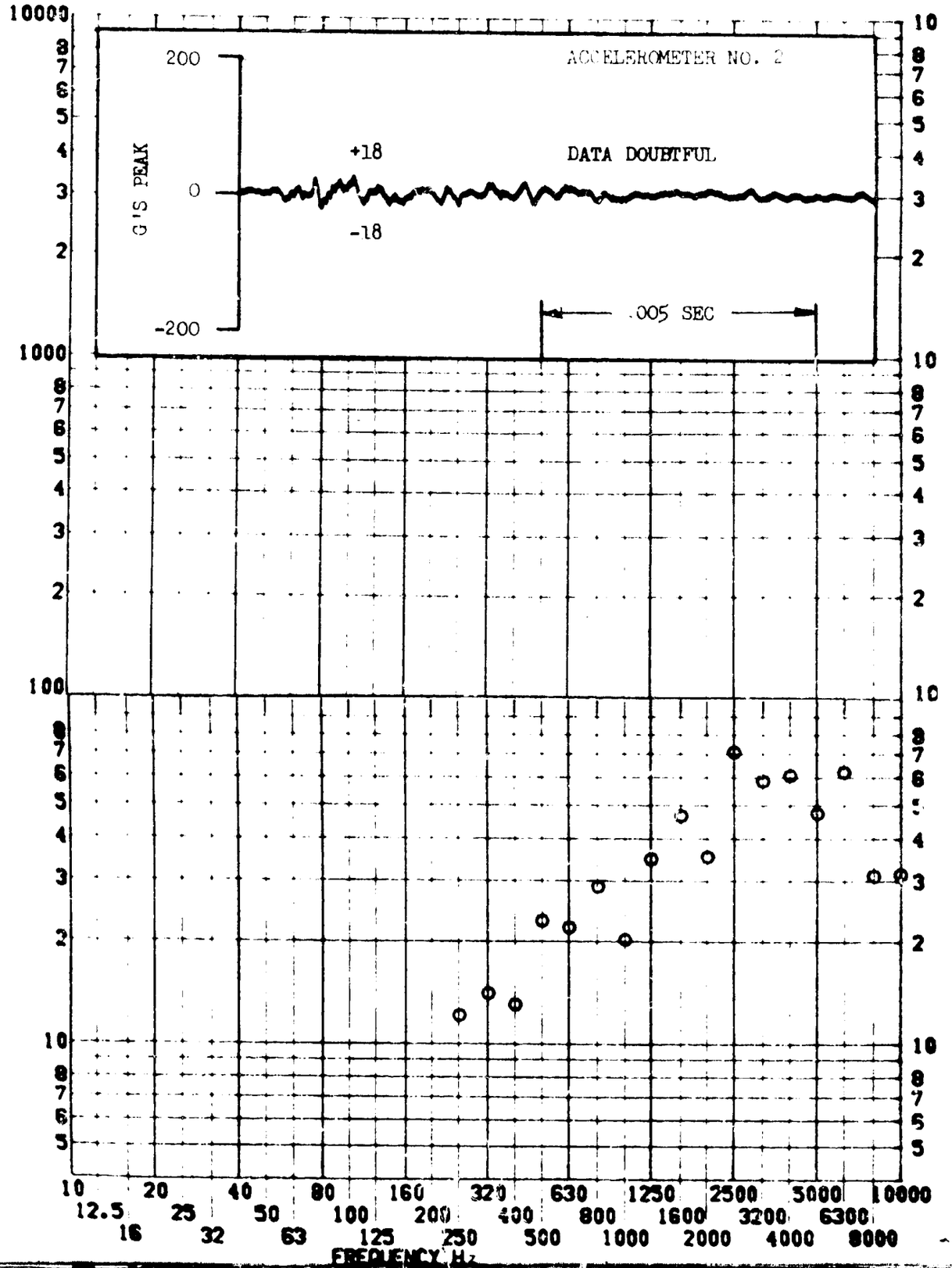

SHOCK TEST ANALYSIS DATA SHEET II.B.2.13

TEST ITEM 867-76
SERIAL NO.
SHOCK AXIS LATERAL
PART NO. STRUCTURE
TEST DATE 2 NOV 1960
SHOCK NO. 1

RESPONSE G-S

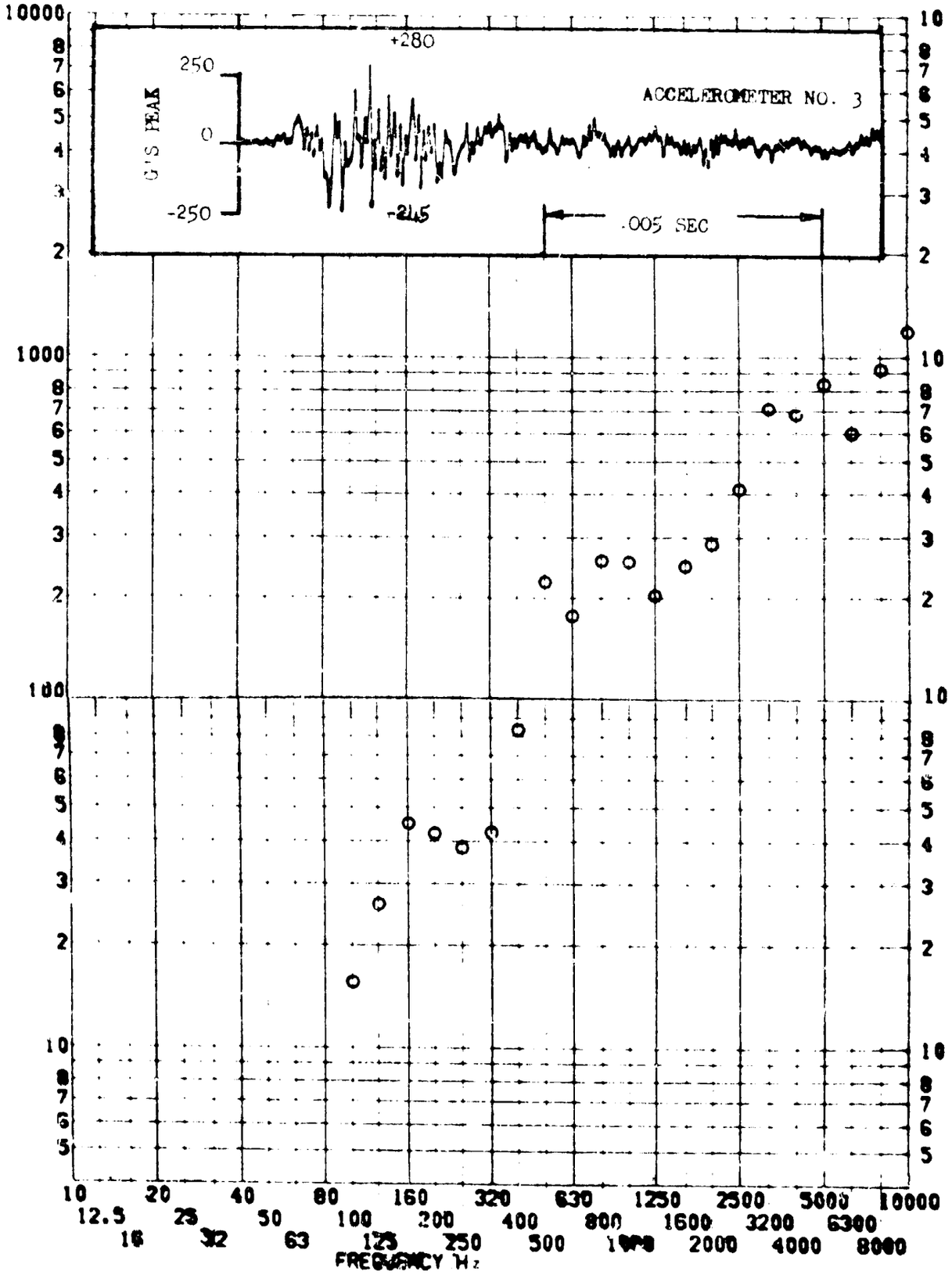

SHOCK TEST ANALYSIS DATA SHEET [illegible]

TEST ITEM 868-78 — PART NO. [illegible]
SERIAL NO. — TEST DATE [illegible] 1968
RESPONSE G-S SHOCK AXIS LATERAL — SHOCK NO. 2

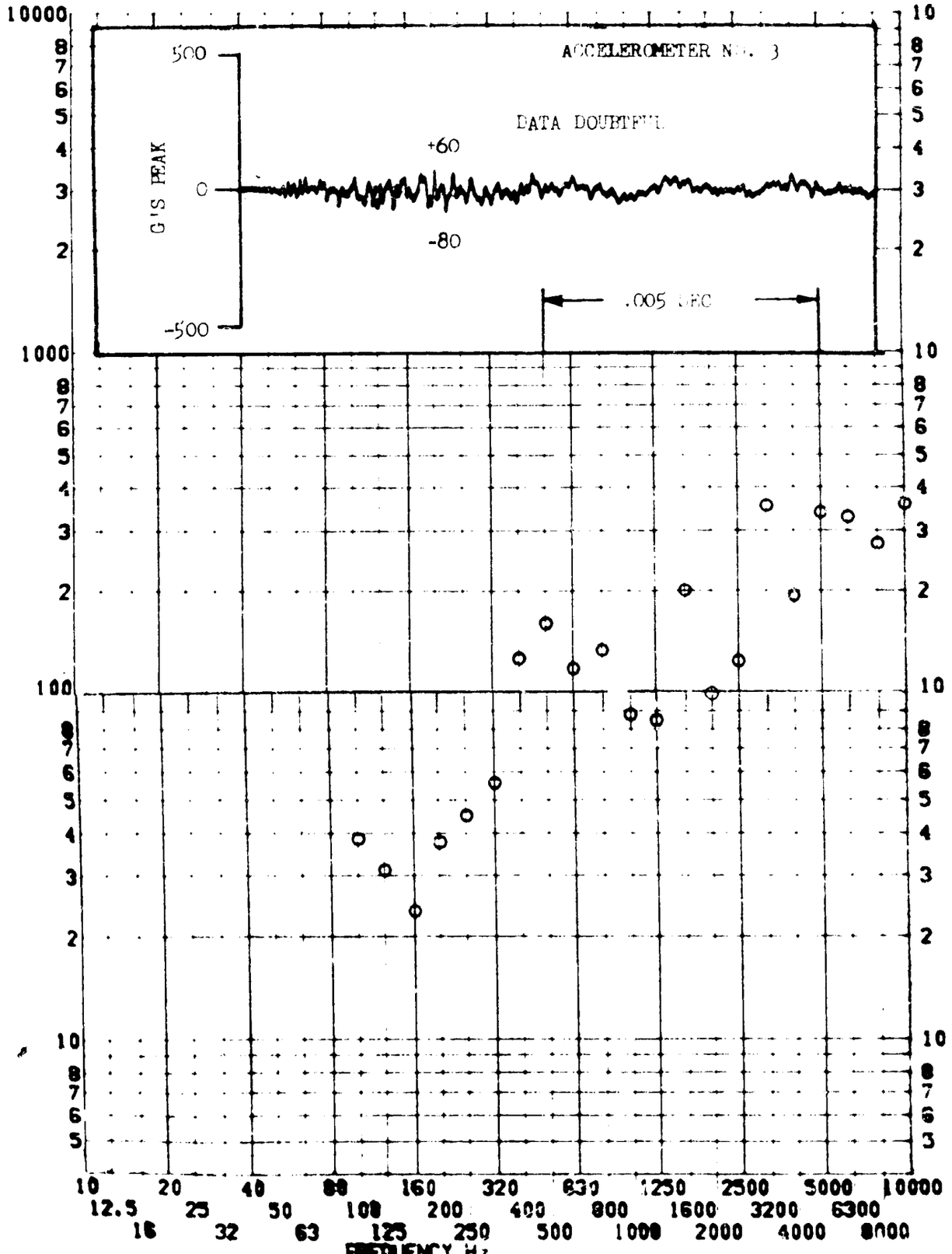

SHOCK TEST ANALYSIS DATA SHEET II.B.2.15

TEST ITEM 867-79
SERIAL NO.
SHOCK AXIS LATERAL

PART NO. STRUCTURE
TEST DATE 2 NOV 1964
SHOCK NO. 3

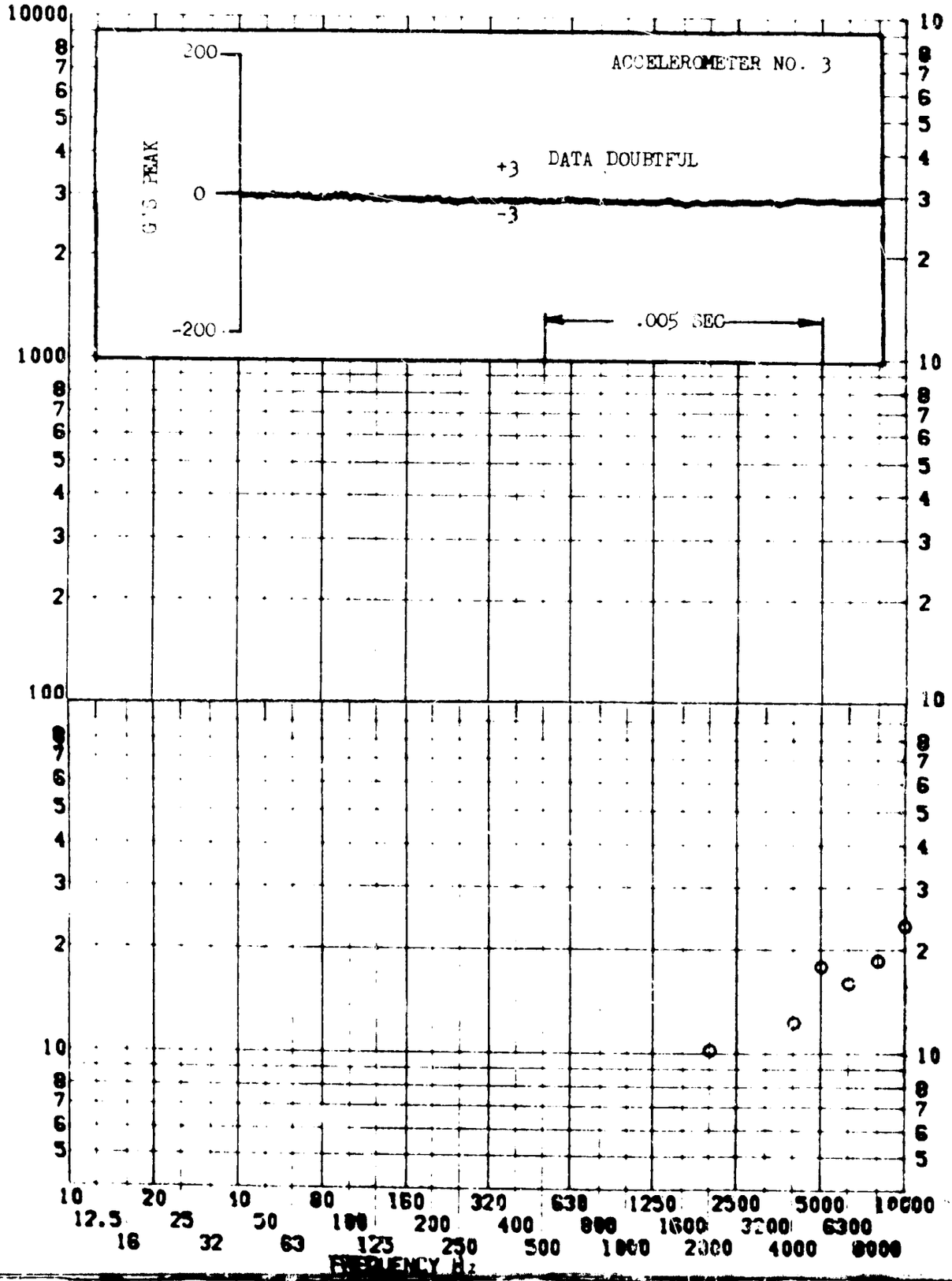

SHOCK TEST ANALYSIS DATA SHEET II.B.2.16

TEST ITEM 868-77 — PART NO. STRUCTURE
SERIAL NO. — TEST DATE 2 NOV 1964
RESPONSE G-S SHOCK AXIS LATERAL — SHOCK NO. 4

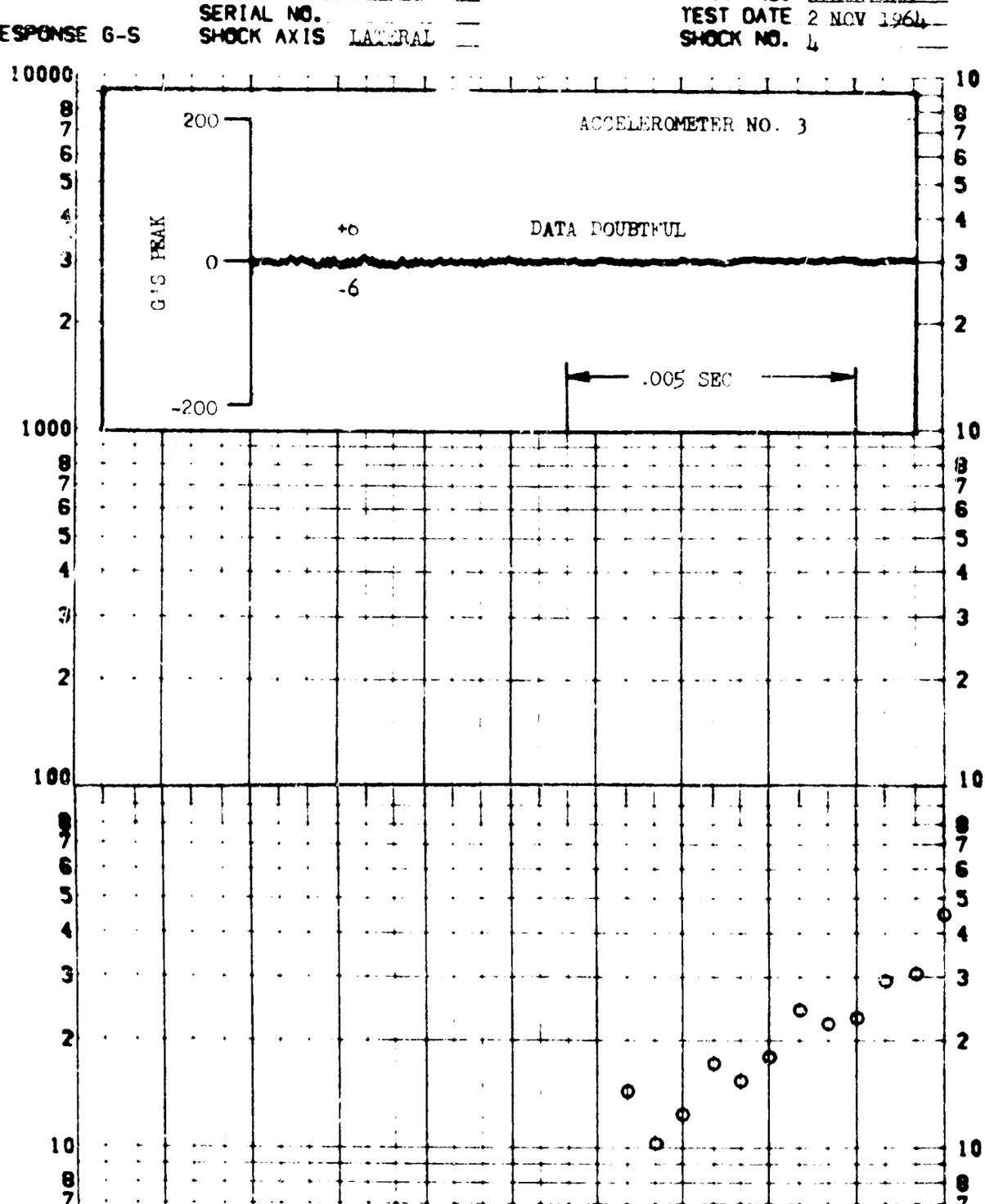

SHOCK TEST ANALYSIS DATA SHEET II.B.2.17

TEST ITEM 867-80
SERIAL NO.
SHOCK AXIS RADIAL

PART NO. STRUCTURE
TEST DATE 2 NOV 1964
SHOCK NO. 1

RESPONSE G-S

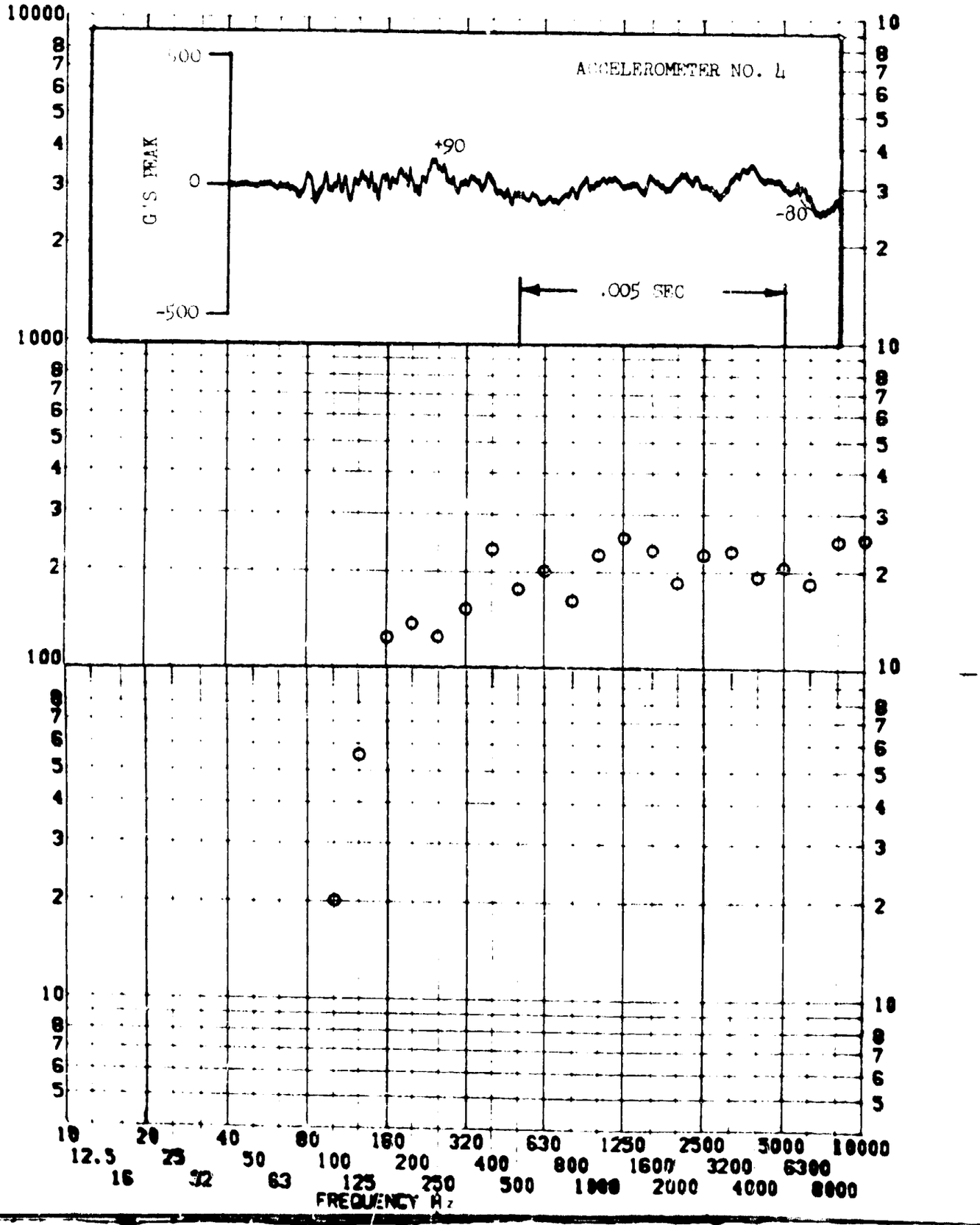

SHOCK TEST ANALYSIS DATA SHEET

TEST ITEM 867-82
SERIAL NO.
SHOCK AXIS AXIAL

PART NO. STRUCTURE
TEST DATE 2 NOV 1964
SHOCK NO. 2

RESPONSE G-S

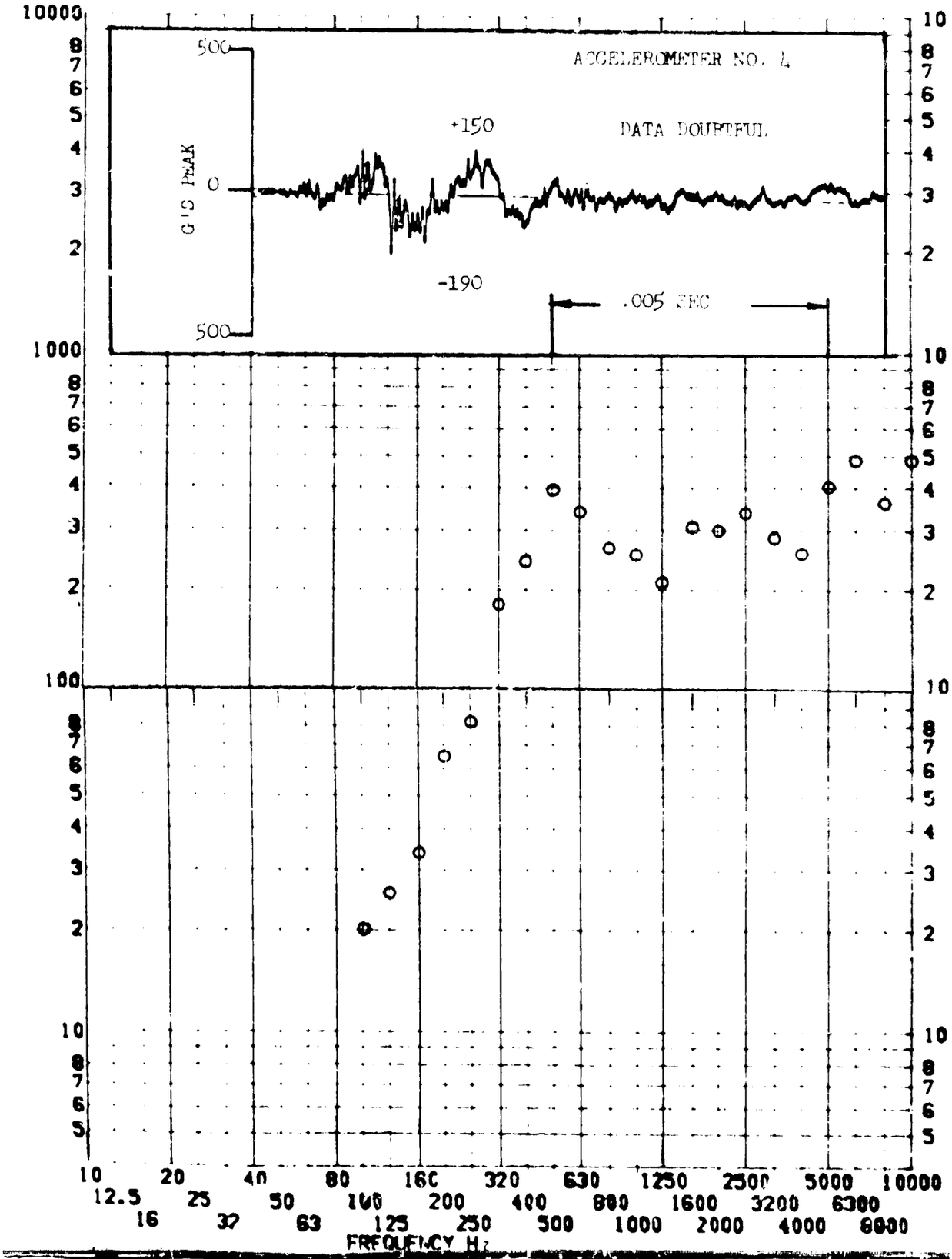

SHOCK TEST ANALYSIS DATA SHEET II.B.2.29

TEST ITEM 867-83 PART NO. STRUCTURE
SERIAL NO. TEST DATE 2 NOV [illegible]
SHOCK AXIS RADIAL SHOCK NO. 3

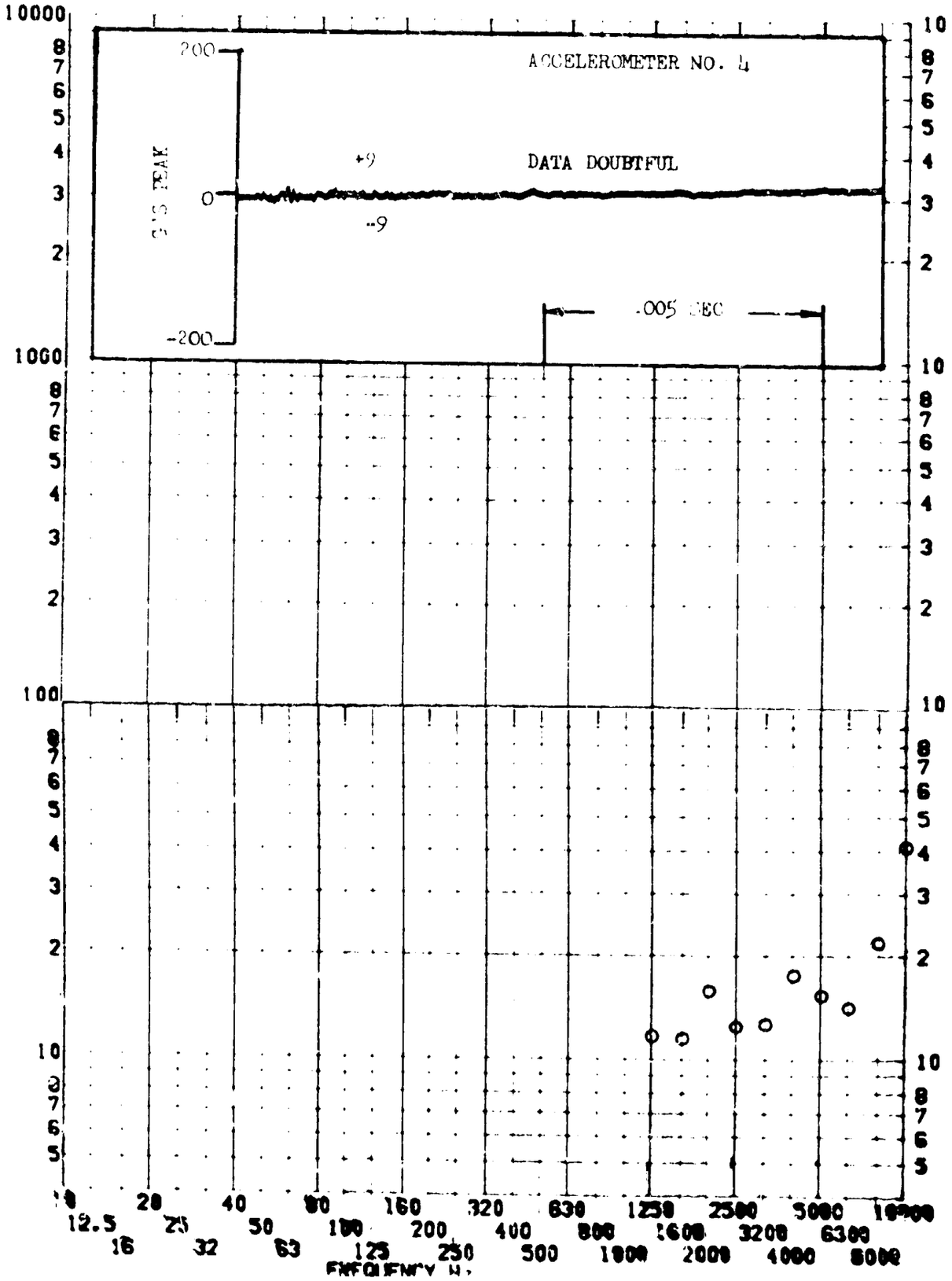

SHOCK TEST ANALYSIS DATA SHEET

TEST ITEM 867-81
SERIAL NO.
SHOCK AXIS RADIAL
PART NO.
TEST DATE
SHOCK NO. 4

RESPONSE G-S

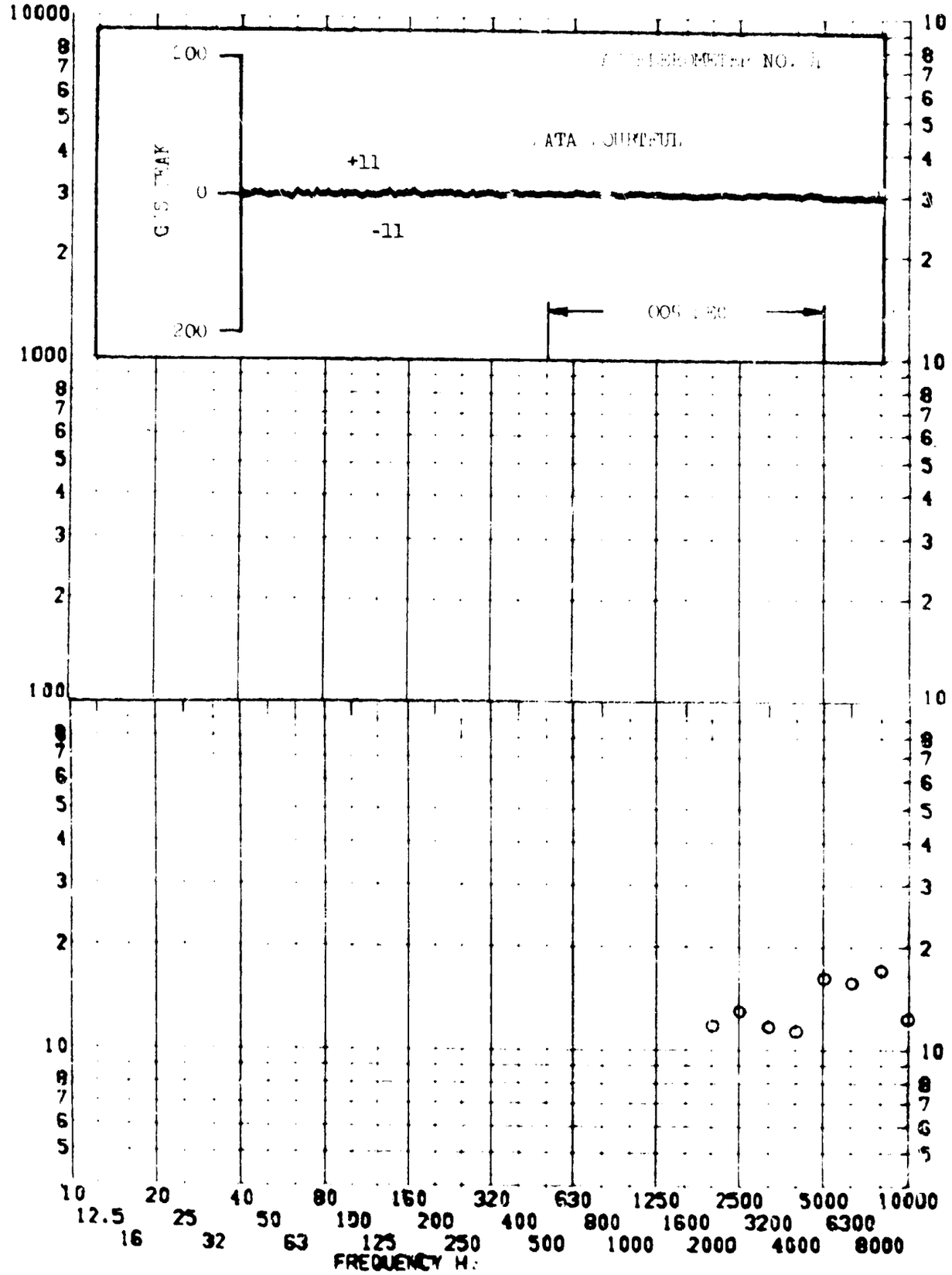

SHOCK TEST ANALYSIS DATA SHEET EI.B.2.21

TEST ITEM 867-84
SERIAL NO.
SHOCK AXIS LATERAL

PART NO. [illegible]
TEST DATE [illegible]
SHOCK NO. 1

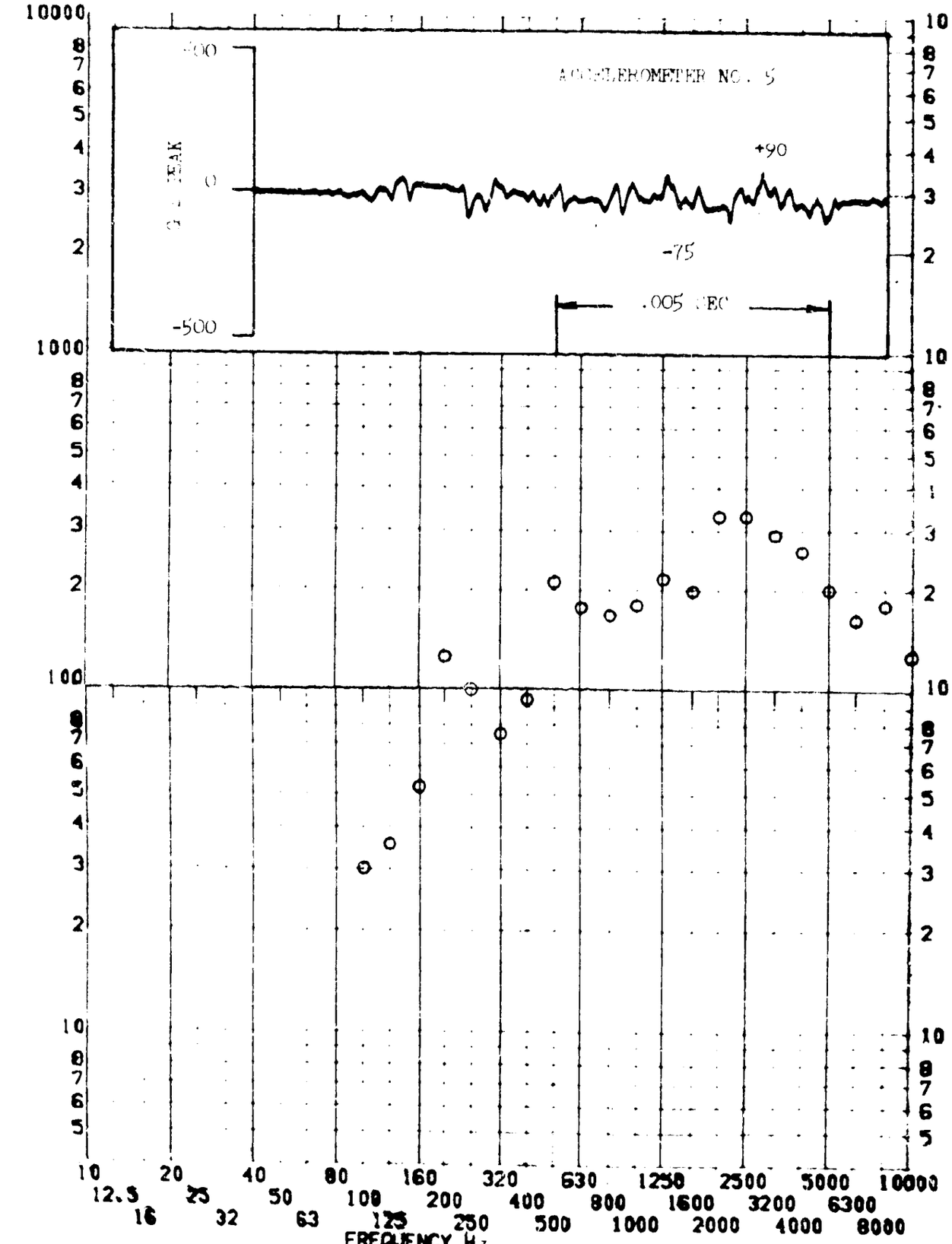

SHOCK TEST ANALYSIS DATA SHEET II.B.2.22

TEST ITEM 867-86
SERIAL NO.
SHOCK AXIS LATERAL

PART NO. [illegible]
TEST DATE 2 NOV 1968
SHOCK NO. 2

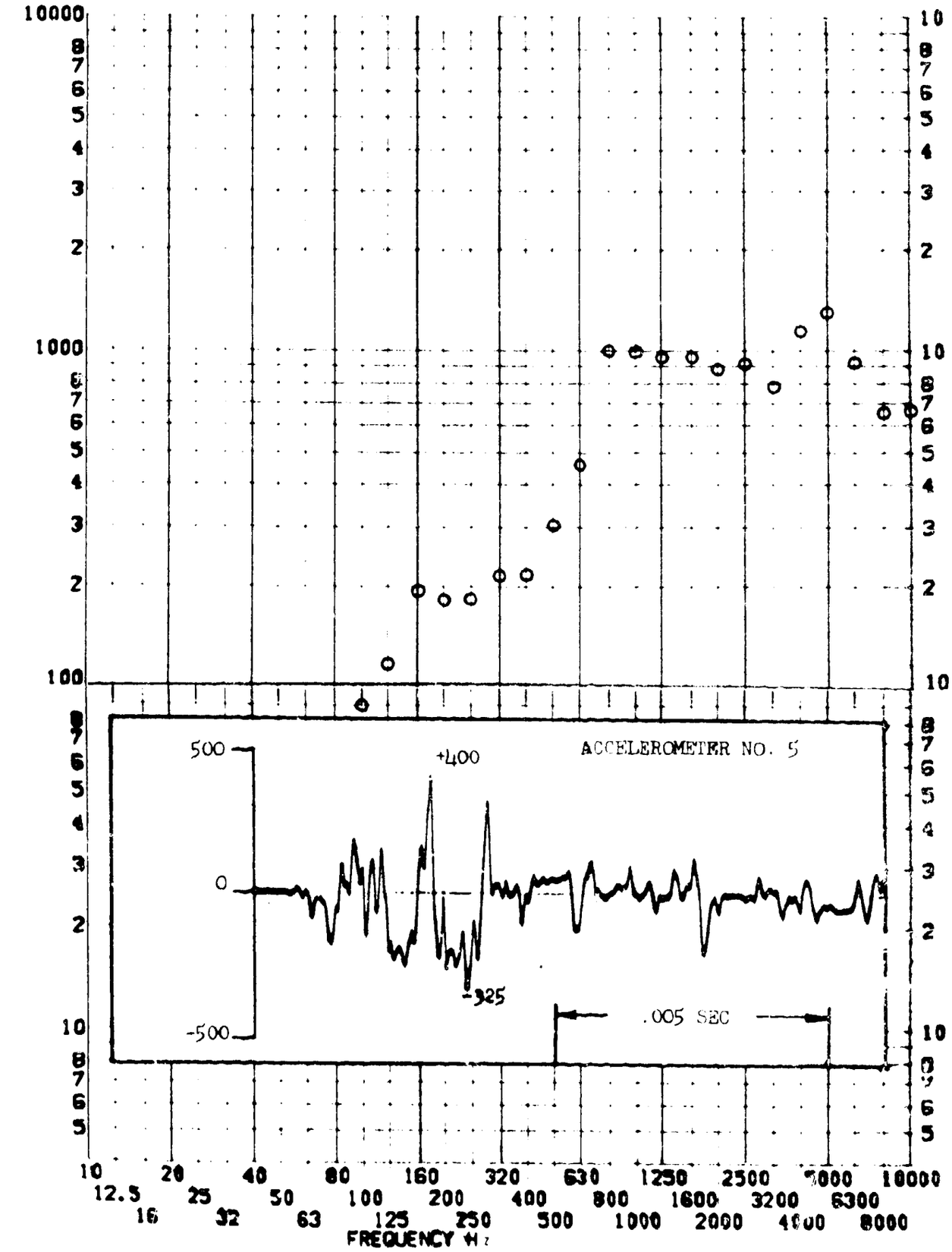

SHOCK TEST ANALYSIS DATA SHEET II.B.2.23

TEST ITEM 867-87
SERIAL NO.
SHOCK AXIS LATERAL

PART NO. STRUCTURE
TEST DATE 2 NOV 1962
SHOCK NO. 3

RESPONSE G-S

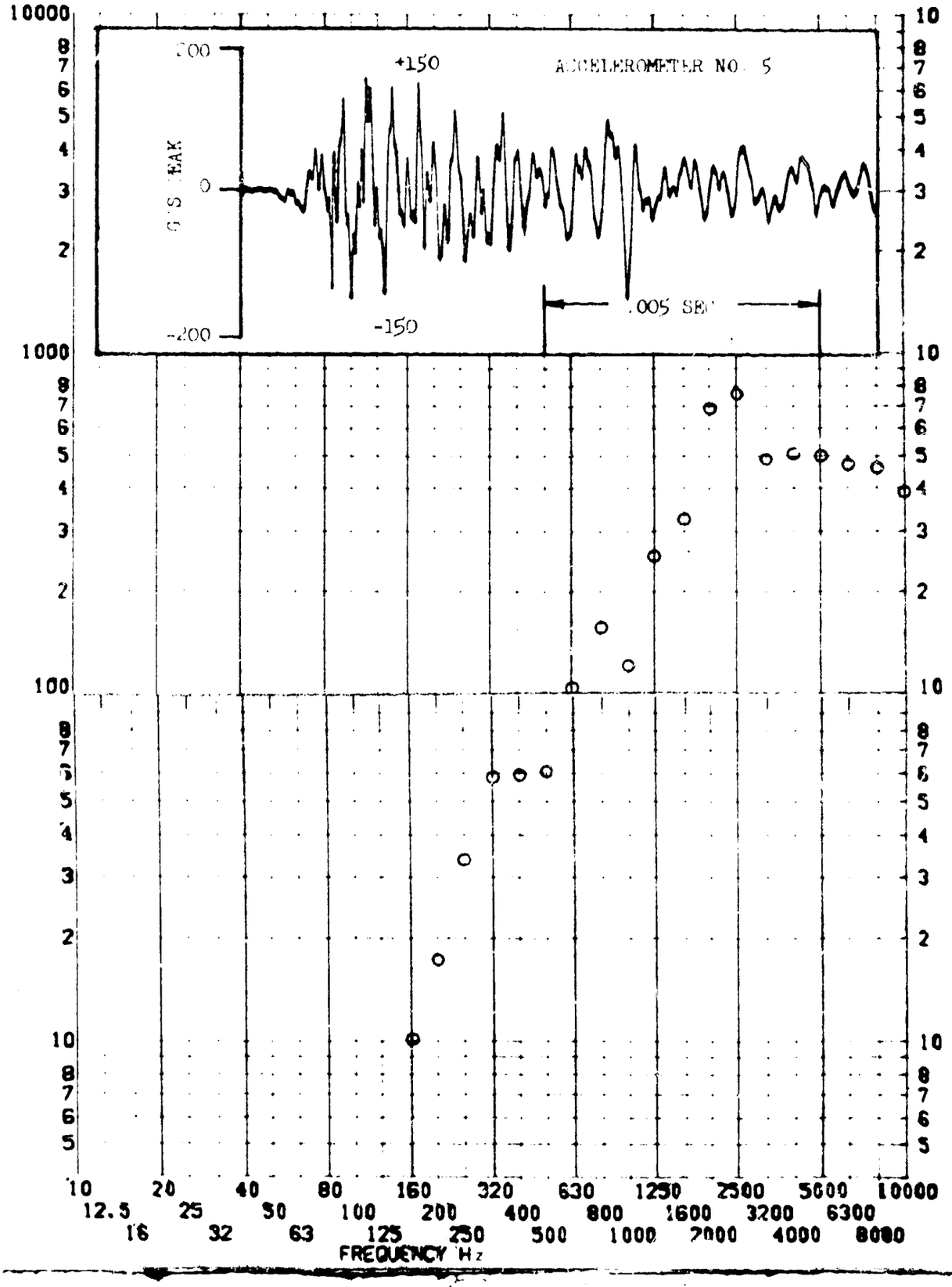

SHOCK TEST ANALYSIS DATA SHEET

TEST ITEM 067-85
SERIAL NO.
SHOCK AXIS LATERAL

PART NO. STRUCTURE
TEST DATE 2
SHOCK NO. 4

RESPONSE G-S

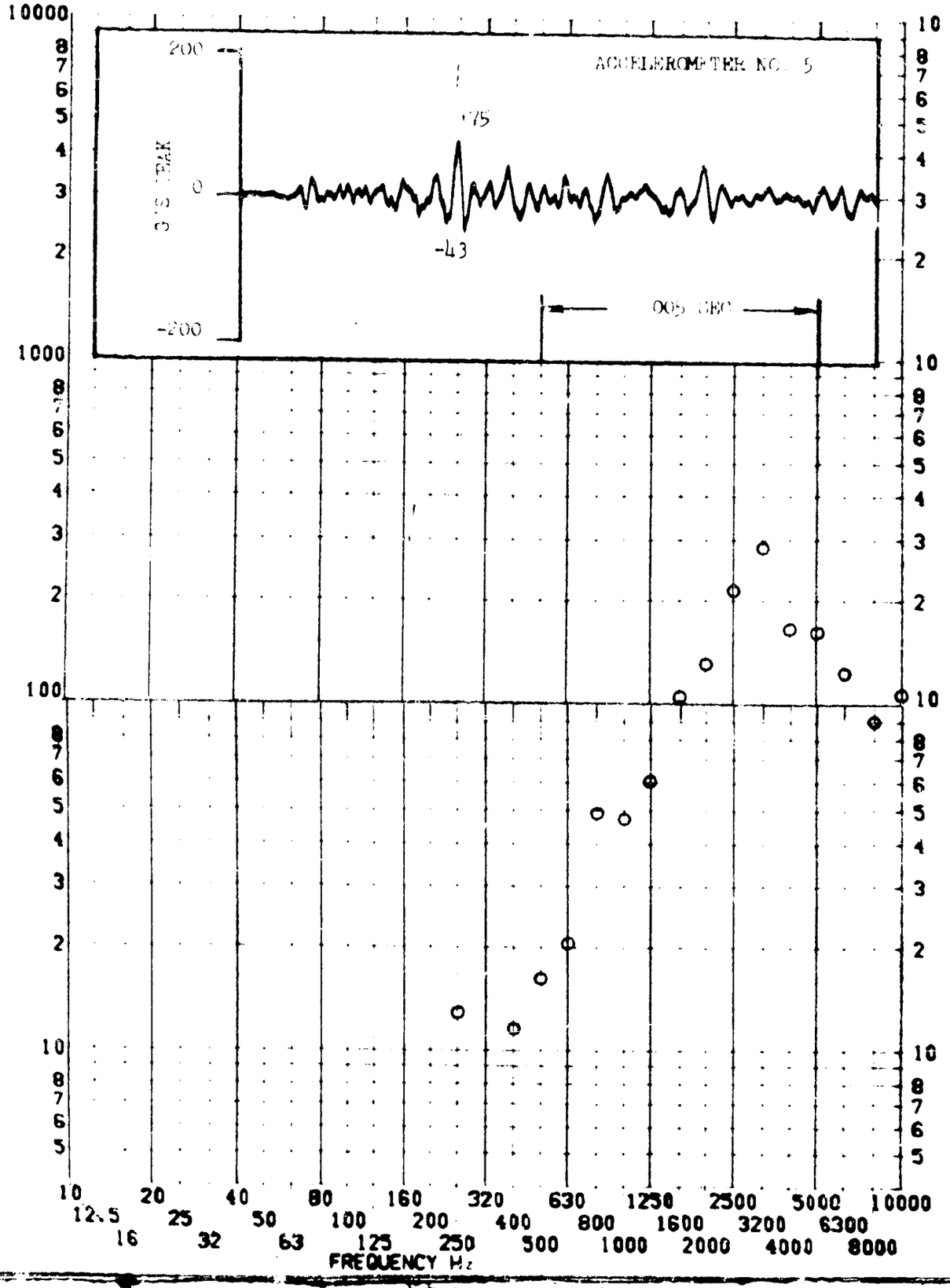

SHOCK TEST ANALYSIS DATA SHEET 11.8.2.15

TEST ITEM 86-88
SERIAL NO.
SHOCK AXIS RADIAL

PART NO. STRUCTURE
TEST DATE 2 NOV 196[illegible]
SHOCK NO. 1

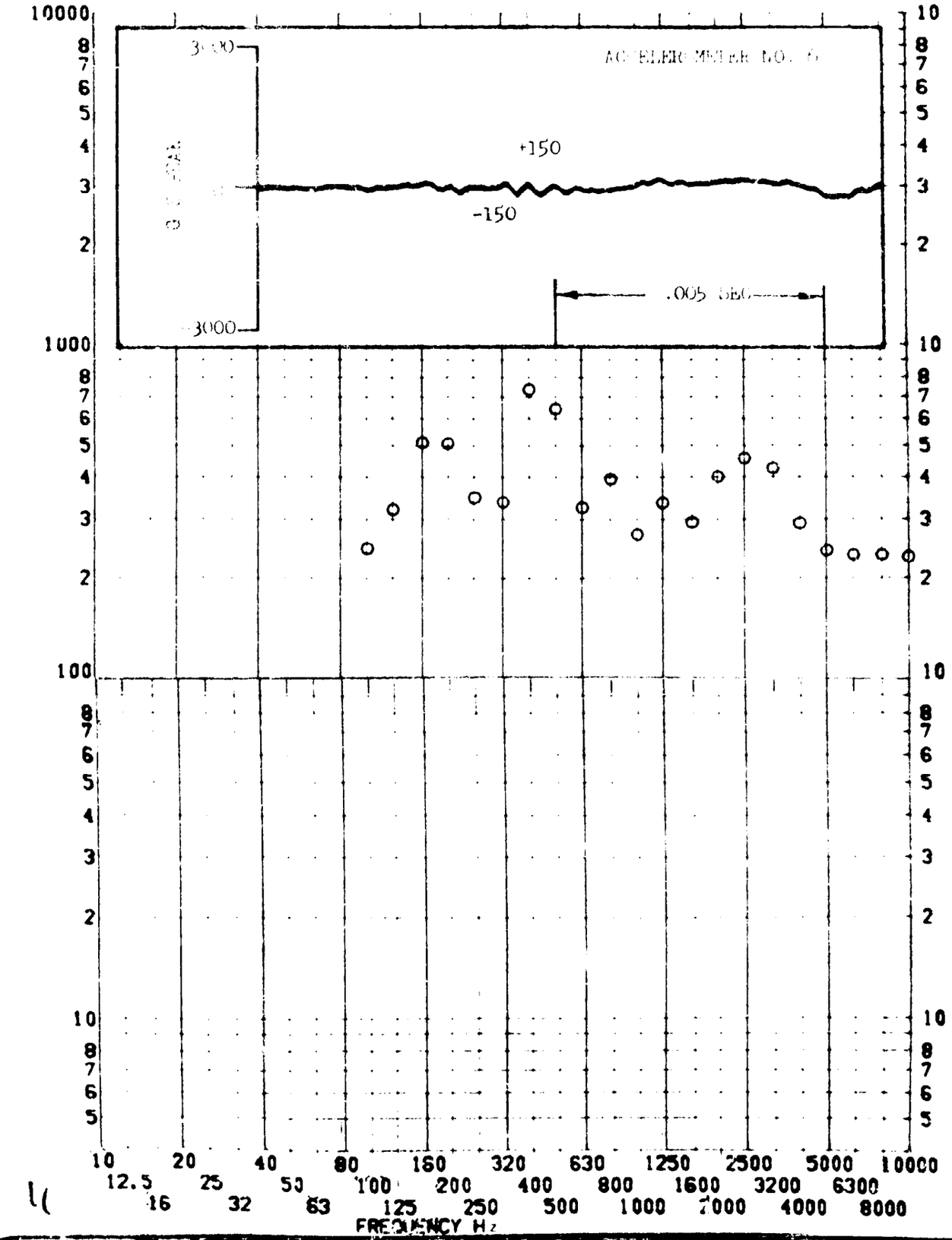

SHOCK TEST ANALYSIS DATA SHEET 11.B.2.25

TEST ITEM 867-90
SERIAL NO.
SHOCK AXIS RADIAL

PART NO. SPACECRAFT
TEST DATE 2 NOV 1969
SHOCK NO. 2

RESPONSE G-S

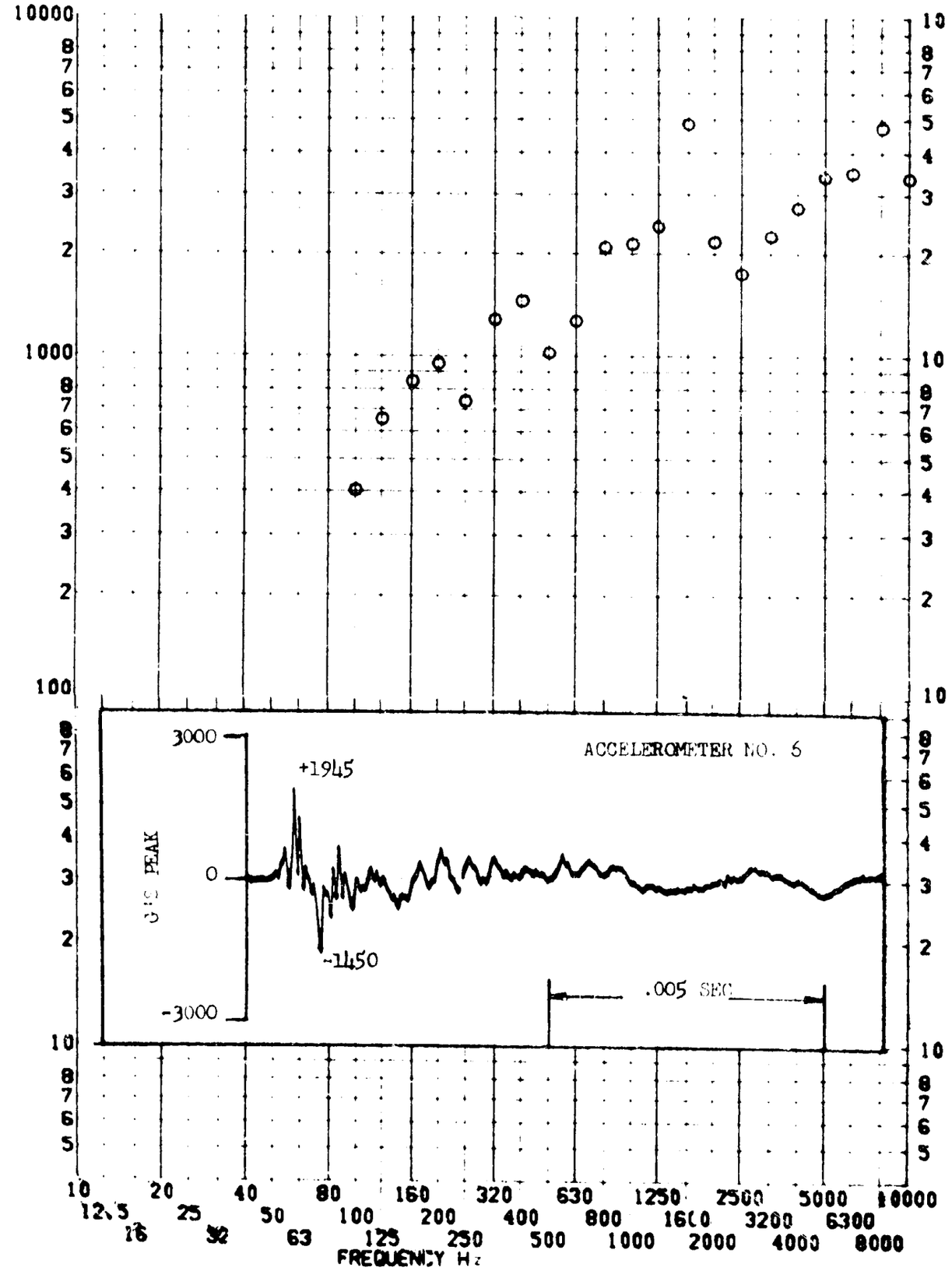

SHOCK TEST ANALYSIS DATA SHEET

TEST ITEM 867-91
SERIAL NO.
SHOCK AXIS RADIAL

PART NO. STRUCTURE
TEST DATE 2 NOV 1968
SHOCK NO. 3

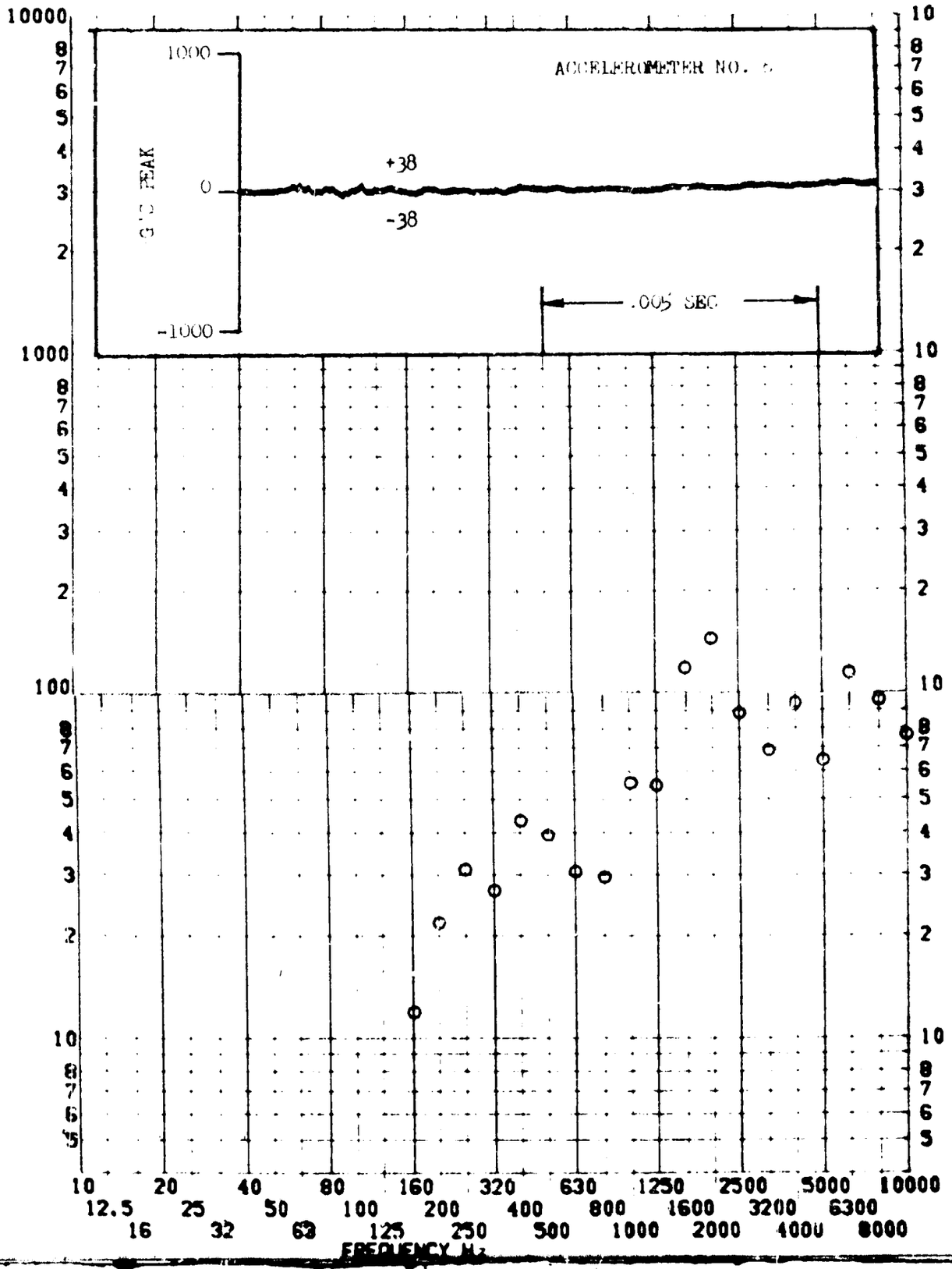

SHOCK TEST ANALYSIS DATA SHEET 11.8.2.38

TEST ITEM 867-92
SERIAL NO.
SHOCK AXIS TANGENTIAL

PART NO. STRUCTURE
TEST DATE [illegible]
SHOCK NO. 1

RESPONSE G-S

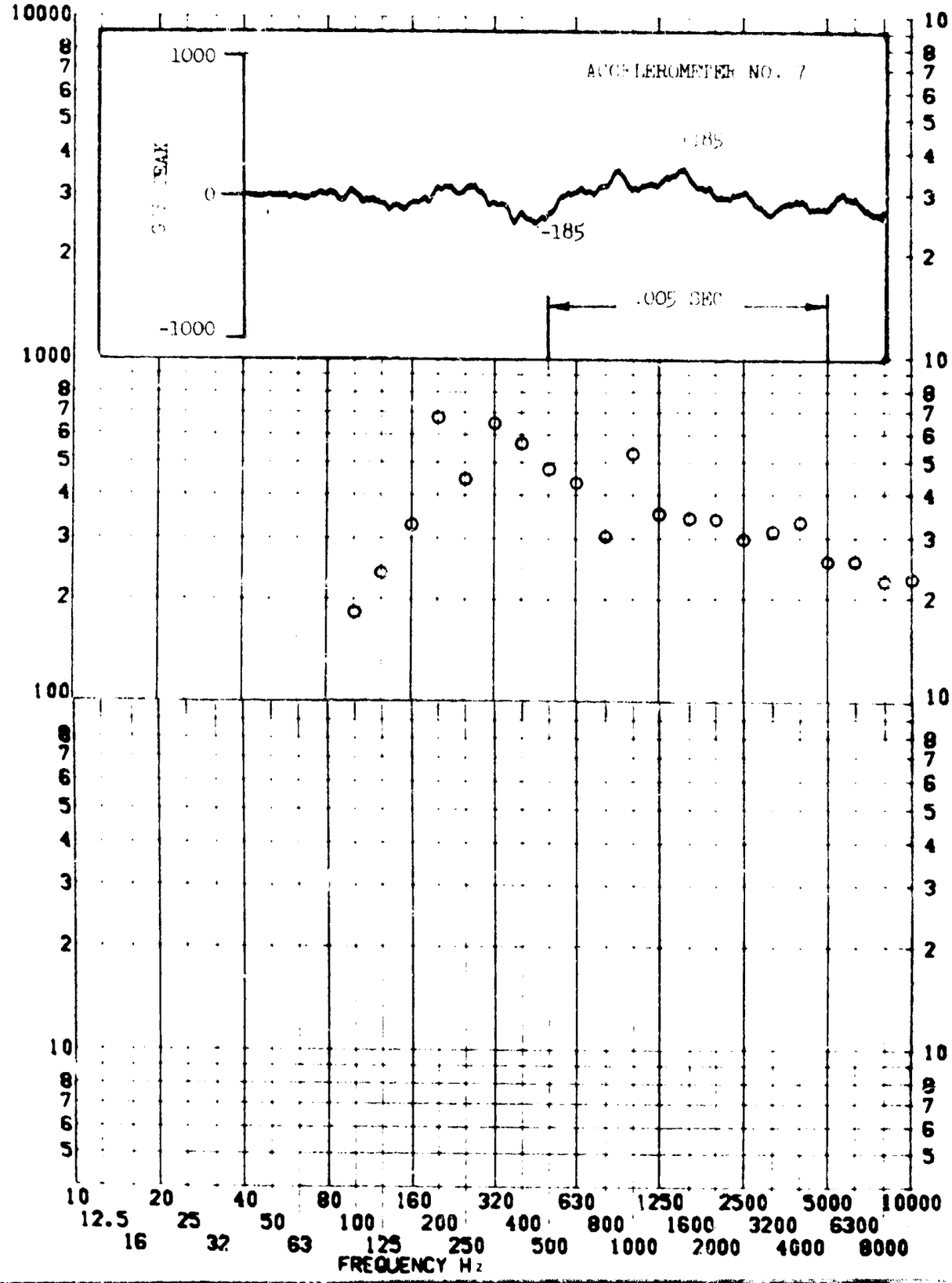

SHOCK TEST ANALYSIS DATA SHEET 11.8.2.29

TEST ITEM 867-9[illegible]
SERIAL NO.
SHOCK AXIS TANGENTIAL

PART NO. [illegible]
TEST DATE 2 NOV [illegible]
SHOCK NO.

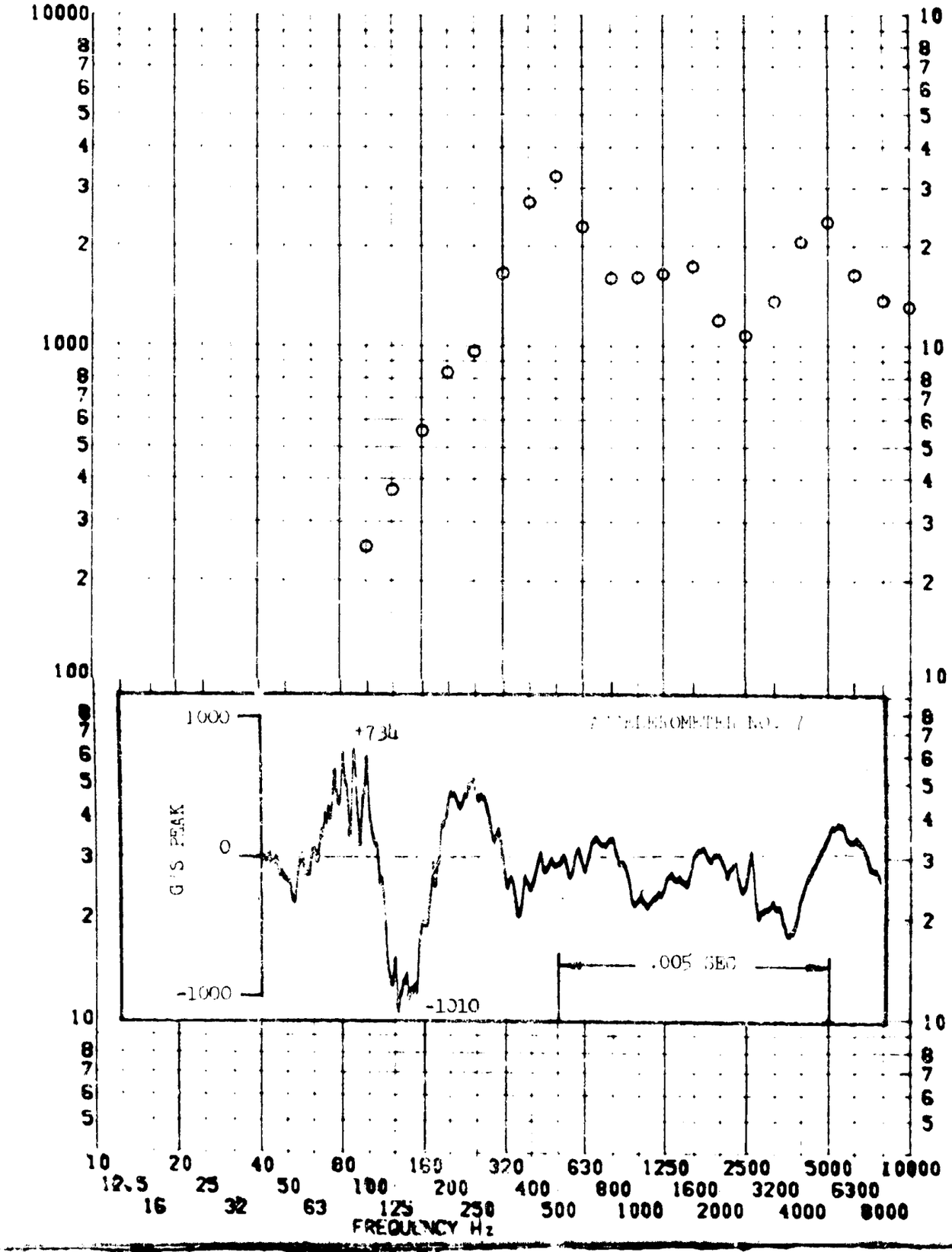

SHOCK TEST ANALYSIS DATA SHEET II.B.2.-0

TEST ITEM 867-95
SERIAL NO.
SHOCK AXIS TANGENTIAL

PART NO. STRUCTURE
TEST DATE 2 NOV 1969
SHOCK NO. 3

RESPONSE G-S

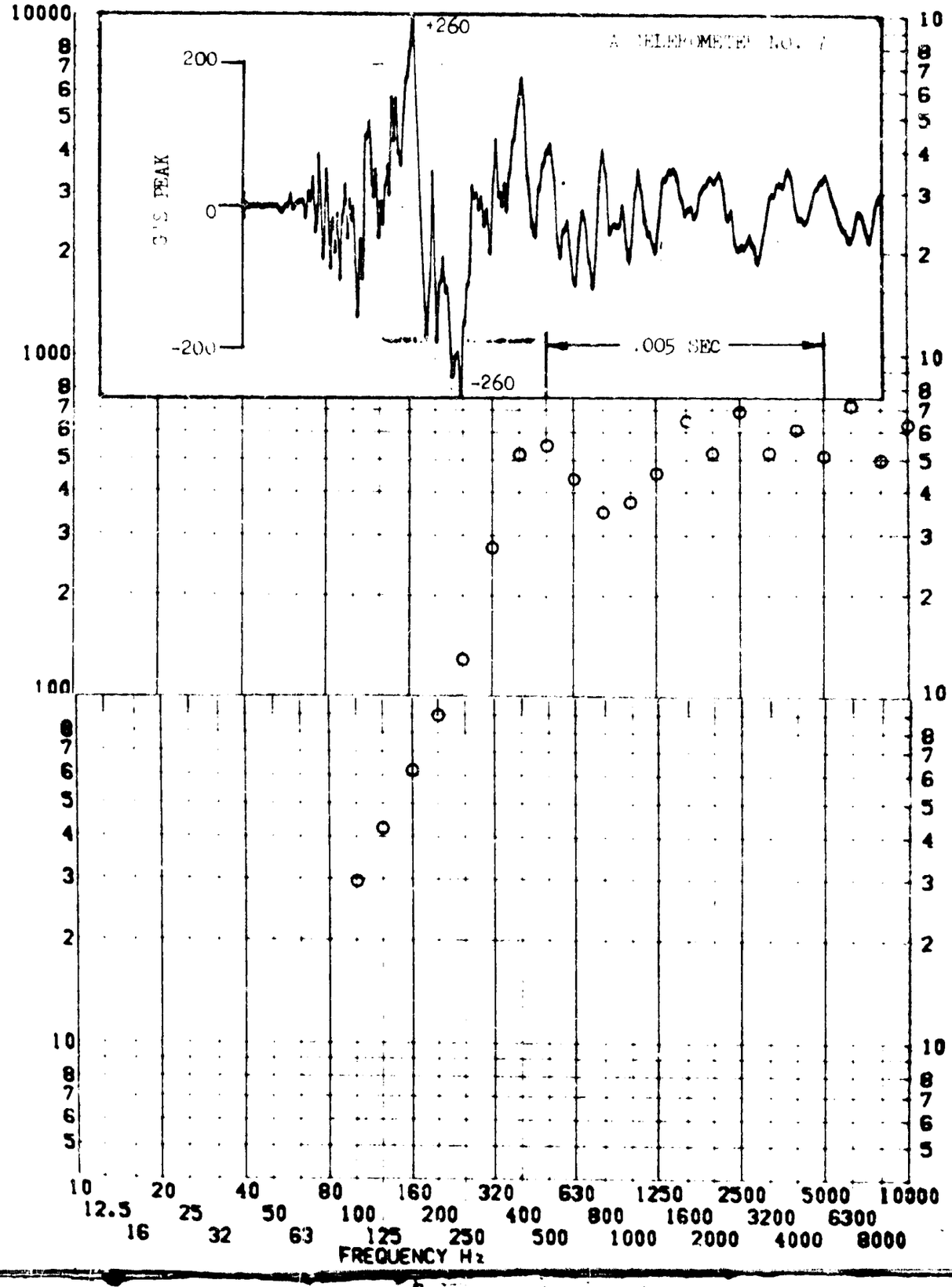

SHOCK TEST ANALYSIS DATA SHEET [illegible].2.31

TEST ITEM 867-93 PART NO. STRUCTURE
SERIAL NO. TEST DATE 2 [illegible] V 1964
RESPONSE G-S SHOCK AXIS TANGENTIAL SHOCK NO. 4

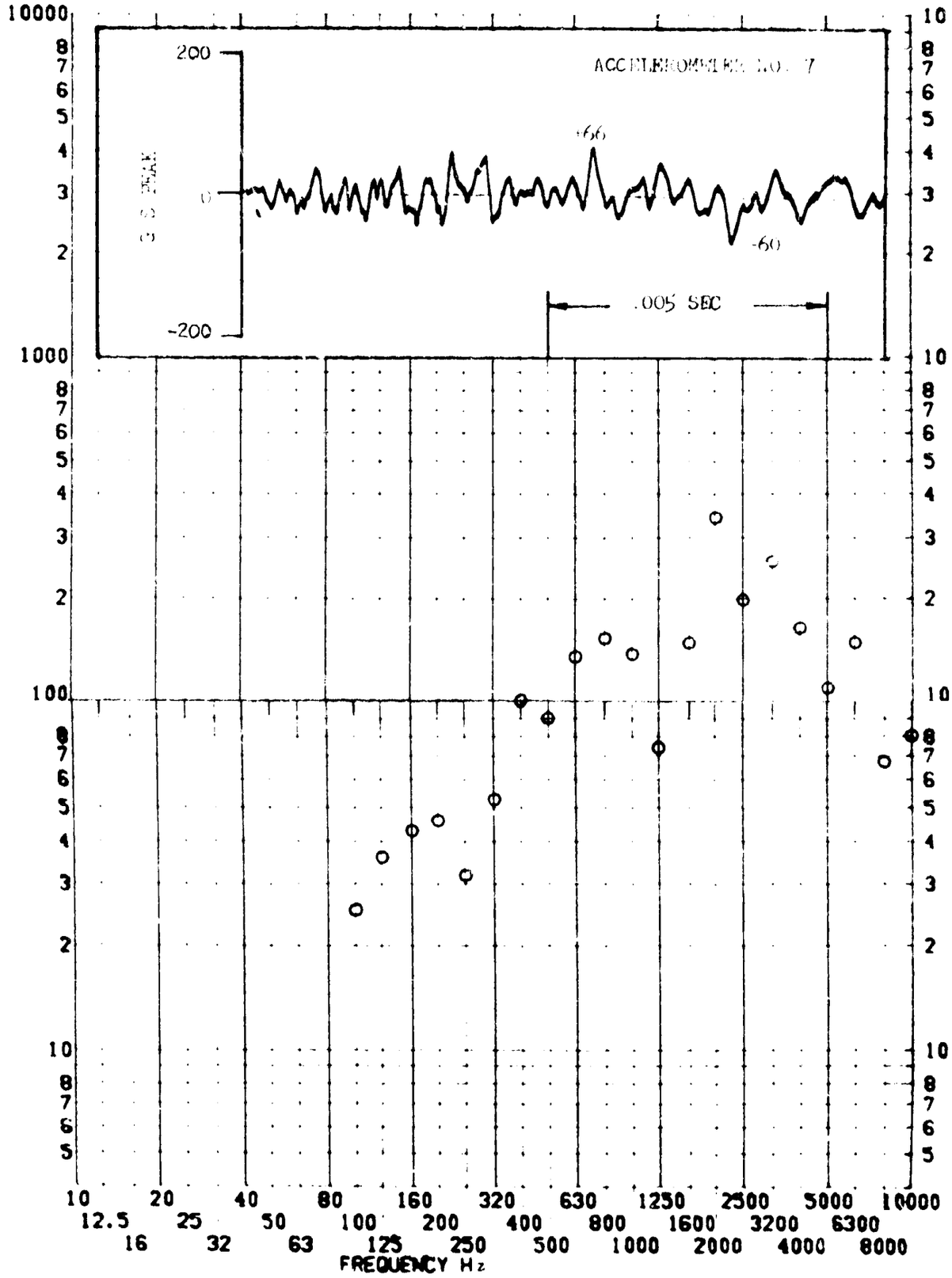

SHOCK TEST ANALYSIS DATA SHEET

T.P.2.32

TEST ITEM 867-6
SERIAL NO.
SHOCK AXIS LATERAL

PART NO.
TEST DATE
SHOCK NO.

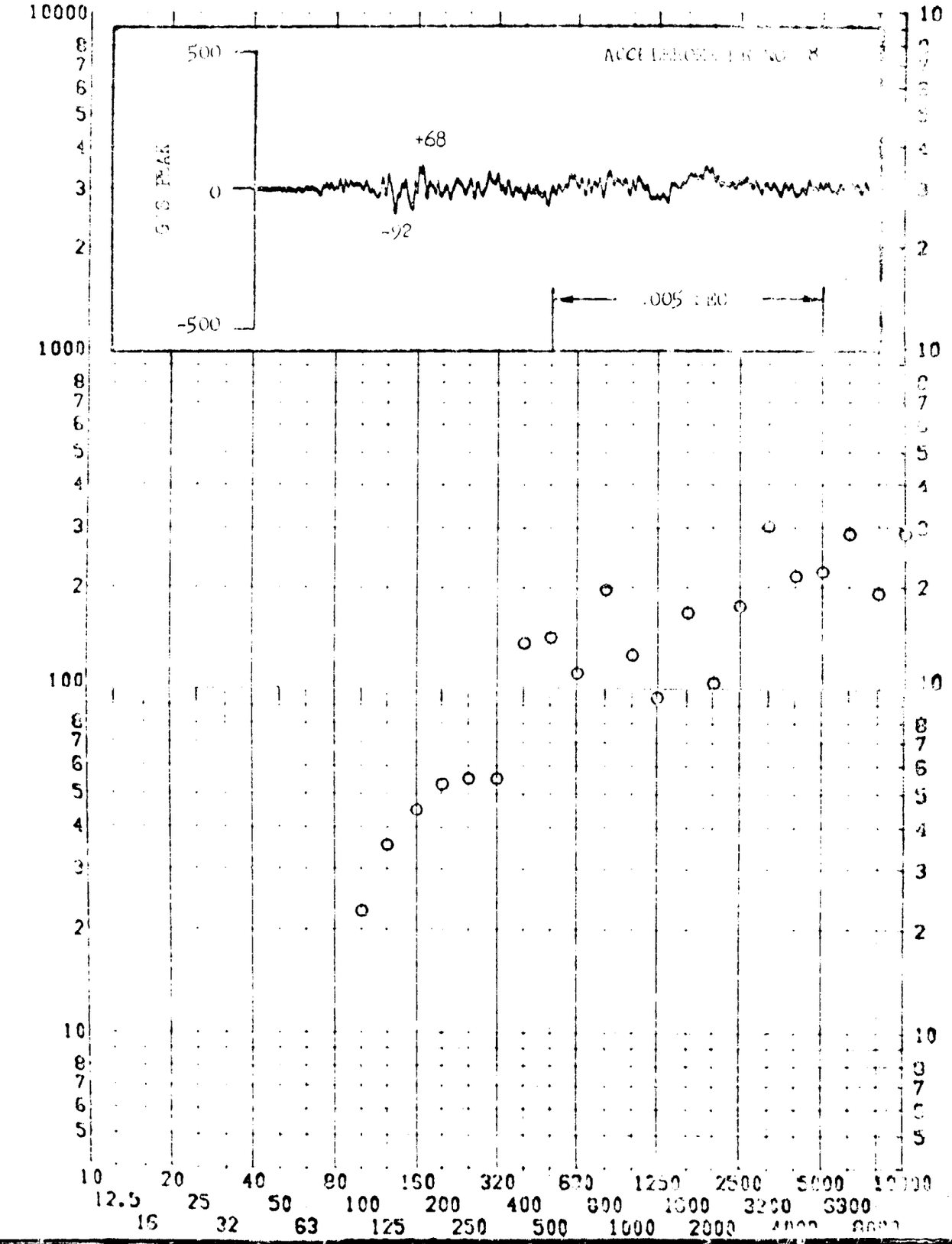

SHOCK TEST ANALYSIS DATA SHEET 11.P.2.33

TEST ITEM 867-8
SERIAL NO.
SHOCK AXIS LATERAL

PART NO. STRUCTURE
TEST DATE 2 [illegible] 1969
SHOCK NO. 2

RESPONSE G-S

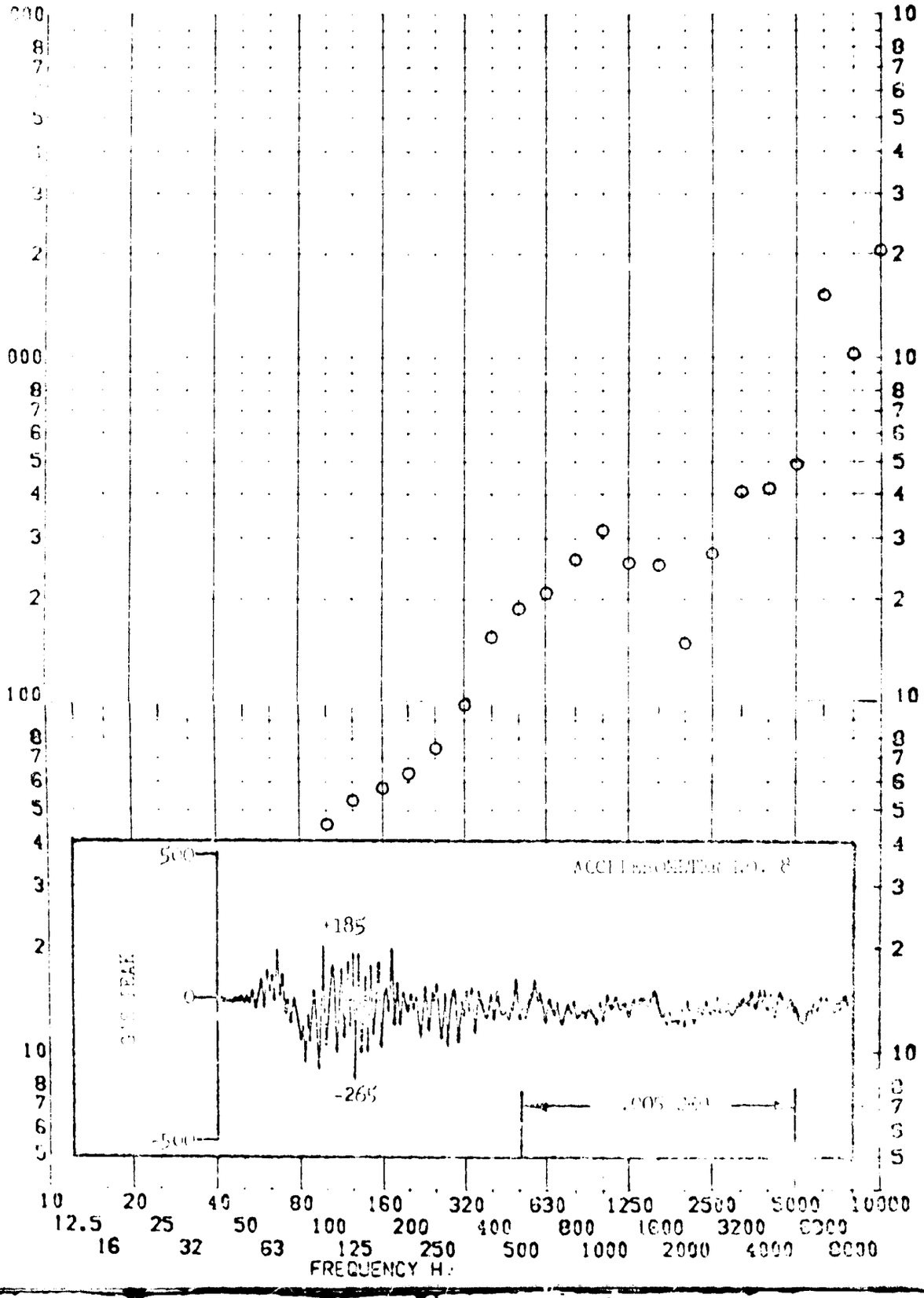

SHOCK TEST ANALYSIS DATA SHEET

TEST ITEM 367-[illegible]
SERIAL NO.
SHOCK AXIS LATERAL

PART NO. STRUCTURE
TEST DATE [illegible] NOV 1968
SHOCK NO. 3

RESPONSE G-S

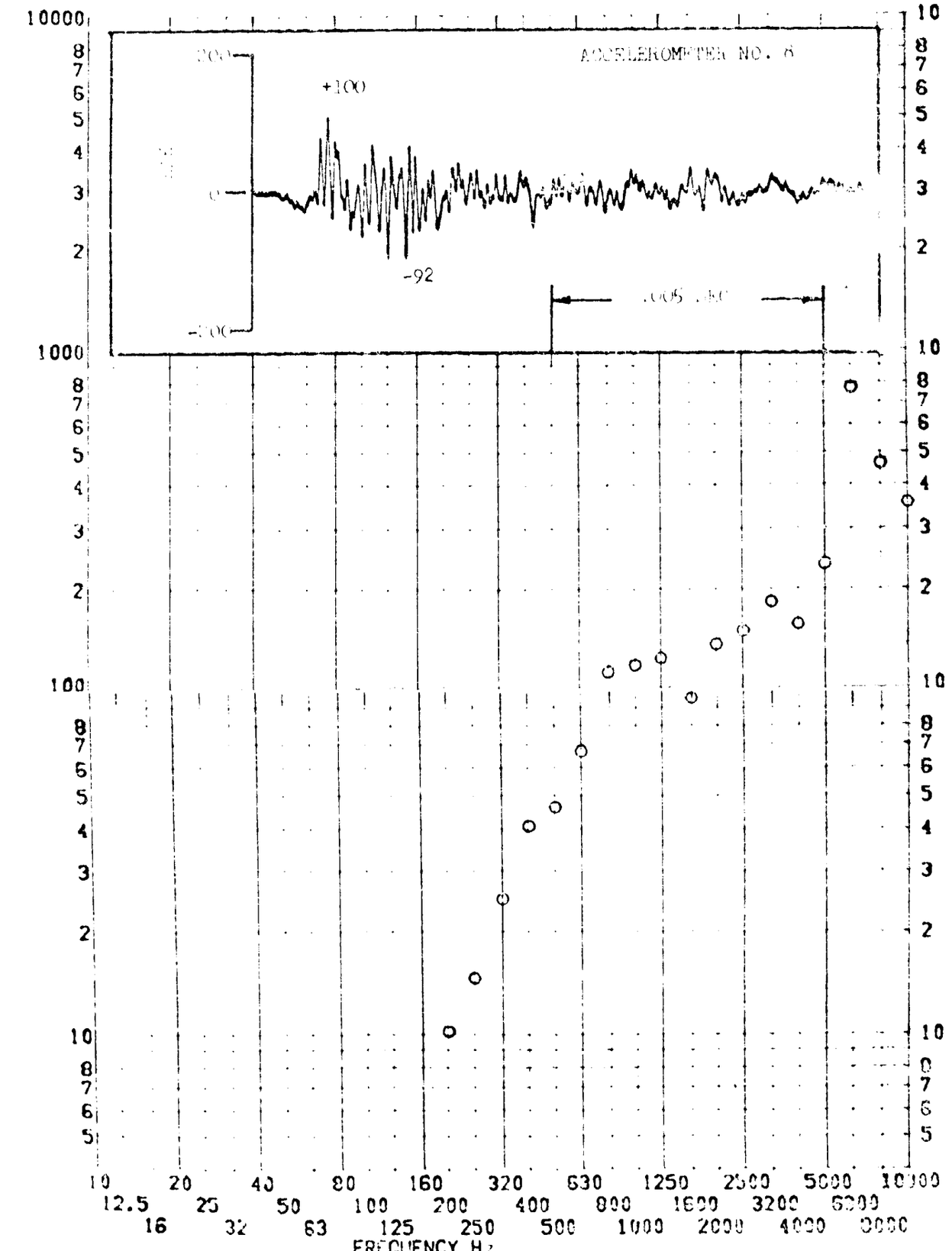

SHOCK TEST ANALYSIS DATA SHEET 11.5.2.35

TEST ITEM 867-97
SERIAL NO.
SHOCK AXIS

PART NO. STRUCTURE
TEST DATE 2 NOV 1964
SHOCK NO. 4

RESPONSE G-S

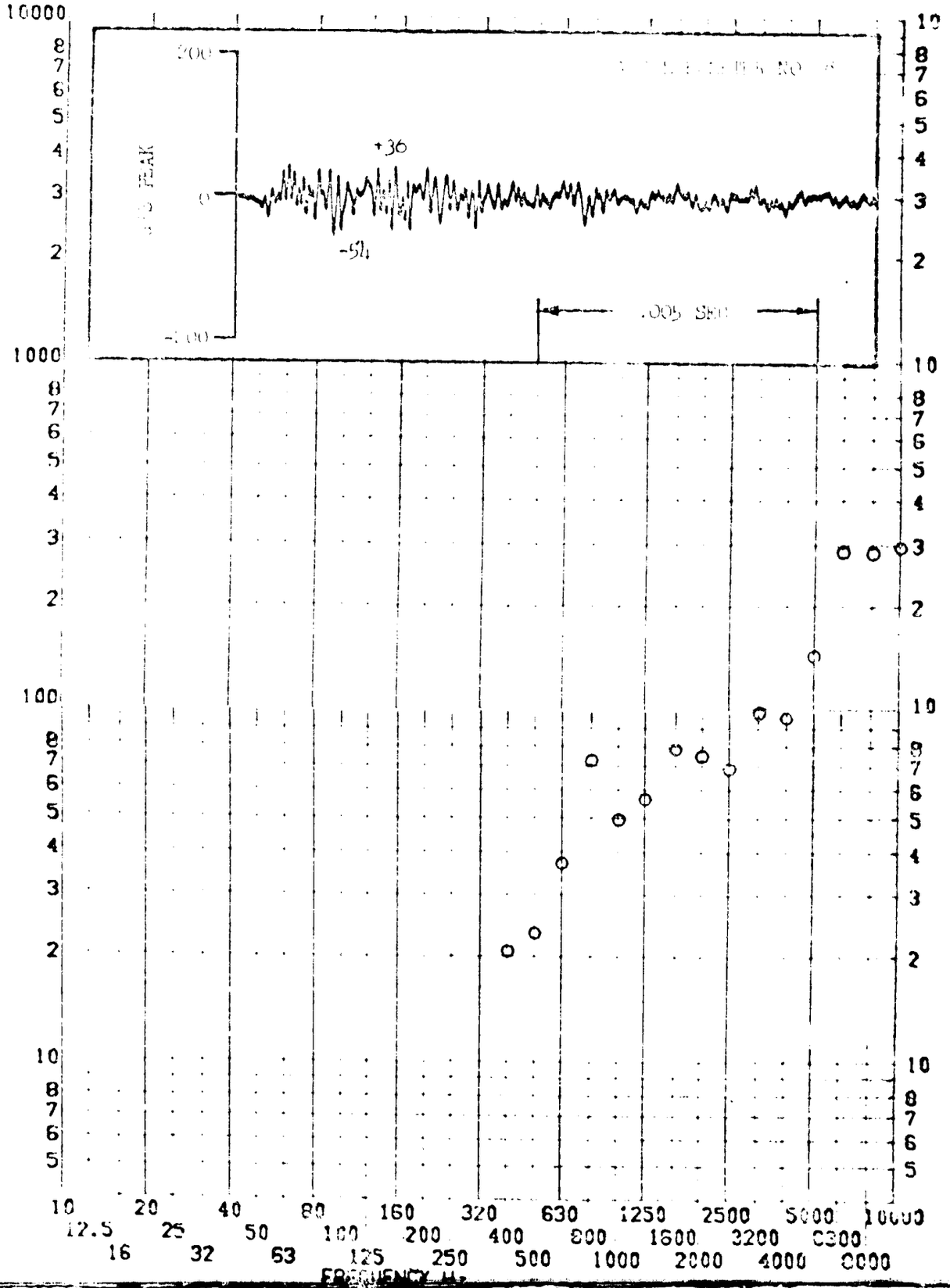

SHOCK TEST ANALYSIS DATA SHEET II.B.2.3[illegible]

TEST ITEM [illegible] PART NO. TRUSS

SERIAL NO. TEST DATE [illegible]

RESPONSE G-G SHOCK AXIS TANGENTIAL SHOCK NO.

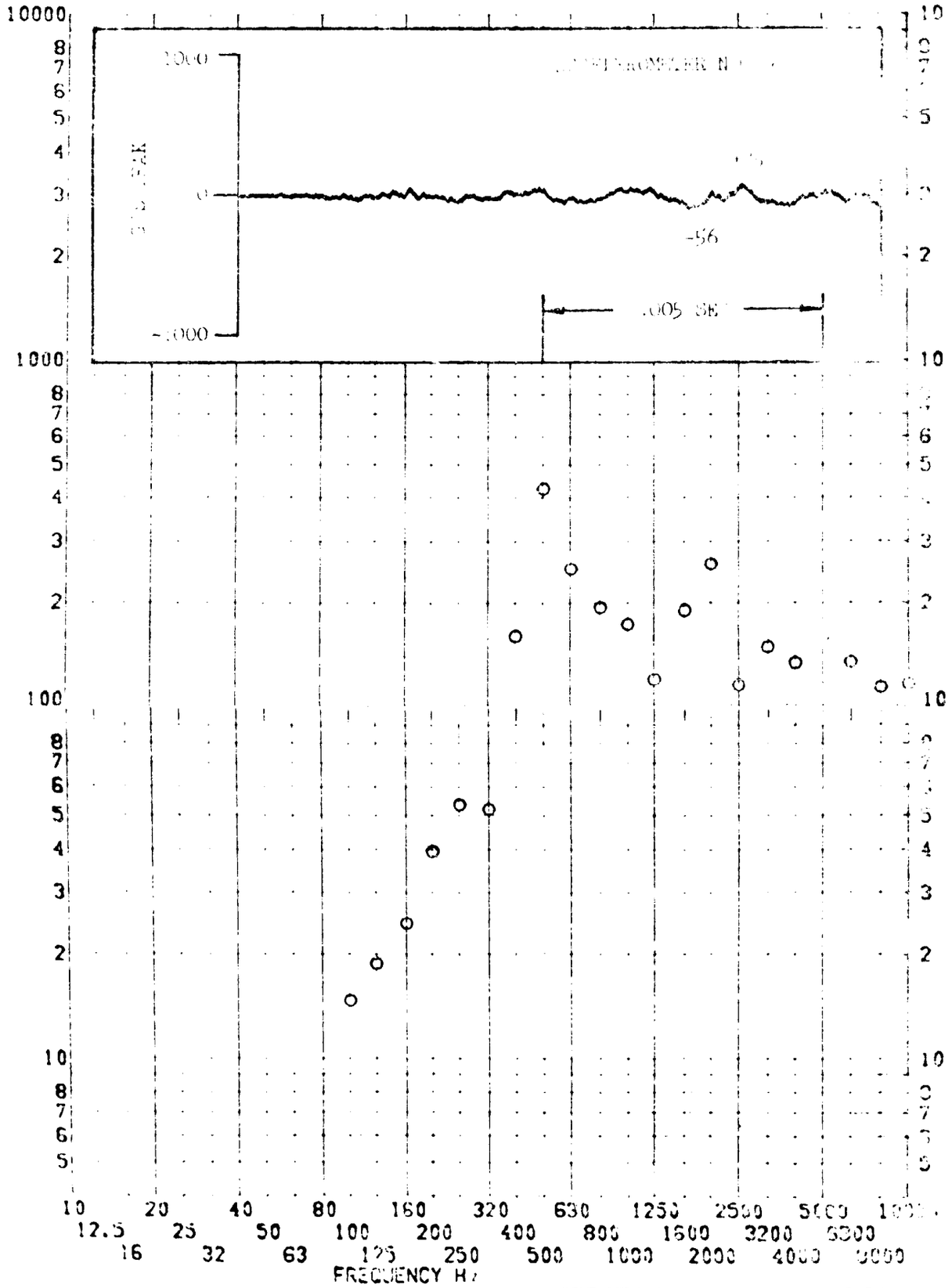

SHOCK TEST ANALYSIS DATA SHEET II.B.2.37

TEST ITEM 867-102
SERIAL NO.
SHOCK AXIS TANGENTIAL

PART NO. STRUCTURE
TEST DATE 3 NOV 1964
SHOCK NO. 2

RESPONSE G-S

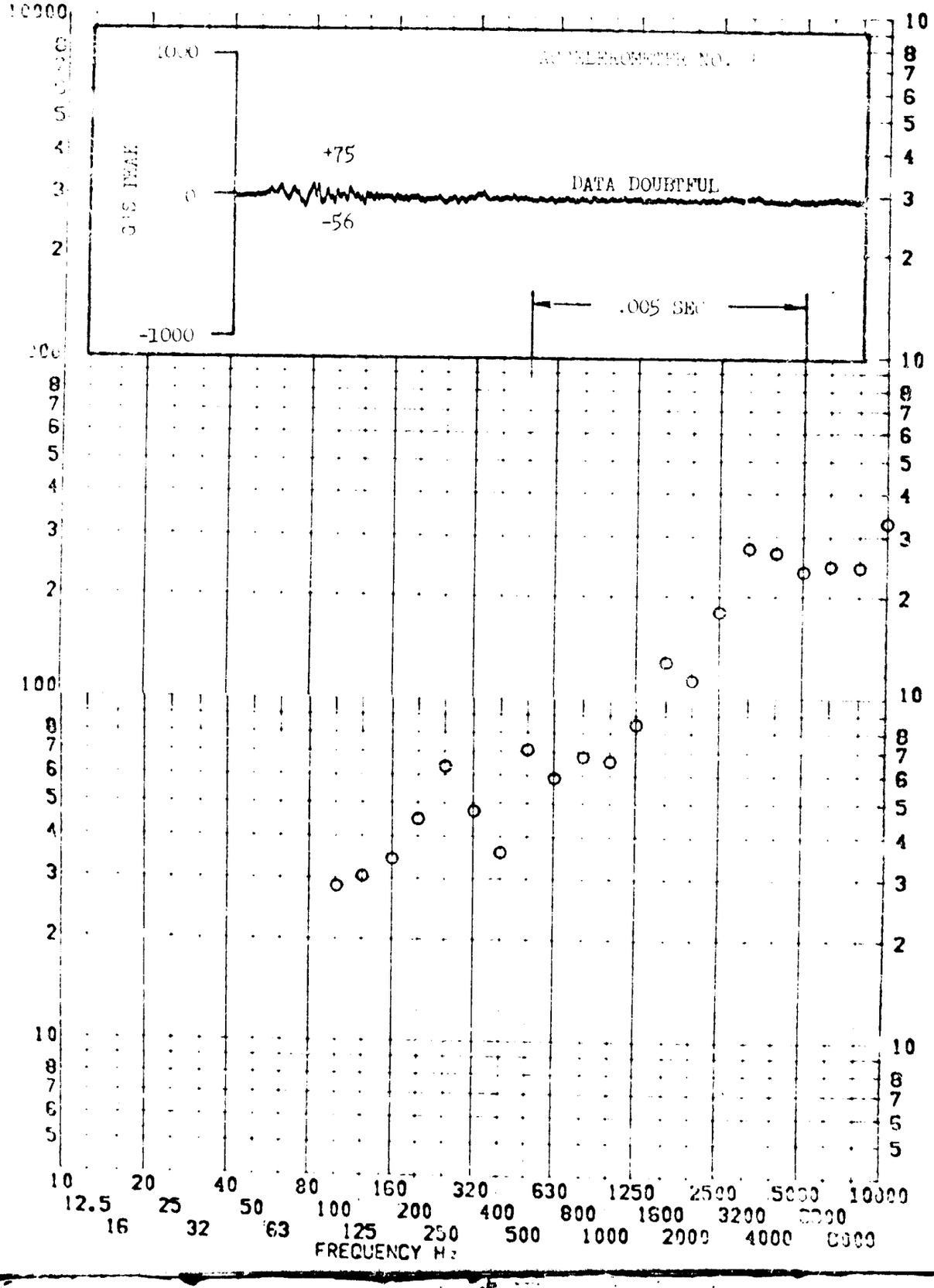

SHOCK TEST ANALYSIS DATA SHEET

TEST ITEM 807-303
SERIAL NO.
SHOCK AXIS TANGENTIAL

PART NO.
TEST DATE 3 NOV 1964
SHOCK NO. 3

RESPONSE G-S

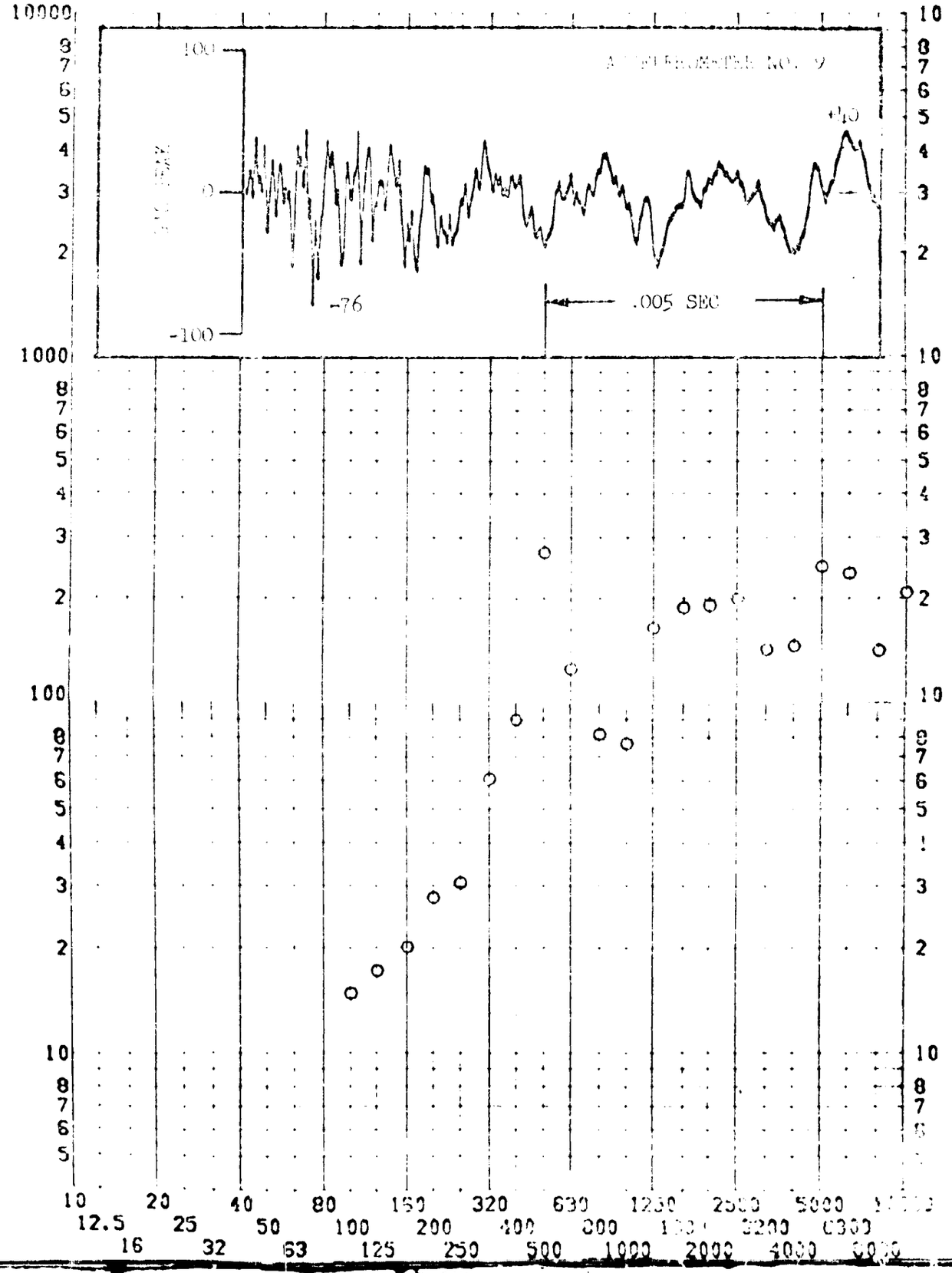

SHOCK TEST ANALYSIS DATA SHEET

TEST ITEM
SERIAL NO.
SHOCK AXIS

PART NO.
TEST DATE
SHOCK NO.

RESPONSE G-S

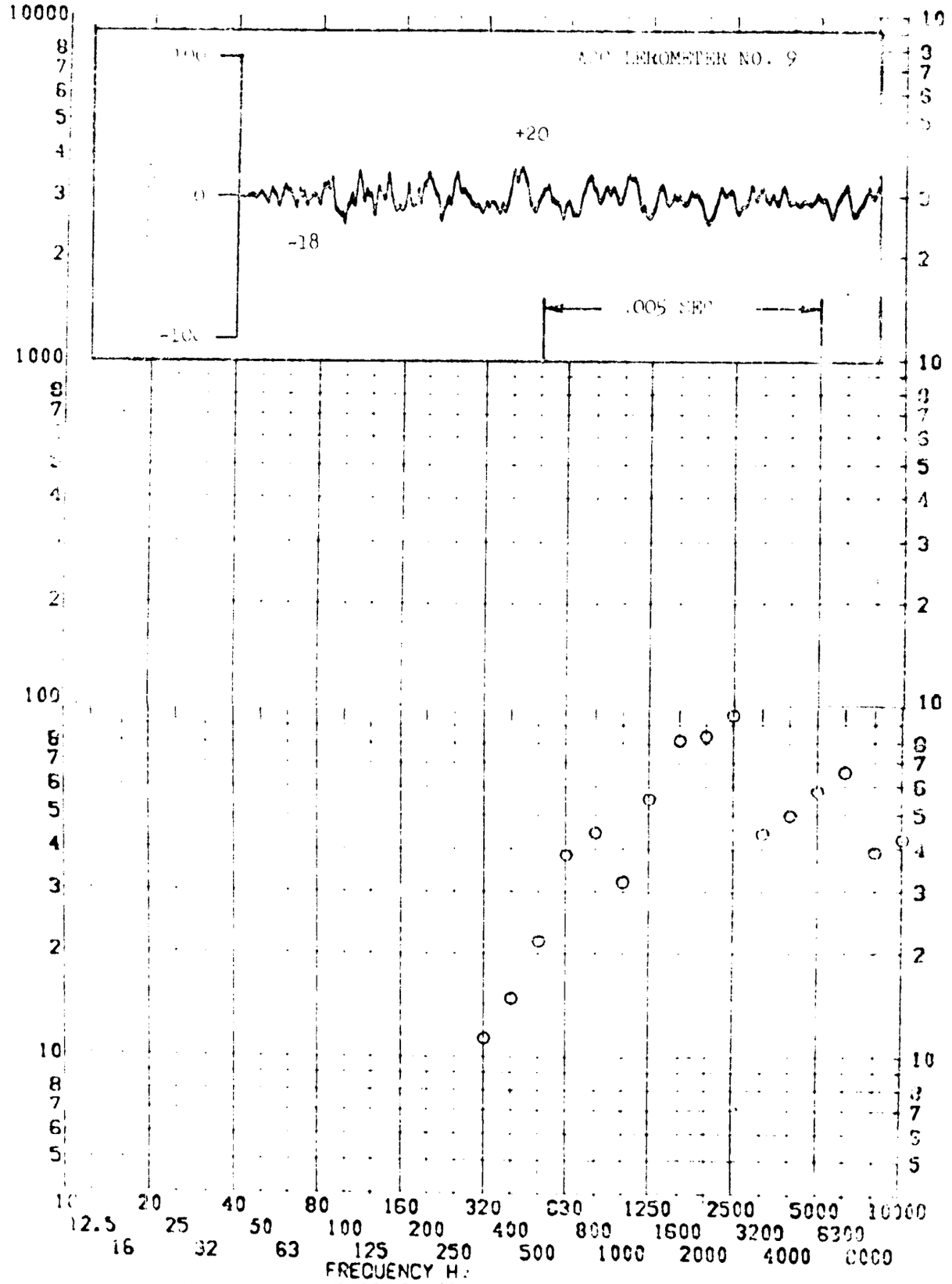

SHOCK TEST ANALYSIS DATA SHEET [illegible]

TEST ITEM [illegible]
SERIAL NO.
SHOCK AXIS [illegible]

PART NO. [illegible]
TEST DATE 2 [illegible] 196[illegible]
SHOCK NO. [illegible]

RESPONSE G-S

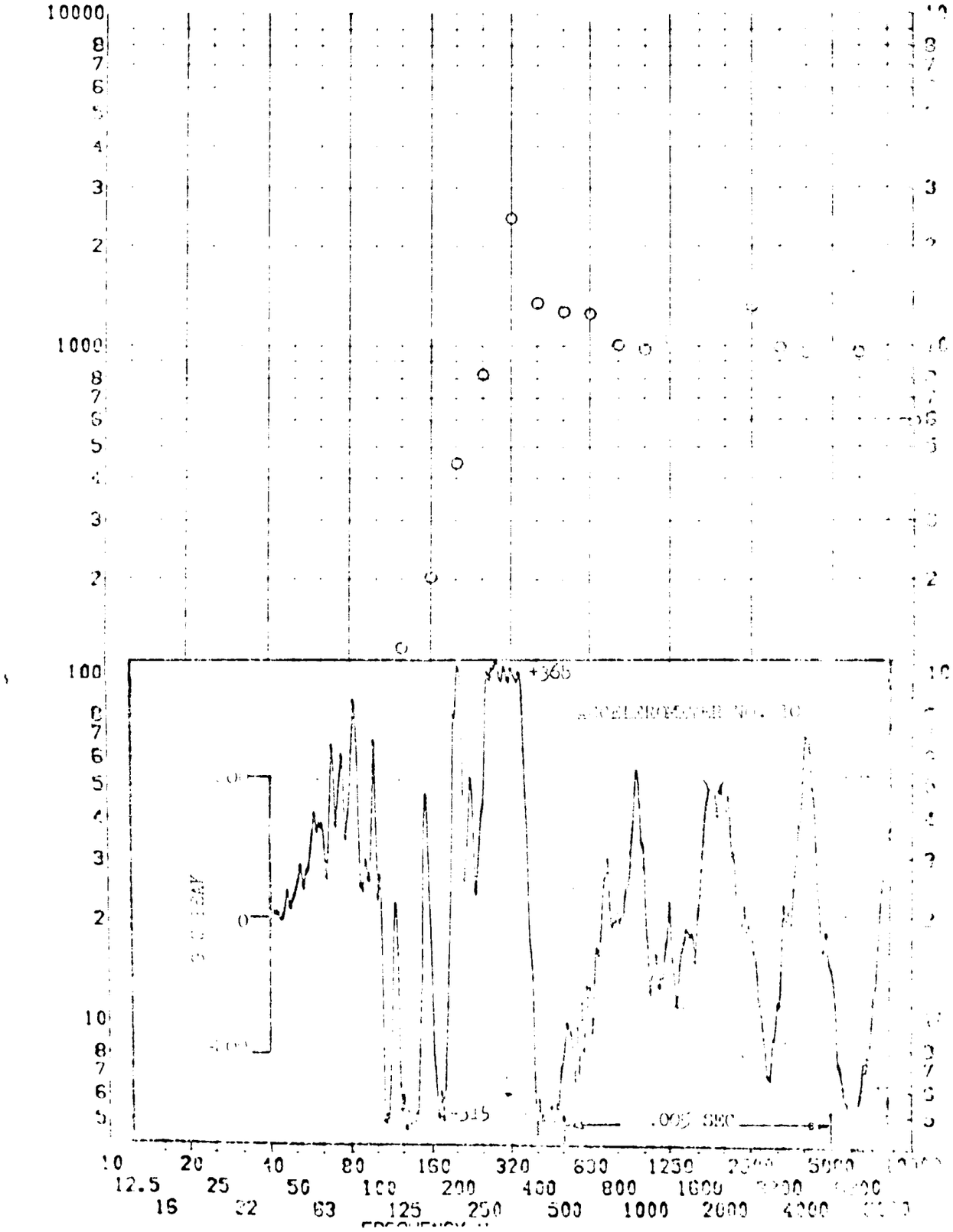

SHOCK TEST ANALYSIS DATA SHEET

TEST ITEM
SERIAL NO.
SHOCK AXIS

PART NO.
TEST DATE
SHOCK NO.

RESPONSE G-S

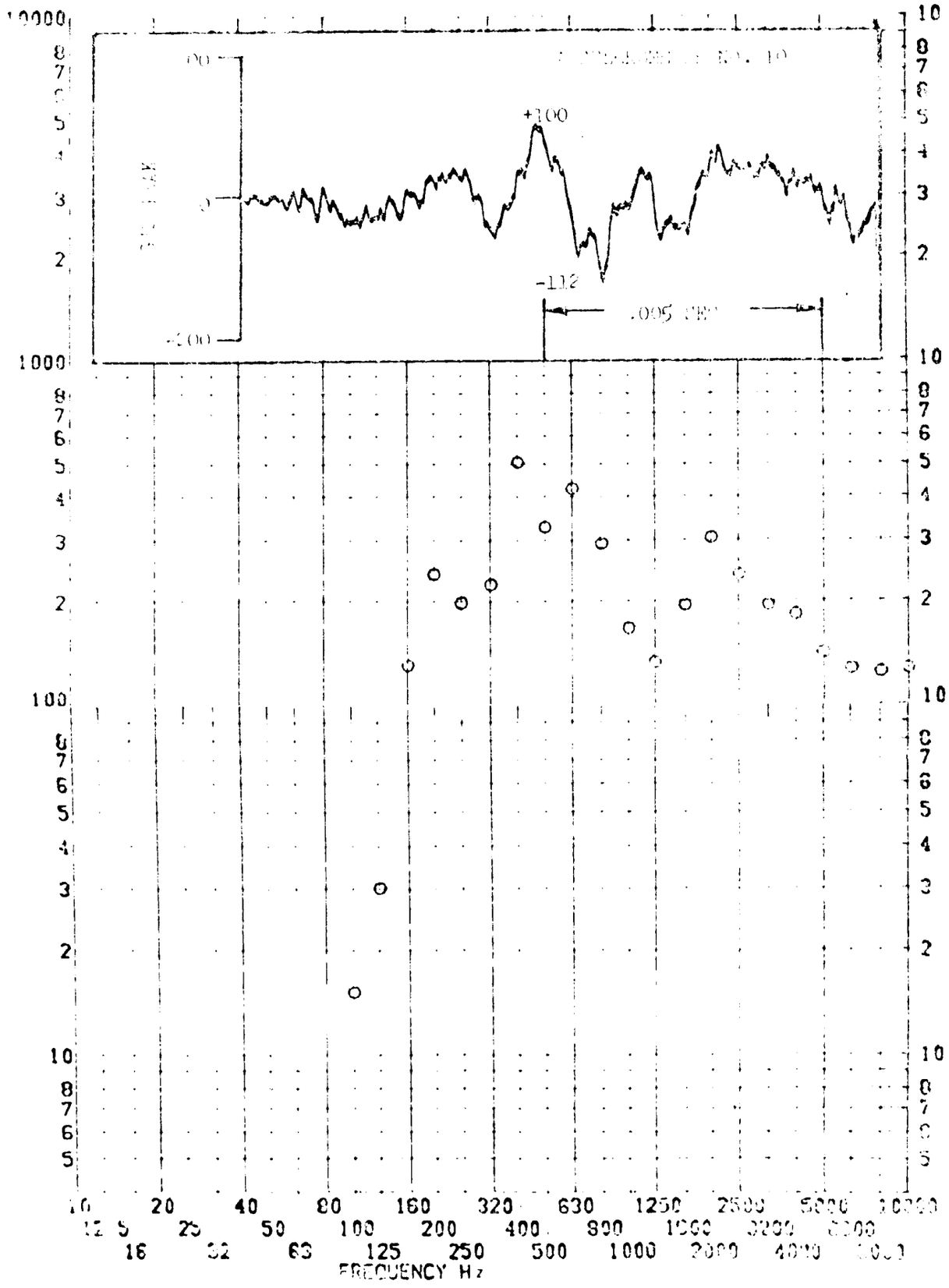

SHOCK TEST ANALYSIS DATA SHEET [illegible]

TEST ITEM [illegible] PART NO. [illegible]
SERIAL NO. TEST DATE [illegible]
RESPONSE G-S SHOCK AXIS [illegible] SHOCK NO. 3

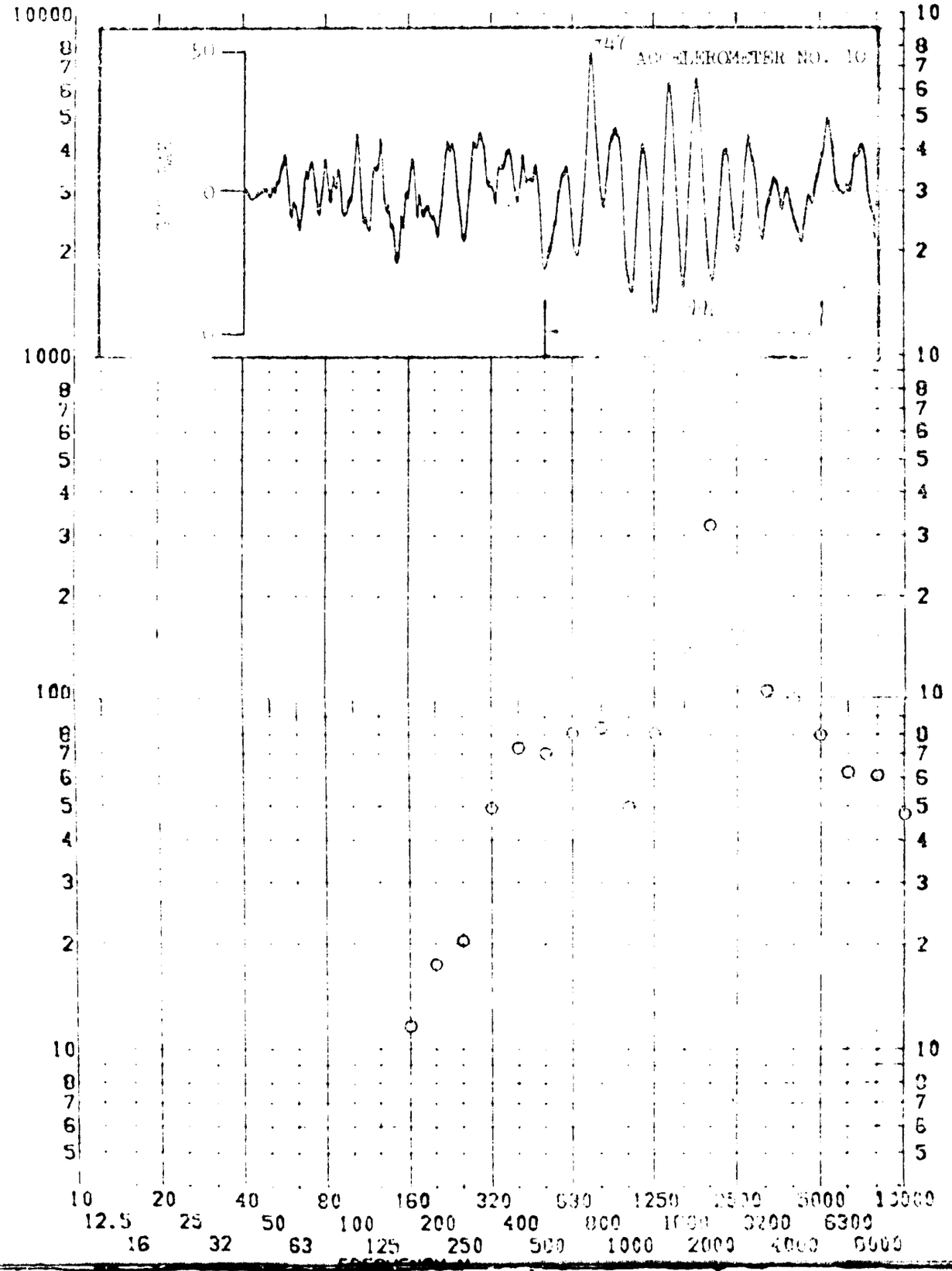

SHOCK TEST ANALYSIS DATA SHEET 11.B.2.43

TEST ITEM 85°-105 PART NO. STRUCTURE

SERIAL NO. TEST DATE 2 NOV 1964

RESPONSE G-S SHOCK AXIS TANGENTIAL SHOCK NO. 1

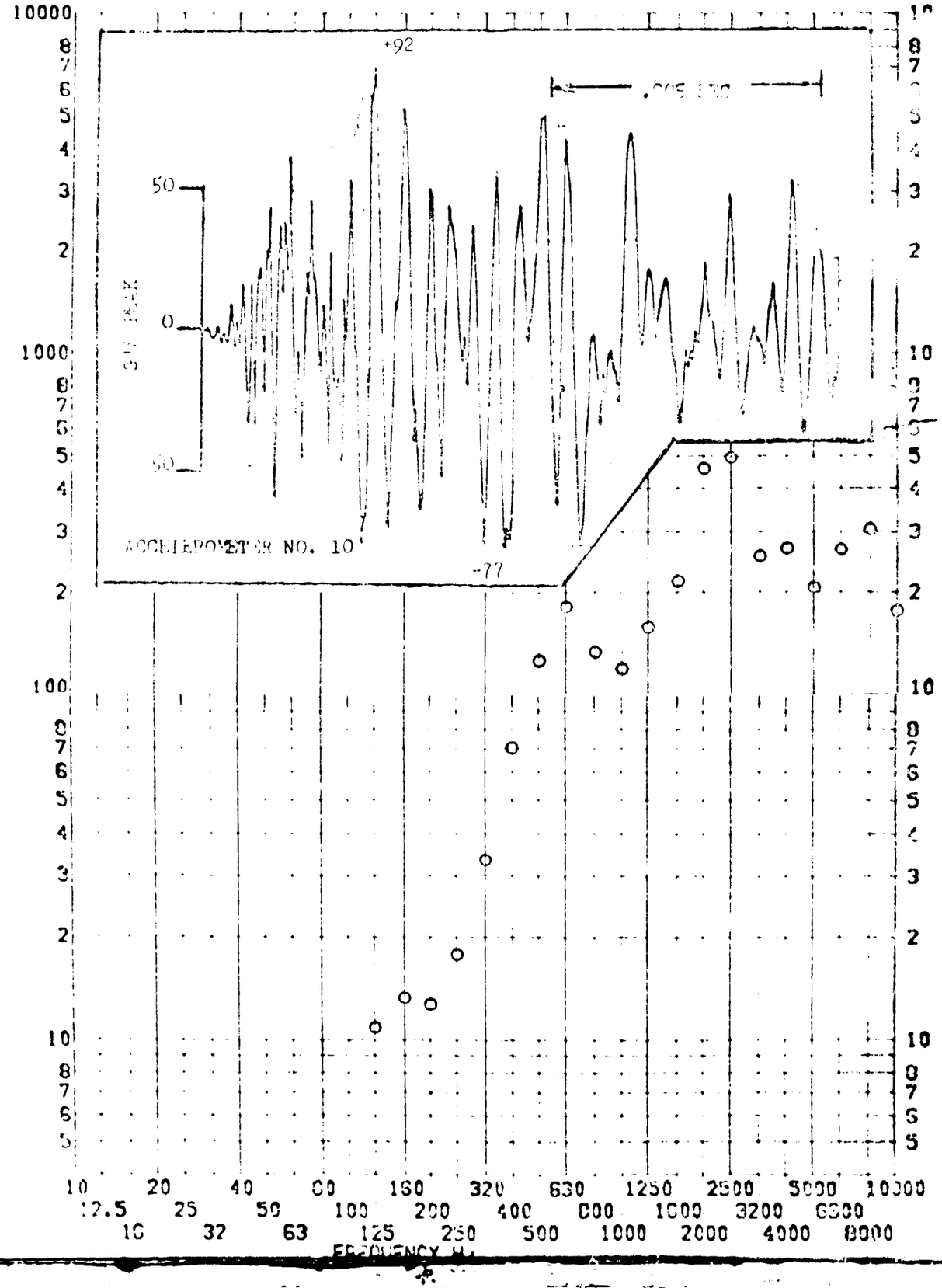

SHOCK TEST ANALYSIS DATA SHEET II.B.2.bb

TEST ITEM [illegible]
SERIAL NO.
SHOCK AXIS [illegible]

PART NO. [illegible]
TEST DATE 2 NOV 1[illegible]
SHOCK NO. 1

RESPONSE G-S

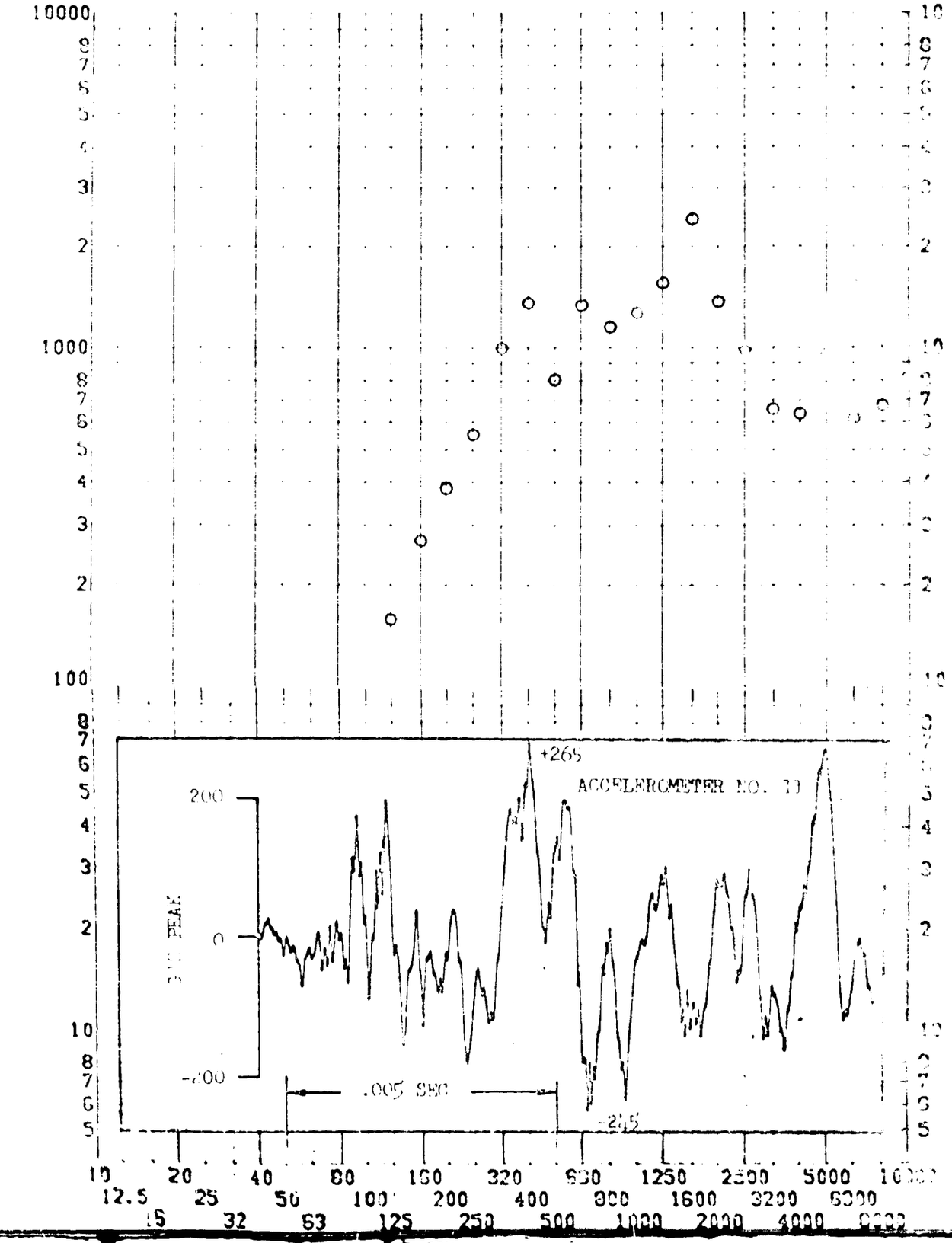

SHOCK TEST ANALYSIS DATA SHEET 11.8.2.45

TEST ITEM 867-110 — PART NO. [illegible]
SERIAL NO. — TEST DATE 2 NOV 1964
SHOCK AXIS RADIAL — SHOCK NO. 2

RESPONSE G-S

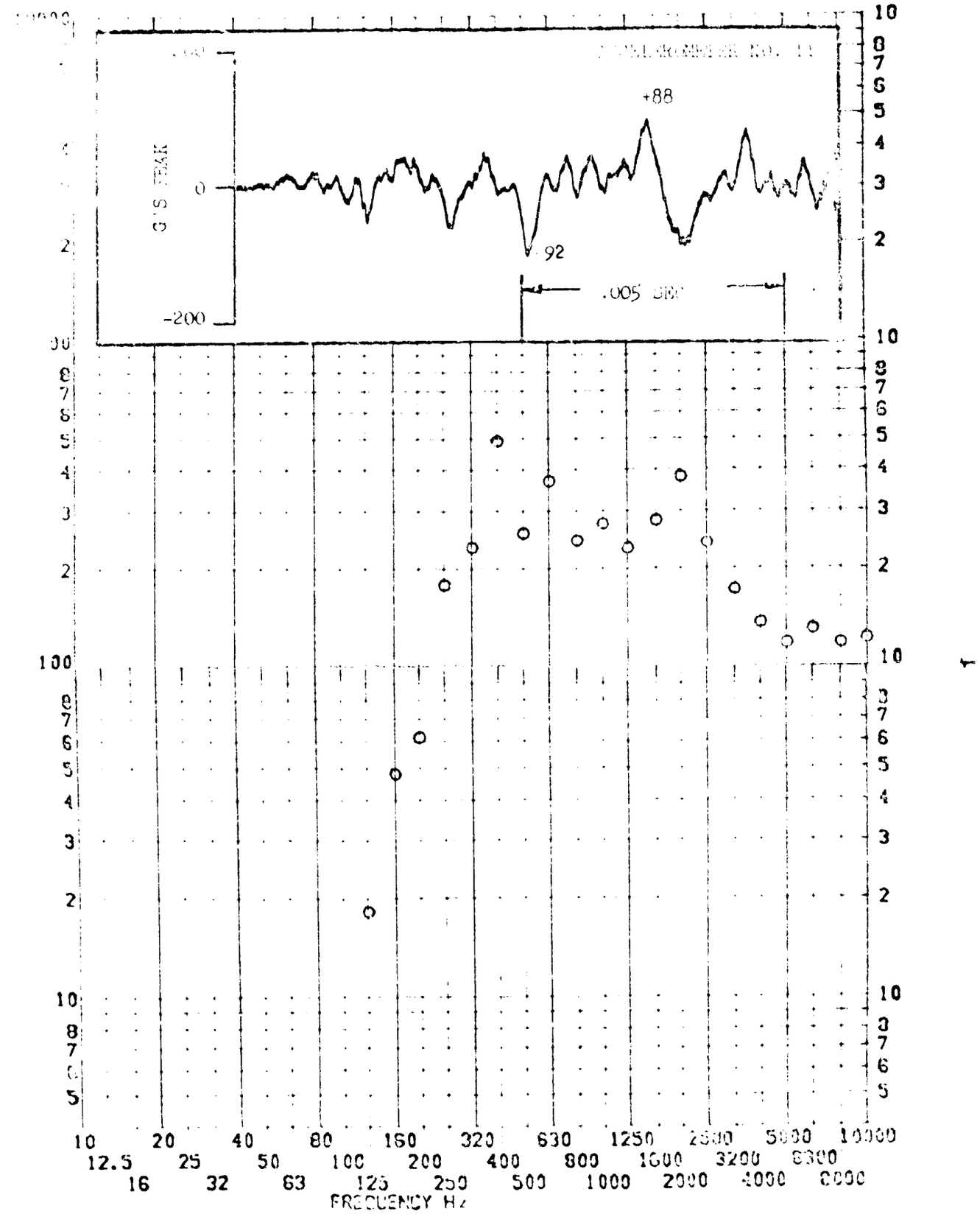

SHOCK TEST ANALYSIS DATA SHEET 11.0.2.46

TEST ITEM 867-111
SERIAL NO.
SHOCK AXIS

PART NO. STRUCTURE
TEST DATE 2 NOV 1964
SHOCK NO. 3

RESPONSE G-S

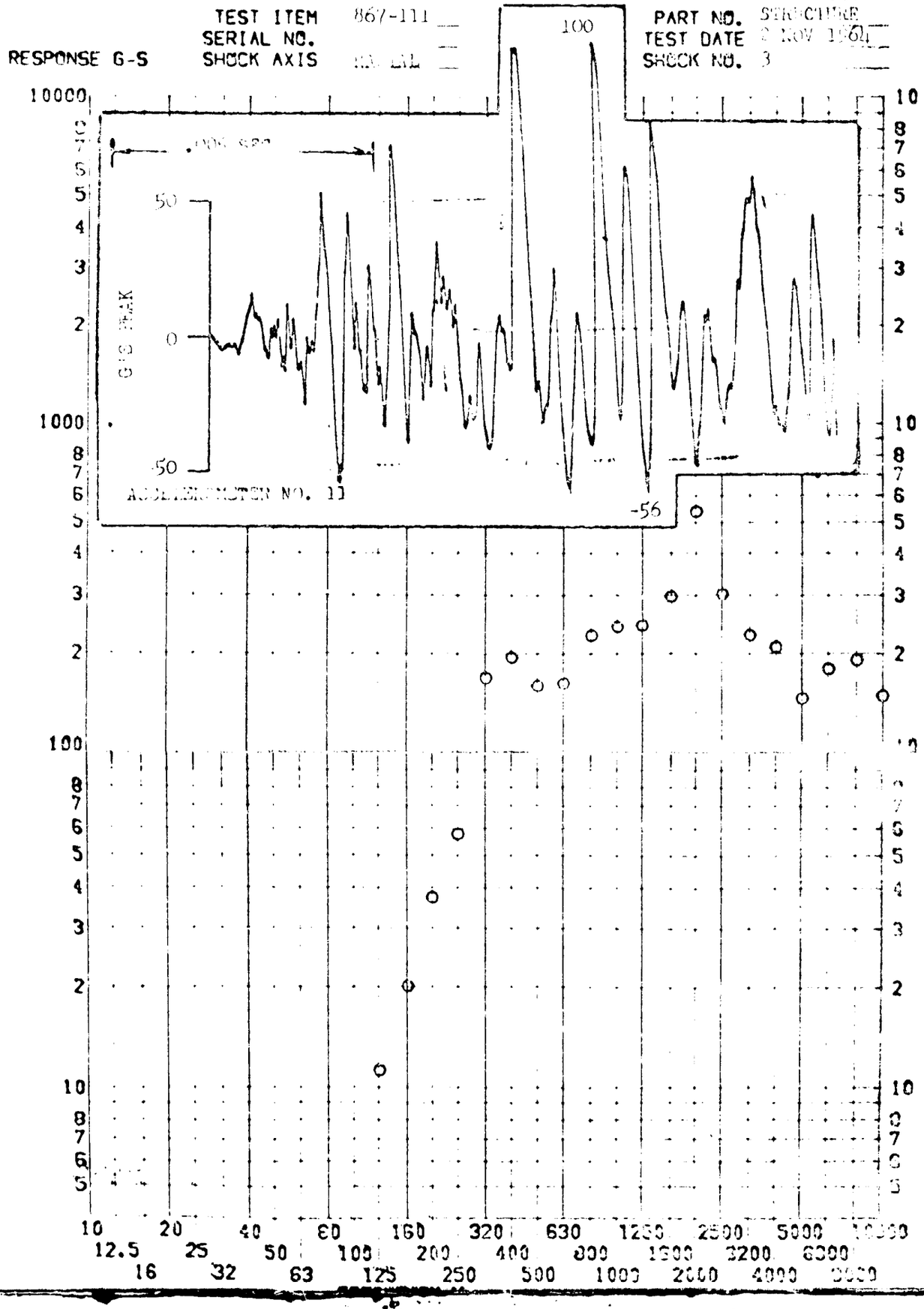

SHOCK TEST ANALYSIS DATA SHEET FT.B.2.47

TEST ITEM 66,-109
SERIAL NO.
SHOCK AXIS RADIAL

PART NO. STRUCTURE
TEST DATE 2 NOV 1964
SHOCK NO. 1
ACCELEROMETER NO. 11

RESPONSE G-S

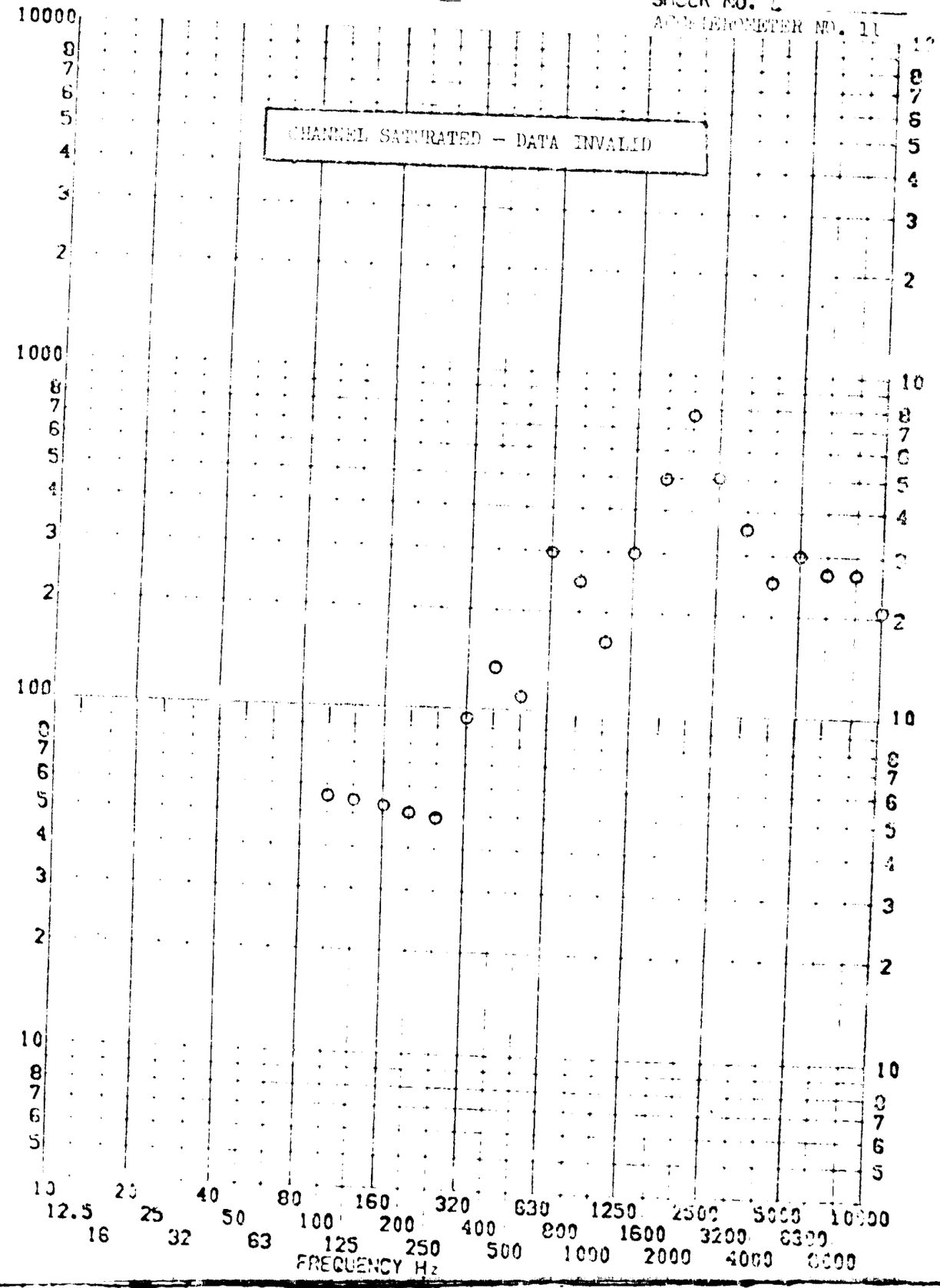

SHOCK TEST ANALYSIS DATA SHEET 11 [illegible] 18

TEST ITEM [illegible]
SERIAL NO.
SHOCK AXIS TANGENTIAL
PART NO. [illegible]
TEST DATE 2 NOV [illegible]
SHOCK NO. 1

RESPONSE G-S

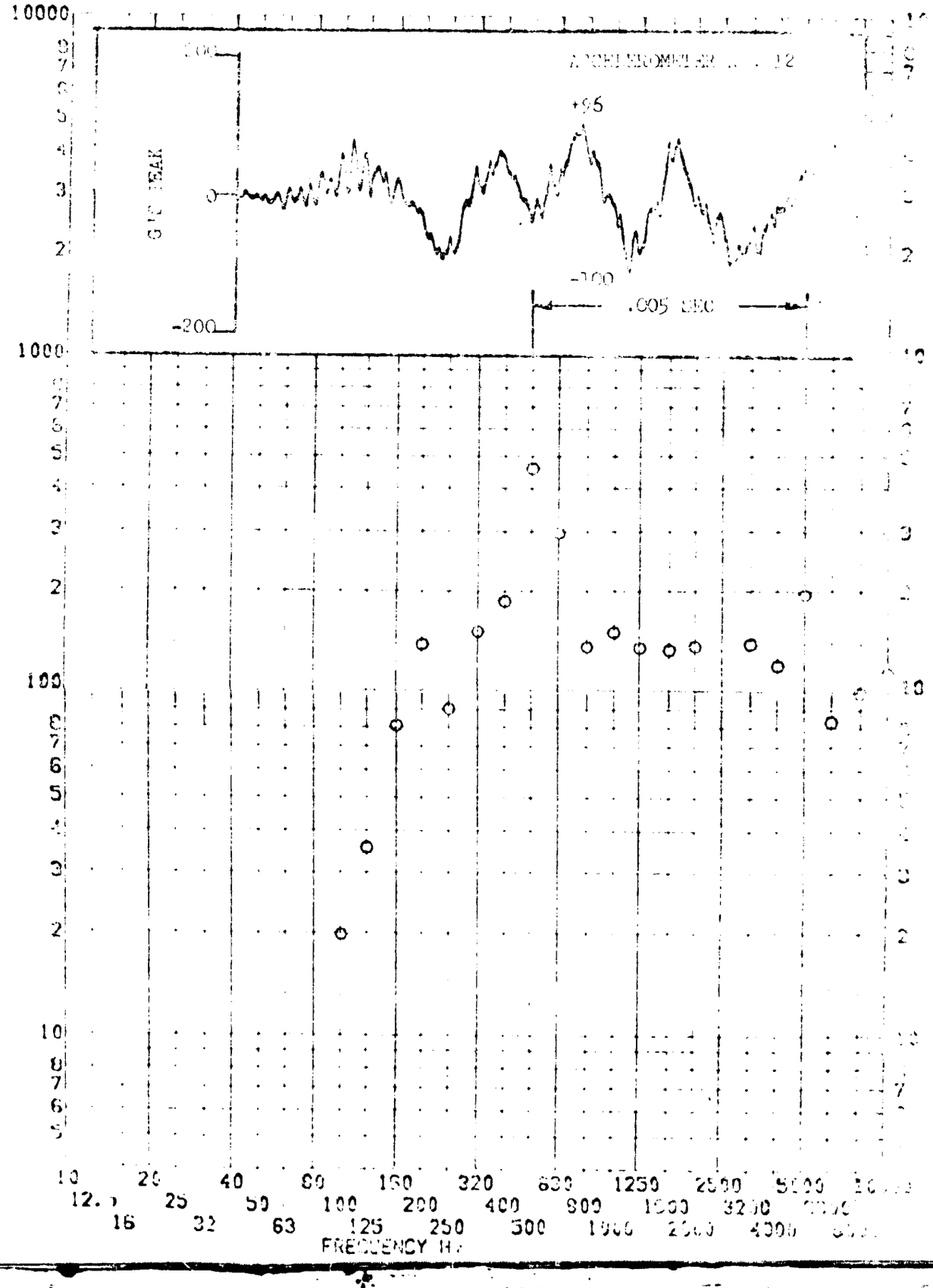

SHOCK TEST ANALYSIS DATA SHEET II.B.2.49

TEST ITEM 867-114 PART NO. STRUCTURE
SERIAL NO. TEST DATE 2 NOV 1964
SHOCK AXIS TANGENTIAL SHOCK NO. 2

SENSE G-S

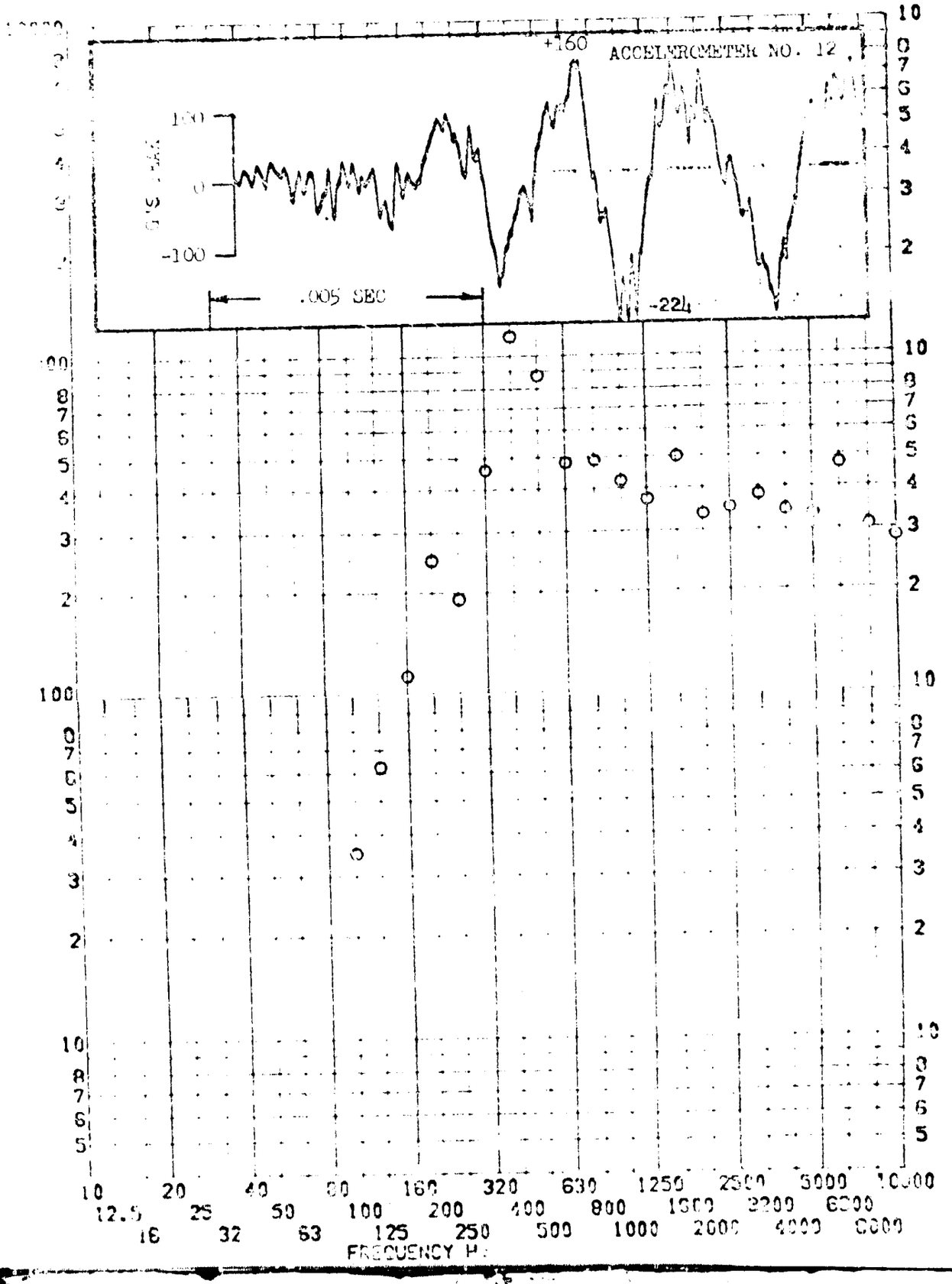

SHOCK TEST ANALYSIS DATA SHEET II.B.2.50

TEST ITEM 867-115
SERIAL NO.
SHOCK AXIS TANGENTIAL

PART NO. STRUCTURE
TEST DATE 3 NOV 1964
SHOCK NO. 3

RESPONSE G-S

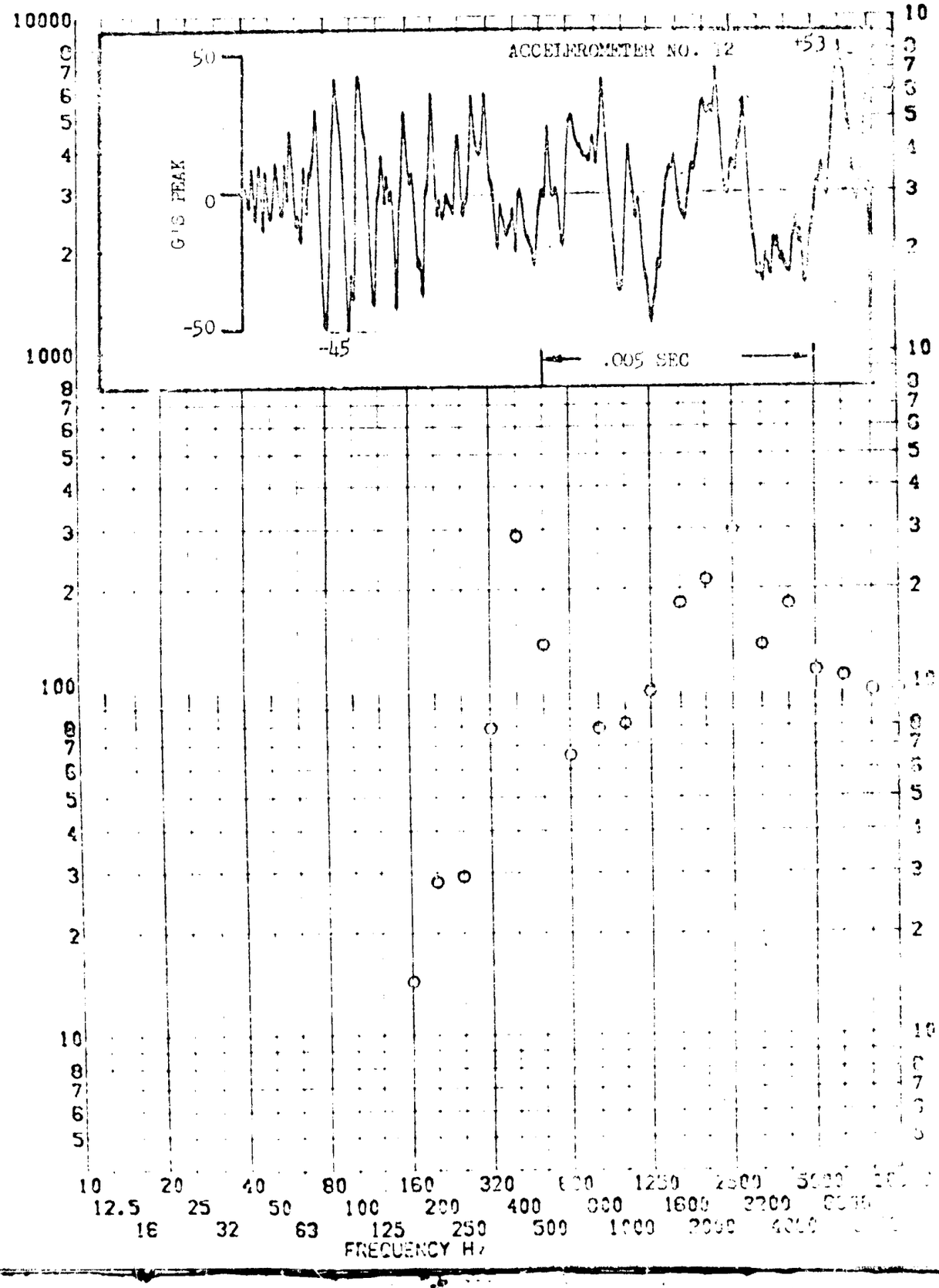

SHOCK TEST ANALYSIS DATA SHEET II.B.2.51

TEST ITEM 867-113
SERIAL NO.
SHOCK AXIS TANGENTIAL

PART NO. STRUCTURE
TEST DATE 2 NOV 1964
SHOCK NO. 4

RESPONSE G-S

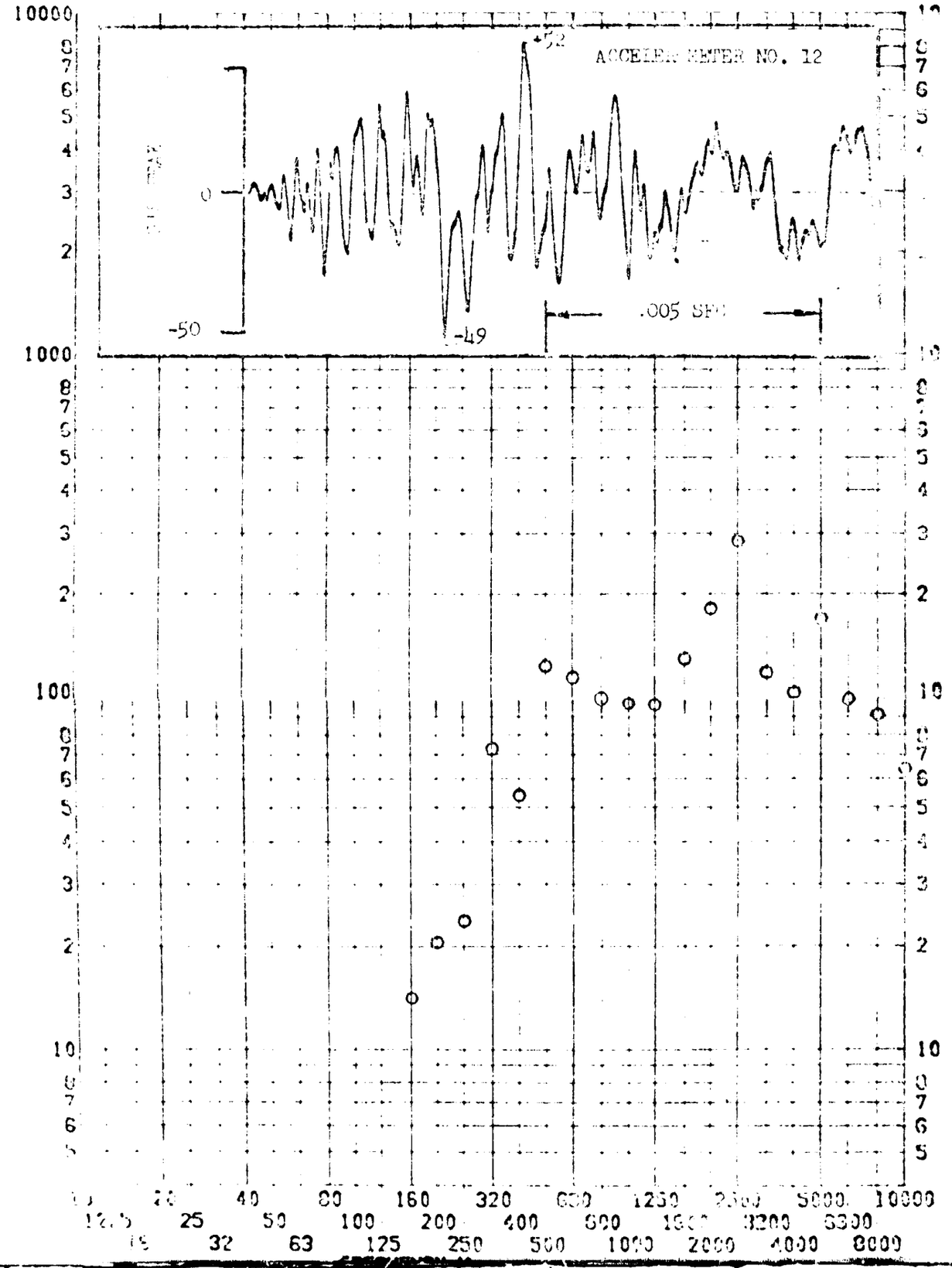

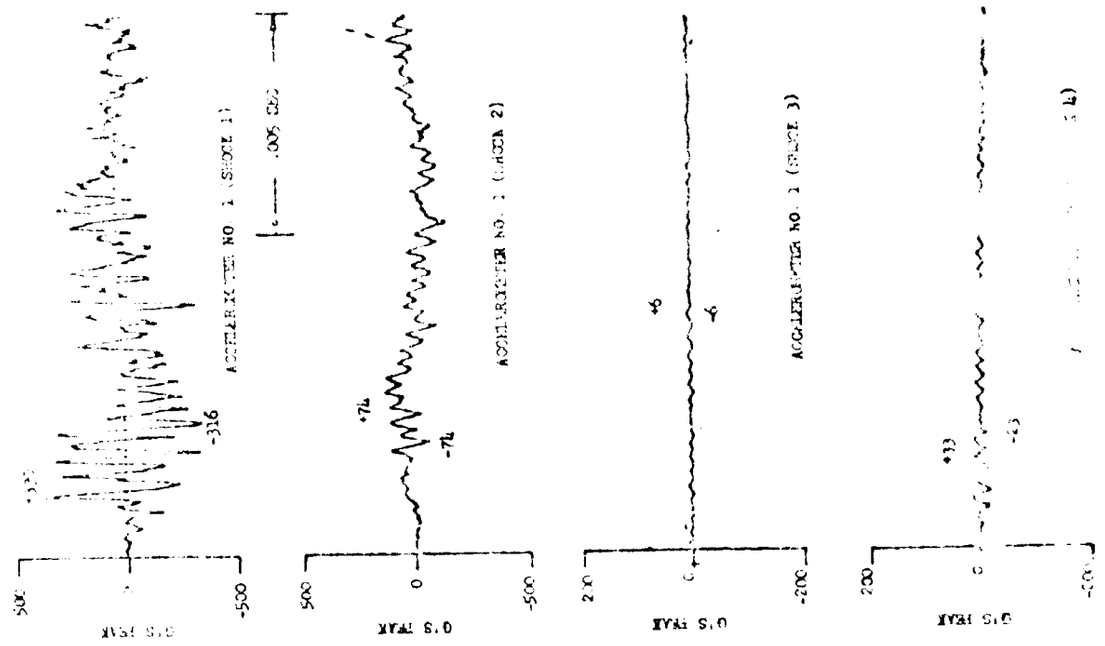
ACCELEROMETER NO. 1 (SHOCK 1)
ACCELEROMETER NO. 2 (SHOCK 2)
ACCELEROMETER NO. 3 (SHOCK 3)
G'S PEAK

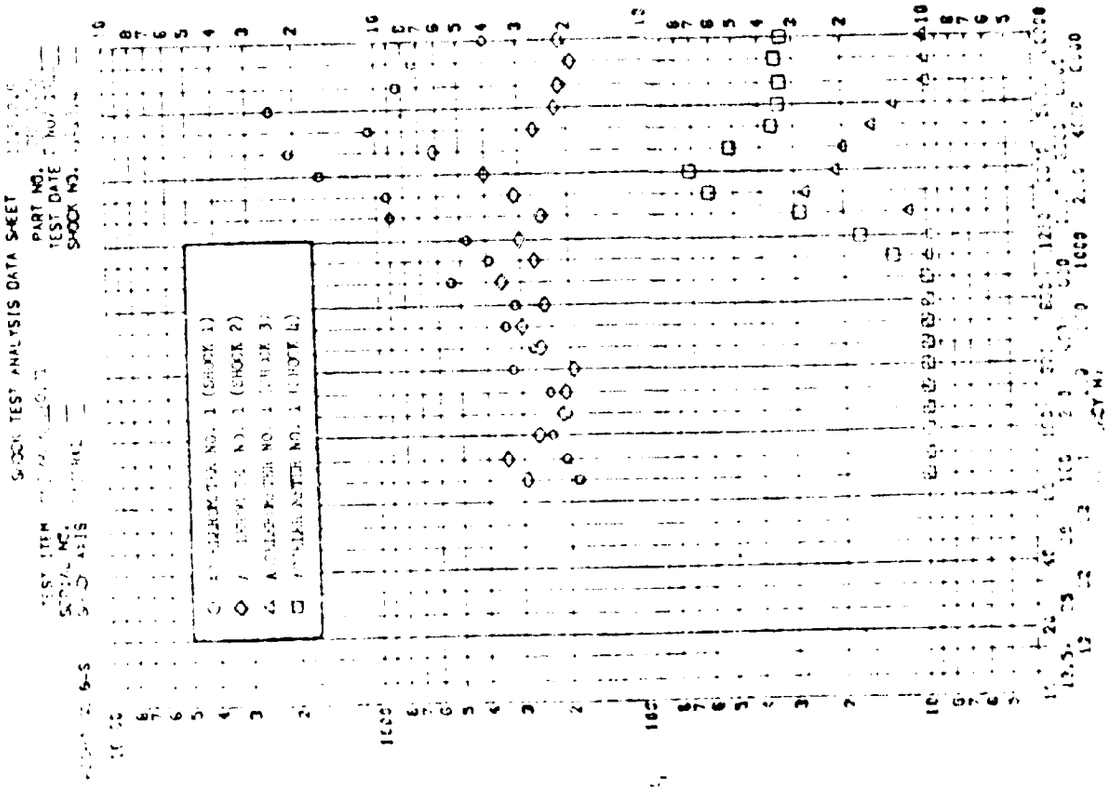
SHOCK TEST ANALYSIS DATA SHEET
PART NO.
TEST DATE
SHOCK NO.
TEST ITEM
SERIAL NO.
ACCELEROMETER NO. 1 (SHOCK 1)
ACCELEROMETER NO. 2 (SHOCK 2)
ACCELEROMETER NO. 3 (SHOCK 3)
ACCELEROMETER NO. 4 (SHOCK 4)

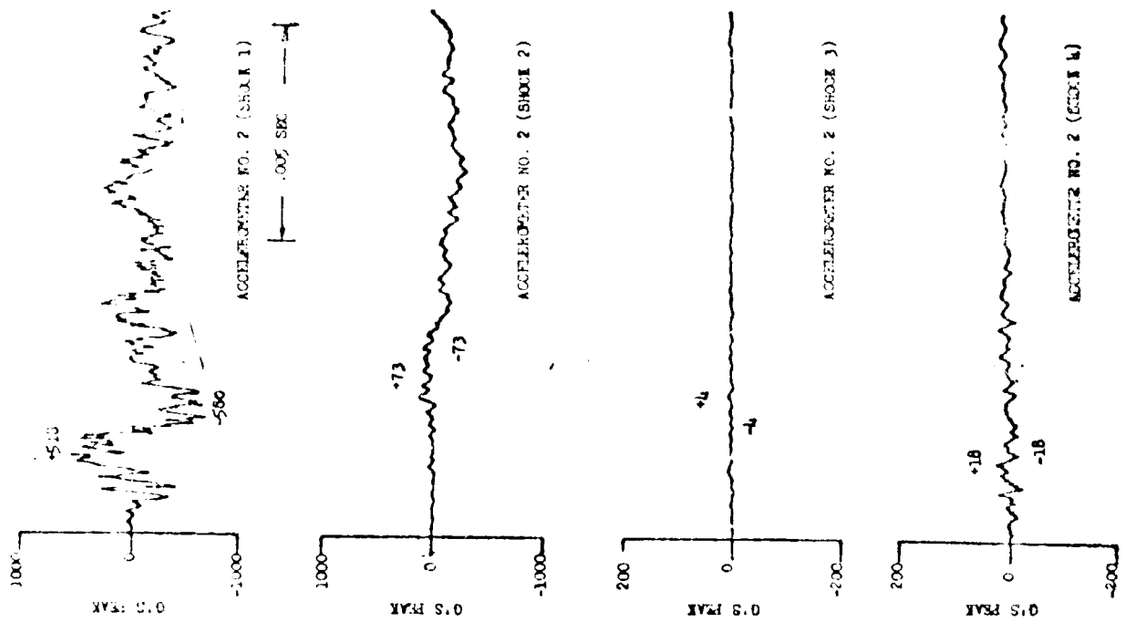
ACCELEROMETER NO. 2 (SHOCK 1)
100 G SEC
+510
-580
ACCELEROMETER NO. 2 (SHOCK 2)
+73
-73
ACCELEROMETER NO. 2 (SHOCK 3)
+4
-4
ACCELEROMETER NO. 2 (SHOCK 4)
+18
-18
0'S PEAK

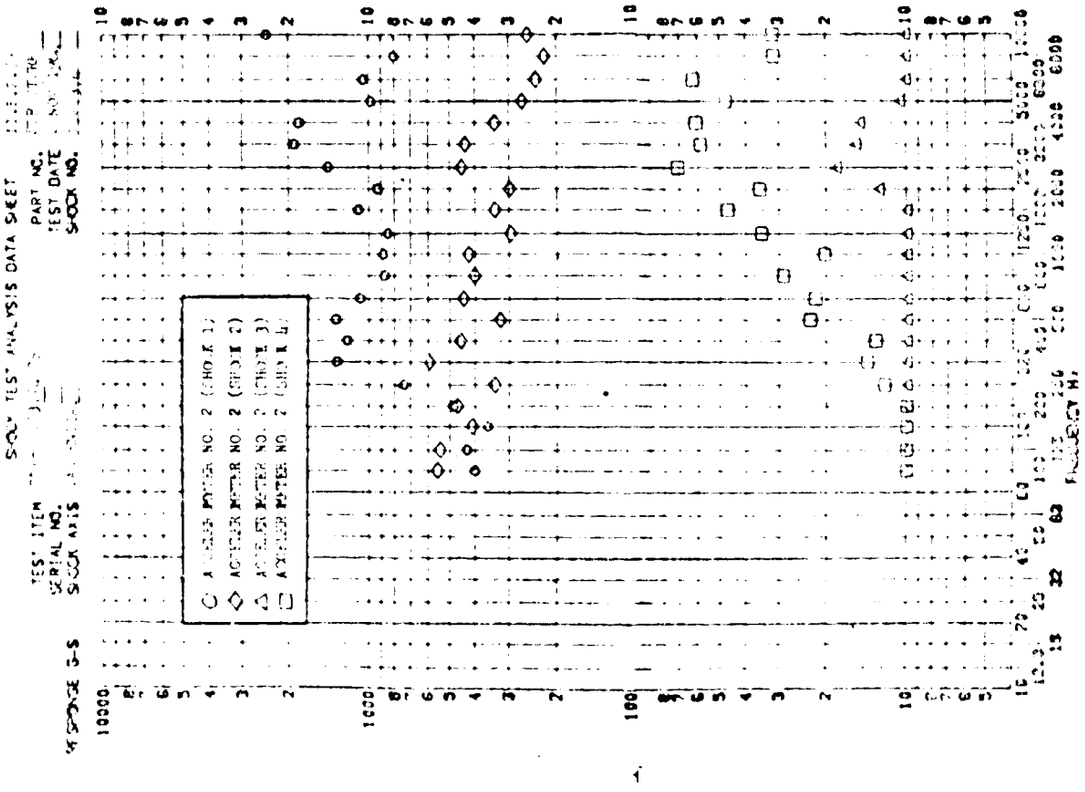
SHOCK TEST ANALYSIS DATA SHEET
TEST ITEM
SERIAL NO.
SHOCK AXIS
PART NO.
TEST DATE
SHOCK NO.
SPECIFICATION G-S
FREQUENCY HZ

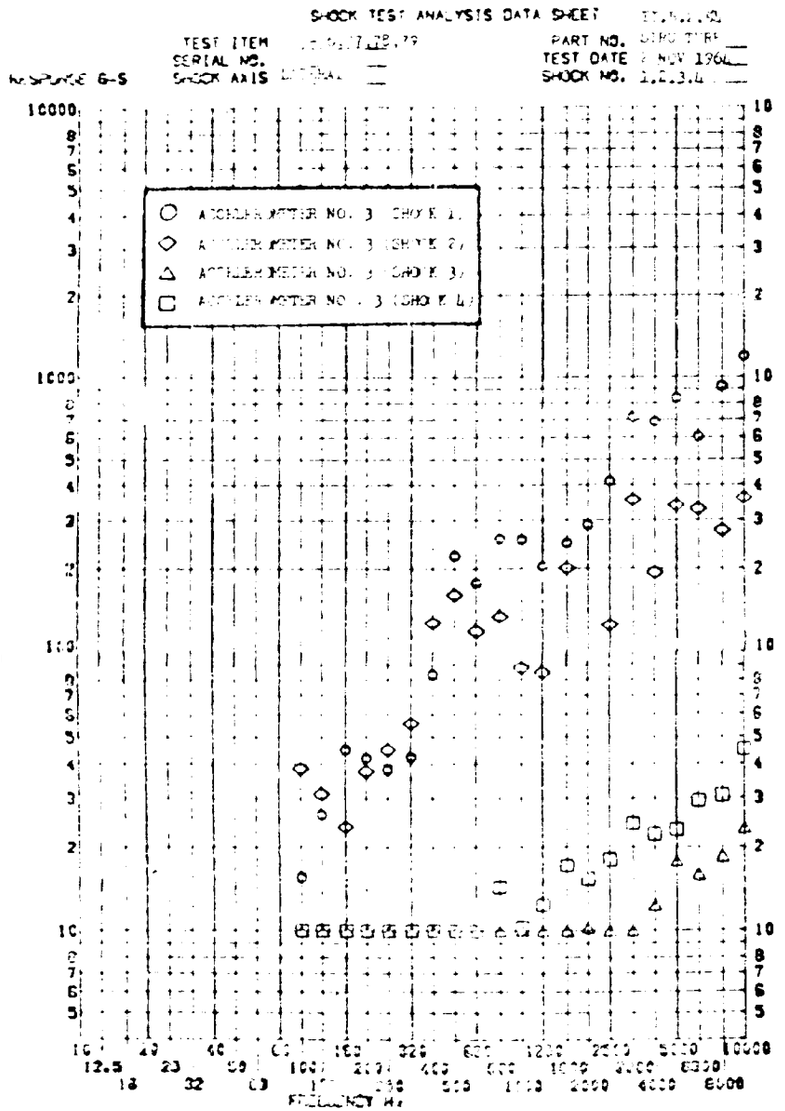
SHOCK TEST ANALYSIS DATA SHEET
TEST ITEM
SERIAL NO.
SHOCK AXIS
PART NO.
TEST DATE
SHOCK NO.
G-S
ACCELEROMETER NO. 3 (SHOCK 1)
ACCELEROMETER NO. 3 (SHOCK 2)
ACCELEROMETER NO. 3 (SHOCK 3)
ACCELEROMETER NO. 3 (SHOCK 4)
FREQUENCY Hz

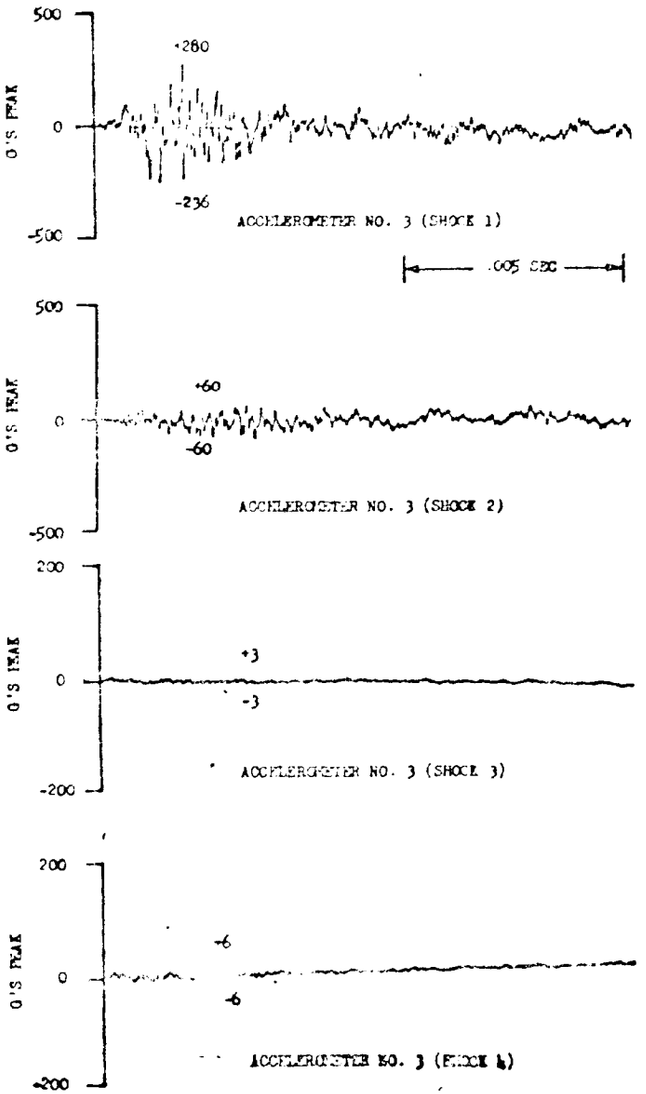
500
+280
0
-236
-500
G'S PEAK
ACCELEROMETER NO. 3 (SHOCK 1)
.005 SEC
500
+60
0
-60
-500
G'S PEAK
ACCELEROMETER NO. 3 (SHOCK 2)
200
+3
0
-3
-200
G'S PEAK
ACCELEROMETER NO. 3 (SHOCK 3)
200
+6
0
-6
-200
G'S PEAK
ACCELEROMETER NO. 3 (SHOCK 4)

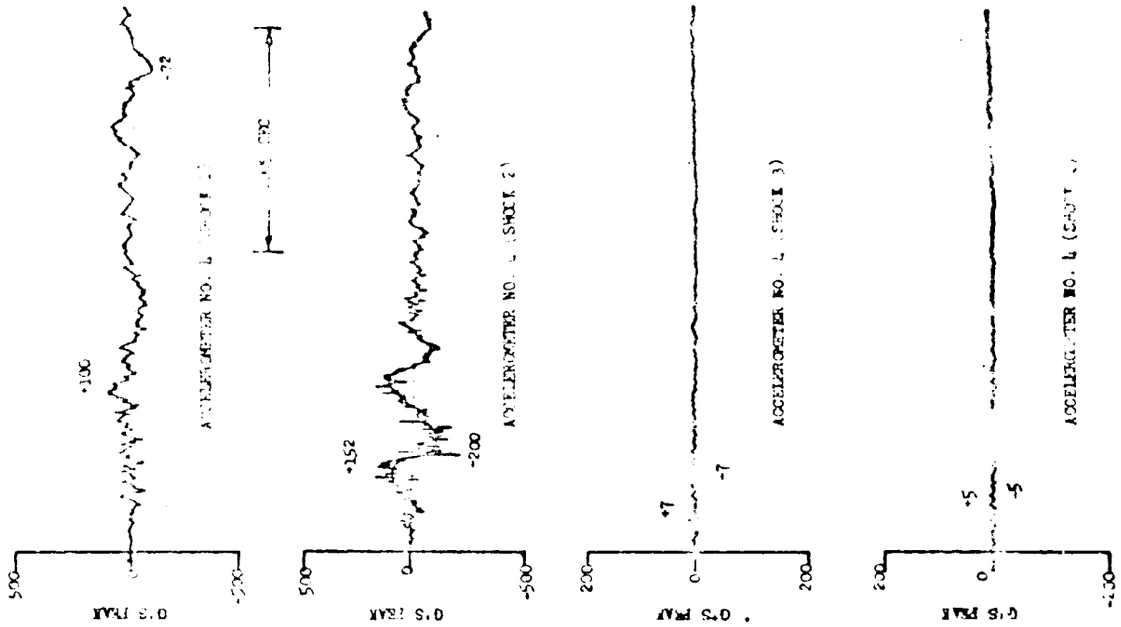
+100
-22
+152
-200
+7
-7
+5
-5
500
0
-500
200
-200

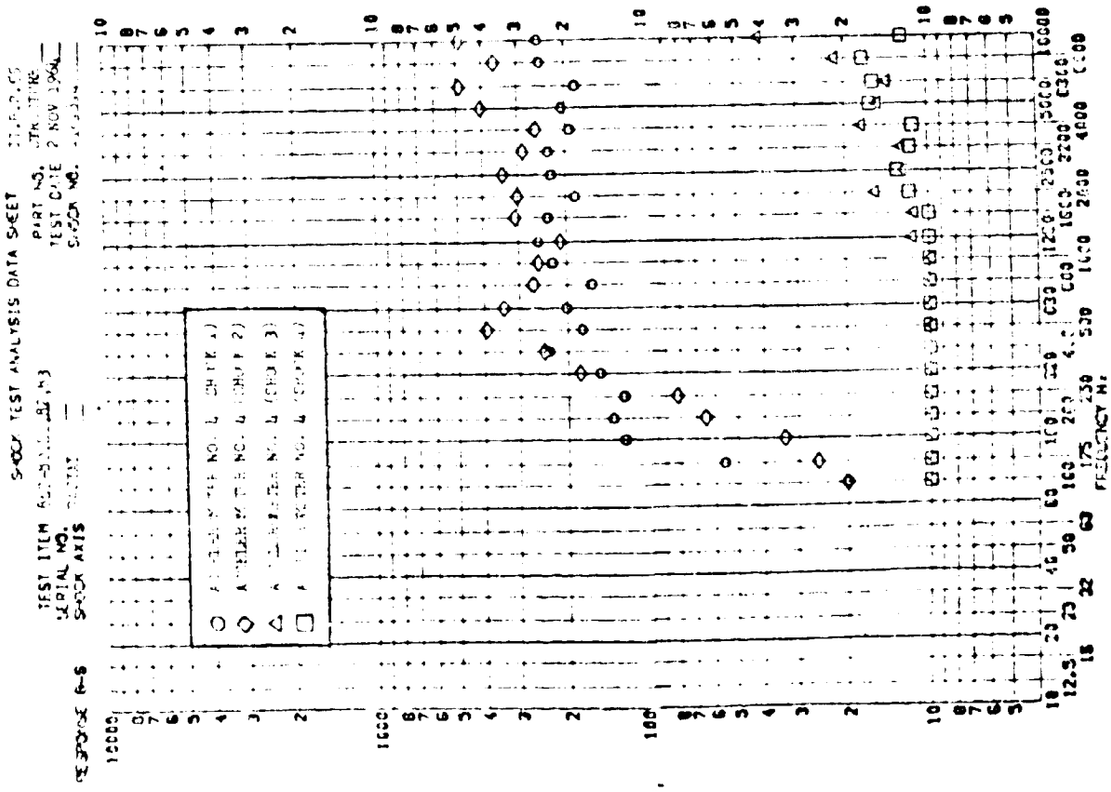
SHOCK TEST ANALYSIS DATA SHEET
TEST ITEM
PART NO.
TEST DATE 2 NOV 1968
SHOCK NO.
SHOCK AXIS
RESPONSE G-S
FREQUENCY Hz

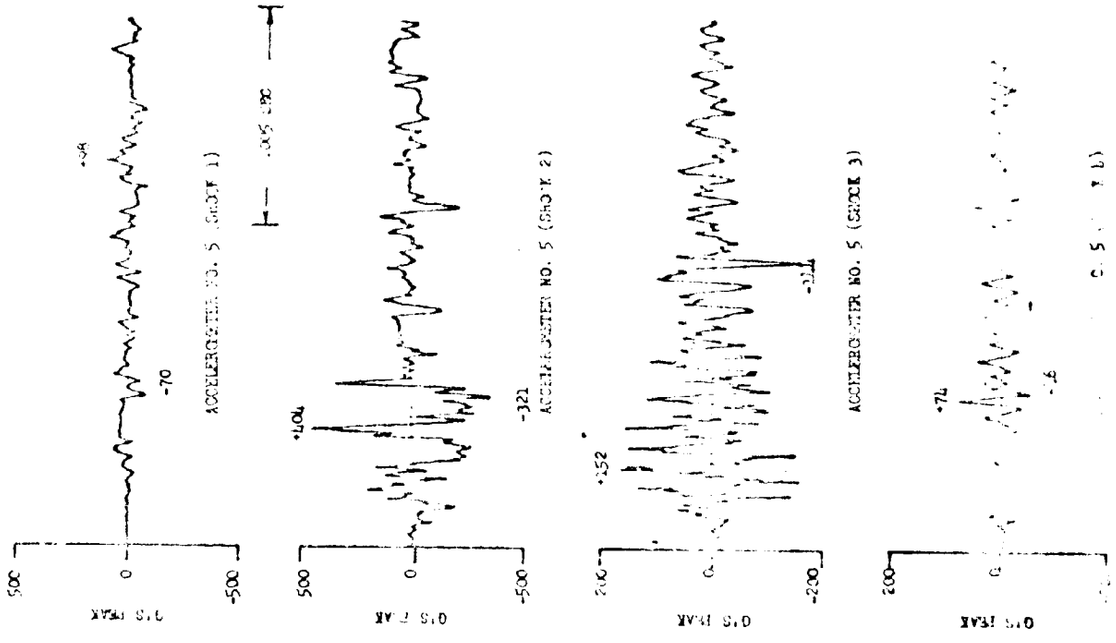
ACCELEROMETER NO. 5 (SHOCK 1)
ACCELEROMETER NO. 5 (SHOCK 2)
ACCELEROMETER NO. 5 (SHOCK 3)
0'S PEAK
500
0
-500
200
-200
+94
-70
+404
-321
+52
-74
-6

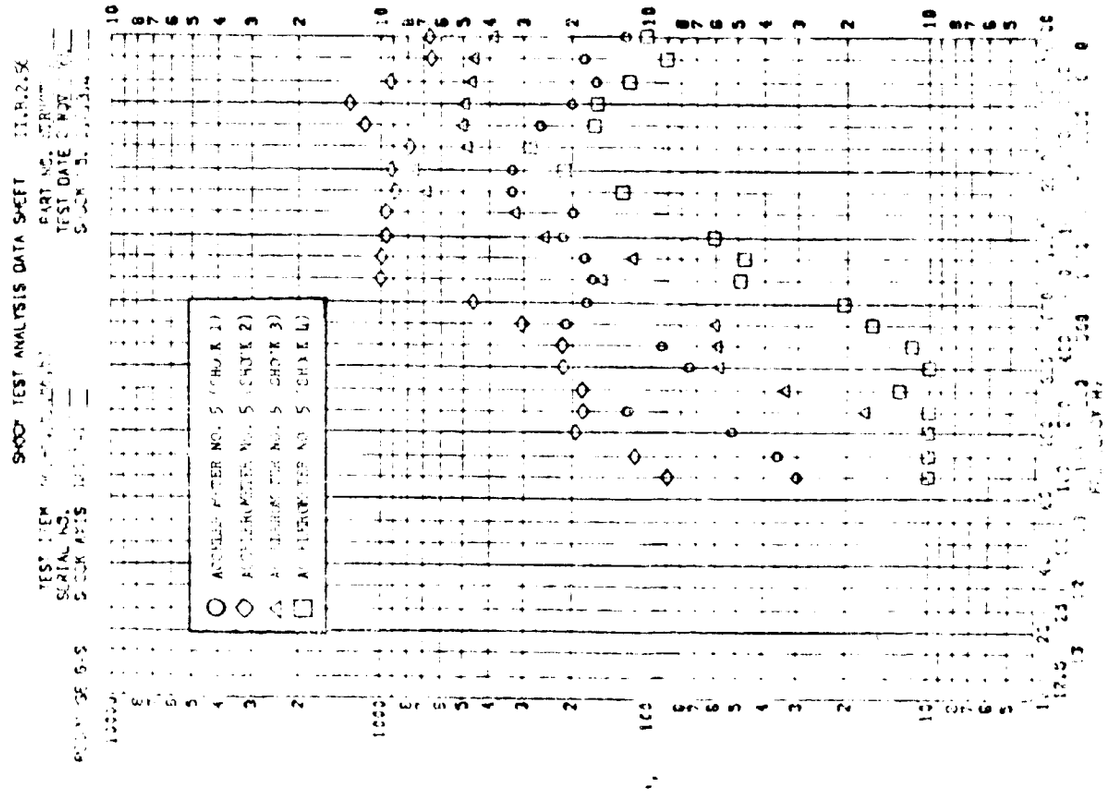
SHOCK TEST ANALYSIS DATA SHEET
TEST ITEM
SERIAL NO.
ACCELEROMETER NO. 5 (SHOCK 1)
ACCELEROMETER NO. 5 (SHOCK 2)
ACCELEROMETER NO. 5 (SHOCK 3)
ACCELEROMETER NO. 5 (SHOCK 4)

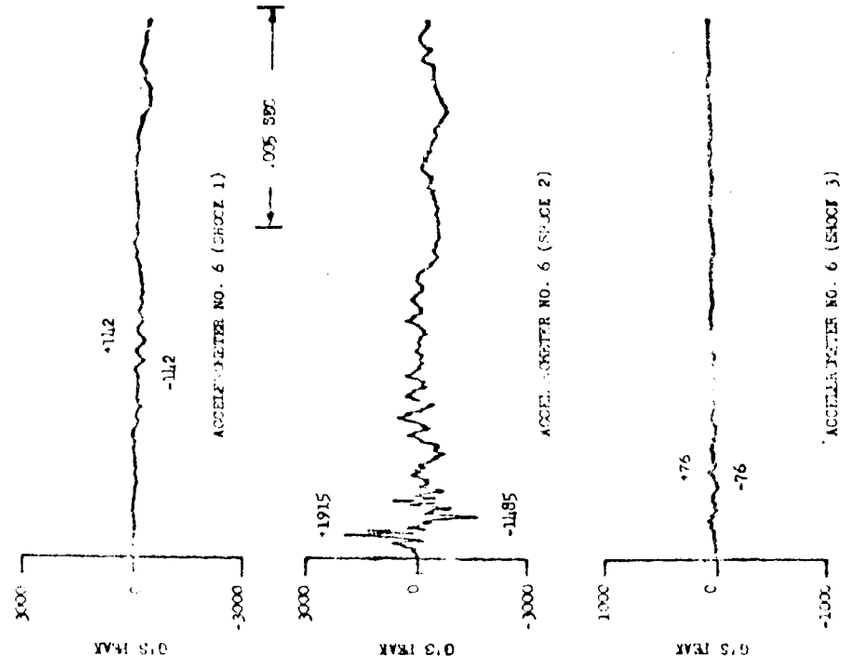
ACCELEROMETER NO. 6 (SHOCK 1)
ACCELEROMETER NO. 6 (SHOCK 2)
ACCELEROMETER NO. 6 (SHOCK 3)
.005 SEC
+112
-112
+1915
-1485
+76
-76
3000
0
-3000
1500
-1500
0.3 IRAR
0.3 IRAR
0.3 IRAR

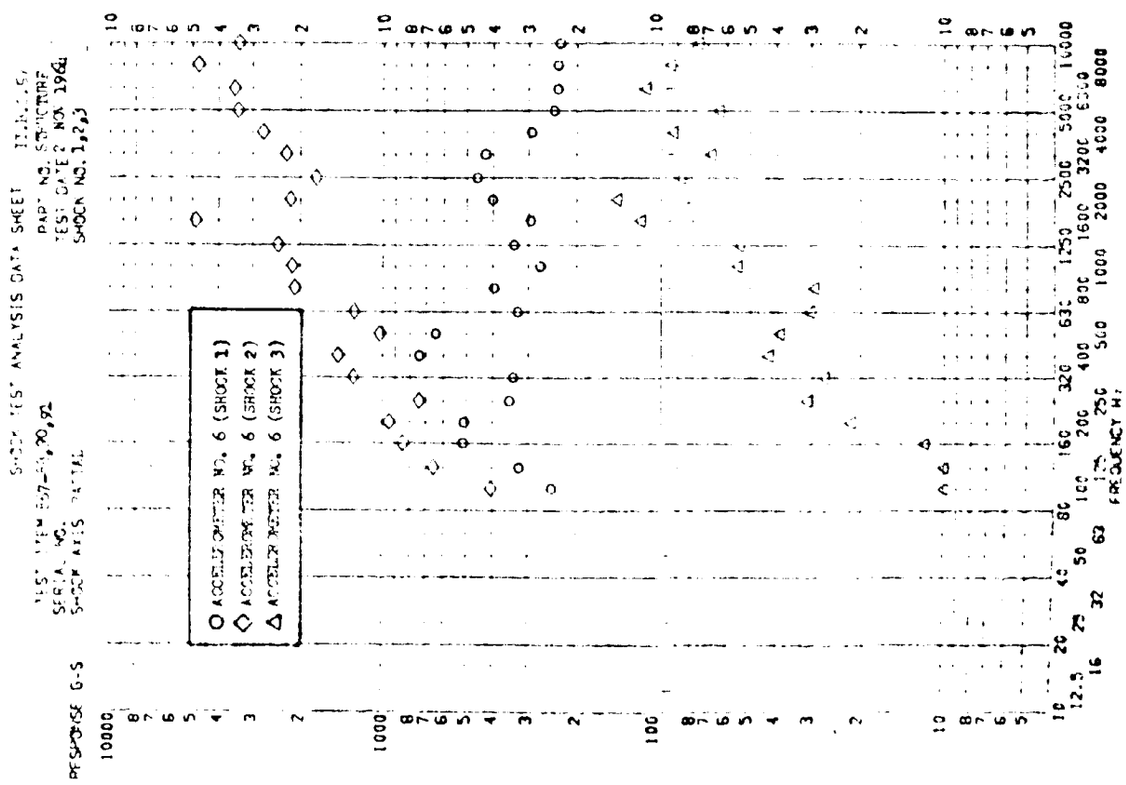
SHOCK TEST ANALYSIS DATA SHEET
PART NO. STRUCTURE
TEST DATE 2 NOV 1968
SHOCK NO. 1,2,3
ACCELEROMETER NO. 6 (SHOCK 1)
ACCELEROMETER NO. 6 (SHOCK 2)
ACCELEROMETER NO. 6 (SHOCK 3)
RESPONSE G-S
FREQUENCY Hz

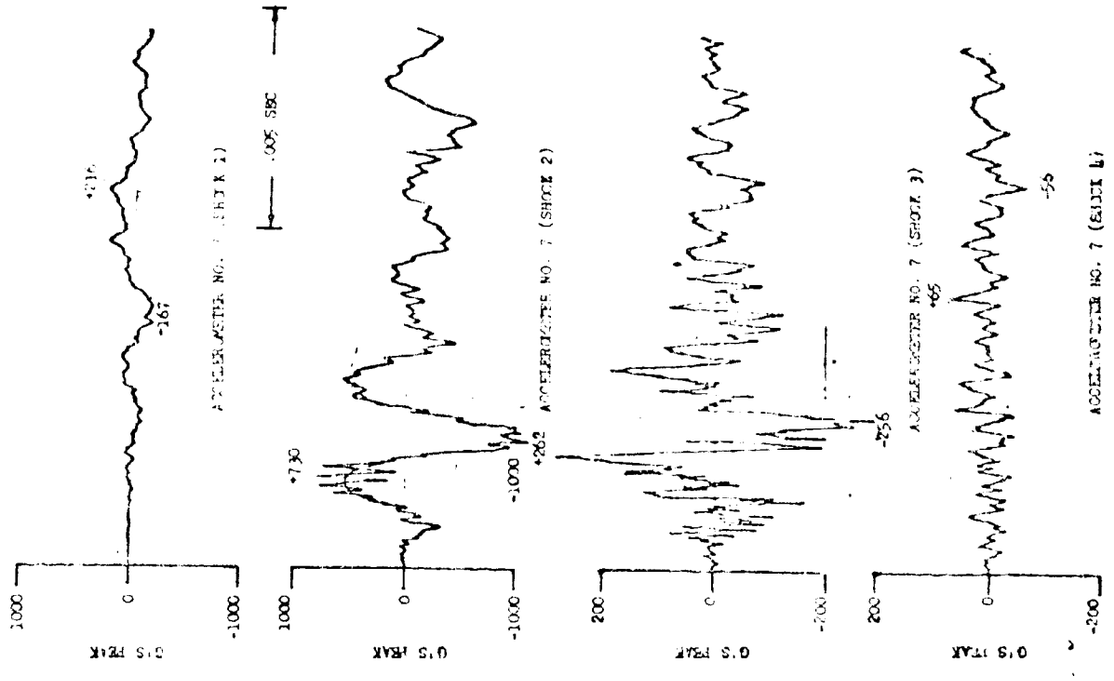
.005 SEC
ACCELEROMETER NO. 7 (SHOCK 1)
ACCELEROMETER NO. 7 (SHOCK 2)
ACCELEROMETER NO. 7 (SHOCK 3)
ACCELEROMETER NO. 7 (SHOCK 4)
G'S PEAK
+730
-1000
+262
-256
+65
-59

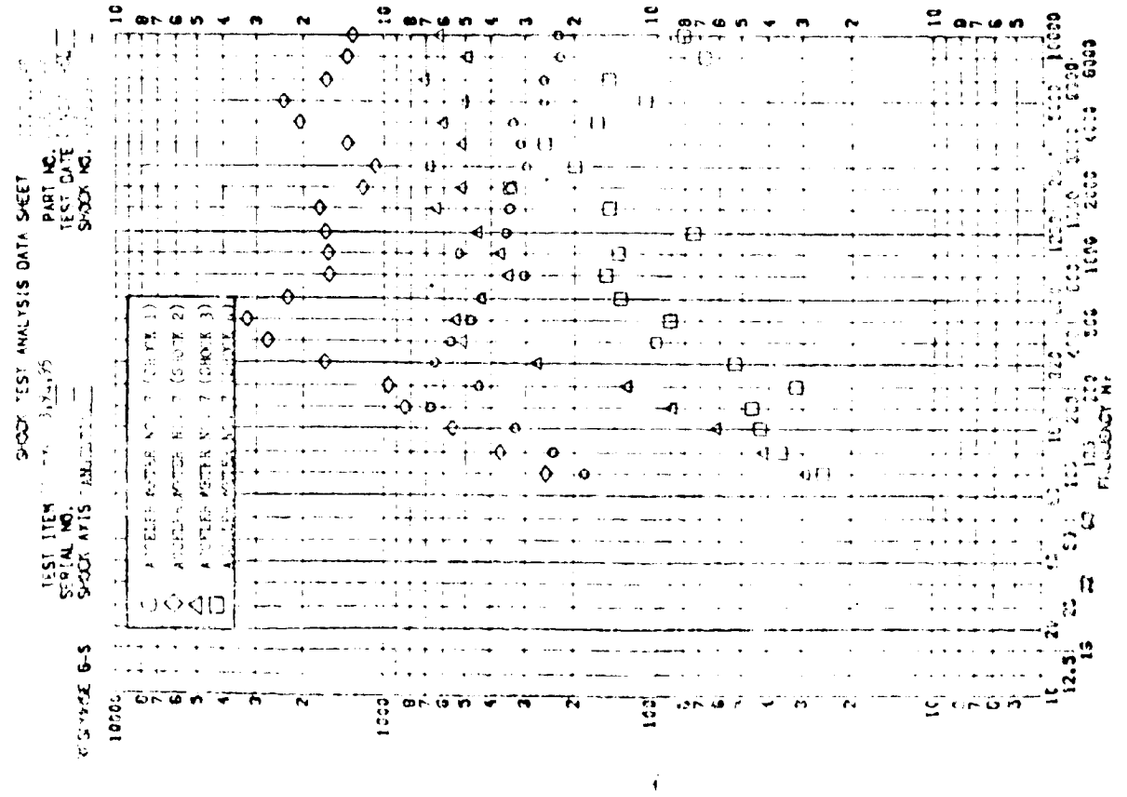
SHOCK TEST ANALYSIS DATA SHEET
TEST ITEM
SERIAL NO.
SHOCK AXIS
PART NO.
TEST DATE
SHOCK NO.
FREQUENCY, Hz

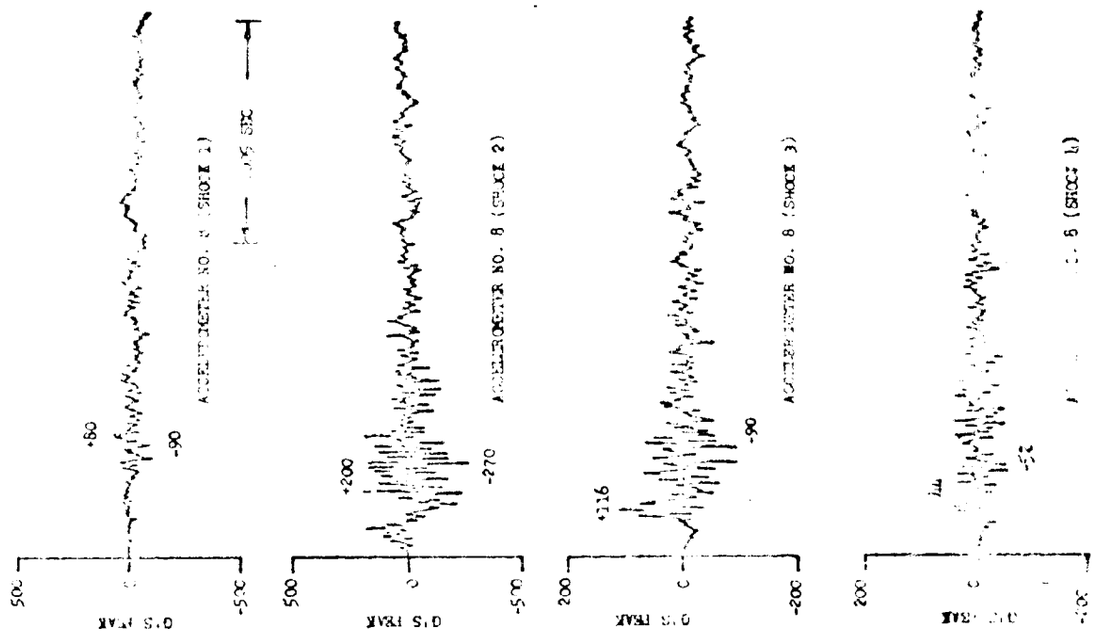
+80
-90
+200
-270
+116
-90
-52
500
0
-500
200
0
-200

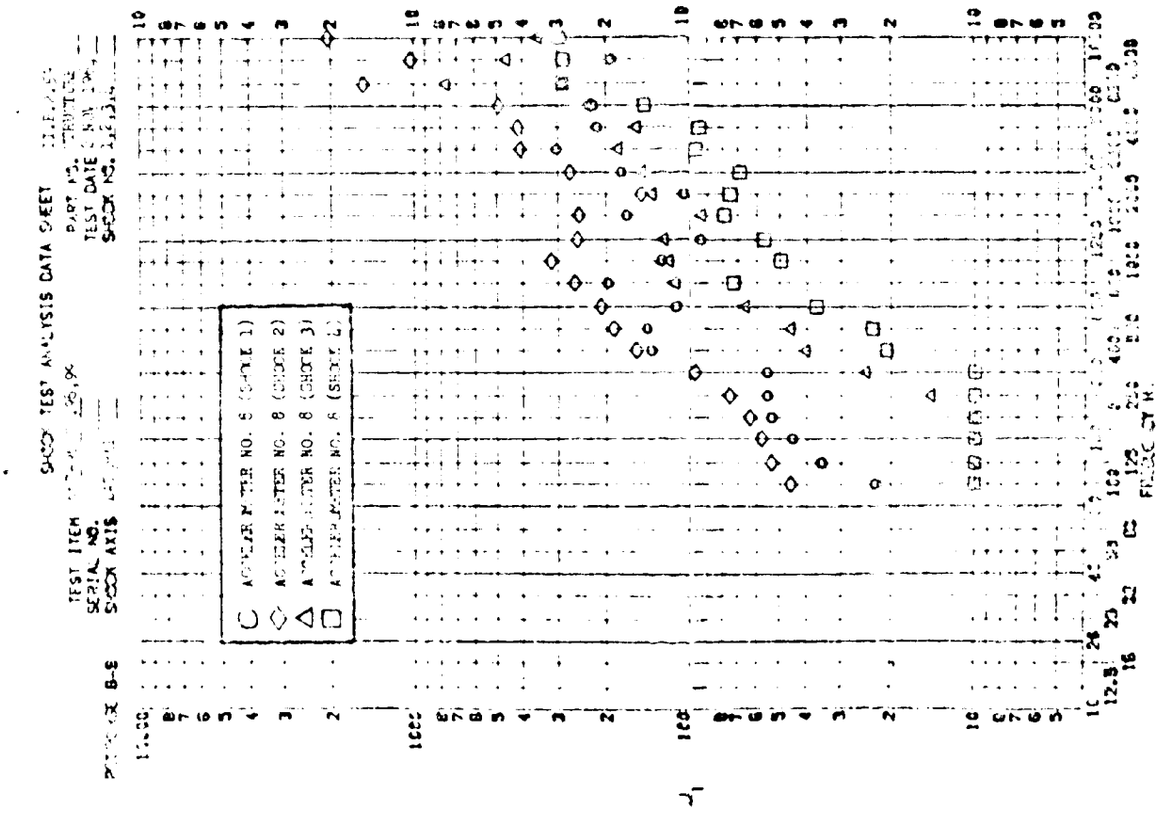
SHOCK TEST ANALYSIS DATA SHEET
TEST ITEM
SERIAL NO.
SHOCK AXIS
PART NO.
TEST DATE
SHOCK NO.
ACCELEROMETER NO. 8 (SHOCK 1)
ACCELEROMETER NO. 8 (SHOCK 2)
ACCELEROMETER NO. 8 (SHOCK 3)
ACCELEROMETER NO. 8 (SHOCK 4)
FREQUENCY

SHOCK TEST ANALYSIS DATA SHEET

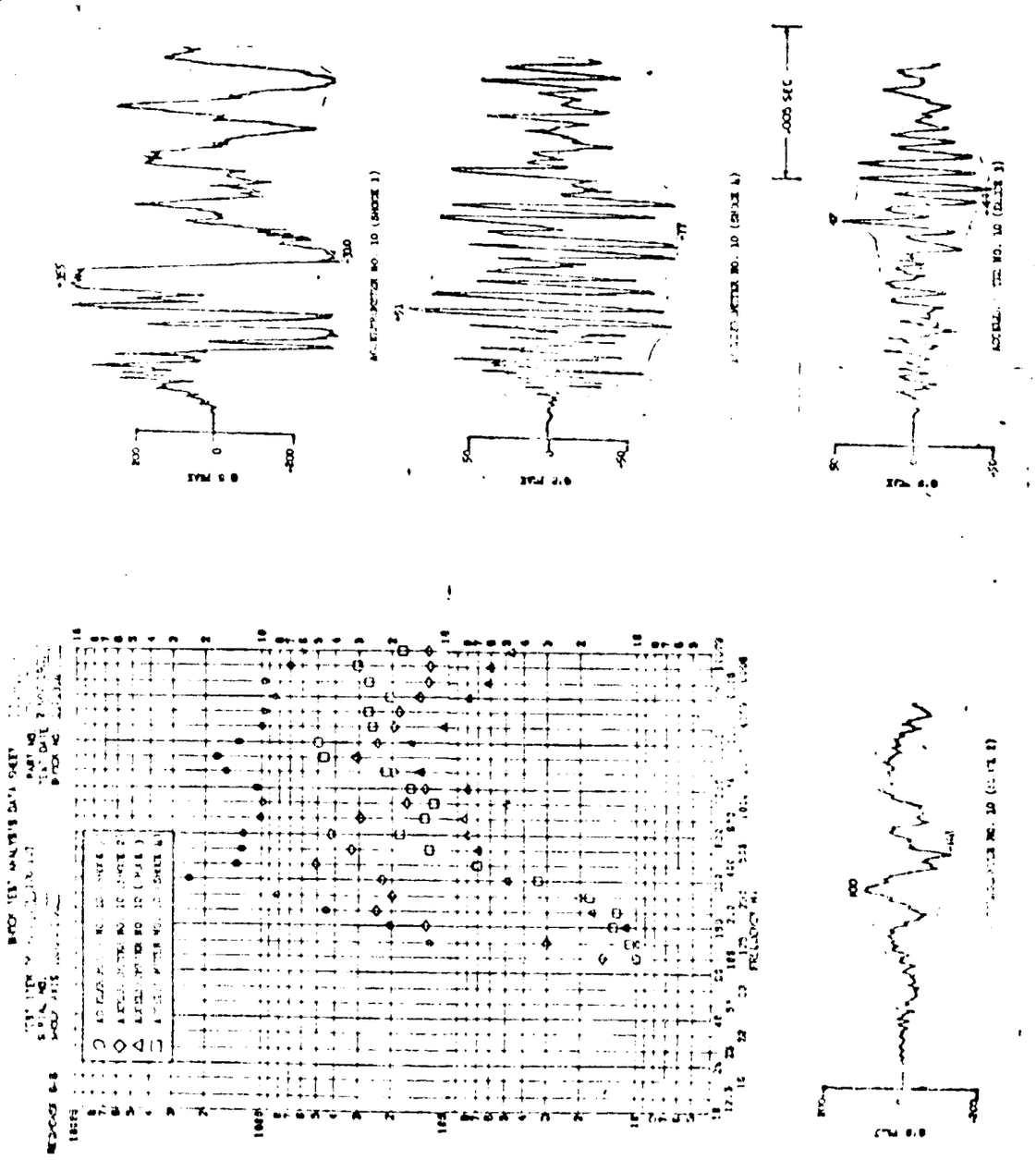

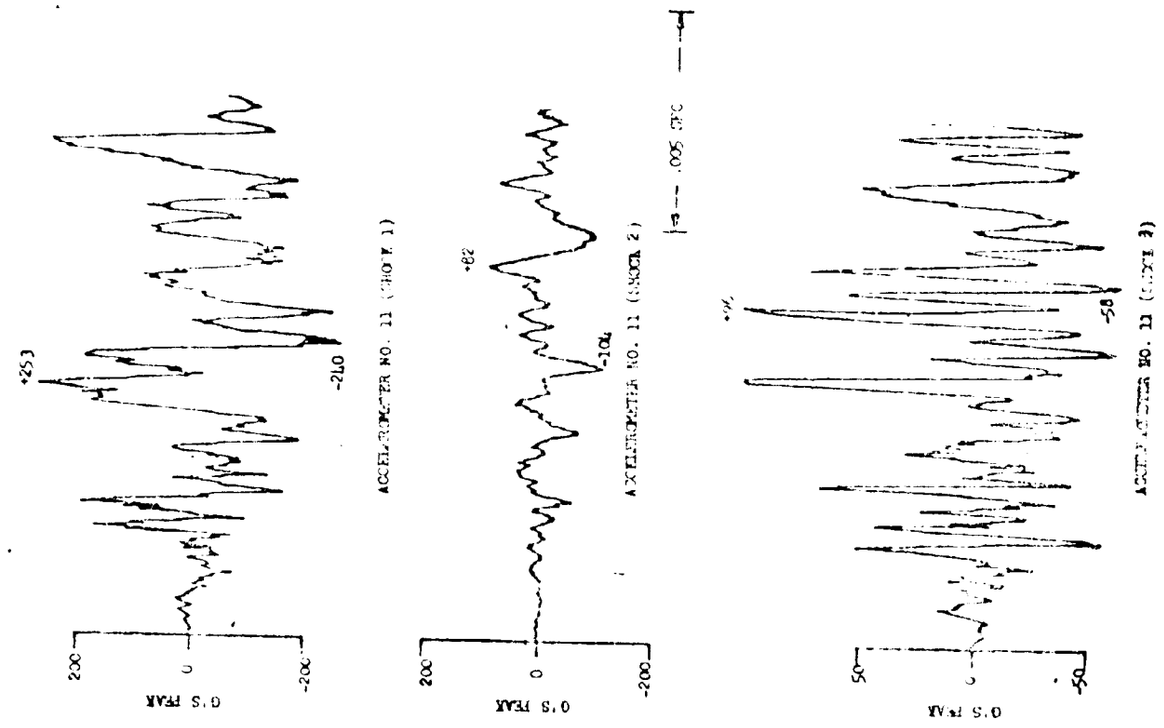
+253
-210
200
0
-200
G'S PEAK
ACCELEROMETER NO. 11 (SHOCK 1)
+82
-104
ACCELEROMETER NO. 11 (SHOCK 2)
.005 SEC
+58
-58
50
0
-50
G'S PEAK
ACCELEROMETER NO. 11 (SHOCK 3)

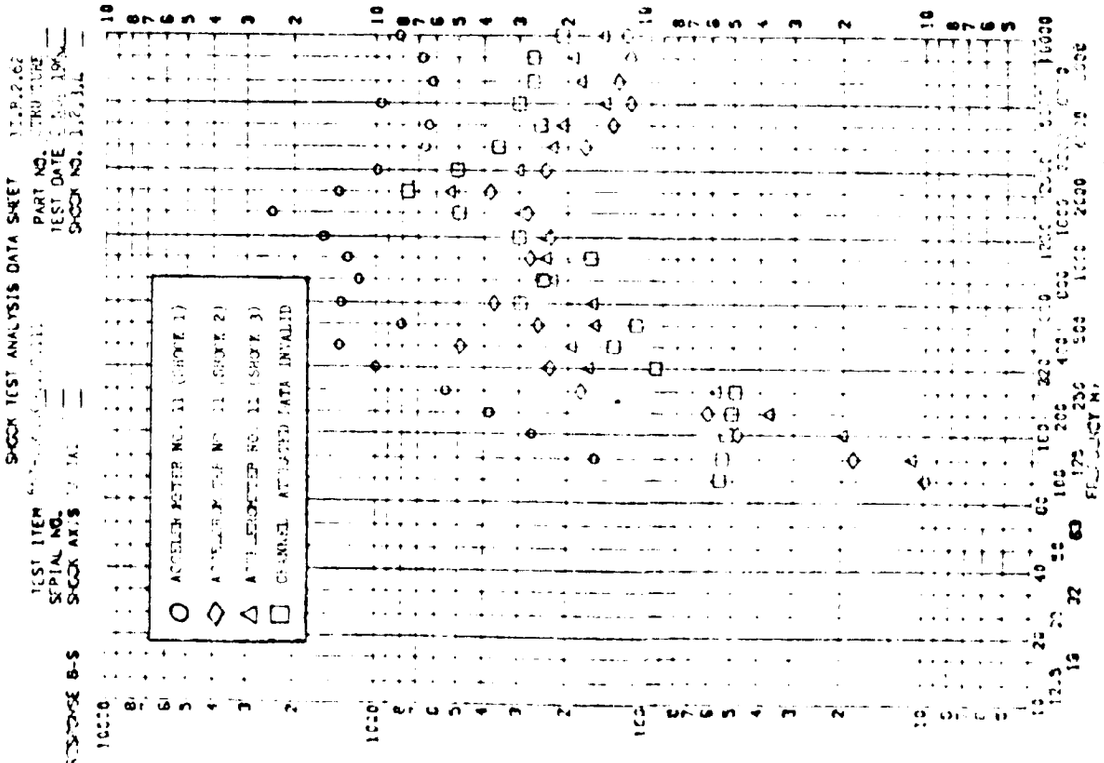
SHOCK TEST ANALYSIS DATA SHEET
TEST ITEM
SERIAL NO.
SHOCK AXIS
PART NO.
TEST DATE
SHOCK NO.
ACCELEROMETER NO. 11 (SHOCK 1)
ACCELEROMETER NO. 11 (SHOCK 2)
ACCELEROMETER NO. 11 (SHOCK 3)
CHANNEL ATTENUATED DATA INVALID

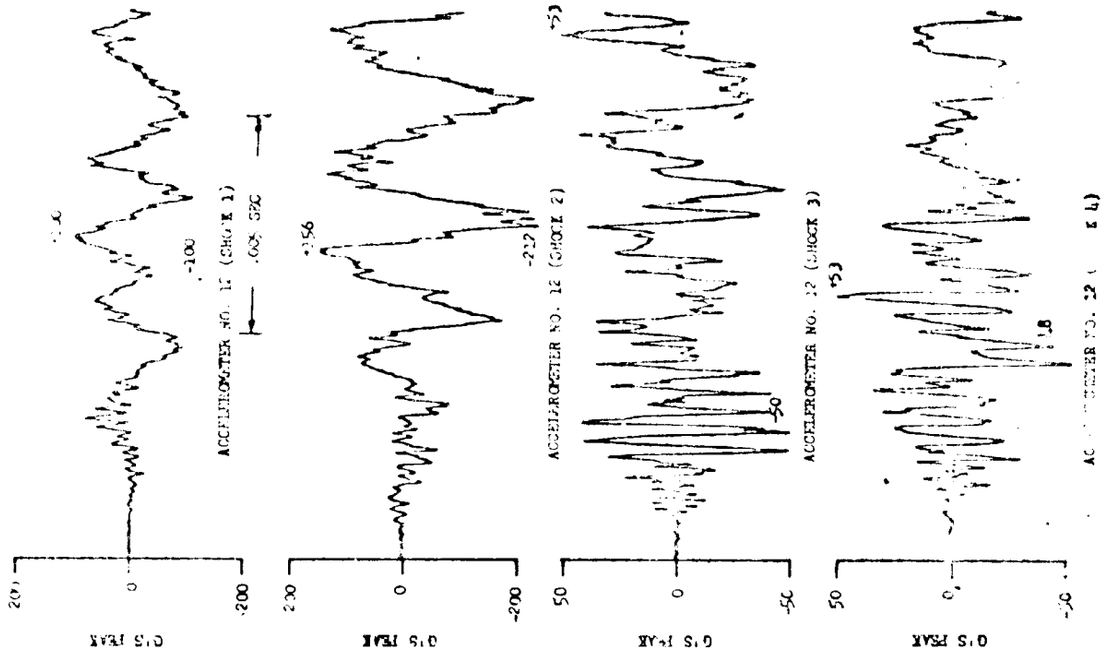
ACCELEROMETER NO. 12 (SHOCK 1)
ACCELEROMETER NO. 12 (SHOCK 2)
ACCELEROMETER NO. 12 (SHOCK 3)
G'S PEAK

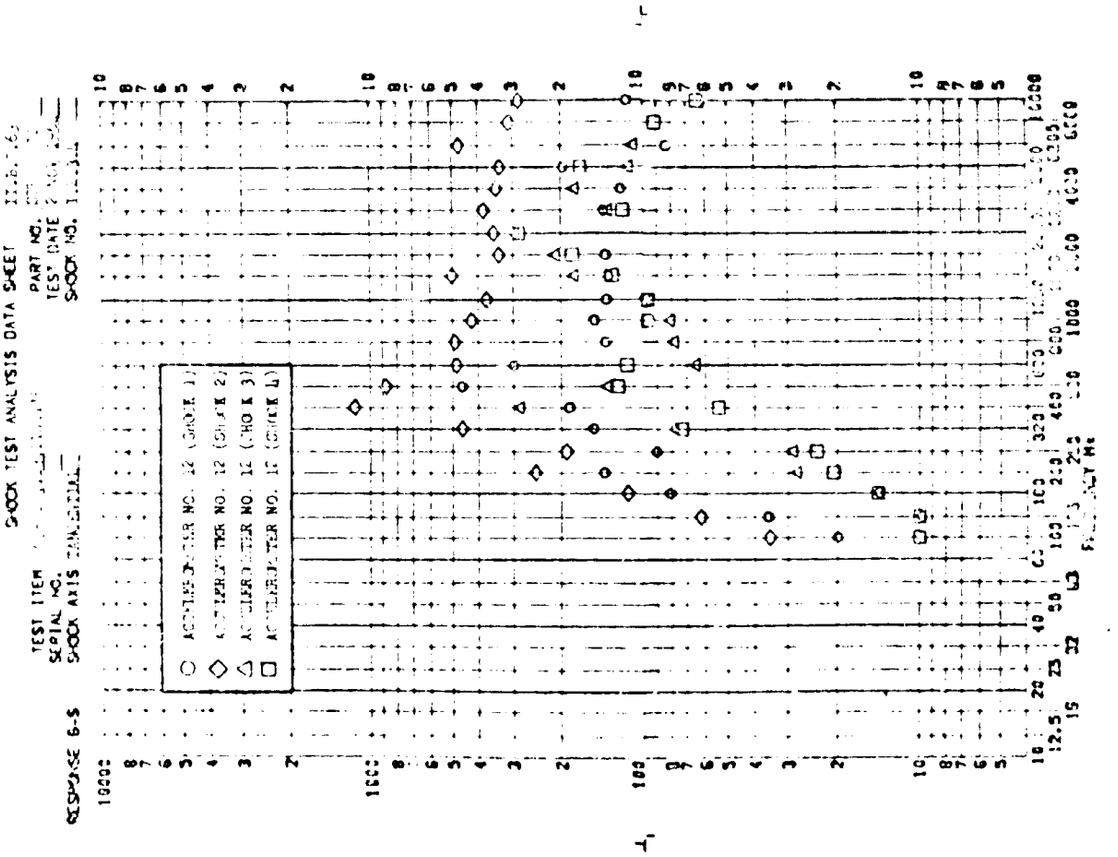
SHOCK TEST ANALYSIS DATA SHEET
TEST ITEM
SERIAL NO.
SHOCK AXIS
PART NO.
TEST DATE
SHOCK NO.
RESPONSE G-S
ACCELEROMETER NO. 12 (SHOCK 1)
ACCELEROMETER NO. 12 (SHOCK 2)
ACCELEROMETER NO. 12 (SHOCK 3)
ACCELEROMETER NO. 12 (SHOCK 4)

SECTION NO. II.B.3

REPORT NO. 1353

SUBJECT:

FAIRING JETTISON USING EXPLOSIVE NUT

SECTION II.B.3

SUMMARY

The fairing deployment mechanism described in this section is a further development of the type shown in Section II.B.2. In order to reduce the intensity of the pyrotechnic shock, the design is modified to use an explosive nut instead of a pin puller to trigger release of the fairing. The energy necessary for jettisoning is provided by a compression spring.

The pyrotechnic tests were carried out on an actual forward equipment frame. Two firings were performed but an instrumentation failure prevented data recording of the first firing. All data presented here is due to firing No. 2 in which eleven accelerometers were recorded.

Shock attenuation versus distance from the shock source was established on the basis of shock spectrum peak g's in each octave band. Due to limited data and data scatter, only an approximation of the reduction trend could be established.

Accelerometer No. 9 indicates a response level higher than expected. Although the exact cause of this high reading is not known, it is assumed that some local resonance is responsible for it. Accelerometers No. 1 and 2 show evidence of some zero shift which was corrected in the data reduction process.

With respect to the standard pin pusher jettison mechanism, the separation nut spring activated mechanism environment is reduced to 1% at low frequencies and 10% at high frequencies.

This system has been incorporated into the design of a flight vehicle where it operated succesfully in several launches.

TABLE OF CONTENTS

SECTION II.B.3

LIST OF TABLES

SECTION II.B.3

LIST OF FIGURES

SECTION II.B.3

LIST OF FIGURES (Cont.)

SECTION II.C.3

II.B.3.1 INTRODUCTION

In order to reduce the shock environment in the forward equipment rack, created by the jettison of the horizon sensor fairing, a new fairing release mechanism was designed and tested.

The test general arrangement is shown on Figure II.B.3.1 and the fairing release mechanism on Figure II.B.3.2. The ejection device consists essentially of a compression spring held by a separation explosive nut. Firing of the nut releases the retaining bolt, thus freeing the spring which imparts an impulse to the fairing, throwing it clear from the vehicle.

II.B.3.2 DISCUSSION AND ANALYSIS

II.B.3.2.1 Test Configuration and Instrumentation

An actual forward equipment rack, containing all internal structure supporting mass simulated equipment, was used for this test. One piece of equipment contained functional flight hardware.

Figure II.B.3.1 shows the general arrangement of the test specimen and location of all accelerometers.

Figure II.B.3.2 shows the fairing release mechanism. The explosive separation nut is placed inside an explosion proof catcher in order to retain debris and vent gases to the outside. The spring ejection mechanism is used in conjunction with a fall-away hinge. Firing of the nut releases the bolt thus freeing the spring which imparts to the fairing rotational and translational accelerations such that it will be thrown clear from the vehicle.

The instrumentation comprises 11 accelerometers (Table II.B.3.1) attached at various points of the structure as shown on Figure II.B.3.1 in order to provide a general mapping of the shock environment. Accelerometers 8 and 11 were placed on the box containing functional flight hardware.

Instrumentation failure prevented data acquisition during the first firing. All data presented here was recorded during the second firing. Firing data is given in Table II.B.3.2.

Shock spectrum and oscillogram data are presented in Figures II.B.3.1 to II.B.3.13.

II.B.3.2.2 Technical Discussion

Upon completion of the test, inspection of the specimen showed that no failure occurred. Over the frequency range, the accelerometer readings were affected by two types of disturbances, namely: piezocrystal zero shift and circuit noise. Piezocrystal zero shift occurred on accelerometers 1 and 2 while circuit noise obliterated the low frequency response of accelerometers 3, 4, 5, 8 and 11.

Reduction of the test data was performed on the UNIVAC 1108 after digitizing the analog tape. This data reduction provided some correction for piezocrystal zero shift.

II.B.3.2.3 Analysis

The shock level attenuation versus distance from the source has been approximated on the basis of shock spectrum peak value in each octave band over the range 200 cps to 6400 cps. This is shown on Figure II.B.3.1 with the numerical data given on Table II.B.3.1 and II.B.3.4.

It will be noted that accelerometer 9 consistently recorded acceleration levels higher than other accelerometers closer to the shock source. This data has been verified and found to be sound. It is assumed that accelerometer 9 was reading the response of some local high amplification system or structure resonating at about 500 cps.

The curve presented on Figure II.B.3.1 is only an approximation of a trend which indicates that considerably more work is needed in this area.

II.B.3.3 CONCLUSION

The separation nut, spring activated fairing ejection system has been tested successfully and provided useful data to assess the environment level produced by its operation.

Comparison of this environment with that produced by other fairing ejection systems is given in Section II.B.4 where it is shown that with respect to the standard pin pusher jettison mechanism the separation nut spring activated mechanism environment is reduced to 1% at low frequencies and 19% at high frequencies.

This system has been incorporated into the design of a flight vehicle where it operated successfully in several launches.

TABLE II.B.3.1

ACCELEROMETERS AND LOCATIONS

Accelerometer No.	Station (inches)	Direction	Distance to Shock Source (inches)	Accelerometer Type
1	247	X	5.0	ENDEVCO 2225
2	247	Y	5.0	ENDEVCO 2225
3	247	Z	5.0	ENDEVCO 2225
4	247	X	5.0	ENDEVCO 2225
5	247	Z	5.0	ENDEVCO 2225
6	247	X	59.0	ENDEVCO 2225
7	247	Z	59.0	ENDEVCO 2225
8	257	Z	14.0	ENDEVCO 2225
9	287	Z	59.0	ENDEVCO 2225
10	247	Y	38.0	ENDEVCO 2225
11	267	X	25.0	ENDEVCO 2225

TABLE II.B.3.2

SUMMARY OF TESTS

Test No.	Explosive Size	Test Purpose	Shock Isolation
1*	XP nut**	Environmental Data	None
2	XP nut**	Environmental Data	None

* Data recording failure.

** Explosive nut. Ref: Hi-Shear No. SN-7323-2B

TABLE II.B.3.3

SUMMARY OF PEAK G READINGS FROM OSCILLOGRAMS

Accelerometer No.	Axis	Distance from Shock Source	Location	Peak G Reading Test 1	Test 2
1	Long.	5.0	Frame - Sta. 247	Data recording failure	150
2	Lat.	5.0	Frame - Sta. 247		200
3	Vert.	5.0	Frame - Sta. 247		245
4	Long.	5.0	Frame - Sta. 247		150
5	Vert.	5.0	Frame - Sta. 247		65
6	Long.	59.0	Frame - Sta. 247		12
7	Vert.	59.0	Frame - Sta. 247		6
8	Vert	14.0	Equipment Box - Sta. 257		36
9	Vert.	69.0	Bracket - Sta. 287		21
10	Lat.	38.0	Frame - Sta. 247		30
11	Long.	25.0	Equipment Box - Sta. 267		90

FORM LMSC 8787.2

TABLE II.6.3.4

DETERMINATION OF SHOCK ATTENUATION VERSUS DISTANCE FROM SOURCE

Symbol	Accelerometer / Octave (cps)	PEAK G FROM SHOCK SPECTRUM									% OF MAX. AT 5.00" NORMALIZED			
		1_x	2_y	3_z	4_x	5_z	6_x	7_z	9_z	10_y	6_x	7_z	9_z	10_y
⊙	200 to 400	75	36	17	13	20	6.2	4	22	7.5	8.27	0	29.33	10.0
◇	400 to 800	87	39	38	30	39	22	18	78	16	25.29	20.69	89.65	18.39
△	800 to 1600	140	95	140	69	59	74	22	72	45	52.86	15.71	51.43	32.14
▽	1600 to 3200	200	480	160	200	180	74	35	102	92	15.42	7.29	21.25	19.17
◈	3200 to 6400	220	480	500	300	300	45	32	102	103	9.0	6.4	20.4	20.6
	Distance from Source (Inches)	5"	5"	5"	5"	5"	59"	59"	69"	38"	59"	59"	69"	36"

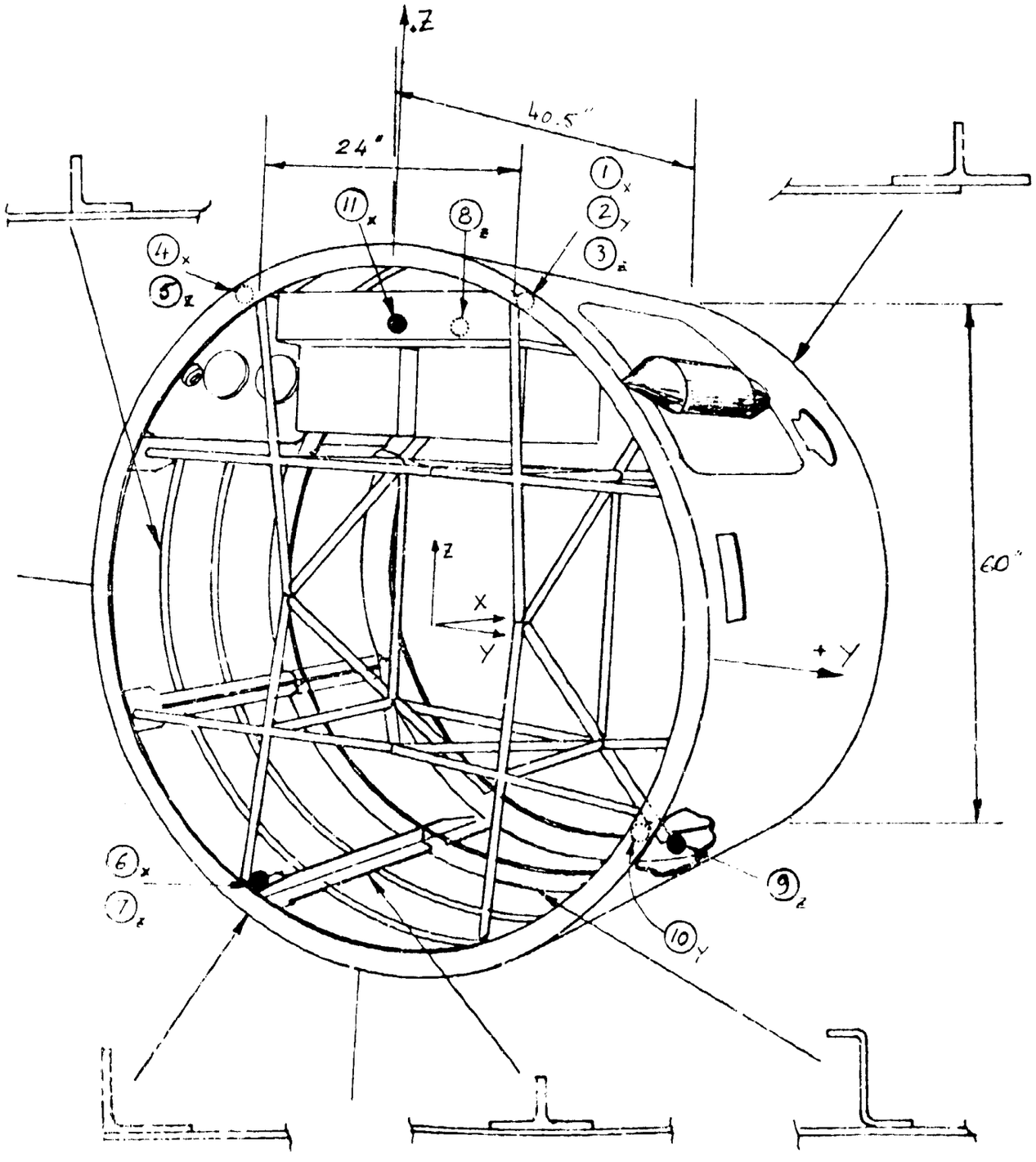

Figure II.B.3.1 TEST CONFIGURATION AND INSTRUMENTATION LOCATIONS

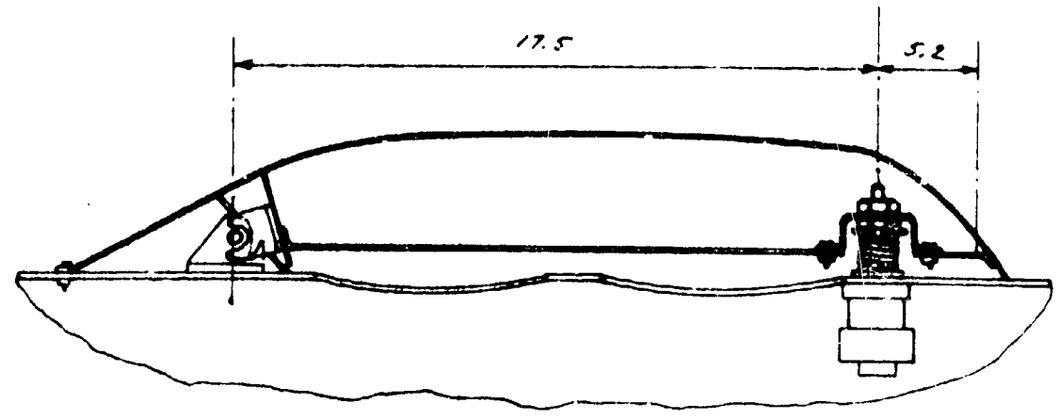

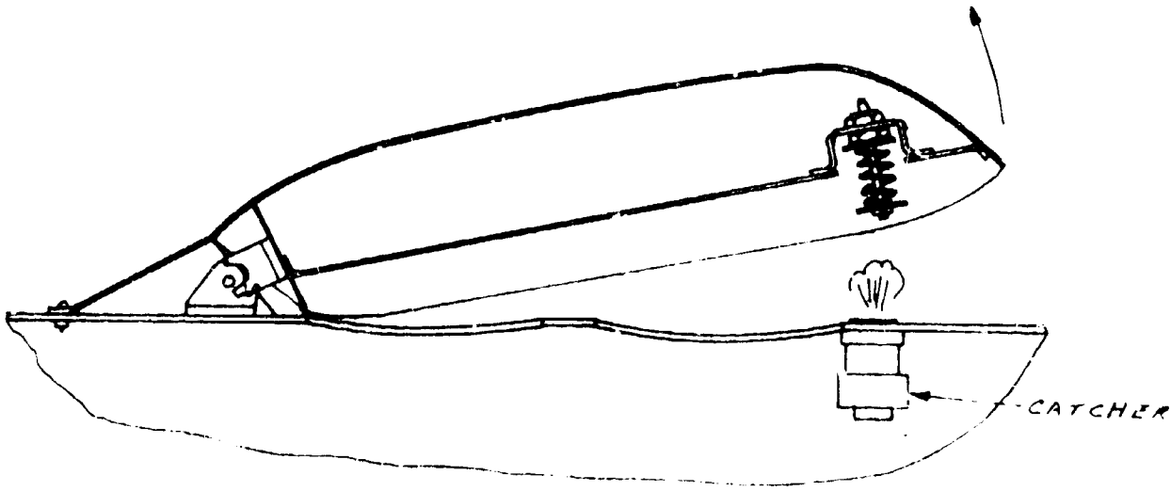

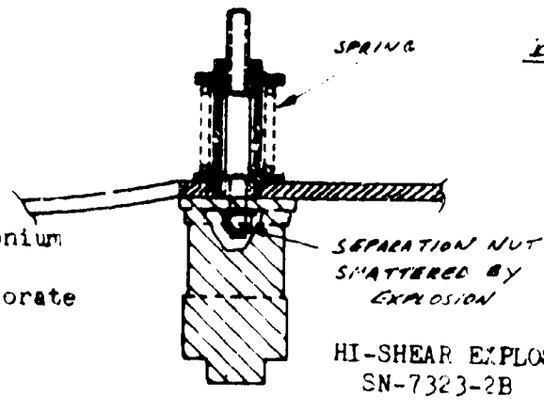

DETAILS OF RELEASE MECHANISM

EXPLOSIVE CONTENTS:

110 mg potassium perchlorate and zirconium

600 mg potassium perchlorate and titanium hydrate

HI-SHEAR EXPLOSIVE NUT SN-7323-2B

Figure II.B.3.2 FAIRING EJECTION MECHANISM

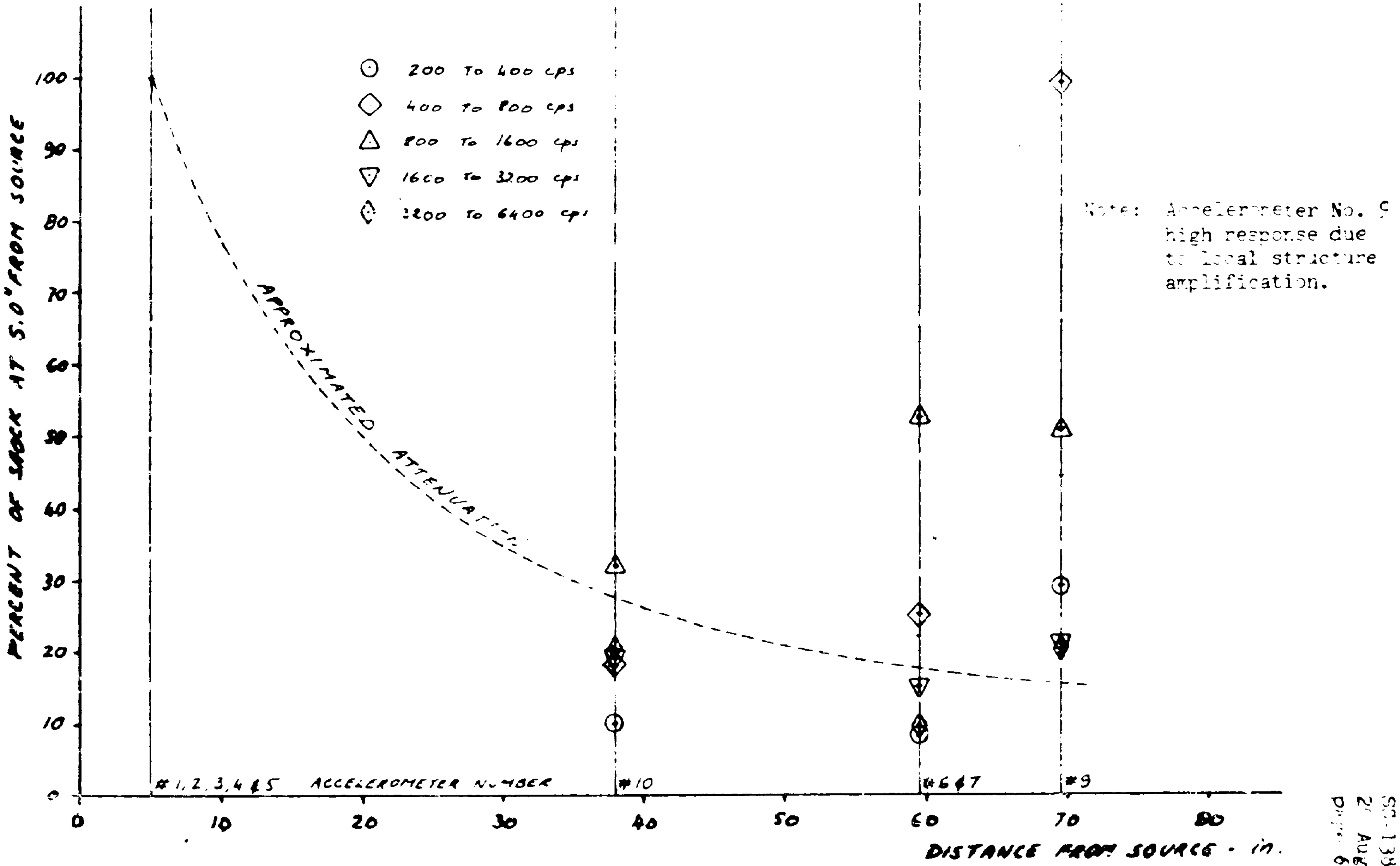

Figure II.B.3.3 ATTENUATION BASED ON SHOCK SPECTRUM PEAK LEVEL IN EACH OCTAVE BAND

SHOCK TEST ANALYSIS DATA SHEET NO. II.B.3.4

TEST ITEM 1353-40
SERIAL NO.
SHOCK AXIS LONGITUDINAL

PART NO. STRUCTURE
TEST DATE 12-20-68
SHOCK NO. 1

RESPONSE G-S

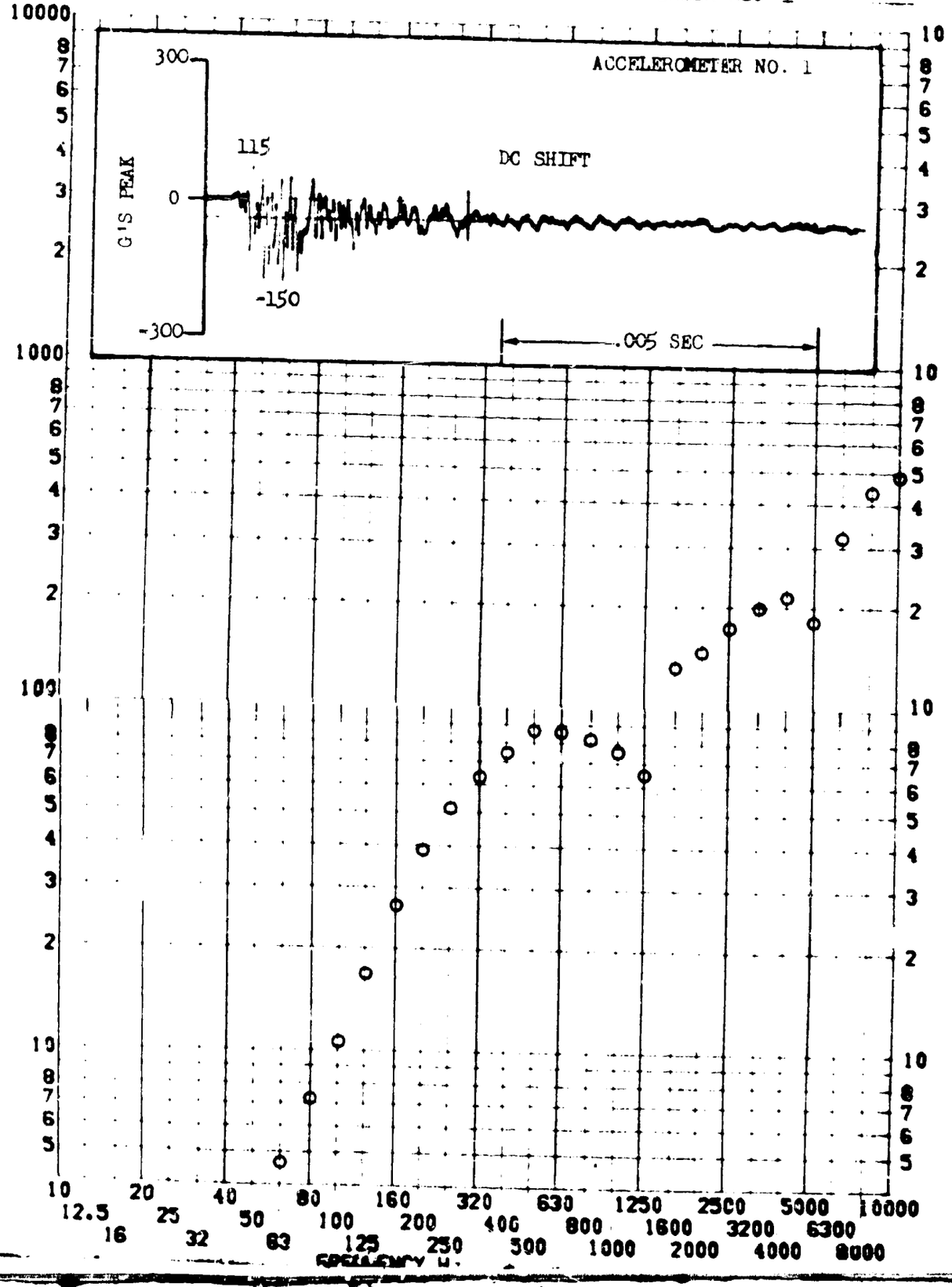

SHOCK TEST ANALYSIS DATA SHEET NO. II.B.3.9

TEST ITEM 1353-41
SERIAL NO.
SHOCK AXIS LATERAL

PART NO. STRUCTURE
TEST DATE 12-20-68
SHOCK NO.

RESPONSE G-S

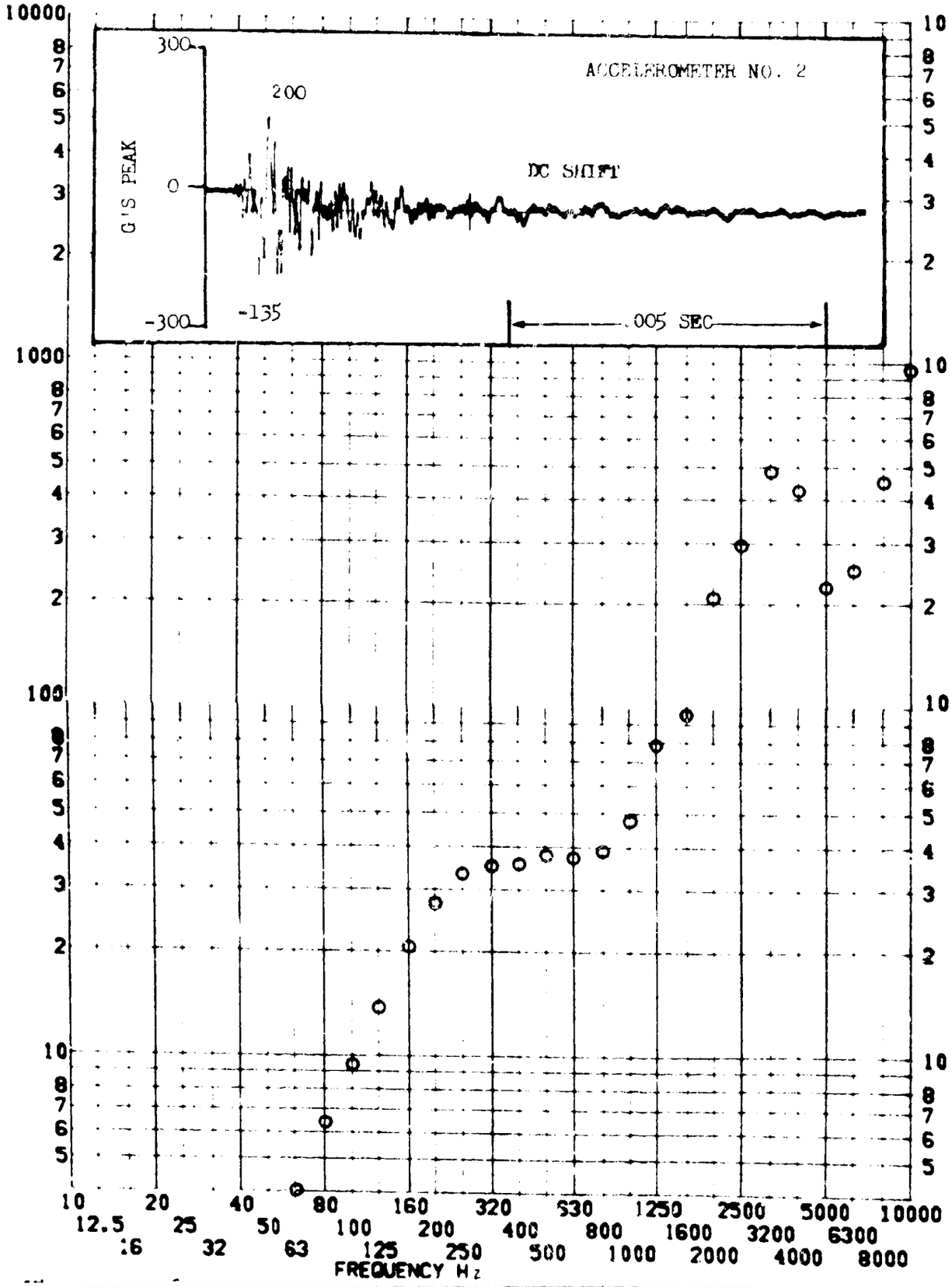

SHOCK TEST ANALYSIS DATA SHEET NO. II.B.3.6

TEST ITEM 1353-42
SERIAL NO.
SHOCK AXIS VERTICAL

PART NO. STRUCTURE
TEST DATE 12-20-68
SHOCK NO. 1

RESPONSE G-S

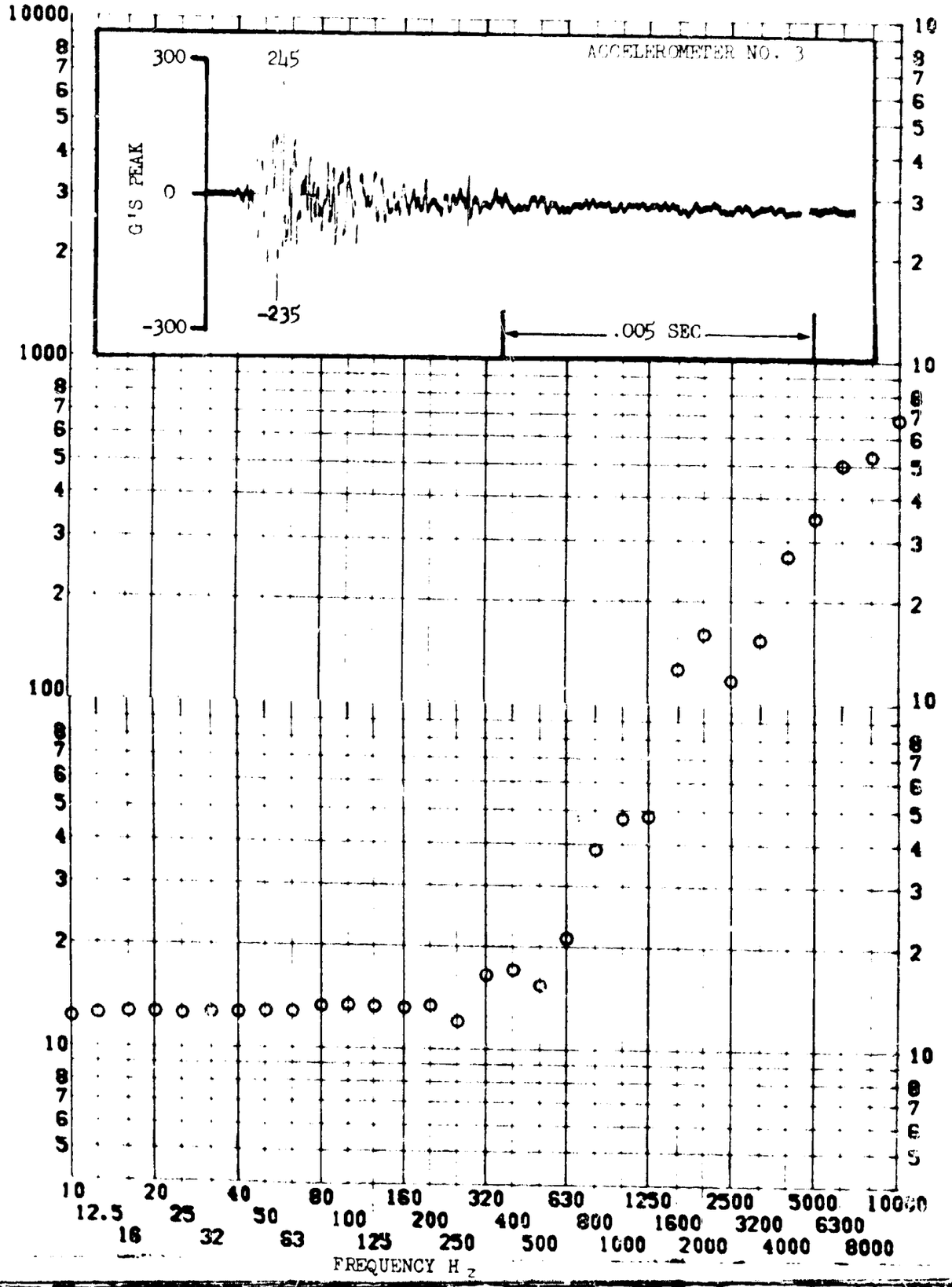

SHOCK TEST ANALYSIS DATA SHEET NO. II.B.3.7

TEST ITEM 1353-43
SERIAL NO.
SHOCK AXIS LONGITUDINAL

PART NO. STRUCTURE
TEST DATE 12-20-68
SHOCK NO. 1

RESPONSE G-S

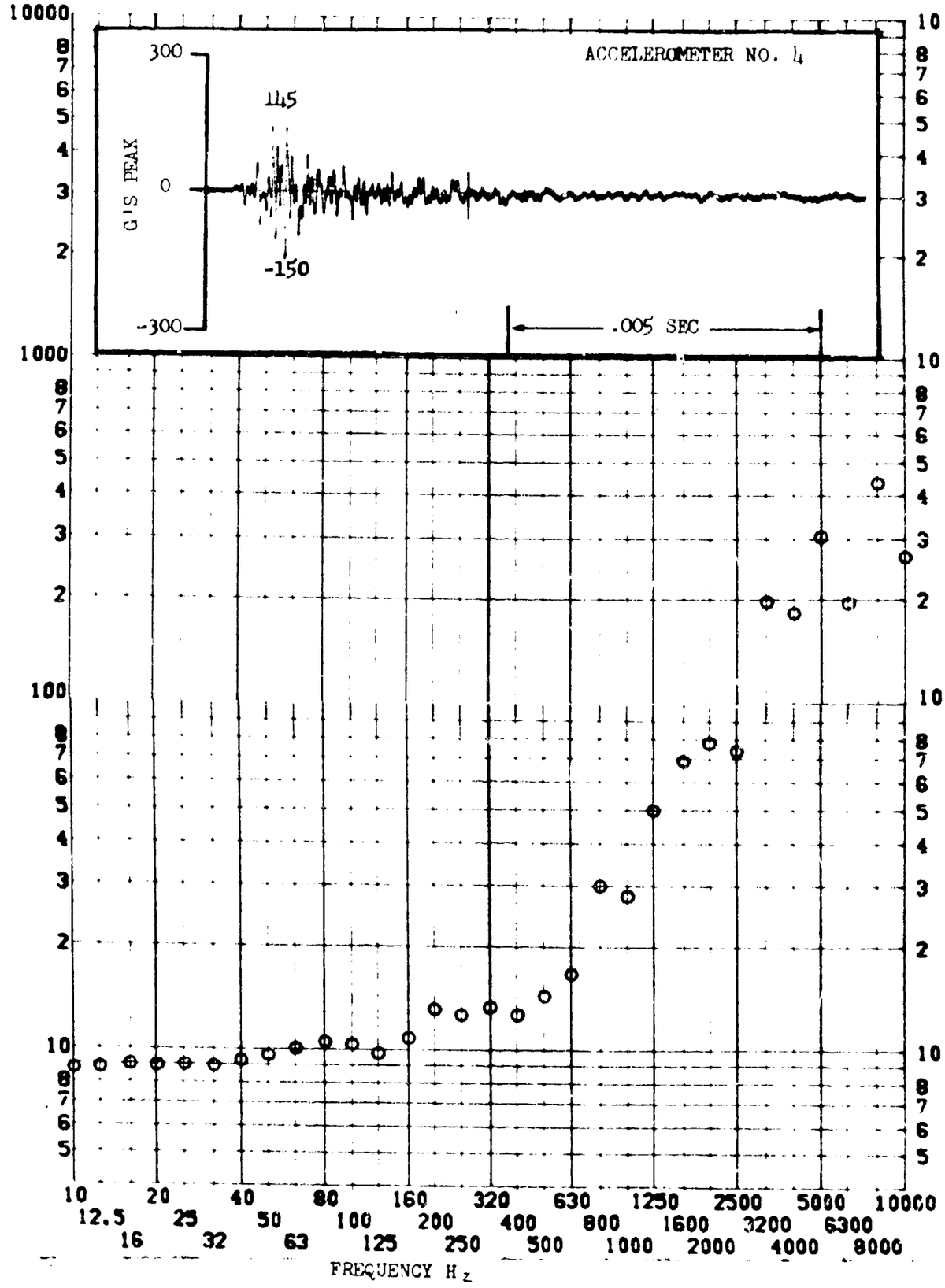

SHOCK TEST ANALYSIS DATA SHEET NO. I.U.B.3.8

TEST ITEM 1353-44
SERIAL NO.
SHOCK AXIS VERTICAL

PART NO. STRUCTURE
TEST DATE 12-20-68
SHOCK NO. 1

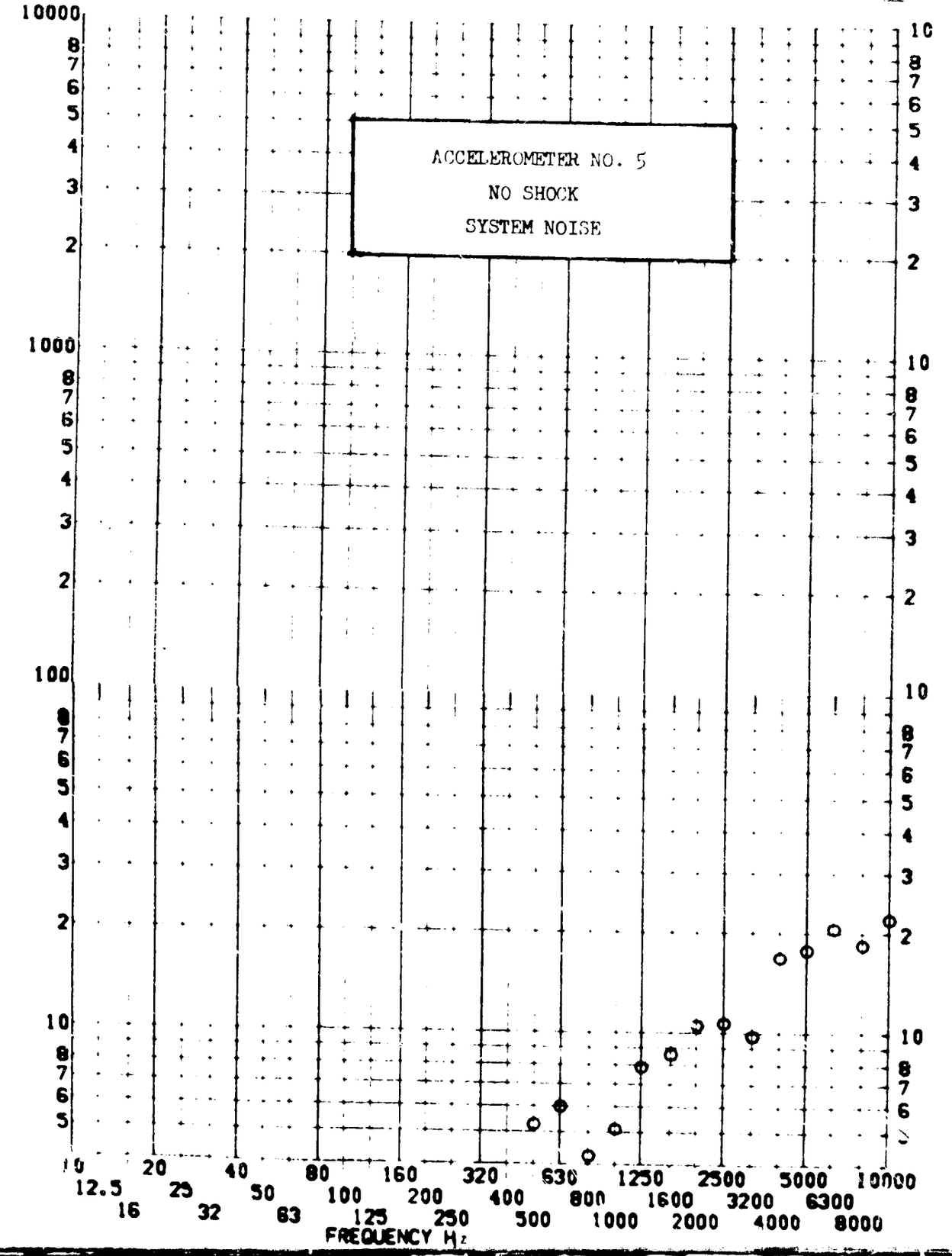

SHOCK TEST ANALYSIS DATA SHEET NO. II.B.3.9

TEST ITEM 1353-45 PART NO. [illegible]
SERIAL NO. TEST DATE 12-20-68
SHOCK AXIS VERTICAL SHOCK NO. 1

RESPONSE G-S

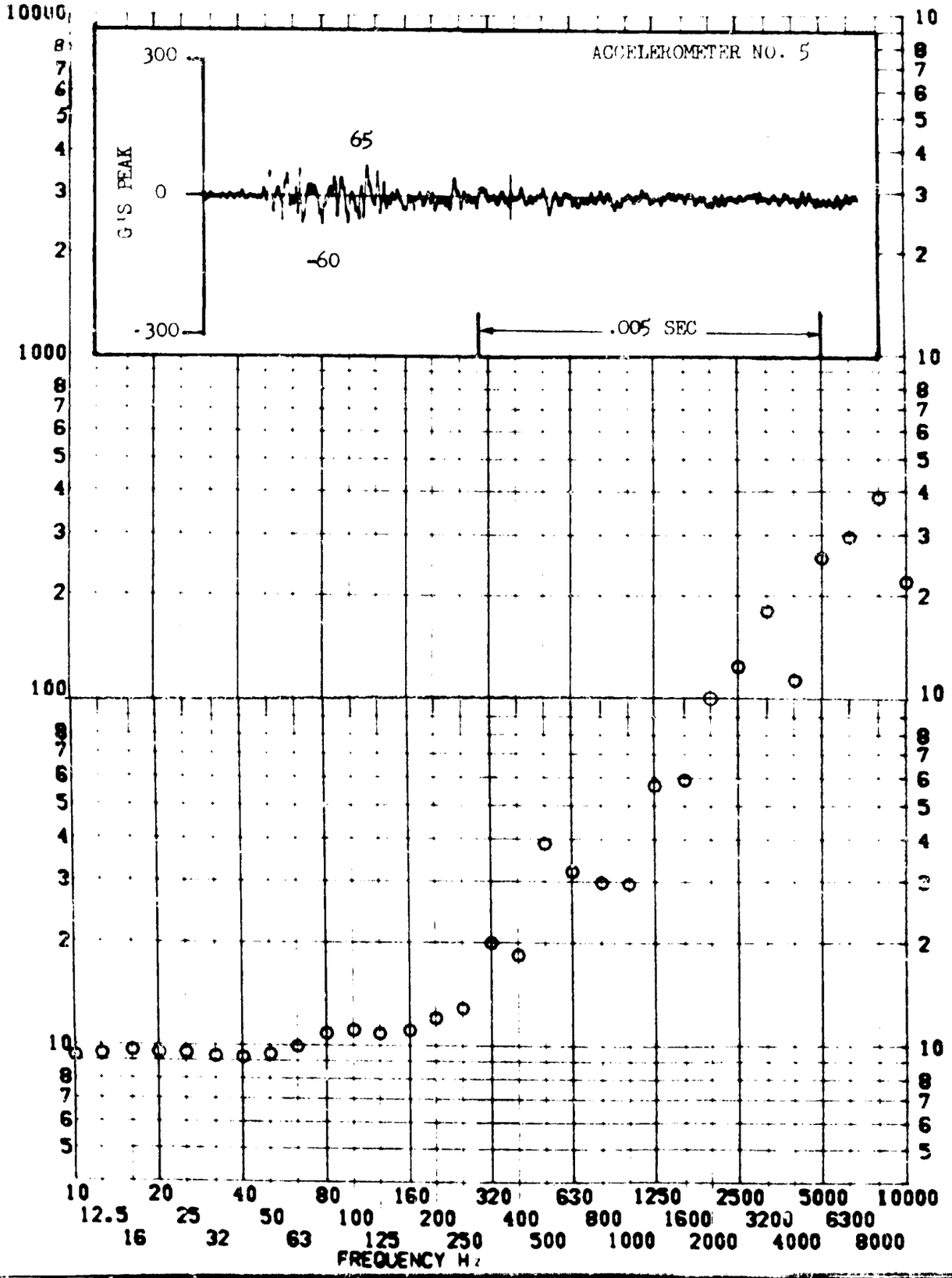

SHOCK TEST ANALYSIS DATA SHEET NO. II.B.3.10

TEST ITEM 1353-44,45 PART NO. STRUCTURE
SERIAL NO. TEST DATE [illegible] 1968
SHOCK AXIS VERTICAL SHOCK NO. 1

RESPONSE G S

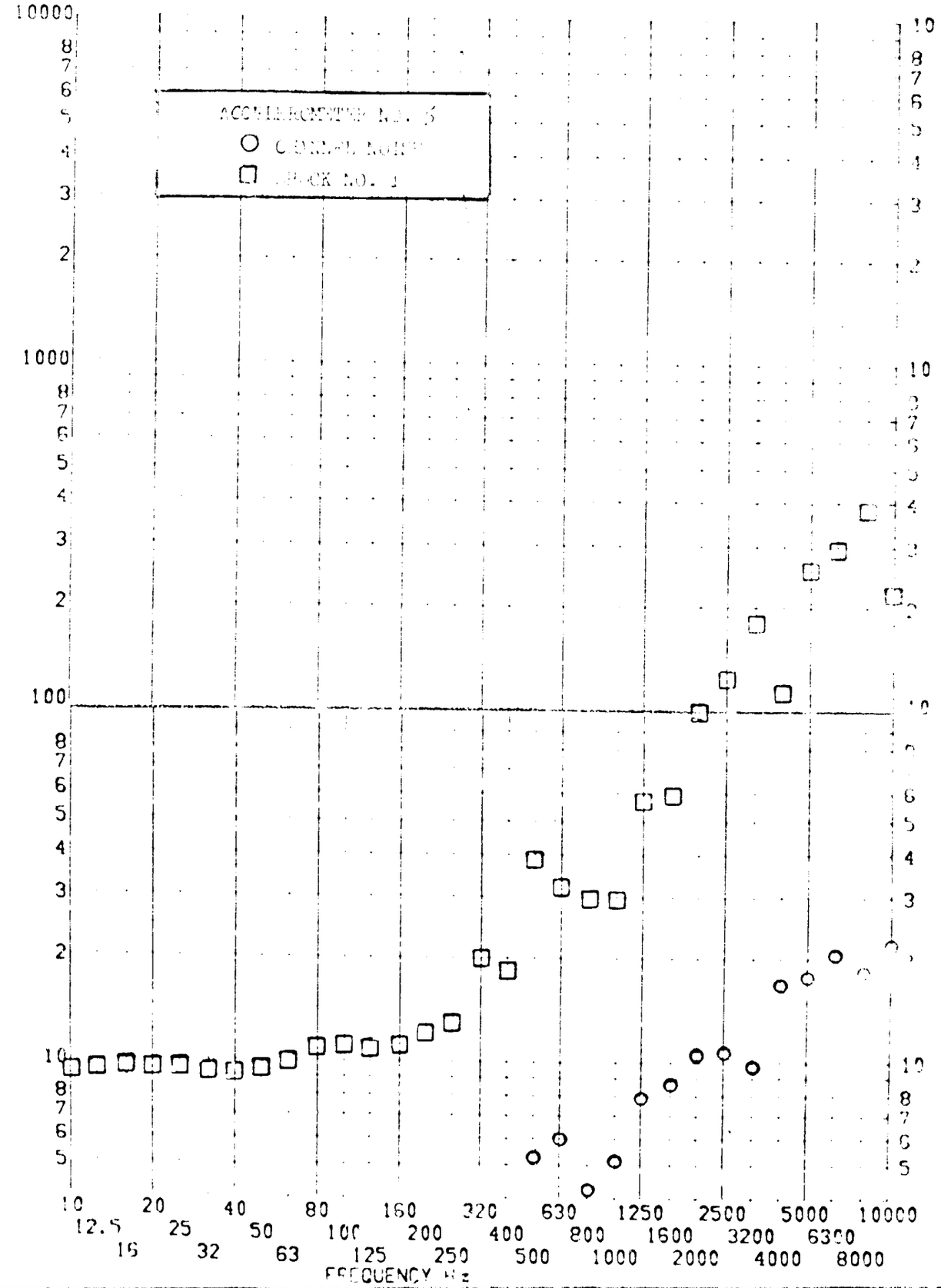

SHOCK TEST ANALYSIS DATA SHEET NO. II.B.3.11

TEST ITEM 1353-46
SERIAL NO.
SHOCK AXIS LONGITUDINAL

PART NO. STRUCTURE
TEST DATE 12-20-68
SHOCK NO. 1

RESPONSE G-S

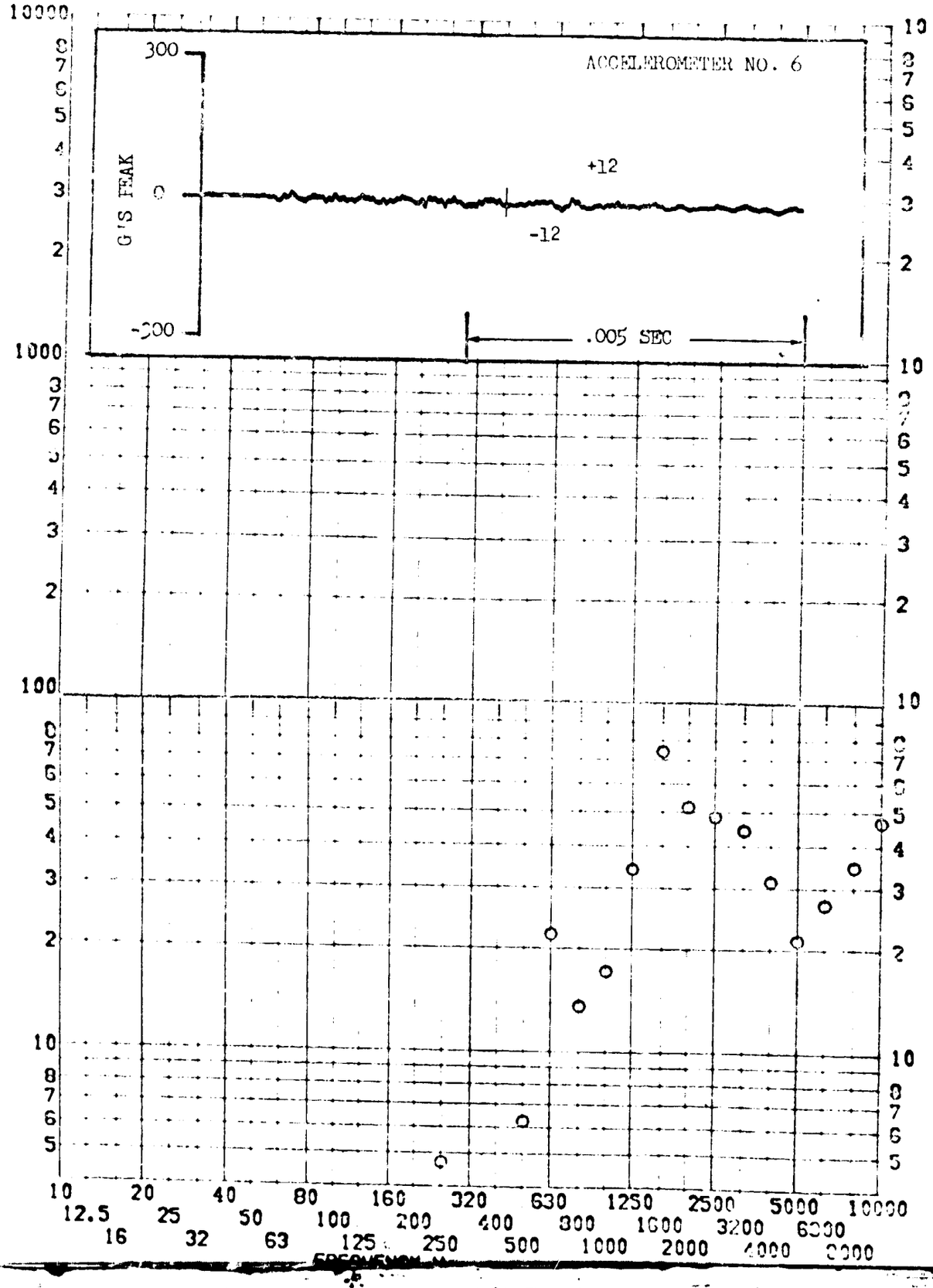

SHOCK TEST ANALYSIS DATA SHEET NO. II.B.3.12

TEST ITEM 1353-17
SERIAL NO.
SHOCK AXIS VERTICAL

PART NO. STRUCTURE
TEST DATE 12-20-62
SHOCK NO. 1

RESPONSE G-S

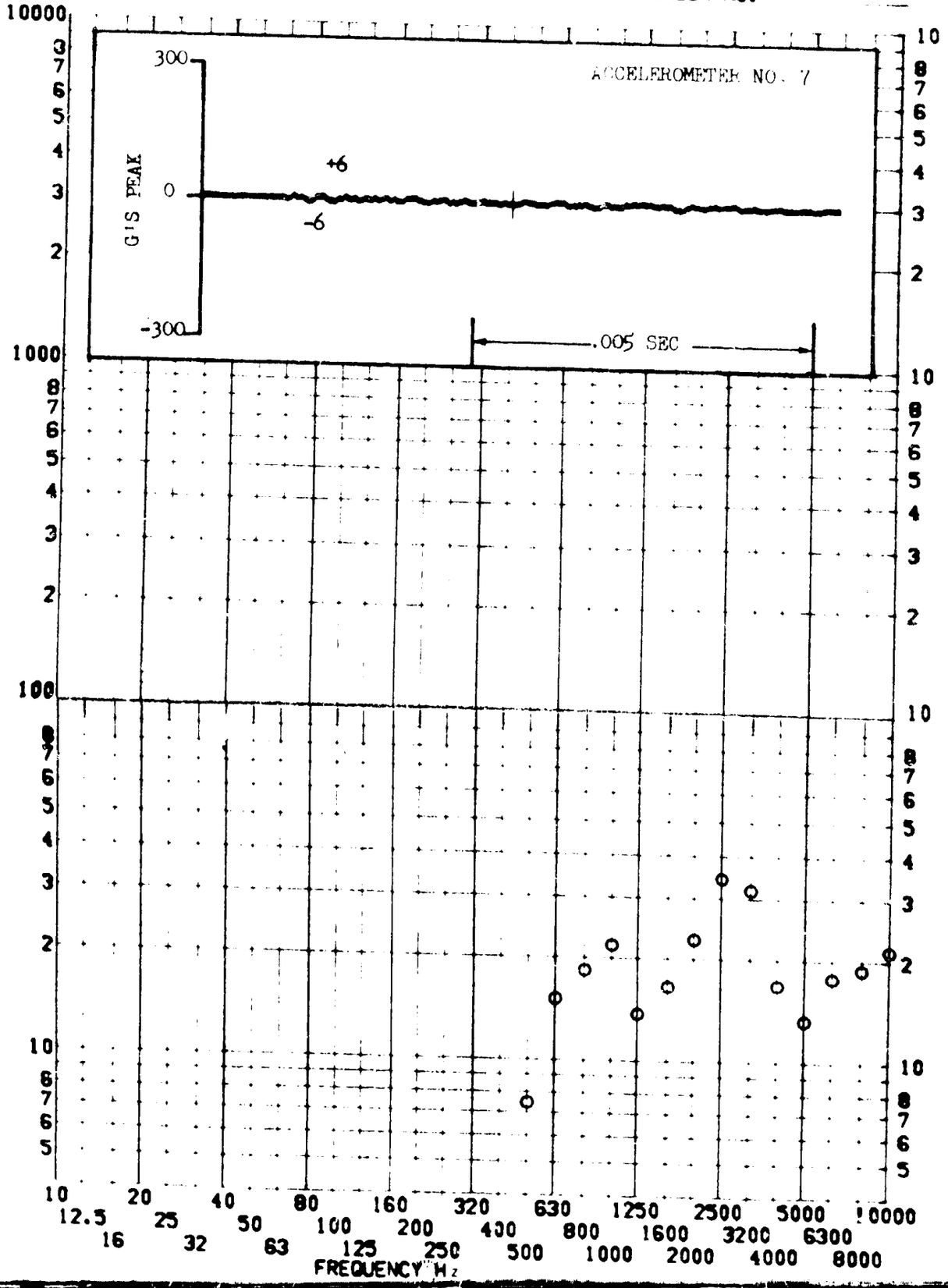

SHOCK TEST ANALYSIS DATA SHEET NO. II.B.3.13

TEST ITEM 1353-48
SERIAL NO.
SHOCK AXIS VERTICAL

PART NO. STRUCTURE
TEST DATE 12-20-68
SHOCK NO. 1

RESPONSE G-S

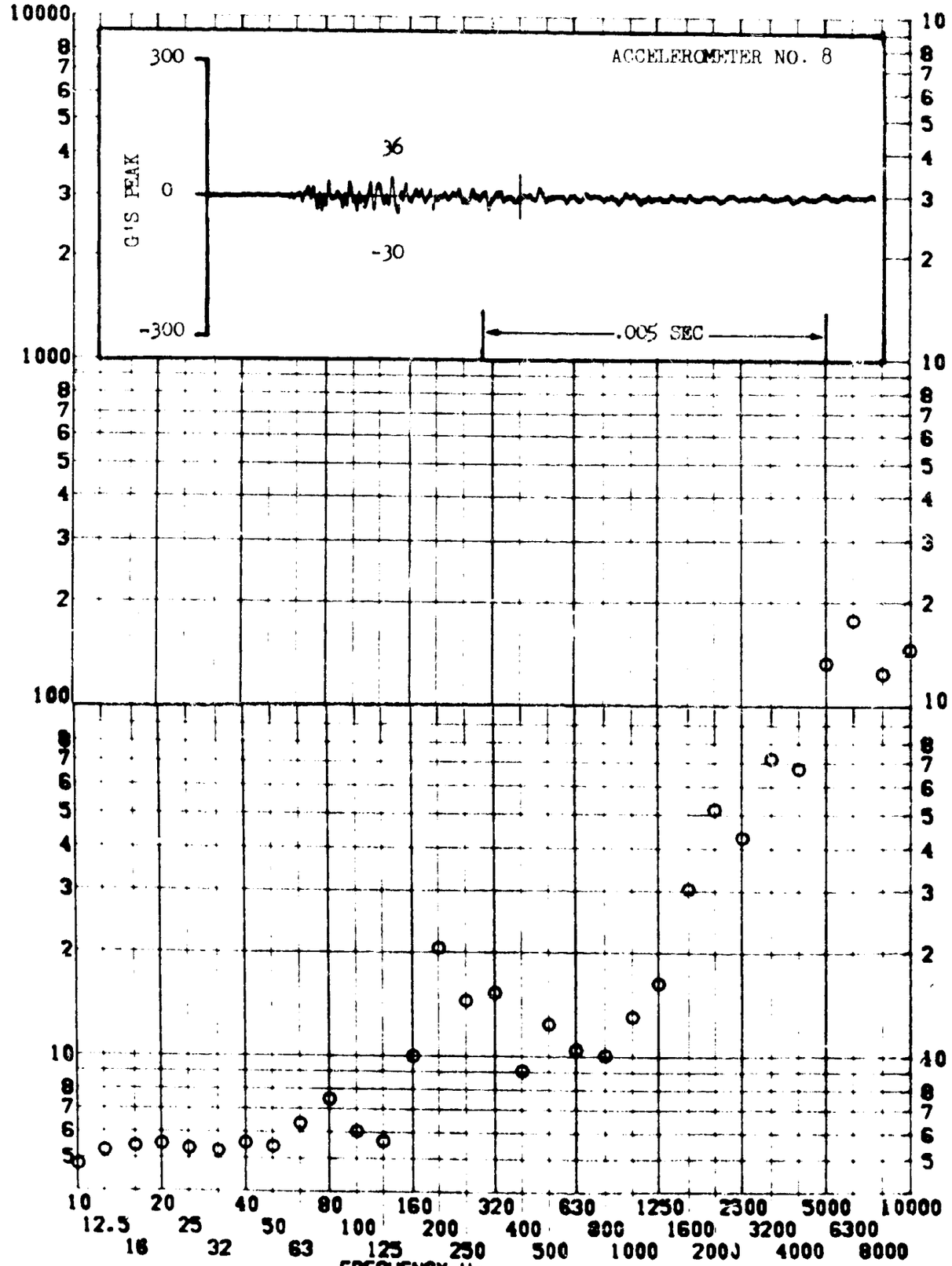

SHOCK TEST ANALYSIS DATA SHEET NO. H.B.

TEST ITEM 1353-49
SERIAL NO.
SHOCK AXIS VERTICAL

PART NO. STRUCTURE
TEST DATE 2-26-68
SHOCK NO.

RESPONSE G-S

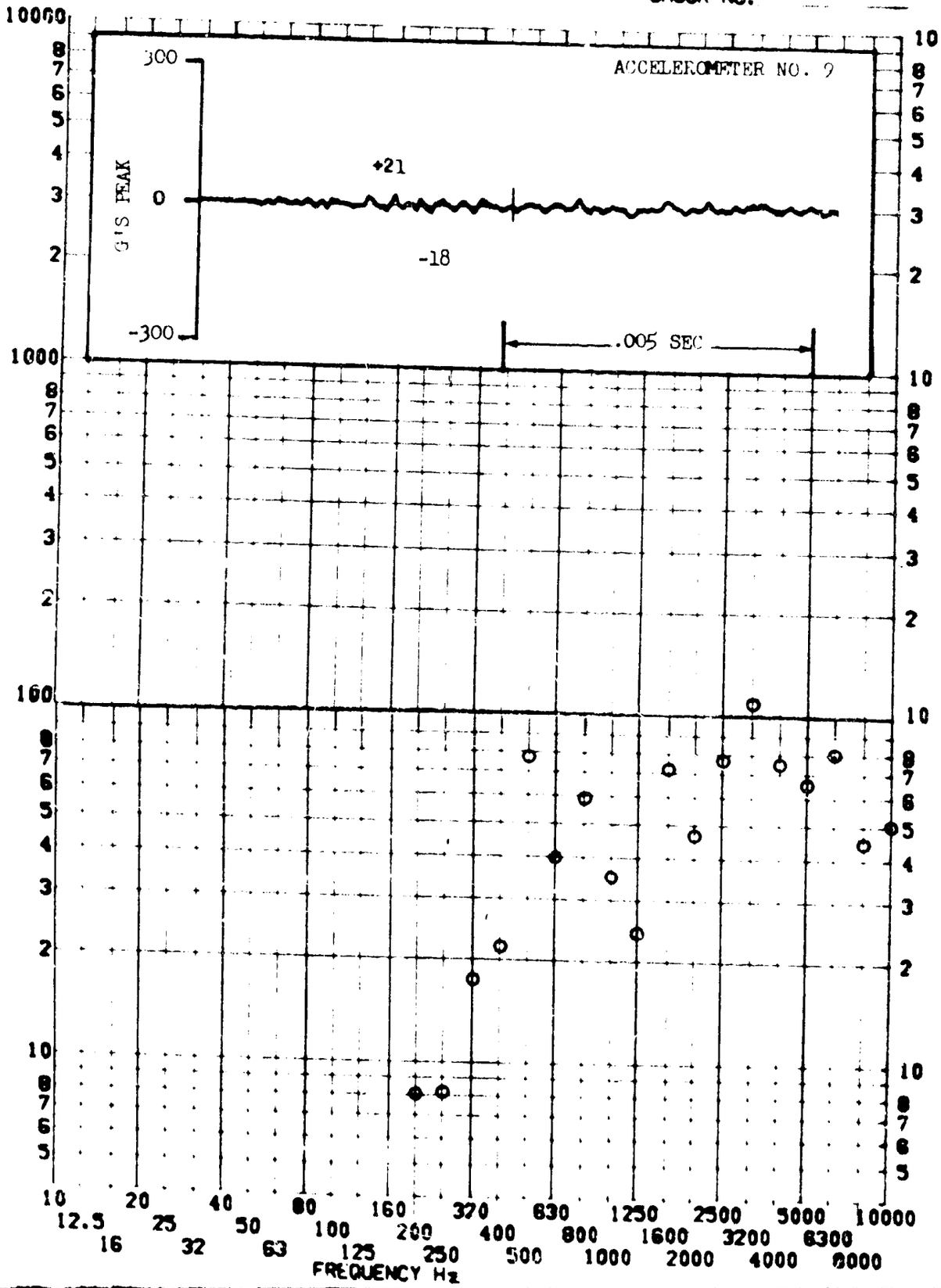

SHOCK TEST ANALYSIS DATA SHEET NO. II.3.3.1

TEST ITEM 1353-50
SERIAL NO.
SHOCK AXIS LATERAL

PART NO. STRUCTURE
TEST DATE 12-20-68
SHOCK NO. 1

RESPONSE G-S

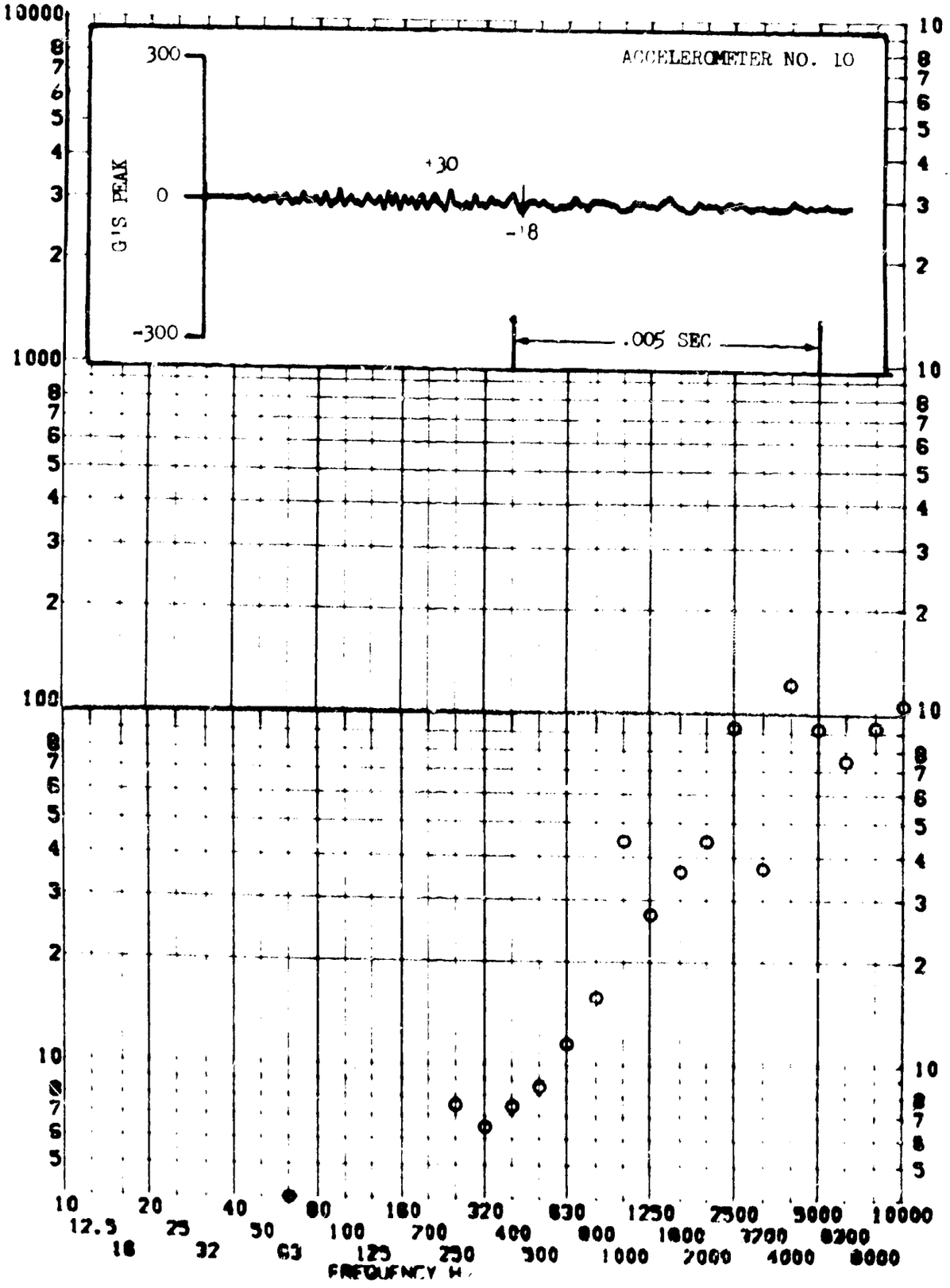

SHOCK TEST ANALYSIS DATA SHEET NO. I.B.3.1

TEST ITEM 1353-51
SERIAL NO.
SHOCK AXIS LONGITUDINAL

PART NO. TRUCTURE
TEST DATE 2-20-68
SHOCK NO.

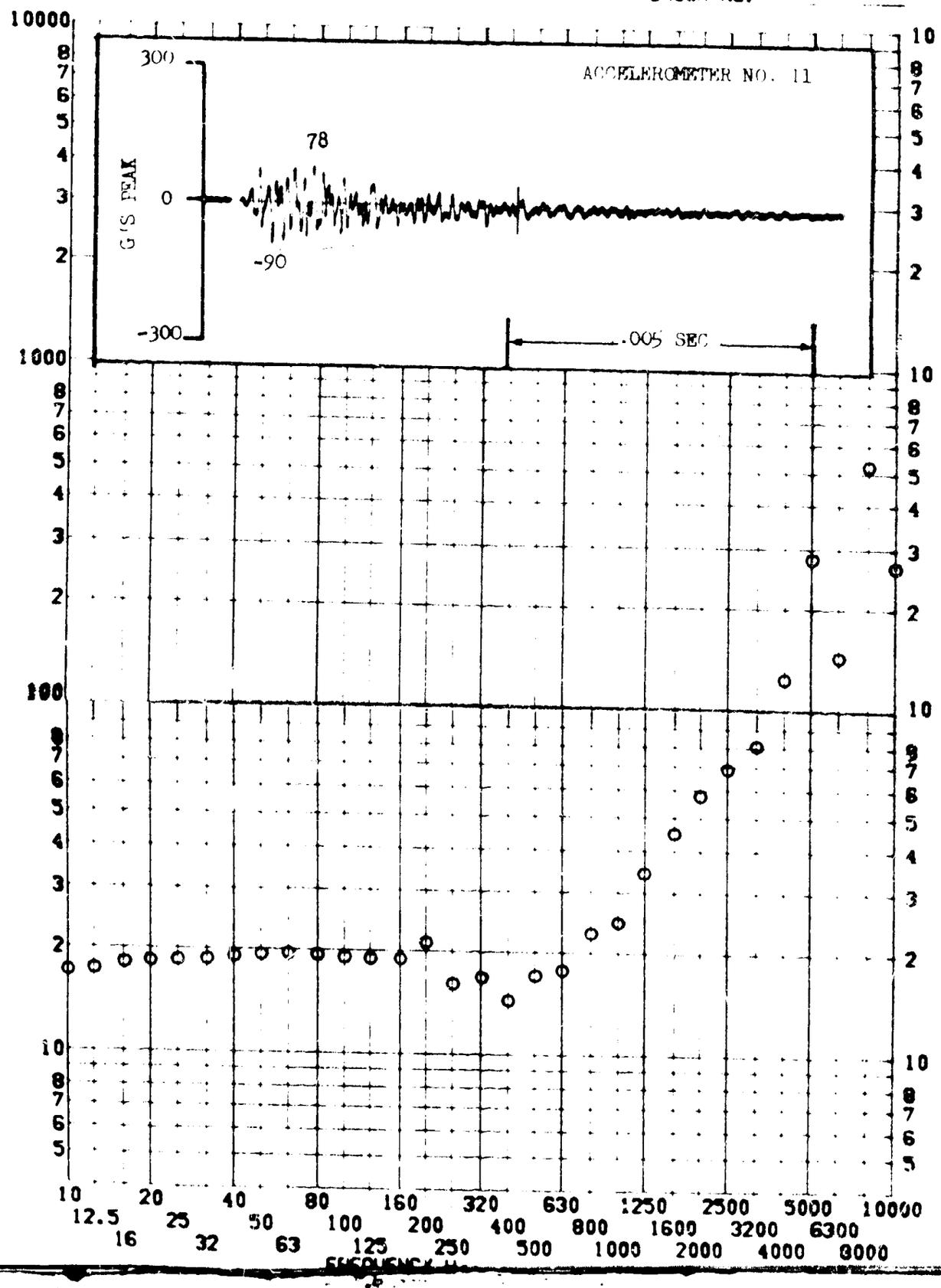

II.B.4 DISCUSSION AND ANALYSIS

II.B.4.1 Pin Actuators

Pin pushers were originally selected for the operation of the fairing deployment mechanism because of their very high reliability and design simplicity. These devices, for safety purposes, are activated by two squibs, each containing one grain of explosive. Upon firing the squibs, high pressure gases are generated which impart a high velocity to the actuator piston. At the end of its stroke, the piston is arrested by striking the actuator housing. This mechanical shock, combined with the explosion shock wave forms the shock environment generated by the pin actuator. Attempts were made to reduce the shock of piston striking its housing by interposing a variety of resilient materials at the interface and by external isolation of the pin pusher. These modifications, however, failed to provide an improvement significant enough to justify their introduction into the design.

A more complete description and analysis of pin actuators is presented in Section II.C of this report.

II.B.4.2 Comparison of the Three Deployment Mechanisms

II.B.4.2.1 Standard Pin Pusher Mechanism (Section II.B.1)

The standard deployment mechanism consists of two pin pushers mounted normally to the vehicle skin with the fairing attached directly to the free part of the actuator pin. In operation, a mass consisting of the complete fairing and the two actuator free pins is accelerated by the expansion of the explosion gases pushing against the face of the piston. Since the mass set in motion is fairly large, its acceleration is relatively slow and the shock extends over a significant length of time. This is in contrast with the firing of a pin actuator in the no load condition which provides a sharp load peak over a very small length of time. The pin pusher deployment mechanism is therefore prone to excite more structural resonances.

II.B.4.2.2 Spring-Pin Puller Mechanism (Section II.B.2)

It was realized that the energy needed to expel the fairing was relatively small, much less than that provided by two pin pushers. The energy which can be stored into a compression spring is sufficient to propel the fairing and the use of a fall-away hinge allows operating with one spring only. The fairing was redesigned along these lines with the release of the spring controlled by a pin puller for reliable operation

II.B.4.2.3 Spring-Explosive Nut Mechanism (Section II.B.3)

Although the spring loaded deployment mechanism performed well, the use of the pin puller release system provided an unnecessarily high energy expenditure and correspondingly high shock environment level.

Without sacrificing reliability, an explosive nut was substituted for the pin puller and this device, having no moving part, eliminated one of the major shock sources (piston striking the housing) thereby reducing by a significant amount the shock environment level.

II.B.4.3 Analysis

The analysis presented here consists of a comparison of the shock environment level provided by the various design modifications, in order to provide an approximate rating of each device. Using data taken from the three reports, the following table gives in percentage the shock environment level for each mechanism.

SHOCK ENVIRONMENT LEVELS VERSUS DEVICE
IN PERCENT OF STANDARD PIN-PUSHER LEVELS

Freq. Band Octave	200/400	400/800	800/1600	1600/3200	3200/6400
Standard pin pusher	100	100	100	100	100
Improved pin pusher	*	*	*	*	*
Spring - pin puller	19	37	50	94	72
Spring - explosive nut	1	1	2	19	19

* Improved pin puller level: 61 percent based on peak g's only.

II.B.5 CONCLUSION

The standard pin-pusher fairing deployment mechanism has been flown repeatedly with complete reliability. Its only disadvantage is the high pyrotechnic shock environment it generates.

The spring - explosive-nut fairing deployment mechanism is considered a significant improvement over the original design and has also been flown successfully.

All other deployment mechanisms described in this section were interim designs considered in the course of development.

END

DATE

FILMED

APR 1 1971